

BIOCHEMICAL ENGINEERING AND BIOTECHNOLOGY

SECOND EDITION

GHASEM D. NAJAFPOUR

*Biotechnology Research Lab., Faculty of Chemical Engineering,
Noshirvani University of Technology, Babol, Iran*



ELSEVIER

AMSTERDAM BOSTON HEIDELBERG LONDON NEW YORK OXFORD
PARIS SAN DIEGO SAN FRANCISCO SINGAPORE SYDNEY TOKYO

Elsevier

Radarweg 29, PO Box 211, 1000 AE Amsterdam, Netherlands
The Boulevard, Langford Lane, Kidlington, Oxford OX5 1GB, UK
225 Wyman Street, Waltham, MA 02451, USA

Copyright © 2015, 2007 Elsevier B.V. All rights reserved.

No part of this publication may be reproduced or transmitted in any form or by any means, electronic or mechanical, including photocopying, recording, or any information storage and retrieval system, without permission in writing from the publisher. Details on how to seek permission, further information about the Publisher's permissions policies and our arrangements with organizations such as the Copyright Clearance Center and the Copyright Licensing Agency, can be found at our website: www.elsevier.com/permissions.

This book and the individual contributions contained in it are protected under copyright by the Publisher (other than as may be noted herein).

Notices

Knowledge and best practice in this field are constantly changing. As new research and experience broaden our understanding, changes in research methods, professional practices, or medical treatment may become necessary.

Practitioners and researchers must always rely on their own experience and knowledge in evaluating and using any information, methods, compounds, or experiments described herein. In using such information or methods they should be mindful of their own safety and the safety of others, including parties for whom they have a professional responsibility.

To the fullest extent of the law, neither the Publisher nor the authors, contributors, or editors, assume any liability for any injury and/or damage to persons or property as a matter of products liability, negligence or otherwise, or from any use or operation of any methods, products, instructions, or ideas contained in the material herein.

ISBN: 978-0-444-63357-6

British Library Cataloguing in Publication Data

A catalogue record for this book is available from the British Library

Library of Congress Cataloging-in-Publication Data

A catalog record for this book is available from the Library of Congress

For Information on all Elsevier publications
visit our website at <http://store.elsevier.com/>



Working together
to grow libraries in
developing countries

www.elsevier.com • www.bookaid.org

Author Biography

Author of *Biochemical Engineering & Biotechnology* is a distinguished professor in chemical engineering and the chairman of Biotechnology Research Center, Babol Noshirvani University of Technology, Iran. He is an educated scholar from University of Arkansas, United States with strong background in biological processes. He is deeply involved in research and teaching in biochemical engineering subjects and has conducted many practical researches in the fields of biofuel and biochemical engineering.



He has served as academic member of University of Mazandaran, visiting professor at University of Waterloo, Canada and University of Arkansas, United States, University Science Malaysia (USM, Penang), and Babol Noshirvani University of Technology. He also spent his sabbatical leave at University of Arkansas, United States (1992–1993). He has expanded his scientific research activities on single cell protein, microbial fuel cells, renewable energy, and synthetic fuels. Since 2005, he was qualified and appointed as professor in the faculty of chemical engineering at Babol Noshirvani University of Technology, Iran.

Currently, Prof. Najafpour is serving as editor-in chief in some international journals including: *International Journal of Engineering*, *World Applied Sciences Journal*, *Middle East Journal of Scientific Research*, and *Iranica Journal of Energy and Environment* since 2006. In addition, he is the editor of *Journal of Environmental Chemistry and Ecotoxicology*, academic journals, since 2007. He is an active member of numerous international institutes, editor and reviewer of number of international journals, and many scientific societies. He is often invited to many international conferences as keynote speaker. In the past decades, he has supervised more than 145 post graduate and 28 Ph.D. students. He has published more than 350 research papers in international journals and has written eight books in the field of Chemical Engineering and Biotechnology. In year 2006, he has published the first edition of his book with Elsevier entitled *Biochemical Engineering & Biotechnology*. He has won number of awards for research achievements and was the winner of gold medal for the Invention/Innovation Exhibition sponsored by Ministry of Science, Technology Malaysia (2004). His researches for formulation of transparent soap and natural biodegradable liquid detergent from palm oil's fatty acids, was patented with SIRIM Berhad, Malaysia (2003). Currently, he is supervising number of Ph.D. scholars and conducting top research projects on microbial fuel cells, biodiesel, biohydrogen, biofuel from algae, bioethanol from agro-wastes, enzyme technology, renewable energy, heterogeneous catalytic processes, wastewater engineering, and biological treatment processes.

Book Audience and Overview

WHO SHOULD READ THIS BOOK?

The intersection between biology and engineering has resulted in a number of fields, two of which are biochemical engineering and biomedical engineering. Thus, one would like to use this book to broaden his or her knowledge in interdisciplinary area of engineering/technology and biology/medicine. The field biochemical engineering is relatively new; in past two decades more research activities have been developed. I believe more and more research activities will be focused in this area in near future. The extended material exactly deals with application of biotechnology, as the related bioprocess may lead to commercialization.

This book is focused on practical knowledge and research outcome, which is used to justify the theoretical concepts. Bioseparation and environmental issues are incorporated as case studies related to bioprocesses. Beside case studies, the book contains many examples and solved problems, which help readers to understand all industrial aspects and applications in biotechnology. The second edition broadens the knowledge of research scientists on "Biochemical Engineering and Biotechnology" to learn fundamentals of biotechnology and apply research outcome in commercial scale. The knowledge in this book is not limited to any geographic region.

Most of currently available books in this field are very complicated or may not explain the detail of processes. In my opinion, detail information in this book

offers the greatest advantage over other available sources. Students and those who are getting familiar with biological and biotechnological processes need to know about biosciences, some examples, and case studies to improve their information and knowledge. This book illustrates several successful research and case studies conducted in this area, which would be very helpful to give an insight to readers.

The present book is more attractive to chemical engineers academics, professionals, and postgraduate students, while it is recommended for senior undergraduates. All chapters give more understanding of the related knowledge to specific field of biotechnology. The related case studies are incorporated with original research data that would help to develop advance research technology and innovation.

This book is a useful guide for all scientists to apply theoretical bases and also to conduct research in bioprocesses. The book explains many concepts and presents highly qualitative and quantitative results in biological processes. It concentrates on application of biology and biochemistry in engineering aspects. The details of bioengineering concepts would be the following: enzyme and microbial growth kinetics; bioreactor design and actual applications in process scale-up; downstream product recovery; biological products separation and purification; and production of value-added products such as enzymes from wastes, antibiotics, and other fermentative products.

The target audience (mainly undergraduate and graduate students of biochemical engineering) needs to understand the basic concepts and theoretical and practical knowledge with appropriate depth and breadth about this topic. This book combines the theoretical basis of biochemical engineering with original research data. This is a great beneficial to the reader.

The second edition of the present book should serve as a useful reference for research scientists currently conducting research in the area of chemical, physical, and biological treatment of industrial wastewater.

This book contains important and interesting topics in the field of bioprocess. Extensive applications of biotechnology in biochemical engineering are included. The second edition has been certainly improved, which may attract special attention of many

scientists around the world. The revised book emphasizes on practical aspects and case studies. It contains useful guidelines for young research scientists to develop their research activities. I believe this book can deliver practical knowledge and contribute to special fields of bioprocesses.

The new chapters added to the second edition are novel and related to recent topics in biotechnology. Additional case studies from recent researches are useful and can give insight to the readers to broaden their future work. Addition of new chapters may enhance the quality of the work. More discussion on pathway of microorganisms is also incorporated. Identifying the pathway of organisms may assist engineers to know the growth factors and enzymes related to enhance series of biological reactions to achieve high yield of end products.

Preface

PREFACE TO THE SECOND EDITION

First and foremost, I want to thank the Almighty for mercy who blessed me and gave me the strength to accomplish this work. I would like to thank my colleagues Dr H. Younesi, Dr M. Mohammadi, and Dr H. Zare, who have assisted me in drawing some of the figures. I am also very thankful to my colleagues who have contributed to some parts of the chapters: Dr A.A. Ghoreyshi, Dr M. Rahimnejad, and Dr M. Jahanshahi from Babol Noshirvani University of Technology and Dr M. Tabatabaei from Agricultural Biotechnology Research Institute of Iran. Also special thanks go to Dr H. Younesi, Dr W.S. Long, Dr M. Esfahanian, Mr M.H. Shahavi, Professor A.H. Kamaruddin, Professor S. Bhatia, Professor A.R. Mohamed, and Professor A.L. Ahmad for their valuable contribution to case studies.

I would like to acknowledge my friends in Malaysia: Dr W.S. Long, Professor A.H. Kamaruddin, School of Chemical Engineering, Universiti Sains Malaysia, for the feedbacks and editing parts of this book. I also wish to acknowledge the following individuals who have positively influenced my professional and educational endeavors over the years: Professor J.L. Gaddy, Professor Mark Townsend, Professor K.E. Starling, Professor C.M. Sliepcevich, Professor S. Ellaison, and Professor Ed. Clausen. Nor should I forget the person who has accelerated this work and given lots of

encouragement: Dr. Kostas Marinakis and Ms Christine McElvenny at Elsevier.

PREFACE TO THE FIRST EDITION

In the new millennium, extensive application of bioprocesses has created an environment for many engineers to expand their knowledge and interest in biotechnology. Microorganisms produce alcohols and acetone, which are used in industrial processes. Knowledge related to industrial microbiology has been revolutionized by the ability of genetically engineered cells to make many new products. Genetic engineering and gene mounting have been developed for the enhancement of industrial fermentation. Finally, application of biochemical engineering in biotechnology has become a new way of making commercial products.

This book demonstrates the application of biological sciences in engineering with theoretical and practical aspects. These 20 chapters give more understanding of the knowledge related to the specified field, with more practical approaches and related case studies with original research data. It is a book for students to follow the sequential lectures with detailed explanations, and solve the actual problems in the related chapters.

There are many graphs that present actual experimental data, and figures and tables, along with sufficient explanations. It is a

good book for those who are interested in more advanced research in the field of biotechnology, and a true guide for beginners to practice and establish advanced research in this field. The book is specifically targeted to serve as a useful text for college and university students; it is mostly recommended for undergraduate courses in one or two semesters. It will also prove very useful for research institutes and postgraduates involved in practical research in biochemical engineering and biotechnology.

This book has suitable biological science applications in biochemical engineering and the knowledge related to those biological processes. The book is unique, with practical approaches in the industrial field. I have tried to prepare a suitable textbook using a direct approach that should be very useful for students in following the many case studies. It is unique in having solved problems, examples and demonstrations of detailed experiments, with simple design

equations and required calculations. Several authors have contributed to enrich the case studies.

During the years of my graduate studies in the United States at the University of Oklahoma and the University of Arkansas, several lecturers and professors from School of Chemical Engineering gave me much knowledge and assisted me in my academic achievements. I have also had the opportunity to learn many things from different people, in different schools at the University of Oklahoma. I am very thankful for their courage and guidance. My vision in research and my success are due to these two great scholars at the University of Arkansas; supervised my research projects; they are always remembered.

Ghasem D. Najafpour
Biotechnology Research Lab., Faculty of
Chemical Engineering, Noshirvani
University of Technology, Babol, Iran.

Industrial Microbiology

OUTLINE

1.1 Introduction	1	1.9 Production of Vinegar	13
1.2 Role of Biotechnology	2	1.10 Production of Amino Acids (Lysine and Glutamic Acid) and Insulin	14
1.3 Role of Biosciences	5	1.10.1 Stepwise Amino Acid Production	14
1.4 Microbe Functions	5	1.10.2 Insulin	15
1.5 Process Fermentation	7	1.11 Antibiotics, Production of Penicillin	15
1.6 Application of Fermentation Processes	9	1.12 Production of Enzymes	16
1.7 Bioprocess Products	10	1.13 Production of Baker's Yeast	16
1.7.1 Biomass	10	References	18
1.7.2 Cell Products	11		
1.7.3 Modified Compounds (Biotransformation)	11		
1.8 Production of Lactic Acid	11		

1.1 INTRODUCTION

Microorganisms have been identified and exploited for more than a century. The Babylonians and Sumerians used yeast to prepare alcohol. There is a great history beyond fermentation processes that explains the applications of microbial processes that resulted in the production of food and beverages. In the mid-19th century, Louis Pasteur understood the

role of microorganisms in fermented food, wine, alcohols, beverages, cheese, milk, yogurt and other dairy products, fuels, and fine chemical industries. He identified many microbial processes and discovered the first principal role of fermentation, which was that microbes require substrate to produce primary and secondary metabolites and end products.

In the new millennium, extensive application of bioprocesses has created an environment for many engineers to expand the field of biotechnology. One of the useful applications of biotechnology is the use of microorganisms to produce alcohols and acetone, which are used in industrial processes. The knowledge related to industrial microbiology has been revolutionized by the ability of genetically engineered cells to make many new products. Genetic engineering and gene mounting have been developed in the enhancement of industrial fermentation. Consequently, biotechnology is a new approach for making commercial products using living organisms. Furthermore, knowledge of bioprocesses has been developed to deliver fine-quality products.

The application of biological sciences in industrial processes is known as bioprocess. Today, most biological and pharmaceutical products are produced in well-defined industrial bioprocesses. For instance, bacteria are able to produce most amino acids that can be used in food and medicine. There are hundreds of microbial and fungal products purely available in the biotechnology market. The microbial production of amino acids can be used to produce L-isomers; chemical production results in both D- and L-isomers. Lysine and glutamic acid are produced by *Corynebacterium glutamicum*. Another food additive is citric acid, which is produced by *Aspergillus niger*. Table 1.1 summarizes several widespread applications of industrial microbiology to deliver a variety of products in applied industries.

The growth of cells on a large scale is called industrial fermentation. Industrial fermentation is normally performed in a bioreactor, which controls aeration, pH, and temperature. Microorganisms use an organic source and produce primary metabolites such as ethanol, which are formed during the cells' exponential growth phase. In some bioprocesses, yeast or fungi are used to produce advanced valuable products. Those products are considered as secondary metabolites, such as penicillin, which is produced during the stationary phase. Yeasts are grown for wine- and bread-making. There are other microbes such as *Rhizobium*, *Bradyrhizobium*, and *Bacillus thuringiensis* that are able to grow and use carbohydrates and organic sources originating from agricultural wastes. Vaccines, antibiotics, and steroids are also products of microbial growth.

1.2 ROLE OF BIOTECHNOLOGY

Biotechnology is an interdisciplinary area that governs the application of biology and chemistry in engineering sciences. In fact, it is the knowledge of the exploitation of living microorganisms and their by-products, such as enzymes, secondary metabolites, and any product from the pathway of living organisms. These biobased products are expanding as safe food additives, medicines, and cosmetics.

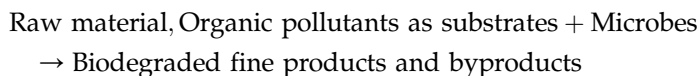
In the past decades, the application of biotechnology focused only on animal biotechnology or plant cell technology and horticulture. But today, the development of biotechnology has enhanced and moved beyond the borders. The knowledge has expanded in many fields of engineering as well as in advance biomaterial and nano-biotechnology products.

TABLE 1.1 Industrial products produced by biological processes¹

Fermentation products	Microorganism	Applications
Ethanol (nonbeverage)	<i>Saccharomyces cerevisiae</i>	Fine chemicals
2-Ketogluconic acid	<i>Pseudomonas</i> sp.	An intermediate in ascorbic acid (vitamin C) production; a precursor for isoascorbic acid synthesis
Pectinase, protease	<i>Aspergillus niger</i> , <i>A. aureus</i>	Clarifying agents in fruit juice
Bacterial amylase	<i>Bacillus subtilis</i>	Modifying starch, sizing paper
Bacterial protease	<i>B. subtilis</i>	Desizing fibers, spot remover
Lipase	<i>Candida rugosa</i>	Esterification of fat and lipids
Protease	<i>Bacillus subtilis</i>	Hydrolysis of protein
Lysine	<i>Micrococcus glutamicus</i>	Food additives
Dextran	<i>Leuconostoc mesenteroides</i>	Food stabilizer
Sorbose	<i>Gluconobacter suboxydans</i>	Manufacturing of ascorbic acid
Cobalamin (vitamin B12)	<i>Streptomyces olivaceus</i>	Food supplements
Glutamic acid	<i>Brevibacterium</i> sp.	Food additive
Gluconic acid	<i>Aspergillus niger</i>	Pharmaceutical products
Lactic acid	<i>Rhizopus oryzae</i>	Foods and pharmaceuticals
Lactic acid	<i>Lactobacillus delbrueckii</i>	food additives and chemicals
Citric acid	<i>Aspergillus niger</i> or <i>A. wentii</i>	Food products, medicine
Acetone-butanol-ethanol	<i>Clostridium acetobutylicum</i>	Solvents, chemical intermediate
Insulin, interferon	Recombinant <i>E. coli</i>	Human therapy
Coagulated milk	<i>Streptococcus thermophilus</i> , <i>Lactobacillus bulgaricus</i>	Yogurt-starting culture
Yeast and rennet	<i>Lactobacillus bulgaricus</i>	Cheese and yogurt production
Microbial protein (single cell protein)	<i>Candida utilis</i>	Food supplements
Single cell protein (SCP)	<i>Pseudomonas methylotroph</i> <i>Oxidizing bacteria</i> , fungus <i>Fusarium</i>	Food supplements
Penicillin	<i>Penicillium chrysogenum</i>	Antibiotics
Cephalosporin	<i>Cephalosporium acremonium</i>	Antibiotics
Erythromycin	<i>Streptomyces erythreus</i>	Antibiotics

In the mid-19th century, Louis Pasteur well understood the industrial application of microorganisms to deliver useful products while implementing various bioprocesses. The raw materials were used as substrates and nutrients for microorganisms to draw suitable products. The products were used by humans, and the even rate of productions was at commercial scale. Microorganisms under normal condition produce large number of chemicals, pharmaceuticals, and food-grade products. Other applications of microorganisms are clearly stated in

mining and bioleaching. The metals are leached out from low grade ores. In the removal of organic pollutants, microorganisms are safely used for many treatment processes and bioremediation. They are able to remove obnoxious pollutants from an aqueous phase. In biofilters, pollutants are removed from air streams through filter media. Biodegradation of volatile organic compounds in a biofilter easily takes place by the consortia of living microorganisms in the filter bed. Applications of microorganisms are expended in many biological processes for economical and environmental reasons. In general, the industrial application of microbes can be summarized in a simple reaction:



In most cases, microorganisms are used to convert waste organic material to useful and stable products. The organisms used in the treatment processes are non-pathogens with no side effect on human health. For instance, dairy waste (whey), pulp, and paper wastes are often used for the propagation of microorganisms.

Industrial fermentations are used in large-scale tanks, often with a capacity of 15–50 m³. From the metabolism of the microorganisms in growth media, the heterogeneous phase of cell mass exists in a broth of culture, while targeted products are liberated. The desired cell products must be recovered in downstream processing via separation and purification of products in aqueous or solid phases for recovery of the product in crystallized or precipitated matter, as solid products are easily recovered and removed from downstream. The commercial products are cell mass with intercellular products. Enzymes are categorized as intracellular and extracellular products. The cell products and secondary metabolites can be used as essential compounds for cell growth. Intermediate metabolites may not be essential as nutrients for cell growth. The biobased products originated from microorganisms are used as chemicals and pharmaceutical compounds, such as antibiotics, interferon, hormones, insulin, and steroid drugs. The genetically engineered bacteria or gene-mounted cells are able to produce strictly the targeted product for the treatment and drug purposes. Mass production of food supplements is performed via bacteria, yeast, fungi, and algae. The cheap raw materials are used for the production of food supplements that are commercially viable in large-scale production. The production of amino acids is a practical example; among amino acids, glutamic and folic acids are fermented from dairy waste. Beverage industries are the oldest large-scale production plants to produce nonalcoholic and alcoholic drinks. Also, bacteria are used for the production of vaccines and antigens. The annotated cell bodies are used as an antigen for the generation of the antibody for the immunization of patients and to protect them from diseases. One of the commercial applications of industrial microorganisms is for oil spillage clean up and removal of coastal pollutants. The organisms having high tolerance to hydrocarbons and aromatics can degrade and use hydrocarbon sources, while inorganic nitrogen sources are balanced for maximum cell growth. Industrial applications of microorganisms with the designated product are summarized in [Table 1.1](#). The most biobased products are lactic acid and amino acids such as lysine and glutamic acids. The detailed descriptions of each product are discussed in different chapters and in related bioprocesses.

Various types of carbon sources, such as corn syrup, potato starch, molasses, and whey, are often used for the production of lactic acid. If starch is used, then the natural polymer must be hydrolyzed to monomeric sugar via enzymatic hydrolysis. The monosaccharides liberated from hydrolysis are used for the fermentation process.

1.3 ROLE OF BIOSCIENCES

In past centuries, the boundary of the knowledge of applied sciences was expanded, which resulted in an evolution of interdisciplinary areas like biobased majors that have assisted engineering sciences to develop the more extended field of applied sciences. In the 1960s, engineers never thought of getting involved in microorganisms in processes. Expansion of process deals with biological knowledge and fundamental biological sciences; in most treatment processes, microbes and bacteria are involved. The use of enzymes in biobased refineries for the production of biofuels and pharmaceutical products created an advance technology for life improvements. The idea of the replacement of fossil fuel with clean fuel such as biohydrogen has been discussed in recently published articles. The combustion of hydrogen never generates any air pollution. Even for desulfurization of natural gas, the process does not require chemical solvents for sorption processes because sulfur gases are used by microbes and sulfur is removed from the natural gas stream. In traditional chemical engineering, even simple unit operation and mass transfer were sufficient to derive the process, while modern process engineers cannot live without the biological knowledge and application of microorganisms in their daily routine life. Therefore, the identification, isolation, propagation, and mass cultivation of potent organisms are required for many processes. Living organisms most often act as biocatalysts in many biochemical and biological processes. In fact, microorganisms play a major role. Today, the expansion of biological research developed molecular biology. In this field, metabolic engineering and genetic engineering serve to broaden engineers' knowledge for a breakthrough in production level and process yield enhancement. For instance, applications of recombinant organisms in the fields of medicine and pharmaceutical sciences are successful cases of biosciences. In addition, knowledge of microbiology for degradation of toxic organic compounds and pesticides by microbial strains in an anaerobic process has created an environment for bioconversion of organic chemicals to methane and carbon dioxide to be used as energy sources. If microbiology is divided into basic and application sciences, then one can directly use applied microbiology in the field of bioprocesses. On the other hand, enzymes and hormones or intermediate cell metabolites as products of living organisms are used in many bioprocesses.

1.4 MICROBE FUNCTIONS

Microbes are defined as creatures that cannot be observed by naked eyes. Their morphology is easily seen under microscopes. Microorganisms are categorized as bacteria, fungi, algae, and protozoa. Also, a virus is identified as a living organism that may cause infection. Microorganisms are classified based on their morphology, physiology, structure

of cell wall, cell divisions, and propagation of cells. The impact of microorganisms on human life may be categorized as useful, nonpathogens, and pathogens. The nonpathogens class of organisms may live in a friendly environment without causing any disease, while pathogens cause infection. The nonpathogen class of organisms is used in human food and beverages. This class of organisms is used for the production of hormones, interferon, enzymes, and many pharmaceutical products. These organisms are often used in many industrial processes for the production of food, fuels, and fine chemicals. A single organism is able to live independently and perform in a network; the organisms may act in an organ for a specific function. The manifestation of life may come through evolution, as each organ carries out specific tasks to function and operate in a living system.

Microorganisms based on morphology and structure for the beginners are quite similar, all having cell walls to protect the cell materials. The cytoplasm of a cell is enclosed by the cell wall; even cell components inside the cell may be identified or unidentified. All cells are able to function perfectly as life is expected from a living organism.

The term cell was introduced in past centuries. Cells are surrounded by boundaries that are known as the cell wall. The wall protects the cell content, also known as cytoplasm, and the cell organs inside the cell. The organ may be formed by the unification of number of cells; most often this looks like honey bees' cell structure with defined cell walls, as a mass of cells are unanimously gathered to act for specific function.

Cells are living organisms; they are unique, and all cell components are identified. The colloidal material inside the cell is known as cytoplasm encapsulated by the cell wall. The cell components inside the cell can be clearly observed by electronic microscope. Cells are replicated in a suitable environment, and nutrients are essential for cell growth. The cell wall is permeable to nutrients inside the media; the cell duplicates in a defined time, which is an indicator of growth known as doubling time.

Microorganisms having biological activities require nutrient sources such as carbon, nitrogen, and phosphate. Most of the organisms must obtain energy from carbon sources. Some of the organisms are able to use nitrogen from air and fix nitrogen as nitrate or generate amino acids for the synthesis of protein. They are able to produce complex nitrogenous compounds. Some other organisms use inorganic and organic nitrogen for protein synthesis.

Microorganisms are able to use a number of carbon sources with a wide metabolic reaction. They are adapt to many sources of nutrients. The use of inexpensive nutrients may create an opportunity for microbes to convert waste to useful products. Especially in industrial waste, organic sources are available that easily can be converted to the desired product in the presence or absence of oxygen via fermentation.

An organism can have commercial products listed in four categories:

1. Single cells
2. Large molecules, such as enzymes
3. Primary metabolites
4. Secondary metabolites.

The primary and secondary metabolites in a bioprocess can be estimated based on projected pathways for the production of intracellular and extracellular by-products.

Four classes of organisms are used in industrial processes. They are yeasts, molds, single bacteria, and *actinomycetes* (fungi). Yeast and molds are well developed in industrial

processes. Mold and *actinomycetes* have a filamentous shape growing in a branched system. They are not like individual cells. Yeasts compared with single cells are much bigger, while they are observed in single individual cells. Fungi show up in a filamentous shape known as hyphae. For instance, *Candida utilis* is a type of fungus having industrial applications, such as single cell protein. Molds are certainly known for their antibacterial activities. This group, including *Aspergillus oryzae* and *A. niger* and genera of *Penicillium*, are well known. The strict anaerobes and prokaryote cell, *Streptomyces*, are the most filamentous fungi-producing antibiotics. The organisms are eukaryote like fungi and plant cells. The distinct point of eukaryote cells is the nucleus, the cell surrounded by the membrane. All organs in the cell are identified under electronic microscope. They have more than one chromosome with defined mitochondria. The mitochondria of the cell are responsible for cell energy, and all chemical reactions are carried out in this center. In contrast, organisms without a distinct nucleus are known as prokaryote cells. Bacteria and microbes are prokaryote; the cells are single isolated units, much smaller than a eukaryote cell. The sizes of eukaryote cells are most probably 10 times bigger than prokaryotes. In a prokaryotic cell, the nucleus materials are spread out inside the cell, and cell organs are not identified. Among anaerobic prokaryote cells, the *Clostridium* species may produce toxin like botulism synthesized by *C. botulinum* and *C. butericum*; they are notorious living organisms that cause serious health problems for human beings. In the fermentation of an organic substrate, the pathways of organisms are always questionable. Organisms in terms of product delivery are known as homofermentative and heterofermentative. The homofermentative organism delivers one significant or principal product, while heterofermentative organisms may generate two or more products through the pathway of organisms. For example, yeasts are able to ferment 6-carbon sugar, either glucose or fructose, to 2 mol of ethanol and 2 mol of carbon dioxide. The pathway of the organism can be influenced by the composition of the media. If yeast refused to produce alcohol due to the acidic pH of the media, then the microbial pathway will shift to lactic acid production. If the fermentation media is contaminated with any *Lactobacillus* species, then glucose is converted to lactic acid. In fact, the heterofermentative culture is able to convert glucose to several products, such as lactic acid, ethanol, and carbon dioxide, through an alternative microbial pathway. *Clostridium acetobutylicum* is a heterofermentative that can produce two major products. This organism is able to use glucose and produce a mixture of acetone, ethanol, isopropanol, and butanol. The culture is aerobic; a certain fraction of substrate is used and converted to a metabolite, then the remaining fraction is converted to a beneficial cell biomass or protein. However, in full oxidation with an excess amount of oxygen, all substrates are oxidized to carbon dioxide and water through a pathway known as glucolysis. The fact is the aerobic process not only ends in carbon dioxide and water, but also delivers significant molecules as an energy carrier that are used for synthesis of biomolecules.

1.5 PROCESS FERMENTATION

The term “fermentation” was obtained from the Latin verb *fervere*, which describes the action of yeast or malt on sugar or fruit extracts and grains. The “boiling” observed during fermentation is due to the production of carbon dioxide bubbles from the aqueous phase under the anaerobic catabolism of carbohydrates in the fermentation medium. The art of

fermentation is defined as the chemical transformation of organic compounds with the aid of enzymes. The ability of yeast to make alcohol was known to the Babylonians and Sumerians before 6000 BC. The Egyptians discovered the generation of carbon dioxide by brewer's yeast in the preparation of bread. The degradation of carbohydrates by microorganisms is followed by the glycolytic or Embden–Meyerhof–Parnas pathway.^{2,3} Therefore, the overall biochemical reaction mechanisms to extract energy and form products under anaerobic conditions are called fermentation processes. In the process of ethanol production, carbohydrates are reduced to pyruvate with the aid of nicotinamide adenine dinucleotide; ethanol is the end product. Other fermentation processes include the cultivation of acetic acid bacteria for the production of vinegar. Lactic acid bacteria preserve milk; the products are yogurt and cheese. Various bacteria and molds are involved in the production of cheese. Louis Pasteur, who is known as the father of the fermentation process, in the early 19th century defined fermentation as life without air. He proved that existing microbial life came from preexisting life. There was a strong belief that fermentation was strictly a biochemical reaction. Pasteur disproved the chemical hypothesis. In 1876, he had been called by the distillers of Lille in Great Britain to investigate why the content of their fermentation product turned sour.⁴ Pasteur found microbial contamination of the yeast broth under his microscope. He discovered organic acid formation, such as lactic acid before ethanol fermentation. His greatest contribution was to establish different types of fermentation by specific microorganisms, enabling work on pure cultures to obtain pure product. In other words, fermentation is known as a process with the existence of strictly anaerobic life; that is, life in the absence of oxygen. The process is summarized in the following steps:

- Action of yeast on extracts of fruit juice or malted grain: The biochemical reactions are related to generation of energy by catabolism of organic compounds.
- Biomass or mass of living matter (living cells) in a liquid solution with essential nutrients at suitable temperature and pH grows up: As a result, the content of biomass increases with time.

In World War I, Germany was desperate to manufacture explosives and needed glycerol for this. They had identified glycerol in alcohol fermentation. Carl Neuberg discovered that the addition of sodium bisulphate to the fermentation broth favored glycerol production at the expense of ethanol. Germany quickly developed industrial-scale fermentation, with a production capacity of about 35 tons per day.⁴ In Great Britain, acetone was in great demand; it was obtained by anaerobic fermentation of acetone–butanol–ethanol using *C. acetobutylicum*.

In large-scale fermentation production, contamination of pure culture with other organisms and bacteriophage or virus is the major problem. Microorganisms are capable of performing a wide range of metabolic reactions using various sources of nutrients. That makes the fermentation processes suitable for industrial applications with inexpensive nutrients. Molasses, corn syrup, waste products from the crystallization of sugar industries, and the wet milling of corn are valuable broths for the production of antibiotics and fine chemicals. We will discuss many industrial fermentation processes in the coming Chapter. First, we will focus on the fundamental concepts of biochemical engineering rather than the applications.

There are various industries using biological processes to produce new products, such as antibiotics, chemicals, alcohols, lipid, fatty acids, and proteins. Deep understanding of the bioprocess may require actual knowledge of biology and microbiology in the applications of the above processes. It is very interesting to demonstrate bench-scale experiments and make use of large-scale advanced technology. However, the application of the bioprocess in a large-scale and the control of microorganisms in 100,000 l of media may not be quite so simple to manage. Therefore, trained engineers are essential and in high demand; this can be achieved by knowledge enhancement in the sheathe bioprocesses. To achieve such objectives, we may need to explain the whole process to the skilled labor and trained staff to implement bioprocess knowhow in biotechnology.

1.6 APPLICATION OF FERMENTATION PROCESSES

Man has been using the fermentative abilities of microorganisms in various forms for many centuries. Yeasts were first used to make bread; later, their use expanded to the fermentation of dairy products to make cheese and yogurt. Today, more than 200 types of fermented food products are available in the market. There are several active biological processes in the industry producing high-quality products, such as various antibiotics, glutamic acid, citric acid, acetic acid, and butyric and propionic acids. Synthesis of proteins and amino acids, lipids and fatty acids, simple sugar and polysaccharides such as xanthan gum and glycerol, and many more fine chemicals and alcohols is carried out through bioprocesses with suitable industrial applications. The knowledge of bioprocess is an integration of biochemistry, microbiology, and engineering science applied in industrial technology. Application of viable microorganisms and cultured tissue cells in an industrial process to produce specific products is known as bioprocess. Thus, fermentation products and the ability to cultivate large amounts of organisms are the focus of bioprocess, and such achievements may be obtained using vessels known as fermenters or bioreactors. The cultivation of large amounts of organisms in fermenters and bioreactors with related fermentation products is the major focus of bioprocess.

A bioreactor is a vessel in which an organism is cultivated and grown in a controlled manner to form the by-product. In some cases, special organisms are cultivated to produce very specific products such as antibiotics. The laboratory scale of a bioreactor is in the range of 2–100 l, but in commercial processes or in a large-scale operation, this might be up to 100 m³.^{5,6} Initially, the term “fermenter” was used to describe these vessels, but in strict terms, fermentation is an anaerobic process, whereas the major proportion of fermenters use aerobic conditions. The term “bioreactor” has been introduced to describe a fermentation vessel for growing the microorganisms under aerobic or anaerobic conditions.

Bioprocess plants are an essential part of the food, fine chemical, and pharmaceutical industries. Use of microorganisms to transform biological materials to fermented foods, cheese, and chemicals has its antiquity. Bioprocesses have been developed for an enormous range of commercial products, as listed in [Table 1.1](#). Most of the products originate from relatively cheap raw materials. The production of industrial alcohols and organic solvents mostly originates from cheap feed stocks. The more expensive and special bioprocesses are in the production of antibiotics, monoclonal antibodies, and vaccines. Industrial enzymes and living

cells such as baker's yeast and brewer's yeast are also commercial products obtained from bioprocess plants.

1.7 BIOPROCESS PRODUCTS

Major bioprocess products are in the area of chemicals, pharmaceuticals, energy, food, and agriculture, as depicted in [Table 1.2](#). The table shows the general aspects, benefits, and applications of biological processes in these fields. Most fermented products are formed in three types. The main categories are now discussed.

1.7.1 Biomass

In such bioprocesses, the aim is to produce a biomass or mass of cells such as microbes, yeast, and fungi. The commercial production of biomass has been seen in the production

TABLE 1.2 Products and services provided by biological processes

Sector	Product and service	Remark
Chemicals	Ethanol, acetone, butanol	Bulk
	Organic acids (acetic, butyric, propionic and citric acids)	
	Enzymes	Fine
	Perfumeries Polymers	
Pharmaceuticals	Antibiotics	
	Enzymes	
	Enzyme inhibitors	
	Monoclonal antibodies	
	Steroids Vaccines	
Energy	Ethanol (gasohol)	Nonsterile
	Methane (biogas)	
Food	Dairy products (cheese, yogurts, etc.)	Nonsterile
	Baker's yeast	
	Beverages (beer, wine)	
	Food additives	
	Amino acids	
	Vitamin B Proteins (SCP)	
Agriculture	Animal feeds (SCP)	Nonsterile
	Waste treatment	
	Vaccines	
	Microbial pesticides	
	Mycorrhizal inoculants	

of baker's yeast, which is used in the baking industry. Single cell protein (SCP) is produced as a biomass enriched in protein.⁷ An algae called *Spirulina* has been used for animal food in some countries. SCP is used as a food source produced from renewable resources such as whey, cellulose, starch, molasses, and a wide range of plant waste.

1.7.2 Cell Products

Products are produced by cells with the aid of enzymes and metabolites known as cell products. These products are categorized as either extracellular or intracellular. Enzymes are one of the major cell products used in industry. Enzymes are extracted from plants and animals. Microbial enzymes can be also produced in large quantities by conventional techniques. Enzyme productivity can be improved by mutation, selection, and perhaps genetic manipulation. The use of enzymes in industry is very extensive, especially in baking, cereal-making, coffee, candy, chocolate, corn syrup, and dairy products as well as the fruit juice and beverage industry. The most common enzymes used in the food industries are amylase in baking; protease and amylase in beef products; pectinase and hemicellulase in the coffee industry; catalase, lactase, and protease in dairy products; and glucose oxidase in the fruit juice industry.

1.7.3 Modified Compounds (Biotransformation)

Almost all types of cells can be used to convert an added compound into another compound, involving many forms of enzymatic reaction including dehydration, oxidation, hydroxylation, amination, isomerization, etc. These types of conversion have advantages over chemical processes in that the reaction can be very specific and performed at moderate temperatures. Examples of transformations using enzymes include the production of steroids, the conversion of antibiotics, and prostaglandins. Industrial transformation requires the production of large quantities of an enzyme; the half-life of enzymes can be improved by immobilization, and extraction can be simplified by the use of whole cells. In any bioprocess, the bioreactor is not an isolated unit, but is a part of an integrated process with upstream and downstream components. The upstream consists of storage tanks, growth, and media preparation followed by sterilization. Also, seed culture for inoculation requires upstream processing, with sterilized raw material, mainly sugar and nutrients, required for the bioreactor to operate. Sterilization of the bioreactor can be done by steam at 15 pounds per square inch gauge at 121 °C or using any disinfectant chemical reagent such as ethylene oxide. The downstream processing involves extraction of the product and purification as normal chemical units of operation.⁸ The solids are separated from the liquid, and the solution and supernatant from the separation unit may go for further purification after the product has been concentrated.

1.8 PRODUCTION OF LACTIC ACID

Lactic acid was produced from sour milk. It is believed that Louis Pasteur was the first scientist who identified fermentation of sour milk to lactic acid. The bioconversion was

found through homolactic fermentation; as a result, maltose is converted to lactate. Lactic acid is known as an acidulent, a flavoring agent for food preservation, and in the dairy industry it is used as feedstock for production of polylactic acid, which is known as a biodegradable polymer. Lactic acid is also used for the preservation of vegetables such as carrots and radishes. The world annual demand for lactic acid is approximated to be 150,000 (metric) tons. The lactic acid production via fermentation is mostly carried out by the *Lactobacillus* species, which is a stereoisomer of L(+) and D(−), or a mixture of racemic DL lactic acid. The separation process for a specific isomer is expensive and tedious. More than 100 species of *Lactobacillus* are identified as potential organisms for the production of lactic acid. The most popular species of lactic acid producers are *Lactobacillus bulgaricus*, *Lactobacillus plantarum*, *Lactobacillus brevis*, *Lactobacillus helveticus*, *Lactobacillus delbrueckii*, *Lactobacillus casei*, *Lactobacillus paracasei*, and *Lactobacillus manihotivorans*. Generally, *Lactobacillus* are homofermentative and can produce a high concentration of lactic acid, while heterofermentatives may convert 50% of substrate to lactic acid. Several carbohydrates, such as corn and potato starch, molasses, and whey, can be used to produce lactic acid. Starch must first be hydrolyzed to glucose by enzymatic hydrolysis; then fermentation is performed in the second stage. The choice of carbohydrate material depends on its availability, and pretreatment is required before fermentation. We shall describe the bioprocess for the production of lactic acid from whey. Inexpensive raw material for the production of lactic acid is recommended. It is customary to convert a significant proportion of cheese whey to lactic acid. Fermentation of lactic acid in suspended growth is more favorable than solid state fermentation (SSF). It is believed that fungi are more suitable for SSF, while the use of *Lactobacillus* species in suspended growth and submerged culture is more favorable for the fermentation process.

Large quantities of whey constitute a waste product in the manufacturing process of dairy products such as cheese. From the standpoint of environmental pollution, it is considered a major problem, and the disposal of untreated wastes may create environmental disasters. It is desirable to use whey to make some useful product. Whey can be converted from being a waste product to something more desirable that can be used for the growth of certain bacteria because it contains lactose, nitrogenous substances, vitamins, and salts. Organisms can use lactose and grow on cheese wastes; the most suitable of them are *Lactobacillus* species such as *L. bulgaricus*, which is the most suitable species for whey. This organism grows rapidly, is homofermentative, and thus is capable of converting lactose to the single end-product of lactic acid. Stock cultures of the organism are maintained in a skimmed milk medium. A three to five volume% of inoculum is prepared and transferred to the main bioreactor, and the culture is stored in pasteurized, skimmed milk at an incubation temperature of 43 °C. During fermentation, pH is controlled by the addition of a slurry of lime to neutralize the product to prevent any product inhibition. The accumulation of lactic acid would retard the fermentation process because of the formation of calcium lactate. After two days of complete incubation, the material is boiled to coagulate the protein and then filtered. The solid filter cake is a useful, enriched protein product that may be used as an animal feed supplement. The filtrate containing calcium lactate is then concentrated by removing water under vacuum, followed by purification of the final product. The flow diagram for this process is shown in Figure 1.1.

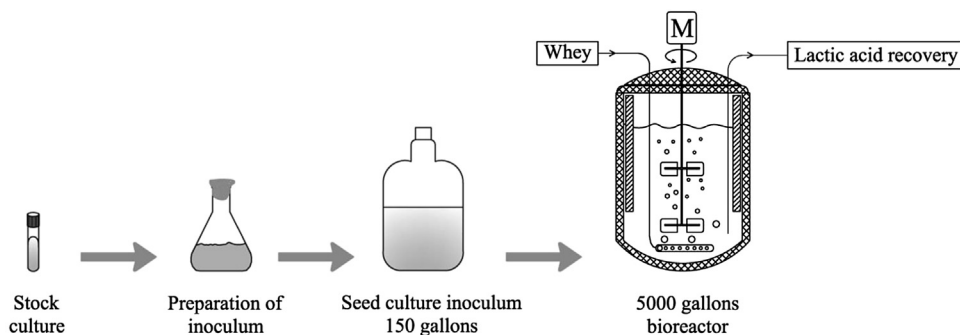


FIGURE 1.1 Production of lactic acid from whey.

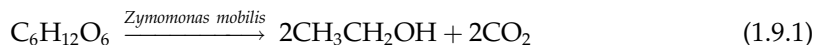
1.9 PRODUCTION OF VINEGAR

The sugars in fruits such as grapes are fermented by yeasts to produce wines. In wine-making, lactic acid bacteria convert malic acid into lactic acid in malolactic fermentation in fruits with high acidity. *Acetobacter* and *Gluconobacter* oxidize ethanol in wine to acetic acid (vinegar).

The word “wine” is derived from the French term *vinaigre* meaning “sour wine.” It is prepared by allowing a wine to get sour under controlled conditions. The production of vinegar involves two steps of biochemical changes:

1. Alcoholic fermentation in fermentation of a carbohydrate
2. Oxidation of the alcohol to acetic acid.

There are several kinds of vinegar. The differences between them are primarily associated with the kind of material used in the alcoholic fermentation, e.g., fruit juices, sugar, and hydrolyzed starchy materials. Based on US Department of Agriculture definitions, there are a few types of vinegar, namely vinegar, cider vinegar, and apple vinegar. The products are made by the alcoholic and subsequent acetous fermentations of the apple juice. The acetic acid content is about 5%. Yeast fermentation is used for the production of alcohol. The alcohol is adjusted to 10–13%, then it is exposed to acetic acid bacteria (*Acetobacter* species), by means of which oxygen is required for the oxidation of alcohol to acetic acid. The desired temperature for *Acetobacter* is 15–34 °C. The reaction is:



The oxidation of ethanol to acetic acid for the production of vinegar is not a fully oxidative process, but the aerobic organism is able to convert glucose to gluconic acid via incomplete oxidation. The derived adenosine triphosphate from limited oxidation is growth associated; finally, with the aid of supplementary nutrients in the media, the organisms are able to complete the biochemical reaction to acetic acid production.

1.10 PRODUCTION OF AMINO ACIDS (LYSINE AND GLUTAMIC ACID) AND INSULIN

Many microorganisms can synthesize amino acids from inorganic nitrogen compounds. The rate and amount of some amino acid production may exceed the cells' need for protein synthesis, in which the excess amino acids are excreted into the media. Some microorganisms are capable of producing certain amino acids such as lysine, glutamic acid, and tryptophan. The primary metabolites are used by specific organism to synthesize next components. Some aerobic organism like *C. glutamicum* can produce lysine. The mutants of *C. glutamicum* are able to produce a high concentration of lysine; the appreciable concentration may reach to 50 g l^{-1} . Lysine is one of the 20 essential amino acids for synthesis of protein molecule. The low molecular weights of cell products as primary metabolites are essential for the cell growth. Another group of microbial products known as secondary metabolites are not directly involved in the synthesis of biomolecules like antibiotics. Secondary metabolites are also produced by certain microorganisms; they are not fast-growing organisms, as the precious byproducts appear at a late stage of the growth cycle. The primary metabolites are involved in biosynthesis of the cell, while the secondary metabolites are mostly considered useful biological products that are easily marketable and have numerous applications. The secondary metabolites may contribute certain action as anti-survival of organisms. The detailed action of secondary metabolites can be inhibitory competitors in the growth system. The organisms go through rapid growth in the initial stage; when further growth is halted by the depletion of essential nutrients in the medium, then organisms enter the next phase. The secondary metabolites are often used for control and survival; therefore, they are more beneficially used for drug and pharmaceutical products.

1.10.1 Stepwise Amino Acid Production

Lysine is an essential amino acid for the nutrition of humans that is used as a supplementary food with bread and other foodstuffs. This amino acid is a biological product that is also used as a food additive and cereal protein. One of the commercial methods for production of lysine consists of a two-stage process using two species of bacteria as follows:

- Step 1: Formation of diaminopimelic acid (DAP) by *E. coli*
- Step 2: Decarboxylation of DAP by *Enterobacter aerogenes*.

The carbon sources for production of amino acids are corn, potato starch, molasses, and whey. If starch is used, it must be hydrolyzed to glucose to achieve higher yield. *Escherichia coli* is grown in a medium consisting of glycerol, corn steep liquor, and diammonium phosphate under aerobic conditions with controlled temperature and pH for an incubation period of three days.

Many species of microorganisms, especially bacteria and fungi are capable of producing large amounts of glutamic acid. Glutamic acid is produced by microbial metabolites of *Micrococcus*, *Arthrobacter*, and *Brevibacterium* through the Krebs cycle. Monosodium glutamate is known as a flavor-enhancing amino acid in food industries. The medium generally used for its production consists of a carbohydrate, peptone, inorganic salts, and biotin.

The concentration of biotin has a significant influence on the yield of glutamic acid. The α -ketoglutaric acid is an intermediate in the tricarboxylic acid cycle or the Krebs cycle and is the precursor of glutamic acid. The conversion of α -ketoglutaric acid to glutamic acid is accomplished in the presence of glutamic acid dehydrogenase (GDH), ammonia, and nicotinamide adenine dinucleotide phosphate (NADPH) as follows^{2,9}:



The living cells assimilate nitrogen by incorporating it into α -ketoglutaric acid, then to glutamic acid and glutamine.

1.10.2 Insulin

In the human body, one-third of glucose from dietary sources is converted to glycogen in the liver. About half the carbohydrates from dietary sources are converted to glycogen in muscle tissues. The remaining carbohydrates are immediately oxidized for body energy requirements. Both glucose uptake and glycogen synthesis are stimulated by a peptide hormone produced in the pancreas known as insulin, which is the most important hormone to regulate carbohydrate and fat metabolism in the human body. The hormone stimulates glycogen breakdown and release of glucose from the liver. In fact, insulin acts reciprocally when blood sugar is high to respond and regulate blood glucose, ensuring that blood sugar concentration is at a relatively constant and safe level (110 mg dl^{-1}). The extra glucose is polymerized may be stored in the liver and muscles as glycogen.

Insulin is one of the important pharmaceutical products produced commercially by genetically engineered bacteria. Before this development, commercial insulin was isolated from animal pancreatic tissue. Microbial insulin has been available since 1982. The human insulin gene is introduced into a bacterium like *E. coli*. Two major advantages of insulin production by microorganisms are that the resultant insulin is chemically identical to human insulin and it can be produced in unlimited quantities.

1.11 ANTIBIOTICS, PRODUCTION OF PENICILLIN

The commercial production of penicillin and other antibiotics is the most dramatic manifestation in industrial microbiology. The annual bulk production of penicillin is about 15,000 metric tons, with an annual sales market of more than US\$400 million.¹⁰ The worldwide bulk sales of the four most important groups of antibiotics, namely penicillin, cephalosporin, tetracycline, and erythromycin, are $\text{US\$}4.2 \times 10^3$ millions per annum.¹¹ The mold isolated by Alexander Fleming in the early 1940s was *Penicillium notatum*. He noted that this species killed his culture of *Staphylococcus aureus*. The production of penicillin is now done by a better penicillin-producing mold species, *Penicillium chrysogenum*. Development of submerged culture techniques enhanced the cultivation of the mold in a large-scale operation using a sterile air supply. *P. chrysogenum* can produce 1,000 times more penicillin than Fleming's original culture.¹⁰ Various waste materials, including molasses, corn steep liquor, waste product from the sugar industry, and wet milling corn, can be used for the production of penicillin.

Streptomycin is commonly produced by *Actinomycetes*. The major steps in the commercial production of penicillin are:

1. Preparation of inoculum
2. Preparation and sterilization of the medium
3. Inoculation of the medium in the fermenter
4. Forced aeration with sterile air during incubation
5. Removal of mold mycelium after fermentation
6. Extraction and purification of the penicillin.

1.12 PRODUCTION OF ENZYMES

Many molds synthesize and excrete large quantities of enzymes into the surrounding medium. Enzymes are proteins; they are denatured by heat and extracted or precipitated by chemical solvents like ethanol and by inorganic salts like ammonium sulfate.¹² Coenzymes are also proteins combined with low molecular mass organics like vitamin B. It is industrially applicable and economically feasible to produce, concentrate, extract, and purify enzymes from cultures of molds such as *Aspergillus*, *Penicillium*, *Mucor*, and *Rhizopus*. Mold enzymes such as amylase, invertase, protease, and pectinase are useful in the processing or refining of a variety of materials. Amylases hydrolyze starch to dextrin and sugars. They are used in preparing sizes and adhesives, desizing textiles, clarifying fruit juices, manufacturing pharmaceuticals, and other purposes. Invertase hydrolyzes sucrose to form glucose and fructose (invert sugars). It is widely used in candy-making and the production of noncrystallizable syrup from sucrose, which is partly hydrolyzed by this enzyme. The proteolytic enzymes such as protease are used for bating in leather processing to obtain a fine texture. Protease is also used in the manufacturing of liquid glue, degumming of silks, and clarification of beer protein. It is used in laundry detergents and as an adjunct to soaps. Pectinase is used in the clarification of fruit juice and to hydrolyze pectins in the retting of flax for the manufacturing of linen. Apoenzyme is the protein portion of enzyme that is inactive. The reaction between low molecular mass coenzymes and apoenzyme gives active holoenzyme:



1.13 PRODUCTION OF BAKER'S YEAST

The use of yeast as a leavening agent in baking dates back to the early histories of the Egyptians, Greeks, and Romans. In those days, leavened bread was made by mixing some leftover dough from the previous batch of bread with fresh dough. In modern baking, pure cultures of selected strains of *Saccharomyces cerevisiae* are mixed with bread dough to bring about desired changes in the texture and flavor of bread. Characteristics of *S. cerevisiae* strains are selected for commercial production of baker's yeast. These strains have the ability to ferment sugar in the dough vigorously and rapidly. The selected strains must be stable and

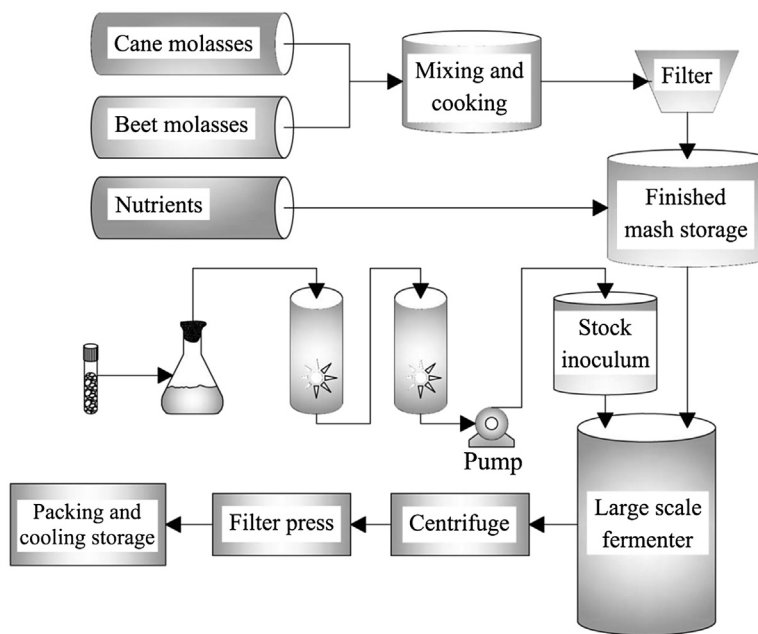


FIGURE 1.2 Commercial production of baker's yeast.

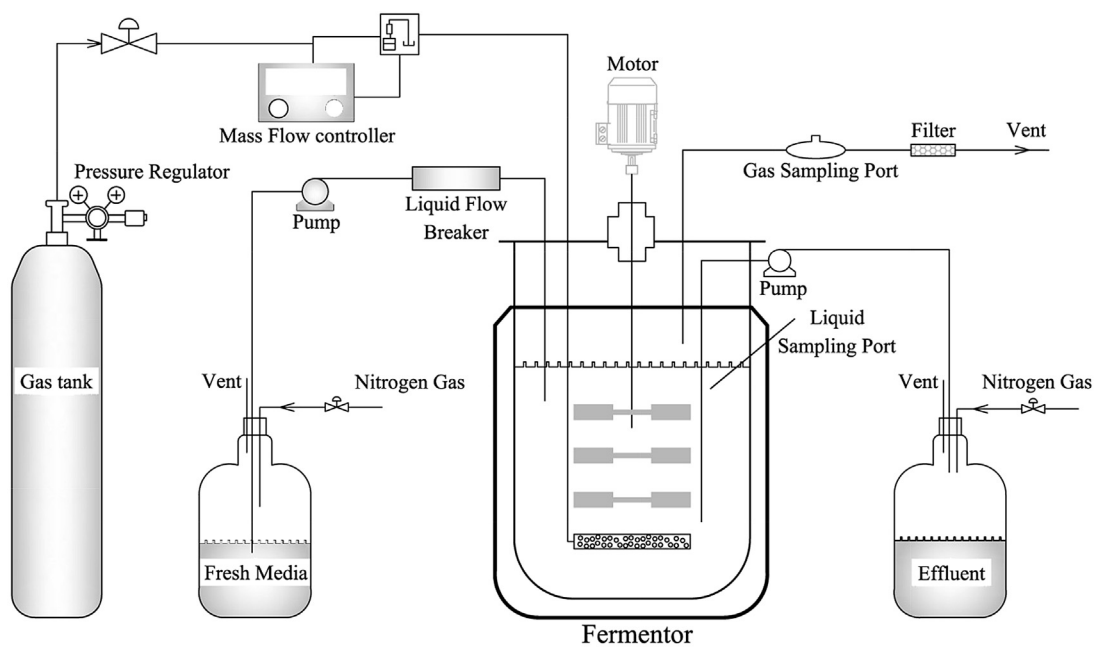


FIGURE 1.3 One complete set of fermenters with all accessory controlling units.

produce carbon dioxide, which results from the fermentation process for leavening or rising the dough. The quality of bread depends on the selected strain of yeast, the incubation period, and the choice of raw materials. Sugars in bread dough are fermented by yeast to ethanol and CO₂, and the CO₂ causes the bread to rise.

In the manufacturing of baker's yeast, the stock strain is inoculated into a medium containing molasses and corn steep liquor. The pH of the medium is adjusted to be slightly acidic at pH 4–5. The acidic pH may retard the bacterial growth. The inoculated medium is aerated during the incubation period. At the end, the cells are harvested by centrifuging out the fermentation broth and recovered by filter press. A small amount of vegetable oil is added to act as a plasticizer, and then the cell mass is molded into blocks. The process is shown in [Figure 1.2](#).

A full set of bioreactor with pH and temperature controllers are shown in [Figure 1.3](#). The complete set of fermenters with all accessory controlling units creates a good opportunity to provide suitable production of biochemical products with variation of process parameters. Pumping fresh nutrients and operating in batch, fed batch, and continuous mode are easy and suitable for producing fine chemicals, amino acids, and even antibiotics.

References

1. Phaff HJ. *Sci Am* 1981;**245**:77.
2. Baily JE, Ollis DF. *Biochemical engineering fundamentals*. 2nd ed. New York: McGraw-Hill; 1986.
3. Aiba S, Humphrey AE, Millis NF. *Biochemical engineering*. 2nd ed. New York: Academic Press; 1973.
4. Demain AL, Solomon AN. *Sci Am* 1981;**245**:67.
5. Ghose TK. *Bioprocess computation in biotechnology*. Ellis Horwood Limited Series in biochemistry and biotechnology, vol. 1. New York: Ellis Horwood Limited; 1990.
6. Scragg AH. *Bioreactors in biotechnology: a practical approach*. Ellis Horwood Limited Series in biochemistry and biotechnology. New York: Ellis Horwood Limited; 1991.
7. Bradford MM. *J Anal Biochem* 1976;**72**:248.
8. Doran PM. *Bioprocess engineering principles*. New York: Academic Press; 1995.
9. Shuler ML, Kargi F. *Bioprocess engineering: basic concepts*. New Jersey: Prentice-Hall; 1992.
10. Pelczar MJ, Chan ECS, Krieg NR. *Microbiology*. New York: McGraw-Hill; 1986.
11. Aharonowitz Y, Cohen G. *Sci Am* 1981;**245**:141.
12. Thomas LC, Chamberlin GJ. *Colorimetric chemical analytical methods*. Salisbury (United Kingdom): Tintometer Ltd; 1980.

Enzyme Technology

OUTLINE

2.1 Introduction	20	Nomenclature	38
2.2 Enzyme Elementary Reaction Rate	21	2.12 Solve Problems	39
2.3 Enzyme Classifications	28	References	40
2.4 Enzymes Specific Function	30	2.13 Case Study: Solid-State Fermentation of Sugarcane Bagasse in a Tray Bioreactor for Production of Lipase Using <i>Rhizopus oryzae</i>	41
2.5 Enzymes Act as Catalysts	30	2.13.1 Introduction	41
2.6 Inhibitors of Enzyme-Catalyzed Reactions	31	2.13.2 Material and Methods	42
2.7 Industrial Application of Enzymes	33	2.13.2.1 Bioreactor Setup	43
2.8 Coenzymes	35	2.14.2.2 Solid-State Fermentation and Sample Preparation	43
2.9 Effect of pH on Enzyme Activities	37	2.13.3 Results and Discussion	44
2.10 Enzyme Unit Activities	37	References	49
2.11 Enzyme Deactivation	37		

SUBCHAPTER

2.1

Introduction

An enzyme is a protein or an organic compound that is similar to a protein and has catalytic activities. An enzyme acts very specifically with a specified functional group that acts as an active site. An enzyme $[E]$ interacts with substrate $[S]$ and as a result, an enzyme–substrate complex $[ES]$ as an intermediate compound is formed. The initiation reactions are reversible, and equilibrium is reached. Then, the intermediate compound goes through irreversible reaction to yield a product and a free enzyme. The liberated enzyme searches for a substrate to form an $[ES]$. The defined reaction mechanism proceeds until substrates are converted to products. In fact, presence of the enzyme in the reaction media is to accelerate the reaction rate. The concept of reaction as energy involved is similar to the mechanism of catalytic reaction.¹

Most enzymes are named according to the reaction involved. Generally, all enzymes carry the name of the reaction with a suffix as “ase,” for instance, an amylolytic enzyme that reacts with amylose is named amylase; that means the enzyme that hydrolyzes amylose is named amylase. Also, the organic configuration is similar to carbohydrates that are specified for the enzyme as well. Another example is the enzyme that catalyzes the decomposition of urea is named as urease. The enzyme that reacts with tyrosine is known as tyrosinase. The name of enzyme interacting with a substrate like uric acid is uricase.

The enzymatic reactions may take place in homogeneous or heterogeneous phases. It depends on the enzyme and substrate phases or conditions. In general, three cases may occur. If enzyme is soluble and the substrate is in the liquid phase, which is called the homogeneous phase, the enzyme and substrate interact in a single liquid phase. In this case, both enzyme and substrate are soluble in an aqueous phase. In the case of solid-state fermentation (SSF), a solid substrate like rice bran or soya beans uses a specific culture, say *Aspergillus niger*, live in liquefied nutrients. The solid substrate should contain desired moisture, and the SSF process successfully delivers the enzyme. This process is known as heterogeneous, as more than one phase exists.

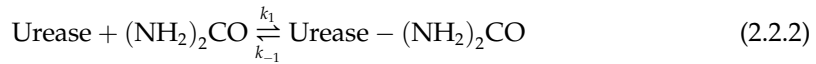
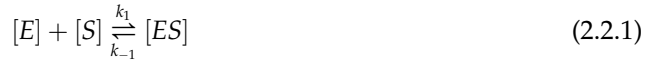
For the production of enzymes, a number of bioreactors are involved. Tray bioreactors are often employed for SSF. The leachates from solid media are collected for recovery of an enzyme. In this case, enzymes are available in an aqueous phase while substrates remain in the solid phase. In the heterogeneous case, either enzyme or substrates are in solid or liquid phases. In the case of SSF, the organisms utilize a substrate to generate biomass and an enzyme. The enzyme may be involved in further enzymatic reaction. The enzyme or organisms must penetrate into a solid substrate for the liquefaction of

the solid, and as a result of washing, solid products are isolated. In SSF, the liberated enzymes are washed off the solid bed, while cell biomass is washed off along with the liberated enzyme.

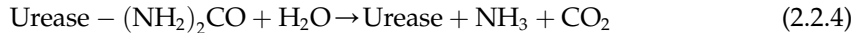
Whereas, the third case may be the inverse of the second case, as substrate is available in the liquid phase while an enzyme is insoluble or in solid phase (insoluble enzyme plus soluble substrate). An example of a type II reaction is the use of amylase, lipase, and protease in laundry detergents. The soluble enzymes interact with the insoluble substrate attached to the surface of cloth, and as a result, the product is soluble. For the type III enzymatic reaction, the enzyme is insoluble; the enzyme is immobilized on a solid support and then packed in a column. The soluble substrate has to pass through the bed of enzymes. Most often, the second type of soluble substrates are preferred. For the simple case, both enzyme and substrate are in an aqueous phase.

2.2 ENZYME ELEMENTARY REACTION RATE

Let us define the substrate $[S]$ to be urea, $(\text{NH}_2)_2\text{CO}$, and the suitable enzyme $[E]$ for hydrolysis of urea would be urease. The product is defined as $[P]$, CO_2 and NH_3 . The mechanism of the reaction for the enzyme-substrate complex is written as follows:



In the next step, as the intermediate compound is hydrolyzed, urease is released; the product would be ammonia and carbon dioxide. The reaction is irreversible, expressed as follows:



The rate of utilization of substrate $-r_s$ is stated as follows:

$$-r_s = k_1[E][S] - k_{-1}[ES] \quad (2.2.5)$$

At equilibrium for constant intermediate concentration, the rate of change of intermediate with respect to time reached to zero is stated as:

$$r_{E.S} = 0 = k_1[E][S] - k_{-1}[ES] - k_s[\text{H}_2\text{O}][ES] \quad (2.2.6)$$

The rate of hydrolysis of the intermediate complex is:

$$r_p = k_s[ES][\text{H}_2\text{O}] \quad (2.2.7)$$

Based on equilibrium, one can calculate the intermediate $[ES]$ according to following relation:

$$[ES] = \frac{k_1[E][S]}{k_{-1} + k_s[H_2O]} \quad (2.2.8)$$

Where part of the initial enzyme concentration is active and the remaining is attached to the substrate as an intermediate complex $[E_o] = [E] + [ES]$, one can define the free enzyme part as $[E] = [E_o] - [ES]$; now we can substitute the free enzyme $[E]$ in the above equation, which results in the following relation:

$$k_1([E_o] - [ES])[S] = [ES](k_{-1} + k_s[H_2O]) \quad (2.2.9)$$

Rearrange Eqn (2.2.6), then solve for $[ES]$:

$$[ES] = \frac{k_1[E_o][S]}{k_{-1} + k_s[H_2O] + k_1[S]} \quad (2.2.10)$$

In the course of hydrolysis, the concentration of water compared to enzyme and substrate is in excess; therefore, once can assume a new constant $k' = k_s[H_2O]$. Then, substitute the constant into Eqn 2.2.10, which yields:

$$-r_s = \frac{k'k_1[E_o][S]}{k_{-1} + k' + k_1[S]} \quad (2.2.11)$$

Let us define a constant known as Michaelis–Menten constant $K_M = k_{-1} + k'$ and $k'k_1[E_o]$ as maximum specific rate:

$$V_{max} = k'k_1[E_o] \quad (2.2.12)$$

Finally, Eqn 2.2.11 simplifies and reduces to a well-known equation called the Michaelis–Menten rate equation, stated as follows:

$$V = \frac{V_{max}S}{K_M + S} \quad (2.2.13)$$

For a given enzyme concentration, the rate of substrate utilization can be calculated by the above equation. Figure 2.1 shows the rate of substrate consumption versus substrate concentration.

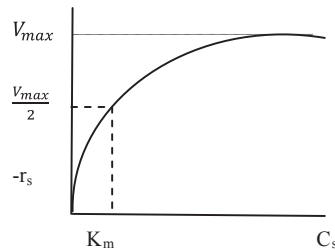


FIGURE 2.1 Illustration of Michaelis–Menten parameters.

When substrate concentration is low in comparison to K_M , the rate equation shifts to first order:

$$-r_s = \frac{V_{max}S}{K_M} \quad (2.2.14)$$

While at high concentration of substrate, the rate of enzyme reaction may reach constant rate at maximum value; that means $-r_s = V_{max}$. For the case of substrate S is equal to K_M , the rate is half of the maximum rate, as is indicated in the preceding illustrated figure.

$$-r_s = \frac{V_{max}}{2} \quad (2.2.15)$$

The parameters in the rate model V_{max} and K_M are used to characterize the enzymatic reaction. The value of V_{max} is dependent on enzyme concentration; whereas, K_M is independent. For a batch bioreactor, the rate is given as follows:

$$-\frac{dC_{urea}}{dt} = -r_{urea} = \frac{V_{max}C_{urea}}{K_M + C_{urea}} \quad (2.2.16)$$

Integration, while separating variables to define batch residence time for enzymatic reaction, yields:

$$t = - \int_{C_i}^{C_s} \frac{K_M + C_{urea}}{V_{max}C_{urea}} dC_{urea} \quad (2.2.17)$$

$$t = \frac{K_M}{V_{max}} \ln \frac{C_i}{C_s} + \frac{C_i - C_s}{V_{max}} \quad (2.2.18)$$

The preceding equation in terms of conversion is written by substitution $C_s/C_i = 1 - X$.

$$t = \frac{K_M}{V_{max}} \ln \frac{1}{1 - X} + \frac{C_i X}{V_{max}} \quad (2.2.19)$$

The preceding equation is multiplied by $\frac{V_{max}}{K_M t}$, then rearranged:

$$\frac{1}{t} \ln \frac{1}{1 - X} = \frac{V_{max}}{K_M} - \frac{C_i X}{K_M t} \quad (2.2.20)$$

To obtain K_M and V_{max} in a batch bioreactor, a linearized model of the Michaelis–Menten rate equation is used. To define batch residence time, a similar expression for substrate concentration is given below:

$$\frac{1}{t} \ln \frac{S_o}{S} = \frac{V_{max}}{K_M} - \frac{S_o - S}{K_M t} \quad (2.2.21)$$

The slope and intercept of the line drawn in [Figure 2.2](#) are defined for K_M and V_{max} .

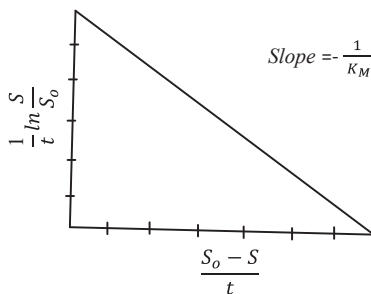


FIGURE 2.2 Linear plot of Eqn 2.2.21.

EXAMPLE 1**Evaluate Michaelis–Menten rate constants**

Determine Michaelis–Menten rate constants, V_{max} for a urease enzymatic reaction. The reaction rate is given as a function of substrate concentration given in the Table E.1.1

TABLE E.1.1 Urea concentration and rate of urea consumption

C_{urea} (mol l ⁻¹)	0.2	0.02	0.01	0.005	0.0025
$-r_{\text{urea}}$ (mol (l s) ⁻¹)	1.1	0.55	0.375	0.2	0.1

Solution

The Michaelis–Menten rate model is linearized for a double reciprocal equation that is known as the Lineweaver–Burk plot, which is described by the following equation:

$$\frac{1}{-r_s} = \frac{S + K_m}{V_{max}S} = \frac{1}{V_{max}} + \frac{K_m}{V_{max}} \left(\frac{1}{S} \right) \quad (\text{E.1.1})$$

The plot of reciprocal reaction rate versus reciprocal of substrate should be a straight line. Let us calculate double reciprocal values as given; data are summarized in the following Table E.1.2

TABLE E.1.2 Calculated inverse urea and inverse rate

C_{urea} (mol l ⁻¹)	$-r_{\text{urea}}$ (mol (l s) ⁻¹)	$1/C_{\text{urea}}$ (l mol ⁻¹)	$1/-r_{\text{urea}}$ (l s mol ⁻¹)
0.20	1.1	5.0	0.93
0.02	0.55	50	1.82
0.01	0.375	100	2.67
0.005	0.2	200	500
0.0022	0.093	455	10.75

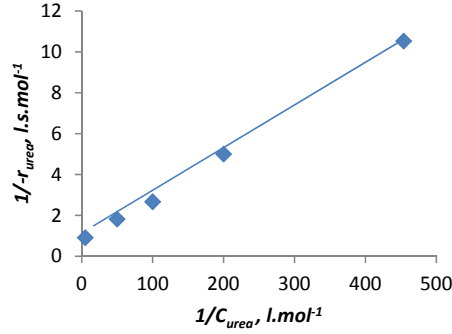


FIGURE E.1.1 Lineweaver–Burk plot for enzyme linear rate model.

From Figure E.1.1, the slope of the line is $\frac{K_M}{V_{\max}} = 0.02 \text{ s}$, $K_M = 0.025 \text{ mol l}^{-1}$ and the intercept is 0.8; the maximum rate is $V_{\max} = 1.25 \text{ mol (l s)}^{-1}$. Now substitute kinetic parameters into the rate equation. The result is the rate model for enzyme kinetics.

$$-r_{\text{urea}} = \frac{1.25 C_{\text{urea}}}{0.025 + C_{\text{urea}}} \quad (\text{E.1.2})$$

EXAMPLE 2

Given Michaelis–Menten kinetics for a concentration of enzyme $[E]$, assume specific gravity of an enzyme solution that has K_M value of 6.2 v/v%. The initial and final substrate concentrations were 1.4 and 0.2 $\mu\text{mol ml}^{-1}$, respectively. Also given is the maximum rate for the enzyme $V_{\max} = 5.6 \mu\text{mol (ml min)}^{-1}$. Density of the solution is 0.9 g cm^{-3} and average molecular weight of 300 g mol^{-1} ; total concentration $C_T = 0.003 \text{ mol ml}^{-1}$ or 3000 $\mu\text{mol ml}^{-1}$. Define batch reaction time for the given information about the enzyme kinetic activities.

Solution

Michaelis–Menten rate is defined as:

$$\begin{aligned} -r_s &= -\frac{dC_s}{dt} = \frac{V_{\max} C_s}{K_M + C_s} \\ C_s &= C_{s0}(1 - X) \\ 0.2 &= 1.4(1 - X); \quad X = 0.86 \\ -\int_{1.4}^{0.2} \frac{K_M + C_s}{C_s} dC_s &= \int_0^t \frac{V_{\max}}{C_T} dt = \int_0^t \frac{5.6}{3000} dt \\ \frac{5.6 \times 10^{-3}}{3} t &= K_m \ln \frac{1.4}{0.2} + (1.4 - 0.2) \\ t &= \frac{6.2 \ln 7 + 1.2}{5.6 \times 10^{-3}/3} = 7106 \text{ min} = 118.4 \text{ h} \end{aligned}$$

EXAMPLE 3

For an enzymatic hydrolysis of a lipid, a 5 l batch bioreactor for conversion of 95% is used, while initial substrate concentration is 0.5 mol l^{-1} , and enzyme reaction has utilized an 80 ng l^{-1} . The reaction is carried out isothermally. Experimental data for the reaction is provided in the [Table E.3.1](#)

TABLE E.3.1 Data collected in enzyme rate studies

$C_S \text{ (mol l}^{-1}\text{)}$	$-r_S \text{ (mol (l s)}^{-1}\text{)}$	$1/C_S \text{ (l mol}^{-1}\text{)}$	$1/-r_S \text{ (l s mol}^{-1}\text{)}$
1.0	1.15	1.0	0.87
0.1	0.67	10	1.49
0.05	0.43	20	2.33
0.025	0.22	40	4.55
0.01	0.10	100	10.0

Determine batch kinetics reaction time.

Solution

Given batch residence time for the enzymatic hydrolysis, the related expression is as follows:

$$t = \frac{K_M}{V_{max}} \ln \frac{1}{1-X} + \frac{C_i X}{V_{max}} = \frac{2004}{1.43} \ln \frac{1}{0.05} + \frac{0.5(0.95)}{1.43} = 4.6 \text{ s}$$

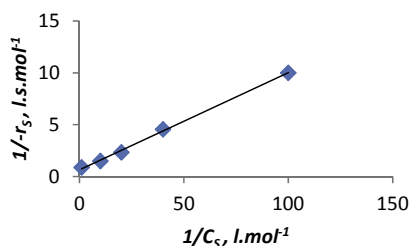


FIGURE E.3.1 Linearized Lineweaver–Burk plot.

From [Figure E3.1](#) the slope of the line is $\frac{K_M}{V_{max}} = 0.92 \text{ s}$, $K_M = 2.05 \text{ mol l}^{-1}$ and the intercept is 0.7; the maximum rate is $V_{max} = 1.43 \text{ mol (l s)}^{-1}$. Now substitute kinetic parameters into the rate equation; the results are in the rate model for enzyme kinetics.

EXAMPLE 4

Define enzyme kinetic parameters given experimental data as urea is liberated with respect to time:

Time (min)	2	2.5	3.2	4	10
Urea concentration (g l^{-1})	0.12	0.43	0.95	2.70	12.0

Solution

The rate is calculated based on the change of concentration of urea release with respect to time differences. The calculated rate and double reciprocals are stated in [Table E.4.1](#).

TABLE E.4.1 For given experimental data, calculated inverse substrate and rate

Time (min)	C_s (g l^{-1})	$-r_s$ (g (l min)^{-1})	$1/C_s$ (l g^{-1})	$1/-r_s$ (l min g^{-1})
2	0.12	0.06	8.33	16.67
2.5	0.43	0.17	2.33	5.88
3.2	1.15	0.36	0.87	2.78
4	2.67	0.67	0.37	1.49
10	11.40	1.14	0.088	0.88

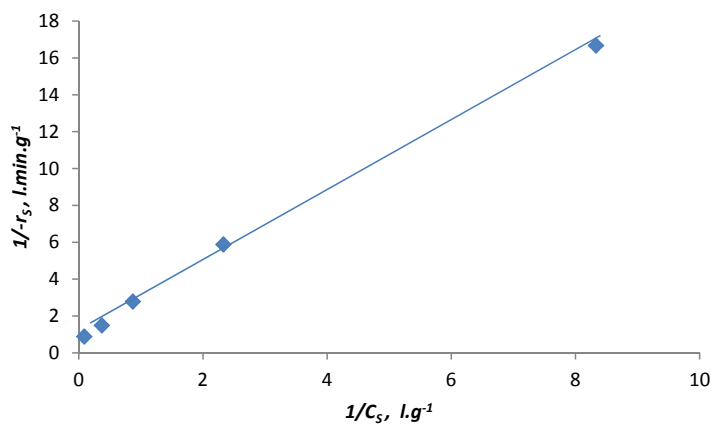


FIGURE E.4.1 Inverse rate, $1/-r_s$ versus $1/C_s$.

Plot of inverse rate, $1/-r_s$ versus $1/C_s$ resulted $V_{max} = 1.25 \text{ g (l min)}^{-1}$ and $K_M = 2.4 \text{ g l}^{-1}$; the plotted data are shown in [Figure E.4.1](#).

The energy stored in the protein as biomolecules is known as the activation energy; it may assist as the biochemical reaction proceeds. In a living system, an enzyme functions in a specific temperature and pH. Enzymes have remarkable properties; as enzyme are catalyzed and speed up the reaction rate, the rate may increase by a magnitude of one million. Enzymes, in contrast to inorganic catalyst, act in a very specific manner and often function for a very selective, exact reaction. In pharmaceutical applications, enzymes are used to activate a specific medicine by shifting a functional group of a medicine. Because the actions of enzymes are highly selective, side reactions or side products are rarely produced. Enzymes are known as very precise catalysts that conserve energy in biochemical reactions. The free energy involved for enzymatic reaction is much lower than noncatalytic reaction.

Enzymes are known for being very unique, and they have active sites for interacting with an exact functional group coupled with a substrate. That is why enzymes work like a lock and key model. Several amino acids are involved in participation of the active site and catalytic activities. As a result, energy is transferred to the enzyme–substrate complex; that energy can lower the energy formation of the product, and then products are released. That means the energy required for the reaction transferred by the enzyme enhances the product to be released. The catalytic activity of an enzyme depends on an interaction between the active site amino acids and the substrate. It may be possible in some other enzyme nonprotein components to be responsible for their catalytic activities. For instance, enzyme cofactors are acting ions in enzymes; these ions are like Fe^{2+} , Zn^{2+} , Mg^{2+} , Mn^{2+} or a complex of organics known as coenzymes. If a protein component of the enzyme is lacking an essential cofactor, it is known as “apoenzyme.” Once an enzyme is bounded to cofactors, it is called holoenzyme.²

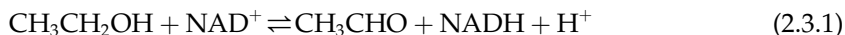
The rate of an enzyme acting as a catalyst can be regulated in a desired environment. The enzyme activities may be enhanced by activators or promoters, and also, the activities can be reduced by enzyme inhibitors. This means the activity of an enzyme can be regulated by cofactors and bonds to any ions for extra charges. For example, hexokinase is an enzyme that can catalyze the adenine triphosphate in the phosphorylation of carbohydrates known as hexose, a six-carbon sugar. The enzyme will bind to D-glucose, not to L-hexose. This is a specific action of the enzyme on a specified carbohydrate. The prefixes D- and L- for carbohydrates are related to shifting polarized sugar isomers. In fact, photons of light can move the isomer structure of D-glucose carbohydrates as the molecule can shift the polarized light to the right and L-hexose shifts the light to the left, like α -L-fucose (6-deoxy-L-galactose).¹

2.3 ENZYME CLASSIFICATIONS

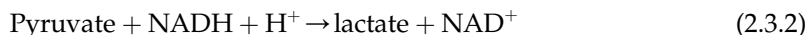
Enzymes are classified based on their specific function. In biological processes and living systems, certainly a huge number of biochemical reactions occur under enzymatic activities.³ These enzymes are categorized based on the reaction and specific function, product formation, or substrate consumption. There are six groups of enzymes identified based on enzyme activities and enzyme-specific special function:

1. Oxidation and reduction enzymes: These enzymes are involved in oxidation and reduction and are often called oxidoreductase. The common conversion of *oxidases*, *reductases*, and *hydrogenases* is ketones/keto-acids to chiral alcohols. For instance, in the oxidation of ethanol, the alcohol is converted to aldehydes, while nicotinamide adenine

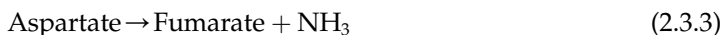
dinucleotide (NAD^+) is reduced to nicotinamide adenine dinucleotide hydrogenase (NADH). The reaction in living systems requires an enzyme to oxidize ethanol while NAD^+ is reduced.



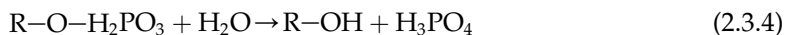
The enzymatic reaction catalyzed by lactate dehydrogenase can be stated as follows:



Aspartate ammonia lyase (aspartase) can convert aspartic acid to fumaric acid; the reaction is stated as follows:

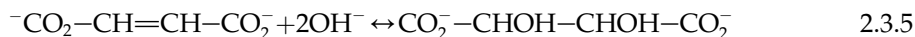


2. Enzymes involved in transfer reactions: The second group of enzymes is known as "transferase." This group of enzymes transfers a functional group from one molecule to another one. For example, in an enzyme known as "phosphatase," the phosphate group is moved from adenosine triphosphate (ATP) to an other compound.
3. Hydrolase enzymes: These enzymes are able to hydrolyze a polysaccharide to a monomeric sugar. In fact, the purpose of a hydrolase enzyme is to catalyze the reaction of a water molecule with a polymer. For example, amylose is reacted with amylase in the presence of water, and as a result, glucose is liberated. Another example is a reaction of phosphatase breaking a phosphate group to liberate phosphoric acid while alcohol is formed.

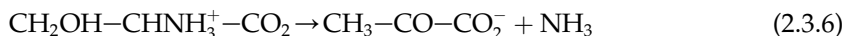


The enzymes act as digestive function while breaking the peptide bond in proteins. The most common hydrolytic enzyme, for instance reaction, of water with cellulose fiber, monomeric sugar is formed.

4. Enzymes for the removal or formation of a double bond: The formation or removal of a double bond with a group transfer occurs by an enzyme having the suffix of "lyase," which includes the amino group, water, and ammonia. For example, an enzyme known as decarboxylase is able to remove CO_2 from alpha- or beta-ketoacids:

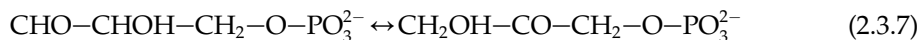


Such a type of enzyme is able to remove double bonds to deliver a saturated organic structure. Another example is the removal of the ammonia group from an amino acid. In this case, serine is converted to pyruvate:



5. Isomerization of functional groups: This group of enzymes is able to catalyze chemical structure as the position of functional group is shifting, while the molecule contains the same number of atoms; the only changes occur on the configuration of the molecule as some functional groups are displaced. Such changes are called isomerization. For example, the enzyme known as phosphate isomerase is able to shift the aldehyde group

($-\text{CHO}$) to ketone from ($-\text{CO}-$). The reaction of isomerization in glyceraldehyde-3-phosphate is shown next:



In addition, the following reactions demonstrate how the isomerase enzyme can catalyze reactions. For instance, triose phosphate isomerase can convert dihydroxyacetone to glyceraldehyde-3-phosphate.



Also, an especial enzyme is able to convert optical isomers; for example, alanine racemase may convert L-alanine to D-alanine.



6. Single bond formation by eliminating the elements of water: Enzymes known as hydrolases act in breaking down bonds by adding water molecules. However, ligases respond in a converse reaction by removing a water molecule from two functional groups to form a single bond. Synthetases are a subclass of ligases used for hydrolysis of ATP to drive this formation. For example, *aminoacyl-transfer RNA synthetases* join amino acids to transfer RNAs for protein synthesis.

2.4 ENZYMES SPECIFIC FUNCTION

Enzymes that are able to function outside of living cells are known as biological catalysts acting in vitro. The enzymatic activities of enzymes are associated with a protein structure because enzymes have active sites with which bind to substrate. Generally, digestive enzymes are pure protein structures. For example, urease is a pure protein. Pepsin, trypsin, and chymotrypsin are known as digestive enzymes. Lysozymes are active enzymes found in tears, saliva, and egg whites that digest the cell wall of some bacteria. The structure of a lysozyme is in crystalline form, which was defined by X-ray crystallography. That was the beginning of the field of structure biology. Enzymes are globular proteins arranged from amino acid residues. The activities of enzymes are determined by their three-dimensional structure of proteins.

2.5 ENZYMES ACT AS CATALYSTS

Most enzymes are known as active catalysts, acting fast, and the rate of reactions is millions of times faster than uncatalyzed reactions. In fact, enzymes function similar to metal oxide catalysts. The enzymes-like catalysts are not consumed by the catalytic reaction, while the catalyst can lower the required activation energy to perform the reaction.

Besides the catalytic activities of enzymes, in comparison to metal oxide catalysts, they act very specifically on a substrate. Enzymes are highly selective for interaction with their specific substrate. The activities of enzymes are affected by other molecules. If any molecules

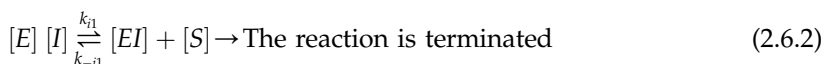
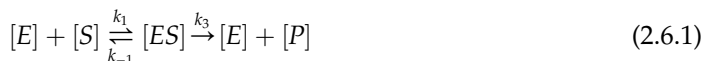
interfere with the enzyme reaction, the rate is affected by the specific molecules, known as inhibitors. The inhibitors can decrease enzyme activities. On the contrary, any molecules that increase or promote the enzymatic activities are known as enzyme activators. Many drugs and poisons act as inhibitors. Sometimes, the promoters can be a physical effect such as pH, temperature, or concentration of substrate.

Some enzymes are commercially used for the synthesis of antibiotics. There are four enzymes used in liquid and powder detergents. The purpose of these commercial enzymes is to interact and break down the dirt in the form of proteins and fats attached to the cloth. Therefore, most of these four enzymes are protease, lipase, amylase, and cellulase. Another well-defined application of enzymes is meat tenderizers; these enzymes break down the long chain of protein molecules to a small size; as a result, the meat became more tender, and then can easily be chewed.

2.6 INHIBITORS OF ENZYME-CATALYZED REACTIONS

Molecules that are able to retard or reduce enzyme activities are called inhibitors. These molecules can be food preservatives, drugs, and antibiotics. Enzyme inhibitors may be seriously involved in metabolic pathways and interrupt any biochemical or biological activities. On the contrary, for therapy, inhibitors may be used to control enzyme activities. For example, antibiotics are used to eliminate or reduce activity of specific enzymes. For protecting specific drugs, inhibitors are temporarily used. Enzyme inhibitors may occupy the active site of a free enzyme and strictly reduce enzyme activities. The function of inhibitors in any enzyme reaction is well understood. Inhibitors may influence enzyme rate constants, either by directly acting to reduce maximum specific growth rate (V_{max}) or by increasing the Michaelis–Menten constant (K_m). There are two distinct inhibitors acting on enzyme kinetic constants. Competitive and noncompetitive inhibitors are easily identified based on Lineweaver–Burk plots. In a competitive inhibitor, the value of V_{max} is unchanged by the addition of inhibitor concentration in the enzymatic reaction; that means the intercept of the plot does not change. Conversely, a noncompetitive inhibitor causes the reduction of the value of maximum specific growth rate, while the value of Michaelis–Menten constant remains unchanged. It is possible that both constants change due to the type of inhibitors; such inhibitors are known as mixed inhibitors. The details of the three types of inhibitors are discussed next.

Competitive Inhibitors: In this type of inhibitors; there is serious competition for substrate and inhibitors to interact with active sites of the free enzymes to form an enzyme–inhibitor complex $[EI]$. Competitive inhibition, having constant $1/V_{max}$, is shown in Figure 2.3. The reactions are illustrated as follows:



In this case, substrate and inhibitors often compete for binding to the free sites of enzymes. The concentration of enzyme–inhibitor complex depends on the concentration of inhibitors

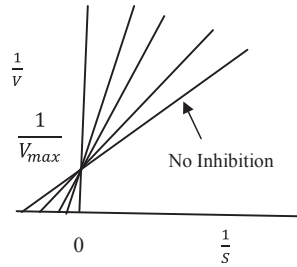


FIGURE 2.3 Competitive inhibition having a constant $1/V_{max}$.

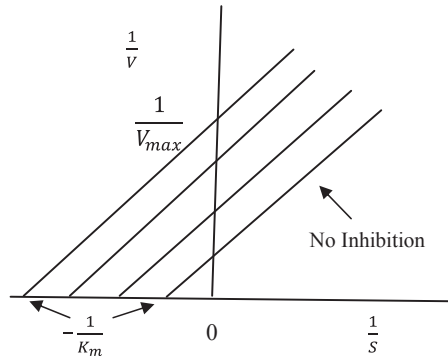


FIGURE 2.4 Uncompetitive inhibitors.

and the dissociation coefficient or equilibrium constants of $K_i = \frac{[E][I]}{[EI]} = \frac{k_{-i}}{k_{i1}}$; since enzymes are associated with inhibitors, enzymes activities are reduced while the active sites of enzymes are occupied with inhibitors. That reduces the affinity of the substrate to interact with active sites of enzymes.

Figure 2.4 shows uncompetitive inhibitors having constant slopes. The first line from the bottom has no inhibition; while the concentration of inhibitors increased as the value of maximum specific growth deceased. Notice that the value of K_m is not constant. In uncompetitive inhibitors, the inhibitors are not involved with the interaction of free sites, but they may take the advantage of binding to the complex formed as an enzyme-substrate $[ES]$, and the further $[EIS]$ complex is formed. This complex may terminate the reaction and cause to reduction of the activity of the enzyme.

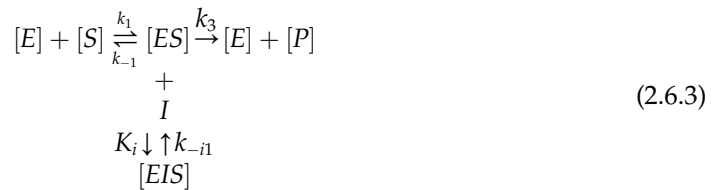


Figure 2.5 depicts noncompetitive inhibition for constant K_m , while the concentration of inhibitors increased and the value of maximum specific growth deceased. For the case of

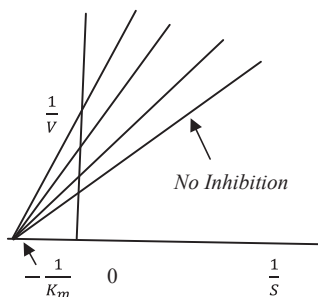
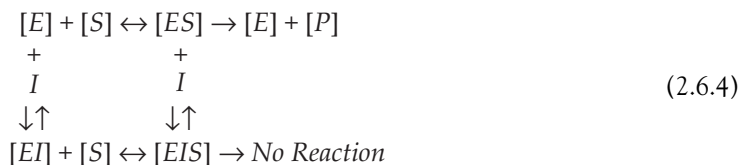


FIGURE 2.5 Noncompetitive inhibitors.

noncompetitive or mixed inhibitors, the enzyme interacts with the substrate and inhibitors to form an enzyme–substrate complex $[ES]$ while an enzyme–inhibitor complex also formed. Once the reaction proceeds, more complex enzyme–inhibitor–substrates $[EIS]$ are formed. At this stage, the reaction is terminated while inhibitors block the active sites of enzymes.



The rate of enzymatic reaction depends on substrate concentration and product formation. High concentrations of substrate and product may cause any sort of inhibition, as the enzymes are occupied by high levels of substrate or product; such phenomena may easily happen in a batch process.

2.7 INDUSTRIAL APPLICATION OF ENZYMES

Enzymes are used in chemical industries, food processing, cosmetics, and pharmaceutical use. In fact, enzymes are used as catalysts at atmospheric pressure and mild temperature; however, limitations with enzymes regarding denaturation may occur at high temperatures. The thermal tolerance of enzymes is produced to function and catalyze at relatively high temperature. An additional limitation of enzymes is the lack of stability in organic solvents. The nature of the enzyme is that of a protein; organic solvents may destroy the structural configuration of the enzyme. Enzymes are also sensitive to the pH of media. In other words, enzyme activities may be maximized at optimal pH. The demonstration of enzyme activities is dependent on their function. Amylases, which originate from fungi and plants, are commonly used in food processing. These enzymes are often used for production of sugar from starch. Also for the production of high fructose corn syrup, amylolytic enzymes are often used. In a baking process, enzymes are used to break down the starch content of flour; then, the polysaccharides are reduced to monomeric sugar. Yeasts are used for fermenting

carbohydrates to generate intermediate metabolites and carbon dioxide. The fermented product may be enriched with protein, and even proteases are used to liberate folic acid or other useful amino acids for the production of biscuits. The enriched flour is used for production of amino acids and other intermediate metabolites. In fermentation, carbon dioxide is generated; therefore, instead of baking soda, yeasts are used in bakeries and the food industry.

In preparation of predigested baby foods, use of trypsin is common. In the brewing industry, enzymes from barley are released in the course of the mashing stage of beer production. The enzyme breaks down starch and proteins to produce monosaccharides, peptides, and amino acids. The process is enriched via fermentation of yeasts. The industrial enzymes prepared from barley are widely used in the brewing process. These enzymes are perfectly substituted for the enzyme naturally found in barley.

Enzymes such as amylase, glucanase, and proteases are used for the saccharification of polysaccharides and proteolysis of proteins in malt. An enzyme, such as β -glucanase or arabinoxylanase, is used for the improvement of wort and beer filtration. Also, amyloglucosidases and pullulanases are implied in low-caloric beer to adjust the fermentation. Use of protease in clarification and removal of the cloudiness of stored beer is absolutely effective. The fermentation efficiency may be enhanced by the reduction of diacetyl, which is conducted in the enzymatic process by acetolactate decarboxylase. Normally, fruit juices are clarified by addition of enzymes known as cellulase and pectinase.

Enzymes are directly involved in cheese manufacturing, which are used to hydrolyze protein. In fact, the rennin, which is derived from the stomachs of young ruminant calves and lambs, is rich in proteolytic enzymes. The extracted enzymes from ruminants are used in dairy industries. There are many enzymes generated from *Lactobacillus* species used in dairy products. For instance, lipase is used for production of cheese to enhance ripening of the blue mold cheese.

The enzymes involved in most starch industries are amylase, amyloglucosidase, and glucoamylase. All of these enzymes are used for the hydrolysis of starch, which break down carbon-carbon bonds and liberate monomeric sugars like glucose and fructose in the form of various syrups that are products of starch industries.

The enzyme known as glucose isomerase is used to convert glucose to fructose. This enzyme is often used for production of highly enriched fructose syrups from starchy materials. These syrups are enhanced with sweetening properties and lower calorific values than sucrose for the same level of sweetness.

Applications of several enzymes in pulp and paper industries are well known. These enzymes are amylases, xylanases, cellulases, and ligninases. All of the amylolytic enzymes are used to degrade starch in order to reduce viscosity, sizing, and also used for paper coating. Xylanases may reduce the consumption of bleaches used for decolorizing; cellulase is also used for smoothening fibers. The lignin-degrading enzymes are used to remove lignin from softened paper. Use of cellulase in the biofuel industry is clearly demonstrated for the bioconversion of cellulose to reduced sugars. The monomeric carbohydrates are fermented to ethanol.

One of the main uses of enzymes is for the cleaning purposes as biological detergents. These enzymes are primarily proteases produced in an extra cellular cell synthesis, using for washing and presoaking conditions. The enzyme directly acts on protein stains on clothes. For liquid detergent, a combination of four enzymes is used, such as primary proteases,

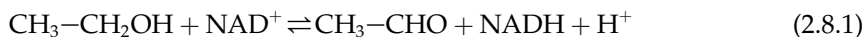
amylases, lipases, and cellulases. Also, these enzymes as a combination of four different enzymes are often used as laundry detergents. In addition, the mixture of four enzymes such as amylases, lipases, proteases, and cellulases are used in biological detergents for the purpose of cleaning and softening in washing machines to remove residues of starch, fats, and protein stains. Proteases are used in solution for the cleaning of contact lenses to remove proteins from the surface of the contact lens and to prevent infections. Another industrial application of an enzyme is the use of catalase in the rubber industry. This enzyme is used for the generation of oxygen from peroxide which is used for conversion of latex to foam rubber. Even proteases are used in the photographic industry for dissolving gelatin from scrap film for the recovery of sliver.

DNA ligase and polymerases are used for the manipulation of DNA in genetic engineering. Several enzymes are also used in pharmacology, agriculture, and medicine for the purpose of drug, digestion, and polymerase chain reactions; no one can ignore the role of the enzyme in pharmaceutical uses.

One of the enzymes that is able to break down polysaccharides and also to destroy the bacteria cell wall is known as lysozyme. In fact, the enzyme is able to hydrolyze the glycosidic bond β (1–4) from N-acetylmuramic acid to N-acetylglucosamine in peptidoglycans of the cell wall. Similarly, hydrolysis of the linkage of poly-N-acetylglucosamine as chitin, which is found in the exoskeletons insects, is a cell wall component of most fungi and can be accomplished by lysozyme. This enzyme is found in tears and, obviously, protects eyes from any bacterial infection. Lysozyme is found in the egg white (albumen) of hens eggs; the enzyme is a protein of a single polypeptide chain; it consists of 129 amino acids.¹ The enzyme catalyzes the hydrolysis reaction of most lipopolysaccharide compounds of most microbial cell walls. That means, the enzyme has the ability to lyse the cell walls of microorganisms.

2.8 COENZYMES

Enzymes catalyze a wide variety of biochemical reactions. Enzymes even speed up oxidation–reduction reactions as catalytic activities are associated with small molecules known as cofactors. The cofactor as a core center of the enzyme essentially acts as a chemical functional group binds with specific identified compounds. The cofactor may be metal ions such as $\text{Fe}^{3+}/\text{Fe}^{2+}$ and Zn^{2+} that are involved in catalytic activities of enzymes. An organic molecule such as nicotinamide adenine dinucleotide (NAD^+) serves a specific group with catalytic activities for oxidation–reduction reactions catalyzed by dehydrogenases. A typical reaction catalyzed by alcohol dehydrogenase is shown as follows:



The forms of NAD^+ and NADP^+ are known as the first coenzymes were recognized. They are involved in a large number of enzymatic reactions. The conversion of NAD^+ to reduced form of NADH is accompanied by marked alteration in the spectrophotometric properties of the coenzyme. NAD^+ is a coenzyme associated with a given molecule such as a co-substrate. The reduced forms of NAD^+ are NADH and NADPH . They are involved in the transfer of a hydroxide group, a hydrogen molecule with two electrons, between substrate and coenzyme. Such reactions may proceed via an actual transfer of hydroxide ion. Nicotinic acid, as known

TABLE 2.1 Vitamins function as coenzymes

Vitamin	Coenzyme	Reaction-mediated and metabolic roles
Biotin	Biocytin	Carboxylation, nonphotosynthetic fixation of carbon dioxide
Cobalamin, B ₁₂	Adenosyl cobalamin, B ₁₂	Alkylation, intermolecular rearrangements
Coenzyme A	CoA	Acyl transfer
Folic acid	Tetrahydrofolate	One carbon group transfer
Lipoic acid	Lipoic acid	Acyl transfer
Nicotinamide	Nicotinamide	Oxidation–reduction
Niacin	Nicotinamide adenine dinucleotide, NAD ⁺	Redox-active
Pantothenate, B ₃	CoA	Acyl transfer
Pyridoxine, B ₆	Pyridoxal phosphate	Amino group transfer
Riboflavin, B ₂	Flavin dinucleotide, FAD	Oxidation–reduction
Thiamine, B ₁	Thiamine pyrophosphate, TPP	Aldehyde transfer
Vitamin A	Retinol, carotenoid	Vision
Vitamin K	Vitamin K	Carboxylation of glutamate residues
Vitamin C	Ascorbic acid	Oxidation–reduction
Vitamin D	Ergocalciferol, β -carotene, ergosterol, steroid	Photolysis, photochemical reaction, calcium adsorption
Vitamin E	Tocopherol, terpenes	Reducing agent

as niacin, is available in cereals and meat, and is precursor of NAD⁺ and NADP⁺. The most prominent coenzyme in living system for transfer of the acyl group is coenzyme A (CoA). Other cofactors known as prosynthetic groups are associated with proteins via covalent bonds. For instance, the heme molecule in hemoglobin is tightly bounded to its protein. There is a covalent bond between heme and an Fe²⁺ ion and histidine (His). The heme molecule has a high affinity to bind with oxygen. The core of this molecule is Fe²⁺-Fe³⁺, surrounded by four porphyrin rings. The porphyrin ring is not only present in heme, but it is also appears in chlorophylls of green plant cells. For oxidation and reduction, shifting may occur from Fe²⁺ to Fe³⁺ inside the heme in a reversible reaction for oxyhemoglobin or reduced (redox) forms of globins.

Table 2.1 represents vitamins functioning as coenzymes. The coenzymes are considered as growth factors as they show up in supplementary nutrients in media for microbial growth. They may act as growth stimulants in specific cases. It is known that microorganisms are not able to synthesis some molecules; most of these biomolecules are vitamins. In the human diet, deficiency of nicotinic acid (niacin) causes a disease known as “pellagra.” The symptoms of pellagra are diarrhea, dermatitis, and dementia appearing in the human being. Most animals are able to synthesis nicotinamide from an amino acid known as tryptophan.

Vitamins are classified into two groups: those that are soluble in water and those vitamins that are insoluble in water (but are soluble in fats and lipids). The vitamins in the human diet that may act as coenzyme precursors are classified as water soluble vitamins. In the contrary, those vitamins that are insoluble in water, but soluble in fat or lipids such as vitamins A and D, are not considered as coenzymes. Vitamin D is a steroid. Among steroids, ergosterol is easily converted to vitamin D. Vitamin A is a carotenoid, whereas, vitamins D and E are derivatives of terpenes. Although these vitamins are essential in trace amounts in the human diet, but they may not be involved in catalytic activities similar to other coenzymes. The human system is unable to synthesize the supplementary vitamins. Some of these vitamins are synthesized by bacteria; these organisms are normal inhabitants in the human digestive system. It is believed that the superfluous cellular systems through evolution may lose the ability to synthesize these types of vitamins.

2.9 EFFECT OF pH ON ENZYME ACTIVITIES

Most enzymes are active only within a narrow range of pH, typically 5–9.⁴ The effect of pH may be related to a combination of several factors such as energy involved in binding the substrate to an active site on the enzyme, ionization of amino acid residues involved in catalytic activity of the enzyme, ionization of substrate and variation of protein structure due to ionic strength of the media. The rate of the enzymatic reaction due to variation of pH may lead to a normal bell curve, where a maximum rate is obtained at optimum pH of the solution. The optimal pH value may be related to pKs of ionized amino acids involved in the structure of the enzyme. Based on pKs values, it is probably possible to project the optimal pH of an enzyme by having the amino acid compositions in the structure of protein. Enzymes at extreme values of acidic or basic pH cause denaturation of protein.

2.10 ENZYME UNIT ACTIVITIES

The most common unit used for defining enzyme activities is the amount of transformation of 1.0 μmole of substrate per minute at 25 °C under optimum conditions. The specific activity of the enzyme is the number of units per mg of enzyme. The value for a specific activity is constant when the enzyme is pure. The turn over number for an enzyme is the number of substrate molecules transformed by a single active site on the enzyme. The molar activity of an enzyme with a single active site can be calculated from its maximum specific rate value, V_{max} . An international unit for enzyme activity is introduced by “Enzyme Commission” that is defined as the amount of enzyme activity transforms per 1 mol per second of substrate; known as “kat.”.

2.11 ENZYME DEACTIVATION

Enzymes are proteins; their stability is often reported by half-life. The half-life is the duration of time required by the use of an enzyme as the enzyme's activities decline to half of its

initial activities. The rate of enzyme deactivation is proposed as the first order of enzyme concentration:

$$r_d = -\frac{dE_a}{dt} = k_d E_a \quad (2.11.1)$$

where r_d is rate of enzyme deactivation, E_a is the active enzyme concentration, and k_d is the deactivation rate constant. Integrating the above equation and carrying out separation of variables results in an expression for active enzyme concentration with respect to time:

$$\begin{aligned} -\int_{E_{a0}}^{E_a} \frac{dE_a}{E_a} &= k_d \int_0^t dt \\ E_a &= E_{a0} e^{-k_d t} \end{aligned} \quad (2.11.2)$$

where E_{a0} is the concentration of active enzyme at time zero. The concentration of active enzyme decreases with respect to time. The maximum rate is defined as V_{max} ; the value is decreasing as the activation of enzyme decreases. The half-life of the enzyme, t_h , is defined based on following expression:

$$t_h = \frac{\ln 2}{k_d} \quad (2.11.3)$$

The rate of deactivation is temperature-dependent as its dependency is described by Arrhenius' law:

$$k_d = A e^{-\frac{E_d}{RT}} \quad (2.11.4)$$

where A is the Arrhenius constant, and E_d is the activation energy for enzyme deactivation. As the temperature increases, the activity of the enzyme decreases; that is most probably due to denaturation of the enzyme at high temperature.

NOMENCLATURE

- A Arrhenius constant (min^{-1})
- E_a Active enzyme concentration (mg l^{-1})
- E_d Deactivation energy for enzyme (J mol^{-1} or cal mol^{-1})
- k_d Deactivation rate constant (min^{-1})
- K_M Michaelis–Menten constant (mol l^{-1} or g l^{-1})
- R Ideal gas constant, $1.987 \text{ cal (mol K)}^{-1}$ or $8.3144 \text{ J (mol K)}^{-1}$
- r_d Rate of enzyme deactivation (mg (l min)^{-1})
- T Absolute temperature (K)
- t_h Half-life of enzyme (min)
- V_{max} Maximum specific rate value (mol (l s)^{-1})

2.12 SOLVE PROBLEMS

1. An enzyme known as catalase is used to accelerate decomposition of hydrogen peroxide to yield oxygen and water. The concentration of hydrogen peroxide with respect to time is given as follows (Table P.1):

TABLE P.1 Concentration of H₂O₂ with respect to time

Time (min)	0	10	20	50	100
Concentration of hydrogen peroxide (mol l ⁻¹)	0.02	0.0178	0.0158	0.0106	0.005

- a. Determine the Michaelis–Menten parameters
- b. Total enzyme concentration with respect to the above case is tripled. What would be the substrate concentration after 20 min?
2. A pesticide has inhibited the activity of an enzyme *A*, which is used to react with substrate “*S*,” the rate with and without an inhibitor is given in the following table:
 - a. What are the K_M and V_{max} in the presence and absence of the inhibitor?
 - b. What kind of inhibition exists? Explain what sort of inhibitor you have selected (Table P.2).

TABLE P.2 Enzyme rate data

S (mol l ⁻¹)	v_o (mol (l min) ⁻¹), no inhibitor	v_o (mol (l min) ⁻¹), with inhibitor
3.3×10^{-4}	5.6×10^{-5}	3.7×10^{-5}
5.0×10^{-4}	7.1×10^{-5}	4.7×10^{-5}
6.7×10^{-4}	8.8×10^{-5}	6.1×10^{-5}
1.65×10^{-3}	1.29×10^{-4}	1.05×10^{-4}
2.3×10^{-3}	1.51×10^{-4}	1.2×10^{-4}
3.2×10^{-3}	1.69×10^{-4}	1.27×10^{-4}

3. The kinetics of the enzymatic reaction of disaccharides such as lactose is affected by β -galactosidase concentration. The reaction may be inhibited with high product concentration. The projected rate is:

$$\mu = \frac{\mu_m S}{K_m(1 + p/K_i) + S}$$

For easy recovery of enzyme from milk, the enzyme solution was entrapped with nitro-cellulose membrane with diameter of 30 μ m (microcapsules).

TABLE P.3 Enzyme activities

Time (min)	Enzyme activity ($\mu\text{mol (ml min)}^{-1}$)	
	Soluble enzyme	Immobilized enzyme
0	0.86	0.45
3	0.79	0.44
6	0.7	0.43
9	0.65	0.43
15	0.58	0.41
20	0.46	0.40
25	0.41	0.39
30	—	0.38
40	—	0.37

Determine the kinetic constants while inhibition is holding.

- At 350 K, the rate of an enzymatic reaction is eight times the rate of the same enzyme reaction at 270 K. Find the activation energy of the above stated enzyme reaction using Arrhenius' law. Arrhenius' law shows the temperature dependency of rate constant based on

$$k = k_0 e^{-\frac{E}{RT}}$$

where R is ideal gas constant, $8.3144 \text{ J (mol K)}^{-1}$.

- Amylase is often produced by *Endomycopsis biospora*; the enzyme is immobilized on polyacrylamide gel. Enzyme activities for soluble and immobilized enzymes are compared at 80°C . Our experimental data for the rate equation in both cases were obtained. The data are summarized in Table P.3. What is the half-life for each form of enzyme?

Hint: Please compare enzyme activities by half-life and also $E = E_0 e^{-k_d t}$.

References

- Voet D, Voet JG, Pratt CW. *Fundamentals of biochemistry: life at the molecular level*. New York: John Wiley & Sons; 2006.
- Doran PM. *Bioprocess engineering principles*. New York: Academic Press; 1995.
- Shuler ML, Kargi F. *Bioprocess engineering, basic concepts*. New Jersey: Prentice-Hall; 1992.
- Baily JE, Ollis DF. *Biochemical engineering fundamentals*. 2nd ed. New York: McGraw-Hill; 1986.

SUBCHAPTER

2.13

Case Study: Solid-State Fermentation of Sugarcane Bagasse in a Tray Bioreactor for Production of Lipase Using *Rhizopus oryzae**

2.13.1 INTRODUCTION

Lipases (glycerol ester hydrolases EC 3.1.1.3) are well-known biocatalysts participating in the hydrolysis reaction to produce fatty acids and monoacylglycerols from triacylglycerols. The reaction occurs in the water–oil interface. Numerous industrial applications of lipase such as the food industry, pharmaceuticals, cosmetics, wastewater treatment, and the leather industry have been reported in literature.^{1–5} Yield of lipase production is associated with several parameters including type of fermentation, substrate varieties, the strain of microorganism, as well as fermentation environment, i.e., the bioreactor.^{6–8}

Cellulosic and lignocellulosic agricultural wastes such as sugarcane bagasse can be used as potential substrates for lipase production.⁹ Their usage offers two advantages: first, it helps to omit or reduce environmental pollution caused by their disposal into open spaces. Second, it results in the production of value-added products (such as enzymes) from invaluable sources.

Solid-state fermentation (SSF) and submerged fermentation (SmF) are regarded as two suitable fermentation techniques for the production of enzymes, including lipases. The former is defined as the cultivation of microorganisms in the absence of free-flowing water, while in the latter, fermentation occurs in the liquid media. In the last two decades, various studies have considered lipase production in solid-state fermentation, most probably due to some superiorities of this technique compared to submerged fermentation. By using agro-industrial residues, high yields of product formation and simple technology have made SSF economically feasible.

Bacteria, fungi, and yeasts are three main microorganisms which yield lipase. However, due to low water activity in SSF, fungi and yeasts are well adapted to fermentation conditions. Thus, the studies concerning lipase synthesis in SSF are mainly focused on fungi and yeasts as potential microorganisms. Several strains of potential lipase-producing fungi, such as *Aspergillus*, *Rhizopus*, *Penicillium*, *Rhizomucor* and *Geotrichum*, are reported in the studies.¹⁰

*This case study was partially written with contributions from:

Zahra Vaseghi, Biotechnology Research Lab., School of Chemical Engineering, Noshirvani University of Technology, Babol, Iran.

In large scale, various types of bioreactors have been developed in order to perform solid-state fermentation; the most popular systems are tray, packed bed, stirred bed, rotating drum, and fluidized bed bioreactor, among which, the static tray bioreactor, also known as koji bioreactor has been successfully applied in SSF. A comprehensive control on the process parameters in bioreactors is necessary for achieving maximum product efficiency. There are some important operational variables including temperature, moisture in the incubating chamber, depth of bed, and maintenance of circulating air within the chamber. Meanwhile, the design features of the bioreactor include the dimensions of trays and chamber, the distance between trays, the presence of a cooling surface, etc. The tray bioreactor, as is apparent from its name, consists of a number of trays situated in the chamber with equal tray spacing. Depending on operational goal, different approaches can be applied in tray bioreactors: The first approach considers the whole inner space of the chamber as a single bioreactor, which requires homogeneity of fermentation materials throughout each individual tray. On the other hand, having identical operating conditions in trays is almost impossible, mainly owing to manual and technical errors. Thus, most researchers apply the second approach, which is measuring enzymatic activities of individual trays, followed by comparing and analyzing the obtained results with each other.

In this case study, a tray bioreactor with full control over temperature and humidity was fabricated for lipase production using *Rhizopus oryzae* PTCC 5176. Sugarcane bagasse, which is an abundant waste substance in the north of Iran, was employed as a substrate in the fermentation process. Operational conditions of the fabricated tray bioreactor were varied, and lipase activities were measured accordingly. Several parameters were investigated for maximizing enzyme yields in SSF, such as temperature and moisture content of the incubating chamber and the height of the solid substrate bed. Furthermore, the effect of particle size, initial moisture content, and supplementation of substrate with additional carbon and nitrogen sources were also investigated.

2.13.2 MATERIAL AND METHODS

All the materials used in this study were analytical grades except olive oil, which was food grade, and were provided from the local market. Yeast extract, peptone, di-potassium hydrogen phosphate, $\text{MgSO}_4 \cdot 7\text{H}_2\text{O}$, sodium chloride, triton X-100, and glucose were purchased from Merck (Darmstadt, Germany); while para nitrophenyl palmitate was supplied from Sigma-Aldrich. Sugarcane bagasse was prepared from a local animal food company located in Ghaemshahr, Iran.

The *Rhizopus oryzae*, PTCC 5176, employed in the present study was supplied from Iranian Research Organization for Science and Technology (IROST), Tehran, Iran. The strain was cultivated on a complex agar medium with the composition of (g l^{-1}) yeast extract (1.0), dipotassium hydrogen phosphate (1.0), $\text{MgSO}_4 \cdot 7\text{H}_2\text{O}$ (0.2), peptone (4), glucose (10.0), and agar (15.0) at 30 °C for 24 h and was maintained at 4 °C. *R. oryzae* was grown in a 1000 ml Erlenmeyer flask in a medium containing (g l^{-1}) yeast extract (1.0), dipotassium hydrogen phosphate (1.0), $\text{MgSO}_4 \cdot 7\text{H}_2\text{O}$ (0.2), peptone (4), and glucose (10.0) at pH value of 8.0 (pH meter, HANA 211, Romania) in an incubator shaker at 30 °C and 180 rpm for the incubation period of 48 h.

2.13.2.1 Bioreactor Setup

The bioreactor ($45 \times 35 \times 55$ cm), which was fabricated from Plexiglas, contained three aluminum trays in series ($35 \times 25 \times 5$ cm), two of which were perforated and filled with sugarcane bagasse as solid substrate. Meanwhile, the surfaces of these trays were covered with a linen cloth for uniform distributions of fluid heat and mass transfers. The third tray, which was located in the bottom of the chamber, was fully filled with nutrient solution. The trays were located inside the chamber with equal tray spacing (18.3 cm). A heating element was installed in the cabinet while connected to a temperature controller (SAMWON ENG, accuracy $\pm 0.2\% + 1$ digit, Korea). The nutrient solution was circulated along the bioreactor by means of an external peristaltic pump (ETATRON, Italy) and uniformly distributed on the top tray by an injection nozzle at a constant flow rate. On the other hand, the pump power supply was connected to a humidity controller (DS FOX, accuracy $\pm 2\%$, Korea) in order to maintain the required moisture content in the bioreactor. For obtaining the highest accuracy to record the bioreactor environmental conditions, the temperature and humidity controller probes were placed approximately in the middle of the bioreactor chamber. Meanwhile, for maintenance of uniform temperature, four small circulating fans (PC fan 12 V, 0.18 A, 1.68 W) were installed inside the cabin beside the top and middle trays. The main characteristic of the fabricated tray bioreactor was that all the operational variables for lipase production were fully controlled for the achievement of maximum yields of lipase and cell growth. It should be noted that all of the raw materials and media used in the fabricated bioreactor were autoclaved at 121°C for 20 min in order to prevent microbial contamination. In addition, the cabin was initially disinfected by an oxidizing chemical (bleaching agent). The schematic of the bioreactor along with all of its units is shown in [Figure 2.6](#).

2.14.2.2 Solid-State Fermentation and Sample Preparation

Paper bags that contained 5 g of dried sugarcane bagasse were placed on the top and middle trays. Fungus seed culture was cultivated in an Erlenmeyer flask for 48 h and then uniformly spread over the surface of sugarcane bagasse with the same ratio of 3:1 (i.e., the ratio of fungous suspension (v) to a solid substrate (w)). In order to provide appropriate moisture content within the bioreactor, the nutrient solution containing yeast (1 g l^{-1}) and dipotassium hydrogen phosphate (0.2 g l^{-1}) was distributed over the surface of the top tray, and then the solution penetrated through the bed, leaving from small holes in the bottom of the top tray. In the next stage, the nutrient solution may reach the solid samples of the middle tray until it poured into its original source of media, the bottom tray. This liquid cycle continued until the humidity controller reached the set point. In fact, two distinct purposes were followed by the above action: First, the presence of liquid kept the inner environment of the bioreactor always humid. Second, the media provided the required substances other than the solid substances that existed in the sugarcane bagasse. These actions may assist the microorganism to grow in a more accelerated manner. Moreover, it was assumed that the humidity of fermented solids on the bed was equal to the overall humidity within the bioreactor during the fermentation process. The experiments were conducted in an incubation period of five days from the bioreactor startup. The activity of the crude enzyme

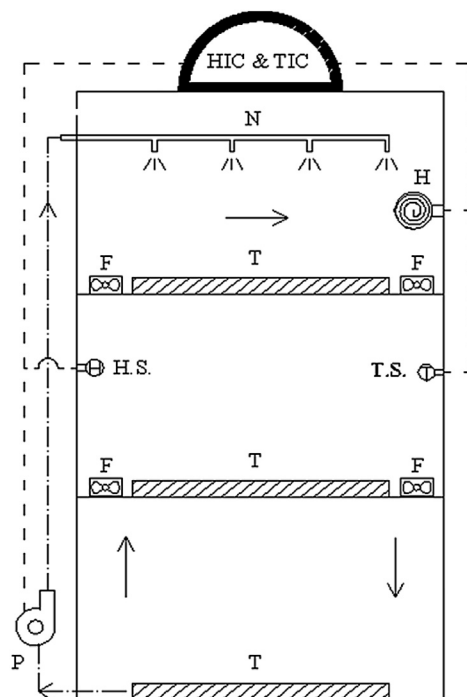


FIGURE. 2.6 Schematic diagram of the tray bioreactor setup. H, heater; T, tray; F, fan; P, pump; N, nozzle; T.S., temperature sensor; H.S., humidity sensor; T.I.C., temperature indicator and controller; H.I.C., humidity indicator and controller.

obtained was analyzed and reported based on the colorimetric method using *p*-nitrophenyl palmitate as substrate.

Samples were taken every 24 h for evaluation of lipase activity. In order to have representative samples, paper bags containing inoculated substrates were placed at the same locations on the trays in all of the experimental runs. The extraction of the enzyme from the fermented solid residues required transferring the solid sample into liquid media, which was followed by the use of NaCl (1%), triton X-100 (1%) solution in a 100 ml Erlenmeyer flask. The suspension was kept in a rotary shaker for 2 h at 30 °C and 180 rpm. Solid substrate was then filtered with Whatman filter paper (No. 41; diameter of 125 mm) and was separated from the enzymatic suspension by means of a vacuum pump (PLATINUM, USA). Since there was no solid phase in the bottom tray, the extraction of the enzyme from this tray did not require the previous step, and the enzymatic solution was used for direct measurement of enzyme activity.

2.13.3 RESULTS AND DISCUSSION

The effect of various fermentation times (24, 48, 72, 96, and 120 h) on production of lipase was studied. Experiments were conducted at several fermentation temperatures (25, 35, and

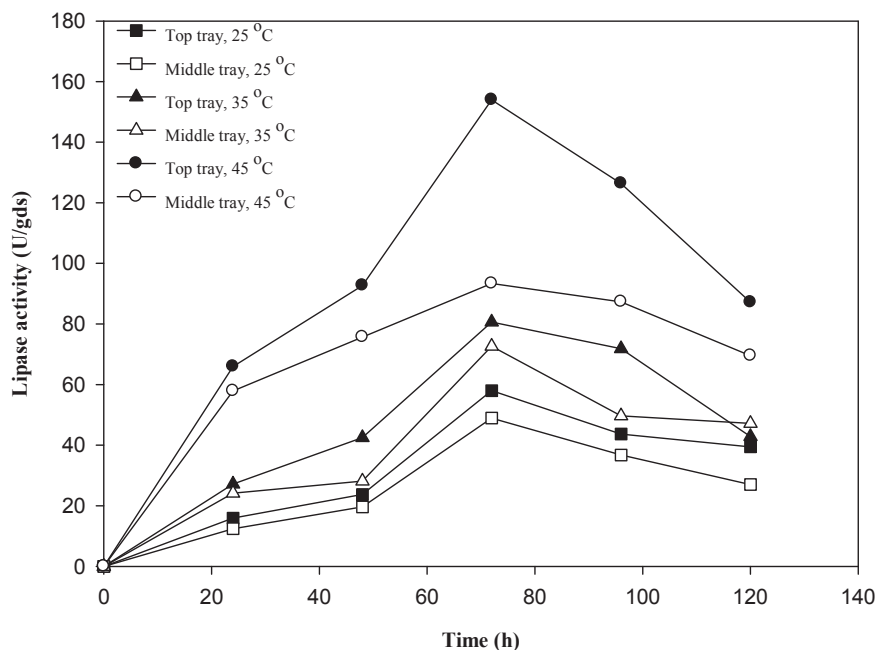


FIGURE. 2.7 Time course of lipase production by *Rhizopus oryzae* at 25, 35, and 45 °C.

45 °C). As is apparent from Figure 2.7, maximum yields of lipases were obtained after 72 h of fermentation. When the fermentation period exceeded 72 h, a gradual decrease in lipase activity was observed that was mainly due to reduced penetration rate of nutrients and diffusion of air through the solid bed of biomass. The results also demonstrated that as the incubation temperature shifted from 25 to 45 °C, lipase activity appreciably increased as a result of temperature dependency of microorganism growth and the related extracellular cell products. Maximum lipase activities achieved for the three tested thermal points 25, 35, and 45 °C were 58.23, 82.94, and 157.67 U per gds, respectively. Since the lipases produced in the tray located at the bottom of the bioreactor did not show significant changes in enzyme activities as compared to those produced in the top and middle trays, they was not depicted in the figure.

The effect of temperature on lipase production was also investigated. The temperature of the incubating chamber was adjusted at the values ranging from 25 to 50 °C with an increment of 5 °C. Lipase activity was assayed under several incubating temperatures after a 72-hour incubation. Interestingly, enzyme activity peaked at 45 °C (153.97 U gds⁻¹). This temperature was high enough to increase lipase extraction efficiency without causing the enzyme to be denatured. Another important parameter that must be taken into consideration in the analysis of enzyme activities is the estimation of total protein. Since enzymes are proteins, measurement of total protein leads to determining the order of enzyme activities among sample enzymatic solutions. In this way, the obtained results of enzyme activities are known to be more reliable. Furthermore, from a comparative point of view between the two trays, a

TABLE 2.2 Effect of cabin temperature on activity and total protein of lipase produced by *Rhizopus oryzae*

Temperature (°C)	Lipase activity (U gds ⁻¹)		Total protein (mg g ⁻¹)	
	Top tray	Middle tray	Top tray	Middle tray
25	33.17	28.07	0.43	0.29
30	52.48	43.37	0.54	0.43
35	62.17	48.78	0.99	0.88
40	122.67	70.07	1.19	1.09
45	153.97	123.37	2.17	1.89
50	105.47	62.57	0.99	0.58

higher protein content and lipase activity was achieved in the top tray with *Rhizopus oryzae*; that was probably due to a suitable supply of nutrients and oxygen transfer to the bed of the top tray (Table 2.2).

Humidity of the cabin was adjusted on the values ranging from 70 to 90% with an increment of 5% by means of a humidity controller, and its effect on lipase activity was investigated. Meanwhile, the temperature of the cabin was set at 35 °C. For the incubation period of 72 h, maximum values for lipase activity and total protein were achieved at 80% humidity (Table 2.3). As it was previously stated, the humidity of the bioreactor was provided by circulation of the nutrient solution in the bottom tray by means of an external pump. Provision of higher amounts of humidity required more circulation of nutrient solution in the chamber which subsequently led to domination of liquid media followed by formation of semi-solid media in the trays. However, the productivity of lipase in solid media (solid-state fermentation) is much higher than liquid media (submerged fermentation).

In tray bioreactors, depth of the solid bed influences the productivity extensively. This issue is of great importance when transport phenomena such as nutrient, oxygen, and heat

TABLE 2.3 Effect of cabin humidity on activity and total protein of lipase produced by *Rhizopus oryzae*

Humidity (%)	Lipase activity (U gds ⁻¹)		Total protein (mg g ⁻¹)	
	Top tray	Middle tray	Top tray	Middle tray
70	77.97	74.03	1.16	0.91
75	86.77	76.57	1.58	1.20
80	99.77	92.87	1.89	1.71
85	61.32	59.68	1.57	1.48
90	57.18	56.08	0.76	0.62

TABLE 2.4 Effect of bed depth on activity and total protein of lipase produced by *Rhizopus oryzae*

Bed depth (cm)	Lipase activity (U gds ⁻¹)		Total protein (mg g ⁻¹)	
	Top tray	Middle tray	Top tray	Middle tray
0.5	116.76	109.38	2.08	1.99
1.0	105.56	95.36	1.65	1.62
1.5	97.98	94.17	1.53	1.50
2.0	96.97	88.38	1.46	1.37
2.5	96.77	82.77	1.41	1.02
3.0	96.35	81.37	1.31	0.94

transfer within the solid bed are considered. In the present case study, this parameter was studied by making paper bags of different dimensions. The height of bagasse in paper bags was varied between 0.5 and 3.0 cm, and the corresponding lipase activities and total proteins were evaluated after 72 h of fermentation at 35 °C. As is obvious in Table 2.4, the produced lipase had the most activity at 0.5 cm bed depth. When the height of the bed increased, the metabolic heat produced during fermentation, accumulated over the bed surface. As the generated heat was beyond the fans' power to be uniformly distributed through the chamber, a temperature gradient was formed over the bed. In lower bed heights, a wet, linen cloth was extended on the trays to help tackle this problem. However, it caused an indirect contact between the trays and solid particles of sugarcane bagasse that subsequently prevented pore blockage. In addition, by increasing the depth of the bed, the mycelium created during the fermentation period accumulated over the tray, and bed caking occurred. This was mainly problematic in providing appropriate air circulation in the chamber. As a result, microbial growth was only observed in a thin layer of bagasse that was in near contact with the fungus solution. Mixing the substrate with the fungus solution prior to fermentation onset is a helpful tool for solving this problem. However, it should be noted that inappropriate mixing may cause shear damage to the fungus structure.

The effect of initial moisture content of the solid substrate on the activities of the produced lipases was also studied. Initial moisture of the substrate is defined as the ratio of liquid media (fungus solution) to dried solid media (sugarcane bagasse). In the present case study, initial humidities of 30 to 90% were considered for the samples. It was found that an initial moisture content of 80 and 70% were optimum for the top and middle trays, respectively. The amount of aqueous solution required for providing initial moisture content depends strongly on the type of applied substrate. In this research, increasing initial moisture content from 30 to 80% in the top tray and from 30 to 70% in the middle tray resulted in an enhancement in water activities, which increased the availability of nutrients to the substrate for better bioprocess development and enzyme yields. However, further increase in this parameter resulted in compaction of bagasse and thus reduced the activity of the obtained enzyme. The obtained results concerning initial humidity are summarized in Table 2.5.

TABLE 2.5 Effect of initial moisture of substrate on activity and total protein of lipase produced by *Rhizopus oryzae*

Initial humidity (%)	Lipase activity (U gds ⁻¹)		Total protein (mg g ⁻¹)	
	Top tray	Middle tray	Top tray	Middle tray
30	75.57	73.84	0.86	0.79
40	80.07	78.59	0.97	0.89
50	86.77	83.53	1.33	1.24
60	91.97	90.49	1.35	1.23
70	105.36	99.35	1.69	1.65
80	121.06	90.66	2.12	1.11
90	102.47	85.49	1.40	0.98

TABLE 2.6 Effect of particle size of substrate on activity and total protein of lipase produced by *Rhizopus oryzae*

Particle size (mm)	Lipase activity (U gds ⁻¹)		Total protein (mg g ⁻¹)	
	Top tray	Middle tray	Top tray	Middle tray
Less than 0.18	71.17	62.17	1.22	0.99
0.18–0.335	89.17	82.77	1.93	1.55
0.335–1	99.95	99.93	2.07	1.70
1–2	89.77	86.92	1.27	1.12
Mixture of all sizes	85.98	80.92	1.66	1.53

To investigate the effect of a substrate's particle size, five samples of sugarcane bagasse with particle sizes in the range of 1–2, 0.335–1, 0.18–0.335, less than 0.18 mm in size, and a sample comprised of a mixture of all these particle sizes were tested for lipase activity and total protein measurements. The highest lipolytic activity was observed in the second group (0.335–1 mm). When particle size exceeded this range, lipase activity decreased considerably due to reduced contact surface between substrate particles and fungus solution, which prevented microbial growth. On the other hand, providing suitable aeration is another important term affecting respiration quotient and, thus, influencing microbial growth. That is why considerable activities were not observed for particle sizes less than 0.18 mm. Moreover, as it was expected, lipase activity obtained from using the mixture of all sizes was approximately the average of the four identified sizes. Furthermore, the results obtained from total protein analysis confirmed the correctness of the obtained results concerning lipolytic activities (Table 2.6).

Supplementation of the substrate with carbon and nitrogen sources is another important factor that significantly affected lipase production. In order to enhance lipolytic enzyme production, olive oil and urea were used as the pure carbon and nitrogen sources. In the case of the carbon source, the concentration of oil was varied, and lipase production was monitored after a 72-hour incubation period. Maximum activities of lipase were achieved when sugarcane bagasse was supplemented with 8% (v/w) olive oil, while other parameters remained at the desired or optimum conditions. Activity of the enzymes located at the top and middle trays in this case was found to be 215.16, 199.36 U gds⁻¹. Furthermore, lipolytic activity obtained using urea (2% w/w) as the supplementary nitrogen source was 253.55 and 205.16 U gds⁻¹ for the top and middle trays. As is apparent from the obtained results, nitrogen source plays a more important role in enhancing lipolytic activities than a carbon source such as olive oil. This may be due to the fact that bagasse is rich in carbon sources on its own. Thus, its supplementation with nitrogen sources is a greater help for increasing the activity of the produced enzyme under solid-state fermentation.

References

1. Damaso MCT, Passianoto MA, Freitas SC, Freire DMG, Lago RCA, Couri S. Utilization of agroindustrial residues for lipase production by solid-state fermentation. *Braz J Microbiol* 2008;**39**:676–81.
2. Vaseghi Z, Najafpour GD, Mohseni S, Mahjoub S, Hosseinpour MN. Lipase production in tray bioreactor via solid state fermentation under desired growth conditions. *Iranica J Energy Environ* 2012;**3**:76–82.
3. Singhara RR, Patel AK, Soccol CR, Pandey A. Recent advances in solid-state fermentation. *Biochem Eng J* 2009;**44**:13–8.
4. Rigo E, Ninow JL, Di Luccio M, Oliveira JV, Polloni AE, Remonato D, et al. Lipase production by solid fermentation of soybean meal with different supplements. *LWT Food Sci Technol* 2010;**43**:1132–7.
5. Adinarayana K, Raju K, Zargar MI, Devi RB, Lakshmi PJ, Ellaiah P. Optimization of process parameters for production of lipase in solid-state fermentation by newly isolated *Aspergillus* species. *Indian J Biotechnol* 2004;**3**:65–9.
6. Colen G, Junqueira RG, Moraes-Santos T. Isolation and screening of alkaline lipase-producing fungi from Brazilian savanna soil. *J Microbiol Biotechnol* 2006;**22**:881–5.
7. Hosseinpour MN, Najafpour GD, Younesi H, Khorrami M, Vaseghi Z. Lipase production in solid state fermentation using *Aspergillus niger*: response surface methodology. *Int J Eng* 2012;**25**:151–9.
8. Ali HKQ, Zulkali M. Design aspects of bioreactors for solid-state fermentation: a review. *Chem Biochem. Eng Q* 2011;**25**:255–66.
9. Rodriguez Couto S, Sanroman MA. Application of solid-state fermentation to ligninolytic enzyme production. *Biochem. Eng J* 2005;**22**:211–9.
10. Guatarra MLE, Godoy MG, Castilho LR, Freire DMG. Inoculum strategies for *Penicillin simplicissimum* lipase production by solid state fermentation using a residue from the babassu oil industry. *J Chem Technol Biotechnol* 2007;**82**:313–8.

Gas and Liquid System (Aeration and Agitation)*

OUTLINE

3.1 Introduction	53	3.11 Mass Transfer Limited Process	63
3.2 Aeration and Agitation	53	3.11.1 Oxygen Transport	67
3.2.1 Measurement of DO Concentration	54	3.11.2 Diameter of Gas Bubble Formed D_o	68
3.2.2 Oxygen Transfer Rate	54	Nomenclature	74
3.2.3 Respiration Quotient	55	Greek Symbols	75
3.2.4 Agitation Rate Studies	56	References	75
3.3 Air Sparger	56	3.13 Case Study: Oxygen Transfer Rate Model in an Aerated Tank for Pharmaceutical Wastewater	76
3.4 Agitation and Mixing Phenomena	57	3.13.1 Introduction	76
3.5 Types of Agitator	57	3.13.2 Material and Method	78
3.6 OTR in a Fermenter	58	3.13.3 Results and Discussion	79
3.7 Mass Transfer in a Gas–Liquid System	59	3.13.4 Conclusion	81
3.8 Gas Hold-Up	60	Nomenclature	82
3.9 Mass Transfer Coefficients for Stirred Tanks	61	References	82
3.10 Agitated System and Mixing Phenomena	63		

*This case study was partially written with contributions from:
Maedeh Mohammadi, Faculty of Chemical Engineering, Noushervani University of Technology, Babol, Iran.

3.14 Case Study: Fuel and Chemical Production from the Water–Gas Shift Reaction by Fermentation Processes	83	3.14.4 Mass Transfer Phenomena	91
3.14.1 Introduction	83	3.13.5 Kinetic of Water Gas Shift Reaction	93
3.14.2 Kinetics of Growth in a Batch Bioreactor	84	3.14.6 Growth Kinetics of CO Substrate on <i>C. ljungdahlii</i>	96
3.14.3 Effect of Substrate Concentration on Microbial Growth	88	Nomenclature	98
		Acknowledgments	99
		References	99

SUBCHAPTER

3.1

Introduction

In the biochemical engineering profession, there are various bioprocesses actively involved in the synthesis and production of biological products. Understanding all the processes may require basic knowledge of biology, biochemistry, biotechnology, and real knowledge of engineering processes. Transfer of oxygen is a major concern in many bioprocesses in which air is required for microbial growth, such as production of single-cell protein and antibiotics. Agitation in a fermentation unit is directly related to oxygen transported from the gas phase to the liquid phase followed by oxygen uptake by the individual microbial cell. The activities of microorganisms are monitored by the use of oxygen from the supplied air and the respiration quotient (RQ). In this chapter, mechanisms of oxygen transport are discussed. The details of process operation are also discussed in this chapter.

3.2 AERATION AND AGITATION

Aeration and agitation as the most vital parameters are implemented in most fermentation processes. The word “aerobe” refers to the kind of microorganism that needs molecular oxygen for growth and metabolism. “Aerobic” is the condition of living organisms that survive only in the presence of molecular oxygen. Aerobic bacteria require oxygen for growth and can be incubated to be grown in atmospheric air. Oxygen is a strong oxidizing agent that has the ability to accept electrons for yielding energy, a process known as respiration.

A bioreactor is a reaction vessel in which an organism is cultivated in a controlled manner to produce cell bodies and/or product. Initially the term “fermenter” was used to describe these vessels, but in strict terms, fermentation is an anaerobic process, whereas most fermenters use aerobic processes. Thus, in general terms, “bioreactor” means a vessel in which organisms are grown under either aerobic or anaerobic conditions. In this book, the term “bioreactor” will be used because of its global applications. If a bioreactor or a reaction vessel operates under aerating conditions, the system is called an aerobic bioreactor. In this situation, sterile air is supplied to the bioreactor as a source of intake for respiration of microorganisms. The supplied oxygen is dissolved in the liquid phase. The microorganisms consume the oxygen that is dissolved in the liquid media for respiration and growth. The growth of aerobic bacteria in the fermenter is controlled by the availability of substrate, oxygen, energy sources, and enzymes. Microbial cultures are always known as heterogeneous systems, because cells are solid and nutrients are in the liquid phase. The supplied

oxygen from the gas phase has to penetrate into the microorganism. The rate of oxygen transfer from the gas phase to the liquid phase is important. Several steps are required to let such a phenomenon take place. The oxygen must first travel through the gas–liquid interface, then the bulk of liquid, and finally into the microbial cell.¹

In aerobic processes, air has to be supplied to enhance cell growth, otherwise the limited dissolved oxygen (DO) is used up, and then oxygen limitation may cause a decrease in the cell growth rate. Also, at conditions with high cell densities, the cell growth is limited by the availability of oxygen in the medium, and any failure in providing the required oxygen may retard the cell growth. Thus, the availability of oxygen is a major parameter that needs to be considered for effective microbial cell growth. Microbial activity of aerobic organisms is monitored by the oxygen uptake rate (OUR) from the supplied air or oxygen. The aerobic activity of microbial cultures depends on the local bulk oxygen concentration, the oxygen diffusion coefficient, and the respiration rate of microbes in the aerobic region.

3.2.1 Measurement of DO Concentration

In biochemical engineering processes, measurement of DO is essential. Variation of DO may affect retention time and other process variables such as substrate and product concentrations, retention time, dilution rate, and aeration rate. The availability of oxygen is a major parameter to be considered for effective microbial cell growth rate.

For indicating the availability of oxygen in the liquid phase, the amount of DO should be measured. The concentration of DO in a fermenter is normally measured using a DO electrode, known as DO probe. DO probes are available on the market, and most fermenters are equipped with a DO meter. For aerobic fermentation, the bioreactor must be equipped with a DO meter. There are two types in common use, galvanic electrodes and polarographic electrodes. In both probes, there are membranes that are permeable to oxygen. Oxygen diffuses through the membrane and reaches the cathode, where it reacts to produce a current between anode and cathode proportional to the oxygen partial pressure in the fermentation broth. The electrolyte solutions in the electrode take part in the reactions, and thus the electrode must be located in the bulk of liquid medium.

The concentration of DO in the media is a function of temperature. The higher operating temperature would decrease the level of DO. The solubility of air in water at 10 °C and under atmospheric conditions is 11.5 ppm; as the temperature is increased to 30 °C, the solubility of air drops to 8 ppm. The solubility of air decreases to 7 ppm at 40 °C. Availability of oxygen in the fermentation broth is higher than air, if pure oxygen is used. The solubility of pure oxygen in water at 10 °C and 1 atm pressure is 55 ppm. As the temperature increases to 30 °C, the solubility of pure oxygen drops to 38.5 ppm. The solubility of pure oxygen decreases to 33.7 ppm at 40 °C. Therefore, pure oxygen is commonly used to enhance oxygen availability in the fermentation media.

3.2.2 Oxygen Transfer Rate

Once batch mode studies are completed and the required data are collected, without dismantling the bioreactor, liquid media is prepared with 33 g KH_2PO_4 and 3 g Na_2HPO_4 ,

10 g yeast extract, and 500 g glucose in 10 L of distilled water. The liquid media can be sterilized in an autoclave at 121 °C, 15 psig for 20 min. The liquid media is cooled down to room temperature with an air flow rate of 100 mL min⁻¹. The fluid residence time of 10 h is expected to give maximum cell optical density. Otherwise, the effect of media flow rate has to be carried out separately. This is the basic assumption made in this experiment. The aim of this set of experiments is to determine a suitable air flow rate with variation from 0.025 to 1 vvm. Table 3.1 shows the data collected in a continuous mode of operation for 3.5 days using isolated strains from the waste stream of a food processing plant. The time intervals for sampling are 12 h. The steady-state condition of the system may be reached at about 10 h. If any samples are taken at shorter time intervals, the steady-state condition would not be reached, and then overlapping in the experimental condition may occur.

3.2.3 Respiration Quotient

Measurements of inlet and outlet gas compositions of a culture vessel have been considered as an indicator for cell activities in the fermentation broth. The continuous monitoring of gas analysis would lead us to understand the oxygen consumption rate and carbon dioxide production, which originate from catabolism of carbon sources. Respiration is a sequence of biochemical reactions resulting in electrons from substances that are then transferred to an exogenous electron-accepting terminal. Respiration in a cell is an energy-delivery process in which electrons are generated from oxidation of substrate and transferred through a series of oxidation–reduction reactions to electron acceptor terminals. In biosynthesis, the end products result from a respiration process. Since oxidation of carbonaceous substrate ends with carbon dioxide and water molecules, the molar ratio of carbon dioxide generated from oxidation–reduction to oxygen supplied is known as the RQ:

$$RQ = \frac{dC_{CO_2}/dt}{dC_{O_2}/dt} = \frac{dC_{CO_2}}{dC_{O_2}} \quad (3.2.1)$$

TABLE 3.1 Effect of aeration rate on Baker's yeast production

Air flow rate, mL min ⁻¹	DO, mg L ⁻¹	Optical density, absorbance, λ520 nm	Cell dry weight, mg mL ⁻¹	Protein concentration, mg L ⁻¹	Sugar concentration, g L ⁻¹
50	2	0.20	0.26	1300	16.8
100	4	0.45	0.59	1450	14.5
200	6	0.69	1.24	2500	13.9
500	7.7	1/10 diluted 0.72	3.95	3000	12.5
1000	8	1/10 diluted 0.74	4.63	3100	9.8
1500	8	1/10 diluted 0.77	4.68	3350	8.6
2000	8	1/10 diluted 0.79	4.75	4800	6.7

There are several methods to monitor the off-gas analysis. Online gas chromatography is commonly used. The daily operation for inlet and outlet gases is balanced to project growth in the bioprocess. High operating cost is the disadvantage of the online system. For an online bioreactor, a few important process variables should be monitored continuously. The off-gas analysis provides the most reliable information for growth activities. Measurement of oxygen and carbon dioxide in the off-gas is a fairly standard procedure used for a pilot-scale bioreactor. Knowing air flow rate and exit gas compositions or having a simple material balance can quantify OUR and carbon dioxide production rate, which would lead us to a value for the RQ. The three indicators for growth can be correlated and give cell growth rate. From RQ, the metabolic activity of the bioprocess and the success of a healthy operation can be predicted. The off-gas analysis will show the specific CO₂ production rate, which is used to calculate oxygen consumption rate.

3.2.4 Agitation Rate Studies

In the following experiment, we shall assume that the optimum air flow rate of 0.5 vvm is desired. This means for an aeration vessel with a 2 L working volume, the experiment requires 1000 ml air per minute. The rest of process parameters and media conditions remain unchanged. Another 10 L of fresh aseptic media must be prepared. The operation is continued for 3.5 days at an agitation speed from 100 to 700 rpm; samples are drawn at intervals of 12 h Table 3.2 shows the effect of agitation rate on cell dry weight and protein production using a starchy wastewater stream. The active strain was isolated from a food-processing plant.

3.3 AIR SPARGER

Aerobic bacteria are easily grown at small scale in tubes and flasks by incubating the media under normal atmospheric conditions. However, in large-scale operations, the media has to be exposed to air, and sufficient air must be present for respiration of the living cells. In such case, an air sparger is required to purge compressed air or pressurized air to be bubbled into the media. Air under pressure is supplied through a tube with an end

TABLE 3.2 Effect of agitation rate on Baker's yeast production

Agitation rate, rpm	DO, mg L ⁻¹	Optical density, absorbance, λ520 nm	Cell dry weight, mg mL ⁻¹	Protein concentration, mg L ⁻¹	Sugar concentration, g L ⁻¹
100	2	1/10 diluted 0.22	0.29	1250	15.5
200	3	1/10 diluted 0.36	0.46	1360	14.7
300	5	1/10 diluted 0.45	0.59	1450	13.6
400	6	1/10 diluted 0.65	0.85	1850	12.1
500	8	1/10 diluted 0.79	1.12	2150	11.5
600	8	1/10 diluted 0.82	1.16	2250	10.8
700	8	1/10 diluted 0.83	1.19	2300	8.4

consisting of a perforated plate or “O” ring with very fine holes or orifices. The size of bubbles depends on the size of hole and type of sparger. For very fine bubbles with effective gas dispersion, a microsparger is used in the fermenter. A microsparger is, in fact, a highly porous material and is used instead of a gas sparger. The size of bubbles affects the mass transfer process. Smaller bubble size provides more surface area for gas exposure, so a better oxygen transfer rate (OTR) is obtained. The size of gas bubbles and their dispersion throughout the reactor vessel are critical for bioreactor performance. Although a sparging unit will provide small size bubble and good gas distribution with sufficient agitation, microspargers are often used because the porous media provides an extensive number of fine and uniform bubbles. They are also resistant to plugging of biomass on the outer surface of the sparger.

3.4 AGITATION AND MIXING PHENOMENA

Mixing is a physical operation that creates uniformities in fluids and eliminates any concentration and temperature gradients. If a system is perfectly mixed, there is homogeneous distribution of system properties. Mixing is one of the most important operations in bioprocessing. Efficient liquid mixing is essential in a bioreactor to maintain not only a uniform DO concentration, but also a uniform liquid concentration. To create an optimum environment in the bioreactor, agitation is required for cells to have access to all substrates, including oxygen in aerobic cultures. Another aspect of an agitated system is uniform heat transfer. Most bioreactors must be able to operate at a constant uniform temperature. A jacketed system for cooling, or a cooling coil, is provided for sufficient heat transfer. The objectives of agitation and effective mixing are to circulate the fluid for sufficient time, to disperse the gas bubbles in the liquid, to have small bubbles with high interfacial area, and to maintain uniform conditions for mass and heat transfer operations.

Agitation creates uniformity of gas bubbles in the entire media by placing the agitator in the appropriate position. A few sets of impellers are used to ensure the even distribution of the gas in the fermentation broth. Very high agitation may cause high shear forces that may damage the cell wall and cause cell rupture. If the propagating cells, such as animal cells and plant tissue cultures, are shear-sensitive, special configurations of impellers are required. A wide variety of impellers are available; other shapes of impellers related to mixing and agitation of bioreactors are discussed in the literature.²

3.5 TYPES OF AGITATOR

Gas dispersion is not mainly related to the sparger, but rather is dependent on the type of impeller used for agitation. There are four types of agitator commonly used in bioreactors:

- Disk turbine (Rushton turbine)
- Inclined blade turbine

- Propeller, marine type
- Intermig.

These types of agitators are used in low-viscosity systems ($\mu < 50 \text{ kg m}^{-1} \text{ s}^{-1}$) with high rotational speed. The typical tip speed velocity for turbine and intermig is in the region of 3 m s^{-1} , a propeller rotates faster. These impellers are classified as remote clearance type, having diameters in the range of 25–67% of the tank diameter.

The most common type of agitator is disk turbine. It consists of several short blades mounted on a central shaft. The diameter of a turbine is normally 35–45% of the tank diameter. There are four to six blades for perfect mixing. Turbines with flat blades give radial flow. This is good for gas dispersion in the media where the gas is introduced just below the impeller; it is drawn up to the blades and broken up into uniform fine bubbles.

The propeller agitator with three blades rotates at relatively high speeds of 60–300 rpm; high efficient mixing is obtained. The generated flow pattern is axial flow since the fluid moves axially down to the center and up the side of the tank.

The intermig agitator is the most recently developed agitator. This is an axial pumping impeller in which the blades are mounted at an angle opposite each other. Comparing the mixing properties of disk turbine agitator with an intermig agitator, the intermig agitator has more uniform energy transferred to the fluid in the vessel. Therefore, this type of agitator requires less power and less air input to obtain the same degree of mixing and mass transfer coefficient.

3.6 OTR IN A FERMENTER

The molar flux of oxygen is generalized in a simple equation, with the concentration gradient as the major driving force in the transfer of oxygen from gas and liquid interface to the bulk of liquid. The rate of oxygen transfer in a fermenter broth is influenced by several physical and chemical parameters that change either k_L , the value of interfacial area of bubbles (a), or the concentration gradient known as the driving force for the mass transfer. At low concentrations of the soluble gas, the molar flux of oxygen transported to the fermentation media is³:

$$N_A = k_L a (C_{AL}^* - C_{AL}) \quad (3.6.1)$$

where N_A is the oxygen flux in $\text{kmol m}^{-2} \text{ s}^{-1}$, k_L is the liquid side mass transfer coefficient in $\text{m}^2 \text{ s}^{-1}$, C_{AL}^* is the oxygen concentration in equilibrium with the liquid phase at the interface in kmol m^{-3} , C_{AL} is the oxygen concentration in the bulk of liquid in kmol m^{-3} , and a is the interfacial area in surface area of bubbles per unit volume of broth ($\text{m}^2 \text{ m}^{-3}$). The DO can be measured at one or several points in the vessel, depending on vessel size, using a DO probe. In the large bioreactor, the partial pressure of oxygen in the gas will fall as it passes through the fermentation broth.

$$P_{\log \text{ mean}} = \frac{P_{in} - P_{out}}{\ln(P_{in}/P_{out})} \quad (3.6.2)$$

The equilibrium concentration is evaluated from Henry's law.^{3,4} The equilibrium concentration of oxygen is calculated by the ratio of mean value of pressure over Henry's law constant, H .

$$C^* = \frac{P_{\log \text{ mean}}}{H} \quad (3.6.3)$$

This is the most accurate method of measuring the mass transfer coefficient, and it can be used in the actual fermentation system. It depends on accurate oxygen analyses and accurate measurement of temperature and pressure. For bubble sizes of 2–3 mm diameter in the fermentation broth, the mass transfer coefficient is about 3×10^{-4} to $4 \times 10^{-4} \text{ m s}^{-1}$.

3.7 MASS TRANSFER IN A GAS–LIQUID SYSTEM

The molar flux of oxygen is generalized in a simple equation, with the concentration gradient as the major driving force in the transfer of oxygen from gas and liquid interface to the bulk of liquid. Oxygen transfer at low concentrations is proportional to the oxygen concentration gradient existing on the interface of the gas and liquid bulk phases. The molar flux of oxygen from the gas phase to the liquid phase is stated as:

$$J_{\text{O}_2} = k_g(P_{\text{O}_2} - P_{\text{O}_2,i}) \quad (3.7.1)$$

where J_{O_2} is the molar flux of oxygen in ($\text{mol m}^{-2} \text{ s}^{-1}$), k_g is the mass transfer coefficient in the gas side in ($\text{mol m}^{-2} \text{ atm}^{-1} \text{ s}^{-1}$), P_{O_2} is the oxygen partial pressure in the bulk of gas phase in (atm), and $P_{\text{O}_2,i}$ is the oxygen partial pressure at the interface in (atm). The molar flux of oxygen from the gas–liquid interface to the bulk of liquid is expressed as:

$$J_{\text{O}_2} = k_l(C_i - C_l) \quad (3.7.2)$$

where N_A is oxygen flux in $\text{kmol m}^{-2} \text{ s}^{-1}$, k_L is the mass transfer coefficient in liquid side in (m s^{-1}), C_i is oxygen concentration at the interface in (mol m^{-3}), and C_L is oxygen concentration in the bulk of liquid in (mol m^{-3}). Based on film theory and considering the steady-state condition, the oxygen flux in the gas film is equal to the flux in the liquid film:

$$J_{\text{O}_2} = k_g(P_{\text{O}_2} - P_{\text{O}_2,i}) = k_l(C_i - C_l) \quad (3.7.3)$$

Since it is impossible to measure the interface concentration by knowing the molar flux and mass transfer coefficient, the bulk driving force and equilibrium concentrations should be considered:

$$J_{\text{O}_2} = K_g(P_{\text{O}_2} - P^*) = K_l(C^* - C_l) \quad (3.7.4)$$

where K_g and K_l are the overall mass transfer coefficients in the gas and liquid phase, respectively, P^* is the partial pressure of oxygen in equilibrium with liquid phase, and C^* is the saturation concentration of oxygen in liquid bulk in equilibrium with gas phase. The equilibrium partial pressure of oxygen can be related to the equilibrium concentration of the gas in the liquid using Henry's law as follows:

$$P^* = HC^* \quad (3.7.5)$$

where H is the Henry's constant in ($\text{atm m}^3 \text{mol}^{-1}$). Combing Eqns (3.7.3) and (3.7.4) and considering the Henry's law, the resistances in series are written as:

$$\frac{1}{K_L} = \frac{1}{k_l} + \frac{1}{Hk_g} \quad (3.7.6)$$

For slightly soluble gases, H is defined as a large value ($769.23 \text{ L atm mol}^{-1}$). In such case, the resistance to mass transfer lies on the liquid film side, and the gas phase resistance can be neglected. Thus, the overall mass transfer coefficient for sparingly soluble gases equals to the local mass transfer coefficient: $K_L = k_L$. Thus, the molar flux of oxygen from the gas phase to liquid phase can be expressed as:

$$J_{\text{O}_2} = k_l(C^* - C_l) \quad (3.7.7)$$

The molar flux of oxygen in the gas phase to liquid phase is also stated as:

$$N_a = k_g(P_{\text{O}_2} - P_{\text{O}_{2,i}}) \quad (3.7.8)$$

where k_g is the mass transfer coefficient at the gas side in $\text{kmol m}^{-2} \text{atm}^{-1} \text{s}^{-1}$, P_{O_2} is the oxygen partial pressure at the bulk of gas phase in atmospheres, and $P_{\text{O}_{2,i}}$ oxygen partial pressure at interface. It is impossible to measure the interface concentration by the molar flux without knowing the mass transfer coefficient.

$$N_A = K_L(C^* - C_L) \quad (3.7.9)$$

where K_L is the overall mass transfer coefficient, then, Henry's law is

$$P = HC^* \quad (3.7.10)$$

$$\frac{1}{K_L} = \frac{1}{k_L} + \frac{1}{Hk_g} \quad (3.7.11)$$

For the OTR, the interface area is important. For oxygen bubbles, the surface area of bubbles is defined as:

$$a = \frac{\text{Surface area}}{\text{Volume}} = \frac{\text{m}^2}{\text{m}^3} \quad (3.7.12)$$

By multiplying both sides of Eqns (3.7.9) with (3.7.12), the following equation results:

$$-r_A = K_L a (C^* - C_L) \quad (3.7.12)$$

where, $-r_A$ is the consumption rate of substrate A in $\text{mol L}^{-1} \text{s}^{-1}$.

3.8 GAS HOLD-UP

The fraction of the fluid volume occupied by gas is called gas hold-up: that is, the volume fraction of gas phase to total gas-liquid volume. Small bubbles lead to higher gas hold-up, which is defined by the following equation^{4,5}:

$$\varepsilon = \frac{V_g}{V_l + V_g} \quad (3.8.1)$$

where ε is the gas hold-up, V_g is the volume of gas bubbles in the reactor in (m^3), and V_l is the volume of liquid in the fermenter in (m^3). The interfacial surface area of bubbles, assuming spherical bubbles, can be calculated as:

$$a = \frac{6\varepsilon}{d_b} \quad (3.8.2)$$

where d_b is the average bubble diameter in (m).

3.9 MASS TRANSFER COEFFICIENTS FOR STIRRED TANKS

Agitation of fermentation broth creates a uniform distribution of air in the media. Once a solution is mixed, some energy is exerted into the system. Increasing the input power reduces the bubble size, and this in turn increases the interfacial area. Therefore, the mass transfer coefficient would be a function of power input per unit volume of fermentation broth, which is also affected by the gas superficial velocity.^{2,3} The general correlation is expected to be as follows:

$$k_l a = \alpha \left(\frac{P}{V_l} \right)^y v_s^z \quad (3.9.1)$$

where $k_l a$ is the volumetric mass transfer coefficient in (s^{-1}), α is proportionality factor as a constant, P is the agitator power under gassing condition in (W), V_l is the liquid volume without gassing in (m^3); v_s is the gas superficial velocity in (m s^{-1}), and y and z are empirical constants. Most laboratory fermenters operate with a stirrer power between 10 and 20 kW m^{-3} , whereas large bioreactors operate at 0.5–5 kW m^{-3} . The mass transfer coefficient for coalescing air–water dispersion is:

$$k_l a = 2.6 \times 10^{-2} \left(\frac{P}{V_l} \right)^{0.4} v_s^{0.5} \quad (3.9.2)$$

The above correlation is valid for a bioreactor size of less than 3000 L and a gassed power per unit volume of 0.5–10 kW. For noncoalescing (nonsticky) air–electrolyte dispersion, the exponents of the gassed power per unit volume and gas superficial velocity in the correlation of mass transfer coefficient change slightly. The empirical correlation with defined coefficients may come from the experimental data with a well-defined bioreactor with a working volume of less than 5000 L and a gassed power per unit volume of 0.5–10 kW. The defined correlation is:

$$k_l a = 2 \times 10^{-3} \left(\frac{P}{V_l} \right)^{0.7} v_s^{0.2} \quad (3.9.3)$$

This empirical correlation was obtained from the experimental data with a well-defined bioreactor with a working volume of less than 5000 L and a gassed power per unit volume of 0.5–10 kW.

In general, coalescing systems are those in which the water is relatively pure; noncoalescing systems are those in which a small amount of electrolytes presents in the system.

The presented correlations do not take into account either the nonNewtonian behavior of biological fluids or the effect of antifoam and the presence of solids. A correlation may be applied to a nonNewtonian filamentous fermentation in the following form²:

$$k_L a = \alpha \left(\frac{P}{V_L} \right)^{0.33} v_s^{0.56} \quad (3.9.4)$$

Comparing this with the equations for Newtonian fluids shows that the oxygen transfer coefficient for nonNewtonian fluids is less sensitive to power input changes. Kawase and Moo-Young obtained the constants for nonNewtonian systems as $0.37 < y < 0.80$ and $0.20 < z < 0.84$. Then, this justification may be applied for the specific bioreactor used and cannot be applicable for general cases.⁶ Thus, more power input is required to reach the same mass transfer coefficient value as that in a Newtonian fluid. The addition of antifoam has a significant effect on the value of the mass transfer coefficient. Antifoam reduces the interfacial free energy at the interface between air and water. Therefore, the surface tension and the bubble size are reduced, leading to higher values of interfacial area per unit volume (a). However, k may decrease due to liquid movement near the interface. This means that the mobility of the liquid could decrease at the interface, and a film of liquid generates a resistance between the liquid and gas systems. Figure 3.1 shows the linear dependency of the mass transfer coefficient to the air flow rate as volume of air per volume of liquid media per min; customary for fermentation to be shown in vvm ($\text{L L}^{-1} \text{ min}^{-1}$) for 10, 100 and 1000 L fermenters. A higher mass transfer coefficient can be obtained as the air flow rate is increased.

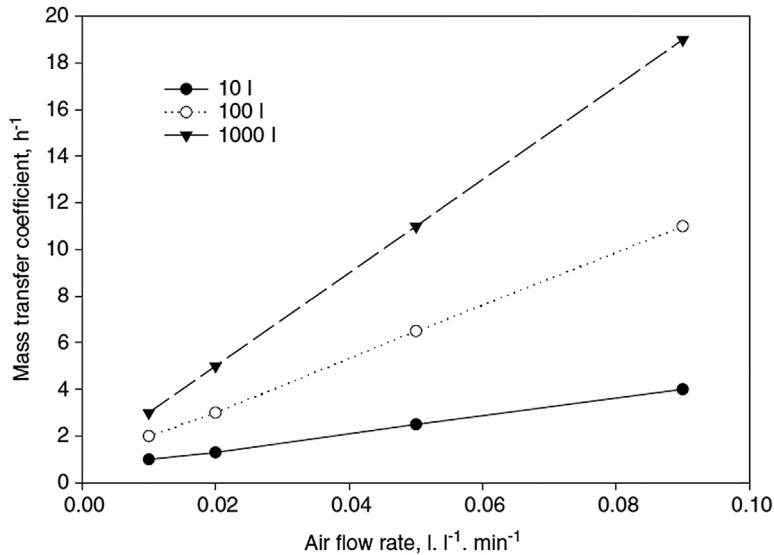


FIGURE 3.1 Effect of air flow rate on oxygen transfer coefficients, $K_L a$. ($\text{L L}^{-1} \text{ min}^{-1}$ = liters of air per liter of liquid per min).

3.10 AGITATED SYSTEM AND MIXING PHENOMENA

The following treatment of agitation is restricted to fluids that approximate to Newtonian fluids. Because mixing is a complex process, the variables involved are considered together in a dimensionless group known as the Reynolds number (Re). Re is used to characterize the behavior of flow:

$$Re = \frac{\text{Inertia forces}}{\text{Viscous forces}} = \frac{\rho D_i^2 N}{\mu} \quad (3.10.1)$$

where D_i is the impeller diameter in m, N is the rotational speed of impellers in round per second (rps), ρ is the fluid density in kg m^{-3} , and μ is the viscosity of the fluid in $\text{kg m}^{-1} \text{s}^{-1}$. Fully turbulent flow exists above a Reynolds number of 10^4 , whereas fully laminar flow exists below 100; in between is the transitional region. Another group of dimensionless variables that are used to characterize mixing in a vessel is the Froude number (Fr), which takes gravitational forces into account:

$$Fr = \frac{\text{Inertia forces}}{\text{Gravity forces}} = \frac{N^2 D_i}{g} \quad (3.10.2)$$

where g is gravitational acceleration in m s^{-2} . A third group, which is related to energy required by the agitator, is the power number. This shows the power consumption for stirring. The power consumption is related to fluid properties, the density and viscosity of the fluid, the stirrer rotation rate, and the impeller diameter. Several well-known studies have shown the relation between power number and Reynolds number; the laminar region is a straight line, but it depends on the shape of the impellers.^{2,4,5} Marine propellers require less energy compared with flat blade turbine disks. The power in the turbulent region is proportional to $N_i^3 D_i^5$; therefore the power number is the ratio of power for the aerated fluid and the nonaerated powered system, which is:

$$N_{Po} = \frac{P \cdot g_c}{N^3 D_i^5 \rho} \quad (3.10.3)$$

where P is agitator power in W. The power number for laminar flow is proportional to the inverse of the Reynolds number, $N_{Po} \approx k_1/Re_i$; for turbulent flow, the agitation power is proportional to $K_2 N^3 D_i^5 \rho$, where units for agitation power are in W, kW, or hp.

3.11 MASS TRANSFER LIMITED PROCESS

The transfer of oxygen from the gas phase to the liquid phase becomes “mass transfer limited” when sufficient oxygen is not supplied to the fermentation broth, especially in cultures with high cell density. Some actual cases are.

- In a large-scale fermenter for penicillin production.
- In production of extracellular biopolymers such as xanthan gum.
- In wastewater treatment with an activated sludge system.

Gas and liquid systems are described by solubility of gas in the liquid phase. The solubility of oxygen at room temperature is about 10 ppm; therefore, the concentration of oxygen is 10 ppm (oxygen flux, N_A). The solubility of oxygen at 0 °C is double that at 35 °C. Also, the solubility decreases if the electrolyte concentration is increased. The concentrations of oxygen in the gas phase and liquid phase are related to each other by the Raoult–Dalton equilibrium law:

$$\overline{P_{Ag}} = y_A P_A = x_{AL} H_A \quad (3.11.1)$$

The above relation is rewritten in terms of concentration:

$$HC_{l,i} = C_{g,i} \quad (3.11.2)$$

Based on film theory, the oxygen flux in the gas film is equal to flux in the liquid film:

$$N_A = K_g (C_g - C_{g,i}) = K_l (C_{l,i} - C_l) \quad (3.11.3)$$

where C_{li} is oxygen concentration at interface. Let us define C_l^* oxygen concentration at equilibrium with the liquid phase. Henry's law in terms of oxygen concentration at equilibrium is

$$HC_l^* = C_g \quad (3.11.4)$$

The molar flux in terms of equilibrium concentration is:

$$N_A = K_L (C_l^* - C_l) \quad (3.11.5)$$

where K_L is the overall mass transfer coefficient. If we simplify all the resistances in liquid and gas phases, then the resistances in series are written as:

$$\frac{1}{K_L} = \frac{1}{k_l} + \frac{1}{H} \frac{1}{k_g} \quad (3.11.6)$$

If k_g is larger than k_l , then the resistance to mass transfer lies on the liquid film side. Oxygen absorption rate is:

$$\begin{aligned} Q_{O_2} &= (\text{flux}) \left(\frac{\text{interfacial area}}{\text{volume}} \right) \\ Q_{O_2} &= k_l (C_l^* - C_l) \left(\frac{A}{V} \right) \end{aligned} \quad (3.11.7)$$

The interfacial area per unit volume and $a' = A/V$ is incorporated into Eqn (3.11.7):

$$Q_{O_2} = k_l a' (C_l^* - C_l) \quad (3.11.8)$$

The minimum oxygen utilization rate is $x\mu_{\max}/Y_{O_2}$. If the system is mass-transfer limited, C_l approaches zero. Then the amount of oxygen absorbed is exactly equal to the amount of oxygen consumed. Equations (3.11.8) leads to the following:

$$k_l a' (C_l^* - C_l) = \frac{x\mu}{Y_{O_2}} \quad (3.11.9)$$

Using the Monod rate for the specific growth rate in Eqn (3.11.9), it is reduced to the following equation:

$$k_L a' (C_l^* - C_l) = \frac{x}{Y_{O_2}} \left(\frac{\mu_{\max} C_l}{K_{O_2} + C_l} \right) \quad (3.11.10)$$

Rearranging Eqn (3.11.10) yields the following equation:

$$Y_{O_2} k_L a' (C_l^* - C_l) = x \mu_{\max} \left(\frac{C_l}{K_{O_2} + C_l} \right) \quad (3.11.11)$$

if $C_l < C_l^*$, then the concentration profile for oxygen in the liquid phase is:

$$C_l = C_l^* \left[\frac{Y_{O_2} K_{O_2} k_L a' / x \mu_{\max}}{1 - Y_{O_2} C_l^* k_L a' / x \mu_{\max}} \right] \quad (3.11.12)$$

EXAMPLE 1

Calculate Cell Density in an Aerobic Culture

A strain of *Azotobacter vinelandii* was cultured in a 15 m³ stirred fermenter for the production of alginate. Under current conditions, the mass transfer coefficient, $k_L a$, is 0.18 s⁻¹. Oxygen solubility in the fermentation broth is approximately 8×10^{-3} kg m⁻³.⁹ The specific OUR is 12.5 mmol g⁻¹ h⁻¹. What is the maximum cell density in the broth? If copper sulfate is accidentally added to the fermentation broth, which may reduce the OUR to 3 mmol g⁻¹ h⁻¹ and inhibit the microbial cell growth, what would be the maximum cell density in this condition?

The OUR is defined as¹⁰:

$$OUR = q_{O_2}(x) = k_L a (C_{AL}^* - C_{AL}) \quad (E1.1)$$

Solution

We make an assumption based on the fact that all of the DO in the fermentation broth is used or taken by microorganisms. In this case, the DO goes to zero. The value for C_{AL} can be zero because it is not given in the problem statement. Also, the cell density has to be maximized. Therefore the above assumption is valid. In the above equation, x represents the cell density; that is:

$$x_{\max} = \frac{k_L a C_{AL}^*}{q_{O_2}} \quad (E1.2)$$

Substituting values into Eqn (E2.2), the maximum biomass production is calculated as follows:

$$x_{\max} = \frac{(0.18 \text{ s}^{-1})(8 \times 10^{-3} \text{ kg m}^{-3})}{\left(\frac{12.5 \text{ mmol}}{\text{g} \cdot \text{h}} \right) \left(\frac{1 \text{ mol}}{1000 \text{ mmol}} \right) \left(\frac{32 \text{ g}}{1 \text{ mol}} \right) \left(\frac{1 \text{ kg}}{1000 \text{ g}} \right)} = \frac{12960 \text{ g}}{\text{m}^3} \text{ or } 12.96 \text{ g L}^{-1}$$

Assuming the solubility of oxygen does not affect C_{AL}^* or k_{La} , the factor affected on the OUR that is $12.5/3 = 4.167$, then x_{\max} is:

$$x_{\max} = (12.96)(4.167) = 54 \text{ g L}^{-1}$$

To achieve the calculated cell densities, other conditions must be favorable, such as substrate concentration and sufficient time.

EXAMPLE 2

Effect of Carbon Source in Penicillin Production

The carbon source affects oxygen demand. In penicillin production, oxygen demand for glucose is $4.9 \text{ mol L}^{-1} \text{ h}^{-1}$. The lactose concentration is $6.7 \text{ mol L}^{-1} \text{ h}^{-1}$; sucrose is $13.4 \text{ mol L}^{-1} \text{ h}^{-1}$. The yield of oxygen per mole of carbon source for CH_4 is $Y_{\text{O}_2/\text{C}} = 1.34$, $Y_{\text{O}_2/\text{C}}$ for paraffins = 1, and $Y_{\text{O}_2/\text{C}}$ for hydrocarbon $(\text{CH}_2\text{O})_n = 0.4$. The mass transfer coefficient k_{La} is for gas–liquid reactions, and the film thickness where the mass transfer takes place is δ .

In such cases, the rate of oxygen transfer to the fermentation broth is less than oxygen consumption by the cells:

$$\delta \times \text{rate}|_{\text{film}} < k_l(C^* - C_l) \quad (\text{E2.1})$$

where δ is the film thickness of the mass transfer given as:

$$\delta = \frac{D_{\text{O}_2}}{k_l} \quad (\text{E2.2})$$

where D_{O_2} is the oxygen diffusion coefficient in $(\text{m}^2 \text{ s}^{-1})$. The reaction rate is based on the elementary rate, which means rate is proportional to substrate concentration to definite exponent:

$$-r_{\text{O}_2} = k_r(C^*)^\alpha \quad (\text{E2.3})$$

where r_{O_2} is the oxygen reaction rate in $(\text{mol m}^{-3} \text{ s}^{-1})$ and k_r is the rate constant. Substituting the rate expression and (E2.2) into Eqn (E2.1) leads to an inequality for mass transfer coefficient in the liquid phase:

$$\frac{D_{\text{O}_2}}{k_l} \times k_r(C^*)^\alpha < k_l(C^* - C_l) \quad (\text{E2.4})$$

By rearranging Eqn (E2.4) then solving for k_l , we obtain:

$$k_l > \left[\frac{k_r(C^*)^\alpha D_{\text{O}_2}}{C^* - C_l} \right]^{\frac{1}{2}} \quad (\text{E2.5})$$

For “mass transfer limited” fermentation with very little DO in the broth, $C_l < C^*$; thus Eqn (E2.5) is simplified, and the above inequality becomes:

$$k_l > \left[\frac{k_r(C^*)^\alpha D_{\text{O}_2}}{C^* - C_l} \right]^{\frac{1}{2}} \quad (\text{E2.6})$$

given a value for $\alpha = 0.5$.

$$k_l > \left[\frac{k_r (C^*)^{0.5} D_{O_2}}{C^* - C_l} \right]^{\frac{1}{2}} \quad (E2.7)$$

The mass transfer coefficient is calculated for a given diffusivity coefficient and reaction rate constant at the equilibrium concentration of oxygen.

When oxygen is continuously transported and removed from the liquid phase, we may obtain the moles of oxygen used in the bioreactor considering the ideal gas law ($PV = nRT$) as:

$$OUR = [F_{g,in} \times P_{O_{2,in}} - F_{g,out} P_{O_{2,out}}] / VRT \quad (E2.7)$$

where OUR is the oxygen uptake rate in ($\text{mol m}^{-3} \text{s}^{-1}$), F_g is the volumetric oxygen flow rate in ($\text{m}^3 \text{s}^{-1}$), and P_{O_2} is the partial pressure of oxygen. Using the ideal gas law ($PV = nRT$), we then solve for moles of oxygen used in the bioreactor. The moles of gas transferred are calculated by the ideal gas law:

$$n_A = \frac{F_A}{V} = \frac{P_A V}{RT} \quad (E2.8)$$

3.11.1 Oxygen Transport

Molar transformation of oxygen is proportional to the concentration gradient of oxygen at the gas–liquid interface and oxygen dissolved in the bulk liquid phase:

$$N_{O_2} = N_A = k_l (C_i^* - C_l) \quad (3.11.1.1)$$

where N_{O_2} is oxygen flux in $\text{kmol m}^{-2} \text{s}^{-1}$, k_l is the liquid side mass transfer coefficient in m s^{-1} , C_i^* is the oxygen concentration at interface in kmol m^{-3} , and C_l is the oxygen concentration in the bulk of liquid. The molar transformation of oxygen in the gas phase is proportional to the pressure gradient:

$$N_{O_2} = k_g (P_{O_2} - P_i^*) \quad (3.11.1.2)$$

where k_g is the gas side mass transfer coefficient in $\text{kmol atm}^{-1} \text{m}^{-2} \text{s}^{-1}$, P_i^* atm^{-1} is the interfacial partial pressure of oxygen, and P_{O_2} is the partial pressure of oxygen in bulk gas. The resistances in series, which are associated with Henry's law, are explained earlier (3.11.6). For the slightly soluble gas, H is greater than $4 \times 10^4 \text{ bar mol}^{-1}$, the mass transfer coefficient for gas phase, k_g , is large, and we may neglect the resistance created by the gas film; then it would be a perfect assumption to state $K_L = k_l$. The interfacial surface area created by the gas bubbles is:

$$a_i = \frac{\text{surface area of gas bubbles}}{V_L} \quad (\text{m}^2 \text{m}^{-3}) \quad (3.11.1.3)$$

The molar flux is given by Eqn (3.5.1).

Gas hold-up is defined as $H_o = \text{bubble volume}/\text{reactor volume}$, which is the volume of gas per unit volume of reactor. Assume the system is an agitated vessel. Let us use Richard's data to define gas hold-up³:

$$\left(\frac{P}{V}\right)^{0.4} (V_s)^{0.5} = 7.63h + 2.37 \quad (3.11.1.4)$$

where P is power in hp, V is ungassed liquid volume in m^3 , V_s is gas superficial velocity in m h^{-1} and h is the volume void fraction.

EXAMPLE 3

Calculated Gas Hold-up

Calculate the gas hold-up for an agitated and aerated system with power input of 18 hp in an 80 m^3 vessel; tank diameter is 4 m, with gas superficial velocity of 2.6 m min^{-1} .

$$\left(\frac{18}{80}\right)^{0.4} (2.6 \times 60 \text{ min h}^{-1})^{0.5} = 7.63H + 2.37 \quad (\text{E3.1})$$

The gas hold-up can be defined by the above definition using the gas height per volume of tank, where H is 0.6 m for aeration and height of liquid 6.5 m

$$H_o = \frac{V_g}{V_g + V_L} = \frac{0.6 \text{ m}}{0.6 + 6.5 \text{ m}} = 0.085 \quad (\text{E3.2})$$

The calculated gas hold-up is 8.5%.

3.11.2 Diameter of Gas Bubble Formed D_o

As gas flows with fixed volumetric flow rate through an orifice gas sparger, bubbles are formed with diameter D_o . Analysis of bubble formation is based on the balance of buoyant force, as the bubbles leave the orifice and rise through the media $(\pi\Delta\rho g D_o^3)/6$, with the rest of the forces resulting from the surface tension, $\pi\sigma d$. Buoyant force-rest of force.

$$\frac{\pi g \Delta \rho D_o^3}{6} = \pi \sigma d \quad (3.11.2.1)$$

$$D = \left[\frac{6\sigma d}{g\Delta\rho} \right]^{\frac{1}{3}} \quad (3.11.2.2)$$

The interfacial area:

$$a = H \left(\frac{6}{D} \right) \quad (3.11.2.3)$$

Bubble residence time

$$t_b = \frac{H_L}{u_t} = \frac{\text{Height of liquid}}{\text{Gas terminal velocity}} \quad (3.11.2.4)$$

The terminal velocity for rising bubbles is:

$$u_t = \frac{D^2 \Delta \rho g}{18 \mu} \quad (3.11.2.5)$$

Using the following equation:

$$a' = \frac{1}{V} (nF_0)(t_b) \left(\frac{6}{D} \right) \quad (3.11.2.6)$$

where a' is the interfacial area per unit volume of liquid.

$$a' = \frac{nF_0(H_L/u_t) \times 6}{VD} \quad (3.11.2.7)$$

The oxygen use balanced with growth gives:

$$Y_{O_2} k_L a' (C_l^* - C_l) = x \mu = x \frac{\mu_{\max} C_l}{K_{O_2} + C_l} \quad (3.11.2.8)$$

given $K_S = K_{O_2}$

$$\mu = \frac{1}{x} \frac{dx}{dt} = \frac{\mu_{\max} C_l}{Y_{O_2} (K_{O_2} + C_l)} \quad (3.11.2.9)$$

Useful equations similar to Eqn (3.11.12) for $C_l < C_l^*$ are obtained.

$$C_l = C_l^* \left[\frac{Y_{O_2} K_{O_2} k_L a' / x \mu_{\max}}{1 - Y_{O_2} C_l^* k_L a' / x \mu_{\max}} \right] \quad (3.11.2.10)$$

EXAMPLE 4

Calculation of Cell Density in Aerobic Culture

A strain of *A. vinelandii* is cultured in a 15 m³ stirred fermenter for production of alginate. Under current conditions, the mass transfer coefficient, $k_L a$, is 0.25 s⁻¹. Oxygen solubility in the fermentation broth is approximately 8.5 × 10⁻³ kg m⁻³. The specific OUR is 15 mmol g⁻¹ h⁻¹. What is the maximum cell density in the broth? If copper sulfate is accidentally added to the fermentation broth, which may reduce the OUR to 1.5 mmol g⁻¹ h⁻¹ and inhibit the microbial cell growth, what would be the maximum cell density in such a case?

The OUR is defined as:

$$OUR = (q_{O_2})(x) = k_L a (C_{AL}^* - C_{AL}) \quad (3.11.2.11)$$

Solution

We assume all the DO in the fermentation broth is used or taken by microorganisms. In this case, the DO is zero or the value for C_{AL} is zero, since it is not given in the problem statement. Also, the

cell density has to be maximized; therefore, the above assumption is valid. In the above equation, x represents cell density, which is

$$x_{\max} = \frac{k_L a C_{AL}^*}{q_{O_2}} \quad (3.11.2.12)$$

$$x_{\max} = \frac{(0.25 \text{ s}^{-1})(8.5 \times 10^{-3} \text{ kg m}^3)}{(15 \text{ mmol/g} \cdot \text{h})(1 \text{ h}/3600 \text{ s})(1 \text{ mol}/1000 \text{ mmol})(32 \text{ g}/1 \text{ mol})(1 \text{ kg}/1000 \text{ g})}$$

$$= 15937.5 \text{ g/m}^3 = 15.94 \text{ g L}^{-1}$$

Let us assume the solubility of oxygen does not affect C_{AL}^* or $k_L a$. The factor affected by.

OUR is:

$$15/1.5 = 10$$

then x_{\max} is:

$$x_{\max} = (15.94)(10) = 159.4 \text{ g L}^{-1}$$

To achieve the calculated cell densities, all other conditions must be favorable, such as substrate concentration and sufficient time.

EXAMPLE 5

Oxygen Requirements for Activated Sludge in an Aerated Bioreactor

Oxygen balance for an aerated system with activated sludge is defined by a dynamic model:

$$\frac{dC_{O_2}}{dt} = a \left(\frac{F}{V} \right) (C_{S_0} - C_S) + b\mu x \quad (3.11.2.13)$$

The substrate in this equation is represented by biological oxygen demand (BOD), where V is the reactor volume, x is the cell density or sludge concentration, a is a constant in $\text{kg O}_2 \text{ kg}^{-1} \text{ BOD}$, b is also a constant in $\text{kg O}_2 \text{ kg}^{-1} \text{ MLSS}$, and F is the fresh feed flow rate in $\text{m}^3 \text{ h}^{-1}$. MLSS is the mixed liquor suspended solid in mg l^{-1} , and BOD is 0.4 kg/kg MLSS . The constants for $a = 0.5$ and $b = 0.4$ are given. For a flow rate of $100 \text{ m}^3 \text{ h}^{-1}$ and initial substrate S_0 of $30,000 \text{ ppm}$ (0.03 kg m^{-3}) in an aeration tank volume of $V = 10 \text{ m}^3$, what would the BOD concentration be if an oxygen rate of $0.95 \text{ m}^3 \text{ h}^{-1}$ is supplied, and what would the leaving substrate concentration, S , be?

$$\mu = \frac{\mu_m S}{K_M + S} \quad \text{or} \quad x\mu = \frac{\mu_m x S}{K_M + S} \quad (3.11.2.14)$$

Given rate = $0.75 \text{ kg O}_2 (\text{kg BOD h})^{-1}$

Oxygen flow rate supplied in $0.95 \text{ m}^3 \text{ h}^{-1}$:

$$OTR = (0.95 \text{ m}^3 \text{ h}^{-1}) \left(\frac{1 \text{ kmol}}{22.4 \text{ m}^3} \right) \left(\frac{32 \text{ kg}}{1 \text{ kmol}} \right) = 1.36 \text{ kg h}^{-1}$$

Plug in values into [Eqn \(3.11.2.13\)](#)

$$0.136 \text{ kg m}^{-3} \text{ h}^{-1} = 0.5(10 \text{ h}^{-1})(0.03 \text{ kg m}^{-3} - S) + 0.4(0.75 \text{ kg m}^{-3} \text{ h}^{-1})(0.03 \text{ kg m}^{-3} - S)$$

$$S = 0.004 \text{ kg m}^{-3}$$

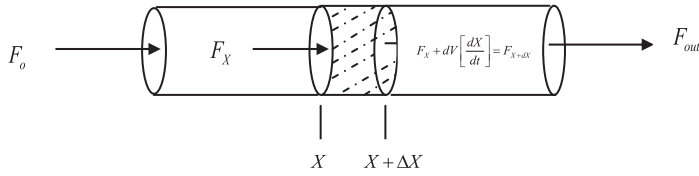


FIGURE 3.2 Schematic diagram of plug flow reactor.

For a plug flow system, we can define all the conditions in inlet and outlet streams as shown in Figure 3.2.

The residence time for an ideal plug flow system is stipulated as:

$$t_p = \int_{x_1}^{x_2} \frac{dx}{(dx/dt)} = \int_0^{x_A} \frac{dx_A}{-r_A} \quad (3.11.2.15)$$

Generally, residence time is obtained by a division of working volume by volumetric flow rate:

$$\tau = \frac{V}{F} \quad (3.11.2.16)$$

The differential form shows the changes occurring along the length of tubular reactor. The plug flow bioreactor as the substrate and the product formed along the length of the tubular bioreactor is shown in Figure 3.3.

$$d\tau = \frac{dV}{F} = \frac{dx}{\left(\frac{dx}{dt}\right)} \quad (3.11.2.17)$$

The concentration profiles for substrate, product, and biomass in a plug flow system are shown in Figure 3.4.

For CSTR, the design equation is given below:

$$\tau_m = \frac{C_{A0}x_A}{-r_A} \quad (3.11.2.18)$$

The rate model for a biological process is given by a Monod rate model.

$$-r_A = \frac{v_{\max}SX}{K_M + S} \quad (3.11.2.19)$$

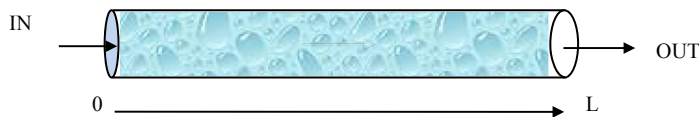


FIGURE 3.3 Schematic diagram of plug flow bioreactor.

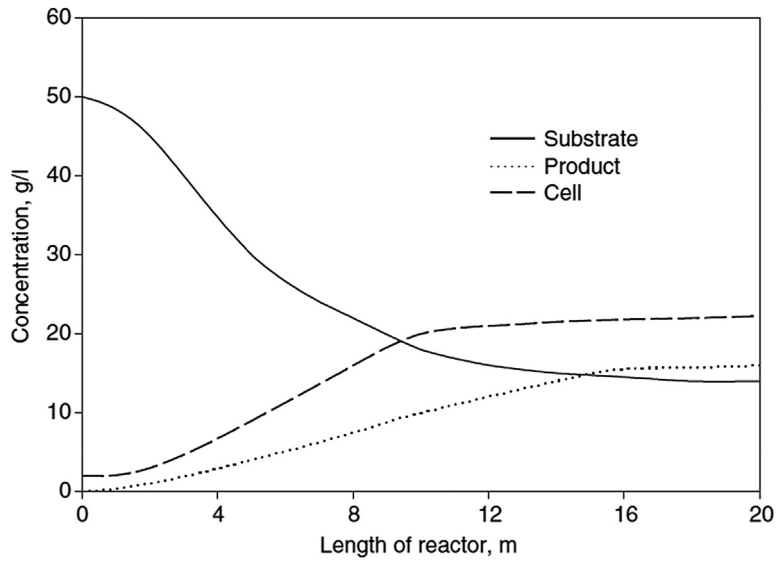


FIGURE 3.4 Substrate, product, and cell concentration versus length of plug flow bioreactor.

Bioreactor with the assumption of tank diameter is equal to the height of the liquid ($D_t = H$). Assume steady-state condition, no cell accumulation, and no death rate:

$$\frac{F}{V}(x_0 - x) + r_x \frac{V}{v} = 0 \quad (3.11.2.20)$$

(Flow rate) (Cell in – Cell out) = rate of cell generation = 0.

Let us define μ , which is known as specific growth rate:

$$\mu = \frac{r_x}{x} \quad (3.11.2.21)$$

Dilution rate is defined as the number of tank volume pass through per unit time, $D = F/V$. The residence time is defined as the time required for one unit volume of reactor to be replaced by the flow rate, $\tau = V/v$. When the feed is sterile, there is no cell entering the bioreactor, which means $x_0 = 0$; the rate may be simplified and reduced to:

$$\mu = D; \quad DX = r_x \quad (3.11.2.22)$$

Steady-state material balance is used for cell mass.

$$\frac{F}{V}x_0 = \frac{F}{V}x - x\left(\frac{r_x}{x}\right) \quad (3.11.2.23)$$

Substituting dilution rate and specific rate into Eqn (3.11.2.23) leads to a useful relation:

$$Dx_0 = (D - \mu)(x) \quad (3.11.2.24)$$

For the case of sterile feed, Eqn (3.11.2.24) reduces to:

$$(D - \mu) = 0 \quad \text{or} \quad D = \mu \quad (3.11.2.25)$$

The general balance equation is given below:

$$V_R \frac{dC_i}{dt} = F(t)[C_{if} - C_i] + r_{fi} \quad (3.11.2.26)$$

At unsteady-state conditions, the change of concentration with respect to time is detectable, $dS/dt \neq 0$, but for steady-state conditions the leaving substrate may be constant. For a plug flow bioreactor, we can treat it like a batch system.

The cell balance is:

$$-\frac{dC_A}{dt} = -r_A \quad (3.11.2.27)$$

The change of cell density with respect to time is given as follows:

$$\frac{dx}{dt} = \frac{r_x}{x} x = \mu x \quad (3.11.2.28)$$

Substituting the specific growth rate into Eqn (3.11.2.28) leads to the following differential equation:

$$\frac{dx}{dt} = \left(\frac{\mu_{\max} S}{K_S + S} \right) X \quad (3.11.2.29)$$

When dilution rate reaches the maximum specific rate ($D = \mu_{\max}$), wash out phenomena may take place.

Balance for substrate S :

$$-\frac{ds}{dt} = \frac{X}{Y} \left(\frac{\mu_{\max} S}{K_S + S} \right) \quad (3.11.2.30)$$

For sterile media in a chemostat:

$$D_{in} = \frac{\mu_{\max} S_0}{K_S + S_0} \quad (3.11.2.31)$$

The substrate concentration is defined as:

$$S = \frac{DK_S}{\mu_{\max} - D} \quad \text{and} \quad Y = \frac{X}{S_0 - S} \quad (3.11.2.32)$$

The biomass is calculated using Eqn (3.11.2.32):

$$X = Y(S_0 - S) = Y \left(S_0 - \frac{DK_S}{\mu_{\max} - D} \right) \quad (3.11.2.33)$$

Yield of biomass is defined as:

$$Y = \frac{\text{mass of cells formed}}{\text{mass of substrate consumed}}$$

The Monod rate equation, $\mu = \frac{\mu_{\max} S}{K_S + S}$, is used to substitute into mass balance. Substituting S into X , the following equation is obtained:

$$Dx_0 + \left(\frac{\mu_{\max} S}{K_S + S} - D \right) X = 0 \quad (3.11.2.34)$$

At steady state condition, the mass balance for substrate S is $\frac{dS}{dt} = 0$, results in the following equation:

$$D(S_0 - S) = \left(\frac{\mu_{\max} S}{K_S + S} \right) \frac{X}{Y} \quad (3.11.2.35)$$

The rate equation is incorporated:

$$D(S_0 - S) = \frac{r_x}{Y} \quad (3.11.2.36)$$

NOMENCLATURE

- a Gas-liquid interfacial area per unit volume of broth, m^{-1}
 C^* Saturation concentration of oxygen in liquid bulk in equilibrium with gas phase, mol m^{-3}
 C_i Oxygen concentration at the interface, mol m^{-3}
 C_l Oxygen concentration in the bulk of liquid, mol m^{-3}
 D_o Orifice diameter, m
 d_b Average bubble diameter, m
 D_{O_2} Oxygen diffusion coefficient, $\text{m}^2 \text{s}^{-1}$
 F_g Volumetric oxygen flow rate, $\text{m}^3 \text{s}^{-1}$
 H Henry's constant, $\text{atm m}^3 \text{mol}^{-1}$
 H_l Height of liquid, m
 J_{O_2} Molar flux of oxygen, $\text{mol m}^{-2} \text{s}^{-1}$
 k_g Mass transfer coefficient in the gas side, $\text{mol m}^{-2} \text{atm}^{-1} \text{s}^{-1}$
 K_g Overall mass transfer coefficient in the gas phase, $\text{mol m}^{-2} \text{atm}^{-1} \text{s}^{-1}$
 k_l Mass transfer coefficient in liquid side, m s^{-1}
 K_l Overall mass transfer coefficient in the liquid phase, m s^{-1}
 k_r Rate constant
 k_{la} Volumetric mass transfer coefficient, s^{-1}
 N_{O_2} Oxygen transfer rate, $\text{mol m}^3 \text{s}^{-1}$
 OUR Oxygen uptake rate, $\text{mol m}^{-3} \text{s}^{-1}$
 P Agitator power under gassing condition, W
 P^* Partial pressure of oxygen in equilibrium with liquid phase, atm
 P_{O_2} Oxygen partial pressure in the bulk of gas phase, atm
 $P_{O_2,i}$ Oxygen partial pressure at the interface, atm
 r_{O_2} Oxygen reaction rate, $\text{mol m}^{-3} \text{s}^{-1}$
 t_b Bubble residence time in liquid, s
 vvm Volume of air per volume of liquid media per min, $\text{L L}^{-1} \text{min}^{-1}$
 V_g Volume of gas bubbles in the reactor, m^3
 V_l Volume of liquid in the fermenter, m^3
 v_s Gas superficial velocity, m s^{-1}
 v_t Gas terminal velocity, m s^{-1}
 y, z Empirical constants

GREEK SYMBOLS

- α proportionality factor as a constant
 δ film thickness of the mass transfer, m
 ϵ gas hold-up
 μ viscosity, $\text{kg m}^{-1} \text{s}^{-1}$
 ρ_l density of liquid, kg m^{-3}
 ρ_g density of gas, kg m^{-3}
 σ interfacial tension of the gas–liquid film, kg s^{-2}

References

1. Baily JE, Ollis DF. *Biochemical engineering fundamentals*. 2nd ed. New York: McGraw-Hill; 1986.
2. Scragg AH. *Bioreactors in biotechnology: a practical approach*. New York: Ellis Horwood Series in Biochemistry and Biotechnology; 1991.
3. Wang DIC, Cooney CL, Deman AL, Dunnill P, Humphrey AE, Lilly MD. *Fermentation and enzyme technology*. New York: John Wiley & Sons; 1979.
4. Doran PM. *Bioprocess engineering principles*. New York: Academic Press; 1995.
5. Shuler ML, Kargi F. *Bioprocess engineering, basic concepts*. New Jersey: Prentice Hall; 1992.
6. Kawase Y, Moo-Young M. Correlations for liquid phase mass transfer coefficients in bubble column reactors with newtonian and non-newtonian fluids. *Can J Chem Eng* 1992;70(1):48–54.

SUBCHAPTER

3.13

Case Study: Oxygen Transfer Rate Model in an Aerated Tank for Pharmaceutical Wastewater

3.13.1 INTRODUCTION

Aerobic wastewater treatment processes remove dissolved and colloidal organic matter from industrial wastewater. The growth and propagation of the microorganisms consume oxygen in the liquid phase. This causes the dissolved oxygen (DO) to be depleted when the microorganisms are in the exponential growth phase. However, the specific oxygen uptake of bacteria increases only slightly with increasing oxygen concentration above a certain critical concentration. To achieve the optimum oxygen transfer rate (OTR), several parameters, such as airflow rate, bubble size, nature of the wastewater, agitation rate, temperature, reaction rate, and propagation of the microorganisms, which influence the mass transfer rate, have to be considered. The activated sludge process for domestic wastewater treatment was first introduced to the world in 1914.¹ Since then, many studies have been conducted to improve the oxygen transfer efficiency. Among the aeration devices introduced are porous diffuser, filter type diffuser, mechanical aeration device, orifice type diffuser, and fine-pore air diffuser. In the United States today, the aerated treatment process has a substantial market. There is a great emphasis on the enhancement of an efficient process, which may lead to intensive research programs. The process aim is to evaluate the design, operation, and control processes while improving overall system performance. The transfer of oxygen from the gas phase to the microorganism takes place in several steps. First, the oxygen must travel through the gas to the gas–liquid interface, then through the bulk liquid, and finally into the microorganism. Some researchers believe that oxygen transfer occurs significantly during bubble formation when the interfacial area exposed to the liquid is constantly renewed. On the other hand, there are other researchers who believe that significant oxygen transfer occurs during the bubble's ascent. However, it is well understood that regardless of where the transfer occurs, the rate of transfer is proportional to the contact time and area of contact between the liquid and the gas. It is found that the overall gas transfer coefficient, $K_L \cdot a$, increases while bubble size decreases down to a diameter of 2.2 mm; further reduction in bubble size results in a decrease of $K_L \cdot a$, although smaller bubbles may increase oxygen transfer efficiency.²

Modeling oxygen transport in the aeration system is important because it can be used as a reference for overall process performance improvement as well as process design and simulation. The oxygen transfer process mentioned above is based on the concentration gradient between the oxygen concentration in the gas phase and in the organism. The basic model for oxygen transfer in a dispersed gas–liquid system is given by Eqn (3.7.3).³ For the gas side, mass transfer can be similarly defined in terms of the gas partial pressure, as explained in the related section.

Since it is usually impossible to measure the local and interface concentrations everywhere in a bioreactor, average values of concentrations or dominant bulk concentrations and overall mass transfer coefficients are used. To know the total OTR in a vessel, the total surface area available for the oxygen transfer has to be determined. Thus, an overall mass transfer coefficient incorporating the surface area of the bubble is used, namely $N_A = K_L \cdot a (C^* - C)$. The value of $K_L \cdot a$ is dependent on the physicochemical properties of the bioreactor media, the physical properties of the bioreactor, and the operating conditions of the vessel. The magnitude of $K_L \cdot a$ can be controlled by the agitation rate and the airflow rate. Oxygen is the substrate that enhances microbial growth; however, above a certain concentration, the microbial growth becomes independent of the oxygen concentration.

In a short period, at a quasisteady-state condition, OTR to microbial cells would be equal to oxygen molar flow transfer to the liquid phase⁴:

$$\frac{dC}{dt} = K_L \cdot a (C^* - C) - Q_{O_2} x \quad (3.13.1.1)$$

At steady-state condition the oxygen concentration profile would be an exponential model:

$$\frac{C - C^*}{C_o - C^*} = e^{-K_L \cdot a \cdot t} \quad (3.13.1.2)$$

In reality, oxygen concentration never reaches the concentration defined in the proposed model, because the microbial activities at optimal and maximum cell density would reach the point where oxygen depletion takes place.⁵

The volumetric mass transfer coefficient, $K_L \cdot a$, for a continuous stirred tank bioreactor can be correlated by power input per unit volume, bubble size, which reflects the interfacial area, and superficial gas velocity.^{3,6} The general form of the correlations for evaluating $K_L \cdot a$ is defined as a polynomial equation given by Eqn (3.9.1).

The mass transfer coefficient is expected to relate gas power per unit volume and gas terminal velocity. Measurement of gas bubble velocity is troublesome in the experimental stage of aeration. Extensive research has been conducted for an explanation of the above correlation. Gas–liquid mass transfer in low-viscosity fluids and in agitated vessels has been reviewed and summarized as stated in Section 3.9³:

1. For coalescing air–water dispersion, when liquid is relatively pure, the mass transfer coefficient was estimated from Eqn (3.9.2) for the defined range of liquid volume and power per unit volume:

$$V_l \leq 2.6 \text{ m}^3; \quad 500 < P_g/V_l < 10,000 \quad (3.13.1.3)$$

2. For noncoalescing air–electrolyte dispersion, when there is a small amount of electrolyte in the system, the mass transfer coefficient may be correlated using Eqn (3.9.3), with the following condition for liquid volume and power per unit volume:

$$V_l \leq 4 \text{ m}^3; \quad 500 < P_g/V_l < 10,000 \quad (3.13.1.4)$$

The above correlations may not be valid for nonNewtonian behavior of biological fluids, nor for the effect of antifoam or in the presence of solids. A correlation proposed in the literature as stated in Eqn (3.9.4)³ may be true for aerobic nonNewtonian fluid filamentous media of fermentation broth.

The industrial wastewater used in the current experiment is considered as noncoalescing air–electrolyte dispersion. Thus, the equations discussed above would be used as a theoretical model for the estimation of oxygen transfer rate in the liquid phase.

3.13.2 MATERIAL AND METHOD

The nonpenicillin wastewater from a pharmaceutical company was collected and used in the batch aeration wastewater treatment experiment. The pharmaceutical wastewater had a clear orange color and a strong odor, contained toxic chemicals, and had a COD value in the range of 3000–30,000 mg L⁻¹. The pH of the wastewater was neutralized and monitored for each experimental run, because the bacteria would have a higher rate of propagation at neutral pH.

Two different sizes of aerated tanks with working volumes of three and 15 L were used. An aeration pump (model 8500, 6 W) with low, medium, and high rates of oxygenation was used for the small tank. A gas-flow meter (Cole Parmer, model 6G08 R4) with a flow range of 0–70 mL min⁻¹ was used for setting the desired airflow rate. Air bubbles entered the bottom of the tank through a gas sparger and maintained the wastewater highly aerated. A stirrer (Cafamo digitalm model RZR2000) in the range of 100–600 rpm was used for complete aeration in the small aeration tank. Also, a 15 L aeration unit (model TR01, with a stirrer model RW20DZM.n, 72W, KIKA from Labortechnik, Malaysia) was used for the large aeration tank. A high-shear dispersing impeller with a diameter of 82 mm was used in the large system. A DO meter (model HI9145 microprocessor, Hanna Instrument, Portugal) was used to detect and measure the amount of DO in the large aeration tank.

The organism was isolated from the wastewater that was used as the seed culture. The medium for seed culture as a starter of each experimental run was prepared by dissolving 1.0 g of glucose and 1.0 g of peptone in 100 mL of distilled water. The nutrients and minerals were obtained from Merck. The medium was sterilized in an autoclave at 121 °C, 15 psig steam pressure for 20 min.

Periodic samples were taken at the starting point after introducing the inocula on the first, second, and third day of each experimental run. The optical cell density, COD, carbohydrate concentration, and DO were monitored for various airflow rates. The COD was measured by the closed reflux colorimetric method at 600 nm with a spectrophotometer, using potassium dichromate as a reducing reagent.⁷ All organic chemicals that were present in the wastewater could be detected as equivalent to carbohydrates by a chemical reducing agent, 3,5-dinitrosalicylic acid, which was detected by the spectrophotometer at 540 nm wavelength.^{8,9}

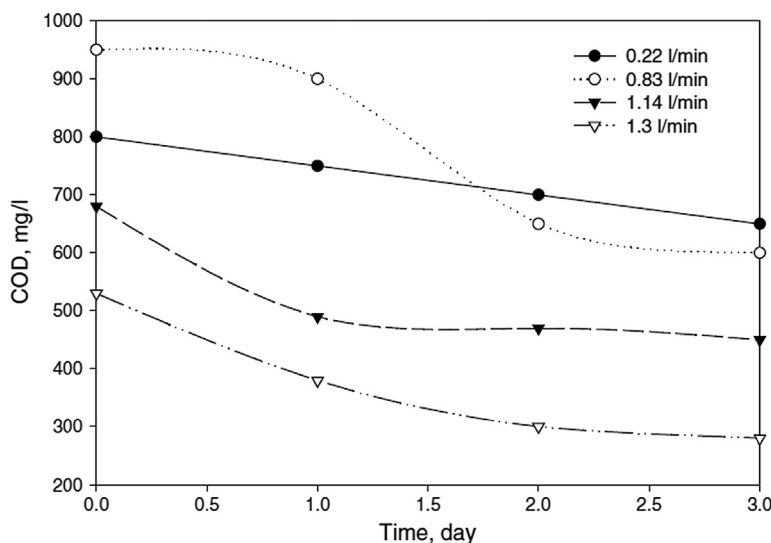


FIGURE 3.5 COD reduction for small aeration tank with various airflow rates.

3.13.3 RESULTS AND DISCUSSION

An experimental run was conducted to study the effect of airflow rate in a 3 L aeration wastewater treatment tank. Nutrients were added to the treatment tank to ensure sufficient bacterial growth. In each experiment, the cell optical density, COD, and the concentration of chemicals equivalent to carbohydrates were monitored for the duration of aeration.

Based on the experimental results shown in Figure 3.5, the COD curves showed sharp reduction on the first day of the treatment, and the rates were gradually reduced when the aeration was extended until the third day. The data show that higher reduction of COD was achieved with the higher airflow rates. An airflow rate of 1.3 L min^{-1} yielded the highest percentage of COD reduction, about 58%. On the other hand, the percentage of carbohydrate consumption also presented similar trend with the airflow rate. Reduction of chemical equivalent to carbohydrate for the small aeration tank with airflow rates of 0.22, 0.83, and 1.3 L min^{-1} is shown in Figure 3.6. The highest percentage of carbohydrate reduction, i.e., 90%, was obtained with an airflow rate of 1.3 L min^{-1} . The results indicated that the aerobic wastewater treatment process with the airflow rate of 0.22– 1.14 L min^{-1} was under oxygen transfer limitation; further process improvement can be achieved by increasing the airflow rate.

Further experiments were conducted in a large aeration tank, 15 L batch system to study the cell dry weight, COD, carbohydrate, DO, and oxygen transfer modeling. Two different airflow rates, 5 and 10 L min^{-1} , were applied. However, owing to the failure and operation limitation of the system, the system could only operate for 8 h a day. The COD, cell dry weight, carbohydrate, and DO concentrations for the experimental run with an airflow rate of 5 L min^{-1} are presented in Figure 3.7.

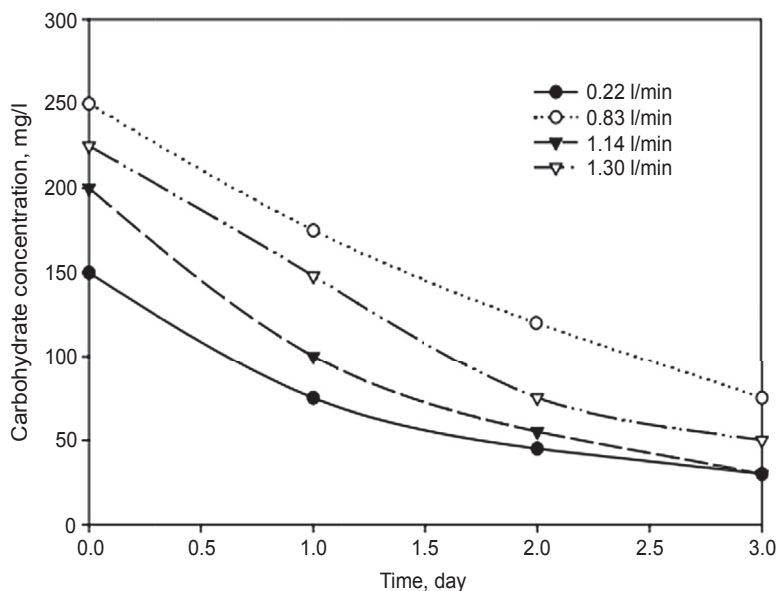


FIGURE 3.6 Reduction of carbohydrate in an aeration tank at various flow rates.

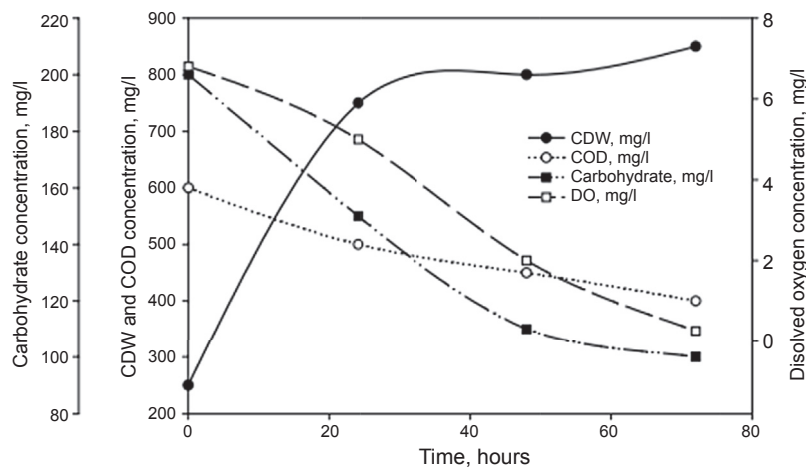


FIGURE 3.7 COD, cell dry weight (CDW), carbohydrate, and dissolved oxygen concentration in a 15 L aeration tank at an airflow rate of 5 L min^{-1} .

It was expected that the DO for the 5 L min^{-1} system would decrease with time because the system was running in an oxygen-limited condition. The concentration of the oxygen approached zero percent on the third day of the experiment. Although the system was running in an oxygen transfer limiting condition, the microbes achieved maximal growth at 24 h. The reduction of COD and carbohydrate were 40 and 74%, respectively. The

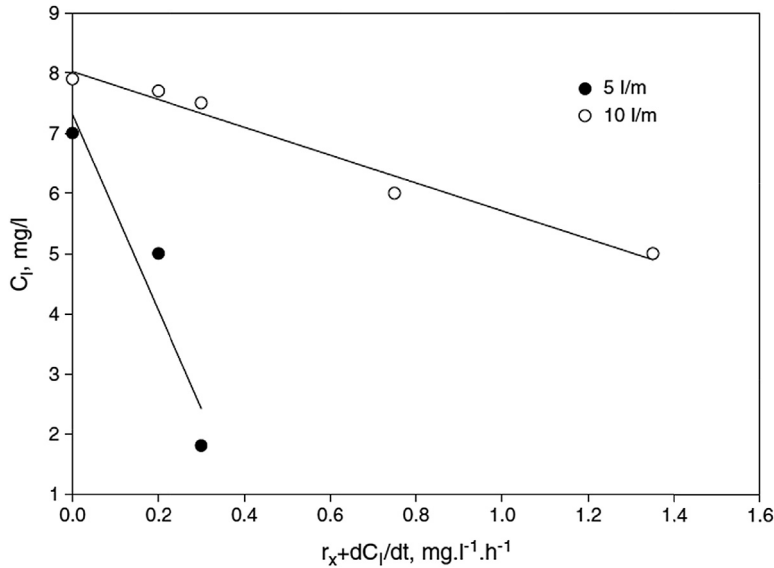


FIGURE 3.8 Experimental data for DO concentration level in liquid phase at 5 and 10 L min⁻¹.

experimental results showed that the system required more aeration. Therefore, an airflow rate of 5 L min⁻¹ was not sufficient, and the calculation of $K_L \cdot a$ might cause error.

When the airflow rate was doubled, there was sufficient oxygen for optimum microbial growth. Theoretically, under sufficient aeration conditions, the concentration of DO in the system should be constant; however, because of the reason mentioned above, the DO curve showed a drop in the oxygen concentration from 24 to 30 h. The DO was available at around 5–8 mg L⁻¹ during the aeration. The oxygen transfer coefficient $K_L \cdot a$ for the above system can be estimated by applying the following mathematical model (3.13.3.1). A graph of C_L against $(-r_X + dC_L/dt)$ was plotted as presented in Figure 3.8 for the 15 L aeration tank system with 5 and 10 L min⁻¹ limitation. The experimental data as presented in Figure 3.5 show good agreement for 10 L min⁻¹ airflow rate. The oxygen transfer coefficient for 5 and 10 L min⁻¹ airflow rate was 0.0509 and 0.3918 h⁻¹, respectively. The superficial gas velocity (v_s) for the turbulent flow region was predicted to be around 0.18 and 1.3 m s⁻¹ for the airflow rates of 5 and 10 L min⁻¹, respectively, for the given correlation. The experimental data were compatible with the theoretical correlation.

$$\frac{dC_L}{dt} = K_L \cdot a(C^* - C_L) - rx \quad (3.13.3.1)$$

3.13.4 CONCLUSION

$K_L \cdot a$ and v_s for the 10 L min⁻¹ airflow rate for the 15 L aeration system were 0.0509 h⁻¹ and 1.3 m s⁻¹, respectively. From the experimental results, the microbial growth was not at the

optimum stage for the reasons mentioned earlier. Nevertheless, a reduction of around 95% can be achieved for carbohydrate reduction. However, further studies should be carried out for optimization of the treatment and to improve COD reduction for pharmaceutical wastewater treatment.

NOMENCLATURE

- C_o Initial concentration, mg L^{-1}
 C Concentration, mol m^{-3}
 C_L Concentration in the bulk of liquid, mol m^{-3}
 x Biomass concentration, g L^{-1}
 N_A Molar rate, $\text{mol m}^{-3} \text{ h}^{-1}$
 $K_L \cdot a$ Mass transfer coefficient in liquid phase, h^{-1}
 C^* Oxygen concentration in equilibrium with liquid phase at the interface, mol m^{-3}
 Q_{O_2} Oxygen absorption rate, $\text{mol L}^{-1} \text{ h}^{-1}$
 P_g Gassed power, W
 V_l Volume of liquid in the fermenter, m^3
 $-r$ Consumption rate of substrate, $\text{mol L}^{-1} \text{ s}^{-1}$
 t Time, h

References

1. Eckenfelder WW. *Industrial water pollution control*. 3rd ed. New York: McGraw-Hill; 2000. p. 341.
2. Scragg AH. *Bioreactors in biotechnology*. New York: Ellis Horwood; 1997.
3. Deronzier G, Duchene Ph, Heduit A. *Wat Sci Technol* 1998;**38**(3):35.
4. Badino Jr CA, Facciotti MCR, Schmidell WJ. *Chem Technol Biotechnol* 2000;**75**:469.
5. Chern J-M, Yu C-F. *Indust Eng Chem Res* 1997;**36**:5447.
6. Bailey J, Ollis DF. *Biochemical engineering fundamentals*. New York: McGraw-Hill; 1986.
7. Greenberg AE, Clesceri LS, Eaton AD. *Standard methods for the examination of water and wastewater*. 18th ed. Washington, DC: American Public Health Association, American Water and Wastewater Association, Water Environment Federation; 1992.
8. Summers JB. *J Biol Chem* 1924;**62**:248.
9. Thomas LC, Chamberlin GJ. *Colorimetric chemical analytical methods*. Salisbury, United Kingdom: Tintometer Ltd; 1980.

SUBCHAPTER

3.14

Case Study: Fuel and Chemical Production from the Water–Gas Shift Reaction by Fermentation Processes*

3.14.1 INTRODUCTION

Synthesis gas (syngas), a mixture of primarily CO, H₂, and CO₂ is a major building block in the production of fuels and chemicals.^{1,2} Syngas is produced from several sources, including coal, oil shale, tar sands, heavy residual oil, or low-grade natural gas.^{3,4} Catalytic processes are used to convert syngas components into a variety of fuels and chemicals, such as hydrogen, methane, methanol, ethanol, acetic acid, etc.⁵ Microorganisms are used as suitable biocatalysts to convert syngas into chemicals and fuels. Biological processes, although generally slower than chemical reaction, have several advantages over catalytic processes, such as higher specificity, higher yields, lower energy cost, and generally greater resistance to catalyst poisoning. Furthermore, the irreversible character of biological reactions allows complete conversion and avoids thermodynamic equilibrium.^{5,6}

Anaerobic bacteria are able to grow autotrophically on syngas components. They follow specific pathways to produce fuels and chemicals from inorganic waste gases.⁷ The reaction occurs under mild conditions, ambient temperature, and pressure with the formation of specific products.⁸ However, direct production of fuels and chemicals by gasification technology is economically unfavorable and requires a very large plant.^{9,10} Suitable microorganisms may be used for production of fuels and chemicals from bioconversion of syngas. Fermentation needs substrates such as CO or CO₂ to provide energy for bacterial growth, maintenance, and by-products such as organic acid, alcohols, and hydrogen that result from microbial metabolism.^{11,12} A recent investigation was conducted using suitable microorganisms to produce acetic acid and ethanol from H₂, CO, and CO₂. The organism must be anaerobic and grow either chemolithotrophically on CO and H₂/CO₂ or chemoorganotrophically with carbon sources such as fructose, malate, glutamate, or pyruvate. It has been reported that

*This case study was partially written with contributions from:

Habibollah Younesi, Department of Environmental Science, Faculty of Natural Resources, Tarbiat Modares University, Noor, Iran;

Abdul Rahman Mohamed, School of Chemical Engineering, Engineering Campus, Universiti Sains Malaysia, 14300 Nibong Tebal, Pulau Pinang, Malaysia.

CO, H₂, and CO₂ can be converted to acetate by several bacteria such as *Clostridium aceticum*, *Acetobacterium woodii*, *Clostridium ljungdahlii*, and *Clostridium thermoaceticum*.^{13–15}

Generally, bacteria in the fermentation process require substrates like glucose, sucrose, malate, or acetate as carbon sources to obtain energy for growth and maintenance for synthesis of organic acids, alcohols, and hydrogen, which are liberated in the course of microbial metabolism.^{3,16} It is believed that for oxidation of CO, acetyl coenzyme A is required to enter CO into the citric acid cycle. *Rhodospirillum rubrum* is capable of producing carbon monoxide dehydrogenase (CODH) to facilitate the oxidation process.¹⁷ It was stated that synthetic gases were converted to molecular hydrogen with the aid of several photosynthetic bacteria, for instance *C. aceticum*, *A. woodii*, *C. ljungdahlii*, and *C. thermoaceticum*, which are able to produce fuels and chemicals.^{12,13}

Purple nonsulfur phototrophic anaerobic bacteria use light (photons) to produce hydrogen by a biological route. The metabolites of photosynthetic bacteria are organic acids or carbon monoxide as the energy source. Bacteria grown on carbon monoxide produce molecular hydrogen and carbon dioxide and generate no by-product. The CODH from methanogenic bacteria is the key enzyme in CO metabolism.¹⁸ It has been reported that light and acetate are present during hydrogen formation, in which light is required for hydrogen evolution and acetate is not consumed during hydrogen production.¹⁹ Reports in the literature state that *R. rubrum* can be grown on organic components. Photoheterotrophic growth is based on most intermediate metabolites in the tricarboxylic acid (TCA) cycle. The major precursor in this pathway is an acetylating agent for the synthesis of other components and coenzyme A (CoA). Acetyl CoA is the key component for entering the TCA cycle. In this cycle, molecular hydrogen and carbon dioxide are continuously evolved.²⁰

In the past decade, an increasing interest in biological utilization of gaseous substrates has developed in several bioprocesses for fuel synthesis.^{18,21} Production of chemicals and fuels from gaseous substrates was demonstrated in biocatalytic processes. It has also been reported that biological processes are used to convert gaseous substrates such as CO/H₂ or CO₂/H₂ to ethanol and acetate at ambient temperature and atmospheric pressure.²² The reactions are generally carried out in the aqueous phase, where microorganisms are suspended as free cells or in flocs. The advantages of microbial processes are stated as the product specificity, yielding few by-products and high process yield. Also, the resistance of biocatalysts has been found to be higher than chemical catalysts. In industrial gas streams, chemical catalysts are easily inhibited by trace contaminants such as H₂S and COS. Therefore, the economic attraction of biological processes in the development of suitable biocatalysts to ferment gaseous substrates to valuable products has been considered.^{23–25}

In the present study, a strictly anaerobic bacterium, *C. ljungdahlii*, was used to investigate ethanol and acetate production by bioconversion of syngas at various total pressures of syngas in a series of batch bioreactors. The significant aspect of this fermentation was to investigate the bioconversion of syngas to commercial fuels. The effects of initial total pressure of syngas on microbial cell population, substrate and product inhibition in the culture were also studied.

3.14.2 KINETICS OF GROWTH IN A BATCH BIOREACTOR

When microbial cells are inoculated into a batch bioreactor containing fresh media, their increase in concentration can be monitored.²⁶ It is common to use the cell dry weight as a

measurement of cell concentration. The simplest relationships describing exponential cell growth are unstructured models. Unstructured models view the cell as an entity in solution, which interacts with the environment. One of the simplest models is that of Malthus^{27,28}:

$$\frac{dx}{dt} = \mu x \quad (3.14.2.1)$$

where x is the cell dry weight in g L^{-1} , μ is specific growth rate in h^{-1} , and t is time in h. This model predicts unlimited growth with time. We can propose an inhibition term to provide limited growth that is dependent on cell concentration. We assume that the limiting substrate is consumed according to first-order kinetics:

$$\frac{dS}{dt} = -k_s S \quad (3.14.2.2)$$

where S is the substrate concentration in g L^{-1} and k_s is first-order rate constant in h^{-1} . We also assume that the substrate is converted with a fixed yield factor:

$$Y_{x/S} = -\frac{\Delta x}{\Delta S} = -\frac{x - x_o}{S - S_o} \quad (3.14.2.3)$$

where $Y_{x/S}$ is yield coefficient in $\text{g cell/g substrate}$, x_o is inoculum concentration, and S_o is initial substrate concentration in g L^{-1} . Rearranging Eqn (3.14.2.3) gives²⁸:

$$S = \frac{x_o + Y_{x/S} S_o - x}{Y_{x/S}} \quad (3.14.2.4)$$

Maximum cell dry weight is inoculum size plus coefficient yield multiplied by inocula concentration, with the assumption that substrate is converted to biomass^{27,29}:

$$x_m = x_o + Y_{x/S} S_o \quad (3.14.2.5)$$

Inserting Eqn (3.14.2.5) into Eqn (3.14.2.4) yields²⁸:

$$S = \frac{x_m - x}{Y_{x/S}} = \frac{x_m}{Y_{x/S}} \left(1 - \frac{x}{x_m} \right) \quad (3.14.2.6)$$

Applying the chain rule principle on the right-hand side of Eqn (3.14.2.2):

$$\frac{dS}{dx} \frac{dx}{dt} = -k S \quad (3.14.2.7)$$

Introducing yield coefficient into Eqn (3.14.2.7):

$$\frac{dx}{dt} = k Y_{x/S} S \quad (3.14.2.8)$$

Inserting Eqn (3.14.2.6) into Eqn (3.14.2.8) gives:

$$\frac{dx}{dt} = k x_m \left(1 - \frac{x}{x_m} \right) \quad (3.14.2.9)$$

Equations (3.14.2.9) contributes to the postulated model that is induced by an inhibition factor for the population growth rate. Assuming that the inhibition is second-order with respect to cell dry weight (x^2), then the equation becomes²⁷:

$$\frac{dx}{dt} = \mu_m x \left(1 - \frac{x}{x_m} \right) \quad (3.14.2.10)$$

where μ_m is the maximum specific growth rate in h^{-1} . This equation is known as the Riccati equation, which can be easily integrated to give the logistic equation:

$$x = \frac{x_o e^{\mu_m t}}{1 - (x_o/x_m)(1 - e^{\mu_m t})} \quad (3.14.2.11)$$

The logistic equation leads to a lag phase, an exponential initial growth rate, and a stationary population of concentration (x_m). In a population, it is often the case that the birth rate decreases as the population itself increases. The reasons may vary from increased scientific or cultural sophistication to a limited food supply.

It is useful to develop a more general population model that accommodates birth and death rates that are not necessarily constant. Initially, living cells are inoculated into the batch bioreactor containing the nutrients to begin the growth process. Suppose that the population changes only by the occurrence of births and deaths, and there is no immigration from the outside environment under consideration. It is customary to track the growth or decline of population in terms of its birth rate and death rate. To describe the above discussion in mathematical form, the Malthus function can be written for the species that is growing after inoculation²⁸:

$$\frac{dx_1}{dt} = \mu x_1 \quad (3.14.2.12)$$

To include a linear decreasing function of the population size, the second-order cell population inhibition is considered:

$$\mu = \mu_m \left(1 - \frac{x_1 x_2}{x_m^2} \right) \quad (3.14.2.13)$$

where x_1 is growing cells in g L^{-1} and x_2 is declining cells as a result of either the toxic byproducts or depletion of nutrient supply. Substituting Eqn (3.14.2.12) into Eqn (3.14.2.13) gives:

$$\frac{dx_1}{dt} = \mu_m x_1 \left(1 - \frac{x_1 x_2}{x_m^2} \right) \quad (3.14.2.14)$$

The products that inhibit the cell population in the bioreactor and promote the cell population give³⁰:

$$\frac{dx_2}{dt} = k x_2 \quad (3.14.2.15)$$

where x_1 and x_2 are cell species in g L^{-1} and k is the decline or promotion constant in h^{-1} . This means that k is negative when the cell population is inhibited by toxic chemicals, and

k is positive when the cell population is promoted by nutrient. Integrating from Eqn (3.14.2.14) yields:

$$x_2 = x_{02}e^{kt} \quad (3.14.2.16)$$

Inserting Eqn (3.14.2.16) into Eqn (3.14.2.14) provides:

$$-\frac{dx_1}{dt} + \mu_m x_1 = x_1^2 \frac{x_{02}\mu_m}{x_m^2} e^{kt} \quad (3.14.2.17)$$

Equation (3.14.2.17) shows the form of the Bernoulli equation that is a first-order differential equation. By substituting Eqn (3.14.2.18):

$$u = \frac{1}{x_1}, \quad \text{and} \quad -\frac{dx_1}{dt} = x_1^2 \frac{du}{dt} \quad (3.14.2.18)$$

u is new dependent variable. Transfer Eqn (3.14.2.17) into the linear equation:

$$\frac{du}{dt} + \mu_m u = \frac{x_{02}\mu_m}{x_m^2} e^{kt} \quad (3.14.2.19)$$

which is a first-order linear differential equation of the form:

$$\frac{dy}{dx} + P(x)y = Q(x) \quad (3.14.2.20)$$

By multiplying through the integration factor $e^{\int P(x)dx}$ the solution is:

$$y = e^{-\int P(x)dx} \left[\int Q(x)e^{\int P(x)dx} dx + B \right] \quad (3.14.2.21)$$

Applying this general procedure to the integration of Eqn (3.14.2.19) gives:

$$u = e^{-\int \mu_m dt} \left[\int e^{\int \mu_m dt} \left(\frac{x_{02}\mu_m}{x_m^2} \right) e^{kt} dt + B \right] \quad (3.14.2.22)$$

Then,

$$u = e^{-\mu_m t} \left[\left(\frac{x_{02}\mu_m}{x_m^2} \right) \int e^{(k+\mu_m)t} dt + B \right] \quad (3.14.2.23)$$

By integrating Eqn (3.13.2.23) we obtain:

$$u = \left(\frac{x_{02}}{x_m^2} \right) \left(\frac{\mu_m}{k + \mu_m} \right) e^{kt} + B e^{-\mu_m t} \quad (3.14.2.24)$$

Substituting Eqn (3.14.2.18) into Eqn (3.14.2.24) yields:

$$x_1 = \frac{1}{\left(\frac{x_{02}}{x_m^2} \right) \left(\frac{\mu_m}{k + \mu_m} \right) e^{kt} + B e^{-\mu_m t}} \quad (3.14.2.25)$$

Solving Eqn (3.14.2.25) for initial value problems and applying pure culture with a single species (x) gives²⁸:

$$x = \frac{x_0 e^{\mu_m t}}{1 - \left(\frac{x_0}{x_m}\right)^2 \left(\frac{\mu_m}{k + \mu_m}\right) [1 - e^{(k + \mu_m)t}]} \quad (3.14.2.26)$$

Equation (3.14.2.26) is the novel population equation, which describes the cell population with inhibition or promotion.^{27,29}

3.14.3 EFFECT OF SUBSTRATE CONCENTRATION ON MICROBIAL GROWTH

Equation (3.14.2.11) predicts the cell dry weight concentration with respect to time. The model shows the cell dry weight concentration (x) is independent of substrate concentration. However, the logistic model includes substrate inhibition, which is not clearly seen from Eqn (3.14.2.11).

Figure 3.9 shows the growth of *R. rubrum* in a batch fermentation process using a gaseous carbon source (CO). The data shown follow the logistic model as fitted by Eqn (3.14.2.11) with the solid lines, which also represent an unstructured rate model without any lag phase. The software Sigma Plot was used to fit model Eqn (3.14.2.11) to the experimental data.

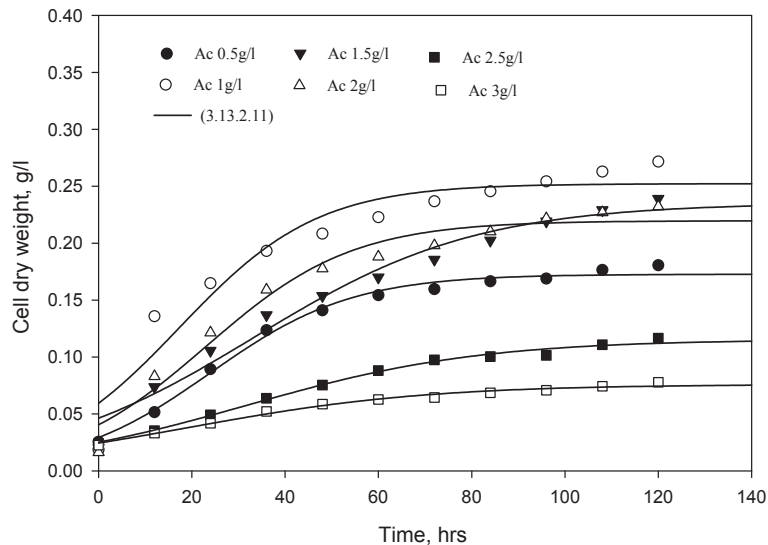


FIGURE 3.9 Cell dry weight of *R. rubrum* grown on various acetate concentrations at an agitation speed of 200 rpm and light intensity of 1000 lux.

An increase in concentration of acetate in the prepared culture media did not improve the cell dry weight at values of 2.5 and 3 g L⁻¹ acetate, as shown in the figure.^{9,13,31} However, the exponential growth rates were clearly observed to change with acetate concentrations of 0.5–2 g L⁻¹ in the culture.^{32,33}

It was found that the substrate consumption rate followed first-order kinetics with respect to substrate concentration.^{34,35} The expression of substrate consumption with time is written in a first-order differential equation.

After separating the variables, Eqn (3.14.2.2) was solved by integration, and the initial conditions were implemented ($t = 0, S = S_0$). The resulting expression is^{36,37}:

$$S = S_0 \exp(-k_S t) \quad (3.14.3.1)$$

where S_0 is the initial substrate concentration in g L⁻¹ and k_S is the substrate consumption rate constant in h⁻¹.

Figure 3.10 shows the time course consumption of varying acetate concentrations in batch culture for 120 h. An alternative way to describe substrate utilization of microorganisms is to use first-order reaction kinetics, i.e. Eqn (3.14.3.1). The software Sigma Plot 5 was used to compare the fitted equation with the experimental data. Acetate concentration (3 g L⁻¹) was slightly decreased, while the reduction of acetate concentration for 1–2 g L⁻¹ was significantly higher. Acetate conversion dropped from 73% to 23% when acetate concentration was doubled from 1.5 to 3 g L⁻¹. This indication may represent inhibition of substrate in the batch

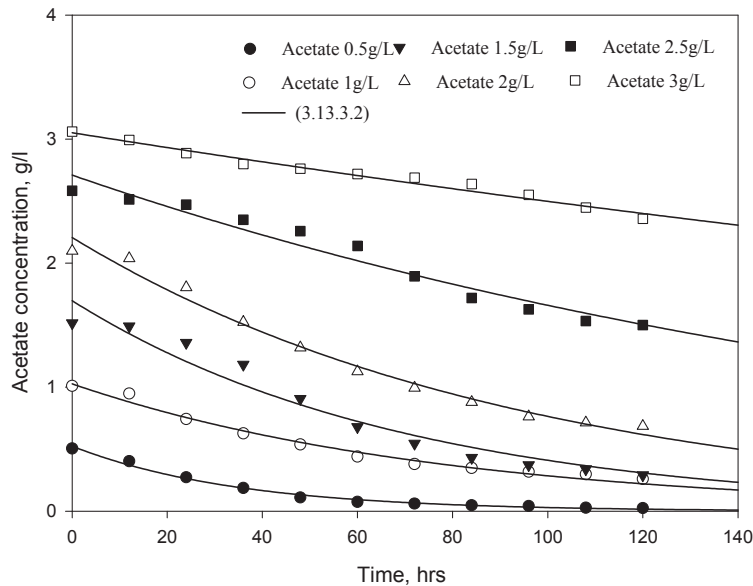


FIGURE 3.10 Acetate reduction in batch cultivation of *R. rubrum* at an agitation speed of 200 rpm and light intensity of 1000 lux.

media to retard the microbial growth rate. The objective of variation in acetate concentration was to investigate and identify a suitable acetate concentration for desired cell population and hydrogen production from synthesis gas.^{38,39}

When microbial cells were incubated into a batch culture containing fresh culture media, an increase in cell concentration was observed. It is common to use cell dry weight as a measurement of cell concentration.^{19,40} The simplest relation describes the exponential growth as an unstructured model. Microbial cell growth is an autocatalytic reaction in which the growth rate is proportional to the cell concentration initially present in the media.⁴¹ In fact, the microbial populations in which there is increase in biomass are accompanied by an increase in the number of cells. The practicalities for growing bacteria in suitable culture depend on both the type of organisms and the system being used, but the microbial growth theory is applied universally.¹⁹ The batch system is a closed system, which would only maintain cell viability for a limited time, and the growth cycle changes progressively from one phase to another in the remaining media and environmental conditions.⁴² The logistic equation leads to an exponential initial growth rate and a stationary population of concentration (x_m). But the logistic equation does not predict the death phase of microorganisms after the stationary phase. In this research, a modified equation was introduced that can predict the death phase of bacteria after the stationary phase. Figure 3.11 shows the simulation of the cell dry weight versus time. The Eqn (3.14.2.1) fitted fairly with experimental data. The simulated value was plotted with various values of k in Figure 3.9, k is a constant value, which is associated with the promotion or decline of the cell population in the batch system. On the other hand, the

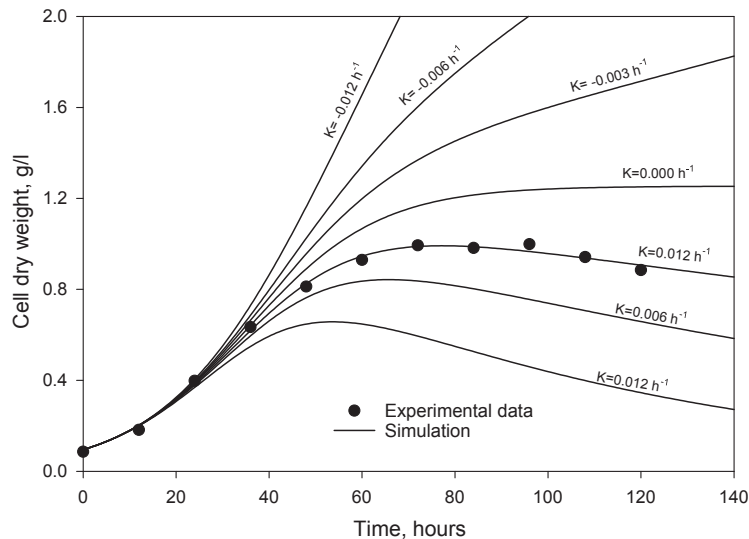


FIGURE 3.11 Growth simulation of *C. ljungdahliae* on synthesis gas in batch bioreactor, the experimental data are average values.

negative value of k shows the decline of cell population, whereas a positive value of k shows the promotion in the cell population. The maximum cell dry weight concentration (x_m) was 1.2 g L^{-1} , when the inhibition value was 0.003 h^{-1} . The maximum cell dry weight reached 1.5 g L^{-1} when the growth inhibition ($k = 0$) was not observed. The determination coefficient of the fit (R^2) was 0.997.

3.14.4 MASS TRANSFER PHENOMENA

The simplest theory involved in mass transfer across an interface is film theory, as shown in Figure 3.12. In this model, the gas (CO) is transferred from the gas phase into the liquid phase and it must reach the surface of the growing cells. The rate equation for this case is similar to the slurry reactor as mentioned by Levenspiel.²⁹

The rate of CO transport from the bulk gas into the gas and liquid films is as follows:

$$r'_{\text{CO}} = k_{\text{CO,gas}} a_i (P_{\text{CO,gas}} - P_{\text{CO,i}}) \quad (3.14.4.1)$$

$$r'_{\text{CO}} = k_{\text{CO,liquid}} a_i (C_{\text{CO,i}} - C_{\text{CO,liquid}}) \quad (3.14.4.2)$$

where r'_{CO} is the rate of mass transfer for component CO in $\text{mol L}^{-1} \text{ h}^{-1}$; $k_{\text{CO,gas}}$ and $k_{\text{CO,liquid}}$ are the mass transfer coefficients in gas and liquid phases in m h^{-1} , respectively; a_i is the interfacial area in $\text{m}^2 \text{ m}^{-3}$; $P_{\text{CO,gas}}$ and $P_{\text{CO,i}}$ are partial pressure of gaseous substrate CO at gas phase and interface in atm, respectively; and $C_{\text{CO,i}}$ and $C_{\text{CO,liquid}}$ are concentrations of component CO in the interface and liquid phase in mol L^{-1} , respectively.

Because the interface region is thin, the flux across a thin film will be at steady state. Therefore, the transfer rate to the gas–liquid interface is equal to its transfer rate through the liquid-side film. Thus:

$$k_{\text{CO,gas}} a_i (P_{\text{CO,gas}} - P_{\text{CO,i}}) = k_{\text{CO,liquid}} (C_{\text{CO,i}} - C_{\text{CO,liquid}}) \quad (3.14.4.3)$$

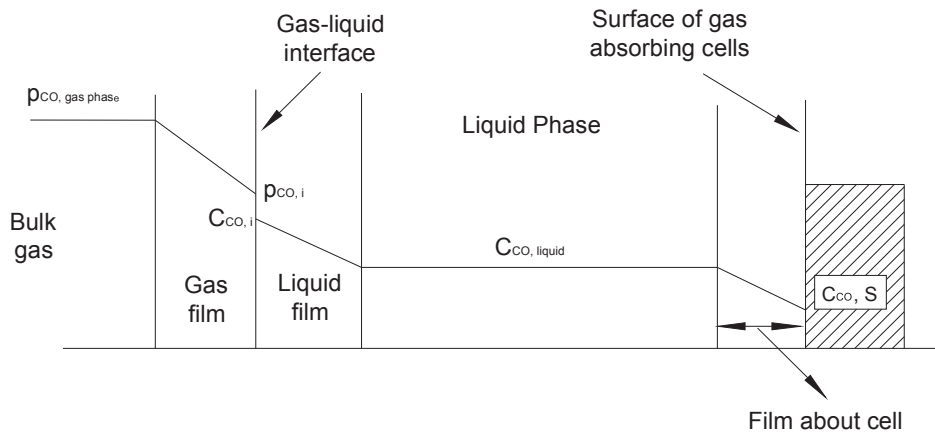


FIGURE 3.12 The film theory for mass transfer.

At the interface, the relation between $P_{\text{CO},i}$ and $C_{\text{CO},i}$ is given by the distribution coefficient, called Henry's constant (H) for gas–liquid systems. Thus:

$$P_{\text{CO},i} = HC_{\text{CO},i} \quad (3.13.4.4)$$

Substituting Eqn (3.14.4.4) into Eqn (3.14.4.3) gives:

$$k_{\text{CO},\text{gas}}a_i(P_{\text{CO},\text{gas}} - P_{\text{CO},i}) = k_{\text{CO},\text{liquid}}a_i\left(\frac{P_{\text{CO},i}}{H} - C_{\text{CO},\text{liquid}}\right) \quad (3.14.4.5)$$

Rearranging Eqn (3.13.4.5) for $P_{\text{CO},i}$ gives:

$$P_{\text{CO},i} = \frac{k_{\text{CO},\text{gas}}a_iP_{\text{CO},\text{gas}} + k_{\text{CO},\text{liquid}}a_iC_{\text{CO},\text{liquid}}}{\frac{k_{\text{CO},\text{liquid}}a_i}{H} + k_{\text{CO},\text{gas}}a_i} \quad (3.14.4.6)$$

Substituting Eqn (3.14.4.6) into Eqn (3.14.4.1) gives:

$$r'_{\text{CO}} = \frac{k_{\text{CO},\text{gas}}a_i k_{\text{CO},\text{liquid}}a_i}{\frac{k_{\text{CO},\text{liquid}}a_i}{H} + k_{\text{CO},\text{gas}}a_i} \left(\frac{P_{\text{CO},\text{gas}}}{H} - C_{\text{CO},\text{liquid}} \right) \quad (3.14.4.7)$$

Rearranging Eqn (3.14.4.7) gives:

$$r'_{\text{CO}} = \frac{1}{\frac{1}{k_{\text{CO},\text{liquid}}a_i} + \frac{1}{Hk_{\text{CO},\text{gas}}a_i}} \left(\frac{P_{\text{CO},\text{gas}}}{H} - C_{\text{CO},\text{liquid}} \right) \quad (3.14.4.8)$$

which results in a relation between the overall mass transfer coefficient, $K_L \cdot a$, and the physical parameters of the two-film transport, k_{gas} and k_{liquid} .

$$\frac{1}{K_L \cdot a} = \frac{1}{k_{\text{CO},\text{liquid}}a_i} + \frac{1}{Hk_{\text{CO},\text{gas}}a_i} \quad \text{and} \quad C^* = \frac{P_{\text{CO},\text{gas}}}{H} \quad (3.14.4.9)$$

For slightly soluble gas, such as CO, Henry's constant is large.^{27,29} Thus, $k_{\text{CO},\text{gas}}$ is considerably larger than $k_{\text{CO},\text{liquid}}$. That makes $K_L \cdot a$ equal to $k_{\text{CO},\text{liquid}}a_i$. Thus, essentially, all the resistances to mass transfer lie on liquid-film side. Therefore:

$$r'_{\text{CO}} = K_L \cdot a (C^* - C_{\text{CO},\text{liquid}}) \quad (3.14.4.10)$$

where $K_L \cdot a$ is the overall volumetric mass transfer coefficient, C^* is the concentration of CO in equilibrium with the bulk gas partial pressure in mol L^{-1} , and $C_{\text{CO},\text{liquid}}$ is the concentration of CO in the bulk liquid in mol L^{-1} .

The reaction rate ($-r_{\text{CO}}$) for a constant volume batch reactor system is equal to the rate of mass transfer (r'_{CO}):

$$r'_{\text{CO}} = -r_{\text{CO}} = -\frac{1}{V_L} \frac{dN_{\text{CO},\text{gas}}}{dt} = -\frac{dC_{\text{CO},\text{gas}}}{dt} = \frac{dC_{\text{CO},\text{liquid}}}{dt} \quad (3.14.4.11)$$

Then, substituting Eqn (3.14.4.11) into Eqn (3.14.4.8) yields:

$$-r_{\text{CO}} = -\frac{1}{V_L} \frac{dN_{\text{CO},\text{gas}}}{dt} = \frac{K_L \cdot a}{H} (P_{\text{CO},\text{gas}} - P_{\text{CO},\text{liquid}}) = \frac{K_L \cdot a}{H} \Delta p \quad (3.14.4.12)$$

where

$$\frac{H}{K_L \cdot a} = \frac{1}{Hk_{\text{CO,gas}}a} + \frac{1}{k_{\text{CO,liquid}}a} \quad (3.14.4.13)$$

Henry's Constant (H) for CO at 30 and 38 °C is 1.116 and 1.226 atm L mmol⁻¹ CO.^{27,29,43}

Based on assumption, the rate of reaction is absolutely controlled by the mass transfer process, the dissolved CO in liquid phase penetrates into the cell, then microorganisms rapidly use the transferred CO in the reaction center. These phenomena may not be justified for the fresh inocula entering the culture media; however, once the culture is dominated by active organisms, the concentration of CO in the gas phase decreases as the propagation of microorganisms increases. Therefore, the concentration of CO in the liquid phase decreases nearly to zero. That justifies making an assumption, i.e. $P_{\text{CO,liquid}} = 0$. This means that the CO molecules available in the liquid phase are rapidly used by the microorganisms. Thus, the rate of mass transfer can be proportional to the partial pressure of CO in the gas phase, as expected by Eqn (3.14.4.12). Therefore, Eqn (3.14.4.12) can be simplified in the regime of mass transfer control by the following expression^{21,23}:

$$-\frac{1}{V_L} \frac{dN_{\text{CO,gas}}}{dt} = \frac{K_L \cdot a}{H} P_{\text{CO,gas}} \quad (3.14.4.14)$$

The plot of the rate of disappearance of CO per volume of liquid in the serum bottles versus partial pressure of CO in the gas phase based on Eqn (3.14.4.14) could give the constant slope value of $K_L \cdot a/H$. Henry's constant is independent of the acetate concentration, but it is only dependent on temperature. The overall volumetric mass transfer coefficient can be calculated based on the above assumption. The data for various acetate concentrations and different parameters were plotted to calculate the mass transfer coefficient.⁴⁴

Figure 3.13 illustrates the mass transfer coefficient for batch-grown *R. rubrum* and was computed with various acetate concentrations at 200 rpm agitation speed, 500 lux light intensity, and 30 °C. As the experiment progressed, there was an increase in the rate of carbon monoxide uptake in the gas phase and a gradual decrease in the partial pressure of carbon monoxide. Also, a decrease in the partial pressure of carbon monoxide was affected by acetate concentration in the culture media. The value of the slope of the straight line increased with the decrease in acetate concentrations, i.e. 2.5–1 g L⁻¹. The maximum mass transfer coefficient was obtained for 1 g L⁻¹ acetate concentration ($K_L \cdot a = 4.3 \text{ h}^{-1}$). The decrease in mass transfer coefficient was observed with the increase in acetate concentration. This was due to acetate inhibition on the microbial cell population as acetate concentration increased in the culture media. The minimum $K_L \cdot a$ was 1.2 h⁻¹ at 3 g L⁻¹ acetate concentration.

3.13.5 KINETIC OF WATER GAS SHIFT REACTION

Since there are various specific growth rates and different values of rate constants while substrate concentration varies, mix inhibition exists. Andrew⁴⁵ incorporated a substrate

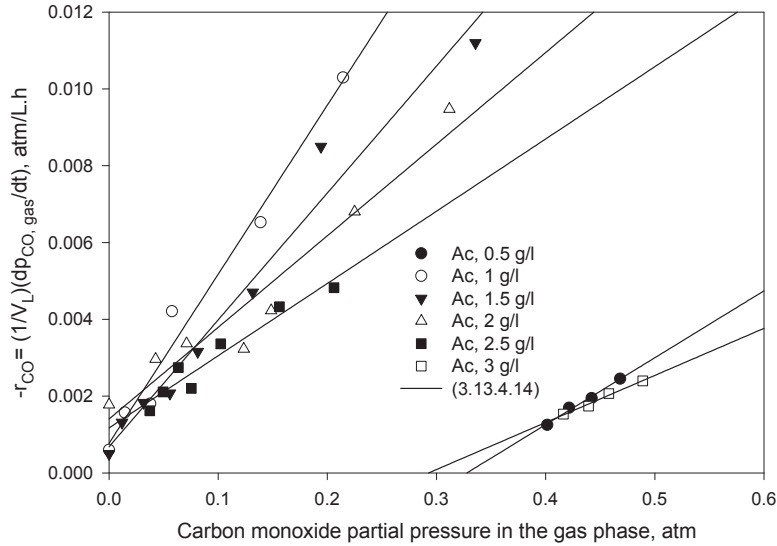


FIGURE 3.13 Rate of CO uptake by *R. rubrum* with various acetate concentrations at agitation speed of 200 rpm and light intensity of 500 lux.

inhibition model¹⁴ in the Monod equation; the modified Monod equations with second-order substrate inhibition are presented in Eqns (3.14.5.1) and (3.14.5.2)^{22,23}:

$$\mu = \frac{\mu_m P_{\text{CO},\text{liquid}}}{K_p + P_{\text{CO},\text{liquid}} + P_{\text{CO},\text{liquid}}^2 / K_i} \quad (3.14.5.1)$$

$$q_{\text{CO}} = \frac{q_m p_{\text{CO},\text{liquid}}}{K'_p + P_{\text{CO},\text{liquid}} + P_{\text{CO},\text{liquid}}^2 / K'_i} \quad (3.14.5.2)$$

where K_i and K'_i are the substrate inhibition constants. To obtain the maximum specific growth rate and Monod constant, a linear model of $1/\mu$ versus $1/P_{\text{CO},\text{liquid}}$ was plotted to fit the experimental data in a linear regression model. Equations (3.14.5.2) and (3.14.5.3) are rearranged for the linearized model to compute the substrate inhibition constants as shown below^{22,23}:

$$\frac{P_{\text{CO},\text{liquid}}}{\mu} = \frac{K_p}{\mu_m} + \frac{P_{\text{CO},\text{liquid}}}{\mu_m} + \frac{P_{\text{CO},\text{liquid}}^2}{\mu_m K_i} \quad (3.14.5.3)$$

$$\frac{P_{\text{CO},\text{liquid}}}{q_{\text{CO}}} = \frac{K'_p}{q_m} + \frac{P_{\text{CO},\text{liquid}}}{q_m} + \frac{P_{\text{CO},\text{liquid}}^2}{q_m K'_i} \quad (3.14.5.4)$$

The experimental data followed the predicted model, and the line represents the above stated function. The presented data indicate that the range of concentrations in this study

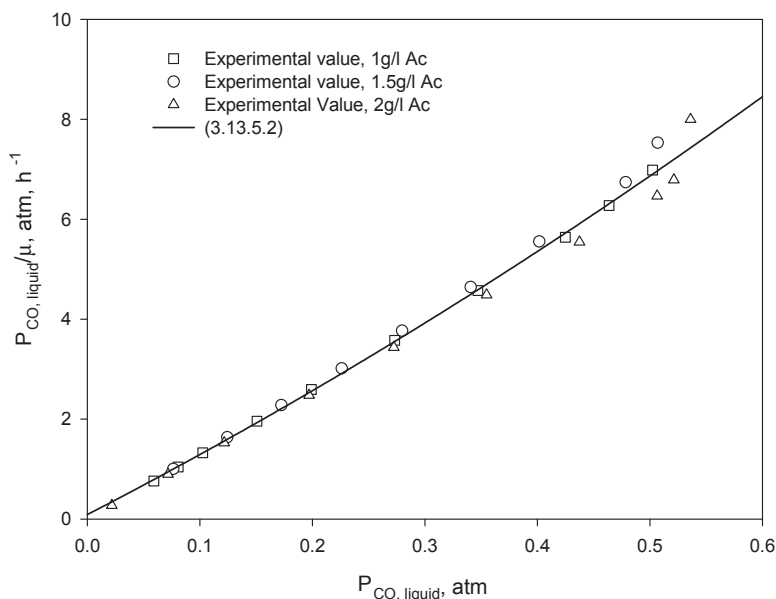


FIGURE 3.14 Quadratic model based on Eqn (3.14.5.2) with substrate inhibition at an agitation speed of 200 rpm and light intensity of 500 lux.

exhibited an observed substrate inhibition. The experimental data from the current studies were observed to fit the predicted model based on Andrew's modified equations.

Figures 3.14 and 3.15 show the kinetic parameter evaluation of Eqns (3.14.5.2) and (3.14.5.4), i.e. μ_m , q_m , K_p , and K'_p . The inhibition phenomena were examined for the growth rate and the rate of CO uptake. The experimental data followed the quadratic manner as presented in the Eqns (3.14.5.2) and (3.14.5.4). The Sigma Plot 5 was used to calculate coefficients of Eqns (3.14.5.2) and (3.14.5.4). The specific growth rate and CO uptake rate was considered at 1, 1.5, and 2 g L⁻¹ acetate concentrations, light intensity of 500 lux, and 200 rpm agitation speed.

Table 3.3 shows the kinetic parameters for cell growth, rate models with or without inhibition, and mass transfer coefficient calculation at various acetate concentrations in the culture. The Monod constant value, K_M , in the liquid phase depends on some parameters, such as temperature, initial concentration of the carbon source, presence of trace metals, vitamin B solution, light intensity, and agitation speeds. The initial acetate concentrations in the liquid phase reflected on the value of Monod constants, K_p and K'_p . The average value for maximum specific growth rate (μ_m) was 0.01 h⁻¹. The value of μ_m was double that reported in the literature.^{46,44} The CO uptake rate (q_m) was 1.1 mmol g_{cell}⁻¹ h⁻¹ for 1 g L⁻¹ acetate. The CO uptake rates were a few times higher than the data previously cited in the literature.⁴⁶ The Monod saturation constant for growth (K_p) was exactly 0.015 atm. The K_p value was very small because of substrate depletion as a result of the fast microbial growth.

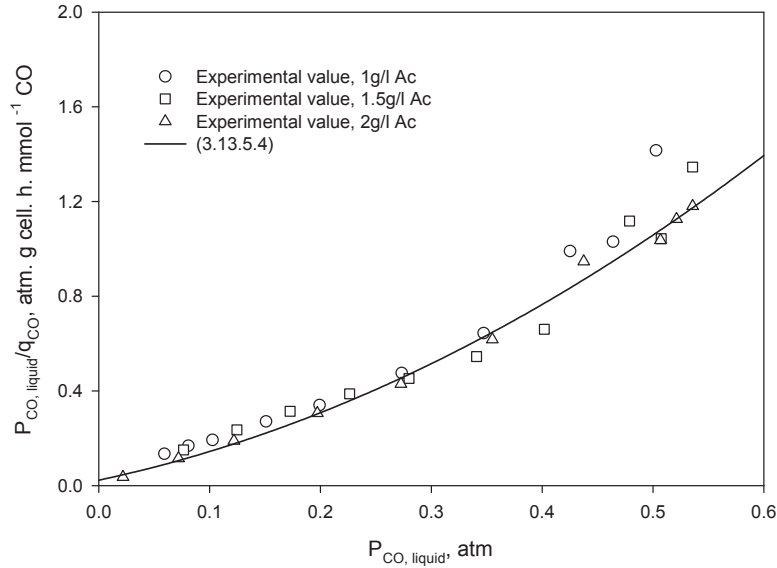


FIGURE 3.15 Quadratic model based on Eqn (3.14.5.4) with substrate inhibition at agitation speed of 200 rpm and light intensity of 500 lux.

3.14.6 GROWTH KINETICS OF CO SUBSTRATE ON *C. LJUNGDAHLII*

Growth-dependence of microbial cells on CO was proposed by the equation of Andrew that substrate inhibition was included as⁴⁵:

$$\mu = \frac{\mu_{m,CO} C_{CO}^*}{K_{CO} + C_{CO}^* + (C_{CO}^*)^2 / K_i} \quad (3.14.6.1)$$

where μ is the specific growth rate in h^{-1} , $\mu_{m,CO}$ is the maximum specific growth rate for CO in h^{-1} , C_{CO}^* is carbon monoxide concentration in the gas phase in equilibrium with the liquid phase in $mmol\ CO.l^{-1}$, K_{CO} is the Monod constant for CO in $mmol\ CO\ L^{-1}$, and K_i is the inhibition constant in $mmol\ CO\ L^{-1}$. C_{CO}^* in the gas phase was calculated based on Henry's law, which relates partial pressure of CO to Henry's law constant ($C_{CO}^* = P_{CO,gas}/H$). In order to maintain maximum cell dry weight, Eqn (3.14.6.1), is used; this equation is modified to drive an expression to predict the CO concentration; which is used for determination of cell dry weight:

$$\frac{C_{CO}^*}{\mu} = \frac{K_{CO}}{\mu_{m,CO}} + \frac{C_{CO}^*}{\mu_{m,CO}} + \frac{(C_{CO}^*)^2}{\mu_{m,CO} K_i} \quad (3.14.6.2)$$

Figure 3.16 shows the quadratic equation of growth-dependence of CO by *C. ljungdahlii* with various initial pressures in experiments repeated three times. It was shown that CO transfer increased by augmentation of CO concentration (C_{CO}) and was easily used by

TABLE 3.3 Kinetic parameters and rate models with and without inhibition mass transfer coefficients

Acetate concentration (g L ⁻¹)	0.5	1.0	1.5	2.0	2.5	3.0
Growth kinetics						
x_0 , g l ⁻¹	0.029	0.059	0.046	0.040	0.025	0.025
μ_m , h ⁻¹	0.066	0.068	0.042	0.064	0.040	0.040
x_m , g L ⁻¹	0.173	0.252	0.235	0.220	0.115	0.076
R^2 , %	99.3	92.7	97.2	97.0	99.3	99.0
Substrate consumption rate						
Ac_0 , g l ⁻¹	0.53	1.03	1.697	2.21	2.71	3.01
k_{Ac} , h ⁻¹	0.029	0.128	0.142	0.011	0.005	0.002
R^2 , %	99.1	98.4	95.4	98.6	96.0	97.6
Biohydrogen yield						
$Y_{H_2/CO}$, %	—	83.0	85.7	70.4	—	—
R^2 , %	—	97.0	99.6	99.1	—	—
Mass transfer						
$K_L \cdot a$, h ⁻¹	—	4.3	3.2	2.3	—	—
R^2 , %	—	96.0	92.0	99.4	—	—
Monod equation						
μ_m , h ⁻¹	—	0.057	0.095	0.125	—	—
K_p , atm	—	0.345	0.403	0.530	—	—
R^2 , %	—	95.0	94.1	94.4	—	—
Andrew's equation						
K_p , atm	—	0.015	—	—	—	—
μ_m , h ⁻¹	—	0.010	—	—	—	—
K_i , atm	—	10.3	—	—	—	—
R^2 , %	—	99.7	—	—	—	—
K'_p , atm	—	0.032	—	—	—	—
q_m , mmol CO g _{cell} ⁻¹ h ⁻¹	—	1.10	—	—	—	—
K'_i , atm	—	13.0	—	—	—	—
R^2 , %	—	99.5	—	—	—	—

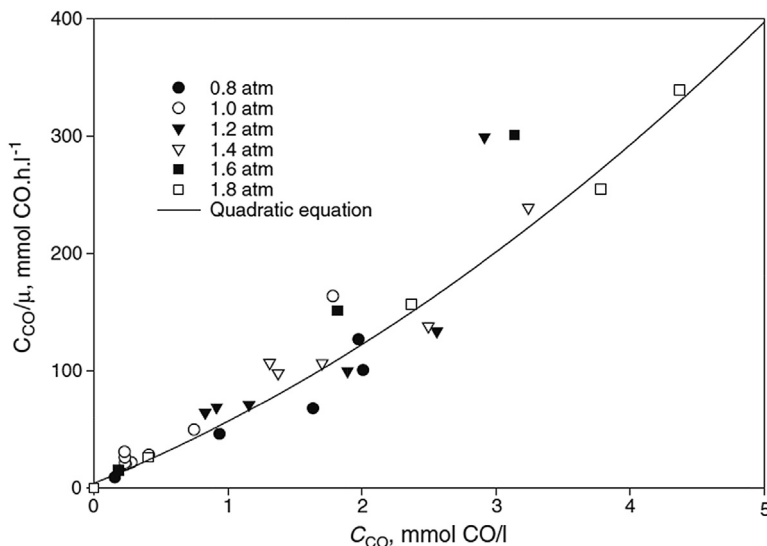


FIGURE 3.16 Growth-dependence on carbon monoxide (CO) concentration represented by the equation of Andrew with various syngas pressures.

C. ljungdahlii in the culture. Cultures of *C. ljungdahlii* exhibited CO inhibition in batch cultivation. The inhibition constant was obtained at $2.0 \text{ mmol CO L}^{-1}$. The reason may be due to the formation of ethanol, which damages the functions of *C. ljungdahlii* in the culture media. The inhibition of ethanol may be reduced by its removal through a continuous process, because ethanol is a volatile product. The maximum specific growth rate and Monod constant for CO were 0.022 h^{-1} and $0.078 \text{ mmol CO L}^{-1}$, respectively.

NOMENCLATURE

- a_i Interfacial area per unit volume of liquid, m^{-1}
 B Integration constant
 C_{AL}^* Equilibrium concentration of A at the liquid phase, mmol g^{-1}
 C_{AL} Concentration of A at liquid phase, mmol g^{-1}
 C_{PR} Carbon dioxide production rate, $\text{mmol g}^{-1} \text{ s}^{-1}$
 C_{CO}^* CO concentration in gas phase equilibrium with liquid phase, mmol CO L^{-1}
 $C_{CO,liquid}$ CO concentration in the liquid phase, mol L^{-1}
 $C_{CO,i}$ CO concentration in the interface, mol L^{-1}
 CO Carbon monoxide
 CO_2 Carbon dioxide
 H Henry's law constant
 H_2 Hydrogen
 k Decline or increase in growth constant by products, h^{-1}
 $k_L \cdot a$ Mass transfer coefficient at liquid phase, s^{-1}
 $k_{CO,gas}$ Mass transfer coefficient in the gas phase, m h^{-1}
 $k_{CO,liquid}$ Mass transfer coefficient in the liquid phase, m h^{-1}
 K_i Inhibition constant for CO, mmol CO L^{-1}

K'_i Substrate inhibition constant for uptake rate, atm
 K_{CO} Monod constant for CO, mmol CO L⁻¹
 k_s First-order rate constant, h⁻¹
 $N_{CO,gas}$ Number of moles of CO component in the gas phase, atm
 $K_L \cdot a$ Overall gas–liquid mass transfer coefficient, h⁻¹
 K_P Monod saturation constant for growth, atm
 K'_P Monod saturation constant for substrate uptake, atm
 $P_{CO,i}$ Partial pressure of CO in interface, atm
 $P_{CO,gas}$ Partial pressure of CO in the gas phase, atm
 $P_{CO,liquid}$ Partial pressure of CO in the liquid phase, atm
 q_{CO} Substrate uptake rate per unit of cell weight, mmol g_{cell}⁻¹ h⁻¹
 q_m Maximum specific substrate uptake rate, mmol g_{cell}⁻¹ h⁻¹
 S_0 Initial substrate concentration, g L⁻¹
 S Substrate concentration, g L⁻¹
 t Time, h
 V_l Volume of liquid phase, L
 x_0 Initial cell concentration, g L⁻¹
 x Cell dry weight concentration, g L⁻¹
 x_m Maximum cell dry weight concentration, g L⁻¹
 $Y_{x/S}$ Yield coefficient of cell substrate, g_{cell} g_{substrate}⁻¹
 μ Specific growth rate, h⁻¹
 μ_m Maximum specific growth rate, h⁻¹
 $\mu_{m,CO}$ Maximum specific growth rate for CO, h⁻¹
OUR Oxygen uptake rate, mmol g⁻¹ s⁻¹
RQ Respiration quotient, mmol CO₂ per mmol O₂
 x Biomass concentration, mg L⁻¹
 x_{max} The maximum specific biomass production, s⁻¹
 q_{O_2} Specific oxygen uptake rate, s⁻¹

Acknowledgments

The present research was made possible through a long-term IRPA grant No.01-02-05-3223EA011, sponsored by the Ministry of Science, Technology and Innovations (MOSTI), Malaysia, and Universiti Sains Malaysia (USM). The authors are thankful to the RCMO and MOSTI scientific panels, Universiti Sains Malaysia and MOSTI for their financial support.

References

1. Younesi H, Najafpour G, Mohamed AR. *Iran J Biotechnol* 2006;**4**(1):45.
2. Mohammadi M, Najafpour GD, Younesi H, Lahijani P, Uzir MH, Mohamed AR. *Renew Sust Energ Rev* 2011;**15**(9):4255.
3. Najafpour G, Ku Ismail KS, Younesi H, Mohamed A, Harun A. *Int J Eng* 2004;**17**:105.
4. Najafpour G, Younesi H, Syahidah Ku Ismail K. *Bioresour Technol* 2004;**92**(3):251.
5. Klasson KT, Ackerson MD, Clausen EC, Gaddy JL. *Enzyme Microb Technol* 1992;**14**(8):602.
6. Younesi H, Najafpour G, Ku Ismail KS, Mohamed AR, Kamaruddin AH. *Bioresour Technol* 2008;**99**(7):2612.
7. Braun M, Mayer F, Gottschalk G. *Arch Microbiol* 1981;**128**(3):288.
8. Najafpour G, Younesi H, Mohamed A. *Malays J Microbiol* 2005;**1**(1):12.
9. Tjattjopoulos GJ, Vasalos IA. *Ind Eng Chem Res* 1998;**37**(4):1410.
10. Najafpour G, Ismail KSK, Younesi H, Mohamed AR, Kamaruddin AH. *Afr J Biotechnol* 2004;**3**(10):503.
11. Asada Y, Miyake J. *J Biosci Bioeng* 1999;**88**(1):1.
12. Jung GY, Kim JR, Park J-Y, Park S. *Int J Hydrog Energy* 2002;**27**(6):601.
13. Kellum R, Drake HL. *J Bacteriol* 1984;**160**(1):466.

14. Klasson KT, Gupta A, Clausen EC, Gaddy JL. *Appl Biochem Biotechnol* 1993;**39-40**(1):549.
15. Mohammadi M, Younesi H, Najafpour G, Rahman Mohamed A. *J Chem Technol Biotechnol* 2012;**87**(6):837.
16. Gonzalez JM, Robb FT. *FEMS Microbiol Lett* 2000;**191**(2):243.
17. Kerby RL, Hong SS, Ensign SA, Coppoc LJ, Ludden PW, Roberts GP. *J Bacteriol* 1992;**174**(16):5284.
18. Phillips J, Clausen E, Gaddy J. *Appl Biochem Biotechnol* 1994;**45-46**(1):145.
19. Najafpour G, Younesi H. *J Pol Min Eng Soc* 2003;**4**(2):29.
20. Tanisho S, Kuromoto M, Kadokura N. *Int J Hydrog Energy* 1998;**23**(7):559.
21. Vega JL, Clausen EC, Gaddy JL. *Biotechnol Bioeng* 1989;**34**(6):774.
22. Vega JL, Antorrena GM, Clausen EC, Gaddy JL. *Biotechnol Bioeng* 1989;**34**(6):785.
23. Vega J, Holmberg V, Clausen E, Gaddy J. *Arch Microbiol* 1988;**151**(1):65.
24. Pezacka E, Wood H. *Arch Microbiol* 1984;**137**(1):63.
25. Mohammadi M, Mohamed A, Najafpour G, Younesi H, Uzir M. *Int J Eng* 2013;**27**(2):185.
26. Mohammadi M, Mohamed AR, Najafpour GD, Younesi H, Uzir MH. *Sci World J* 2014;**2014**.
27. Bailey JE, Ollis DF. *Biochemical engineering fundamentals*. McGraw-Hill; 1986.
28. Younesi H, Najafpour G, Mohamed AR. *Biochem Eng J* 2005;**27**(2):110.
29. Levenspiel O. *Chemical reaction engineering*. Wiley; 1972.
30. Najafpour G, Younesi H. *Enzyme Microb Technol* 2006;**38**(1):223.
31. Najafpour G, Younesi H, Mohamed AR. *Biochem Eng J* 2004;**21**(2):123.
32. Najafpour G, Younesi H. *Int J Eng* 2005;**18**(2):145.
33. Najafpour G, Younesi H, Mohamed AR. *Energy Sources, Part a* 2006;**28**(11):1013.
34. Koku H, Eroğlu İ, Gündüz U, Yücel M, Türker L. *Int J Hydrog Energy* 2002;**27**(11-12):1315.
35. Koku H, Eroğlu İ, Gündüz U, Yücel M, Türker L. *Int J Hydrog Energy* 2003;**28**(4):381.
36. Najafpour G, Younesi H. *World J Microbiol Biotechnol* 2007;**23**(2):275.
37. Pakpour F, Najafpour G, Tabatabaei M, Tohidfar M, Younesi H. *Bioprocess Biosyst Eng* 2013;**1**.
38. Najafpour G, Younesi H. *ASEAN J Chem Eng* 2005;**5**(1):35.
39. Najafpour GD, Younesi H, Mohamed AR, Harun A. *Intern J Eng Sci* 2005;**16**(1):1.
40. Najafpour G, Younesi H, Mohamed A. *Pet Coal* 2003;**45**(3/4):154.
41. Scragg AH. *Bioreactors in biotechnology: a practical approach*. E. Horwood; 1991.
42. Nielsen JH, Villadsen J, Lidén G. *Bioreaction engineering principles*. Kluwer Academic/Plenum Publishers; 2003.
43. Geankoplis CJ. *Transport processes and separation process principles (includes unit operations)*. 4th ed. Prentice-Hall of India Pvt. Limited; 2003.
44. Najafpour G, Younesi H, Ismail K, Mohamed A, Kamaruddin A. *Dev Chem Eng Min Process* 2005;**13**(5-6):549.
45. Andrews JF. *Biotechnol Bioeng* 1968;**10**(6):707.
46. Klasson KT, Lundbäck KMO, Clausen EC, Gaddy JL. *J Biotechnol* 1993;**29**(1-2):177.

PROBLEMS

3.1 The following data were obtained from an aerated tank at 15 °C. (Table Q.1)

Determine the mass transfer coefficient $K_L \cdot a$, using differential equation, solve it with initial condition $t = 0$, $C = C_0$.

TABLE Q.1

Time, min	$C, \text{mg L}^{-1}$
0	0
5	1.8
10	3.2
15	4.4
20	5.5
25	6.4
30	7.2
35	7.9
40	8.4

TABLE Q.2 Oxygen concentration and off-gas analysis

Time (h)	Dissolved oxygen concentration (ppm)	Percentage oxygen in exit air of horizontal rotary fermenter (%)
0	-	21.0
2	6.4	20.8
4	5.6	20.4
6	5.1	20.0
8	2.2	18.7
10	0.5	16.4

Define the concentration profile with respect to time.

$$dC/dt = K_L \cdot a, (C_s - C)$$

where C_s is saturation gas concentration in liquid phase 12 ppm.

- 3.2** Cultivation of a well-known fungus as *Torula utilis* was carried out in a horizontal rotary fermenter (HRF) at 30 °C, air flow rate of $3.5 \times 10^{-3} \text{ m}^3 \text{ s}^{-1}$, and agitation rate of 300 rpm. The working liquid volume reactor was 1.25 L. During cell cultivation, dissolved oxygen concentration in the liquid was monitored using an oxygen probe, and the percentage of oxygen in the fermenter's exit gas was analyzed by a paramagnetic oxygen analyzer (PMOA). The collected data are shown in Table Q.2. From the given data, determine mass transfer coefficient $K_L \cdot a$, r_X and C^* by implementation of oxygen balance method. Hint: The most useful relation would be dynamic balance. Assume air density at 30 °C is 1.23 kg m^{-3} .
- 3.3** Determine oxygen uptakes rates (OUR) and respiration quotient (RQ) of a yeast suspension culture by Warburg constant volume respiration meter. The collected data are given in Table Q.3. Manometer readings were taken at 15 min intervals. The total volume of the manometer filled with mercury in both flasks was $1.8 \times 10^{-6} \text{ m}^3$ (18 ml) Experiment conducted at 25 °C.

TABLE Q.3 Warbug manometer readings

Flask 1		Flask 2	
Left arm, mL	Right arm, mL	Left arm, mL	Right arm, mL
15	15	15	15
15	15	15	15
15	15	14.5	15.5
14.3	15.8	14.7	15.3
13.8	16.2	15	15
13.2	16.8	15	15

Contents of the flasks were:

Flask 1: A 3-mL suspension of yeast with alkali in the central cup.

Flask 2: A 3-mL suspension of yeast (washed cells)

*Flask 3: Blank, distilled water +0.3 mL KOH in the cup.

From the above given data, calculate:

1. The OUR for the yeast suspension
 2. RQ of yeast cell
-

Fermentation Process Control

OUTLINE

4.1 Introduction	104		
4.2 Bioreactor Controlling Probes	105		
4.3 Characteristics of Bioreactor Sensors	106		
4.4 Temperature Measurement and Control	108		
4.5 Dissolved Oxygen Measurement and Control	109		
4.6 pH/Redox Measurement and Control	110		
4.7 Detection and Prevention of Foam	112		
4.8 Biosensors	113		
4.8.1 <i>Biological Element</i>	114		
4.8.2 <i>Immobilization of Biomaterials</i>	115		
4.8.2.1 Adsorption	115		
4.8.2.2 Entrapment	115		
4.8.2.3 Encapsulation	115		
		4.8.2.4 Cross-Linking	116
		4.8.2.5 Covalent Binding	116
		4.8.3 <i>Transducer</i>	117
		4.8.3.1 Thermal Biosensor	117
		4.8.3.2 Optical Biosensor	117
		4.8.3.3 Piezoelectric Biosensor	117
		4.8.3.4 Electrochemical Biosensor	117
		4.8.4 <i>Amperometric Biosensors</i>	118
		4.8.4.1 Response Time	122
		4.8.4.2 Recovery Time	122
		4.8.4.3 Linear Detection Range	122
		4.8.4.4 Limit of Detection	122
		4.8.4.5 Sensitivity	123
		Nomenclature	124
		References	124

4.1 INTRODUCTION*

The growth of an organism in a bioreactor has to be controlled, so the operators must have sufficient information about the state of the organism and the bioreactor conditions. Monitoring a fermentation process may require basic knowledge of the bioprocess, and the running conditions should be recorded. Also, any changes taking place must be reported. As most bioreactors operate under sterile conditions, information can be obtained by taking samples or by in situ measurements. There are direct and indirect measurements of microbial growth. The methods of direct growth measurement are cell optical density, total cell counters, Coulter counter, cell dry weight, packed cell volume, and optical detectors. Growth is based on absorbance/light scattering. The absorbance of the culture is generally measured with a spectrophotometer at a wavelength of about 600 nm.¹ The indirect measurements of cell growth are based on cellular components, measurements of ATP, bioluminescence, substrate consumption and product formation, oxygen uptake rate, respiration quotient, and heat evolution.

There are many types of bioreactors used in bioprocesses such as the continuous stirred tank reactor (CSTR), plug flow column, bubble column bioreactor, packed-bed bioreactor, fluidized-bed bioreactor, trickle-bed bioreactor, tower fermenter, air lift bioreactor, and immobilized bioreactor. The most common form is the simple stirred tank bioreactor. This is a well-stirred tank designed for perfect mixing; under these conditions, the fluid is uniform everywhere. The standard CSTR is normally operated under aerobic conditions. In the CSTR bioreactor, the routine measurement of temperature, pressure, pH, and dissolved oxygen condition is carried out through a set of experimental runs. In equipped bioreactors, the basic instrumentation may provide sufficient information to determine the total mass or volume of the bioreactor contents, the agitation speed, power and torque, redox potential, dissolved carbon dioxide concentration, gas and liquid flow rates into the fermentation vessel, with analysis of oxygen and carbon dioxide contents of the exhaust gas. Basic control facilities normally consist of a temperature controller, pH and dissolved oxygen content controller, and foaming and level controller for steady operation.²

Figure 4.1 shows the usual instrumentation for a bioreactor with an agitating motor and all control units. The vessel is jacketed for cooling and heating, with a separate side unit of temperature-controlled bath. Steam is used for sterilization and elimination of contaminants.

Measurement and control of the fermentation conditions are very important for bioprocess control as they provide knowledge and, hence, a better understanding of the operation. The recorded data can be used to improve the process. Controlling operating conditions is important for maintaining viable cells, and it makes the interpretation of fermentation data easier.

The growth of living organisms is a bioprocess that is regulated by a complex interaction among the physical, chemical, and biological conditions of the living environment of fermentation and the biochemical processes inside the cells. The most important part of the instrumentation is concerned with physical factors such as temperature, pressure, agitation speed, power input, flow rates, and mass quantities. Such measurements are standard in all industrial bioprocesses. Chemical factors are utilized for measuring oxygen and carbon dioxide concentrations in the exit gas and by aqueous phase pH. However, for measurements of

*This case study was partially written with contributions from:

Hossein Zare, Biotechnology Research Lab., Faculty of Chemical Engineering, Noshirvani University of Technology, Babol, Iran.

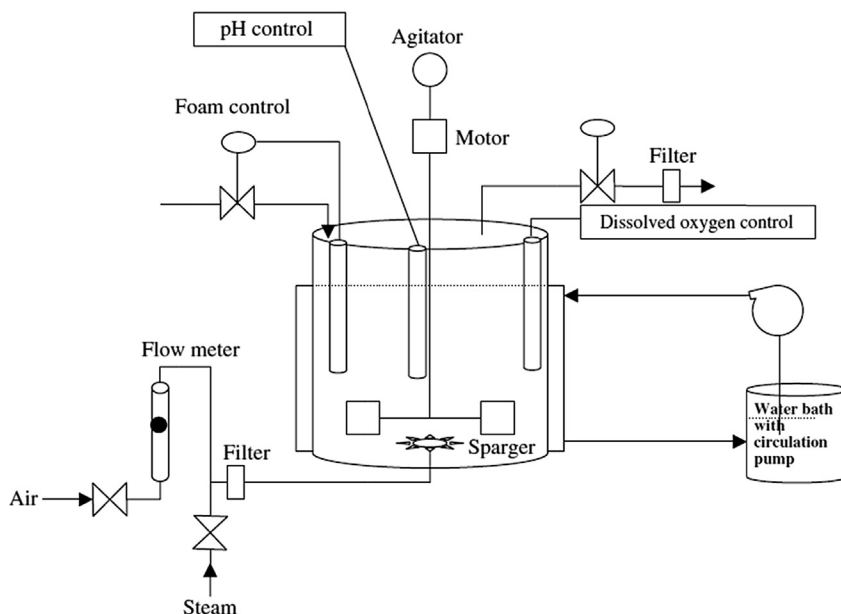


FIGURE 4.1 Instrumentation control for continuous stirred tank (CSTR) bioreactor.

redox potential, dissolved oxygen, and dissolved carbon dioxide concentration, their dependency is more related to the instrumentation of controlled units.

Several different instruments are available for measuring flow rates of gases (the inlet air and the exhaust gas). The simplest instrument is a flow meter for measuring flow rates, such as a rotameter, which provides a visual readout or is fitted with a transducer to give an electrical output. Thermal mass flow meters are increasingly popular, especially for laboratory- and pilot-scale reactors. In these devices, gas flows through a heated section of tubing and the temperature differences across this heated section are directly related to the mass flow rate. The flow rate of the liquid can be monitored with electromagnetic flow meters, but it is very costly. Use of a normal rotameter for low flow rate may cause some error. Therefore, a level sensor is used. As the liquid level reaches the probe, the conductivity of the media surrounding the probe changes, so monitoring is based on the conductance of the liquid level. Such capacitance probes or conductance probes are used to detect foam on the surface of the bioreactor.

Table 4.1 summarizes the physical, chemical, and biological parameters that should be collected during fermentation. The lack of reliable biological sensors in most fermentation processes results in poor feedback of biological information. Biochemical engineers are able to sort out information using material balance to estimate quantities such as respiration quotient, oxygen uptake rate, and carbon dioxide production rate. Analysis of bioreactor off-gas is very important for any material balance that leads us to biological activities of viable organisms in the bioprocess.

4.2 BIOREACTOR CONTROLLING PROBES

In bioprocess plant instrumentation and process control, variables are very important. Reading and processing the information about the biosystem and monitoring the cells are the major aims of the process instrumentation. Controlling pH, measuring the dissolved

TABLE 4.1 Bioreactor operating parameters

Physical	Chemical	Biological and cell properties
Time	pH	Respiratory quotient
Temperature	Redox potential	O ₂ uptake rate
Pressure	Dissolved oxygen	CO ₂ production rate
Agitation speed	Dissolved carbon dioxide	Optical density
Total mass	O ₂ in gas phase	Cell concentration
Total volume	CO ₂ in gas phase	Viability of cells
Volume feed rate	Lipid	Cell morphology
Viscosity of culture	Carbohydrates	Cellular composition
Power input	Enzyme activities	Protein, DNA, RNA
Foam	Nitrogen	ATP/ADP/AMP
Shear	Ammonia, if present	NAD/NADH
Mixing time	Mineral ions	Activities of whole cells
Circulation time	Precursors	Specific growth rate
Gas holdup	Inducers	Specific oxygen uptake rate
Bubble size distribution	Growth stimulants	Specific substrate uptake rate
Impeller flooding	Effective mineral as catalyst	Metabolites
Broth rheology	Products	Growth factors
Gas mixing patterns	Volatile products	Growth inhibitors
Liquid level	Conductivity	Biomass composition
Reactor weight	Off-gas composition	Biomass concentration
Foam level		

oxygen in the fermentation broth, and controlling foam are all considered as major parameters and necessary biological information for large-scale operations. The main objective is to operate a bioreactor without any problems. To do so, we need to be familiar with all the controlling facilities and process instrumentation. Application of biosensors in the bioreactors is very common, so it is good to know how the controlling unit operates.

4.3 CHARACTERISTICS OF BIOREACTOR SENSORS

The sensor in a bioreactor provides knowledge and information on the state of the process and also supplies suitable operational data for the process variables. Some of the physical and chemical effects on the bioreactor have to be translated to electrical signals which can be

amplified and then displayed on a monitor or recorder and used as an input signal for a controlling unit. In practice, the response of most of the processes follows a sigmoidal S-shaped curve. A similar response would be obtained if a dissolved oxygen probe was suddenly removed from a vessel with depleted oxygen levels, the probe transferred to a vessel with water maintained with supplied air passed through the aqueous phase, and the system agitated for sufficient oxygen transfer so that it is saturated in the liquid phase.³ Air bubbles may interfere with sensor signals, and false readings can mislead the bioreactor operation.

The dynamics given by the instrument response signal comprise several processes taking place in series. Thus, the transfer of oxygen from the air into the liquid causes reduction in the rate of mass transfer due to the reduction in the concentration gradient as the existing driving forces. The rate of change of the oxygen concentration in the gas phase is determined by the magnitude of the time constant which depends on the gas volume and the mass transfer coefficient $K_L a$. The rate of change in the dissolved oxygen with time is determined by the magnitude of the time constant for the liquid phase which depends on the volume of the liquid and the mass transfer coefficient. Finally, the time-varying liquid-phase concentration is registered by the dissolved oxygen electrode and is transmitted as an output signal. Again the signal is affected by the electrode time constant. Thus, the process dynamics are determined by a combination of the time constants for gas phase, liquid phase, and the electrode dynamics. Figure 4.2 shows the computer simulation results of such a dynamic aeration experiment. The y -axis shows the response fraction with respect to time. The gas-phase response is typically first-order, and the liquid phase shows some lag or delay on the signal. The electrode response is much more delayed for a slow-acting electrode.⁴

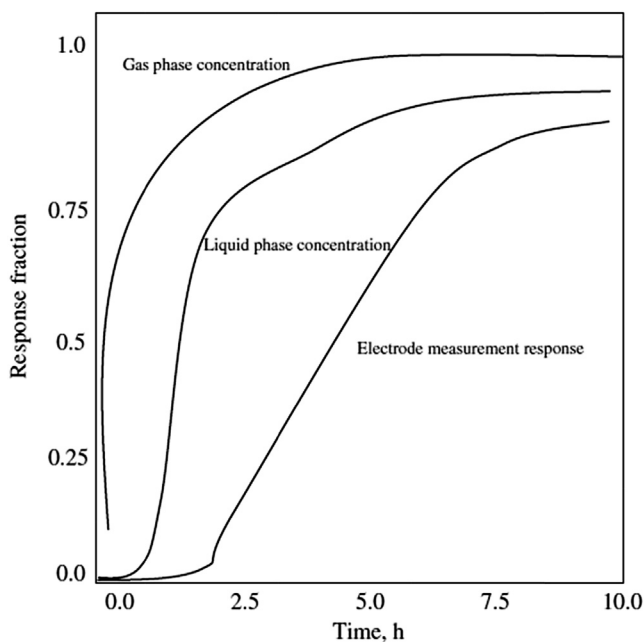


FIGURE 4.2 Computer simulation of a dynamic aeration experiment with a slow dissolved oxygen (DO) electrode.

4.4 TEMPERATURE MEASUREMENT AND CONTROL

Control of temperature for fermentation vessels is required because of the narrow range of optimal temperature. Most fermenters operate around 30–36 °C, but certain fermentations may require control of the temperature in a range of 0.5 °C; this can easily be obtained in large bioreactors.^{4,5} To maintain bioreactor temperature within the limited range, the system may require regulation of heating and cooling by the control system. Heat is generated in the fermenter by dissipation of power, resulting in an agitated system; heat is also generated by the exothermic biochemical reactions. In exothermic reactions, the fermentation vessel requires cooling. At the start and end of the fermentation, the heat generation rate is very low, although the systems are normally heated to achieve the desired temperature. There are many alternatives for measuring and controlling the bioreactor temperature. These include glass thermometers, thermocouples, thermostats, resistance thermometers, and miniature integrated circuit devices. Thermal units capable of giving direct electrical output signals are favored for control purposes. Thermocouples are cheap and simple to use, but they are rather low in resolution and require a cold junction. Thermistors are semiconductors that exhibit a change in electrical conductivity with temperature. They are very sensitive and inexpensive; they give a highly nonlinear output. Modern transistorized, integrated circuits combine the features, but they often display a more linear output. Platinum resistance thermometers are usually preferred as standard. To avoid contamination of the bioreactor, the thermometers are usually fitted into thin-walled stainless-steel pockets which project into the bioreactor. The pockets are filled with a heat-conducting liquid to provide good contact and to speed the instrument response. The resistance thermometer works on a principle that electrical resistance changes with temperature. It requires the passage of a current to develop a measurable voltage which is proportional to the temperature. However, the current should not be so large that it causes heating effects.

The changes in the electrical resistance of the electrical wires to the thermometer can be quite large, with their resistance being affected by changes in the ambient temperature. These effects can be eliminated by using separate wires to supply and sense the current. The advantages of platinum resistance detectors are their high accuracy, high stability, and that the linear output signal can be obtained in normal temperature ranges. The high temperature steam for sterilization may require separate instrumentation within a temperature range of 50–150 °C.⁵

The energy balance for the bioreactor is shown by the following equation. As the fermenter is used batchwise, the heat balance is mathematically expressed as stated in (4.4.1):

$$d\left[\frac{MC_P T}{dt}\right] = \mu X(-\Delta H_X)V - UA[T - T_j] \quad (4.4.1)$$

where M is the total mass of the reactor for the batch system in kg, C_P is the specific heat in $\text{kJ kg}^{-1} \text{K}^{-1}$, T is the temperature of the fermentation in K and t is time in s. Also, the term μX is the rate of cell growth in $\text{kg m}^{-3} \text{s}^{-1}$, V is the working volume of the bioreactor in m^3 and ΔH_X is the exothermic heat generated inside the fermenter in $\text{kJ kg}^{-1} \text{cell}$. Under steady-state conditions of controlled temperature, $dT/dt = 0$, the rate of heat accumulation is zero, and the rate of heat production is equal to the heat transfer by the jacketed system. The rate of heat

production is related to the rate of cell growth. The rate of heat transfer is the mean temperature gradient, $[T - T_j]$, multiplied by overall heat transfer coefficient (U) in $\text{kJ m}^{-2} \text{s}^{-1} \text{K}^{-1}$. T_j is the temperature of the coolant in the jacket in K.

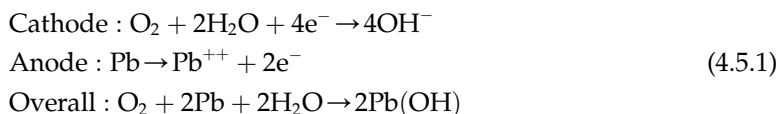
4.5 DISSOLVED OXYGEN MEASUREMENT AND CONTROL

The dissolved oxygen (DO) content of the fermentation broth is also an important fermentation parameter, affecting cell growth and product formation. The rate of oxygen supply to the cell is often limited because the solubility of oxygen in fermentation is low. Unfortunately, measurement and control of dissolved oxygen under bioreactor conditions is a challenging problem. The low solubility of oxygen makes the measurements very difficult. There are several methods to determine the concentration of dissolved oxygen. Most DO probes use a membrane to separate the point of measurement from the broth; all probes require calibration before use. Three main methods are used: (1) the tubing method; (2) use of mass spectrometer probes; and (3) electrochemical detectors. In the tubing method, an inert gas flows through a coil of permeable silicon rubber tubing that is immersed in the bioreactor. Oxygen diffuses from the broth, through the wall of the tubing, and into a flow of inert gas passing through the tube. The concentration gradient exists because of the diffusion of oxygen into the inert gas. Then, the concentration of oxygen gas in the inert gas is measured at the outlet of the coil by an oxygen gas analyzer. This method has a relatively slow rate of response on the order of several minutes. The advantages of this method are its simplicity, and in situ sterilization is easily carried out. In the second method, the membrane of a mass spectrometer probe is used to separate the fermenter contents from the high vacuum of the mass spectrometer. Measurement of oxygen in the mass spectrometer probe and the tubings are based on the ability of the gas to diffuse across the surface of membrane.

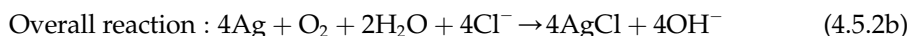
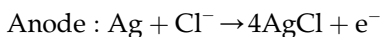
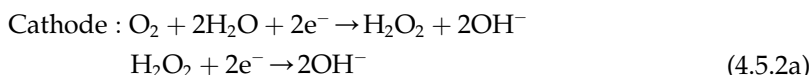
The most common method of measuring dissolved oxygen is based on electrochemical detector. Two types of detectors are commercially available: galvanic and polarographic detectors. Both use membranes to separate electrochemical cell components from the broth. The membrane must be permeable only to oxygen and not to any other chemicals that might interfere with the measurement. Oxygen diffuses from the broth across the permeable membrane to the electrochemical cell of the detector, where it is reduced at the cathode to produce a measurable current or voltage which is proportional to the rate of arrival of oxygen at the cathode. It is important to note that the measurement rate of oxygen arrival at the cathode depends on the rate of arrival at the outer membrane surface, the rate of transfer across the membrane, and the rate of transport from the inner surface of the membrane to the cathode. The rate of arrival at the cathode is proportional to the rate of diffusion of oxygen across the membrane. The rate of diffusion is also proportional to the overall concentration driving force for oxygen mass transfer. We assume the oxygen concentration at the inner surface of the membrane is efficiently reduced to zero. The rate of diffusion is thus proportional to the oxygen concentration in the liquid only. The electrical signal produced by the probe is directly proportional to the dissolved oxygen concentration of the liquid. The probe has to be calibrated for accurate measurements.

In the galvanic detector, the electrochemical detector consists of a noble metal, like silver (Ag) or platinum (Pt), and a base metal, such as lead (Pb) or tin (Sn), which acts as the anode.

The well-defined galvanic detector is immersed in the electrolyte solution. Various electrolyte solutions can be used, but commonly they may be a buffered lead acetate, sodium acetate, and acetic acid mixture. The chemical reaction in the cathode with electrons generated in the anode may generate a measurable electrical voltage, which is a detectable signal for measurements of DO. The lead is the anode in the electrolyte solution that is oxidized. Therefore, the probe life is dependent on the surface area of the anode. The series of chemical reactions occurring in the cathode and anode are stated as follows:



Polarographic electrodes are different from the galvanic type. In this type of electrode, the external negative base voltage is applied between the cathode (Au or Pt) and the anode (Ag/AgCl) so that oxygen is reduced at the cathode according to the sequential reactions stated below. The following reactions take place at cathode and anode, respectively:



An electrical output for a polarographic detector is produced according to the above reactions. Again, various electrolytes can be used for this type of detector, but they are usually based on KCl or AgCl with additional high molecular mass compounds that are added to prevent the loss of electrolyte during sterilization.

4.6 pH/REDOX MEASUREMENT AND CONTROL

Fermenters are generally operated most efficiently. The fermentation process is normally carried out at a constant pH. The pH of a culture medium will change with the metabolic product of microorganisms that are developed in the fermentation media. Therefore, pH control is required during the course of fermentation. The pH has a major effect on cell growth and product formation by influencing the breakdown of substrates and transport of both substrate and product through the cell wall. It is, therefore, a very important factor in fermentation. In fine chemicals, organic acids, amino acids, and antibiotic fermentations, even a small change in the pH can cause a large fall in the productivity. Also, in animal-cell fermentations, the pH is strictly affected by the cell density.

Measurement of pH is based on the absolute standard of the electrochemical properties of the standard hydrogen electrode. The basic part of the electrode is a very thin, glass membrane (0.2–0.5 mm) that reacts with water to form a hydrated gel layer of only 50–500 Å thicknesses. This layer exists on both sides of the membrane and is essential for the correct operation and maintenance of the electrode. Hydrogen ions that exist within the layer are mobile, and any difference between the ionic activities on each side of the

membrane will lead to the establishment of a pH-dependent potential. A constant potential is maintained at the inner surface of the glass membrane by filling the tube of the electrode with a buffered solution of accurately determined and stable composition and with constant and accurate hydrogen ion activity. An Ag/AgCl electrode is generally used as the electrical outlet from this system. As the pH of the process fluid varies, it causes a change in the potential on the outer surface of the membrane. To measure this, a reference electrode is necessary to complete the measurement circuit. In the combined electrode, this is constructed as an integrated part of the electrode assembly and consists of an Ag/AgCl₂ electrode in KCl electrolyte saturated with AgCl₂. The reference electrode must have direct contact with the process liquid to have an electrical continuity in the system. The overall potential measured by the electrode with respect to the hydrogen ions is given by the Nernst equation:

$$E = E_o + \frac{RT}{F} \ln [a_H^+] \quad (4.6.1)$$

where E is the measured potential in volt, E_o is the standard electrode potential in volts, R is the gas constant, F is the Faraday constant, T is the absolute temperature and a_H^+ is the hydrogen ion activity. The second term of (4.6.1) is related to pH, with a proportionality constant instead of ionic activity. The potential terms are translated to pH, leading to the following relation:

$$E = E_o - K[\text{pH} - \text{pH}_0] \quad (4.6.2)$$

where K is the proportionality constant, pH_0 is the reference or base pH. At room temperature, 25 °C (298K), the value for K is 59.15 mV per unit pH. The calomel reference electrode can be prepared with a predictable and reproducible voltage of 0.28 V. The pH of a solution can be determined with an electrode. A typical pH control scheme for a pilot-plant fermenter is shown in Figure 4.3.

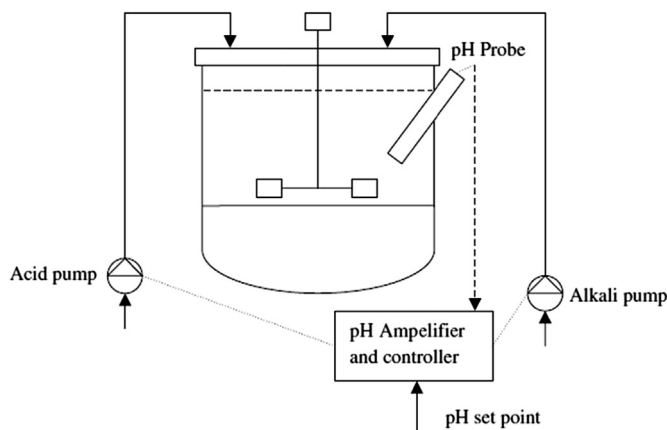


FIGURE 4.3 Instrumentation for a pH control system in a bioreactor.

4.7 DETECTION AND PREVENTION OF FOAM

In a gas and liquid system, when gas is introduced into a culture medium, bubbles are formed. The bubbles rise rapidly through the medium and dispersion of the bubbles occurs at the surface, forming froth. The froth collapses by coalescence, but in most cases the fermentation broth is viscous, so this coalescence may be reduced to form stable froth. Any compounds in the broth, such as proteins, that reduce the surface tension may influence foam formation. The stability of preventing bubbles from coalescing depends on the film elasticity, which is increased in the presence of peptides, proteins, and soaps. On the other hand, the presence of alcohols and fatty acids will make the foam unstable.

Foaming in the bioreactor is a nuisance that reflects on the mass transfer process and must be prevented for many reasons. The problems related to foaming are obvious, if they are due to gas sparging. The problems are the loss of broth, clogging of the exhaust gas system, and possible contamination, a problem that is due to wetting of the gas filters. During fermentation, foaming may occur suddenly. Some foams are easy to destroy and can be removed by a foam breaker; others are quite stable and are relatively hard to remove from the top of the bioreactor. The suppression of foam is usually accomplished by mechanical agitation such as a foam breaker. The mechanical devices operate on the center of the shaft. They are generally blades or disks that are mounted on the same agitator shaft. Chemical antifoams are used to regulate the foam and prevent any foaming on the surface of the broth.

The chemical antifoams are expensive, and minimal amounts must be used. Use of a chemical antifoam may complicate the microbial fermentation process, and some may act as an inhibitor. Therefore, they have to be regulated to eliminate any side effect on the bioprocess. Chemical antifoams are usually based on silicon and act by reducing the interfacial tension of the broth. Mechanical devices have advantages because expensive chemicals do not have to be added to the fermentation broth. However, the addition of antifoam may require the detection of foam. This requires the addition of the necessary amount of antifoam to control any preventive foaming in the bioreactor. Also, ultrasonic waves may be additional means of destroying foam.

Generally, two main types of foam detectors are used. They work by detecting either changes in electrical capacitance or changes in electrical resistance. [Table 4.2](#) shows the application of foam detectors based on various principles such as conductance, thermal conductivity, capacitance, and ultrasonic and rotating disks.

TABLE 4.2 Types of foam detectors, their features and functions

Conductance	An insulated stainless steel electrode that forms one terminal in the circuit.
Thermal conductivity	Two thermistors mounted some distance apart. A current through the thermistors heats them above ambient; foam cool down.
Capacitance	A vertical tube with a central electrode. The height to liquid or foam alters the capacitance.
Ultrasonic	A transmitter and receiver mounted opposite each other in a bioreactor. At 25–40 kHz ultrasound is absorbed by the foam.
Rotating disk	This may double as a foam breaker; foam will slow down the rotation or need an increase in power to maintain speed.

The capacitance foam detector is made of two electrodes which are installed in the bioreactor. They measure the capacitance of the air space above the normal working liquid level in the bioreactor. If foaming occurs, the air-space capacitance is reduced. Detection is by a change in the magnitude of a small alternating electrical current that is applied between the two electrodes. This method is applicable in large-scale bioreactors. The change in electrical current is converted to an output signal from the detectors; the change in current is directly proportional to the amount of foam formed. From evaporation of the liquid media, fouling problems may occur on the electrode by the broth. This may cause some error in foam detection, so regular cleaning is needed to maintain the electrode.

The foam detector based on the resistance method acts on the conductivity of the probe. The length of the probe is coated with some electrically insulating material, leaving the tip of the probe exposed to the media. As the foam builds up, it contacts the tip of the probe, thus completing an electrical circuit and producing an output signal. In the fermentation medium, as the tip of the probe contacts the generated foam, an electrical circuit is generated, and an output signal is produced for foam detection.

Another type of probe is based on the principle of the sudden cooling of the heated element. When foam comes in contact with a heated electrical element, the hot surface detects sudden cooling, which is translated to an output signal. The major problem with the use of a heated element is fouling of the media; the sensitivity decreases while it is used, so such detectors may not be reliable in practice.

The two other foam sensors mentioned above are ultrasound and rotating disks. The ultrasound sensor is composed of a transmitter and a receiver mounted opposite to each other and operates at 25–40 kHz. In the bioreactor, the waves are absorbed by the foam, and the signal is generated. The rotational disk foam sensor is a mechanical foam breaker which is used by increasing the rotational resistance.

The use of a chemical agent as an antifoam is affected by an on–off algorithm with variable dosing time and time delay. If the presence of foam is detected, then the controller first activates a delay timer. This type of foam controller works with some delay and variable dosing time. If at the end of the delay period the foam still presents, then the dosing pump is activated, and chemical agent is added to the bioreactor. If the foam is still detected at the end of this period, the combined system of delay and dosing is reactivated. With this method of control, addition of any unnecessary antifoam is prevented.

4.8 BIOSENSORS

Sensors are essential tools for determination of different chemical and physical quantities such as temperature, pressure, humidity, concentration, etc. In recent years, industrial growth has required rapid measurements of substances, which are conceivable by applying sensors.⁶

Sensors convert the changes in physical and chemical properties into detectable signals which can be recorded by an instrument. For instance, a glass thermometer is a simple and elementary sensor. In a glass thermometer, an increase or decrease in temperature causes expansion or contraction of a liquid volume that can be measured in a calibrated glass tube. Another example of a sensor is the human body. The nose and the tongue are sensors which naturally detect smell and flavors. In the nose, when the chemicals reach olfactory bulbs (which

are biological components), an electrical signal is produced and transmitted to the brain by olfactory nerves. Finally, the brain transduces the produced signals into the sensation of smell.^{7,8}

In sensors, the key constituent is a detection element that is responsible for detecting chemical or physical quantities. If a biological material is used as a detection element, the fabricated sensor is named as a biosensor. In biosensors, the material that is detected by the biosensor is called a substrate or analyte. Bioanalytical assays are environmentally friendly methods for assessment of various substrates.

In the last decades, biosensors have attracted considerable attention because of their simple procedure, and also because of their accurate and fast response. These advantageous features make biosensors applicable in chemical, pharmaceutical, and food industries, environmental monitoring, and medical and health applications.⁹

Carbohydrates (glucose, fructose, sucrose, lactose, etc.), alcohols (methanol, ethanol, propanol, phenol, etc.), organic acids (such as, acetic acid, ascorbic acid, etc.), amino acids (such as arginine, histidine, leucine, and lysine), fatty acids (such as maleic acid and linoleic acid), triglycerides, cholesterol, vitamins, toxic compounds, microbes, bacteria, and viruses are a number of analytes detected by biosensors that have been reported in the literature.^{10–12}

Generally, a biosensor is composed of two main constituents: a biological element and a transducer. However, three more constituents, including an amplifier, processor, and monitoring device, may be used in the fabrication of biosensors.^{13,14} Figure 4.4 shows a schematic diagram of typical biosensor components.

The biological element is a sensitive element to the substrate of interest which reacts with it and causes physicochemical changes. In the transducer, the resulted changes are converted to a measurable signal. If the output signal from the transducer is weak, the response is amplified through an amplifier. A processor converts the value of the biosensor response into the analyte concentration by means of standards prepared via a calibration curve. A monitoring device is used to display the analyte concentration measured by the biosensor.¹⁴

4.8.1 Biological Element

The biological elements used in biosensors include enzymes, microorganism, antibodies, receptors, nucleic acids, cells, tissues, and biologically derived or biomimetic materials. Bioelements selectively react or interact with the analyte of interest; therefore, in biological assays, the undesired effects of interfering materials are insignificant. Bioelements may catalyze the substrate reaction or bind to the detectable analyte.^{12,15}

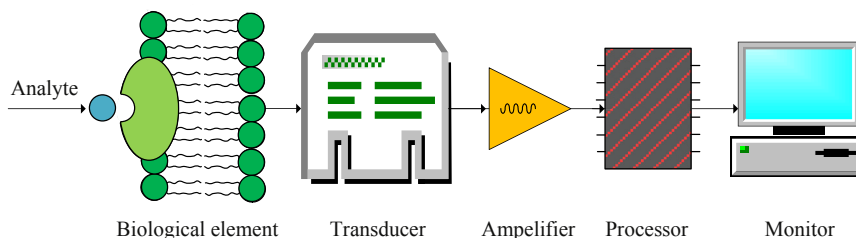


FIGURE 4.4 Schematic diagram of biosensor components.

Enzymes are the most desired biological elements used in the fabrication of biosensors. An enzyme is a complicated and large macromolecule that consists of chains of amino acids linked together. In fact, an enzyme is a highly selective biocatalyst that accelerates the rate and specificity of biochemical reactions. The advantages of enzymatic biosensors are that they possess high selectivity, rapid detection, and high sensitivity.¹⁶

4.8.2 Immobilization of Biomaterials

The immobilization of bioelements plays an important role in the performance of biosensors. The various techniques based on physical (adsorption, entrapment, and encapsulation) and chemical (cross-linking and covalent binding) methods are commonly used for biomaterial immobilization.^{17–19}

4.8.2.1 Adsorption

Adsorption of enzymes and biomaterials by insoluble supports is the simplest method for bioelement immobilization. This technique is based on physical interactions (Van der Waal's forces, hydrogen bonds, and multiple salt linkages) between the enzyme and the surface of solid support.²⁰ In the adsorption method, the enzyme is dropped on the support surface or support is immersed into the enzyme solution. After a certain time, the support is allowed to dry and then is washed with a buffer solution or distilled water to remove the unbound enzymes from the surface. In the adsorption technique, no extra chemicals are used; therefore, this method has low cost and also does not have undesired effects on enzyme activities. Enzyme leakage is the main disadvantage of adsorption method, which is caused by fluctuation of temperature, pH, and ionic strength or induction of analyte.^{20,21} The biosensors based on adsorption method have sufficient repeatability and are useful for disposable diagnostic enzyme kits.

4.8.2.2 Entrapment

Entrapment of enzymes within polymeric matrices is a common method for immobilization. In this method, first, enzyme is added to the monomeric solution, and then the monomer is polymerized. Thermal, sol–gel, and electropolymerization are typical methods used in entrapment technique.²² The pore size of the gel or fiber is such that the matrix prevents leakage of enzyme macromolecules; whereas, the analyte or reaction products can freely diffuse into the matrix and reach enzyme active sites. However, high molecular weight analytes cannot easily penetrate into the matrix.²³ The conditions applied in chemical polymerization and generated free radicals may have damaging effects on enzyme activity. Therefore, the conditions of polymerization need to be carefully controlled. Polypyrrole, polythionine, polyethylene dioxythiophene, natural polymer (chitosan, agar) and calcium alginate are some common materials that are widely used for enzyme entrapment.^{22,24}

4.8.2.3 Encapsulation

Encapsulation of enzyme and biomaterials within the membrane is another method of immobilization. In microencapsulation, the enzyme is surrounded by a continuous film of membrane or polymeric gel to produce spherical beads that contain an enzyme, known as

microcapsuls.²⁰ Encapsulation of enzyme between the coating material and support surface is the most applicable method used in biosensors. In this method, first, the enzyme is placed on the surface of the support, and then a film of membrane is coated on the surface of the deposited enzyme.

The most important membrane and coating materials used for encapsulation are carrageenan, chitosan, sodium alginate, carboxy methyl cellulose (CMC), methylcellulose, cellulose acetate, polycarbonate, polysulfone, polyacrylate, collagen, Teflon, and phospholipids.^{22,25} Applying membranes that selectively allow analytes and products to permeate is a useful and precise technique; however, the biosensors based on this method usually have long response times. Membrane disruption caused by accumulation of side products is another disadvantage of this method.

4.8.2.4 Cross-Linking

This type of immobilization is based on the intermolecular cross-linking of an enzyme, either to other enzyme molecules or to functional groups available on the support. Aggregation of enzymes leads to a bulky mass of enzyme molecules that is insoluble in the supporting electrolyte; therefore, the enzyme leakage resulting from enzyme solubility is significantly reduced.²⁶

The most common reagents used for cross-linking are glutaraldehyde and toluene diisocyanate. The disruptive nature of cross-linking reactions and also the toxicity of cross-linkers adversely affect the conformation of enzyme active sites and cause a decrease in enzyme activity. Hence, the amount of reagent used in cross-linking and the ratio of enzyme to reagent must be precisely controlled. The cross-linking technique is usually used in association with another immobilization method to ensure high performance of immobilization and, consequently, to enhance biosensor stability.²⁷

4.8.2.5 Covalent Binding

The covalent binding method is based on the strong covalent bonds between amino acid side chains of the enzyme and a protein with functional groups available on the support. Since covalent bonds are the strongest chemical bonds, the covalent binding method is more stable than other immobilization methods. The most common functional groups used in covalent bonding are the hydroxyl group ($-\text{OH}$) of the serine, threonine, and tyrosine, the amino group ($-\text{NH}_2$) of lysine, arginine, and histidine, the carboxyl group ($-\text{COOH}$) of glutamic acid and aspartic acid, and the thiol group ($-\text{SH}$) of cysteine.²⁸

In this technique, first, the support is functionalized with specific reagents to create the required functional groups. Then, the enzyme is added to the support for coupling with functional groups. For example, (3-Aminopropyl) triethoxysilane, carbodiimide conjugation, and cyanogen bromide are widely used for producing $-\text{NH}_2$, $-\text{COOH}$, and $-\text{OH}$ functional groups, respectively. Alkylation, peptide binding, diazo linkage, and isourea linkage are the main reaction processes used in the covalent binding method.^{7,22}

The main disadvantage of covalent binding is that some of the enzyme active sites participate in the coupling reaction, which causes the deactivation of the enzyme. However, addition of enzyme inhibitors at the moment of the coupling reaction moderately prevents enzyme active sites from taking part in the reaction.

4.8.3 Transducer

The transducer converts the physicochemical changes resulting from the interaction of the analyte and bioelement into a quantifiable signal. Depending on the transduction mechanism, there are three groups of biosensors:

1. Products resulting from biosensors through the biochemical reaction transfer into the transducer and causing the measurable response.
2. Biosensors that benefit from mediators in order to assist product transfer into the transducer.
3. Biosensors where the bioelement is directly connected to the transducer and product or the response resulting from the biochemical reaction is immediately available through the transducer.²⁹

Based on the transducer, there are different types of biosensors, such as electrochemical, piezoelectric, optical, and thermal biosensors.^{30,31}

4.8.3.1 Thermal Biosensor

Biochemical reactions have definite enthalpy changes, in which the changes of enthalpy affect the temperature. In thermal biosensors, the thermometric detection of the variation in reaction enthalpies is used. For thermal biosensing, a very sensitive thermometer is required that has the ability to detect very small temperature changes. Simple thermometers and thermocouples are not sensitive enough to measure the variation of biochemical reaction enthalpies. Thermopiles and thermistors are commonly used to detect such small variations in temperature.³²

4.8.3.2 Optical Biosensor

Interactions between the analyte and biological element lead to a change in photometric properties. In optical assay, photometric detection is the basis of this method. Mainly, the photometric change may occur in the analyte, biosensor element, or marker that is included in the biosensor. The photometric methods applied in optical biosensors are absorption, reflection spectroscopy and scattering methods, fluorescence and phosphorescence emission, and luminescence.^{33,34}

4.8.3.3 Piezoelectric Biosensor

The piezoelectric method is based on the electrical currents resulting from a vibrating crystal. Crystals have a certain resonant frequency of oscillation. In piezoelectric biosensors, the total frequency of a crystal is related to mass of crystal and the coated bioelement. In this method, the analyte concentration is detected by measuring the variation in resonant frequency resulting from the analyte binding or biochemical reaction. Enzymatic piezoelectric biosensors and piezoelectric immunosensors are the most common piezoelectric biosensors. Crystals (quartz, berlinite, gallium orthophosphate, langasite, etc.), ceramic materials (barium titanate, lead titanate, and lead zirconate titanate) and some organic polymers (polyvinylidene fluoride) are a number of materials used in piezoelectric sensors.^{27,35}

4.8.3.4 Electrochemical Biosensor

The electrochemical method is the most applicable technique in the fabrication of biosensors. The electrochemical biosensors is the leading biosensor that has been commercially

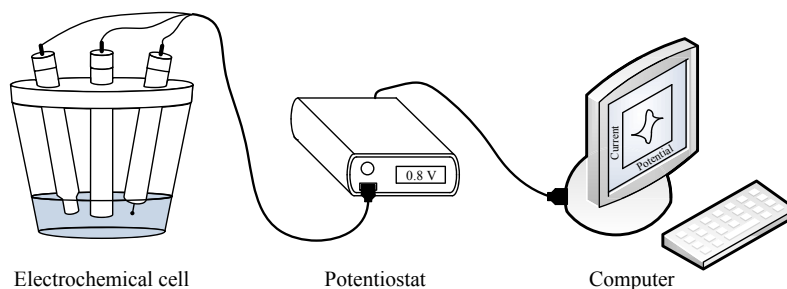


FIGURE 4.5 Schematic diagram of a conventional three-electrode system for electrochemical detection.

developed. An electrochemical biosensor is based on a biochemical reaction that produces or consumes electrons. Amperometry, potentiometry (measuring potential at zero current), and conductometry (measuring conductivity using an alternating current bridge method) are the common methods applied in electrochemical biosensors. The electrochemical transducer usually consists of a conventional three-electrode system, a reference electrode, a counter electrode, and a working electrode.^{36,37} Figure 4.5 shows the schematic diagram of an electrochemical method using a conventional three-electrode system.

4.8.4 Amperometric Biosensors

The amperometry method is suitable for analytes that are able to oxidize or reduce in chemical or biochemical reactions. In the amperometry method, a current signal is produced by applying a fixed potential between the reference electrode and working electrode. Amperometric measurement is carried out in a supporting electrolyte (containing buffer solution at a constant pH) to ensure electron transfer in the electrical circuit. Amperometric biosensors generate a current proportional to the concentration of the analyte of interest.^{38,39} Amperometric measurements may be performed at fixed potential with respect to time or at differential pulse potential. Chronoamperometry is a typical method for amperometry detection where the current response is recorded at a fixed potential with respect to time in an unstirred solution. The unstirred condition is applied to avoid convection and to provide natural mass transfer into the electrode surface.⁴⁰

Voltammetry is a powerful technique for studying electrochemical (oxidation and reduction) behavior of a biosensor in the vicinity of an analyte. In voltammetry, the current is measured while the applied potential between working and reference electrodes is scanned. Linear-sweep is a type of voltammetry in which the applied potential is linearly varied, and the current versus the potential is shown as a voltammogram curve. Cyclic voltammetry is another method which studies the oxidation and reduction of a chemical reaction. In cyclic voltammetry, the potential is varied from an initial value to another value of potential and then reaches again to the starting point with a constant scan rate.⁴¹ The scan rate of the potential is projected by the simple rate equation, $\nu = \frac{dE}{dt}$. Figure 4.6 represents an increase and decrease of potential with respect to time. As illustrated in this figure, the cyclic voltammetry includes two stages of linear sweep in which the potential scan rates are equal with reverse direction.

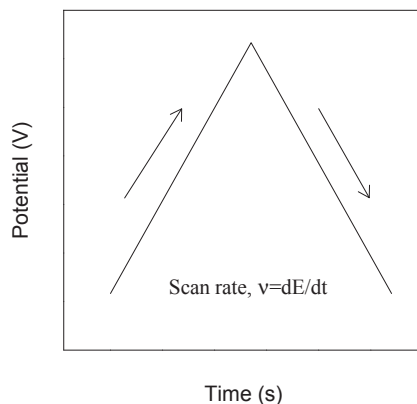


FIGURE 4.6 Sweeping the potential versus time.

Considering that electroactive analyte participate in a redox reaction on the surface of a biosensor electrode, the half-cell redox reaction is given as follows:



where Ox and Red are the oxidized and reduced species in the redox reaction, respectively. Figure 4.7 shows the cyclic voltammogram of a reversible redox reaction which occurs near the electrochemical biosensor. In starting point (A) the current value is low. From point A to B, the current response slightly increases in which this current is known as the background current. Background current is due to residual current from impurities and also double-layer charging. In point B, potential required for oxidation of an analyte is available; therefore, the reduced specie is oxidized. In this stage, the current response increases with increasing potential value and reaches anodic peak current, shown in point C. After that, the substrate is oxidized in the vicinity of the working electrode, and the current response descends to the

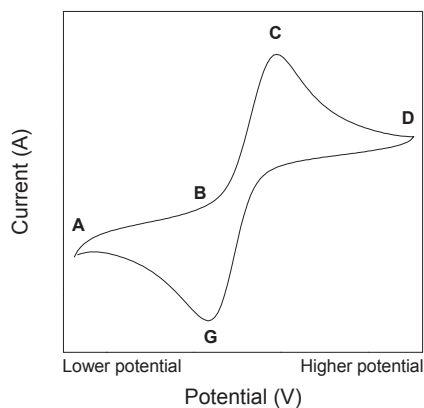


FIGURE 4.7 Cyclic voltammogram of a redox reaction on the electrode surface of a biosensor.

point B. For a reversible reaction, in reverse scan, the reduction of oxidized species occurs, and cathodic peak current (point G) is obtained.^{39,41,42} In cases where the potential first scans with negative slope, locations of anodic and cathodic peak currents are displaced.

The potential corresponding to the peak current obtained in cyclic voltammetry is valuable information which can be applied in amperometric measurements. If the applied potential is adjusted to the peak potential, the current response of the analyte is increasing and the current response related to interfering material is decreasing and, as a result, the sensitivity and accuracy of electrochemical detection are enhanced.

Figure 4.8 depicts a typical current response for chronoamperometry method. In the beginning, the high current is observed, and then the current decays and reaches a steady-state value. This phenomenon is due to the consumption of substrate near the electrode that causes spreading of the diffusion layer and consequently decreases the driving force that results from diffusion.⁴³ In the steady-state region, the current response is almost independent of time. According to Fick's first law of diffusion, the current response is given by the following equation³³:

$$i = \frac{nFADC}{\delta} \quad (4.8.4.2)$$

where i (A) is the current response, n is the number of exchanged electrons, F is Faraday's constant, D ($\text{cm}^2 \text{s}^{-1}$) is the diffusion coefficient of the redox active analyte, A (cm^2) is the surface area of the electrode, C (mol cm^{-3}) is the concentration of the analyte in the supporting solution, and δ (cm) is the thickness of the diffusion layer.

Another useful equation used in chronoamperometric study is the Cottrell equation, which is described as follows:^{41,42}

$$i = \frac{nFACD^{1/2}}{\pi^{-1/2}t^{-1/2}} \quad (4.8.4.3)$$

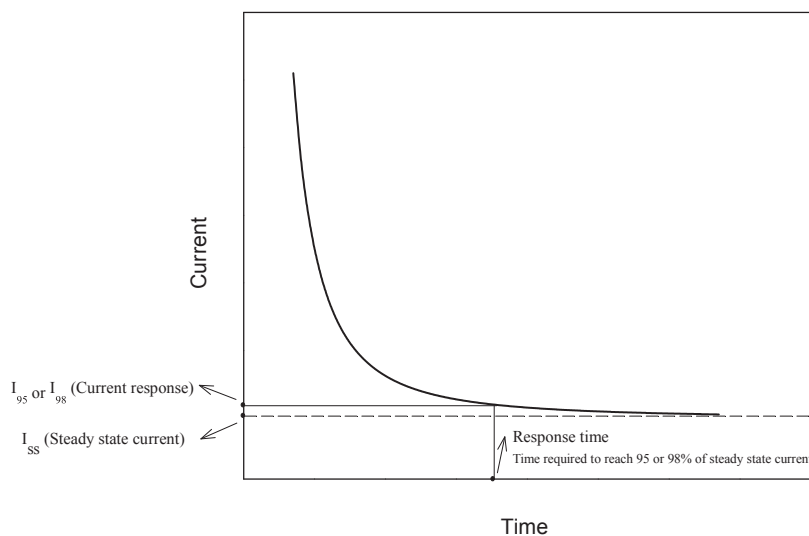


FIGURE 4.8 Chronoamperometry: current response versus time.

If the chemical reaction on the surface of the electrode is a diffusion-controlled process, a linear relationship exists between the current and the reciprocal of the square root of time. By plotting i versus $t^{-1/2}$ and from the slope of the linear plot, the diffusion coefficient of the analyte is calculated. This equation can also be used to determine the number of exchanged electrons, the electrode surface area, or the analyte concentration.

In practice, determining the concentration of analyte using a calibration curve is more precise and applicable. In this method, a chronoamperometric experiment is carried out at different concentrations of analyte. Then, the steady-state current response of each concentration is depicted versus the concentration, and a calibration curve is obtained. In addition, another common method often used for preparing a calibration curve of a biosensor is amperometric; first, the amperometric measurement is performed in the supporting electrolyte in stirred condition. The background current is allowed to decay to a steady-state value, and then aliquots of analyte stock solution are added into the supporting solution. In this method, stirred condition is needed to ensure convective transport for each injection. Figure 4.9 represents a typical amperometric current response with respect to time for each injection of aliquots of analyte solution.

Figure 4.10 represents a typical amperometric current response versus the analyte concentration for enzymatic biosensors. In enzymatic biosensors, the current reaches a maximum value based on the enzyme loading on the electrode surface. The linear range of the current response profile is used as the calibration curve for analytical assays.

In an enzymatic biosensor, the enzyme–substrate kinetic of the biosensor is represented by the Lineweaver–Burk equation state, as follows⁴³:

$$\frac{1}{I_{ss}} = \frac{1}{I_{max}} + \frac{K_M}{I_{max}} \frac{1}{C} \quad (4.8.4.4)$$

where I_{ss} is the steady-state current response after each step of substrate addition, I_{max} is the maximum current response under saturated substrate condition, C is the substrate concentration in the bulk solution, and K_M is the apparent Michaelis–Menten constant. To determine the K_M value of the enzyme electrode from Eqn (4.8.4.4), the reciprocal of steady-state current

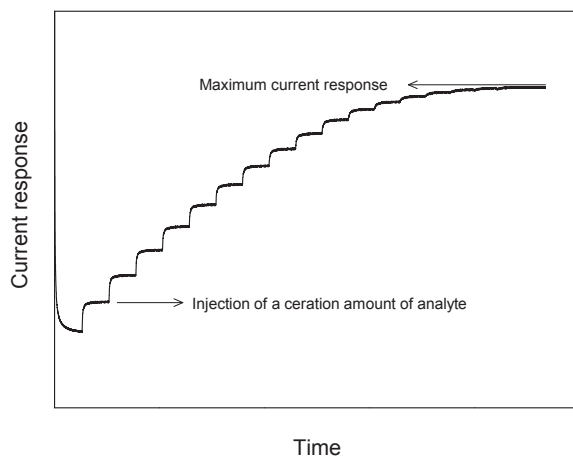
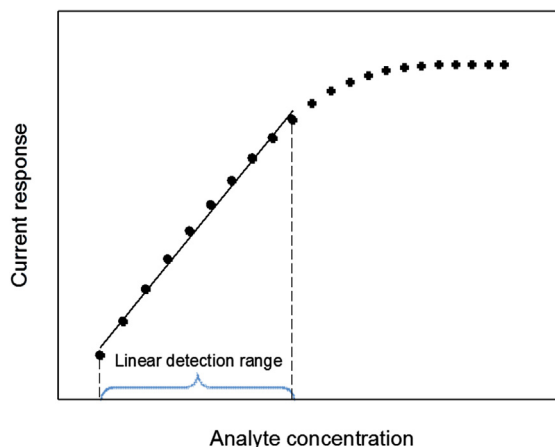


FIGURE 4.9 A typical amperometric current response for adding analyte concentrations with respect to time.

FIGURE 4.10 Amperometric current response versus the concentration of analyte.



response versus the reciprocal of analyte concentration is plotted. From the slope and intercept of the Lineweaver–Burk plot, the K_M is calculated. The low values of K_M show that the biosensor has high affinity to glucose and high activity of immobilized enzyme.

4.8.4.1 Response Time

The response time of a biosensor is the time required to achieve steady-state value. However, in practice, the time required to reach 95%³⁶ or 98%²⁷ of the biosensor response is known as the response time (Figure 4.8). Response times of 3 s to 25 min have been reported in the literature.^{44–46} Since the essence of the sensors is based on the rapid detection, the response times above 5 min are not of interest.

4.8.4.2 Recovery Time

The recovery time is the time required for the biosensor to reach equilibrium state and the signal to return to its base line. In order to remove substrate and product accumulated on the support surface, the biosensor is washed or immersed in a buffer solution.^{7,36}

4.8.4.3 Linear Detection Range

Linear detection range is the range of detection in which the response of the biosensor is linear (Figure 4.10). In biosensors, the wide linear range is of interest that makes the biosensor applicable in a wide range of analyte concentration.

4.8.4.4 Limit of Detection

Limit of detection (LOD) is the lowest concentration of the analyte that can be detected by biosensors. In practice, LOD is usually determined by a signal to noise ratio of 3 ($S/N = 3$). The equation commonly used for determination of LOD is given as follows⁴⁷:

$$\text{LOD} = \frac{3S_b}{m} \quad (4.8.4.5)$$

where S_b is the standard deviation of blank or buffer, and m is the slope of the calibration curve.

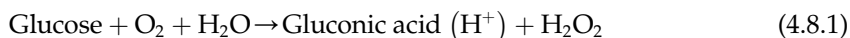
4.8.4.5 Sensitivity

Sensitivity is defined as the current response per unit of analyte concentration and electrode surface. From the definition, it is found that for a certain current response, the biosensor sensitivity is higher for the electrode that has a smaller surface than others.

The biochemical constituents of fermentation broth such as liberated biochemical compounds, oxidation, and reductions have been developed by a wide range of biosensors. A biosensor consists of two main elements. These two elements, the biocatalyst and a transducer, are combined as a single detecting probe in which the transducer and biocatalyst are held together in a very close contact. The biosensor acts as a device as flow passes. It can detect penetration of flow through biocatalysts and measures the biochemical transformation of a given substance, for example, a change in pH. The function of the transducer is to detect such change and to produce an output signal, which is related to the concentration of the measured substance. In fact, a biosensor is a combination of a biological sensor attached to a transducer, which is a simple device that acts specifically with a high sensitivity in measurements.

The application of biosensors in an operating bioreactor is usually based on whole cells or enzyme activities. The perfect function of a biosensor is very dependent on the biological activities of a system. The biocatalytic reaction produces some detectable change that must be converted to an output signal by the transducer. The transducers are usually amperometric and potentiometric devices. Such transducers are included in dissolved oxygen probes and pH electrodes, ion-selective electrodes, and gas-sensing devices. Amperometric detectors operate by measuring the flux of some electrochemical redox activities of the produced biosensor reaction. For example, a dissolved oxygen probe can be used to measure the rate of oxygen flux produced in a catalyzed oxidation reaction. DO probes are a popular form of biosensor transducer. They are used for microbial and enzymatic oxidoreductase reactions. Many enzymatic reactions are associated with the uptake or production of protons. The rate of proton flux can be measured by using a potentiometric detector, which is normally done in a pH probe.

Several biosensors are commercially available. One of the most useful ones is the glucose sensor. The standard sensor determines glucose concentration based on the glucose oxidase enzyme. The chemical reaction for the oxidation of glucose is as follows:



A suitable biosensor can measure the amount of oxygen consumed in the above reaction. The biosensor is constructed by the surrounding tip of the DO probe, which is a glucose permeable membrane and retains glucose oxidase/electrolyte solution in direct contact with the membrane of the DO probe. Normally, the DO probe can measure the rate of oxygen flux in the bulk liquid. The flux across the DO probe membrane to the cathode, where oxygen is reduced, is equal to the rate of oxygen flux reaching and reducing the electrode. The reduced amount of oxygen is equivalent to the rate of glucose that is consumed in the glucose oxidase enzymatic conversion of glucose to gluconic acid.

The use of a catalyst with an oxidase enzyme is an example of the application of a combined enzyme system, which illustrates the wide potential offered by multienzyme electrode systems. Various enzymes can be arranged to work sequentially to transform quite complex substances and eventually to produce a measurable concentration-dependent change that is detected by the output signal and recorded for analysis.

NOMENCLATURE

E Potential, V
 E_o Standard electrode potential, V
 R The gas constant
 K Proportionality constant, mV per unit pH
 T Absolute temperature, K
 v Potential scan rate, V/s
 I Current, A
 F Faraday's constant
 A Surface area, cm^2
 D Diffusion coefficient, $\text{cm}^2 \text{s}^{-1}$
 C Analyte concentration, mol cm^{-3}
 δ Diffusion layer thickness, cm^2
 t Time, s
 I_{SS} Steady-state current, A
 I_{\max} Maximum current response, A
 K_M Apparent Michaelis–Menten constant
 S_b Standard deviation
 m Slope of the calibration curve

References

1. Baily JE, Ollis DF. *Biochemical engineering fundamentals*. 2nd ed. New York: McGraw-Hill; 1986.
2. Scragg AH. *Bioreactors in biotechnology, a practical approach*. Ellis Horwood series in biochemistry and biotechnology; New York: Ellis Horwood Limited; 1991.
3. Wang DIC, Cooney CL, Deman AL, Dunnill P, Humphrey AE, Lilly MD. *Fermentation and enzyme technology*. New York: John Wiley & Sons; 1979.
4. Doran PM. *Bioprocess engineering principles*. New York: Academic Press; 1995.
5. Stanbury PF, Whitaker A. *Principles of fermentation technology*. New York: Pergamon Press; 1987.
6. Ho CK, Robinson A, Miller DR, Davis MJ. Overview of sensors and needs for environmental monitoring. *Sensors* 2005;5(1):4–37.
7. Eggins BR. *Biosensors: an introduction*. Chichester (UK): Wiley; 1996.
8. Nicholas J, White D. *Liquid-in-glass thermometry. Traceable temperatures: an introduction to temperature measurement and calibration*. 2nd ed., Wiley: 1999. 255–293.
9. Wang J. Glucose biosensors: 40 years of advances and challenges. *Electroanalysis* 2001;13(12):983–8.
10. Mello LD, Kubota LT. Review of the use of biosensors as analytical tools in the food and drink industries. *Food Chem* 2002;77(2):237–56.
11. Rodriguez-Mozaz S, de Alda MJL, Barceló D. Biosensors as useful tools for environmental analysis and monitoring. *Anal Bioanal Chem* 2006;386(4):1025–41.
12. Vo-Dinh T, Cullum B. Biosensors and biochips: advances in biological and medical diagnostics. *Fresenius' J Anal Chem* 2000;366(6–7):540–51.
13. Berggren C, Bjarnason B, Johansson G. Instrumentation for direct capacitive biosensors. *Instrum Sci Technol* 1999;27(2):131–9.
14. Davis J, Huw Vaughan D, Cardosi MF. Elements of biosensor construction. *Enzyme Microb Technol* 1995;17(12):1030–5.
15. Mohanty SP, Kougiannos E. Biosensors: a tutorial review. *Potentials IEEE* 2006;25(2):35–40.
16. Newman JD, Setford SJ. Enzymatic biosensors. *Mol Biotechnol* 2006;32(3):249–68.
17. Bourdillon C, Laval JM, Thomas D. Enzymatic electrocatalysis: controlled potential electrolysis and cosubstrate regeneration with immobilized enzyme modified electrode. *J Electrochem Soc* 1986;133(4):706–11.
18. Krajewska B. Application of chitin-and chitosan-based materials for enzyme immobilizations: a review. *Enzyme Microb Technol* 2004;35(2):126–39.

19. Olea D, Viratelle O, Faure C. Polypyrrole-glucose oxidase biosensor: effect of enzyme encapsulation in multi-lamellar vesicles on analytical properties. *Biosens Bioelectron* 2008;**23**(6):788–94.
20. Guisan JM. *Immobilization of enzymes and cells*, Vol. 22. Springer; 2006.
21. Mathewson PR, Finley JW. *Biosens Design Application*, Vol. 511. 1992.
22. Bickerstaff Jr GF. *Immobilization of enzymes and cells*. Springer; 1997.
23. Guisán JM, Penzol G, Armisen P, Bastida A, Blanco RM, Fernandez-Lafuente R, et al. Immobilization of enzymes acting on macromolecular substrates. In: *Immobilization of enzymes and cells*. Springer; 1997. p. 261–75.
24. Dempsey E, Diamond D, Collier A. Development of a biosensor for endocrine disrupting compounds based on tyrosinase entrapped within a poly (thionine) film. *Biosens Bioelectron* 2004;**20**(2):367–77.
25. Wijffels RH, Buitelaar R, Bucke C, Tramper J. *Immobilized cells: basics and applications*, Elsevier Science; 1996.
26. Cooper J, Cass T. *Biosensors*, Vol. 268. Oxford University Press; 2004.
27. Canh TM. *Biosensors*. US: Springer; 1994.
28. Williams R, Blanch H. Covalent immobilization of protein monolayers for biosensor applications. *Biosens Bioelectron* 1994;**9**(2):159–67.
29. Mulchandani A, Bassi AS. Principles and applications of biosensors for bioprocess monitoring and control. *Critical Rev Biotechnol* 1995;**15**(2):105–24.
30. Patel P. (Bio) sensors for measurement of analytes implicated in food safety: a review. *Trac Trends Anal Chem* 2002;**21**(2):96–115.
31. Si W, Han Z, Lei W, Wu Q, Zhang Y, Xia M, et al. Fast electrochemical determination of imidacloprid at an activated glassy carbon electrode. *J Electrochem Soc* 2014;**161**(1):B9–13.
32. Ramanathan K, Danielsson B. Principles and applications of thermal biosensors. *Biosens Bioelectron* 2001;**16**(6):417–23.
33. Bilitewski U, Turner A. *Biosensors in environmental monitoring*. CRC Press; 2003.
34. Riboh JC, Haes AJ, McFarland AD, Ranjit Yonzon C, Van Duyne RP. A nanoscale optical biosensor: real-time immunoassay in physiological buffer enabled by improved nanoparticle adhesion. *J Phys Chem B* 2003;**107**(8):1772–80.
35. Pramanik S, Pinguang-Murphy B, Osman NAA. Developments of immobilized surface modified piezoelectric crystal biosensors for advanced applications. *Int J Electrochem Sci* 2013;**8**:8863–92.
36. Ronkainen NJ, Halsall HB, Heineman WR. Electrochemical biosensors. *Chem Soc Rev* 2010;**39**(5):1747–63.
37. Thevenot DR, Toth K, Durst RA, Wilson GS. Electrochemical biosensors: recommended definitions and classification. *Pure Appl Chem* 1999;**71**(12):2333–48.
38. Frew JE, Hill HAO. Electrochemical biosensors. *Anal Chem* 1987;**59**(15):933A–44A.
39. Grieshaber D, MacKenzie R, Vörös J, Reimhult E. Electrochemical biosensors-Sensor principles and architectures. *Sensors* 2008;**8**(3):1400–58.
40. Scheller F, Schubert F. *Biosensors*. Elsevier; 1991.
41. Allen JB, Larry RF. *Electrochemical methods: fundamentals and applications*. Department of chemistry and biochemistry university of Texas at Austin. John Wiley & Sons, Inc; 2001.
42. Greef R, Peat R, Peter L, Pletcher D, Robinson J. *Instrumental methods in electrochemistry*. Chichester (England): Ellis Horwood Ltd; 1985.
43. Wang Y, Ma X, Wen Y, Zheng Y, Duan G, Zhang Z, et al. Phytic acid-based layer-by-layer assembly for fabrication of mesoporous gold film and its biosensor application. *J Electrochem Soc* 2010;**157**(1):K5–9.
44. Yang VC-M, Ngo TT. *Biosensors and their applications*. Springer; 2000.
45. Gomathi P, Kim MK, Park JJ, Ragupathy D, Rajendran A, Lee SC, et al. Multiwalled carbon nanotubes grafted chitosan nanobiocomposite: a prosperous functional nanomaterials for glucose biosensor application. *Sensors Actuators B Chem* 2011;**155**(2):897–902.
46. Rogers KR, Mulchandani A, Zhou W. Biosensor and chemical sensor technology: process monitoring and control []. In: *ACS symposium series (USA)*; 1995.
47. Reddaiah K, Madhusudana Reddy T. Electrochemical biosensor based on silica sol–gel entrapment of horseradish peroxidase onto the carbon paste electrode toward the determination of 2-aminophenol in non-aqueous solvents: a voltammetric study. *J Mol Liq* 2014;**196**:77–85.

Growth Kinetics

OUTLINE

5.1 Introduction	129	5.7.6 Biomass Balances (Cells) in a Bioreactor	141
5.2 Indirect Measurements of Cell Growth	129	5.7.7 Material Balance in Terms of Substrate in a Chemostat	142
5.2.1 Fluorescence Spectroscopy	129	5.7.8 Modified Chemostat	143
5.2.2 Specific Growth Rate	130	5.7.9 Fed Batch Culture	144
5.3 Cell Growth in Batch Culture	131	5.8 Enzyme Reaction Kinetics	145
5.4 Growth Phases	131	5.8.1 Mechanisms of Single Enzyme with Dual Substrates	147
5.5 Kinetics of Batch Culture	132	5.8.2 Kinetics of Reversible Reactions with Dual Substrate Reaction	151
5.6 Growth Kinetics for Continuous Culture	133	5.8.3 Reaction Mechanism with Competitive Inhibition	152
5.7 Material Balance for Continuous Stirred Tank Reactor (CSTR)	137	5.8.4 Noncompetitive Inhibition Rate Model	153
5.7.1 Rate of Product Formation	139	5.9 Unstructured Kinetic Model	173
5.7.2 Continuous Culture	140	Nomenclature	179
5.7.3 Disadvantages of Batch Culture	140	References	180
5.7.4 Advantages of Continuous Culture	140		
5.7.5 Growth Kinetics, Biomass, and Product Yields, $Y_{X/S}$ and $Y_{P/S}$	140		

5.11 Case Study: Enzyme Kinetic Models for Resolution of Racemic Ibuprofen Esters in a Membrane Reactor	181	5.11.3 Enzyme Kinetics for Rapid Equilibrium System (Quasi-Equilibrium)	187
5.11.1 Introduction	181	5.11.4 Derivation of Enzymatic Rate Equation from Rapid Equilibrium Assumption	187
5.11.2 Enzyme Kinetics	182	5.11.5 Verification of Kinetic Mechanism	189
5.11.2.1 Substrate and Product Inhibitions Analyses	182	References	191
5.11.2.2 Substrate Inhibition Study	183		
5.11.2.3 Product Inhibition Study	185		

SUBCHAPTER

5.1

Introduction

Microbial growth is considered for the observation of the living cell activities. It is important to monitor cell growth and biological and biocatalytic activities in cell metabolism. Several methods are available to predict cell growth by direct or indirect measurements. Cell dry weight, cell optical density (OD), cell turbidity, cell respiration, metabolic rate, and metabolites are quite suitable for analyzing cell growth, substrate utilization, and product formation. The rate of cell growth is described in this chapter. Various bioprocesses are modeled for substrate utilization and product formation. Growth kinetics in batch and continuous culture is examined in detail.

5.2 INDIRECT MEASUREMENTS OF CELL GROWTH

Biological fluorophores including proteins, pigments, and many metabolites such as nicotinamide adenine dinucleotide hydrogenase (NADH) represents cell activities. Biological compounds including nucleotides, riboflavin, NADH, nicotinamide adenine dinucleotide phosphate-oxidase, and flavin adenine dinucleotide are fluorophores at specific wavelengths of 310–520 nm are fluorescence with properties that can be detected and measured as counts for cell growth activities. The cell population can be determined by fluorescence spectroscopy. The method has advantages as it is relatively specific, sensitive, and accurate for online measurements.

5.2.1 Fluorescence Spectroscopy

Certain cellular components exhibit fluorescence property, which is defined as the ability to absorb light with spectral longer fluorescence wavelength. The fluorescence light intensity depends on concentration of fluorophase, which is described by the Lambert–Beer law:

$$Fl = \phi \cdot I_{\phi} \cdot (1 - e^{-a \cdot C \cdot d}) \quad (5.2.1.1)$$

Where Fl is intensity of fluorescence light (W cm^{-2}), ϕ is the fluorescence yield and I_{ϕ} is the excitation light intensity (W cm^{-2}), a is molar absorption coefficient ($\text{mol}^{-1} \text{cm}^{-1}$), C is fluorophore concentration (mol l^{-1}), and d is path length (cm). Because nonlinear relation exist for fluorescence with respect to concentration of fluorophore, one can use the linearized segment of the above relation for small concentration of fluorophore over a small path. The relation can be simplified as:

$$Fl = \phi / I_{\phi} \cdot a \cdot C \cdot d \quad (5.2.1.2)$$

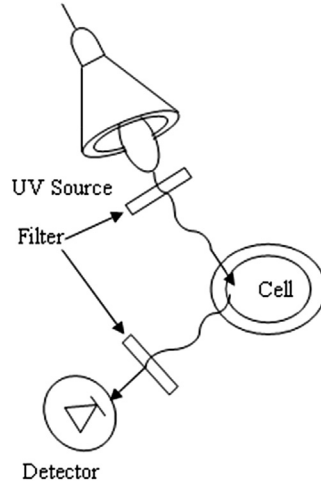


FIGURE 5.1 The principle of fluorescence for measurements and detection of cell growth.

The cell activities can be detected by oxygen uptake rate and respiration quotient (RQ) for utilization of oxygen and liberation of carbon dioxide. The detection can be conducted online for the bioreactor in continuous operation. Figure 5.1 demonstrates the principle of fluorescence used for measurements and detection of cell growth.

5.2.2 Specific Growth Rate

Cell growth is easily detected once cells are rapidly propagated at exponential phase, whereas cell weight is doubling at certain time interval; then the number of doubling after time t is defined as:

$$n = \frac{t}{t_d} \quad (5.2.2.1)$$

Where n is the number of doubling, t is incubation time, and t_d is doubling time for the specific organism.

$$\ln\left(\frac{x}{x_0}\right) = (\ln 2)\left(\frac{t}{t_d}\right) = 0.693\left(\frac{t}{t_d}\right) \quad (5.2.2.2)$$

Plot of $\ln \frac{x}{x_0}$ versus time t resulted slope of $\frac{0.693}{t_d}$, which is defined as specific growth rate (h^{-1}).

For batch culture, the specific growth rate is:

$$\begin{aligned} \mu &= \frac{0.693}{t_d} \\ \mu &= \frac{1}{X} \frac{dX}{dt} \end{aligned} \quad (5.2.2.3)$$

The outcome of the above expression demonstrates exponential growth phase for the living organism:

$$x = x_0 e^{0.693(\frac{t}{t_d})} \quad (5.2.2.4)$$

5.3 CELL GROWTH IN BATCH CULTURE

Batch culture is a closed system without any inlet or outlet streams, as nutrients are prepared in a fixed volume of liquid media. The inocula are transferred and then the microorganisms gradually grow and replicate. As the cell propagates, the nutrients are depleted and end products are formed. The microbial growth is determined by cell dry weight (g l^{-1}) and cell OD (absorbance at a defined wavelength, λ_{nm}). A growth curve can be divided into four phases, as shown in Figure 5.2. As inocula are transferred to the fermentation media, cell growth starts rapidly in the media. The lag phase shows almost no apparent cell growth. This is the duration of time represented for adaptation of microorganisms to the new environment, without much cell replication and with no sign of growth. The length of the lag phase depends on the size of the inocula. It is also results from the shock to the environment when there is no acclimation period. Even high concentrations of nutrients can cause a long lag phase. It has been observed that growth stimulants and trace metals can sharply reduce the lag phase. Figure 5.3 shows the influence of magnesium ions on the reduction of lag phase in a culture of *Aerobacter aerogenes*. The lag phase in the batch culture of *A. aerogenes* was drastically reduced from 10 h to zero when the concentration of Mg^{2+} was increased from 2 to 10 mg l^{-1} . There are many other factors believed to affect the lag phase. These are discussed in more detail in microbiology textbooks.¹

5.4 GROWTH PHASES

Once there is an appreciable amount of cells and they are growing very rapidly, the cell number exponentially increases. The optical cell density of a culture can then be easily detected; that phase is known as the exponential growth phase. The rate of cell synthesis

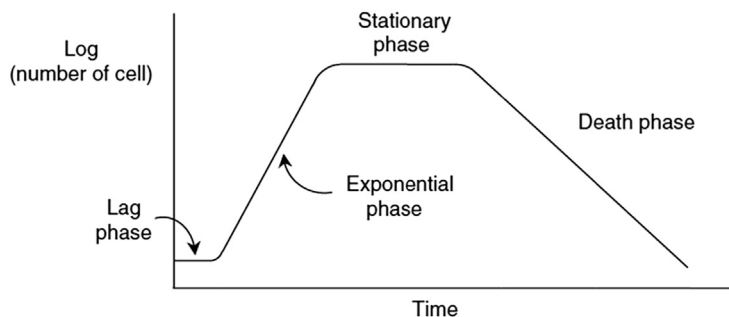
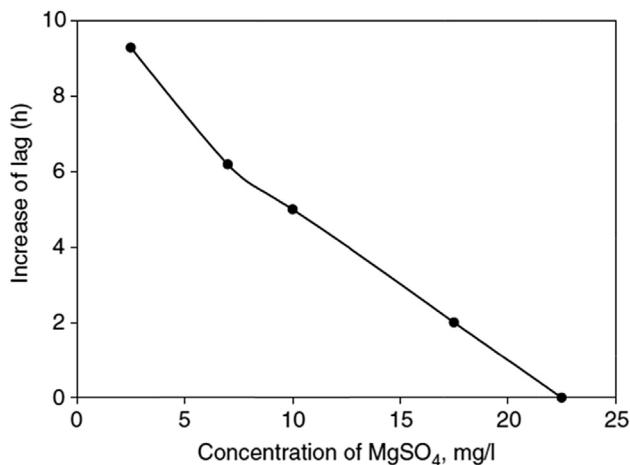


FIGURE 5.2 Typical batch growth curve of a microbial culture.

FIGURE 5.3 Influence of $[\text{Mg}^{2+}]$ on the lag phase in *Aerobacter aerogenes* culture.



sharply increases; the linear increase is shown in the semilog graph with a constant slope representing a constant rate of cell population. At this stage, carbon sources are utilized and products are formed. Finally, rapid utilization of substrate and accumulation of products may lead to stationary phase in which the cell density remains constant. In this phase, cells may start to die as the cell growth rate balances the death rate. It is well known that the biocatalytic activities of the cell may gradually decrease as they age, and finally autolysis may take place. The dead cells and cell metabolites in the fermentation broth may create toxicity, so deactivating remaining cells. At this stage, a death phase develops while the cell density drastically drops if the toxic secondary metabolites are present. The death phase shows an exponential decrease in the number of living cells in the media while nutrients are depleted. In fact the changes are detected by monitoring the pH of the media.

5.5 KINETICS OF BATCH CULTURE

The batch culture is a simple, well-controlled vessel in which the concentration of nutrients, cells, and products vary with time as the growth of the microorganism proceeds. Material balance in the reactor may assist in following the biochemical reactions occurring in the media. In batch fermentation, living cells propagate and many parameters of the media go through sequential changes with time as the cells grow. The following parameters are monitored while the batch process continues:

- Cells and cell by-product
- Concentration of nutrients
- Desirable and undesirable products
- Inhibition
- pH, temperature, substrate concentration

The objective of a good process design is to minimize the lag phase period and maximize the length of exponential growth phase. The substrate balance in a batch culture for component i in the culture volume of V_R and change of molar concentration of C_i is equal to the rate of formation of product:

$$\frac{d}{dt}(V_R \cdot C_i) = V_R \cdot r_{fi} \quad (5.5.1)$$

where V_R is the culture volume, assumed to be constant while no liquid media is added or removed, C_i is the molar concentration of component i and r_{fi} is the rate of product formation. Then Eqn (5.5.1) is reduced to:

$$\frac{dC_i}{dt} = r_{fi} \quad (5.5.2)$$

The rate of product formation, r_{fi} , depends upon the state of the cell population, environmental condition, temperature, pH, media composition, and morphology with cell age distribution of the microorganism.^{2,3} A similar balance can be formulated for microbial biomass and cell concentration. The exponential phase of the microbial growth in a batch culture is defined by:

$$\frac{dX}{dt} = \mu X \quad (5.5.3)$$

There is no cell removal from the batch vessel and the cell propagation rate is proportional to specific growth rate, μ (h^{-1}), using the differential growth equation the cell concentration with respect to the time is:

$$X(t) = X_0 e^{\mu t} \quad (5.5.4)$$

5.6 GROWTH KINETICS FOR CONTINUOUS CULTURE

The fermentation system can be conducted in a closed system as batch culture. The batch system growth kinetics and growth curve are explained in Sections 5.3 and 5.4. The growth curve is the best representation of a batch system. Disadvantages exist in the batch system such as substrate depletion with limited nutrients or product inhibition growth curve. The growth environment in the batch system has to follow all the phases projected in the growth curve. Besides nutrient depletion, toxic by-products accumulate. Even the composition of media with exponential growth is continuously changing; therefore, it will never be able to maintain any steady-state condition. The existing limitation and toxic product inhibition can be removed if the system is an open system and the growing culture is in a continuous mode of operation. In engineering, such a system is known as an open system. There would be an inlet medium as fresh medium is pumped into the culture vessel and the excess cells are washed out by the effluents, leaving the continuous culture from the fermentation vessel. The advantages of continuous culture are that the cell density, substrate, and product concentrations remain constant while the culture is diluted with fresh media. The fresh media is sterilized or filtered and there are no cells in the inlet stream. If the flow rate of the fresh media

gradually increases, the dilution rate also increases while the retention time decreases. At a high flow rate, the culture is diluted and the cell population decreases; with the maximum flow rate when all the cells are washed out, the composition of the inlet and outlet conditions remain about the same. In this condition, a washout phenomenon takes place. In continuous culture, the flow rate is adjusted in such a way that the growth rate and the cell density remain constant. There are two types of culture vessel: chemostat and biostat, and both are open systems.^{4,5} Detailed explanations are given in the following section.

1. Chemostat (growth rate controlled by dilution rate, D , h^{-1})
2. Turbidostat (constant cell density that is controlled by the fresh medium)

1. Chemostat. The nutrients are supplied at a constant flow rate and the cell density is adjusted with the supplied essential nutrients for growth. In a chemostat, growth rate is determined by the utilization of substrates like carbon, nitrogen, and phosphorus. A simple chemostat with feed pump, oxygen robe, aeration, and the pH controlling units is shown in Figure 5.4. The system is equipped with a gas flow meter. Agitation and aeration provided suitable mass transfer. The liquid level is controlled with an outlet pump.

Fresh medium is pumped into the culture vessel. The liquid level is controlled as the overflow is drained to a product reservoir.

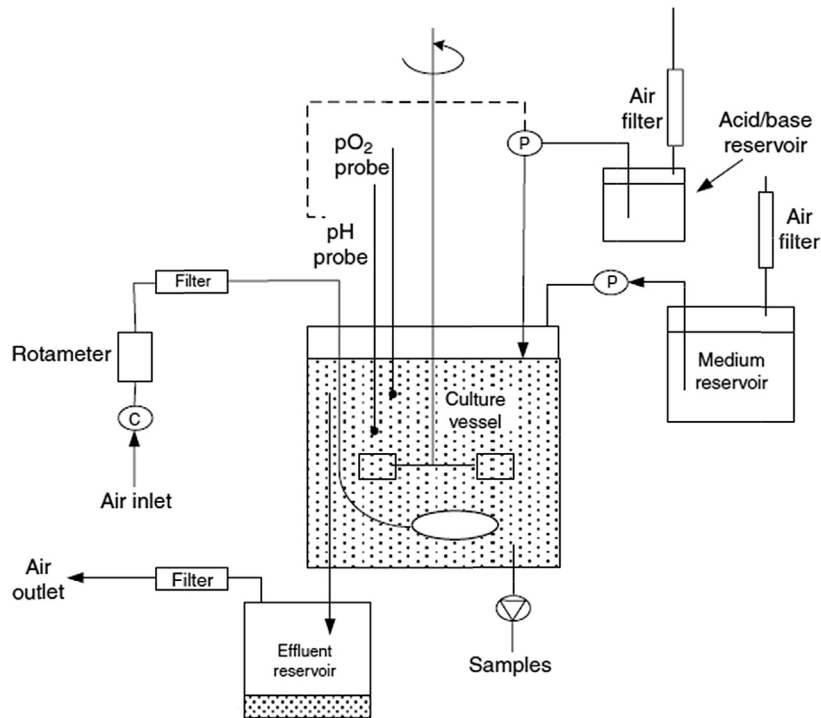


FIGURE 5.4 Schematic diagram of continuous culture with control units in a constant volume chemostat.

For constant volume of the fermentation vessel, a liquid level controller is used. The system is also designed with an outlet overflow to keep the liquid level constant. Figures 5.5–5.7 show various mechanisms for constant-volume bioreactors. An outlet pump is customarily used to maintain a constant flow rate. Complex systems are designed to control the mass of the generated cells; photocells or biosensors are used to monitor the OD of the cells (Figure 5.8). Cell concentration is controlled by the supplied nutrients and the flow rate of fresh media. The substrate concentration and the retention time in the fermentation vessel may dictate the cell density. Besides the nutrients and the controlling dilution rate, there are several physiological and process variables involved in the kinetics and the design of a bioreactor.^{6,7} These parameters are temperature, pH, redox (reduction and oxidation) potentials, dissolved oxygen, substrate concentration, and many process variables. In a chemostat, cell growth rate is determined by an expression that is based on substrate utilization, mainly C, N, and P with trace amounts of metals and vitamins. The advantages of continuous culture are that the essential nutrients can be adjusted for maximum growth rate and to maintain steady-state conditions. There is a determined relation between cell concentration and dilution rate. At a steady state, cell concentration is maximized with optimum dilution

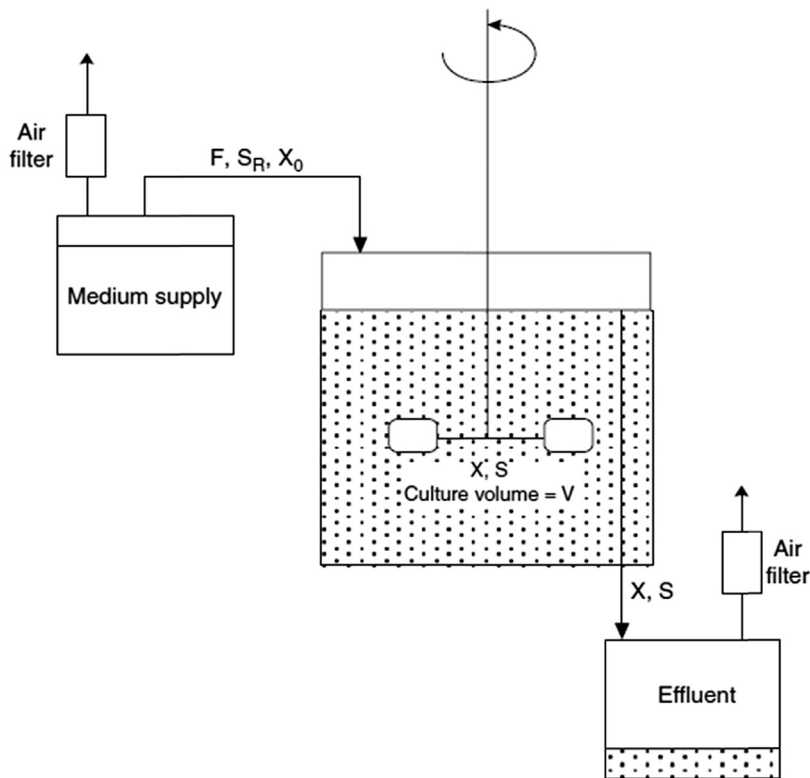


FIGURE 5.5 Chemostat without pumps maintained at a constant level.

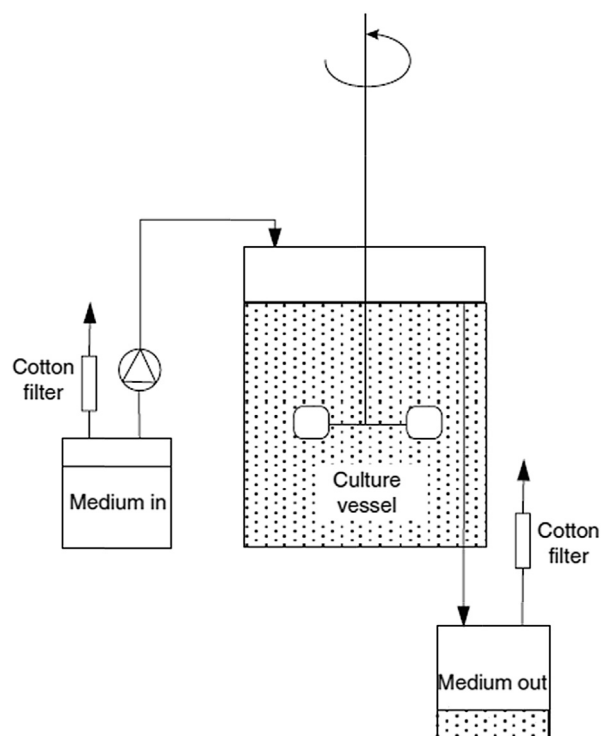


FIGURE 5.6 Chemostat with feed pump overflow drainage maintained at a constant level.

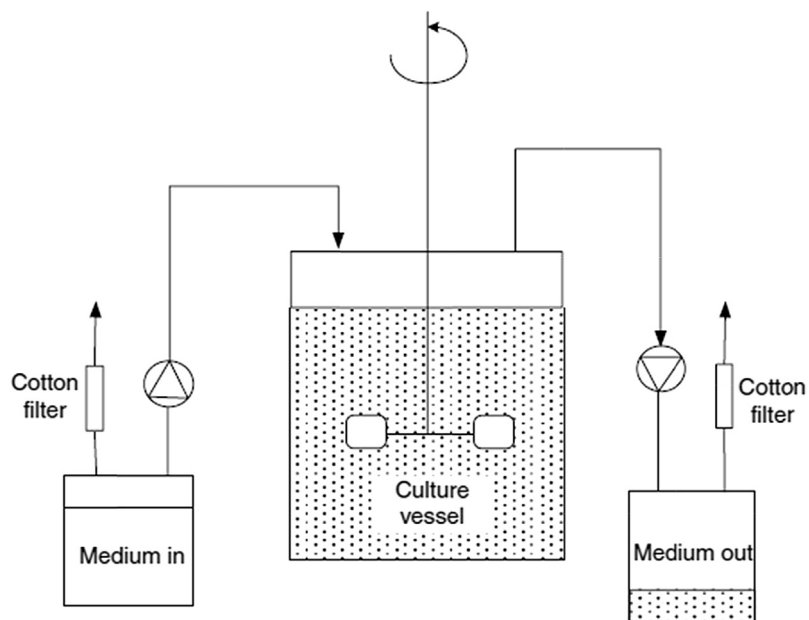


FIGURE 5.7 Chemostat using single medium inlet feed and outlet pumps.

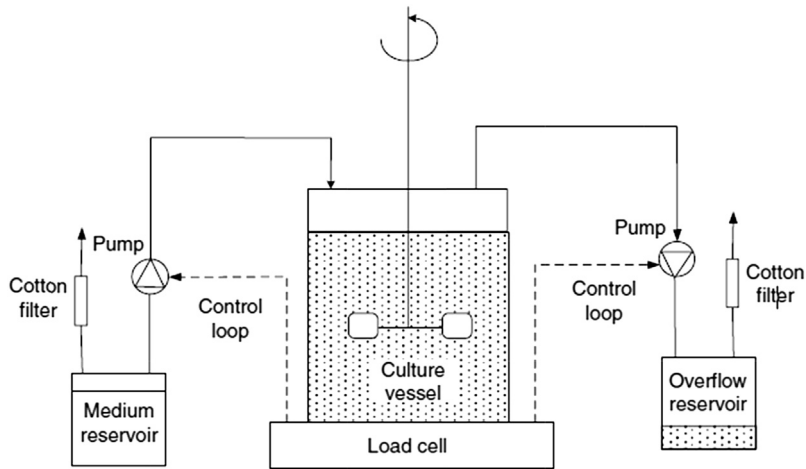


FIGURE 5.8 Chemostat with inlet and outlet control loops, feed, and product pump with cell loading and recycling.

rate. There is also a critical dilution rate where all the cells are washed out and there is no chance for the microorganisms to replicate; this is known as the maximum dilution rate.

2. **Biostat.** This is also known as a turbidostat. It is a system in which cell growth is controlled and remains constant while the flow rate of fresh media does not remain constant. Cell density is controlled based on set value for turbidity, which is created by the cell population while fresh media is continuously supplied. A turbidostat is shown in Figure 5.9.

In a chemostat and biostat or turbidostat, even with differences in the supply of nutrients and/or fresh media, constant cell density is obtained. The utilization of substrate and the kinetic expressions for all the fermentation vessels are quite similar. It is possible to have slight differences in the kinetic constants and the specific rate constants.^{3,4} Figure 5.10 shows a turbidostat with light sources. The system can be adapted for photosynthetic bacteria.

The continuous cultures of chemostat and biostat systems have the following criteria:

- Medium and cells are continuously changing
- The cell density (ρ_{cell}) is constant
- Steady-state growth
- Open system

The system is balanced for cell growth by removing old culture and replacing it with fresh medium at the same rate.

5.7 MATERIAL BALANCE FOR CONTINUOUS STIRRED TANK REACTOR (CSTR)

At a steady-state condition for chemostat operation, change of concentration is independent of time. Material balance for the fermentation vessel is:

$$\text{In} - \text{Out} + \text{Reaction rate} = \text{Accumulation}$$

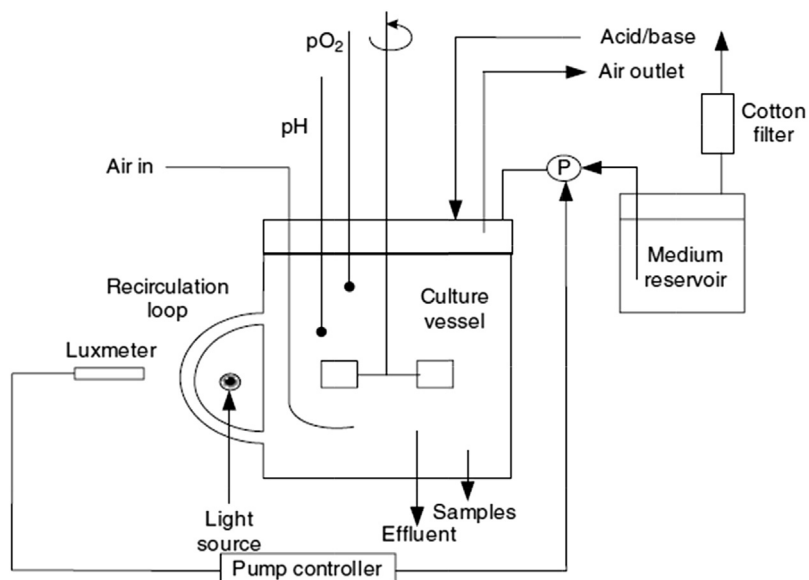


FIGURE 5.9 Biostat with a light source used detects cell turbidity and bacterial optical density.

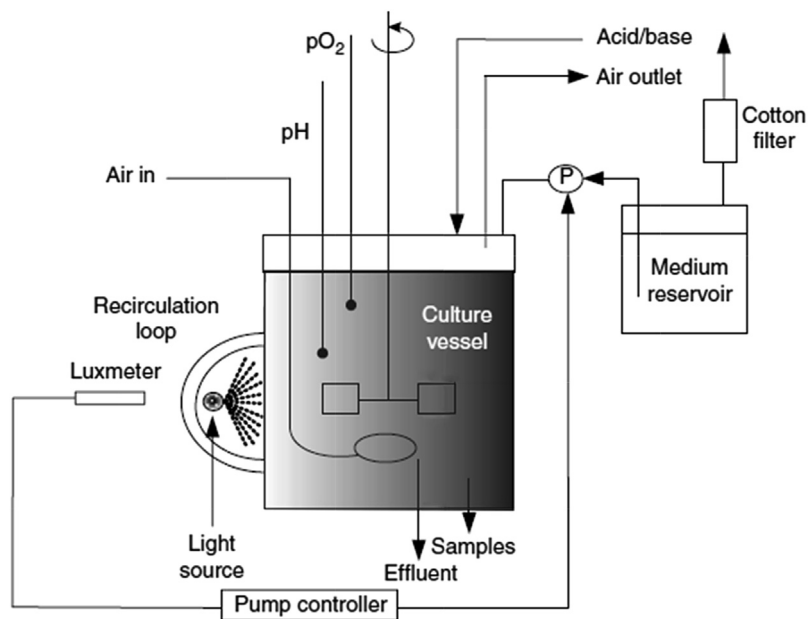


FIGURE 5.10 Continuous culture with light source used for photosynthetic bacteria, turbidostat.

At a steady-state condition, there is no accumulation; therefore, the material balance is reduced to:

$$F(C_{if} - C_i) + V_R \cdot r_{fi} = 0 \quad (5.7.1)$$

where C_{if} is the molar concentration in feed stream, C_i is the molar concentration in the outlet stream, and $-r_{fi} = \frac{dC_{fi}}{dt}$ is the rate of feed stream or consumption rate

$$r_{fi} = \frac{F}{V_R} (C_i - C_{if}) = D(C_i - C_{if}) \quad (5.7.2)$$

The rate of formation of a product is easily evaluated at steady-state condition for inlet and outlet concentrations, where D is the dilution rate, defined as $D = \frac{F}{V_R}$, which characterizes the inverse retention time in the CSTR unit. The dilution rate is equal to the number of fermentation vessel volumes that pass through the vessel per unit time. D is the reciprocal of the mean residence time.

The kinetic of cell growth for prediction of growth rate is projected by the net growth rate, which is:

Rate of cell dry weight.

$$dX/dt = \text{growth rate} - \text{cell removal rate} - \text{cell death rate}$$

In a continuous culture:

$$dX/dt = \mu X - DX - \alpha X \quad (5.7.3)$$

where α is the specific death-rate constant.

5.7.1 Rate of Product Formation

Similarly, the rate of product formation is defined as:

$$\frac{dP}{dt} = q_p X - DP - \beta P \quad (5.7.1.1)$$

where q_p is the specific growth rate for product formation and β is the denaturation of product coefficient and the specific rate of product formation. For a special case, the specific growth rate for product formation is simplified and reduced to:

$$q_p = \frac{1}{X} \frac{dP}{dt} \quad (5.7.1.2)$$

If the cells are in the exponential growth period and there is no cell death rate, then $\alpha \approx 0$. The net cell concentration is:

$$\frac{dX}{dt} = \text{growth} - \text{output} = \mu X - DX \quad (5.7.1.3)$$

At a steady-state condition, the biomass concentration remains constant, that is, $dX/dt = 0$, and Eqn (5.7.1.3) concludes to $\mu = D$; therefore, the specific growth rate is equal to the dilution rate.

5.7.2 Continuous Culture

Exponential growth in a batch culture may be prolonged by addition of fresh medium to the fermentation vessel. In a continuous culture, the fresh medium has to be displaced by an equal volume of old culture, then continuous cell production can be achieved.

5.7.3 Disadvantages of Batch Culture

There are several disadvantages to batch culture. The nutrient in the working volume becomes depleted; the other major problem is the limitation and depletion of the substrate. Because there is no flow stream to take effluent out, as the system is closed, toxins form there. A disadvantage related to substrate depletion is that the growth pattern may reach the death phase quickly in an old culture. The long duration of the batch system for slow growth results in exhaustion of essential nutrients and an accumulation of metabolites as by-products. Exhaustion of nutrients and substrate may cause the system to become retarded. The technical problem resulting in changes to media composition may directly affect the microbial exponential growth phase. Inhibition is another factor affecting the bioprocess, which causes the reaction rate shift. As a result, inhibition may slow down bio-catalytic activities. Product inhibition may block enzyme activities, and the cells become poisoned by the by-product. One common disadvantage of the batch process is that one has to carry out a cycle for production: the product should be sent for downstream processing, then the system has to be cleaned and recharged with fresh feed, so the process is highly labor intensive for downtime and cleaning.

5.7.4 Advantages of Continuous Culture

There are several advantages to continuous culture, where all the problems associated with the batch culture are solved. First, the growth rate is controlled and the cells are well maintained, because fresh media are replaced by old culture while the dilution is taking place. As a result, the effect of physical and chemical parameters on growth and product formation can easily be examined. The biomass concentration in the cultured broth is well maintained at a constant dilution rate. The continuous process results in substrate-limited growth and cell growth—limiting nutrients. The composition of the medium can be optimized for maximum productivity; in addition secondary metabolite production can also be controlled. The growth kinetics and kinetic constants are accurately determined. The process leads to reproducible results and reliable data. High productivity per unit volume is achieved. The continuous culture is less labor-intensive, and less downtime is needed. Finally, steady-state growth can be achieved, even if mixed cultures are implemented.

5.7.5 Growth Kinetics, Biomass, and Product Yields, $Y_{X/S}$ and $Y_{P/S}$

The yield is defined as ratio of biomass to the mass of substrate. The ethanol fermentation from sugar is simplified based on the following reaction:



The rates of biomass production and product formation are:

$$\frac{dX}{dt} = \frac{dX}{ds} \frac{ds}{dt} = -Y_{X/S} \cdot \frac{dS}{dt} \quad \text{and} \quad \frac{dP}{dt} = -Y_{P/S} \cdot \frac{dS}{dt} \quad (5.7.5.2)$$

where the yields of biomass and product are:

$$Y_{X/S} = -\frac{\Delta X}{\Delta S} \quad \text{and} \quad Y_{P/S} = -\frac{\Delta P}{\Delta S} \quad (5.7.5.3)$$

For instance, the theoretical yield of ethanol fermentation based on fermentation of glucose results in 2 mol of ethanol:

$$\frac{2 \text{ mol EtOH}}{\text{mol C}_6\text{H}_{12}\text{O}_6} = \frac{2 \times 46}{180} = 0.511 \frac{\text{g EtOH}}{\text{g C}_6\text{H}_{12}\text{O}_6}$$

The effect of substrate concentration on specific growth rate (μ) in a batch culture is related to the time and μ_{\max} ; the relation is known as the Monod rate equation. The cell density (ρ_{cell}) increases linearly in the exponential phase. When substrate (S) is depleted, the specific growth rate (μ) decreases. The Monod equation is described in the following equation:

$$\mu = \mu_m \frac{S}{K_S + S} \quad (5.7.5.4)$$

where μ is the specific growth rate, μ_m is the maximum specific growth rate in h^{-1} , K_S is saturation or Monod constant and S is substrate in g l^{-1} . The linearized form of the Monod equation is:

$$\frac{1}{\mu} = \left(\frac{K_S}{\mu_m} \right) \frac{1}{S} + \frac{1}{\mu_m} \quad (5.7.5.5)$$

The average biomass concentration is defined as the product of yield of biomass and change of substrate concentrations in inlet and outlet streams. The biomass balance is:

$$\bar{X} = Y_{X/S}(-\Delta S) = Y_{X/S}(S_i - S_o) \quad (5.7.5.6)$$

where S_i and S_o are inlet and outlet concentrations in mol l^{-1} . Rate expression is based on the Monod equation for substrate utilization, given by the rate Eqn (5.7.5.4):

$$\mu K_S + \mu S = \mu_{\max} S \quad \text{or} \quad \mu K_S = (\mu_{\max} - \mu) S \quad (5.7.5.7)$$

The rate equation was solved for substrate concentration in the product stream. Rearrangement of Eqn (5.7.5.7) results in an equation for substrate in terms of specific rate:

$$S = \frac{K_S \mu}{\mu_{\max} - \mu} \quad (5.7.5.8)$$

Finally, at a steady-state condition, as has been stated previously Eqn (5.7.1.3), the rate of substrate consumption is equal to the biomass generation, with the assumption of zero death rate:

$$\mu = D \Rightarrow S_o = \frac{K_S D}{\mu_{\max} - D} \quad (5.7.5.9)$$

5.7.6 Biomass Balances (Cells) in a Bioreactor

The material balance for cells in a continuous culture chemostat is defined as:

$$\text{cell accumulation} = \text{cell in} - \text{cell out} + \text{cell growth} - \text{cell death} \quad (5.7.6.1)$$

$$\frac{dX}{dt} = \left(\frac{F}{V}\right)(X_o - X) + \mu X - \alpha X \quad (5.7.6.2)$$

where F is the flow rate in h^{-1} , V is the working volume of the bioreactor in l , X is the cell concentration in g l^{-1} , μ is the specific growth rate in h^{-1} , K_e or K_d equal a , known as the specific death rate in h^{-1} , and D or F/V is the dilution rate in h^{-1} . Because in the exponential phase, steady-state growth has been achieved and the specific growth rate is much greater than the specific death rate, then Eqn (5.7.6.2) is simplified and reduced to a point where the specific growth rate is equal to the dilution rate:

$$\frac{dX}{dt} = -DX + \mu X \quad (5.7.6.3)$$

At a steady-state condition, biomass concentration is constant or cell density is stable at fixed dilution rate:

$$\begin{aligned} \frac{dX}{dt} &= 0 \\ 0 &= X(\mu - D) \end{aligned} \quad (5.7.6.4)$$

Then, $\mu = D$. Such condition is valid only at steady condition. As the fresh medium flow rate increases, cell concentration may gradually decreases because of high dilution rate. There is a specific dilution rate known as critical dilution rate where a washout phenomenon takes place. At the critical dilution rate there is not enough time for the microorganisms to replicate.

5.7.7 Material Balance in Terms of Substrate in a Chemostat

The substrate balance is given based on following equation:

$$-\frac{dS}{dt} = \left(\frac{F}{V}\right)(S_{in} - S_{out}) - \underbrace{\left(\frac{\mu}{Y_{X/S}}\right)X}_{\text{cell growth}} - \underbrace{\left(\frac{q_P}{Y_{P/S}}\right)X}_{\text{product formed}} - \underbrace{mX}_{\text{maintenance may negligible}} \quad (5.7.7.1)$$

In general, $\mu \gg m$, so we can therefore neglect the last term. For steady-state conditions, no additional product is formed, which means there are no changes in substrate and product concentrations:

$$-\frac{dS}{dt} = 0 \quad \text{and} \quad \left(\frac{q_P}{Y_{P/S}}\right) = 0 \quad (5.7.7.2)$$

Simplify Eqn (5.6.7.1) substituting $F/V = D$ and then $\mu = D$ resulted in:

$$0 = D(S_{in} - S_{out}) - \left(\frac{\mu X}{Y_{X/S}}\right) \quad (5.7.7.3)$$

Rearranging this equation yield:

$$\bar{X} = Y_{X/S}(S_{in} - S_{out}) \quad (5.7.7.4)$$

For a steady-state condition, dilution rate and outlet substrate concentration are defined:

$$D = \mu_m \frac{S}{K_S + S} \Rightarrow S_{out} = \frac{K_S D}{\mu_m - D} \quad (5.7.7.5)$$

Substituting Eqn (5.7.7.5) into Eqn (5.7.7.4):

$$\bar{X} = Y_{X/S} \left(S_{in} - \frac{K_S D}{\mu_m - D} \right) \quad (5.7.7.6)$$

For unsteady state when $\mu \neq D$:

$$\frac{dX}{dt} = X(\mu - D) \quad (5.7.7.7)$$

The equation with respect to substrate is:

$$\frac{dX}{dt} = X \left(\mu_m \frac{S}{K_S + S} - D \right) \quad (5.7.7.8)$$

5.7.8 Modified Chemostat

With cell recycling, chemostat efficiency is improved. To maintain a high cell density, the cells in the outlet stream are recycled back to the fermentation vessel. Figure 5.11 represents a chemostat unit with a cell harvesting system. The separation unit is used for harvesting the cells and recycling then to the culture vessel to increase the cell concentration. The material balance in a constant volume chemostat is derived based on cell balance as shown in the following equations. Material balance in a chemostat with recycle, ρ_{cell} :

$$\frac{dX}{dt} = \left(\frac{F}{V} \right) [X_o - X(1 + \tau)] + \mu X + \left(\frac{F}{V} \right) \cdot cX \quad (5.7.8.1)$$

where τ = recycle ratio.

c = the factor by which the outlet stream is concentrated before return.

For steady-state, $\frac{dX}{dt} = 0$

$$\mu = D(1 + \tau - c) \quad (5.7.8.2)$$

Multiple stages of continuous culture are designed to use the outlet of the first vessel as the inoculum for the next stage. If intermediate metabolites are used as feed for another micro-organism, sequential continuous culture is useful. The dilution rate for each vessel may be different to the other vessel. It is also possible to supply different nutrients for each stage of fermentation vessel. It is common to operate earlier stages as aerobic and subsequent stages in an anaerobic condition. In addition, if unused substrate leaves the product stream, it can be used in the next stage even at low substrate concentration. The kinetic representation may show a slower rate and even drop to zero order. Figure 5.12 shows two stages of a chemostat in operation.

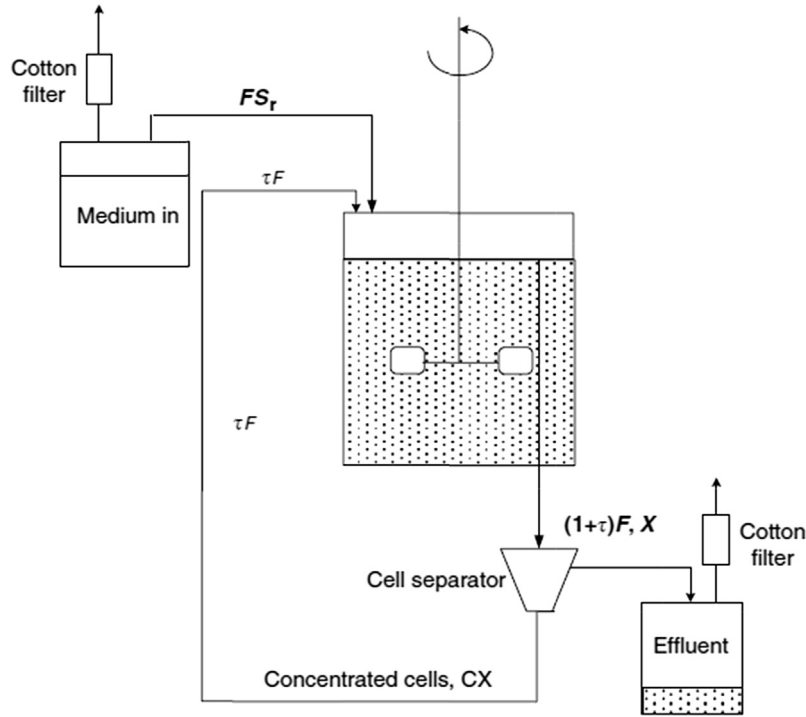


FIGURE 5.11 Chemostat with a cell recycle stream.

5.7.9 Fed Batch Culture

Culture with continuous nutrient supply can be operated in two modes: (1) variable volume and (2) fixed volume. For variable volume, feed rate F_{in} is not the same as outlet flow rate, when the system is fed batch that means $F_{out} = 0$.

$$\frac{d}{dt}(XV) = \mu XV - F_{out}X \quad (5.7.9.1)$$

$$\frac{dV}{dt} = F_{in} - F_{out} \quad (5.7.9.2)$$

and dilution rate,

$$D = \frac{F_{in}}{V} \quad (5.7.9.3)$$

Material balance for substrate:

$$\frac{dS}{dt} = \frac{F}{V}[S_i - (1 + \tau)S_o + S_o] - \frac{\mu}{Y_{X/S}}S_o \quad (5.7.9.4)$$

For a steady-state condition, $\frac{dS}{dt} = 0$

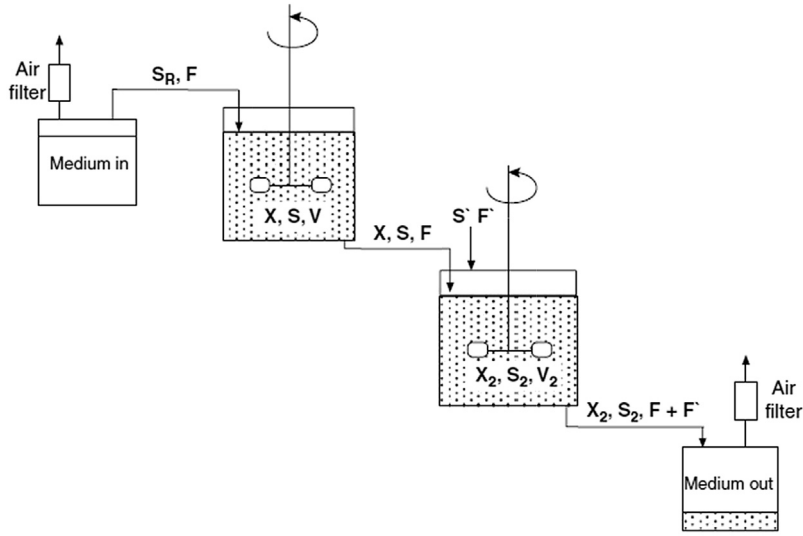


FIGURE 5.12 Two stages of CSTR fermentation vessels in series.

$$\bar{X} = \frac{D}{\mu} Y_{X/S}(S_i - S_o) \quad (5.7.9.4)$$

Substituting μ :

$$\bar{X} = Y_{X/S}(S_i - S_o)/(1 + \tau - c) \quad (5.7.9.6)$$

$$\frac{dX}{dt} = \left(\mu - \frac{F_{in}}{V} \right) X = (\mu - D)X \quad (5.7.9.7)$$

For a quasi-steady state, the specific growth rate reaches the media dilution rate, $\mu \approx D$. If $F_{in} > F_{out}$, the specific growth rate may decrease.

- Fed batch is used to overcome substrate limitations, especially for the production of antibiotics.
- Avoid substrate inhibition, which can allow a periodic shift of the growth rate.

5.8 ENZYME REACTION KINETICS

Most enzymes catalyze reactions follow Michaelis–Menten kinetics. The rate can be described on the basis of the concentration of the substrate and the enzymes. For a single enzyme and single substrate, the rate equation is:



$$v = -\frac{dS}{dt} = \frac{v_{\max}S}{K_M + S} \quad (5.8.3)$$

$$\frac{1}{v} = \frac{K_M}{v_{\max}} \frac{1}{S} + \frac{1}{\mu_{\max}} \quad (5.8.4)$$

where v is rate of substrate consumption in $\text{mol l}^{-1} \text{h}^{-1}$, v_{\max} is the maximum specific growth rate in h^{-1} , S is substrate concentration in g l^{-1} , and K_M is Michaelis–Menten constant in g l^{-1} . A double reciprocal plot or a well know Lineweaver–Burk plot of $1/\mu$ versus $1/S$ is shown in Figure 5.13. For batch reaction, there is no inlet or outlet stream.

$$m_i = m_o = 0 \quad (5.8.5)$$

$$-r_A = -r_s = \frac{1}{V} \frac{d(SV)}{dt} = \frac{-v_{\max}S}{K_m + S} \quad (5.8.6)$$

where V is the volume of batch reactor which is constant volume.

The rate equation based on substrate utilization is:

$$-\frac{dS}{dt} = \frac{v_{\max}S}{K_m + S} \quad (5.8.7)$$

By separation of variables;

$$-\int_0^t dt = \int_{S_o}^{S_f} \frac{K_m + S}{v_{\max}S} ds \quad (5.8.8)$$

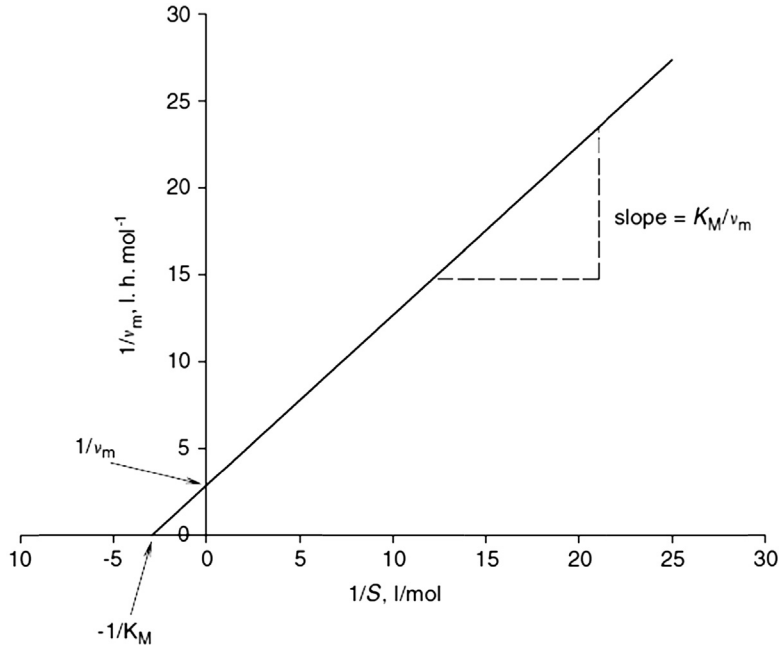


FIGURE 5.13 Single enzyme with different substrates.

then, fractionation and integration resulted in:

$$-t = \frac{K_m}{v_{\max}} \ln \frac{S_f}{S_o} + \frac{1}{v_{\max}} (S_f - S_o) \quad (5.8.9)$$

Batch reaction time is calculated based on following relation:

$$t_{\text{batch}} = \frac{K_m}{v_{\max}} \ln \frac{S_o}{S_f} + \frac{(S_f - S_o)}{v_{\max}} \quad (5.8.10)$$

where S_o is the initial substrate concentration in g l^{-1} and S_f is the final substrate concentration in g l^{-1} .

5.8.1 Mechanisms of Single Enzyme with Dual Substrates

The kinetics of double substrates with defined dissociation constants are given as:



where K_1 is the equilibrium constant or dissociation constant.



Similarly, for a second substrate, the reaction is carried out and the second product is formed.



where K_2 is the equilibrium or dissociation constant.



Overall enzyme balance and equilibrium constants are defined for the intermediate substrate and enzyme complex. The total enzyme concentration is the sum of free and conjugated enzymes with the substrates.

$$e_o = E + ES_1 + ES_2 \quad (5.8.1.5)$$

The intermediates, complexes of ES_1 and ES_2 , are defined based on equilibrium constants.

$$K_1 = \frac{[E][S_1]}{[ES_1]} \Rightarrow [ES_1] = \frac{[E][S_1]}{K_1} \quad (5.8.1.6)$$

$$K_2 = \frac{[E][S_2]}{[ES_2]} \Rightarrow [ES_2] = \frac{[E][S_2]}{K_2} \quad (5.8.1.7)$$

The initial and total enzyme concentrations are defined based on measurable components given as:

$$e_o = E \left(1 + \frac{S_1}{K_1} + \frac{S_2}{K_2} \right) \quad (5.8.1.8)$$

The free enzyme can also be defined based on the following equation:

$$E = \frac{e_o}{\left(1 + \frac{S_1}{K_1} + \frac{S_2}{K_2}\right)} \quad (5.8.1.9)$$

The rate equation for first substrate:

$$-\frac{ds_1}{dt} = v_1 = k'_1[ES_1] = \frac{k'_1[E][S_1]}{K_1} \quad (5.8.1.10)$$

The rate is defined with respect to dual substrates:

$$v_1 = \frac{k'_1 e_o [S_1]}{K_1} \bigg/ \left(1 + \frac{S_1}{K_1} + \frac{S_2}{K_2}\right) \quad (5.8.1.11)$$

The rate equation for the second substrate is:

$$-\frac{ds_2}{dt} = v_2 = k'_2[ES_2] = \frac{k'_2[E][S_2]}{K_2} \quad (5.8.1.12)$$

The second rate is also defined as follows:

$$v_2 = \frac{k'_2 e_o [S_2]}{K_2} \bigg/ \left(1 + \frac{S_1}{K_1} + \frac{S_2}{K_2}\right) \quad (5.8.1.13)$$

Overall reaction rates for dual substrates are the sum of the rates of dissociation of two substrates.

$$v_T = -\frac{dS_T}{dt} = -\left(\frac{dS_1}{dt} + \frac{dS_2}{dt}\right) = e_o \left(\frac{k'_1 S_1}{K_1} + \frac{k'_2 S_2}{K_2}\right) \bigg/ \left(1 + \frac{S_1}{K_1} + \frac{S_2}{K_2}\right) \quad (5.8.1.14)$$

If one substrate vanishes, then the rate is based on the concentration of the total substrate present in the reaction vessel; so, if S_2 is zero, then the total substrate concentration S_{T_o} is the concentration of substrate involved in the reaction.

$$v_T = \frac{e_o k_1 S_{T_o}}{K_1 + S_{T_o}} \quad (5.8.1.15)$$

Otherwise, if one of the substrate increases, the other substrate decreases. If S_2 increases, then S_1 has to decrease. The simplified rate, which is very similar to that for a single substrate, is given as follows:

$$v_T = \frac{e_o k_2 S_{T_o}}{K_2 + S_{T_o}} \quad (5.8.1.16)$$

In general, enzymes are proteins and carry charges; the perfect assumption for enzyme reactions would be multiple active sites for binding substrates with a strong affinity to hold on to substrate. In an enzyme mechanism, the second substrate molecule can bind to the enzyme as well, which is based on the free sites available in the dimensional structure of the enzyme. Sometimes, large amounts of substrate cause the enzyme-catalyzed reaction to diminish; such

a phenomenon is known as inhibition. It is good to concentrate on reaction mechanisms and define how the enzyme reaction may proceed in the presence of two different substrates. The reaction mechanisms with rate constants are defined as:



The dissociation constant is related to the equilibrium constant, given by. $k_1 = \frac{k_{-1}}{k_1}$



$$K_2 = \frac{k_{-2}}{k_2} = \frac{[ES][S]}{[ES_2]} \quad (5.8.1.19)$$



The total enzyme concentration is the sum of free and conjugated enzymes with substrates.

$$e_o = E + ES_1 + ES_2 \quad (5.8.1.21)$$

When the enzyme–substrate complex is stabilized, it may reach a fixed concentration; therefore, there is no more change in ES :

$$-\frac{d[ES]}{dt} = k_2[ES][S] - k_2[ES_2] + k_{-1}[ES] - k_1[E][S] - k[ES] = 0 \quad (5.8.1.22)$$

The rate equation for the enzyme complex leads to product in Eqn (5.8.1.22) is defined as:

$$v = k[ES] \quad (5.8.1.23)$$

ES_2 was obtained from Eqn (5.8.1.19):

$$[ES_2] = \frac{[ES][S]}{k_2} \quad (5.8.1.24)$$

Incorporating Eqn (5.8.1.24) into Eqn (5.8.1.22), after simplification it is reduced to:

$$(k_{-1} - k_2)[ES] = k_1[E][S] \quad (5.8.1.25)$$

Substituting Eqn (5.8.1.24) into Eqn (5.8.1.22), the rate of enzymatic reaction with dual substrates is obtained:

$$v = \frac{k k_1[E][S]}{k_{-1} - k_2} \quad (5.8.1.26)$$

The reaction mechanisms may assist us in obtaining a suitable rate equation. Based on the enzyme reaction mechanism given by Eqn (5.8.1.18) for the intermediate enzyme–substrate complex, the following equations are derived for ES :

$$-\frac{d(ES)}{dt} = k_1[E][S] - k_{-1}[ES_1] - k_2[ES][S] + k_{-2}[ES_2] = 0 \quad (5.8.1.27)$$

From the equilibrium constant, the free enzyme concentration must be defined. We know the total enzyme concentration is the sum of the conjugated enzymes with substrates and the free enzymes.

$$e_o = E + ES + ES_2 \Rightarrow E = e_o - ES - ES_2 \quad (5.8.1.28)$$

Substituting Eqn (5.8.1.28) into Eqn (5.8.1.27), then solving for intermediate enzyme–substrate complex:

$$k_1[e_o][S] - (k_1 + k_{-1})[ES] + (k_{-2} - k_1)[ES_2] - k_2[ES][S] = 0 \quad (5.8.1.29)$$

$$k_1 e_o [S] = (k_1 + k_{-1})[ES] - \left[\left(\frac{k_{-2} - k_1}{k_2} \right) - k_2 \right] [ES][S] \quad (5.8.1.30)$$

The enzyme–substrate complex is used by substituting ES into Eqn (5.8.1.23):

$$v = k[ES] = \frac{ke_o[S]}{1 + K_1 - \left[\left(\frac{k_2}{k_1} - 1 \right) - \frac{k_2}{k_1} \right] [S]} \quad (5.8.1.31)$$

At equilibrium conditions the rate constant for Eqn (5.8.1.17) is:

$$K_1 = \frac{[E][S]}{[ES]} \quad (5.8.1.32)$$

The intermediate enzyme–substrate complex is defined as:

$$[ES] = \frac{[E][S]}{K_1} = \frac{e_o S - ES_2 - ES_2 S}{K_1} \quad (5.8.1.33)$$

The second equilibrium constant for the Eqn (5.8.1.18) is also defined as:

$$K_2 = \frac{[ES][S]}{[ES_2]} \quad (5.8.1.34)$$

where the total enzyme is $e_o = E + ES + ES_2$

$$E = e_o - ES - ES_2 \quad (5.8.1.35)$$

Let us eliminate ES_2 by substituting $ES_2 = e_o - E - ES$ into Eqn (5.8.1.27). Equation (5.8.1.34) gives:

$$K_2 e_o - K_2 E - K_2 [ES] = [ES][S] \quad (5.8.1.36)$$

Equation (5.8.1.32) leads to:

$$K_1 [ES] = [E][S] \quad (5.8.1.37)$$

The free enzyme concentration is:

$$[E] = \frac{K_1 [ES]}{[S]} \quad (5.8.1.38)$$

Substituting Eqn (5.8.1.38) into Eqn (5.8.1.36) results in:

$$K_2 e_o - K_2 \frac{K_1 [ES]}{[S]} - K_2 [ES] = [ES][S] \quad (5.8.1.39)$$

The intermediate complex ES is defined:

$$[ES] = K_2 e_o / \left[S + K_2 - \frac{K_2 K_1}{[S]} \right] \quad (5.8.1.40)$$

The enzyme rate equation with two dissociation relations at equilibrium yields:

$$v = k e_o / \left[1 + \frac{[S]}{K_2} + \frac{K_1}{[S]} \right] \quad (5.8.1.41)$$

Now, maximize the rate at a specific substrate concentration:

$$\frac{dv}{dt} = 0 = -\frac{1}{K_2} + \frac{K_1}{S_2} \Rightarrow \frac{K_1}{S_2} = \frac{1}{K_2} \quad (5.8.1.42)$$

Maximum substrate concentration is defined by the square root of the dissociation constants.

$$S_{\max} = \sqrt{K_1 K_2} \quad (5.8.1.43)$$

At a high substrate concentration, the rate can be simplified and a linearized model is obtained:

$$\frac{1}{v} = 1 + \frac{[S]}{K_2} / k e_o \quad (5.8.1.44)$$

A graph of $1/v$ versus S is plotted and the slope is $1/K_2 k e_o$. There is an intercept in the graphical presentation to identify another constant. From the previous equation, K_2 can be calculated, which is similar to S_{\max} , where S_{\max} means that the substrate concentration gives the maximum rate.

5.8.2 Kinetics of Reversible Reactions with Dual Substrate Reaction

The reaction mechanisms for reversible reactions are slightly different. In the previous section, the second part of the reaction that leads to product was irreversible. However, if all the steps in enzyme reactions were reversible, the resulting rates may be affected.



where k_1 is the rate constant for forward and k_{-1} the rate constant for backward reactions. The second reaction is:



where k_2 is the rate constant for forward and k_{-2} the rate constant for backward reactions. For dual substrates, the reaction mechanisms may be complicated if the enzyme–substrate complex of the first substrate reacts with the second substrate; then the dissociation constant of K_{12} is defined to present the equilibrium, and vice versa the dissociation constant for the reaction of second substrate–enzyme complex with the first substrate is K_{21} .

$$e_o = e + ES_1 + ES_2 + ES_1S_2 \quad (5.8.2.3)$$

The rate equation for reversible reactions with two substrates is defined.

$$v = ke_o / \left(1 + \frac{K_{21}}{S_1} + \frac{K_{12}}{S_2} + \frac{K_2 K_{21}}{S_1 S_2} \right) \quad (5.8.2.4)$$

Assume:

$$K_1 K_{12} = K_2 K_{21} \quad (5.8.2.5)$$

$$v = \frac{ke_o S_2 S_1}{S_1 S_2 + K_{21} S_2 + K_{12} S_1 + K_2 K_{21}} = \frac{ke_o S_2 S_1}{(K_{12} + S_2)(K_1^* + S_1)} \quad (5.8.2.6)$$

For the special case, the rates are simplified to more familiar rates and result in the following:

$$v = \frac{v_{\max}^* S_1}{K_1^* + S_1} \quad (5.8.2.7)$$

where v_{\max}^* and K_1^* are the apparent maximum rate and Michaelis constant, respectively.

$$v_{\max}^* = \frac{ke_o S_2}{K_{12} + S_2} \quad (5.8.2.8)$$

$$K_1^* = \frac{K_1 K_2 + K_{12} S_2}{K_{12} + S_2} \quad (5.8.2.9)$$

If one substrate is in great excess, K_{12} is small or $S_2 \gg K_{12}$ then $v_{\max} = ke_o$ and $K_1^* \approx K_{21}$. In this case, we can simplify the rate to:

$$v = \frac{ke_o S_1}{K_{21} + S_1} \quad (5.8.2.10)$$

5.8.3 Reaction Mechanism with Competitive Inhibition

Generally inhibitors are competitive or noncompetitive with substrates. In competitive inhibition, the interaction of the enzyme with the substrate and competitive inhibitor instead of the substrate can be analyzed with the sequence of reactions taking place; as a result, a complex of the enzyme–inhibitor (EI) is formed. The reaction sets at equilibrium and the final step shows the product is formed. The enzyme must get free, but the enzyme attached to the inhibitor does not have any chance to dissociate from the EI complex. The EI formed is not available for conversion of substrate; free enzymes are responsible for that conversion.

The presence of inhibitor can cause the reaction rate to be slower than the ordinary reaction, in the absence of the inhibitor. The sequence of reaction mechanisms is:



where K_s and K_i are dissociations for the Michaelis–Menten rate constant and the inhibition constant, respectively:



The total enzyme concentration is the sum of all enzymes as free, and those conjugated as ES and EI :

$$e_o = E + ES + EI \quad (5.8.3.4)$$

The reaction rate model is based on total enzyme, substrate, and inhibitor concentrations.

$$v = \frac{ke_o S}{S + K_s \left(1 + \frac{I}{K_i}\right)} \quad (5.8.3.5)$$

Comparison of the ordinary Michaelis–Menten relation with Eqn (5.8.3.5) shows that the inhibitor did not influence specific growth rate, v_{\max} , but the Michaelis–Menten constant was affected by the inhibitor and resulted in a constant, known as the apparent Michaelis constant.

$$K_m^{app} = K_s \left(1 + \frac{i}{K_i}\right) \quad (5.8.3.6)$$

where K_m^{app} is apparent Michaelis constant. The rate constant is increased by the presence of a competitive inhibitor. The inhibitor causes the reaction rate to slow down. The competitive inhibitor can be unaffected or eliminated by increasing the substrate concentration.

5.8.4 Noncompetitive Inhibition Rate Model

The noncompetitive inhibitor is defined by the following sequence of reactions:



In such inhibition, the inhibitor and the substrate can simultaneously bind to the enzyme. The nature of the enzyme–inhibitor–substrate binding has resulted in a ternary complex defined as EIS . The K_s and K_i are identical to the corresponding dissociation constants. It is also assumed that the EIS does not react further and is unable to deliver any product P . The rate equation for noncompetitive inhibition, v_{\max} , is influenced:

$$v = \frac{ke_o S / \left(1 + \frac{i}{K_i}\right)}{S + K_s} \quad (5.8.4.3)$$

The maximum specific growth rate is retarded with noncompetitive inhibitor. The apparent specific growth rate, v_{\max}^{app} , is smaller than the ordinary specific growth rate, v_{\max} .

$$v_{\max}^{app} = \frac{ke_o}{1 + \frac{i}{K_i}} \quad (5.8.4.4)$$

If the complex of ESI can be dissociated to product, the rate equation would result in mixed competitive and noncompetitive inhibitors:



$$v = \frac{v_{\max}^{app} S}{S + K_m^{app}} \quad (5.8.4.6)$$

The competitive and noncompetitive inhibitors are easily distinguished in a Lineweaver–Burk plot. The competitive inhibitor intercepts on the $1/v$ axis, whereas the noncompetitive inhibitor intercepts on the $1/S$ axis. The reaction of inhibitors with substrate can be assumed as a parallel reaction, whereas the undesired product is formed along with desired product. The reactions are shown as:



Because enzyme is not shown in the reaction, we assume an elementary rate equation may explain the previous reactions. The simple kinetics are discussed in most fermentation technology and chemical reaction engineering textbooks.^{8–10}

EXAMPLE 1

An enzyme is produced for manufacturing a sun protection lotion. Given kinetic data for the enzyme reaction with $v_{\max} = 2.5 \frac{\text{mmol}}{\text{m}^3\text{s}}$, $K_m = 8.9 \text{ mM}$, and initial substrate $S_i = 12 \text{ mM}$, what would be the time required for 95% conversion in a batch bioreactor?

Solution

$$V_{\max} = \left(2.5 \frac{\text{mmol}}{\text{m}^3\text{s}}\right) \left(\frac{3600 \text{ s}}{\text{h}}\right) \left(\frac{1 \text{ m}^3}{1000 \text{ L}}\right) = 9 \frac{\text{mmol}}{\text{hL}}$$

$$t_{\text{batch}} = \frac{8.9 \text{ mM}}{9 \text{ mM/h}} \ln \frac{12}{0.6} + \frac{(0.95)(12)}{9} = 4.23 \text{ h}$$

EXAMPLE 2

Calculate K_m and V_{\max} for given substrate concentrations and rates in Table E.2.1. The inverse rate and substrate concentrations are calculated in Tables E.2.1 and E.2.2.

Solution

Let us inverse the substrate concentration and reaction rate as shown in Tables E.2.2 and E.2.3. In evaluation of kinetic parameters, the double reciprocal method is used for linearization of the Michaelis–Menten Equation (5.7.3) (Figure E.2.1).

1. Use the Lineweaver–Burk plot as defined in the following relation:

$$\frac{1}{v} = \frac{1}{v_{\max}} + \frac{K_m}{v_{\max}} \frac{1}{S} \quad (\text{E.2.1})$$

$$\text{Slope} = \frac{22500 - 10000}{1.875 \times 10^5 - 2.5 \times 10^4} = 0.077$$

$$v_{\max} = 1.25 \times 10^{-4} \text{ mol l}^{-1} \text{ min}^{-1}$$

$$\frac{K_m}{v_{\max}} = 0.077 \quad (\text{E.2.2})$$

$$K_m = 9.6 \times 10^{-5} \text{ mol l}^{-1}$$

2. Use another form of linear graphical presentation to evaluate K_m and v_{\max} based on the following relation:

$$\frac{S}{v} = \frac{K_m}{v_{\max}} + \frac{1}{v_{\max}} S \quad (\text{E.2.3})$$

This method tends to create a cluster of data near the origin as shown in [Figure E.2.2](#).

TABLE E.2.1 Substrate concentration and reaction rate

$S \text{ (mol l}^{-1}\text{)}$	$v \text{ (mol l}^{-1} \text{ min}^{-1}\text{)}$
4.10×10^{-3}	1.77×10^{-4}
9.50×10^{-4}	1.73×10^{-4}
5.20×10^{-4}	1.25×10^{-4}
1.03×10^{-4}	1.06×10^{-4}
4.90×10^{-5}	8.00×10^{-5}
1.06×10^{-5}	6.70×10^{-5}
5.10×10^{-6}	4.30×10^{-5}

TABLE E.2.2 The inverse substrate concentration and reaction rate

$1/S \text{ (l mol}^{-1}\text{)}$	$1/v \text{ (l min mol}^{-1}\text{)}$
243.9	5650
1052.6	5780
1923.0	8000
9708.7	9434
20,408.1	12,500
94,339.6	14,925
196,078.4	23,256

TABLE E.2.3 Data collected and calculated for the fate model

$S \text{ (mol l}^{-1}\text{)}$	$v \text{ (mol l}^{-1} \text{ min}^{-1}\text{)}$	$S/v \text{ (min)}$	$v/S \text{ (min}^{-1}\text{)}$
4.10×10^{-3}	1.77×10^{-4}	23.00	0.044
9.50×10^{-4}	1.73×10^{-4}	5.50	0.182
5.20×10^{-4}	1.25×10^{-4}	4.20	0.240
1.03×10^{-4}	1.06×10^{-4}	0.97	1.030
4.90×10^{-5}	8.00×10^{-5}	0.60	1.670
1.06×10^{-5}	6.70×10^{-5}	0.16	6.250
5.10×10^{-6}	4.30×10^{-5}	0.12	8.330

$$\text{Slope} = \frac{22.5 - 6.0}{3 \times 10^{-3}} = 5500$$

$$v_{\max} = 1.82 \times 10^{-4} \text{ mol l}^{-1} \text{ min}^{-1}$$

$$K_m = \frac{0.5}{5500} = 9.1 \times 10^{-5} \text{ mol} \cdot \text{l}^{-1}$$

For the Eadie–Hofstee plot, both coordinates contain rates that are subjected to the greatest error, as indicated in Figure E.2.3.

$$v = v_{\max} - K_m \frac{v}{S} \quad (\text{E.2.4})$$

A plot of v/S versus y is presented in Figure E.2.3 for defining slope and intercept, K_m and v_{\max} , respectively.

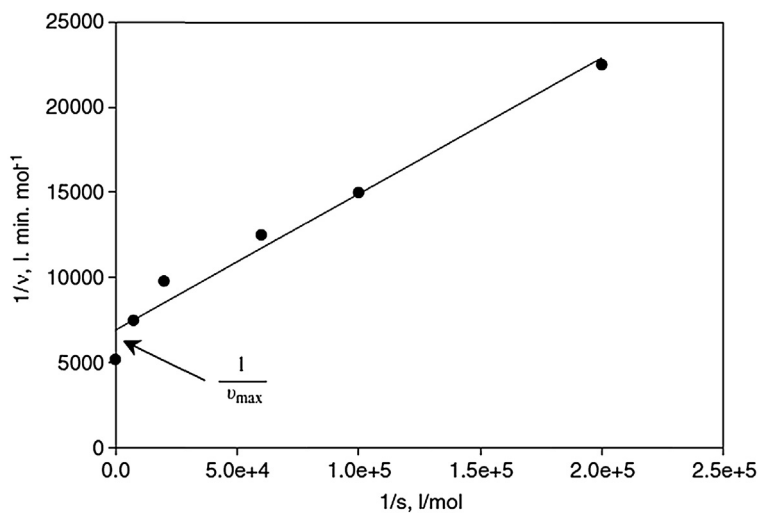


FIGURE E.2.1 Lineweaver–Burk plot.

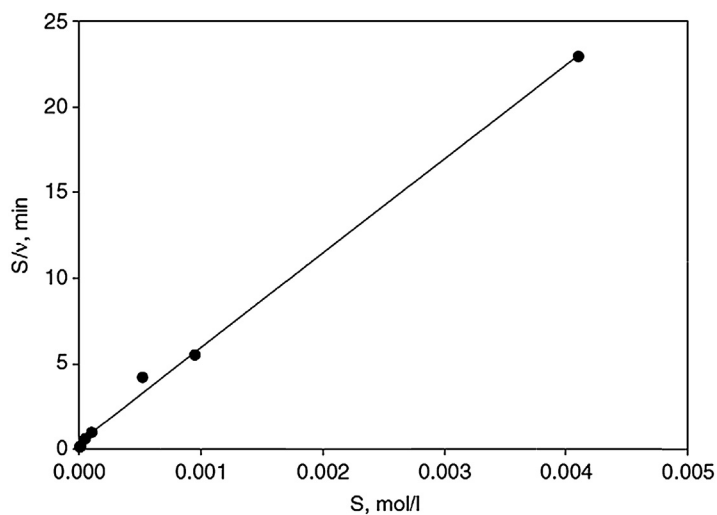


FIGURE E.2.2 Linear model for the Monod rate equation with populated data at the origin.

A linearization model is used to explain the equation of a simple straight line⁹:

$$y = bx + a \quad (\text{E.2.5})$$

where

$$b = \frac{\sum_i^N x_i y_i - N \bar{x} \bar{y}}{\sum_i^N x_i^2 - N \bar{x}^2} \quad (\text{E.2.6})$$

$$a = \bar{y} - b \bar{x} \quad (\text{E.2.7})$$

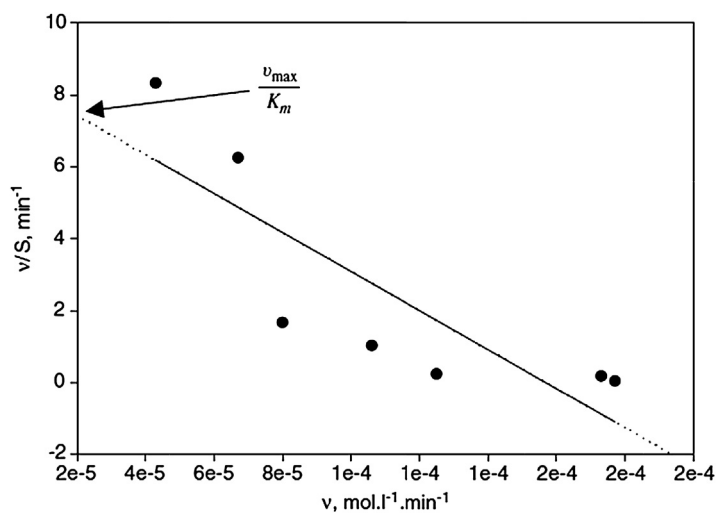


FIGURE E.2.3 Eadie-Hofstee plot.

\bar{x} , \bar{y} are average values of x_i and y_i

$$\text{Slope of the line} = \frac{1}{K_m}$$

$$K_m = 6.5 \times 10^{-5} \text{ mol} \cdot \text{l}^{-1}$$

$$v_{\max} = 18 \times 10^{-4} \text{ mol} \cdot \text{l}^{-1} \cdot \text{min}^{-1}$$

EXAMPLE 3

In batch enzyme reaction kinetics, given $K_m = 10^{-3} \text{ M}$ and substrate concentration $S_0 = 3 \times 10^{-5} \text{ M}$, after 2 min, 5% of the substrate was converted. How much of the substrate was consumed after 10, 20, 30, and 60 min?

Solution

For $S_0 \ll K_m$, the rate model is reduced to a first-order rate equation. The Michaelis–Menten rate equation is:

$$v = \frac{v_{\max} S}{K_m + S} \quad (\text{E.3.1})$$

The simplified first-order rate is:

$$-\frac{dS}{dt} = V_m^* S \quad (\text{E.3.2})$$

Carry out integrations:

$$-\int_{S_0}^S \frac{dS}{S} = V_m^* \int_0^t dt \quad (\text{E.3.3})$$

$$\ln \frac{S}{S_0} = -V_m^* t \quad (\text{E.3.4})$$

The concentration profile is predicted by the following equation.

$$S = S_0 e^{-V_m^* t} \quad (\text{E.3.5})$$

At time equal to 2 min:

$$\frac{S}{S_0} = 1 - X_E \quad (\text{E.3.6})$$

$$C_A = C_{A_0} (1 - X_A) \quad (\text{E.3.7})$$

$$\frac{S}{S_0} = 0.95 \quad (\text{E.3.8})$$

$$e^{-2V_m^* t} = 0.95 \quad (\text{E.3.9})$$

$$\begin{aligned}
 v_m &= -\frac{\ln 0.95}{2} \\
 &= 0.2565 \text{ min}^{-1} \\
 \frac{S}{S_o} &= e^{-2.02565t}
 \end{aligned} \tag{E.3.10}$$

Conversion:

$$X_A = 1 - \frac{S}{S_o} = 1 - e^{-0.02565t} \tag{E.3.11}$$

For $t = 10$ min, $X_A = 1 - e^{-0.2565} = 0.226$ or 22.6%.

For $t = 20$ min, $X_A = 1 - e^{-0.02565(20)} = 0.401$ or 40.1%.

For $t = 30$ min, $X_A = 1 - e^{-0.02565(30)} = 0.5367$ or 53.67%.

For $t = 60$ min, $X_A = 1 - e^{-0.02565(60)} = 0.785$ or 78.5%.

EXAMPLE 4

In a complex enzyme reaction, multiple substrate–enzyme complexes are formed. Assume the following reaction mechanisms are taking place in three consecutive stages:



Develop a suitable rate expression using the Michaelis–Menten rate equation and the quasi-steady-state approximations for the intermediate complexes formed.

Solution

Equilibrium dissociation constants are defined as:

$$K_1 = \frac{k_2}{k_1} = \frac{[E][S]}{[ES_1]} \tag{E.4.2}$$

$$K_2 = \frac{k_4}{k_3} = \frac{[ES_1]}{[ES_2]} \tag{E.4.3}$$

$$v = k_5[ES_2] \tag{E.4.3}$$

$$[ES_2] = \frac{[ES_1]}{K_2} \tag{E.4.5}$$

$$[ES_1] = \frac{[E][S]}{K_1} \tag{E.4.6}$$

$$v = \frac{k_5}{K_2}[ES_1] = \frac{k_5}{K_1 K_2}[E][S] \tag{E.4.7}$$

The total enzyme concentration is:

$$E_0 = E + ES_1 + ES_2 = E + \frac{[E][S]}{K_1} + \frac{[E][S]}{K_1 K_2} = E \left(1 + S \left[\frac{1}{K_1} + \frac{1}{K_1 K_2} \right] \right) \tag{E.4.8}$$

$$E = \frac{e_o}{1 + \left(\frac{K_2+1}{K_1 K_2}\right)[S]} \quad (\text{E.4.9})$$

$$K_{\text{obs}} = K_{\text{apparent}} = \frac{K_1 K_2}{K_2 + 1} \quad (\text{E.4.10})$$

$$v_{\text{max}} = \frac{k_5 e_o}{K_2 + 1} \quad (\text{E.4.11})$$

The final rate expression is:

$$v = \frac{e_o k_5}{K_1 K_2} \times \frac{[S]}{\left(1 + \left(\frac{K_2+1}{K_1 K_2}\right)[S]\right)} = \frac{k_5 e_o [S]}{K_1 K_2 + (K_2 + 1)[S]} = \frac{\left(\frac{k_5 e_o}{K_2 + 1}\right)}{\left(\frac{K_1 K_2}{K_2 + 1}\right) + [S]} \quad (\text{E.4.12})$$

EXAMPLE 5

Pesticide inhibition on an active enzyme has been reported, which caused enzyme activities to reduce. The collected data with and without inhibition are presented in [Tables E.5.1 and E.5.2](#). Determine the rate model with and without inhibitor (see [Table E.5.1](#)). Also define the type of inhibition.

Solution

Plot both sets of data as a Lineweaver–Burk plot for competitive inhibition (see [Figure E.5.1](#)):

$$v = \frac{k e_o S}{S + K_s \left(1 + \frac{i}{K_i}\right)} \quad (\text{E.5.1})$$

The mechanism of the enzyme with substrate in the present of inhibitor is:

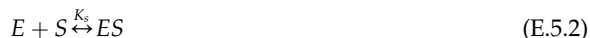
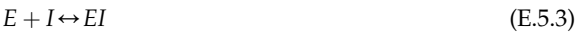


TABLE E.5.1 Substrate concentration and enzymatic rate calculation with and without inhibition

$S \text{ (mol l}^{-1}\text{)}$	$v \text{ (no inhibitor)}$ $\text{(mol l}^{-1} \text{ min}^{-1} \times 10^6\text{)}$	$v^* \text{ (inhibitor)}$ $\text{(mol l}^{-1} \text{ min}^{-1} \times 10^6\text{)}$
3.30×10^{-4}	56	37
5.00×10^{-4}	71	47
6.70×10^{-4}	88	61
1.65×10^{-3}	129	103
2.21×10^{-3}	149	125

TABLE E.5.2 Inverse substrate concentration and inverse enzymatic rate calculation with and without inhibition

1/S (l mol ⁻¹)	v (no inhibitor) (mol l ⁻¹ min ⁻¹ × 10 ⁶)	1/v	v* (inhibitor) (mol l ⁻¹ min ⁻¹ × 10 ⁶)	1/v* (l min mol ⁻¹)
3030	56	17,857	37	27,027
2000	71	14,085	47	21,277
1492	88	11,363	61	16,393
606	129	7752	103	9709
452	149	6711	125	8000



$e_o = E + [ES] + [EI]$ (E.5.5)

Without inhibition:

$$v = \frac{k e_o S}{S + K_s} = \frac{k e_o S}{S + 8.4 \times 10^{-3}}$$
 (E.5.6)

$$K_s^{app} = K_s \left(1 + \frac{i}{k_i} \right)$$
 (E.5.7)

$$1.5 \times 10^{-3} = 8.4 \times 10^{-4} \left(1 + \frac{i}{k_i} \right)$$
 (E.5.8)

$$\frac{i}{k_i} = 0.786$$
 (E.5.9)

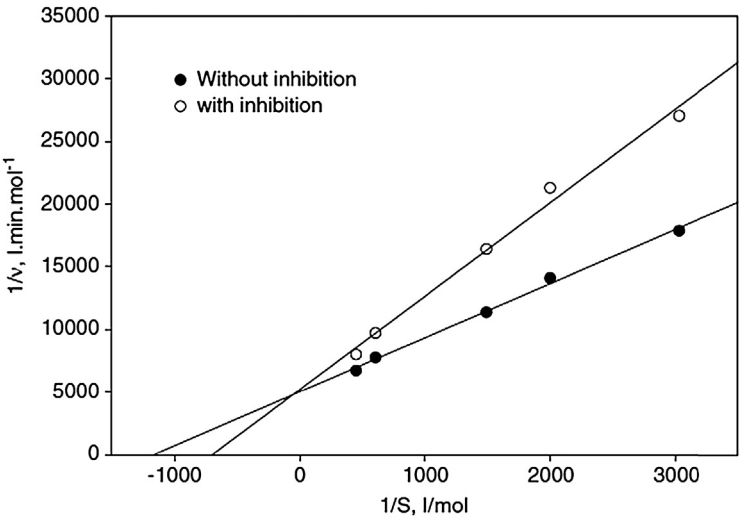


FIGURE E.5.1 Competitive inhibition based on the Lineweaver–Burk model.

$$k_i \frac{i}{0.786} = \frac{10^{-5}}{0.786} = 1.73 \times 10^{-3} \mu \quad (\text{E.510})$$

Plug in a number:

$$88 \times 10^{-6} = \frac{ke_o \times 6.7 \times 10^{-4}}{6.7 \times 10^{-4} + 8.4 \times 10^{-3}} \quad (\text{E.511})$$

$$ke_o = 1.2 \times 10^{-3} \text{ min}^{-1}$$

$$61 \times 10^{-6} = \frac{1.2 \times 10^{-3} \times 6.7 \times 10^{-4}}{6.7 \times 10^{-4} + 8.4 \times 10^{-3} \left(1 + \frac{i}{k_i}\right)} \quad (\text{E.512})$$

$$\frac{i}{k_i} = 0.49 \quad (\text{E.513})$$

The reading from the plot for the rate without inhibition:

$$\text{Slope : } \frac{(18 - 5) \times 10^3}{3100} = 4.2$$

$$k_{app} = 1.5 \times 10^{-3}$$

For the data plotted with inhibition:

$$\text{Slope : } \frac{(27 - 5) \times 10^3}{3000} = 7.3$$

$$\frac{K_2}{v_{\max}} = 4.2$$

$$K_s = 8.4 \times 10^{-4} \text{ mol l}^{-1}$$

$$v_{\max} = 2 \times 10^{-4} \text{ mol min}^{-1}$$

Based on the graphical presentation, this is a competitive inhibition.

EXAMPLE 6

The RQ is often used to estimate metabolic stoichiometry. Using quasi-steady-state and by definition of RQ , develop a system of two linear equations with two unknowns by solving a matrix under the following conditions: the coefficient of the matrix with yeast growth ($\gamma = 4.14$), ammonia ($\gamma_N = 0$), and glucose ($\gamma_S = 4.0$), where the evolution of CO_2 and biosynthesis are very small ($\sigma = 0.095$). Calculate the stoichiometric coefficient for $RQ = 1.0$ for the previous biological processes.

Solution

At a quasi-steady-state condition:

$$\frac{d[\text{NADH} + \text{H}^+]}{dt} = \frac{v_s}{2} \times a - 2b - \frac{1}{2} \left[v_s - v_s(1 + \sigma) - \frac{\delta}{n} \times v_N \right] = 0 \quad (\text{E.6.1})$$

$$RQ = \frac{\text{moles of CO}_2}{\text{moles of O}_2} = \frac{a + \sigma}{b} \quad (\text{E.6.2})$$

$$\begin{cases} \frac{v_s a}{2} - 2b = \frac{1}{2} \left[v_B - v_s(1 + \delta) - \frac{\delta}{n} v_N \right] \\ a - b(RQ) = -\sigma \end{cases} \quad (\text{E.6.3})$$

The mathematical solution for this system is set as given by the following matrix:

$$\begin{bmatrix} \frac{v_s}{2} & -2 \\ 1 & -(RQ) \end{bmatrix} \begin{bmatrix} a \\ b \end{bmatrix} = \begin{bmatrix} \frac{1}{2} & v_B - v_s(1 + \delta) - \frac{\sigma}{n} v_N \\ -\sigma \end{bmatrix} \quad (\text{E.6.4})$$

At a singular point, let:

$$\begin{bmatrix} \frac{v_s}{2} & -2 \\ 1 & -(RQ) \end{bmatrix} = 0 \quad (\text{E.6.5})$$

$$-(RQ)\left(\frac{v_s}{2}\right) - (-2)(1) = 0 \quad (\text{E.6.6})$$

$$RQ = \frac{4}{v_s} \quad (\text{E.6.7})$$

For anaerobic fermentation, $v_s = 4$ then $RQ = 1.0$.

$$\begin{bmatrix} 2 & -2 \\ 1 & -1.05 \end{bmatrix} \begin{bmatrix} a \\ b \end{bmatrix} = \begin{bmatrix} \frac{1}{2} [4.14 - 4(1 + 0.095) - 0] \\ -0.095 \end{bmatrix} = \begin{bmatrix} -0.12 \\ -0.095 \end{bmatrix}$$

$$a = 0.64, \quad b = 0.7 \quad (\text{E.6.8})$$

$$\begin{bmatrix} 2 & -2 \\ 1 & -1.05 \end{bmatrix} \begin{bmatrix} a \\ b \end{bmatrix} = \begin{bmatrix} -0.12 \\ -0.095 \end{bmatrix} \quad (\text{E.6.9})$$

$$a = 0.52, \quad b = 0.58$$

Increasing RQ with very small changes causes, the constants a and b to change in the reaction.

EXAMPLE 7

For single- and multiple-substrate kinetics, single-substrate glucose, 30 g l^{-1} and dual substrates glucose and lactose with each carbohydrate at a concentration of 15 g l^{-1} or total.

A carbohydrate concentration of 30 g l^{-1} was used in sterilized media (Table E.7.1). The cell OD was measured at wavelength 420 nm . The following data for single and double substrates were obtained. If OD is linear in cell density with a value of 0.175 equal to $0.1 \text{ mg cell dry weight per milliliter}$, evaluate the specific growth rate, lag phase, and yield of biomass.

TABLE E.7.1 Optical density (OD) for single and double substrates

Time (h)	OD (single)	OD (double)	Time (h)	OD (single)	OD (double)
0.0	0.05	0.05	4.5	0.89	0.44
0.5	0.08	0.06	5.0	1.05	0.49
1.0	0.11	0.07	5.5	1.05	0.51
1.5	0.14	0.08	6.0	1.06	0.53
2.0	0.20	0.10	6.5	1.06	0.61
2.5	0.27	0.14	7.0	1.08	0.85
3.0	0.38	0.19	7.5	1.08	1.04
3.5	0.50	0.27	8.0	1.08	1.04
4.0	0.71	0.33	—	—	—

$t_{\text{lag}} = 1 \text{ h}$ for dual substrate.

$t_{\text{lag}} = 0$ for single substrate.

Solution

$$\frac{1}{n} \frac{dn}{dt} = \mu \quad (\text{E.7.1})$$

$$N(t) = N_0 e^{\mu_m t} \quad (\text{E.7.2})$$

For $t = 5 \text{ h}$:

$$\left(\frac{0.1}{0.175} \right) (1.05) = N(S) = \left(\frac{0.005}{0.175} \right)$$

$$1.05 = 0.05 e^{5\mu_m}$$

$$\ln 21 = 5\mu_m$$

$$\mu_m = 0.609 \text{ h}^{-1}$$

$$N(0) = 0.05 \left(\frac{0.1 \text{ g dry cell}}{0.175} \right) = \frac{0.005}{0.175}$$

$$\mu_m = 0.61 \text{ h}^{-1} \text{ for single substrate (Figure E7.1)} \quad (\text{E.7.3})$$

For $t = 8 \text{ h}$:

$$\mu_m = \frac{\left[\ln \left(\frac{1.04}{0.05} \right) \right]}{8}$$

$$\mu_m = 0.38 \text{ h}^{-1} \text{ for double substrate}$$

Therefore, yield is:

$$Y = \frac{(1.04) \left[\frac{0.1}{0.175} \right]}{30} = 0.02$$

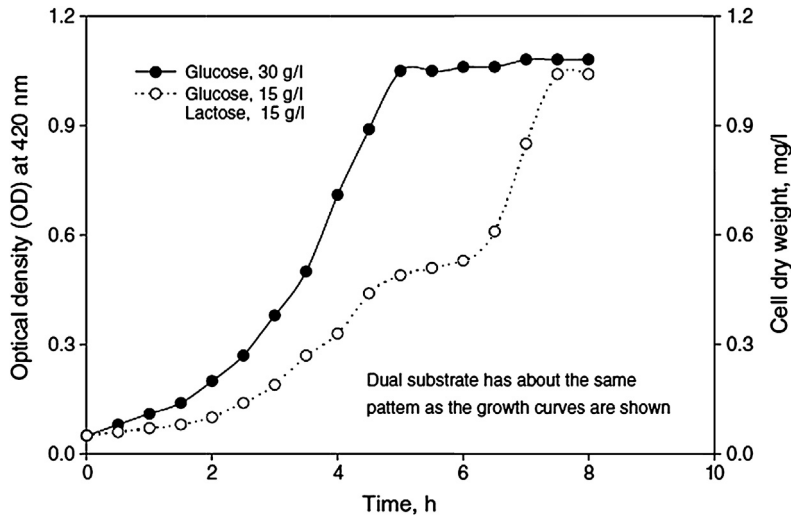


FIGURE E.7.1 Single and double substrate growth model.

The shape of dual substrates with the same total concentration of sugar and lactic acid shows two stages such as stepwise utilization of dual substrates has taken place in the cells.

Multiple lag phases were observed in Figure E.7.1 when the medium contained multiple carbon sources. This phenomenon is known as diauxic growth, which is caused by shifting in the metabolic pathway of the cell using glucose and lactose. After one source of carbon as substrate is exhausted (glucose), the cell diverts metabolisms from one source to another source of energy supply. After 6 h of fermentation, the second substrate—in this case, lactose—is used for energy supply. The most possible explanation is known as catabolic repression; such a phenomenon is used for synthesis of cell secondary metabolites.

EXAMPLE 8

Monod kinetics are considered in a CSTR with an organism growing with an initial substrate concentration of 50 g l^{-1} and kinetic parameters of $K_s = 2 \text{ g l}^{-1}$ and $\mu_{\max} = 0.5 \text{ h}^{-1}$. (1) What would be the maximum dilution rate for 100% yield of biomass with maximum rate? (2) If the same dilution is used, what would be number of CSTRs in series?

Solution

1.

$$D_{\max} = \mu_{\max} \left[1 - \sqrt{\frac{K_s}{K_s + S_0}} \right] \quad (\text{E.8.1})$$

$$\begin{aligned}
 &= (0.5 \text{ h}^{-1}) \times \left[1 - \sqrt{\frac{2}{2 + 50}} \right] \\
 &= 0.402 \text{ h}^{-1}
 \end{aligned} \tag{E.8.2}$$

2. For the first tank, use Eqn (5.7.7.5), obtained from the steady-state condition, then solve for substrate concentration profile. The outlet substrate concentration was calculated as:

$$\begin{aligned}
 S_1 &= \frac{DK_s}{\mu_{\max} - D} \\
 &= \frac{(0.402)(2)}{0.5 - 0.402} \\
 &= 8.2 \text{ g} \cdot \text{l}^{-1}
 \end{aligned} \tag{E.8.3}$$

Biomass concentration is obtained from definition as substrate is utilized; it is converted to cells or biomass:

$$X = Y_{X/S}(S_{in} - S_{out}) \tag{E.8.4}$$

Now substitute the outlet concentration of substrate, resulting in the following equation:

$$\begin{aligned}
 X_1 &= Y \left[S_0 - \frac{DK_s}{\mu_{\max} - D} \right] \\
 X_1 &= (1) \left[50 - \frac{(0.402)(2)}{0.5 - 0.402} \right] = 41.8 \text{ g} \cdot \text{l}^{-1}
 \end{aligned} \tag{E.8.5}$$

For the subsequent tanks, use the steady-state mass balance on substrate:

$$D(S_{feed} - S) - \frac{1}{Y_{X/S}} \mu X = 0 \tag{E.8.6}$$

$$D(S_1 - S_2) - \frac{\mu_{\max} S_2 X_2}{Y(S_2 + K_s)} = 0 \tag{E.8.7}$$

$$X_2 - X_1 = Y(S_1 - S_2) \tag{E.8.8}$$

$$X_2 = X_1 + Y(S_1 - S_2) \tag{E.8.9}$$

$$D(S_1 - S_2) - \frac{\mu_{\max} S_2 [X_1 + Y(S_1 - S_2)]}{Y(S_2 + K_s)} = 0 \tag{E.8.10}$$

Solve for substrate concentration:

$$D(Y)(S_1 - S_2)(S_2 + K_s) = \mu_{\max} S_2 [X_1 + Y(S_1 - S_2)] \tag{E.8.11}$$

$$(0.402)(1)(8.2 - S_2) = 0.5(S_2)[X_1 + Y(8.2 - S_2)] \tag{E.8.12}$$

$$(0.5)S_2^2 + 22.51S_2 - 6.6 = 0 \tag{E.8.13}$$

Solving the quadratic equation, the meaningful substrate concentration is:

$$S_2 = 0.29 \text{ g l}^{-1}$$

N = two tanks

EXAMPLE 9

For the design of a CSTR with inhibition, consider the following rate is valid for a CSTR as a fermentation vessel.

Given the following data:

Initial substrate concentration, $S_0 = 10 \text{ g l}^{-1}$

Inlet cell concentration for sterile media, $X_0 = 0$.

The rate constant, $K_S = 1 \text{ g l}^{-1}$

The inhibitory constant, $K_i = 0.01 \text{ g l}^{-1}$

The inhibitor concentration, $[I] = 0.05 \text{ g l}^{-1}$

The $\mu_{\max} = 0.5 \text{ h}^{-1}$ and yield of biomass on substrate $Y_{X/S} = 0.1 \text{ g cells/g substrate}$.

Solution

The rate model with inhibition is given by Eqn (5.8.3.5).

$$r_X = \frac{\mu_{\max} S X}{K_S + S + \frac{i}{K_i} K_S} \quad (\text{E.9.1})$$

$$D = \mu = \frac{\mu_{\max} S}{S + K_S \left(1 + \frac{i}{K_i}\right)} \quad (\text{E.9.2})$$

$X_0 = 0$ for sterile feed.

$$X = Y_{X/S}(S_0 - S) \quad (\text{E.9.3})$$

Rearrangement of the rate model and the equation is solved for substrate S:

$$S = \frac{DK_S + DK_S \left(\frac{i}{K_i}\right)}{\mu_{\max} - D} \quad (\text{E.9.4})$$

With defined values of inhibition concentration, rate constant, and given dilution rate, the substrate concentration is calculated based on Eqn (E.9.4). The tabulated data are given in Table E.9.1.

For substrate ratio with no inhibition and with inhibition, the following equation is simplified.

$$\frac{S}{S_i} = \frac{\frac{DK_S}{(\mu_{\max} - D)}}{\frac{DK_S + DK_S \left(\frac{i}{K_i}\right)}{(\mu_{\max} - D)}} = \frac{1}{1 + \left(\frac{i}{K_i}\right)} \quad (\text{E.9.5})$$

Cell productivity can be achieved by multiplying Eqn (E.9.2) to X:

$$DX = \mu X = \frac{\mu_{\max} S [Y_{X/S}(S_0 - S_i)]}{S_i + K_S \left(1 + \frac{i}{K_i}\right)} \quad (\text{E.9.6})$$

The rate equation without inhibition is:

$$(DX)_i = \frac{\mu_{\max} S_i}{S_i + K_S} \quad (\text{E.9.7})$$

TABLE E.9.1 Dilution rate, substrate concentration, cell dry weight, and productivity in a CSTR with and without inhibition

$D \text{ (h}^{-1}\text{)}$	$[I] = 0 \text{ g l}^{-1}$		$[I] = 0.05 \text{ g l}^{-1}$		$XD \text{ (g l}^{-1} \text{ h}^{-1}\text{)}$	
	$S \text{ (g l}^{-1}\text{)}$	$X \text{ (g l}^{-1}\text{)}$	$S \text{ (g l}^{-1}\text{)}$	$X \text{ (g l}^{-1}\text{)}$	$i = 0$	$i = 0.05$
0.05	0.11	0.99	0.67	0.93	0.0495	0.0465
0.10	0.25	0.98	1.50	0.85	0.0980	0.0850
0.15	0.43	0.96	2.57	0.74	0.1290	0.1110
0.20	0.67	0.93	4.00	0.60	0.1860	0.1200
0.25	1.00	0.90	6.00	0.40	0.2250	0.1000
0.30	1.50	0.85	9.00	0.10	0.2550	0.0300
0.35	2.33	0.77	—	—	0.2700	—
0.40	4.00	0.60	—	—	0.2400	—
0.45	9.00	0.10	—	—	0.0450	—

$$\frac{XD}{(XD)_i} = \left(\frac{S}{S_i}\right) \left(\frac{S_o - S}{S_o - S_i}\right) \left(\frac{S_i + K_S \left(1 + \frac{I}{K_i}\right)}{K_S + S}\right) \quad (\text{E.9.8})$$

For the special case, the equation without any inhibition the maximum dilution rate is:

$$D_{\max} = \mu_{\max} \left[1 - \sqrt{\frac{K_S}{S_o + K_S}} \right] \quad (\text{E.9.9})$$

The maximum dilution rate with inhibition is:

$$D_{\max} = \mu_{\max} \left[1 - \sqrt{\frac{K_S \left(1 + \frac{I}{K_i}\right)}{S_o + K_S \left(1 + \frac{I}{K_i}\right)}} \right] \quad (\text{E.9.10})$$

Given inhibition concentration as $[I] = X/10$.

Without inhibition (Figures E.9.1–E.9.3):

$$D_{\max} = \frac{\mu_{\max} S_o}{S_o + K_S} \quad (\text{E.9.11})$$

With inhibition (Figures E.9.1–E.9.3):

$$D_{\max} = \frac{\mu_{\max} S_o}{S_o + K_S \left(1 + \frac{I}{K_i}\right)} \quad (\text{E.9.12})$$

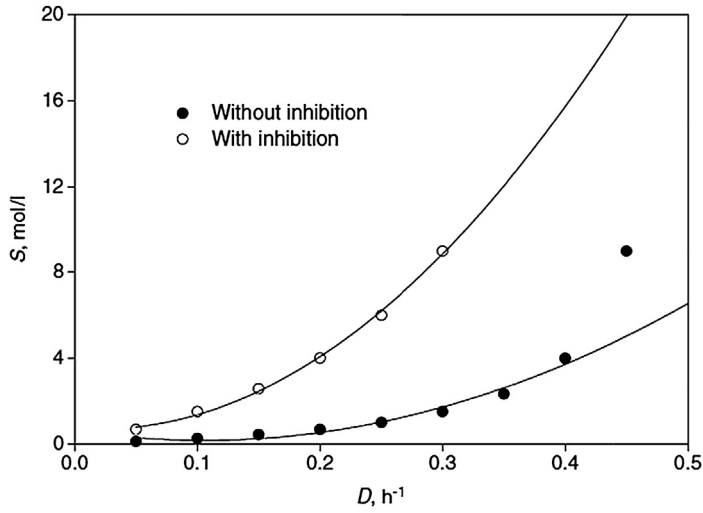


FIGURE E.9.1 Substrate concentration versus dilution rate in a CSTR bioreactor.

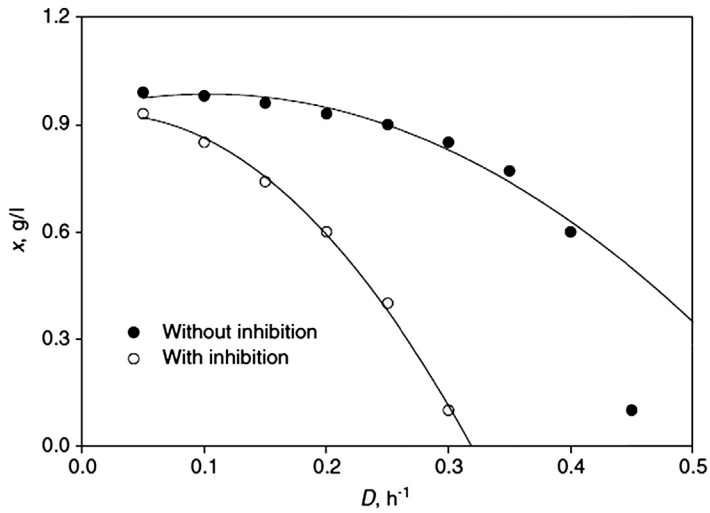


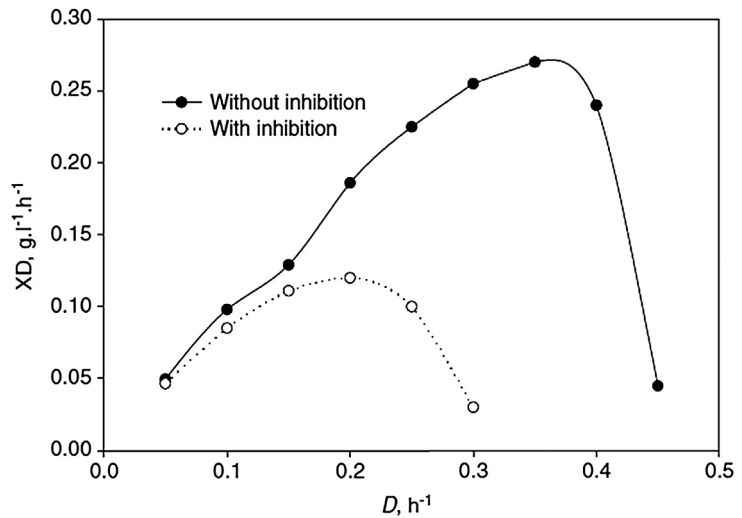
FIGURE E.9.2 Cell dry weight concentration versus dilution rate in a CSTR bioreactor.

$$D = \frac{\mu_{\max} S}{S + K_S \left(1 + \frac{x}{10K_i}\right)} = \frac{\mu_{\max} S}{S + K_S \left(1 + \frac{Y(S_0 - S)}{10K_i}\right)} \quad (\text{E.9.13})$$

$$S = \frac{DK_S \left(1 + \frac{1}{K_i}\right)}{\mu_{\max} - D} = \frac{DK_S \left(1 + \frac{Y(S_0 - S)}{10K_i}\right)}{\mu_{\max} - D} \quad (\text{E.9.14})$$

$$XD = DY(S_0 - S) \quad (\text{E.9.15})$$

FIGURE E.9.3 Productivity versus dilution rate in a CSTR bioreactor.



EXAMPLE 10

Microbial growth was discovered with replication of each cell to three daughter cells. With the growth data, define the mean time for the cell divisions. Table E.10.1 shows the cell dry weight increases with culture incubation time.

Solution

$$\frac{1}{X} \frac{dX}{dt} = \mu \quad (\text{E.10.1})$$

Because the population triples:

$$M_{cell} = 3M_{cell,0} \quad (\text{E.10.2})$$

$$X = X_0 e^{-\mu t} \quad (\text{E.10.3})$$

Then, generation time would be:

$$t = \frac{1}{\mu} \ln \frac{3X_0}{X_0} = \frac{\ln 3}{\mu} \quad (\text{E.10.4})$$

Table E.10.2 gives natural logarithm of cell dry weight.

The previous data are plotted in Figure E.10.1.

Thus, the generation time can be calculated from the slope of Figure E.10.1.

TABLE E.10.1 Microbial growth in a batch fermentation bioreactor

Time (h)	0.00	0.50	1.00	1.50	2.0
Cell dry weight (g l^{-1})	0.09	0.15	0.25	0.35	0.55

TABLE E.10.2 Natural logarithm of the cell dry weight concentration

T	$\ln X$
0.0	-2.303
0.5	-1.900
1.0	-1.470
1.5	-1.080
2.0	-0.670

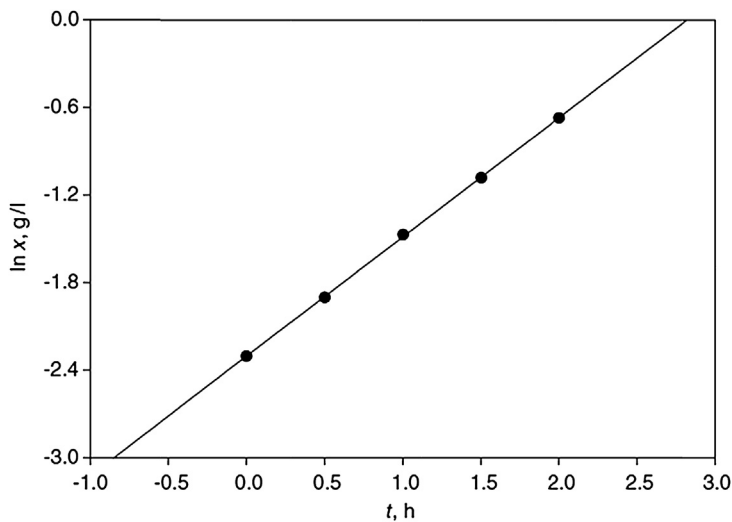


FIGURE E.10.1 Plot of natural logarithm of the cell dry weight concentration versus time in the batch bioreactor fermentation.

EXAMPLE 11

For enzymatic reaction, kinetic data may lead to fitting experimental data for projection of suitable rate model. It was proposed to apply Eadie–Hofstee model for the given data in [Table E.11.1](#). Determine kinetic constants for the given data.

TABLE E.11.1 Given and calculated kinetic data for rate model

C_S , Substrate concentration (g l^{-1})	r , Rate (g (l h)^{-1})	r/C_S (h^{-1})
10	2.6	0.26
16.8	3.2	0.19
27.7	3.6	0.13
32.2	3.7	0.115
43.3	3.9	0.09
50	4.0	0.08
66.1	4.3	0.065

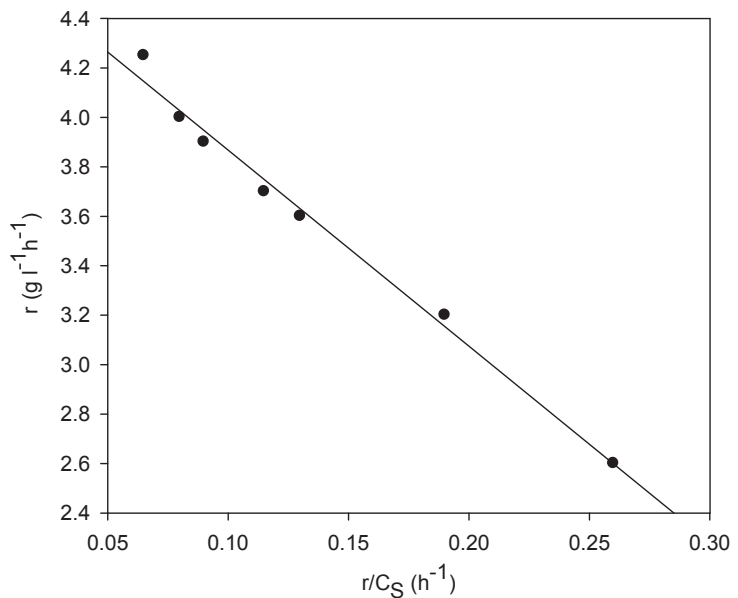
The rate equation for Eadie–Hofstee model is stated as follows:

$$v = v_{\max} - K_m \left(\frac{v}{C_S} \right) \quad (\text{E.11.1})$$

Solution

The plotted data for rate versus r/C_S resulted in a straight line because the slope is $-K_m$ and intercept is V_{\max} . This is known as Eadie–Hofstee plot. However, the inverse rate may approach infinity as substrate concentration decreases, which gives inconsistent measurements. From the plotted data, the value of V_{\max} is $4.25 \text{ g (l h)}^{-1}$ and the slope of the fitted data is defined as $K_m = 15.74 \text{ g l}^{-1}$ (Figure E.11.1).

FIGURE E.11.1 Eadie–Hofstee plot rate versus rate-to-substrate ratio.



5.9 UNSTRUCTURED KINETIC MODEL

Before discussing the principal concepts of kinetic model for growth, one has to know the precise application of each model, the potential to predict for special cases or use in projection of suitable bioreactor design, or sizing for production of desired product.

Generally, media consist of essential nutrients that are directly affecting on microbial cell growth. In fact, extensive research papers are tied up with media optimization and parameters to enhance cell cultivation in fermentation broth. About medium composition, for this topic special attention paid and detail is discussed in Chapter 9.

The simple relation in batch culture is defined by the rate cell production as a function of cell concentration.

$$\frac{dX}{dt} = f(X) \quad (5.9.1)$$

Malthus has defined the nature of biomass production as a linear function of cell concentration with proportionality constant of μ stated here:

$$f(X) = \mu X \quad (5.9.2)$$

Where μ is a specific growth rate and acts as a constant and X is cell concentration. Substitute the previously function in Malthus expression; then carry integration:

$$\int_{X_0}^X \frac{dX}{X} = \mu \int_0^t dt \quad (5.9.3)$$

$$\ln \frac{X}{X_0} = \mu t \quad \text{or} \quad X = X_0 e^{\mu t}$$

The cell concentration profile is perfect prediction for exponential phase, whereas the lag and stationary phases were ignored. In another rate model, inhibition term is incorporated; as the mode is shown inhibition has prevented cell growth or has negative impact on growth rate. That is Riccati equation:

$$\frac{1}{X} \frac{dX}{dt} = k(1 - \beta X) \quad \text{for I.C. } X(0) = X_0 \quad (5.9.4)$$

Rearrange the above expression by separation of variables, partial fraction, and then integration results in the Logistic model:

$$\int_{X_0}^X \frac{dX}{X(1 - \beta X)} = \int_{X_0}^X \frac{dX}{X} + \int_{X_0}^X \frac{\beta dX}{1 - \beta X} = \int_0^t k dt$$

$$\ln\left(\frac{X}{X_0}\right) + \ln\left(\frac{1 - \beta X_0}{1 - \beta X}\right) = \ln\left(\frac{X}{X_0}\right) \left(\frac{1 - \beta X_0}{1 - \beta X}\right) = kt \quad \text{or} \quad \frac{X(1 - \beta X_0)}{X_0(1 - \beta X)} = e^{kt} \quad (5.9.5)$$

Now solve for X :

$$X = \frac{X_O e^{kt}}{1 - \beta X_O (1 - e^{kt})} \quad (5.9.6)$$

Where $\beta = X_O / X_m$ is constant and is a ratio of initial cell density and maximum cell mass. This equation represent a sigmoidal curve leads to stationary phase at $t = k$ and $X_S = 1/\beta$; at this point, the curve is shifting the shape of concave up to concave downward similar to "S" shape curve. Application of the Logistic model for inhibitory effect is explained exactly when toxin is generated by microorganism. The rate of toxin production is proportional to the cell growth rate.

$$\begin{aligned} \frac{dC_t}{dt} &= \alpha \frac{dX}{dt}; \quad C_t(0) = 0 \\ C_t &= \alpha(X - X_O) \end{aligned} \quad (5.9.7)$$

When the mass initial cell concentration is $dC_t/dt = qX$, then:

$$\alpha \frac{dX}{dt} = qX \quad (5.9.8)$$

Separate variables and then result in similar expression as the Logistic model:

$$\frac{dX}{dt} = \frac{q}{\alpha} X = kX(1 - \beta X) \quad (5.9.9)$$

Another unstructured model that leads to prediction of the stationary phase would be at the condition of nutrient exhaustion, in which it is assumed constant yield as nutrients and cell mass are balanced. Such a case for bacterial or yeast inhibited by product or having a volatile product such as a high concentration of acetone and ethanol, the cell growth would be enhanced by the removal of product either by evaporative or extractive distillation; similar principles are applied in a membrane bioreactor for ethanol and lactic acid productions. Very promising results were obtained in a membrane bioreactor for instant removal of ethanol and lactic acid. Such a technique can remove product inhibition. The Logistic model is not able to predict death or declined phase. A model developed by Italian mathematician Volterra explains the death phase stated as follows:

$$f(X) = \mu X + \int_0^t k(t, r) X(r) dr \quad (5.9.10)$$

Where t and r are variables involved in terms of physical expansion with respect to cell growth. Volterra has extended the Verlhurst model by multiplication of a term that influenced cell population resulted in a growth rate as follows:

$$\frac{dX}{dt} = kX(1 - \beta X) + k_o \int_0^t X(r) dr; \quad \text{I.C. } X(0) = X_O \quad (5.9.11)$$

The influential term would be concentration of components as nutrients in a culture medium as shown here:

$$\frac{dC}{dt} = k(t)X(t) \quad \text{I.C. } C(0) = 0 \quad (5.9.12)$$

When the value of k_o is positive, the nutrient components promoting cell growth rate, whereas for negative value decline in cell concentration, inhibition significantly affects cell growth rate. The advantages of unstructured model is the equation has no capability to explain the lag phase and has no detail information on significant term to define influential parameter affecting on cell growth. The model is unable to give insight of the growth mechanisms or unable to explore the stepwise biochemical reaction to clarify the pathway of growing cells.

It is well understood that there is strong relations between substrate and specific growth rate. In continuous culture, the rate of utilization of substrate is balanced with specific growth rate:

$$\mu X = D(S_i - S_f) = \frac{\mu_{\max} SX}{K_S + S} \quad (5.9.13)$$

Compared with growth curve based on type of carbon and nitrogen sources; the trends are quite similar, whereas the rate can be in different scales. Based on the definition for cell mass incorporated in yield calculation, the biomass balance is stated as follows:

$$\begin{aligned} \mu X &= DY_{X/S}(S_{in} - S_{out}) \\ \frac{dX}{dt} &= \frac{\mu_{\max} SX}{K_S + S} \end{aligned} \quad (5.9.14)$$

Because the feed is in sterile condition, it does not contain any cell; the biomass balance in the bioreactor leads to the following equation while in a steady-state condition:

$$\begin{aligned} \mu &= D \\ D(S_O - S) - \frac{\mu_{\max} SX}{Y_{X/S}(K_S + S)} &= 0 \\ X &= \frac{Y_{X/S}D(S_O - S)(K_S + S)}{\mu_{\max} S} \end{aligned} \quad (5.9.15)$$

Other related rate models for specific growth rate are known as Monod, Tessier, Moser, Andrews, and Contois are often used for projection of cell growth in fermentation broth. Monod rate equation demonstrates cultivation with substrate limitation, whereas some limitations exist. Andrews described a rate model while taking into account substrate inhibition. This model was designed to resolve the existing limitation in Monod rate equation. [Tables 5.1–5.4](#) categorized several useful unstructured models in all of these models effective variables such as substrate, biomass, and product concentrations are involved. Based on effective variables on rate model all are divided in five groups. Therefore we would identify them as substrate or product dependent because the concentrations of substrate and or product are appeared in the proposed model.

Tessier and Moser models for growth represent algebraic solutions that are more complicated than the Monod rate equation. The Contois model is somehow similar to Monod rate, except it has an apparent Michaelis constant that is proportional to biomass concentration (X). In fact, from the simplified model, one can conclude that specific growth rate is proportional to inverse concentration of biomass ($\mu \propto X^{-1}$). The specific growth rate may be inhibited by medium composition such as high substrate concentration or product formed. A rate model with substrate inhibition was proposed by Haldane as a second-order substrate inhibition affected on growth represented by the following equation:

$$\mu = \frac{\mu_{\max} S}{K_S + S + S^2/k_I} \quad (5.9.16)$$

The kinetic model developed by Hinshelwood was adopted for ethanol fermentation to describe cell growth and product inhibition. The equation looks like the Monod rate model was slightly modified by multiplying a correction factor influenced by ethanol concentration as product term:

$$\mu = \mu_{\max} \left(\frac{S}{K_S + S} \right) \left(1 - \frac{P}{P_m} \right) \quad (5.9.17)$$

TABLE 5.1 Unstructured rate model depending on a substrate concentration

Kinetic model	Rate equation	Description
Monod	$\mu = \frac{\mu_{\max} S}{K_S + S}$	Simple model as a base is selected
Tessier	$\mu = \mu_{\max} \left(1 - e^{-\frac{S}{K_S}} \right)$	The growth rate is very sensitive to a low substrate concentration
Moser	$\mu = \frac{\mu_{\max} S^\lambda}{K_S + S^\lambda} = \mu_{\max} (1 + K_S S^{-\lambda})^{-1}$	A model that strongly depends on a substrate
Ming	$\mu = \frac{\mu_{\max} S^2}{K_S + S^2}$	This is a special case of Moser when $\lambda = 2$
Andrews and Haldane	$\mu = \frac{\mu_{\max} S}{K_S + S + S^2/k_I}$	This model incorporated inhibition term
Chen and Hashimoto	$\mu = \frac{\mu_{\max} S}{k(S_O - S) + S} = \frac{\mu_{\max} S}{kS_O + S(1 - k)}$	These two models have slightly differences on apparent saturation constant
Yue	$\mu = \frac{\mu_{\max} S}{K_S + S + k(S_O - S)} = \frac{\mu_{\max} S}{K_S + kS_O + S(1 - k)}$	

TABLE 5.2 Unstructured rate model depending on either on a cell and/or substrate concentration or both

Kinetic model	Rate equation	Description
Verlhurst	$\mu = \mu_{\max} \left[1 - \frac{X}{X_m} \right]$	Growth rate is related to biomass concentration
Contois	$\mu = \frac{\mu_{\max} S}{\beta X + S}$	Saturation term is a function of biomass concentration
Staniskis	$\mu = k_1 S - k_2 X$	Rate is linear function of substrate and biomass

TABLE 5.3 Unstructured rate model depending on product concentration

Kinetic model	Rate equation	Description
Aiba	$\mu = \mu_{\max} e^{-k_1 P}$	Specific rate is inversely incorporated with product concentration.
Jerusaliwski	$\mu = \mu_{\max} \left[\frac{P}{K_p + P} \right]$	The model is similar to Monod rate except instead of substrate and product concentration is used.
	$\mu = K_p \mu_{\max} \left[\frac{P}{K_p + P} \right]$	
Hagglund	$\mu = k'_1 - k'_2 \left[\frac{P}{k'_3 + P} \right]$	Linear plus Monod style with product concentration.
Westerhoff	$\mu = a + b \ln S$	Linear model with log function of substrate.
Herbert	$\mu = (\mu_{\max} + m) \left(\frac{S}{K_S + S} \right) - m$	Apparent maximum specific growth rate with additional correction terms.

TABLE 5.4 Unstructured rate model depending on substrate and product concentration

Kinetic model	Rate equation	Description
Aiba	$\mu = \mu_{\max} \left[\frac{S}{K_S + S} \right] e^{-k_1 P}$	In conjunction with Monod rate correction term applied by the use of product concentration.
Hinshelwood	$\mu = \mu_{\max} \left(\frac{S}{K_S + S} \right) \left(1 - \frac{P}{P_m} \right)$	Monod rate is corrected with product inhibition.
Hansford	$\mu = \left(\frac{\mu_{\max} S}{K_S + S} \right) \left(\frac{K_p}{K_p + Y_{X/S}(S_O - S)} \right)$	The model incorporated substrate and product inhibition.
Ghose and Tyagi	$\mu = \frac{\mu_{\max} S}{K_S + S + S^2/k_I} \left[1 - \frac{P}{P_L} \right]$	Substrate and product inhibitions are incorporated in Monod rate.
Jin	$\mu = \mu_{\max} \left[\frac{S}{K_S + S} \right] e^{-(k_1 P + k_2 S)}$	Both product and substrate are applied in exponential function for correction of Monod rate.
Severly	$\mu = \left(\frac{\mu_{\max} S}{K_S + S} \right) \left(\frac{k_p}{k_p + P} \right) \left[1 - \frac{P}{P_L} \right]$	Monod rate with product inhibition rate model.
Dourado	$\mu = \frac{\mu_{\max} S}{K_S + S + S^2/k_I} \left(\frac{k_p}{k_p + P} \right) \left[1 - \frac{P}{P_L} \right]$	Similar to the Severly model, but substrate inhibition is incorporated.

Where μ is the specific growth rate, μ_{\max} is the maximum specific growth rate of biomass, K_S is the substrate affinity or saturated constant, and P_m is the maximum concentration of ethanol may cause inhibition and reduce cell growth rate. Also, in ethanol fermentation, inhibition may be due to high product and substrate concentrations. The following model may be useful for rate equation, which is very close to the Severly model.

$$\mu = \left(\frac{\mu_{\max} S}{K_i + S} \right) \left(\frac{K_p}{K_p + P} \right) \quad (5.9.18)$$

The Hansford model incorporated substrate and product inhibition, whereas as the correction term was applied on the Monod rate equation. In continuous culture of *Saccharomyces cerevisiae* for ethanol fermentation, high glucose concentration (200 g l^{-1}) was used. The following model proposed by Hansford for ethanol production with inhibition was successfully applied.

$$\mu = \left(\frac{\mu_{\max} S}{K_S + S} \right) \left(\frac{K_P}{K_P + Y_{X/S}(S_O - S)} \right) \quad (5.9.19)$$

The model for multiple substrates is introduced by multiplication of concentrations of dual substrates. The projected model is stated as follows:

$$\mu = \mu_{\max} \left(\frac{S_1}{K_1 + S_1} \right) \left(\frac{S_2}{K_2 + S_2} \right) \quad (5.9.20)$$

Deviation from exponential growth phase may occur at any time when significant amount of nutrients were used or toxin concentration developed in the media. In that case, the maximum specific growth rate was no longer valid. To demonstrate the analysis of such an event, the rate of toxin formation is defined as the rate of nutrient composition is proportional to mass of cell until a stationary phase is reached. The rate of formation of toxin is:

$$\frac{da}{dt} = -k_a X \quad (5.9.21)$$

Based on mass balance, $a_O = \frac{k_a}{\mu} (X_S - X_O)$; the exponential growth is defined as $X = X_O e^{\mu t}$; if the substrate concentration is defined as $X_S = X_O + \frac{\mu}{k_a} a_O$ where X_S is depend on initial nutrient level. If toxin concentration is accumulated causes slow growth.

$$\frac{dX}{dt} = kX[1 - f(\text{toxin concentration})] \quad (5.9.22)$$

Where toxin may linearly decrease with growth rate.

$$\frac{1}{X} \frac{dX}{dt} = k(1 - bC_t) \quad (5.9.23)$$

Where C_t represents toxin concentration and b is constant. It was assumed that toxin production is dependent on cell biomass concentration as stated here:

$$\begin{aligned} \frac{dC_t}{dt} &= qX \\ C_t &= q \int_0^t X dt; \quad \text{I.C.: } t = 0, \quad C_t = 0 \end{aligned} \quad (5.9.24)$$

Now substitute toxin concentration into the previous equation for a result of the biomass concentration:

$$\frac{dX}{dt} = kX \left(1 - bq \int_0^t X dt \right) \quad (5.9.25)$$

The effective specific growth rate is

$$\mu_{eff} = \frac{1}{X} \frac{dX}{dt} = k \left(1 - bq \int_0^t X dt \right) \quad (5.9.26)$$

When cell growth is halted, that means $\mu_{eff} = 0$; then:

$$\left(1 - bq \int_0^t X dt \right) = 0; \quad \frac{1}{bq} = \int_0^t X dt$$

When $C_t = 1/b$, then $dX/dt = 0$; this means constant biomass. Also, it means that the toxicated medium has to be diluted with nontoxicated nutrients. If the growth is halted due to decrease or exhaustion of nutrients; then dilution with a non-nutrient does not improve the growth. For the death phase projection is defined as follows:

$$X = X_0 e^{-k_d t} \quad (5.9.27)$$

NOMENCLATURE

- μ Specific growth rate, h^{-1}
- μ_{\max} Maximum specific growth rate, h^{-1}
- ρ_{cell} Cell density, g l^{-1}
- v Specific growth rate constant, $\text{g l}^{-1} \text{h}^{-1}$
- C_i Molar concentration of component i , g l^{-1}
- C_{if} Molar concentration in feed, g l^{-1}
- D or F/V Dilution rate, h^{-1}
- F Flow rate, h^{-1}
- i Inhibition concentration, g l^{-1}
- k_2 Rate constant for forward, h^{-1}
- k_{-2} Rate constant for backward, h^{-1}
- K_m^{app} Apparent Michaelis constant, g l^{-1}
- K_d Specific death rate, h^{-1}
- K_i Inhibition constant, g l^{-1}
- K_S Saturation or Monod constant g l^{-1}
- r_{fi} Rate of product formation, $\text{g l}^{-1} \text{h}^{-1}$
- S Substrate concentration, g l^{-1}
- V_R Culture volume, m^3
- V Working volume of the bioreactor, l
- X Cell concentration, g l^{-1}
- X_0 Initial biomass concentration, g l^{-1}
- y_{\max}^{app} Apparent maximum specific growth rate constant, h^{-1}
- $Y_{p/S}$ Yield of product
- $Y_{X/S}$ Yield of biomass

References

1. Pelczar MJ, Chan ECS, Krieg NR. *Microbiology*. New York: McGraw-Hill; 1986.
2. Baily JE, Ollis DF. *Biochemical engineering fundamentals*. 2nd ed. New York: McGraw-Hill; 1986.
3. Wang DIC, Cooney CL, Deman AL, Dunnill P, Humphrey AE, Lilly MD. *Fermentation and enzyme technology*. New York: John Wiley & Sons; 1979.
4. Scragg AH. *Bioreactor in biotechnology, a practical approach*. New York: Ellis Horwood Series in Biochemistry and Biotechnology; 1991.
5. Doran PM. *Bioprocess engineering principles*. New York: Academic Press; 1995.
6. Ghose TK. *Bioprocess computation in biotechnology*, vol. 1. New York: Ellis Horwood Series in Biochemistry and Biotechnology; 1990.
7. Shuler ML, Kargi F. *Bioprocess engineering, basic concepts*. New Jersey: Prentice Hall; 1992.
8. Stanbury PF, Whitaker A. *Principles of fermentation technology*. Oxford: Pergamon Press; 1984.
9. Levenspiel O. *Chemical reaction engineering*. 3rd ed. New York: John Wiley & Sons; 1999.
10. James ML, Smith GM, Wolford JC. *Applied numerical methods for digital computation*. New York: Harper & Row; 1977.

SUBCHAPTER

5.11

Case Study: Enzyme Kinetic Models for Resolution of Racemic Ibuprofen Esters in a Membrane Reactor*

5.11.1 INTRODUCTION

In this case study, an enzymatic hydrolysis reaction, the racemic ibuprofen ester, i.e., (R)- and (S)-ibuprofen esters in equimolar mixture, undergoes a kinetic resolution in a biphasic enzymatic membrane reactor (EMR). In kinetic resolution, the two enantiomers react at different rates; lipase originated from *Candida rugosa* shows a greater stereo-preference toward the (S)-enantiomer. The membrane module consisted of multiple bundles of polymeric hydrophilic hollow fiber. The membrane separated the two immiscible phases (i.e., organic in the shell side and aqueous in the lumen). Racemic substrate in the organic phase enacted with immobilized enzyme on the membrane where the hydrolysis reaction took place, and the product (S)-ibuprofen acid was extracted into the aqueous phase.

In this case study, the kinetic behavior of the immobilized system was analyzed while the following parameters were taken into account:

1. the rate equations for native enzymes and immobilized enzymes are not necessarily the same because of microenvironment and shear stress effects;
2. within the reaction layer, the substrate should diffuse, then mass transfer and enzymatic reaction occur simultaneously, giving rise to substrate concentration profiles at levels lower than the feed concentration; and
3. external mass transfer resistances have to be taken into account, depending on the operating conditions and the reactor configuration.

The values of the Michaelis–Menten kinetic parameters, V_{\max}^{app} and K_m^{app} characterize the kinetic expression for the microenvironment within the porous structure. Kinetic analyses of the immobilized lipase in the membrane reactor were performed because the kinetic parameters cannot be assumed to be the same values as for the native enzymes.

*This chapter was written with contributions from:

Wei Sing Long, Institute of Thermodynamics, Helmut-Schmidt University, Hamburg, Germany;
Azlina Harun Kamaruddin, Subash Bhatia, School of Chemical Engineering, Engineering Campus,
Universiti Sains Malaysia, 14300 Nibong Tebal, Pulau Pinang, Malaysia.

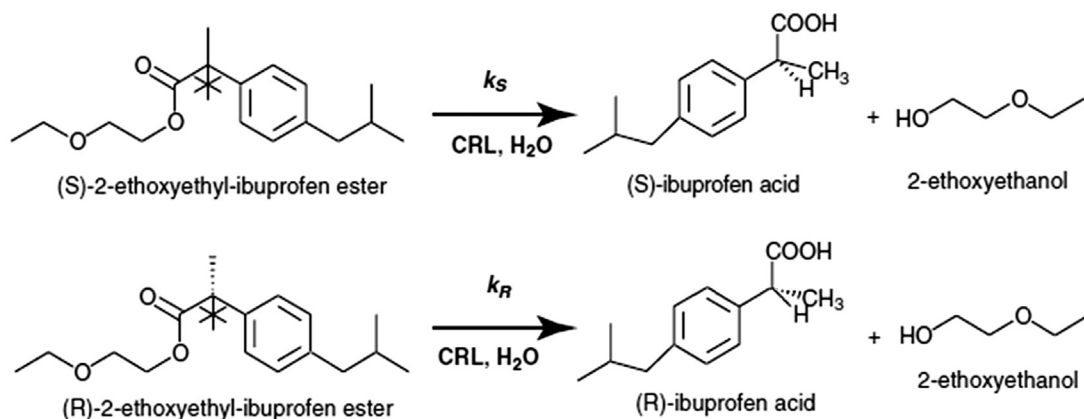


FIGURE 5.14 Lipase-catalysed hydrolysis of racemic ibuprofen ester. CRL, *Candida rugosa* lipase.

The reaction under investigation is the enzymatic hydrolysis of racemic ethoxyethylibuprofen ester. The (R)-ester is not active in the above reaction,^{1–3} thus simplifying the reaction mechanism, as shown in Figure 5.14. Because both enantiomers are converted according to first-order kinetics, the conversion of one enantiomer is independent of the conversion of the other.⁴

5.11.2 ENZYME KINETICS

The initial reaction rate (v_0) obtained from each substrate concentration was fitted to Michaelis–Menten kinetics using *enzyme kinetics*. Pro (EKP) Software (ChemSW product, Singapore) was obtained for estimates V_{\max} and K_m of free lipase reaction and V_{\max}^{app} and K_m^{app} and for immobilized lipase reaction. Hanes–Woolf and Simplex methods were used for the evaluation of kinetic parameters owing to their strength in error handling when experimental data are subject to random errors.⁵

5.11.2.1 Substrate and Product Inhibitions Analyses

Substrate and product inhibitions analyses involved considerations of competitive, uncompetitive, noncompetitive, and mixed inhibition models. The kinetic studies of the enantiomeric hydrolysis reaction in the membrane reactor included inhibition effects by substrate (ibuprofen ester) and product (2-ethoxyethanol) while varying substrate concentration (5–50 mmol l⁻¹). The initial reaction rate obtained from experimental data was used in the primary (Hanes–Woolf plot) and secondary plots ($1/V_{\max}$ versus inhibitor concentration), which gave estimates of substrate inhibition (K_{IS}) and product inhibition constants (K_{IP}). The inhibitor constant (K_{IS} or K_{IP}) is a measure of enzyme–inhibitor affinity. It is the dissociation constant of the enzyme–inhibitor complex.

Table 5.5 presents the intrinsic kinetic parameters (K_m and V_{\max}) for the free lipase system and apparent kinetic parameters (K_m^{app} and V_{\max}^{app}) for the immobilized lipase in the EMR using

TABLE 5.5 Kinetic parameters for enzymatic membrane reactor (EMR) and free lipase system

EMR		Free lipase system	
V_{\max}^{app} (mmol l ⁻¹ h ⁻¹)	K_m (mmol l ⁻¹)	V_{\max} (mmol l ⁻¹ h ⁻¹)	K_m (mmol l ⁻¹)
3.27	36.47	2.83	63.43

fixed 2 g l⁻¹ lipase concentration. The immobilized lipase showed higher maximum apparent reaction rate and greater enzyme–substrate (*ES*) affinity compared with free lipase.

5.11.2.2 Substrate Inhibition Study

The inhibition analyses were examined differently for free lipase in a batch and immobilized lipase in membrane reactor system. Figure 5.15 shows the kinetics plot for substrate inhibition of the free lipase in the batch system, where $[S]$ is the concentration of (S)-ibuprofen ester in isooctane and v_o is the initial reaction rate for (S)-ester conversion. The data for immobilized lipase are shown in Figure 5.16; that is, the kinetics plot for substrate inhibition for immobilized lipase in the EMR system. The Hanes–Woolf plots in both systems show similar trends for substrate inhibition. The graphical presentation of rate curves for immobilized lipase shows higher values compared with free enzymes. The value for the maximum specific growth rate in the immobilized enzyme reactor was 15% higher than the free enzyme system. The K_{IS} values calculated by EKP software are presented in Table 5.6. The inhibition constant (K_{IS}) in EMR was 49.52 mmol l⁻¹, higher than the value obtained in batch system (43.07 mmol l⁻¹).

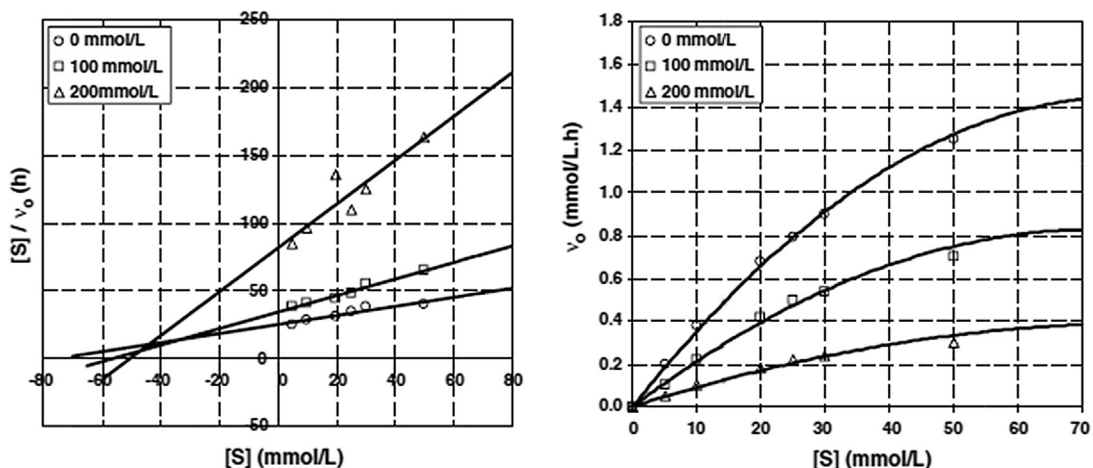


FIGURE 5.15 Substrate inhibition plots for batch system with top left corner showing the concentration of substrate inhibitor designated by $[S^*]$ (left: Hanes-Woolf; right: curve fit).

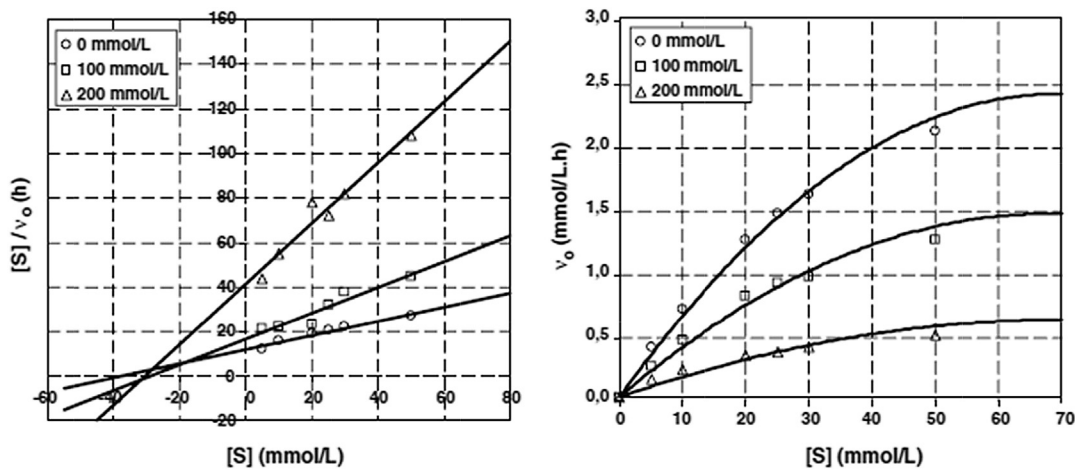


FIGURE 5.16 Substrate inhibition plots for enzymatic membrane reactor system with top left corner showing the concentration of substrate inhibitor designated by [S*] (left: Hanes-Woolf; right: curve fit).

TABLE 5.6 K_{IS} value for free lipase and enzymatic membrane reactor (EMR)

	Inhibition	K_{IS} (mmol l ⁻¹)
Free lipase	Uncompetitive	43.07
EMR	Uncompetitive	49.52

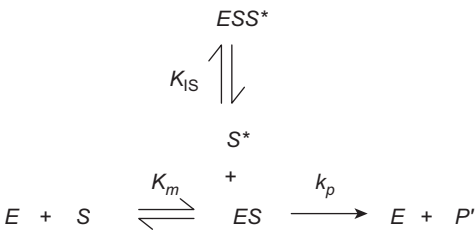


FIGURE 5.17 Enzyme mechanism with uncompetitive substrate inhibition.

A possible substrate inhibition in the system was uncompetitive inhibition, as determined by EKP software. The mechanism of this kind of inhibition is presented in Figure 5.17. As ES interact with S* it forms ESS* where S* is a sort of inhibitory substrate as illustrated in Figure 5.17. The reduction of K_m^{app} was caused by a possible uncompetitive inhibition, because excessive substrate binds to the ES complex forming the ternary ESS* complex, as depicted in Figure 5.17. This phenomenon showed an apparent increase in the affinity of the enzyme against the substrate as a result of more substrate being bound to the enzyme, i.e., the ESS* formation, thus leading to a reduction in V_{max}^{app} . This uncompetitive inhibition effect was in agreement with the literature that substrate inhibition in enzyme-catalyzed reactions

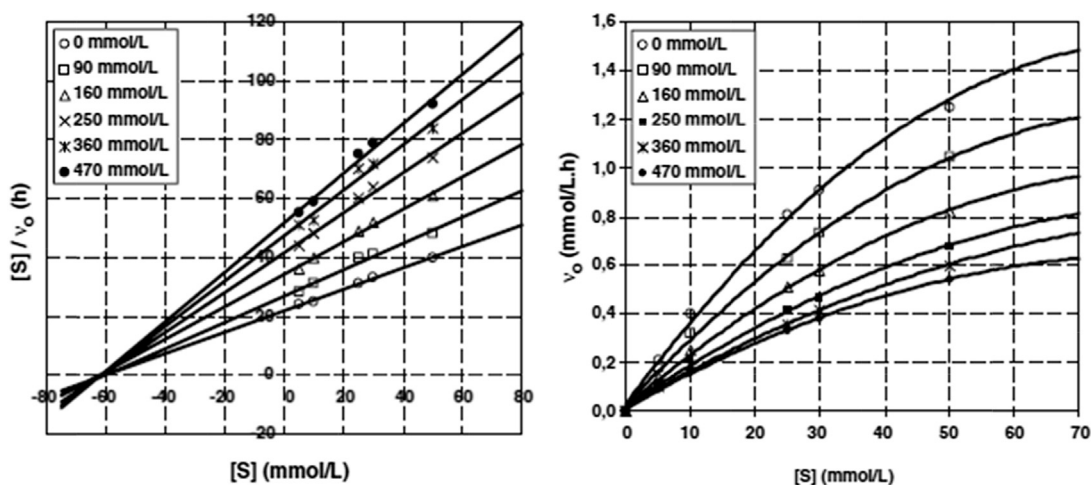


FIGURE 5.18 Free lipase in batch system: product inhibition plots (left: Hanes-Woolf; right: curve fit).

decreases the reaction rate for Michaelis–Menten kinetics, resulting in the drop of racemate conversion.³ Matson and Lopez, Xiu and Jiang, and Xiu et al.^{4,6,7} found that when substrate inhibition took place, the conversion dropped and the enantiomeric reaction rate decreased, causing the optimal time for terminating the reaction for a racemic resolution to become longer. Uncompetitive inhibitor binds to the ES complex, hence pulling the equilibrium of the substrate binding reaction to the right (Figure 5.18), causing an apparent increase in the ES affinity and a decrease in the value of K_m^{app} . In other words, the inhibitor and substrate each bound to the enzyme independently.

5.11.2.3 Product Inhibition Study

The 2-ethoxyethanol was a by-product, as shown in Figure 5.13. The formation rate of 2-ethoxyethanol was the same as the conversion rate of the (S)- or (R)-ibuprofen ester: 1 mol of 2-ethoxyethanol was formed when 1 mol of ester was catalyzed. A known concentration of 2-ethoxyethanol was added in the organic phase before the start of the reaction for product inhibition. The plots of the kinetics for the free lipase system are presented in Figure 5.18 and immobilized enzyme (EMR) in Figure 5.19, respectively. The K_{IP} value was $337.94 \text{ mmol l}^{-1}$ for the free lipase batch system and $354.20 \text{ mmol l}^{-1}$ for immobilized lipase in the EMR. The product inhibition constants (K_{IP}) for the two systems are given in Table 5.7. The 2-ethoxyethanol was found to be a noncompetitive inhibitor to the substrate as determined by the EKP software, with the mechanism shown in Figure 5.20.

In a noncompetitive inhibition, the substrate (S) and inhibitor (I) have equal potential to bind to the free enzyme (E). The inhibitor forms a ternary complex with ES , whereas the substrate will form another ternary complex with enzyme–inhibitor (EI). Because the noncompetitive inhibitor had no effect on the binding of substrate to the enzyme, the K_m value remained consistent (or unchanged). There are two different ways for the formation of ESI ternary complex; this complex would not form the product and therefore

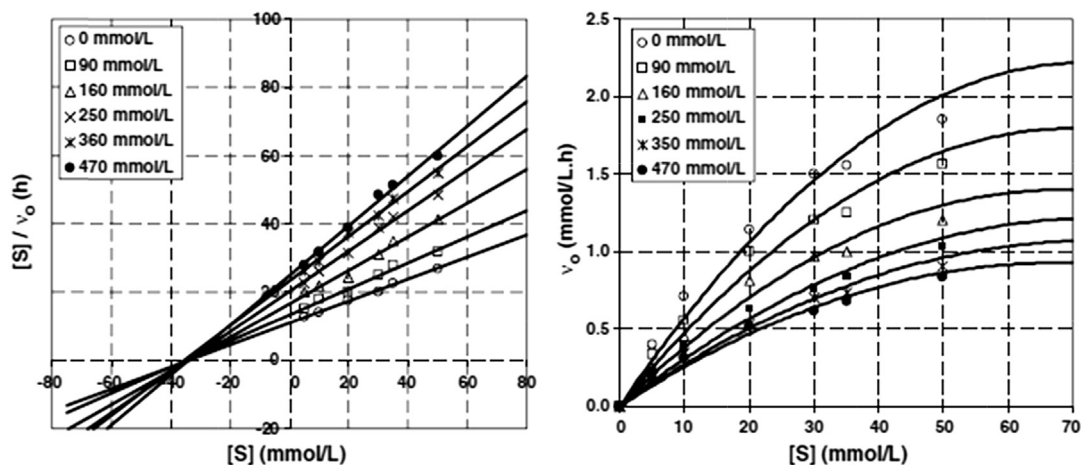


FIGURE 5.19 Immobilized lipase in enzymatic membrane reactor: product inhibition plots (left: Hanes-Woolf; right: curve fit).

TABLE 5.7 K_{IP} value for batch system and enzymatic membrane reactor (EMR)

	Product inhibition	K_{IP} (mmol l ⁻¹)
Batch system	Noncompetitive	337.94
EMR	Noncompetitive	354.20

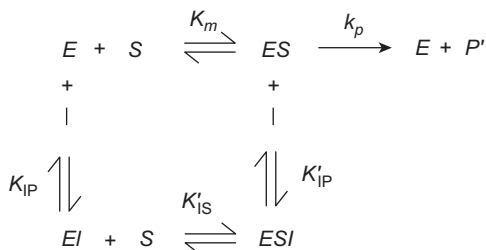


FIGURE 5.20 Enzyme mechanism with noncompetitive product inhibition.

was decreased. A noncompetitive inhibitor had no effect on substrate binding or the ES affinity, therefore, the apparent rate constant (K_m^{app}) was unchanged.⁵ A possible reason for product inhibition was because of the nature of 2-ethoxyethanol, which is miscible in both aqueous buffer and organic solvent. K_{IP} was larger than K_{IS} by an order of magnitude, i.e., K_{IP} was 337.94 mmol l⁻¹ for the free lipase system and 354.20 mmol l⁻¹ for EMR, whereas K_{IS} was 43.07 mmol l⁻¹ for the batch system and 49.52 mmol l⁻¹ for EMR.

5.11.3 ENZYME KINETICS FOR RAPID EQUILIBRIUM SYSTEM (QUASI-EQUILIBRIUM)

Enzyme reaction kinetics were modeled on the basis of rapid equilibrium assumption. Rapid equilibrium condition (also known as quasi-equilibrium) assumes that only the early components of the reaction are at equilibrium.^{8–10} In rapid equilibrium conditions, the enzyme (E), substrate (S), and ES , the central complex equilibrate rapidly compared with the dissociation rate of ES into E and product (P'). The combined inhibition effects by 2-ethoxyethanol as a noncompetitive inhibitor and (S)-ibuprofen ester as an uncompetitive inhibition resulted in an overall mechanism, shown in Figure 5.21.

5.11.4 DERIVATION OF ENZYMIC RATE EQUATION FROM RAPID EQUILIBRIUM ASSUMPTION

The mechanism involved the overall conversion of $[S]$ to $[P]$. The reverse reaction is insignificant because only the initial velocity in one of the forward direction is concerned. The mass balance equation expressing the distribution of the total enzyme is:

$$[E]_t = [E] + [ES] + [EI] + [ESI] + [ESS^*] \quad (5.11.4.1)$$

The rate-dependent equation was expressed in the form:

$$v = k_p [ES] \quad (5.11.4.2)$$

where v indicates the initial rate of the product-forming species. The rate equation was divided by $[E]_t$:

$$\frac{v}{[E]_t} = \frac{k_p [ES]}{[E]_t = [E] + [ES] + [EI] + [ESI] + [ESS^*]} \quad (5.11.4.3)$$

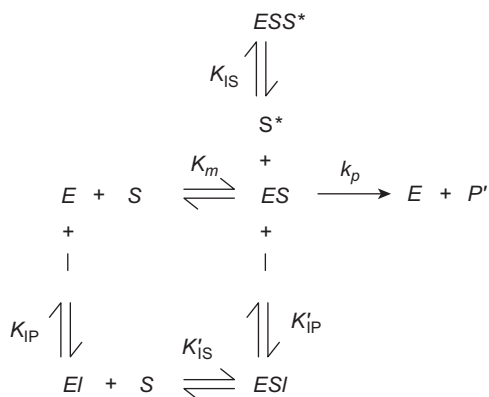


FIGURE 5.21 Kinetics mechanism with uncompetitive substrate inhibition and noncompetitive product inhibition.

where $[E]_t$ contains a total of five enzyme species of one free and four complexes of enzyme, substrate, and inhibitor. The concentration of each enzyme species was expressed in terms of free enzyme, E . This was accomplished by rearranging the expressions for the various equilibria. In this case, there are four equilibria:

$$K_m = \frac{[E][S]}{[ES]} \Rightarrow [ES] = \frac{[S]}{K_m} [E] \quad (5.11.4.4)$$

$$[EI] = \frac{[E][I]}{K_{IP}} \quad (5.11.4.5)$$

$$[ESI] = \frac{[E][S][I]}{K_m K_{IP}} \quad (5.11.4.6)$$

$$[ESS^*] = \frac{[E][S][S^*]}{K_m K_{IS}} \quad (5.11.4.7)$$

Each enzyme complex in the rate-dependent equation was substituted by the previous equations in terms of $[E]$. After canceling $[E]$ and substituting $k_p[E]_t = V_{\max}$, the following rate equation was obtained.

$$\frac{v}{V_{\max}} = \frac{\frac{[S]}{K_m}}{1 + \frac{[I]}{K_{IP}} + \frac{[S][I]}{K_m K_{IP}} + \frac{[S]}{K_m} + \frac{[S][S^*]}{K_m K_{IS}}} \quad (5.11.4.8)$$

The previous equation can be transformed into the Michaelis–Menten equation by multiplying the numerator and denominator by K_m :

$$\frac{v}{V_{\max}} = \frac{[S]}{(K_m + [S]) \left(1 + \frac{[I]}{K_{IP}}\right) + \frac{[S][S^*]}{K_{IS}}} \quad (5.11.4.9)$$

In the present work, $[I] = [P]$ and $[S^*] = [S]$, so the equation becomes:

$$v = \frac{V_{\max}[S]}{(K_m + [S]) \left(1 + \frac{[P]}{K_{IP}}\right) + \frac{[S]^2}{K_{IS}}} \quad (5.11.4.10)$$

This rate equation is in agreement with that reported by Madhav and Ching.³ This rapid equilibrium treatment is a simple approach that allows the transformations of all complexes in terms of $[E]$, $[S]$, K_{IS} , and K_{IP} , which only deal with equilibrium expressions for the binding of the substrate to the enzyme. In the absence of inhibition, the enzyme kinetics is reduced to the simplest Michaelis–Menten model, as shown in [Figure 5.22](#).



FIGURE 5.22 First-order reaction kinetics mechanism without inhibitions.

The rate equation for the Michaelis–Menten model is given in ordinary textbooks and is as follows¹¹:

$$v = \frac{V_{\max}[S]}{[S] + K_m} \quad (5.11.4.11)$$

5.11.5 VERIFICATION OF KINETIC MECHANISM

The velocity equation for rapid equilibrium system was easily derived by inverting the numerator and denominator of Eqn (5.11.4.10):

$$\frac{V_{\max}}{v} = \left(\frac{K_m + [S]}{[S]} \right) \left(1 + \frac{[P]}{K_{IP}} \right) + \frac{[S]}{K_{IS}} \quad (5.11.5.1)$$

$$\frac{1}{v} = \frac{1}{V_{\max}} \left(1 + \frac{K_m}{[S]} \right) \left(1 + \frac{[P]}{K_{IP}} \right) + \frac{1}{V_{\max}} \frac{[S]}{K_{IS}} \quad (5.11.5.2)$$

$$\frac{1}{v} = \frac{1}{V_{\max}} \frac{1}{K_{IP}} \left(1 + \frac{K_m}{[S]} \right) [P] + \frac{1}{V_{\max}} \left(1 + \frac{K_m}{[S]} + \frac{[S]}{K_{IS}} \right) \quad (5.11.5.3)$$

Plotting $1/v$ against $[P]$ will result in a Dixon plot, which is plotted at different fixed $[S]$ with the slope:

$$\frac{1}{V_{\max}} \frac{1}{K_{IP}} \left(1 + \frac{K_m}{[S]} \right) \quad (5.11.5.4)$$

and the y -intersect:

$$\frac{1}{V_{\max}} \left(1 + \frac{K_m}{[S]} + \frac{[S]}{K_{IS}} \right) \quad (5.11.5.5)$$

The plotting of Dixon plot and its slope replot (see Eqn (5.11.5.9)) is a commonly used graphical method for verification of kinetics mechanisms in a particular enzymatic reaction.⁹ The proposed kinetic mechanism for the system is valid if the experimental data fit the rate equation given by Eqn (5.11.4.4). In this attempt, different sets of experimental data for kinetic resolution of racemic ibuprofen ester by immobilized lipase in EMR were fitted into the rate equation of (5.11.5.6). The Dixon plot is presented in Figure 5.23.

Dixon plot:

$$\frac{1}{v} = \frac{1}{V_{\max}^{app}} \frac{1}{K_{IP}} \left(1 + \frac{K_m^{app}}{[S]} \right) [P] + \frac{1}{V_{\max}^{app}} \left(1 + \frac{K_m^{app}}{[S]} + \frac{[S]}{K_{IS}} \right) \quad (5.11.5.6)$$

The slope and intersect of the illustrated plot were determined and compared with values calculated from Eqn (5.11.5.7) and Eqn (5.11.5.8):

$$\text{Slope} = \frac{1}{V_{\max}^{app}} \frac{1}{K_{IP}} \left(1 + \frac{K_m^{app}}{[S]} \right) \quad (5.11.5.7)$$

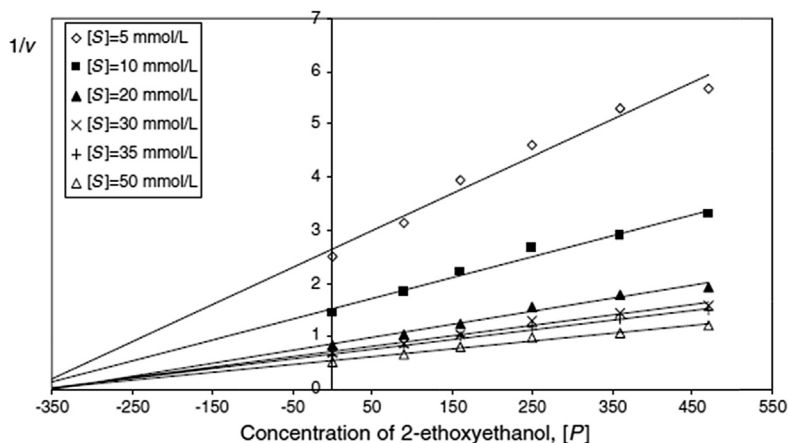


FIGURE 5.23 Dixon plot: $1/v$ versus $[P]$ at different initial substrate concentrations.

$$\text{Intersect} = \frac{1}{V_{\max}^{\text{app}}} \left(1 + \frac{K_m^{\text{app}}}{[S]} + \frac{[S]}{K_{IS}} \right) \quad (5.11.5.8)$$

The experimental values fit the velocity equation with insignificant deviation in the slope and intersect values at maximum error of $\pm 5.94\%$ (see Table 5.8). The corresponding slope replot given by Eqn (5.11.5.9) was plotted in Figure 5.24.

$$\text{Slope replot} = \frac{K_m^{\text{app}}}{V_{\max}^{\text{app}} K_{IP}} \left(\frac{1}{[S]} \right) + \frac{1}{V_{\max}^{\text{app}} K_{IP}} \quad (5.11.5.9)$$

$$\text{Slope} = \frac{K_m^{\text{app}}}{V_{\max}^{\text{app}} K_{IP}} \quad (5.11.5.10)$$

TABLE 5.8 Comparison between graphical value (Figure 5.23) and calculated value

[S] (mmol l^{-1})	Slope			Intersect		
	From Figure 5.23	Calculated from (5.11.5.9)	Error (%)	From Figure 5.23	Calculated from (5.11.5.8)	Error (%)
5	0.0070	0.00720	2.7	2.6509	2.567	3.23
10	0.0039	0.00400	2.5	1.5292	1.4828	3.10
20	0.0024	0.00244	1.64	0.9360	0.9870	5.17
30	0.0020	0.00190	5.26	0.8140	0.8630	5.68
35	0.0018	0.00176	2.27	0.7911	0.8406	5.94
50	0.0015	0.00150	0.00	0.7852	0.8276	5.19

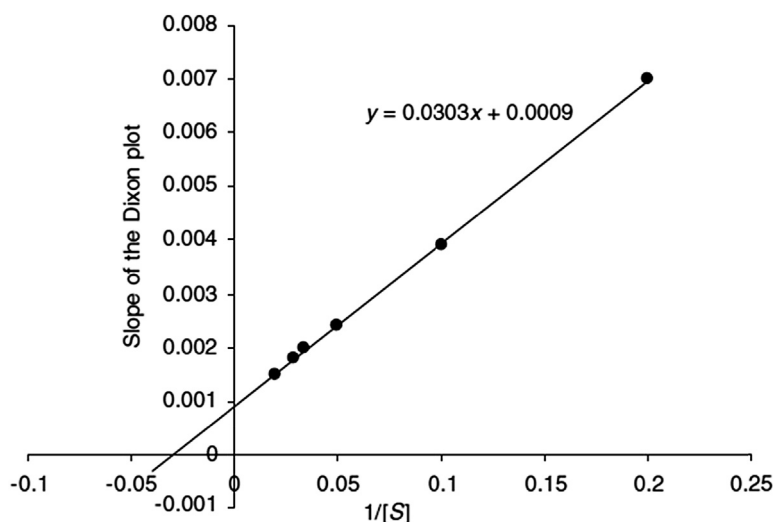


FIGURE 5.24 Slope replot: the slope of the Dixon plot was plotted against $1/[S]$.

TABLE 5.9 Slope replot (slope of Dixon plot versus $1/[S]$)

Slope replot (Figure 5.24)	Slope		Intersect		
	Calculated from (5.11.5.10)	Error (%)	Slope replot (Figure 5.24)	Calculated from (5.11.5.11)	Error (%)
0.0303	0.0315	3.81	0.0009	0.00086	4.65

$$\text{Intersect} = \frac{1}{V_{\max}^{\text{app}} K_{IP}} \quad (5.11.5.11)$$

The values determined from Figure 5.23 agree well with the values calculated from the equations (Table 5.9), with an error of $\pm 3.81\%$ for the slope and $\pm 4.65\%$ for the intersect, respectively. The obtained experimental data were consistent with the proposed enzymatic reaction and the reaction mechanisms with uncompetitive substrate inhibition and the noncompetitive product inhibition model.

References

1. Battistel E, Bianchi D, Cesti P, Pina C. *Biotechnol Bioengng* 1991;**38**:659.
2. Giorno L, Molinari R, Natoli M, Drioli E. *J Membr Sci* 1997;**125**:177.
3. Madhav MV, Ching CB. *J Chem Technol Biotechnol* 2001;**76**:941.
4. Xiu G-H, Jiang L, Li P. *Biotechnol Bioengng* 2001;**74**:29.
5. Chaplin MF, Bucke C. In: *Enzyme technology*. London: Cambridge University Press; 1990.
6. Matson SL, López JL. In: *Frontiers in bioprocessing*. Florida: CRC Press; 1990.
7. Xiu G-H, Jiang L. *Ind Eng Chem Res* 2000;**39**:4054.
8. Segel IH. *Enzyme kinetics: behavior and analysis of rapid equilibrium and steady-state enzyme systems*. New York: John Wiley & Sons; 1975.

9. W.S. Long, (Ph.D. thesis), Universiti Sains Malaysia, Penang, Malaysia, 2004.
 10. Long WS, Azlina Harun K, Bhatia S. *Chem Eng Sci* 2005;**60**:4957.
 11. Voet D, Voet JG. *Fundamentals of biochemistry*. 3rd ed. New York: John Wiley; 2004.

PROBLEMS

- 5.1. In a chemostat, *Escherichia coli* has been cultivated in an aerobic condition using glucose as the limiting substrate with an initial sugar concentration of 1.05 g l^{-1} .
 a. Based on given data in Table Q.1, determine μ_m and K_s .
 b. If the cell is represented by formula as $\text{C}_5\text{H}_7\text{NO}_2$, find $Y_{\text{O}_2/\text{x}}$ (mass of oxygen/mass of cells) and maximum oxygen consumed for maximum biomass concentration.
- 5.2. Determine the kinetic coefficients k , K_s , μ_{max} , Y , and k_d from the following data obtained in bench-scale bioreactor with solid recycle (Table P.5.2).

TABLE Q.1 Biomass and limiting substrate concentrations with respect to dilution rate

Dilution rate (h^{-1})	Limiting substrate, C_s (g l^{-1})	x (g l^{-1})
0.05	0.0006	0.45
0.12	0.013	0.44
0.24	0.033	0.42
0.31	0.041	0.44
0.43	0.064	0.42
0.53	0.102	0.43
0.60	0.122	0.41
0.71	0.241	0.38
0.79	0.250	0.35

TABLE P.5.2 Experimental data

Run no.	S_o (mg l^{-1})	S (mg l^{-1})	θ (day)	x_r (mg VSS l^{-1})	θ_c (day)
1	400	10	0.167	3950	3.1
2	400	14.3	0.167	2865	2.1
3	400	21.0	0.167	2100	1.6
4	400	49.5	0.167	1050	0.8
5	400	101.6	0.167	660	0.6

Bioreactor Design

OUTLINE

6.1 Introduction	193	6.8.1 Monod Model for a Chemostat	205
6.2 Bioreactors: Background	194	6.9 Temperature Effect on Rate Constant	209
6.3 Type of Bioreactor	195	6.10 Scale-Up of Stirred-Tank Bioreactor	210
6.3.1 Airlift Bioreactors	196	6.11 Biological Transport of Oxygen through Cells	217
6.3.2 Airlift Pressure Cycle Bioreactors	197	6.11.1 Estimation of Mass Transfer Coefficient	218
6.3.3 Loop Bioreactor	197	6.11.2 Mass Transfer in Aerated and Agitated Vessels	221
6.4 Stirred Tank Bioreactor	198	Nomenclature	223
6.5 Bubble Column Fermenter	201	References	223
6.6 Airlift Bioreactors	202		
6.7 Heat Transfer	203		
6.8 Design Equations for CSTR Fermenter	205		

6.1 INTRODUCTION

To design a bioreactor, some objectives must be defined. The decisions made in design of the bioreactor could have a significant impact on overall process performance. Knowledge of reaction kinetics is essential for understanding how a biological reactor works. Knowledge

of other areas of bioprocess engineering such as mass and energy balances, mixing, mass transfer, and heat transfer is also required.

The bioreactor is the heart of any biochemical process in which enzymes, microbial, mammalian, or plant cell systems are used for the manufacture of a wide range of useful biological products. The performance of any bioreactor depends on many functions, such as those listed below:

• Biomass concentration	• Nutrient supply
• Sterile conditions	• Product removal
• Effective agitations	• Product inhibition
• Heat removal	• Aeration
• Correct shear conditions	• Metabolisms/microbial activities

There are three groups of bioreactors currently in use for industrial production:

1. Nonstirred, nonaerated system: about 70% of bioreactors are in this category.
2. Nonstirred, aerated system: covers about 10% of bioreactors.
3. Stirred and aerated systems: about 20% of the bioreactors in industrial operation.

Nonstirred, aerated vessels are used in the process for traditional products such as wine, beer, and cheese production. Most of the newly found bioprocesses require microbial growth in an aerated and agitated system. The percentage distribution of aerated and stirred vessels for bioreactor applications is shown in [Table 6.1](#). The performances of various bioreactor systems are compared in [Table 6.2](#). Because these processes are kinetically controlled, transport phenomena are of minor importance.

Nonstirred, nonaerated vessels are used for traditional products such as wine, beer, and cheese. Most of the new products require growth of microorganisms in aerated, agitated vessels.

6.2 BIOREACTORS: BACKGROUND

The main objective of a properly designed bioreactor is to provide a controlled environment to achieve optimal growth and/or product formation in the particular cell system

TABLE 6.1 Percentage distribution of aerated and stirred vessels in bioreactor applications

Type of bioreactor application	%
Nonstirred, nonaerated	76
Nonstirred, aerated	11
Stirred, aerated	13
Total	100

TABLE 6.2 Performances of bioreactors

Concentration (kg m ⁻³)	Productive bioreactors		Wastewater treatment	
	10–50		Aerobic	Anaerobic
	Molds	bacteria/yeast	5	50
Viscosity	High	Low	Low	Low
Oxygen consumption	High	High	Low	Absent
Mass transfer	Low	High	Low	Absent
Heat production metabolic (kW m ⁻³)	3–15	3–15	0.03–0.14	Negligible
Power consumption, hp	3–15	Fewer than 5	0.02–05	Negligible

employed. Frequently the term “fermenter” is used in the literature to refer to a “bio-reactor.”^{1–3} The performance of any bioreactor depends on many functions including:

- In a growth-associated bioprocess, the biomass concentration must be high enough to achieve a high product yield.
- Sterile conditions must be maintained for a pure culture system.
- Effective agitation is required for perfect mass transfer and uniform distribution of substrate and microbes in the working volume of a bioreactor.
- Efficient heat transfer is needed to operate the bioreactor at constant temperature, as the desired optimal microbial growth temperature.
- Creation of the correct shear conditions. High shear rate may be harmful to shear-sensitive organisms and disrupt their cell wall; low shear may also be undesirable because of unwanted flocculation and aggregation of the cells, or even growth of organisms on the reactor wall and stirrer.

6.3 TYPE OF BIOREACTOR

Aerobic bioreactors are classified into four categories; division of the aerated system depends on how the gas is distributed.

- Stirred tank reactor: the most common type of bioreactor used in industry. A draught is fitted which provides a defined circulation pattern.
- Airlift pressure cycle bioreactor: the gas is circulated by means of pressurized air.
- Loop bioreactor: a modified type of airlift system in which a pump transports the air and liquid through an internal or external loop in the vessel.
- Immobilized system: the air circulates over a film of microorganisms that grows on a solid surface. In an immobilized bioreactor, particulate biocatalysts for enzyme production and conversion of penicillin to 6-aminopenicillanic acid are used.

- Fluidized bed: when packed beds are operated in an up-flow mode, the bed expands at high flow rates; channeling and clogging of the bed are avoided. Normal application is wastewater biological treatment and the production of vinegar.
- Trickle bed: another variation of the packed bed; fluid is sprayed onto the top of the packing and trickles down through the bed. Air is introduced at the base; because liquid does not flow continuously throughout the column, air moves easily around the wetted packing media. This type of bioreactor is widely used for aerobic wastewater treatment, nitrification, and denitrification for further treatment of wastewater.
- Fed-batch mixed reactor: starting with a relatively dilute solution of substrate this provides control over the substrate concentration. High organic loading rates are avoided. Fed batch is successfully used for baker's yeast production to overcome catabolite repression and to control oxygen demand. It is also used routinely for production of penicillin.
- Batch mixed reactor: There are three principal modes of bioreactor operation: (a) batch; (b) fed batch; (c) continuous.

Industrial bioreactors can easily withstand up to 3 atm positive pressure. Large fermenters are equipped with a lit vertical sight glass for inspecting the contents of the bioreactor. Side parts for pH, temperature, and dissolved oxygen sensors are the minimum requirements for monitoring the cell growth. A steam sterilization sample port is provided. Mechanical agitators are installed on the top or bottom of the tank for adequate mixing.

Choice of operating strategy has a significant effect on substrate conversion, product susceptibility to control contamination, and process reliability.

$$\text{Mass balance : } \frac{dm}{dt} = m_i - m_o + r_p - r_s \quad (6.3.1)$$

where r_p is the rate of product formation and $-r_s$ is the rate of substrate consumption. The design emphasis of this section will be on stirred tank bioreactors, which are the most common type used commercially in many bioprocess industries.

6.3.1 Airlift Bioreactors

In an airlift fermenter, mixing is accomplished without any mechanical agitation. Airlift bioreactors are used for tissue culture because the tissues are shear sensitive and normal mixing is not possible due to generation of shear forces. There are many forms of airlift bioreactors. In the usual form, air is fed into the bottom of a central draught tube through a sparger ring, thus reducing the apparent density of the liquid in the tube relative to the annular space within the bioreactor. The flow passes up through the draught tube to the head space of the bioreactor, where the excess air and the by-product, CO_2 , disengage. The degassed liquid then flows down the annular space outside the draft to the bottom of the bioreactor. Cooling can be provided by either making the draught tube an internal heat exchanger or with a heat exchanger in an external recirculation loop. The advantages of airlift bioreactors are:

1. In low shear, there is low mixing which means the bioreactor can be used for growing plant tissues and mammalian cells.
2. Because there is no agitation, sterility is well maintained.

3. In a large vessel, the height of liquid can be as high as 60 m, the pressure at the bottom of the vessel will increase the oxygen solubility, and the value of K_La will increase.
4. Extremely large vessels can be constructed. In one single cell protein plant, the reactor had a total volume of 2300 m³ (a column of 7 m diameter and 60 m height with a reactor working volume of 1560 m³). Further, in this reactor the microorganisms were grown on methanol for SCP, and the biochemical reactions resulted in an extremely large heat release. It was not possible to remove such a high exothermic heat of reaction with a conventional stirred-tank design. In applications of airlift bioreactors there are various types of fermenters. The most common bioreactors are airlift pressure cycle, internal loop, and external loop.

6.3.2 Airlift Pressure Cycle Bioreactors

The gas is circulated by means of pressurized air. In airlift bioreactors, circulation is caused by the motion of injected gas through a central tube, with fluid recirculation through the annulus between the tube and the tower or vice versa. Figure 6.1 shows an airlift bioreactor with an internal loop cycle of fluid flow.

6.3.3 Loop Bioreactor

A modified type of airlift system with gas and liquid flow patterns is a loop bioreactor in which a pump transports the air and liquid through the vessel. Here, an external loop is used, with a mechanical pump to remove the liquid. Gas and circulated liquid are injected into the

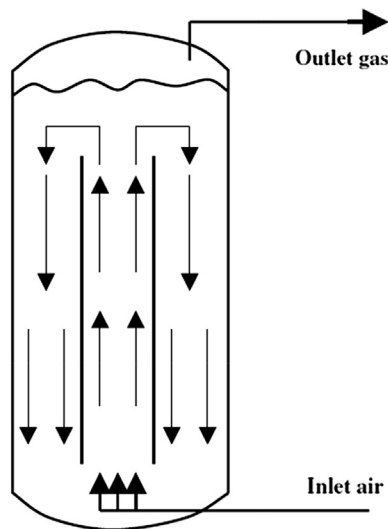


FIGURE 6.1 Gas and liquid flow pattern with internal loop cycle.

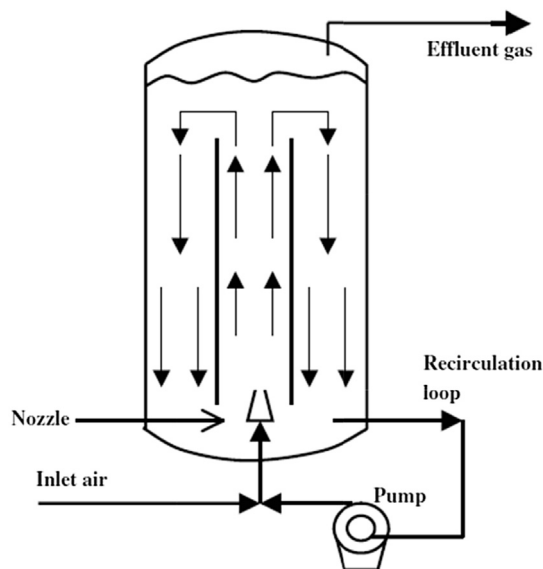


FIGURE 6.2 Airlift bioreactor with external recirculation pump.

tower through a nozzle. Figure 6.2 depicts an airlift bioreactor that operates with an external recirculation pump.

6.4 STIRRED TANK BIOREACTOR

The most important bioreactor for industrial application is the conventional mixing vessel, which has the dual advantage of low capital and low operating costs. Figure 6.3 is a schematic diagram for the stirred tank bioreactor. Vessels for laboratory experiments with volumes up to 20 l are made of glass. For larger volumes, construction is made of stainless steel. The height:diameter ratio of the vessel can vary between 2:1 and 6:1, depending largely on the amount of heat to be removed, and the stirrer may be top or bottom driven. All tanks are fitted with baffles, which prevent a large central vortex from being formed as well as improve the mixing behavior in the vessel. Four baffles are used for vessels less than 3 m in diameter, and six to eight baffles are used in larger vessels. The width of the baffle is usually between $T/10$ and $T/12$, in which T is the tank diameter.^{4,5}

Height of vessel to diameter:

$$\frac{H}{D_t} = 2 : 1 \text{ and } 6 : 1 \quad (6.4.1)$$

Diameter of vessel to baffle:

$$10 < \frac{D_t}{D_b} < 12 \quad (6.4.2)$$

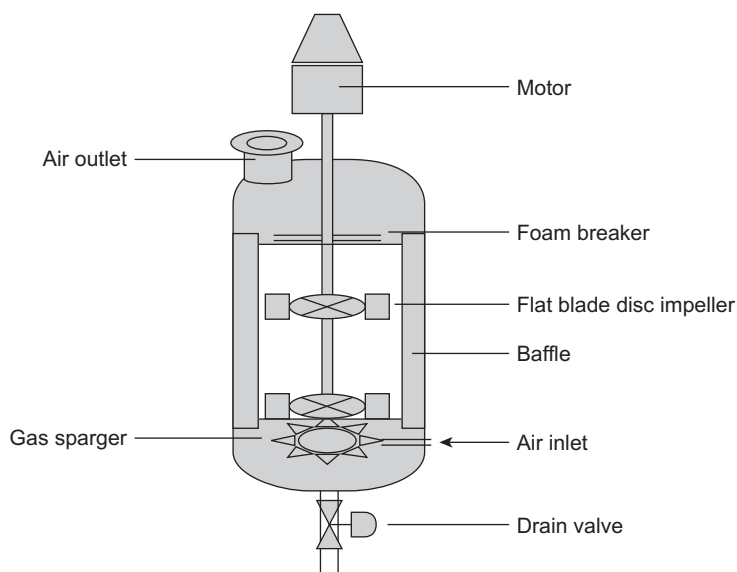


FIGURE 6.3 Stirred tank bioreactor.

The diameter of the tank, D_{tank} , is less than 3 m; four baffles of 15–20 cm may prevent formation of any central vortex. Typically, 75% of the designed reactor volume is used as working volume. In a fermentation vessel about 75% of the total CSTR volume is filled with liquid, and the remaining 25% is used for gas space. If sufficient gas space exists and foaming takes place, there is no chance for immediate contamination. If the vessel height is equal to the diameter ($H = D$), one agitator is sufficient. If the vessel height is twice the diameter ($H = 2D$) or more, additional sets of agitators should be mounted on the same shaft, separated by a defined distance. Installation of multiple sets of impellers improves mixing and mass transfer. Spargers should always be located near the bottom of the vessel with a distance $D_i/2$ below the agitator, where D_i is the diameter of the impellers. Power input per unit volume of fermentation vessel for a normal fermenter should be greater than 100 W m^{-3} , and the impeller tip speed ($\pi N D_i$) should be greater than 1.5 m s^{-1} . Let us define a dimensionless number that is known as the Froude number, Fr ; the value of the stated dimensionless number must be greater than 0.1:

$$Fr = \frac{N^2 D_i}{g} < 0.1 \quad (6.4.3)$$

High agitation and aeration cause major problems such as foaming, which may lead the fermentation vessel to unknown contamination. Antifoam and chemical agents cannot be always added for the reduction of foam: it may cause inhibitory effects on the growth of microorganisms, so the simplest devices have rakes mounted on the stirrer shaft and located on the surface of the fluid. If heat removal is a problem, as it can be in large bioreactors greater than 100 m^3 , up to 12 baffles can be used, through which coolant passes.

Careful consideration must be given to agitator design within a bioreactor because it controls the operation of the bioreactor.

The most common type of agitator used is the four-bladed disk turbine. However, research on the hydrodynamics of the system has shown that other disk turbine agitators with 12, 18, or concave blades have advantages.

Considerable research has been undertaken in gas/liquid systems with no solids present and where shear is not a problem. In systems that are shear sensitive and where solids are present, there are advantages in using an inclined bladed turbine. The number of agitators mounted on the shaft will be dependent on the height of liquid in the vessel. For specification of the correct number of agitators on the shaft, the height of liquid in the vessel should be equal to liquid height. Desired mixing with one set of agitators may occur. If the height of liquid is two or three times that of the tank diameter ($H = 2T$ or $3T$), additional agitators should be mounted on the same shaft. The sets of impellers are separated by a distance ϕ ; then $\phi = T$, where T represents tank diameter. Installation of multisets of impellers improves mixing and enhances mass transfer.

High turbulence is required for efficient mixing; this is created by the vortex field which forms behind the blades. For all the gas to flow through this region it must enter the vessel close to and preferably underneath the disk; hence it is recommended that spargers should always be placed near the impellers. The location is about a distance of $D_i/2$ below the agitator, where D_i is the impeller diameter.

The centrifugal force will draw the gas into the system, which ensures that sufficient turbulence is created. For this, a power input greater than 100 W m^{-3} is required from the agitator.⁶ Alternatively, a tip speed (πND_i) greater than 1.5 m s^{-1} or a Froude number ($N^2 D_i/g$) greater than 0.1 is often used, where N is the agitator speed in Hz, and g is gravitational acceleration in m s^{-2} .

The design of a gas inlet device is of only secondary importance for the capture and dispersal of the gas by the agitator. For efficient mass transfer, a multiple-orifice ring sparger is generally used with a gas outflow diameter of $3D_i/4$. However, it is only slightly better than a single open-pipe sparging located centrally beneath the disk.

Foaming is often a problem in large-scale aerated systems. Antifoam cannot always be added for the disappearance of foam because it may interfere with the living system and inhibit the growth of microorganisms. However, there are several mechanical methods by which the foam can be broken up. The simplest devices have rakes mounted on the stirrer shaft located on the surface of the liquid. A more sophisticated device is the "Funda-foam system," in which the foam is destroyed by centrifugal forces. The nutrient solution held in the foam flows back into the bioreactor, and the air released from the foam leaves the vessel.

There should be a minimum number of openings in the bioreactor so that sterility can be maintained. Small openings must be made leak proof with an O-ring, and larger openings fitted with gaskets. One of the most difficult areas to seal effectively is the point where the agitator shaft passes into the vessel; here a double mechanical shaft seal should be fitted. If possible the joints of all the parts connected within the sterile vessel as well as all of the pipes both inside and outside the bioreactor should be welded. There should not be any direct connection between the nonsterile and the sterile area; that is, sampling devices and injection ports must be accommodated in steam-sterilization closures. Most often, steam is applied to ensure the sterilized condition in sampling points.

6.5 BUBBLE COLUMN FERMENTER

For the production of baker's yeast, beer, and vinegar, bubble column fermenters are used. They are also often used for sufficient aeration and treatment of wastewater. In designing such a bioreactor, the height of liquid to tank diameter ($H:D$) is about 2:1, a common ratio of $H:D$ is also about 3:1; in bakers' yeast production the ratio of $H:D$ is 6:1. In bubble columns the hydrodynamics and mass transfer depend on the size of the bubbles and how they are released from the sparger. The upward liquid velocity at the center of the column, for the column diameter range 10 cm to 7.5 m ($0.1 < D < 7.5$ m), and the superficial gas velocity are in the range of $0 < u_{gas} < 0.4 \text{ m s}^{-1}$.⁷ The liquid velocity is correlated with the following equation:

$$U_{liquid} = 0.9 [g D u_{gas}]^{0.33} \quad (6.5.1)$$

The gas superficial velocity is defined as the ratio of gas flow rate to column cross-sectional area:

$$U_{gas} = \frac{Q_{gas}}{A} \quad (6.5.2)$$

The mixing time is calculated by

$$t_{mixing} = 11 \left(\frac{H}{D} \right) \left(\frac{g u_g}{D^2} \right)^{-0.33} \quad (6.5.3)$$

where H is the height of bubble column and D is the column diameter. Figure 6.4 shows a simple column with an air sparger installed at the bottom of the column which allows sufficient air to pass through the liquid.

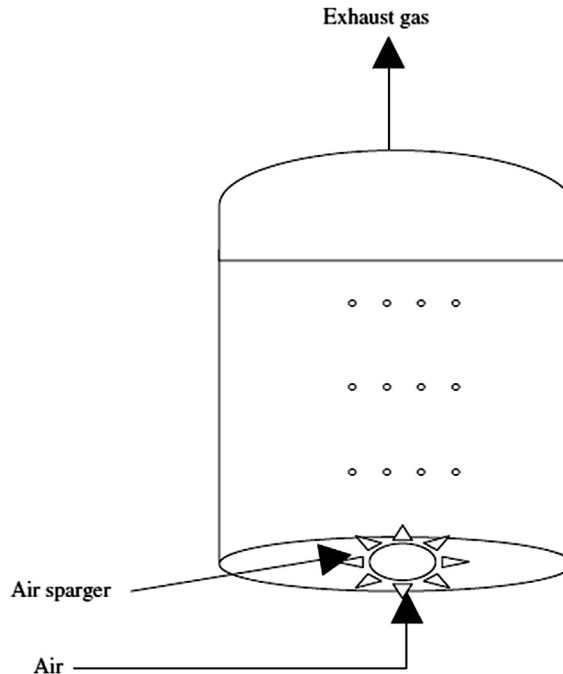


FIGURE 6.4 Bubble column bioreactor.

6.6 AIRLIFT BIOREACTORS

In an airlift fermenter, mixing is accomplished without any mechanical agitation. An airlift fermenter is used for tissue culture, because the tissues are shear sensitive and normal mixing is not possible. With the airlift, because the shear levels are significantly lower than the stirred vessels, it is suitable for tissue culture. The gas is sparged only up to the part of the vessel cross-section called the riser. Gas is held up; fluid density decreases causing liquid in the riser to move upward and the bubble-free liquid to circulate through the down-comer. The liquid circulates in airlift reactors as a result of the density difference between riser and down-comer.

There are many forms of airlift bioreactors. In the usual form, air is fed into the bottom of a central draught tube through a sparger ring, so reducing the apparent density of the liquid in the tube relative to the annular space within the bioreactor. The flow passes up through the draught tube to the head space of the bioreactor, where the excess air and the by-product, CO_2 , disengage. The degassed liquid then flows down the annular space outside the draft to the bottom of the bioreactor. In general, airlift bioreactors have the following features:

- Internal-loop vessels
- Draft tubes
- External loop or outer loop.

The cooling duty can be provided either by making the draught tube an internal heat exchanger or with a heat exchanger in an external circulation loop. The mass transfer coefficient for an external loop airlift fermenter is estimated by the following correlations⁸:

$$K_L a < 0.32 u_g^{0.7} \quad (6.6.1)$$

The height of airlift reactors is typically about 10 times the diameter of the column ($H = 10D$). For deep-shaft systems the ratio of $H:D$ is about 100. For large fermenters (500 m^3), a bubble column is an attractive choice, because it is simple and cheap to operate. The main disadvantages of airlift reactors are:

1. High capital cost for large-scale vessels.
2. High energy costs. Although an agitator is not required, a greater air throughput is necessary, and the air must be at a higher pressure, particularly on a large scale. In addition, the efficiency of gas compression is low.
3. As the microorganisms circulate through the bioreactor, the conditions change, and it is impossible to maintain consistent levels of carbon source, nutrients, and oxygen throughout the vessel.
4. The separation of gas from the liquid is not very efficient when foam is present. In the design of an airlift bioreactor, these disadvantages must be minimized. If the feed comes in at only one location, the organism would experience continuous cycles of high growth, followed by starvation. This would result in the production of undesirable by-products, low yields, and high death rates. Therefore, particularly on a large scale, multiple feed points should be used. Similarly, air should be admitted at various points up the column. However, the air must mainly enter from the bottom to circulate the fluid through the reactor.

6.7 HEAT TRANSFER

The temperature in a vessel can be controlled by removing heat by means of water circulating through a jacket on the outside of the vessel and/or by passing the water through hollow baffles situated in the vessel. With an airlift bioreactor the heat can be removed through the hollow draught tube. The rate at which heat is transferred is given by

$$Q = UA\Delta T \quad (6.7.1)$$

where Q is heat transferred in W, U is the overall heat transfer coefficient in $\text{W m}^{-2} \text{K}^{-1}$, A is the surface area for heat transfer in m^2 , and ΔT is the log mean temperature; in approximation that is the temperature difference between media and cooling water in K. The coefficient U may represent the conductivity of the system, which depends on the system geometry, fluid properties, flow velocity, wall material, and thickness. The overall resistance to heat transfer is the reciprocal of the overall heat transfer coefficient. It is defined as the sum of the individual resistances to heat transfer as heat passes from one fluid to another, and can be written as

$$\frac{1}{U} = \frac{1}{h_o} + \frac{1}{h_i} + \frac{1}{h_{of}} + \frac{1}{h_{if}} + \frac{1}{h_w} \quad (6.7.2)$$

where, h_o is the outside film coefficient, h_i is the inside film coefficient, h_{of} is the outside fouling film coefficient, h_{if} is the inside fouling film coefficient, h_w is the wall heat transfer coefficient (which is k/x), k is the thermal conductivity of the wall, and x is the wall thickness in m. The units for all film coefficients are $\text{W m}^{-2} \text{K}^{-1}$. This equation is applicable for all cases except a thick-walled tube where a correction factor must be used. The outside and inside film coefficients can be evaluated from semiempirical correlations of the form

$$Nu = k(\text{Re})^a(\text{Pr})^b \quad (6.7.3)$$

where Nu is Nusselt number, the ratio of convective to conductive heat transfer coefficients. The terms k , a , and b are constants. Re is Reynolds number, which is the ratio of inertial over viscous forces, and Pr is Prandtl number, which is the ratio of kinematic viscosity over the thermal diffusivity. The dimensionless numbers involved in the above correlation are stated as

$$Nu = \frac{hD_t}{k} \quad (6.7.4)$$

$$\text{Re} = \frac{D_i V \rho}{\mu} \quad \text{or} \quad \frac{D_i^2 N \rho}{\mu} \quad (6.7.5)$$

$$\text{Pr} = \frac{C_p \mu}{k} = \frac{\nu}{\alpha} \quad (6.7.6)$$

where D_t is the vessel diameter, D_i is the impeller diameter, all in m; ρ is the density in kg m^{-3} , μ is the viscosity in $\text{kg m}^{-1} \text{s}^{-1}$, ν the kinematic viscosity in $\text{m}^2 \text{s}^{-1}$, k is the thermal conductivity in $\text{W m}^{-1} \text{K}^{-1}$, h is the convective heat transfer coefficient in $\text{W m}^{-2} \text{K}^{-1}$, C_p is the specific heat in $\text{J kg}^{-1} \text{K}^{-1}$, α is the thermal diffusivity in $\text{m}^2 \text{s}^{-1}$, V is the velocity in m s^{-1} , and N is the impeller speed in Hz. The above equation applies to turbulent

conditions for Newtonian fluids. In stirred-tank bioreactors, normally turbulent conditions are attained. However, non-Newtonian behavior can occur, especially if polysaccharides pass into the broth. An extensive literature survey of heat transfer correlations for both Newtonian and non-Newtonian single-phase systems has been introduced by many researchers. They have shown that for holdups of less than 15%, the rates of heat transfer with gas addition are very close to the values obtained without gas addition.^{8,9} Gas holdup is defined as the volume of gas in the vessel per vessel volume, and can be calculated with the equation

$$\varepsilon = K \left(\frac{P_g}{V_L} \right)^{0.48} (v_s)^{0.4} \quad (6.7.7)$$

where P_g is power consumed by gassed liquid in W, V_L is liquid volume without gassing, v_s is the superficial gas velocity in m s^{-1} , and K is a constant. Other correlations for gas holdup are defined in the literature.^{10,11}

The calculation of heat transfer film coefficients in an airlift bioreactor is more complex, as small reactors may operate under laminar flow conditions whereas large-scale vessels operate under turbulent flow conditions. It has been found that under laminar flow conditions, the fermentation broths show non-Newtonian behavior, so the heat transfer coefficient can be evaluated with a modified form of the equation known as the Graetz–Leveque equation,⁹

$$Nu = 1.75\delta^{0.33} Gz^{0.33} \quad (6.7.8)$$

where δ is correction for non-Newtonian behavior equal to $(3n+1)/4n$, where n is the flow behavior index of power-law fluid. Gz is the Graetz number, a dimensionless number related to mass flow rate, heat capacity, and conductive heat transfer coefficient.

$$Gz = \frac{m' C_p}{kL} \quad (6.7.9)$$

where m' is the mass flow rate of fluid in the tube in kg s^{-1} , and C_p is specific heat in $\text{J kg}^{-1} \text{K}^{-1}$, k is thermal conductivity in $\text{W m}^{-1} \text{K}^{-1}$, and L is the length along the tube in m. This equation is most accurately applied in the initial stages of the bioreactor. In later stages growing *Xanthomonas campestris*, the value of the film coefficients were up to 45% lower than predicted by the Graetz–Leveque equation, because of fouling of the heat transfer surface. However, with *Aspergillus niger*, values of up to four times those predicted by the non-Newtonian form of Graetz–Leveque equation were observed. The enhancement was found to be dependent on cell concentration and morphology of the microorganisms. That was probably due to the increased turbulence of the boundary layer caused by the aggregated mycelial. The overall heat transfer coefficient is dependent on the agitation rate in the vessel, throughput of the liquid and gas in an airlift bioreactor, and the rate of circulation of cooling water in the jacket. The expected value of the overall heat transfer coefficient including all resistance for a nonfouling system should be in the range of $500\text{--}1500 \text{ W m}^{-2} \text{K}^{-1}$. In case of any problems, for instance, mammal and plant cells, which are shear sensitive the vessel side turbulence must be reduced; consequently, the heat transfer coefficient will be lowered. In such cases, the heat transfer will increase only by providing more heat transfer area. Additional effective surface area can be obtained by having a vessel with a large height:diameter

ratio, because the volume of a vessel is proportional to the height multiplied by the cross-sectional area, whereas the surface area is the external area of the vessel that is αHD , where α is the proportionality factor. Where the total heat transferred must be calculated, the power of the agitator should be included, because a considerable amount of energy is converted to heat in the vessel.

Small temperature differences, ΔT , in a bioreactor are usually easily stabilized, unless refrigerated cooling water is used; which means that the product of overall heat transfer coefficient and the heat transfer area, "UA," must be large. Therefore, the heat transfer area can be maximized by having cooling water in the baffles as well as in the jacket of the bioreactor.

6.8 DESIGN EQUATIONS FOR CSTR FERMENTER

In designing a bioreactor, material balance is used for all the streams associated with the fermentation vessel. The biomass at inlet and outlet and the generated biomass must be balanced while the fermentation proceeds. The cell balance without any cell accumulation is shown in the equation

$$F(X_0 - X) + Vr_x = 0 \quad (6.8.1)$$

where X is viable cell in the effluent stream and X_0 is viable cell in the feed stream, F is the volumetric flow rate, V is the reactor working volume, and r_x is the rate of cell formation per unit volume. The rate equation is explained in detail by a Monod rate model. The Monod rate equation is well known in microbial growth kinetics.

$$\mu = \frac{\mu_{\max} S}{K_s + S} \quad (6.8.2)$$

where μ is the specific growth rate, μ_{\max} is the maximum specific growth rate, and K_s is the Monod constant.

6.8.1 Monod Model for a Chemostat

A Monod rate model is used to demonstrate the rate of biomass generation. We neglect the cell death rate. Let us denote the ratio of biomass rate of generation to biomass concentration, r_x/X , that is, the specific growth rate; μ also denotes the dilution rate; D is defined as number of tank volumes passed through per unit time, F/V . After substitution of D and μ into Eqn (6.8.1), the following equation is obtained:

$$DX_0 = (D - \mu)X \quad (6.8.1.1)$$

Substituting specific growth rate based on the Monod rate equation into Eqn (6.8.2), the rearranging results in

$$\left(\frac{\mu_{\max} S}{K_s + S} - D \right) X + DX_0 = 0 \quad (6.8.1.2)$$

For sterile media with suitable nutrients in the absence of any organisms.

$$X_o = 0, \quad 0 = (D - \mu)X$$

Biomass generated is considered as $X \neq 0$; therefore $D - \mu = 0$.

$$D = \mu \quad (6.8.1.3)$$

At steady state, substrate utilization is balanced with a rate equation:

$$F(S_i - S) = \left(\frac{\mu_{\max} S}{K_s + S} \right) V \quad (6.8.1.4)$$

When the volume of the vessel is divided by the flow rate, retention time and dilution rate are defined in the following equation:

$$\frac{V}{F} = \tau = \frac{1}{D} \quad (6.8.1.5)$$

Plug in Eqn (6.8.1.5) to Eqn (6.8.1.4):

$$D(S_i - S) = \left(\frac{\mu_{\max} S}{K_s + S} \right) \quad (6.8.1.6)$$

Solve Eqn (6.8.1.6) for dilution rate or substrate concentration, as follows:

$$\left(\frac{\mu_{\max} S}{K_s + S} \right) = D \quad \text{or} \quad S = \frac{DK_s}{\mu_{\max} - D} \quad (6.8.1.7)$$

Material balance in terms of cell density is written as

$$\frac{d\rho_{\text{cell}}}{dt} = \frac{F}{V}(\rho_i - \rho_o) + (\mu - \alpha)\rho_{\text{cell}} \quad (6.8.1.8)$$

Under steady-state conditions, $d\rho/dt = 0$ for a sterile fermenter, inlet cell mass is zero ($\rho_i = 0$), Eqn (6.8.1.8) is simplified and reduced to dilution rate, which is similar to Eqn (6.8.1.3) above. Substrate balance may also lead to the same results as the following relations:

$$\frac{dS}{dt} = \frac{F}{V}(S_i - S) - \frac{\mu\rho_{\text{cell}}}{\text{Yield of cell}} - m\rho_{\text{cell}} - \frac{q_p\rho_{\text{cell}}}{Y_{p/s}} \quad (6.8.1.9)$$

Under steady-state conditions, where $dS/dt = 0$ and $m\rho_{\text{cell}} \ll m\rho_{\text{cell}}/Y$, Eqn (6.8.1.9) can be simplified and leads to substrate balance with growth rate:

$$D(S_o - S) = \frac{\mu\rho_{\text{cell}}}{Y} \quad (6.8.1.10)$$

For the special case when $\mu = D$, the substrate balance equation reduces to yield of substrate to cell biomass:

$$\rho_{\text{cell}} = Y(S_i - S) \quad (6.8.1.11)$$

Let us define yield factor, Y :

$$Y = \frac{\text{mass of cell formed}}{\text{mass of substrate consumed}}$$

By rearrangement of Eqn (6.8.1.11) and when yield factor is inserted, it becomes the same equation as in Eqn (6.8.1.2):

$$DX_0 + \left(\frac{\mu_{\max} S}{K_s + S} - D \right) X = 0$$

Substituting into the mass balance yields, the cell mass balance is arranged. Under steady-state conditions:

$$D(S_0 - S) = \frac{\mu_{\max} SX}{Y(K_s + S)} = 0 \quad (6.8.1.12)$$

For sterile conditions X_0 is zero, because no microbe is present in the feed stream and the feed is sterile without any contamination.

$$0 = (D - \mu)X \quad (6.8.1.13)$$

When the cell concentration is appreciable, the dilution rate must reach a specific rate ($X \neq 0, D = \mu$). The cell mass concentration is defined in Eqn (6.8.1.13) as the dilution rate approaches zero; the cell density is the product of yield and initial substrate concentration:

$$Y = \frac{X}{S_0 - S} \quad (6.8.1.14)$$

Substituting Eqn (6.8.1.7) into Eqn (6.8.1.14), the biomass concentration is defined:

$$X = Y(S_0 - S) = Y \left(S_0 - \frac{DK_s}{\mu_{\max} - D} \right) \quad (6.8.1.15)$$

As the dilution rate increases, the concentration level of final substrate will linearly increase with D , and D approaches μ_{\max} . The result of a high dilution rate would cause the cell density to drop. When $D = \mu_{\max}$, $X = 0$. This phenomenon is known as wash out.

$$D_{\max} = \frac{\mu_{\max} S_0}{K_s + S_0} = \mu_{\max} \left(1 - \sqrt{\frac{K_s}{K_s + S_0}} \right) \quad (6.8.1.16)$$

Near the wash out, the reactor is very sensitive to variations of dilution rate D . A small change in D gives a relatively large shift in X and S . The rate of cell production per unit volume of reactor is DX . These quantities are shown in Figure 6.5, where there is a sharp maximum in the curve of DX . We can compute maximal cell rate by taking the derivative of DX with respect to D , then solving the equation. The derivative of DX with respect to D is defined as

$$\frac{d(DX)}{dD} = 0 \quad (6.8.1.17)$$

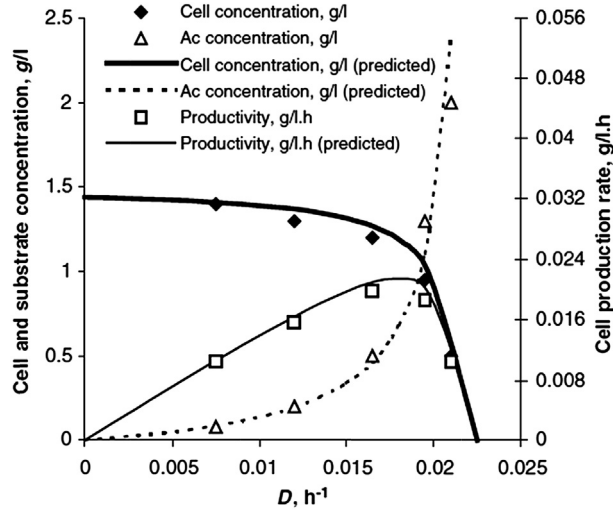


FIGURE 6.5 Effect of dilution rate on cell density, substrate concentration, and cell production rate.

$$\frac{d(XD)}{dD} = \frac{d}{dD} \left[YD \left(S_0 - \frac{DK_s}{\mu_{\max} - D} \right) \right] = 0 \quad (6.8.1.18)$$

After differentiation, the result is simplified for initial substrate concentration with respect to dilution rate:

$$S_0 - \frac{DK_s}{\mu_{\max} - D} - \frac{DK_s(\mu_{\max} - D) + D^2 K_s}{(\mu_{\max} - D)^2} = 0 \quad (6.8.1.19)$$

$$S_0 - \frac{DK_s}{\mu_{\max} - D} - \frac{DK_s \mu_{\max}}{(\mu_{\max} - D)^2} = 0$$

Rearranging Eqn (6.8.1.19) gives a second-order equation with respect to D :

$$\left(\frac{D}{\mu_{\max}} \right)^2 (S_0 + K_s) + S_0 - 2 \frac{D}{\mu_{\max}} (S_0 + K_s) = 0 \quad (6.8.1.20)$$

Solving the quadratic equation will lead to Eqn (6.8.1.21):

$$\frac{D}{\mu_{\max}} = \frac{(S_0 + K_s) \pm \sqrt{(S_0 + K_s)^2 - 4S_0(S_0 + K_s)}}{2(S_0 + K_s)} = 1 \pm \sqrt{1 - \frac{S_0}{S_0 + K_s}} \quad (6.8.1.21)$$

$$\frac{D}{\mu_{\max}} = 1 - \sqrt{\frac{K_s}{K_s + S_0}}$$

6.9 TEMPERATURE EFFECT ON RATE CONSTANT

Generally, in an equation of a chemical reaction rate, the rate constant often does not change with temperature. There are many biochemical reactions that may be influenced by temperature and the rate constant depends on temperature as well. The effect of temperature on reaction rate constant may follow Arrhenius' law. The differential form of rate constant is shown as follows:

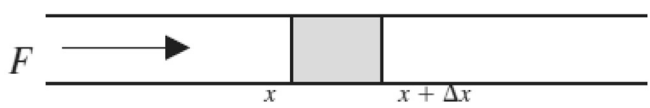
$$\frac{d \ln k}{dT} = \frac{E}{RT^2} \quad (6.9.1)$$

Integration may lead to a relation for rate constant with temperature dependency in the form of Arrhenius' law:

$$k = Ae^{-E/RT} \quad (6.9.2)$$

For a plug flow reactor, differential volume moves along the length. The following equation may express the material balance for a plug flow reactor:

dV



$$FX + dV \left(\frac{dx}{dt} \right)_{growth} = F(x + dx) \quad (6.9.3)$$

The integration may simply express the residence time for PFR:

$$t_p = \int_{x_1}^{x_2} \frac{dx}{\left(\frac{dx}{dt} \right)_{growth}} = \int_0^{x_A} \frac{dx_A}{-r_A} \quad (6.9.4)$$

$$\tau = \frac{V}{F}$$

The differentiation of Eqn (6.9.4) results in the following expression for plug and mixed flow reactors:

$$dt_p = \frac{dV}{F} = \frac{dx}{\left(\frac{dx}{dt} \right)_{growth}} \quad (6.9.5)$$

$$\text{For CSTR } \tau_{mix} = \frac{x_2 - x_1}{\left(\frac{dx}{dt} \right)_{growth}}$$

The result in Eqn (6.9.5) shows a discrete time, which is numerically used for a PFR bioreactor.

6.10 SCALE-UP OF STIRRED-TANK BIOREACTOR

A general rule, which is often applied in scale-up, is that of geometric similarity between the small and the large vessels. However, as shown in Table 6.3, the relevant parameters that affect mixing can vary widely between the two scales. The pilot scale is a base line; the parameters in the second column are given a numerical value of 1. Several strategies were used to observe the effect of design parameters on the scale-up process. The third column considers the situation with geometric similarity and where constant power per unit volume was implemented in the design calculation. The new volume is 1250 times the old volume, and the linear dimension scale-up is 5:1.

The important parameters that affect mixing and growth of a microorganism are summarized as follows:

- Oxygen transfer rate (mass transfer coefficient).
- Power per unit volume, agitation, and mixing.
- Volumetric flow rate of gas per unit volume of reactor.
- Maximum shear rate, average shear rate and mixing time, impeller tip velocity, ND_i .
- Pumping rate per unit volume, N .
- Heat transfer, Reynolds number, and surface area of the vessel.

Referring to Table 6.3, it can be seen that with geometric similarities in self controls there is no mixing variable. In practice, we would select the important criterion that needs to be controlled and then size the vessel accordingly.

Let us summarize the results of Table 6.3. In column 2, constant power per unit volume is maintained, giving larger mixing times and maximum shear rates than those in the pilot-scale vessel, but with a lower average shear rate. In column 3, a constant impeller speed and mixing time are maintained, which gives an increase in the power per unit volume of 6.25 times. This is not on scale-up as the maximum shear is also considerably increased. If constant tip

TABLE 6.3 Various parameters on scale-up using geometric similarities

Property	Pilot scale (100 l)	Constant P/volume constant	Plant-scale ND_i^2	(125,000 l) Constant ND_i	Constant N_{Re}
Power, P (hp)	1.0	15.63	7800	6.25	0.005
P/volume	1.0	1.00	6.25	0.005	4×10^{-6}
N , mixing time ⁻¹	1.0	0.48	1.00	0.005	2×10^{-3}
D_i , m	1.0	2.50	2.50	2.50	2.50
Agitator flow discharge, $Q \propto ND_i^2$	1.0	7.50	15.63	6.25	2.50
ND_i	1.0	1.20	2.50	1.00	0.40
Reynolds number $\rho ND_i^2 / \mu$	1.0	3.00	6.25	2.50	1.00
Froude number $N^2 D_i / g$	1.0	0.60	2.50	1.00	0.0003

$\omega = ND_i^2$, impeller speed (Hz); $N^2 D_i^3 \propto$ power; $ND_i \propto$ average shear rate; $N \propto$ 1/mixing time.

velocity is maintained, as shown in column 4, the power per unit volume is drastically decreased and consequently the mass transfer rate of oxygen to microorganisms. In all of these scale-up calculations, the Reynolds number is increased. In column 5, an attempt was made to maintain a constant Reynolds number, which resulted in a dramatic fall in the power requirement and an increase in mixing time. The extremely low Reynolds number caused very low agitation and low power input. This is usually not a practical situation, and generally the Reynolds number always increases in the scale-up process. The special criteria chosen for the scale-up process are based on three concepts:

- Constant power/unit volume.
- Constant gas flow rate/unit volume.
- Geometric similarity of the vessel.

These criteria have been found to give comparable growth and product rates compared with the pilot-scale operation. If we need to control maximum shear, the value of ND_i should be the same in both the pilot- and the large-scale vessels.

EXAMPLE 1

A bacterial fermentation was carried out in a reactor containing broth with average density $\bar{\rho} = 1200 \text{ kg m}^{-3}$ and viscosity 0.02 N s m^{-2} . The broth was agitated at 90 rpm and air was introduced through the sparger at a flow rate of 0.4 vvm. The fermenter was equipped with two sets of flat blade turbine impellers and four baffles. The dimensions of vessel, impellers, and baffle width were as follows:

Tank diameter, $D_t = 4 \text{ m}$;

Impeller diameter, $D_i = 2 \text{ m}$;

Baffle width, $W_b = 0.4 \text{ m}$;

Also, the liquid depth was $H = 6.5 \text{ m}$.

Determine: (a) ungassed power, P ; (b) gassed power, P_g ; (c) $K_L a$; (d) gas holdup.

Solution

Let us define the ratio of tank diameter to impeller diameter:

$$\frac{D_t}{D_i} = \frac{4}{2} = 2 \quad (\text{E.1.1})$$

Also, the ratio of the height of the liquid level to impeller diameter is:

$$\frac{H_L}{D_i} = \frac{6.5}{2} = 3.25 \quad (\text{E.1.2})$$

$$n = \frac{90 \text{ rpm}}{60} = 1.5 \text{ rps} \quad (\text{E.1.3})$$

Now define the Reynolds number:

$$N_{\text{Re}} = \frac{ND_i^2 \rho}{\mu} = \frac{(1.5)(2)^2(1200)}{0.02} = 3.6 \times 10^5 \quad (\text{E.1.4})$$

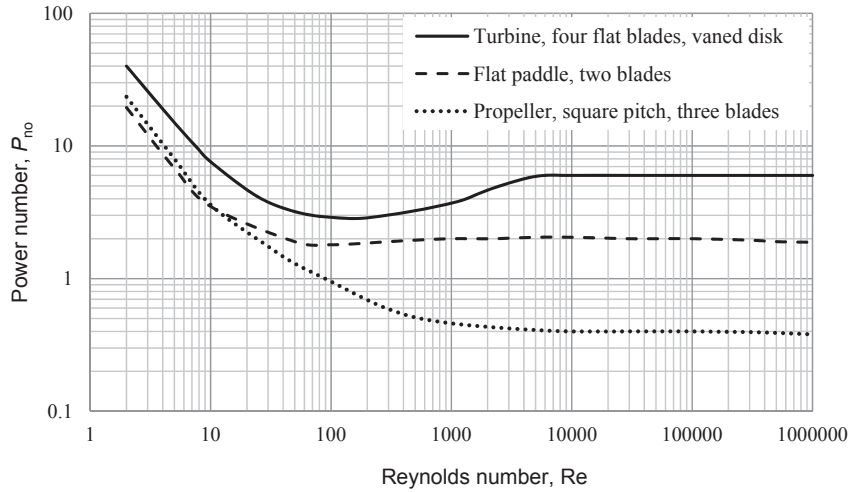


FIGURE 6.6 Power number versus Reynolds number for various impellers (flat blades, turbine, vaned disk, and marine propeller).

The Reynolds number is greater than 10^4 ; therefore, the flow is turbulent. Based on a power number defined in the turbulent regime, the power number is defined as about 6 (from Figure 6.6).

$$N_p = 6 = \frac{P g_c}{\rho N^3 D_i^5} = \frac{P \times 9.81}{(1200)(1.5)^3 (2)^5} \quad (\text{E.1.5})$$

Power is calculated as

$$P = \frac{(6)(1.5)^3 (2)^5 (1200)}{9.81} = \left(79266 \frac{\text{kg.m}}{\text{s}}\right) \left(\frac{\text{hp}}{745.7W}\right) = 106.3 \text{ hp} \quad (\text{E.1.6})$$

Correction factors are used to define actual power:

$$f_c = \sqrt{\frac{\left(\frac{D_t}{D_i}\right)^* \left(\frac{H_t}{D_i}\right)^*}{\left(\frac{D_t}{D_i}\right) \left(\frac{H_t}{D_i}\right)}} = \sqrt{\frac{2 \times 3.25}{3 \times 3}} = 0.85 \quad (\text{E.1.7})$$

For two sets of impellers with application of a correction factor, ungassed power is

$$P = (2)(0.85)(106.3) = 180.7 \text{ hp} \quad (\text{E.1.8})$$

Dimensionless aeration rate is defined as

$$N_a = \frac{F_g}{N_i D_i^3} \quad (\text{E.1.9})$$

$$F_g = 0.4(\text{volume}) = 0.4(4)^2 \left(\frac{\pi}{4}\right) (6.5) = 32.67 \frac{\text{m}^3}{\text{min}} = 0.5445 \frac{\text{m}^3}{\text{s}} \quad (\text{E.1.10})$$

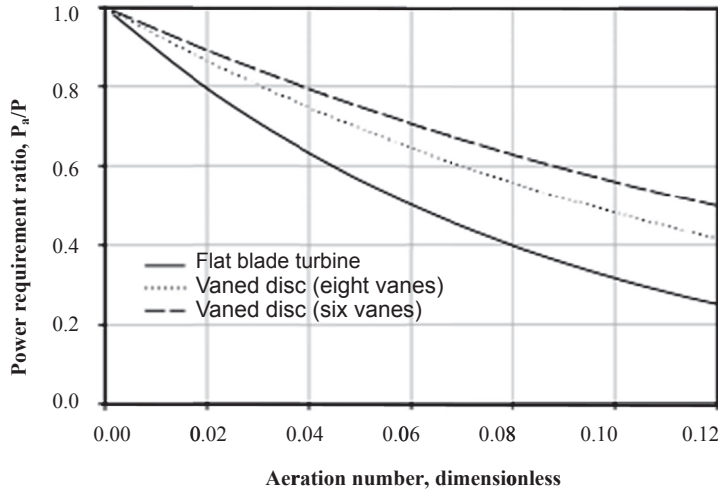


FIGURE 6.7 Ratio of power requirement for aerated versus nonaerated systems.

$$N_a = \frac{0.5445}{(1.5)(2)^3} = 4.5 \times 10^{-2} \quad (\text{E.1.11})$$

Using the plot of P_g/P versus N_a (Figure 6.7), the ratio of gassed power to ungassed power is defined.

$$\frac{P_g}{P} = 0.58 \quad (\text{E.1.12})$$

The gassed power is

$$P_g = 0.58(180.7) = 104.8 \text{ hp.}$$

The gas superficial velocity is

$$V_s = \frac{32.67}{(4)^2 \left(\frac{\pi}{4}\right)} = 2.6 \frac{\text{m}}{\text{min}} \quad (\text{E.1.13})$$

The mass transfer coefficient is defined as turbulent:

$$K_L a = 2 \times 10^{-3} \left(\frac{P_g}{V}\right)^{0.6} V_s^{0.667} = 2 \times 10^{-3} \left(\frac{104.8}{81.68}\right)^{0.6} (260 \text{ cm} \cdot \text{min}^{-1})^{0.667} = 0.095 \text{ s}^{-1} \quad (\text{E.1.14})$$

$$\text{Gas hold up, } H_o = \frac{\text{Bubble volume}}{\text{Reactor volume}} \quad (\text{E.1.15})$$

Gas holdup is defined as volume of gas per unit volume of reactor. For air in water, Richard's equation is defined as follows:

$$\left(\frac{P}{V}\right)^{0.4} (V_s)^{0.5} = 7.63H + 2.37 \quad (\text{E.1.16})$$

$$\left(\frac{180.7}{81.68}\right)^{0.4} \left(2.6 \times 60 \frac{\text{min}}{\text{h}}\right)^{0.5} = 7.63H + 2.37 \quad (\text{E.1.17})$$

$H = 1.94 \text{ m}$ for aeration.

$$H_o = \frac{V_g}{V_g + V_L} = \frac{1.94}{1.94 + 6.5} = 0.23 \quad (\text{E.1.18})$$

Gas holdup = 23%.

EXAMPLE 2

The Monod rate model is valid for a CSTR bioreactor with maximum specific growth rate of 0.5 h^{-1} and $K_s 2 \text{ g L}^{-1}$. What would be a suitable dilution rate under steady-state conditions, where there is no cell death if initial substrate concentration is 50 g L^{-1} and yield of biomass on substrate is 100%.

Solution

The Monod rate is

$$\begin{aligned} \mu &= \frac{\mu_{\max} S}{K_s + S} \rightarrow D = \frac{\mu_{\max} S}{K_s + S} \\ S_{\text{out}} &= \frac{K_s D}{\mu_{\max} - D} \\ Y_{x/s} &= 1 \\ S_0 &= 50 \text{ g L}^{-1} \end{aligned} \quad (\text{E.2.1})$$

Substrate balance:

$$-\frac{ds}{dt} = \frac{F}{V} (S_{\text{in}} - S_{\text{out}}) - \left(\frac{\mu}{Y_{x/s}}\right) X - \left(\frac{q_p}{Y_{p/x}}\right) X$$

Assume no death rate, under steady-state conditions:

$$-\frac{ds}{dt} = 0, \quad \mu = D, \quad \frac{F}{V} = D$$

Use Eqn (6.8.1.15) under steady-state conditions and rearrange to obtain DX :

$$\begin{aligned} q_p &= 0, \quad \bar{X} = Y_{x/s} (S_{\text{in}} - S_{\text{out}}) \\ D(S_{\text{in}} - S_{\text{out}}) &= \left(\frac{\mu_{\max} S}{K_s + S}\right) \left(\frac{1}{Y_{x/s}}\right) X \\ \rightarrow \bar{D} &= Y_{x/s} \left(S_0 - \frac{K_s D}{\mu_m - D}\right) \end{aligned}$$

Take derivative $d(DX)/dD = 0$ to obtain a value for maximum dilution rate:

$$D_{\max} = \mu_{\max} \left(1 - \sqrt{\frac{K_s}{K_s + S}} \right) = 0.5 \left(1 - \sqrt{\frac{2}{52}} \right) = 0.4 \text{ h}^{-1}$$

$$\frac{d(D\bar{X})}{dD} = Y_{x/s} \left(S_0 - \frac{K_s D}{\mu_m - D} \right) - \left[\frac{K_s(\mu_m - D) - K_s D}{(\mu_m - D)^2} \right] D$$

$$\text{Get } D_{\max} = \mu_{\max} \left(1 - \sqrt{\frac{K_s}{K_s + S}} \right)$$

Then calculate the substrate concentration at leaving stream:

$$S_{out} = \frac{K_s D}{\mu_{\max} - D} = \frac{2(0.4)}{0.5 - 0.4} = 8 \text{ g L}^{-1}$$

EXAMPLE 3

A 20 m³ working volume of a bioreactor is used for production of penicillin. What would be the sugar concentration (S_0) you choose if oxygen transfer rate is not the limiting reactant?

Given data:

Impeller speed = 1.5 rps (90 rpm)

Number of blades = 8; flat, turbine types of blade

$\mu = 1 \text{ mPa s}$

$\rho = 1.2 \times 10^3 \text{ kg m}^{-3}$

Aeration rate = 1 vvm

Ratio of gassed to ungassed power, $P_g/P = 0.4$

Driving force for OTR = $6 \times 10^{-3} \text{ kg m}^{-3}$

Specific O₂ uptake = 0.65 mmol O₂ per kg cell

Also, the kinetic data are given as $v_{\max} = 0.5 \text{ h}^{-1}$

Specific sugar consumption rate of cells = $1.0 \text{ kg (kg cell)}^{-1} \text{ h}^{-1}$

Solution

Given data:

$D_{\text{tank}} = 2.4 \text{ m}$

Data:

$D_{\text{tank}} = 2.4 \text{ m}$

$D_i = D_{\text{tank}}/3 = 0.8 \text{ m}$; for three sets of impellers.

Impeller speed 150 rpm; assume broth viscosity is 1 cp and the specific gravity of the broth is 1.2 (density 1200 kg m⁻³); aeration rate is 1 vvm; given ratio of gassed power to ungassed system is 0.4; specific oxygen uptake is 0.65 mmol O₂ (kg cell)⁻¹; OTR = $6 \times 10^{-3} \text{ kg m}^{-3}$.

$$D_{\text{tank}}/D_i = 3$$

$D_i = 0.8$ m, three sets of impellers are used

$$\mu = 1 \text{ mpas}$$

$$\rho = 1200 \text{ kg m}^{-3}$$

$$P_g/P = 0.4, v_{\text{max}} = 0.5 \text{ h}^{-1}.$$

Specific sugar consumption rate of cells = $1.0 \text{ kg (kg cell)}^{-1} \text{ h}^{-1}$.

Mass transfer is calculated by the empirical correlation defined for non-Newtonian filamentous fermentation:

$$K_L a = 2 \times 10^{-3} \left(\frac{P_g}{V} \right)^{0.6} V_s^{0.667}$$

$$K_L a = s^{-1}$$

$$\frac{P_g}{V} = \frac{\text{Gassed power}}{\text{volume}}; \frac{\text{hp}}{\text{m}^3}$$

$$V_s = \text{gassuperficial velocity, } \frac{\text{cm}}{\text{min}}$$

Read power number versus Reynolds number in a turbulent region is based on the geometry of the impellers. The lowest power number is less than 1, for marine propellers. For flat bladed turbines in a turbulent region, the power number is equal to 6. The power graph is illustrated in Figure 6.6.

$$N_p = 6 = \frac{P_{g_c}}{N^3 D_i^5 \rho}$$

$$\text{Ungassed power, } P = \frac{6 P N^3 D_i^5}{g_c} = \frac{6 \times 1200 \times (1.5)^3 (0.8)^5}{9.81} = 811.68 \text{ kg m s}^{-1}$$

$$P = \frac{811.68}{745.7} = 1.09 \text{ hp}$$

For three sets of impellers, $3(1.09) = 3.27 \text{ hp}$.

$$P_g = 0.4(3.27) = 1.3 \text{ hp}$$

The Correction factor for nongeometrical similarity is

$$f_c = \sqrt{\frac{\left(\frac{D_i}{D_i}\right)^* \left(\frac{H_i}{D_i}\right)^*}{\left(\frac{D_i}{D_i}\right) \left(\frac{H_i}{D_i}\right)}} = \sqrt{\frac{3 \times \frac{4.42}{0.8}}{3 \times 3}} = 1.36$$

$$P = (3 \text{ sets of impellers})(1.36)(1.09) = 4.45 \text{ hp}.$$

For the agitated and aerated vessel, the ratio of power requirements for aerated versus non-aerated systems is expressed by a dimensionless number known as the aeration rate; the value is obtained from Figure 6.7.

$$N_a = \frac{F_g}{N_i D_i^3}$$

$$N_a = \frac{0.333}{(2.5)(0.8)^3} = 0.26$$

$$F_g = 20 \text{ m}^3 \text{ min}^{-1} = 0.333 \text{ m}^3 \text{ s}^{-1}$$

$$P_g = 0.4(20.56) = 8.2 \text{ hp}$$

$$V_s = \frac{20 \text{ m}^3 \text{ min}^{-1}}{\frac{\pi}{4}(2.4)^2 \text{ m}^2} = 4.42 \text{ m min}^{-1} = 7.4 \times 10^{-2} \text{ m s}^{-1}$$

$$K_L a = 2 \times 10^{-3} \left(\frac{8.2}{20} \right)^{0.6} (442 \text{ cm.s}^{-1})^{0.667} = 6.18 \times 10^{-2} \text{ s}^{-1}$$

$$OTR = K_L a (C^* - C)$$

$$OTR = x q_{O_2} = (6.18 \times 10^{-2})(6 \times 10^{-3}) = 4.09 \times 10^{-4} \text{ kg m}^{-3} \text{ s}^{-1}$$

Maximum cell concentration, $OTR = x q_{O_2}$

$$q_{O_2} = (0.65 \times 10^{-3})(32 \times 10^{-3}) = 2.08 \times 10^{-5} \text{ kg O}_2 (\text{kg cell s})^{-1}$$

$$x_s = x = \frac{4.09 \times 10^{-4}}{2.08 \times 10^{-5}} = 19.66 \text{ kg m}^{-3}$$

$$x_s = x_0 + \frac{\mu_m}{q_s} C_s = 0 + \frac{0.5}{1.0} C_s$$

$$C_s = \frac{19.66}{0.5} = 39.33 \text{ kg m}^{-3}$$

6.11 BIOLOGICAL TRANSPORT OF OXYGEN THROUGH CELLS

Based on study, cells and their components act as biocatalysts, In fact, the biosystem operates at the Thiele module near to unity. This means that the cells are potent to operate at maximum rate without any diffusion limitations. If carbon sources as fuel supplied to the cells without oxygen limitation, the cells behave aerobically while nutrients in the presence of plenty of oxygen are utilized for energy. In the case of gas and liquid systems, mass transfer considerably increased at high concentrations of oxygen available in the vicinity of the cell. The transport of oxygen depends on the driving forces existing for oxygen concentration gradient inside and outside of the cell. The availability of oxygen depends on the solubility of oxygen in the aqueous phase like culture media. Aerobic activities and cell respiration may be related to the bulk concentration of oxygen, as the gas must diffuse through the media and reach the cell neighborhood. The respiration rate is the cell oxygen uptake for the necessary biosynthesis. The oxygen uptake may differentiate the living organisms with the

dying cells. The strict aerobes such as fungi and mold in the form of mycelia can be good evidence of the oxygen sensitivity of the cell for living. In the process of transferring a gaseous substrate such as synthesis gas, methane and oxygen; the gas must be dissolved in fermentation broth in a continuous manner for cell demands and bioconversion. In the operation of a high cell population and dense cell concentrations oxygen limitations exist due to lack of sufficient mass transfer. Such problems in large-scale fermentations for production of single cell proteins, xanthenes gum, extracellular biopolymers, and penicillin production may be serious due to insufficient oxygen transfer. One should consider the cell oxygen demand; how fast oxygen must be transferred from gas bubbles to the cell. In this case the cell may face a series of resistance before oxygen reaches the cell. This involves the effective process parameters, which are such as bubble size, temperature, hydrodynamic of the flow, cellular activities and cell density, composition of the solution, and interfacial area for mass transfer.

The concept of mass transfer in film theory is valid in biological systems. For a rising bubble, there are seven resistances involved in the process of mass transfer:

1. Diffusion of bulk oxygen to the gas–liquid interface
2. Concentration gradient of oxygen in the gas film
3. Diffusion of oxygen at the gas–liquid interface
4. Transport of oxygen through liquid film
5. Transport of oxygen through the bulk of liquid
6. Transport through the cell membrane
7. Transport inside the cell for consumption at the reaction site.

The respiratory oxygen utilization for different substrates may vary because pathways of substrate utilization for energy and anabolisms might be different. It has been reported that nutrients and various carbon sources affected the oxygen consumption rate. The oxygen demands for *Penicillium* sp. utilizing carbon sources of lactose, sucrose, and glucose were 4.9, 6.7, and 13.4 mmol (L h)^{−1}, respectively.¹² The yields of oxygen with respect to carbon source, $Y_{O_2/C}$, for methane, fats, and carbohydrate were 1.34, 1.0, and 0.4, respectively.¹³ The transported oxygen is used for growth and oxidation of organic substrates to deliver cell energy requirements for biotransformation, biosynthesis, and primary and secondary metabolites. After glucose exhaustion in living organisms, biological transformations of organic compounds are involved in energy conversion. This means that nutrients are converted to intermediate products which are used as energy sources. In the final stage, in an aerobic process, oxygen molecules are required for product formation.

6.11.1 Estimation of Mass Transfer Coefficient

Estimation of mass transfer coefficient in aerated systems with bubbles is necessary to determine the oxygen uptake rate. In an aerated system with gas bubbles, useful correlations for mass transfer coefficients were introduced in the literature. Dimensionless groups such as Reynolds number, $Re = \frac{\rho_l D u}{\mu_l}$, and Peclet number, $Pe = uD/D_{O_2}$, are commonly used for generating a useful correlation. The term “ u ” in these dimensionless groups is related to the velocity of the gas bubbles relative to liquid velocity. Specifically for gas bubble velocity,

the difference of the densities of bubble and liquid may have an influence on the increasing bubble velocity. Therefore, the Grashof number should cover the density differences. The mass transfer correlations are also related to the Grashof number, $Gr = \frac{D^3 \rho_l (\rho_l - \rho_g)}{\mu_l^2}$, and Schmidt number, $Sc = \frac{\mu_l}{\rho_l D_{O_2}}$, as Sherwood number, Sh , is a function of Gr and Sc :

$$Sh = \frac{k_l D_b}{D_{O_2}} = f(Gr, Sc) \quad (6.11.1.1)$$

where D_b is bubble diameter.

For the the case of very low Reynolds number, the special case of mass transfer for small bubbles in fermentation broth containing active agent,

$Re \ll 1$ and $Pe \gg 1$ or $Pe > 1 > Re$; $\frac{uD}{D_{O_2}} \gg 1 \gg \frac{\rho_l D u}{\mu_l}$, the proposed correlation for $Sc > 1$ is

$$Sh = Pe^{1/3} = \left(\frac{uD_b}{D_{O_2}} \right)^{1/3} \quad (6.11.1.2)$$

For sphere bubbles and small Reynolds number, the terminal velocity of a bubble is:

$$u_t = \frac{D_b^2 \Delta \rho g}{18 \mu_b} \quad (6.11.1.3)$$

Substitute u_t in the above correlation; then, regroup it for the dimensionless group. This resulted in an expression similar to that discussed in previous section. This correlation is used for a single bubble.

$$Sh = \left(\frac{D_b^3 \Delta \rho g}{18 \mu_l D_{O_2}} \right)^{1/3} = \left(\frac{D_b^3 \rho_l \Delta \rho g}{18 \mu_l^2} \right)^{1/3} \left(\frac{\mu_l}{D_{O_2}} \right)^{1/3} = 0.38 (Gr Sc)^{1/3} \quad (6.11.1.4)$$

The above correlation is grouped into Gr and Sc . As proposed earlier, the groups of Gr and Sc are known as Rayleigh number (Ra). For a single bubble, very large Reynolds number, and noncirculating spheres the correlation is

$$Sh = 2.0 + 0.6 Re^{1/2} Sc^{1/3} \quad \text{for } Re \gg 1 \quad (6.11.1.5)$$

Note that, Sherwood number varies with the square root of flow velocity. This may indicate that there should be a difference on hydrodynamic regions for Reynolds number greater than or less than unity. The mass transfer resulted in fluid in motion or hydrodynamic mixing. When a group or massive number of bubbles appears at the interface of gas and liquid, then sufficient mass transfer must occur. The mass transfer coefficient for bubbles compared to the single bubble is about 20% reduced.

Calderbank and Moo-Young¹⁴ have proposed two correlations to describe their experimental data for the absorption of soluble gas into liquid, when the gas was consumed at the liquid phase. The identification of two regions was small bubbles with critical diameter of $D_c = 2.5$ mm.

For region I, as $D < D_c$

$$Sh = 0.31 Gr^{1/3} Sc^{1/3} = 0.31 Ra^{1/3} \quad (6.11.1.6)$$

For region II as $D > D_c$

$$Sh = 0.42Gr^{1/3}Sc^{1/2} \quad (6.11.1.7)$$

Change of exponent for Sc is due to change of hydrodynamic regime. For Newtonian fluid μ is constant, independent of shear rate due to agitation speed, bubble velocity, and other fluid parameters. For changing to region II, $D > D_c$, the bubble shape changed from spherical to hemisphere or cap shape. The critical bubble diameter in a solution with surfactant from 2.5 mm changed to 7 mm. The changes for non-Newtonian fluid can be gradually observed. Mass transfer for small particles is estimated by Sherwood number ($Sh = 2$); whereas for gas oil floc the Sherwood number is defined as

$$Sh = 2 + 0.31 Ra^{1/3} \quad (6.11.1.8)$$

This means that $Sc = 1$, $\gamma = D_{O_2}$.

Maximum bubble size is a dimensionless constant times surface tension (σ) divided by dynamic pressure (τ). The relation for maximum stable bubble size and fluid flow properties is explained by a dimensionless group known as Weber number, We :

$$We = \tau \frac{D}{\sigma} \quad (6.11.1.9)$$

When $D = D_c$, the Weber number is unity for a clean air–water system $We = 1$; the dynamic pressure is $\tau = \rho_l u_t^2/2$; u_t is bubble terminal velocity. For turbulent shear stress acts on bubble size D_c resulting in the following correlation:

$$D_c = \alpha' \frac{\sigma^{0.6}}{\left(\frac{P}{V}\right)^{0.4} \rho_l^{0.2}} \quad (6.11.1.10)$$

Overall mass transfer coefficient for agitated and aerated vessels as discussed before; the mass transfer is influenced by gas terminal velocity and $\left(\frac{P}{V}\right)$. As indicated, the calculation for determination of the mass transfer coefficient is not simple because defining the $\left(\frac{P}{V}\right)$ and gas terminal velocity is also not simple. The mass transfer coefficient in a bubble column was proposed by Akita and Yoshida¹⁵, stated as follows:

$$\frac{k_l[aD_{tank}]}{D} = 0.6 Sc^{1/2} Bo^{0.62} Ga^{0.31} H^{1.1} \quad (6.11.1.11)$$

Here Bo is bond number $Bo = gD_{tank}^2 \rho_l / \sigma$ and Ga is Galileo number $Ga = gD_{tank}^3 / u_t^2$.

For tower diameter less than 60 cm the correlation is perfectly fitted whereas for tank diameter greater than 60 cm the correlation is useful.

The volumetric mass transfer coefficient for an airlift bioreactor is defined by Bello et al.¹⁶:

$$k_{la} = \frac{0.0005 \left(\frac{P}{V}\right)^{0.8}}{1 + A_d/A_r} \quad (6.11.1.12)$$

where the A_d/A_r in airlift is ratio of the area of down-comer to the area of riser. For small $P/V < 1$, the term for power per unit volume vanishes. The modified correlation is

$$k_l a = 0.12 u_l^{0.624} \left(\frac{u_g}{2u_g + 47} \right) \quad (6.11.1.13)$$

where $k_l a$ is in s^{-1} , and u_l and u_g are liquid and gas velocity in $cm\ s^{-1}$.

6.11.2 Mass Transfer in Aerated and Agitated Vessels

For aerated and agitated vessels under turbulent conditions, the correlations for mass transfer coefficients are projected by Sherwood number, which is a function of Reynolds and Schmidt numbers.

$$Sh = \frac{k_l D}{D_{O_2}} = f(Re, Sc) \quad (6.11.2.1)$$

Calderbank¹⁷ has proposed a correlation for the turbulent aeration in fermentation equipment.

$$Sh = 0.13 Sc^{\frac{1}{3}} Re^{\frac{3}{4}} \quad (6.11.2.2)$$

$$k_l = 0.13 \left(\frac{\gamma}{D_{O_2}} \right)^{1/3} (Re)^{3/4} \left(\frac{D_{O_2}}{D_b} \right) \quad (6.11.2.3)$$

Sherwood number correlated in terms of power per unit reactor volume is

$$Sh \propto \left(\frac{P}{V} \right)^{1/4} \quad (6.11.2.4)$$

The mass transfer coefficient is

$$k_l = 0.13 \left(\frac{\alpha^3 \mu_l \left(\frac{P}{V} \right)}{\rho_l D} \right)^{1/4} Sc^{-2/3} \quad (6.11.2.5)$$

EXAMPLE 4

Determine the mass transfer coefficient for an operating bioreactor: working volume is 100 L, and diameter of the vessel is 50 cm. The system is mixed by a turbine impeller with diameter of 15 cm and agitation rate of 180 rpm. The diffusivity of air through media is $0.5 \times 10^{-5} cm^2\ s^{-1}$. The air flow rate is $8\ L\ min^{-1}$. The media have a specific gravity of 1.2 and the viscosity of broth is $0.01\ g\ (cm\ s)^{-1}$. The bubble diameter is 1 mm.

Solution

Given:

$$V = 100 \text{ L}$$

$$D_{\text{tank}} = 50 \text{ cm}$$

$$H_L = 51 \text{ cm}$$

$$D_i = 15 \text{ cm}$$

$$N_i = 180 \text{ rpm} = 3 \text{ rps}$$

$$D_{O_2} = 0.5 \times 10^{-5} \text{ cm}^2 \text{ s}^{-1}$$

$$F_g = 0.5 \text{ vvm}$$

$$\mu_l = 0.01 \text{ g (cm s)}^{-1}$$

$$\rho = 1.2 \text{ g.cm}^{-3}$$

$$Re_i = \frac{\rho N_i D_i^2}{\mu_l} = \frac{(1.2)(3 \text{ rps})(15)^2}{0.01} = 8.1 \times 10^4$$

Because we know that the agitated vessel is turbulent flow, the select flat blade turbine disk type impeller for reading dimensionless power number from the illustrated graph is obtained:

Power number = six.

$$P_{no.} = \frac{Pg}{\rho_l N_i^3 D_i^5} \quad (\text{E.4.1})$$

$$P = \frac{6(1200)(3)^3(0.15)^5}{9.81} = 1.5 \text{ kg m s}^{-1}$$

As the calculated power in terms of hp is very low, for the bioreactor the select motor for mixing is 1 hp. Aeration number is defined as

$$N_a = \frac{F_g}{N_i D_i^3} \quad (\text{E.4.2})$$

$$N_a = \frac{50000 \text{ cm}^3 \text{ min}^{-1}}{180 \times 15^3 \text{ cm}^3 \text{ min}^{-1}} = 0.082$$

For flat blade turbine impellers $P_g/P = 0.6$ read off from the graph power required aerated versus nonaerated systems. If ungas power is $P = 1 \text{ hp}$, then the gas power would be $P_g = 0.6 \text{ hp}$. The gas superficial velocity is defined as gas flow rate divided by the cross-sectional area of the tank:

$$u_s = \frac{F_g}{\frac{\pi}{4}(D_t)^2} \quad (\text{E.4.3})$$

$$u_s = \frac{0.05 \text{ m}^3 \text{ min}^{-1}}{\pi(0.25)^2 \text{ m}^2} = 0.25 \text{ m min}^{-1} = 15.3 \text{ m h}^{-1}$$

For aerated and agitated vessel using Richards' data projected in gas hold correlation:

$$\left(\frac{P_g}{V}\right)^{0.4} u_s^{1/2} = 7.63H + 2.37 \quad (\text{E.4.4})$$

$$\left(\frac{0.6}{0.1}\right)^{0.4} (15.3)^{\frac{1}{2}} = 7.63H + 2.37$$

The calculated gas holdup is $H = 0.74$ as volume void fraction. Diameter of the bubble is calculated based on the following correlation:

$$D_b = \left(1.452 \times 10^{-2} \frac{\sigma}{\Delta\rho}\right)^{\frac{1}{2}} \quad (\text{E.4.5})$$

D_b is in cm, and σ is gas–liquid surface tension in dynes cm^{-1} . The surface tension of water is related to temperature as given according to the expression¹⁸

$$\sigma = 0.1232[1 - 0.00146T] \quad (\text{E.4.6})$$

where σ is N m^{-1} and T is in K. For $T = 330\text{K}$, $\sigma = 0.064 \text{ N m}^{-1}$.

$$D_b = \left(1.452 \times 10^{-2} \times \frac{64}{1198.77}\right)^{\frac{1}{2}} = 0.028 \text{ cm}$$

Now, calculate mass transfer coefficient:

$$k_l = 0.13 \left(\frac{\mu_l}{\rho_l D_{O_2}}\right)^{\frac{1}{3}} (\text{Re})^{\frac{3}{4}} \left(\frac{D_{O_2}}{D_b}\right) \quad (\text{E.4.7})$$

$$k_l = 0.13 \left(\frac{0.01}{1.2 \times 0.5 \times 10^{-5}}\right)^{\frac{1}{3}} (81000)^{0.75} \left(\frac{0.5 \times 10^{-5}}{0.028}\right) = 1.32 \text{ s}^{-1}$$

NOMENCLATURE

- r_p Rate of product formation, $\text{g L}^{-1} \text{ h}^{-1}$
 $-rs$ Rate of substrate consumption, $\text{g L}^{-1} \text{ h}^{-1}$
 Fr Froude number, dimensionless
 g gravity, m s^{-2}
 N rotational speed, Hz
 D_i Impeller diameter, m
 N_p Power number, dimensionless
 V_s Gas superficial velocity, cm min^{-1}
 N_a Dimensionless aeration rate

References

1. Demain AL, Solomon AN. *Sci Am* 1981;**245**:67.
2. Aiba S, Humphrey AE, Millis NF. *Biochemical engineering*. 2nd ed. New York: Academic Press; 1973.
3. Phaff HJ. *Sci Am* 1981;**245**:77.

4. McCabe W, Smith J, Harriott P. *Unit operations of chemical engineering*. 6th ed. New York: McGraw-Hill; 2000.
5. Wang DIC, Cooney CL, Deman AL, Dunnill P, Humphrey AE, Lilly MD. *Fermentation and enzyme technology*. New York: John Wiley & Sons; 1979.
6. Baily JE, Ollis DF. *Biochemical engineering fundamentals*. 2nd ed. New York: McGraw-Hill; 1986.
7. Doran PM. *Bioprocess engineering principles*. New York: Academic Press; 1995.
8. Scragg AH. *Bioreactor in biotechnology, a practical approach*. New York: Ellis Horwood Series in Biochemistry and Biotechnology; 1991.
9. Blakebrough N, McManamey WJ, Tart KR. *Trans Inst Chem Eng* 1978;**56**:127.
10. Shuler ML, Kargi F. *Bioprocess engineering, basic concepts*. New Jersey: Prentice Hall; 1992.
11. Ghose TK. *Bioprocess computation in biotechnology*, vol. 1. New York: Ellis Horwood Series in Biochemistry and Biotechnology; 1990.
12. Finn R. Agitation and aeration. In: *Biochemical and biological engineering science*, Vol. 1. New York: Academic Press, Inc.; 1967. p. 69–99.
13. Bailey JE, Ollis DF. *Biochemical engineering fundamentals*. 2nd ed. Chemical Engineering Education; 1986.
14. Calderbank P, Moo-Young M. The continuous phase heat and mass-transfer properties of dispersions. *Chem Eng Sci* 1961;**16**(1):39–54.
15. Akita K, Yoshida F. Bubble size, interfacial area, and liquid-phase mass transfer coefficient in bubble columns. *Ind Eng Chem Process Des Dev* 1974;**13**(1):84–91.
16. Bello RA, Robinson CW, Moo-Young M. Liquid circulation and mixing characteristics of airlift contactors. *Can J Chem Eng* 1984;**62**(5):573–7.
17. Calderbank P, editor. *Mass transfer in fermentation equipment. Biochemical and biological engineering science*, Vol. 1. New York: Academic Press Inc.; 1967. p. 102.
18. Welty JR, Wicks CE, Rorrer G, Wilson RE. *Fundamentals of momentum, heat, and mass transfer*. John Wiley & Sons; 2009.

PROBLEMS

- 6.1. A 25 m³ working volume of bioreactor is used for production of antibiotics. The oxygen is not limited in this bioprocess. The aeration rate is 1 vvm. Assume that the physical property of water can be used, e.g., viscosity of water is 1 cP.

- a. What would be the required power input?
- b. What is the oxygen transfer rate (OTR)?

Given data and useful formula:

$$P_g/P = 0.4$$

$$\text{Equilibrium concentration of oxygen} = 6 \times 10^{-3} \text{ kg/m}^3$$

$$\text{Angular velocity is 60 rpm}$$

$$\text{One hp} = 745.7 \text{ kg m/s.}$$

$$\text{CO}_2 \text{ in fact is concentration of oxygen O}_2$$

$$\text{Power no.} = 6 = \frac{P_g}{\rho N_i^3 D_i^5}$$

$$\text{OTR} = k_L \cdot a (C_{O_2}^* - C_{O_2})$$

$$k_L \cdot a = 2 \times 10^{-3} \left(\frac{P_g}{V} \right)^{0.6} V_s^{0.667}$$

$$\text{unit of mass transfer coefficient, s}^{-1}$$

$$\frac{P_g}{V}, \text{ hp m}^{-3}$$

$$V_s, \text{ cm min}^{-1}$$

- 6.2. Oxygen transport in the bioreactor is considered; an unstirred aerated Chemostat, with working volume of 1 l and 10 orifices is mounted in the bottom. Each orifice is 1 mm diameter with and air flow rate of 15 ml min⁻¹. What would be the rate of biomass growth for oxygen limiting?

Useful equations, data, and physical properties are given below:

$\mu_{\max} = 0.5 \text{ h}^{-1}$	$K_S = 0.1 \text{ mM}$	$\sigma = 72 \text{ g s}^{-2}$
$g = 980 \text{ cm s}^{-2}$	$\mu_{\text{gas}} = 2 \times 10^{-4} \text{ g (cm s)}^{-1}$	$D = 5 \times 10^{-6} \text{ cm}^2 \text{ s}^{-1}$
$\mu_{\text{liq}} = 10^{-2} \text{ g (cm s)}^{-1}$	$P_{\text{gas}} = 1.4 \text{ g L}^{-1}$	$H_L = 10 \text{ cm}$
$Y_{\text{O}_2/X} = 1 \text{ g O}_2/\text{g cell}$	$X = 1 \text{ g L}^{-1}$	$k_L \cdot a = 2 \times 10^{-3} \left(\frac{P_g}{V} \right)^{0.6} V_S^{0.667}$

Forces are balanced:

$$g\Delta\rho D_{\text{bubble}} = 6\sigma d_{\text{orifice}}$$

Rising terminal velocity of bubbles: $u_t = \frac{gD_b^2\Delta\rho}{18\mu_{\text{liq}}}$

Hint: Use the dynamic model for oxygen balance and Fick's as well. Additional data may use physical properties of water.

- 6.3. In a bioreactor, utilization of methane as substrate in the presence of oxygen on a continuous basis is given by the following cell growth rate equation, which is used for SCP production based on gaseous dual substrates:

$$r_x = \mu_{\max} \left(\frac{S_1}{K_1 + S_1} \right) \left(\frac{S_2}{K_2 + S_2} \right)$$

where S_1 substrate is oxygen and the S_2 is methane. The following data are provided:

$K_1 = K_2 = 0.5 \text{ mg L}^{-1}$, $Y_1 = 1.25 \text{ g cell (g O}_2\text{)}^{-1}$, $Y_2 = 2 \text{ g cell (g methane)}^{-1}$, $\mu_m = 0.8 \text{ h}^{-1}$.

Under washout conditions the steady-state substrate concentrations are $S_1 = 0.015$ and $S_2 = 0.007 \text{ g L}^{-1}$. Write overall mass balance for the gas and liquid system. Determine hydraulic retention time; τ for the wash out phenomena may happen at a high liquid flow rate. Assume that the system is well mixed.

- 6.4. Consider a 5 L unstirred aerated bioreactor with 10 orifices mounted in the bottom of the reactor (e.g., Biostat B). If each orifice is 1 mm in diameter and has an airflow rate of 15 mL min⁻¹, what specific cell growth rate will be maintained if oxygen is limited? Neglect cell break up and coalescence and assume that the media are sufficiently dilute; it behaves like pure water. Hint: Buoyant force is equal to the rest of the existing forces.

$\mu_{\max} = 0.5 \text{ h}^{-1}$	$K_S = 0.1 \text{ mM}$	$\sigma = 72 \text{ g s}^{-2}$
$g = 980 \text{ cm s}^{-2}$	$\mu_{\text{gas}} = 2 \times 10^{-4} \text{ g (cm s)}^{-1}$	$DD = 0.5 \times 10^{-4} \text{ cm s}^{-2}$
$H_L = 15 \text{ cm}$	$\mu_{\text{liq}} = 10^{-2} \text{ g (cm s)}^{-1}$	$X = 1.0 \text{ g cells L}^{-1}$
$\rho_{\text{gas}} = 1.4 \text{ g L}^{-1}$		$Y_{\text{O}_2/X} = 1.0 \text{ g O}_2 (\text{g cell})^{-1}$

TABLE Q.5 Batch culture data

Culture time (h)	Alcohol concentration of the broth (g L ⁻¹)
12	
15	
18	
21	
27	
33	
42	
48	
51	
54	
57	
60	
66	
72	

6.5. Given batch fermentation data for rate equation in Table Q.5. We are planning to use such data for designing a continuous bioreactor in a single vessel with a working volume of 100 L. Determine alcohol concentration in the broth when operated at a flow rate of 4 L h⁻¹.

Downstream Processing

OUTLINE

7.1 Introduction	228	7.9.2 Continuous Extraction	
7.2 Downstream Processing	228	Column Process, Rotating	
7.3 Filtration	231	Disk Contactors	240
7.3.1 Theory of Filtration	231	7.10 Adsorption	242
7.4 Centrifugation	233	7.10.1 Ion-Exchange Adsorption	242
7.4.1 Theory of Centrifugation	233	7.10.2 Langmuir Isotherm	
7.5 Sedimentation	235	Adsorption	243
7.6 Flotation	237	7.10.3 Freundlich Isotherm	
7.7 Emerging Technology for Cell		Adsorption	243
Recovery	238	7.10.4 Fixed-Bed Adsorption	243
7.8 Cell Disruption	238	7.11 Chromatography	244
7.9 Solvent Extraction	239	7.11.1 Principles of Chromatography	246
7.9.1 Product Recovery by Liquid		7.12 Crystallization Process	253
–Liquid Extraction	240	7.13 Freeze-Drying	255
		Nomenclature	255
		References	256

7.1 INTRODUCTION

Bioprocess engineering treats raw materials and generates useful products. Most bioprocesses involve one or more of the following processes: centrifugation, chromatography, cooling, crystallization, dialysis, distillation, drying, evaporation, filtration, heating, humidification, membrane separation, milling, mixing, precipitation, centrifugation, solid handling, and solvent extraction. A particular sequence of unit operations and bioprocesses is used for the manufacture of an extra pure pharmaceutical product.

Fermentation broths are complex, aqueous mixtures of cells, comprising soluble extracellular and intracellular products and any unconverted substrate or unconvertible components. Recovery, separation, purification, and extraction of products are important in bioprocess engineering. In particular, separation is a useful technique; it depends on product, its solubility, size of the process, and product value. Purification of high-value pharmaceutical products using chromatography such as hormones, antibodies, and enzymes is expensive and difficult to scale up for commercialization.¹ The necessary steps to follow a specific process depend on the nature of the product and the characteristics of the fermentation broth. There are a few steps for product recovery; the following processes are discussed, which are considered as an alternative for the product recovery from fermentation broth.

Initially, fermentation broth has to be characterized based on the viscosity of the fluid. If the presence of biomass or cells causes trouble, the biomass and cells have to be removed. If the product is stored inside the cells, the cells must be ruptured and the product must be freed. Intracellular protein can easily be precipitated, settled or filtered. In fact, the product in diluted broth may not be economical enough for efficient recovery. Enrichment of the product from the bioreactor effluents for increasing the product concentration may reduce the cost of product recovery. There are several economical methods for pure product recovery, such as crystallization of the product from the concentrated broth or liquid phase. Even small amounts of cellular proteins can be lyophilized or dried from crude solution of biological products such as hormone or enzymes.^{2,3} Advanced technology has to be implemented to reduce downstream processing costs.

7.2 DOWNSTREAM PROCESSING

In downstream processing of a fermentation unit for enzyme production with a feed stream of sugar at a concentration of 35 g l^{-1} , the expected product to be recovered is α -amylase. The concentration of enzyme is very low, about several 100 milligrams per liter in the fermentation broth. Solvent extraction is a suitable process to recover a small amount of enzyme. The chance of some enzyme being intracellular is high; therefore, cells are ruptured to liberate intracellular enzyme, which can then interact with organic solvents. [Figure 7.1](#) shows a simple diagram for a jacketed fermentation vessel for operation at constant temperature.

Bioprocess includes the bioreactor and a subsequent section for product recovery. The particular separation techniques are useful for any given bioprocess, which depends not only on the size, charge, and solubility of the product but also on the size of the process and product value. For example, various forms of gel filtration, gel chromatography, and ion exchangers are used to purify highly valuable pharmaceutical biological compounds such as

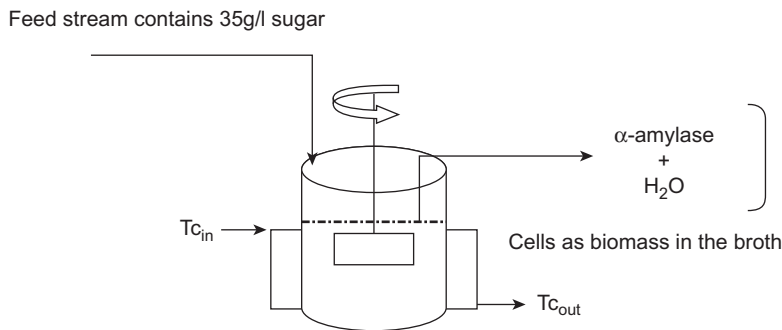


FIGURE 7.1 Schematic of jacketed fermentation vessel for enzyme production.

hormones, interferon, antibiotics, and enzymes. This chapter emphasizes product recovery from fermentation products. Our discussion on separation and purification will cover several bioprocesses, such as solvent extraction and recovery of whole or part of the microbial products. The ultimate challenge is to select the best combination of substrate, enzyme, or organism, bioreactor, and separation of the specific product. Each separation depends on initial broth characteristics such as viscosity, product concentration, impurities, and undesired particulates, and final product concentration required detail information for crystallization of the desired compound from the concentrated liquid product for the dried powder.

It is often desirable to recover product and to select a suitable strain of microorganism that produces an extracellular rather than an intracellular product. If the product stays inside the cells, the cells must be ruptured, to liberate the intracellular enzyme, after which extraction or purification is performed to recover the valuable product. The fermentation broth has to be processed and pass through several stages of separation and purification. The product requires a sequence of operations for high purification. The usual steps to follow are stated as follows:

1. Removal of insoluble particulates using various separation techniques. Common operations are filtration, centrifugation, and/or settling/sedimentation/decanting.
2. Primary isolation is done to increase product concentration. Solvent extraction, absorption, precipitation, and ultrafiltration are the best known. Ultrafiltration can discriminate at the molecular level. During primary isolation, desired product concentration increases considerably and substances of widely differing polarities are separated from the product.
3. Product purification. For production of highly pure product the impurities have to be removed for further product concentration such as chromatography and adsorption. These operations often select for impurity removal as well as further product concentration. Approaches include fractional precipitation. Other alternatives such as chromatography and adsorption are also considered as methods of process purification.
4. Final product isolation and drying of the crystallized products are carried out in drum drying, spray drying, or freeze-drying. The last steps must provide the desired product in a form suitable for final formulation and blending, or for direct shipping. Processes of centrifugation, freeze-drying/lyophilization, or organic solvent removal are commonly used.

For antibiotic production, the fermentation broth needs to be treated in a pretreatment tank to produce crude and highly purified antibiotic products. The bioprocesses involved

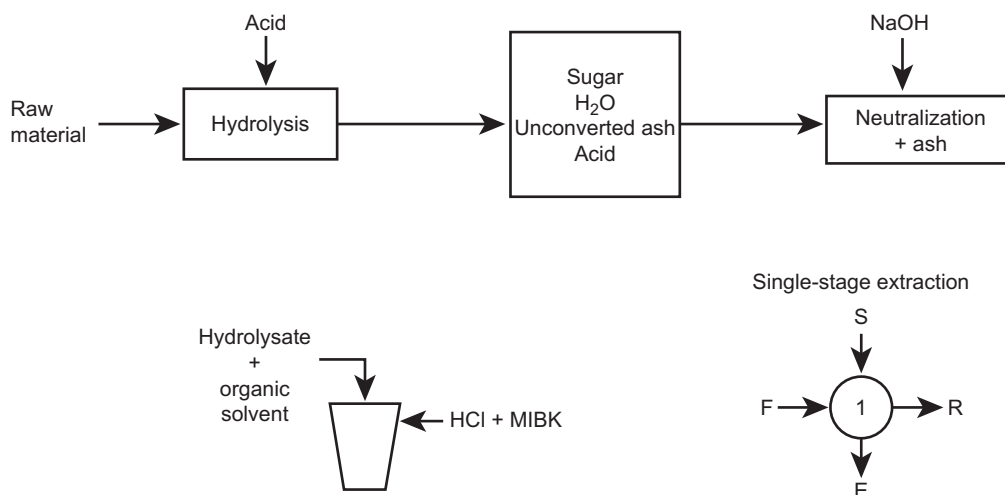
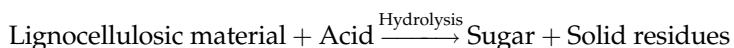


FIGURE 7.2 Acid recovery by liquid–liquid method.

in producing antibiotics are spray or continuously dried crude solids and pure solid in the form of crystalline antibiotic.

Another case of bioprocess engineering is production of an alternative and renewable fuel from agricultural wastes. Lignocellulosic materials are an abundant and renewable source of energy; in acid hydrolysis, sugar is the desired product. The acid can be neutralized by adding sodium hydroxide or any bases; the sugar may not be fermentable in the presence of salts. Solvent extraction is normally performed to recover acid and reuse/recycle acid for the hydrolysis process. Once fermentable sugar is obtained, it is useful to carry out fermentation for ethanol, organic acid, enzyme, or antibiotic production. Figures 7.2 and 7.3 show the common separation and extraction processes that are involved in purification of enzyme and fermentable sugar for the related bioprocesses.



When the fermentation broth enters the downstream units, it has high viscosity and needs pretreatment. Addition of chemicals and coagulating aids for cell flocculation such as poly- electrolytes, CaCl_2 , and colloidal clay are useful pretreatment methods to recover

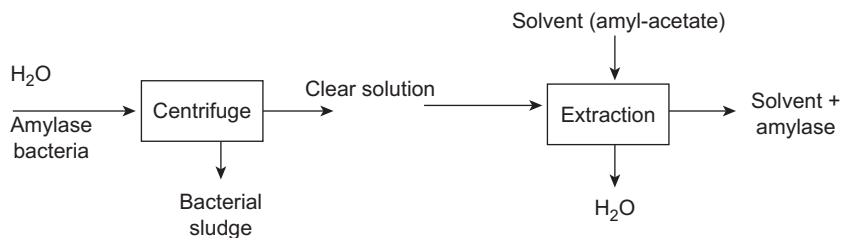


FIGURE 7.3 Centrifugation and solvent extraction for enzyme recovery from downstream.

product from downstream. Settling solids are often used in large-scale wastewater treatment processes as well as traditional fermentation industries. Generally, simple centrifugation produces a cell-concentrated stream of 15% w/v. Also, filtration produces more concentrated cell sludge of up to 20–35% w/v.⁴

7.3 FILTRATION

In filtration, solid particles are separated from a fluid–solid mixture by forcing the fluid through a filter medium or filter cloth, which retains the solid particles. As a result, solids are retained by filter media and the filtrate is obtained, which is a clear solution without any solid particles. The solid particles deposited on the filter form a layer, which is known as filter cake. The deposited solids create resistance, which reduces filter flux. The depth of the filter cake gradually increases as more solids are retained. The filter cake may create more resistance to further filtration. Filtration can be performed using either vacuum or positive-pressure equipment. The exerting differential pressure across the filter separates fluid from solid and is called the filtration pressure drop. Ease of filtration depends on particle properties and fluid filtrates. The compactions of particles are soft or hard, compressible or non-compressible, and the viscosity of the fluid may create different resistances. Fermentation broths are troublesome and hard to filter, because of the non-Newtonian behavior of the broth. Most microbial filter cakes are compressible. When the filter pores are clogged by cell bodies, then the high pressure drop results in major problems in the filtration of fermentation broth. Then more pressure is created and gradually the filtration rate drops.

Filter aids are widely used in the fermentation industry to improve the efficiency of filtration. A filter aid is a precoated filter medium to prevent blockage or blinding of the filter by solids, which would otherwise wedge themselves into the pores of the cloth. Filter aid can be added to the fermentation broth to increase the porosity of the cake as it forms. This is only recommended when the fermentation product is extracellular. Filter aids add to the cost of filtration. The minimum quantity needed to achieve the desired condition must be experimentally established. Fermentation broths can be pretreated to improve filtration characteristics. Heating may denature proteins while enhancing the filterability of mycelial broths such as in penicillin production. Alternatively, electrolytes may be added to promote coagulation of colloids into larger, denser particles, which are easier to filter. Finally, the filtration process is affected by the viscosity and composition of the broth, and the cell cake.⁵

Plate filters are suitable for filtration of batch fermentation broth; accumulated biomass must be cleaned periodically. A rotary-drum vacuum filter is used for a continuous system. This type of filter can be used for the removal of *Penicillium* and *Streptomyces* mycelia in the production of penicillin and streptomycin, respectively.⁵ In these processes, the rotary-drum filter is used with a pre-coated cloth filter with filter aid; the filter cake is removed by a knife blade that scrapes the cake from the rotating drum.

7.3.1 Theory of Filtration

Assume laminar flow of filtrate of liquid through the filter cake. The rate of filtration is usually measured as the rate at which liquid filtrate is collected. The filtration rate depends on the area of the filter cloth, the viscosity of the liquid, the pressure drop across the filter, and

filter cake resistance. At any instant during filtration, the rate of filtration is given by the following equation:

$$\frac{1}{A} \frac{dV_f}{dt} = \frac{\Delta p}{\mu_c \left[\alpha \left(\frac{W}{A} \right) + r_m \right]} \quad (7.3.1.1)$$

where A is the filter area, V_f is the volume of filtrate, t is the filtration time, ΔP is the pressure drop across the filter, μ_c is the fluid viscosity, and W is the mass of solids in the filter cake. Where W is defined as:

$$W = \text{mass of solids in the cake} = \left[\frac{\rho\omega}{1-m\omega} \right] V_f = \frac{m\omega}{1-m\omega} \quad (7.3.1.2)$$

where m is the ratio of mass of wet cake over mass of dry cake and ω is the solid mass fraction.

Also from (7.3.1.1), r_m is the filter media resistance and α is the average specific cake resistance. If the filter cake is incompressible, α is constant; for compressible cake α is defined as:

$$\alpha = \alpha'(\Delta P)^S \quad (7.3.1.3)$$

where S is cake compressibility, and α' is constant, depending on the size of particles in the cake. For incompressible solids, S is about zero; for highly compressible solids, S is about 1. For convenient integration, rewrite (7.3.1.1) in its reciprocal form:

$$A \frac{dt}{dV_f} = \mu_f \alpha \left(\frac{\rho\omega}{1-m\omega} \right) \frac{V_f}{A\Delta p} + \frac{\mu_f r}{\Delta P} \quad (7.3.1.4)$$

The separation of variables is used for suitable integrations, which result in the following equations:

$$A \int dt = \left(\frac{\mu_f \alpha \rho \omega}{1-m\omega} \right) \left(\frac{1}{A\Delta P} \right) \int V_f dV_f + \frac{\mu_f r}{\Delta P} \int dV_f \quad (7.3.1.5)$$

$$(A)(t) = \frac{\mu_f \alpha}{2A\Delta P} \left(\frac{\rho\omega}{1-m\omega} \right) V_f^2 + \left(\frac{\mu_f r}{\Delta P} \right) V_f \quad (7.3.1.6)$$

Use of an initial condition for calculation for defining integration constant at $t = 0$, $V_f = 0$, gives the integration constant as zero. By division of the above equation with V_f we can obtain a linear model, which we can plot and obtain the slope and intercepts. The modified equation after division of (7.3.1.6) is:

$$\frac{t}{V_f/A} = \frac{\mu_f \alpha \rho \omega}{2\Delta P(1-m\omega)} \cdot \frac{V_f}{A} + \frac{\mu_f r}{\Delta P} \quad (7.3.1.7)$$

Now (7.3.1.7) is linear, as $\frac{t}{V_f/A}$ versus $\frac{V_f}{A}$, the linearized model is ($y=k_1x + k_2$):

$$\frac{t}{V_f/A} = k_i \left(\frac{V_f}{A} \right) + k_2 \quad (7.3.1.8)$$

where $k_1 = \frac{\mu_c \alpha \rho \omega}{2\Delta P(1-m\omega)}$ and $k_2 = \frac{\mu_c r_m}{\Delta P}$.

The slopes of the above lines depend on physical properties of the fermentation broth such as viscosity, density, mass fraction, and pressure drop. The pH for the filtration of fermentation broth in the production of streptomycin using *Streptomyces griseus* may show an additional effect; neutralizing pH should eliminate such effect.

In general, fungal mycelia are filtered relatively easy, because mycelia filter cake has a sufficiently large porosity. Yeast and bacteria are much more difficult to handle because their small sizes can clog up the filter pores. Alternative filtration methods, which eliminate the filter cake, are becoming more acceptable for bacterial and yeast separation. Microfiltration is achieved by developing large cross-flow fluid velocities across the filter surface while the velocity vector normal to the surface is relatively small. Buildup of filter cake and problems of high cake resistances are therefore prevented. Microfiltration is not discussed in this section.

7.4 CENTRIFUGATION

Centrifugation is used to separate materials of different densities when a force greater than gravity has been implemented, such as centrifugal forces. Centrifugation may be used to remove cells from fermentation broth; yeast, for example, is harvested in a centrifuge unit. For dilute suspensions each cell may be treated as a single particle in an infinite fluid. In the concentrated fluid with suspended solids, the particle's motion is influenced by neighboring particles. A continuous process is commonly used in separation of solid particles from fermentation broth. The particle's velocity correlates with the hindered settling particles (u_h), the single particle's velocity (u_o), and the volume fraction of particles (ϵ_p). The correlation is stated as follows:

$$\frac{u_h}{u_o} = \frac{1}{1 + \beta \epsilon_p^{1/3}} \quad (7.4.1)$$

The empirical relations for β in the above equation derived for various ranges of ϵ_p are:

$$\beta = \begin{cases} 1 + 3.05\epsilon_p^{2.84} & 0.15 < \epsilon_p < 0.5, \text{ irregular particles} \\ 1 + 2.29\epsilon_p^{3.43} & 0.2 < \epsilon_p < 0.5, \text{ spherical particles} \\ 1 - 2 & \epsilon_p < 0.15, \text{ dilute suspensions} \end{cases} \quad (7.4.2)$$

Another type of centrifuge is known as a scroll conveyer centrifuge. By comparing several types of continuous centrifuges, the scroll type of centrifuge has an important feature of the decanter, which is able to handle large solid particles without any clogging. The decanter centrifuge is used for recovery of large mold pellets and the large throughput capacity of the nozzle. The settled solid is easily removed with a scroll centrifuge.

7.4.1 Theory of Centrifugation

The particle's velocity in a particular centrifuge is compared with the settling velocity that occurs under the influence of gravity and the effectiveness of centrifugation. The terminal

velocity during gravity settling of a small particle in dilute suspension is given by Stoke's law:

$$u_g = \left(\frac{\rho_p - \rho_f}{18\mu} \right) D_p^2 g \quad (7.4.1.1)$$

where u_g is the sedimentation velocity under gravity, ρ_p is the density of the particle, ρ_f is the density of the fluid, μ is the viscosity of the fluid, D_p is the diameter of the solid particle, and g is gravitational acceleration. In (7.4.1.1) the centrifugal force is implemented to obtain terminal velocity in the centrifuge:

$$u_c = \left(\frac{\rho_p - \rho_f}{18\mu} \right) D_p^2 \omega^2 r \quad (7.4.1.2)$$

where u_c is the particle velocity in the centrifuge, ω is the angular velocity of the bowl in rad s^{-1} , and r is the radius of the bowl or centrifuge drum. The ratio of velocity in the centrifuge to velocity under gravity (u_c/u_g) is called the centrifuge effect or g -number, and is denoted as Z ; therefore:

$$Z = \frac{\omega^2 r}{g} \quad (7.4.1.3)$$

The force developed in a centrifuge is Z times the force of gravity and is often expressed as so many g -forces. Industrial centrifuges have Z factors from 300 to 16,000. In a small laboratory centrifuge, Z may be up to 500,000. The particle velocity in a given centrifuge can be increased by increasing the centrifuge angular velocity (ω); by increasing the particle diameter (D_p); by increasing the density differences between particle and liquid ($\Delta\rho = \rho_p - \rho_f$); and by decreasing suspension viscosity (μ).

However, where the particles reach the walls of the bowl, the separation is also affected by the time of exposure to the centrifugal forces. In continuous flow and devices such as the disc stack centrifuge, the residence time increases by decreasing the feed flow rate. Performance of centrifuges of different size can be compared by using a parameter known as the sigma factor (Σ). For a continuous centrifuge, the sigma factor is related to the feed flow rate:

$$\Sigma = \frac{Q}{2u_g} \quad (7.4.1.4)$$

where Q is the volumetric flow rate and u_g is the terminal velocity of the particles in a gravitational field. The sigma factor physically represents the cross-sectional area of a gravity settler with the same sedimentation characteristics as the centrifuge. For two centrifuges with equal particle velocities, the performance of their effectiveness is related by their flow rate:

$$\frac{Q_1}{\Sigma_1} = \frac{Q_2}{\Sigma_2} \quad (7.4.1.5)$$

where subscripts 1 and 2 denote the two centrifuges. Equation (7.4.1.5) can be used to scale-up centrifuge equipment. The sigma factor depends on centrifuge design. Figure 7.4

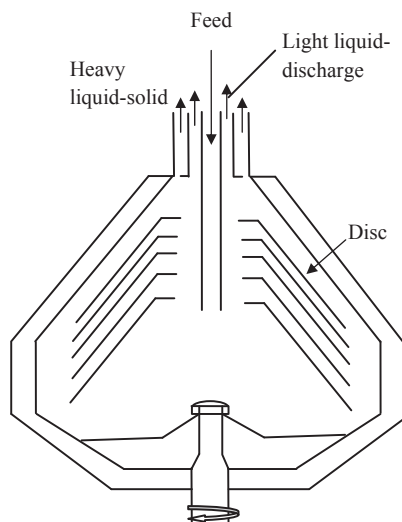


FIGURE 7.4 Disc stack bowl centrifuge for continuous separation of solids.

shows a simplified stack bowl centrifuge. For a disc-stack bowl centrifuge, Σ is defined as:

$$\Sigma = \frac{2\pi\omega^2(N-1)}{3g \tan \theta} (r_2^3 - r_1^3) \quad (7.4.1.6)$$

where ω is the angular velocity in rads s^{-1} , N is the number of discs in the stacks, r_2 is the outer radius of the disc, r_1 is the inner radius of the disc, and θ is half of the cone angle of the disc. For a tubular bowl centrifuge the above equation has to be modified.

7.5 SEDIMENTATION

When cells have a high tendency to aggregate closely (coagulate) or to form multicellular flocs with the aid of polyvalent cations or extracellular polymers, the recovery of cell biomass becomes simple and easily applicable by the sedimentation process. Such aggregation provides cell recycle streams in activate sludge wastewater treatment; and several highly flocculent yeast strains are used in brewing beer and single-cell protein production. In fact, we need to remove cells from fermentation broth, so sedimentation is considered as a downstream processing method. Alum, lime, and poly-electrolytes are commonly used to create macro-flocs. There are several natural and chemical coagulants used for aggregating suspended cells in bioprocesses. Figure 7.5 shows that cells are removed from fermentation broth and the sludge of coagulants with biomass settles as sludge. The clear solution is analysed for enzyme activity and further process purification is needed for enzyme recovery.

The nature of chemical coagulants is such that the macrofloc may possess certain charges; for example lime (CaO), alum (Al_2O_3), and flocculating polyvalent cations carry positive charges, which interact with proteins. The interactions are simply illustrated in Figure 7.6.

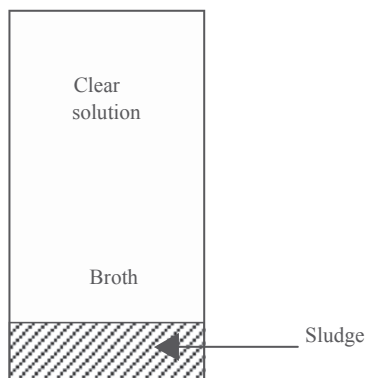
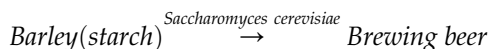


FIGURE 7.5 Sedimentation and settled sludge.

It is necessary to define settleable solids and the settling velocity. Let us take barley and use the polysaccharide content of it with a well-known yeast for brewing beer. It is ideal to use a natural settling tank to have a clear solution; we can generate bioflocs that settle down the biomass faster than usual sedimentation. Figure 7.7 shows the free-falling solid particles in a fluid. When cells have a high tendency to aggregate, with the aid of polyvalent cations, cell biomass recovery becomes possible.



In brewing beer and SCP production, several highly flocculent yeast strains are used. The special yeast strains are easily separated without the use of any expensive separation process.⁶ The settling velocity is defined by:

$$u_s = kC^{-m} \quad (7.5.1)$$

where m is an empirical constant in the range 1.7–2.6. Once the cell concentration achieves a large value, C_{\max} , further concentration occurs at a negligible rate, as seen in an activated sludge process. The relative abilities of sedimentation, centrifugation, filtration, and drying to achieve dewatering up to a desired level are important in determining which processes are appropriate. For example, centrifugation at $Z = 3000$ removes all the floc water, giving a pellet with 5% moisture; further dewatering may be required after cell lysis. Increased sedimentation rates may be possible in inclined tubes or narrow channels, leading to evolution of a clear fluid zone at the top of the channel or tube.

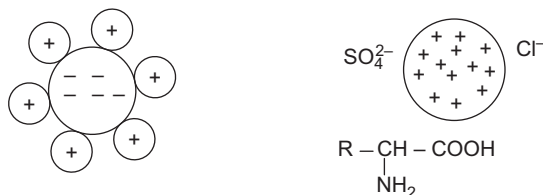


FIGURE 7.6 Floc with positive or negative charges.

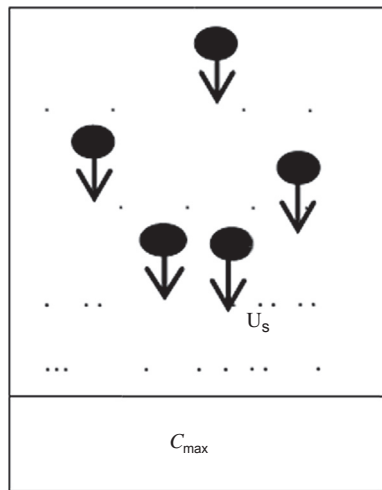


FIGURE 7.7 Solid particles with free-falling velocity.

7.6 FLOTATION

Flotation is another method to remove solid (cells) from fermentation broth, using air bubbles to float protein. We may use different kinds of high shear-force devices to make homogeneous solutions for liberating intracellular enzymes. Figure 7.8 shows several types of impeller for homogenization. Nonmechanical methods are also used to break down the cell wall and to release intracellular enzymes or proteins. Listed below are several methods that fracture cell walls and release cell content:

- Osmotic shock
- Freezing
- Solvent
- Detergents
- Based on shear forces: high-pressure homogenizer
- Manton Gaulin homogenizer works at high pressure, about 550 atm
- Lysis of cells for intracellular products
- Cell wall lysed with organic solvent extraction

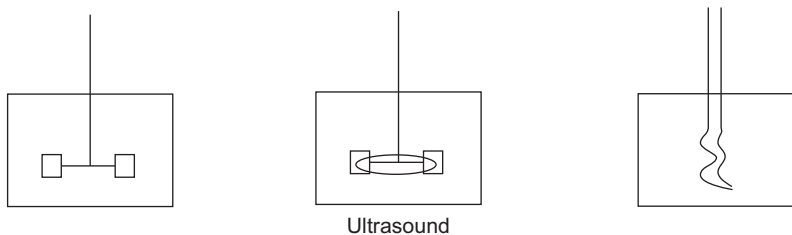


FIGURE 7.8 Various impeller shapes.

7.7 EMERGING TECHNOLOGY FOR CELL RECOVERY

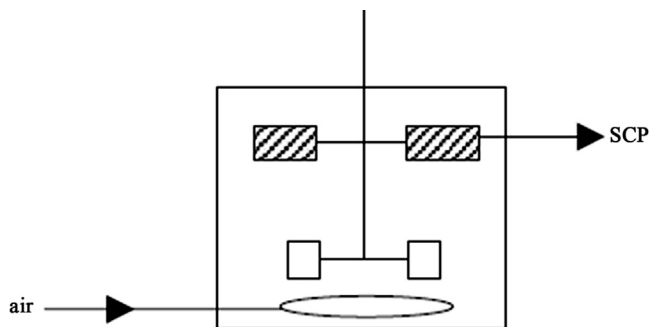
Particulates can be removed from aqueous suspension by attachment to rising air bubbles. This method is known as flotation, which is widely used for recovery of small particles from aqueous suspension minerals. This method is used in beer processing. A related technique for flotation uses air–water surface tension to strip out proteins from the broth solution and accumulate them in a high protein. English beer is prepared for cell separation by air flotation. Flotation is applied to concentrate *Acinetobacter cerificans* for production of SCP. *Acinetobacter cerificans* is a suitable microorganism used in the production of single cell protein (SCP). The synthesized protein is concentrated by aeration using the flotation method.^{7,8} Figure 7.9 shows an aeration vessel with agitation and mechanical foam breakers.

Application of charges and filtration may separate protein very efficiently. Electrokinetic deposition uses voltage gradients of 1050 V/cm to produce solid biomass with densities of up to 40% w/v.

7.8 CELL DISRUPTION

Downstream processing of fermentation broths usually begins with separation of cells by filtration or centrifugation. In centrifugation, a vertical rotor, horizontal rotor, or even disc types are used. Sedimentation and coagulation are used in downstream processing. A combination of bioprocesses is required for product recovery. Separation of products such as ethanol, citric acid, and antibiotics is extracellular but harvesting and recovery of enzymes inside the cells requires cell rupture. Cells are broken down by lysis of the cell wall. Cell disruption is used for downstream product recovery. Removal of biomass from the extracted product is necessary. The selection of a process such as filtration, batch or continuous, vacuum filtration, cross-flow, etc. is based on the nature of the product. Biomass separated from the fermentation broth is discarded or sold as a byproduct. For example, the products of recombinant proteins, which remain inside the cells, must be ruptured to release the intracellular products. Two categories of well-defined methods for cell rupturing are mechanical grinding with abrasives, high-speed agitation, high-pressure pumping, and ultrasound; and nonmechanical methods such as osmotic shock, freezing and thawing, enzymatic digestion of cell walls, and treatment with solvents and detergents.

FIGURE 7.9 Aeration vessel with foam breaker for SCP production.



A widely used technique for cell disruption is high-pressure homogenization. Shear forces generated in this treatment are sufficient to completely disrupt many types of cell. A common type is the Manton–Gaulin homogenizer.^{9,10} In this system, a high-pressure pump incorporates an adjustable valve with a restricted orifice through which the cells are forced at a pressure of up to 550 atm. The homogenizer is of general applicability for cell disruption. The homogenizing valve can become blocked when used with highly filamentous organisms. Stages involved for product recovery are:

- Lysis of cells for intracellular product recovery
- Extraction of lysed or ground cells
- Removal of unconverted soluble substrate
- Removal of biomass from extracted product
- The choice of filtration (batch, continuous vacuum, cross-flow, etc.)
- Centrifuge (vertical rotor, horizontal rotor)
- Sedimentation (and/or coagulation)

The process depends on broth conditions (temperature, pH, ionic strength), medium components, and final state of the desired product.

7.9 SOLVENT EXTRACTION

Many antibiotics have excellent solubility in organic solvents and they are water immiscible. A multistage extraction separates the aqueous phase from the organic phase. Extraction can provide concentrated and purified products.

A typical penicillin broth contains 20–35 mg l⁻¹ of antibiotic. Filtration is used to remove mycelial biomass from fermentation broth. The filtration may be subjected to filter-aided polymers. Neutralization of penicillin at pH 2–3 is required. Amyl acetate or butyl acetate is used as an organic solvent to remove most of the product from the fermentation broth. Finally, penicillin is removed as sodium penicillin salt and precipitated in a butanol–water mixture.

Extraction of penicillin from the fermentation broth is normally done using organic solvents such as butyl acetate, amyl acetate methyl isobutyl ketone, and methyl ethyl ketone (MEK). Isolation of erythromycin using pentyl or amyl acetate is another example of solvent extraction. For recovery of steroids, solvent extraction is used. Purification of vitamin B₁₂ and isolation of alkaloids such as morphine and codeine from raw plant materials are used in solvent extraction methods. Two phases are formed: the separated organic and aqueous phases. Vigorous mixing requires perfect contact of liquid phases and turbulences to facilitate solute transfer from the aqueous phase to the organic phase. However, organic solvents are undesirable for the isolation of proteins. Two phases are produced when a particular polymer plus salt are dissolved in water above certain concentrations. When biomolecules and cell fragments are distributed in the aqueous phase, one phase contains protein and cell fragments are confined to other phase. The extracted phase goes to other unit for precipitation or crystallization. The partition coefficient ($k = C_{Au}/C_{Al}$) is constant, where C_{Au} is the equilibrium concentration of component “A” in the upper phase and C_{Al} is the equilibrium concentration of “A” in the lower phase. If $k > 1$, component “A” favors the upper

phase; if $k < 1$, component “A” favors the lower phase. For effective separation in a single stage of extraction, $k \geq 3$ is required; for low k , a large volume of solute is also required. The yield is defined as the ratio solute extracted over the original amount of solute in the feed:

$$Y_u = \frac{C_{Au}}{V_o C_{Ao}} = \frac{V_u C_{Au}}{V_u C_{Au} + V_l C_{Al}} \quad (7.9.1)$$

where V_o is the original volume, V_u is the upper-phase volume, and V_l is the lower-phase volume.

7.9.1 Product Recovery by Liquid–Liquid Extraction

Solvent extraction is popular for recovery of fermentation products downstream. Antibiotics are dissolved in an organic solvent, which may be precipitated by converting antibiotic to salt form and separating it from the organic solvents. Simple alcohol (R-OH, CH₃OH, C₂H₅OH), propanol, butanol, and ketones are used in pharmaceutical industries. A simple separation funnel to show the two phases are clearly separated is shown in [Figure 7.10](#). Two sequential stages of extraction with fresh solvent are shown in [Figure 7.11](#).

$$S + F = R + E \quad (7.9.1.1)$$

7.9.2 Continuous Extraction Column Process, Rotating Disk Contactors

Organic solvents are used to extract antibiotics. The characteristics of antibiotics and product from extraction processes are summarized below:

- Water immiscible
- Multistage extraction
- Purification provides highly concentrated products.

Stages of the extraction process using fermentation broth for product recovery are listed below:

- 20–35 g l⁻¹ Antibiotic.
- Filtration: to remove mycelia with addition of polymer to get clear filtrate.

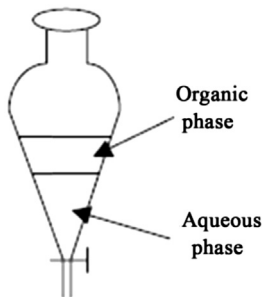


FIGURE 7.10 Single-stage extraction in a separation funnel.

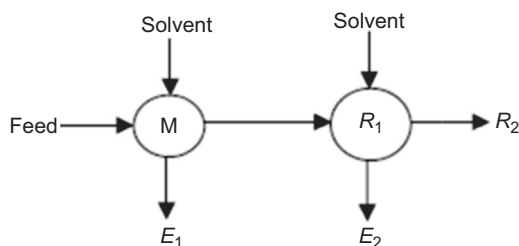


FIGURE 7.11 Sequence of single stages of extraction with fresh solvent.

- Neutralization: penicillin, pH about 2–3.
- Solvent extraction: using suitable solvent such as amyl acetate, a salt solution of penicillin is obtained.
- Precipitation of antibiotics is done with butyl acetate, an isobutyl ketone, and mineral ions such as Na^+ .
- Crystallization: solid product can easily be filtered.

Erythromycin is extracted by an organic solvent such as pentyl acetate. Similarly, steroids, vitamin B₁₂, morphine, and codeine are extracted with organic solvents. Countercurrent extraction columns are used. Figure 7.12 shows the countercurrent extraction column with a ternary diagram for material balance and equilibrium curve.

The mixture of feed and solvent has been identified as the crossing lines of material balance and tie line connecting the desired product in organic and aqueous phases.

$$M = S + F \quad \text{and} \quad M' = \frac{S}{F} \quad (7.9.2.1)$$

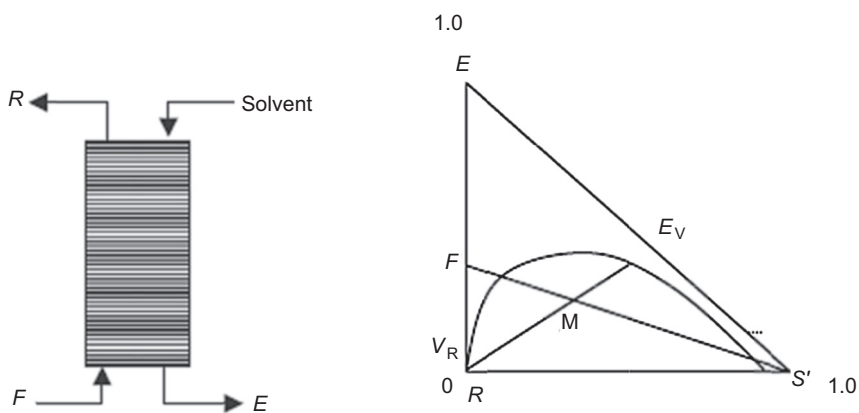


FIGURE 7.12 Countercurrent extraction column with material balance in the ternary diagram.

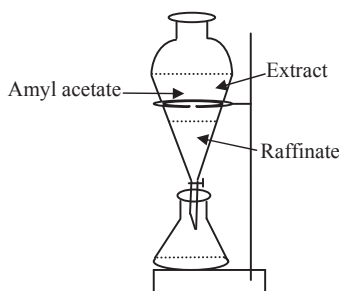


FIGURE 7.13 Separation of extract and raffinate layers.

Equilibrium data must be obtained for material balance showing raffinate and extracted phases. A simple separation funnel for single-stage extraction using amyl acetate as organic solvent is shown in Figure 7.13.

The equilibrium constant is defined by K , $K = y/x$, and the portion coefficient is also defined by K as a ratio of C_{Au}/C_{Al} , which is constant. Based on the value of K , single or multi-stage extractions are performed to do a perfect job in bioseparation.

Another parameter used to characterize two-phase partitioning is the purification factor, defined as:

$$\delta_c = \frac{\text{Concentration of product in the preferred phase}}{\text{Initial product concentration}} \quad (7.9.2.2)$$

$\delta_c = C_{Al}/C_{Ao}$, where product is shown in the lower phase, and $\delta_c = C_{Au}/C_{Ao}$, where product partitions to the upper phase. When single-stage extraction does not give sufficient recovery, repeated extraction can be carried out in a chain or cascade of contacting and separation units.

7.10 ADSORPTION

In general, adsorption is physical process as a surface phenomenon, where gas or liquid is concentrated on the surface of solid particles or fluid interfaces. There are many adsorption systems.

7.10.1 Ion-Exchange Adsorption

Adsorption beds of activated carbon for the purification of citric acid, and adsorption of organic chemicals by charcoal or porous polymers, are good examples of ion-exchange adsorption systems. Synthetic resins such as styrene, divinylbenzene, acrylamide polymers, and activated carbon are porous media with total surface area of $450\text{--}1800 \text{ m}^2 \text{ g}^{-1}$. There are a few well-known adsorption systems such as isothermal adsorption systems. The best-known adsorption model is Langmuir isotherm adsorption.

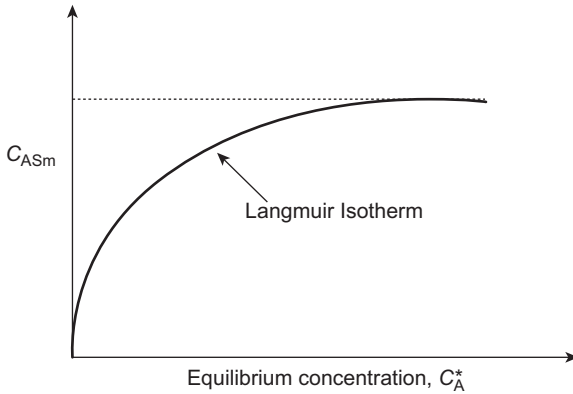


FIGURE 7.14 Langmuir isotherm adsorption model.

7.10.2 Langmuir Isotherm Adsorption

Adsorption, like extraction, depends on equilibrium relationships. Isothermal adsorption is projected by Langmuir isotherms. The model is illustrated in Figure 7.14, which is based on the linear model of the following equation:

$$C_{As}^* = \frac{C_{ASm} k_A C_A^*}{1 + k_A C_A^*} \quad (7.10.2.1)$$

where, C_{As}^* is the equilibrium concentration ($\text{kg solute kg}^{-1} \text{ solid}$) and C_{ASm} is the maximum loading of adsorbate.

7.10.3 Freundlich Isotherm Adsorption

Another useful model for isothermal adsorption is Freundlich model, which is presented by the following equation:

$$C_{As}^* = k_F C_A^{*1/n} \quad (7.10.3.1)$$

where k_F and n are constants based on the characteristics of the particular adsorption system. If adsorption is favorable, the value of n is greater than 1. For n less than 1, the adsorption process is not favourable. Figure 7.15 shows the adsorption of ion exchangers, downflow pattern. The bed has an adsorption zone with respect to time and is saturated with solute.

7.10.4 Fixed-Bed Adsorption

Fixed-bed adsorption may give a higher adsorption area per unit volume than any other type of adsorber. The point of saturation of the bed is called the breakthrough point. By knowing this point, one can determine operation schedules. In designing fixed-bed adsorber, the quantity of resin and the time required for adsorption of a given quantity of solute must be estimated.

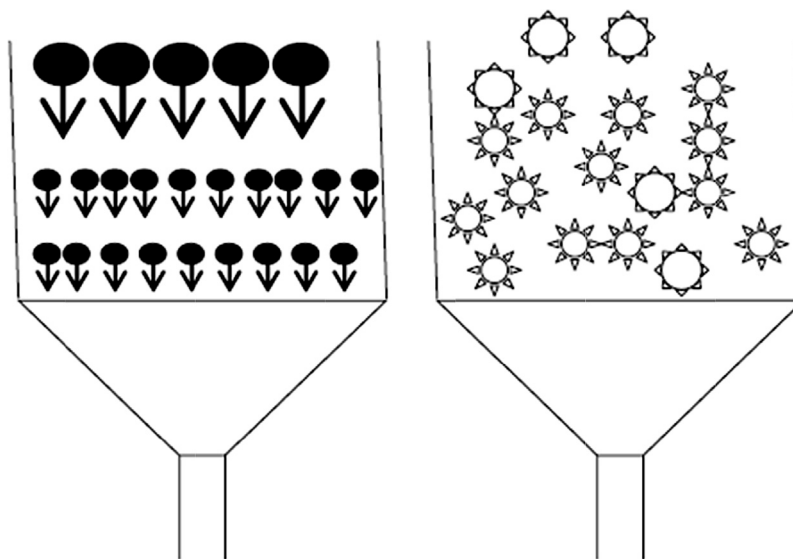


FIGURE 7.15 Ion exchange adsorption bed.

The overall rate of mass transfer from liquid to internal surface is given by the following expression:

$$\frac{\partial C_{As}}{\partial t} = \frac{K_L a}{1 - \varepsilon} (C_A - C_A^*) \quad (7.10.4.1)$$

where C_{As}^* is the concentration of “A” at equilibrium, and the void function is defined as a fractional volume—that is, the ratio of the empty space volume in the bed and the total volume $\varepsilon = (V_T - V_S)/V_T$, where V_T is the total volume and V_S the volume of resin in the packed bed.

7.11 CHROMATOGRAPHY

Chromatography is a separation procedure for resolving mixtures and isolating components. The basis of chromatography is differential migration and the selective retardation of solute molecules during passage through the bed of resin particles. The fluid carrying the solutes through the column used for elution is known as the mobile phase. The material that stays inside the column and effects the separation is called the stationary phase. In gas chromatography (GC), the mobile phase is a gas. GC is widely used as an analytical tool to separate relatively volatile components. For instance, separation of three solutes from a mixture that is injected into a column would lead to three separate peaks identified by the detectors on the outlet analysis.

Chromatography is a high-resolution technique; therefore the method is suitable for recovery of high-purity therapeutics and pharmaceuticals. Different chromatographic methods are

available for purification of proteins, amino acids, nucleic acids, alkaloids, vitamins, steroids, and many other biological materials. These methods are adsorption chromatography, partition chromatography, ion-exchange chromatography, gel chromatography, and affinity chromatography. These methods differ in the principal mechanism by which the molecules are retarded in the chromatography column. There are several distinct methods of chromatography:

- Adsorption chromatography.
- Partition chromatography.
- Ion-exchange chromatography, such as carboxy methyl cellulose (CMC), agarose, and/or dextrin.
- Gel chromatography or molecular sieve chromatography, such as polyacrylamide gels.
- Affinity chromatography, which is the binding of biomolecules with the matrix bed, often used for antibodies and antigens.

In adsorption chromatography, the bed has special characteristics to adsorb solutes. The recommended beds for adsorption chromatography are silica gel, alumina, and charcoal.

In ion-exchange chromatography, agarose, dextrose, and carboxy methyl cellulose (CMC) are used as the media beds for separation. In gel chromatography the bed is mainly molecular sieves such as polyacrylamide gels. In affinity chromatography, the separating bed is a binding biomolecular matrix that is able to attract antibodies or antigen, so there is good affinity for separating the product. The gel is defined as porous material that is cross-linked, such as dextrin agarose and polyacrylamide gel. As flow passes through the bed, differentiation and separation based on molecular size occur. The large molecules are completely trapped while small molecules move through the gel matrix. The small molecules are able to penetrate into the pore of the packed bed. The intermediate-sized molecules are separated from large and small molecules. At the end of the process, three zones are eluted with buffers for backwash to separate original samples to three proportions with molecular cut-off. The capacity of the column is given by the following equation:

$$k = \frac{V_e - V_o}{V_o} \quad (7.11.1)$$

where k is known as the capacity of the column, and the solvent volume for eluting the bed is defined with V_e ; also V_o is the void volume, the free volume, outside of the bed particles; V_i is known as internal volume of liquid in the pores of the particles; and V_s is the volume of the gel itself. These equations are normally applied for partition coefficient, ion exchange, and affinity chromatography. In gel filtration, the separation is a function of effective molecular size, elution volume, and total gel volume. The total volume of the gel column is:

$$V_{total} = V_o + V_i + V_s$$

$$V_e = V_o + k_p V_i$$

where V_e is the volume of eluting solvent, V_o is the void volume outside the particles, V_i is the internal volume of liquid in the pores of the particles, and V_s is the volume of the gel itself. For two solutes k_1 and k_2 are capacity factors for solutes 1 and 2, respectively. The relative

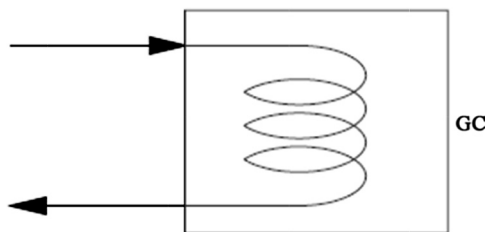


FIGURE 7.16 GC column in an insulated box.

retention, $\delta = \frac{k_2}{k_1}$, is the ratio of two capacities; also known as selectivity. Also, k_p is the gel partition coefficient, $k_p = (V_e - V_o)/V_i$, where V_i is internal volume of liquid in the pore of particles, which is defined by multiplication of “ a ” mass of dry gel with W_r :

$$V_i = aW_r = \frac{W_r \rho_g}{1 + W_r \rho_w} (V_T - V_o) \quad (7.11.2)$$

where W_r is the water regain value, that is, the volume of water taken up per mass of dry gel; ρ_g is the density of wet gel; and ρ_w is the density of water.

7.11.1 Principles of Chromatography

The basis of chromatography is in the differential migration of chemicals injected into a column. The carrier fluid takes the solutes through the bed used for elution (mobile phase). The bed is the stationary phase. Based on mobility, the retention-time detectors identify the fast- and slow-moving molecules. According to internal or external standards with defined concentration, all unknown molecules are calculated in a developed method by software. GC columns are installed in an oven that operates at a specified temperature. A diagram of an oven with a GC column is shown in [Figure 7.16](#).

Example 1

A 30-ml sample of broth from penicillin fermentation is filtered in the laboratory on a 3 cm² filter at a pressure drop of 5 psi. The filtration time is 4.5 min. Previous studies have shown that the filter cake of *Penicillium chrysogenum* is significantly compressible with $S = 0.5$. If 500 l of fermentation broth from a pilot plant have to be filtered in 1 h, what size of filter is required for pressure drops of 5, 10, and 15 psi? Neglect the resistance exerted by the filter medium.

Solution

Since the filter resistance in the filter medium is neglected, the second part of [Equation \(7.3.1.5\)](#) is neglected. Let us define a new constant, C , equal to the mass of solid deposited on the filter per volume of filtrate:

$$C = \frac{\rho \omega}{1 - m \omega} \quad (E.1.1)$$

Equations (7.3.1.5) was modified as the second part is neglected, so the filtration time per unit volume is:

$$\frac{t}{V_f} = \frac{\mu_c \alpha \rho \omega}{2\Delta P(1 - m\omega)} \frac{V_f}{A^2} \quad (\text{E.1.2})$$

The obtained equation is written with respect to pressure drop:

$$\frac{t}{V_f} = \frac{\mu_e \alpha' \Delta P^{s-1} C}{2A^2} \quad (\text{E.1.3})$$

The area for a laboratory-scale filter is calculated by:

$$\begin{aligned} \mu_e \alpha' c &= \frac{2A^2 t}{(\Delta P)^{s-1} V_f^2} \\ \mu_e \alpha' c &= \frac{2(3\text{cm}^2)^2 (4.5\text{min})}{(5\text{psi})^{0.5-1} (30\text{cm}^3)^2} \\ \mu_e \alpha' c &= 0.201 \frac{(\text{psi})^{0.5} \text{min}}{\text{cm}^2} \end{aligned}$$

The area for a pilot-scale filter is obtained according to defined pressure drop.

For a pressure drop of 5 psi, the filter area is:

$$\begin{aligned} A^2 &= \frac{\mu_e \alpha' c (\Delta P)^{s-1} V_f^2}{2t} \\ A^2 &= \frac{(0.201)(5)^{0.5-1} (500,000\text{cm}^3)^2}{120\text{min}} \\ A &= 1.37 \times 10^4 \text{cm}^2 \quad \text{or} \quad 1.37\text{m}^2 \end{aligned}$$

For pressure drop of 10 psi, the filter area is:

$$\begin{aligned} A^2 &= \frac{\mu_e \alpha' c (\Delta P)^{s-1} V_f^2}{2t} \\ &= \frac{(0.20125)(10)^{0.5-1} (500,000\text{cm}^3)^2}{120\text{min}} \\ A &= 1.15 \times 10^4 \text{cm}^2 \quad \text{or} \quad 1.15\text{m}^2 \end{aligned}$$

The value for area A for a pressure drop of 15 psi is reduced: A .

$$\begin{aligned} &\frac{(0.20125)(15)^{0.5-1} (500,000\text{cm}^3)^2}{120\text{min}} \\ &= 1.04\text{m}^2 \end{aligned}$$

Having a differential pressure in the above filtration process, and increasing the pressure drop from 5 to 10 and then 15 psi, the filter area was reduced by 19 and 11%, respectively. One of the main reasons why an increase in the pressure drop results in less filter area may be due to compression of the filter cake and the porosity of the filter.

Example 2

Filtration of 300 ml of fermentation broth was carried out in a laboratory-sized filter with a pressure drop of 10 psi. The filtration took 20 min. Based on previous studies, the filter cake obtained from *Penicillium chrysogenum* was compressible with the exponent “ s ” in the equation for calculation of filter area equal to 0.5.

1. What size of filter is required to carry out filtration of 1 m³ broth from a pilot plant in 20 h and at a pressure drop of 20 psi?
2. What is the percentage increase in filter area if the pressure drop is reduced to 10 psi?

Solution

$$\frac{t}{V_f} = \frac{\mu\alpha c}{2A^2\Delta P} \cdot V_f = \frac{\mu\alpha'c\Delta P^{s-1}}{2A^2} \cdot V_f$$

$$\alpha = \alpha'\Delta P^s$$

$$\mu\alpha'c = \frac{2A^2t}{(\Delta P)^{s-1}V_f^2} = \frac{2(10)^2(20)}{(10)^{0.5-1}(300)^2} = 0.1405$$

$$A = \left[\frac{(\mu\alpha'c)\Delta P^{-0.5}V_f^2}{2t} \right]^{1/2} = \left[\frac{(\mu\alpha'c)\Delta P^{-0.5}}{2t} \right] V_f$$

$$= \left[\frac{0.1405(20)^{-0.5}}{2 \times 2 \times 60} \right]^{1/2} (10^6 \text{ cm}^3) = 1.14 \times 10^4 \text{ cm}^2 = 1.14 \text{ m}^2$$

$$\frac{A_1}{A_2} = \left[\left(\frac{\Delta P_1}{\Delta P_2} \right)^{-0.5} \right]^{1/2} = \left(\frac{1}{2} \right)^{-0.25} = 1.189 \quad (\text{E.2.1})$$

An 18.9% increase in the area of the filter was obtained.

$$\frac{A_1}{A_2} = \frac{(\mu\alpha'c/2t)_1^{0.5} \left[(20)^{-0.5} \right]^{1/2}}{(\mu\alpha'c/2t)_2^{0.5} \left[(20)^{-0.5} \right]^{1/2}} = \frac{0.473}{0.56} = 0.84$$

$$A_2 = \frac{A_1}{0.84} = \frac{1.14}{0.84} = 1.356 \text{ m}^2 \quad (\text{E.2.2})$$

The ratio of $\frac{A_2}{A_1} = \frac{1.356}{1.14} = 1.189$, which is approximately an increase in filter surface area of 19%.

Example 3

In a batch production of penicillin, 40 m³ capacity of the plant, sterile air is required to be supplied. The bioreactor requires 1 vvm (volume of air/volume of broth. min). The incoming air contains 3000 cells m⁻³ of air, for 100 h operation. Calculate the depth of filter, if the penetration of bacteria is one in one million.

Solution

Assume $D_{\text{filter}} = 60$ cm, based on availability of filter air flow rate,

$$F_{\text{air}} = (40 \text{ m}^3)(1 \text{ vvm})(60 \text{ min h}^{-1}) = 2400 \text{ m}^3 \text{ h}^{-1}$$

$$\text{Microbial load} = (3000 \text{ cells/m}^3)(2400) = 7.2 \times 10^8 \text{ cells}$$

$$\text{Cross-sectional area of filter, } A = (\pi/4)(0.6)^2 = 0.028 \text{ m}^2$$

$$\text{Air velocity} = (2400)/(0.028) = 8488 \text{ m h}^{-1}$$

$$N_t = N_o e^{-kt} \quad (\text{E.3.1})$$

$$\ln(N_1/N_2) = kL \quad (\text{E.3.2})$$

$$\ln[(7.2 \times 10^8)/(10^{-6})] = kL$$

$$N_1 = 7.2 \times 10^8 \text{ cells}$$

$$N_2 = 1 \text{ cell in } 10^6 \text{ cells} = 10^{-6} \text{ cells}$$

where L represents the length of filter, and k is the rate constant based on filter bed material = 84.

$$L = (1/k) \ln 7.2 \times 10^{14} = (1/84) \ln 7.2 \times 10^{14} = 0.4 \text{ m}$$

Example 4

Microbial cells are separated from a culture broth at a flow rate of $3.35 \times 10^{-3} \text{ m}^3 \text{ s}^{-1}$. Assume the cells are spherical with average diameter of 1 μm . Select a centrifuge that can perform this separation. Given data: $\rho_{\text{cell}} = 1.1 \rho_{\text{water}}$, $\rho_{\text{water}} = 997 \text{ kg m}^{-3}$ at 25 °C; $\rho_{\text{broth}} = 3\rho_{\text{water}}$, and the viscosity of water is $0.9 \times 10^{-3} \text{ N.s.m}^{-2}$.

Solution

$$Z = \frac{\omega^2 r}{g} \quad (\text{E.4.1})$$

$$u_c = \left(\frac{\rho_p - \rho_g}{18\mu} \right) D_p^2 \omega^2 r = Zu \quad (\text{E.4.2})$$

$$x = u_c t = Zu_g \left(\frac{V}{F} \right) \quad (\text{E.4.3})$$

$$\frac{VZ}{x} = \frac{F}{u_g} = S$$

$$S = \frac{F}{u_g} = \frac{F(18\mu)}{D_p^2(\rho_{cell} - \rho_{water})}$$

$$S = \frac{(3.35 \times 10^{-3} m^3/s)(18 \times 0.9 \times 10^{-3} \times 3N \cdot s/m^2) \left(\frac{Kg \cdot m}{N \cdot s^2} \right)}{(1 \times 10^{-6} m)^2 (1.1 - 1)(997 Kg/m^3)(9.81 m/s^2)} = 1.65 \times 10^5 m^2$$

$$S = 2\Sigma$$

$$\Sigma = 83250 m^2 \quad (E.4.4)$$

Example 5

Microbial cell recovery is carried out in a continuous disc-stack centrifuge. The centrifuge is operated at 5000 rpm for separation of baker's yeast. At a feed rate of 60 l min^{-1} , 50% of the cells are recovered. At constant speed, solid recovery is inversely proportional to flow rate.

1. What flow rate is required to recover 90% of cells if the centrifuge speed is fixed at 5000 rpm?
2. What operating speed is required to recover 90% of cells if the flow rate in the centrifuge is maintained at 60 l min^{-1} ?

Solution

$$\frac{S_1\%}{S_2\%} = \frac{Q_2}{Q_1}, \quad Q_2 = 33.33 \text{ l min}^{-1}$$

$$\frac{Q_2}{Q_1} \frac{\Sigma_2}{\Sigma_1} = \frac{\omega_2^2}{\omega_1^2} = \frac{(5000)^2}{\omega_1^2} = \frac{60}{33.33}$$

$$\omega_2 = 6708 \text{ rpm} \quad (E.5.1)$$

When we need to remove cells from fermentation broth, sedimentation is considered as a downstream processing method. Alum, lime, and polyelectrolyte are commonly used.

Example 6

Enzyme Recovery Using Aqueous-Phase Extraction

Extraction for enzyme recovery is a common process. A polyethylene glycol–dextrose mixture is used to recover α -amylase from the fermentation broth. Given a partition coefficient of 4.2, calculate the maximum enzyme recovery when:

$$(a) \quad \frac{V_u}{V_1} = 5 \quad (E.6.1)$$

$$(b) \quad \frac{V_u}{V_1} = 0.5 \quad (\text{E.6.2.})$$

Solution

$$Y_u = \frac{V_u C_{Au}}{V_u C_{Au} + V_1 C_{A1}} = \frac{V_u}{V_u + V_1 \left(\frac{C_{A1}}{C_{Au}} \right)} = \frac{V_u}{V_u + (V_1/K)} \quad (\text{E.6.3})$$

Define K :

$$K = \frac{C_{Au}}{C_{A1}}$$

$$(a) \quad Y_u = \frac{V_u/V_1}{\frac{V_u}{V_1} + \frac{1}{K}} = \frac{5}{5 + \frac{1}{4.2}} = 0.95 \quad \text{or} \quad 0.95\% \text{ yield}$$

$$(b) \quad Y_u = \frac{0.5}{0.5 + \frac{1}{4.2}} = 0.68$$

The yield for a lower value of upper-phase volume was 68%. Increase in the relative volume of the extracting phase enhanced the recovery.

Example 7

Antibody Recovery by the Adsorption Method

Cell-free fermentation broth contains $8 \times 10^{-5} \text{ mol l}^{-1}$ immunoglobulin C. Ninety percent of antibody is recovered by adsorption on nonpolar resin:

$$C_{As}^* = 5.5 \times 10^{-5} C_A^{0.35} \quad (\text{E.7.1})$$

where C_{As}^* is solute adsorbed/ cm^3 and C_A^* is the liquid-phase solute concentration in mol/l . What is the minimum quantity of resin required to treat 2 m^3 of broth in a single-stage tank? The minimum quantity of resin required when 90% recovery of immunoglobulin occurs at equilibrium.

The rest is $0.1 \times 8 \times 10^{-5} = 8 \times 10^{-6} \text{ mol l}^{-1} = C_A^*$

$$\begin{aligned} C_{As}^* &= 5.5 \times 10^{-5} (8 \times 10^{-6})^{0.35} \\ &= 9.05 \times 10^{-7} \text{ mol.cm}^{-3} \end{aligned} \quad (\text{E.7.2})$$

This is the resin capacity. Amount of antibody adsorbed is:

$$0.9(8 \times 10^{-5} \text{ mol/l})(2 \text{ m}^3 \times 1000 \text{ l/m}^3) = 1.44 \times 10^{-1} \text{ mol} \quad (\text{E.7.3})$$

The volume of resin required is.

$$\frac{0.144 \text{ mol}}{9.05 \times 10^{-7} \frac{\text{mol}}{\text{cm}^3}} = 1.59 \times 10^5 \text{ cm}^3 \approx 0.16 \text{ m}^3 \quad \text{resin required} \quad (\text{E.7.4})$$

Example 8***Hormone Separation in Gel Filtration***

Gel chromatography is used for hormone separation. A pilot-plant scale gel chromatography column packed with Sephadex, G-25 (Sigma–Aldrich) is used to separate two hormones, A and B. The column is 5 cm in diameter and 35 cm in height; the void volume is 40% of the total column volume, water retained by gel bed $w_r = 3 \times 10^{-3} \text{ m}^3 \text{ kg}^{-1}$ dry Sephadex, density of wet gel $\rho_g = 1.25 \times 10^3 \text{ kg m}^{-3}$. The partition coefficients are $k_{PA} = 0.38$ and $k_{PB} = 0.15$. If the eluting flow rate is 0.7 l h^{-1} , what are the retention times for hormones A and B?

Solution

$$V_T = \pi r^2 h = \pi (2.5 \times 10^{-2} \text{ m})^2 (0.35 \text{ m}) = 6.87 \times 10^{-4} \text{ m}^3$$

Use Equation (7.11.2):

$$V_i = \frac{(3 \times 10^{-3} \text{ m}^3/\text{kg})(1.25 \times 10^3 \text{ kg/m}^3)}{1 + (3 \times 10^{-3}) \times 1000} \times (0.6 \times 6.87 \times 10^{-4}) = 3.86 \times 10^{-4} \text{ m}^3$$

$$V_{eA} = V_0 + K_{PA} V_i = (0.4)(6.87 \times 10^{-4}) + 0.38(3.86 \times 10^{-4}) = 4.215 \times 10^{-4} \text{ m}^3$$

$$V_{eB} = V_0 + K_{PB} V_i = (0.4)(6.87 \times 10^{-4}) + 0.15(3.86 \times 10^{-4}) = 3.33 \times 10^{-4} \text{ m}^3$$

$$\tau_A = \frac{4.215 \times 10^{-4} \text{ m}^3}{\left(\frac{0.7\text{l}}{\text{h}}\right)\left(\frac{\text{m}^3}{1000\text{L}}\right)\left(\frac{\text{h}}{60\text{min}}\right)} = 36 \text{ min}$$

$$\tau_B = \frac{3.33 \times 10^{-4} \text{ m}^3}{\left(\frac{0.7\text{l}}{\text{h}}\right)\left(\frac{\text{m}^3}{1000\text{L}}\right)\left(\frac{\text{h}}{60\text{min}}\right)} = 28.5 \text{ min} \quad (\text{E.8.1})$$

Example 9***Cell Filtration of Fermentation Broth***

A shake-flask broth was filtered with a filtration unit and all the process conditions and variables are defined in the following table.

Process Variables	Values
Filter area, A	10 cm^2
Viscosity, μ_c	2 cp
Pressure drop, DP	0.3 atm
Density, ρ	1.1 g cm^{-3}
Solid mass fraction, v	0.001
Ratio of masses of wet cake over dry cake, m	2.5

1. Evaluate the specific cake concentration, α , and the resistance coefficient, r , of the filter, for two different filtration times and volumes of filtration solution $[t(s), V(\text{ml})] = [(30, 38), (60, 52)]$.
2. What size filter would be needed to process 100 m^3 broth in 10 min?

Solution

1. Using the filtration Equation (7.3.1.7):

$$\begin{aligned}\frac{t}{V_f/A} &= \frac{\mu_c \alpha \rho V_f w}{2\Delta P(1 - mw)A} + \frac{\mu_c r}{\Delta P} \\ \frac{t}{V_f/10\text{cm}^2} &= \frac{(2 \times 10^{-2} \text{g/cm.s})\alpha(1.1)(0.001)V_f}{2(0.3\text{atm})(1 - 2.5 \times 0.001)10\text{cm}^2} + \frac{(2 \times 10^{-2} \text{g/cm.s})r}{0.3\text{atm}} \\ \frac{t}{V_f} &= \frac{2.2 \times 10^{-7}}{0.5985} \times V_f \alpha + 6.67 \times 10^{-3} r \\ \frac{30}{38} &= 0.79 = 1.4 \times 10^{-5} \alpha + 6.67 \times 10^{-3} r \\ \Rightarrow \alpha &= 7 \times 10^4 \frac{\text{atm.s}^2.\text{cm}^2}{\text{g}^2} \\ \Rightarrow r &= -\frac{0.187}{6.67} \times 10^3 \\ \frac{60}{52} &= 1.15 = 1.91 \times 10^{-5} \alpha + 6.67 \times 10^{-3} r \quad (\text{E.9.1})\end{aligned}$$

2. Scale-up calculation:

$$\frac{t}{V_f/A} = \frac{\mu_c \alpha \rho V_f w}{2\Delta P(1 - mw)A} + \frac{\mu_c r}{\Delta P}$$

7.12 CRYSTALLIZATION PROCESS

In all crystallization processes at a supersaturated condition, both nucleation and crystal particles are formed. This means crystal at first must form and then grow. As the crystal is introduced, nucleation occurs. Crystallization and nucleation were developed on the basis of an extremely pure solution for nucleus formation. There are five identified sources of nucleation that may be considered in industrial crystallization units:

1. Homogeneous nucleation
2. Heterogeneous nucleation
3. Attrition
4. Contact nucleation
5. Seeding

Generally, homogeneous and heterogeneous nucleation occur in ultra-pure solutions at a highly supersaturated condition; while seeding is a surrogate form of nucleation. In attrition,

small crystalline particles are formed; the identifiable fine crystalline matter is separated and returned to the body of solids as discrete particles. Their presence may increase the level of mechanical energy input into the crystallization system. The crystallization rate is reduced to a very low-value product, decreased size as particles are separated from the existing solids. Attrition can occur even whether or not supersaturation condition is present.

Crystallization can be analyzed from the point of view of purity, yield energy, supersaturation, rate of nucleation, and growth. In formation of crystals, two steps are taking place:

1. Nucleation, that is, formation of new crystal; even called seeding
2. Growth of macroscopic size of fine crystals

The driving potential is the supersaturation condition, which may be generated by the solubility of solute with increasing temperature by introducing salts and organic substances; the saturated condition becomes supersaturated by cooling and reduction of temperature. Evaporating a proportion of solvent and cooling may assist the process easily to reach to supersaturated condition. When solubility is very high, a supersaturated condition may be generated by the addition of a third component. The added component may act with solvent to reduce the solubility of the solute. Such a process is called salting; it may create precipitation of the solute in the aqueous phase and crystalline products are formed.

There are differences between supersaturated solutions for growing crystals and the solution at equilibrium with solute, shown as:

$$\Delta y = y - y_s$$

$$\Delta C = C - C_s$$

$$\Delta C = \rho y - \rho_s y_s = \rho \Delta y$$

where Δy is the difference in mole fraction of the solute in solution and saturation point. The y and y_s are the mole fractions of solute in solution and the saturation point, respectively. If the difference between ρ and ρ_s is negligible, then the concentration ratio is:

$$\alpha = \frac{C}{C_s} = 1 + \frac{\Delta y}{y_s}$$

$$N = k_m e^{-\Delta E_n/RT}$$

The number of crystals per unit length (mm), $\frac{dN}{dL}$ *numbers*/*mm* is:

$$n = \lim_{\Delta L \rightarrow 0} \frac{\Delta N}{\Delta L}$$

where N is number of crystals, L is the unit length of crystals (mm), and ΔE_n is the activation energy.

$$n = n_0 e^{-L/RT}$$

The crystal growth rate, G (mm h⁻¹); $\Delta L = G\Delta t$; retention time $\tau = V/Q$.

$$-\frac{dn}{dL} = \frac{nQ}{GV_c}$$

where, Q is volumetric flow rate, V_c is the total volume of liquid in the crystallizer, and Δt is the time interval involved in formation of each crystal. Separation variables; then integration with initial point n_0 at $L = 0$

$$-\frac{dn}{n} = \frac{1}{G\tau} dL; \text{ resulted in } \ln \frac{n_0}{n} = \frac{L}{G\tau}; n = n_0 e^{-L/G\tau}; \text{ nucleation rate is defined.}$$

The quantity $L/G\tau$ is dimensionless; can be introduced as dimensionless length.

7.13 FREEZE-DRYING

Cells are not crystallized, but the by-products of cells for purified state are crystallized. Antibiotics and many pharmaceutical products are in crystal form. An alternative method for determination of cell dry weight is to remove intercellular and intracellular water; such a method is freeze-drying or lyophilization of cells. The known volume of sample culture is placed in a pre-weighed freeze-drying flask, which is rapidly frozen under vacuum refrigeration. The flask is connected to a vacuum pump. The frozen water is directly vaporized from solid to vapor phase under vacuum condition. The flask after drying is weighed. Then, the cell dry weight can be determined. This method avoids heat decomposition of cells, especially plant cells and filamentous fungi. The cell dry weight is determined for a culture grown on simple media. However, complex media may contain appreciable amount of solids, such as the media, cell debris, dead cells, and living cells. The freeze-dried cells are still in living condition and can be viable if the culture is hydrated; therefore, cells are stored at lyophilized condition. In fact, protein and any biological products are very heat sensitive; a drying process such as lyophilization is recommended. Since microorganisms are stored and dried for easy transportation, the only condition for returning them back to living condition is hydration of the lyophilized culture. The lyophilized cell samples are in a pure state and sterile condition. One can transfer the lyophilized culture in front of flame by sterile loop, or hydrate it with sterile media for propagation, viable activities, and live in sterilized media after proper incubation.

NOMENCLATURE

- r_m Filter media resistance
- a Average specific cake resistance
- m Ratio of mass of wet cake over mass of dry cake
- ω Solid mass fraction
- A Filter area, m^2
- V_f Volume of filtrate, ml
- t Filtration time, min
- τ Retention time, min
- ΔP pressure drop across the filter, Pa
- μ_c Fluid viscosity, cP
- W Mass of solids in the filter cake, kg
- u_h Hindered settling particles, $m\ s^{-1}$
- u_o Particles velocity, $m\ s^{-1}$
- v_p Volume fraction of particles
- u_g Sedimentation velocity, $m\ s^{-1}$
- u_c Particle velocity in the centrifuge, $m\ s^{-1}$

- r_p Density of particle, kg m^{-3}
 r_f Density of fluid, kg m^{-3}
 μ Viscosity of fluid, cP
 D_p Diameter of solid particle, mm
 g Gravitational acceleration, m s^{-2}
 ω Angular velocity of the bowl, rad s^{-1}
 Q Volumetric flow rate, ml h^{-1}
 u_g Terminal velocity of the particles, m s^{-1}
 Σ Performance of centrifuge, sigma factor
 N Number of discs in stacks of centrifuge
 r_1, r_2 Inner and outer radius of the discs, cm
 θ Half of the cone angle of the disc
 C_{As}^* Equilibrium concentration ($\text{kg solute kg solid}^{-1}$)
 C_{ASm} Maximum loading of adsorbate, g l^{-1}
 C_{Au} Equilibrium concentration of A in upper phase, g l^{-1}
 C_{Al} Equilibrium concentration of A in lower phase, g l^{-1}
 V_o Original volume, ml
 V_u Upper phase volume, ml
 V_l Lower phase volume, ml
 W_r Water regain value, g
 ρ_g Density of wet gel, kg m^{-3}
 ρ_w Density of water, kg m^{-3}
 V_T Total volume, m^3
 V_S Volume of resin, m^3
 C_A^* Concentration of A at equilibrium, g l^{-1}
 Δy Difference in mole fraction of the solute in solution and saturation point
 y Mole fractions of solute in solution
 y_s Mole fraction at saturation point
 E_n Activation energy
 α Concentration ratio
 N The number of crystals per unit length
 L Length, mm
 G Crystal growth rate, mm h^{-1}
 Q Volumetric flow rate, $\text{m}^3 \text{h}^{-1}$
 V_c Total volume of liquid in the crystallizer, m^3
 Δt Time interval involved in formation of each crystal, min
 n Population density of crystals

References

1. Aiba S, Humphrey AE, Millis NF. *Biochemical engineering*. 2nd ed. New York: Academic Press; 1973.
2. Baily JE, Ollis DF. *Biochemical engineering fundamentals*. 2nd ed. New York: McGraw-Hill; 1986.
3. Bradford MM. *Anal Biochem* 1976;**72**:248.
4. Doran PM. *Bioprocess engineering principles*. New York: Academic Press; 1995.
5. Dominguez M, Mejia A, Gonzalez JB. *J Biosci Bioeng* 2000;**89**:409.
6. Najafpour GD, Klasson KT, Ackerson MD, Clausen EC, Gaddy JL. *Biores Technol* 1994;**48**:65.
7. Driessen FM, Ubbels J, Stadhouders J. *Biotech Bioengng* 1977;**19**:821.
8. Stanbury PF, Whitaker A. *Principles of fermentation technology*. Oxford: Pergamon Press; 1984.
9. Shuler ML, Kargi F. *Bioprocess engineering, basic concepts*. New Jersey: Prentice Hall; 1992.
10. Pelczar Jr MJ, Chan ECS, Krieg NR. *Microbiology*. 6th ed. New York: McGraw-Hill; 1993.

Immobilization of Microbial Cells for the Production of Organic Acid and Ethanol

OUTLINE

8.1 Introduction	259	8.6.1 Introduction	267
8.2 Immobilized Microbial Cells	260	8.6.2 Materials and Methods	268
8.2.1 Carrier Binding	261	8.6.2.1 Experimental Reactor System	268
8.2.2 Entrapment	261	8.6.2.2 Determination of Glucose Concentration	270
8.2.3 Cross-Linking	262	8.6.2.3 Detection of Ethanol	271
8.2.4 Advantages and Disadvantages of Immobilized Cells	262	8.6.2.4 Yeast Cell Dry Weight and Optical Density	271
8.3 ICR Experiments	263	8.6.2.5 Electronic Microscopic Scanning of Immobilized Cells	271
8.4 ICR Rate Model	263	8.6.2.6 Statistical Analysis	271
Nomenclature	266	8.6.3 Results and Discussion	272
References	266	8.6.3.1 Evaluation of Immobilized Cells	272
8.6 Case Study: Ethanol Fermentation in an Immobilized Cell Reactor Using <i>Saccharomyces cerevisiae</i>	267	8.6.3.2 Batch Fermentation	278

8.6.3.3 <i>Relative Activity</i>	278	8.7.1 Immobilization of Microorganisms by Covalent Bonds	284
8.6.3.4 <i>Reactor Setup</i>	279		
8.6.3.5 <i>Effect of High Concentration of Substrate on Immobilized Cells</i>	279	8.7.2 Oxygen Transfer to Immobilized Microorganisms	284
8.6.4 Conclusion	281	8.7.3 Substrate Transfer to Immobilized Microorganisms	285
Nomenclature	282	8.7.4 Growth and Colony Formation of Immobilized Microorganisms	286
Acknowledgment	282	8.7.5 Immobilized Systems for Ethanol Production	288
References	282	Reference	289
8.7 Fundamentals of Immobilization Technology, and Mathematical Model for ICR Performance	284		

SUBCHAPTER

8.1

Introduction

Microorganisms are biocatalysts actively used in the fermentation process where product and biomass are obtained from fermentable sugars. The cells are harvested and reused. The immobilization of cells has been practiced in the production of vinegar. Enzymes and whole cells can be bound to solid support, fixed in the form of an active layer. When substrate passes over the surface, enzymatic reactions change the substrate to the desired product. Enzymes and suitable microorganisms are used in manufacturing food flavors, additives, medicines, and other goods and produced by variety of microbial metabolites. Immobilized cells may perform different from an equivalent mass of freely suspended cells.¹ They may produce extracellular polymers, which are usually lumped together with cells in dry biomass measurements, resulting in overestimation of the activity of immobilized biomass.² In addition, cell location in the form of biofilm can affect its quality and activity, because profiles of environmental conditions such as substrate concentration often exit. However, in many studies results for freely suspended cultures have been used to model immobilized cell bioreactors, usually without a lot of attention to assessing the quality of the biomass in the system. Typically these models allow for the effect of difficult limitations in and around the biofilm and assume that the immobilized cells have the same quality and activity as the suspended cell culture, regardless of the position in the biofilm.

In fact, significant substrate concentration gradients may exist for cells immobilized in biofilm. Cells located close to the nutrient supply are likely to maintain higher quality and activity compared to cells located relatively further away, leading to differentiation in the quality or activity of the immobilized cell population. This difference is more pronounced if there are starvation regions. In practice, zero substrate concentration may exist inside the biofilm, because in these regions the cell physiology may be markedly different from that of the freely suspended cells.

The cells' activities have been described based on a multispecies biofilm model and the microbial kinetics by a mathematical model. Using this model predicts that the biomass on the external surface of the biofilm has higher activity than the biomass near the solid support surface and that condition may occur, after the biofilm has reached a critical depth or formed a thick multilayer of the biofilm. The model was based on microbial growth kinetics determined by Wang et al.² However, no experimental results were presented in either of these studies to verify the model predictions, nor was the predicted immobilized biomass activity compared with that of freely suspended cells in a comprehensive way.

Wang et al.² and Najafpour et al.^{3,4} worked with immobilized microbial cells of *Nitrobacter agilis*, *Saccharomyces cerevisiae*, and *Pseudomonas aeruginosa* in gel beads, respectively. They

found that the cells retained more than 90% of their activity after immobilization using specific oxygen uptake rate ($\text{mg O}_2 \text{ g}^{-1} (\text{dry biomass}) \text{ h}^{-1}$) as the biomass activity indicator. Such differences in immobilized biomass and activity between free and immobilized biomass depend strongly on the particular characteristics of the microbial systems and their interaction with the support matrix.

8.2 IMMOBILIZED MICROBIAL CELLS

Since 1978, several papers have examined the potential of using immobilized cells in ethanol production. Microbial cells are advantageously used for industrial purposes, such as *Escherichia coli* for the continuous production of L-aspartic acid from ammonium fumarate.^{5,6} Enzymes from microorganisms are classified as extracellular and intracellular. If whole microbial cells can be immobilized directly, procedures for extraction and purification can be omitted and the loss of intracellular enzyme activity can be kept to a minimum. Whole cells are used as a solid catalyst when they are immobilized and attached to a solid support.

The entire work on immobilization can be categorized in two groups; the first group of research work emphasized on preparation and techniques of immobilization. The second category focused on application immobilized cell as biocatalyst in biochemical reactions or in bioconversion process. In this chapter, a brief technique of cell preparation and immobilization is introduced. However, application of the prepared immobilized cell in fermentation process is the major concern. Even duration of the use of immobilized cell and testing the biocatalysts activities in the bioprocess was under extensive investigation. The overall immobilization techniques are illustrated in Figure 8.1.⁵

There are three general methods available for the immobilization of whole microbial cells: carrier binding, cell entrapment, and cross-linking.

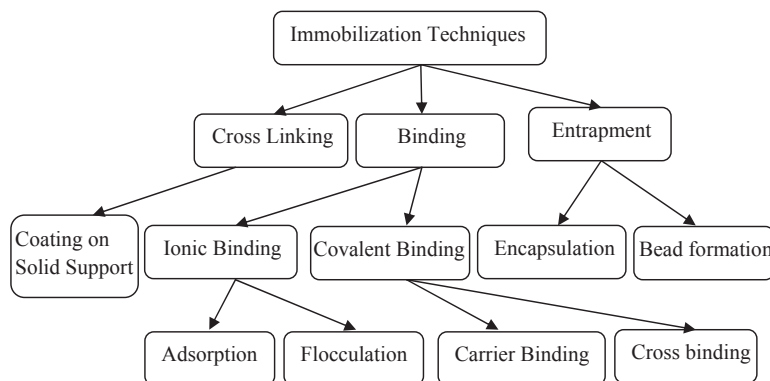


FIGURE 8.1 Techniques of cell immobilization.

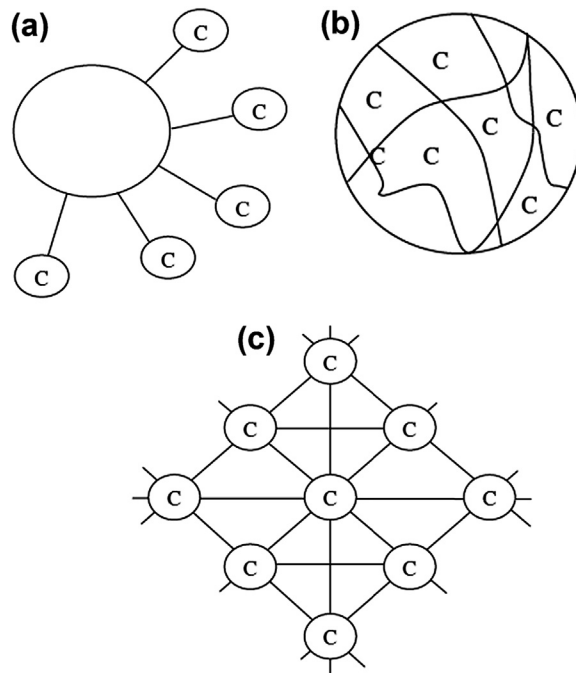


FIGURE 8.2 Alternative methods used to immobilize cells: (a) carrier binding; (b) entrapment; and (c) cross-linking.³

8.2.1 Carrier Binding

As shown in Figure 8.2(a), the carrier binding method is based on binding microbial cells directly to water-insoluble carriers. The binding is due to ionic forces between the microbial cells and the water-insoluble carriers. This technique has rarely been used, because of lyses during the enzyme reactions. Microbial cells may leak from the carrier, thereby disrupting the immobilization. Therefore, this method has not been applied successfully.⁶

8.2.2 Entrapment

In applying entrapment, microbial cells are directly entrapped into polymer matrices (Figure 8.2(b)). This method has been applied to several microorganisms by using gelatin, agar, polyacrylamide gel, calcium alginate, etc., as the entrapping agents.^{5,6} The following matrices are used extensively to immobilize microbial cells:

- Collagen
- Gelatin
- Agar
- Alginate
- Carrageenan

- Cellulose triacetate
- Polyacrylamide
- Polystyrene

In this method, microbial cells are apparently lysed within the entrapping agent, but they retain the desired enzymatic activity. To perform an efficient immobilization, the type and concentration of a bifunctional reagent for entrapment should be optimized. The advantage of this method is that cell leakage may act as a diffusion barrier, thus causing difficulty in transferring substrate and product through the matrix.^{4,7,8}

8.2.3 Cross-Linking

Microbial cells immobilized by cross-linking with bi- or multifunctional reagents such as glutaraldehyde have been reported to be successful, but active immobilizations have not been obtained with other reagents such as toluenediisocyanate.⁷ The microbial cell wall is composed of lipoproteins, with lipopolysaccharide extending from the cell membrane. Glutaraldehyde reacts with lysine within the protein in the lipid bilayer of the cell membrane.

Furthermore, gelatin is physically absorbed on a solid support, which provides a covalent link between the microbial cells and the gelatin layer which is tightly bound to a solid support by absorption (Figure 8.2(c)).

Glutaraldehyde has been used as cross-linking reagent for ethanol production. Maximum achieving rate was reported as high as $7.4 \text{ g l}^{-1} \text{ h}^{-1}$ ethanol produced from glucose.⁹ The major advantage of the cross-linking method is that the immobilization reagent does not act as diffusion barrier. Actually, a thin film of cells is provided in this system, making it ideal for many applications.^{10,11}

8.2.4 Advantages and Disadvantages of Immobilized Cells

There are several advantages for an immobilized cell system over a batch or CSTR system. The first and most obvious benefit is the capability of recycling or reusing the microorganisms because they are retained in the reactor as the product leaves the reactor. Second, immobilization can be easily used for a continuous process maintaining high cell density, thus providing a high productivity.¹²

Third, nutrient depletion and inhibitory compounds do not, in general, have a large effect on the immobilized cells because the cells are fixed by immobilization. In batch and CSTR fermentation, nutrient depletion, inhibition and accumulation of toxic by-products are major problems, but immobilized cells are usually unaffected by toxic by-products.

However, there are disadvantages for using immobilized cells. The cell may contain numerous catalytically active enzymes, which may catalyze unwanted side reactions. Also, the cell membrane itself may serve as a diffusion barrier and may reduce productivity. The matrix may sharply reduce productivity if the microorganism is sensitive to product inhibition. One of the disadvantages of immobilized cell reactors (ICRs) is that the physiological state of the microorganism cannot be controlled.

8.3 ICR EXPERIMENTS

The ICR experiments were undertaken to determine the performance of immobilized *Propionibacterium acidipropionici* in a plug-flow tubular reactor. The productivity of the ICR was evaluated by measuring glucose and xylose consumption, and propionic and acetic acid production, along the length of the reactor.³

The Raschig rings were sterilized and dip-coated in sterile 20% gelatin and 1.5% agar solution. The coated rings were dried; the dried coated rings were randomly packed in the column. The packing was sprayed with a 2.5% glutaraldehyde solution. An alternative procedure to prepare the packing was also tested and proved to be satisfactory. In the latter method, the reactor column was filled with clean Raschig rings. A hot gelatin-agar solution was passed through the column and allowed to wet the entire packing surface. When the coating was dried, the glutaraldehyde solution was passed through the column in a similar fashion. The column was allowed to stand for 24 h and then washed with sterile, distilled water. The reactor was sterilized by passing ethylene oxide through the column. The ethylene oxide was allowed to stand in the column for 8 h before the system was purged with sterile nitrogen. The feed and product tubing were autoclaved using steam at 15 psig.

After sterilization, a 24-h incubated seed culture was pumped through the column. An adaptation time of about 48 h was allowed for the establishment of a film of microorganisms cross-linked to the surface Raschig rings. The Raschig rings served as solid support. Feed media were then pumped into the reactor. An accurate calculation of the retention time in the reactor was difficult, because growth and carbon dioxide evolution may take a significant fraction of avoid volume of the ICR, resulting in a false retention time. The microbial film thickness could be controlled by periodically passing sterile nitrogen or carbon dioxide through the column, to stop cell overgrowth.

A feed concentration of 15 g glucose and 15 g xylose per liter was used over a feed rate of 20–200 ml h⁻¹. Samples were taken at successive points along the reactor length, and the usual analysis for glucose and xylose consumption, organic acid production, and cell density were done. A kinetic model for the growth and fermentation of *P. acidipropionici* was obtained from these data.

Analytical procedures were set up to measure cell density, sugar concentration, and organic acid concentration. The turbidity of the culture (optical density) was determined by reading the absorbance with spectrophotometer and cell counts. Sugar concentration as a single substrate was measured by an industrial digital analyzer. Total sugar was evaluated by a reducing agent such as dinitrosalicylic acid in alkaline solution. An orange color was produced which was read on a spectrophotometer at 540 nm. Organic acids were determined by a gas chromatograph, with a flame ionization detector.

8.4 ICR RATE MODEL

Table 8.1 presents the results of the ICR retention time studies, sugar concentration (dual substrate) studies, and cell density. The kinetic model for ICR was derived on the basis of a first order reaction, plug flow, and steady-state behavior.

TABLE 8.1 Continuous fermentation of dual substrate (glucose, xylose) in immobilized cell reactor at 36 °C

Retention time (h)	Length of reactor (cm)	Substrate concentration (g l ⁻¹)		Organic acid concentration (g l ⁻¹)		Reaction rate of glucose (g l ⁻¹ h ⁻¹)	Cell density (cells ml ⁻¹)
		Glucose	Xylose	Propionic acid	Acetic acid		
28	0	15	15	—	—		
	15	6.28	10	1.3	7.78	0.31	9 × 10 ¹¹
	35	4.52	8.6	1.98	8.45	0.37	9 × 10 ¹¹
	60	2.13	7.2	2.7	12.4	0.46	9 × 10 ¹¹
	85	1.36	5.4	3.25	17.2	0.49	9 × 10 ¹¹
	110	1.14	3	3.95	19.1	0.495	9 × 10 ¹¹
20	0	15	15	—	—		
	15	7.1	11	1.2	6.45	0.395	9 × 10 ¹¹
	35	4.72	9.8	1.46	8.1	0.514	9.5 × 10 ¹¹
	60	2.21	7.9	1.87	12	0.64	9.5 × 10 ¹¹
	85	1.5	7.15	2.12	16.4	0.675	9.5 × 10 ¹¹
	110	1.2	5.8	2.4	18	0.69	9.5 × 10 ¹¹
12	0	15	15	—	—		
	15	9.3	14.5	2.59	1.33	0.475	1 × 10 ¹⁰
	35	6.02	14	3.26	2.37	0.75	2 × 10 ¹⁰
	60	3.62	13	4.5	2.45	0.95	3 × 10 ¹⁰
	85	2.65	12	5.07	2.5	1.03	3 × 10 ¹⁰
	110	2.3	10	5.36	2.54	1.06	5 × 10 ¹⁰
5	0	15	15	—	—		
	15	9.8	15	0.5	0.58	1.04	6 × 10 ¹⁰
	35	7.27	14.5	0.6	0.76	1.55	1.8 × 10 ¹⁰
	60	6.05	14	0.65	1.2	1.79	5 × 10 ¹⁰
	85	5.84	14	0.7	1.36	1.83	5 × 10 ¹⁰
	110	5.2	13.5	0.8	1.65	1.96	6 × 10 ¹⁰

$$r_A = kC_A \quad (8.4.1)$$

$$u \frac{dC_A}{dz} = r_A \quad (8.4.2)$$

where r_A is the reaction rate, k is the rate constant, C_A is the sugar concentration, z is the axial reactor length, and u is the bulk fluid velocity. Substituting Eqn (8.4.1) into Eqn (8.4.2) yields:

$$u \frac{dC_A}{dz} = kC_A \quad (8.4.3)$$

Equation (8.4.3) is a linear first-order differential equation of concentration and reactor length. Using the separation of variables technique to integrate Eqn (8.4.3) yields:

$$\ln\left(\frac{C_A}{C_{A_0}}\right) = \frac{kz}{u} \quad (8.4.4)$$

Figure 8.3 shows a plot of $\ln C_A/C_{A_0}$ as a function of dimensionless reactor length for the fermentation data obtained at a feed concentration of 15 g l^{-1} glucose and 15 g l^{-1} xylose at different retention times. A straight line is obtained at each retention time. The value of the slope increases with increasing retention time owing to decreasing velocity through the column. Table 8.2 also indicates that the rate constant in the first-order reaction is fixed with different retention times.

The same feed composition was experimented in CSRT; it was found that the ICR flow rate was five to eight times faster than the CSTR. The overall conversion of sugars in the ICR at a 12-h retention time was 60%, at this retention time, the ICR was eight times faster than CSTR, but in the CSTR an overall conversion rate of 89% was obtained. At the washout rate for the chemostat, the ICR resulted in a 38% conversion of total sugars. Also, the organic acid production rate in the ICR was about four times that of the CSTR. At a higher retention time of

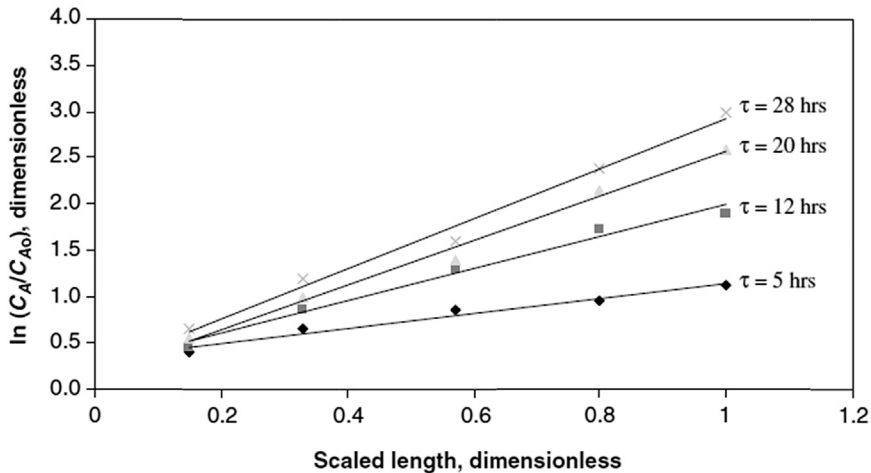


FIGURE 8.3 Model test for immobilized cell reactor using *Propionibacterium acidipropionici*.

TABLE 8.2 Immobilized cell reactor kinetic model for immobilized *Propionibacterium acidipropionici*¹⁰

Retention time τ (h)	Flow rate (ml h ⁻¹)	Rate constant (h ⁻¹)
5	214	0.70
8	135	0.69
12	90	0.68
20	55	0.68
28	38	0.51

28 h, the conversion of glucose in the ICR and CSTR were about the same, but the conversion of xylose reached 75% in the ICR and 86% in the CSTR.

NOMENCLATURE

- C_A Sugar concentration (g l⁻¹)
 k Rate constant (l h⁻¹)
 r_A Reaction rate (g l⁻¹ h⁻¹)
 u Bulk fluid velocity (cm h⁻¹)
 z Axial reactor length (cm)

References

1. Gikas P, Livingston AG. *Biotechnol Bioeng* 1997;**55**:660.
2. Wang DIC, Cooney CL, Demain ADL, Dunnill P, Humphrey AE, Lilly MD. *Fermentation and enzyme technology*. New York: John Wiley & Sons; 1979.
3. Najafpour GD. *J Sci I R Iran* 1990;**1**:172.
4. Najafpour GD, Younesi H. *Bioresour Technol* 2004;**92**:251.
5. Chibata I. Immobilized microbial cells with polyacrylamide gel, carrageenan and their industrial applications. In: *Immobilized microbial cells*. Washington (DC): American Chemical Society; 1979 [chapter 3].
6. Chibata I. *Microb Technol* 1979;**11**:361.
7. Brodelius P, Mesback K. *Adv Appl Microbiol* 1982;**28**:1.
8. Mark RR, Muzzio FJ, Buettner HM, Sebastian CR. *Biotechnol Bioeng* 1996;**49**:223.
9. Sitton OC, Gaddy JL. *Biotechnol Bioeng* 1980;**22**:1735.
10. Najfpour GD. *Propionic and acetic acid fermentation using propionibacterium acidipropionici in batch and continuous culture* [Ph.D. thesis]. Fayetteville (AR): University of Arkansas; 1983.
11. Najafpour GD. *Resour Conserv* 1987;**13**:187.
12. Senthuran A, Senthuran V, Mattiasson B, Kaul R. *Biotechnol Bioeng* 1997;**55**:841.

SUBCHAPTER

8.6

Case Study: Ethanol Fermentation in an Immobilized Cell Reactor Using *Saccharomyces cerevisiae**

8.6.1 INTRODUCTION

Owing to diminishing fossil fuel reserves, alternative energy sources need to be renewable, sustainable, efficient, cost-effective, convenient, and safe.¹ In recent decades, microbial production of ethanol has been considered as an alternative fuel for the future because fossil fuels are depleting. Several microorganisms, including *Clostridium* sp. and yeast, the well-known ethanol producers *Saccharomyces cerevisiae* and *Zymomonas mobilis*, are suitable candidates to produce ethanol.^{2,3}

Microorganisms under anaerobic growth conditions have the ability to use glucose by the Embden–Meyerhof–Parnas pathway.⁴ Carbohydrates are phosphorylated through the metabolic pathway; the end products are 2 mol of ethanol and carbon dioxide.⁵

During batch fermentation of *S. cerevisiae*, other influential parameters can adversely influence the specific rate of growth, and inhibition can be caused either by product or substrate concentration. The viability of the *S. cerevisiae* population, its specific rate of fermentation, and the sugar uptake rate are directly related to the desired medium condition.⁶ It has been reported by Nagodawithana and Steinkraus,⁷ that the addition of ethanol to the cultured media was less toxic for *S. cerevisiae* than ethanol produced by cell bodies. This indicates that there are other metabolic by-products that can cause inhibition and may show impurity of ethanol produced in the fermentation system. Also, the death rates were lower with addition of pure ethanol than the similar condition with the endogenously produced ethanol concentration.⁷

Use of biofilm reactors for ethanol production has been investigated to improve the economics and performance of fermentation processes.⁸ Immobilization of microbial cells for fermentation has been developed to eliminate inhibition caused by high concentrations of substrate and product, also to enhance productivity and yield of ethanol. Recent work on ethanol production in an immobilized cell reactor (ICR) showed that production of ethanol

*This case study was partially written with contributions from:

Habibollah Younesi, Department of Environmental Science, Faculty of Natural Resources, Tarbiat Modares University, Noor, Iran.

using *Z. mobilis* was doubled.⁹ The immobilized recombinant *Z. mobilis* was also successfully used with high concentrations of sugar (12–15%).¹⁰

The potential use of immobilized cells in fermentation processes for fuel production has been described previously. If intact microbial cells are directly immobilized, the removal of microorganisms from downstream product can be omitted and the loss of intracellular enzyme activity can be kept to a minimum level.¹¹

Recently, immobilized biomass activity has been given more attention, because it has been acknowledged to play a significant role in bioreactor performance.¹² Frequently, immobilized cells are subjected to limitations in the supply of nutrients. Thus, because of the presence of heterogeneous materials such as immobilized cells, there is no convective flow inside the beads and the cells can receive nutrients only by diffusion.¹³ Immobilization of cells to a solid matrix is an alternative means of high biomass retention. The cells divide within and on the core of the matrix.¹⁴ Alginate is widely used in food, pharmaceutical, textile, and paper products. Alginate is used in these products for thickening, stabilizing, gel, and film forming. Sodium alginate is a linear polysaccharide, normally isolated from many strains of marine brown seaweed and algae, named “alginate.” The copolymer consists of two uronic acids or polyuronic acids. It comprises primarily D-mannuronic acid (M) and L-glucuronic acid (G). Alginic acid can be either water-soluble or nonwater-soluble depending on the type of the associated salt. Interchange of sodium ions with calcium ions in the solution may follow solidification of sodium alginate in calcium chloride solution. The sodium salt, other alkaline metals, and ammonia are soluble in water, whereas the polyvalent cations salts (e.g., calcium) are not water-soluble, except for magnesium ions.

The purpose of this research was to obtain high ethanol production with high yields of productivity and to lower the high operating costs. The ICR column fermenter was used with *S. cerevisiae* by an entrapment technique using alginate as a porous wall to retain the yeast cells. The effect of initial glucose concentration on the production of ethanol by *S. cerevisiae* was evaluated. The yield for large-scale ethanol production was compared with the ethanol produced in batch fermentation using the same microorganism.

8.6.2 MATERIALS AND METHODS

8.6.2.1 Experimental Reactor System

The ICR was a plug flow tubular column, constructed with a nominal diameter of 5 cm, internal diameter of 4.6 cm, Plexiglas of 3 mm wall thickness, and 85 cm length. The medium was fed to the ICR column from a feed tank located above the column. A variable-speed Masterflex pump, model L/S Easyload (Cole-Parmer, Vernon Hills, IL, USA) was used to transfer feed medium from a 20 l polypropylene autoclavable Nalgene carboy (Cole-Parmer), the carboy was serving as reservoir. The effluent from the column was collected in a 20-l polypropylene autoclavable carboy serving as product reservoir. A flow breaker was installed between the column and feed pump, which prevented growth of microorganisms and contamination of feed line and feed tank. Samples from the ICR column were taken from the inlet and outlet compartments of the column. A 16-h culture was harvested at exponential growth phase and mixed with 2% sodium alginate. The slurry of yeast culture was converted

to droplet form while it was dripped into a 6% bath of calcium chloride using a 50-ml syringe. Once the slurry was added to the bath, beads of calcium alginate with entrapped cells were formed.¹¹ The bed consisted of uniformly packed 5-mm beads. The solidified beads were transferred to the column. About 70% of the column was packed. The extra space was counted for bed expansion by the fresh media. The void volume was measured by volume of distilled water pumped through the bed. The packed ICR column was used in continuous mode for the duration of fermentation. The fresh feed was pumped in an up flow manner, whereas sugar and ethanol concentration was monitored during the course of continuous fermentation. The working volume of ICR after random packing was 740 ml. The bed volume was about 660 ml. The experimental set up of the ICR is shown in Figure 8.4. There was no evidence of cell leakage from the beads to the surrounding media, the matrix was permeable

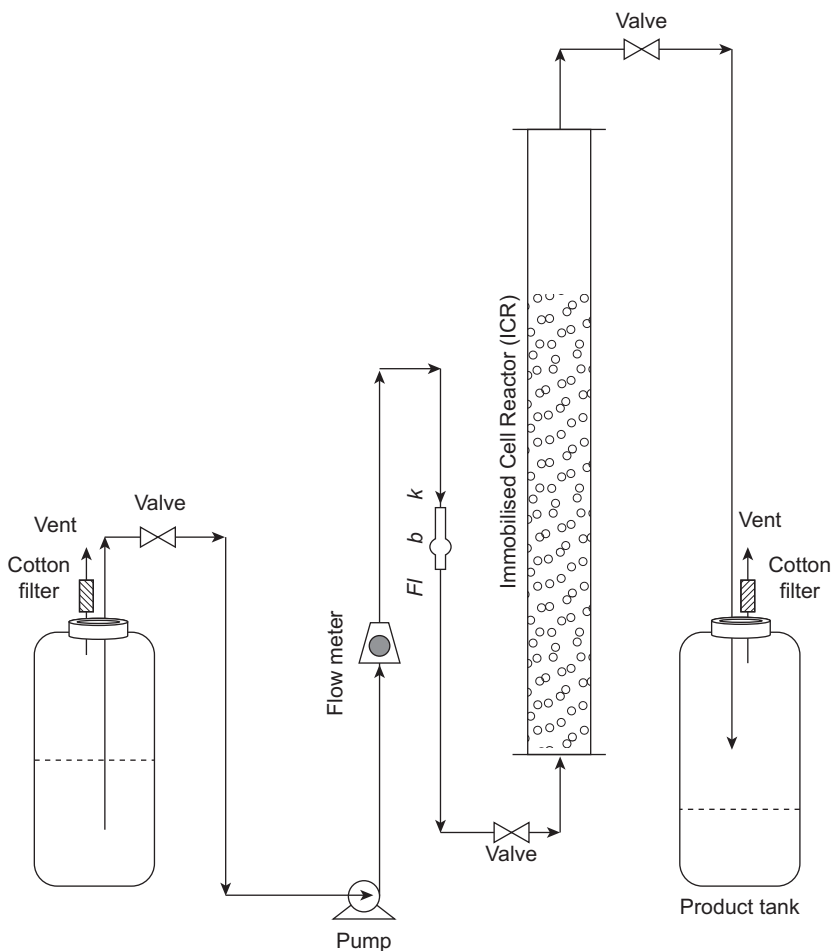


FIGURE 8.4 Schematic diagram of immobilized cell reactor experimental setup. Reprinted from Najafpour et al.¹⁵ Copyright with permission from Elsevier.

TABLE 8.3 Physical properties and appearance of *Saccharomyces cerevisiae* beads

Alginate (wt%)	1.5	2	3	6
Beads diameter (mm)	5	4.9–5	4.8–4.9	4.5
Growth, diameter expansion after 72 h	50–60%	25–30%	20–25%	No expansion
Diffusion problem	Nil	Nil	Nil	May exists
Cell activity	Active	Fully active	Fully active	Partly active
Physical appearance	Easy to break	Flexible, hard enough to stand	Flexible and hard	Very hard
Stability	Not stable	Good stability	Stable and rigid	Very rigid

to substrate and product, and cell growth and glucose conversion were monitored in the ICR. Overgrowth of beads after a few days of operation was controlled. Carbon dioxide was purged to eliminate overgrowth of beads. The major overgrowth occurred at the entrance region, in about the first 30 cm length of the column where the sugar concentration was very high. High sugar concentrations of 25, 35, 50, and 150 g l⁻¹ were used.

Microbial overgrowth was controlled with carbon dioxide passed through the bed. There was a maximum 30% increase in the beads' diameter at the lower part of column, where the glucose concentration was at a maximum. The void volume was measured by passing sterilized water. In addition to the carbon source, the feeding media consisted of 1 g l⁻¹ yeast extract pumped from the bottom of the reactor, while the flow rate was constant for a minimum duration of 24 h.

A seed culture of *S. cerevisiae* ATCC 24860 (American Type Culture Collection, Manassas, VA, USA) was grown in a media of 5 g glucose, 0.5 g yeast extract, 1.5 g KH₂PO₄, and 2.25 g Na₂PO₄ phosphate buffer up to a total volume of 500 ml using distilled water. The media was sterilized at 121 °C for 15 min. The stock culture of the microorganisms was transferred to the broth media for preparation of seed culture.

Sodium alginate (Fisher Scientific, Manchester, UK) was prepared by dissolving 10 g of powder form in 500 ml of distilled water. A separate solution of 120 g of calcium chloride was dissolved in 2 l of distilled water. Sodium alginate and calcium chloride solution were autoclaved at 121 °C for 15 min. The sterilized sodium alginate solution and the high cell density of the grown seed culture were thoroughly mixed. Beads were prepared by droplet from pipette with about 5 mm diameter in a sterilized calcium chloride solution. The cell density of the seed culture for bead preparation was 3.1 g l⁻¹. The wet and dry weight of beads incubated for 16 h were measured as 3.28 and 0.5 g, respectively. The moisture content of the beads was 85%. The physical properties and appearance of the *S. cerevisiae* beads are summarized in Table 8.3.

8.6.2.2 Determination of Glucose Concentration

To determine the concentration of inlet and outlet glucose in the ICR, a reducing chemical reagent, 3,5-dinitrosalicylic (DNS) acid 98% solution, was used. The DNS solution was prepared by dissolving 10 g of 3,5-DNS acid in 2 M sodium hydroxide solution. A separate

solution of 300 g sodium potassium tartrate solution was prepared in 300 ml of distilled water. The hot alkaline 3,5-dinitrosalicylate solutions were added to sodium potassium tartrate solution. The final volume of DNS solution was made up to 1 l with distilled water. A calibration curve was prepared with 2 g l⁻¹ glucose solution.^{16,17}

8.6.2.3 Detection of Ethanol

Ethanol production in the fermentation process was detected with gas chromatography, HP 5890 series II (Hewlett-Packard, Avondale, PA, USA) equipped with a flame ionization detector and GC column Porapak QS (Alltech Associates Inc., Deerfield, IL, USA) 100/120 mesh. The oven and detector temperatures were 175 and 185 °C, respectively. Nitrogen was used as carrier gas. Isopropanol was used as an internal standard.

8.6.2.4 Yeast Cell Dry Weight and Optical Density

In batch fermentation, approximately 2 ml sample was harvested every 2 h. The absorbance of each sample during batch fermentation was measured at 620 nm using spectrophotometer, Cecil 1000 series (Cecil Instruments, Cambridge, UK). The cells dry weight was obtained using a calibration curve. The cell dry weight was proportional to cell turbidity and absorbance at 620 nm. The cell concentration (dry weight) of 2.1 g l⁻¹ was obtained from the 24 h culture broth, the free cell samples with absorbance of 1.6 at 620 nm.

8.6.2.5 Electronic Microscopic Scanning of Immobilized Cells

For electronic micrographs, samples were taken from fresh beads and 72 h beads from the ICR column. The samples were dipped into liquid nitrogen for 10 min, then freeze-dried for 7 h (EMITECH, model IK750, Cambridge, UK). The sample was fixed on an aluminium stub and coated with gold–palladium by a Polaron machine model SD515 (EMITECH) at 20 nm coating thickness. Finally the sample was examined under scanning electron microscope (SEM) using a Stereoscan model S360 (SEM-Leica Cambridge, Cambridge, UK). The SEM images of beads before and after use in ICR are shown in [Figures 8.5 and 8.6](#).

8.6.2.6 Statistical Analysis

The size of beads was uniform and consistent, the mean diameter of beads with 3% alginate and based on measurement of 20 samples was 4.85 mm, with a standard deviation of 0.3 mm and calculated variance of 0.1 mm. The standard deviation was less than 5%. The data for the batch fermentation experiment with 50 g l⁻¹ glucose are presented in [Figures 8.7–8.9](#); they were replicated three times. The data for ICR with 25, 35, 50, and 150 g l⁻¹ glucose that were conducted at a wide range of flow rates are shown in [Figures 8.10–8.14](#), which were repeated in additional runs. The standard deviations of collected data for the batch experiments were approximately 5%, and the standard deviation for the ICR experimental data with a sugar concentration of 50 g l⁻¹ was approximately 10%. Data were analyzed in a spreadsheet, Microsoft Excel 2000. The error analysis for the ICR data with a substrate concentration of 150 g l⁻¹ was slightly higher but it was in the range of 10–12%.

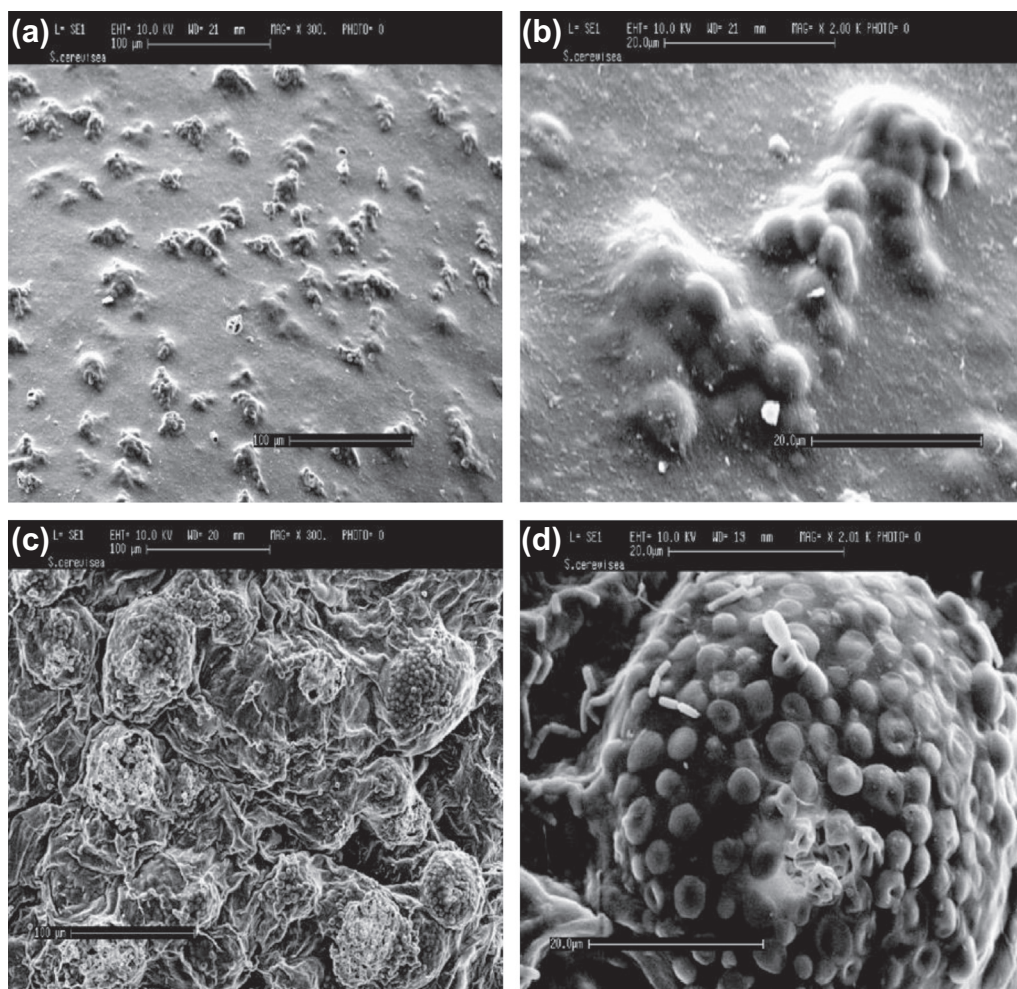


FIGURE 8.5 Electron micrographs of the outer surface of immobilized *Saccharomyces cerevisiae* beads. (a) Outer surface of the fresh beads with magnification of 300 μm . (b) Outer surface of the fresh beads with magnification of 2000 μm . (c) Outer surface of the used beads after 72 h with magnification of 300 μm . (d) Outer surface of the used beads after 72 h with magnification of 2000 μm . Reprinted from Najafpour et al.¹⁵ Copyright with permission from Elsevier.

8.6.3 RESULTS AND DISCUSSION

8.6.3.1 Evaluation of Immobilized Cells

In preparing immobilized cells, 1.5, 2, 3, and 6% alginate was used. By pressing them manually, the hardness and rigidity of the beads were tested. The physical criteria of the prepared beads are summarized in Table 8.3. The suitable alginate concentration based on activity of the beads for ethanol production was 2%. The weight percentage of alginate was related

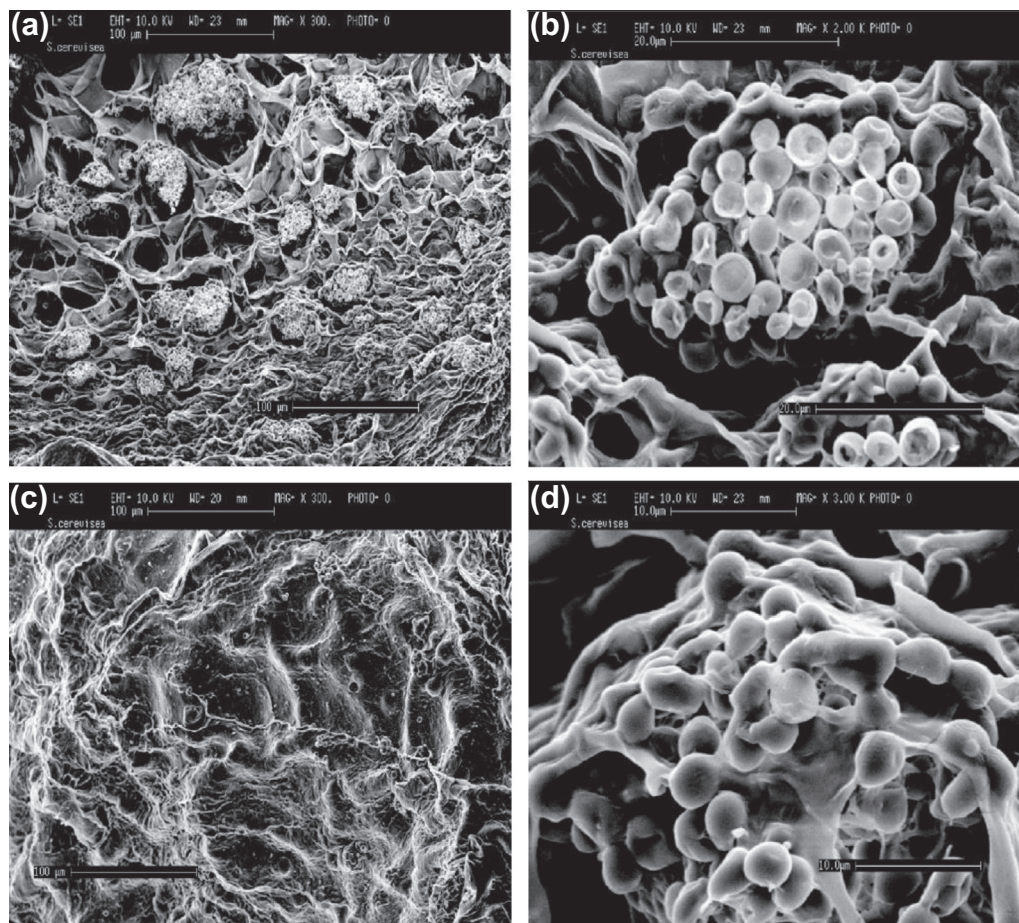


FIGURE 8.6 Electron micrographs of the inner surface of immobilized *Saccharomyces cerevisiae* beads. (a) Inner surface of the fresh beads with magnification of 300 μm . (b) Inner surface of the fresh beads with magnification of 2000 μm . (c) Inner surface of the used beads after 72 h with magnification of 300 μm . (d) Inner surface of the used beads after 72 h with magnification of 2000 μm . Reprinted from Najafpour et al.¹⁵ Copyright with permission from Elsevier.

to substrate and product penetration into the beads and return to bulk of fluid. Beads with low alginate (1.5%) were too soft and easily breakable. The soft beads were pressed once they were loaded in the ICR column. Therefore they were unable to be used successfully; also, the soft beads faced problems such as overgrowth and expansion of their diameter when grown in sugar solution. The high alginate beads (6%) were very hard and almost unbreakable by pressing manually. They were very rigid; therefore, diffusion was the most probable cause since ethanol production declined. The 2% alginate was used because the beads were strong enough to hold the weight of packing in the ICR column. The packed beads were used in the ICR column for 10 days. The prepared beads were refrigerated for 2 weeks and activated in sugar solution. The storage condition and ICR column were

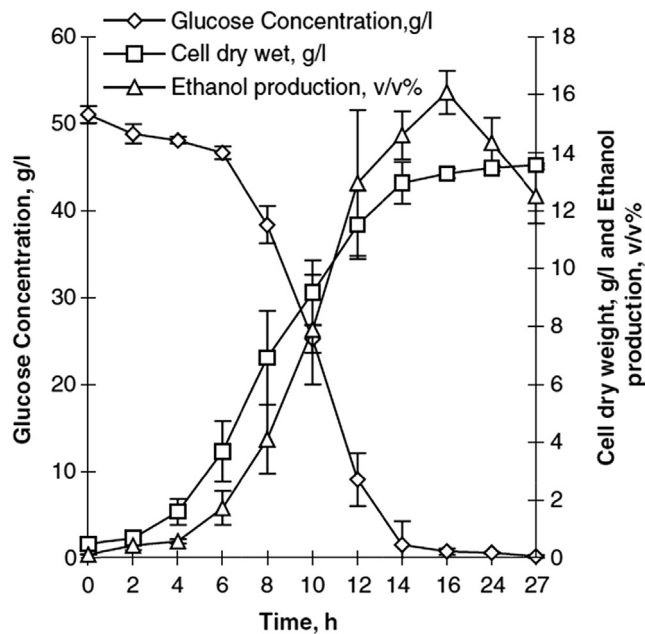


FIGURE 8.7 Glucose concentration, cell density, and production of ethanol in batch fermentation with initial concentration of 50 g l^{-1} glucose versus time. Reprinted from Najafpour et al.¹⁵ Copyright with permission from Elsevier.

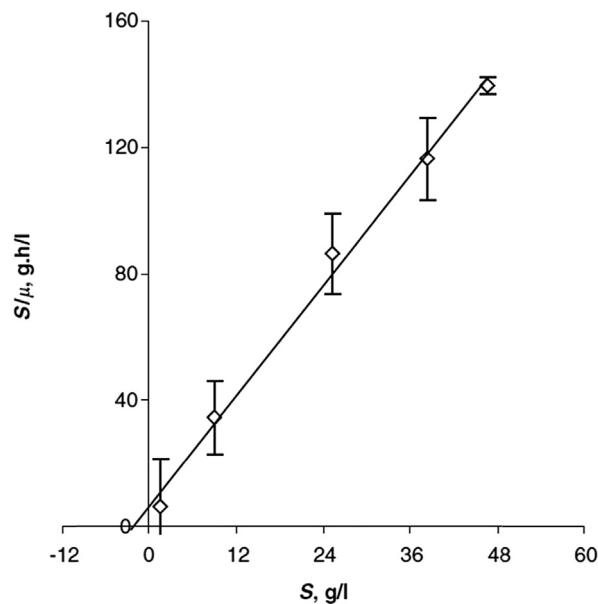


FIGURE 8.8 Kinetic model for batch fermentation, Langmuir-Hanes plot. Reprinted from Najafpour et al.¹⁵ Copyright with permission from Elsevier.

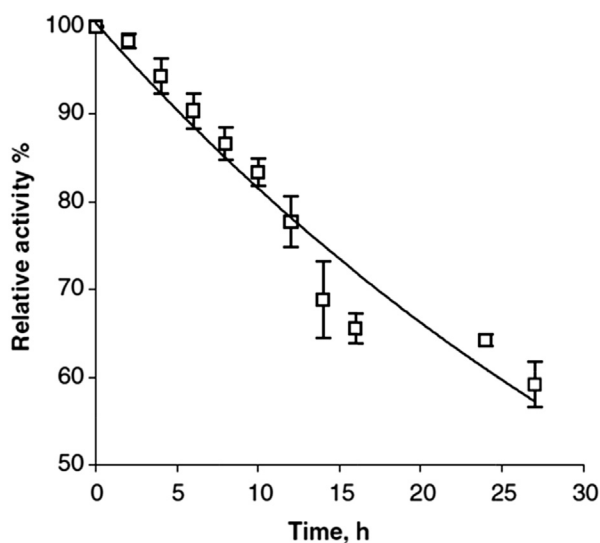


FIGURE 8.9 Relative activities of *Saccharomyces cerevisiae* in batch fermentation. Reprinted from Najafpour et al.¹⁵ Copyright with permission from Elsevier.

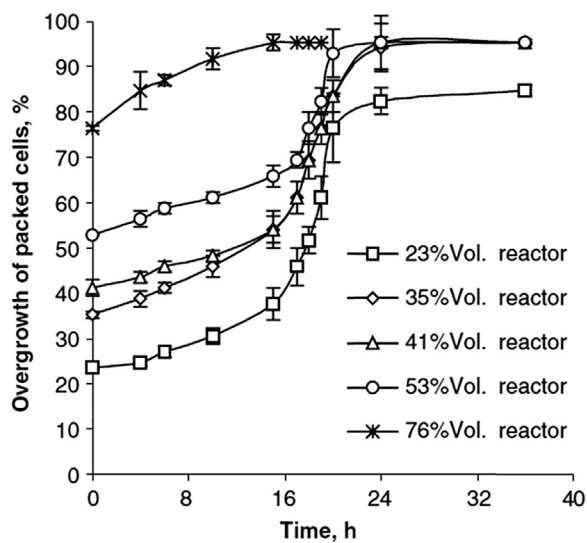


FIGURE 8.10 Percentage growth of immobilized cells with various initial beads loading. Reprinted from Najafpour et al.¹⁵ Copyright with permission from Elsevier.

nonsterile; therefore, there was the possibility of contamination in the packing of the ICR and in the activation process.

A series of electron micrographs were taken from the fresh and 72 h immobilized beads. The outer and inner surfaces of the beads are shown in Figures 8.5 and 8.6, respectively.

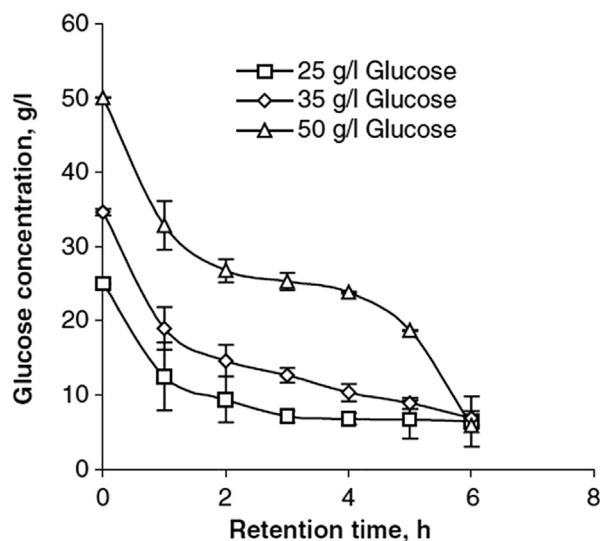


FIGURE 8.11 Consumption of glucose in the immobilized cell column. Reprinted from Najafpour et al.¹⁵ Copyright with permission from Elsevier.

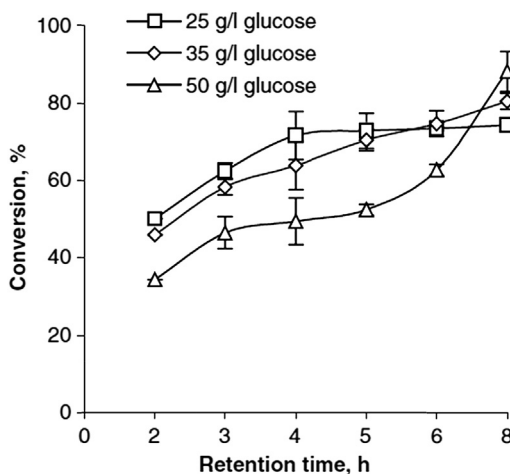


FIGURE 8.12 Conversion versus retention time in the immobilized cell column. Reprinted from Najafpour et al.¹⁵ Copyright with permission from Elsevier.

These micrographs were used as a comparative indicator for yeast growth on the surface of the solid support (2% calcium alginate). There was no apparent leakage of cells from the beads into the bulk of the fluid. It was also apparent that, by 72 h in the ICR, the yeast was growing on the outer surface. Therefore, the active sites were potentially available for

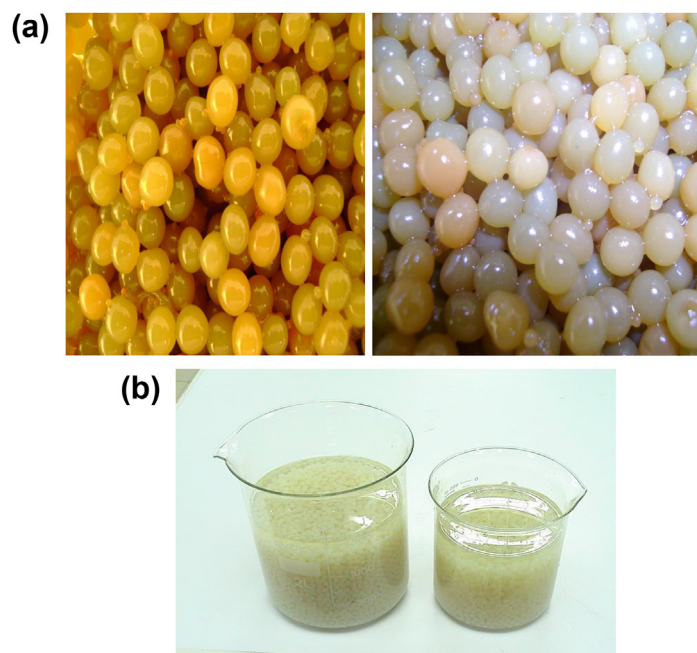


FIGURE 8.13 Active and fresh beads of *Saccharomyces cerevisiae*. (a) Active *S. cerevisiae* beads in ethanol fermentation after 14 days in continuous operation. (b) Fresh prepared beads of *S. cerevisiae*.

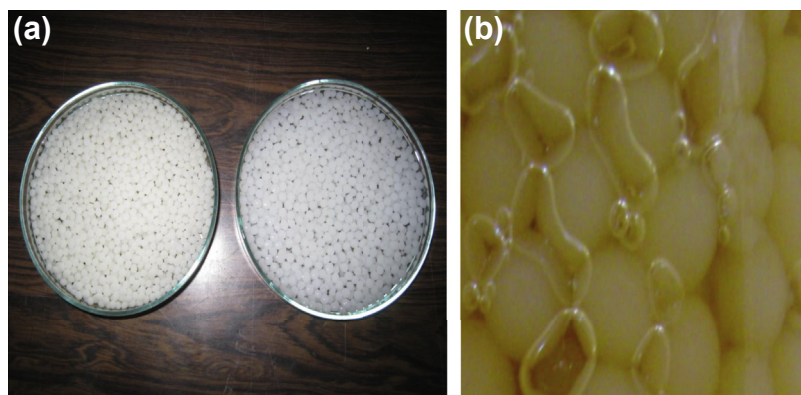


FIGURE 8.14 Fresh prepared beads and active beads of *Lactobacillus bulgaricus* in production of lactic acid from whey. (a) Fresh beads. (b) Active used beads.

ethanol production without diffusion problems. The outer surface of fresh and 72 h immobilized cell beads at magnifications of 300 and 2000 are shown in Figure 8.5. A comparison between fresh and 72-h beads indicates that the cells were present on the surface, with a few contaminants from a bacillus-type organism, as shown in Figure 8.5(d). This may have occurred during the transfer stage.

The inner surface of the beads before and after use was compared. The cells were initially trapped inside the beads; after 72 h the cells apparently migrated from the inner side to the surface. The micrographs of the inner sides of the beads before and after use, at magnifications of 300 and 2000, are shown in Figure 8.6. After 72 h the cells appeared to form new colonies on the surface of the alginate layer. By contrast, the surfaces were completely covered with colonies after 72 h of ethanol production in the ICR.

8.6.3.2 Batch Fermentation

Ethanol fermentation in batch experiments was carried out in triplicate with 50 g l⁻¹ glucose solution as the sole carbon source for *S. cerevisiae*. The purpose of the batch experiment was to compare the amount of glucose concentration and ethanol production in batch fermentation and the ICR. The concentration of glucose was gradually decreased, whereas the cell density and ethanol production were increased for 27 h, as shown in Figure 8.7. There was a lag phase of 4–6 h; the glucose consumption was low at this stage. Subsequently the concentration profile drastically decreased during batch fermentation after 8–16 h. Because the cell density was initially low, sugar consumption was also low. The resulting cell growth curve from the batch experiment was a typical sigmoidal (S-) shape. The maximum cell density of *S. cerevisiae* in batch fermentation was 13.7 g l⁻¹ with 50 g l⁻¹ glucose concentration. The average yield of biomass and product on substrates ($Y_{X/S}$ and $Y_{P/S}$) were 33 and 32%, respectively. The rate of ethanol productivity for 24 h was 1.4 g l⁻¹ h⁻¹. A Langmuir–Hanes plot based on the Monod rate equation is presented in Figure 8.8. The Monod kinetic model can be used for microbial cell biocatalyst and is described as follows:

$$\frac{S}{\mu} = \frac{K_s}{\mu_m} + \frac{S}{\mu_m} \quad (8.6.3.2.1)$$

The terms K_s and μ_m are defined as the Monod constant and maximum specific growth rate, respectively. The data generated in this study were linearly fitted with the model as a function of concentration produced during the exponential phase versus time (Figure 8.8). From the plot, the maximum specific growth rate and Monod constant were determined to be 0.35 h⁻¹ and 2.23 g l⁻¹, respectively. The large value of the Monod constant may suggest that at high concentrations of substrate, more influence on the cell–substrate complex dissociation occurred than cell–substrate complex formation.

8.6.3.3 Relative Activity

The economics of an immobilized cell process depend on the lifetime of the microorganism and a continued level of clean product delivered by the fixed cells. It is important to eliminate the free cells from the downstream product without the use of any units such as centrifuge or filtration processes. Because the cells are retained in the ICR, the activity of intracellular

enzymes may play a major role. It is assumed that the deactivation of the enzyme at constant temperature follows a first-order equation as shown here:¹⁸

$$A_t = A_0 \exp(-k_d t) \quad (8.6.3.3.1)$$

where A_t and A_0 are activities of enzymes at time t and initial time zero, respectively. Also, k_d is the dissociation constant. The plot of relative activity versus time in batch fermentation with free cells is shown in Figure 8.9. The value of k_d was 0.36 h^{-1} (Figure 8.9). According to the first-order dissociation rate constant, the half-life of the *S. cerevisiae*, ($\tau_d = \ln 2/k_d$), in batch fermentation suspended cells with 50 g l^{-1} of glucose was 1.95 h. The free cells were apparently completely deactivated after 60 h in batch operation. The data indicate that the free cells were deactivated rapidly compared with immobilized cells when used in a continuous mode for more than 7 days.

8.6.3.4 Reactor Setup

The volume of reactor without beads was 1.4 l. The column was loaded with the solidified uniform beads of *S. cerevisiae*. The void volume of the reactor was 660 ml when it was packed with immobilized beads. The growth of beads with different proportions of column packing is shown in Figure 8.10. A fresh feed of 10 g l^{-1} glucose solution was pumped from the bottom of the reactor. The optimum amount of packing obtained was 65–70% of the reactor volume. The trend of the collected data resembles the growth curve of yeast in suspended cell culture. The diameters of the beads increased with the increase in *S. cerevisiae* cell density, which indicates that *S. cerevisiae* was growing within the solid support. Under these circumstances, substrate would be easily consumed at the solid surface coated with immobilized yeast cells. Thus, it was expected that substrate concentration at the surface would be less than the concentration of substrate in the bulk fluid. The main objective was to determine whether substrate penetrated into the beads. Because the matrix of beads was quite porous, it was assumed that the concentration gradient was the major force that influenced the mass transfer process in immobilized cells of *S. cerevisiae*. Therefore, the immobilized yeast system was preferred compared with free cells in the solution. Moreover, economic aspects of immobilized yeast must be considered as it eliminates the need for the extra unit for free-cell removal from the product stream. The other advantages of the immobilization system are that the substrate may not accumulate on the surface of the beads and that there was no evidence of cell leakage from the beads.

The actual image of fresh and active beads before and after *S. cerevisiae* in ethanol production and *Lactobacillus bulgaricus* in lactic acid production from whey are shown in Figures 8.13 and 8.14, respectively.

8.6.3.5 Effect of High Concentration of Substrate on Immobilized Cells

The fermentation was performed with various sugar concentrations to increase product concentrations. The initial sugar concentrations were 25, 35, and 50 g l^{-1} . The sugar consumption profile in the ICR is presented in Figure 8.11. The sugar consumption trends of various glucose concentrations were similar, with a sharp reduction of substrate occurring within the first 3 h. A range of 55–75% of the sugars was reduced within a 3 h retention time. A 6-h

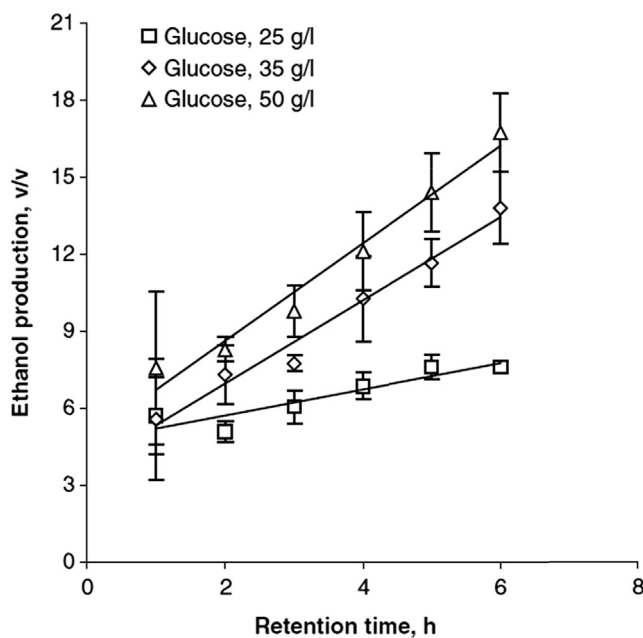


FIGURE 8.15 Ethanol production versus retention time in the immobilized cell column. Reprinted from Najafpour et al.¹⁵ Copyright with permission from Elsevier.

retention time indicated that this was the most suitable time to achieve high sugar consumption. A longer retention time was required for higher sugar concentrations of up to 150 g l^{-1} in the ICR column (7 h) (Figure 8.15). The amount of cell immobilized with calcium alginate was determined by the cell dry weight of immobilized cells and the assumption that 98% of the beads were considered to be loaded with active cells. Beads were measured before loading in the ICR column.

Conversion of glucose versus dilution rate, used in the continuous fermentation process with immobilized *S. cerevisiae*, is shown in Figure 8.12. As the sugar concentration increased, the conversion may have decreased. At very high sugar concentrations, the conversion of sugar decreased. The maximum sugar conversion at 6 h retention time was obtained as 74.3, 80.5, and 88.2% for 25, 35, and 50 g l^{-1} glucose concentrations, respectively.

At high concentrations of sugar, conversion was highly influenced by dilution rate. The conversion decreased to less than 10% once the dilution rate approached wash out. The sugar conversion at low sugar concentrations appeared to be much less sensitive to feed dilution rate. The conversion for 25 g l^{-1} glucose was constant at 74% for a retention time of greater than 3 h (Figure 8.12). The trend of the data with 50 g l^{-1} sugar showed that conversion increased with retention time. At a higher sugar concentration, it required a longer retention time to achieve higher conversion.

Reactor productivity was obtained by dividing final ethanol concentration with respect to sugar concentration at a fixed retention time. It was found that the rates of 1.3, 2.3, and

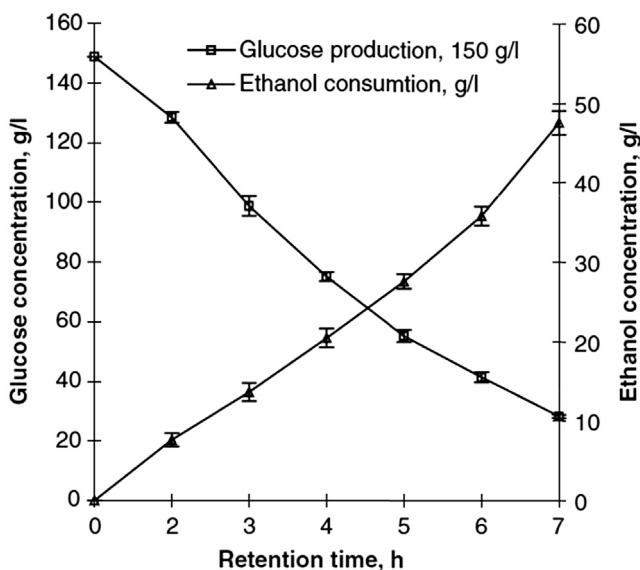


FIGURE 8.16 Glucose concentration and ethanol production versus retention time in immobilized cell reactor with initial substrate concentration of 150 g l^{-1} glucose. Reprinted from Najafpour et al.¹⁵ Copyright with permission from Elsevier.

$2.8 \text{ g l}^{-1} \text{ h}^{-1}$ for 25, 35, and 50 g l^{-1} glucose concentrations were optimal. Ethanol productivities with various substrate concentrations were linearly dependent on retention time (Figure 8.16). The proportionality factor may have increased while the substrate concentration increased. As the sugar concentration doubled, the slope of the line for ethanol productivity with 50 g l^{-1} sugar increased fivefold. These results indicate that the ICR column has a high capacity to produce very high concentrations of ethanol. The final ethanol concentrations with 25 and 50 g l^{-1} of glucose were 7.6 and 16.73 v/v, respectively.

A high glucose concentration of 150 g l^{-1} was used in continuous fermentation with immobilized *S. cerevisiae*; the obtained data for sugar consumption and ethanol production with retention time are shown in Figure 8.14. As the retention time gradually increased, the glucose concentration dropped, whereas the ethanol concentration profile showed an increase. The maximum ethanol concentration of 47 g l^{-1} was obtained with a retention time of 7 h. The yield of ethanol production was approximately 38% compared with batch data, where only an 8% improvement was achieved.

8.6.4 CONCLUSION

Continuous ethanol production in an ICR was successfully done with high sugar concentrations. In batch fermentation, when the concentration of glucose was 50 g l^{-1} , substantial substrate inhibition occurred. The advantage of the ICR was that the inhibition of substrate

and product were not apparent even with a 150 g l^{-1} glucose solution in the fresh feed (data not shown). The ICR system exhibited a higher yield of ethanol production (38%) than the batch system. The ICR column gave a high performance to processing feed with concentrated sugar. Most of ICR experimental runs resulted in a glucose consumption of 82–85%. The results indicate that the immobilization of *S. cerevisiae* possesses the capacity not only to use high concentrations of sugar, but also to yield higher ethanol productivities during the course of continuous fermentation. Ethanol production in the ICR column increased fivefold, as the glucose concentration was doubled from 25 to 50 g l^{-1} . The new findings in the present investigation confirmed the application of concentrated feed with a higher rate of ethanol production, because the cell loaded into the gel matrices of sodium alginate shown in the SEM micrographs eliminated the free cells from the ethanol product stream.

NOMENCLATURE

- A_0 Initial activity of bacterium ($\text{U g}^{-1} \text{ cell}$)
 A_t Activity of bacterium at time t ($\text{U g}^{-1} \text{ cell}$)
 C Microorganisms cell concentration (g l^{-1})
 k_d Dissociation constant (h^{-1})
 K_s Monod constant (g l^{-1})
 S Substrate concentration (g l^{-1})
 T Time (h)
 μ Specific growth rate ($\text{g l}^{-1} \text{ h}^{-1}$)
 μ_m Maximum specific growth rate (h^{-1})

Acknowledgment

The present research was made possible through an Intensive Research Priority Area (IRPA) grant No. 03-02-05-9016, sponsored by the Universiti Sains Malaysia. We thank the Research Creativity & Management Office, Universiti Sains Malaysia, Penang, Malaysia. Special thanks go to the Ministry of Science Technology and Environment (MOSTE), Kuala Lumpur, Malaysian government, for their financial support for IRPA.

References

1. Chum LH, Overend RP. *Fuel Bioprocess Technol* 2001;**17**:187.
2. Flickinger MC, Drew SW. In: *Encyclopedia of bioprocess technology: fermentation, biocatalysis, and bioseparation*, vol. 2; 1999. p. 939.
3. Gunasekaran P, Raj KC. *Ethanol fermentation technology — Zymomonas mobilis*; 2001. <http://ces.iisc.ernet.in/curscinev/july10/articles14.htm>.
4. Baily JE, Ollis DF. *Biochemical engineering fundamentals*. New York: McGraw-Hill; 1986 [chapter 3].
5. Ingram LO, Gomez PF, Lai X, Moniruzzaman M, Wood BE. *Biotechnol Bioeng* 1998;**58**:204.
6. Holzberg I, Finn RK, Steinkraus KH. *Biotechnol Bioeng* 1967;**9**:413.
7. Nagodawithana TW, Steinkraus KH. *J Appl Env Microbiol* 1976;**31**:158.
8. Vega JL, Clausen EC, Gaddy JL. *J Enzyme Microb Technol* 1988;**10**:390.
9. Takamitsu I, Izumida H, Akagi Y, Sakamoto M. *J Ferment Bioeng* 1993;**75**:32.
10. Yamada T, Fatigati MA, Zhang M. *Appl Biochem Biotechnol* 2002;**98**:899.
11. Najafpour G. Organic acids for biomass by continuous fermentation. *Resour Conserv* 1987;**17**:187.
12. Gikas P, Livingston AG. *Biotechnol Bioeng* 1997;**55**:660.
13. Riley MR, Muzzio FJ, Buettner HM, Reyes SC. *Biotechnol Bioeng* 1996;**49**:223.

14. Senthuran A, Senthuran V, Mattiasson B, Kaul R. *Biotechnol Bioeng* 1997;**55**:841.
15. Najafpour GD, Younesi H, Ku Ismail KS. Ethanol fermentation in immobilized cell reactor (ICR) using *Saccharomyces cerevisiae*. *Bioresour Technol* 2004;**92**(3):251.
16. Summers JB. *J Biol Chem* 1924;**62**:248.
17. Miller GL. *Anal Chem* 1959;**31**:426.
18. Yuan YJ, Wang SH, Song ZX, Gao RC. *J Chem Technol Biotechnol* 2002;**77**:602.

SUBCHAPTER

8.7

Fundamentals of Immobilization Technology, and Mathematical Model for ICR Performance

It is well-known that pure enzymes change their behavior and stability when they are immobilized. In the past two decades, the immobilization of microorganisms, cells, and parts of cells has gradually been introduced into microbiology and biotechnology. The cell immobilization techniques are modifications of the techniques developed for enzymes. However, the larger size of microbes has influenced the techniques. As for immobilized enzymes, two broad types of method have been used to immobilize microorganisms: attachment to a support and entrapment.

8.7.1 IMMOBILIZATION OF MICROORGANISMS BY COVALENT BONDS

By these methods microorganisms are cross-linked by chemical substances, e.g., by glutaraldehyde. The surfaces (especially the proteins) of microorganisms are linked with the surfaces of other microorganisms by aldehyde groups of glutaraldehyde. Yeast cells, for instance, react with free ϵ -amino group or N-terminal amino groups to form imines. Another reaction mechanism was proposed for a conjugated addition of amino groups to double linkages of α - and β -unsaturated oligomers, which are present in commercial aqueous solutions of glutaraldehyde. This mechanism may explain the stability of the linkages. By this chemical linking, growth inhibition and toxic influences on the microorganisms are very intensive. These reactions are only partly understood and can lead to decay or death of the microorganisms.

8.7.2 OXYGEN TRANSFER TO IMMOBILIZED MICROORGANISMS

Availability of oxygen is one of the most important parameters that are different for immobilized and free microorganisms. Free organisms can get oxygen directly from the surrounding air or, in most technical processes, from the liquid, especially water, which contains dissolved oxygen. The molar transfer of oxygen with respect to time, dO_2/dt , can be described by the following equation:

$$\frac{dO_2}{dt} = K_L a (C_g - C_L) \quad (8.7.2.1)$$

K_La is the volumetric oxygen mass transfer coefficient, owing to the oxygen transfer from the gas phase or air, C_g , to the surface of the cells, C_x or to the transfer of oxygen dissolved in water to the surface of the cells. In principle, the same formula can be applied to immobilized microorganisms, but here the conditions are quite different. The adsorbed cells form microbial films or varying thickness during a short incubation time. Oxygen has to be transferred into these microfilms, and because of this, zones of different oxygen concentrations exist in the films, in which the growth of the microorganisms varies in direct relation to the oxygen concentration. Using the unsteady-state model, the maximum oxygen penetration depth for highly packed immobilized cells has been reported to be in the range of 50–200 μm .

8.7.3 SUBSTRATE TRANSFER TO IMMOBILIZED MICROORGANISMS

In an immobilized cell bioreactor, significant substrate concentration gradients may exist. Cells are located close to the nutrient supply, which are likely to maintain higher quality and activity than cells located relatively further away, leading to differentiation in the quality or activity of the immobilized cell population. This differentiation is more pronounced if there are starvation regions (practically zero substrate concentration) inside the reactor. Typical approaches for measuring diffusivities in immobilized cell systems include bead methods, diffusion chambers, and holographic laser interferometry. These methods can be applied to various support materials, but they are time-consuming, making it onerous to measure effective diffusivity (D_{eff}) over a wide range of cell fractions. Owing to the mathematical models involved, the deconvolution of diffusivities can be very sensitive to errors in concentration measurements. There are mathematical correlations developed to predict D_{eff} as a function of diffusivities in broth and inside the cells (D_0 , D_c). The relation can also be used to extrapolate D_{eff} measurements from one cell fraction to any other cell fraction. Various values of D_0/D_c have been compiled in Table 8.4 for a variety of immobilized cell systems. These diffusivity ratios for specific systems (i.e., diffusing species, cell type, and gel material) facilitate the prediction of D_{eff} values for a wide range of operating conditions. For a few systems, the diffusivity ratios are very large (∞). The infinite diffusivity

TABLE 8.4 Methods of immobilization

Attachment	Aggregation of floc for formation of cross-linking
Without support cross-linking	Covalent binding
With support	Adsorption to ion-exchangers or inorganic sorbent
	Biofilm formation
Entrapment	Organic polymer
	Inorganic polymer
	Semipermeable membrane

TABLE 8.5 Microbial cells covalently linked to various supports

Species	Support	Product
<i>Acetobacter</i>	Metal hydroxides	Acetic acid
<i>Aspergillus niger</i>	Glycidyl methacrylate	Gluconic acid
<i>Micrococcus luteus</i>	CM-cellulose	Urocanic acid
<i>Saccharomyces cerevisiae</i>	Aminopropyl silica	Ethanol
<i>S. cerevisiae</i>	Hydroxyalkyl methacrylate	Killer toxin
<i>S. cerevisiae</i>	Cellulose	Ethanol
<i>Zygosaccharomyces lactis</i>	Hydroxyalkyl methacrylate	β -Galactosidase

ratio corresponds to a diffusing solute that does not enter the cells (i.e., $D_c = 0$); such cases were observed with large molecules of disaccharide (galactose), polysaccharides and cells of *Zymomonas mobilis* (Table 8.5).

8.7.4 GROWTH AND COLONY FORMATION OF IMMOBILIZED MICROORGANISMS

It was pointed out by several scientists that immobilized microorganisms differ in their growth rates and show altered morphological forms of colonies. Adsorbed cells form micro- and macrofilms in which the microorganisms in the outer region have a different morphology than in the inner region. These microfilms often show different colony forms in relation to their density. Thick films have a slimy character; thin films often show the presence of individual microorganisms. These characteristics can be observed with bacteria, yeast, and with molds. They are caused by differing oxygen concentrations and limited concentrations of nutrients. By referring to our previous work on ICR,¹ a mathematical model for ICR performance may be obtained by applying a mass balance over a differential volume element of the column:

$$\varepsilon \frac{\partial C_A}{\partial t} + u \frac{\partial C_A}{\partial z} = r_A \quad (8.7.4.1)$$

where ε is the void volume of the packed column, C_A is the substrate concentration (g l^{-1}), u represents the bulk fluid velocity (cm h^{-1}), z is the axial reactor length (cm), and r_A denotes the rate of substrate transfer to microbial film ($\text{g l}^{-1} \text{h}^{-1}$).

Assuming plug-flow and steady-state behavior, Eqn (8.7.4.1) reduces to:

$$u \frac{\partial C_A}{\partial z} = r_A \quad (8.7.4.2)$$

Plug-flow behavior has been shown in this type of reactor by tracer studies (Table 8.6).

The reaction rate for simple fermentation systems is normally given by the Monod equation. This model indicates that the specific conversion rate is constant when applied to an

TABLE 8.6 Experimental studies of diffusion in immobilized cell systems and their associated values of D_0/D_c

Cell type	Immobilization	Solute	D_0/D_c
<i>Saccharomyces cerevisiae</i>	Ca-alginate	Glucose	0.1
Baker's yeast	Ca-alginate	Glucose	10.6
Ehrlich ascites tumor	Agar, collagen	Glucose	2.4
<i>Zymomonas mobilis</i>	K-carrageenan, Ca-alginate	Glucose	∞
<i>Pseudomonas aeruginosa</i>	Ca-alginate	Glucose	2.3
<i>Saccharomyces cerevisiae</i>	Ca-alginate	Glucose	2.8
Plant	Ca-alginate	Sucrose	∞
Baker's yeast	Ca-alginate	Galactose	15.8
<i>Zymomonas mobilis</i>	Ca-alginate	Galactose	∞
Baker's yeast	Ca-alginate	Lactose	∞
Ehrlich ascites tumor	Agar, collagen	Lactic acid	6.7
<i>Clostridium butyricum</i>	Polyacrylamide, agar collagen	Hydrogen	3.2
<i>Escherichia coli</i>	Natural aggregates	Nitrous oxide	3.9
<i>S. cerevisiae</i>	Fermentation media	Oxygen	2.3
<i>S. cerevisiae</i>	Ca-alginate, Ba-alginate	Oxygen	0.1
<i>Escherichia coli</i>	Fermentation media	Oxygen	2.2
<i>Penicillium chrysogenum</i>	Fermentation media	Oxygen	5.6
<i>Bacillus amyloliquefaciens</i>	Ca-alginate, PVA-SbQ gel	Oxygen	1.8
<i>S. cerevisiae</i>	Ca-alginate	Ethanol	0.1
Baker's yeast	Ca-alginate	Ethanol	∞

immobilized cell system (Table 8.7). If a first-order rate equation for sugar consumption is used, Eqn (8.7.4.2) yields:

$$u \frac{\partial C_A}{\partial z} = kC_A \quad (8.7.4.3)$$

Equation (8.7.4.3) is a linear first-order differential equation for concentration and reactor length. After separation of variables, the equation can be integrated as:

$$\int_{C_{A_0}}^{C_A} \frac{dC_A}{C_A} = \int_0^z \frac{k dz}{u} \quad (8.7.4.4)$$

TABLE 8.7 Ethanol productivity from immobilized systems

System	Feed sugar concentration (g l ⁻¹)	% of Feed sugar utilization	Dilution rate (h ⁻¹)	Max. ethanol productivity (g l ⁻¹ h ⁻¹)
<i>Saccharomyces cerevisiae</i> carrageenan	Glucose 100	86	1.0	43
<i>S. cerevisiae</i> Ca-alginate	Glucose 127	63	4.6	53.8
<i>S. cerevisiae</i> Ca-alginate	Molasses 175	83	0.3	21.3
<i>S. cerevisiae</i> Carrier A	Molasses 197	74	0.35	25
<i>Zymomonas mobilis</i> Ca-alginate	Glucose 150	75	0.85	44
<i>Zymomonas mobilis</i> Ca-alginate	Glucose 100	87	2.4	102
<i>Z. mobilis</i> carrageenan	Glucose 150	85	0.8	53
<i>Z. mobilis</i> flocculation	Glucose 100			120
<i>Z. mobilis</i> borosilicate	Glucose 50			85
<i>Z. mobilis</i> carrageenan-locust bean gum	Whey-lactose 50	98		178

Integration of the above differential equation yields:

$$\ln(C_A/C_{A_0}) = \frac{kz}{u} \quad (8.7.4.5)$$

Thus a linear relation between $\ln(C_A/C_{A_0})$ and the reactor length should exist if the model accurately describes the immobilized cell reactor. The experimental data fitting the model were discussed previously.

8.7.5 IMMOBILIZED SYSTEMS FOR ETHANOL PRODUCTION

The most significant advantage of immobilized cell systems is the ability to operate with high productivity at dilution rates exceeding the maximum specific growth rate (μ_{\max}) of the microbe. Several theories have been proposed to explain the enhanced fermentation capacity of microorganisms as a result of immobilization. A reduction in the ethanol concentration in the immediate microenvironment of the organism owing to the formation of a protective layer or specific adsorption of ethanol by the support may act to minimize end product inhibition. Alternatively, substrate inhibition may be diminished in the case of a gel matrix, if the rate of fermentation meets or exceeds the rate of glucose diffusion to the cell. A third possibility is that alteration of the cell membrane during immobilization provides improved transfer of substrate into and product out of the microbe.

The effect of temperature on the rate of ethanol production is markedly different for free and immobilized systems. Thus while a constant increase in rate is observed with free *S.*

cerevisiae as temperature is increased from 25 to 42 °C, a maximum occurs at 30 °C with cells immobilized in sodium alginate. The lower temperature optimum for immobilized systems may result from diffusional limitations of ethanol within the support matrix. At higher temperatures, ethanol production exceeds its rate of diffusion so that accumulation occurs within the beads. The achievement of inhibitory levels then causes the declines observed in the ethanol production rate.

Significant differences are also apparent for the effect of pH on the fermentation rate. The narrow pH optimum characteristic of a free cell system is replaced by an extremely broad range upon immobilization. This effect stems from the gradient pH that exists within the bead.

Reference

1. Najafpour GD. *Resour Conserv* 1987;13:187.

Material and Elemental Balance

OUTLINE

9.1 Introduction	291	9.6 Conservation of Mass Principle	309
9.2 Media Preparation for Fermentation	292	9.6.1 Acetic Acid Fermentation Process	312
9.2.1 Medium Formulation	293	9.6.2 Xanthan Gum Production	314
9.2.2 Preparation of Anaerobic Media	295	9.6.3 Stoichiometric Coefficient for Cell Growth	317
9.2.3 Preparation of Minimal Media and Standard Media	301	9.7 Embden–Meyerhof–Parnas Pathway	318
9.3 Growth of Stoichiometry and Elemental Balances	303	9.7.1 Description of Glycolysis	319
9.4 Energy Balance for Continuous Ethanol Fermentation	305	References	326
9.5 Mass Balance for Biological Processes	306		

9.1 INTRODUCTION

All microorganisms require nutrients for propagation and to produce metabolites as useful byproducts. Medium is supplied to the reaction vessel while the products leave through effluent for downstream processing. Balancing individual elements assists us in understanding biocatalytic activities and monitoring the downstream process. Nutrients are supplied in aqueous media with carbon, nitrogen, and phosphorus sources. Mineral elements, vitamins, and oxygen are also provided to enhance microbial growth. Once a system is selected, we

balance the inlet and outlet compositions. Knowledge of microbial elemental compositions such as C, H, N, S, P, Mg, Na, and K is required to solve the elemental balance equation. Normally trace metals and minerals such as Fe, Cu, Zn, Co, Mn, and Mo are required in small quantities, which act as growth stimulants with sufficient energy sources to provide adenosine triphosphate (ATP) as needed, for biochemical reactions to precede and progress.¹ Carbohydrates as substrates are used in the cells to generate energy and carry out biosynthesis. An adequate carbon source is essential to ensure cell growth. Nutrients are frequently added into the media in substantially excessive amounts than are required by the cell, but the amount of trace metals and minerals supplied is limited.²⁻⁴

For any viable microorganism in a fermentation process, we should be able to respond to the following questions:

- What would the respiration quotient be related to the concentration of CO₂ generated in the fermentation process, known as off gas?
- What fraction of substrate is consumed and how much substrate is converted to biomass and end products?
- If the process is aerobic, how much O₂ is required?
- What would the oxygen transfer rate be?

To answer these questions, the media used to propagate and culture organisms are discussed; then, mass balance is required for microorganisms to determine conversion and how much air has to be supplied into the fermentation broth. The substrate consumption or production rates must be set as a starting point. To provide suitable answers to these statements, we may approach the questions by reviewing a few biological processes and illustrating the assumptions and process conditions.

9.2 MEDIA PREPARATION FOR FERMENTATION

A recent survey showed that many research papers are published for the purpose of identifying suitable a media composition for maximum growth and productivity. Various software packages have been developed to optimize the chemical composition of media. Appropriate media for cultivating microorganisms are necessary to contain carbon, nitrogen, and phosphorous sources. The media have to be prepared in advance before inoculum is transferred to them. Media have to meet certain requirements to provide a suitable environment for an organism to have safe and sustainable growth. All organisms are required to live in water while necessary nutrients are available for the organism in the aqueous phase. Water acts as the desired environment for keeping all nutrients in the soluble phase. Based on the concentration of gradients, nutrients diffuse through the cell wall. In addition, the energy source for all viable cells is supplied by a carbon source and nitrogen and phosphorous compounds are required for the biosynthesis of essential compounds such as amino acids and nucleic acids. Enzymes have an important role as biocatalysts and energize biochemical reactions to be formed. Most enzymes for an active state require a center core of metal ions (e.g., Co, Cu, Mn, Mo, Zn, Fe, and B). For certain organisms, vitamins and supplementary nutrients are essential to secure cell growth. Some organisms are unable to synthesize nucleic acids, amino acids, and vitamins. Therefore, specific growth factors are identified and

incorporated as supplements into media. In addition, media should have mineral and trace metals for enzymes to function properly. Most organisms such as yeast can easily grow in simple media consisting of glucose as a carbon source; yeast extract for the purpose of nitrogen supply and phosphate buffer provides a medium stability of pH and phosphorylate carbohydrates. A carbon source is used as the energy requirement for the synthesis of biomolecules through anabolism and catabolism, which may assist organism in selecting a living respiration path. The yield of biomolecule generation for one organism may be different from that of others.

9.2.1 Medium Formulation

In designing media for the propagation of organisms in synthesizing energy and biomolecules, knowledge of the elemental composition of an organism, including C, H, O, N, and P, and S and trace metal elements, is required. In fact, in the growing media elemental balance is essential to determine the ability of an organism to synthesize a product.

Media for the growth of bacteria requires carbon and nitrogen sources plus supplements of yeast extract, meat extract, and peptone. For a yeast cell to grow, common media would be yeast extract (1%), peptone (2%), plus glucose: media with three components. The addition of 1.5% agar is used for plate agar to culture organisms on a Petri dish. The yeast extract (1%), malt extract (1.5%), and bacto-agar (1.5%) is known as YM agar medium for culturing most organisms. It is recommended to incubate the inoculated medium at 32 °C. Bacteria form colonies on plate agar; one can identify the purity of a culture by inspecting the appearance of the colony while filamentous organisms such as fungi form spores; therefore, colony counting may not be suitable for such organisms.

McInerney et al.⁵ proposed enriched complex media for growing anaerobic methanogenic bacteria to convert fats into biogas as a energy source. Mixtures of all vitamins are stirred for several hours without heating; then, they are dispensed into plastic storage bottles and kept in a freezer for future use. The vitamin solution has to be refrigerated for short or long durations of use. Metal ions and trace minerals essential for growth are summarized in Table 9.1.

TABLE 9.1 Mixture of stock solution of trace metals and minerals⁵

PFN minerals	g l ⁻¹	PFN trace metals	g l ⁻¹
KH ₂ PO ₄	10.0	ZnSO ₄ ·7H ₂ O	0.1
MgCl ₂ ·6H ₂ O	6.6	MnCl ₂ 0·4 H ₂ O	0.03
NaCl	8.0	H ₃ BO ₃	0.3
NH ₄ Cl	8.0	CoCl ₂ ·6H ₂ O	0.2
CaCl ₂ ·2H ₂ O	1.0	CuCl ₂ ·H ₂ O	0.01
		NiCl ₂ ·6H ₂ O	0.02
		Na ₂ MoO ₄ ·2H ₂ O	0.03
		FeCl ₂ ·4H ₂ O	1.5
		Na ₂ SeO ₃	0.01

TABLE 9.2 Vitamin stock solution⁶

B Vitamins	mg l ⁻¹
Biotin	20
Folic acid	20
Pyridoxal HCl	10
Lipoic a. (thioctic a.)	60
Riboflavin	50
Thiamine HCl	50
Ca-D-pantothenate	50
Cyanocobalamine	50
<i>p</i> -Aminobenzoic acid	50
Nicotinic acid	50

The metal ions and trace minerals are introduced as Pfennig (PFN) metals and PFN trace metals, respectively. The mineral media for use are dispensed into 100-ml quantities in serum bottles and autoclaved for 20 min for further use.

Genthner et al.⁶ investigated the impact of effective vitamins in the growth of anaerobic bacteria; the stock solution of vitamins is shown in Table 9.2. The basal media used for anaerobic bacteria (*Peptostreptococcus*) products are summarized in Table 9.3.

TABLE 9.3 Basal media composition in 1000 ml solution

Composition	g l ⁻¹	^a g l ⁻¹
Glucose or sodium acetate	10	6
Yeast extract	1	0.5
PFN minerals	50 ml	30 ml
PFN trace metals	1 ml	1 ml
B vitamins	5 ml	5 ml
Resazurin (0.1%)	1 ml	—
NaHCO ₃	2.5	2.4
Ammonium chloride		2.6
Distilled water	1000 ml	1000 ml

Note: Use full volume of water to allow for some loss during boiling.

^aCultured *Rhodospirillum rubrum* for hydrogen production.

9.2.2 Preparation of Anaerobic Media

The preparation of media for strict anaerobe organisms is not easy, especially using the media to bioconvert synthesized gas to hydrogen. A mixture of all ingredients for media preparation, except NaHCO_3 , is prepared in a separate boiling flask. Place cotton into the mouth of a 1 ml pipette with a gas mixture of 80% N_2 and 20% CO_2 flowing through the pipette; degas the hot clear media solution to prevent the presence of any dissolved oxygen. Otherwise, place it in a boiling flask and hang it above the gas burner, about 10 cm from the flame. Bring the solution to the boiling point and then boil it for 2 min to drive off dissolved O_2 . After boiling, leave the flushing pipette in the neck of the flask, flow it with $\text{N}_2:\text{CO}_2$ to prevent O_2 from being pulled into the flask as it cools. When the solution has cooled to about 50°C , add the NaHCO_3 to the flask (the media color will change to bright pink). Flush the pipette with a 16 G 1.5 needle in the neck of the flask several times. Place gas lines into the bottles or tubes before, while, and after filling, for about 30 s. Carefully pull out the gas line while inserting a rubber septum and crimp an aluminum seal over the rubber septum. The prepared bottled media are autoclaved for 20 min. The pH of prepared media for gas bioconversion after autoclaving is about 7. Table 9.4 shows the composition of media for anaerobic bacteria.

To prepare basal media, details are listed as follows:

1. For basal medium without yeast extract, add only 0.2 g NaHCO_3 /100 ml medium. The media final pH is about 7.
2. For basal medium without yeast extract plus 5 ml/100 ml medium of filtered sludge, add 0.25 g NaHCO_3 /100 ml medium to get a media final pH of about 7.
3. For basal medium without yeast extract plus 1.5% sodium acetate, add 0.25 g NaHCO_3 /100 ml medium to obtain a media final pH of about 7. Always check the pH on a finished bottled medium. Withdraw 1 ml with a sterile syringe and put the solution into a 2 ml conical centrifuge tube. Check the pH of the sampled medium. Use the bottle of medium at a later time. The pH can change from time to time if the $\text{CO}_2\%$ varies or if the distilled water composition has changed.

For media preparation, distribute serum bottles under anaerobic conditions; special precautions are required. First, all ingredients are mixed except sodium bicarbonate (NaHCO_3); then, boil the solution. Cool it off with a gas mixture of $\text{N}_2:\text{CO}_2$, 80:20%. Cool to about room

TABLE 9.4 Anaerobic media composition for variable volume

Media composition	400 ml	500 ml	600 ml	750 ml	800 ml
Yeast extract, g	0.4	0.5	0.6	0.75	0.8
PFN minerals, ml stock	20	25	30	37.5	40
PFN trace minerals, ml	0.4	0.5	0.6	0.75	0.8
B vitamins, ml stock	2.0	2.5	3.0	3.75	4.0
Resazurin (0.1%), ml	0.4	0.5	0.6	0.75	0.8
NaHCO_3 , g	1.0	1.25	1.5	0.88	2.0

TABLE 9.5 Media for methanogenic bacteria, composition of media in 1000 ml

NH ₄ Cl	2.7 g
FeSO ₄	0.01 g (dissolve 0.1 g in 10 ml distilled water)
Sodium acetate	2.5 g (optional)
NaHCO ₃	2 g
Mineral solution I	50 ml
Mineral solution II	50 ml
Trace metals III	10 ml
B vitamins IV	10 ml
Resazurin (0.1%)	1 ml

TABLE 9.6 Minerals, trace metals and vitamin composition for the preparation of media

Mineral I	g l ⁻¹	B vitamins IV	mg l ⁻¹
K ₂ HPO ₄	6	Biotin	2.0
Mineral II	g l ⁻¹	Folic acid	2.0
KH ₂ PO ₄	6.0	Pyridoxine HCl	10.0
(NH ₄) ₂ SO ₄	6.0	Riboflavin	5.0
NaCl	12.2	Nicotinic acid	5.0
MgCl ₂ ·6H ₂ O	4.0	Ca-pantothenate	5.0
MgSO ₄ ·7H ₂ O	2.6	Cyanocobalamin (vitamin B ₁₂)	0.10
		<i>p</i> -Aminobenzoic acid	5.0
		Lipoic acid (thioctic acid)	5.0

temperature and then add NaHCO₃ before bottling anaerobically. The final pH of the prepared media is about 7. The bottled media are autoclaved for 20 min. The media composition of methanogenic bacteria is listed in Table 9.5. Table 9.6 introduces media with minerals, trace metals, and vitamins. The composition of mineral solutions I and II and vitamin combinations are summarized in Table 9.6. Table 9.7 shows several combinations of trace metal ions effective for microbial growth.

For media preparation, mix all ingredients except NaHCO₃ and boil for 2 min with 80% N₂:20% CO₂. Cool and add NaHCO₃ before bottling anaerobically. The pH of media before boiling is 6.6, after boiling the pH drops to 5.8, whereas after adding NaHCO₃ the pH is nearly neutral (6.97). The pH after autoclaving is 7. The solution of 0.25 g NaHCO₃ in 100 ml will rise to pH 7 or even slightly greater than 7. The minimal medium used for methanogenic bacteria is shown in Table 9.8. Table 9.9 lists minerals and vitamins required for microbial growth. Table 9.10 shows different constituents of the complex media.

TABLE 9.7 Different combinations of trace metal ions used as growth stimulants

Trace metals III	G l ⁻¹
CoCl ₂	0.1
Na ₂ MoO ₄ ·2H ₂ O	0.024
NiCl ₂ ·6H ₂ O	0.024
Nitrilotriacetate	1.5; adjust pH with KOH, then add to other minerals
Na ₂ SeO ₃	0.024 in 10 ml concentrated HCl (optional)

TABLE 9.8 Minimal media composition for 500 and 1000 ml

Components	Grams per 1000 ml	Grams per 500 ml
NH ₄ Cl	2.7 g	1.35 g
NaHCO ₃	2 g	1.0 g
Mineral solution I	50 ml	25 ml
Mineral solution II	5 ml	25 ml
Wolfe's minerals III	1 ml	5 ml
Wolfe's vitamins IV	1 ml	5 ml
Resazurin (0.1%)	0.1 ml	0.5 ml
Distilled water	88 ml	470 ml to allow under gas boiling

TABLE 9.9 Combinations of minerals and vitamins used in complex media

Mineral I	g l ⁻¹	Wolfe's vitamins IV	mg l ⁻¹
K ₂ HPO ₄	6.0	Biotin	2.0
		Folic acid	2.0
Mineral II	g l ⁻¹	Pyridoxine HCl	10.0
KH ₂ PO ₄	6.0	Riboflavin	5.0
(NH ₄) ₂ SO ₄	6.0	Nicotinic acid	5.0
NaCl	12.0	Ca-pantothenate	5.0
CaCl ₂ ·H ₂ O	1.6	Vitamin B ₁₂	0.10
MgSO ₄ ·7H ₂ O	2.4	<i>p</i> -Aminobenzoic acid	5.0
		Thioctic (lipoic) acid	5.0
		Thiamine HCl	5.0

TABLE 9.10 Complex media with different constituents

Wolf's minerals III	g l ⁻¹		g l ⁻¹
Nitrilotriacetic acid	1.5	ZnSO ₄	0.01
MgSO ₄	3.0	CuSO ₄	0.01
MnSO ₄	0.5	AlK(SO ₄) ₂	0.01
NaCl	1.0	H ₃ BO ₃	0.01
FeSO ₄	0.1	Na ₂ MoO ₄	0.01
CaCl ₂	0.1	NiCl ₂ ·6H ₂ O	0.024
CoCl ₂	0.1		

TABLE 9.11 Complex medium with defined chemical composition in 100 ml medium

Minerals	5.0 ml
Trace metals	0.5 ml
B vitamins (same solution as basal medium)	2.0 ml
Amino acid solution (2 mg l ⁻¹ of each in final medium)	12.5 ml
Resazurin solution (0.1%)	0.1 ml
Distilled water	80 (+5) ml

Note that some methanogenic bacteria can grow well by adding sodium acetate. An exact amount of sodium acetate, 0.25 g in 100 ml medium, is added, or 0.5 ml of 2 M sodium acetate (sterile) may be added to 50 ml of the prepared medium. Table 9.11 shows rich medium with known chemical compositions.

In mixing the basal medium, the pH is adjusted to 5 before boiling. Other cultures may require pH 6–7. The required carbon source such as synthesized gas should be added after inoculation. The mixture of amino acids mostly contains valine, threonine, arginine, histidine, methionine, lysine, leucine, cysteine, glutamic acid, phenylalanine, serine, asparagines, and tryptophan; each amino acid has a concentration of 16 mg·l⁻¹. Table 9.12 shows a complex medium for anaerobic culture. The media required trace metal ions and amino acids.

For a culture, if it is grown in culture tubes, a gas flow of helium over the medium instead of N₂/CO₂ is used. Add a synthesized gas pressure of 10–15 psi as carbon source. As synthesized gas is used, the He should maintain a positive pressure in the bottle or tubes; this should not produce a vacuum inside the bottle or tube. For growth in bottles, autoclave with purge gas of N₂/CO₂ in the gas phase; then, synthesized gas after inoculation is used. Initially the culture is flushed and then charged. Several suggested ATCC media for certain organisms are listed in the following tables (see Tables 9.13–9.16).

TABLE 9.12 Chemical composition of a complex medium

Trace metals	g l ⁻¹	Grams in 500 ml	Minerals	Grams in 500 ml	g l ⁻¹
Nitrilotriacetate	1.5	0.75	(NH ₄) ₂ SO ₄	5.0	10.0
MgSO ₄ ·7H ₂ O	6.1	3.05	NH ₄ Cl	5.0	10.0
MnSO ₄ ·H ₂ O	0.5	0.25	KH ₂ PO ₄	68.0	136.0
NaCl	1.0	0.5			
FeSO ₄ ·7H ₂ O	0.1	0.05			
CoCl ₂ ·6H ₂ O	0.1	0.05			
CaCl ₂ ·2H ₂ O	0.1	0.05			
ZnCl ₂	0.1	0.05			
CuCl ₂ ·xH ₂ O	0.01	0.005			
AlK(SO ₄) ₂ ·12H ₂ O	0.01	0.005			
H ₃ BO ₃	0.01	0.005			
Na ₂ MoO ₄ ·2H ₂ O	0.01	0.005			
NiCl ₂ ·6H ₂ O	0.05	0.025			
Na ₂ SeO ₃	0.0005	0.00025			

TABLE 9.13 ATCC medium for culturing *Rhodocyclus gelatinosus*

Composition	Grams in 100 ml	Grams in 300 ml	g l ⁻¹
K ₂ HPO ₄	0.1	0.3	1.0
MgSO ₄ ·7H ₂ O	0.1	0.3	1.0
Yeast extract	1.0	3.0	10.0
PFN minerals (trace)	0.1 ml	0.3 ml	1.0 ml
Resazurin (0.1%)	0.1 ml	0.3 ml	1.0 ml
PFN vitamins	0.5 ml	1.5 ml	5.0 ml

TABLE 9.14 ATCC medium with yeast malt extract for *Streptomyces* sp.

Composition	Grams in 100 ml	Grams in 300 ml	g l ⁻¹
Yeast extract	0.4	1.2	4.0
Malt extract	1.0	3.0	10.0
Glucose	0.4	1.2	4.0
Agar	2.0	6.0	10.0

TABLE 9.15 ATCC medium with peptone—yeast extract for *Brevibacterium lactofermentum* and *Zymomonas mobilis*

Components	%	Components	%
Glucose	1	Glucose	2
Bacto-peptone	1		
Yeast extract	1	Yeast extract	1
NaCl	0.5	KH ₂ PO ₄	0.2

TABLE 9.16 ATCC medium for *Acetobacterium*

Composition	Grams in 100 ml	Grams in 300 ml	Grams in 500 ml
Yeast extract	0.1	0.3	0.5
NH ₄ Cl	0.1	0.3	0.5
MgSO ₄ ·7H ₂ O	0.01	0.03	0.05
KH ₂ PO ₄	0.04	0.12	0.2
K ₂ HPO ₄	0.04	0.12	0.2
Wolfe's vitamins	1 ml	3 ml	5 ml
Wolfe's mineral	1 ml	3 ml	5 ml
Fructose (2.5 ml of a 20% solution)	0.5 ml	1.5 ml	2.5 ml
Resazurin (0.01%)	0.1 ml	0.3 ml	0.5 ml
NaHCO ₃	0.3	0.9	1.5

Adjust the pH to 7.2 and prepare the medium through the usual anaerobic technique. After boiling, add 0.2 g NaHCO₃ in 100 ml solution; the final pH is 7.

Fructose is sterilized separately and added after autoclaving. The pH of the medium is adjusted to 6.7. Media are prepared by the usual anaerobic technique. The preparation of tris maleate buffer solution and composition of Wolfe's mineral solution are shown in [Tables 9.17 and 9.18](#), respectively.

TABLE 9.17 Tris maleate buffer solution

Solution A: 250 ml l ⁻¹	25 ml	62.5 ml	125 ml	250 ml
Solution B: 200 ml l ⁻¹	20 ml	50 ml	100 ml	200 ml
Distilled water to volume	53 ml	132.5 ml	265 ml	530 ml

TABLE 9.18 Wolfe's mineral solution

Composition	g l ⁻¹
Nitriloacetic	1.5
MgSO ₄	3.0
MnSO ₄	0.5
NaCl	1.0
FeSO ₄	0.1
CaCl ₂	0.1
CoCl ₂	0.1
ZnSO ₄	0.1
CuSO ₄	0.01
AlK(SO ₄) ₂	0.01
H ₃ BO ₃	0.01
Na ₂ MoO ₄	0.01

The media rough pH estimation will be about 6.7.

Solution A: Contains 0.2 M Tris acid maleate; add 24.2 g tris (hydroxymethyl) aminomethane, 23.2 g maleic acid, or 19.6 malic anhydride in 1 l distilled water.

Solution B is 0.2 M NaOH, which is 8 g NaOH dissolved in 1 l distilled water MgSO₄·7H₂O. prepare a 1% solution. Use 10 ml l⁻¹ to get 0.01%. Store in a refrigerator. For MnSO₄·H₂O: prepare a 0.1% solution. Use 10 ml l⁻¹ to get 0.001%. Store in a refrigerator.

9.2.3 Preparation of Minimal Media and Standard Media

Minimal medium contains the essential nutrients for growth of bacterial species. The medium is often used for a particular microbial species of heterotroph organism that has no nutritional requirements beyond core sources of carbon (dextrose) and nitrogen for the synthesis of amino acids and nucleic acids. Auxotroph organisms with nutritional requirements may not be able to grow on minimal medium. The medium components are glucose as the carbon source and nitrogen source. Often, ammonium chloride is used as the nitrogen source because most bacterial species are unable to use atmospheric nitrogen to convert to an amine group. In fact, nitrogen is used to synthesize amino acids for proteins and bases for nucleic acids. Mineral ions and trace metals are present in the medium as core nutrients such as sodium, potassium, calcium, phosphorus and magnesium. Phosphate buffer 0.1 M solution (sodium phosphate, Na₂HPO₄·7H₂O and potassium phosphate, KH₂PO₄) is prepared (Table 9.19).

The pH of medium is adjusted to 6.8 by gassing with a mixture of N₂ and CO₂. The medium is dispensed into serum bottles under mixed gas of 80% N₂ and 20% CO₂ and then

TABLE 9.19 Modified minimal medium ATCC medium

Components	g l^{-1}
NH_4Cl	0.1
$\text{MgSO}_4 \cdot 7\text{H}_2\text{O}$	0.2
$\text{CaCl}_2 \cdot 2\text{H}_2\text{O}$	0.1
K_2HPO_4	0.05
NaHCO_3	20 mM
Thiosulfate	10 mM
Wolfe's mineral solution (see Table 9.18)	10 ml
Vitamin solution (see Table 9.9)	10 ml
Distilled water	1000 ml

For solid medium 1.5% agar is added.

TABLE 9.20 Standard medium for growth of *Candida* sp

Composition	g l^{-1}	Mineral I	g l^{-1}
Maltose	1.0	Maltose	1.0
NaNO_3	3.0	NH_4Cl	1.89
K_2HPO_4	1.0	K_2HPO_4	1.0
$\text{MgSO}_4 \cdot 7\text{H}_2\text{O}$	0.5	$\text{MgSO}_4 \cdot 7\text{H}_2\text{O}$	0.5
KCl	0.5	KCl	0.5
$\text{FeSO}_4 \cdot 7\text{H}_2\text{O}$	0.01	$\text{FeSO}_4 \cdot 7\text{H}_2\text{O}$	0.01
Agar	15.0	Agar	15.0
pH adjusted to 5.6		pH adjusted to 5.6	

TABLE 9.21 Standard medium peptone, glucose, yeast extract for *Propioni bacterium*

Medium composition	100 ml	250 ml	500 ml	1000 ml
Peptone	1 g	2.5 g	5 g	10 g
Yeast extract	1 g	2.5 g	5 g	10 g
Glucose	1 g	2.5 g	5 g	10 g
$\text{MgSO}_4 \cdot 7\text{H}_2\text{O}$	1 ml	2.5 ml	5 ml	10 ml
$\text{MnSO}_4 \cdot \text{H}_2\text{O}$	1 ml	2.5 ml	5 ml	10 ml

TABLE 9.22 Preparation of standard medium with bioextract for *Saccharomyces cerevisiae*

Nutrient components	g l ⁻¹
C ₆ H ₁₂ O ₆	10
(NH ₄) ₂ SO ₄	2.6
K ₂ HPO ₄	1.0
KH ₂ PO ₄	0.5
Na ₃ PO ₄ ·12H ₂ O	3.66
MgSO ₄	0.2
CaCl ₂ 2H ₂ O	0.01
Yeast extract (Difco)	0.5
Peptone	2.0
Glucose	20.0

autoclaved for 20 min. The vitamin and mineral solutions are added after autoclaving 100 µl per 100 ml of medium. For growth the serum bottle is supplied with synthesized gas for 40–60% gas space.

The standard media are designed based on a simple concept of energy and synthesis sources with minimal bases. Tables 9.20–9.22 are a universal standard media composition for *Candida* sp., *Propioni bacterium*, and *Saccharomyces cerevisiae*, respectively.

9.3 GROWTH OF STOICHIOMETRY AND ELEMENTAL BALANCES

Even though cell growth is a complex process, it has to follow the laws of conservation of mass and energy. Nutrients, organic compounds, and other elements for life are involved in metabolic activities. As a result, cells grow, energy is generated, biosynthesis is accomplished, and products are formed. From these examples, the law of conservation of mass can be successfully used to determine unknown components. Cell growth also obeys the law of conservation of mass. Living matter mainly consists of four major elements: C, H, O, and N. These are the four major elements found in carbohydrates, lipids, and proteins used in metabolic processes of cells. The biological products of aerobic growth are carbon dioxide and H₂O. Each element is balanced with the amount removed from the environment. In other words, the amount of metabolic product formed or the amount of heat released by cell growth is proportional to the amount of the substrate consumed and CO₂ formed. Because metabolic products and organic compounds are different from the cell material released into the medium, nutrients and substrates are depleted from the medium; as a result, cells grow and products are formed. Macroscopically, a cell is considered a system in which cell growth is independent of biochemical reaction pathways.

Employing the overall growth rate, as substrate has to penetrate into the system based on concentration gradient and the product and additional biomass leave the system, cell growth is achieved.

Cell growth and metabolic activities are similarly described as a simple chemical reaction. It is also necessary to establish a definite formula for dry cell matter. The elemental composition of certain strains of microorganism is defined by an empirical formula, $\text{CH}_\alpha\text{O}_\beta\text{N}_\delta$. The general biochemical reaction for biomass production is based on consumption of organic substrate, as shown below. Substrate oxidation is simplified in the following biochemical oxidation:



About 95% of *Escherichia coli* is C, H, O, and N. The chemical formula for cell composition and the stoichiometric coefficients in (9.2.1) depend on the media composition and the environment surrounding the cell.^{2,4} All major elements in the above equation have to be balanced.

The stoichiometric coefficients are then identified by simultaneously solving the system of equations:

C balance: $w = c + d$.

H balance: $x + bg = ca + 2e$.

O balance: $y + 2a + bh = c\beta + 2d + e$.

N balance: $z + bi = c\delta$.

Notice that we have five unknown coefficients (a , b , c , d , and e) but four equations. This means we need an additional equation to solve a system of five equations with five unknowns. An important and measurable parameter in a living system is the respiration quotient (RQ), which is defined as moles of CO_2 produced per mole of O_2 uptake.^{1,2}

$$\text{Respiratory quotient (RQ)} = \frac{\text{Moles of } \text{CO}_2 \text{ produced}}{\text{Moles of } \text{O}_2 \text{ consumed}} = \frac{d}{a} \quad (9.3.2)$$

The chemical composition of strains of microorganisms depends on the chemical composition of the media. Even for single strains of organisms such as *E. coli* grown in different media, the fractional composition of C, N, O, and H are different if the media compositions are different.^{2,7} There are a few environmental factors known as growth-rate limitations that affect cell growth and environmental conditions. If a specific nutrient in the medium is suddenly increased, does the growth rate of the cell increase? First, it is necessary to briefly discuss sources needed for microbial growth, and then to respond directly to the points. Often the composition of media is based on a single component that is growth-rate limiting. This means that changing the concentration of the specified nutrient may influence cell growth, and depleting the specified nutrient may retard the growth pattern. Growth can also be inhibited by the product formed. On the other hand, changing the concentrations of components of the medium causes relatively insignificant changes in the alteration of the growth rate. In reality this may not be true because cell growth does not depend on a single substrate; even the growth of cells is extended on yeast extracts. Cell metabolism is not limited to carbohydrate catabolism: fats, lipids, and proteins are involved in the generation

of energy for biosynthesis. The elemental composition of selected microorganisms can be defined as^{2,4}:

Escherichia coli: $\text{CH}_{1.77}\text{O}_{0.49}\text{N}_{0.24}$.

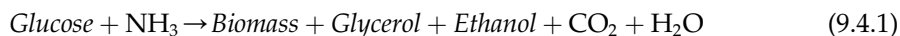
S. cerevisiae: $\text{CH}_{1.64}\text{O}_{0.52}\text{N}_{0.16}$.

Candida utilis: $\text{CH}_{1.83}\text{O}_{0.54}\text{N}_{0.10}$.

When RQ is given, the stoichiometric coefficients can be solved simultaneously.^{4,8}

9.4 ENERGY BALANCE FOR CONTINUOUS ETHANOL FERMENTATION

Saccharomyces cerevisiae is anaerobically grown in a continuous culture at 30 °C. Glucose is used as the substrate and ammonia as the nitrogen source. A mixture of glycerol and ethanol is produced. The following reaction is proposed for the related bioprocess^{4,6}:



The basis of the calculation is operation for 1 h. Necessary data are presented in Table 9.23. The energy balance is based on the first law of thermodynamics:

$$\sum n_{in}h_{in} - \sum n_{out}h_{out} + (-\Delta H_{rxn}) = \delta Q - \delta W \quad (9.3.2)$$

Assume an isothermal operation in which no work done by the system. Then, the first law simplifies to:

$$\delta Q = -\Delta H_{rxn} \quad (9.4.3)$$

Before energy balance is calculated, we need to make mass balance. Figure 9.1 shows the material balance for ethanol and glycerol fermentation. Put simply, mass into the system equals mass out of the system. The mass of carbon dioxide is calculated by adding the

TABLE 9.23 Heat of combustion in fermentation process for production of glycerol and alcohol

Component	Δh_c° , kJ gmol ⁻¹	Molecular mass	kJ kg ⁻¹
Glucose	-2805.0	180	-1.558×10^4
NH ₃	-382.6	14	-2.251×10^4
Glycerol	-1655.4	92	-1.799×10^4
Ethanol	-1366.8	46	-2.971×10^4

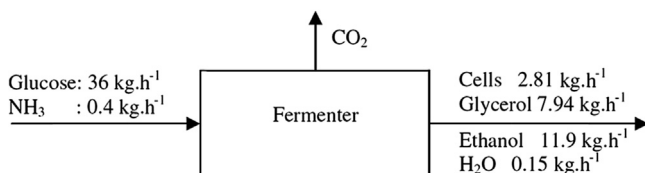


FIGURE 9.1 Flow sheet for ethanol and glycerol fermentation.

mass of the dry cell, the mass of glycerol, the mass of ethanol, and the mass of water at the product stream and then subtracting the sum from the feed stream. As a result, the mass of carbon dioxide is obtained. The heat of reaction is calculated by the following equation:

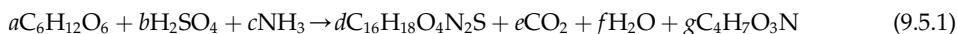
$$\begin{aligned}
 -\Delta H_{rxn} &= \sum n_i h_{c,products}^0 - \sum n_i h_{c,reactants}^0 & (9.4.4) \\
 -\Delta H_{rxn} &= 36(-1.558 \times 10^4) + 0.4(-2.251 \times 10^4) - 7.14(-1.799 \times 10^4) \\
 &\quad - 2.81(-2.12 \times 10^4) - 11.9(-2.971 \times 10^4) = -1.392 \times 10^4 \text{ kJ} \\
 Q &= -1.392 \times 10^4 \text{ kJ}
 \end{aligned}$$

Because heat is generated as the system liberates energy, this reaction is considered exothermic.

9.5 MASS BALANCE FOR BIOLOGICAL PROCESSES

EXAMPLE 1

A batch process is customary for producing antibiotics. A submerged culture is used to propagate fungus with suitable carbohydrate resources. This assumption is based on simplicity in calculations and the normal use of penicillin in the pharmaceutical industry. Assume that we are required to produce an antibiotic, 1 kmol penicillin G (334 kg) per batch. The general equation for the production of penicillin G and biomass is:



Our next assumption is related to process yield; yields of product and biomass are 20% and 50%, respectively ($Y_{P/S} = 0.2$, $Y_{X/S} = 0.5$). Do the material balance of antibiotic production based on the given data.

Solution

Moles of penicillin G produced are based on a stoichiometric relation, as given in (9.5.1).

$$d = \frac{334 \text{ kg}}{334 \frac{\text{kg}}{\text{kmol}}} = 1 \text{ kmol}$$

Also, moles of glucose needed in penicillin production are based on a stoichiometric relation:

$$a = \frac{334 \text{ kg penicillin G}}{0.2 \frac{\text{kg penicillin G}}{\text{kg glucose}} \times 180 \frac{\text{kg}}{\text{kmol}}} = 9.28 \text{ kmol}$$

The third product is the cell biomass. Moles of biomass produced are given by:

$$g = \frac{0.5 \times (9.28 \text{ kmol glucose}) \times 180 \frac{\text{kg}}{\text{kmol}}}{117 \frac{\text{kg}}{\text{kmol}}} = 7.14 \text{ kmol}$$

Moles of the remaining components are found using elemental balance. The method has been discussed, so now we balance for each element.

N balance: $c = (2 \times d) + (1 \times g)$,

S balance: $b = 1 \times d$,

C balance: $(6 \times a) = (16 \times d) + (1 \times e) + (4 \times g)$,

Overall balance: $(180 \times a) + (98 \times b) + (17 \times c) = (334 \times d) + (44 \times e) + (18 \times f) + (117 \times g)$.

The known variables are substituted into the equations to get values for c , b , e , and f . Upon solving these equations simultaneously, the unknown coefficients are obtained.

Moles of ammonia required:

$$C = 9.14 \text{ kmol}$$

Moles of sulfuric acid required:

$$B = 1 \text{ kmol}$$

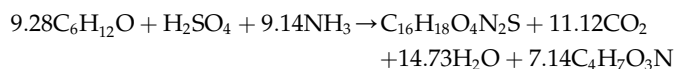
Moles of carbon dioxide released:

$$E = 11.12 \text{ kmol}$$

Moles of water produced:

$$F = 14.73 \text{ kmol}$$

Therefore, the stoichiometric coefficients for the projected equation in production of penicillin G are:



Material balance is carried out at the inlet and outlet of the fermenter, summarized in [Table 9.24](#). Based on the results presented in this table, the error for calculation of the mass balance is less than 1%—negligible in fact—so the method is reliable and useful for process design.

TABLE 9.24 Summary of material balance for inlet and outlet of the fermenter

Substance	Inlet (kg)	Outlet (kg)
Glucose	1670.40	0.00
H ₂ SO ₄	98.00	0.00
NH ₃	155.38	0.00
Penicillin G	0.00	334.00
CO ₂	0.00	489.28
Water	167.04	432.18
Biomass	0.00	835.38
Total	2079.18	2090.84

TABLE 9.25 Density and mass fraction of inlet and outlet of the fermenter

Substance	Density (kg m ⁻³)	Inlet (kg)	Outlet (kg)	Mass fraction	
				Inlet	Outlet
Glucose	1544	1670.40	0.00	0.80	—
H ₂ SO ₄	1834	98.00	0.00	0.05	—
NH ₃	597.1	155.38	0.00	0.07	—
Penicillin G	3420	0.00	334.00	—	0.16
CO ₂	110.1	0.00	489.28	—	0.23
Water	1000	167.04	432.18	0.08	0.21
Biomass	1013	0.00	835.38	—	0.40
Total		2079.82	2090.84	1.00	1.00

$$Error = \frac{2090.84 - 2079.18}{2090.84} \times 100\% = 0.56\%$$

The density and mass fraction of the inlet and outlet of the fermenter are shown in [Table 9.25](#).

EXAMPLE 2

In a continuous wastewater treatment plant, 10^5 kg of cellulose and 10^3 kg of bacteria enter into the digestion unit as a feed stream on a daily basis, whereas 10^4 kg of cellulose and 1.5×10^4 kg of bacteria leave in the effluent. The rate of cellulose digestion is 7×10^4 kg day⁻¹. The bacterial growth rate is 2×10^4 kg day⁻¹. The cell death rate by cell autolysis is 5×10^2 kg day⁻¹. Do the material balance for cellulose and bacteria based on the given data.

Solution

Basis: 1-day operation.

Cellulose Balance

Cellulose in the wastewater stream is not generated but it is consumed and biomass is produced by the microbial population as a substrate for energy.

$$[\text{Cellulose in}] - [\text{cellulose out}] + [\text{cellulose generation}] - [\text{cellulose consumption}] \\ = [\text{cellulose accumulation}]$$

$$\text{In} - \text{Out} + \text{Generation} - \text{Consumption} = \text{Accumulated cellulose}$$

$$10^5 - 10^4 + 0 - 7 \times 10^4 = 20,000 \text{ kg cellulose}$$

Biomass Balance

Applying the same concept for mass balance, the mass of sludge accumulated is:

$$\text{Cell in} - \text{cell out} + \text{growth rate} - \text{death rate} = \text{cell accumulation}$$

$$10^3 - 1.5 \times 10^4 + 2 \times 10^4 - 5 \times 10^2 = 5,500 \text{ kg bacteria}$$

9.6 CONSERVATION OF MASS PRINCIPLE

Based on the law of conservation of mass, mass is neither created nor destroyed, except in nuclear reactions. Therefore, in a definite system, mass in is equal to mass out.

EXAMPLE 1

Humid air with O_2 is prepared for gluconic acid fermentation. The humid air has been prepared by a special humidification chamber in which $1.5 \text{ l} \cdot \text{h}^{-1}$ of liquid water enters; at the same time dry air and $15 \text{ mol} \cdot \text{min}^{-1}$ dry O_2 enter the chamber. The exiting gas stream contains 1% (w/w) water. Draw and label the flow sheet and do the material balance for the humidifier.

Solution

The air humidification flow diagram for material balance is shown in [Figure 9.2](#). The mass flow rate for water into the humidification unit is:

$$1.5 \frac{\text{l}}{\text{h}} \times \frac{10^3 \text{ g}}{1 \text{ l}} \times \frac{1 \text{ h}}{60 \text{ min}} = 25 \text{ g} \cdot \text{min}^{-1} \text{H}_2\text{O}$$

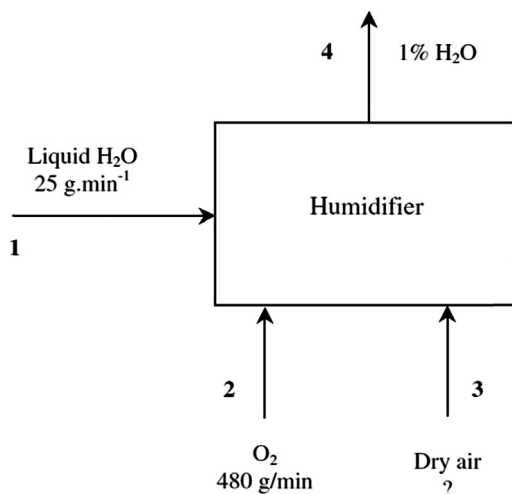


FIGURE 9.2 Flow diagram for oxygen enrichment and air humidification.

The mass flow rate for dry oxygen is:

$$15 \frac{\text{gmol}}{\text{min}} \times \frac{32 \text{ g}}{\text{gmol}} = 480 \text{ g min}^{-1} \text{O}_2$$

Basis of calculation: 1 min.

Water Balance

The mass of water in is equal to the mass of water out, because the enriched air with oxygen should have only 1% humidity. Therefore, the mass of humid air can be calculated as tie element:

$$\begin{aligned} 25 &= 0.01 m_4 \\ \Rightarrow m_4 &= 2500 \text{ g Humid air rich with O}_2 \end{aligned}$$

Overall Material Balance

Total mass in is equal to total mass out:

$$\begin{aligned} m_1 + m_2 + m_3 &= m_4 \\ 2500 &= 25 + 480 + m_3 \\ m_3 &= 1995 \text{ g} \end{aligned}$$

The mass flow rate of dry air in is 1995 g min^{-1} .

EXAMPLE 2

A fermentation broth containing *Streptomyces kanamyceticus* cells is filtered by a vacuum rotary filter. The feed rate is 120 kg h^{-1} ; each kilogram of broth contains 60 g of cells. To improve filtration, filter aids are added at a rate of 10 kg h^{-1} . The concentration of kanamycin in the broth is 0.05%. The filtrate is collected at a rate of 112 kg h^{-1} . The concentration of kanamycin in the filtrate is 0.045%. The filter cake contains cells, and filter aid is continuously removed from the filter cloth.

- What is the moisture content in the filter cake?
- If the concentration of kanamycin in the filter cake is the same as in the filtrate, how much kanamycin is absorbed per kilogram of filter aid?

Solution

Basis of calculation: 1-h operation.

The simplified flow diagram of continuous filtration with stream lines of material balance is shown in [Figure 9.3](#). Mass in is equal to mass out:

$$\begin{aligned} 120 + 10 &= 112 + M \text{ filter cake} \\ M \text{ filter cake} &= 18 \text{ kg h}^{-1} \end{aligned}$$

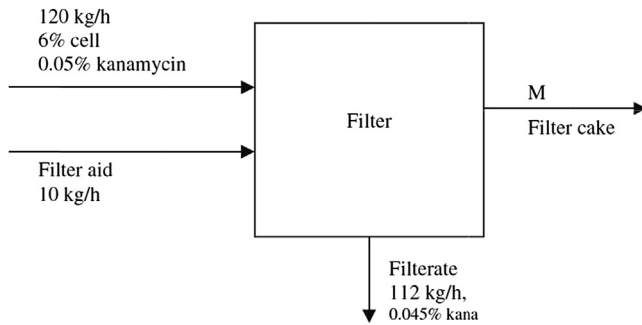


FIGURE 9.3 Flow sheet for continuous filtration.

H₂O Balance

The mass of water at inlet streams is equal to the mass of water at the filtrate and filter cake.

$$\begin{aligned} 120[(1 - 0.06) - 0.0005] &= 112.74 \text{ kg} \\ &= 112(1 - 0.00045) + \text{cake moisture} \\ M(\text{H}_2\text{O in the filter cake}) &= 0.79 \end{aligned}$$

The filter cake moisture content is calculated as:

$$\frac{0.79}{18} \times 100 = 4.4\% \text{ moisture}$$

The mass of water in the filtrate is $112 - 0.05 = 111.95 \text{ kg}$

Amount of kanamycin in the moisture $= 0.79(0.00045) = 3.6 \times 10^{-4} \text{ kg}$

Kanamycin Balance

The mass of kanamycin in is equal to the mass of kanamycin out.

$$\begin{aligned} 0.0005 \times 120 &= (112)(0.00045) + (0.79)(0.00045) + M_{k,abs.} \\ M_{k,abs.} &= 0.06 - 0.05075 = 9.245 \times 10^{-3} \text{ kg} \end{aligned}$$

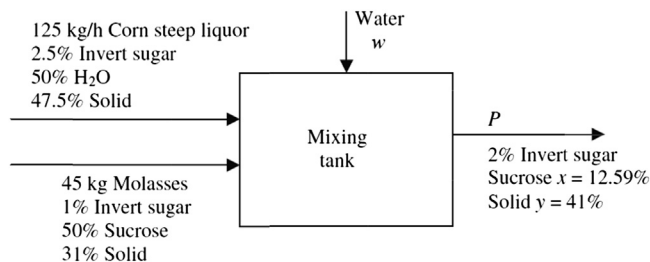
$$\text{Kanamycin absorbed per kilogram filter aid} = \frac{9.245}{10} = 9.245 \times 10^{-4} \text{ kg kg}^{-1}$$

EXAMPLE 3

Various sources of carbohydrates are used in the fermentation processes. Molasses and corn steep are the most common carbon sources used to generate energy for biosynthesis. Having the correct composition and desired concentration is necessary in actual experimental work.

Corn steep liquor contains 2.5% invert sugars and 50% water. The rest of the feed is considered residual solids. Beet molasses containing 50% sucrose, 1% invert sugar, and 18% water and the remaining solids are mixed with corn steep liquor in a mixing tank. Water is added to produce a

FIGURE 9.4 Flow sheet for diluting sugar and mixing tank.



diluted mixture with 2% invert sugar, 125 kg corn steep liquor, and 45 kg molasses, which is fed into an enzymatic hydrolysis tank.

- How much water is required?
- What is the concentration of sucrose in the final mixture?

Solution

A flow diagram for diluting carbohydrates, corn steep liquor, and molasses in the mixing tank is shown in Figure 9.4.

Mass Balance

Let us assume that mass in is equal to mass out.

$$125 + 45 + W = P$$

Now we can balance the invert sugar:

$$(0.025 \times 125) + (0.01 \times 45) = 0.02 P$$

$$P = 178.75 \text{ kg}$$

$$W = 8.75 \text{ kg}$$

The next step is to take sucrose into the balance:

$$(0.5)(45) = (x)(P)$$

$$(0.5)(45) = 178.75x$$

The concentration of sucrose in the product mixture is $x = 0.1259$ or 12.59% of the product.

The residual solids in corn steep, molasses, and the diluted mixture are also balanced:

$$(0.31)(45) + (0.475)(125) = 178.75y$$

$$y = 0.41$$

The amount of solid in the product mixture is 41%.

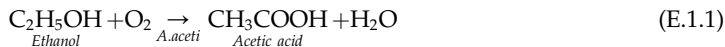
9.6.1 Acetic Acid Fermentation Process

In fermentation for the production of acetic acid, ethyl alcohol is used in an aerobic process. In an ethanol oxidation process, the biocatalyst *Acetobacter aceti* was used to convert ethanol into acetic acid under aerobic conditions. A continuous fermentation for vinegar

production was proposed for use of nonviable *A. aceti* immobilized onto the surface of alginate beads.

EXAMPLE 1

The production rate of acetic acid is 2 kg h^{-1} , where the maximum acetic acid concentration is 12%. Air is pumped into the fermenter with a molar flow rate of $200 \text{ mol} \cdot \text{h}^{-1}$. The chemical reaction is presented in (E. 1.1) and the flow diagram is in Figure 9.5. Determine the minimum amount of ethanol intake and identify the required mass balance for the given flow sheet. The ethanol biochemical oxidation reaction using *A. aceti* is:



The process flow diagram for the fermentation of ethyl alcohol is shown in Figure 9.5. Assuming steady-state condition, the air intake has no moisture, and that the volume and molar fractions are about the same, ethanol is not going to vaporize while fermentation is taking place. Assume the only biochemical reaction that takes place is acetic acid production, which means ethanol is not used for maintenance or ATP generation. No side reactions occur. Relative molecular masses are: ethanol 46, acetic acid 60, oxygen 32, and water $18 \text{ g} \cdot \text{mol}^{-1}$. Also, air consists of 21% oxygen and 79% nitrogen.

Solution

The basis for calculation is 1 h operation and 2 kg acetic acid produced.

Mass flow rate of air: $(0.2 \text{ kg mol h}^{-1})(28.84 \text{ kg} \cdot \text{kg mol}^{-1}) = 5.768 \text{ kg h}^{-1}$.

Mass flow rate of O_2 : $0.2 \times 0.21 \times 32 = 1.344 \text{ kg h}^{-1}$.

Mass flow rate of N_2 : $0.2 \times 0.79 \times 28 = 4.424 \text{ kg h}^{-1}$.

Sum of $\text{O}_2 + \text{N}_2$: $1.344 \text{ kg h}^{-1} + 4.424 \text{ kg h}^{-1} = 5.768 \text{ kg h}^{-1}$.

The product stream with 12% acetic acid has a mass flow rate of:

$$P = \frac{2}{0.12} = 16.67 \text{ kg h}^{-1}$$

Moles of acetic acid are calculated as:

$$\frac{2 \text{ kg}}{60 \text{ kgmol kg}^{-1}} = 3.333 \times 10^{-2} \text{ kgmol}$$

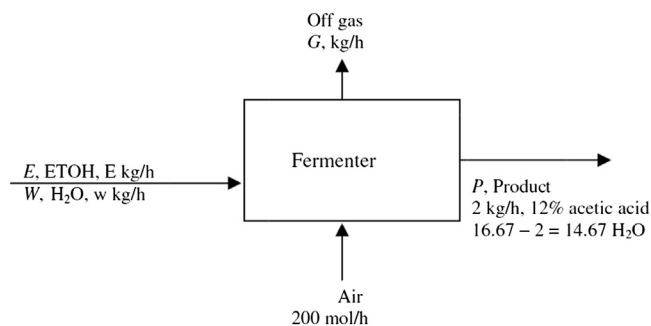


FIGURE 9.5 Flow sheet for acetic acid production.

From the reaction stoichiometry, for each mole of acetic acid, 1 mol of oxygen is used. So the equal molar oxygen consumption is:

$$(3.333 \times 10^{-2})(32) = 1.067 \text{ kg O}_2 \text{ consumed}$$

$$\text{Excess amount of O}_2 = 1.344 - 1.067 = 0.277 \text{ kg h}^{-1}$$

The off gas stream consists of all inlet nitrogen plus excess oxygen.

Off gas, G , is the sum of excess oxygen plus inert nitrogen.

$$G = \text{N}_2 + \text{excess O}_2 = 4.424 + 0.277 = 4.701 \text{ kg}$$

$$\text{Off gas composition is } 0.277/4.701 = 0.059, 5.9\% \text{ O}_2 \text{ and } 94.1\% \text{ N}_2$$

Water Balance

The sum of water at the inlet stream and water generated by the chemical reaction is equal to water at the outlet stream.

$$\text{H}_2\text{O in} + \text{H}_2\text{O generated} = \text{H}_2\text{O out}$$

$$\text{Mass of H}_2\text{O generated: } (3.333 \times 10^{-2})(18 \text{ kg} \cdot \text{kg mol}^{-1}) = 0.6 \text{ kg.}$$

$$\text{Water at inlet stream: } 14.67 \text{ kg} - (0.6 \text{ kg, H}_2\text{O generated}) = 14.07 \text{ kg.}$$

Ethanol Balance

Ethanol concentration at the inlet plus ethanol generated is equal to ethanol in the outlet stream as unreacted reactant plus ethanol consumed. For each mole of acetic acid, 1 mol ethanol is used. The mass of ethanol used is:

$$\text{Mass of ETOH consumed} = (3.333 \times 10^{-2})(46 \text{ kg} \cdot \text{kgmol}^{-1}) = 1.533 \text{ kg Ethanol}$$

Assume all of the ethanol (100%) is taken by the bacteria and that there is no ethanol generation or evaporation. This means that ethanol in is equal to ethanol consumed in the oxidation process.

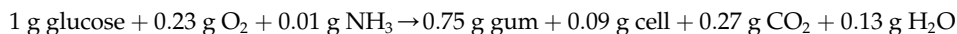
$$\text{Ethanol in} = \text{ethanol consumed} = 1.533 \text{ kg ETOH}$$

9.6.2 Xanthan Gum Production

EXAMPLE 1

Xanthan gum is produced using *Xanthomonas campestris* in a batch culture. Laboratory experiments have shown that for each gram of glucose used by the bacteria, 0.23 g oxygen and 0.01 g ammonia are consumed whereas 0.75 g gum, 0.09 g cells, 0.27 g gaseous CO_2 , and 0.13 g H_2O are formed. Other components such as phosphate can be neglected. A medium containing glucose and ammonia dissolved in 20,000 l of water is pumped into a CSTR fermenter and inoculated with *X. campestris*. Air is pumped; the off gas recovered during the entire batch is 1250 kg. The final gum concentration is 3.5 wt%. What is the percentage of excess air and how much glucose and ammonia are required?

Reaction stoichiometry per unit mass of glucose:



Solution

Figure 9.6 shows the schematic diagram for production of xanthan gum with inlet and outlet streams.

Overall Mass Balance

$$F + A = 1250 + P$$

The amount of glucose required is:

$$1 \text{ kg glucose} \times \left(\frac{0.035P}{0.75 \text{ g gum}} \right) = 0.0467P \text{ kg glucose}$$

The mass of oxygen based on reaction stoichiometry is:

$$0.23 \text{ kg O}_2 \times \left(\frac{0.035P}{0.75 \text{ g gum}} \right) = 0.0107P \text{ kg O}_2$$

The amount of ammonia needed is:

$$0.01 \text{ kg NH}_3 \times \left(\frac{0.035P}{0.75 \text{ g gum}} \right) = 0.00047P \text{ kg NH}_3$$

Products

The mass of the cell with respect to the mass of the product stream is:

$$0.09 \text{ kg cells} \times \left(\frac{0.035P}{0.75 \text{ g gum}} \right) = 0.0042P$$

The mass of carbon dioxide generated is:

$$0.27 \text{ kg CO}_2 \times \left(\frac{0.035P}{0.75 \text{ g gum}} \right) = 0.0126P \text{ kg CO}_2$$

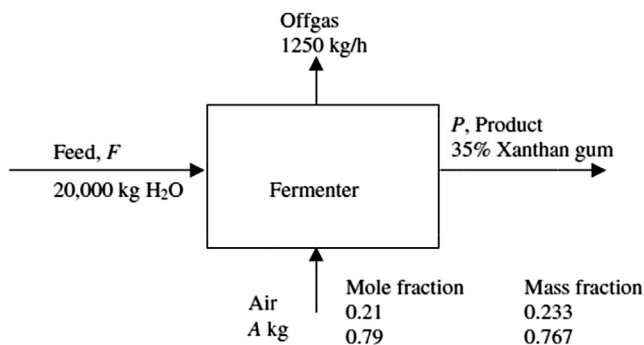


FIGURE 9.6 Flow sheet for xanthan gum production.

The amount of water according to reaction stoichiometry is:

$$0.13 \text{ kg H}_2\text{O} \times \left(\frac{0.035P}{0.75 \text{ g gum}} \right) = 0.00607P \text{ kg H}_2\text{O}$$

O₂ Balance

The mass of oxygen in the inlet air stream is equal to the oxygen consumed and the excess oxygen leaving the outlet stream.

$$0.233A = \text{O}_2 \text{ out} + 0.0107P \text{ O}_2 \text{ used}$$

The outlet stream:

$$\text{O}_2 \text{ out} = 0.233A - 0.0107P$$

N₂ Balance

The mass of nitrogen at the inlet is equal to the mass of nitrogen in the outlet steam.

$$0.707A = \text{N}_2 \text{ out}$$

The mass of carbon dioxide generated is equal to the mass of CO₂ at the outlet stream.

$$\text{CO}_2 \text{ out} = \text{CO}_2 \text{ generated} = 0.0126P$$

Off Gas Balance

$$1250 = (0.233A - 0.0107P) + 0.767A + 0.0126P$$

$$\text{O}_2 = \text{N}_2 - \text{CO}_2$$

$$1250 = A + 1.9 \times 10^{-3}P$$

The mass of air is:

$$A = 1250 - 0.0019P$$

$$\bar{m} = (0.0467 + 0.00047)/P + 20,000$$

$$20,000 + 0.04717P + A = 1250 + P$$

Substitute A into the above equation, then solve for P :

$$20,000 + (1250 - 0.0019P) = 0.9528P + 1250$$

$$P = 20,949 \text{ kg}$$

Replace P in the above equation and then solve for A :

$$A = 1250 - 0.0019(20,949) = 1210.2 \text{ kg}$$

Solve for \bar{m} :

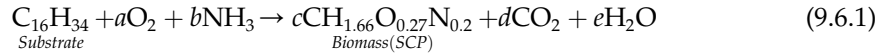
$$\bar{m} = 20,988.2 \text{ kg}$$

$$P = 87.986 \text{ kg cell} + 263.96 \text{ kg CO}_2 + 127.1 \text{ kg H}_2\text{O}$$

$$\begin{aligned}\text{Off gas} &= 57.8 \text{ kg O}_2 + 928.2 \text{ kg N}_2 + 263.96 \text{ kg CO}_2 \\ \text{Excess air} &= \frac{57.8}{224.15} \times 100 = 25.8\% = \frac{57.8}{0.0107(20949)} \times 100\end{aligned}$$

9.6.3 Stoichiometric Coefficient for Cell Growth

Stoichiometric coefficients for cell growth for the production of single cell protein (SCP) from hexadecane are given by the following reaction:



where $\text{CH}_{1.66}\text{O}_{0.27}\text{N}_{0.2}$ represents the chemical composition of the cell biomass.

EXAMPLE 1

Based on the stoichiometric relation of the above equation for SCP production, if $\text{RQ} = 0.43$, find the stoichiometric coefficients a , b , c , d , and e in (9.9).

Solution

C balance: $16 = c + d \rightarrow d = 16 - c$.

H balance: $34 + 3b = 1.66c + 2e$.

O balance: $2a = 0.27c + 2d + e$.

N balance: $b = 0.2c$.

RQ: $0.43 = d/a \rightarrow d = 0.43a$.

$d = 0.43a = 16 - c$.

Substituting and rearranging:

$$34 + 0.6c = 1.66c + 2e$$

$$2a = 0.27c + 2(16 - c) + e \quad 2a = 0.27c + 32 - 2c + e$$

$$74.4 - 4.65c + 2c - 0.27c = 32 + e$$

$$2(e + 2.92c = 42.4) \quad c = 10.63$$

$$-(2e + 1.06c = 34) \quad d = 5.37$$

$$a = 12.49$$

$$b = 2.13$$

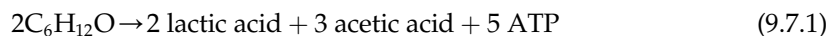
$$e = 2(12.49) + 0.27(10.63) - 2(5.37) = 11.37$$

Therefore, the exact stoichiometric coefficients for the above reaction are:



9.7 EMBDEN–MEYERHOF–PARNAS PATHWAY

The metabolic pathway for bacterial sugar fermentation proceeds through the Embden–Meyerhof–Parnas pathway. The pathway involves many catalyzed enzyme reactions that start with glucose, a six-carbon carbohydrate, and end with 2 mol of three carbon intermediates, pyruvate. The end pyruvate may go to lactate or be converted into acetyl Co–A for the TCA cycle. The fermentation pathways from pyruvate and the resulting end products are shown in Figures 9.7 and 9.8. The overall catabolism of glucose into lactate and acetate, in which 2 mol of glucose yields 2 mol of lactic acid, 3 mol of acetic acid, and 5 mol of ATP, are shown below:



Reactions involve several enzymes that have to follow in sequence for lactic acid and alcohol fermentation. This is known as the catabolic pathway of glucose, with emphasis on energetic and energy carrier molecules such as ATP, ADP, and nicotine adenine dinucleotide. In this pathway, the six-carbon substrate yields two three-carbon intermediates known as primary metabolites, each of which converts through a sequence of reactions into the stable end product of pyruvic acid.

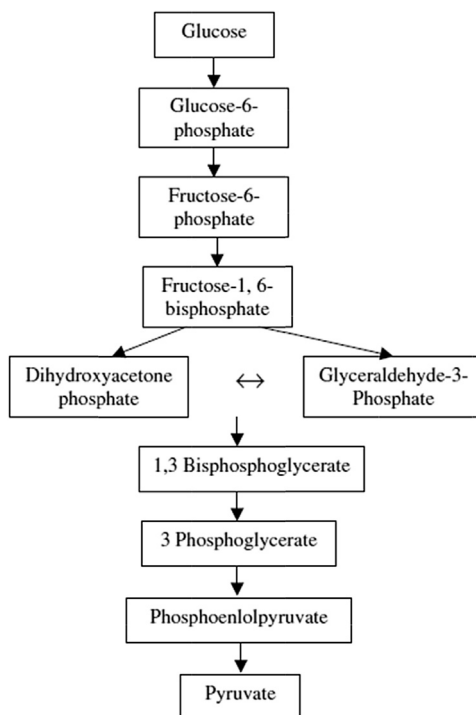


FIGURE 9.7 Glyconeogenesis illustrated in the Embden–Meyerhof–Parnas pathway.

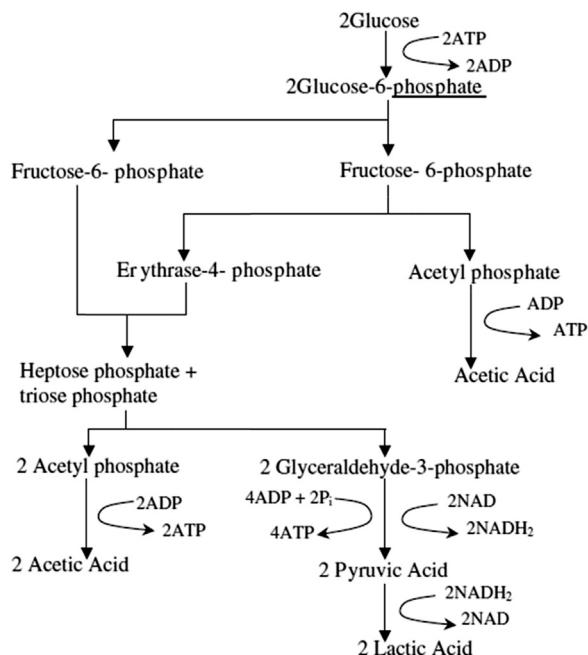
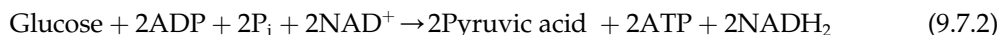


FIGURE 9.8 Fermentation of glucose to acetate or lactate via the Embden–Meyerhof–Parnas pathway.

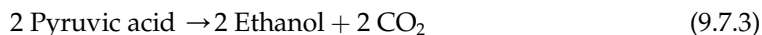
9.7.1 Description of Glycolysis

Glycolysis under anaerobic conditions to ethanol fermentation of pyruvate occurs in the presence of a biocatalyst such as yeast, which occurs as an alternative pathway in homolactic fermentation for lactic production. In addition, pyruvate in aerobic respiration for oxidative phosphorylation through the TCA cycle is converted into carbon dioxide and water molecules. The fermentation of glucose to ethanol by yeast has resulted in useful end products. The theoretical yield of ethanol fermentation is 51.1%. Control of the metabolic pathway is possible by facilitating the fermentation conditions. The optimal pH and temperature for ethanol production, with the aid of *S. cerevisiae*, are 5.6 and 32 °C, respectively. The overall reaction of glucose to pyruvate is as follows:



The detailed pathway for bioconversion of glucose into pyruvate is illustrated in Figure 9.9 with energy carrier biomolecules is as follows:

The overall reaction for ethanol fermentation from pyruvate is as follows:



The alternative pathways for the oxidative phosphorylation process, anaerobic fermentative alcoholic and anaerobic homolactic fermentative, are shown in Figure 9.10. The media

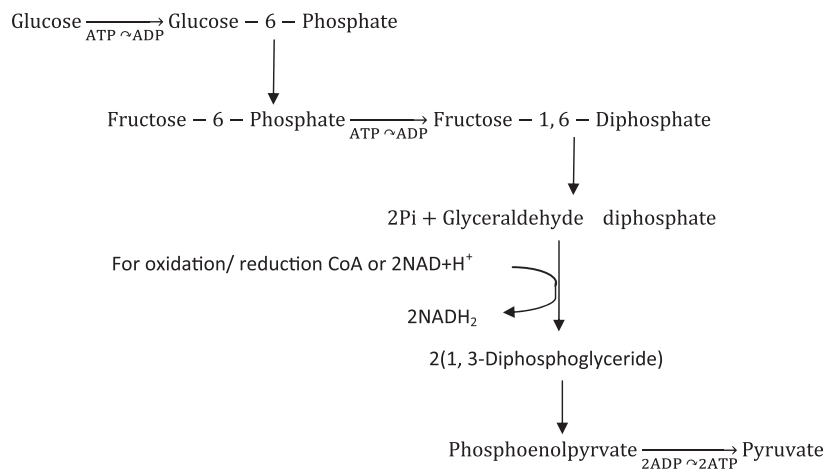


FIGURE 9.9 Pathway of glucose to pyruvate bioconversion.

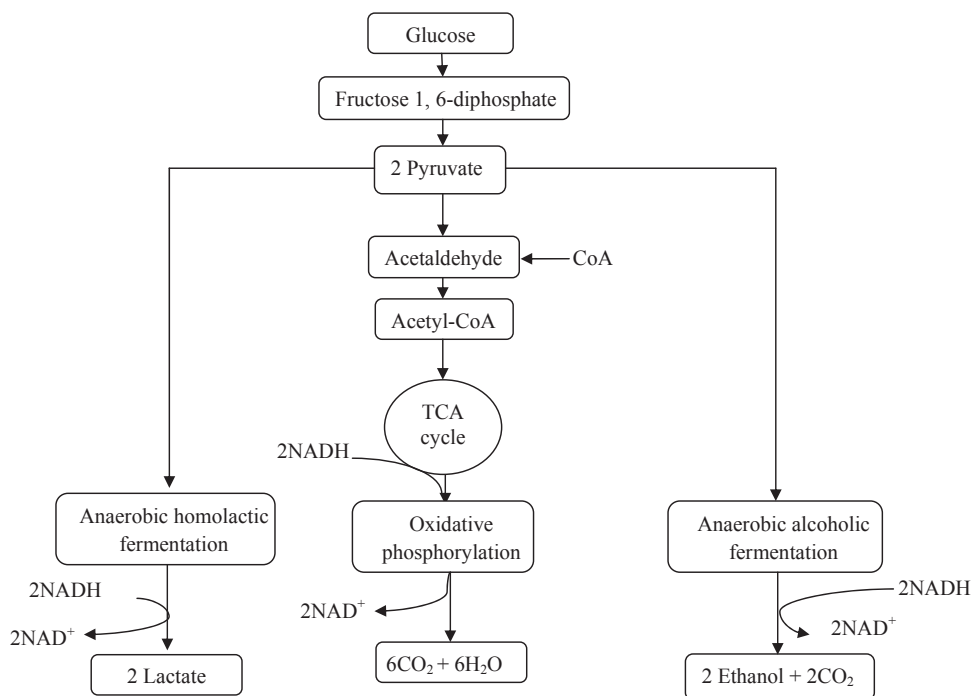


FIGURE 9.10 Pathway of glycolysis in anaerobic fermentation and oxidative phosphorylation.

composition and fermentation conditions for the cell propagation and anabolisms should be investigated to determine how the organism can select specific pathways for a desired end product.

EXAMPLE 1

There was an old and outdated fermenter in our school warehouse. The dean of the school wanted the equipment to be used for undergraduate students to learn about bioprocess concepts. The technician ran the equipment experimentally but forgot to weigh the glucose carbon source and did not analyze the ethanol. The product stream was analyzed as follows: lactic acid 10 mol, acetic acid 5 mol, carbon dioxide 15 mol, and hydrogen 10 mol. It was expected that sugar oxidized, converted to pyruvic acid, and then was sent through the Embden–Meyerhof–Parnas pathway. No product except ethanol was formed. The problem was adjusted by pH control and restarting the process with no contamination. How many moles of ethanol were in the waste product stream? The overall biological reaction is summarized as:



Solution

Carbon balance: $6a = 2c + 30 + 10 + 15$.

Hydrogen balance: $12a + 2b = 6c + 60 + 20 + 20$.

Oxygen balance: $6a + b = c + 30 + 10 + 30$.

$$\begin{cases} 6a - 2c = 55 \\ 12a + 2b - 6c = 100 \\ 6a + b - c = 70 \end{cases}$$

Rearrange the first equation for $-2c$ gives:

$$\begin{cases} -2c = -6a + 55 \\ 12a + 2b - 6c = 100 \\ 6a + b - c = 70 \end{cases}$$

Then, substitute the first equation into the second and third equations:

$$\begin{cases} 12a + 2b - 3 \times 6a + 3 \times 55 = 100 \\ 12a + 2b - 6a + 55 = 140 \end{cases}$$

Add both sides:

$$\begin{cases} -6a + 2b = -65 \\ 6a + 2b = 85 \end{cases}$$

Solving the above equation for b yields:

$$+4b = +20$$

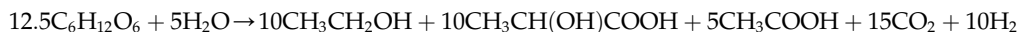
$$b = 5$$

$$a = 12.5$$

$$c = \frac{6a - 55}{2}$$

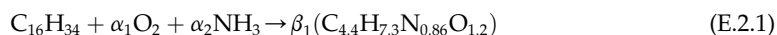
$$c = 10$$

Substitute the values of a , b , and c into Eqn (E. 1.1); the defined equation is:



EXAMPLE 2

Assume that cells can convert 67% of carbon source to biomass. Hexadecane and glucose are used as carbon sources. Calculate the stoichiometric coefficients of the following reactions:



Solution

Figure 9.11 shows the flow sheet for stoichiometry and material balance in a cell. According to the problem, two thirds of the carbon source goes to biomass.

$$\frac{2}{3}(16) = 4.4\beta_1$$

Therefore:

$$\beta_1 = 2.424$$

The remainder of the carbon source, one third, goes to carbon dioxide:

$$\frac{1}{3}(16) = \beta_2 = 5.333$$

Nitrogen balance: $a_2 = 0.86 \beta_1 = 2.085$,

H₂ balance: $34 + 3a_2 = 7.3 \beta_1 + 2 \beta_3$,

$\beta_3 = 11.28$,

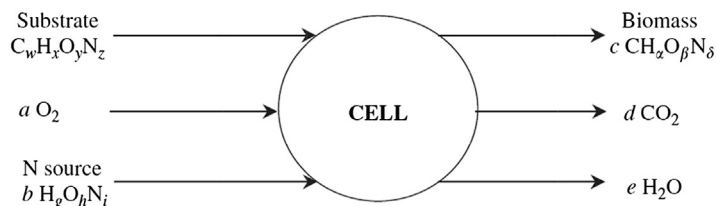
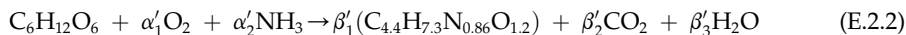


FIGURE 9.11 Flow sheet for stoichiometry and material balance in a cell.

O₂ balance: $2a_1 = 1.2 B_1 + 2 B_2 + B_3 = 1.2(2.424) + 2(5.333) + 11.28$,
 $a_1 = 12.43$.

Glucose oxidation to SCP:



$$C - balance: \frac{2}{3}(6) = 4.4\beta_1$$

$$\beta'_1 = 0.909$$

$$\frac{1}{3}(6) = \beta_{21} = 2.0$$

$$N_2 Balance: \alpha'_2 = 0.86\beta'_1 = 0.78$$

$$H_2 Balance: 12 + 3\alpha'_1 = 7.3\beta'_1 + 2\beta'_3$$

$$12 + 3(0.78) = 7.3(0.909) + 2\beta'_3$$

$$\beta'_3 = 3.85$$

$$O_2 Balance: 6 + 2\alpha'_1 = 1.2\beta'_1 + 2\beta'_2 + \beta'_3$$

$$2\alpha'_1 = 1.2(0.909) + 2 \times 2 + 3.85 - 6$$

$$\alpha'_1 = 1.47$$

Cells are able to use chemical energy efficiently. Like any actual process, energy retained in the substrate is released as heat.

EXAMPLE 3

From the above biomass production, calculate the yield coefficients. Based on the definition, the yield of biomass on glucose means how much biomass is produced per gram of glucose used in a cell. The yield of biomass on glucose is calculated as follows:

$$Y_{X/S} = \frac{\text{Biomass}}{\text{Glucose}} \quad (E.3.1)$$

$$Y_{X/S} = \frac{0.909(4.4 \times 12 + 7.3 + 0.86 \times 14 + 1.2 \times 16)}{180}$$

$$Y_{X/S} = \frac{83.03}{180} = 0.46 \text{ g cell g}^{-1} \text{ glucose}$$

The yield of biomass produced per gram of oxygen consumed is:

$$Y_{X/O_2} = \frac{83.03}{2 \times 1.47 \times 16} = 1.76 \text{ g cells g}^{-1} \text{ oxygen}$$

Cells use energy from substrate in an efficient way, like a real chemical process. Some of the energy is released as heat. The generated metabolic heat has to be removed from the bioreactor; the temperature must be controlled for optimal cell growth. Also, the liberated heat is proportional to the cell growth. The yield factor Y_Δ is defined as grams of cell produced per kilocalorie of heat

evolved. This is analogous to the yield of biomass to the substrate and the heat of combustion of the substrate and cell, ΔH_s , and ΔH_c , respectively. The following equation relates the yield factor to the yield of biomass and the net heat evolved resulting from cell growth.

$$Y_{\Delta} = \frac{Y_{X/S}}{\Delta H_s - Y_{X/S} \Delta H_c} \quad (\text{E.3.2})$$

Given heat of combustion of sugar:

$$\Delta H_s = \frac{673 \text{ kcal mol}^{-1}}{180} = 3.74 \text{ kcal g}^{-1} \text{ biomass}$$

Heat of combustion of cell:

$$\Delta H_c = 5.8 \text{ kcal g}^{-1} \text{ dry cell mass}$$

Now substitute the values into (E.3.2) to obtain the yield factor.

$$Y_{\Delta} = \frac{0.46}{3.74 - 0.46 \times 5.8} = 0.43 \text{ kcal g}^{-1} \text{ biomass}$$

The yield of biomass to substrate for hexadecane is obtained.

$$Y_{X/S} = \frac{2.424(91.34)}{226} = 0.988 \text{ g cell g}^{-1} \text{ glucose}$$

The molecular mass of $\text{C}_{16}\text{H}_{34}$ is 226.

$$Y_{X/\text{O}_2} = \frac{221.4}{12.43 \times 32} = 0.56 \text{ g cell g}^{-1} \text{ O}_2$$

$$Y_{\Delta} = \frac{0.988}{11.2 - 0.988} = 0.18 \text{ g cell g}^{-1} \text{ glucose}$$

ΔH_s is the possible heat evolved from oxidation of hexadecane.

EXAMPLE 4

Citric Acid Production in Solid-State Fermentation

Citric acid is manufactured by submerged cultures of *Aspergillus niger* in a batch reactor operated at 30 °C. For an incubation period of 2 days, 2500 kg glucose and 860 kg oxygen were consumed to produce 1500 kg citric acid, 500 kg biomass, and other byproducts. Ammonia was used as the nitrogen source. Power input to the system by mechanical agitation was about 15 kW. Approximately 100 kg of water evaporated during the 2 day operation.

Estimate the energy consumption for cooling requirements.

Solution

Figure 9.12 shows the flow diagram for production of citric acid in solid-state fermentation. The basis of calculation is 1500 kg citric acid.

$$\Delta H_{\text{evap., H}_2\text{O}} \text{ at } 30^\circ\text{C, steam table} = 2430.7 \text{ kJ kg}^{-1}$$

$$\text{Heat of reaction at } 30^\circ\text{C} = -460 \text{ kJ mol}^{-1} \text{ O}_2 \text{ used}$$

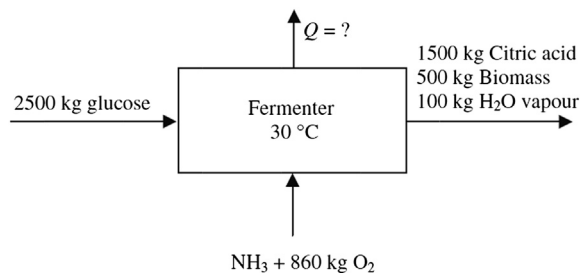
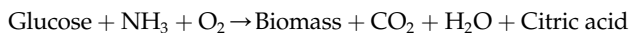


FIGURE 9.12 Flow sheet for citric acid production in solid-state fermentation.

Fermentation reaction:



Mass is balanced at the beginning and end of the process. The evaporated water in solid-state fermentation may not be required for energy balance.

$$\text{Mass}_{\text{beginning}} = \text{Mass}_{\text{end}} + \text{H}_2\text{O}_{\text{vap}}$$

The first law of thermodynamics is valid for the energy balance.

$$-\Delta H_{\text{rxn}} - m_{\text{H}_2\text{O}} \Delta H_{\text{evap}} = \delta Q - \delta W \quad (\text{E.4.2})$$

$$-\Delta H_{\text{rxn}} = (-460)(861 \text{ kg})(1000 \text{ g kg}^{-1})(1 \text{ gmol } 32 \text{ g}^{-1}) = -1.24 \times 10^7 \text{ kJ}$$

Heat lost by vaporization of 100 kg H₂O:

$$m_v \Delta H_{\text{evap}} = (100 \text{ kg})(2430.7) = 2.43 \times 10^5 \text{ kJ}$$

Mechanical work:

$$W_s = (15 \text{ kW})(\text{kJ s}^{-1}/1 \text{ kW}^{-1})(2 \text{ days})(24 \text{ h day}^{-1})(3600 \text{ s h}^{-1}) = 2.59 \times 10^6 \text{ kJ}$$

$$Q = 1.24 \times 10^7 - 2.43 \times 10^5 + 2.59 \times 10^6 = 1.47 \times 10^7 \text{ kJ (removed heat)}$$

EXAMPLE 5

Penicillin G Production

To calculate the yield for penicillin G (Pen G) production based on material and energy balance using the biosynthesis pathway as proposed by the following stoichiometry reaction:



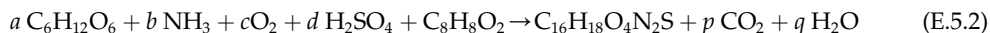
where a , b , c , d , e , n , p , and q are the stoichiometric coefficients and PAA stands for phenyl-acetic acid. In this reaction, the theoretical yield of penicillin G production is 1.1 g Pen G per gram of

glucose. The projected formula for Pen G and PAA are $C_{16}H_{18}O_4N_2S$ and $C_6H_5-CH_2-COOH$, respectively. The respiration quotient is defined as:

$$RQ = \frac{CO_2}{O_2} = 4; \quad Y_{PenG/glucose} = 1.113g \text{ PenG } g^{-1} \text{ glucose}$$

Solution

Let us define clearly that for each mole of Pen G 1 mol of PAA is required. We shall rewrite the above formula, replace the desired formula for Pen G and PAA, and then apply the elemental mass balance:



Sulfur balance $d = 1$, nitrogen balance $b = 2$, and $RQ = 4 = p/c$ results in $p = 4c$.

Carbon balance: $6a + 8 = 16 + p$.

Hydrogen balance: $12a + 6 + 2 + 8 = 18 + 2q$.

Oxygen balance: $6a + 2c + 4 + 2 = 4 + 2p + q$.

Substitute p in the above equation.

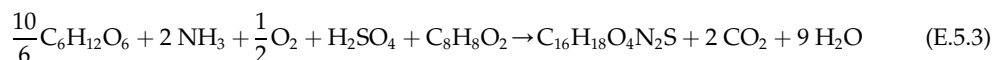
$$6a = 8 + 4c.$$

$$12a = 2 + 2q; \quad q = 6a - 1.$$

$$6a = -2 + 6c + q = -2 + 6c + 6a - 1 \text{ resulting in } 6c = 3; \quad c = 0.5.$$

$$\begin{aligned} a &= \frac{10}{6} \\ 6a &= 8 + 4(0.5) = 10; \\ q &= 6\left(\frac{10}{6}\right) - 1 = 9 \end{aligned}$$

The stoichiometric coefficients are defined and substituted into the proposed reaction:



The theoretical yield seems to be high because glucose is not the single carbon source for the production of Pen G. In fact, for 1 mol of Pen G, 1.67 mol of glucose and 1 mol of PAA are required. The actual theoretical yield should be based on the total carbon sources:

$$Y = 334 / (300 + 136) = 0.766$$

The fact is that *Penicillin* sp. requires nutrients for growth and maintenance; therefore, the yield cannot be greater than 1. It must be lower than 0.7.

References

1. Aiba S, Humphrey AE, Millis NF. *Biochemical engineering*. 2nd ed. New York: Academic Press; 1973.
2. Bailly JE, Ollis DF. *Biochemical engineering fundamentals*. 2nd ed. New York: McGraw-Hill; 1986.
3. Blanch HW, Clark SD. *Biochemical engineering*. New York: Marcel Dekker; 1996.
4. Doran PM. *Bioprocess engineering principles*. New York: Academic Press; 1995.
5. McInerney MJ, Bryant MP, Pfennig N. Anaerobic bacterium that degrades fatty acids in syntrophic association with methanogens. *Arch Microbiol* 1979;**122**(2):129–35.

6. Genthner B, Davis C, Bryant MP. Features of rumen and sewage sludge strains of *Eubacterium limosum*, a methanol- and H_2 - CO_2 -utilizing species. *Appl Environ Microbiol* 1981;**42**(1):12–9.
7. Shuler ML, Kargi F. *Bioprocess engineering, basic concepts*. New Jersey: Prentice-Hall; 1992.
8. Ghose TK. *Bioprocess computation in biotechnology*, vol. 1. New York: Ellis Horwood Series in Biochemistry and Biotechnology; 1990.

PROBLEM

1. *Clostridium acetobutylicum* is carried out in anaerobic fermentation, to convert glucose into biomass cells, acetone (C_3H_6O), butanol ($C_4H_{10}O$), butyrate ($C_4H_8O_2$), acetate ($C_2H_4O_2$), ethanol (C_2H_6O), CO_2 , and H_2 . The product analysis is obtained from using 100 mol of glucose and 11.2 mol of NH_3 as the nitrogen source, shown below.

With formed product	Moles
Cells	13
Butanol	56
Acetone	22
Butyric acid	0.4
Acetic acid	14
CO_2	221
H_2	135
Ethanol	0.7

Determine the elemental composition of the cells.

Application of Fermentation Processes

OUTLINE

10.1 Introduction	330	10.11 Analytical Method for Ethanol Analysis	338
10.2 Production of Ethanol by Fermentation	330	10.12 Refractive Index Determination	338
10.3 Benefits from Bioethanol Fuel	331	10.13 Cell Dry Weight Measurements	339
10.4 Stoichiometry of Biochemical Reaction	331	10.14 Yield Calculation	339
10.5 Optical Cell Density	332	10.15 Batch Fermentation Experiment	340
10.6 Kinetics of Growth and Product Formation	333	10.16 Continuous Fermentation Experiment	341
10.7 Preparation of Stock Culture	334	10.17 Media Sterilization	342
10.8 Inoculum Preparation	335	10.18 Batch Experiment	342
10.9 Inoculation of Seed Culture	336	10.18.1 Optical Cell Density, Ethanol, and Carbohydrate Concentration	342
10.10 Analytical Method for Sugar Analysis	337	10.18.2 Continuous Ethanol Fermentation Experiment	343
10.10.1 Quantitative Analysis	337	10.19 Expected Results	343
10.10.2 Analysis of Mixed Sugar by Ultraviolet	337	References	344
Sample Preparation	338		

10.1 INTRODUCTION

In World War I, Germany needed to synthesize glycerol to manufacture explosives. It was found that glycerol was generated in alcoholic fermentation. Nearburg discovered that the addition of sodium bisulfite to the fermentation broth was favored and enhanced the production of glycerol at the expense of ethanol. German scientists quickly developed industrial-scale fermentation with a yield capacity of 1000 tons of glycerol per month.^{1,2}

Ethanol is an essential chemical used as a raw material for a vast range of applications including chemicals, fuel (bioethanol), beverages, pharmaceuticals, and cosmetics. The feedstock for ethanol generally comes from renewable sources such as starch (from wheat, barley, maize, potato, cassava, sweet potato, etc.) and molasses or syrups originating from sugar beet or sugar cane, and so forth. The second generation of bioethanol uses raw material feedstock not related to human food sources: nonfood base raw material such as cellulose and organic wastes. Cellulose is natural polymer of glucose, which is the major constituent of almost all plants and is a renewable source by plantations. For instance, wood is made of cellulose, hemicellulose, and lignin. Hemicellulose is a hetero-polymer of glucose and xylose (hexose and pentose). Cellulosic material should be hydrolyzed and converted to a monomer of fermentable sugar for ethanol fermentation. The strategy for producing renewable and inexpensive raw material involves ethanol fermentation in a single or two-step process. In a single step, pure or mixed cultures of organisms are used to break down cellulose and then ferment the resulting sugar solely into ethanol. Organisms that have such a capability are apparently rare; therefore, a two-step process has to be implemented. In this process, one organism breaks polymeric sugar into monomers. The alternative approach is a single operation unit to break down cellulose and ferment the resulting sugar into ethanol. An organism is required to deliver enzymes for enzymatic hydrolysis while ethanol fermentation is taking place. Such a phenomenon in a single organism may not be possible unless investigators present species of organisms genetically engineered with induction and incorporation enzyme-producing genes into ethanol producers to take two different metabolic pathways for saccharification while an anaerobic pathway for ethanol production is in progress. Then, in the fermentation of sugar, a second organism is used to produce bioethanol. The six-carbon sugar is easily fermented by bacteria or yeast into ethanol. It is believed that there are more efficient bacteria such as *Zymomonas mobilis* and *Thermoanaerobacter ethanolicus* for the bioconversion of carbohydrates to ethanol. Bioethanol is produced via fermentation technology. The fermentation product downstream is processed with subsequent enrichment by distillation/rectification and dehydration.

Bioethanol is becoming a viable solution as a source of renewable energy because it is considered a non-fossil fuel. It may originate from renewable agricultural sources, resulting in clean combustion without emissions into the atmosphere.

10.2 PRODUCTION OF ETHANOL BY FERMENTATION

Carbohydrates obtained from grain, potato, or molasses are fermented by yeasts to produce ethanol in the production of beer, alcohols, and distilled spirits. Fermentation of sugar using *Saccharomyces cerevisiae* produces ethanol under anaerobic conditions. The batch

fermentation system is affected by high substrate and product inhibition. Glucose concentration has a major role in increasing the concentration of ethanol and the cell growth rate in the fermentation broth. Cell density, ethanol concentration, and glucose concentration are measured. Industrial-grade sugars and molasses are used to produce bioethanol. Today, alcohol technologies are well developed. Many integrated extractive distillation, evaporative vacuum distillation, membrane separation, and purification techniques have enhanced ethanol production plants, and the process is considered economically feasible for competing with fossil fuel prices.

In the process of integration in bioethanol production, a membrane bioreactor (MBR) is designed to reduce ethanol distillation and purification costs. This means that while ethanol is produced in a bioreactor, the synthesized bioethanol is vaporized and extracted in a liquefied nitrogen gas trap. This process is developed to eliminate substrate and production inhibitions resulting from the use of high sugar concentrations in fresh feed and high ethanol produced in a fermentation broth. A breakthrough invention may occur in the next stage of technology development while we can demonstrate a commercial plant working with MBRs. For knowledge-based research, an MBR is developed and necessary data are collected for the fabricated MBR; details of the design process and experimental data are further discussed in a case study in Chapter 16.

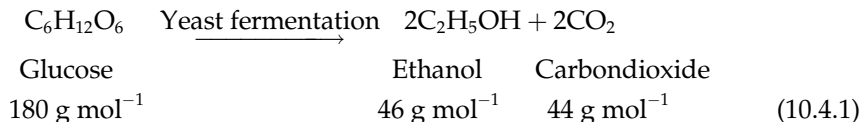
10.3 BENEFITS FROM BIOETHANOL FUEL

Alcoholic fermentation and ethanol production by *S. cerevisiae* have been well known for a few decades. Many obligate aerobic fungi, such as common molds of the genera *Aspergillus*, *Fusarium* species and *Mucor*, are also well known for their ability to produce ethanol.² Benefits are:

- Use of renewable resources
- Cleaner environment owing to cleaner combustion
- No net carbon dioxide emissions
- Expanded market opportunities in agriculture
- Less dependence on crude oil

10.4 STOICHIOMETRY OF BIOCHEMICAL REACTION

The following biochemical reaction represents sugar fermentation. Ethanol is the end product, which may be used as a useful bioprocess chemical.



Two popular microorganisms can produce a high concentration of alcohol: one is bacteria and the other is yeast. Their tolerance to high concentrations of ethanol and substrates is stated in the literature.^{3–5} The most common ones are *Z. mobilis* and *S. cerevisiae*. Ethanol

can also be produced from any organic waste; *Kluyveromyces marxianus* is able to produce ethanol from cheese whey permeate. Feedstock from cellulose is hydrolyzed into fermentable sugar; then in single or two-step fermentation, ethanol is produced. The most common organisms applied in different processes for ethanol fermentation are *S. cerevisiae*, *Z. mobilis*, *T. ethanolicus*, *Clostridium thermocellum*, *Clostridium thermohydrosulfuricum*, *Clostridium thermosaccharolyticum*, *Monilla* species, and *Fusarium* species.

10.5 OPTICAL CELL DENSITY

Cell growth is identified by cell density. Cell concentration is an indication of the viability of a microorganism. It is possible to distinguish between viable and nonviable cells by staining the culture sample with a stain such as methylene blue or trypan blue. The dead cells will be stained. The cell population or total number of cells may be counted on a cell count slide under a microscope as a defined volume of diluted culture introduced into a special slide known as a hemocytometer slide. Typically, the area under one small square is $2.5 \times 10^{-3} \text{ mm}^2$ and the depth under the glass slide cover is 0.1 mm. There are 25 small squares in one square and the total number of small squares is 625. The total volume of the counting slide is 0.156 mm^3 . In 1 ml of culture the number of cells is counted and defined. Because there is no uniform distribution of cell counting and it is impossible to count all boxes, random selection of five boxes is done. Certainly there is error in this method: Cells may aggregate and form clumps, and counting fungus mycelia is not simple so this method is not reliable for filamentous fungi. Another method of measuring cell population and cell distribution is to use a Coulter counter. An electrode is placed in the diluted culture sample while the reference electrode is under vacuum. The current is generated in presence of living cells in the diluted sample, detected by the analyzing electrode. The principles of a Coulter counter for total cell concentration measurements are shown in Figure 10.1.

Nephelometry and turbidity are the suitable approaches for determining the amount of cloudiness, or turbidity based on measurements of absorption, transmission, and light scattering owing to the presence of molecules causing turbidity or cloudiness in a solution.

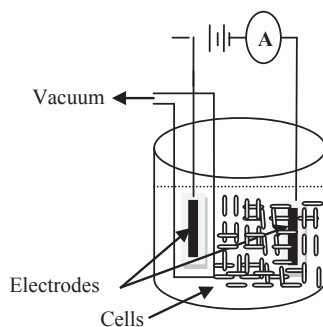


FIGURE 10.1 Coulter counter principle for total cell measurements.

Nephelometric and turbidimetric methods are techniques used in microbiology to determine the levels of cell density equivalent to accumulated broth proteins. Turbidity meters are used as an alternative method for a densely populated culture to identify cell density. In an alternative method, cell colony counters are used to culture a dilute sample in a Petri dish with nutrient agar medium for an identified number of colonies. The most accurate method is cell dry weight versus optical cell density, which cell light absorbance in a spectrophotometer at a defined wavelength. The optical cell density of *S. cerevisiae* is measured at a wavelength of 580 nm. Other wavelengths such as 600 nm or less may also be used, but one must be consistent by testing the sample at maximum absorbance. A growth curve is developed based on the incubation time and cell dry weight. A standard calibration curve is needed before an actual experiment. A calibration curve should be generated to relate the absorbance to the cell dry weight. The usual rules of operating a spectrophotometer are often applied. For example, the accuracy of the method is greatest when the absorbance readings are in the range of 0.1–1.3. For a given culture sample, a good spectrophotometer should yield a linear relation between the number of cells and the absorbance. However, optical density is also a function of cell morphology such as size and shape, because the amount of transmitted or scattered light depends strongly on these factors. Consequently, an independent calibration curve is required for each condition in accurate research work, since the cell size and shape depend on the specific growth rate and the nutrient composition. As a rule of thumb, an optical density of one unit corresponds to approximately 1 g l^{-1} of dry cell. This is also commonly referred to as the turbidity measurement. This simple assumption involved in the above techniques is that fresh culture may consist of viable organisms; therefore, it is necessary to apply these methods for an incubated culture less than 24 h.

10.6 KINETICS OF GROWTH AND PRODUCT FORMATION

It has been suggested that fungi grow in a filamentous form at an exponential rate with a constant specific growth rate (μ) until some substrate becomes growth limiting, according to the Monod equation^{4,6}:

$$\mu = \frac{\mu_{\max} S}{K_s + S} \quad (10.6.1)$$

where μ_{\max} is the specific growth rate of the organism in h^{-1} , K_s is the saturation constant in kg m^{-3} , and S is the concentration of the limiting substrate in kg m^{-3} . The cell-specific growth (μ) is a function of time in a typical batch culture; once the organism passes the delay or lag phase it follows an accelerating pattern known as the exponential growth phase until μ reaches a stable constant value known as the stationary phase, where it is at a zero rate from where nutrient depletion started. One can evaluate rate expression in three cases:

1. When S is much greater than K_s , the reaction falls into zero order where $\mu = \mu_{\max}$
2. When the value of S is equal to the Monod constant; $\mu = \mu_{\max}/2$
3. The value of S is low compared with the saturation constant, and thus the rate equation falls into first-order kinetics.

TABLE 10.1 Values for saturation constant for several organisms with identified desired substrate

Microorganism	Substrate	K_s , mg l ⁻¹
<i>Escherichia coli</i>	Glucose	6.8×10^{-2}
<i>E. coli</i>	Lactose	20
<i>Aspergillus niger</i>	Glucose	5
<i>Candida utilis</i>	Glycerol	4.5
<i>Saccharomyces cerevisiae</i>	Glucose	25
<i>Pseudomonas</i> sp.	Methanol	0.7
<i>Klebsiella aerogenes</i>	Carbon dioxide	0.4

The saturation constant may be expressed as the affinity of the organism for the substrate. A high K_s value means low affinity for a substrate whereas for a low value it is the reverse. At a low saturation constant, the rate is a function of substrate, which is mostly related to vitamins and trace metal act as substrates. Table 10.1 represents some typical values for a saturation constant that vary from one organism to another; the type of substrate may also reflect values of K_s preferred by organisms for the desired substrate.

The ethanol fermentation performance and bioprocess criteria are summarized below:

- High conversion yield
- High ethanol tolerance
- Resistance to inhibitors in a hydrolyzed product
- No oxygen requirement
- Low fermentation pH
- Broad substrate usage range

10.7 PREPARATION OF STOCK CULTURE

It is best to store organisms in pure culture for a long time without a lack of nutrients. A nutrient broth may not last for weeks. Solid media nutrients with agar in slants are used for stock culture to preserve organisms for a long duration. Normally freeze-dried culture obtained from the American Type Culture Collection (ATCC) (Rockville, MD) is hydrated and grown in broth media, and is then transferred to a culture tube with slant agar.⁷ Figure 10.2 shows a stock culture on slant agar in a sealed tube that can be stored and kept in a refrigerator for a minimum of 4–6 months.

Several steps are involved in transferring pure culture from a broth cultured on slants. It should be an aseptic technique without transfer of any contaminants. An inoculating loop is flamed on a Bunsen burner until it is red hot. It is then cooled off on a corner of the media before touching and picking up any colony of organism to be introduced into the culture broth. A full loop of cultivated culture is brought in front of the flame and then transferred to the surface of the slanted agar with continuous streaking; it is incubated at 30 °C until



FIGURE 10.2 Stock culture of *Rhodospirillum rubrum* on slant agar (a photosynthetic bacterium hydrogen producer).

growth is visible as colonies appear on the surface. The stock culture tube can then be kept in a refrigerator and is good for use within 6 months. Renewal is necessary for a 6-month-old stock culture.

10.8 INOCULUM PREPARATION

To have stock culture in a slant, a single isolated colony of yeast should be found on the Petri dish from which the culture can be transferred to the fermentation media. This technique may ensure that the stock culture is not contaminated with other organisms.

Take a loop full of the creamy culture off the agar plate. Dip the loop into a 250-ml flask containing 100 ml of 5.0 g l⁻¹ glucose and 1 g l⁻¹ yeast extract. Swirl the loop in the nutrient solution to dislodge the selected culture from the loop.

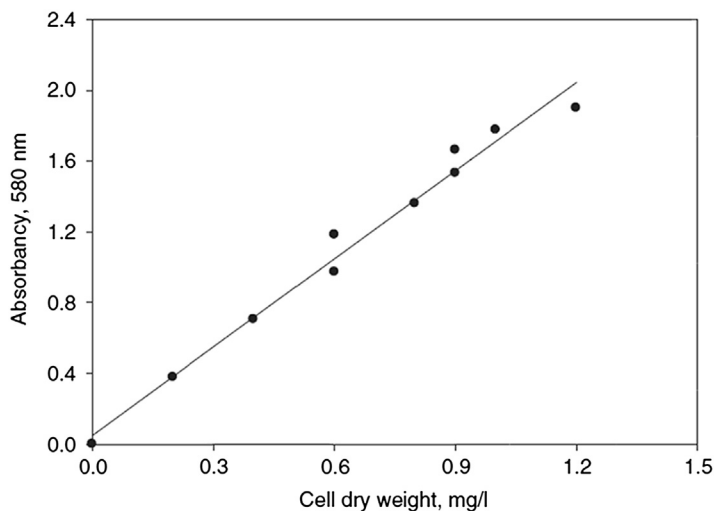
Flame the neck of the flask and the cotton plug before inserting the plug back into the flask. Also, flame the loop to kill residual microorganisms.

Place the flask in a temperature-controlled shaker at 37 °C. The exponential growth phase will last from 2 to 24 h after inoculation. The exact time and duration depend on the physiological condition of the inoculum. The data in Table 10.2 are plotted and a growth curve is obtained for an exponentially growing culture. Figure 10.3 shows the typical growth curve obtained for a viable organism.

TABLE 10.2 Data sheet for batch fermentation at constant agitation

Time, h	Absorbance, λ_{520} nm	Cell concentration, g l ⁻¹	Concentration of carbohydrates, g l ⁻¹	Ethanol concentration, g l ⁻¹
0	0.0	0.0	31.5	—
6	0.68	0.5	27.78	1.85
8	1.0	0.78	21.5	3.8
12	1.4	1.1	14.3	5.8
24	1.9	1.55	11.0	8.9

FIGURE 10.3 Standard curve for cell density defined based on growth of *Saccharomyces cerevisiae*.



10.9 INOCULATION OF SEED CULTURE

Seed culture of *S. cerevisiae* (ATCC 24,860) is grown in a rich medium composed of 1 g glucose, 0.1 g peptone, 1 g yeast extract, 0.33 g KH_2PO_4 , and 0.03 g Na_2HPO_4 in 100 ml distilled water. The media is autoclaved at 121 °C and 15 psig for 20 min. The stock culture from ATCC media is transferred to a prepared seed culture. The pH of the medium is adjusted to 5.5 using 0.03 M phosphate buffer solution. A pH meter (model WTW, Wissenschaftlich-Technische-Werkstaetten, 82,362, Weilheim, Germany) is used to read pH and control it in

FIGURE 10.4 A 50-ml seed culture is used for inoculation of batch fermenter.



the experiment. Figure 10.4 shows a typical seed culture prepared for inoculation of batch fermentation. The transformation is carried out in front of a flame with a sterile syringe.

10.10 ANALYTICAL METHOD FOR SUGAR ANALYSIS

10.10.1 Quantitative Analysis

For each fermentation broth sample, the glucose concentration is measured with 3,5-dinitrosalicylic acid (DNS) reagent. The DNS solution is prepared by dissolving 10 g DNS in 200 ml of 2 M NaOH. A separate solution of 300 g sodium potassium tartrate is prepared in 500 ml of distilled water; mixing and heating is required. The hot salt solution (sodium potassium tartrate) is added to the DNS. The volume of the solution is made up to 1 l by adding distilled water. A standard glucose solution (2 g l^{-1}) is prepared a day in advance for any structural deformation or changes. A calibration curve is prepared. A straight line can easily be obtained in the range of 200–1600 mg l^{-1} glucose.

10.10.2 Analysis of Mixed Sugar by Ultraviolet

Normally, analysis of a mixture of carbohydrates, high-performance liquid chromatography as an analytical tool is recommended. Because the process may be hectic and expensive, simple ultraviolet (UV) spectrophotometry was developed to analyze mixture of pentose and hexose (xylose and glucose). A standard salt solution as reagent was prepared by dissolving sodium chloride (12 g) and boric acid (2 g) in 100 ml distilled water. The mixture of sugars with salt reagent and sulfuric acid are detectable with UV at a desired wavelength. The method follows Beer's law. The absorbance of each sample reads at two defined wavelengths. At given wavelengths, the following systems of equations are given:

$$\begin{aligned} A_{310} &= G_{310}C_1 + X_{310}C_2 \\ A_{340} &= G_{340}C_1 + X_{340}C_2 \end{aligned} \quad (10.10.2.1)$$

Also, the solutions in form of metrics are defined for glucose and xylose concentrations:

$$\text{Glucose } C_1 = \frac{\begin{vmatrix} A_{310} & X_{310} \\ A_{340} & X_{340} \end{vmatrix}}{\begin{vmatrix} G_{310} & X_{310} \\ G_{340} & X_{340} \end{vmatrix}} \quad \text{Xylose } C_2 = \frac{\begin{vmatrix} G_{310} & A_{310} \\ G_{340} & A_{340} \end{vmatrix}}{\begin{vmatrix} G_{310} & X_{310} \\ G_{340} & X_{340} \end{vmatrix}} \quad (10.10.2.2)$$

Given the slope of these straight lines, the concentrations for glucose and xylose are defined by the solution of metrics, as follows:

$$\begin{aligned} \text{Glucose Concentration } (\text{g l}^{-1}) &= \frac{A_{310}X_{340} - X_{310}A_{340}}{G_{310}X_{340} - X_{310}G_{340}} \times \text{dilution rate} \\ \text{Xylose Concentration } (\text{g l}^{-1}) &= \frac{G_{310}A_{340} - G_{340}A_{310}}{G_{310}X_{340} - X_{310}G_{340}} \times \text{dilution rate} \end{aligned} \quad (10.10.2.3)$$

where A_{340} and A_{310} stand for absorbance at a defined wavelength; G_{340} , G_{310} , X_{340} , and X_{310} represent glucose and xylose, respectively, at the specified wavelength. Also, C_1 and C_2 are concentrations of components 1 and 2: glucose and xylose, respectively. A standard solution of mixed sugars may be prepared according to the mixture of glucose and xylose, as follows:

Mixture of glucose and xylose solution			
Glucose, g l ⁻¹	0.03	0.06	0.09
Xylose, g l ⁻¹	0.06	0.1	0.14

Sample Preparation

Remove solids from the samples by means of filtration, using Whatman filter paper for a clear sample. Dilute the sample to a 1:500 ratio with distilled water. Mix 0.5 ml of diluted sample with 0.5 ml of the salt reagent in a clean dried test tube; use a micropipette for exact sampling. Mix the mixture well using a tube vortex mixer for 10 s. Add 8 ml concentrated sulfuric acid to each test, mixing for 10 s. Then heat the sample with reagent and acid in a 70 °C water bath. Degas the sample after 20 min, mix it for 10 s, and then return it to the water bath for 30 min of heating. Finally, cool the sample in ice water to stop the reaction. Allow the samples to return to room temperature. The UV spectrophotometer should be read at 15–20 min. The spectrophotometer mode is on absorbance with a response of 0.5. Turn the power on, turn on both lamps, and enter two wavelengths for absorbance reading at 310 and 340 nm. When the system is ready and stable, start to read UV absorbance of each sample. Blank for zero absorbance is concentrated sulfuric acid.

10.11 ANALYTICAL METHOD FOR ETHANOL ANALYSIS

The ethanol concentration in the fermentation broth is determined using gas chromatography (GC) (HP 5890 series II with HP Chemstation data processing software, Hewlett Packard, Avondale, PA) with a Poropak Q Column, and a Hewlett Packard model 3380A integrator. A flame ionization detector is used to detect the ethanol. The oven temperature is maintained at 180 °C and the injector and detector temperature are maintained at 240 °C. The sample taken from the fermentation media has to be filtered and an internal standard must be added for analysis based on internal standard methods; otherwise, the area under the peak must be compared with known standard samples for calculation based on external standard methods.

10.12 REFRACTIVE INDEX DETERMINATION

The refractive index (RI) is used to analyze the sample. It can also be used to help to determine the percentage of a chemical (such as ethanol) in an aqueous solution. The RI is always reported to four decimal places. An example of the RI scale is shown in [Figure 10.5](#). The correct reading from the RI of the sample would be 1.3764.

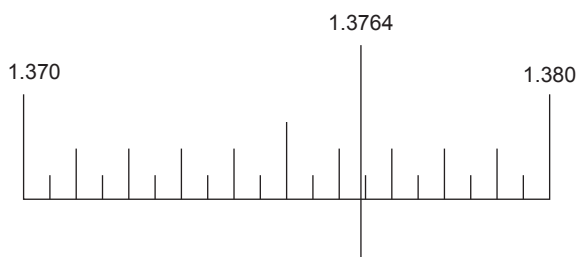


FIGURE 10.5 Refractive index reading for ethanol solution.

10.13 CELL DRY WEIGHT MEASUREMENTS

About 5 ml of sample is withdrawn from the fermentation broth for every 4–6 h. The absorbance reading of the sample at 580 nm is measured using a Hitachi U-2000 spectrophotometer. The sample is filtered through Whatman filter paper with a pore size of 2.5 μm and diameter of 47 mm. The dry weight of cells is measured to monitor the microbial cell population and cell density. A plot of optical density reading from the spectrophotometer against cell dry weight can be obtained. The cell density, a standard calibration curve for *S. cerevisiae* at a wavelength of 580 nm, has been experimentally determined, as shown earlier.

10.14 YIELD CALCULATION

Normally, the yield is the ratio of the products over the reactants. In the fermentation process, carbon sources are used while the desired product as metabolites and cell mass are formed. The yield coefficient is defined as the mass of cells or product per unit mass of consumed nutrient. The yield of the cell mass or biomass produced per gram of carbohydrate or any other carbon source and the yield of the desired product per unit mass of substrate is defined as follows:

$$Y_{X/S} = \frac{\Delta X}{\Delta S} \quad (10.14.1)$$

$$Y_{P/S} = \frac{\Delta P}{\Delta S} \quad (10.14.2)$$

In an aerobic process for the complete oxidation of glucose as full energy is released: $\Delta G^\circ = -2850 \text{ kJ mol}^{-1}$. The energy released via alcoholic fermentation (ethanol) results in $\Delta G^\circ = -235 \text{ kJ mol}^{-1}$. Because 2 mol ethanol is produced per mole of glucose, a yield of 51% is obtained. In fact, the exact theoretical yield cannot be achieved because some of the substrate is consumed for biomass production; however, a 90–95% theoretical yield is achievable. To calculate the yield percentage, one needs to know the theoretical value that can be obtained, based on material balance and whether 100% of the reactant(s) is converted to product. After obtaining the experimental value (actual yield), divide it by the theoretical value and then multiply by 100 to get the percentage yield.⁸

$$\text{Yield\%} = \frac{\text{Experimental value}}{\text{Theoretical value}} \times 100 \quad (10.14.3)$$

10.15 BATCH FERMENTATION EXPERIMENT

It is simple to perform batch fermentation in a small flask with a volume of, say, 200 ml. Our target is to use a 2-l B. Braun fermenter. All accessories are shown in Figure 10.6. The fermentation vessel only, as shown in Figure 10.7, with about 250 ml of media without accessories but with some silicon tubing attached with a filter for ventilation, is autoclaved at 121 °C for 10 min at 15 psig.⁹ After that, the system is handled with special care and all

FIGURE 10.6 Continuously stirred tank fermenter: experimental setup with instrumentation, controllers, and effluent.

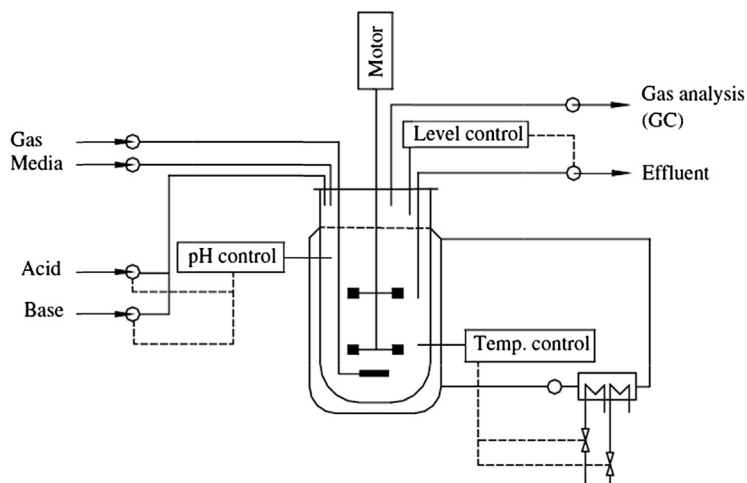
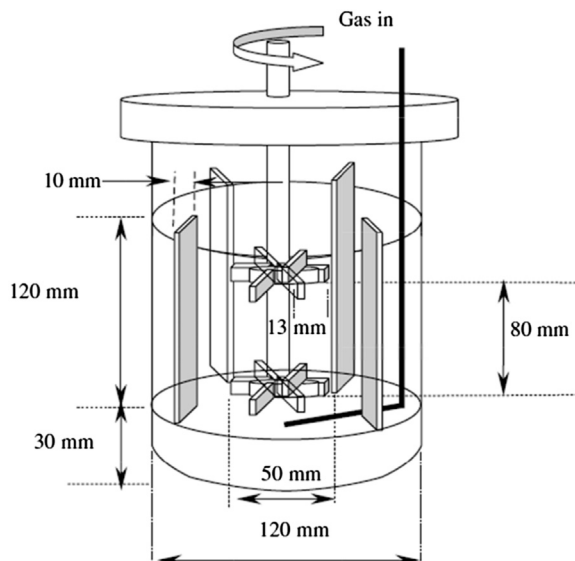


FIGURE 10.7 Geometrical dimensions of B. Braun fermentation vessel.



accessories are attached. Media are separately sterilized and pumped into the vessel. Inoculum is transferred and the batch experiment is started right after inoculation of the seed culture. An initial sample is withdrawn for analysis.

10.16 CONTINUOUS FERMENTATION EXPERIMENT

The experiment is accomplished with a 2-l B. Braun fermenter biostat (Germany) equipped with DO and pH meters. Temperature and level controllers are sensitive, with highly accurate response from the sensors installed in the vessel. [Figure 10.8](#) shows a complete continuous fermentation setup used in photosynthetic production. A small modification of the sampling port is necessary to change the sample jar with a stainless-steel tube sample port connected with a rubber septum, which is gas tight. A simple syringe needle is used to take liquid samples aseptically. The original fabricated sampling jar must be attached to on-line steam to prevent contamination while liquid is withdrawn. The fermentation vessel is jacketed and an external heating and cooling water bath is provided with the fermentation unit to control the temperature, set at 32 °C. Because ethanol fermentation requires no oxygen, neither air nor pure oxygen is supplied. The CO₂ is vented from the carboy by installing a sterilized air filter.

Draw a sample at the time intervals proposed in [Table 10.2](#). The fermentation should last for approximately 24 h before the culture enters the stationary phase.

- A 5-ml sample is adequate to analyze optical density, glucose/sucrose concentration, and ethanol concentration. For sugar analysis you may dilute 1 ml of sample and 9 ml of distilled water to have a suitable concentration range for DNS analysis.



FIGURE 10.8 Complete laboratory setup of biostat, B. Braun fermenter with external feed pumps, and product reservoirs.

- Save a drop of the sample on a slide for later microscopic examination of the purity of the culture.
- Initially, when the cell density is still low, the optical density of the sample can be measured without dilution with water. Perform this step quickly with a spectrophotometer at 580 nm. Then, filter out the cells from the sample. Afterward, withdraw 1 ml of the sample by pipetting from the culture vessel and then put it into a test tube for optical density measurement. Force the remaining sample through a filter. Normally a sterile syringe is used to withdraw the sample. A suitable filter case fitted on the tip of syringe is used to remove cells. The filtered sample is used for analysis by GC. Ethanol is determined by GC. Otherwise, the RI method is easy to use but it may not be accurate for research purposes.
- The clear filtrate is collected in a tightly capped sampling vial for later analysis. Freezing the filtrate will better preserve the existing condition.
- If a 1-ml sample is saved for optical density measurement, dilute the sample with 5 ml of water. Record the optical density.

10.17 MEDIA STERILIZATION

The prepared nutrient must be sterilized. Usually, this is done by autoclaving. However, autoclaving is not a practical sterilization method for the formulation used in this experiment. The heat of autoclaving may caramelize the sugar and darken the nutrient to a brown color. In addition, vitamins will be destroyed by the heat. Furthermore, the loss of liquid as a result of boiling during autoclaving will change the concentration of various nutrient components, including the rate-limiting carbon source. Evaporation loss is especially severe when ethanol is the designated carbon source. Even with all of the disadvantages of an autoclave, it is still customary to use autoclave routine equipment with some modifications, such as for a fast program or to sterilize sugar and media separately.

Instead, membrane filtration may be used to sterilize the nutrient in this experiment. This can be accomplished by drawing the nutrient from a mixing jar and forcing it through an inline filter (0.2 μm pore size) either by gravity or with a peristaltic pump. The sterilized medium is fed into an autoclaved nutrient jar with a rubber stopper fitted with a filtered vent and a hooded sampling port.

For each run, calculate and plot the cell biomass concentration, glucose concentration, ethanol concentration, and pH as a function of time. Identify the major phases in batch fermentation: lag, exponential, stationary, and death phases.

10.18 BATCH EXPERIMENT

10.18.1 Optical Cell Density, Ethanol, and Carbohydrate Concentration

Measure the optical cell density of *S. cerevisiae* at a wavelength of 520 nm. Try to collect data based on information required in [Table 10.2](#). Draw a growth curve based on incubation time and cell dry weight. The cell concentration indicates microorganism growth. A standard calibration curve is needed before an actual experiment.

10.18.2 Continuous Ethanol Fermentation Experiment

The batch experiment had neither incoming fresh media nor a product stream leaving the fermentation vessel. A complete experimental setup with a B. Braun Biostat, is shown in this laboratory experimental setup. The continuous flow of media requires a feed tank and product reservoir. The batch process has many disadvantages, such as substrate and product inhibition, whereas in the continuous process the fresh nutrients may remove any toxic by-product formed.

10.19 EXPECTED RESULTS

1. The parameters of the Monod cell growth model are needed: For instance, the maximum specific growth rate and Monod rate constant for cells, and the Michaelis–Menten constant for enzymes are required for a suitable rate equation. Based on data presented in [Tables 10.2 and 10.3](#), the kinetic parameters for the experimental data in ethanol production are obtained. It is customary to have a linear model and to plot a double reciprocal model known as the Lineweaver–Burk plot. From the data obtained, it is easy to see that at a retention time of more than 12 h, the rate of substrate uptake is low, whereas at a low retention time of 4–8 h, the rate of glucose uptake is much higher than $\tau = 24$ h. That is most probably because of the limited substrate available in the fermentation broth. From the given data, it is recommended that the substrate concentration be increased to a much higher value. Let us propose that $90\text{--}110\text{ g l}^{-1}$ is the target for a high production rate, whereas we need to define the desired retention time.
2. Another parameter for living organisms is the media pH, which may change during the course of the fermentation. The change in pH results from product formation and metabolites being liberated from the cells. The question is whether the change in pH coincides with the different batch growth phases. The answer may not be clear, because it depends on the activity of the microorganisms and the media absorbing the metabolites. In ethanol fermentation, maximum ethanol productivity is obtained at a pH range of 5.6–5.8. The fermentation media composition is 10% glucose, 0.1% yeast extract, 0.44% KH_2PO_4 , and 0.044% Na_2HPO_4 for the ethanol producer *S. cerevisiae*. There is a direct relation between the media composition and the pH of the media and microbial growth

TABLE 10.3 Data sheet for continuous ethanol fermentation, $S_0 = 35\text{ g l}^{-1}$

Media flow rate, ml h^{-1}	Retention time, τ , h	Cell density, g l^{-1}	Substrate concentration S , g l^{-1}	$1/S$, g^{-1}	$-r_A$, Rate of substrate uptake, $\text{g l}^{-1}\text{ h}^{-1}$	$1/-r_A$	Ethanol concentration, g l^{-1}
83	24	2.30	8.3	0.12	1.11	0.90	8.9
125	16	1.95	9.5	0.105	1.59	0.63	6.9
167	12	1.45	13.0	0.077	1.83	0.55	5.2
250	8	1.03	20.5	0.049	1.81	0.55	3.8
500	4	0.38	27.5	0.036	1.88	0.53	1.5

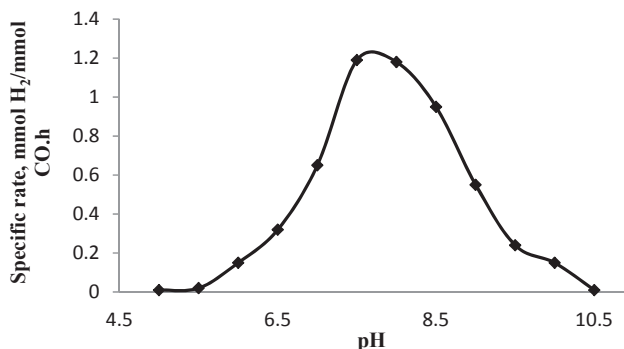


FIGURE 10.9 Specific rate of hydrogen production versus pH.

and productivity. In addition, the pH of the media is directly affected by the kinetic data of hydrogen production in the bioconversion of synthesis gas through a water–gas shift reaction. In this reaction, *Rhodospirillum rubrum* was used as the biocatalyst. To determine the effect of pH in rate studies, complex media were used with malic acid as the carbon source. The pH was adjusted to the desired value using 1M sodium hydroxide solution. The range of pH was 3–12. The data in Figure 10.9 illustrate the specific rate of hydrogen production from synthesis gas with respect to a variable pH; the desired pH for the maximum specific rate of hydrogen production is in the narrow range of 7.5–8.

3. Identification of the major elements of life for living organisms is necessary for a deep understanding of the growth pattern, i.e., nutrient requirement, in a typical yeast cell. Trace metals and minerals act as cofactors in enzyme activities, so the amount of each element such as Zn, Cu, Co, Mg, Mn, and Mo in a typical yeast cell may have a major role. In fact, these essential elements or trace metals may need to be represented in very small amounts, even micrograms, in our synthetic medium formulation. From the relative ratios of the elements present in the media, we may be able to identify the limiting substrate. It is well known that the carbon source is the limiting substrate in application of kinetic models such as the Monod rate model.

References

1. Demain AL, Solomon AN. *Sci Am* 1981;245:67.
2. Phaff HJ. *Sci Am* 1981;245:77.
3. Aiba S, Humphrey AE, Millis NF. *Biochemical engineering*. 2nd ed. New York: Academic Press; 1973.
4. Baily JE, Ollis DF. *Biochemical engineering fundamentals*. 2nd ed. New York: McGraw-Hill; 1986.
5. Blanch HW, Clark SD. *Biochemical engineering*. New York: Marcel Dekker; 1996.
6. Doran PM. *Bioprocess engineering principles*. New York: Academic Press; 1995.
7. Pelczar MJ, Chan ECS, Krieg NR. *Microbiology*. New York: McGraw-Hill; 1986.
8. Scragg AH. Bioreactors in biotechnology, a practical approach. In: *Ellis Horwood series in biochemistry and biotechnology*; 1991. New York.
9. Shuler ML, Kargi F. *Bioprocess engineering, basic concepts*. New Jersey: Prentice-Hall; 1992.

Production of Antibiotics

OUTLINE

11.1 Introduction	346	11.12 Submerged Culture	354
11.2 Herbal Medicines and Chemical Agents	347	11.12.1 <i>Growth Kinetics in Submerged Culture</i>	354
11.3 The History of Penicillin	348	11.13 Bioreactor Design and Control	355
11.4 Production of Penicillin	349	11.14 Estimation of Dimension of Fermenter	356
11.5 Microorganisms and Media	349	11.15 Determination of the Reynolds Number	358
11.6 Inoculum Preparation	349	11.16 Determination of Power Input	358
11.7 Filtration and Extraction of Penicillin	352	11.17 Determination of Oxygen Transfer Rate	359
11.8 Experimental Procedure	352	11.18 Design Specification Sheet for the Bioreactor	361
11.9 Fermenter Description	352	References	361
11.10 Analytical Method for Bioassay and Detection of Antibiotic	352		
11.11 Antibiogram and Biological Assay	353		

11.1 INTRODUCTION

Antibiotics are classified based on their mechanism of action or their function in a host. Some antibiotics are bactericides (an agent that destroys bacteria) whereas others are bacteriostatic, meaning they may inhibit the growth of organisms and multiplication of bacteria but do not kill them. In fact, they act by interfering with the synthesis of folic acid inside the cell anabolism. Another method of classifying antibiotics is based on mode of action as antibiotics interact with an antigen. There are four modes of actions: (1) inhibition of cell wall synthesis, (2) damage of the membrane of the cell surrounded by cytoplasm, (3) inhibition of nucleic acid protein synthesis, and (4) inhibition of specific enzyme systems.

Penicillin, cephalosporin, cytosine, vancomycin, and bacitracin are among the antibiotics that act as inhibitors of cell wall synthesis or biosynthesis of the peptidoglycan structure of the cell wall. These antibiotics hinder the formation of the peptidoglycan polymer, thus formation of the cell wall for cell synthesis is inhibited.

All prokaryote cells have a common peptidoglycan structure in their cell walls. The biopolymers are responsible for cell shape and wall strength. The peptidoglycan polymer alternatively builds subunits of N-acetylmuramic acid, which is similar to N-acetylglucosamine. Pyruvic acid in between units serves as chain reaction for cross-linking of the cell wall with the biopolymer. There are four side chain units that act as cross-linking agents of the cell wall structure: L-alanine, D-glutamic acid, diaminopimelic acid (a compound like an amino acid), and D-alanine. The peptidoglycan content of the cell wall of different strains of bacteria may vary. The contents of cell walls of more than 50% of Gram-positive bacteria and less than 10% of Gram-negative bacteria are the biopolymer of peptidoglycan.

There are a number of bacteria not susceptible to penicillin or inhibition of the cell wall; the biosynthesis of peptidoglycan is not working in the antibiotic mechanisms; that is due to absence of these biopolymers in the cell wall structure. For instance, in *Mycoplasma*, the cell wall is completely lacking peptidoglycan structures. Therefore, penicillin is not able to function as an inhibitor in such organisms. The rigidity of the cell wall and the shape of the cell depend on the content of the peptidoglycan polymer. If an organism is unable to synthesize such a biopolymer for its cell wall, then its replication is hindered. Such mechanisms of action certainly work for Gram-positive bacteria.

Penicillins are known as β -lactam antibiotics and have a related structure with different properties and activities. The antibiotic, with various side chains of chemicals attached to main core of the antibiotic, makes different generations of penicillin. Some strains of bacteria are resistant to penicillin as a result of enzymes produced that break down and inactivate antibiotics. One such enzyme is penicillinase, which deactivates penicillin. The enzyme is synthesized by group of Gram-negative bacteria. In addition, penicillin is deactivated by heat, sodium hydroxide, and strong acid solutions. Among the penicillins, which are much more resistant to acid, may act more efficient would be penicillin V. It is now known that a new generation of a synthesized penicillin with active side chains may be a bactericide; it kills the bacteria rather than inhibits their growth. The bacteria may be destroyed from osmotic damage of the unprotected outer wall, which means that penicillin may not be a suitable antibiotic for the treatment of Gram-negative bacteria because of its cell wall composition, which is completely different than others. However, a high biopolymer content of peptidoglycan of Gram-positive bacteria is a suitable target for penicillin to act as an inhibitor of biosynthesis of the cell wall.

Antibiotics are produced by fermentation. The process may take a few days to obtain an extractable amount of product. Antibiotic production is done in a batch process. Oxygen transport is the major concern; therefore, sufficient polymeric sugar and protein with a trace amount of elemental growth factors are used to enhance production yield. An antibiogram test is used to observe the amount of antimicrobial agent in the fermentation broth. A bioassay determines the activity unit of the bactericides.

11.2 HERBAL MEDICINES AND CHEMICAL AGENTS

Herbal medicine was used in ancient treatments. Natural chemicals extracted from herbs were used. For 17 centuries, natural quinine extracted from the bark of a particular tree known as *cinchona* was used to treat malaria. Native Americans and southern Asians were able to fight malaria by chewing the bark of cinchona trees. Over time, chemical agents were identified and used for treating patients. Toxic compounds such as mercury were used to treat syphilis for 18 centuries. Even arsenic compounds were used to cure many diseases without great danger to the patient. Arsphenamine and neoarsphenamine were also used to treat patients with syphilis. Investigation of chemotherapy expanded into a wide range of compounds. Chemotherapy is known as the treatment of disease with chemicals called *chemotherapy agents*. Treatment with chemicals had been practiced for many centuries. During the mid 1950s, the first generation of sulfonamide was used successfully against certain bacteria, which was a great victory in the field of medicine. Antibiotics as chemotherapy agents were discovered. The action of drugs or chemical agents was to destroy germs, to control the growth of microorganisms, or to prevent microbial growth, with the aim of treating a patient. The chemical substances had selective toxicity, and overdosing created complications for the host. The side effects of chemicals were monitored based on observed symptoms during and after treatment. The drug targeted specific germs and parasites. In general, germicides are not selective in their mechanisms and often interfere with the immune system. Inactivation of germs and parasites with antigens and antibody mechanisms played a major role in the development of germicides and antiseptic agents. The action was similar to the inactivation of protein antigens—by destroying, killing, or deactivating any unknown bodies penetrating the host. The action of chemotherapeutic agents in a host can be summarized as follows:

- The antibiotic agents may destroy or prevent the germs or parasites, without creating any injury to the host cell or with only minimal toxicity to the host.
- The chemical agents should contact the parasite by prevention or by diffusion through the cells and tissues of the host at suitable doses and effective concentrations.
- The action should not disturb the immune system, such as cell defense actions (known as *phagocytosis*) production of antibodies, which takes place naturally in the presence of parasites.
- These agents profoundly prevent production of bacterial nucleic acids and inhibit genetic replication.

Sulfonamides are very useful in treating bacterial infections, especially the infectious agents of known microorganisms such as meningococci and *Shigella*, respiratory infections caused by streptococci and staphylococci, and urinary tract infections resulting from Gram-negative microorganisms. Sulfonamide drugs are strongly recommended for rheumatic fever, endocarditis, and urinary tract infections after any surgery.¹

11.3 THE HISTORY OF PENICILLIN

The original organism for producing penicillin, *Penicillium notatum*, was isolated by Alexander Fleming in 1926 as a chance contaminant while culturing other organisms. However, all the penicillin-producing strains were isolated and purified from an infected cantaloupe obtained from a market in Peoria, Illinois.¹ The infecting organism was *Penicillium chrysogenum*. The original wild strain of *Penicillium* produces a yellow pigment devoid of antibiotic properties that colors the final product. Production of antibiotics by mutants does not produce any pigment and yields a colorless end product.

The chemotherapeutic agent extracted or obtained from secondary metabolites of living cells is known as an *antibiotic*. The terms *antibiotic* and *antibiosis* were introduced during the 20th century when Alexander Fleming, during the 1930s, accidentally found mold contaminating a culture while he was cultivating microorganisms. At the time, Fleming was culturing *Staphylococcus aureus* on a plate with a thin agar layer. His cultured plate was contaminated with a mold. The amazing part of his work was that he found no microbial growth within a radius of 3–5 cm of the mold.² Normally, any contaminated culture is taken out of the investigation cycle, but Fleming was curious and decided to continue his investigation. He wanted to know why there was no growth in presence of the mold. He needed to know what the toxic metabolite was that killed the organisms in the neighborhood of the mold. He found that the cell metabolites were able to lyse and dissolve the cell walls of the microorganisms. He identified the contaminants as mold. Later, the mold was identified as *Penicillium* sp. Fleming named the drug *penicillin*, which was isolated from *P. notatum*. Fleming had discovered a new antibiotic, and for his great contribution he was awarded the Nobel Prize, in the field of medicine and physiology in 1945. His discovery answered his question of why the colony of *Staphylococcus* did not grow in presence of *P. notatum*.

The commercial production of penicillin and other antibiotics is the most dramatic example of industrial microbiology. The annual production of bulk penicillin is about 33 million lb, with an annual sales market of more than US\$344 million.¹

Production of penicillin has been superseded by a better antibiotic-producing mold species: *P. chrysogenum*. The development of submerged culture techniques has enhanced the cultivation of the mold in large-scale operations using a sterile air supply. The development of advanced fermentation technologies lead in to utilize suitable nutrient resources, potential strain of microorganisms and the biosynthesis of organic compounds stated as follows:

- Streptomycin is produced by *Actinomycetes*.
- Molasses, corn steep liquor, waste product from the sugar industry, and wet milling corn are used for the production of penicillin.
- *P. chrysogenum* can produce 1000 times more penicillin than Fleming's original culture.^{1,3,4}

The major steps in the commercial production of penicillin are as follows:

1. Preparation of inoculum.
2. Preparation and sterilization of medium.
3. Inoculation of the medium in the fermenter.
4. Forced aeration with sterile air during incubation.
5. Removal of mold mycelium after fermentation.
6. Extraction and purification of the penicillin.

11.4 PRODUCTION OF PENICILLIN

There is only one choice for the antibiotic production process: the synthesis of benzylpenicillin (penicillin G, originally known as *penicillin*). This, the most renowned antibiotic and the first one manufactured in bulk, is still prescribed universally.⁵ Although originally made by surface liquid culture, penicillin G is now produced by airlift fermentation under aerated conditions.

Penicillin G is not a typical fermented antibiotic; it is made by the fungus *P. chrysogenum*. The number of antibiotics from fungal sources is few, although they do include penicillin G and V, and cephalosporin C. These three antibiotics are the major starting materials for the semisynthetic β -lactam antibiotics. The systemic antifungal antibiotic griseofulvin is also of fungal origin. Most antibiotics are produced by fermentation using fungi, including streptomycin and the tetracycline family, among numerous others. Streptomycin is the next important antibiotic after penicillin G that is available for clinician use. It has played an important role in the fight against tuberculosis.¹

Penicillin production occurs as batched fermentation, during which a volume of sterile medium in a vessel is inoculated. The broth is fermented for a defined period, then the tank is emptied and the products are separated to obtain the antibiotic. The vessel is then recharged for batch operation with medium and the sequence is repeated, as often as required. Continuous fermentation is not a common practice in the antibiotics industry. The antibiotic concentration rarely exceeds 20 g/L and may be as low as 0.5 g/L.

11.5 MICROORGANISMS AND MEDIA

A mutant strain⁶, P2-4, derived from *Penicillium chrysogenum* ATCC 48271 has been used in solid-state fermentation for penicillin production. Also a series of experimental studies in a 2-L B Braun airlift fermenter. A complex growth medium for *P. chrysogenum* was prepared. The medium contained 20 g sucrose, 10 g lactose, 5 g peptone, 13 g $(\text{NH}_4)_2\text{SO}_4$, 3 g KH_2PO_4 , 0.5 g Na_2SO_4 , 0.55 g ethylenediamine tetraacetic acid, 0.25 g $\text{MgSO}_4 \cdot 7\text{H}_2\text{O}$, 0.05 g $\text{CaCl}_2 \cdot 2\text{H}_2\text{O}$, 0.25 g $\text{Fe}_2\text{SO}_4 \cdot 7\text{H}_2\text{O}$, 0.02 g $\text{MnSO}_4 \cdot 4\text{H}_2\text{O}$, 0.02 g $\text{ZnSO}_4 \cdot 7\text{H}_2\text{O}$, 0.01 g $\text{Na}_2\text{MoO}_4 \cdot 2\text{H}_2\text{O}$, and 0.005 g $\text{CuSO}_4 \cdot 5\text{H}_2\text{O}$ in 1000 mL distilled water. The medium was sterilized in an autoclave at 121 °C for 30 min.

11.6 INOCULUM PREPARATION

Most fungi sporulate on suitable agar media, but a large surface area is required to produce sufficient spores. A roll-bottle technique is used to produce spores of *P. chrysogenum*, with 300 mL medium containing 3% agar sterilized in a 1-L cylindrical bottle. After autoclaving, the medium is cooled to 45 °C and rotated on a roller mill so that a layer of agar formed on the cylinder wall. The inoculum used for inoculation was of a spore suspension is incubated at 24 °C for 6–7 days.

Submerged culture is common for sporulation of fungi such as *P. chrysogenum*. Sporulation is induced by inoculating 300 mL of a spore suspension in a 1-L shaking flask containing spores from a well-sporulated agar culture, which is then incubated for a sufficient time.

At this stage, a 2-L fermenter is inoculated with a pure inoculum (300 mL) and harvested in the fast-growing (logarithmic) phase, so that a high cell density is obtained in the culture. The organism *P. chrysogenum* grows in a filamentous (hypha) form, with branching occurring to a greater or lesser extent. The B Braun airlift fermenter is used for production. A pressurized air filter is used to circulate the mycelia in an internal loop pattern. Air is supplied continuously and bubbles lose oxygen as they rise up the column. At the same time, carbon dioxide and other gaseous metabolites are released in the overhead gas compartment. The production of penicillin G is very sensitive to temperature, with a tolerance of less than 1 °C. Heat is generated by the metabolism of nutrients and has to be removed by a well-controlled cooling system. Cooling coils are used for isothermal operation. The fermentation vessel is fitted with several probes to detect foaming, to monitor temperature, to control the media level, and to record parameters such as pH. The rate of airflow through the fermenter is measured, and the exhaust gases that emerge from the top of the vessel may also be analyzed. Originally, all penicillin G was manufactured using lactose in this way, and some manufacturers still prefer this technique.

Calcium, magnesium, phosphates, and trace metals added initially are usually sufficient to last throughout fermentation, but the microorganisms need an additional supply of nitrogen and sulfur to balance the carbon feed. Nitrogen is often supplied as ammonia gas. Ammonium ions can contribute to pH control, with carbon metabolism being acidogenic and balanced by the alkalinity of the ammonia. Sulfate is usually supplied in common with the sugar feed and the flow is adjusted with suitable feed stream ratios.

All feed streams are sterilized before being entered into the fermentation vessel. Contaminants resistant to the antibiotic rarely find their way into the fermenter. When they find a way to contaminate media, their effects are so catastrophic that prevention is of paramount importance. A resistant, β -lactamase-producing, fast-growing bacterial contaminant can destroy the penicillin.⁵ The contaminants not only consume nutrients intended for the fungus, but also cause loss of pH control and interfere with the subsequent extraction process.

A Petri dish culture of penicillin is shown in [Figure 11.1\(a\)](#). The action of the antibiotic shows an overlay plate, in which a central colony of the fungus *P. notatum* was allowed to grow on agar for 4–5 days. The plate was then overlain with a thin film of molten agar containing cells of the yellow bacterium *Micrococcus luteus*. The production of penicillin by the fungus creates a clear zone free of organisms, which means the antibiotic activities of penicillin cause growth inhibition of the yellow bacterium. [Figure 11.1\(b\)](#) shows the typical asexual sporing structures of a species of *Penicillium*. The spores are produced in chains from flask-shaped cells (phialides), which are found at the tips of a brushlike aerial structure.¹

Penicillin has an interesting mode of action in that it prevents the cross-linking of small peptide chains in the peptidoglycan—the main cell wall polymer of bacteria. Preexisting cells are unaffected, but all newly produced cells grow abnormally. The newly formed cells are unable to maintain their wall rigidity and are susceptible to osmotic lysis.

The clinical aspects of several antibiotics such as penicillin G, cephalosporin, and many other antibiotics are summarized in [Table 11.1](#). The potential microorganisms for the production of various antibiotics and their activities onsite or the mode of action of the antibiotics are also listed.

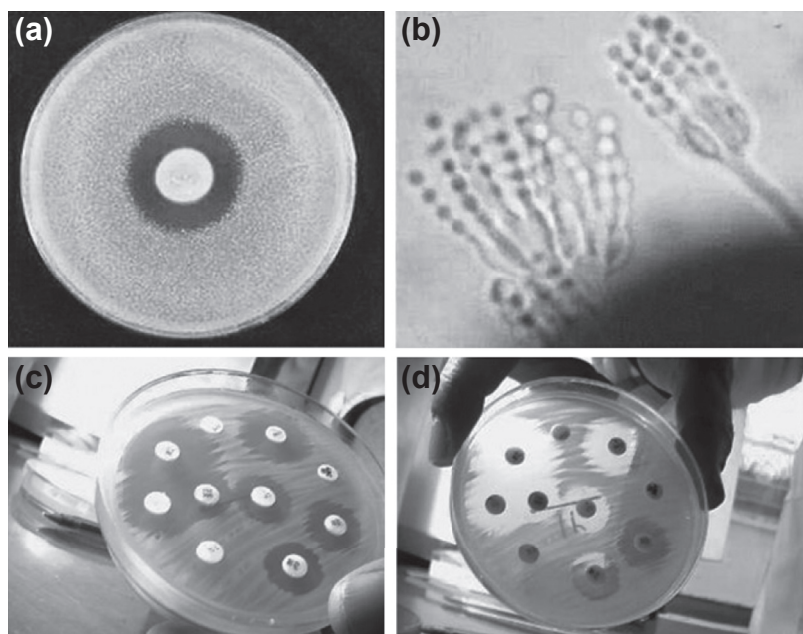


FIGURE 11.1 (a) Action of penicillin. (b) Structure of a species of *Penicillium*. (c) An antibiogram testing several antibiotics is effective, as noted by the surrounding clear space. (d) Unsuccessful antibiotic surrounded with cell growth at the 2, 7, and 11 O'clock positions.

TABLE 11.1 Clinically important antibiotics and the producing microorganism³

Antibiotic	Producer organism	Activity	Site or mode of action
Penicillin	<i>Penicillium chrysogenum</i>	Gram-positive bacteria	Wall synthesis
Cephalosporin	<i>Cephalosporium acremonium</i>	Broad spectrum	Wall synthesis
Griseofulvin	<i>Penicillium griseofulvum</i>	Dermatophytic fungi	Microtubules
Bacitracin	<i>Bacillus subtilis</i>	Gram-positive bacteria	Wall synthesis
Polymyxin B	<i>Bacillus polymyxa</i>	Gram-negative bacteria	Cell membrane
Amphotericin B	<i>Streptomyces nodosus</i>	Fungi	Cell membrane
Erythromycin	<i>Streptomyces erythreus</i>	Gram-positive bacteria	Protein synthesis
Neomycin	<i>Streptomyces fradiae</i>	Broad spectrum	Protein synthesis
Streptomycin	<i>Streptomyces griseus</i>	Gram-negative bacteria	Protein synthesis
Tetracycline	<i>Streptomyces rimosus</i>	Broad spectrum	Protein synthesis
Vancomycin	<i>Streptomyces orientalis</i>	Gram-positive bacteria	Protein synthesis
Gentamicin	<i>Micromonospora purpurea</i>	Broad spectrum	Protein synthesis
Rifamycin	<i>Streptomyces mediterranei</i>	Tuberculosis	Protein synthesis

11.7 FILTRATION AND EXTRACTION OF PENICILLIN

At harvest, the cells are removed. Penicillin G is the cell product in the solution that is an extracellular product, with a host of other metabolites and medium constituents. The first step in harvesting penicillin is to remove the cells by filtration. This stage is done under conditions that avoid contamination of the filtrate with enzymes, which may destroy the antibiotic. The β -lactamase-producing microorganisms could react with the antibiotics, which may cause serious or total loss of the product.⁵ The next stage is to isolate penicillin G. Solvent extraction is the generally accepted process. In aqueous solution at a pH of 2–2.5, there is a high partition coefficient in favor of certain organic solvents, such as amyl acetate, butyl acetate, and methyl isobutyl ketone. The extraction has to be done quickly because penicillin G is very unstable at low pH values. The penicillin is then extracted back into an aqueous buffer at a pH of 7.5. The partition coefficient now strongly favors the aqueous phase. The solvent is recovered by distillation for reuse.

11.8 EXPERIMENTAL PROCEDURE

The inoculate was prepared in 250-mL flasks containing 100 mL growth medium, which was inoculated with 10 mL of spore suspension. The mixture was shaken at 250 g and the temperature was controlled at 26 °C for 48 h. Then, 110 mL of the resulting mycelia suspension was used to inoculate a 1000 mL broth in the airlift fermenter. The sterilized media were pumped slowly into the bioreactor at a flow rate of about 100 mL h⁻¹ until 2 L working volume was used completely. Aeration rates of 0.5, 1, and 2 vvm (1, 2, and 4 L of air per min) were used.^{7,8} Samples were taken at 24 h intervals and evaluated for biomass, sugars, and antibiotic concentrations.

11.9 FERMENTER DESCRIPTION

A 2-L B Braun airlift fermenter with a working volume of about 2000 mL is used. Sterile air is sparged through a sintered plate located near the bottom of the central concentric tube. There is no mechanical stirring; only the air nozzle was forced through the central tube, and the flow was directed to the annulus tube side. Aeration causes circulation of the media; the flow was gentle without serious shear forces. Temperature was maintained at 26 °C.

11.10 ANALYTICAL METHOD FOR BIOASSAY AND DETECTION OF ANTIBIOTIC

The extracted antibiotic was used in an antibiogram test. Petri dishes of *Bacillus subtilis* ATCC 6633 are cultured for bioassay of penicillin. Small circular paper filters (3–5 mm) are placed at different positions on the surface of the agar. The small circular filters were

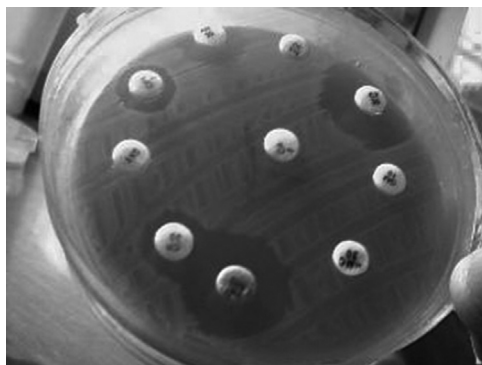


FIGURE 11.2 Antibioqram test diffusion of antibiotic on agar layer, preventing microbial growth.

sterilized earlier. A few drops of concentrated and extracted antibiotic were poured on the filter. The small circular filter held the antibiotic after incubation for 24 h. There was a clear circle around the paper filter without any microbial growth. This bioassay is called an *antibioqram*. Figure 11.2 shows an antibioqram test diffusion of antibiotic on an agar layer, which prevents microbial growth. Normally, an antibioqram is used for clinical purposes to identify a suitable antibiotic for infected patients. High-performance liquid chromatography is commonly used for quantitative analysis. The carbohydrate concentration is determined using the dinitrosalicylic acid method.⁹ The biomass is evaluated by measuring the total solid concentration. Cell dry weight may represent the growth curve in the fermentation broth. The samples were centrifuged at 4500 rpm for 20 min, and the sediment was washed with distilled water and dried in an oven at 105 °C to determine cell dry weight.

11.11 ANTIBIOGRAM AND BIOLOGICAL ASSAY

Antibiotic activities are examined by transfer of seed culture of *B. subtilis* on nutrient agar on a Petri dish. The seed culture for *B. subtilis* is a simple basal media of 1 g glucose, 1 g peptone, and 1 g yeast extract; it does not require a complex medium. The antibioqram test for diffusion of the antibiotic product obtained with solvent extraction using amyl acetate or methyl *iso*-butyl ketone is then distilled and concentrated for bioassay. A few drops of antibiotic are tested according to the antibioqram test shown in Figure 11.1. The Petri dish media is a simple basal media with 3% agar. The Petri dishes are prepared in advance and stored in a refrigerator so they are ready to use for microbial growth tests. The Petri dishes inoculated with *B. subtilis* are incubated at 32 °C. The clear area around the antibiotic shows that *B. subtilis* is unable to grow near the antibiotic. The activities are scaled from +1 to +4, based on the radius of the clear circle of 5–10 mm without any microbial growth.

11.12 SUBMERGED CULTURE

11.12.1 Growth Kinetics in Submerged Culture

The use of stirred fermenters with automatic control of the culture environment is the most suitable technique to evaluate bacterial or fungal kinetics. Cultures can be operated in discontinuous mode (batch cultures). The growth curve of the batch culture of a micro-organism can be divided into six phases (Figure 11.3): the lag phase (phase I), the accelerating growth phase (phase II), the exponential growth phase (phase III), the declining growth phase (phase IV), the stationary phase (phase V), and the death phase or lytic decline phase (phase VI). The growth curve is often represented by mathematical models.¹⁰ In the case of media limitation, the Monod equation is most often used to describe growth rate:

$$\mu = \frac{\mu_m S}{K_s + S} \quad (11.12.1.1)$$

where μ_m is the maximum specific growth rate per hour and K_s is the saturation constant in grams per liter. For special cases when $K_s \ll S$, then $S/(K_s + S) \approx 1$ and the growth is stable at the stationary phase. If the value of K_s is relatively high compared with the substrate concentration (S), when substrate concentration decreases, a decelerating growth phase is reached. Values of growth rate (μ) are dependent on a combination of media–fungus, but most often the projected value is between 0.1 and 0.4 h^{-1} . Values of K_s can be determined by plotting $1/\mu_m$ against $1/S$. The linear rate equation becomes a Lineweaver–Burk plot:

$$\frac{1}{\mu} = \frac{K_s}{\mu_m} \frac{1}{S} + \frac{1}{\mu_m} \quad (11.12.1.2)$$

Figure 11.4 shows the growth curve with the log, stationary, and death phases for micro-organism growth. In the case of nonexponential growth (Figure 11.4), the value of K_s can be approximated from the curve $\mu = f(S)$. Growth of fungi in batch culture is difficult to trace

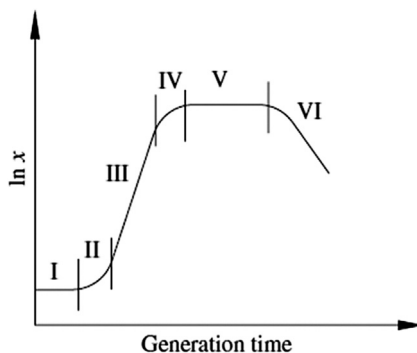


FIGURE 11.3 Batch growth curve with various phases.

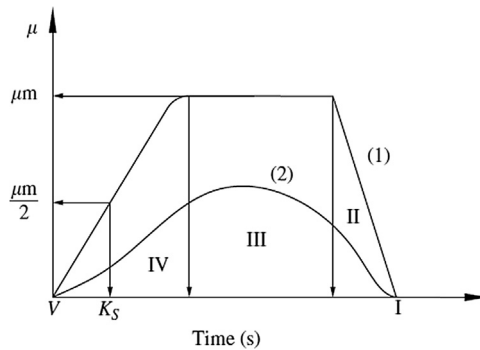


FIGURE 11.4 Nonexponential growth curve in a batch culture.

because of the exponential increase in biomass concentration for the organism, with more than five doubling times. After a certain growth time, the fungus eventually modifies the physicochemical condition of its environment and, correspondingly, growth slows the process as a result of low substrate concentration, limitation of nutrients, low oxygen transfer rate, product inhibition, and accumulation of undesired products. Morphologically, linear growth can be correlated with a blockage of the branching, when branching of the mycelium or the fermentation of blastospores (yeastlike cells) induces an exponential increase of the biomass.

11.13 BIOREACTOR DESIGN AND CONTROL

Incubation control necessitates the precise control of several influential parameters, which are the primary process variables and growth conditions¹¹:

- Temperature
- Agitation
- pH
- Dissolved oxygen
- Pressure
- Airflow
- Nutrients
- Redox

The pH is typically controlled by acid–alkali feeds. Dissolved oxygen and redox loops are controlled as a cascade loop using airflow, agitation, pressure, auxiliary feed, or a combination thereof. The control of these and any other parameter is most usually done in fermenter vessels designed specifically for this purpose and that accommodate various working volumes, depending on the yield and production requirements. Laboratory-scale vessels have a capacity of 10 L or less, whereas clinical trials and production vessels may be as large as several thousand liters.

The actual incubation of the culture is known as the fermentation process, which is part of the batch cycle. A complete fermentation cycle typically includes the following steps, depending predominantly on bioreactor design:

- Sterilization of empty vessel and piping using direct steam injection
- Medium charging
- Indirect sterilization by steam injected into the vessel jacket
- Cooling and jacket drain
- Preinoculation of vessel environment under control
- Inoculation (injection of a small sample of the monoculture)
- Incubation of the fermentation process
- Harvest of the product (extraction process)

A control system must, therefore, provide flexibility in such a way that the results are accurate and repeatable. Also, precise control of the fermentation environment is necessary and includes the following:

- Precise loop control with set point profile programming
- Recipe management system for easy parameterization
- Sequential control for vessel sterilization and more complex control strategies
- Secure collection of online data from the bioreactor for analysis and evidence
- Local operator display with clear graphics and controlled access to parameters

A conventional batch fermenter and the important parts of the fermentation vessel are shown in [Figure 11.5](#).

11.14 ESTIMATION OF DIMENSION OF FERMENTER

Suppose a fermenter has a working volume of 10 m^3 ($V_{\text{working}} = 10 \text{ m}^3$); let us add 20% overdesign as a safety factor. The total volume (V) is

$$V = \frac{V_{\text{working}}}{0.8} = \frac{10 \text{ m}^3}{0.8} = 12.5 \text{ m}^3$$

The volume of a fermenter for a cylindrical system is defined as

$$V = \frac{\pi}{4} \times D_t^2 \times H_L \quad (11.14.1)$$

where D_t is the diameter of the tank in meters and H_L is the height of the fermentation vessel. Let us take the ratio of the liquid level to the tank diameter to be $H_L:D_t$, 2:1; therefore,

$$V = \frac{\pi}{4} \times D_t^2 \times 2D_t \quad (11.14.2)$$

$$V = 0.5\pi \times D_t^3 = 12.5 \text{ m}^3$$

Solving for tank diameter, D_t , and liquid height,

$$D_t = 2.0 \text{ m}$$

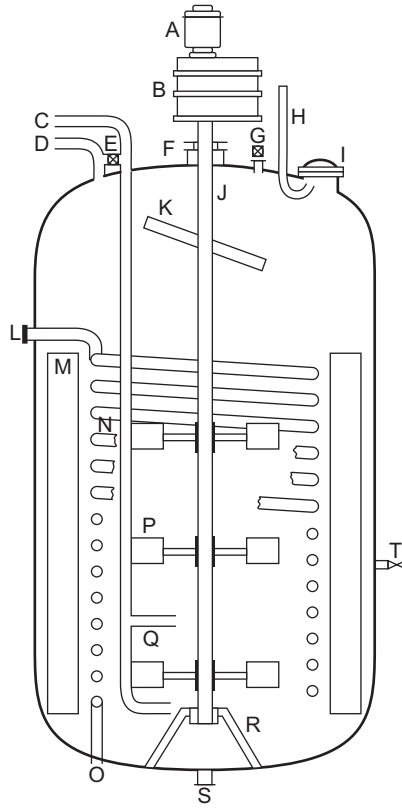


FIGURE 11.5 Conventional batch fermenter: A, agitator motor; B, speed reduction unit; C, air inlet; D, air outlet; E, air bypass valve; F, shaft seal; G, sight glass with light; H, sight glass clean-off line; I, manhole with sight glass; J, agitator shaft; K, paddle to break foam; L, cooling water outlet; M, Baffle; N, Cooling coil; O, cooling water inlet; P, mixer; Q, sparger; S, outlet; T, sample valve.

$$H_L = 2 \times D_t = 2 \times 2.0 = 4.0 \text{ m}$$

The diameter of the impeller is set to one-third of the tank diameter:

$$D_i = \frac{D_t}{3} = \frac{2.0 \text{ m}}{3} = 0.67 \text{ m}$$

Let us take the required aeration as 1.0 vvm. The volumetric flow of air for a 12.5 m^3 fermenter is defined as

$$F_g = 1.0 \text{ vvm} \times 12.5 \text{ m}^3 = 12.5 \frac{\text{m}^3}{\text{min}} \times \frac{1 \text{ min}}{60 \text{ s}} = 0.21 \text{ m}^3 \text{ s}^{-1}$$

The gas superficial velocity is defined as the ratio of gas flow rate to vessel cross-sectional area:

$$U_s = \frac{F_g}{A} = \frac{12.5 \frac{\text{m}^3}{\text{min}}}{\frac{\pi}{4}(2.0)^2 \text{ m}^2} \times \frac{60 \text{ min}}{1 \text{ h}} = 238.73 \text{ m h}^{-1}$$

11.15 DETERMINATION OF THE REYNOLDS NUMBER

To calculate the Reynolds number, let us define an average density at the inlet using weight fractions:

$$\rho_{\text{ave.in}} = (0.80 \times 1544) + (0.05 \times 1834) + (0.07 \times 597.1) + (0.08 \times 1000)$$

$$\rho_{\text{ave.in}} = 1448.70 \text{ kg m}^{-3}$$

Also, the average density of the outlet stream is

$$\rho_{\text{ave.in}} = (0.16 \times 3420) + (0.23 \times 110.1) + (0.21 \times 1000) + (0.40 \times 1013)$$

$$\rho_{\text{ave.in}} = 1187.72 \text{ kg m}^{-3}$$

The highest density of the solution is used to determine the Reynolds number. The broth is viscous and viscosity is assumed to be $\mu = 0.1 \text{ Pa s}^{-1}$. The rotational speed of the impeller is set at $N = 150 \text{ rpm} = 2.5 \text{ rps}$.

The Reynolds number is calculated based on provided data:

$$\text{Re} = \frac{\rho N D_i^2}{\mu} = \frac{(1448.70 \frac{\text{kg}}{\text{m}^3}) \times (2.5 \text{ rps}) \times (0.67 \text{ m})^2}{(0.1 \text{ Pa s}^{-1})}$$

$$\text{Re} = 16,258$$

The high Reynolds number represents the turbulent flow regime.

11.16 DETERMINATION OF POWER INPUT

First it is necessary, using knowledge of the flow regime, to read the power number directly from a power graph (as discussed in Chapter 6 and illustrated in Figure 6.6). The reading for Reynolds numbers greater than 16,000 is $P_{no} = 6$. The equation for the power number is

$$P_{no} = \frac{P_g}{\rho N_i^3 D_i^5} = 6 \quad (11.16.1)$$

Therefore, ungassed power is calculated as

$$P = \frac{6 \times (1448.70 \frac{\text{kg}}{\text{m}^3}) \times (2.5 \text{ rps})^3 \times (0.67 \text{ m})^5}{9.81 \frac{\text{m}}{\text{s}^2}} = 1869.2 \text{ kg m s}^{-1}$$

$$P = 1557.66 \frac{\text{kg m}}{\text{s}} \times \frac{1 \text{ hp}}{745.7 \frac{\text{kg m}}{\text{s}}} = 2.5 \text{ hp}$$

That is the input power required for one set of impellers. Correction factors (f_c) for nongeometric similarity are required to include the effect of known factors in precise calculations.

$$f_c = \sqrt{\frac{\left(\frac{D_t}{D_i}\right)^* \left(\frac{H_L}{D_i}\right)^*}{\left(\frac{D_t}{D_i}\right) \left(\frac{H_L}{D_i}\right)}} \quad (11.16.2)$$

where the parameter in designing the bioreactor is set at $D_t/D_i = 3$ and $H_L/D_i = 3$. On substitution, for the previous cases the correction factor is calculated as

$$f_c = \sqrt{\frac{\left(\frac{2.0}{0.67}\right) \left(\frac{4.0}{0.67}\right)}{3 \times 3}} = \sqrt{\frac{3 \times 6}{3 \times 3}} = 1.414$$

Therefore, the actual power with the correction factor is

$$P^* = 1.414 \times P = 1.414 \times 2.09 \text{ hp} = 3.54 \text{ hp}$$

The dimensionless aeration rate is defined by the following equation:

$$N_a = \frac{F_g}{N_i D_i^3} = \frac{0.21 \frac{\text{m}^3}{\text{s}}}{(2.5 \text{ rps}) \times (2.0 \text{ m})^3} = 0.0105 \quad (11.16.3)$$

Read the ratio of gassed power to ungassed power from Figure 6.7. The reading from the graph is $P_g/P = 0.9$. The gassed power for the motor to rotate is

$$P_g = 0.9 \times 3.54 \text{ hp} = 3.2 \text{ hp}$$

11.17 DETERMINATION OF OXYGEN TRANSFER RATE

The mass transfer coefficient for noncoalescing air bubbled in the fermentation broth in a turbulent regime is discussed frequently in the literature.⁶ The volumetric mass transfer coefficient is defined by the following correlation:

$$K_L a = 2 \times 10^{-3} \left(\frac{P_g}{V_L} \right)^{0.6} (V_S)^{0.667} \quad (11.17.1)$$

where the gas superficial for the previous case is calculated as $V_S = 0.21 \text{ m}^3 \text{ s}^{-1}$ per $\pi (2 \text{ m})^2$, and the vessel working volume is

$$V_L = 4\pi \text{ m}^2 \times 4 \text{ m} = 16\pi \text{ m}^3$$

Substituting V_S and V_L into the previous equation allows one to determine the volumetric mass transfer coefficient. The volumetric mass transfer coefficient is calculated as

$$K_L a = 2 \times 10^{-3} \left(\frac{2.664 \text{ hp}}{16\pi \text{ m}^3} \right)^{0.6} \times \left(\frac{0.21 \text{ m}}{4\pi \text{ s}} \right)^{0.667} = 2.24 \times 10^{-5} \text{ s}^{-1}$$

TABLE 11.2 Fermenter design specification sheet

Fermenter			
Identification:	Item:	Fermenter	Date: 24-02-2005 By: Nicky Teoh
Function:	To produce Penicillin G from the raw materials fed		
Operation:	Batch		
Type	Batch reactor		
Material handled:	Inlet		Outlet
Quantity (kg)	2079.81		2090.84
Composition			
Penicillin G	—		334.0
Water	167.04		432.18
Glucose	1670.40		—
H ₂ SO ₄	98.00		—
NH ₃	155.38		—
CO ₂	—		489.28
Biomass	—		835.38
Pressure (bar)	1.00		1.00
Temperature (°C)	25.00		25.00
Design data:			
Tank	Turbine		
Height (m)	4.0	Turbine impeller diameter, m	0.67
Diameter (m)	2.0	Impeller speed, rpm	150
Capacity safety factor (%)	20.0		
Capacity (m ³)	12.5	Ungassed power, hp	2.96
Operating pressure (bar)	1.0	Gassed power, hp	2.664
Operating temperature (°C)	32.0	Oxygen transfer rate, kg > m ⁻³ > s ⁻¹	1.344 × 10 ⁻⁷
Material of construction	Stainless steel		
Utilities:	Chilled water		
Tolerances:	Rules of thumb and heuristics		

The simple equation for the oxygen transfer rate is based on the driving forces existing for the equilibrium value for oxygen concentration and the dissolved oxygen available in the liquid phase:

$$OTR = K_L a (C_1^* - C_1) \quad (11.17.2)$$

The assumption was made that the equilibrium value for oxygen was $C_1^* = 6$ ppm and all oxygen available in the liquid phase was used by microorganisms ($C_1 = 0$), which means the growth was mass transfer limited, the organisms were growing fast, and the limited oxygen transfer can retard the biological process. The oxygen transfer rate is calculated as

$$OTR = 2.24 \times 10^{-5} (6 \times 10^{-3} - 0) = 1.344 \times 10^{-7} \text{ kg O}_2 \text{ m}^{-3} \text{ s}^{-1}$$

11.18 DESIGN SPECIFICATION SHEET FOR THE BIOREACTOR

The characteristics and design specification sheet for the bioreactor are summarized in [Table 11.2](#).

References

1. Pelczar MJ, Chan ECS, Krieg NR. *Microbiology*. 6th ed. New York: McGraw-Hill; 1993.
2. Baily JE, Ollis DF. *Biochemical engineering fundamentals*. 2nd ed. New York: McGraw-Hill; 1986.
3. Stanbury PF, Whitaker A. *Principles of fermentation technology*. New York: Pergamon Press; 1987.
4. Demain AL, Solomon NA. *Sci Am* 1981;**245**:67.
5. Voet D, Voet JG. *Biochemistry*. 3rd ed. New York: John Wiley; 2004.
6. Dominguez M, Mejia A, Revah S, Barrios-Gonzalez J, World J. *Microbiol Biotechnol* 2001;**17**(7):751–756.
7. Scragg AH. *Bioreactors in biotechnology, a practical approach*. Ellis Horwood series in biochemistry and biotechnology; 1991. New York.
8. Ghose TK. *Bioprocess computation in biotechnology*. Ellis Horwood series in biochemistry and biotechnology, vol. 1; 1990. New York.
9. Miller GL. *Anal Chem* 1959;**31**:426.
10. Doran PM. *Bioprocess engineering principles*. New York: Academic Press; 1995.
11. Shuler ML, Kargi F. *Bioprocess engineering, basic concepts*. New Jersey: Prentice-Hall; 1992.

Production of Citric Acid

OUTLINE

12.1 Introduction	363	12.7.1 Cell Dry Weight	368
12.2 Production of Citric Acid in Batch Bioreactors	364	12.7.2 Carbohydrates	369
12.2.1 Microorganism	365	12.7.3 Citric Acid	369
12.3 Factors Affecting Mold Growth and the Fermentation Process	365	12.8 Processes for Recovery and Purification of Citric Acid	369
12.4 Starter or Seeding an Inoculum	367	12.9 Experimental Run	369
12.5 Seed Culture	367	12.10 Kinetic Model in Batch Citric Acid Fermentation	371
12.6 Citric Acid Production	367	Nomenclature	373
12.7 Analytical Method	368	References	373

12.1 INTRODUCTION

Citric acid is an intermediate organic compound in the tricarboxylic acid (TCA) cycle and is found naturally in citrus fruits, pineapples, and pears and crystallized as calcium citrate. It is an important chemical used in medicines, flavoring extracts, food, candies, and the manufacture of ink and dyes. It also is used in detergents as a surfactant in the form of trisodium citrate. Citric acid is a six-carbon TCA that was first isolated from lemon juice. It is used for various purposes in the food and beverage industry, as pharmaceuticals, and for other

industrial uses. It is an organic carboxylic acid and can be extracted from the juice of citrus fruits by adding calcium oxide (lime) to form calcium citrate, which is an insoluble precipitate that can be collected by filtration; the citric acid can be recovered from its calcium salt by adding sulfuric acid. Citric acid is mainly produced by fermentation. There are many potent microorganisms including fungi, yeast, and bacteria that are able to produce citric acid by fermentation. It also is obtained by fermentation of glucose with the aid of the mold *Aspergillus niger*. Citric acid is used in soft drinks and also used as food additives. Its salts, the citrates, have many uses; for example, ferric ammonium citrate is used in making blue print paper. Sour salt, used in cooking, is citric acid. Most citric acid is produced by fungal (*A. niger*) fermentation. For production of enzymes from fungi, nitrogen and phosphate sources are specifically involved in synthesis and liberation of enzymes. *A. niger* is a potential organism for the synthesis of oxalate and citrate as members of TCA cycle while limitation of nitrogen and phosphate sources may influence on concentration of organic acid production. In addition, metal ions such as copper, iron, and manganese may be influential in the high productivity of citric acid. *Aspergillus niger* may propagate in the form of mycelia, which may cause clogging problems in a continuous system. Yeast such as *Saccharomycopsis lipolytica*, however, does not form mycelia; the organism is very stable with a high citric acid yield on glucose. The disadvantage of yeast in the production of citric acid is the by-product of isocitric acid, which is also synthesized in parallel as a side reaction. *Candida lipolytica* grown on normal paraffin mixture continuously produced citric acid. The process yield by weight is significantly higher than other carbon sources. Other species such as *Candida guilliermondii* use molasses for the production of citric acid. The rate of productivity of organic acid is estimated to be $0.35 \text{ g (L h)}^{-1}$.¹ In fact, citric acid is considered a secondary metabolite, which is synthesized via the TCA cycle. The production rate may be enhanced if the organisms are under catalytic repression by limiting nitrogen sources such as ammonia. Chemical synthesis of citric acid is possible, but it is not cheaper than fungal fermentation. However, a small amount of citric acid is still produced from citrus fruits in Mexico and South America, where they are available economically. There are basically three different types of batch fermentation process used in industry. Two very common and practical fermentation processes are the liquid surface culture and the submerged fermentation process. The second process, submerged culture fermentation, is more popular. Continuous fermentation has been studied at the laboratory scale.^{1,2}

12.2 PRODUCTION OF CITRIC ACID IN BATCH BIOREACTORS

Citric acid fermentation of cane molasses is created through submerged fermentation in a 2 L biostat stirred fermenter (B. Braun). A strain of *A. niger* is the most widely used for commercial production. *A. niger* is also highly recommended in this study, and can be obtained from American Type Culture Collection (ATCC; Rockville, Maryland, USA). Molasses from cane sugar is used with the addition of trace metals at the desired concentration.

The sources of sugar and initial pH of the media play a major role in citric acid production. Submerged and surface cultures are customarily used with cheap but purified and high-concentration sources of sugars. A variety of sugars may serve as the substrate for the production of citric acid; however, molasses and cane sugar are generally used in fermentation processes. Carbohydrates, along with nutrients, are incorporated into a medium with necessary

trace metals and minerals. The medium is sterilized and then inoculated with the mold spores. The process is aerobic; adequate mixing and aeration for supply of oxygen is required. Air passes through a suitable filter in a sterile condition then is supplied to a large-scale fermentation tank. The strain of mold used, the composition of the medium, the necessary amount of oxygen supply, the incubation temperature, and pH affect the yield of citric acid produced.

12.2.1 Microorganism

Aspergillus niger (ATCC 11414) can be used for citric acid fermentation. It should be ordered from the ATCC. The culture was maintained on 10.0% sterilized molasses obtained from Central Sugar SDN BHD (pH 5.8). The slant stock cultures of *A. niger* are stored at 5 °C in the refrigerator. All the culture media, unless otherwise stated, are sterilized at 121 °C (15 psig pressure) for 15 min.

Aspergillus niger utilizes beet molasses, fructose, glucose, and starch hydrolysates as substrates for fermentation. Inoculation proceeds by introducing the active inoculum at its optimum stage. The substrate is used at a concentration of 10–15%. The production stage usually lasts for 5 days and takes place in stirred, aerated fermenters at 30 °C. Agitation is in the middle range, about 200 rpm. Regulation of the dissolved oxygen concentration in the medium is done by the air supply, pressurized air, and impeller speed; regulation of the pH value; and regulation of the level of free potassium hexacyano ferrate in the medium. The trace metal potassium hexacyano ferrate is used for surface fermentation in citric acid production.³ The media used for fermentation in batch culture consists of 30–150 g glucose, 0.1 g yeast extract, 0.3–1.3 g ammonium chloride, 0.3 g monopotassium phosphate, 0.2 g magnesium sulfate, and 0.0001 g thiamine hydrochloride in one liter. The medium pH is adjusted to 5.5 then autoclaved to create a sterile medium.

Although *A. niger* has mainly been used in citric acid production, other strains of fungi, various kinds of yeast, and some bacteria are known to accumulate citric acid in the medium. The reasons for choosing *A. niger* over other potential citrate-producing organisms are that cheap raw materials (molasses) can be used as substrate and a high product yield can be obtained. There is general agreement in the literature that the pelleted form is desirable for acid production. An ideal 1.2- to 2.5-mm-diameter pellet configuration is formed after 5 days. The pellet form is a favorable spore. Pellet cultures have low viscosity, causing improved bulk mixing and aeration conditions and lower oxygen consumption than cultures composed mainly of filamentous forms. Furthermore, problems of wall growth and pipe blockage are reduced and the separation of biomass from culture liquid by filtration is considerably enhanced by the pellet form.

12.3 FACTORS AFFECTING MOLD GROWTH AND THE FERMENTATION PROCESS

Trace element nutrition is one of the most important factors affecting the yields (grams of citric acid per gram of sugar) from citric acid fermentation. In particular, the levels of manganese, iron, copper, and zinc are critical. If the levels of these trace elements are correct, other factors have less pronounced effects. Conversely, the medium will not allow high production unless the trace element content is controlled carefully. Manganese (Mn^{2+} ions) in the nutrient medium plays a key role in the accumulation of large amounts of citrate by *A. niger*. When the

Mn^{2+} concentration is maintained below 0.02 mM (which does not affect growth rate or biomass yield), large amounts of citric acid are produced. It has been found that up to 0.5 mg iron per liter of medium is essential for high yields of citric acid by *A. niger* while the organism utilizes sucrose in the submerged culture. The medium with 40% sucrose was purified with an ion exchanger; resistance measured 3.5 M Ω , and it was diluted to 14.2% sugar content. The medium composition is KH_2PO_4 , 0.014%; $\text{MgSO}_4 \cdot 7\text{H}_2\text{O}$, 0.1%; $(\text{NH}_4)_2\text{CO}_3$, 0.2%; FeCl_3 , 0.05% and pH is adjusted to 2.6 using diluted HCl solution. Excess amounts of Fe^{3+} may drastically reduce the yield of citric acid from 88 to 39%. The effect of iron ions on the yield of citric acid is shown in Figure 12.1.

Aspergillus niger normally produces many useful secondary metabolites; citric and oxalic acids are stated as the dominant products. Limitation of phosphate and certain metals such as copper, iron, and manganese results in a predominant yield of citric acid. The additional iron may act as a cofactor for an enzyme that uses citric acid as a substrate in the TCA cycle; as a result, intermediates of the TCA cycle are formed.

The presence of excess iron favors the production of oxalic acid. Copper ions play an important role in reducing the deleterious effect of iron on citric acid production. It also has been reported that copper ions can successfully counteract the addition of manganese to citric acid fermentation media and are inhibitors of cellular manganese uptake. It was found that copper is an essential requirement for citric acid production. An optimum concentration of Cu^{2+} is 40 ppm for high yields. Low concentrations of zinc in the fermentation medium are generally favored in most media for citric acid production. It was reported that zinc deficiencies promote citric acid production. The zinc ion plays a role in the regulation of growth and citrate accumulation. At high zinc concentrations (about 2 μM) the cultures are maintained

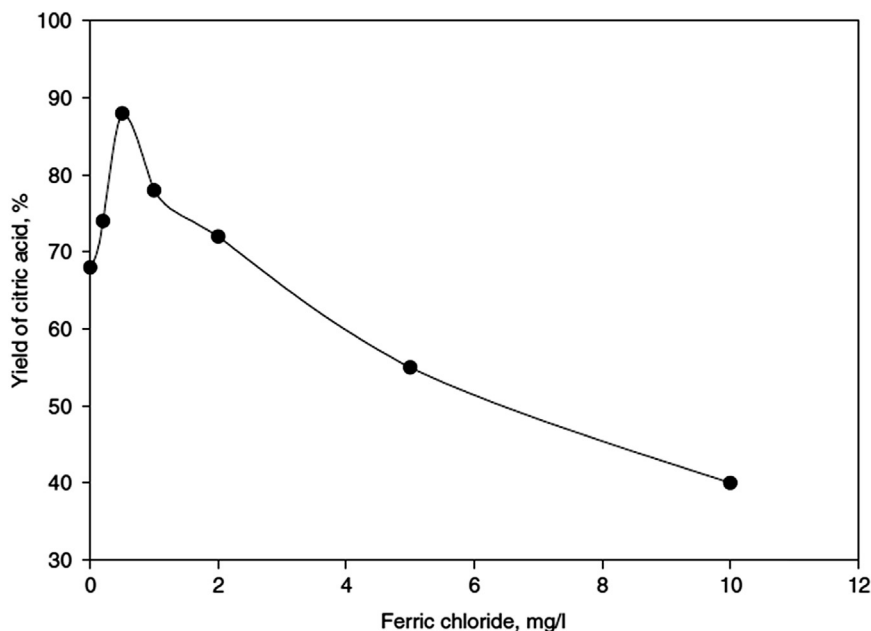


FIGURE 12.1 Effect of iron concentration on yield of citric acid by *Aspergillus niger*.

in the growth phase, but when the medium becomes zinc deficient ($<0.2 \mu\text{M}$), growth is terminated and citric acid accumulation begins. The addition of zinc to citrate-accumulating cultures results in their reversion to the growth phase. Because molasses (beet or cane) contains inhibitory amounts of metal ions such as zinc, iron, and copper, it is absolutely necessary either to remove these ions or to render them ineffective by pretreatment. The most commonly used methods of pretreatment are the addition of ferro- or ferricyanide to precipitate iron, zinc, copper, and manganese; decreasing the available manganese content to below 0.002 ppm; or passing the medium over ion exchange resin.

12.4 STARTER OR SEEDING AN INOCULUM

From the beginning of the experiment Petri dishes of nutrients are prepared with a media composition of 50 g glucose; 2 g monopotassium sulfate; 1 g magnesium sulfate heptahydrate; 8 g peptone, 2 g yeast extract, 20 g agar, and 1000 mL distilled water. Media and Petri dishes are sterilized separately. It is recommended each Petri dish be wrapped separately in aluminum foil. Media must be distributed in the presence of a flame. The stock culture is transferred to the Petri dish for cultivation. The conidia are harvested then transferred to the defined media for *A. niger*. Also, cultivation can be done in a cotton-clogged head of a flask with desired media in a shaker for good aeration. After 18 h of growth, mycelia in the form of short and fat hyphae, known as small pellets, develop. If Petri dishes are used, one should wait for 2 days for spore formation. The conidia are washed with 1% saline solution (sodium chloride 10 g L^{-1}) and collected in an Erlenmeyer flask in sterilized media. Aseptic transformation is required.

12.5 SEED CULTURE

A seed culture is prepared as sterile media, and the stock culture is induced for spore formation. Ferrocyanide (200 ppm) in a medium containing 100 g L^{-1} sugar is used as the basal fermentation medium. The sugar solution must be pretreated and filtered and then passed through a cation and anion exchange column. After determining the media, the sterile media is inoculated. The culture conditions are typically incubation temperature (30°C), initial pH (6.0), air supply of $1\text{--}2 \text{ dm}^3 \text{ min}^{-1}$ (0.5–1.0 vvm), agitation intensity (200 rpm), and batch experiment time about 3–5 days. The yield of citric acid is about 67–70%. The pH gradually drops to an acidic condition, which retards the process. Since it has been shown that the nature and quantity of trace metals, carbon and nitrogen source, air supply, and media pH are very important for successful citric acid fermentation, all these factors are considered in the course of fermentation. Standard media for yeast and fungi are used. The composition is shown in [Table 12.1](#).

12.6 CITRIC ACID PRODUCTION

Citric acid fermentation of cane molasses by submerged fermentation is performed in a 2 L B. Braun stirred fermenter (2-L working volume). A strain of *A. niger* (ATCC 11414) obtained from

TABLE 12.1 Initial media composition for seed culture preparation

Media composition	Concentration
Ammonium chloride	50 mg L ⁻¹
Monopotassium phosphate	30 mg L ⁻¹
Magnesium sulfate heptahydrate	20 mg L ⁻¹
Ferrous sulfate heptahydrate	10 mg L ⁻¹
Zinc chloride	10 mg L ⁻¹
Copper(II) sulfate pentahydrate	10 mg L ⁻¹
Distilled water	1000 mL

the ATCC is used in this study. Ferrocyanide-treated molasses (ferrocyanide 200 ppm) medium containing 100 g L⁻¹ sugar is used as the basal fermentation medium. Different cultural conditions such as incubation temperature (30 °C), initial pH (6.0), air supply (1.0 L L⁻¹ min⁻¹), agitation intensity (200 rpm), and incubation time (about 5 days) are optimized for enhanced citric acid production. A maximum amount of anhydrous citric acid with 100 g L⁻¹ of substrate is in the range of 71–88 g L⁻¹. If the product is removed as it is formed, the yield can be maximized. Final pH and cell dry weight are about 2.1 and 10 g L⁻¹, respectively.

Aspergillus niger remains the organism of choice for the production of citric acid. In a submerged fermentor, either purified compressed air or oxygen and agitation are used. Molasses is a desirable raw material for citric acid fermentation because of its availability and relatively low price.

Incubation temperature plays an important role in the production of citric acid. Temperatures between 25 and 30 °C are usually used for culturing of *A. niger*, but at temperatures above 35 °C citric acid formation is inhibited because of the increased production of by-product acids and the inhibition of culture development. Citric acid production by *A. niger* is sensitive to the initial pH of the fermentation medium. The maximum production of citric acid (6.5%) was obtained at pH 5.4 in the molasses medium. The appropriate pH is important for the progress and successful termination of fermentation. The citric acid produced by *A. niger* is extremely sensitive to trace metals present in the molasses. Trace metals such as iron, zinc, copper, and manganese present a critical problem in submerged fermentation. The organisms need major elements such as carbon, nitrogen, phosphorus, and sulfur, in addition to various trace elements, for growth and citric acid production.^{4,5}

12.7 ANALYTICAL METHOD

12.7.1 Cell Dry Weight

Cells, spores, and mycelia are filtered (0.45 µm), the filter is dried in an oven at 80 °C, and the cell dry weight is determined according to the procedure explained in chapters 5 and 10 for the measurements of cell growth and cell optical density.

12.7.2 Carbohydrates

Sugars are estimated with a reducing 3,5-dinitrosalicylic acid (DNS) reagent based on the colorimetric method developed in chapter 10 section 10 for analytical method. The samples are determined by the color that develops, which is detected by a spectrophotometer at a wavelength of 540 nm. In large-scale operations, mycelia are separated by a rotary drum filter.

12.7.3 Citric Acid

The citric acid obtained from fermentation is removed from the culture by precipitation. The fermentation broth is harvested and then filtered in a rotary vacuum filter to remove *A. niger* mycelium. The precipitation is formed by adding 200 g L⁻¹ calcium hydroxide at 70 °C. The pH of solution is adjusted to 7.2. Tricalcium citrate tetrahydrate is collected by filtration. The tricalcium citrate as filter cake of rotary vacuum filter is dissolved in sulfuric acid at 60 °C with 0.1% excess, the solid retained is calcium sulfate, and the free citric acid is obtained. The free concentration of citric acid is determined with an enzymatic kit available from Merck. Gas chromatography/high-performance liquid chromatography is recommended for high accuracy of any research work.⁵

12.8 PROCESSES FOR RECOVERY AND PURIFICATION OF CITRIC ACID

In commercial plants, calcium hydroxide solution should not have magnesium ions because magnesium citrate is more soluble and would remain in the solution. The filtered calcium citrate is dissolved in sulfuric acid just to precipitate the insoluble calcium sulfate and release citric acid in the solution. To remove any impurities, the solution is passed through activated carbon for decolorization, then is passed through cation and anion exchange resins. The aqueous citric acid is evaporated to the point of crystallization at 36 °C. The crystals of citric monohydrate are separated from the continuous centrifuges; then the crystals are dried at 60 °C for marketing purposes.

12.9 EXPERIMENTAL RUN

Based on the above discussion we are now ready to start a real experiment. Molasses is transferred from the sugar industry and kept in a cool room. The ATCC culture order arrived and has been hydrated. Stock culture was prepared and aseptic transfer successful. Prepare spores and fungal conidia/small pellets in a Petri dish or cotton-plugged flask for 48 h. Harvest the spores in a separate flask with media for propagation. Once in the separated flask, the concentration of spores has reached about 3 million per liter. It is now ready to be transferred to a 2 L B. Braun biostat fermenter. The minimum volume of harvested spores in the flask is 300 mL. Media must be prepared based on sufficient carbon source with 10 g L⁻¹ sugar, nitrogen sources, and trace metals, as explained earlier and defined in

TABLE 12.2 Experimental run for production of citric acid

Time (h)	Dissolved oxygen (mg L ⁻¹)	Citric acid concentration (g L ⁻¹)	Cell dry weight (g L ⁻¹)	Sugar concentration (g L ⁻¹)
0	8	0	0.1	10
12	7	0.4	0.3	9
24	7	0.9	0.5	8
36	6	1.35	0.7	7
48	6	2.1	1	6
60	5	2.9	1.1	4
72	5	3.6	1.2	2
84	4	3.9	1.3	1
96	4	4	1.3	1
108	6	4	1.3	1
120	7	4	1.3	1

Table 12.1. Air or pure oxygen is supplied to ensure the availability of oxygen for sufficient aeration. The experimental data obtained are reported in Table 12.2.

Production of citric acid using *S. lipolytica* at a high substrate concentration in batch resulted in a high concentration of citric acid. *Saccharomycopsis lipolytica* is sensitive to nitrogen source (ammonia) while citric acid is produced. Figure 12.2 illustrates that the glucose

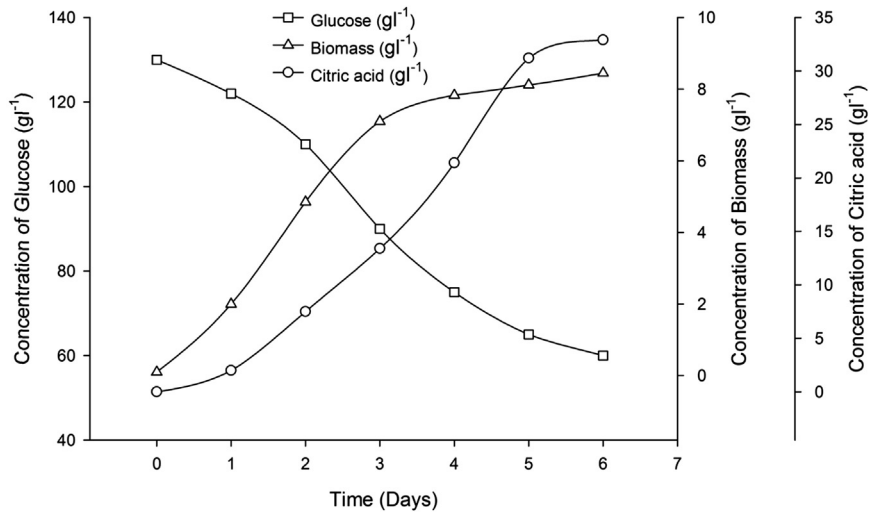


FIGURE 12.2 Substrate, biomass, and citric acid concentration profiles using *Saccharomycopsis lipolytica* in batch culture.

concentration profile reduces with respect to incubation time—maximum reduction occurred in 3–4 days—while cell density also exponentially increased. Once biomass concentration reaches a stable condition then the concentration of the product is gradually increased. From the concentration of cell dry weight and citric acid, one can see the increasing trend of product formation. Therefore, citric acid production is associated with cell growth. Significant concentration of citric acid as the targeted product is detected after 48 h of incubation. High concentration of citric acid may encourage longer fermentation for maximum citric acid production. The yield of citric acid at optimum media composition with a desired nitrogen source based on substrate utilization is calculated to be 71%.

12.10 KINETIC MODEL IN BATCH CITRIC ACID FERMENTATION

The typical growth of *A. niger* or *S. lipolytica* in citric acid production shows rapid growth in an optimum medium composition. These organisms may be adapted to medium to eliminate any lag phase. In the late stage of exponential growth, the organism demonstrates excessive mass of cells in batch culture. The cell may gain sufficient age at the stationary phase. The best harvesting time would be the upper part of the sigmoid exponential growth curve. The cell growth for citric acid production is divided into two parts: growth of hyphae and pellet formation. Cell growth is identified as the tropho phase, in which the cell is actively growing; this means cells are able to demonstrate synthesis of primary metabolites in the tropho phase, whereas in the idio phase the culture in a stationary point can produce secondary metabolites. In fact, most of the important metabolites often used in the pharmaceutical industry are categorized as secondary metabolites. In kinetic modeling, the simplest type, known as the unstructured model and based on either substrate or product, is introduced. Because cell growth is a complex phenomenon—we are unable to explain or illustrate in terms of equations how the cell growth mechanisms function. The model only considers the entire cell mass as a single component while ignoring all sequences of biochemical reactions and enzymes catalyzing synthesis or anabolism. The only major concern would be substrate utilization for biomass growth. Therefore, the simple growth model is useful for a single component involved in the stoichiometric relation between the substrate and product. In the fermentation process, when the product is formed, the rate of formation is associated with cell growth. This means that, without the presence of cell mass, synthesis may not occur. The modified growth rate model, known as the Leudeking–Piret equation, is used. The model consists of two parts; the first part is based on cell concentration (X) and the second part is the rate of biomass accumulation (r_X), as stated below:

$$r_P = \alpha X + \beta r_X \quad (12.10.1)$$

where α and β are proportionality constants. In the course of citric acid production, ammonium ions or a nitrogen source should be used by the growing cells; the production may not be detected in an early stage as the lag phase. Then the rate of production is proportional to the biomass growth rate:

$$r_P = k r_X \quad (12.10.2)$$

where r_X is the biomass growth rate. The model predicts different types of cells exist in fermentation broth, such as mycelium in hyphae and the pellet. Each type of cell have different rate of productivity. Based on the above concepts discussed for Leudeking-Piret model, an equation similar to equation (12.10.1) is written:

$$r_P = k_1 r_X + k_2 X \quad (12.10.3)$$

where k_1 and k_2 represent growth- and nongrowth-associated constants. The expanded form of the Leudeking–Piret model can be rewritten incorporating yield based on biomass and product:

$$\frac{1}{Y_{P/s}} \frac{dP}{dt} = \frac{k_1 r_X}{Y_{X/s}} \frac{dX}{dt} + k_2 X \quad (12.10.4)$$

The rate for substrate utilization is stated as follows:

$$\begin{aligned} -\frac{dS}{dt} &= \frac{1}{Y_{X/s}} \frac{dX}{dt} + \frac{1}{Y_{P/s}} \frac{dP}{dt} + k_2 X \\ \frac{dS}{dt} &= -\gamma \frac{dX}{dt} - \eta X \end{aligned} \quad (12.10.5)$$

$$\text{where } \gamma = \frac{1}{Y_{X/s}} + \frac{\alpha}{Y_{P/s}}; \quad \eta = \frac{\beta}{Y_{P/s}} + k_2$$

A simplified model representing cell metabolite has been developed using the main reaction inside of the cell. In this regard, biomass and product yields are the main concern; the actual biomass and product yields should not exceed one as stated as follows:

$$Y_{P/s} + Y_{X/s} \leq 1 \quad (12.10.6)$$

Rearrangements and integration resulted, as follows:

$$\begin{aligned} \ln \left[\frac{X(t)}{X_S - X(t)} \right] &= k t - \ln \left[\frac{X_S - X_o}{X_o} \right] \\ \ln \left[\frac{X(t)}{X_S - X(t)} \times \frac{X_S - X_o}{X_o} \right] &= k t \end{aligned} \quad (12.10.7)$$

where $X(t)$ is the biomass concentration with respect to time, X_S is the biomass at the stationary phase, and X_o is the initial biomass at inoculation or the starting point. The above equation resembles exponential growth while we consider biomass concentration with respect to time.

The logistic model describes the growth kinetic of *S. lipolytica*. The logistic equation leads to an explanation of the lag phase, an exponential phase, and stationary phases. The specific growth rate predicted by the model is explained by the following equation:

$$\frac{dx}{dt} = \mu_{max} x \left(1 - \frac{x}{x_{max}} \right) \quad (12.10.8)$$

where μ_{max} is the maximum specific growth rate (h^{-1}) and x_{max} is the maximum cell dry weight concentration (g L^{-1}). The above expression is known as the Riccati equation, which is integrated to give the following logistic equation:

$$x = \frac{x_0 \exp(\mu_{max} t)}{1 - \left(\frac{x_0}{x_{max}}\right)(1 - \exp(\mu_{max} t))} \quad (12.10.9)$$

The logistic growth kinetic model successfully predicted the batch culture for citric acid production. The maximum specific growth rate and maximum cell concentration as the kinetic parameters with an initial substrate (glucose) concentration of 50 g L^{-1} were 0.25 h^{-1} and 4.71 g L^{-1} , respectively. The model can project a rate constant of 1.6 g (L h)^{-1} for an initial cell concentration of 100 mg L^{-1} and an incubation period of 10 h.

NOMENCLATURE

X Cell concentration, g L^{-1}

$X(t)$ Biomass concentration with respect to time, g L^{-1}

X_S Biomass at stationary phase, g L^{-1}

X_0 Initial biomass at inoculation, g L^{-1}

r_X Rate of biomass accumulation, g (L h)^{-1}

$Y_{p/s}$ Product yield, that is mass of product per unit substrate, g g^{-1}

$Y_{X/s}$ Biomass yield, mass of cell produced per unit mass of substrate, g g^{-1}

k_1 and k_2 Growth- and nongrowth-associated constants; depends on unit used

References

1. Baily JE, Ollis DF. *Biochemical engineering fundamentals*. 2nd ed. New York: McGraw-Hill; 1986.
2. Doran PM. *Bioprocess engineering principles*. New York: Academic Press; 1995.
3. Schmauder HP, editor. *Methods in biotechnology*. UK: Taylor & Francis; 1997.
4. Stanbury PF, Whitaker A. *Principles of fermentation technology*. Oxford: Pergamon Press; 1984.
5. Matthews RF, Braddock RJ. *Food Technol* 1987;**41**:57.

Bioprocess Scale-up

OUTLINE

13.1 Introduction	375	13.4 Continuous Stirred Tank Reactor Chemostat versus Tubular Plug Flow	388
13.2 Scale-up Procedure from Laboratory Scale to Plant Scale	376	13.5 Dynamic Model and Oxygen Transfer Rate in Activated Sludge	399
13.2.1 Scale-up for Constant K_{La}	377	13.6 Aerobic Wastewater Treatment	410
13.2.2 Scale-up Based on Shear Forces	378	13.6.1 Substrate Balance in a Continuous System	412
13.2.3 Scale-up for Constant Mixing Time	379	13.6.2 Material Balance in Fed Batch	413
13.2.4 Scale-up Based on Physical Concepts	381	Nomenclature	415
13.3 Bioreactor Design Criteria	384	References	416
13.3.1 General Cases	384		
13.3.2 Bubble Column	384		

13.1 INTRODUCTION

Microbial processes are developed and implemented in many ways. These processes are operated at different scales, such as bench, pilot, and plant scales. For economic reasons, large-scale bioprocesses should not be disturbed, and any modification to the running processes may not be considered. For research, many small-scale processes are developed to

screen and develop better strains, improve existing culture, use efficient media, and handle the process more efficiently with maximum productivity. The role of biochemical engineers in microbial processes is well defined. First, they should have a clear understanding of the bioprocess and know the action of biocatalysts to stimulate biochemical reactions. Second, they should maintain optimal growth and the environmental conditions required to obtain maximum production yield. The microbial environment involves substrate and product concentrations, media composition, pH, and temperature. There are many physical and chemical parameters involved in the growth environment once the organisms are propagated in a well-advanced bioreactor with instrumentation control. The process parameters are the flow dynamics and chemical dynamics of the biochemical system such as mass transfer, mixing, shear generated by agitation, power input, dilution rate, nutrients, and growth stimulants. The chemical parameters of the process are well controlled and optimized for growth kinetics; physical factors are based on process design. The process design, geometric shape, and size of the bioreactor are affected by dilution rate and substrate consumption rate. The operating parameters are well controlled. Changing bioreactor size must follow certain rules to meet special criteria. Most bioprocess designers have attempted to follow only vessel geometric similarities and some dimensionless numbers. However, only increasing volume and dimensions by keeping some dimensionless number constant may not satisfy the needs of bioprocess design.

13.2 SCALE-UP PROCEDURE FROM LABORATORY SCALE TO PLANT SCALE

The usual procedure for scale-up of a fermenter based on concepts is well known. The following criteria are translated between two scales of operation. They are selected as a procedure for scale-up.

1. Similar Reynolds number or momentum factors.
2. Constant power consumption per unit volume of liquid, P_g/V .
3. Constant impeller tip velocity, ND_i .
4. Equal liquid mixing and recirculation times, t_m .
5. Constant volumetric of mass transfer coefficient, K_La .
6. Keep all environmental factors for the microorganism constant.

Based on the practical history of scale-up, most fermentation processes for alcohol and organic acid production have followed the concepts of geometric similarity and constant power per unit volume. From the above concept, and as a strong basis for translation of process criteria, only physical properties of the process were considered in the scale-up calculation. For power consumption in an agitated vessel, there is a fixed relation between impeller speed, N , and impeller diameter, D_i . The constant power per unit volume for a mechanical agitated vessel is given by:

$$\frac{P}{V} = \frac{\rho N^3 D_i^5}{D_i^3} \quad \text{for } Re \geq 10^4 \quad (13.2.1)$$

The power per unit volume is constant. From power consumptions in a bench-scale bioreactor, the necessary agitation rate is calculated for the scale-up ratio, using Eqn (13.2.1). The choice of criterion is dependent on what type of fermentation process has been studied. The following equation expresses relations for the impeller size and agitation rate in small and large bioreactors:

$$N_1^3 D_{i,1}^5 = N_2^3 D_{i,2}^5 \quad (13.2.2)$$

The agitation rate is proportional to impeller diameter to the power of 2/3.

$$N_2 = N_1 \left(\frac{D_{i,1}}{D_{i,2}} \right)^{2/3} \quad (13.2.3)$$

Similarly, that is true for the rotational speed of a large tank, which is related to a small tank with the ratio of impeller diameter of large and small tanks to the power of 2/3.

$$\text{rpm}_2 = \text{rpm}_1 \left(\frac{D_{i,1}}{D_{i,2}} \right)^{2/3} \quad (13.2.4)$$

The characteristics of an agitated vessel with impeller spacing are illustrated in Figure 13.1.

13.2.1 Scale-up for Constant $K_L a$

The mass transfer coefficient $K_L a$ is constant; the general correlation is considered by many to be proportional to the power per unit volume with constant exponent, and gas superficial velocity to another constant power as shown below:^{1,2}

$$K_L a = \alpha \left[\left(\frac{P_g}{V_L} \right)^a (V_s)^b \right] \quad (13.2.1.1)$$

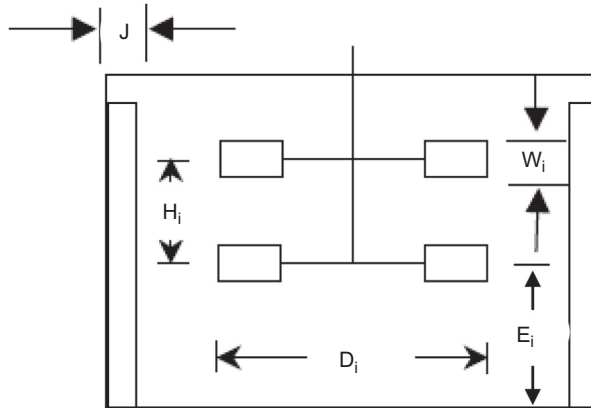


FIGURE 13.1 Characteristics of agitated vessel with impeller spacing.

TABLE 13.1 Constants in mass transfer correlation for various fermenter size

Fermentation vessel size, l	a	b
5	0.95	0.67
500	0.60–0.7	0.67
50,000	0.40–0.5	0.50

There has to be a relation between K_La with aeration rate and agitation speed, and scale-up factor has to be determined. To eliminate the effect of viscous forces, the rheology of the media and broth for a large vessel has to be similar to that of a bench-scale vessel. For scale-up based on geometric similarity, the constant values a and b are proposed for the mass–transfer correlation in Table 13.1.

The oxygen transfer rate (OTR) is calculated based on oxygen concentration gradient, by determination of the oxygen level in the liquid phase and the equilibrium value.

$$\text{OTR} = K_La(C_{AL}^* - C_{AL}) - XQ_{O_2} \quad (13.2.1.2)$$

At steady-state condition, the change of oxygen concentration with time approaches zero. The value of K_La should be estimated by a correlation developed for various sizes of fermentation vessel.

$$K_La = \frac{XQ_{O_2}}{C_{AL}^* - C_{AL}} \quad (13.2.1.3)$$

where Q_{O_2} is OTR and X is biomass concentration.

13.2.2 Scale-up Based on Shear Forces

The scale-up calculation is based on constant shear forces, in which shear is directly related to impeller tip velocity. Shear forces are defined as.

$$\tau = \mu \frac{du}{dx} \quad (13.2.2.1)$$

where τ is the shear stress, du/dx is the shear rate, and μ is the fluid viscosity. Since the shear is defined as S , which is proportional to ρND_i , the concept of constant impeller tip velocity and constant power per unit volume were applied. Now introduce variable S for impeller tip velocity ND_i into Eqn (13.2.2), then multiply both sides and divide by impeller diameter, so that the power equation is reduced to shear forces related to impeller diameter:

$$S_L = S_S \left(\frac{D_{i,L}}{D_{i,S}} \right)^{1/3} \quad (13.2.2.2)$$

The constant shear concept has been applied for bioreactor scale-up that uses mycelia, in which the fermentation process is shear sensitive and the broth is affected by shear rate of impeller tip velocity. For instance, in the production of novobiocin, the yield of antibiotic production is dependent on impeller size and impeller tip velocity.

The impeller is a device in which shear forces are transmitted to the fermentation broth. Since the process is sensitive to a high agitation rate, it is necessary that the special bioreactor be scaled up, based on shear forces for maximizing product yield, such as antibiotics.

This is the main reason for keeping the impeller tip speed constant; in practice, it is recommended that this is in the range $0.25\text{--}0.5\text{ m s}^{-1}$. If the above conditions hold, it is not necessary to follow the geometric similarity constraint; however, it may violate the rule of power consumption per unit volume. Therefore keeping the impeller at a constant speed and keeping K_La constant may be required for special case studies for bioreactor design in antibiotic fermentation.

13.2.3 Scale-up for Constant Mixing Time

The problem associated with poor mixing in a large vessel was identified as low dissolved oxygen in the aerated vessel. The mixing time has been correlated with turbulent flow. In a large-scale operation, the corrected function for mixing time incorporates the actual mixing time with impeller speed, tank diameter, and liquid height. The function of mixing, $f(t)$ is defined as constant mixing time:

$$f(t) = t_m(ND_i^2)^{2/3}g^{1/6}D_i^{1/2}Y^{1/2}D_i^{3/2} \quad (13.2.3.1)$$

where t_m is the mixing time, g is gravity, D_t is the tank diameter, and Y is the depth of the liquid. Substitute Eqn (13.2.2) into Eqn (13.2.2.2) as power per unit volume is constant; the resulting equation is the mixing time:

$$\frac{t_{mL}}{t_{mS}} = \left[\left(\frac{N_S}{N_L} \right)^4 \left(\frac{D_{iL}}{D_{iS}} \right) \right]^{1/6} \quad (13.2.3.2)$$

That is proportional to impeller diameter to the power of 0.65. Then, solving for mixing time:

$$t_{mL} = t_{mS} \left(\frac{D_{iL}}{D_{iS}} \right)^{11/18} = t_{mS} \left(\frac{D_{iL}}{D_{iS}} \right)^{0.65} \quad (13.2.3.3)$$

Equation 13.2.3.3 is used for geometric similarity, where t_{mS} and t_{mL} represent the mixing time for small and large fermentation vessels. Mixing and mixing time have been major concerns for several investigators, because large-scale vessels may not have uniform mixing, whereas in small vessels mixing is not a problem. The mixing time in large vessels has been correlated based on dimensional analysis.

In 1953, Rushton proposed a dimensionless number that is used for scale-up calculation. The dimensionless group is proportional to N_{Re} , as shown by the following equation:^{2,3}

$$\psi = k(N_{Re})^a \quad (13.2.3.4)$$

where the Reynolds number for an agitated vessel was defined as:

$$Re = \frac{\rho ND_i^2}{\mu} \quad (13.2.3.5)$$

Since the process is more complex, the proposed method may not be valid for scale-up calculation. The combination of power and Reynolds number was the next step for correlating power and fluid-flow dimensionless number, which was to define the power number as a function of the Reynolds number. In fact, the study by Rushton summarized various geometrics of impellers, as his findings were plotted as dimensionless power input versus impeller Reynolds number; the plot is known as a power graph. The plot is presented in Figure 6.6, Chapter 6. Equation 13.2.3.6 correlates the power number as a function of the Reynolds number.

$$N_p = k(Re)^{-m} \quad (13.2.3.6)$$

In fact, the power number is a dimensionless number that is the ratio of ungassed power to gassed power in a normal bioreactor.³

$$N_p = \frac{Pg_c}{\rho N^3 D_i^5} \quad (13.2.3.7)$$

where P is ungassed power, in W or hp.

In a mixed agitated vessel with a high agitation rate, a vortex often forms at the center of the vessel. To prevent a central vortex in tanks less than 3 m in diameter, four baffles, each with a baffle width of 15–20 cm, are necessary. A basic assumption is to select a ratio of liquid height to tank diameter from 2:1 to 6:1.

$$\frac{H_L}{D_t} = 2 : 1 - 6 : 1 \quad (13.2.3.8)$$

It is common for an agitated vessel to have the tank diameter equal to the liquid working volume.

$$\frac{H_L}{D_t} = 1 \quad (13.2.3.9)$$

Also, select a ratio of tank diameter to baffle width from 10 to 12:

$$\frac{D_t}{D_b} = 10 - 12 \quad (13.2.3.10)$$

A suitable impeller interspacing (H_i) is preferred for good mixing that has to be in distance of less than $2D_i$:

$$D_i < H_i < 2D_i \quad (13.2.3.11)$$

It is well understood that mixing and mass transfer is affected by agitation and aeration rates. Typically, in an agitated vessel, the working volume is about 75% of nominal continuous stirred tank reactor (CSTR) volume.

13.2.4 Scale-up Based on Physical Concepts

For bioreactor scale up, an aerated and agitated vessel for a gas and liquid system, a specific fermentation in a bench-scale fermenter is preformed. The proposed operation focused on large-scale fermentation while the same geometrical design is applied. The problem associated with a large vessel would be mass transfer limitation; proper aeration is required. An estimation of mass transfer coefficient for desired agitation is important for sufficient mixing. It was assumed that for either small- or large-scale bioreactor operations there were no significant changes in physical properties of fermentation media. In addition, to eliminate any side effects, both small and large systems are geometrically similar. The mass transfer coefficients for small and large scales are defined as follows:

$$\frac{(k_L a)_{\text{Small}}}{(k_L a)_{\text{Large}}} = \frac{(F/V)_1}{(F/V)_2} \left(\frac{H_{L1}}{H_{L2}} \right) \left(\frac{d_{B2}}{d_{B1}} \right)^{2/3} \left(\frac{\gamma_{B2}}{\gamma_{B1}} \right)^{1/2} \quad (13.2.4.1)$$

where F/V stands for volume of gas per volume of liquid per minute (vvm) or rate of aeration, H_L is liquid level, d_B is bubble diameter, and $\gamma = \rho/\mu$ is kinematic viscosity of the fluid. Let us denote that the subscript 1 and 2 represent small and large systems, respectively. Assume bubble size and kinematic viscosity of media in both systems are the same while no significant changes were observed; then the above equation is simplified:

$$\frac{(F/V)_1}{(F/V)_2} = \left(\frac{H_{L2}}{H_{L1}} \right) \quad (13.2.4.2)$$

Let us define a volumetric scale factor of 125, and aeration rate in small fermenter is 1 vvm; then what would be the aeration in large-scale fermenter? The volumetric scale-up is 125; then, the scale-up ratio of liquid height would be $\frac{H_{L2}}{H_{L1}} = 5$.

$$\frac{1 \text{ vvm}}{(F/V)_2} = 5; \quad (F/V)_2 = 0.2 \text{ vvm}$$

However, the effect of emerged and segregated oxygen bubbles in an aerated system may disregard the above assumptions. For a bench-scale aerated vessel, the above correlation should be corrected by liquid height ratio $\left(\frac{H_{L1}}{H_{L2}} \right)^{2/3}$; then, the corrected aeration rate for segregated bubbles would be:

$$(F/V)_2 = 5^{-2/3} = 0.34$$

That means, instead of 0.2 vvm oxygen, 0.34 vvm oxygen is required in large-scale aerated vessel. The concept of scale-up is based on constant physical properties of broth

during the course of fermentation, while keeping geometric similarities for aerated systems. This means in a baffled bioreactor, we need to keep media composition, temperature, pH, and dissolved oxygen concentration constant. The proportionality factors in terms of power, aeration, and many other useful terms used for scale-up are stated below:

$$P \propto N^3 D_i^5 \quad (13.2.4.3)$$

where P stands for power, N is angular velocity, and D_i is diameter of the impeller. Also for gassed power (P_g) and ungassed power (P) as a function of aeration number is:

$$\frac{P_g}{P} = f(N_a) \quad 13.2.4.4$$

Where N_a is aeration number in terms of scale, proportional factors are used as stated below:

$$N_a = \frac{F_g}{ND_i^3} \quad (13.2.4.5)$$

$$F_g \propto ND_i^3$$

$$\frac{P}{V} \propto N^3 D_i^2$$

$$V \propto D_i^3$$

$$\frac{F_g}{V} \propto N$$

(13.2.4.6)

where F_g/V is the liquid circulation rate occur inside the fermenter. Also, the impeller tip velocity represents the liquid shear rate, which is stated as:

$$v \propto ND_i \quad (13.2.4.7)$$

The Reynolds number, $Re = ND_i^2 \rho / \mu$, can be simplified for proportionality factor used for scale up calculation shown below:

$$Re \propto ND_i^2 \quad (13.2.4.8)$$

Table 13.2 summarizes all physical properties for small- and large-scale fermenters using a scale-up factor of 125. The physical properties of a large-scale bioreactor, including P , P/V , F , F/V , ND_i , and Re are calculated for constant D_i , while N is varied from 0.1 to 2.

To explain the given numbers in the above table, we had to follow up exactly the proportional factors given for scale-up. In the first row of the above table, the numbers are based on the power calculation given in second row. Just multiply the numbers by a scale-up factor of 125. The angular velocity, N for large-scale, reduced power to 25, then the velocity is reduced by 1/5 and the last value is 0.2/5, which is equal to 0.04. The gas volumetric flow rate (F) is

TABLE 13.2 Relations based on physical properties as a base for scale up⁴

Property	Small scale, 100 l			Large scale, 12.5 m ³			
N	1.0	0.1	0.34	0.5	0.67	1.0	2
P	1.0	3.125	125	390	940	3125	25,000
P/V	1.0	0.025	1.0	3.125	7.5	25	200
D_i	1.0	5.0	5.0	5.0	5.0	5.0	5.0
F	1.0	12.5	42.5	62.5	83.75	125	250
F/V	1.0	0.1	0.34	0.5	0.67	1.0	2
ND_i	1.0	0.5	1.7	2.5	3.35	5.0	10
$\frac{ND_i^2 \rho}{\mu}$	1.0	2.5	8.5	12.5	16.75	25	50

proportional to ND_i for $N = 0.34$ and $D_i = 5$, the calculated F is 42.5 for the other given values just followed N -values. For F/V , just divide the given F -values by volume of scale-up factor. The next row, ND_i , can be calculated for the given N and D_i . The last row, Re , is proportional to ND_i , just multiply the above row by D_i .

Scale-up based on constant power per unit volume:

$$\left. \frac{P}{V} \right|_{Small} = \left. \frac{P}{V} \right|_{Large}$$

$$N_1^3 D_{i,1}^2 = N_2^3 D_{i,2}^2 \quad (13.2.4.9)$$

$$N_2 = N_1 \left(\frac{D_{i,1}}{D_{i,2}} \right)^{2/3} = 5^{2/3} = 0.34$$

In scale-up for constant power, the proportional factor for scale-up would be D_i^2 :

$$\frac{P_2}{P_1} = \frac{N_2^3 D_{i,2}^5}{N_1^3 D_{i,1}^5} \quad (13.2.4.10)$$

In the above equation, substituting $\frac{N_2^3}{N_1^3} = \left(\frac{D_{i,1}}{D_{i,2}} \right)^2$ resulted in an expression of power ratio that would be in terms of impeller diameter:

$$\frac{P_2}{P_1} = \left(\frac{D_{i,1}}{D_{i,2}} \right)^2 \left(\frac{D_{i,2}}{D_{i,1}} \right)^5 = \left(\frac{D_{i,2}}{D_{i,1}} \right)^3 \quad (13.2.4.11)$$

The scale-up for power ratio ends up to be the same scale-up factor for volumetric proportion that is 125 for the above case.

13.3 BIOREACTOR DESIGN CRITERIA

The bioreactor is the major piece of equipment used in biochemical processes. It differs totally from a simple chemical reaction vessel. To control physical operating parameters and microbial environmental conditions, there are several influential variables:

- Biomass concentration
- Sterile condition
- Effect of agitation and mass transfer
- Heat removal for temperature control
- pH control of the media
- Correct shear conditions.

Bioreactors in terms of operation and specific criteria are well defined. The most useful and applied types of bioreactor are:

- CSTR
- Air lift: air is used for fluid circulation by pressurized air
- Loop reactor: modified air lift, pump transport the air and fluid through the vessel
- Immobilized system: air and fluid circulate over a film of microorganisms grown on a solid support
- Tower fermenter
- Membrane bioreactor.

13.3.1 General Cases

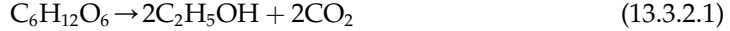
If the height of liquid, H_L , is equal to D_t , one set of agitators is enough to obtain sufficient mixing. For H_L equal to $2D_t$ or $3D_t$, additional sets of agitators separated by distance H_i are required, mounted on the same shaft. Spargers are placed at a distance $D_i/2$ from the bottom of the tank. Power input is greater than 100 W m^{-3} , and the tip impeller speed is $\pi N D_i$ greater than 1.5 m s^{-1} . Also, the Froude number is $\frac{N^2 D_i}{g}$ greater than 1.0. H_i is impeller interspacing.

Foam in the bioreactor is troublesome: it can reduce the OTR. Antifoam is used to prevent foam formation. However, excess antifoam may cause growth inhibition in the course of fermentation. The simplest device is known as a foam breaker, which is mounted on the stirrer shaft located on the surface of liquid. It is a flat blade.

13.3.2 Bubble Column

For production of baker's yeast, beer, vinegar, and, in wastewater treatment, bubble columns are used. Generally these columns should be long enough so that bubbles are used as they rise while passing through the column. Column diameters range from 10 cm to 7.5 m. The height of the column is three to six times greater than the diameter. The common

height and diameter ratio (H/D) is in the range 2–6. The H/D ratio that is commonly used is 3:1; the ratio especially used for baker's yeast production is 6:1. Hydrodynamics and mass transfer in bubble columns are dependent on the bubble size and the bubble velocity. As the bubble is released from the sparger, it comes into contact with media and microorganisms in the column. In sugar fermentation, glucose is converted to ethanol and carbon dioxide:



The superficial gas velocity is the air flow rate per unit cross-sectional area of the column. The superficial gas velocity is less than 0.4 m s^{-1} , and the media flow rate is based on liquid velocity. Then, the column may have a hydraulic retention time that is a function of fluid velocity and column diameter. The liquid velocity is given by⁵:

$$U_L = 0.9(dDU_g)^{0.33} \quad (13.3.2.2)$$

where U_g is the upward gas bubble velocity at the center of the column, the gas superficial velocity is in the range of $0 < U_g < 0.4 \text{ m s}^{-1}$, and the column diameter is in the range $0.1 < D < 7.5 \text{ m}$. The hydraulic retention time is obtained by division of column height and the actual liquid velocity; while the gas terminal velocity is defined by air flow rate over cross sectional area:

$$U_g = \frac{\text{Air flow rate}}{\text{Cross sectional area}} = \frac{Q_g}{A} \quad (13.3.2.3)$$

The mixing time, t_m , is given by²:

$$t_m = 11 \left(\frac{H_L}{D} \right) \left(\frac{gU_g}{D^2} \right)^{-0.33} \quad (13.3.2.4)$$

where H_L is the height of bubble column.

EXAMPLE 1

Let us have a bubble column with an H/D ratio of 3, diameter 0.5 m, and a gas flow rate of $0.1 \text{ m}^3 \text{ h}^{-1}$, which gives a superficial gas velocity of $1.42 \times 10^{-4} \text{ m s}^{-1}$. What would the liquid media flow rate be?

Solution

Once the superficial gas velocity is defined, then liquid velocity is given by Eqn (13.3.2.2):

$$U_g = \frac{Q_g}{A} = \frac{4(0.1 \text{ m}^3 \text{ h}^{-1})}{\pi(0.5)^2 \text{ m}^2} = 0.51 \text{ m h}^{-1} = 1.42 \times 10^{-4} \text{ m s}^{-1}$$

$$U_L = 0.9[(9.81)(0.5)(1.42 \times 10^{-4})]^{0.33} = 0.082 \text{ m s}^{-1}$$

Equation (13.3.2.4) is used to calculate mixing time.

$$\tau_m = 11 \left(\frac{1.5}{0.5} \right) \left(\frac{(9.81)(1.42 \times 10^{-4})}{(0.5)^2} \right)^{-0.33} = 183 \text{ h}$$

Based on mixing time, the liquid media flow rate is:

$$Q_L = \frac{V}{\tau} = \frac{(1.5 \text{ m})(0.5)^2 \pi \text{ m}^2 / 4}{183 \text{ h}} = 1.61 \times 10^{-3} \text{ m}^3 \text{ h}^{-1}$$

EXAMPLE 2

Calculate the speed of an impeller and the power requirements of a production-scale bioreactor with 60 m³ using two different methods. Also, match the volumetric mass transfer coefficient. The following optimum conditions were obtained with a small-scale fermenter of volume 0.3 m³ and 60% of the vessel working. The density of broth, ρ_{broth} , 1200 kg m⁻³, working volume 0.18 m³, aeration rate of one volume of gas per volume of liquid (1 vvm), OTR 0.25 kmol m⁻³ h⁻¹, liquid height inside the vessel, H_L , 1.2 D_t . Two sets of standard, flat-blade turbine impellers were installed.

Solution

$$V_1 = \frac{\pi}{4} \times D_t^2 (1.2D_t) = 0.3\pi D_t^3$$

Diameter of the vessel:

$$D_t = \left(\frac{V_1}{0.3\pi} \right)^{1/3} = \left(\frac{0.18}{0.3\pi} \right)^{1/3} = 0.576 \text{ m}$$

Diameter of the impeller:

$$D_{i,1} = \frac{1}{3} \times D_t = \frac{0.576}{3} = 0.192 \text{ m}$$

The height of liquid media was assumed to be 1.2 times the diameter of the fermentation vessel.

$$H_{L,1} = 1.2 \times 0.576 = 0.691 \text{ m}$$

Diameter of the larger vessel:

$$D_{t2} = \left(\frac{V_1}{0.3\pi} \right)^{1/3} = \left(\frac{60}{0.3\pi} \right)^{1/3} = 3.36 \text{ m}$$

The impeller size for the larger vessel is:

$$D_{i2} = \frac{0.36}{3} = 1.12 \text{ m}$$

and the liquid media height in the second fermenter is:

$$H_{L2} = 1.2 \times 3.36 = 4.03 \text{ m}$$

Assume the fermentation broth has the same viscosity as water:

$$\overline{\mu}_1 = 1 \text{ cp}$$

Aeration rate for 1 vvm is:

$$F_1 = 1 \times 0.18 = 0.18 \text{ m}^3 \text{ min}^{-1} = 3 \times 10^{-3} \text{ m}^3 \text{ s}^{-1}$$

Gas superficial velocity is:

$$U_s = \frac{0.18 \times 60}{\frac{\pi}{4}(0.576)^2} = 41.45 \text{ m h}^{-1}$$

Let us take average values for the partial pressure of oxygen.

$$\overline{P_{O_2}} = \frac{1 \text{ atm} + \left(1 + \frac{H_L \text{ m}}{10.3 \text{ m}} \text{ atm}\right)}{2} \times 0.21 = 0.213 \text{ atm}$$

The OTR is:

$$(K_v \overline{P_{O_2}}) = 0.25 \text{ kmol m}^{-3} \text{ h}^{-1}$$

The mass transfer coefficient is:

$$K_v = \frac{0.25}{0.213} = 1.174 \text{ kmol m}^{-3} \text{ h}^{-1} \text{ atm}^{-1}$$

Use the imperial correction based on the following equation for mass transfer in the bioreactors.

1,2 The general equation for evaluation of $K_L a$ is:

$$K_L a = x \left(\frac{P_g}{V} \right)^y (U_s)^z \quad (\text{E.2.1})$$

where x , y , and z are empirical constants. For Newtonian fluids, noncoalescing broth, and gas bubbles, the following correlation is valid for a working volume of less than 4 m^3 and a power per unit volume of $500\text{--}10,000 \text{ W m}^{-3}$.

$$K_v = 0.002 \left(\frac{P_g}{V} \right)^{0.7} U_s^{0.5} \quad (\text{E.2.2})$$

For the gassed power per unit volume, $\left(\frac{P_g}{V} \right)$ is 630.7 W ; the gassed power, P_g , was 0.15 hp . Since the flow regime is turbulent, the power number obtained from Figure 6.6, power number versus Reynolds number, Re , reads $P_{no} = 6$. For two sets of impellers:

$$N_p = 2(6) = 12 \quad (\text{E.2.3})$$

$$P_1 = \frac{12 \times 1200 \times N_1^3 \times (0.192)^5}{9.81} = \frac{0.383 N_1^3 \text{ W}}{745.7 \text{ W hp}^{-1}} = 5 \times 10^{-4} N_1^3 \text{ hp}$$

Using Michel and Miller's correction factor for power calculation^{6,7}:

$$P_{g1} = 0.5 \left\{ \frac{P_1^2 N_1 D_{i1}^3}{F_l^{0.56}} \right\}^{0.45} \quad (\text{E.2.4})$$

Knowing the power input, we can calculate the rotational speed:

$$P_{g1} = 0.5 \left\{ \frac{(5 \times 10^{-4})^2 (N_1^3)^2 (0.192)^3}{(3 \times 10^{-3})^{0.56}} \right\}^{0.45} = 0.15$$

$$N_1 = 10 \text{ rps}$$

$$N_1 = 600 \text{ rpm}$$

The power input for an ungassed system is:

$$P_1 = 5 \times 10^{-4} N_1^3 = 5 \times 10^{-4} (10)^3 = 0.5 \text{ hp}$$

$$\frac{P_g}{P} = \frac{0.15}{0.5} = 0.3$$

For constant power input based on geometric similarity of the vessels, the agitation rate is calculated.

$$\frac{\rho N_1^3 D_{i1}^5}{V_1} = \frac{\rho N_2^3 D_{i2}^5}{V_2} \quad (\text{E.2.5})$$

$$\left(\frac{N_2}{N_1}\right)^3 = \left(\frac{V_2}{V_1}\right) \cdot \left(\frac{D_{i1}}{D_{i2}}\right)^5 \quad (\text{E.2.6})$$

$$N_2 = N_1 \left(\frac{V_2}{V_1}\right)^{1/3} \left(\frac{D_{i1}}{D_{i2}}\right)^{5/3} = 600 \left(\frac{60}{0.3}\right)^{1/3} \left(\frac{0.192}{1.12}\right)^{5/3} = 185 \text{ rpm} \leftarrow$$

For constant input velocity for a large system:

$$N_2 = N_1 \left(\frac{D_{i1}}{D_{i2}}\right) = 600 \left(\frac{0.192}{1.12}\right) = 103 \text{ rpm} \leftarrow$$

13.4 CONTINUOUS STIRRED TANK REACTOR CHEMOSTAT VERSUS TUBULAR PLUG FLOW

The performance of a biochemical reactor is designed and evaluated based on the reaction rate equation. The rate of biomass generation is based on the Monod rate model:

$$q_x = \frac{k C_s x}{K_s + C_s} = \frac{k x S}{a + S} \quad (13.4.1)$$

where $S = \frac{C_s}{C_{sf}}$ and $a = \frac{K_s}{C_{sf}}$ are dimensionless, K_s is the Monod rate constant, g l^{-1} , and kx represents the maximum specific growth rate, $\text{g l}^{-1} \text{h}^{-1}$. The fresh media dilution rate for cell production is D , h^{-1} .

$$D = \frac{q_x}{x} = \frac{q_x S}{C_{sf} - C_s} \quad (13.4.2)$$

The substrate concentration is defined as:

$$x = Y_{x/s} (C_{sf} - C_s); \quad S = \frac{C_s}{C_{sf}} \quad (13.4.3)$$

$$x = (1 - S) Y_{x/s} C_{sf}$$

The yield is incorporated into Eqn (13.4.1).

$$q_x = \frac{kS}{a + S} (1 - S) Y_{x/s} C_{sf} \quad (13.4.4)$$

EXAMPLE 1

A special CSTR fermentation known as a chemostat bioreactor is used for microbial cell growth. The rate of biomass generation is given by:

$$q_x = \frac{4}{3} \frac{C_s x}{C_s + 4} \frac{\text{g cells}}{\text{m}^3 \text{ h}} \quad (\text{E.1.1})$$

We wish to compare the performance of two reactor types, plug flow versus CSTR with a substrate concentration of $C_{sf} = 60 \text{ g m}^{-3}$ and a biomass yield of $Y_{x/s} = 0.1$. In a plug flow bioreactor with a volume of 1 m^3 and a volumetric flow rate of $2.5 \text{ m}^3 \text{ h}^{-1}$, what would the recycle ratio be for maximum q_x compared with corresponding results and rate models proposed for the chemostat?

Solution

To maximize q_x , we need to take the derivative of the following function; if $\frac{S(1-S)}{a+S}$ is maximum, then the derivative must be set to zero.

$$\frac{d}{dS} \left[\frac{S(1-S)}{a+S} \right] = \frac{(1-2S)(a+S) - S(1-S)}{(a+S)^2} = 0 \quad (\text{E.1.2})$$

$$(1-2S)(a+S) - S(1-S) = 0 \quad (\text{E.1.3})$$

$$S^2 + 2aS - a = 0 \quad (\text{E.1.4})$$

$$S = -a + \sqrt{a+a^2} \quad (\text{E.1.5})$$

The quadratic equation is solved for a .

$$a = \frac{K_m}{C_{sf}} = \frac{4}{60} = \frac{1}{15}$$

$$Y_{x/s} = 0.1$$

Maximum cell production is obtained in a chemostat at:

$$\begin{aligned} S &= -a + \sqrt{a+a^2} = -\frac{1}{15} + \sqrt{\frac{1}{15} + \left(\frac{1}{15}\right)^2} = 0.2 \\ S &= \frac{C_s}{C_{sf}} = 0.2 \\ \frac{1}{q_x} &= \frac{4+C_s}{C_s \times x} \times \frac{3}{4} \end{aligned} \quad (\text{E.1.6})$$

Now we can generate data by plug-in numbers in the above equation. We need to illustrate inverse rate versus substrate concentration. After the data are plotted, we can justify a suitable type of bioreactor.

$$X = Y_{x/s}(C_{Cf} - C_s) = 0.1(60 - 12) = 4.8$$

The performance data for plug versus mix reactors were obtained. The data were collected as the inverse of q_x versus inverse of substrate concentration. Table E.1.1 shows the data based on obtained kinetic data. From the data plotted in Figure E.1.1, we can minimize the volume of the chemostat. A CSTR works better than a plug flow reactor for the production of biomass. Maximum q_x is obtained with a substrate concentration in the leaving stream of 12 g m^{-3} .

$$S = \frac{1}{5} = \frac{C_s}{60}$$

Then, the substrate concentration is:

$$C_s = 12 \text{ g m}^{-3}$$

In a tubular bioreactor design with infinite recycle ratio, the plug flow operation may leads to a CSTR, that behave like chemostat. The recirculation plug flow reactor is better than a chemostat, with maximum productivity at $C_s = 3 \text{ g m}^{-3}$. Combination of plug flow with CSTR that behave like a chemostat was obtained from the illustration of minimized curve with maximum rate at $C_{sf} = 3 \text{ g m}^{-3}$. In a plug flow reactor, the value for C_s is reduced from 12 to 3 g m^{-3} , then the retention time and rate model with recycle ratio in a plug flow reactor can be written as:

$$\tau = \frac{C_{sf} V}{v_o} = -(R+1) \int_{\frac{C_{sf} + RC_s}{R+1}}^{C_s} \frac{dC_s}{\frac{4\mu_{\max} C_s}{3(C_s+4)}} \quad (\text{E.1.7})$$

$$\frac{K_m}{S_f} \ln \left(\frac{C_{sf} + RC_s}{RC_s} \right) + \ln \left(\frac{R+1}{R} \right) = \frac{R+1}{R} \times \frac{K_m}{f+R} + \frac{1}{R} \quad (\text{E.1.8})$$

TABLE E.1.1 Substrate concentration versus inverse biomass concentration

Substrate concentration, $C_s \text{ (g m}^{-3}\text{)}$	Inverse of biomass rate $1/q_x \text{ (m}^3 \text{ g}^{-1} \text{ h}^{-1}\text{)}$
3	0.31
5	0.25
10	0.21
15	0.21
20	0.225
25	0.25
30	0.28
35	0.33
40	0.41
45	0.54
50	0.81
55	1.61

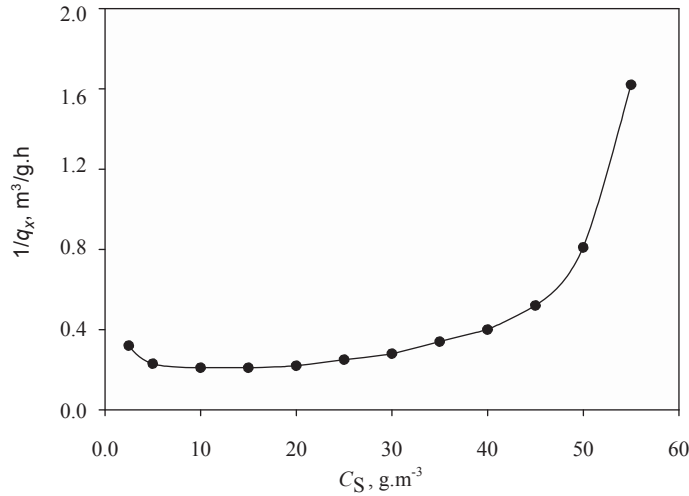


FIGURE E.1.1 Performance plot for plug versus mix reactor.

where S_f is the inlet to outlet substrate ratio, R is the recycle ratio, and f is the ratio of inlet to outlet substrate concentration. Solve R by trial and error, with calculation for right- and left-hand sides with the assumption of a value for R :

$$\frac{4/3}{60/3} \ln\left(\frac{60 + 2.5(3)}{2.5(3)}\right) + \ln\left(\frac{2.5 + 1}{2.5}\right) = \frac{2.5 + 1}{2.5} \times \frac{4/3}{20 + 2.5} + \frac{1}{2.5}$$

Let us plug in $f = 20$, $k_m = \frac{4}{3}$, and $R = 2.5$ into Eqn (E.1.9), then calculate $k\tau$

$$k\tau = (R) \left[\ln\left(\frac{R+1}{R}\right) + \frac{K_m}{f} \ln\left(\frac{C_{sf} + RC_s}{R}\right) \right] \quad (\text{E.1.9})$$

$$k\tau = (2.5) \left[\ln\left(\frac{3.5}{2.5}\right) + \frac{4/3}{20} \ln\left(\frac{60 + 2.5(3)}{2.5}\right) \right]$$

$$k\tau = 1$$

EXAMPLE 2: APPLIED CALCULATION METHOD FOR SCALE-UP

The bioreactor will be scaled up by a factor of 125. It is necessary to discuss the effect of operating variables resulting from constant power per unit volume, agitation rate, and speed tip velocity, N_{Re} . The data for a small-scale bioreactor volume of 100 L fermenter with 132 rpm and additional data are given below:

$$V_1 \times 125 = V_2 = 12.5 \text{ m}^3$$

$$\frac{P}{V} = \text{Constant} \quad (\text{E.2.1})$$

$$N_i D_i = \text{Constant} \quad (\text{E.2.2})$$

Factoring for scale-up, we make some assumptions and may use a few known correlations to progress our calculations. Let us say $P \propto V = D_i^3$, $H/D = 1$, and $D/D_i = 3$. Also, use constant power per unit volume for the small- and large-scale bioreactor.

$$\frac{P}{V} \approx (N_i^3 D_i^2)_{\text{Small}} = (N_i^3 D_i^2)_{\text{Large}} \quad (\text{E.2.3})$$

Since we assumed power per unit volume is constant, it is possible $(N_i D_i)_1$ may not be equal with $(N_i D_i)_2$. Now calculate the agitation rate for a large vessel.

$$N_{i2} = N_{i1} \left(\frac{D_{i1}}{D_{i2}} \right)^{2/3} = 132 \left(\frac{1}{5} \right)^{2/3} = 45 \text{ rpm}$$

$$\frac{H}{V} \propto \frac{N_i D_i^3}{D_i^3}$$

$$V = \frac{\pi}{4} H D^2 = \frac{\pi D^3}{4} = \frac{9}{4} \pi D_i^3$$

Now assume $H \approx D$, $D = 3D_i$, and bioreactor volume is proportional to impeller diameter to the power of $V \propto D_i^3$. The Reynolds number is written as:

$$\text{Re}_i = \frac{\rho N D_i}{\mu} \quad (\text{E.2.4})$$

The power for laminar flow is proportional to agitation rate, N^2 , and if the flow is turbulent, the power is proportional to $\sim N^3 D_i^2$. Let us assume the mass transfer coefficients remain constant ($K_L a$ unchanged):

$$\frac{D_i}{D_t} = 0.33$$

$$N D_i = 0.5 \text{ m s}^{-1}$$

Also assume the height of liquid media is 1.2 times the tank diameter.

$$\frac{H}{D_t} = 1.2$$

$$V_s = 100 \text{ l} = \frac{1.2 \times 9}{4} \pi D_i^3$$

The diameter of small tank is 68.28 cm. Since the impeller is one third of the tank diameter, $D_i = 22.76 \text{ cm}$.

$$\text{Re}_i = \frac{\rho V D_i}{\mu} = \frac{(1 \text{ g cm}^{-3})(50 \text{ cm s}^{-1})(22.76 \text{ cm})}{0.01 \text{ g (cm s)}^{-1}} = 113800 \text{ Turbulent flow} \quad (\text{E.2.5})$$

Power is defined for a well-agitated vessel with a mechanical stirrer; then read power number for turbulent flow from Figure 6.6, Chapter 6:

$$P_{no} = \frac{P \cdot g_c}{\rho N^3 D_i^5} = 6$$

$$ND_i = 0.5$$

$$N = \frac{0.5}{0.2276} = 2.2 \text{ rps} \quad (\text{E.2.6})$$

Calculate power for a small-scale vessel:

$$P_{Small} = 3.98 \text{ W} \quad (\text{E.2.7})$$

The power for a large vessel is based on a scale factor value of 125, which is calculated as the following:

$$P_{Large} = 125 \times 3.98 = 497.5 \text{ W} \quad (\text{E.2.8})$$

For mass transfer calculation:

$$K_L a = \text{Constant}$$

$$V_s = 100 \text{ l} \quad D_i = 22.76 \text{ cm} \quad D_t = 68.28 \text{ cm}$$

$$ND_i = 0.5$$

$$N_i = \frac{0.5}{0.2276} = 2.2 \text{ rps} = 132 \text{ rpm} \quad (\text{E.2.9})$$

When $Re = 113,800$ for turbulent flow, the power number versus Re , we can read:

$$P_{no} = 6$$

$$P_{NO} = \frac{P \cdot g}{\rho N_i^3 D_i^5}$$

$$P_{Small} = \frac{6 \times 1000 \times 2.2^3 \times 0.2276^5}{9.81} = 3.98 \text{ W}$$

$$\frac{3.98}{0.1} = 39.8 \frac{\text{W}}{\text{m}^3}$$

Scale-up factor = 125.

$$\frac{P_s}{P_l} = \frac{(N_i^3 D_i^5)_s}{(N_i^3 D_i^5)_l} = \frac{1}{125} \quad (\text{E.2.10})$$

The power required for a large vessel is:

$$P_l = 3.98 \times 125 = 497.5 \text{ W} \quad \text{or} \quad 0.67 \text{ hp} \quad (\text{E.2.11})$$

The power per unit volume of small bioreactor is

$$P/V = 3.98/0.1 = 39.8 \text{ W m}^{-3} \quad (\text{E.2.12})$$

The volume of a large vessel is.

$$V_L = 2450/196 = 12.5 \text{ m}^3$$

$$\left(\frac{D_{iL}}{D_{iS}}\right)^2 = 25$$

$$D_{iL} = (0.84 \text{ m})$$

$$\frac{\pi}{4}D_i^3 = \frac{\pi}{4}(2.515)^3 = 12.5 \text{ m}^3 \quad (\text{E.2.13})$$

We have understood the following concepts are true; our calculations also support the fact that power per unit volume is constant.

$$ND_i \neq \text{constant} \quad N^3 D_i^2 = \text{constant}$$

$$V_L = 125V_S$$

$$D_{i,L} = \sqrt[3]{\frac{12.5 \times 4}{\pi}} \quad D_{i,L} = 2.515 \text{ m} \quad D_{i,L} = 0.84 \text{ m}$$

$$N_{i,L} = N_{i,S} \left(\frac{D_{i,S}}{D_{i,L}}\right)^{2/3} = (3.125) \left(\frac{0.16}{0.8}\right)^{2/3} = 1 \text{ rps}$$

$$\text{Re}_{i,L} = \frac{\rho N_i D_i^2}{\mu} = \frac{(1000)(0.84)^2(1)}{0.001 \frac{\text{Kg}}{\text{m s}}} = 7.06 \times 10^5$$

$$P_{no} = 6$$

$$\text{Power} = 0.5 \text{ hp} \quad (\text{E.2.14})$$

EXAMPLE 3: POWER CALCULATION

A 20-m³ working volume of bioreactor is used for production of penicillin. What is the initial substrate concentration, so that you choose when there is a limitation in sufficient OTR and there are no limiting reactants?

Bioreactor Characteristics and Given Data

$D_{\text{tank}} = 2.4 \text{ m}$	Turbine
$D_i = 0.8 \text{ m}$	$\mu_{\text{broth}} = 1 \text{ mPa s}$
$N_i = 2.3 \text{ rps}$	$\rho = 1.2\rho_{\text{H}_2\text{O}}$
Number of blades = 8	Aeration rate = 1 vvm
$P_g/P = 0.4$	

If you aerate a bioreactor, power consumption is much less than a nonaerated bioreactor.

Oxygen concentration: $6 \times 10^{-3} \text{ kg m}^{-3}$.

Oxygen uptake rate, OUR: $0.65 \text{ mmol O}_2 \text{ kg}^{-1} \text{ cell}$.

Specific growth rate, ν_{\max} : 0.5 h^{-1} .

Specific sugar consumption rate = $1.0 \text{ kg kg}^{-1} \text{ cell h}^{-1}$.

The mass transfer coefficient is calculated by the following correlation:

$$K_L a (\text{s}^{-1}) = 2 \times 10^{-3} \left(\frac{P_g}{V} \right)^{0.6} V_S^{0.667} \quad (\text{E.3.1})$$

where P_g/V is the power per unit volume (hp m^{-3}), and V_S is the gas superficial velocity (cm min^{-1}).

Solution

The flow regime is turbulent because the Reynolds number is large.

$$N_{\text{Re}} = \frac{\rho D v}{\mu} = \frac{\rho D_i (N_i D_i)}{\mu} = \frac{1200(0.8)^2(2.3)}{0.1} = 1.92 \times 10^4$$

Read power number N_p from the graph P_{no} versus Re : $N_p = 6$.

$$\begin{aligned} N_p &= \frac{P g_c}{\rho N^3 D_i^5} \Rightarrow P = N_p \rho N^3 D_i^5 / g_c \\ &= 6 \times 1200 \times (2.5)^3 \times (0.8)^5 / 9.81 \\ &= \frac{3758 \text{ Kg m/s hp}}{745.7 \text{ Kg m/s}} = 5.04 \text{ hp} \end{aligned}$$

Correction factor for non-geometrical similarity:

$$\begin{aligned} f_c &= \sqrt{\frac{(D_t/D_i)^* (H_L/D_i)^*}{(D_t/D_i)(H_L/D_i)}} = \sqrt{\frac{3 \times 5.53}{3 \times 3}} = 1.36 \\ (D_t/D_i)^* &= \frac{2.4}{0.8} = 3 \\ (H_L/D_i)^* &= \left(\frac{20 \text{ m}^3}{(2.4)^2 \left(\frac{\pi}{4} \right) \text{ m}^2} \right) / 0.8 \text{ m} = 4.42/0.8 = 5.53 \end{aligned}$$

The power input for three sets of impellers in a single shaft is: $P = (5.04 \text{ hp})(1.36)(\text{three sets of impellers}) = 20.5 \text{ hp}$.

$$\text{Aeration rate} = N_a = \frac{F_g}{N_i D_i^3}$$

$$F_g = 20 \text{ m}^3 \text{ min}^{-1} = 1 \text{ vvm} \times V_L = 0.333 \text{ m}^3 \text{ s}^{-1}$$

Given gassed power is 40% of ungassed power.

$$P_g/P = 0.4 \quad P_g = 0.4 \times 20.5 = 8.2 \text{ hp}$$

$$N_a = \frac{F_g}{N_i D_i^3} = \frac{0.333}{2.5 \times (0.8)^3} = 0.26$$

$$V_S = \frac{20 \text{ m}^3 \text{ min}^{-1}}{\frac{\pi}{4} \times (2.4)^2 \text{ m}^2} = 4.42 \text{ m min}^{-1} = 7.4 \times 10^{-2} \text{ m s}^{-1} \quad (\text{E.3.2})$$

The mass transfer coefficient is calculated.

$$K_L a = 2 \times 10^{-3} \left(\frac{8.2 \text{ hp}}{20} \right)^{0.6} (442)^{0.667} = 0.068 \text{ s}^{-1} \quad (\text{E.3.3})$$

With an assumption of oxygen concentration at the interface, equilibrium with the liquid phase is 6 ppm, and the OTR is calculated.

$$\text{OTR} = K_L a (C_{\text{O}_2}^* - C_{\text{O}_2}) = (0.068) (6 \times 10^{-3}) = 4.09 \times 10^{-4} \text{ kg m}^{-3} \text{ s}^{-1}$$

$$\text{OTR} = x q_{\text{O}_2} = (0.65 \times 10^{-3}) (32 \times 10^{-3}) x$$

$$\text{OUR} q_{\text{O}_2} = 2.08 \times 10^{-5} \text{ kg O}_2 \text{ kg}^{-1} \text{ cell}^{-1} \text{ s}^{-1}$$

$$x = \frac{4.09 \times 10^{-4}}{2.08 \times 10^{-5}} = 19.66 \text{ kg m}^{-3} \quad (\text{E.3.4})$$

Cell Balance:

$$19.66 = x_s = x_o + \frac{\mu_{\max}}{q_s}$$

$$C_s = \frac{19.66}{0.5} = 39.3 \text{ kg m}^{-3} \quad (\text{E.3.5})$$

EXAMPLE 4

Scale-up Calculations

Calculate mass transfer, gas hold-up, and gassed and ungassed power for the fermenter with the given data:

$$\rho_{\text{broth}} = 1200 \text{ kg m}^{-3} \quad \mu = 0.002 \text{ N s m}^{-2} \quad N_i = 90 \text{ rpm}$$

$$D_t = 4 \text{ m} \quad D_i = 2 \text{ m} \quad w_b = 0.4 \text{ m} \quad H_L = 6.5 \text{ m}$$

Air is sparged with 0.4 vvm; it is equipped with two sets of impellers and a flat-blade turbine with four baffles.

Calculate: (a) power, P ; (b) power, P_g ; (c) $K_L a$; (d) gas hold-up.

Solution

$$(D_t/D_i)^* = 2$$

$$(H_L/D_i)^* = \frac{6.5}{2} = 3.25$$

$$N = 90 \text{ rpm}/60 = 1.5 \text{ rps}$$

$$N_{\text{Re}} = \frac{ND_i^2 \rho}{\mu} = \frac{1.5 \times 2^2 \times 1200}{0.002} = 3.6 \times 10^6$$

Read N_p from Figure 6.6, Chapter 6, power versus Re, for a turbulent regime, $N_p = 6$.

$$6 = \frac{P \times 9.81}{(1.5)^3 (2)^5 (1200)} \Rightarrow P = 105 \text{ hp}$$

Correction factor for non-geometrical similarity:

$$f_c = \sqrt{\frac{(D_t/D_i)^* (H_L/D_i)^*}{(D_t/D_i)(H_L/D_i)}} = \sqrt{\frac{2 \times 3.25}{3 \times 3}} = 0.85 \quad (\text{E.4.1})$$

$$P = 2 \times 0.8 \times 105 = 168 \text{ hp}$$

The gas flow rate is:

$$F_g = 0.4(4)^2 \left(\frac{\pi}{4}\right) (6.5) = 32.67 \text{ m}^3 \text{ min}^{-1} = 0.5445 \text{ m}^3 \text{ s}^{-1}$$

The aeration number is:

$$N_a = \frac{F_g}{N_i D_i^3} = \frac{0.5445}{1.5 \times (2)^3} = 0.045$$

Reading gassed power to ungassed power ratio from the plot for the ratio of P_g/P , defined in Figure 6.6, Chapter 6:

$$\frac{P_g}{P} = \frac{P_a}{P} = 0.74$$

The gassed power is always less than the ungassed power.

$$P_g = 0.74P = 0.74(168) = 124.3 \text{ hp}$$

The mass transfer coefficient for turbulent flow is:

$$K_L = 2 \times 10^{-3} \left(\frac{P_g}{V_L}\right)^{0.6} V_s^{0.667} \quad (\text{E.4.2})$$

$$K_L a = 2 \times 10^{-3} \left(\frac{124.3 \times 754.7 \text{ W hp}^{-1}}{26\pi}\right)^{0.6} \left(\frac{0.54}{4\pi}\right)^{0.667} = 58.62 \text{ s}^{-1}$$

where the gas and liquid velocities are:

$$V_s = \frac{0.5445 \text{ m}^3 \text{ s}^{-1}}{4\pi \text{ m}^2} \quad V_L = 4\pi \times 6.5 = 26\pi = 81.68 \text{ m}^3$$

EXAMPLE 5

Calculate mass transfer coefficient in a 60 m^3 fermenter with a gas and liquid interfacial area of $\alpha = 0.3 \text{ m}^2 \text{ m}^{-3}$, given $\rho_{\text{broth}} = 1200 \text{ kg m}^{-3}$. The small reactor has working volume of 0.18 m^3 , 1 vvm aeration rate. The OTR is $0.25 \text{ kmol m}^{-3} \text{ h}^{-1}$. There are two sets of impellers, and flat-blade turbine types of impeller were used, $H_L = 1.2D_t$. Find the exact specifications of a large fermenter.

$$V = 0.18 = \frac{\pi}{4} D_t^2 (1.2D_t) = 0.3\pi D_t^3$$

The diameter of the tank is:

$$D_t = \left(\frac{0.18}{0.3\pi} \right)^{1/3} = 0.576 \text{ m}$$

Also, the impeller diameter is:

$$D_i = \frac{1}{3} D_t = 0.576/3 = 19.2 \text{ cm}$$

The liquid media height is:

$$H_L = 1.2 \times 0.576 = 0.691 \text{ m}$$

The large tank diameter is:

$$D_{t_2} = \left(\frac{V_2}{0.3\pi} \right)^{1/3} = \left(\frac{60}{0.3\pi} \right)^{1/3} = 3.36 \text{ m}$$

and the impeller for the large tank is:

$$D_{i_2} = 3.36/3 = 1.12 \text{ m}$$

$$H_{L_2} = 1.2 \times 3.36 = 4.03 \text{ m}$$

The air flow rate is:

$$F_1 = 1 \times 0.18 \text{ m}^3 \text{ min}^{-1} = 3 \times 10^{-3} \text{ m}^3 \text{ s}^{-1}$$

Gas superficial velocity:

$$U_s = \frac{0.18 \times 60}{(\pi/4)(0.576)^2} = 41.45 \text{ m h}^{-1}$$

Oxygen partial pressure:

$$\overline{P_{\text{O}_2}} = 1 \text{ atm} + \left(1 + \frac{H_L m}{10.3 \text{ in}} \text{ atm} \right) \times 0.21 = 0.213 \text{ atm}$$

$$\text{OTR} = K_L \cdot \overline{P_{\text{O}_2}} \Rightarrow K_{L_1} = \frac{0.25 \text{ kmol m}^{-3} \text{ h}^{-1}}{0.213 \text{ atm}} = 1.174 \text{ kmol m}^{-3} \text{ h}^{-1} \text{ atm}^{-1}$$

$$H : D = 3 : 1 = 6 : 1$$

The column diameter is in the range of $0.1 < D < 7.5 \text{ m}$.

The mass transfer for freely rising gas bubbles is governed by conservation of mass and momentum balance. When the distance, velocity, and concentration of substances provide the major driving forces for fluid motion, three dimensionless numbers explain the mass transfer. The dimensionless numbers are the Schmidt number, the Grashof number, and the Sherwood number. The Schmidt number relates viscous forces with mass diffusivity. The Grashof number deals with free convection and buoyant forces. The Rayleigh number results from the multiplication of the Schmidt number and the Grashof number. Finally, the Sherwood number is the ratio of conductive forces and mass diffusivity. Based on the analogy in mass transfer, the Sherwood number is similar to the Nusselt number in heat transfer. The Sherwood number can be correlated with the Schmidt and Grashof numbers for calculating mass transfer coefficients in a mathematical expression.

$$Sc = \frac{\nu}{D_{O_2}} \quad (E.5.1)$$

$$Sh = \frac{k_l D}{D_{O_2}} \quad (E.5.2)$$

$$Gr = \frac{D^3 \Delta \rho g}{18 \mu_l^2} \quad (E.5.3)$$

and the Rayleigh number:

$$Gr \cdot Sc = Ra = \frac{D^3 \Delta \rho g}{\mu_l D_{O_2}} \quad (E.5.4)$$

Calderbank's correlation for turbulent flow aeration shows mass transfer is proportional to D_i^2 and $Re^{3/4}$:

$$Sh = 0.13 Sc^{1/3} Re^{3/4} \quad (E.5.5)$$

$$U_g = \frac{Q_g}{A} \quad (E.5.6)$$

13.5 DYNAMIC MODEL AND OXYGEN TRANSFER RATE IN ACTIVATED SLUDGE

The oxygen requirements for an activated sludge system with aeration and agitation for complete mixing are shown by a mathematical model as the rate of oxygen transferred is equal to the difference of inlet and outlet concentration plus the oxygen used for generation of biomass:

$$V \frac{dC_{O_2}}{dt} = a \cdot \bar{\mu} (C_{SO} - C_S) + b V X \quad (13.5.1)$$

where V is aeration tank volume in m^3 , and dC_{O_2}/dt is oxygen accumulation rate in $kg O_2 m^{-3} day^{-1}$, a , and b are empirical constants ($kg O_2 kg^{-1} BOD$) and ($kg O_2 kg^{-1} MLSS day^{-1}$), respectively. Also constant is the flow rate of fresh wastewater ($m^3 day^{-1}$); MLSS stands for mixed liquor suspended solids, C_S is the BOD in effluent from aeration tank ($kg BOD m^{-3}$), C_{SO} is BOD in fresh wastewater, and X is the sludge concentration in the aeration tank ($kg MLSS m^{-3}$).

EXAMPLE 1

In a specific activated sludge plant, the organic load is carried out at 0.8 kg BOD per kg MLSS day⁻¹ with an 80% BOD removal efficiency. Values for the above mathematical model are as follows. The fresh feed flow rate is 1 m³ h⁻¹, the initial BOD concentration is 20,000 ppm and V is 10 m³. The yield of biomass on substrate is 0.5 g g⁻¹ BOD.

$$a = 0.55 \text{ kg O}_2 \text{ kg}^{-1} \text{ BOD}$$

$$b = 0.35 \text{ kg O}_2 \text{ kg}^{-1} \text{ MLSS day}^{-1}$$

What is the oxygen requirement per kg BOD removal?

Solution

Making oxygen balance for the aeration tank, the dynamic transfer rate of oxygen is obtained:

$$V \frac{dC_{O_2}}{dt} = a \cdot \bar{\mu} (C_{SO} - C_S) + b V X \quad (\text{E.1.1})$$

Dividing the oxygen balance by the volume of the aeration tank and concentration of biomass, XX , the above equation will be simplified as follows:

$$\frac{1}{X} \frac{dC_{O_2}}{dt} = a \frac{\bar{\mu}}{VX} (C_{SO} - C_S) + b \quad (\text{E.1.2})$$

$$\frac{\bar{\mu} C_{SO}}{VX} = \frac{\left(\frac{\text{m}^3}{\text{day}}\right) \left(\frac{\text{kg BOD}}{\text{m}^3}\right)}{\left(\text{m}^3\right) \left(\frac{\text{kg MLSS}}{\text{m}^3}\right)} \quad (\text{E.1.3})$$

$$\frac{\text{kg BOD}}{\text{kg MLSS day}} = 0.8 \leftarrow \text{BOD loading} \quad (\text{E.1.4})$$

$$\frac{1}{X} \frac{dC_{O_2}}{dt} = \frac{a \cdot \bar{\mu} \cdot C_{SO}}{VX} \left(1 - \frac{C_S}{C_{SO}}\right) \quad (\text{E.1.5})$$

The BOD removal is 80%.

$$\frac{80}{100} = \frac{C_{SO} - C_S}{C_{SO}} = \left(1 - \frac{C_S}{C_{SO}}\right) \quad (\text{E.1.6})$$

$$0.8 = 1 - \frac{C_S}{C_{SO}} \quad (\text{E.1.7})$$

$$C_S = 0.2 C_{SO} \quad (\text{E.1.8})$$

$$\frac{1}{X} \frac{dC_{O_2}}{dt} = 0.4 \times 0.55(0.8) + 0.35 = 0.526 \frac{\text{kg O}_2}{\text{kg MLSS} - \text{day}} \quad (\text{E.1.9})$$

Now we can increase the BOD removal efficiency with decreasing organic loading. What would the amount of oxygen required per kg BOD removal be, with 90% removal efficiency? Given data for constant coefficient $a = 0.5$ and $b = 0.3$:

$$\frac{1}{X} \frac{dC_{O_2}}{dt} = a \left(\frac{F}{V}\right) \cdot \frac{1}{X} (C_{SO} - C_S) + b \quad (\text{E.1.10})$$

Given BOD loading:

$$\frac{FC_{SO}}{VX} = \frac{(\text{m}^3 \text{ day})(\text{kg BOD m}^{-3})}{(\text{m}^3)(\text{kg MLSS m}^{-3})} = 0.4 \quad (\text{E.1.11})$$

$$\frac{C_{SO} - C_S}{C_{SO}} = 0.9 \Rightarrow 1 - \frac{C_S}{C_{SO}} = 0.9 \quad (\text{E.1.12})$$

$$C_S = 0.1C_{SO}$$

$$\frac{1}{X} \frac{d\text{CO}_2}{dt} = 0.5 \times 0.4 \times 0.9 + 0.3 = 0.48 \text{ kg of O}_2 \text{ kg}^{-1} \text{ MLSS}^{-1} \text{ day}^{-1}$$

In fact, the more organic load there is, the more oxygen is needed in the treatment process.

EXAMPLE 2

A bioreactor of $V = 20 \text{ m}^3$ working volume produces penicillin. What sugar concentration will you choose if OTR is not limited? Hint: If you aerate a bioreactor, the power consumption is less than a nonaerated bioreactor, and the specific sugar consumption rate is $1 \text{ kg kg}^{-1} \text{ cell h}^{-1}$.

Given Data

$D_t = 2.4 \text{ m}$	Three sets of impellers
$D_i = 0.8$	$\mu = 1 \text{ mPa s}$
$N_i = 2.5 \text{ rps}$	$\rho = 1200 \text{ kg m}^{-3}$
Number of blades = 8, turbine	Aeration rate = 1 vvm
$P_g/P = 0.4$	OTR = $6 \times 10^{-3} \text{ kg m}^{-3}$
Specific O ₂ uptake = $0.63 \text{ mmolO}_2 \text{ kg}^{-1} \text{ cell}$	$\nu_m = 0.5 \text{ h}^{-1}$

Solution

Let us find the Reynolds number.

$$\text{Re} = \frac{\rho N D_i^2}{\mu} = \frac{1200 \times 0.8^2 \times 2.5}{0.1} = 1.9 \times 10^4$$

When flow is turbulent, the power number is obtained from Figure 6.6, Chapter 6, using Re from power curves.

$$N_p = P_{no} = 6$$

$$P_{no} = 6 = \frac{P \cdot g}{\rho N_i^3 D_i^5} \Rightarrow P = \frac{6 \rho N_i^3 D_i^5}{g} = \frac{6 \times 1200 \times 2.5^3 \times 0.8^5}{9.81} = 5 \text{ hp}$$

Ungassed power = 5×3 sets of impellers = 15 hp.

Correction factor for scale-up using non-geometry similarity:

$$f_c = \sqrt{\frac{(D_t/D_i)^*(H_L/D_i)^*}{(D_t/D_i)(H_L/D_i)}} = \sqrt{\frac{3 \times 5.53}{3 \times 3}} = 1.36$$

$$D_t/D_i = 3$$

$$H_L/D = 3$$

$$(H_L/D_i)^* = \left[(20)/(2.4)^2(\pi/4) \right] / 0.8 = 5.53$$

Gassed power, $P_g = 0.4 (15)(1.36) = 8.14$ hp.

For three sets of impellers using aeration:

$$V_s = \frac{20 \text{ m}^3 \text{ min}^{-1}}{(\pi/4)(2.4)^2 \text{ m}^2} = 4.4 \text{ m}^3 \text{ min}^{-1} = 7 \times 10^{-2} \text{ m}^3 \text{ s}^{-1}$$

The mass transfer coefficient for a turbulent regime is:

$$K_L a = 2 \times 10^{-3} \left(\frac{8.14}{20} \right)^{0.6} (442)^{0.667} = 6.8 \times 10^{-2} \text{ s}^{-1}$$

The OTR is:

$$\text{OTR} = K_L a (C_i^* - C_l) = 6.8 \times 10^{-2} (6 \times 10^{-3} - 0)$$

$$\text{OTR} = x q_{O_2} = 4.07 \times 10^{-4} \text{ kg O}_2 \text{ m}^{-3} \text{ s}^{-1}$$

$$q_{O_2} = \left(6 \times 10^{-3} \frac{\text{kg}}{\text{m}^3} \times \frac{1}{32} \right) \text{ kg O}_2 \text{ kg}^{-1} \text{ cell m}^{-3} \text{ s}^{-1}$$

$$2.08 \times 10^{-3} = 0.65 \times 10^{-3} \frac{\text{mol O}_2}{\text{kg cell}} \times \frac{32 \text{ kg}}{\text{kmol}}$$

Biomass concentration is calculated.

$$X = \frac{4.07 \times 10^{-4}}{2.08 \times 10^{-5}} = 19.56 \text{ kg cell m}^{-3}$$

What is your desired sugar concentration?

To answer the above question, we need to know the yield of biomass on the substrate. Based on the availability of oxygen, there is a good chance of sufficient biomass being generated; therefore, nutrients and carbon sources must be available to carry on the process.

EXAMPLE 3

Let us scale-up a small fermenter with a volume (V) of 0.3 m^3 . The scale-up factor is 200-fold. The large fermenter has a volume (V_2) of 60 m^3 . The working volume is 60% of the nominal volume; that is, $V_L = 0.18 \text{ m}^3$

Aeration rate = 1 vvm.

Density, $\rho = 1200 \text{ kg m}^{-3}$.

Oxygen transfer rate, $\text{OTR} = 0.25 \text{ kmol m}^{-3} \text{ h}^{-1}$.

$$H_L/D_t = 1.2.$$

Two sets of impellers, turbine and flat blade.

The usual procedures for scaling up are summarized as following:

1. Reynolds number
2. Power consumption per unit volume of liquid
3. Tip velocity of an impeller, $N_i D_i$
4. Liquid circulation time, mixing time
5. Volumetric oxygen transfer coefficient

Solution

$$V_l = \frac{\pi}{4} D_t^2 (1.2 D_t) = 0.18 \text{ m}^3$$

$$D_t = \left(\frac{0.18}{0.3\pi} \right)^{1/3} = 0.576 \text{ m}$$

$$D_i = 1/3 D_t = 0.192 \text{ m}$$

$$H_{L_1} = 1.2 \times 0.576 = 0.691 \text{ m}$$

Large reactor:

$$D_{t_2} = \left(\frac{V_2}{0.3\pi} \right)^{1/3} = \left(\frac{60}{0.3\pi} \right)^{1/3} = 3.36 \text{ m}$$

and:

$$D_i = \frac{3.36}{3} = 1.12 \text{ m}$$

$$H_{L_2} = 1.2 \times 3.36 = 4.03 \text{ m}$$

Air flow rate:

$$F_1 = 1 \times 0.18 \text{ m}^3 \text{ min}^{-1} = 3 \times 10^{-3} \text{ m}^3 \text{ s}^{-1}$$

Gas supply velocity:

$$U_s = \frac{0.18 \times 60}{(\pi/4)(0.576)^2} = 41.45 \text{ m h}^{-1}$$

$$\bar{P}_{O_2} = \frac{1 \text{ atm} + \left(1 + \frac{H_L}{10.3} \right)}{2} = 0.213 \text{ atm}$$

$$\text{OTR} = K_v \cdot \bar{P}_{O_2}$$

$$K_v = \frac{0.25 \text{ kmol m}^{-3} \text{ h}^{-1}}{0.213 \text{ atm}} = 1.174 \text{ kmol m}^{-3} \text{ h}^{-1} \text{ atm}^{-1}$$

$$K_v = 0.0318 \left(\frac{P_g}{V} \right)^{0.95} U_s^{0.67} = 1.174$$

$$P_g = 3.22V = 3.22 \times 0.18 = 0.58 \text{ hp}$$

For turbulent flow, the power number is about six, and for two sets of impellers it will be doubled.

$$\text{Re} \rightarrow N_p = 6 \times 2 = 12$$

$$N_p = \frac{P_1 g}{\rho N_1^3 D_i^5} \Rightarrow P_1 = 12 \times 1200 \times N_1^3 (0.192)^5 / 9.81 = 0.383 N_1^3 \text{ hp}$$

If you have access to the graph P_g/P that is good, read the gassed power to ungassed power ratio off of the graph.

Read aeration number (N_a) from Figure 6.7, Chapter 6. Now we make use of Miller's correlation for gassed power calculations⁵:

$$P_g = 0.5 \left(\frac{P_1^2 N_1 D_{i1}^3}{F^{0.56}} \right)^{0.43}$$

$$0.58 = 0.5 \left(\frac{(0.383)^2 (N_1^3)^2 N_1 D_{i1}^3}{(3 \times 10^{-3})^{0.56}} \right)^{0.43} \Rightarrow N_1 = 116 \text{ rpm}$$

$$P_1 = 0.383 N_1^3 = 0.383 (116)^3 = 2.75 \text{ hp}$$

$$P_g/P = 0.58/2.75 = 0.21$$

Power input constant, geometric similarities:

$$\begin{aligned} \frac{\rho N_2^3 D_{i1}^5}{V_1} &= \frac{\rho N_2^3 D_{i2}^5}{V_2} \Rightarrow \left(\frac{N_2}{N_1} \right)^3 = \left(\frac{V_2}{V_1} \right) \left(\frac{D_{i1}}{D_{i2}} \right)^5 \\ N_2 &= N_1 \left(\frac{V_2}{V_1} \right)^{1/3} \left(\frac{D_{i1}}{D_{i2}} \right)^{5/3} = 116 \left(\frac{60}{0.3} \right)^{1/3} \left(\frac{0.192}{1.12} \right)^{5/3} = 35 \text{ rpm} \end{aligned}$$

Constant impeller tip velocity:

$$N_1 D_{i1} = N_2 D_{i2}$$

$$N_2 = N_1 \left(\frac{D_{i1}}{D_{i2}} \right) = 116 \left(\frac{0.192}{1.12} \right) = 20 \text{ rpm}$$

$$P_g/V = 0.58/0.18 = 3.22 \text{ hp}$$

$$P_g = \left(\frac{0.58}{0.18} \right) \times (36 \text{ m}^3) = 116 \text{ hp}$$

$$P = 2.75 \left(\frac{36}{0.18} \right) = 550 \text{ hp}$$

EXAMPLE 4: FILTER AND AIR FILTRATION

A batch production of penicillin of 40 m³ capacity is required to supply sterile air through a bioreactor at one volume of air per volume of culture per min (1 vvm). Incoming air contains 3000 bacteria per cubic meter of air for 1 h operation. Calculate the filter depth, if the penetration of bacteria is one in one million.

Solution

Assuming:

$$D_{\text{filter}} = 60 \text{ cm based on availability}$$

Air flow rate:

$$F_{\text{air}} = (40 \text{ m}^3)(1 \text{ vvm})60 \text{ min h}^{-1} = 2400 \text{ m}^3 \text{ h}^{-1}$$

$$\text{Microbial load} = 3000 \text{ cell m}^{-3}$$

$$\text{Cell rate} = 2400 \times 3000 = 7.2 \times 10^6 \text{ cell h}^{-1}$$

$$\text{Filter cross-sectional area} = (\pi/4)(0.6)^2 = 0.0283 \text{ m}^2$$

$$\text{Air velocity} = \frac{\text{Volumetric flow rate}}{A} = \frac{2400}{0.0283} = 8488 \text{ m h}^{-1}$$

Removal of organisms may follow the following exponential format of equation with implantation of initial condition, resulted as follows:

$$N_t = N_o e^{-kt}$$

$$\ln \frac{N_1}{N_2} = kL$$

$$\ln \frac{7.2 \times 10^6}{10^{-6}} = kL \quad (\text{E.4.1})$$

$$N_1 = 7.2 \times 10^6 \text{ cells}$$

$$N_2 = 1 \text{ cell in } 10^6 \text{ cells} = 10^{-6} \text{ cells}$$

where L is the length of filter, and k is rate constant for bed materials 40 m⁻¹ and/or 84 m⁻¹. The length of the filter is based on filter materials: for a large k , a shorter length of filter was obtained.

$$L = \frac{1}{k} \ln(7.2 \times 10^{12}) = \frac{1}{40} \ln(7.2 \times 10^{12}) = 0.74 \text{ m}$$

$$L = \frac{1}{84} \ln(7.2 \times 10^{14}) = 0.35 \text{ m}$$

EXAMPLE 5

In a batch fermentation of ethanol, kinetic data were collected as product formed. The data are shown in Table E.5.1. The data will be used to design a continuous bioreactor (CSTR) with a 100 l working volume.

1. If the feed rate, F , is $5 \times 10^{-3} \text{ m}^3 \text{ h}^{-1}$, calculate the ethanol concentration in the product stream. Keep in mind there was no ethanol in the feed stream.
2. If the product yield is 45%, what would the sugar concentration in the feed stream be?

Experimental data are shown in Table E.5.1.

The data are plotted in Figure E.5.1.

Use material balance for ethanol production:

$$\frac{dC_p}{dt} = D(C_{P_0} - C_p) + r_p \quad (\text{E.5.1})$$

At steady-state condition, the product concentration remained constant, $dC_p/dt = 0$. Initially there was no ethanol in the feed stream, $C_{P_0} = 0$. When there is no accumulation, the balance equation is reduced to:

$$D(-C_p) + r_p = 0 \quad (\text{E.5.2})$$

TABLE E.5.1 Ethanol production in batch fermentation with respect to inoculation time

Time (h)	Ethanol (g l^{-1})
0	0.0
10	2.0
15	4.0
18	6.2
21	10.0
27	16.0
33	30.0
42	56.5
48	75.7
51	85.0
54	96.0
57	103.5
60	107.3
66	110.5
72	113.0

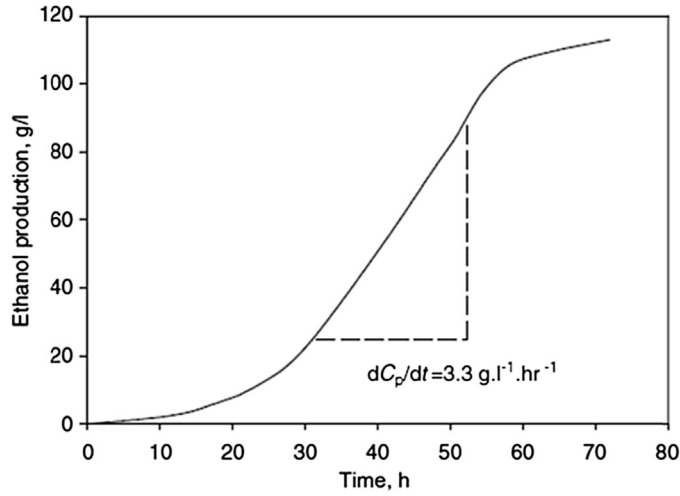


FIGURE E.5.1 Ethanol concentration profile with respect to fermentation time in batch mode of operation.

$$r_p = DC_p = \frac{F}{V} C_p \quad (\text{E.5.3})$$

$$C_p = \frac{V}{F} r_p \quad (\text{E.5.4})$$

Since there were no significant changes in temperature, then it was assumed that there was no wall temperature effect.

$$\left(\frac{\mu}{\mu_w} \right)^{0.14} = 1 \quad (\text{E.5.5})$$

From plotted data:

$$\frac{dC_p}{dt} = 3.3 \text{ g l}^{-1} \text{ h}^{-1} \quad (\text{E.5.6})$$

$$\frac{V}{F} r_p = \left(\frac{dC_p}{dt} \right) \frac{V}{F} = \frac{F}{V} C_p \quad (\text{E.5.7})$$

$$C_p = \left(\frac{0.1 \text{ m}^3}{5 \times 10^{-3} \text{ m}^3 \text{ h}^{-1}} \right) (3.3 \text{ g l}^{-1} \text{ h}^{-1}) = \frac{330}{5} \text{ g l}^{-1} = 66 \text{ kg m}^{-3}$$

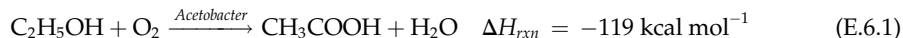
Ethanol concentration in the product stream is 66 g l^{-1} .

$$Y_{p/s} = 0.45$$

$$S_o = \frac{C_p}{Y_{p/s}} = \frac{66}{0.45} = 147 \text{ g l}^{-1}$$

EXAMPLE 6: VINEGAR PRODUCTION IN A JACKETED BIOREACTOR

Ethanol is oxidized to acetic acid in the production of vinegar using *Acetobacter*. The reaction is exothermic:



The biochemical reaction rate followed the Monod rate model, with a Monod rate constant of $k_S = 6.2 \times 10^{-6} \text{ g cm}^{-3}$ and a specific growth rate of $\nu_{\text{max}} = 6.67 \times 10^{-7} \text{ g cm}^{-3} \text{ s}^{-1}$.

Design the bioreactor with a suitable heat transfer area.

Given data	
$N = 500 \text{ rpm} = 30000 \text{ rph}$	$T = 32^\circ\text{C} = 90^\circ\text{F}$
$D_i = 0.75 \text{ ft}$	$k = 0.356 \text{ Btu h}^{-1} \text{ ft}^{-1} \text{ }^\circ\text{F}^{-1}$
$\rho = 62.4 \text{ lbm ft}^{-3}$	$C_p = 1 \text{ Btu lb}^{-1} \text{ }^\circ\text{F}^{-1}$
$\mu = 1 \text{ cp} = 2.42 \text{ lbm ft}^{-1} \text{ h}^{-1}$	$H_L = \frac{4}{3} D_t$

Solution

$$-r_s = \frac{\nu_{\text{max}} S}{K_S + S} \quad (\text{E.6.2})$$

$$K_S = 6.2 \times 10^{-6} \text{ g cm}^{-3} \text{ and } \nu_{\text{max}} = 6.67 \times 10^{-7} \text{ g cm}^{-3} \text{ s}^{-1}$$

Figure E.6.1 shows the jacketed bioreactor.

From the graph, the overall heat transfer coefficient for the jacketed vessel⁸ is:

$$U \approx 100 \text{ Btu h}^{-1} \text{ ft}^{-2} \text{ }^\circ\text{F}^{-1}$$

$$\text{Re} = \frac{\rho N D_i^2}{\mu} \quad (\text{E.6.3})$$

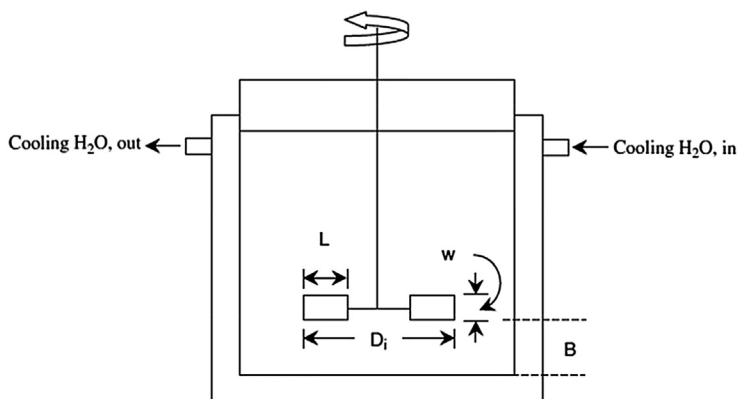


FIGURE E.6.1 Diagram of jacketed vessel with impeller location.

For turbulent flow:

$$Nu = \frac{hD_t}{k} = 0.36 Re^{2/3} Pr^{1/3} \quad (E.6.4)$$

$$\frac{h_1}{h_2} = \left(\frac{D_1}{D_2}\right)^{1/2} \left(\frac{N_1}{N_2}\right) \quad (E.6.5)$$

The power for the fermentation vessel was projected by the following general equation:

$$\text{Power (hp)} = 1.29 \times 10^{-4} D^{1.1} L^{2.72} N^{2.86} w^{0.3} H^{0.6} \mu^{0.14} \rho^{0.86} \quad (E.6.6)$$

$$Re = \frac{\rho N D_i^2}{\mu} = \frac{(62.4)(30000)(0.75 \text{ ft})^2}{2.42} = 4.3 \times 10^3$$

From Kern⁸ page 718, for the given Re , read the Nusselt number, $hD/k = 2000$.

$$\frac{D_i}{D_t} = \frac{1}{3}$$

$$h = \frac{2000 \times 0.356}{3 \times 0.75} = 600 \text{ Btu h}^{-1} \text{ ft}^{-2} \text{ }^\circ\text{F}^{-1}$$

Assuming the thickness of jacket is one inch, the film coefficient in the cold side of tube is estimated to be:

$$h_{\text{cold water}} \approx 550 \text{ Btu h}^{-1} \text{ ft}^{-2} \text{ }^\circ\text{F}^{-1}$$

The clean design over all heat transfer coefficients is defined as:

$$U_c = \frac{h_i h_o}{h_i + h_o} = \frac{550 \times 600}{1150} = 300 \text{ Btu h}^{-1} \text{ ft}^{-2} \text{ }^\circ\text{F}^{-1}$$

The dirt factor is assumed:

$$R_d = 0.005$$

$$\frac{1}{U_D} = \frac{1}{U_c} + R_d = \frac{1}{300} + 0.005 = 0.0083$$

$$U_D = 120 \text{ Btu h}^{-1} \text{ ft}^{-2} \text{ }^\circ\text{F}^{-1}$$

The inlet and outlet temperature of the jacketed bioreactor is shown in [Figure E.6.2](#). The log mean temperature is:

$$\Delta T_{\text{ln}} = \frac{(T - t_{c_{in}}) - (T - t_{c_{out}})}{\ln\left(\frac{T - t_{c_{in}}}{T - t_{c_{out}}}\right)} \quad (E.6.7)$$

$$\Delta T_{\text{ln}} = \frac{(32 - 15) - (32 - 25)}{\ln\left(\frac{17}{7}\right)} = 11.27 \text{ }^\circ\text{C}$$

Heat transfer is based on the resistance theory for the composite wall. The heat transfer overall coefficient is calculated.

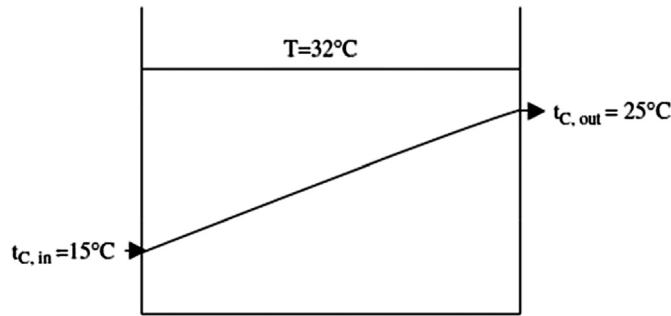


FIGURE E.6.2 Temperature pattern in a jacketed bioreactor for log mean temperature.

$$\frac{1}{U} = \frac{1}{h_i} + \frac{\Delta x}{k} + \frac{1}{h_o} \quad (\text{E.6.8})$$

Heat transfer area:

$$A = \pi [(D^2/4) + (DH_L)] = \pi [(2.25)^2/4 + 3(2.25)] = 25.18 \text{ ft}^2 \quad (\text{E.6.9})$$

$$Q = AU_D \Delta T_{\ln} \quad (\text{E.6.10})$$

$$Q = (25.18)(120)(1.8)(11.27) = 61,300 \text{ Btu h}^{-1}$$

The temperature differences in cooling water is $10 \text{ K} = 18\text{R}$.

$$Q_{\text{cooling}} = m_{\text{H}_2\text{O}} C_P \Delta t \quad (\text{E.6.11})$$

$$61,300 \text{ Btu h}^{-1} = m_{\text{H}_2\text{O}} (1 \text{ Btu lb}_m ^{\circ}\text{F})(18\text{R})$$

$$m_{\text{H}_2\text{O}} = 3405 \text{ lb}_m \text{ h}^{-1}$$

The mass flow rate of cooling water through energy balance as heat transfer from the reactor is equal to heat absorbed by cooling water $= 3405 \text{ lb}_m \text{ h}^{-1}$.

13.6 AEROBIC WASTEWATER TREATMENT

The well-known aerobic downflow process is a trickled bed filter. Attached growth is used in the biological treatment of wastewater. Air passes through the bed while the liquid is forced down by gravity. Figure 13.2 shows the liquid gas system for the mass transfer process in a biological filter. The system is known as attached growth. Modes of bioreactor operation are:

- Batch
- Fed batch
- Continuous.

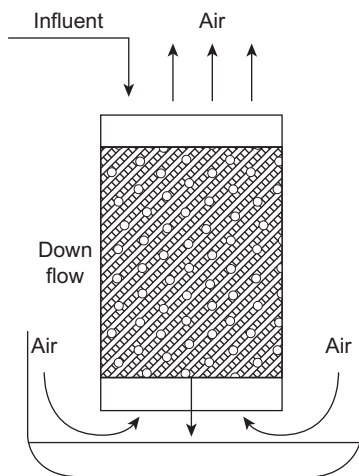


FIGURE 13.2 Liquid gas mass transfer process in biological filter, attached growth system.

For mass balance:

$$\frac{dm}{dt} = m_i - m_o + r_p - r_s \quad (13.6.1)$$

For batch operation:

$$m_i - m_o = 0 \quad (13.6.2)$$

$$-r_s = -r_A = -\frac{1}{V} \frac{d(SV)}{dt} = \frac{n_{\max} S}{K_M + S} \quad (13.6.3)$$

$$-r_A = -\frac{dC_A}{dt} \quad (13.6.4)$$

$V = \text{constant}$:

$$\frac{dS}{dt} = -\frac{v_{\max} S}{K_M + S} \quad (13.6.5)$$

$$-\int_0^t dt = \int_{S_0}^S \left(\frac{K_M + S}{v_{\max} S} \right) dS \quad (13.6.6)$$

$$-t_{\text{batch}} = \frac{K_M}{n_{\max}} \ln \frac{S_f}{S_o} + \frac{1}{n_{\max}} (S_f - S_o) \quad (13.6.7)$$

where S_0 and S_f are initial and final substrate concentration in mol l^{-1} .

13.6.1 Substrate Balance in a Continuous System

Substrate balance:

$$\frac{dS}{dt} = \frac{F}{V}(S_I - S) - \underbrace{\frac{\mu \rho_{cell}}{Y_{x/s}}}_{\text{Yield of cell}} - m \rho_{cell} - \underbrace{\frac{q_p \rho_{cell}}{Y_{p/s}}}_{\text{Nutrient maintenance}} \quad (13.6.1.1)$$



At steady-state condition:

$$\frac{dS}{dt} = 0 \quad (13.6.1.3)$$

$$m \rho_{cell} \leq \frac{\mu \rho_{cell}}{Y_{s/x}} \quad (13.6.1.4)$$

$$\begin{aligned} D(S_i - S) &= \frac{\mu \rho_{cell}}{Y_{x/s}} \text{ for SCP} \\ &= \frac{\mu \rho_{cell}}{Y_{x/s}} + \frac{q_p \rho_{cell}}{Y_{p/s}} \text{ for ethanol} \end{aligned} \quad (13.6.1.5)$$

When:

$$\mu = D \quad (13.6.1.6)$$

$$\rho_{cell} = Y_{x/s}(S_i - S) \quad (13.6.1.7)$$

$$\begin{aligned} \frac{d \ln k}{dT} &= \frac{E}{RT^2} \\ k &= k_0 e^{-\frac{E}{RT}} \end{aligned} \quad (13.6.1.8)$$

EXAMPLE 1

For production of an enzyme used for synthesis of a sun protection lotion, the required kinetic data and constants are:

$$v_{\max} = 2.5 \text{ mmol m}^{-3} \text{ s}^{-1}$$

$$K_m = 8.9 \text{ mmol l}^{-1}$$

$$S_o = 12 \text{ mmol l}^{-1}$$

Find the reaction time for 95% conversion of raw materials. $t_{batch} = ?$ for $x_A = 0.95$.

Solution

$$v_{\max} = \left(\frac{2.5 \text{ mmol}}{\text{m}^3 \text{ s}} \right) \left(\frac{3600 \text{ s}}{\text{h}} \right) \left(\frac{1 \text{ m}^3}{1000 \text{ l}} \right) = \frac{9 \text{ mmol}}{\text{l h}}$$

$$\begin{aligned} t_{\text{batch}} &= \frac{K_m}{v_{\max}} \ln \frac{S_o}{S_f} + \frac{S_o - S_f}{v_{\max}} \\ &= \frac{8.9}{9} \ln \frac{12}{(1 - 0.95)(12)} + \frac{0.95 \times 12}{9} \\ &= 4.2 \text{ h} \end{aligned}$$

13.6.2 Material Balance in Fed Batch

In fact, fed batch is a batch system operating without any outlet stream. The differences in substrate in and out are equal to the rate of product generation.

$$\frac{F}{V}(S_i - S) = \left(\frac{v_{\max} S}{K_M + S} \right) \frac{V}{V} \quad (13.6.2.1)$$

The retention time:

$$\tau = \frac{1}{D} = \frac{V}{F} \quad (13.6.2.2)$$

$$D(S_i - S) = \frac{v_{\max} S}{K_m + S} \quad (13.6.2.3)$$

$$\underbrace{\frac{d\rho_{\text{cell}}}{dt}}_{\text{At steady state}=0} = \frac{F}{V} \left(\rho_i - \underbrace{\rho_o}_{\text{sterile system}} \right) + \left(\underbrace{\mu}_{\text{growth}} - \underbrace{\alpha}_{\text{death}} \right) \rho_{\text{cell}} \quad (13.6.2.4)$$

The simplified material balance would lead to growth rate:

$$\mu = \frac{F}{V} \quad (13.6.2.5)$$

EXAMPLE 1

A 10-m³ bioreactor with $H/D = 2.5D$, 75% working volume, with two sets of standard flat blade impellers was used for a baker's yeast production unit. The operating dilution rate was set at 0.5 h⁻¹. The rate equation satisfying the reactor design was a Monod model with $\mu_{\max} = 0.65$ h⁻¹ and $k_S = 3$ kg m⁻³. The initial substrate concentration was 65 g l⁻¹ with 1 vvm aeration, a broth density of 1200 kg m⁻³, and a viscosity $\mu = 0.02$ N s m⁻². The yield of biomass on glucose was 0.5 g cell g⁻¹ glucose. Calculate power consumption for a 90 rpm agitation rate and OTR of 0.05 g l⁻¹. State the controlling resistance in the mass transfer process.

Solution

The flow regime is turbulent flow. Read the value for the power number using Figure 6.6, Chapter 6.

$$10 = \frac{\pi}{4}(2.5D)D^2$$

$$D_t = 1.7 \text{ m}$$

$$D_i = 0.57 \text{ m}$$

$$\text{Re} = \frac{(1.5 \text{ rps})(0.57)^2(1200)}{0.02 \frac{\text{N s}}{\text{m}^2}} = 2.9 \times 10^4$$

The flow regime is turbulent flow. Read the value for the power number using Figure 6.6 in Chapter 6.

$$N_p = 6$$

$$N_a = \frac{F_g}{ND_i^3} = \frac{7.5 \text{ m}^3 \text{ min}^{-1}}{(90 \text{ rpm})(0.57)^3} = 0.45$$

where N_a is known as the aeration number; then use Figure 6.7 in Chapter 6 to find the ratio of gassed power to ungassed power.

$$\frac{P_g}{P} = 0.95$$

$$N_p = \frac{Pg_c}{\rho n^3 D_i^3}$$

$$P = \frac{6 \times 1200(1.5)^3(0.57)^3}{9.81} = 149 \frac{\text{kg m}}{\text{s}}$$

$$= \frac{149}{745.7} = 0.2 \text{ hp}$$

Conversion factor:

$$1 \text{ hp} = 745.7 \text{ kg m s}^{-1}$$

$$P = 2 \times 0.2 = 0.4 \text{ hp}$$

$$P_g = 0.95(0.4) = 0.38 \text{ hp}$$

$$\frac{P_g}{V_L} = 0.051 \text{ w l}^{-1}$$

OTR:

$$\text{OTR} = K_L a (C - C_L) = 7.9 \times 10^{-4} (0.03) = 4 \times 10^{-5} \text{ kg m}^{-3} \text{ s}^{-1}$$

Given:

$$K_L a = 2 \times 10^{-3} V_s^{0.7} \left(\frac{P_g}{V_L} \right)^{0.2}$$

$$V_s = \frac{7.5 \text{ m}^3 \text{ min}^{-1}}{(\pi/4)(1.72)^2} = 3.23 \text{ m min}^{-1} = 194 \text{ m h}^{-1}$$

$$K_L a = 2 \times 10^{-3} (323 \text{ cm min}^{-1})^{0.7} (0.051)^{0.2} = 7.9 \times 10^{-4} \text{ s}^{-1}$$

Liquid film was the controlling resistance.

NOMENCLATURE

N	Impeller speed, rpm
D_i	Impeller diameter, m
Q_{O_2}	Oxygen transfer rate, mmol min ⁻¹
X	Biomass concentration, g l ⁻¹
P_g/V	Power per unit volume, hp m ⁻³
ND_i	Impeller tip velocity, m s ⁻¹
t_m	Mixing time, min
$K_L a$	Mass transfer coefficient, h ⁻¹
τ	Shear stress, Pa
$\frac{du}{dx}$	Shear rate, s ⁻¹
μ	Fluid viscosity, cp
$\frac{N_i D_i}{g}$	Froude Number, dimensionless
\hat{H}_i	Impeller interspacing, cm
U_g	Upward gas bubble velocity, m s ⁻¹
g	Gravity, m s ⁻²
OTR	Oxygen transfer rate, kmol m ⁻³ h ⁻¹
V_S	U_S Gas superficial velocity, m s ⁻¹
K_m	Monod rate constant, g l ⁻¹
ν_{\max}	Maximum specific growth rate, mmol m ⁻³ s ⁻¹
$k_x k_x$	Maximum specific growth rate., g l ⁻¹ h ⁻¹
D	Fresh media dilution rate, h ⁻¹
F	Flow rate, ml min ⁻¹
$MLSS$	Mixed liquor suspended solids, kg m ⁻³
V	Volume, m
$Y_{X/S}$	Yield of biomass on substrate
S_f	Inlet to outlet substrate ratio
R	Recycle ratio
f	Ratio inlet to outlet substrate concentration

References

1. Scragg AH. *Bioreactors in biotechnology, a practical approach*. Ellis Horwood series in biochemistry and biotechnology. 1991. New York.
2. Wang DIC, Cooney CL, Deman AL, Dunnill P, Humphrey AE, Lilly MD. *Fermentation and enzyme technology*. New York: John Wiley & Sons; 1979.
3. Baily JE, Ollis DF. *Biochemical engineering fundamentals*. 2nd ed. New York: McGraw-Hill; 1986.
4. Aiba S, Humphrey AE, Millis NF. *Biochemical engineering*. 2nd ed. New York: Academic Press; 1973.
5. Doran PM. *Bioprocess engineering principles*. New York: Academic Press; 1995.
6. Michel BJ, Miller SA. *AIChE J* 1962;**8**:262.
7. Stanbury PF, Whitaker A. *Principles of fermentation technology*. Oxford: Pergamon Press; 1984.
8. Kern D. *Process heat transfer*. New York: McGraw Hill; 1950. p. 717.

Single-Cell Protein

OUTLINE

14.1 Introduction	418	14.9.3 Mixing of the Coomassie Plus Protein Assay Reagent	425
14.2 Dissolved Oxygen in Single-Cell Protein Production	419	14.9.4 Standard Calibration Curve	426
14.3 Batch and Continuous Fermentation for Production of Single-Cell Protein	419	14.9.5 Standard Calibration Curve for Starch	426
14.3.1 Analytical Methods for Measuring Protein Content of Baker's Yeast	420	14.10 Single-Cell Protein Processes	426
14.3.2 Seed Culture	420	14.11 Nutritional Value of Single-Cell Protein	428
14.4 Batch Experiment for Production of Baker's Yeast	421	14.12 Organisms and Substrates for Single-Cell Protein Production	429
14.5 Separation of Microbial Biomass	421	14.12.1 Cellulose	430
14.6 Background	422	14.12.2 Starch	431
14.7 Production Methods	422	14.12.3 Whey (Lactose)	431
14.8 Media Preparation for Single-Cell Protein Production	424	14.12.4 Glucose	431
14.9 Analytical Methods	424	14.12.5 Alkanes	431
14.9.1 Coomassie-Protein Reaction Scheme	425	14.12.6 Methane/Methanol	431
14.9.2 Preparation of Diluted Bovine Serum Albumin Standards	425	14.13 Advantages and Disadvantages of Single-Cell Protein	432
		14.14 Preparation for Experimental Run	433
		References	433

14.1 INTRODUCTION

The term single-cell protein (SCP) is used to describe protein derived from cells or protein extracted from various microorganisms such as yeast, fungi, algae, and bacteria, which are grown for mass production from various inexpensive carbon sources such as agricultural wastes for the synthesis of food for humans or animals. The dried cells of microorganisms or the whole organism is harvested and consumed. This is a rich protein source that can be used as a human food supplement and in animal feeds. SCP production may have great potential for feeding the ever-increasing world population. Massive quantities of SCP can be produced in a single day. As a source of protein, it is very promising, with potential to satisfy the world shortage of food as the population increases. SCP may be enriched with a high content of proteins, fats and carbohydrates, nucleic acids, and vitamins. However, the disadvantage of SCP as a human food source is the high content of nucleic acids, which may cause serious problem in the human digestive track due to the limited capacity for the complete digestion of nucleic acids. SCP may be more attractive for animal food usage due to the flexibility of animal food and soft regulations for animal feedstock. Over the past decades, a variety of raw materials have been tested for SCP production, including carbon dioxide, methane, methanol, ethanol, various sugars, and even petroleum hydrocarbons and agricultural and industrial wastes. Several carbon sources are used as energy sources for microorganisms growing and producing SCP. In some cases, raw material requires pretreatment or hydrolysis before use. Waste sources of carbon used for SCP production are customary and cheap. SCP technology is a suitable process for converting waste materials to useful biomass containing protein. The broth is concentrated protein that is dried with limited moisture; it is stored for use as food or feed for humans and animals. Waste recycling has been advanced as a method for preventing environmental decay and increasing food supplies. It may be possible to convert waste streams into valuable products by separation and recovery or by biological conversion.¹⁻⁴ Many products are produced biologically from food process waste. The potential benefits of successful recycling of agricultural wastes are enormous. It may be the only method for large-scale protein production that does not require a concomitant increase in energy consumption. In addition, it may be the most effective method for producing animal and human food from lignocellulose materials, although they have little nutritive value and are therefore used for fuel production. One advantage of the biological process is the flexibility of the microorganisms to adapt to different feedstock. Therefore, when combined with the treatment of process waste streams, the biological conversion of these wastes to products can be both environmentally and economically favorable. In the production of antibiotics, sufficient growth of fungi in submerged cultures has created potential sources of biomass as SCP and as flavor additives to replace mushrooms; the biomass contains 50–65% protein.^{1,5} Production of mushroom from lignocellulosic waste seems to be a suitable and economical process because the raw material is inexpensive and available in most countries. Petroleum-based SCP was produced based on oxidation of methane to synthesize methanol; then, methanol as a carbon source was fed to the bioreactor using bacterium known as *Methylophilus methylotrophus* for biomass production, an 80% enriched produced protein known as Pruteen. Large scale production of SCP from petroleum may not be economical due to the high costs of petroleum. Extensive research has been conducted on the use of food processing wastes such as potato and orange peels for the

production of SCP. One has to be very careful in using fungi species, since the synthesis of secondary metabolites may cause food poisoning. Fungi are easily able to produce toxin and aflatoxins with the improper storage of animal feedstock; for instance, *Aspergillus flavus* as a secondary metabolite synthesizes toxins that are highly carcinogenic.

This chapter discusses the present status of microbial SCP production from agricultural wastes and describes some of the technical and economical problems related to the production processes that must be overcome for large-scale application to be possible.

14.2 DISSOLVED OXYGEN IN SINGLE-CELL PROTEIN PRODUCTION

In fermentation broth, the dissolved oxygen (DO) concentration is kept constant, while the production of SCP may reach the steady state condition, and the viable protein is continuously harvested. The concentration of protein is proportional to the oxygen uptake rate. Control of DO would achieve steady SCP production. Variation of DO may affect retention time and other process variables such as substrate and product concentrations, retention time, dilution rate, and aeration rate. Microbial activities are monitored by the oxygen uptake rate from the supplied air or oxygen. Microbial cells in the aerobic condition take up oxygen from the gas and then liquid phases. The rate of oxygen transfer from the gas phase to the liquid phase is important. At high cell densities, the cell growth is limited by the availability of oxygen in the medium. The growth of aerobic bacteria in the fermenter is then controlled by the availability of oxygen, substrate, energy sources, and enzymes. Air has to be supplied for the aerobic process to enhance the cell growth. Oxygen limitation may cause a reduction in the growth rate. The supplied oxygen from the gas phase has to penetrate into the microorganism. Several steps are required to let such a phenomenon take place. The oxygen first must travel through the gas–liquid interface, then the bulk of liquid, and finally into the microbial cell.

The above data show that in the case of high oxygen demand for SCP production, oxygen is drastically depleted after an incubation period of 12–24 h. Therefore, pure oxygen is commonly used when the DO level drops to 2 ppm; additional oxygen may enhance oxygen availability in the fermentation media.

Several DO probes are available. Some well-known branded fermenters, like New Brunswick, Bioflo series, and the B. Braun Biotstat B fermenters are equipped with a DO meter. This unit has a 2-l fermentation vessel equipped with a DO meter and pH probe, an antifoam sensor, and level controllers for harvesting culture. The concentration of DO in the media is a function of temperature. A higher operating temperature would decrease the level of DO. A microsparger is used to provide sufficient small air bubbles. The air bubbles are dominated in the media using a suitable gas sparger.

14.3 BATCH AND CONTINUOUS FERMENTATION FOR PRODUCTION OF SINGLE-CELL PROTEIN

The fermentation vessel is a jacketed vessel with a defined working volume. The media are made of phosphate buffer at a neutral pH with 3.3 g KH_2PO_4 and 0.3 g Na_2HPO_4 , 1 g yeast

extract, and 30 g glucose in 1 l of distilled water. The media should be sterilized in a 20-l carboy. The fermentation vessel with a working volume of 2 l may have 500 ml media initially sterilized by steam under 15 psig and 121 °C. The seed culture is transferred to the fermentation vessel with filtered and pressurized air; the production of SCP is monitored by pumping fresh nutrients and supplying air. Continuous culture with constant volume and controlled dilution rate is conducted in SCP production, as fresh and sterilized media are pumped into the culture vessel. It is desirable to control pH, temperature, and aeration with a constant air flow rate. The most common continuous culture system is the chemostat. The word chemostat refers to the constant chemical environment at a steady-state condition.⁶ Another continuous culture vessel is the turbidostat, in which the cell concentration in the culture vessel is kept constant by monitoring cell optical density. The chemostat experiment is carried out for 24 h at a constant temperature of 32 °C and by controlling pH and monitoring DO concentration. The medium consists of an excess amount of nutrients that is required to synthesize the desired concentration of SCP. The growth limiting nutrient controls the steady-state SCP production rate. The data for optical density, DO level, cell dry weight, and measurements of protein and carbohydrates are carried out at 8, 12, 16, and 24 h in batch mode. The continuous operation is extended for another 24 h to monitor all parameters and measure SCP. The results should be compared with batchwise production. The expected results for reduction of sugar in real experiments were similar. The data were obtained by aeration of pharmaceutical wastewater. A well-known reagent for determination of carbohydrates, dinitrosalicylic acid, was used to reduce the organic chemicals in the aforementioned wastewater for the course of three days incubation.^{7,8} The method of measurement will be discussed in the following sections. If the aforementioned experiments are conducted, they may lead us to a new set of data that are totally different, and only the reduction trend would be about the same. SCP production has to be determined by experimentation, and research is needed to obtain the data. Maximum carbohydrate reduction took place after 24 h of aeration. Since the carbon source was initially low, the rate of biomass production was not appreciable.

The role of DO in the treatment system is absolutely vital. Therefore, the DO level must be maintained at not less than three to four ppm in the wastewater for effective aeration. SCP production is very oxygen-dependent. The results would be very satisfactory if pure oxygen was used.

14.3.1 Analytical Methods for Measuring Protein Content of Baker's Yeast

Protein concentration can be determined using a method introduced by Bradford,⁹ which uses Pierce reagent 23,200 (Pierce Chemical Company, Rockford, IL, USA) in combination with an acidic Coomassie Brilliant Blue G-250 solution to absorb at 595 nm when the reagent binds to the protein. A 20-mg l⁻¹ bovine serum albumin (Pierce Chemical Company, Rockford, IL, USA) solution will be used to prepare a standard calibration curve for determination of protein concentration. The sample for analysis of SCP is initially homogenized or vibrated in a sonic system to break down the cell walls.

14.3.2 Seed Culture

How do we start the real experiment? A 100-ml seed culture is prepared in advance. A 100-ml media consists of 0.1 g yeast extract and 1 g glucose with 0.33 g KH₂PO₄ and 0.03 g

Na_2HPO_4 . It is sterilized, then the microorganism, *Saccharomyces cerevisiae* (ATCC 24,860), on a yeast and malt extracts (YM) slant tube used as stock culture is transferred to the sterile cooled media.¹⁰ The inoculated media is incubated and harvested after 24 h. The first stage of the work is the batch experiment, which is then changed to a continuous experimental run with glucose as a carbon source and the microorganism, *S. cerevisiae*, as an organism sensitive to aeration. The last stage demonstrates how agitation plays an important role in the mass transfer process.

14.4 BATCH EXPERIMENT FOR PRODUCTION OF BAKER'S YEAST

The fermentation vessel is a jacketed vessel with a working volume of 2 l. The media is made of phosphate buffer at neutral pH with 3.3 g KH_2PO_4 and 0.3 g Na_2HPO_4 , 1 g yeast extract, and 50 g glucose in 1 l of distilled water. The media should be sterilized in a 20-l carboy. The fermentation vessel with 500 ml media is initially sterilized under 15 psig steam at 121 °C for 20 min. The seed culture is transferred to the fermentation vessel, and the feed is gradually pumped in at a flow rate of 350 ml h⁻¹. The filtered pure oxygen or pressurized air is continuously supplied. The production of baker's yeast should be monitored for 48 h by batch experiment at a constant temperature of 32 °C, controlling pH and monitoring DO level. Sufficient air is blown at a flow rate of 2000 ml min⁻¹ (1 vvm).^{11,12}

Data collection for optical density, DO level, cell dry weight, protein, and carbohydrates is done at 6, 12, 18, 24, 36, and 48 h in batch mode, as projected in Table 14.1.

14.5 SEPARATION OF MICROBIAL BIOMASS

Bacteria, yeast, and algae are produced in massive quantities of protein sources as food for animals and humans.¹ SCP is considered a major source of feed for animals. The production of valuable biological products from industrial and agricultural wastes is considered through the bioconversion of solid wastes to added-value fermented product, which is easily marketable as animal feedstock. However, the waste streams cause pollution and threaten the

TABLE 14.1 Batch production of baker's yeast with air flow rate of one vvm and an agitation speed of 350 rpm

Time, hours	DO, mg l ⁻¹	Optical density, absorbance, λ_{520} nm	Cell dry weight, mg ml ⁻¹	Protein concentration, g l ⁻¹	Sugar concentration, g l ⁻¹	Yield, $Y_{x/s}$
0	7.9	0.00	0.00	0.00	32.0	—
6	5.6	0.28	0.14	0.83	30.0	0.42
12	4.1	0.50	0.29	4.75	21.0	0.43
18	2.4	1.55	1.10	8.90	13.0	0.47
24	1.5	2.00	1.45	11.15	5.0	0.41
36	1.1	4.20	2.00	11.95	1.7	0.40
48	0.2	4.45	2.65	12.35	0.5	0.39

environment can be considered as a raw material for SCP production using suitable strains of microorganisms.

14.6 BACKGROUND

It is evident that the conversion of photosynthetically produced organic compounds into human and animal food is the limiting process in human food production. The worldwide annual production of organic material by photosynthesis has been estimated to be between 25 and 50 tons.^{5,6} Any practical method capable of converting a small fraction of this yield into human food should find wide application and go a long way to reducing chronic food shortages.

The growth of microorganisms, more rapid than that of the higher plants, makes them very attractive as high-protein crops; whereas only one or two grain crops can be grown per year, a crop of yeasts or molds may be harvested weekly, and bacteria may be harvested daily. The use of microorganisms as a source of protein for human and animal food is not a new development. Traditional foods and feeds such as cheese, sauerkraut, miso, and silage have a high content of microorganisms to which their nutritional properties are due in part. The high-quality proteins synthesized during the growth of these microorganisms compare favorably with those derived from the better grains.^{1,3} There are many convincing reports on the availability of essential amino acids and the protein quality of SCP. Although there are few data on animal feeding trials using SCP produced from lignocellulose wastes, there is a large and growing body of information about SCP from petroleum and methanol. This information should be applicable to SCP from agricultural wastes, with proper allowance for the undesirable contaminants in the sources. In petroleum, there has been concern about accumulation of carcinogenic hydrocarbons. In agricultural wastes, there is concern about accumulation of pesticides and herbicides. The guidelines for testing SCP as a major supplement in animal diets should be consulted for further details on feeding trials. Many more feeding trials will be needed before SCP from lignocellulose wastes is accepted for routine feeding.

The main carbon source for production of SCP is petroleum. It has been used by many companies around the world. Other potential substrates for SCP include bagasse, citrus wastes, sulphite waste liquor from pulp and paper, molasses, animal manure, whey, starch, sewage, and agricultural wastes.

14.7 PRODUCTION METHODS

Some of the proposed methods for conversion of agricultural wastes into animal feed are presented in [Table 14.2](#). These methods will be briefly evaluated in the following. First, a distinction should be made between the production of SCP from the lignocellulose parts of the plant and the production of SCP from the soluble carbohydrates of many agricultural wastes. At present, there are many plants around the world that operate for the production of SCP. The Ceres Ecology Corporation of Chino, California, in the United States will process waste from more than 100,000 dairy cattle for feed recycling and for control of salt in

TABLE 14.2 Methods for conversion of cellulosic agricultural wastes into animal feed

Treatment	Microorganism	Substrate	Protein produced	Fiber used
Dilute alkali	None	Straw	No	Yes
Aerobic mesophiles, 25 °C	<i>Cellulomonas</i>	Bagasse	Yes	Yes
Mold growth, 25 °C	<i>Trichoderma viride</i>	Waste paper	Yes	Yes
Aerobic thermophiles, 55 °C	<i>Thermoactinomyces</i>	Fermented livestock wastes	Yes	Yes

groundwater. Other plants in Toulouse (France), Zacantecos (Mexico), and Sterling (Colorado, USA) use processes that depend on an anaerobic fermentation in a silo or covered ditch. The manure undergoes a lactic acid fermentation due to the action of anaerobic bacteria (chiefly streptococci and lactobacilli), and a typical silage odor results in place of the odor of manure. The processing of poultry for production of prepared food generates waste containing fats and starchy materials. The waste is used in a biological process to be converted to SCP using several microorganisms.^{3,4} These short-time anaerobic fermentation processes do not use the fiber and are therefore a partial solution to the waste problem. The fibrous residue may be used as a soil conditioner before or after composting. Figure 14.1 shows the various types of waste produced annually.

Rates of soluble sugar use of 10–30 g per liter per hour have been reported for SCP production by yeast. Rates of 5–15 g per liter per hour have been claimed for the use of selected hydrocarbons. For the process of SCP production under present market conditions to be an economical, the rate of use of cellulose must be at least 1–5 g per liter per hour. As no pilot plants have been operated, it is not possible to report commercial rates, but laboratory-scale fermenters have been run at 1 g per liter per hour on pretreated wastes. It has been reported

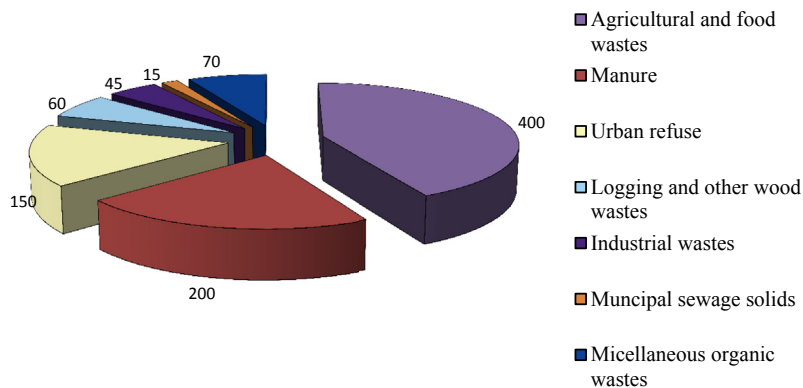


FIGURE 14.1 Solid wastes in the United States in units of tons per year.

that gram-negative aerobic bacteria, *Cellulomonas* sp., grow rapidly on cellulose at 25–30 °C, but cannot use lignin or lignocellulose. Therefore, extensive pretreatment of lignocellulosic material such as rice husks with hot alkali is required.^{7–9} The microorganism must be harvested by centrifugation. Amino acid analysis and animal feeding trials have shown that a high-quality SCP can be produced. Enzymes produced by the mold *Trichoderma viride* are used for production of soluble sugars from waste paper cellulose. Yeasts or bacteria for SCP production can then ferment these sugars. The enzyme reaction takes place in four steps:

1. Pretreatment of waste by ball milling or hot alkali
2. Enzyme production by growth of *T. viride* on pretreated cellulose
3. Depolymerization of cellulose by *T. viride* enzymes
4. SCP production by yeast or bacteria.

Several potential and mutant strains of *T. viride* have been identified in SCP production. Their capacity for amyloletic enzyme production was enhanced several fold in SCP from lignocellulosic resources. The process of bioconversion of agricultural wastes to SCP appeared to be too complex to find an economic application for agricultural waste.

14.8 MEDIA PREPARATION FOR SINGLE-CELL PROTEIN PRODUCTION

Sago starch in Malaysia is abundant, inexpensive, and common as raw material for SCP production. Fifty grams of sago starch is dissolved in 1 l of 0.1 M NaOH solution. The mixture is heat-treated until it is absolutely dissolved in deionizer water with 4 g of NaOH, then the pH is adjusted to 7. Supplementary nutrients are added: 3.3 g KH_2PO_4 , 0.3 g Na_2HPO_4 , and yeast extract; the media is autoclaved and used as feed for a fermenter. One hundred milliliters of seed culture are prepared a day in advance for inoculation of fermentation. *Saccharomycopsis fibuligera* ATCC9947 or ATCC9266 is grown in a media comprising 0.33 g KH_2PO_4 , 0.03 g Na_2HPO_4 , 0.1 g yeast extract, and 1 g glucose in 100 ml distilled water. The seed culture is harvested after 24 h of incubation at 32 °C. The microorganism is purchased from ATCC, and after hydration is kept in a stock culture of YM media (Difco, USA) slants. The inoculum for seed culture is the organism transferred from the prepared slant media.

The culture medium used for growth of *Penicillium javanicum* has been reported by Burrell and his coworkers.¹⁰ The recommended medium for cultivation of the fungi without any alteration contains the following chemical composition in 1 l solution: fumaric acid, 2.0 g, $(\text{NH}_4)_2\text{SO}_4$, 2.5 g; $\text{KH}_2\text{PO}_4 \cdot 2\text{H}_2\text{O}$, 1.0 g; MgSO_4 , 0.5 g; $(\text{NH}_4)\text{Fe}(\text{SO}_4)_2 \cdot 12\text{H}_2\text{O}$, 0.2 mg; $\text{ZnSO}_4 \cdot 7\text{H}_2\text{O}$, 0.2 mg; $\text{MnSO}_4 \cdot \text{H}_2\text{O}$, 0.1 mg; thiamine hydrochloride, 0.1 mg; and a suitable carbon source.

14.9 ANALYTICAL METHODS

Protein concentration can be determined by using the method of Bradford,⁹ which uses Pierce reagent 23,200 (Pierce Chemical Company, Rockford, IL, USA) in combination with an acidic Coomassie Brilliant Blue G-20 solution to absorb at 595 nm when reagent

binds to the protein. A 20 mg l^{-1} bovine serum albumin (Pierce Chemical) solution was used as the standard. Starch concentration was measured by the orcinol method,^{4,9–11} using synthetic starch as the reference. A yellow-to orange color is obtained and measured at 420 nm when orcinol reacts with carbohydrates. Absorbance is determined by spectrometry.

14.9.1 Coomassie–Protein Reaction Scheme

This protein assay works by forming a complex between the protein and the Coomassie dye. When bound to the protein, the absorbance of the dye shifts from a wavelength of 465–595 nm (λ_{595}). The reagent generates a stronger blue color that is detected at the specified wavelength. You will first generate a standard curve using the protein bovine serum albumin (BSA) by measuring the absorbance at 595 nm of a series of standards of known concentration. Next, you will measure the absorbance at wavelength of λ_{595} for all of your samples and determine its concentration by comparison with the standard curve.

Protein + Coomassie G-250 in acidic medium \rightarrow protein–dye complex (blue; measured at 595 nm)

14.9.2 Preparation of Diluted Bovine Serum Albumin Standards

Prepare a fresh set of protein standards by diluting the 2.0 mg per ml BSA stock standard (stock solution) as shown in Table 14.3. There will be sufficient volume for three replications of each diluted BSA standard, if necessary.

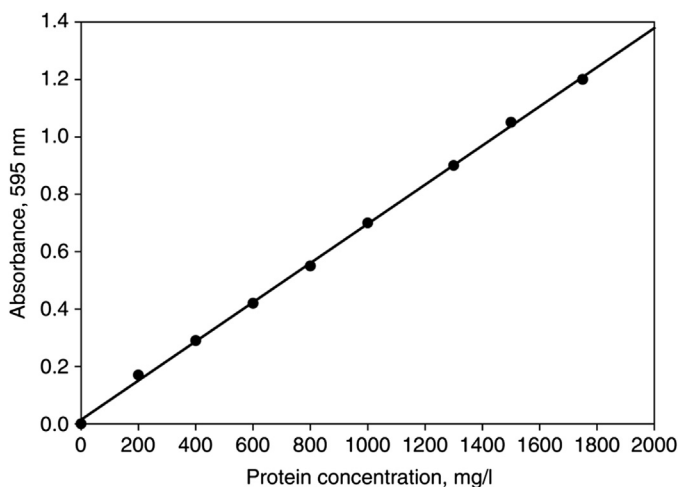
14.9.3 Mixing of the Coomassie Plus Protein Assay Reagent

Allow the Coomassie Plus reagent to come to room temperature. Mix the Coomassie Plus reagent solution just before use by gently inverting the bottle several times. Do not shake.

TABLE 14.3 Preparation of BSA concentration for standard calibration curve

Volume of BSA to add	Volume of diluents (buffer) to add	Final BSA concentration
300 μl of stock	0 μl	Stock – $2000 \mu\text{g ml}^{-1}$
375 μl of stock	125 μl	A – $1500 \mu\text{g ml}^{-1}$
325 μl of stock	325 μl	B – $1000 \mu\text{g ml}^{-1}$
175 μl of A	175 μl	C – $750 \mu\text{g ml}^{-1}$
325 μl of B	325 μl	D – $500 \mu\text{g ml}^{-1}$
325 μl of D	325 μl	E – $250 \mu\text{g ml}^{-1}$
325 μl of E	325 μl	F – $125 \mu\text{g ml}^{-1}$
100 μl of F	400 μl	G – $25 \mu\text{g ml}^{-1}$

FIGURE 14.2 Calibration curve for BSA standard solution.



14.9.4 Standard Calibration Curve

Prepare a standard curve by plotting the average blank corrected 595-nm reading for each BSA standard versus its concentration in mg l^{-1} , using the standard curve; determine the protein concentration for each unknown sample. The calibration curve for the BSA standard is prepared using standard albumin, 50 ml Pierce 23,210 with a concentration of 2 g l^{-1} , diluted with 1 M NaOH solution. Add 1 ml of 1 M NaOH with 0.1 ml of diluted sample plus 5 ml of reagent, protein assay 23,200 Pierce, stirred with a vortex mixer. Read the absorbance with a spectrophotometer at 595 nm. The resulting data for the calibration curve are shown in Figure 14.2.

14.9.5 Standard Calibration Curve for Starch

A standard solution of soluble starch, 2 g l^{-1} well dissolved in an alkali solution, was prepared. With heating, the powder becomes a clear solution. A diluted solution from 200 to 2000 mg l^{-1} was prepared. Dissolved 0.4 g of orcinol (3, five dihydroxy toluene) in 99.6 g of H_2SO_4 (66% acid). Prepare 500 ml orcinol reagent, 170 ml water with 330 ml acid. Add acid to distilled water and gradually dissolve 3.115 g orcinol in the diluted acid solution. Take 0.1 ml of the diluted starch sample with 0.9 ml of distilled water, and then add 2 ml of the prepared orcinol reagent, heated in a boiling water bath for 15 min, stop the reaction by cooling it in an ice water bath. Add 7 ml of distilled water; read the absorbance at 420 nm. Plotting the data can find the given results as projected in Figure 14.3.

14.10 SINGLE-CELL PROTEIN PROCESSES

Using brewer's yeast, *Saccharomyces cerevisiae*, the process was developed for the large-scale production of food. During World War I, a large-scale process for production of SCP

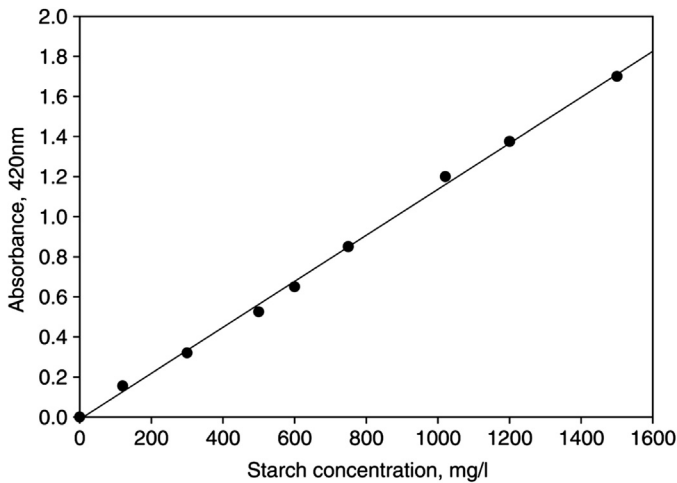


FIGURE 14.3 Standard calibration curve for starch solution.

was developed in Germany. About 60% of food was replaced by massive brewing of yeast, *S. cerevisiae*. In World War II, the yeast-based food made an important contribution in the German diet. The yeast was incorporated mainly into soup and sausages. Special strains of yeast, *Candida arborea* and *Candida utilis*, were predominantly used. In the 1960s, several large-scale plants for the production of SCP were developed by British Petroleum (BP), as the organisms were able to use the aliphatic compounds of petroleum. *Candida lipolytica* was able to convert carbon sources originating from petroleum to protein. *C. lipolytica* was grown on alkanes, a yeast-based food. Other strains and *Candia* also are used for SCP production. For the SCP produced by BP from distilled *n*-alkanes, the cells were separated, salted, dried, and used as animal feed.¹

In the process developed by BP, the protein was named "Toprina." BP planned to go for large-scale production, and the protein was proved toxicologically safe. The rising price of petroleum initiated the plan, but it was unable to contribute to reducing shortages of food and feed sources for humans and animals.^{1,5} Production of an SCP named "Pruteen" from methanol by biooxidation of methane was another a successful case in SCP-process development using *Methylophilus methylotrophus*. However, the whole project of SCP has been a victim of political or economic issues in Europe and Japan. Methane is an abundant and cheap carbon source without any toxicity; it is the main constituent of natural gas and is also produced from anaerobic digestion tanks. There are many biocatalysts involved in methane biooxidation using stable mixed cultures. This mixed culture is one of the best examples of symbiosis. At first, methane in the gas phase is bubbled into the media, then it is biologically oxidized to methanol. Gram-negative bacilli (rod shapes) are used, while methanol is produced in the presence of biocatalysts. Methane is a pure carbon source; it is easily used by several microorganisms such as *Methylomona* and *Methylococcus*. Another species that has been extensively studied is *Methylomonas methanica*. Supplements of nitrogen, trace metals, and minerals are required for optimal growth. Mixed cultures of gram-negative rod-shaped bacilli have the potential to oxidize methane and produce methanol, whereas

other organisms present used methanol as a carbon source to produce SCP. This is an example of symbiosis in mixed culture, by which an intermediate product is formed that is then used by the second organism. *Acinetobacter* and *Flavobacterium* are often used in mixed culture for producing SCP from methane. The fermentation of methanol to SCP was done in an airlift fermenter with sufficient aeration and without any mechanical agitation, using *Methylophilus methylotrophus*. The SCP known as "Pruteen" contained 72% crude protein.¹ The product was marketed for feed as a source of energy, vitamins, and minerals with sufficient protein content. The amino acid analysis was satisfactory, as the methionine and lysine contents of Pruteen were compared to the protein content of white fish meal.

14.11 NUTRITIONAL VALUE OF SINGLE-CELL PROTEIN

The nutritional value of SCP depends on the composition of its amino acids, vitamins, and nucleic acids. The nutrient value of SCP may have a positive and negative impact. The rigid cell wall, the high content of nucleic acids, allergies, and the gastrointestinal effect should be considered as negative impacts. However, with special treatment, it is possible to eliminate these from the product. A long-term use of SCP is required to consider and remove any toxicological effects and carcinogenesis. The positive point for SCP is the high content of protein with sufficient enzymes, minerals, and vitamins.¹²

The protein content of SCP is very high. Dried cells of *Pseudomonas* sp. grown on normal petroleum-based liquid paraffin contain 69% protein. Algae normally possess about 40% protein.^{1,5} The protein content of SCP is absolutely dependent on the raw material used as a carbon source and the microorganisms grown on the media. The proteins of the microorganisms contain all the essential amino acids. Table 14.4 presents the average protein contents of bacteria, yeast, fungi, and algae.

Microorganisms such as yeast and bacteria have a short doubling time, normally in the range of 5–15 min; mold and algae are two to four h. The fast brewing of microorganisms compared with plant cells is a promising point for food replacement and shortage in the new millennium. In terms of amino acids, bacterial protein is similar to fish protein. The yeast's protein is almost identical to soy protein; fungal protein is lower than yeast protein. In addition, SCP is deficient in amino acids with a sulfur bridge, such as cystine, cysteine, and methionine. SCP as a food may require supplements of cysteine and methionine, whereas they have high levels of lysine vitamins and other amino acids. The vitamins of

TABLE 14.4 Cellular composition of SCP from various microorganisms (dry weight per cent)¹³

	Yeast	Bacteria	Fungi	Algae
Protein	45–55	50–65	30–45	40–60
Nucleic acid	6–12	8–12	7–10	3–8
Fat	2–6	1.5–3	2–8	7–20
Ash	5–9.5	3–7	9–14	8–10

TABLE 14.5 Essential amino acid content of the cell protein in comparison with other reference Proteins (weight%)¹⁴

Amino acid	<i>Cellulomonas</i>	<i>Saccharomyces cerevisiae</i>	<i>Penicillium notatum</i>	SCP (BP)	Egg	Cow milk
Lysine	7.6	7.7	3.9	7.0	6.3	7.8
Threonine	5.4	4.8	—	4.9	5.0	4.6
Methionine	2.0	1.7	1.0	1.8	3.2	2.4
Cysteine	—	—	—	—	2.4	—
Tryptophane	—	1.0	1.25	—	1.6	—
Isoleucine	5.3	4.6	3.2	4.5	6.8	6.4
Leucine	7.3	7.0	5.5	7.0	9.0	9.9
Valine	7.1	5.3	3.9	5.4	7.4	6.9
Phenylalanine	4.6	4.1	2.8	4.4	6.3	4.9
Histidine	7.8	2.7	—	2.0	—	—
Arginine	6.4	2.4	—	4.8	—	—

microorganisms are primarily of the B type. Vitamin B₁₂ occurs mostly in bacteria, whereas algae are usually rich in vitamin A. The most common vitamins in SCP are thiamine, riboflavin, niacin, pyridoxine, pantothenic acid, choline, folic acid, inositol, biotin, B₁₂, and P-aminobenzoic acid. Table 14.5 shows the essential amino acid analysis of SCP compared with several sources of protein.

14.12 ORGANISMS AND SUBSTRATES FOR SINGLE-CELL PROTEIN PRODUCTION

SCPs are used as a protein supplement in human diets or animal feeds. Microorganisms such as bacteria, fungi, yeast, and algae are able to use inexpensive raw material as a carbon source like starch, lignocelluloses and organic wastes as energy sources for the cell growth, and proteins along with amino acids, lipids, and vitamins. In fact, SCP has high nutritional value; however, there is a risk of allergic reaction due to the presence of massive cells resulting from the high content of nucleic acids. Production of SCP by any organism that can synthesize similar amino acids profiles like plant or animal proteins, such as algae, is highly recommended.

Inactive dried baker's yeast is used as dietary source of vitamins and trace minerals and is added for supplementary nutrients to enhance microbial cell growth. The dried powder is used for humans as a source of flavor and vitamins. The use of SCP for human food additives is under question because of the high concentration of nucleic acids known as purine and pyrimidine. Generally, in an animal's digestive system, the pathway of nucleic acids catabolism results in uric acid, while in human digestion it may face difficulties.

As algae containing chlorophylls can assimilate carbon dioxide from air using the free energy from the sun, while bacteria have no chloroplast to act as photoautotroph; therefore, they require an organic carbon as a reliable source of energy. *Chlorella sorokiana* and *Chondrus crispus* are capable of assimilating CO₂ in the presence of chloroplast via photosynthesis. *Sce-nedesmus* sp. and *Chlorella pyrenoidosa* are green algae that can use sugarcane and lactose from whey for protein purposes.

Table 14.6 summarizes several organisms and suitable substrate selections for SCP production. For the purpose of selection, identification, and definition of desired substrate for suitable organism, several important substrates are discussed.

14.12.1 Cellulose

Cellulose is an attractive raw material for SCP production because of its abundance. The association of cellulose with lignin in wood makes it difficult to hydrolyze and extract monomeric sugar for SCP production. It should be noted that the use of mixed culture of cellulolytic (*Cellulomonas* sp.) and amylolytic organisms (*Bacillus subtilis*) in aerobic condition for breakdown of cellulose and saccharification of starch is very helpful to supply more carbohydrate to organism for SCP production, especially in the case of potato waste.

TABLE 14.6 Substrate selections for SCP production

Microorganism	Substrate	Remarks
<i>Methylophilus methylotrophus</i>	Methanol	Methane is converted to methanol
<i>Candida</i> sp.	n-Paraffin	Paraffinic compound is used as a carbon source, while gaseous ammonia and other nutrients such as trace metals are added
<i>Kluyveromyces marxianus</i>	Lactose, whey	Whey is deproteinized and used as a suitable substrate; whey contains about 5% lactose, 0.8% protein and 0.2–0.6% lactic acid
<i>Fusarium graminearum</i>	Glucose and molasses	Food-grade glucose was the substrate for production of fungal SCP; medium components include glucose syrup, gaseous ammonia, salts, and biotin
<i>Candida utilis</i>	Sulphite waste liquor	Protein supplement by fermentation of sulphite waste liquor
<i>Paecilomyces varioti</i>	Sulphite waste liquor	Organism grown on sulphite waste liquor
<i>Saccharomyces fibuligera</i> and <i>Candida utilis</i> mixed culture	Starch	<i>S. fibuligera</i> produces the enzyme necessary for starch degradation, enabling co-growth of <i>C. utilis</i> This process is known as simultaneous saccharification and fermentation
<i>Chaetornium cellulolyticum</i>	Cellulose from natural sources and waste wood	Thermal or chemical pretreatment, used in combination with enzymatic hydrolysis, is usually required
<i>Cellulomonas</i> sp. <i>Thermoactinomyces</i>	Bagasse Animal waste	The cultures can be sued in Solid State Fermentation (SSF) and submerged culture for biomass production from lignocellulosic wastes

14.12.2 Starch

SCP from corn and potato starch uses two yeast strains. *Saccharomyces fibuligera* produces the enzyme necessary for starch degradation, followed by the growth of *C. utilis* on hydrolyzed sugar to SCP.

14.12.3 Whey (Lactose)

Whole milk whey or deproteinized whey is a carbohydrate source that creates disposal problems. (High Biological Oxygen Demand (BOD)) Problems associated with whey for SCP production are usually insufficient substrate, seasonal supply variations, and its high water content (>90%), which makes transport prohibitively expensive. While most organisms do not grow on lactose as a carbon source, strains of the yeast *Kluyveromyces marxianus* readily grow on lactose.

14.12.4 Glucose

Food-grade glucose was the substrate for the production of fungal SCP using *Fusarium graminearum*. The strategy adopted was to take advantage of the mycelial fiber content to produce a range of high added-value products, including meat analogues for human consumption.

14.12.5 Alkanes

SCP fermentation process using high alkanes with 10–20% wax from gas oil is considered an economical process. However, the price of crude is rising, and the processes required for the recovery of proteins are exhaustive. Other alkane-based SCP processes were developed, but the only problem related to the presence of the potential carcinogenic residues caused most of the plants never to reach start up for operation.

14.12.6 Methane/Methanol

Methane was initially considered as an SCP raw material, but the gaseous substrates may have purification problems due to limited mass transfer. However, methane is easily converted to methanol through the oxidation process; the solution is cooled for fermentation. Methanol is oxidized via dehydrogenation to formaldehyde, which can either be assimilated for conversion to cell mass or further oxidized to CO₂. The specific growth rate of *Methylophilus methylotrophus* using methanol as a substrate is approximated to be 0.5 h⁻¹, and the cell yield is 0.5 g/g. Cells are recovered by agglomeration followed by centrifugation, flash drying, and grinding. The bacterial SCP product for animal feed with 80% protein is named Pruteen.

The key criteria for SCP production are the selection of suitable strains. The desired and selected organism required suitable carbon and nitrogen sources, with additional supplementary nutrients. In general, fungi have the capacity to degrade a wider range of complex plant materials, particularly plant polysaccharides. They can tolerate a low pH level, which contributes to reduced infections in the fermenter. Bacteria, in general, produces a more favorable protein composition than yeast or fungi. The protein content in bacteria can range from 60 to 80%,

TABLE 14.7 Protein productivities for selected microorganisms

Microorganism	Substrate	Protein productivity
<i>Chaetornium cellulolyticum</i>	1% wheat straw pretreated with caustic soda	0.074 g (l h) ⁻¹
<i>Chaetornium cellulolyticum</i>	4% newspaper pretreated with ball milling	0.023 g (l h) ⁻¹
<i>Myrothecium verrucaria</i>	1% barley straw pretreated with caustic soda	0.038 g (l h) ⁻¹
<i>Trichoderma reesei</i>	5% rice straw pretreated with caustic soda	0.014 g (l h) ⁻¹
<i>Cellulomonas</i> sp.	1% corn stover pretreated with caustic soda	0.089 g (l h) ⁻¹
<i>Alcaligenes faecalis</i>	1% corn stover pretreated with caustic soda	0.088 g (l h) ⁻¹

whereas fungi selected for biomass production and yeast have protein contents in the range of 40–45%. However, the problem associated with high bacterial protein levels is an undesired nucleic acid content. Microorganisms involved in SCP production must be safe and acceptable for food purposes. Some bacterial proteins have amino acid profiles similar to plant/animal protein. *Agaricus bisporus* is able to produce an enzyme for the hydrolysis of lignocellulosic wastes. In addition, *Candida tropicalis* and *C. utilis* are able to assimilate cellulose to liberate monosaccharide and then proteins. *Endomycopsis fibuligira* is one of the amylase producers using amylolytic fungus along with organism such as *C. utilis* to synthesize protein that may enhance SCP production. From the fungus group with amylolytic and cellulolytic enzyme, *Trichoderma viride* can produce extracellular cellulase; while *Paecilomyces variotti* and *Chaetornium cellulolyticum* are in cellulolytic group and can synthesize protein concentrations of 55% and 80%, respectively. The protein productivities of several selected microorganisms are stated in Table 14.7.

14.13 ADVANTAGES AND DISADVANTAGES OF SINGLE-CELL PROTEIN

The addition of SCP to the diet of a milking cow increases milk production and production efficiency by 15%.^{12–17} Microorganisms such as bacteria and yeasts grow rapidly and contain more uric acid than slower-growing plants and animals. Although the uric acid limits the daily intake of SCP for humans and monogastric animals such as pigs and chickens, ruminants such as cattle, sheep, and goats can tolerate higher levels of uric acid or break down urea and excrete it as ammonia.

About 80% of the total cell nitrogen is amino acids, whereas the remaining 20% is possibly fat, ash, and nucleic acids. The concentration of nucleic acids in SCP is higher than in conventional proteins. That is the characteristic of all fast-growing organisms. The problem occurs with the consumption of proteins, roughly 10% of nucleic acids. The high nucleic acid content of SCP results in an increase in uric acid in serum and urine.¹⁸ Uric acid is the final product of purine degradation in humans. Most mammals, reptiles, and mollusks possess the enzyme uricase, and they are able to oxidize uric acid to allantoin.

acid. High uric acid levels in humans causes gout. That disease results from the elevation of uric acid in body fluid. Its manifestation is painful inflammation of arthritic joints. In animals with urease and allantoinase, the biodegradation of uric acid is accelerated, and the end product is ammonia. In the human body, the lack of such enzymes causes the catabolism of uric acid to be terminated, and uric acid has to be excreted in urine through the kidneys.^{19,20}

The removal and reduction of the nucleic acid content of various SCPs is achieved by chemical treatment with sodium hydroxide solution or high salt solution (10%). As a result, crystals of sodium urate form and are removed from the SCP solution.^{21,22} The quality of SCP can be upgraded by the destruction of cell walls. That may enhance the digestibility of SCP. With chemical treatment, the nucleic acid content of SCP is reduced.

The presence of uricase assists the uric acid to be hydrolyzed, and the end product of purine degradation is completed with the addition of uricase.

14.14 PREPARATION FOR EXPERIMENTAL RUN

1. Prepare seed culture and use it for inoculation of 2 l airlift and 2 l B Braun biostat B using soluble starch or glucose.
2. Perform fermentation for 24 h in a batch system.
3. Monitor DO level and control pH at 6.7–7 by using 0.2 M phosphate buffer solution.
4. Measure SCP based on standard methods and analysis explained above.
5. Determine yield of SCP-based carbon sources.
6. Take usual samples at intervals of 4–6 h.
7. Measure carbon sources remaining.

References

1. Rose AH. *Sci Am* 1981;**245**:127.
2. Tamime AY, Deeth HC. *J Food Prot* 1980;**43**:939.
3. Driessen FM, Ubbels J, Stadhouders J. *Biotechnol Bioengng* 1977;**19**:821.
4. Najafpour GD, Klasson KT, Ackerson MD, Clausen EC, Gaddy JL. *Biores Technol* 1994;**48**:65.
5. Pelczar Jr MJ, Chan ECS, Krieg NR. *Microbiology*. 6th ed. New York: McGraw-Hill; 1993.
6. Stanbury PF, Whitaker A. *Principles of fermentation technology*. Oxford: Pergamon Press; 1984.
7. Wang DIC, Cooney CL, Deman AL, Dunnill P, Humphrey AE, Lilly MD. *Fermentation and enzyme technology*. New York: John Wiley & Sons; 1979.
8. Thomas LC, Chamberlin GL. *Colorimetric chemical analytical methods*. Salisbury, UK: Tintometer Ltd; 1980. p. 31.
9. Bradford MM. *Anal Biochem* 1976;**72**:248.
10. Burrel RG, Clayton CW, Gallegly ME, Lilly VG. *Phytopathol* 1966;**6**:422.
11. Miller GL. *Anal Chem* 1959;**31**:426.
12. Lichtfield JH. In: Mateles, Tannenbaum, editors. *The production of fungi. Single-cell protein I*. Cambridge (MA): M.I.T., Press; 1968.
13. Miller MB, Litsky W. *Single cell protein in industrial microbiology*. New York: McGraw-Hill; 1976.
14. Han YW, Duhlap CE, Callihan CD. *Food Technol* 1971;**25**:130.
15. White PS, Handler, Smith EL. *Principles of Biochemistry*. 4th ed. New York: McGraw-Hill; 1968.
16. Voet D, Voet JG. *Biochemistry*. 3rd ed. New York: John Wiley; 2004.
17. Zee JA, Simard RE. *Appl Microbiol* 1974;**29**:59.

18. Yakoub Khan M, Umar Dahot M, Yousuf Khan M. *J Islam Acad Sci* 1992;5:39.
19. Scragg AH. *Bioreactors in biotechnology, a practical approach*. New York: Ellis Horwood Series in Biochemistry and Biotechnology; 1991.
20. Ghose TK. *Bioprocess computation in biotechnology*, vol. 1. New York: Ellis Horwood Series in Biochemistry and Biotechnology; 1990.
21. Doran PM. *Bioprocess engineering principles*. New York: Academic Press; 1995.
22. Shuler ML, Kargi F. *Bioprocess engineering, basic concepts*. New Jersey: Prentice Hall; 1992.

Sterilization

OUTLINE

15.1 Introduction	435	15.8.4 Sterilization Steps in a Programmed Autoclave	448
15.2 Control of Microbial Population by Physical Agents	436	15.8.5 Safety Recommendation in Autoclave Operation	449
15.3 Death Rate of Living Organisms	437	15.9 Dry Heat Sterilization	450
15.4 Batch Sterilization	437	15.10 Sterilization with Filtration	450
15.5 Continuous Sterilization	439	15.11 Microwave Sterilization	450
15.6 Hot Plates	441	15.12 Electron Beam Sterilization	451
15.7 High-Temperature Sterilization	442	15.13 Chemical Sterilization	451
15.8 Sterilized Media for Microbiology	442	15.14 Low-Temperature Sterilization	452
15.8.1 Sterilization of Media for Stock Cultures	447	Nomenclature	452
15.8.2 Sterilization of Bacterial Media	447	References	452
15.8.3 Sterilize Petri Dishes	448		

15.1 INTRODUCTION

The control or elimination of living organisms is performed by either physical and/or chemical agents. Since most of the targeted biological products are conducted in pure culture, sterilization should be done prior to any operation. In fact, sterilization is the action of

eliminating microorganisms from a medium. Sterility is the absence of any detectable and viable microbes in a culture medium or in the gas phase. Sterilization is a process that destroys all living organisms, spores, and viruses in a pressurized vessel at high temperatures.^{1–3} This means that heat as a physical agent is used to denature the protein content of the cell. In the food and dairy industries, sterilization is commonly used to preserve food products. At the laboratory scale, huge steel vessels with live streams at 105 kPa (15 psig) are commonly used for 20–30 min. This is a closed system known as an autoclave; therefore, it is batch sterilization. The temperature is raised to 121 °C when air is initially flushed out and all live streams are replaced. Wet steam is usually used for effective autoclaving. The high temperature and long duration may kill all living microorganisms, spores, and viruses. When medium is prepared, to eliminate bacterial and fungal contaminants it must be heat treated at high pressure. Even at high temperatures the fungal spores may survive if only heat is used. Therefore, media are autoclaved at 121 °C and 105 kPa (15 psig). In fact, an autoclave is used like a pressure cooker, which is a convenient and economical autoclaving equipment.

Overheating the prepared media may have a negative impact, causing the media pH to be unstable. Acid pH is very sensitive to overheating. Overheating in media containing sugars causes the carbohydrate to be caramelized. These media may have a reverse impact, reducing bacteriological performance. Gelatinous media or any nutrient agar at acidic pH is hydrolyzed. This is due to the acidic conditions of catalytic activities or excess amounts of protons breaking down the solid media and extra sugars forming. This may cause substrate inhibition on the growth of organisms on solid slant media.

15.2 CONTROL OF MICROBIAL POPULATION BY PHYSICAL AGENTS

Physical agents such as high temperature or heating may cause reduction of the microbial population. Other physical agents such as osmotic pressure, radiation, and surface tension may also cause the reduction of a microbial population. Filtration is one of the physical agents that can be effectively used in bioprocesses, especially in downstream processing for recovery of biological products and reduction of microbial cells. The term control of a microbial population is strictly used for reduction of the number of living organisms in cultured media. Let us have an incineration unit working at high temperature in a defined volume of microbial culture with a billion of cells per unit volume of culture suddenly exposed and dumped into an incinerator. Phase transition occurs in a short while. All masses of organisms and germs are transferred to vapor and ash. Deformation of cells instantaneously occurs. In such a case, the rate of control of microbial cells has no meaning because at very high temperatures we are unable to detect reduction and destruction of cells with respect to time. Vice versa, let us synthesize a unique organic compound similar to an amino acid. The organic compound is introduced into a medium with growing culture as cells and proteins are formed. Based on similarities existing between the chemical agent and the amino acid, all are involved in the synthesis of a new biomolecule. In this process, the chemical agents are used in the biosynthesis. Once the new molecule is built, it is expected to function in the cell; at this stage the biomolecule is deprotected. It can act as a bactericide. Therefore, the synthesized molecule causes the deactivation of the newborn cell. These mechanisms

are used in medicine for control of a cell population. The synthesized molecules are purposely used. The response for cell growth control may take some time but it works effectively. In this case, the rate of control of an organism has great value in reducing the microbial population. Also, the death rate can be calculated by measurements of cell populations with respect to time. It is well understood that microorganisms are removed, killed, or inhibited by means of physical and chemical agents. Application of these agents for various processes may require specific techniques. It is also necessary to focus exactly on the type of process to find out how to control microorganisms in an effective and efficient manner.

15.3 DEATH RATE OF LIVING ORGANISMS

If a chemical agent is also added to a culture with a high population of living cells for sterilization, the concentration of the chemical is directly related to the time required for the removal of living cells. The action of disinfection for the required time is defined as the death rate. The rate of death is defined as how fast the organisms are destroyed. The number of cells removed with respect to time is also known as the death rate. Let us assume we have shotgun targeting of cell bodies in densely populated living organisms. The question is how fast can we destroy the cells or prevent propagation of living organisms.

The physical agents, for instance, can be filtration or even heating. Any physical process which can eliminate organisms without a chemical reaction is called physical sterilization. Heating is one of the methods of action at high temperatures. Protein materials are denatured at high temperatures; even a fast death rate is achieved. Let us focus on pasteurization of milk. The operation of controlling the population of organisms in an enriched media of nutrients known as milk is carried out at 65–67 °C for a duration of 20–30 min. The slow heating is required to preserve all precious nutrients present in the milk. As the temperature increases, the duration of milk's exposure to heating at 95 °C must be shortened to a few minutes. For high temperatures of around 130–137 °C, the contact time of hot-plate sterilization must be even less than 30 s.

If organisms are suddenly exposed to high temperatures, let us say in incineration, the destruction of cells is instantaneous; therefore, it is not possible to determine the death rate. Another example is a droplet of populated culture introduced into an acidic solution. In such cases determination of death rate is not possible. [Figure 15.1](#) illustrates the surviving organisms with respect to temperature and exposure time. In fact, it was found that the heat effectiveness was much greater than chemical agents for reduction of the cell population.

15.4 BATCH STERILIZATION

Batch sterilization uses steam to eliminate living organisms. Heat losses, heating, and cooling are major steps, and it is a time-consuming process. It requires air to be evacuated and replaced with steam. First the chamber is flashed with pressurized steam. With this technique we can get rid of the existing air. Steam sterilization is performed in a jacketed vessel by supplying steam and maintaining the set pressure and temperature at a constant level for a fixed duration. Batch sterilization wastes energy and overcooks the medium. There is no conservation of energy; therefore, the process may not be economical for implementation on a large-scale. Batch sterilization is commonly used at bench and laboratory scales as the diagram shows in [Figure 15.2](#).

FIGURE 15.1 Survival of organism with increasing temperature, decreasing cell population.

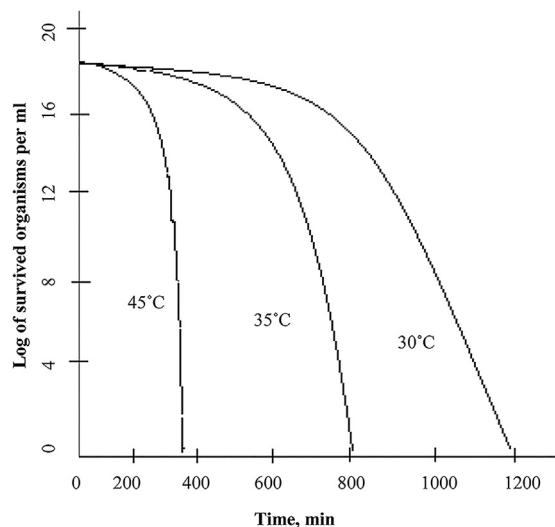
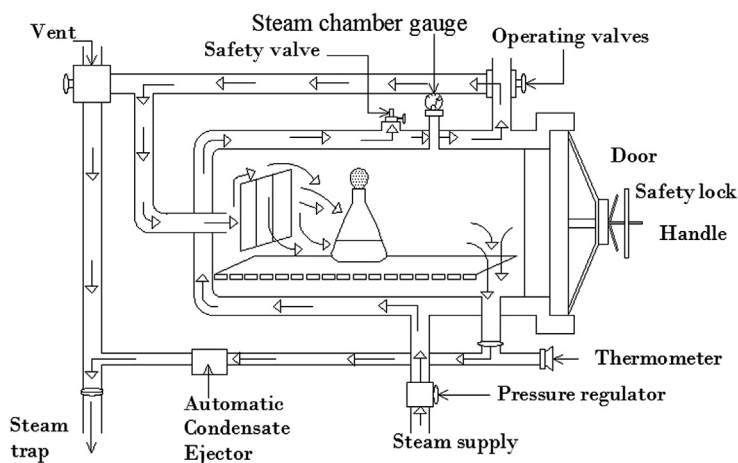


FIGURE 15.2 Pressurized steam sterilizer (autoclave).



Batch media sterilization is performed in an autoclave. Basically, it is a huge steam cooker. Steam enters the jacket of the surrounding chamber. When the pressure from the steam has been built up in the jacket, a venting valve for the outlet of chamber air is closed and the inlet valve allows the steam to enter the chamber. The pressure of the chamber is increased to 105 kPa (15 psig). At this point the sterilization time begins to count down. Usually 15–30 min is used, depending on the type and volume of media. For instance, sterilization of 1 l of media at 121 °C requires 20 min. Larger volumes may require longer retention times for sterilization. There are recommended holding times of 20, 10, and 3 min for 121, 126, and 134 °C, respectively. As the temperature increase, the holding time is sharply reduced. Even at temperatures above 143 °C, it may take a few

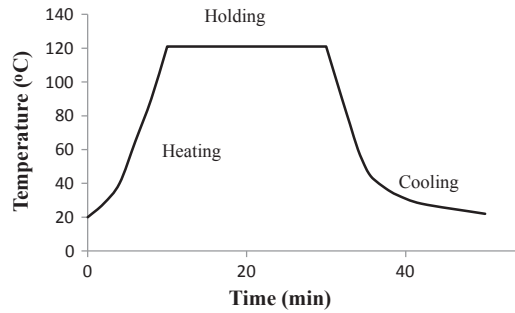


FIGURE 15.3 Batch sterilization temperature–time profiles.

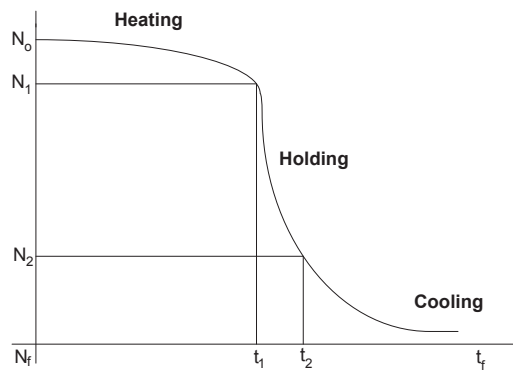


FIGURE 15.4 Reduction of cell population in batch sterilization.

seconds for sterilization. The high pressure in a closed container allows the temperature to exceed 121 °C.

In batch sterilization, a typical temperature distribution with respect to time is shown in Figure 15.3. Temperature variations in heating, holding, and cooling time periods are illustrated in this figure. The rate of cell population reduction for batch sterilization with respect to time is shown in Figure 15.4. In Figure 15.4, N_0 is initial cell population. The time for holding starts from t_1 with a cell population of N_1 and ends at t_2 with a population of N_2 ; the death rate is gradually continued while the system is cooling.

15.5 CONTINUOUS STERILIZATION

One method for continuous sterilization of medium for fermentation is the direct use of live steam by injection of steam into the medium. The heat exchanger is eliminated. The medium stays in a loop for a predetermined holding time until the entire medium is sterile. The problem with directly injecting steam is dilution of medium as it is initially cold. However, it has better heat economy, because it comes from substituting heat exchangers for direct

steam injection. To utilize all the supplied heat, preheaters or heat economizers are used. Instead of having a cold water stream to cool the sterile media, the lower temperature, unsterile media stream takes the primary heat from the warm stream, cooling the sterile media. Continuous sterilization has a holding coil for detention long enough to kill all the microorganisms. The medium from a make-up vessel flowing through the exchanger is held in the coil, and then goes through the heat exchanger, heating more unsterile medium while becoming cool itself, as it is collected in a sterile fermenter. Figure 15.5 presents the sequence of piping that media go through, along with steam. Finally, the media are collected in a vacuum flash drum. In addition, in Figures 15.6 and 15.7 are seen schematic diagrams for continuous sterilization using direct injection of steam and indirect application of steam

FIGURE 15.5 Continuous sterilization.

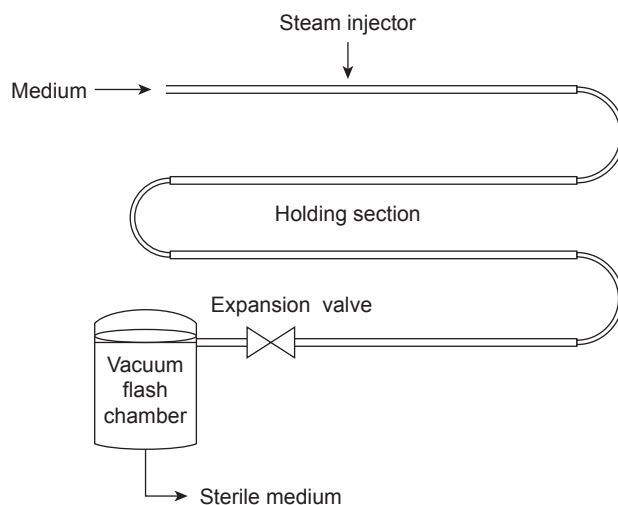
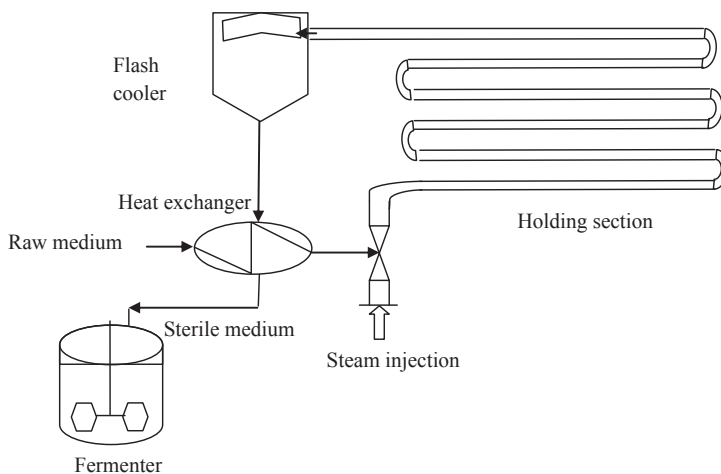


FIGURE 15.6 Continuous sterilization with direct steam injection and flash cooler.



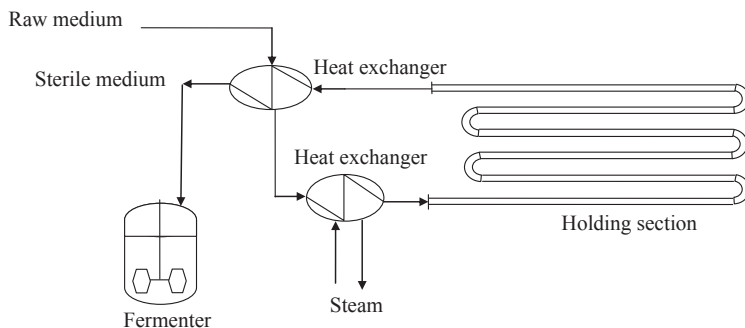


FIGURE 15.7 Continuous sterilization using steam heat exchanger.

through heat exchangers and economizers to supply fresh and sterilized media for fermentation.

Heat economizers are important for a large-scale plant unit in continuous sterilization. For a small-scale bioreactor use of direct steam injection is much simpler to operate. A heat exchanger is then needed with cooling water to bring the medium back to ambient temperature. Therefore, jacketed vessels are commonly used with cooling water. There are advantages and disadvantages to batch and continuous sterilization. The energy savings are related to the use of an economizer and direct stream or indirect sterilization. In a large-scale system, economy and role decide which one is the most suitable process to be implemented. For each case the specific design must be evaluated in terms of the thermal efficiency and fixed costs involved.

15.6 HOT PLATES

In directing steam heating, continuous sterilization is preferable. The medium passed through preheaters may reach about 90°C , and then very quickly sterilization may take place at 140°C . Figure 15.8 shows a countercurrent hot-plate heat exchanger that is normally used

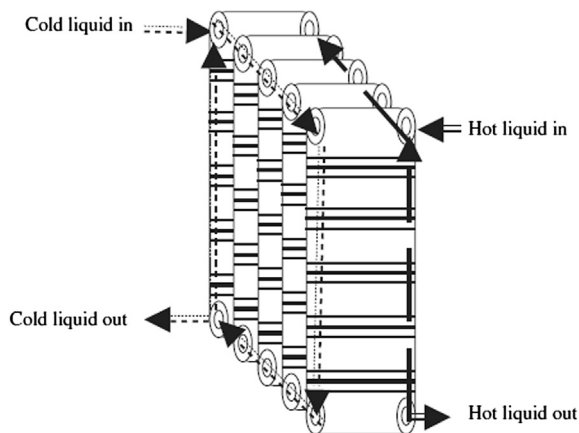


FIGURE 15.8 Countercurrent hot-plate heat exchanger.

for continuous sterilization. Hot-plate heat exchangers are extremely efficient and easily maintained if any fouling or scale deposition takes place. Normally fouling is a serious problem, occurring by deposition of proteins on the hot surface of the exchanger, which causes reduction in the overall heat transfer coefficient. Plate exchangers are easily separated and cleaned. Special care must be taken when the media contain any agglomerated particles. Correlation is required to calculate the suitable residence time for sterilization. The choice of a suitable sterilization process is based on economics and cost of the heat exchangers to reduce energy consumption. In a suitable exchanger, the larger the heat transfer coefficient, the greater the energy recovery.

15.7 HIGH-TEMPERATURE STERILIZATION

Fast sterilization is performed at high temperatures. High-temperature sterilization requires short holding times. This technique is used in the fast preparation of nutrient media for industrial bioprocesses and in pasteurizing milk. A short retention time may favor media with heat-sensitive proteins and cause less damage to the biochemical composition of the media than more prolonged times at lower temperatures. The ability of high temperatures to perform rapid sterilization is related to activation energies. That is affected by how fast bacteria are killed in an elevated temperature. On the other hand, long sterilization at high temperatures may destroy the protein and biochemical composition of the media. Short duration sterilization at high temperatures are more lethal to organisms and less chemically damaging than longer sterilization processes at lower temperatures. Sterilization at high temperature is recommended for 3 min at 134 °C. It is preferable to sterilize for more than 20 min at 115 °C in a conventional operation.

15.8 STERILIZED MEDIA FOR MICROBIOLOGY

Sterile media are used for pure culture. The media used to culture microorganisms depend on the living conditions of the microorganisms. Media compositions must be identified based on the needs of the organisms for carbon, nitrogen, and phosphorus. Nutrients such as protein and sugars are added at wide ranges of pH. The acidic, neutral, and alkaline conditions are defined based on differentiation of microbes in their biochemical reactions. Color indicators are used to observe any transition of pH. Buffer is used in the media to maintain constant pH. Growth factors and growth stimulants are also used to accelerate microbial growth and to maintain exponential growth. The most common medium in the liquid phase is nutrient broth; in the solid phase, nutrient agar is used to propagate microorganisms.

When microbiological media are prepared, it must be sterilized before any inoculation of organisms. Sterilization is used to eliminate any microbial contamination that may originate from air, glassware, or hands. Microbes propagate quite quickly: within a few hours there will be thousands of organisms reproduced in the media. To control the growth of unwanted organisms, the media must be sterilized quickly before any microbes start to utilize the nutrients. The sterilization process makes the medium absolutely free of contaminants and guarantees that the medium will stay sterile, so that it is used only for the desired organisms.

The kinetics of culture media sterilization describes the rate of destruction of microorganisms by steam using a first-order chemical reaction rate model. As the population of microorganisms (N) decreases with time, the rate is defined by the equation

$$-\frac{dN}{dt} = k_d N \quad (15.8.1)$$

where N is the number of viable organisms present in the culture media, t is the retention time or sterilization time, and k_d is the reaction rate constant as it is known for a specific death rate. Using separation of variables and integrating with initial conditions ($N = N_0$ at $t = 0$), the following useful expression is obtained

$$N(t) = N_0 e^{-k_d t} \quad (15.8.2)$$

where N_0 is the number of viable organisms present in the media at the starting point before sterilization. Now take the natural log of (Eqn 15.8.2); it is reduced to a linear model:

$$\ln \frac{N(t)}{N_0} = -k_d t \quad (15.8.3)$$

The graphical presentation of the equation shows a straight line with a negative slope for k_d . As the death rate constant follows Arrhenius' law,¹ the death rate constant is temperature dependent. The value of k_d is about 0.02 min^{-1} at 100°C ; the death rate constant increases by 10-fold at 110°C and 100-fold at 120°C .^{3–6}

$$k_d = k_0 e^{-E/RT} \quad (15.8.4)$$

$$\ln \frac{k_d}{k_0} = -\frac{E}{RT} \quad (15.8.5)$$

where k_0 is the death rate constant at a reference temperature also known as Arrhenius' constant, R is the gas constant, T is the absolute temperature, E is the activation energy, which is 60–70 kcal per mole for microorganisms, 100–150 kcal per mole for spores, and 30–40 kcal per mole for media with vitamins and protein solution.² Figure 15.9 shows the linear model

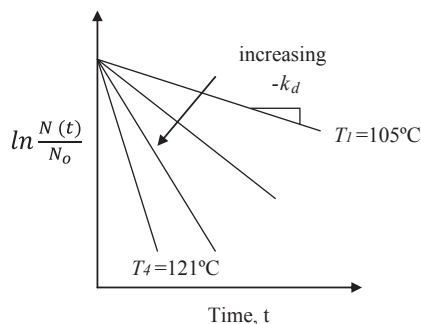


FIGURE 15.9 The loss of cell viability at various temperatures.

for (Eqn 15.8.3), the loss of cell viability at various temperatures. The actual data can be plotted; the slope of the line shall define the value for specific death rate, k_d . As the temperature increases from 105 to 121 °C, the value for the slope of the line sharply increases. This means that the number of viable cells at a fixed time of sterilization will drastically decrease as the temperature increases by 16 °C.

During sterilization, for the specific death rate (k_d) is not constant, the medium temperature in the course of sterilization (heating, holding, and cooling), the rate constant is dependent on temperature. The rate constant temperature dependency according to Arrhenius law can be integrated stated as follows:

$$\nabla_{\text{total}} = \ln \frac{N_o}{N} = k_o \int_0^t e^{-E/RT} dt \quad (15.8.6)$$

In batch sterilization, the heating, holding, and cooling cycle all contribute toward reduction of contaminant organisms; therefore, total sterilization time is the sum of three proportions involved in sterilization.

$$\nabla_{\text{total}} = \nabla_{\text{heating}} + \nabla_{\text{holding}} + \nabla_{\text{cooling}} \quad (15.8.7)$$

$$\nabla_{\text{heating}} = \ln \frac{N_o}{N_1} = k_o \int_0^{t_1} e^{-E/RT} dt \quad (15.8.8)$$

$$\nabla_{\text{holding}} = \ln \frac{N_1}{N_2} = k_o \int_{t_1}^{t_2} e^{-E/RT} dt \quad (15.8.9)$$

$$\nabla_{\text{cooling}} = \ln \frac{N_f}{N_2} = k_o \int_{t_2}^{t_f} e^{-E/RT} dt \quad (15.8.10)$$

Normally, heating, holding, and cooling periods may take 20%, 75%, and 5% of total sterilization time. In general, cell contaminants start to decrease at any temperature greater than 85 °C; the rate of decreasing would be sharp at temperatures above 121 °C. In fact high temperatures cause faster denaturation of cell protein; as temperature increases the holding time decreases.

EXAMPLE 1

Assume that initial medium contaminants are 100 million cells per milliliter of medium, and total volume for sterilization is 10 m³. Let us sterilize the medium with a number of viable cells, one out of 1000. That is the probability level; it means out of 1000 times of sterilization once is not sterilized.

- Calculate sterilization time.
- If Del factors for heating and cooling are defined, also k_d for the contaminants is defined 2.5 min⁻¹, what would be the required time in holding zone?

Solution

$$N_o = 10^8 \text{ cells ml}^{-1}$$

$$N = 10^{-3} \text{ number of cells after sterilization}$$

$$V_{\text{total}} = 10^7 \text{ ml}$$

$$\nabla_{\text{total}} = \ln \frac{N_o}{N} = \ln \frac{(10^8)(10^7)}{10^{-3}} = \ln 10^{18} = 43.75$$

$$\text{Del factor } \nabla = k_d t$$

It has been estimated that the Del factors for heating and cooling are 9.8 and 10.2, respectively. Then the Del factor for holding would be 23.75; while the holding time at 121 °C is 9.5 min.

For continuous sterilization, instead of holding time, use the ratio of length of holding section to average medium velocity ($t = L/U$); while average medium velocity is the ratio of volumetric flow rate over the cross-sectional area of sterilization pipe. One can define:

$$\frac{N_{x=L}}{N_o} = e^{-k_d L/U} \quad (15.8.11)$$

where $N_{x=L}/N_o$ is degree of sterility. Let us define dimensionless Damköhler number (Da) or reaction number, $N_R = k_d L/U$; Peclet number, $N_{Pe} = UL/D_z$, where D_z is axial dispersion coefficient ($\text{cm}^2 \text{s}^{-1}$). The axial dispersion of flow in the design of a continuous sterilizer is critical, because dispersion of bulk flow of medium through the sterilization pipe is presented by Peclet number. Flow of medium in continuous sterilization for Reynolds number is normally greater than 2100; which is turbulent. Figure 15.10 demonstrates the variation of Peclet

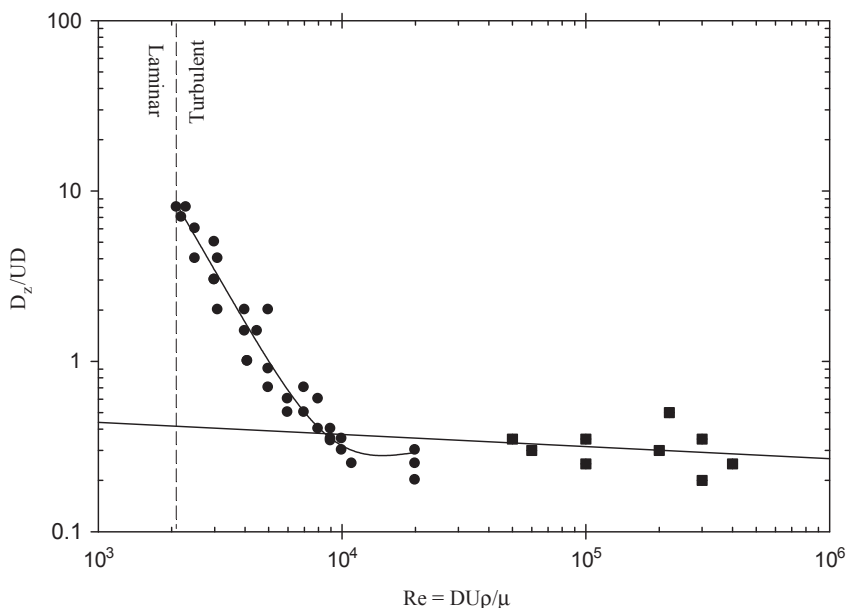
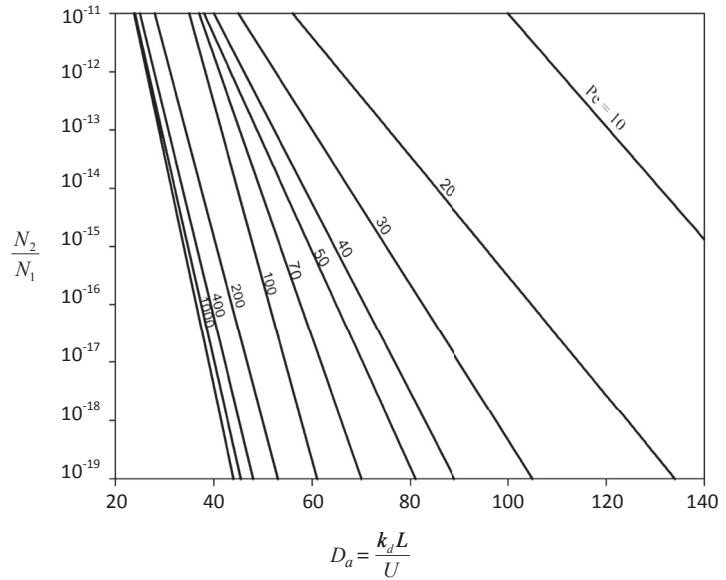


FIGURE 15.10 Inverse Peclet number versus Reynolds number for experimental and theoretical projections.

FIGURE 15.11 Thermal destruction of organisms with respect to Damköhler number and Peclet number.



number with respect to Reynolds number, while the fluid behaves turbulent. Also, the plot of sterility versus reaction number for an exact value of Peclet number resulted in a straight line. The solution of the dispersion model for continuous sterilization is complicated; therefore, the illustrated plot of $N_x = L/N_o$ versus N_R gives the solution of the projected model. Figure 15.11 depicts the thermal destruction of microorganisms in the sterilization process with respect to Damköhler number and Peclet number.

EXAMPLE 2

Continuous Sterilization

A fresh medium with fixed flow rate of $2.5 \text{ m}^3 \text{ h}^{-1}$ is going through a continuous sterilization system by an indirect steam heat source in a heat exchanger. The medium contains a bacterial contaminant concentration of six millions cells per milliliter of medium; the activation energy and Arrhenius constant for heat destruction are 300 kJ mol^{-1} and $1.5 \times 10^{38} \text{ h}^{-1}$, respectively. The risk of survival of contamination is one organism out of 100 days' operation composition. The sterilization pipe diameter is 15 cm and length of heat pipe is 20 m; assume that the density of medium is the same as the density of pure water and the viscosity of medium is $3.3 \text{ kg m}^{-1} \text{ h}^{-1}$. What would be the required sterilization temperature?

$$N_1 = \frac{6 \times 10^6 \text{ cells}}{\text{ml}} \frac{10^6 \text{ ml}}{1 \text{ m}^3} \frac{2.5 \text{ m}^3}{\text{h}} \frac{24 \text{ h}}{\text{day}} (100 \text{ days}) = 3.6 \times 10^{16}$$

$$\frac{N_2}{N_1} = \frac{1}{3.6 \times 10^{16}} = 2.78 \times 10^{-17}$$

The average medium velocity in a sterilizing pipe is

$$U = \frac{2.5 \text{ m}^3 \text{ h}^{-1}}{\pi \left(\frac{0.15}{2}\right)^2} = 141.47 \text{ m h}^{-1}$$

$$\text{Re} = \frac{\rho U D}{\mu} = \frac{(1000 \text{ kg m}^3)(141.47 \text{ m h}^{-1})(0.15 \text{ m})}{3.3 \text{ kg m}^{-1} \text{ h}^{-1}} = 6.43 \times 10^3$$

In order to calculate Peclet number, D_z should be determined. According to Figure 15.10, based on experimental values for a conservative design of a sterilizer for determination of D_z using the inverse function of Peclet number versus Reynolds number shows straight lines in turbulent flow; let us select the experimental curve as it gives an exact value for $1/\text{Pe}$ for a calculated value of Re ; that may lead to a large value of D_z . Read off from the presented graph for a given Reynolds number resulted in

$$D_z/UD = 0.6$$

$$D_z = 0.6(141.47 \text{ m h}^{-1})(0.15 \text{ m}) = 12.73 \text{ m}^2 \text{ h}^{-1}$$

$$\text{Pe} = \frac{UL}{D_z} = \frac{(141.47 \text{ m h}^{-1})(20 \text{ m})}{12.73 \text{ m}^2 \text{ h}^{-1}} = 222$$

From Figure 15.11, for a given Peclet number and N_2/N_1 ratio, a Damköhler number of about 45 is obtained. Then, calculate k_d :

$$k_d = \frac{UD_a}{L} = \frac{(141.47 \text{ m h}^{-1})(45)}{20 \text{ m}} = 318.31 \text{ h}^{-1}$$

Based on given expression (Eqn 15.8.4), the sterilization temperature is defined by the following equation:

$$\ln \frac{k_d}{k_\theta} = -\frac{E}{RT}$$

$$T = \frac{\frac{-E}{R}}{\ln \frac{k_d}{k_\theta}} = \frac{\frac{-300 \times 10^3 \text{ J mol}^{-1}}{8.314 \text{ J K}^{-1} \text{ mol}^{-1}}}{\ln \frac{318.31 \text{ h}^{-1}}{1.5 \times 10^{38} \text{ h}^{-1}}} = 439.3 \text{ K or } 166^\circ \text{C}$$

15.8.1 Sterilization of Media for Stock Cultures

To clear slant tubes, culture agar solution is prepared. To have clear agar solution, boil agar solution till it is clear. Agar is a polysaccharide. It is not soluble in cold water, so heating helps to dissolve it in water. Once the solution is dispensed in the tube, it goes for sterilization. Agar is in the solid state at room temperature, about 35°C .

15.8.2 Sterilization of Bacterial Media

Often, sterilization of culture media is performed in an autoclave at temperatures between 121 and 134°C . It is valuable to know the damage caused to the medium by heating it. Heating the culture medium containing peptides, sugars, vitamins, minerals, and metals results in

nutrient destruction, either a thermal degradation or a reaction between the components of the media. Protein in the media is denatured by high temperature, and sugars are easily caramelized. During the heat treatment, toxic compounds are formed, which may retard or inhibit the microbial growth. For minimal damage to the ingredients of the media, it is important to optimize and minimize the heating and holding time of the sterilization process, respectively.

15.8.3 Sterilize Petri Dishes

There are several ways to handle petri dishes. The standard dishes are 15–20 mm deep and 12–15 cm in diameter. They are normally available in glass and also transparent plastic. Petri dishes are individually wrapped. The medium is separately sterilized while we add the sterilized medium to the petri dishes in front of a flame. It is recommended to use 20–25 ml of medium in each petri dish. These are all called culture dishes. The medium contains about 1.5–2% agar. After the medium cools off it solidifies. The petri dishes with the nutrient agar should be sterilized and stored in a refrigerator.

It is common to sterilize the media and petri dishes separately. When the medium is cooled to about 55 °C, in front of a flame or in a laminar flow chamber, lift the lid of the dish enough to pour about 25 ml of the medium to the desired depth and lower the lid in place. It is best to gently move the petri dish in a way that spreads a thin layer of agar uniformly without any air bubbles. Distribution of media in the petri dishes should be done in front of a flame. Most plastic petri dishes are made of polystyrene and are not autoclaveable. Plastic petri dishes are easily deformed during sterilization at high temperatures. Some plastic dishes can be autoclaved, but they are more expensive. Please follow the instructions given by the manufacturer or obtain information from catalogs.

It is recommended to autoclave glass dishes and medium separately. If your dishes are autoclaveable, you may dispense the agar into the dish and then autoclave it. In this case it is best to cool the dishes in the autoclave or in the pressure cooker to reduce the amount of water that will condense on the cover of the dish.

15.8.4 Sterilization Steps in a Programmed Autoclave

In a fully equipped autoclave, when we execute a sterilization program with the microprocessor, its screen is showing which cycle of the process is under operation. The control in an old system was poor and most operation was handled manually; however, in recent fabricated units detailed information about the temperature and time of sterilization and drying is provided. In a modern system a supply of deionized water in the reservoir tank for steam supply is designed to prevent any system frailer. When choosing your autoclave, careful consideration must be given to the options you may need in order to optimize the autoclave's performance and safety.

Figure 15.12 depicts sequence and steps of a complete programmed autoclave. A complete program of sterilization consists of the following phases:

1. Vacuum: Initial vacuum, air is ejected from the autoclave chamber. Vacuum provides efficient air removal at the beginning of the cycle, ensuring that steam penetrates into the load and not be affected by trapped air pockets.

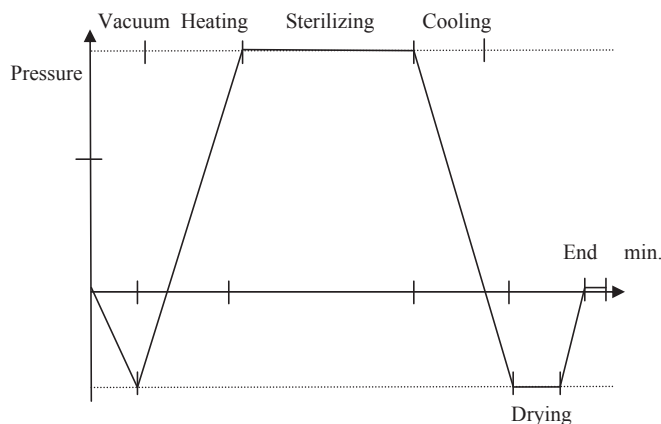


FIGURE 15.12 The sequence of the sterilization program.

2. Filling: Automatically distilled water is filled for the necessary mass of steam supply in the sterilization chamber.
3. Heating: Heating and pressure increase according to program mode.
4. Sterilization completed.
5. Unloading: Automatic unload of the condensate and steam from the sterilization chamber; the condensate may be filtered and dionized water returned to the distilled tank reservoir.
6. Drying and Cooling: The chamber is vacuumed and then the pressure returns to the barometric level. During the cooling stage, vacuum can help to dissipate heat from the load and in some cases can aid in the removal of some moisture from the load. In a cooling system a water jacket is used to speed up the cooling stage of the sterilization cycle.
7. End of sterilization process: Once the gage pressure dropped to near zero, the completion of the sterilization cycle is noted by blinking lights or bibbers; the autoclave doors can be opened.

The controlling system by the microprocessor displays any necessary warning messages when, for example, the water level in the condensers tank is lowered or the bacteriological filter must be changed. The message is blinking on the equipment display monitor. In this way, if any anomaly appears during the execution of the program, the program is aborted and a failure message will appear on the monitor.

Finally, safety is required for operators by filtering all noncondensable gases through a $0.2\ \mu\text{m}$ filter prior to exhaust. Return condensed liquids to the chamber for sterilization. Make sure that nothing is exhausted without being either filtered or sterilized.

15.8.5 Safety Recommendation in Autoclave Operation

Safe operation for autoclave is very important. Volatile samples are unable to resist vaporization; therefore, do not autoclave corrosive chemical solvents, volatile organic compounds, or radioactive materials. Before operating an autoclave, make sure a safe distilled water level exists in the water tank. If autoclave gaskets are deteriorated, replace them before operation.

Do not overload autoclaving material; tubing must be wrapped in aluminum foil. If you autoclaving more than half a tank or carboys of fresh medium, check for siphoning problems; if tubings are in the medium, cotton filters are mounted for avoiding any build up pressure in the feed tank. It is recommended to put all tubing in aluminum foil; avoid any heat damage of silicon tubing. The sterilized feed tank and tubing are connected in front of the flame under sterile conditions. Put glassware in an autoclave basket. Always sterilize sugar separately from supplementary media; avoid caramelization of sugar at high temperature. Then add a carbon source to the medium in front of the flame under sterile conditions.

15.9 DRY HEAT STERILIZATION

Dry heat sterilization is used for equipment that can withstand high temperatures and dry heat but cannot withstand a wet or steam autoclave. This method is often used for glassware as it dries and sterilizes in one operation. The pipettes must be wrapped in dustproof aluminum foil or placed in metal pipette cans. The can lids are removed during heating and replaced after sterilization; that is, before any dust can get in the can. Disposable items are not recommended for dry heat sterilization. This method may only be good for permanent reusable glass pipettes.

Normal laboratory glassware must first be washed and cleaned. It must be rinsed with deionized water. The clean glassware is sterilized in an oven set at 200 °C for 1–4 h. It is suitable to cover glassware with aluminum foil to maintain aseptic conditions after removal of the glassware from the oven. If aluminum foil is not available, special heat-resistant wrapping paper can be used. The sterile glassware must be protected from the air, which has microflora, or any contaminants. Avoid the use of any plastic caps and papers. Detach any labeling tape or other flammable materials, as they are fire hazards.

15.10 STERILIZATION WITH FILTRATION

Certain media components are susceptible to heat; it will be denatured if it is heated. Therefore they must be added to the media after autoclaving. To do so, it is necessary to carry out filtration with components using a 0.22 µm pore size filter that is appropriate to the solvent used. Filters are normally available from Whatman or Fisher Scientific. It is recommended that you consult filter experts or suppliers about the solvent and the special application you are intending to implement for the desired filters for the process. Normally filtration of media is used instead of sterilized media with an autoclave. To filter sterilized media, filter the water using a 0.45 µm pore size filter, before using a 0.22 µm pore size filter for final sterilization.

15.11 MICROWAVE STERILIZATION

Rapid sterilization of media is achieved by using microwave ovens. Most plant tissue culture media can be sterilized using a microwave, although it may not be suitable with a medium containing complex additives such as oatmeal. The high-temperature and

short-time sterilization by microwave heating with a continuous microwave sterilizer was investigated. Spores of *Bacillus stearothermophilus* were used as the biological indicator and also spores having the ability for resistance in a conventional sterilization; whereas the thermal resisting spores had no significant resistance through continuous microwave sterilizer at a high temperature (135 °C).

15.12 ELECTRON BEAM STERILIZATION

Electron beam sterilization is a high-voltage potential established between a cathode and an anode in an evacuated tube. The cathode emits electrons, as a cathodic ray or electron beam. A high intensity of electrons is produced. These electrons are accelerated to extremely high velocities. These accelerated electron intensities have great potential as a bactericide. Most electron beams operate in a vacuum. As a result the unwanted organisms in the media vanish and the media are sterilized.

The electron accelerator equipment producing a high-voltage beam also has various applications in the medical field and for surgical supplies. Electron beam sterilization is a successful technology used for sterilization of disposable medical appliances and devices with a wide range of densities. The electron beam inactivates microorganisms that cause destruction of biomolecules, and results in the death of microbes by an indirect chemical reaction. Irradiation by gamma rays is a similar mechanism. Advanced electronics precisely control the use of electron beams in the sterilization of medical devices. Electron beam sterilization results in less material degradation than with gamma irradiation. Medical products are sterilized in the original shipping containers, saving lots of time and maintaining the integrity of the original package.

15.13 CHEMICAL STERILIZATION

Chemical agents are used to sterilize heat-sensitive equipment. Chemical solutions are used as a suitable method for sterilizing long pipettes and glassware. Normally at the pilot scale in the absence of life, steam and chemical agents are often used. Application of an oxidizing agent such as 10% Chlorox for 20 min or longer proves that the system operates without any contamination. Excess amounts of chemical agent must be removed; otherwise organisms are able to grow in a toxic environment. The bleach (sodium hypochlorite) then needs to be removed by rinsing with sterile water or rubbing with ethyl alcohol, 70% ethanol–water (pH 2) or an alcohol solution of 70% *iso*-propanol without recontaminating the glassware or tools. Ethanol is commonly used for cleaning surfaces. Use of bleach on metal devices is not suitable as it corrodes metals rapidly. Ethylene oxide in the gas phase is commonly used. This is a special chemical effectively used for column bioreactors. It is a volatile compound and strong oxidizing agent. It boils at ambient temperature; therefore, the solution of ethylene oxide (liquid phase) must be stored in a refrigerator (4 °C). An excellent oxidizing agent such as a 3% sodium hypochlorite is used for chemical sterilization of equipment.

15.14 LOW-TEMPERATURE STERILIZATION

Sterilization systems are available operating at low temperatures; such systems utilize effective oxidizing agents such as hydrogen peroxide or ethylene oxide in the gas phase. The application of gas technology to sterilize temperature-sensitive instruments and equipments was developed in past decades. Hydrogen peroxide gas technology is efficiently, effectively, and safely used to sterilize a wide range of instruments. The low-temperature sterilization process is gentle and may take 50–70 min for high assurance of sterilization. The process by-products are oxygen and water vapor, which are nontoxic. Use of toxic gas for sterilization may not be permissible while the generated toxic fume is harmful. Commercially, the hydrogen peroxide gas plasma technology is used for sterilization of devices such as general surgery instruments, rigid and flexible endoscopes, cameras, light cables, battery power drills, and many others. The residual H_2O_2 is safely eliminated while the sterilization process is completed. This process in terms of energy is quite efficient; although hydrogen peroxide must be either supplied or generated in a catalytic electrolysis process. The operation temperature is normally in the range of 10–40 °C and the relative humidity is 30–75%. Sterilization is completed in short and long cycles for durations of 50 and 70 min, respectively.

NOMENCLATURE

- N Number of viable organisms, ml^{-1}
 N_0 Number of viable organisms as contaminants present in the medium, ml^{-1}
 k_d Specific death rate, min^{-1}
 E Activation energy, kcal mol^{-1}
 t Sterilization time, min
 R Gas constant, $1.987 \text{ cal (mol K)}^{-1}$
 T Absolute temperature, K
 D_z Axial dispersion coefficient, $\text{cm}^2 \text{ s}^{-1}$
 U Average medium velocity, cm min^{-1}
 L Length of holding section for sterilization, cm

References

1. Pelczar MJ, Chan ECS, Krieg NR. *Microbiology*. New York: McGraw-Hill; 1986.
2. Scragg AH. *Bioreactors in biotechnology, a practical approach*. New York: Ellis Horwood Series in Biochemistry and Biotechnology; 1991.
3. Doran PM. *Bioprocess engineering principles*. New York: Academic Press; 1995.
4. Shuler ML, Kargi F. *Bioprocess engineering, basic concepts*. New Jersey: Prentice-Hall; 1992.
5. Bailly JE, Ollis DF. *Biochemical engineering fundamentals*. 2nd ed. New York: McGraw-Hill; 1986.
6. Matthews IP, Gibson C, Samuel AH. *J Biomed Mat Res* 1989;**23**:143.

Membrane Reactor

OUTLINE

16.1 Introduction	455	16.3 Membrane and MBR Development	465
16.2 Membrane Bioreactors	457	References	466
16.2.1 MBR Configurations	458	16.4 Case Study: Enhanced Ethanol Fermentation in a Continuous Membrane Bioreactor: Pervaporation Technique	468
16.2.2 Membrane Materials and Modules	459	16.4.1 Introduction	468
16.2.3 Different Applications of MBR	460	16.4.2 Experimental	470
16.2.3.1 Landfill Leachate	460	16.4.2.1 Medium and Microorganism	470
16.2.3.2 Fermentation-Based Products (Lactic Acid)	461	16.4.2.2 Design of Membrane Bioreactor and Pervaporation System	470
16.2.3.3 Biofuel Production	462	16.4.2.3 Membrane	472
16.2.3.4 Bioethanol	462	16.4.2.4 Analysis	472
16.2.3.5 Wastewater Treatment	463	16.4.3 Results and Discussion	472
16.2.4 Membrane Fouling	463	16.4.3.1 Conventional Continuous Fermentation	472
16.2.4.1 Membrane Fouling Classification	464		
16.2.4.2 Membrane Fouling Control	465		

16.4.3.2 Continuous Fermentation with Pervaporation	473	16.5.2 Materials and Methods	485
16.4.3.3 Performance of Membrane Bioreactor with Continuous Pervaporation System	474	16.5.2.1 Preparation of PVA Solution	489
16.4.4 Conclusion	481	16.5.2.2 Preparation of Zirconia- Coated Alumina Membrane	490
Acknowledgments	481	16.5.2.3 Preparation of Porous Ceramic Support	490
References	481	16.5.3 Results and Discussion	491
16.5 Case Study: Inorganic Zirconia γ -Alumina-Coated Membrane on Ceramic Support	483	16.5.4 Conclusion	492
16.5.1 Introduction	483	Acknowledgments	492
		References	493

SUBCHAPTER

16.1

Introduction*

In most traditional processes such as methanol production from synthesis gas, the maximum production yield is restricted by the thermodynamic equilibrium. This restriction is technically overcome by applying a high operating pressure and recycling of unconverted synthesis gas after separation.¹ However, this solution is achieved at the expense of a higher operating cost. Great efforts have been made to improve the methanol synthesis process, among which is the development of Cu/Zn family catalyst. A lower operating pressure can be used in the presence of Cu/Zn family catalyst, which causes a considerable reduction in the operating cost. However, use of such an expensive catalyst may impose a high burden on the process cost, which fades the advantage of catalyst usage. It is clear that a continuous removal of reaction products can improve the production yield without recycling a huge amount of unconverted gas and/or applying a high operating pressure. Various attempts have been made in recent years by in situ removal of product, of which is the selective adsorption of methanol and water on a porous solid in a catalytic fixed bed reactor. A promising alternative technique for the improvement of the methanol production yield is its selective separation within the catalytic reactor using a membrane (membrane reactor (MR)). Indeed, the presence of the membrane as a selective barrier for products causes a continuous permeation of methanol through the membrane, which shifts the reaction toward more methanol production. This, therefore, enhances the conversion yield beyond the equilibrium level.

Indeed, a MR is an apparatus that takes benefits of integration of chemical reaction and membrane-based separation in the same physical device. Thus, the membrane plays two roles: first, it plays the role of separator; and second, it is the place where the reaction occurs.^{1,2} A conventional feature for MRs is in the form a two concentric pipe. The reaction takes place in the inner tube, which is usually filled with catalyst pellets; while, the outer pipe is the permeation side where the permeated products are swept with flowing inert gas. As can be seen in Figure 16.1, there are six membrane reactor concepts that are improvised according to the different problems that can be overcome using membranes within the reactor.^{2,3}

1. Retaining homogenous catalyst
2. Contactor
3. Extractor
4. Energetic coupling

*This case study was partially written with contributions from:

Ali Asghar Ghoreyshi, Kasma Pirzadeh, Maedeh Mohammadi

Faculty of Chemical Engineering, Noshirvani University of Technology, Babol, Iran

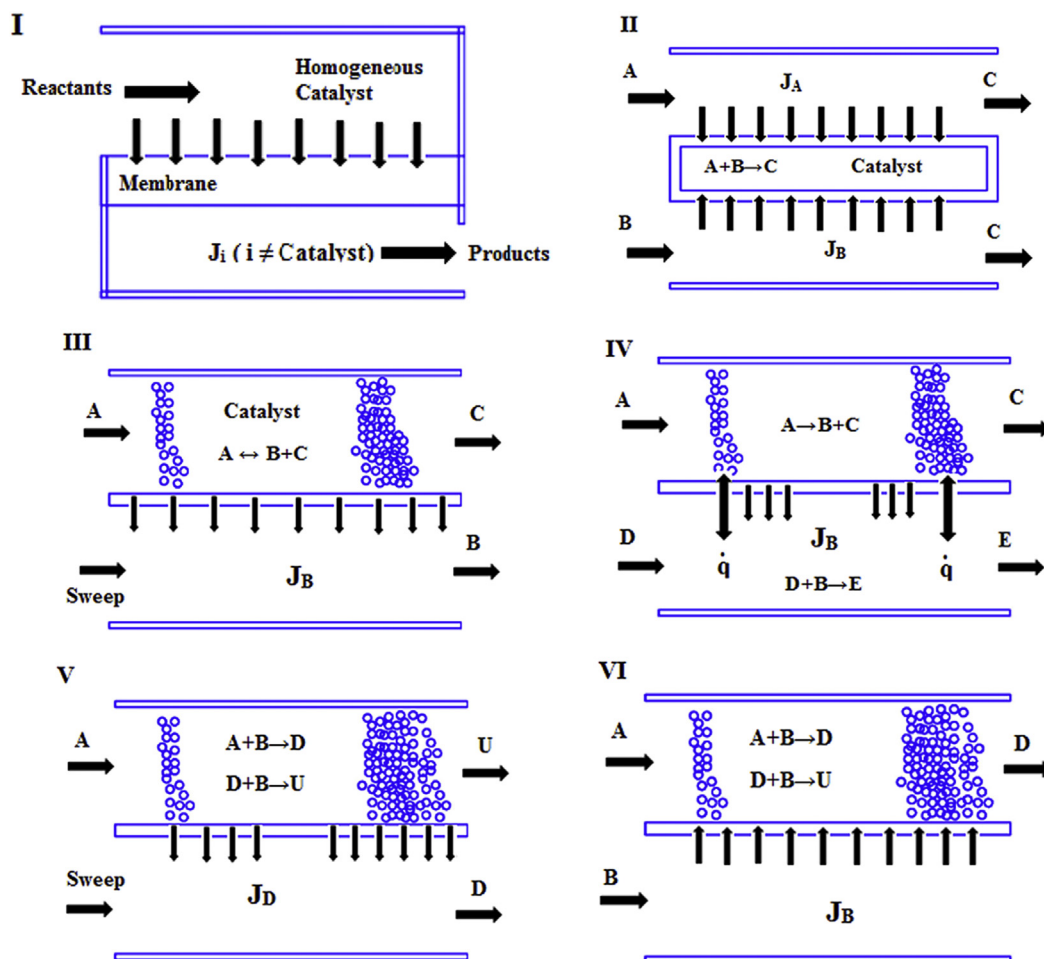


FIGURE 16.1 Different concepts of membrane reactors.

5. Selectivity enhancement through withdrawal of a product
6. Selectivity enhancement through optimized reactant dosing (distributing)

In the first concept, the membrane is exploited to retain soluble (homogeneous) catalysts in the reactor. Therefore, the operation can be implemented continuously without separation and recycling the valuable catalysts.

In type (2), membrane is applied as a contactor, which is a promising and attractive MR principle. In this case, the reactants enter from different sides and react within the membrane.^{4,5} One of the well-understood types of MRs is extractor type (3), in which certain products are selectively removed from the reaction zone. This concept has the capability of increasing the conversion rate if the reactions are reversible.⁶ For improving the driving force and eliminating the permeating products, additional sweeping gases or solvents are required to be used in the extractor principle.

In MR type (4), membrane can also serve as a separator between two segments of the reactor, in which different reactions take place. This type of membrane concept is applied when there is selective transport of certain components that attend in both reactions (for example, component B in Figure 16.1). If both reactions are endothermic or exothermic, additional heat flux over the membrane takes place, which is very attractive from energy point of view.⁷

Concept (5) is somehow similar to concept (3); however, the target component that should be removed by membrane is an intermediate component produced in the reactions series. As a consequence, the membrane selectivity will be improved due to the elimination of the target component.⁸

Type (6), which uses membrane as a distributor of certain reactants, is an interesting approach in which different local concentrations and residence time can be applied in order to increase selectivities. Much effort has begun^{9,10} to exploit the potential of this concept, although this configuration of the membrane has not been industrialized.

16.2 MEMBRANE BIOREACTORS

Technically, membrane bioreactor (MBR) is a promising reactor that combines two sections, biological degradation and solid–liquid separation process, which is implemented by membrane filtration. In the later section, microfiltration (MF) or ultrafiltration (UF) processes are the most common membrane technologies that provide complete physical retention of bacterial flocs and all other suspended particles within the bioreactors.¹¹

The idea of the MBR was first proposed by Yamamoto et al. in 1989 to submerge the membranes in the bioreactor.¹² Until then, MBRs were designed in a manner that the membrane section was placed out of the reactor and operated with high transmembrane pressure to maintain filtration. Also, a cross-flow membrane filtration loop within the MBR was first introduced by Dorr-Olivier Inc.¹¹ The other important changes that happened in recent MBRs were the acceptance of modest fluxes (25% or less as opposed to its first generation) and the idea of using two-phase bubbly flow for controlling fouling problems. In contrast to the first generation of MBR that had high costs for membrane operations, the recent one (submerged configuration) offered lower operating costs along with a continuous decrease in membrane cost, resulting in the popularity of this configuration in the mid-1990s. Since that time, many improvements in MBRs have been introduced. For instance, solid retention times reduced to 10–20 days with mixed liquor suspended solids (MLSS) of 10–15 g l⁻¹; while, in the preliminary configuration it was about 100 days with MLSS 30 g l⁻¹.¹¹

Rapid population growth and restricted availability of freshwater resources around the world have resulted in the popularity of water reclamation techniques. Among water reclamation techniques, MBR is a promising technology that combines biological treatment with a membrane separation process that leads to a considerable reduction in the amount of organic substances and discharged effluent. Fundamentally, two primary sections comprise the MBR system: the biological unit (bioreactor) that is responsible for biodegradation of waste materials, and the membrane unit for separation of clarified water from biomass or microorganisms.¹³ The advantages of the MBR originates from the replacement of a settling

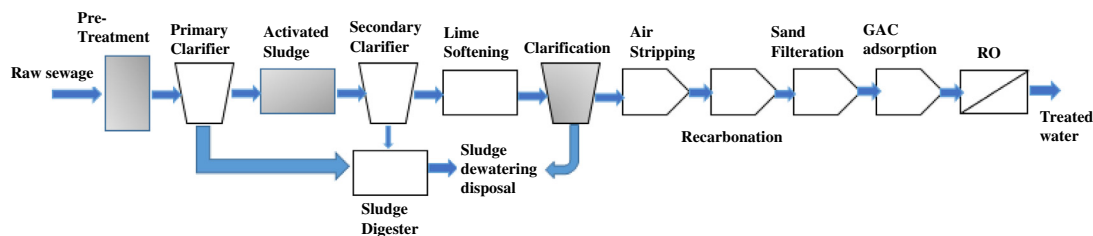


FIGURE 16.2 Conventional system for water treatment.

tank in conventional activated sludge (CAS) processes with membrane filtration device. CAS systems operate based on gravitational settling of microbial flocs from solid–liquid solution, and since the settling ability of biomass at high concentration reduces relatively, MLSS concentration in CAS processes is customarily around 5 g l^{-1} .^{14,15} In contrast, in membrane modules, biomass has the chance to retentate completely, which enables the MBR not only to operate with higher concentration of MLSS ($10\text{--}20 \text{ g l}^{-1}$) but also produces effluents with high quality. Increased MLSS concentration in MBR has other advantages including: (1) working at higher loading rates, (2) smaller reactor size and footprint, and (3) reduced additional sludge generation due to the long retention time.^{16,17} In comparison to the CAS process, MBR offers advantages such as concentrated biomass, high water quality, having low potential in producing sludge and giving high efficiency in removing biological oxygen demand (BOD) and chemical oxygen demand (COD). In conventional systems, the quality of the effluent relies on the settling characteristics of the biomass. This characteristic requires the development of well-settling bacteria; however, maintaining the settling bacteria can be difficult and the mentioned bacteria may not be ideal for treating wastewater.^{18,19} Also, conventional systems are confined with solids concentration of 5 g l^{-1} or less due to the interferences encountered during solids settling; while MBR systems can perform between 5 and 25 g l^{-1} . Furthermore, applying MBRs in large scale will require a notable decrease in the price of membranes. Figure 16.2 illustrates a conventional system for water treatment.²⁰

16.2.1 MBR Configurations

MBRs can be classified into two different configurations: external and submerged systems. In the external configuration, sludge is recirculated from the aeration basin to the outside installed pressure-driven membrane system where suspended solids are collected and recycled back to the bioreactor while the waste stream passes through the membrane. In this configuration, in order to omit the suspended fines and solids that may block the pores, the membranes are frequently backwashed and chemically cleaned. In the submerged configuration, as it is expected, the membrane is submerged in the aeration basin and operated under vacuum conditions. For preventing accumulation of suspended fines on the membrane surface, the membrane is agitated by coarse bubble aeration. The process of membrane recovery in this configuration is somehow similar to the external one, in which the surface of the membrane is either backwashed or relaxed and chemically cleaned when

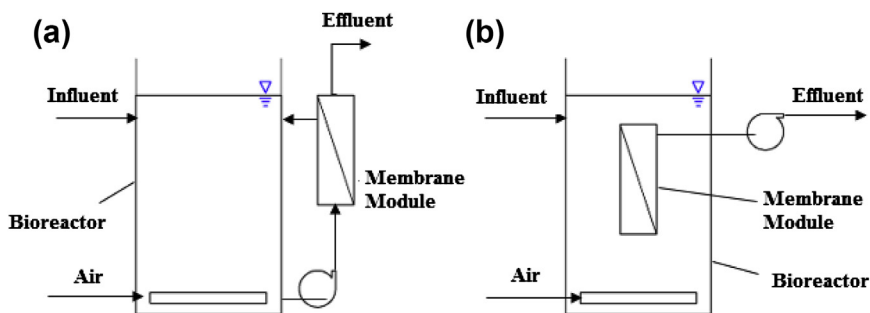


FIGURE 16.3 MBR configurations, (a) external system and (b) submerged.

high pressures are applied. Figure 16.3 shows a schematic view of the two different configurations of MBR.²¹

The advantages of MBRs compared to conventional ones are as follows²²:

1. Reaction and separation units are integrated into a process that results in reduced separation costs and recycle requirements
2. A controlled contact of incompatible reactions
3. Omitting unwanted reactions

16.2.2 Membrane Materials and Modules

Generally, membranes are made from either organic or ceramic materials. Polymeric membranes have the advantage of low production cost; however, they are at risk of fouling and degradation due to the natural variation in their pore size. In contrast, some features such as excellent quality and high durability have made ceramic membranes a better choice for membrane manufacturers. However, they are economically infeasible for large-scale operations in industrial applications.²³ Therefore, most manufacturers use polymeric membranes for application in bioreactors. Table 16.1 summarizes materials mostly used in polymeric membrane fabrication.²⁴

Generally, membranes are manufactured in various modules such as hollow fiber, plate and frame, and spiral; however, among these forms, hollow fiber and plate and frame form are the most common ones for the MBR.

The structure of hollow fibers is such that they are extruded into long fibers and collected in the modules, and then the modules are submerged in the wastewater and permeate passes through the center of the fiber. Plate and frame modules are designed with large membrane sheets loaded in cassettes. In this module, pressure difference is the only driving force that draws permeate through the membrane.

Flow pattern through the MBR system can be either cross-flow or dead-end. In cross-flow pattern, feed moves parallel to the membrane surface, and this flow pattern reduces fouling caused by solid materials. In dead-end flow pattern, feed is fed to the membrane perpendicularly. Feed applied to the membrane may pass through the membrane or maybe rejected as a waste. Since the feed that is applied to the MBR contains a high level of suspended

TABLE 16.1 Polymeric materials and their characteristics

Material	Abbreviation	Advantages	Disadvantages
Polypropylene	PP	Low cost High pH range tolerance	No chlorine tolerance Expensive cleaning chemicals required
Polyvinylidene fluoride	PVDF	High chlorine tolerance Simple cleaning chemicals	Cannot sustain pH >10
Polyethersulfone & polysulfone	PES/PS	Chlorine tolerance Reasonable cost	Brittle material requires support or flow inside to outside
Polyacrylonitrile	PAN	Low cost, typically used for UF membranes	Less chemically resistant than PVDF
Cellulose acetate	CA	Low cost	Narrow pH range Biologically active

materials with high potential of fouling, cross-flow is considered as the best pattern for the MBR.²⁵

16.2.3 Different Applications of MBR

16.2.3.1 Landfill Leachate

Rapid industrial and commercial growth and higher living standards, joined with cumulative production of useless and old-fashioned products, contribute to the accelerated production of solid wastes. In industrialized and developed countries, sanitary landfills are main threats to the environment.²¹ Therefore, landfills require severe surveillance for their design and operation because in long term, generation of leachates can pollute the underground water resources.

There are several factors that can contribute to leachate formation including rainwater filtration, chemical and physical reactions, and inherent moisture of wastes. Landfill leachate (LFL) is a complex and high strength wastewater that is rich in organic matter, ammonia, heavy metals, and toxic materials such as xenobiotic organic compounds.^{26,27}

LFL treatment aims to accomplish the following:

16.2.3.1.1 REMOVAL OF ORGANIC MATTER (BOD AND COD)

As reported in the literature, high BOD removal between 90 and 99% was achieved at various operating conditions and regardless of leachate age. In contrast to the BOD removal, COD removal efficiency varies from 23 to above 90%.

Several processes are used for the treatment of original leachate such as contact aeration, rotating biological reactor, and granular activated carbon (GAC) adsorption. These processes suffer from a variety of drawbacks, including biomass washout, regular replacement of activated carbon, and being in conflict with national regulations concerning wastewater treatment plant. To overcome these problems, a new configuration of processes consisting of a

submerged MBR and a post treatment reverse osmosis (RO) with considerably improved performance was applied. The overall yield of BOD and COD removal in MBR-RO system increased to 97% with effluent COD concentration of 6–72 mg l⁻¹.²⁸

16.2.3.1.2 REMOVAL OF AMMONIA

Nitrogenous compounds are among the most important water pollutants that can cause oxygen depletion and have a negative impact on the environment, resulting in worsening water quality and increasing the level of toxicity to aquatic organisms.²⁹ Removing ammonium nitrogen (NH₃-N) from leachates is always an obstacle in LFL treatment due to the hazards imposed by nitrogenous compounds.

Biological remediation of nitrogen consists of two sequential processes: nitrification and denitrification. In the first step, ammonia is oxidized by autotrophic nitrifiers to nitrite (NO₂⁻), and finally, in the presence of dissolved oxygen, it turns to nitrate (NO₃⁻). Although a biological nitrogen removal system is preferred to a physiochemical system, high amount of ammonia cannot be easily eliminated by biological treatments.^{30,31} However, MBR systems have shown great potential in removing NH₃-N from leachate. The majority of studies have indicated that over 90% of NH₃-N was removed by MBR, and in some cases removal efficiency of 100% was achieved.^{32–34}

16.2.3.1.3 REMOVAL OF ORGANIC MICROPOLLUTANTS

Nowadays, the presence of micropollutants in pharmaceuticals and personal care products has posed harmful effects on human and wild lives. Removal of these persistent organic pollutants from aqueous systems has attracted much attention from various groups including environmentalists and scientific communities.^{35,36}

Since the MBR system has the potential for removing micropollutants from wastewater, great effort has been made to use this system of treatment. The process comprises of an MBR configuration, three bioreactors (a denitrification tank followed by two nitrification units), and an external UF unit. After the permeate was clarified in a GAC adsorption unit, then it was post treated in a combined nanofiltration and powdered activated carbon (NF + PAC) unit. The results of some case studies showed that bisphenol A and nonylphenol removal were 95.3% and 85% in MBR, respectively.³⁷

16.2.3.2 Fermentation-Based Products (Lactic Acid)

Fermentation processes are widely used in the pharmaceutical industry for producing amino acids, antibiotics, and other chemicals. Generally, the fermentation process in batch reactors suffers from low productivity due to the inhibition effects imposed by high concentration of substrates or products.³⁸ Combination of biological reactions and membrane process in single units is a promising technique for the reactions in which the continuous elimination of metabolites is significant for keeping the production at good levels. The continuous separation of products and microorganisms via micro- or ultrafiltration increases the production rate. Some new configurations of MBR couple bacteria immobilization with microfiltration technique and are able to work at high concentrations of microorganisms. In this design, the bacteria are bounded and restricted to the reactor by coaxial membranes. The feed is recirculated in the axial direction, while transformation happens in the radial direction. The bacteria that are usually used in the fermentation process are of the genus *Bacillus* or

Lactobacillus.^{39–41} Since this process can be implemented continuously, it outweighs batch fermentation for the reasons summarized herein:

1. The continuous separation and recycling of the bacteria will shorten the cycle time of the fermentation, because despite the batch fermentation that takes a long time to start up and shut down, in continuous process, negligible time will be lost.
2. The recycling of the cells causes an increase in the cell numbers. High concentration of cells helps the feedstock to be pumped through the fermenter much faster.
3. The continuous removal of lactate via membrane provides the opportunity to the fermenter to eliminate the product inhibition effect and helps the cells to be viable and produce lactate.

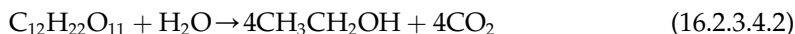
16.2.3.3 Biofuel Production

Fossil fuels are the world's main source of energy and are predicted to be depleted in the not-too-distant future due to high consumption. The great demand for energy production will cause an increase in the price and cost of these supplies. In addition, emissions of greenhouse gases such as carbon dioxide and pollutant gases such as sulfur dioxide (SO₂) and nitrogen oxides (NO_x) lead to air pollution, climate change, and global warming. These obstacles require the development of new policies on clean, efficient, and more environmentally friendly technologies to supply energy. For this reason, renewable energies have become important for sustainable environmental and economic growth. Among the alternative energy sources, bioethanol and biodiesel are widely recognized.^{42–44}

16.2.3.4 Bioethanol

Bioethanol has received a lot of attention as an alternative source of energy. It is currently produced from starches or sugars. The fermentation process is mainly performed in batch bioreactors with the yeast *Saccharomyces cerevisiae*. Ethanol production during this process without cell recycling is about 1.8–2.5 g l⁻¹. If the process of batch fermentation changes to the continuous one and the yeast concentration increases, the productivity will be improved, which would reduce the cost of produced ethanol.⁴⁵ However, yeast recycling in continuous process to reach high productivity is expensive. An MBR can be used for this purpose in very much similar way as it is used for water treatment.^{11,46} In this process, the yeast can be chosen from bakery yeast and the fermentation substrate can be molasses from the sugar industry. The substrate that usually contains sucrose is diluted to minimize the risk and severity of infections. Besides sucrose, the molasses contains glucose, galactose, lactic acid, and acetic acid.

The maximum theoretical amount of ethanol that can be produced in this process can be calculated from the stoichiometric equations of conversion of sugars to ethanol (Eqns (16.2.3.4.1) and (16.2.3.4.2)). The first equation shows the conversion of glucose and galactose to ethanol; the second equation indicates the production of ethanol from sucrose. One kg of glucose and galactose can produce 0.51 kg ethanol; while, 1 kg sucrose can produce 0.54 kg ethanol.



In a typical experiment carried out for ethanol production in batch process, 50% of the theoretical yield was achieved; while, in continuous fermentation, 60% of the maximum theoretical yield was attained; when a continuous submerged MBR was applied, 78% of the theoretical yield was obtained.⁴⁵

16.2.3.5 Wastewater Treatment

One of the main applications of MBRs is in wastewater treatment, which is globally increasing. MBRs produce a low amount of sludge and have the ability to be used for wastewaters with high amounts of BOD and COD.

Among the technologies used for wastewater treatment, anaerobic digestion has received a great deal of attention since it combines contamination reduction and energy generation. In contrast to the aerobic process, in anaerobic treatment sludge handling is considerably lower since it does not need oxygen and the sludge yield is lower. However, application of conventional anaerobic biological systems has been restricted due to the biomass retention obstacles. This problem is one of the most common and important issues in anaerobic technology, which does not provide enough solid retention time for methanogens. Insufficient biomass retention in the conventional system leads to some difficulties. On the one hand, the net production of biomass is low, and on the other hand, inappropriate characteristics of the biomass in conventional anaerobic biological systems lead to the loss of biomass to effluent.⁴⁷

An anaerobic MBR (AnMBR) is a biological treatment process in which there is no oxygen and the membrane is the only means for solid–liquid separation. This kind of MBR offers notable advantages over conventional anaerobic and aerobic systems, which are summarized in Table 16.2. Among the advantages, total biomass retention, excellent effluent quality, and low sludge generation are more salient as opposed to mentioned systems.^{47–49}

There are two configurations for AnMBR: external/side stream and submerged/immersed configuration. Generally, external configuration provides better working conditions, such as more direct hydrodynamic control of fouling, easy replacement of membranes, and high fluxes. However, high energy costs and high cross-flow velocity that have negative effects on the biomass activities are considered to be drawbacks of this configuration.¹¹

Membrane modules that are applied in MBRs can be in the form of MF or UF with either configuration of hollow fiber, flat sheet, or tubular. Hollow fiber membrane modules, due to their high packing density and cost efficiency, are very popular in submerged MBRs. Flat sheet membrane modules are also becoming popular, especially for their good stability, the ease of cleaning, and replacement of defective membranes. A tubular membrane module is made up of several tubular membranes arranged in the form of tubes. The main advantages include low fouling, relatively easy cleaning, and easy handling of suspended solids, while the disadvantages include high capital cost, low packing density, high pumping costs, and high dead volume.^{50,51}

16.2.4 Membrane Fouling

Membrane fouling is the critical issue restricting the widespread application of AnMBR in wastewater treatment. Membrane fouling decreases the system productivity and increases the amount of energy needed for sludge recirculation or gas scouring; the membrane needs

TABLE 16.2 Comparison of conventional aerobic treatment, anaerobic treatment, aerobic MBR and AnMBR

Feature	Conventional aerobic treatment	Conventional anaerobic treatment	Aerobic MBR	AnMBR
Organic removal efficiency	High	High	High	High
Effluent quality	High	Moderate to poor	Excellent	High
Organic loading rate	Moderate	High	High to moderate	High
Sludge production	High	Low	High to moderate	Low
Footprint	High	High to moderate	Low	Low
Biomass retention	Low to moderate	Low	Total	Total
Nutrient requirement	High	Low	High	Low
Alkalinity requirement	Low	High for certain industrial stream	Low	High to moderate
Energy requirement	High	Low	High	Low
Temperature sensitivity	Low	Low to moderate	Low	Low to moderate
Start-up time	2–4 weeks	2–4 months	<1 week	<2 weeks
Bioenergy recovery	No	Yes	No	Yes
Mode of treatment	Total	Essentially pretreatment	Total	Total or pretreatment

to be cleaned frequently, which might reduce the membrane durability and lead to higher replacement cost. Membrane fouling results from interaction between the membrane material and the suspended matters of sludge. Although the membrane used in aerobic MBR can generally be used in AnMBR system, the condition that sludge is suspended in AnMBR system is completely different from that in aerobic compartment. This presents certain unique impacts on membrane fouling characteristics.⁵²

16.2.4.1 Membrane Fouling Classification

Membrane fouling can be classified based on the cleaning practice, as removable and irremovable fouling. Removable fouling refers to fouling that can be removed by physical means, for example, back flushing or relaxation under cross-flow conditions. It occurs due to external deposition of material, which can be separated more easily than an irremovable one. However, irreversible fouling, which is considered as permanent fouling, cannot be removed by any cleaning method and needs to be removed by chemical agents. Irremovable fouling is caused by pore blocking and strongly bounded foulants during membrane filtration.⁵⁰

Membrane fouling can also be classified according to the foulant component to biological, organic, and inorganic fouling. Biological fouling is the result of interaction between biomass and membrane surface. Biological fouling can also occur due to accumulation and adsorption

of soluble microbial products (SMPs) or extracellular polymeric substances (EPSs) on membrane surface and pores.^{19,53}

Organic fouling is attributed to deposition of biopolymers, for example, proteins and polysaccharides on the membrane, while inorganic fouling is attributed to the scalants. Biopolymers can easily deposit on membranes because of their small size at permeate flow. Biopolymers have spatial distribution on the membrane surface. Recent investigations have shown that creation of organic fouling is related to SMPs or EPSs. Main foulants of membranes are biopolymers and organics. In inorganic fouling, the probability of fouling occurrence by them is less during activated sludge filtration.⁵⁰

16.2.4.2 Membrane Fouling Control

The aim of membrane fouling study is to find strategies for controlling membrane fouling and membrane cleaning. Based on the parameters affecting membrane fouling, such as feed characteristics, broth characteristics, membrane characteristics, and operational conditions, these strategies in AnMBR systems can be classified into five groups: (1) pretreatment of feed, (2) optimization of operational conditions, (3) modification of activated sludge, (4) modification of membrane and optimum design of membrane module, and (5) membrane cleaning.⁵⁰

16.3 MEMBRANE AND MBR DEVELOPMENT

Membrane features can impact on the MBR performance; improving membrane characteristics can enhance the performance of MBRs. These characteristics include pore size, surface charge, hydrophilicity/hydrophobicity, material, roughness, etc. For example, narrow pore size can control membrane fouling in MBRs, or polyvinylidene fluoride (PVDF) membrane is the best polyethylene membrane in exclusion of irremovable fouling in MBRs.⁵⁴ As well, hydrophilic membranes have less fouling than hydrophobic ones, because in hydrophobic membranes an interaction can occur between membrane and foulants.⁵⁵ Cost reduction in MBRs is the other development factor. In this case, cheaper filters such as meshes and nonwoven filter cloths can be used when only standard quality of effluent is required. These low-cost filters can improve the economy of the plant, but membrane fouling limits their application. This matter is because of their large pore size and rough surface, which causes entrapping sludge flocs in the fiber matrix and eventually forms hard-to-remove fouling.⁵⁶ In spite of this, membrane fouling can be resolved by improvement of filters to surface roughness, surface charge, and hydrophilicity modification.¹⁹ One of the modification techniques is plasma treatment, which has many advantages. This treatment improves the antifouling property of membranes and has very shallow depth of modification. Although this method is very beneficial, chemical reactions of plasma are complex and hard to understand; therefore, the possibility of its large-scale development is currently low.⁵⁷ In addition to these developments, other membrane modifications for high flux operation and development of cost-effective membranes are required to make the MBR processes economically feasible.⁵⁸

Another new development in separation processes is forward osmosis membrane bioreactor (OSMBR). This novel system uses a submerged forward osmosis (FO) membrane module in a bioreactor. FO membrane works like a barrier for solute transport, and high rejection

of pollutants is provided.⁵⁹ OSMBRs have much higher rejection in lower hydraulic pressures; besides, their fouling rate is lower than pressure-driven systems. The efficiency of this process for total organic carbon and $\text{NH}_4^+ - \text{N}$ removal was above 99 and 98%, respectively.⁶⁰

References

1. Struis R, Stucki S. *Appl Catal A* 2001;**216**(1):117–29.
2. Gallucci F, Basile A. *Membranes for membrane reactors*. John Wiley; 2011.
3. Seidel-Morgenstern A. *Membrane reactors: distributing reactants to improve selectivity and yield*. John Wiley & Sons; 2010.
4. Miachon S, Perez V, Crehan G, Torp E, Ræder H, Bredesen R, et al. *Catal Today* 2003;**82**(1):75–81.
5. Dittmeyer R, Caro J. *Catalytic membrane reactors*. Wiley Online Library; 2008.
6. Pflerle WC. Process for dehydrogenation; 1966, Google Patents.
7. Gobina E, Hou K, Hughes R. *Chem Eng Sci* 1995;**50**(14):2311–9.
8. Kölsch P, Smejkal Q, Noack M, Schäfer R, Caro J. *Catal Commun* 2002;**3**(10):465–70.
9. Mallada R, Menéndez M, Santamaria J. *Catal Today* 2000;**56**(1):191–7.
10. Al-Juaied M, Lafarga D, Varma A. *Chem Eng Sci* 2001;**56**(2):395–402.
11. Le-Clech P, Chen V, Fane TA. *J Membr Sci* 2006;**284**(1):17–53.
12. Yamamoto K, Hiasa M, Mahmood T, Matsuo T. *Water Sci Technol* 1989;**21**(4–5):43–54.
13. Cicek N. *Can Biosyst Eng* 2003;**45**:6.37–49.
14. Delai Sun D, Loong Khor S, Teck Hay C, Leckie JO. *Desalination* 2007;**208**(1):101–12.
15. Muller E, Stouthamer A, van Verseveld HWv, Eikelboom D. *Water Res* 1995;**29**(4):1179–89.
16. Melin T, Jefferson B, Bixio D, Thoeye C, De Wilde W, De Koning J, et al. *Desalination* 2006;**187**(1):271–82.
17. Ng AN, Kim AS. *Desalination* 2007;**212**(1):261–81.
18. Li X-y, Wang X-M. *J Membr Sci* 2006;**278**(1):151–61.
19. Meng F, Chae S-R, Drews A, Kraume M, Shin H-S, Yang F. *Water Res* 2009;**43**(6):1489–512.
20. Côté P, Buisson H, Pound C, Arakaki G. *Desalination* 1997;**113**(2):189–96.
21. Ahmed FN, Lan CQ. *Desalination* 2012;**287**:41–54.
22. Armor J. *J Membr Sci* 1998;**147**(2):217–33.
23. Scott J, Smith K. *Water Res* 1997;**31**(1):69–74.
24. Layson A. Microfiltration- Current know-how and Future Directions IMSTEC, Sydney, Australia; 2003.
25. Alexander K, Guendert D, Pankratz T. Comparing MF/RO performance on secondary and tertiary effluents in reclamation/reuse applications. In: *IDA conference, Paradise Island, Bahamas*; 2003.
26. Renou S, Givaudan J, Poulain S, Dirassouyan F, Moulin P. *J Hazard Mater* 2008;**150**(3):468–93.
27. Baig S, Coulomb I, Courant P, Liechti P. *Ozone Sci Eng* 1999;**21**:1–22.
28. Ahn W-Y, Kang M-S, Yim S-K, Choi K-H. *Desalination* 2002;**149**(1):109–14.
29. Ahn Y-H. *Process Biochem* 2006;**41**(8):1709–21.
30. Wang F, Ding Y, Ge L, Ren H, Ding L. *J Environ Sci* 2010;**22**(11):1683–8.
31. Kim J-H, Guo X, Park H-S. *Process Biochem* 2008;**43**(2):154–60.
32. Sadri S, Cicek N, Van Gulck J. *Environ Technol* 2008;**29**(8):899–907.
33. Li G, Wang W, Du Q. *J Appl Polym Sci* 2010;**116**(4):2343–7.
34. Tsilogeorgis J, Zouboulis A, Samaras P, Zamboulis D. *Desalination* 2008;**221**(1):483–93.
35. Sumpter JP. *Acta Hydroch Hydrob* 2005;**33**(1):9–16.
36. Desbrow C, Routledge E, Brighty G, Sumpter J, Waldoock M. *Environ Sci Technol* 1998;**32**(11):1549–58.
37. Wintgens T, Gallenkemper M, Melin T. *Water Sci Technol* 2003;**48**(3):127–34.
38. Luedeking R, Piret EL. *J Biochem Microbiol Technol Eng* 1959;**1**(4):393–412.
39. Mehaia M, Cheryan M. *Process Biochem* 1987;**22**(6):185–8.
40. Motosugi K, Esaki N, Soda K. *Biotechnol Bioeng* 1984;**26**(7):805–6.
41. Tango M, Ghaly A. *Appl Microbiol Biotechnol* 2002;**58**(6):712–20.
42. Hoekman SK. *Renew Energy* 2009;**34**(1):14–22.
43. Hammond G, Kallu S, McManus M. *Appl Energy* 2008;**85**(6):506–15.

44. Monni S, Raes F. *Environ Sci Policy* 2008;**11**(8):743–55.
45. Thuvander J. Designed, performed and evaluated continuous ethanol fermentation using membrane bioreactors (MBR). [Thesis report]; Lund University, Sweden. Department of Chemical Engineering; 2012.
46. Sutherland K. *Filtr Sep* 2010;**47**(5):14–6.
47. Lin H, Peng W, Zhang M, Chen J, Hong H, Zhang Y. *Desalination* 2013;**314**:169–88.
48. Aquino SF, Hu AY, Akram A, Stuckey DC. *J Chem Technol Biotechnol* 2006;**81**(12):1894–904.
49. Lin H, Xie K, Mahendran B, Bagley D, Leung K, Liss S, et al. *Water Res* 2009;**43**(15):3827–37.
50. Lin H, Chen J, Wang F, Ding L, Hong H. *Desalination* 2011;**280**(1):120–6.
51. Kocadagistan E, Topcu N. *Desalination* 2007;**216**(1):367–76.
52. Meng F, Liao B, Liang S, Yang F, Zhang H, Song L. *J Membr Sci* 2010;**361**(1):1–14.
53. Liao B-Q, Kraemer JT, Bagley DM. *Crit Rev Environ Sci Technol* 2006;**36**(6):489–530.
54. Yamato N, Kimura K, Miyoshi T, Watanabe Y. *J Membr Sci* 2006;**280**(1):911–9.
55. Yu H-Y, Hu M-X, Xu Z-K, Wang J-L, Wang S-Y. *Sep Purif Technol* 2005;**45**(1):8–15.
56. Guan Y, Satoh H, Mino T. *Water Sci Technol* 2006;**54**(10):55–66.
57. Yu H-Y, Xu Z-K, Lei H, Hu M-X, Yang Q. *Sep Purif Technol* 2007;**53**(1):119–25.
58. Shannon MA, Bohn PW, Elimelech M, Georgiadis JG, Mariñas BJ, Mayes AM. *Nature* 2008;**452**(7185):301–10.
59. York R, Thiel R, Beaudry E. Full-scale experience of direct osmosis concentration applied to leachate management. In: *7th international waste management and landfill symposium (Sardinia'99)*, Cagliari, Italy; 1999.
60. Achilli A, Cath TY, Marchand EA, Childress AE. *Desalination* 2009;**239**(1):10–21.

SUBCHAPTER

16.4

Case Study: Enhanced Ethanol Fermentation in a Continuous Membrane Bioreactor: Pervaporation Technique*

16.4.1 INTRODUCTION

Fossil energy sources such as oil, coal, and natural gas are being depleted. Therefore, alternative renewable sources of energy have been considered. In this case, ethanol fermentation from biomass such as cellulose and glucose is a desired alternative energy source.^{1,2} Also, ethanol has extensive applications and is often used in many processes, such as the food industry, brewing process, and medical applications.³ Ethanol as fuel has been used in the world since the early 1900s; the U.S. Clean Air Act, first passed in 1970, specifies a percentage of renewable fuels to be mixed with normal gasoline.⁴

During past decade, almost all industrial-scale ethanol production plants have used conventional ethanol fermentation processes. In conventional continuous fermentation, cell density and dilution rates are low, due to the presence of high ethanol and substrate inhibitions. This may cause limited ethanol productivity. Also, ethanol inhibition is an important limiting factor, but an organism with high tolerance of ethanol permits concentrated glucose substrate to be converted to ethanol. Therefore, improvement of productivity and removal of product-inhibition are required to enhance ethanol fermentation.⁵ Conventional ethanol fermentation process has many disadvantages such as low ethanol concentration, low cell density, low productivity, high capital and labor costs, further purification for achievement of high ethanol concentration, and many more are discussed in literature.^{6,7} To improve the conventional fermentation process, different techniques have been considered. Immobilization of microorganisms in an immobilized cell reactor (ICR) is a relatively new technique for high ethanol production and substrate inhibition in a reasonable retention time.¹ One of the most important and advanced techniques in ethanol production is application of membrane for relatively fast ethanol recovery.

Membrane technology represents one of the most effective and energy-saving processes for ethanol production. Coupling membrane separation with biological process, integrating

*This case study was partially written with contributions from:

Mehri Esfahanian, Department of Chemical Engineering, Islamic Azad University, Qaemshahr Branch, Iran;
Ali Asghar Ghoreyshi, Faculty of Chemical Engineering, Noshirvani University of Technology, Babol, Iran;
Habibollah Younesi, Department of Environmental Science, Faculty of Natural Resources, Tarbiat Modares University, Noor, Iran;
Monireh Fallahi, Faculty of Chemical Engineering, Noshirvani University of Technology, Babol, Iran.

the entire system in a single unit is a very attractive configuration for the process where continuous elimination of metabolites is necessary to maintain high productivity.⁸ MBR is designed to reduce substrate and product inhibitions, and increase cell density and ethanol productivity. The combination of membrane and bioreactor certainly eliminates downstream processing. The major membrane processes are microfiltration, ultrafiltration (UF), reverse osmosis, electrodialysis, gas separation, and pervaporation.⁹ Pervaporation as a useful method has been considered for separation of ethanol/water mixture.⁹

Membranes are shown high ethanol permselective and low water permeabilities in ethanol fermentation. The polymers have been used for ethanol-permselective membranes.¹⁰ The most important and promising polymer membrane that has a high performance for separation of organic chemicals compounds in water is polydimethylsiloxane (PDMS).^{11–14} In addition, PDMS is hydrophobic and has a good chemical stability and biocompatibility. It is suitable for constructing pervaporation membrane bioreactor (MBR), which is applied to bioconversion and separation for biological product.¹⁵

A number of researchers have investigated continuous alcohol fermentation by pervaporation using different mediums, membranes, and configurations at various dilution rates. Nomura et al.⁷ have studied ethanol extraction from fermentation broth by silicalite zeolite membrane. They have investigated the effects of ethanol concentration in feed stream to obtain high ethanol concentration permeation. They have shown that the performance of the silicalite membrane was disturbed during operation time. Cho and Hwang⁵ have investigated integration of continuous ethanol fermentation and membrane separation in the same unit. They have applied silicone rubber hollow fiber membrane that was selective to ethanol. Their dilution rates were in the range of 0.071–0.262 h⁻¹. They achieved a 10–20% increase in ethanol productivity compared to conventional fermentation. Maximum ethanol productivity was approximately 7.3 g ethanol l⁻¹ h⁻¹ at dilution rate of 0.17 h⁻¹. There was an 18% increase in maximum productivity of 6.2 g ethanol l⁻¹ h⁻¹ over conventional continuous fermentation. In addition, pervaporated ethanol concentration was about seven times higher than that of the conventional process. Hoover and Hwang¹⁶ have studied continuous membrane column with pervaporation of alcohols. They have described a mathematical model for capillary membrane pervaporation. Nakao et al.¹⁷ have investigated the continuous ethanol extraction by pervaporation from a MBR. Polytetrafluoroethylene (PTFE) was the selected membrane in their MBR. They have investigated three types of continuous fermentation experiments with a dilution rate of 0.025 h⁻¹: the standard (first) process was conventional free-cell fermentation; the second process was a fermentation in which ethanol was continuously extracted using pervaporation from the MBR; and the third process was ethanol fermentation in which ethanol was extracted by pervaporation and part of the culture was simultaneously removed from the fermentation process. The ethanol yields in three defined fermentation processes were 82, 86, and 95%, respectively. Besides that, they have illustrated that the extracted ethanol concentration in MBRs were six to eight times higher than conventional process.

The main objective of present work was to investigate the enhancement of bioethanol production by integration of conventional fermentation with pervaporation process using a continuous MBR in a comparatively straight-forward application of MBR. For this purpose, first design and fabrication of MBR in laboratory-scale and pervaporation process was completed. Next, two types of continuous fermentation experiments were performed under the same geometrical and physicochemical environment with various dilution rates

with low glucose concentration: conventional continuous fermentation as the standard procedure and continuous fermentation with pervaporation and designed MBR using composite dense PDMS membrane. Finally, based on the results of these two sets of experiments, the effect of ethanol removal on yield and productivity were compared.

16.4.2 EXPERIMENTAL

16.4.2.1 Medium and Microorganism

The microorganism *Saccharomyces cerevisiae* PTCC 24860 was used for ethanol fermentation. The organism was supplied by the Iranian Research Organization for Science and Technology (IROST). For the preparation of seed culture to cultivate microorganisms, the medium was composed of glucose, NH_4Cl , KH_2PO_4 , and yeast extracts: 10, 0.45, 0.2, and 1 g l^{-1} , respectively. The substrate medium was used for ethanol production at optimum condition.¹⁸ The composition of feed tank media was as follows (per liter of pure water): glucose 100 g, yeast extracts 3.0 g, and NH_4Cl 5 g. In addition, potassium hydrogen phthalate 0.1 M and sodium hydroxide 0.1 M were added as a buffer solution to maintain the media pH value of 5.2. Note that the carbon source of the media in batch fermentation before introducing any fresh feed as continuous system was 50 g l^{-1} glucose. These medium were autoclaved at 121°C and 15 psig for 20 min. The inoculum size for batch culture was 3–5% of the working volume.

16.4.2.2 Design of Membrane Bioreactor and Pervaporation System

Figure 16.4(a) shows the design of a laboratory-scale MBR that was fabricated in our Biotechnology Research Lab. Noshirvani University of Technology, Babol, Iran. It could be readily assembled and disassembled between experiments in order to clean and sterilize the various components. A glass column with 30 cm height, 10 cm I.D., and 11 cm O.D. was used as a framework. The flat membrane with useful diagonal of 7.2 cm was fixed at the bottom of the reaction vessel. The bottom of the membrane was evacuated. The DC motor with agitation rate of 200 rpm was used for uniform mixing. Design of the impellers and their configuration was adapted from standard bioreactor design introduced in biochemical engineering and biotechnology texts.¹⁹

Schematic diagrams of the conventional continuous fermentation and continuous pervaporation system to carry out fermentation by well-designed MBR having 40.69 cm^2 effective permeation areas are shown in Figures 16.4(b) and (c), respectively. Fermentation was performed at constant temperature 32°C . The overflow stream was controlled to maintain the constant working volume of 1260 ml in the fermenter, while the fresh feed was continuously pumped. Fermentation broth was well stirred to keep the concentration in the reaction vessel homogeneous. The experiments were conducted at various dilution rates by changing the flow rates of the fresh feed stream. In continuous fermentation with pervaporation, the feed was placed on top of the membrane at atmospheric pressure. The other side of the membrane was evacuated by a vacuum pump (E2M2–Edwards). Vapor-side pressure was kept at lower than 2 mmHg. Permeate vapor was trapped in a liquid nitrogen trap at -196°C .

In these two systems, after 12 h of batch fermentation, when the growth of organism has nearly reached a stationary phase, the fresh media of glucose concentration of 100 g l^{-1} was

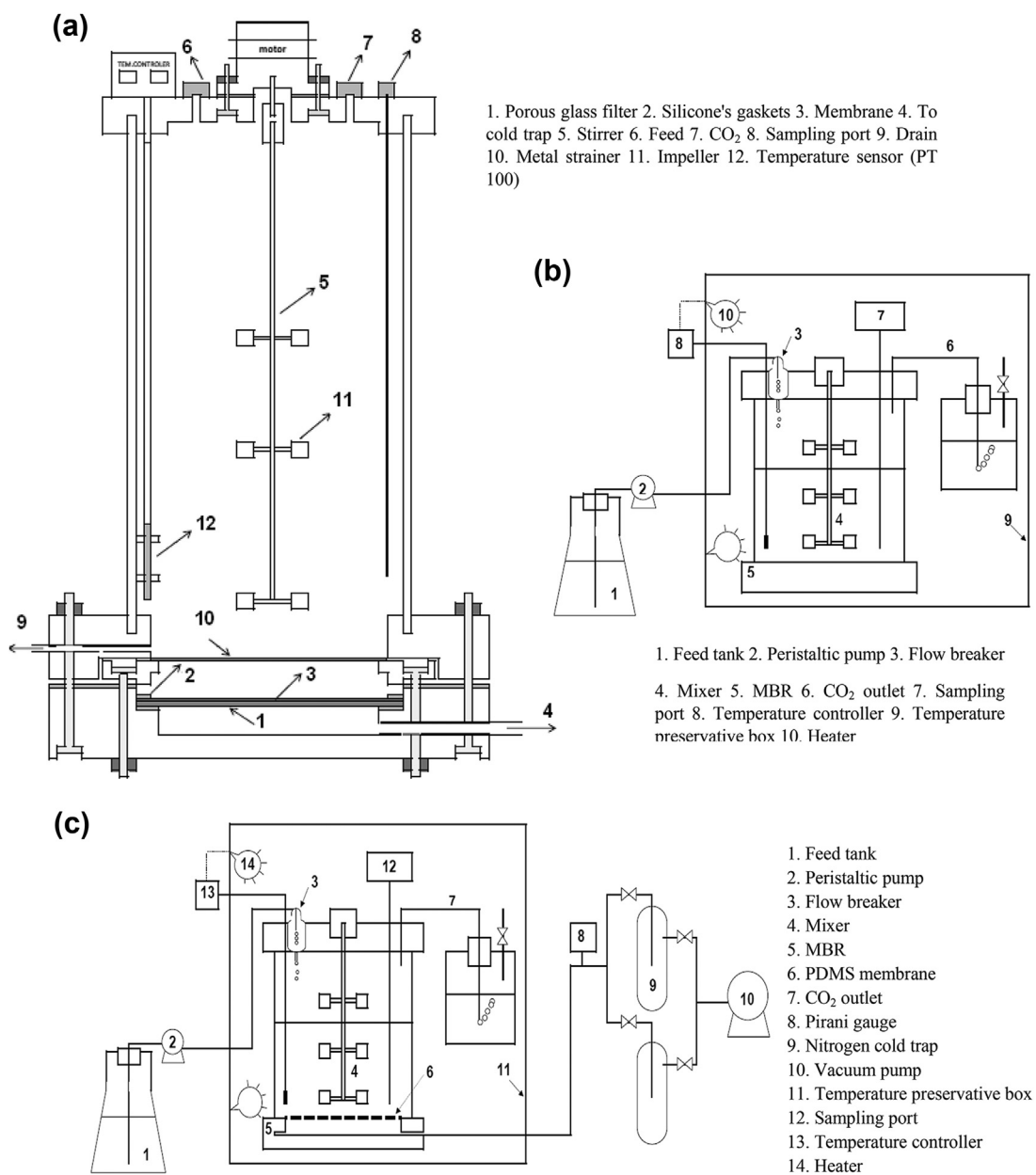


FIGURE 16.4 Schematic diagrams of continuous fermentation system. (a) MBR (b) pervaporation system (c) conventional system.

fed to the bioreactor with defined flow rate. In the pervaporation system, the fresh medium fed to the MBR and pervaporation has started. In continuous operation of MBR, the systems were allowed to come to a steady state condition. Samplings of residue were performed every 4 h to confirm whether the steady state was achieved. When the cell, glucose, and ethanol concentrations remained constant, steady state condition was determined. After sufficient data collection, then for next setting the fresh feed flow rate was changed. The dilution rates of $0.04\text{--}0.24\text{ h}^{-1}$ were based on the ratio of the total working volume of the bioreactor and the calculated and recorded fresh feed flow rates in the range of $50.4\text{--}302.4\text{ ml h}^{-1}$.

16.4.2.3 Membrane

In this work, a dense composite PDMS and asymmetric hydrophobic/organophilic membrane manufactured by Pervatech Corporation (Netherlands), which is well known as being an ethanol-permselective membrane, was used. The membrane was flat sheet form, and it was tested for the enrichment of produced ethanol in continuous fermentation using pervaporation method. The thickness of the membrane was $3\text{--}5\text{ }\mu\text{m}$ PDMS on the top layer, supported by PET with a thickness of $100\text{ }\mu\text{m}$. The intermediate UF membrane was a type of polyimide (PI) with a thickness of $150\text{ }\mu\text{m}$.

16.4.2.4 Analysis

The cell concentration was evaluated via optical density measurement based on developed calibration curve. The optical density was measured at 620 nm using a spectrophotometer (Unico, USA). Determination of glucose concentration was performed in collected 3 ml samples, and the cell from the sample was separated by micro centrifuge at 7000 g for 7 min (Hermle, model: Z 233 M-2 (Germany)). Finally, glucose concentration was determined by colorimetric method using DNS reagent.²⁰ Also, ethanol concentration was measured using a gas chromatograph (Agilent, 7890A) equipped with a flame ionization detector (FID). The stainless steel packed column of 1.83 m length and 2.1 mm I.D., $80/100$ mesh Porapak Q (Supelco, USA) was used. The initial oven temperature was $120\text{ }^{\circ}\text{C}$ held for 1 min . Then, oven temperature was programmed with a rate of $40\text{ }^{\circ}\text{C min}^{-1}$ until it reached $185\text{ }^{\circ}\text{C}$, and remained at the set temperature for 8.5 min . The detector temperature was $225\text{ }^{\circ}\text{C}$. Nitrogen as the carrier gas with a flow rate of 30 ml min^{-1} was used. Also, 2-propanol or propionic acid (Merck, Germany) was prepared in 10% (v/v) as internal standard and added by a micropipette (Labnet, Germany), exactly $50\text{ }\mu\text{l}$ into 0.5 ml of each sample.

16.4.3 RESULTS AND DISCUSSION

16.4.3.1 Conventional Continuous Fermentation

At first, in order to obtain the performance of basic cultivation process, conventional continuous fermentation experiments with dilution rates of $0.04\text{--}0.24\text{ h}^{-1}$ were performed.

The steady state was achieved after cell and ethanol concentrations were steady and kept constant. At the end of a defined steady state, the fresh feed flow rate was subjected to any necessary changes according to the research plan. The obtained data are summarized in [Table 16.3](#). The ethanol concentrations were in the range of 0.41–4.1 %wt (4.10–40.53 g l⁻¹). The ethanol yield is based on cell concentration ($Y_{P/X}$); which was in the range of 1.59–2.05 g ethanol g⁻¹ cell. Also, the ethanol productivities were calculated from 0.75 to 4.27 g (l h)⁻¹ (8–79% of the theoretical value). Maximum productivity was obtained at dilution rate of 0.14 h⁻¹. In addition, increasing dilution rate caused a decrease in the cell and ethanol concentrations. Because of short retention time and a flow rate that was mismatched at final dilution rate (washout), the cell and ethanol concentrations may tend to reach to zero.

16.4.3.2 Continuous Fermentation with Pervaporation

Continuous fermentation processes were carried out in a well-designed MBR. The performance of MBR with regard to ethanol extraction by pervaporation at various dilution rates was investigated. The MBR was very smoothly shifted from one to another steady state condition. In order to secure steady state condition, approximately two to three times fermenter volumes of fresh medium must be pumped through bioreactor. During the course of fermentation, the obtained results showed that ethanol concentration in the permeate vapor was constant that was six to seven times higher than ethanol concentration in the fermentation broth. The ethanol yield based on the cell concentration ($Y_{P/X}$) was computed 1.36 to 1.73 and ethanol concentration was measured between 0.40 wt% and 4.05 wt% (4.01–40 g l⁻¹) in broth and 2.71–22.89 wt% (26.93–215.12 g l⁻¹) in permeate. The ethanol concentration in the broth was lower than in conventional system because of the ethanol extraction by pervaporation and elimination of ethanol inhibition. The cell concentration in MBR was much higher than conventional fermentation, since broth was filtered. The ethanol productivity was in the range of 0.8–4.9 g(l h)⁻¹ (9–91% of the theoretical value). This value was more than the ethanol productivity in conventional continuous fermentation. These are advantages of the new system. The results are summarized in [Table 16.4](#).

TABLE 16.3 Experimental results of conventional continuous fermentation

Dilution rate, h ⁻¹	Concentration in broth, g l ⁻¹			$Y_{X/S}$	$Y_{P/S}$	$Y_{P/X}$	Productivity, g (l h) ⁻¹
	Ethanol	Glucose	Cell				
0.04	40.53	10.96	25.51	0.29	0.46	1.59	1.62
0.09	38.52	15.48	24.00	0.28	0.46	1.61	3.40
0.14	30.50	26.10	20.5	0.28	0.41	1.49	4.27
0.19	18.12	45.88	13.00	0.24	0.33	1.39	2.83
0.24	4.10	71.00	2.00	0.07	0.14	2.05	0.75

TABLE 16.4 Experimental results of continuous fermentation with pervaporation

Dilution rate, h^{-1}	Concentration in broth, g l^{-1}			Ethanol concentration in Permeate g l^{-1}	$Y_{X/S}$	$Y_{P/S}$	$Y_{P/X}$	Productivity g (l.h)^{-1}
	Ethanol	Glucose	Cell					
0.04	40.00	2.50	31.78	215.12	0.33	0.44	1.36	1.97
0.09	37.77	4.03	31.20	203.19	0.32	0.43	1.22	3.96
0.14	29.50	16.31	26.19	168.03	0.31	0.38	1.22	4.90
0.19	17.43	38.34	16.23	108.50	0.26	0.31	1.17	3.11
0.24	4.01	67.45	2.54	26.93	0.08	0.135	1.73	0.8

16.4.3.3 Performance of Membrane Bioreactor with Continuous Pervaporation System

The improvement of MBR by pervaporation was clearly observed since both cases were compared under the same physical and geometrical conditions. The main goals of this research were to find out about membrane effects in the MBR compared to conventional continuous fermentation. Pervaporated ethanol in MBR was clear, glucose-free, and highly concentrated. This stream should be monitored more than as a product of the conventional fermenter. On the other hand, PDMS membrane has been found to be very durable. There was a slightly low tendency for the cells to deposit on membrane and form a biolayer on membrane surface.

Figure 16.5 shows the results of continuous fermentations with a medium containing 100 g l^{-1} glucose. The glucose, cell, cell production rate, and ethanol concentrations were plotted against the dilution rate. The solid line shows the results of continuous fermentation with pervaporation, and the dotted line represents the conventional continuous fermentation. As it was expected, ethanol and cell concentrations decreased with an increase in dilution rate. At high dilution rate or low retention time, there was no sufficient time for cells to replicate; therefore, ethanol production drastically decreased. In addition, the cell production rate increased with an increase in dilution rate to 0.14 h^{-1} and after that it decreased due to cell washout. At low dilution rate, substrate residence time became longer, and consequently the glucose concentrations in both systems were decreased.

When higher cell concentration in the fermenter was obtained, the ethanol production increased. Therefore, if ethanol is not removed from the system, the concentration may gradually increase; accumulation of ethanol may cause product inhibition. This fact that the ethanol concentration in the MBR was kept at approximately the same level as in conventional fermentation implies that ethanol inhibition is removed. It should be noted that the ethanol permselective property of the PDMS membrane facilitated the removal of ethanol inhibition (otherwise ethanol accumulation may take place). As a result, highly concentrated and clean ethanol was obtained by pervaporation. According to the increase of cell densities and the reduction of ethanol inhibition level, along with high residence time, high glucose consumption was accomplished. All of these events are due to positive response of the

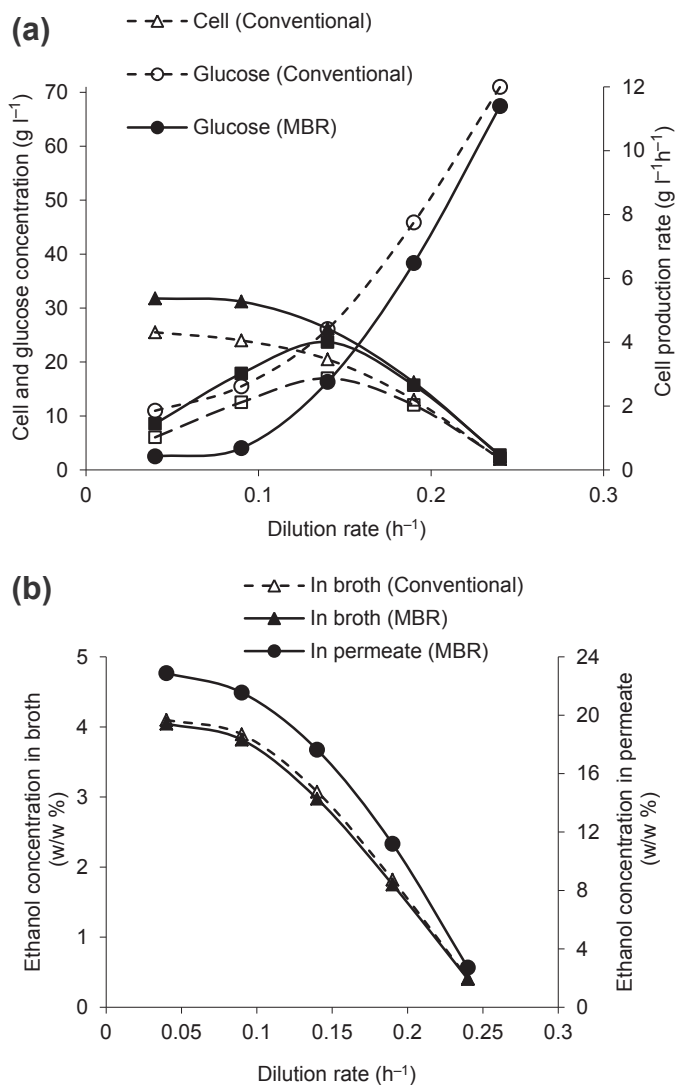


FIGURE 16.5 Changes in glucose, cell, and ethanol concentration as function of dilution rate in continuous fermentation experiments.

membrane. The gap between the solid and dotted lines in Figure 16.5 demonstrates high performance of MBR.

At the dilution rate of 0.04, for instance, the performance of MBR was shown that glucose consumption has increased to 97.5% along with higher cell concentration, while this value was 89% in conventional continuous fermentation. Also, ethanol concentration in MBR was almost the same level as compared with the conventional process. Ethanol concentration in permeate was 215 g l^{-1} , which was approximately six times higher than that in the

conventional bioreactor. One of the most important factors to be considered in conventional fermentation is downstream processing for ethanol recovery, where the cost of recovery is proportional to the amount of liquid to be handled and is inversely harmonized to product concentration. In this work, the integration of continuous fermentation and membrane separation in the same unit enhanced the performance of MBR. In addition, there was no need to have ethanol recovery unit. It was observed that low dilution rate resulted in complete glucose consumption, where at low fresh feed flow rate glucose concentration in the broth nearly reached zero. In MBR with pervaporation technique, complete consumption of substrate occurred when the fresh feed flow rate was low (minimum dilution rate).

As data are illustrated in Figure 16.6(a), with an increase in dilution rate, yield of fermentation was decreased. In MBR, yield of cell density was based on substrate consumption ($Y_{X/S}$), which was more than the conventional process that was due to ethanol permeation, which resulted in high cell concentration in MBR. The yield of the ethanol concentration is based on substrate consumption ($Y_{P/S}$) and cell density ($Y_{P/X}$). The obtained data are illustrated in Figure 16.6(b); the yield in conventional fermentation was less than MBR. It seems that this was due to high glucose consumption and high cell concentration that occurred in MBR. With an increase in dilution rate, $Y_{P/X}$ was decreased until it reached a dilution rate of 0.19 h^{-1} ; after that, the yield was drastically increased. The cell density tends to be zero at high dilution rates, and it seems that the fresh media washed out all of the existing cells in the fermentation broth. The ethanol productivity is the most important factor for the selection of suitable process. For computation of productivity, total ethanol production must be calculated. Total ethanol production was defined as the net weight of ethanol in conventional fermentation and the sum of the net weights of ethanol in the permeate phase and the remaining (the residue) ethanol in the MBR. The ethanol productivity was the total ethanol production divided by the fermenter volume per unit time.

Although the ethanol concentration in the residue stream as shown in Figure 16.5(b) decreases with increasing dilution rate, ethanol productivity actually increases up to the dilution rate of 0.14 as illustrated in Figure 16.7 since the productivity is generally related to the produced ethanol concentration and the dilution rate. After that maximum point, it begins to decrease because of cell washout. The maximum ethanol productivity of the MBR was 4.9 g(l h)^{-1} , which was a 15% increase over the maximum productivity of 4.27 g(l h)^{-1} in conventional continuous fermentation. Interestingly, maximum productivity does not necessarily occur at a dilution rate corresponding to the maximum conversion of substrate or the maximum permeate ethanol concentration. Therefore, optimization is based on productivity, permeate ethanol concentration, residual substrate, etc.

Performance of the membrane used in pervaporation process was deliberated by total flux and the separation factor. The separation factor of the aqueous ethanol solution was defined as follows:

$$\text{Separation factor } (\alpha) = \frac{[C_{Eth}/C_{H_2O}]_{\text{Permeate}}}{[C_{Eth}/C_{H_2O}]_{\text{Feed}}}$$

where C_{Eth} and C_{H_2O} are the weight fractions of ethanol and water, respectively.

As shown in Figure 16.8, the separation factor and total flux across the membrane was almost constant during the continuous fermentation; the obtained values are $7 \text{ g m}^{-2} \text{ h}^{-1}$

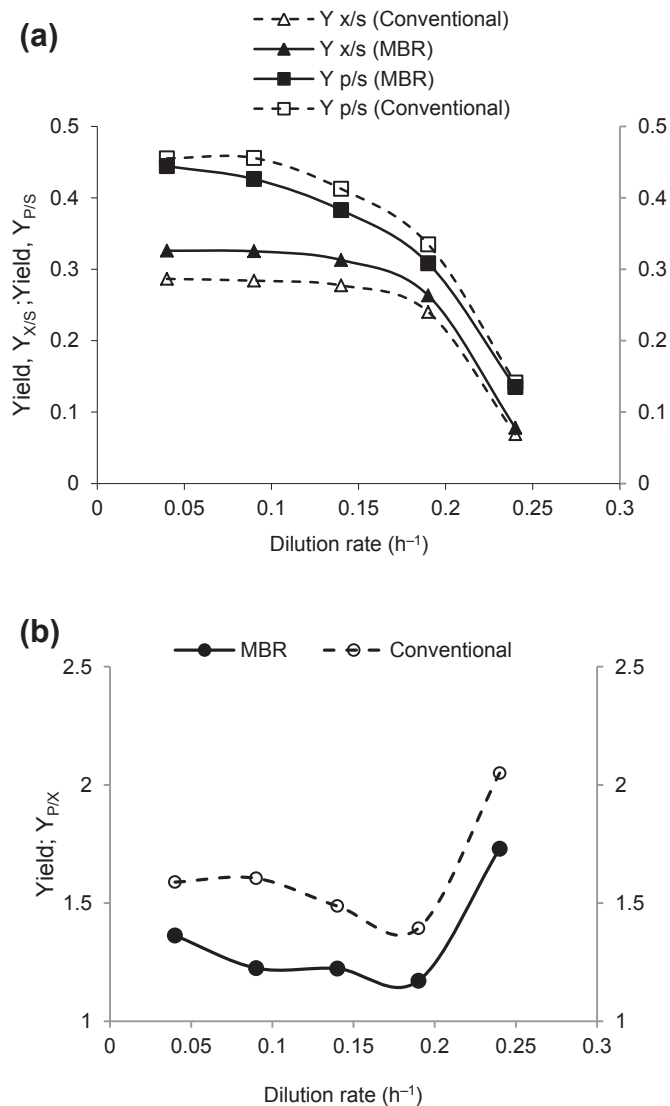


FIGURE 16.6 Changes in yields as function of dilution rate in continuous fermentation experiments.

and $780 \text{ g m}^{-2} \text{ h}^{-1}$, respectively. These values indicated that the PDMS membrane did not show significant changes due to biofouling or deposition of free cells, since there is a slightly low tendency for the cells to form a biofilm layer on the membrane surface. It was found that the composite dense PDMS membrane was quite durable for the long operation time. But it seems that, in long duration, the permeation properties through the membrane could be changed by the adsorption of microorganisms and inorganic salts. Also the additional

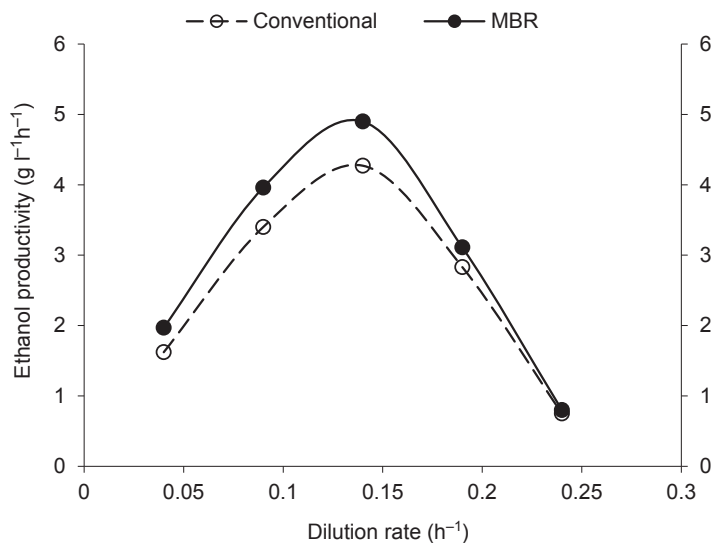


FIGURE 16.7 Changes in ethanol productivity as function of dilution rate in continuous fermentation experiments.

nutrients were not completely consumed and the nonvolatile byproducts are not removed by pervaporation. These technical failures may cause accumulation resistances and fouling in the broth–membrane interface.

The MBR by pervaporation with a rather simple configuration and low glucose concentration in medium for continuous ethanol fermentation at different dilution rates was performed. A dense composite PDMS membrane was chosen for its consistent and stable flux, high ethanol selectivity, and high stability. Ethanol concentration in broth and permeate at dilution rate of 0.04 h^{-1} and glucose concentration of 100 g l^{-1} in the medium were 40 g l^{-1} and 215 g l^{-1} , respectively. The yield of biomass on substrate ($Y_{X/S}$) and the yield of product on substrate ($Y_{P/S}$) were 0.33 and 0.44, respectively. Furthermore, the yield of product on biomass ($Y_{P/X}$) was 1.36. On the other hand, the ethanol productivity of the MBR was 91% of the theoretical value or $1.97 \text{ g (l h)}^{-1}$; this value was 22% higher than conventional continuous fermentation. The obtained values were higher than the reported values by other investigators¹⁷ with media glucose concentration of 200 g l^{-1} . Maximum ethanol productivity was 4.9 g (l h)^{-1} at dilution rate of 0.14 h^{-1} . Pervaporated ethanol concentration was approximately six to seven times higher than that in the broth. This value was consistent and similar to the reported data in the literature.^{5,17}

A 7–22% increase in ethanol productivity was achieved compared to conventional continuous fermentation; this value was higher than reported values by other investigators with different and complex configuration of MBR, membranes, and higher glucose concentration in their media.^{5,17} On the other hand, the productivity was approximately the same as in an experimental investigation with 150 g l^{-1} glucose in medium with an ICR.¹ MBR was able to produce ethanol even at high substrate concentrations ($50\text{--}230 \text{ g l}^{-1}$). Figure 16.9(a)

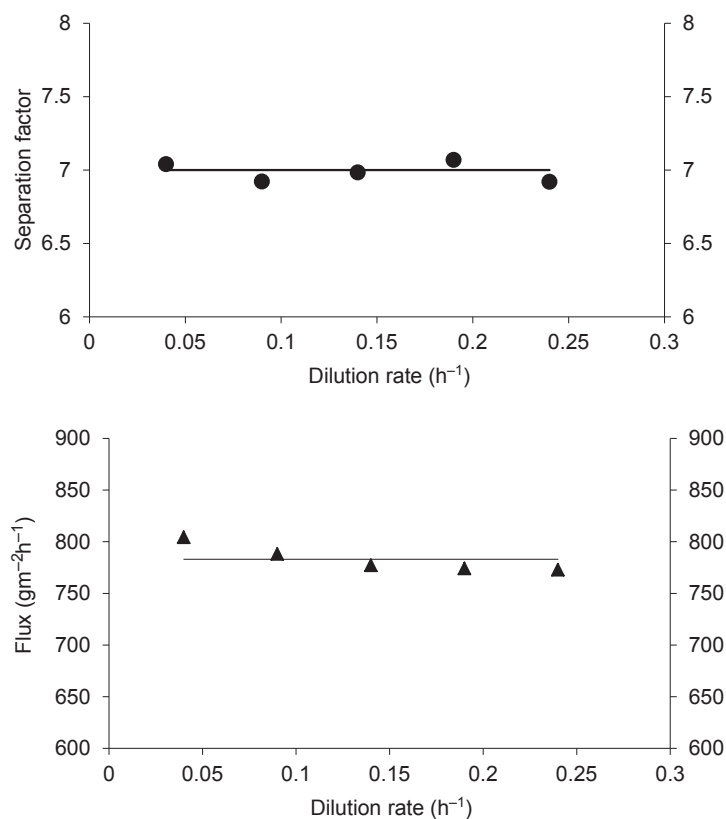


FIGURE 16.8 Pervaporation performance through the permselective polydimethylsiloxane membrane.

shows changes of cell and glucose concentration and ethanol productivity versus substrate concentration. In addition, changes of ethanol concentration in broth and permeate phase are illustrated in Figure 16.9(b). Experiments were performed at optimum dilution rate of 0.14 h^{-1} . Table 16.5 shows ethanol concentrations in broth and permeate with various substrate concentrations. As carbohydrate concentration increased, the ethanol concentrations in permeate also increased, while productivity from $5.04 \text{ g (l h)}^{-1}$ for 170 g l^{-1} substrate decreased to $4.56 \text{ g (l h)}^{-1}$ for 235 g l^{-1} substrate. Decrease in ethanol productivity at very high substrate concentration might be due to MBR limitation as cell densities may gradually accumulate in the retentive broth. In addition, biofouling may form on membrane surface for high dense broth. In order to enhance ethanol productivity in MBR with very high substrate concentration, more than 200 g l^{-1} of either a different type of membrane with high ethanol selectivity must be used or another configuration of MBR with high flux area is required. This issue may require more investigation; further research has to be conducted to justify the existing facts.

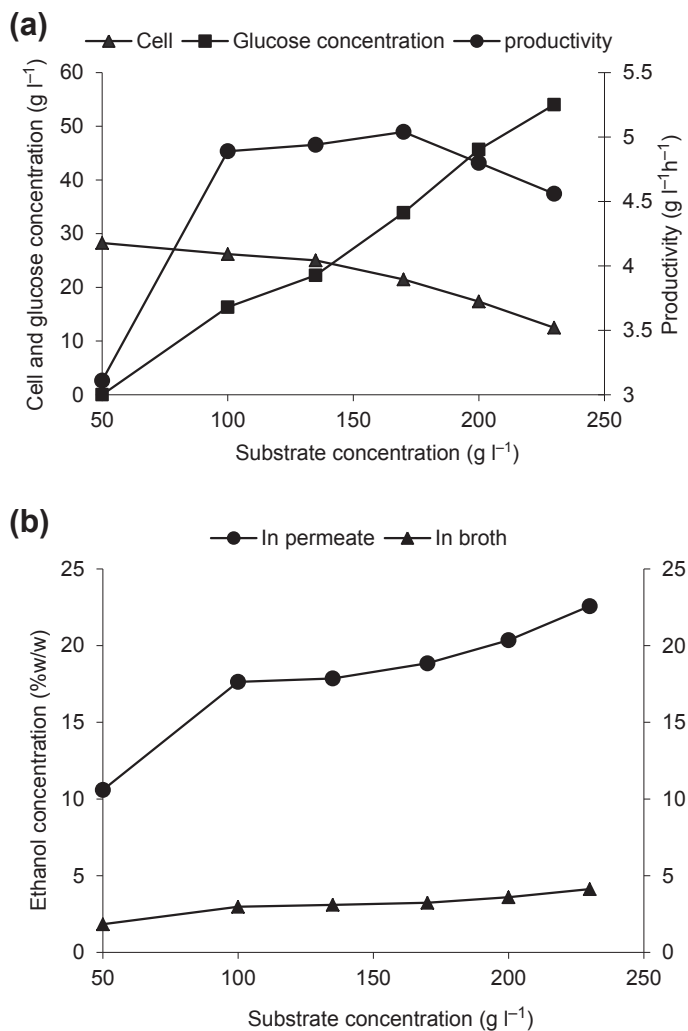


FIGURE 16.9 Profiles of glucose, cell, ethanol concentration, and productivity in membrane bioreactor with high substrate concentration.

TABLE 16.5 Ethanol production in membrane bioreactor with high substrate concentration

Glucose concentration, g l ⁻¹	Ethanol concentration, g l ⁻¹		Cell, g l ⁻¹	Glucose, g l ⁻¹	Productivity, g (l h) ⁻¹
	Broth	Permeate			
50	18.24	102.83	28.26	0	3.11
100	29.50	168.00	26.19	16.31	4.89
135	30.73	170.02	25.02	22.24	4.94
170	32.04	178.97	21.47	33.9	5.04
200	35.59	192.51	17.35	45.67	4.80
230	40.78	212.22	12.48	54.03	4.56

16.4.4 CONCLUSION

It was concluded that MBR can easily be operated without ethanol inhibition with high ethanol productivities using *Saccharomyces cerevisiae* PTCC 24860. The obtained data were compared to conventional continuous fermentation and continuous fermentation with pervaporation. At first, laboratory-scale MBR and pervaporation processes were designed and fabricated. The MBR was easily assembled and disassembled. Also, the proposed model can be easily applied for design of a large-scale MBR for production of ethanol concentration as high as 215 g l^{-1} . A dense PDMS membrane was used for pervaporation of ethanol. A medium containing 100 g l^{-1} glucose was fermented with dilution rates of $0.04\text{--}0.024 \text{ h}^{-1}$. Increase in dilution rate caused an increase in glucose concentrations and decreased cell densities. At 32°C , maximum specific cell growth of 0.14 h^{-1} was achieved. Comparing the MBR performance and conventional continuous fermentation showed that in MBR, ethanol inhibition was removed, cell density was increased, and highly concentrated, and clean ethanol as product was recovered. There was no need to have downstream processing and separation cells. All of these phenomena are counted as advantages of membrane separation resulting in saved energy and making the process viable and economic. In the MBR fermentation system, ethanol productivity was increased by 22%. The permeate stream was free from cells and substrate. It was a highly concentrated ethanol solution, as ethanol concentration reached 215 g l^{-1} . In addition, at high flow rate, the performance of membrane permeation system was similar to the conventional fermentation. Finally, the performance of the pervaporation system illustrated that PDMS membrane was very durable, because there was a little tendency for the cells to form a biofilm layer on the membrane surface.

Acknowledgments

The authors wish to express their special thanks to K. Alinezhad from I.O.O.C company for his technical support and operational assistance. We also thank the Afagh and KGW Isotherm companies for their sincere cooperation and technical supply of equipment and spare parts. We express our special thanks to I.F.C.O for their financial support, which made this research possible.

References

1. Najafpour G, Younesi H, Syahidah Ku Ismail K. Ethanol fermentation in an immobilized cell reactor using *Saccharomyces cerevisiae*. *Bioresour Technol* 2004;**92**:251–60.
2. Melvydas V, Gedminiene G, Jarmalaite I, Capukoitiene B, Nemceva L. Initial analysis of highly competitive yeast strains promising for ethanol industry. *Biologija* 2006;**3**:63–6.
3. Kapse V, Ghosh S, Raghuvanshi F, Kapse S, Khandekar U. Nanocrystalline $\text{NiO} \cdot 0.6\text{ZnO} \cdot 0.4\text{Fe}_2\text{O}_4$: a novel semi-conducting material for ethanol detection. *Talanta* 2009;**78**:19–25.
4. Rendleman CM, Shapouri H, Policy U.S.D.A.O.E., Uses N.. *New technologies in ethanol production*. US Department of Agriculture, Office of the Chief Economist, Office of Energy Policy and New Uses; 2007.
5. Cho CW, Hwang ST. Continuous membrane fermentor separator for ethanol fermentation. *J Membr Sci* 1991;**57**:21–42.
6. Radocaj O. *Ethanol fermentation in a membrane bioreactor*; 1997. University of Toronto. <http://hdl.handle.net/1807/14879>.
7. Nomura M, Bin T, Nakao S. Selective ethanol extraction from fermentation broth using a silicalite membrane. *Sep Purif Technol* 2002;**27**:59–66.

8. Moueddeb H, Sanchez J, Bardot C, Fick M. Membrane bioreactor for lactic acid production. *J Membr Sci* 1996;**114**:59–71.
9. González-Velasco J, González-Marcos J, López-Dehesa C. Pervaporation of ethanol–water mixtures through poly (1-trimethylsilyl-1-propyne) (PTMSP) membranes. *Desalination* 2002;**149**:61–5.
10. Vane LM. A review of pervaporation for product recovery from biomass fermentation processes. *J Chem Technol Biotechnol* 2005;**80**:603–29.
11. Takegami S, Yamada H, Tsujii S. Pervaporation of ethanol–water mixtures using novel hydrophobic membranes containing polydimethylsiloxane. *J Membr Sci* 1992;**75**:93–105.
12. Li L, Xiao Z, Tan S, Pu L, Zhang Z. Composite PDMS membrane with high flux for the separation of organics from water by pervaporation. *J Membr Sci* 2004;**243**:177–87.
13. Xiangli F, Chen Y, Jin W, Xu N. Polydimethylsiloxane (PDMS)/ceramic composite membrane with high flux for pervaporation of ethanol–water mixtures. *Ind Eng Chem Res* 2007;**46**:2224–30.
14. Molina JM, Vatai G, Bekassy-Molnar E. Comparison of pervaporation of different alcohols from water on CMG-OM-010 and 1060-SULZER membranes. *Desalination* 2002;**149**:89–94.
15. Huang Y, Fu J, Pan Y, Huang X, Tang X. Pervaporation of ethanol aqueous solution by polyphosphazene membranes: effect of pendant groups. *Sep Purif Technol* 2009;**66**:504–9.
16. Hoover KC, Hwang ST. Pervaporation by a continuous membrane column. *J Membr Sci* 1982;**10**:253–71.
17. Nakao S, Saitoh F, Asakura T, Toda K, Kimura S. Continuous ethanol extraction by pervaporation from a membrane bioreactor. *J Membr Sci* 1987;**30**:273–87.
18. Esfahanian M, Najafpour GD, Ghoreyshi AA, Younesi H, Ahmad AL. Optimization of ethanol production by *Saccharomyces cerevisiae* as function of pH and temperature: batch fermentation. In: *ICENV 2010, Penang, Malaysia*; 2010.
19. Najafpour GD. *Biochemical engineering and biotechnology*. Elsevier Science; 2006.
20. Thomas LC, Chamberlin GJ, Shute G, Tintometer limited S., England. *Colorimetric chemical analytical methods*. England: Tintometer; 1980.

SUBCHAPTER

16.5

Case Study: Inorganic Zirconia γ -Alumina-Coated Membrane on Ceramic Support*

16.5.1 INTRODUCTION

Membrane separation represents a new type of unit operation, which, ultimately, is expected to be replaced by significant use of conventional separation processes. The advantage of membrane separation lies in its relatively low energy requirements. The reason for low energy consumption is that, unlike conventional processes such as distillation, extraction, and crystallization, it generally does not feature phase transition. The rapid development of membranes in wastewater treatment encourages the development and fabrication of an inorganic membrane. The results expand knowledge and produce various types of ceramic membrane.¹

The ceramic membrane has a great potential and market. It represents a distinct class of inorganic membrane. In particular, metallic-coated membranes have many industrial applications. The potential of ceramic membranes in separation, filtration, and catalytic reactions has favored research on synthesis, characterization, and property improvement of inorganic membranes because of their unique features compared with other types of membrane. Much attention has focused on inorganic membranes, which are superior to organic ones in thermal, chemical, and mechanical stability, and resistance to microbial degradation.

Alumina membranes have recently received considerable attention for their use in a wide range of applications. Alumina is the most cost-effective and widely used material in the family of engineering ceramics. The raw materials from which this high-performance technical-grade ceramic is made are readily available and reasonably priced, resulting in good value for the cost in fabricated alumina shapes, with an excellent combination of properties and an attractive price. For commercial membrane applications, α - Al_2O_3 and γ - Al_2O_3 are the most common membranes. α - Al_2O_3 membranes are well known for their thermal and hydrothermal stabilities beyond 1000 °C.

An inorganic membrane can be prepared by various methods such as sol–gel, phase separation, and leaching.^{2,3} The sol–gel process is considered the most practical method among those used to prepare inorganic membrane. Sol–gel processing is a simple technology in principle but requires considerable effort to become of practical use. The advantage of this technology is

*This case study was partially written with contributions from:

Abdul Latif Ahmad, Membrane Technology, School of Chemical Engineering, Engineering Campus, Universiti Sains Malaysia, Nibong Tebal, Pulau Pinang, Malaysia.

the ability to produce high-purity γ -alumina membranes at low temperatures (400–600 °C). The pore size distribution is very narrow, and additional elements can be added.^{4,5} However, only γ -alumina membranes have the disadvantage of a poor chemical and thermal stability. Below pH 4, they dissolve to form Al^{3+} ions; above pH 12, the membrane will form $\text{Al}(\text{OH})_4^-$. $\gamma\text{-Al}_2\text{O}_3$ has a highly defective spinel structure and can be considered as an AlO_xH_y species, which dissolves more slowly, in low and high pH of the aqueous phase as strong hydroxides behave.

Meanwhile, at higher temperatures (600–900 °C), pore growth occurs. Above 850 °C, the transformation of γ -alumina upon heating is: $\gamma \rightarrow \theta \rightarrow \alpha$ -alumina. The stable $\alpha\text{-Al}_2\text{O}_3$ phase forms above 1000 °C by nucleation and growth.⁶ In the transition of alumina derived from boehmite gels, the pores are as large as the grains. These pores are unable to stop grain boundary migration when $\alpha\text{-Al}_2\text{O}_3$ forms above 1100 °C. Hao et al.⁷ stated that the phase transformation from $\gamma\text{-Al}_2\text{O}_3$ to $\theta\text{-Al}_2\text{O}_3$ occurred at 900 °C for pure alumina membranes. With further heat treatment, 1200 °C and higher, a complete transformation of the $\theta\text{-Al}_2\text{O}_3$ to the high temperature $\alpha\text{-Al}_2\text{O}_3$ phase is observed.

Foreign additives can affect the phase transformation as well as the pore structure at high temperatures. To inhibit dissolution of alumina species or pore growth, the particles are coated with an inert component such as zirconia, titania, and lanthana.¹ It has been reported that the effect of zirconia addition in alumina retarded the grain growth behavior of the alumina membrane. It was found that the ZrO_2 prevents abnormal growth of Al_2O_3 during heat treatment.^{1,3} The effect of zirconia on the phase transformation could be explained by the fact the presence of the zirconia on the γ -alumina surface may reduce the possibility of the nucleation of α -alumina, thus raising the phase transformation temperature.

In this case study, a zirconia-alumina membrane has been developed using the sol–gel technique with and without support.^{6,7} The porous ceramic was prepared to fabricate the membrane support. A thin film of aluminum and zirconium was formed on the porous ceramic support. Unsupported membrane was also prepared. The unsupported membrane was not strong enough to hold a high-pressure gradient; it was very fragile and not useful for independent use. The supported membrane on a highly porous ceramic was quite strong, but the coating covered the solid surface. The ceramic support was strong enough to hold any mechanical forces. Apart from the ceramic support, polyvinyl alcohol (PVA) was prepared to be used as a binder in the preparation of zirconia–alumina membranes to avoid the formation of cracks on the membrane surface. The overall process in the fabrication of membranes is shown in Figure 16.10. The uniform coating and crack-free membranes were examined by scanning electron microscopy (SEM) and light microscope (LM) photographs shown in Figures 16.11–16.14. The main part of the research activities was the preparation and development of an inorganic membrane with and without support (zirconia-coated on γ -alumina). The membrane surface was characterized by SEM and LM.

In preparing the membrane, a clear sol was obtained by the addition of acid into the aluminum sec-butoxide sol to peptize the sol and obtain a stable colloid solution. Aluminum monohydroxides formed by the hydrolysis of aluminum alkoxides, which are peptizable to a clear sol. Peptization was performed by the addition of acid and heat treatment for a sufficient time. It was found that stable sols cannot be obtained when the concentration of the peptization acid is too low.

The critical range for inorganic acids such as nitric, hydrochloric, and perchloric acids is 0.03–0.1 mol/mol of hydroxide. In this study, nitric acid was used as the peptizing agent.

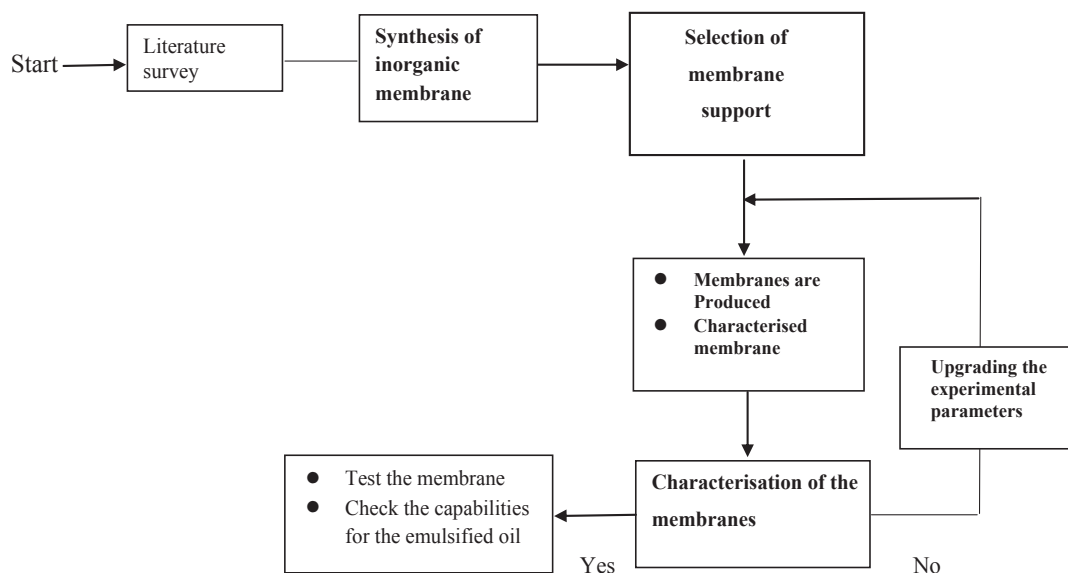


FIGURE 16.10 Overall scheme and stages involved for fabrication of inorganic membrane.

The resulting sols were poured into Petri dishes and dried in an oven at a controlled drying rate to obtain a gel layer. The molar ratio of zirconia salt to alumina was a controlling variable in obtaining crack-free zirconia-coated γ -alumina membranes.^{8–11} Finally, the dried gel was sintered and heat treated at 500 °C for 3 h.

Support materials were prepared by blending the fine power as stated in the later part of this case study. PVA was used as the binder. The organic macromolecule was used to create sufficient pores in the material when burned out after a solid strong support was formed. Drying was performed in a high-temperature furnace. The shape and thickness of the support were based on the mass of the material and the way it was molded.

Once the membrane was successfully produced, it was analyzed for characterization and scanning. The sol–gel technique was successfully used to obtain a crack-free unsupported membrane, which was expected to have pore size of 1–2 nm. The development of the crack-free membrane may not have the same strength without strong, solid support. The next stage of this work was to characterize the fabricated membrane. The objectives of this study were to develop a zirconia-coated γ -alumina membrane with inorganic porous support by the sol–gel method and to characterize the surface morphology of the membrane and ceramic support.

16.5.2 MATERIALS AND METHODS

The fabricated membrane consists of inorganic ceramic material with a fine coating. The support materials were prepared by tape casting or slip casting.⁶ Slips were prepared by

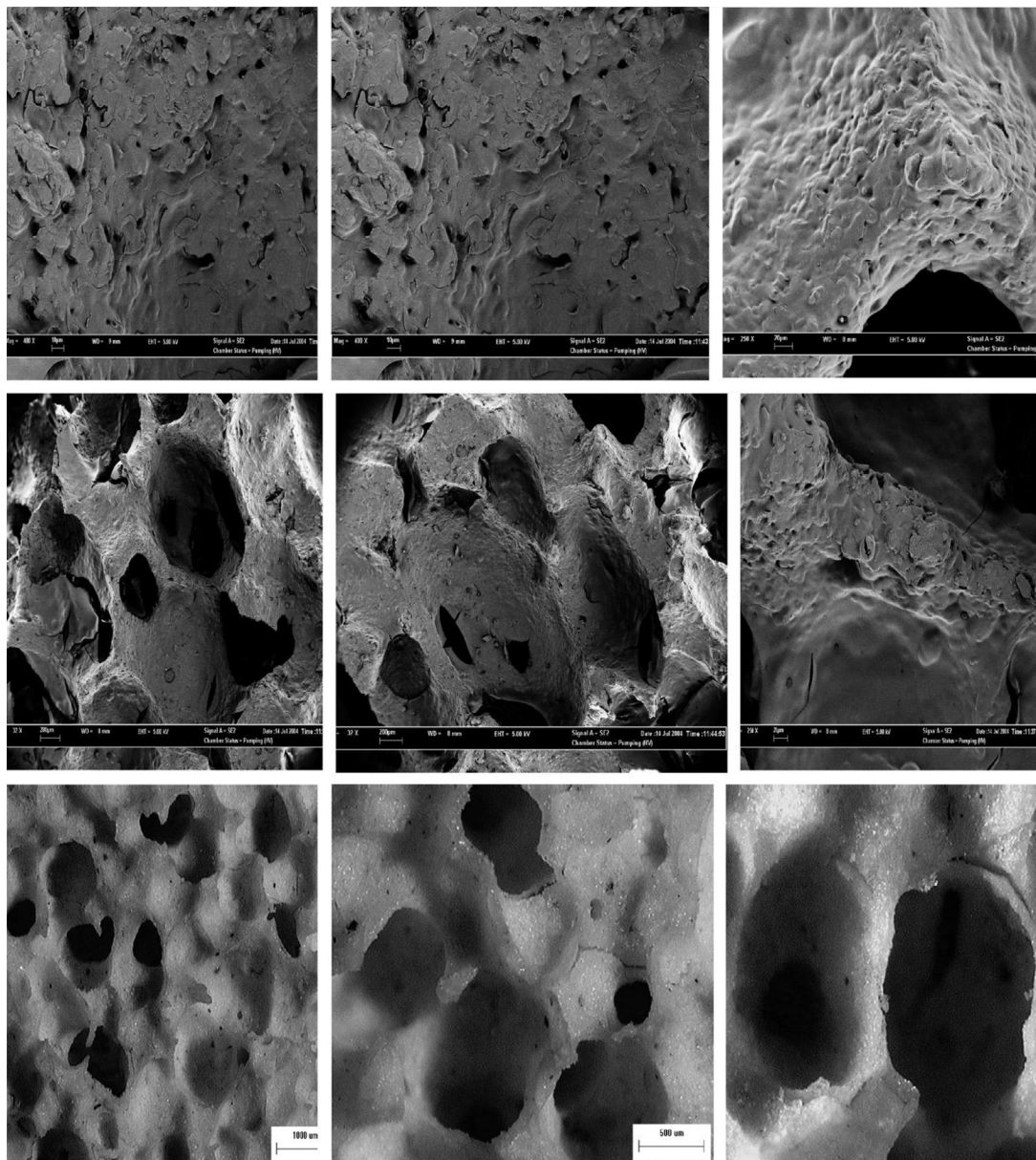


FIGURE 16.11 Nonuniform porous media of the ceramic membrane support.

dispersing the alumina powder in water with the dispersing agent. The slips were homogenized by ball milling for 12–18 h or by ultrasonification for 20 min. The starch was added during vigorous stirring. The addition of starch to the slip created pores⁸ in the material

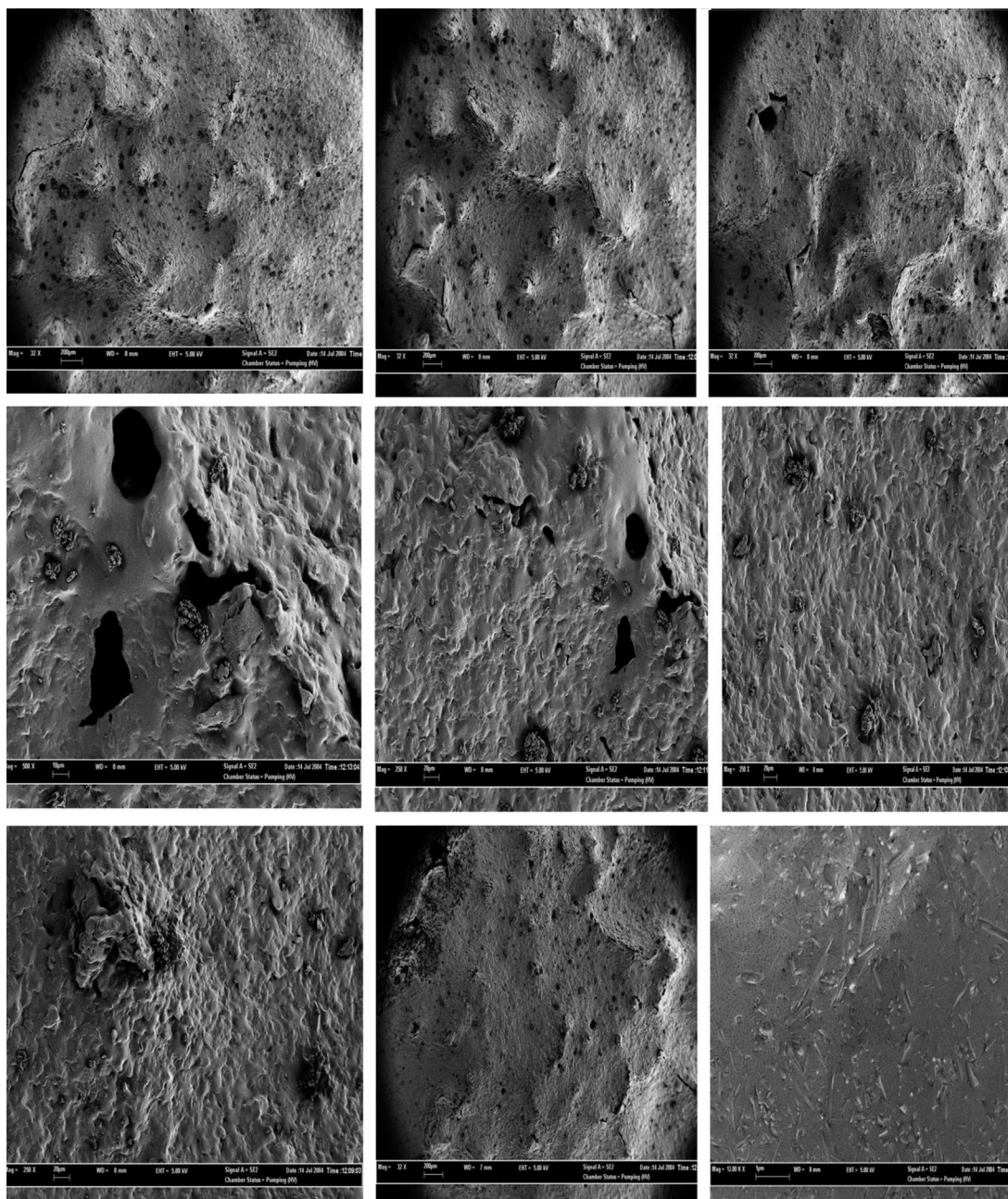


FIGURE 16.12 Alumina-coated on the ceramic membrane.

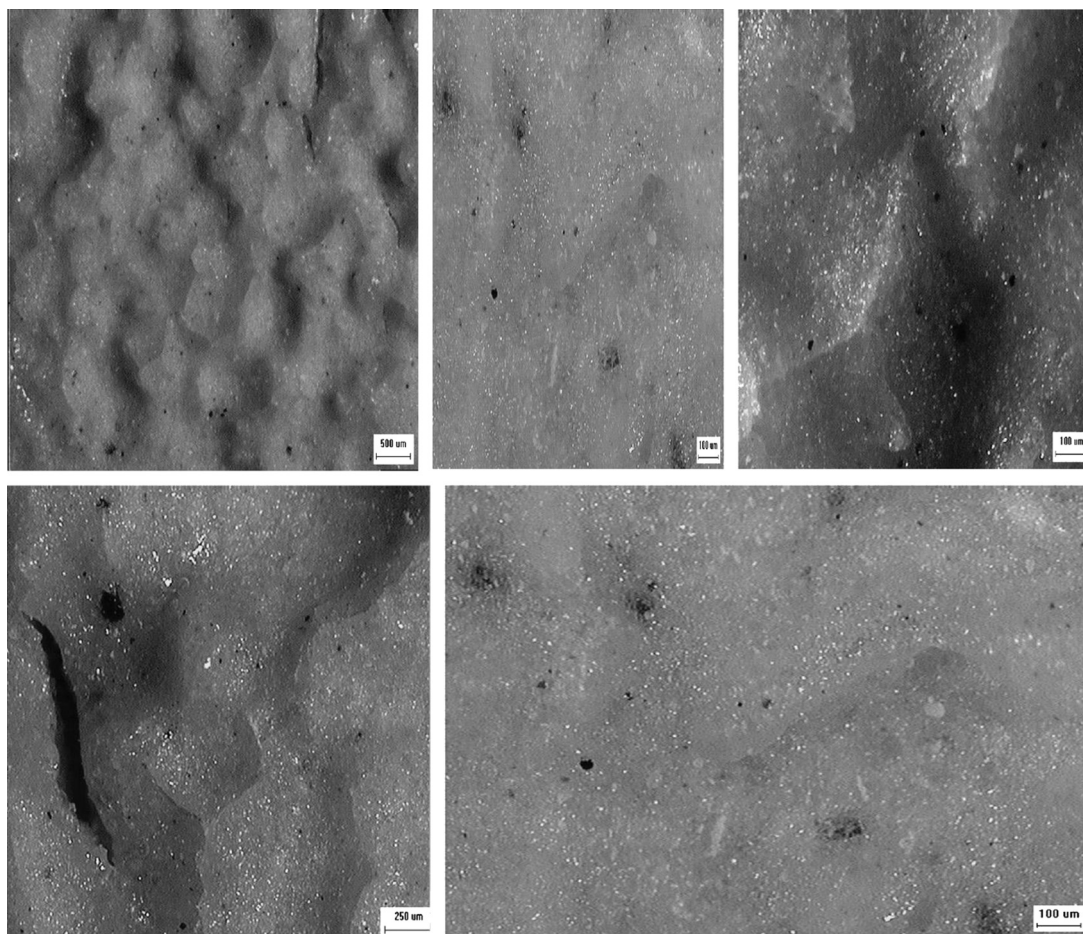


FIGURE 16.13 Zirconia-coated on the ceramic membrane.

when burned out after forming. Then the binder was added while gently stirring the suspension. PVA has been used for a long time as the organic binder of choice in many ceramics applications. The high binding strength, ease of plasticization, water solubility, and cost effectiveness of this polymer have made it a reliable performer.⁸ Drying was provided by application of heat from underneath the tape and by a controlled passage of air over the surface of the tape. Square supports were cut from the tapes and several tapes laminated together in a press at 60 MPa at room temperature to build up the desired thickness of about 1 mm.

Finally, to evaluate the membranes, analysis such as X-ray diffraction (XRD), SEM, TEM, and light scattering were performed at the School of Mineral and Material Engineering, Universiti Sains Malaysia. The last part of the work, testing the produced membrane to remove emulsifier oil from domestic wastewater, was accomplished on a limited budget.

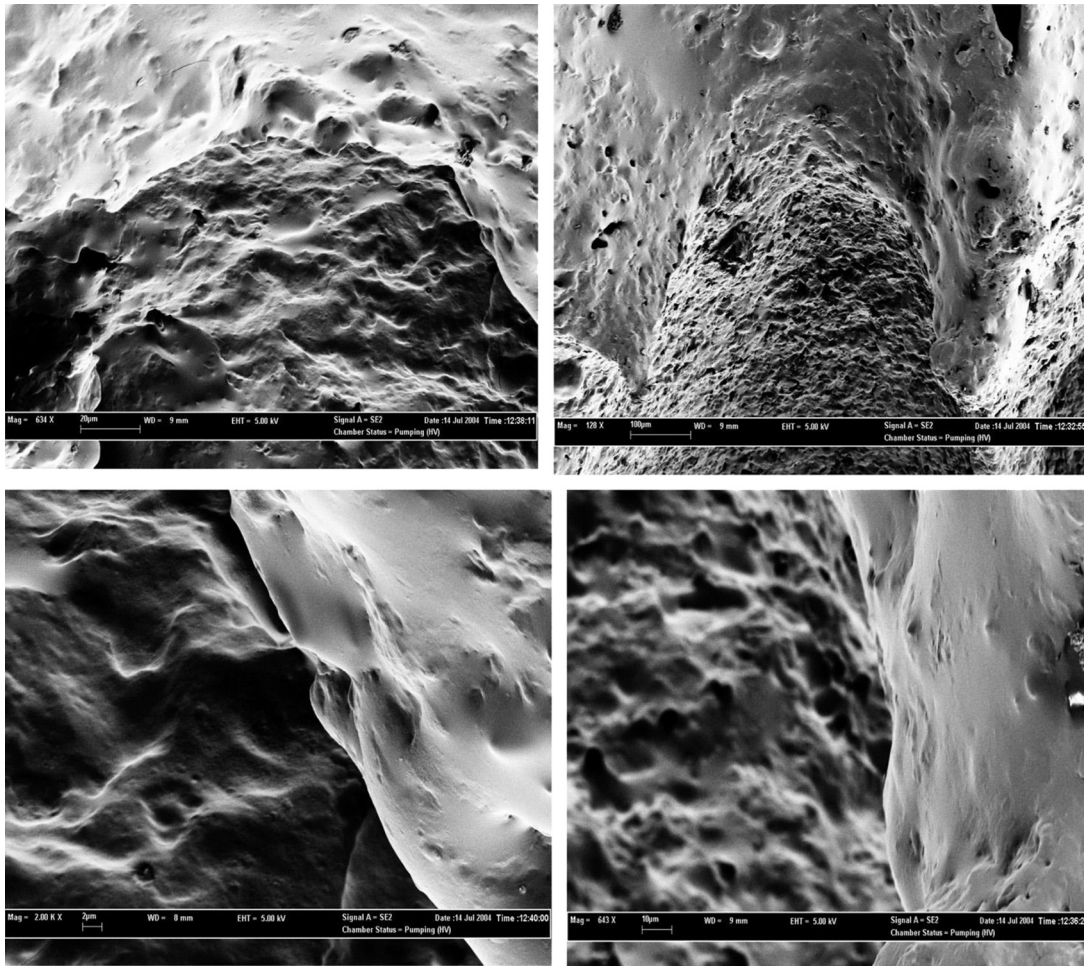


FIGURE 16.14 Mixture of zirconia and alumina-coated on the ceramic membrane.

An experimental rig and membrane module were required. Also, the need for experimental data for the application of the supported membrane may show the real success of this project.

16.5.2.1 Preparation of PVA Solution

PVA was used as a temporary binder owing to its water solubility, excellent binding strength, and clean-burning characteristics. To prepare the PVA solution, 4 g of PVA were added to 100 ml distilled water. The mixture was heated and stirred vigorously until all the PVA was dissolved in the water. This took about half an hour. Peptization was done by addition of 5 ml 1 M HNO_3 to the solution. Finally, the solution was refluxed for 4 h.

The PVA solution was used in the preparation of the zirconia-alumina sol–gel solution. The preparation of the PVA solution can be summarized as follows:

1. 4 g PVA were added to a 250 ml beaker;
2. 100 ml of double-distilled water was stirred vigorously until all the PVA was dissolved;
3. The solution was boiled until all the PVA was dissolved. This step took at least 0.5–1 h;
4. 5 ml of 1 M HNO_3 was added into the solution;
5. The solution was refluxed for 4 h.

16.5.2.2 Preparation of Zirconia-Coated Alumina Membrane

The supported and unsupported membranes were produced by a sol–gel dipping technique. The sol–gel solution was made by using aluminum tri-sec-butoxide and zirconium (IV) oxide. Compared with the pure alumina membrane, the zirconia-coated alumina membrane had high chemical resistances, which allowed steam sterilization and cleaning procedures in the pH range of 0–14. It possessed good pure-heating permeability and high membrane flux in separation and filtration. It had high thermal stability, which was an attractive criterion for catalytic membrane reactors used at high temperatures. The molar ratio of $\text{Al}^{3+}:\text{H}^+:\text{Zr}:\text{H}_2\text{O}$ was 1:0.07:0.15:100, whereas the volumetric ratio on the basis of 100 ml of H_2O is $\text{Al}^{3+}:\text{H}^+:\text{Zr}:\text{H}_2\text{O} = 1:3.88 \text{ ml}:1.0275 \text{ g}:100 \text{ ml}$. The 100 ml of double-distilled water was heated on a hot plate between 80 °C and 85 °C to ensure the formation of $\gamma\text{-AlOOH}$. Aluminum tri-sec-butoxide (14.25 ml) was added to the double-distilled water. The solution was vigorously stirred with a magnetic stirrer until a homogeneous mixture was obtained. HNO_3 (1 M) (3.88 ml) was added to the sol for peptization, and the mixture was again stirred for an additional 15 min. After that, 1.0275 g of ZrO_3 was added into the mixture. The sol was kept at boiling condition in the open flask for 1 h. The PVA solution was added to the mixture according to a PVA: sol ratio of 1:20, and stirred in the mixture continuously. The product was refluxed under continuous stirring at 90 °C for 16–20 h to ensure complete mixing and hydrolysis. The sol was cooled down slowly and left for a few hours. The above steps were repeated with different amounts of ZrO_3 . The sol was dried under ambient conditions until gelation and viscous gel was obtained. The sol was transferred to the support by the dip-coating method to prepare a thin layer of gel on the support. The membrane thickness first increases linearly with the dipping time, until it may reach a limit. It was noted that a thicker and nonuniform gel layer was more liable to crack than a thinner one. A uniform gel layer was obtained by heating and calcination. After dip-coating the sol on the surface of the support, the membrane was heated in the furnace. The furnace temperature started at 30 °C and was raised to 300 °C at a rate of 0.5 °C min^{-1} . The furnace temperature was kept at 300 °C for 0.5 h for relaxation of the gel and to avoid the stress exceeding the elastic strength of the gel. The temperature was raised from 300 to 700 °C at a rate of 0.5 °C min^{-1} . Sintering of the inorganic membrane was done at 700 °C for 5 h. Cooling was conducted at a rate of 1 °C min^{-1} , to ambient temperature, 30 °C.

16.5.2.3 Preparation of Porous Ceramic Support

The preparation of porous ceramic support is summarized in the following sections.

Raw materials.

1. Feldspar potash
2. Ball clay
3. Kaolin
4. Silica power
5. Sodium hexametaphosphate flakes
6. Distilled water
7. PVA 3% solution

Preparation of the PVA solution.

1. 7.5 g of PVA is gradually added to 250 ml of double-deionized water at ambient temperature.
2. Stir the solution until all the PVA is distributed equally.
3. Boil the solution until all PVA is dissolved, and stir the solution carefully. The step should take at least 40 min.
4. After that, 10 ml of 1 M HNO_3 is added to the solution.
5. Reflux the solution for 4 h.

Sieve all the feldspar potash, ball clay, kaolin, and silica powder by mesh, size 90 μm . All the powders were mixed according to mass ratio given below

1. 25% feldspar potash.
2. 25% ball clay
3. 25% kaolin
4. 25% silica powder

Mix 20 g of mixed powder and 25 ml PVA solution to form the concentrated slurry support. A different composition of mixed powder and PVA solution was used.

Dip the sponge in the mixture. After that, put the sponge inside the furnace with the starting temperature at 30 °C, raise the temperature 1 °C min^{-1} up to 1200 °C. Maintain the temperature for 2 h. After heating, decrease the furnace temperature by 1 °C min^{-1} back to 30 °C.

Some experience is needed to perform the last step efficiently. From our previous work, the strength of the ceramic support will increase with a decrease in the amount of dispersion solution.

The advantage of sol–gel technology is the ability to produce a highly pure alumina and zirconia membrane at medium temperatures, about 700 °C, with a uniform pore size distribution in a thin film. However, the membrane is sensitive to heat treatment, resulting in cracking on the film layer. A successful crack-free product was produced, but it needed special care and time for suitable heat curing. Only γ -alumina membrane has the disadvantage of poor chemical and thermal stability.¹²

16.5.3 RESULTS AND DISCUSSION

The vast increase in the application of membranes has expanded our knowledge of fabrication of various types of membrane, such as organic and inorganic membranes.

The inorganic membrane is frequently called a ceramic membrane. To fulfill the need of the market, ceramic membranes represent a distinct class of inorganic membrane. There are a few important parameters involved in ceramic membrane materials, in terms of porous structure, chemical composition, and shape of the filter in use.^{13,14} In this research, zirconia-coated γ -alumina membranes have been developed using the sol–gel technique.

Finally, analytical equipment was used for characterization, such as XRD, SEM, TEM, LM, and light scattering. These were available either in the School of Chemical Engineering or other departments and research centers in the Universiti Sains Malaysia. However, owing to limited access to the high-end analytical equipment to analyze the membrane, the surface morphology of the membrane and the porous ceramic support were only characterized with SEM and LM.

More than 50 samples of successful and unsuccessful membranes for demonstration were fabricated. The successful results are discussed and presented in Figures 16.11–16.14. The porous ceramic supports were fabricated in our research lab.

Figure 16.11 shows SEM micrographs for the porous media of ceramic support at different magnifications. The nonuniformity resulted from the synthetic foam used as a base to absorb the ceramic solution before vaporizing any water from the inorganic mixture. Uniform porous media as a solid support for the membrane was obtained.

Figure 16.12 presents the alumina-coated ceramic membrane. There were opportunities to fabricate a crack-free ceramic membrane coated with γ -alumina. The supported zirconia-alumina membrane on the ceramic support shows an irregular surface. The nonuniform surface of ceramic support caused the irregular surface on the top layer of the membrane. Some of the membrane sol was trapped in the porous ceramic support during coating and caused the irregularity of the membrane surface.

The zirconia membrane was obtained in a unique manner. Figure 16.13 shows light micrographs of the zirconia-alumina membrane coated on the ceramic support. The nonuniform and crater-filled surface of the ceramic support was covered by the zirconia-alumina membrane layer. Zirconia was mounted by very thin or nanolayers on the ceramic membrane.

A combination of alumina and zirconia was used as a strong nanofilm on the ceramic membrane. SEM micrographs are shown in Figure 16.14. Observation by SEM shows that the zirconia–alumina membrane layer was properly adhered and could stand on the top of the porous ceramic support.

16.5.4 CONCLUSION

We have successfully developed a new inorganic ceramic membrane coated with zirconium and alumina. A thin film of alumina and zirconia unsupported membrane was also fabricated. The successful method developed was the sol–gel technique.

Acknowledgments

This research was made possible by an IRPA grant No. 703574, through Universiti Sains Malaysia (USM). We thank USM's Research Creativity and Management Office (RCMO) and the School of Chemical Engineering, Universiti Sains Malaysia, for their support.

References

1. Anderson MA, Gielselmann MJ, Xu Quinyin. *J Membr Sci* 1988;**39**:243.
2. Annika K, Elis C. *J Eur Ceram Soc* 1997;**17**:289.
3. Moreno R. *Am Ceram Soc Bull* 1992;**71**:1647.
4. Gamze GA, Zulal M, Volcan G. *Ceram Int* 1996;**22**:23.
5. Gu YF, Meng GY. *J Eur Ceram Soc* 1999;**19**:1961.
6. Brinker CJ, Schere GW. *The physics and chemistry of sol-gel processing*. Amsterdam: Academic Press; 1990.
7. Hao W, Pan F, Wang T, Zheng S. *J Mat Sci (Shanyang, China)* 2004;**20**:472–4.
8. Lambert CK, Gonzalez RD. *Mat Lett* 1999;**38**:145.
9. Leenars AFM, Keizer K, Burggraaf AJ. *J Mat Sci* 1984;**19**:1077.
10. Huang XR, Meng GL, Hunag ZT, Geng JE. *J Membr Sci* 1997;**133**:145.
11. Karin L, Eva L. *J Eur Ceram Soc* 1997;**17**:359.
12. Larbot A, Fabre JP, Guizard C, Cot L. *J Membr Sci* 1988;**39**:203.
13. Pierre AC. *J Am Ceram Soc* 1987;**70** 28.
14. Yoldas BE. *Ceram Bull* 1975;**54**:289.

Advanced Downstream Processing in Biotechnology

OUTLINE

17.1 Introduction	497		
17.2 Protein Products	497		
17.3 Cell Disruption	498		
17.4 Protein Purification	500		
17.4.1 Overview of Strategies	500		
17.4.2 Dye Ligand Pseudo-affinity Adsorption	500		
17.5 General Problems Associated With Conventional Techniques	501		
17.6 Fluidized Bed Adsorption	502		
17.6.1 Mixing Behavior in Fluidized/Expanded Beds	503		
17.7 Design and Operation of Liquid Fluidized Beds	504		
17.7.1 Hydrodynamic Characterization of Flow in Fluidized/Expanded Beds and Bed Voidage	504		
		17.7.2 Minimum Fluidization Velocity of Particles	505
		17.7.3 Terminal Settling Velocity of Particles	506
		17.7.4 Degree of Bed Expansion	508
		17.7.5 Matrices for Fluidized Bed Adsorption	509
		17.7.6 Column Design for Fluidized Bed Adsorption	510
		17.8 Experimental Procedure	510
		17.9 Process Integration in Protein Recovery	511
		17.9.1 Interfaced and Integrated Fluidized Bed/Expanded Bed System	511

Nomenclature	513	17.11.3 Results and Discussion	518
References	513	17.11.3.1 <i>Bed Expansion</i>	518
17.11 Case Study: Biochemical Characterization of a Custom Expanded Bed Column for Protein Purification	516	17.11.3.2 <i>Mixing of the Liquid Phase (Residence Time Distribution Experiments)</i>	520
17.11.1 Introduction	516	17.11.3.3 <i>Equilibrium Kinetic Studies</i>	520
17.11.2 Materials and Methods	517	17.11.3.4 <i>Expanded Bed Adsorption</i>	522
17.11.2.1 <i>Materials</i>	517	17.11.4 Conclusion	524
17.11.2.2 <i>Adsorbent Contactors</i>	518	References	525
17.11.2.3 <i>Bed Expansion Characteristics</i>	518		
17.11.2.4 <i>Fluidized/Expanded Bed Adsorption</i>	518		

SUBCHAPTER

17.1

Introduction*

In recent decades, advances in biotechnology have increased the potential use of biologically based products. The emergence of new and promising research activities in molecular biology and immunology has promoted a continuous increase in the number of proteins that need to be purified and characterized. A wide variety of proteins are used as diagnostic reagents, such as vaccines, monoclonal antibodies, enzymes, and regulatory factors. The development of simplified and cost-effective bioseparation schemes to eliminate impurities from these products in a highly purified form is a constant major challenge for the continued success and commercialization of biotechnological industries. The series of separation processes used to purify bio-based products can be collectively described by the general term “downstream processing.”^{1,2} The objective is to establish a sequence of operations that will transform the starting material to a state defined by the specification and end use of the desired product. Individual steps should be based on molecular-based knowledge of how individual proteins will behave during purification, to appropriately establish an efficient and economic process. Technologies applicable in such bioprocesses must also accommodate particulate-containing feedstock such as microbial fermentation broths, animal or plant cell cultures, and cell-disruptive feedstock. It is important that the recovery in these processes be done rapidly maintain the native conformation and activity of highly sensitive protein molecules.³ Therefore, the main objectives for the biochemical engineer must encompass the design of an optimal process that: (1) provides the desired quality of the final product, (2) minimizes the total process time and cost through improved operational efficiency, and (3) falls within the constraints of an acceptable market entry.

17.2 PROTEIN PRODUCTS

Advances in biotechnology have enabled the development and use of protein products as pharmaceutical reagents as well as applications in the industrial and domestic spheres.⁴ The domestic market represented by the food and beverage industries requires protein products of low value but with a high-volume demand where the purity of the protein is less

*This chapter was written with contributions from:

Mohsen Jahanshahi, Mohammad Hassan Shahavi, Biotechnology Research Lab., Faculty of Chemical Engineering, Noshirvani University of Technology, Babol, Iran.

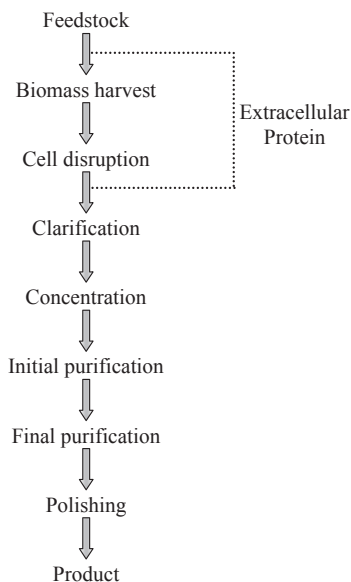


FIGURE 17.1 Conventional downstream processing scheme for the purification of proteins.

important than cost.⁵ This is in contrast to protein products with a market value such as therapeutic enzymes, in which high purity is essential.⁶ Proteins commonly exhibit narrow stability ranges outside of which denaturation occurs. In addition, specific enzymes such as proteases and lipases can make small alterations in protein structure that may lead to substantial changes in their activity and antigenic properties.

A generalized sequence of the discrete unit operations involved in standard downstream processing is depicted in Figure 17.1. In the case of an intracellular product, cell disruption is the first step in the sequence after harvesting the cells (for example, by centrifugation). Here, the cell boundary is permeabilized, punctured, or disintegrated to release the product into the surrounding medium. The cell disruption step is unnecessary in the case of extracellular products, because the products are synthesized within the cells and subsequently excreted naturally into the broth. Each individual technique employed in the purification of proteins has advantages and disadvantages.

However, a diverse combination of separation steps is commonly required; the selection is based on various physical and chemical characteristics of the proteins. Figure 17.1 shows a typical conventional approach adopted for the purification of intracellular and extracellular proteins.

17.3 CELL DISRUPTION

Cell disruption is an essential initial preparative step for the purification of intracellular protein products. Different methods of cell disruption have been reviewed by several researchers,⁷ particularly focusing on large-scale operations.⁸ Different methods of cell disruption that are currently available can be conveniently divided into two main groups: (1) mechanical and (2) non-mechanical. Complete destruction of the cell wall in a nonspecific manner is usually achieved by mechanical means exploiting solid-shear (bead mill) and

liquid-shear forces (high-pressure homogenizer [HPH] or micro-fluidizer). Non-mechanical methods are judged to be more benign and often only perforate or permeabilize cells rather than tearing them apart. For example, chemical and enzymatic methods rely on selective interaction of a substance or enzyme, respectively, with components of the cell wall or the membrane that modify the cell boundary and allow product to seep out. However, such treatment on a large scale may be costly and the waste disposal of process additives may also cause problems. As a result, mechanical methods such as HPHs or bead mills are preferred for large-scale applications.⁹ Homogenization involves the single or multiple passage of a cell suspension at a constant flow rate through an adjustable, restricted orifice discharge valve. As the cells are forced at high pressure through the orifice they are subjected to a combination of cavitations and liquid shear in which operating pressure, cell concentration, and temperature are influential for disruption efficiency.^{10,11}

Mechanical cell disruption in a bead mill has many attractive process characteristics including high disruption efficiency in single-pass operations, high throughput and biomass loading, good temperature control, and commercially available equipment applicable from the laboratory to an industrial scale.¹² In addition, the single-pass and continuous operating characteristics of the bead mill have recommended it as the ideal feedstock generator for immediate and direct sequestration of released products in a fluidized bed.^{13,14} Bead mills consist of a mostly horizontally positioned, closed grinding chamber. Upon a motor-driven agitator shaft, different impellers can be employed in the form of discs, rings, or pins (Figure 17.2).

These can be mounted concentrically or eccentrically and impart kinetic energy from the rotating parts to the grinding elements that are suspended in the cell suspension. Cells are disrupted by shear forces generated by the radial acceleration of these elements (typically ballottini glass or zirconia beads) as well as by bead collisions. Virtually all of the energy input is dissipated as heat, which necessitates efficient cooling of the chamber, achieved by a cooling jacket. The rate of disruption depends on several operational parameters such as agitator speed, suspension throughput, bead size, bead loading, and cell concentration. Many of these parameters have been exhaustively studied using different types and sizes of horizontal bead mill.⁸

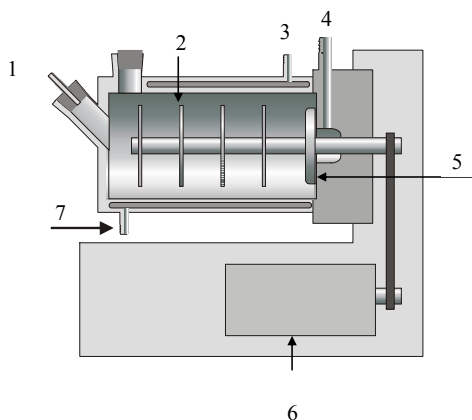


FIGURE 17.2 Sketch of the Dyno Mill KDL-I. 1. Cell suspension inlet; 2. agitator disks; 3. coolant; 4. disruptate outlet; 5. gap separator; 6. motor; 7. coolant.

17.4 PROTEIN PURIFICATION

17.4.1 Overview of Strategies

The initial stages of protein purification stages can be done by exploiting a variety of techniques such as membrane separation, aqueous two-phase partition, and batch adsorption.¹⁵ Membrane separation covers a wide range of fundamentally different processes from micro-filtration to electrodialysis.¹⁶ Common features of these processes include separation occurring between two fluids that are by an interphase made of a membrane. This allows the selective transport of components of the two phases and thus some materials to pass through while others may be retained. Aqueous two-phase partition is a method used for protein separation based on the partition of proteins between two water-rich phases, which are obtained by dissolving two hydrophilic polymers in water or one polymer and salt above a defined concentration.¹⁷ Batch adsorption is performed by contacting adsorbent particles with biological feedstocks in stirred tanks.¹⁸ After product capture, the adsorbent is separated from the broth by decantation washing and then the product is eluted. Batch adsorption is a process characterized by a single equilibrium stage and thus lacks high resolution compared with classical process chromatography.

In addition, the problem of separating the protein-loaded adsorbent from the biomass has to be solved. Primary and final protein purification steps are commonly done by liquid chromatography to achieve further purification of the desired proteins.¹⁹ These techniques have been developed to separate protein products from each other by exploiting their difference with respect to molecular characteristics.⁴ Ion exchange and hydrophobic interaction chromatography is most commonly applied in downstream processing for the primary capture of protein products. The proteins are separated by ion exchange chromatography based on the reversible adsorption of charged groups of the adsorbent phase. In contrast, the basis for hydrophobic chromatography is the interaction between hydrophobic domains of protein and the hydrophobic groups of the adsorbent phase. The principal application of affinity chromatography, which facilitates the selective adsorption of target proteins to biological specific ligands (for example, protein A and antibodies) immobilized on and within the adsorbent phase, makes it well suited for the final stages of purification of protein products.²⁰

However, recent developments²¹ have suggested that the adoption of this high-resolution chromatography system in the earlier stage of downstream processing can facilitate the overall recovery performance (for example, reduce working and processing time). The robust and inexpensive synthetic ligands (for example, triazine dyes) are well suited to such applications (see the following section).

17.4.2 Dye Ligand Pseudo-affinity Adsorption

Historically, chlorotriazine dyes such as Cibacron Blue 3GA, Procion Red H-E7B, Procion Green H-4G, and Yellow H-E3G were designed as cheap chemicals for use in the textile and printing industries. The chemical structure of Cibacron Blue 3 GA is illustrated in [Figure 17.3](#). The chlorotriazine dyes are known to show affinities for several classes of proteins such as dehydrogenase, phosphatransferases, and plasma proteins by virtue of an approximate mimicry of the structure of cofactors nicotinamide adenine dinucleotide and flavin adenine

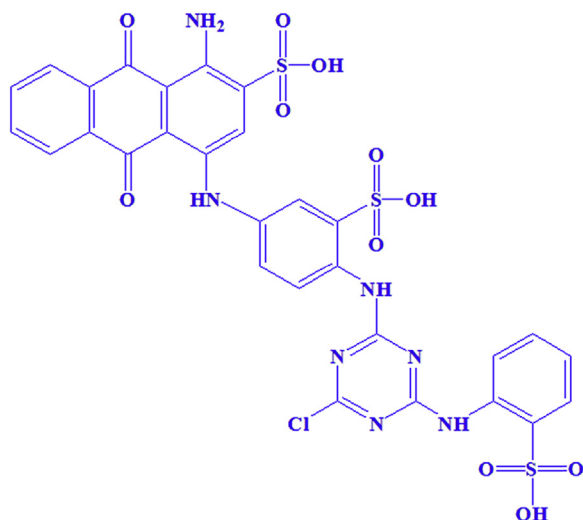


FIGURE 17.3 The chemical structure of Cibacron Blue 3 GA.

dinucleotide.²² As a result, chlorotriazine dyes have been widely exploited as ligands in affinity chromatography for the purification of protein products. In general, dye ligands that tend to show affinities for specific classes of protein (i.e., dehydrogenases, phosphotransferases, plasma proteins, etc.) include reactive dyes belonging to the chlorotriazine group.²³ The dyes provide interactions with enzymes that mimic interactions provided by natural ligands or their chemical analogs. Because of these dyes have no biological relationship with the macromolecules, the terms “pseudo-ligand” and “pseudo-affinity” are commonly used to describe them and their interactions.²⁴ Dissociation constants, K_d , of dye ligands are commonly in the range 10^{-6} to 10^{-7} M, which lies intermediate between ion exchange, 10^{-4} to 10^{-6} M, and truly biospecific ligands, 10^{-6} to 10^{-8} M.²⁵ The dyes are particularly promising pseudo-affinity ligands because they offer several advantages over biospecific ligands including ease of coupling to support matrices, low cost, wide availability, and high-stability operations and sanitization operations.²⁴

17.5 GENERAL PROBLEMS ASSOCIATED WITH CONVENTIONAL TECHNIQUES

From an economic point of view, the number of sequential operations necessary to achieve the desired purity of a protein product contributes significantly to the overall cost of the downstream process. This is because of the capital investment and amount of consumables needed for each step as well as the individual time required for each operation. In addition, the overall yield of the purification is reduced with each additional process step as a result of inherent handling losses of product and/or product activity. It has been estimated that the overall cost of the downstream process is closely correlated to the number of purification steps involved and that cost may account for up to 80% of the final process investment.²⁶

Traditional techniques employed for both harvesting biomass and feedstock clarification are centrifugation and filtration.²⁷ Centrifugation might need to be undertaken twice, whereas an additional depth or microfiltration step is commonly included to ensure a particle-free (99–99.9% in terms of cell clearance) solution that can be fractionated by traditional packed-bed chromatography. Although filtration has been applied successfully in numerous solid–liquid operations, performance is usually diminished as a result of membrane fouling (for example, by cells, cell debris, lipids, and nucleic acids) during operation.²⁸ In addition, combined centrifugation and filtration operations often result in long processing times. Furthermore, the presence of large amounts of insoluble and highly viscous materials (for, cells debris and long chain genomic deoxyribonucleic acid) in the process feedstock can further restrict the clarification performance. This problem is especially critical in the case of a cell disruptate, which results in the generation of cell debris and colloidal materials, and the release of large amounts of intracellular products.²⁹ A rapid method of product capture of the target protein is therefore preferred because the time taken to remove particulates can promote denaturation owing to process conditions that are detrimental to structural integrity: for example, the action of proteases, carbohydrates, or oxidizing conditions. Thus, the development of fast and cost-effective primary recovery steps forms the basis for a successful downstream process, especially in the production of intracellular proteins.

17.6 FLUIDIZED BED ADSORPTION

Fluidized bed adsorption (FBA) has emerged as an efficient recovery method proven to have significant advantages over conventional procedural sequences: for example, discrete feedstock clarification followed by fixed-bed adsorption of the product. In fluidized beds, liquid is pumped upward through a bed of adsorbent beads that, in contrast to a packed bed, are not constrained by an upper flow adapter. Thus, the bed can expand and spaces open up between the adsorbent beads. The increased voidage of the bed allows particulates in the feed to pass freely through the spaces without entrapment (see [Figure 17.4](#)).

Thus, the need for prior removal of cells and/or debris is eliminated. After the adsorption stage, the remaining feedstock and particulates are washed from the adsorbent bed and the product is subsequently eluted either in fluidized or packed-bed mode. As a consequence, clarification, concentration, and initial fractionation are combined into one operation, and thus fluidized beds exhibit great potential for simplifying downstream processes with concomitant savings in capital and operating costs.

Fluidized beds have been used previously for the industrial-scale recovery of the antibiotics streptomycin and novobiocin.³⁰ However, more recently, there has been considerable interest in the use of fluidized beds for the direct extraction of proteins from whole fermentation broths.³¹ In a packed bed, the adsorbent particles are packed within the contactor. The voidage—that is, the inter-particle space—is minimal and thus feedstock clarification is mandatory to avoid clogging of the bed. In a fluidized/expanded bed, the adsorbent bed is allowed to expand by irrigation with feedstock. Bed voidage is increased, allowing the passage of particulates in the feed. The diameters of the adsorbent beads are exaggerated for illustrative clarity.

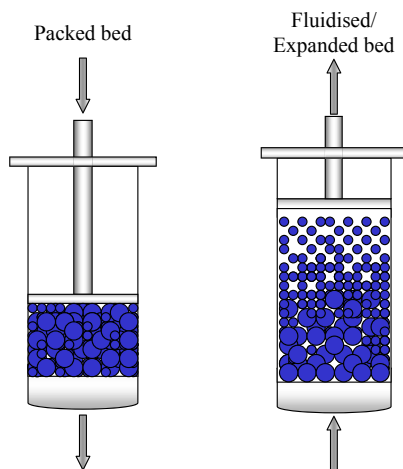


FIGURE 17.4 Adsorbent particles in a packed and a fluidized bed.

17.6.1 Mixing Behavior in Fluidized/Expanded Beds

The conventional chemical engineering view of a fluidized bed is one in which there is a significant degree of mixing in both the solid and fluid phases: for example, in gas fluidized systems.³² In many applications, mixing of the solid phase is desirable, such as to obtain high rates of heat transfer and a uniform temperature within the bed. Gas fluidized beds are characterized by an aggregative behavior in which bubbles of gas pass through a bed of particles that are just fluidized, resulting in considerable mixing of the solid phase as well as distinct bypassing of the gas phase. In general, mixing in liquid fluidized systems is not as severe as in gas fluidized systems. Here, the density differences between the solid and the fluid phase are comparatively small, and thus the bed shows a particulate behavior in which the bed retains a uniform character.³¹

In a packed bed, the adsorbent beads are stationary and liquid flowing through the bed approximates plug flow. Thus, the number of theoretical equilibrium stages (referred to as plates) is maximized, which results in good adsorption and chromatographic performance. As a consequence of the absence of plug flow in the liquid phase, compounded by the mixing of the adsorbent, a fluidized bed would be expected to show inferior adsorption performance compared with that of a packed bed. Thus, for protein recovery in liquid fluidized beds, it is highly desirable to minimize the degree of mixing so as to mimic the adsorption characteristics found in a packed-bed contactor with respect to capacity and resolution.

Several strategies have been reported to limit the mixing of adsorbent particles within liquid fluidized beds. One approach is to divide the bed into sections by introducing baffles into the contactor. Other approaches seek to keep the adsorbent beads in a fixed position or at least localize their movement to achieve a stable fluidised bed that subsequently behaves like a packed bed but with a greater voidage. For example, by using magnetically susceptible adsorbent particles, a fluidized bed can be stabilized by subjecting it to a magnetic field. It is claimed that such beds exhibit little or no back-mixing and can be operated continuously.³³

The practical benefit of this approach, i.e., restricted movement of adsorbent particles and associated uncoupling of the bed expansion from fluidization velocity, was subsequently demonstrated by Zhang.³⁴ In this work, magnetically stabilized fluidized beds were exploited for (1) the direct recovery of the intracellular enzyme glyceraldehydes-3-phosphate dehydrogenase from unclarified yeast disruptates, and (2) the recovery of antibody fragments from *Escherichia coli* fermentation broths. However, this technique requires complicated and relatively expensive equipment, particularly on a large scale.

A simpler approach was designed for the physical properties of the solid phases in such a way that they generate an inherently stable fluidized bed.³⁵ If the adsorbent beads have an appropriate distribution of sizes and/or densities, grading or classification of the adsorbent occurs within the bed, with the larger/denser particles located near the bottom of the bed and the smaller/lighter particles nearer the top. The segregation behavior restricts the local mobility of the fluidized particles. Such a bed exhibits dispersion characteristics similar to a packed bed.³⁶ Thus, the hydrodynamic properties of a fluidized bed are combined with the chromatographic properties of a packed bed. The degree of classification depends on the ratio of the size of the largest and smallest particle within the bed. This ratio has been claimed to be at least 2.2.³⁷

To account for the difference in the dispersion characteristics of the classified, stable fluidized bed and the conventional, well-mixed fluidized bed, the term “expanded bed” has been used by several authors and the leading manufacturer of chromatography media and equipment.³⁸ In the work presented here, the term “fluidized bed” is used synonymously with “expanded bed” to refer to adsorbents fluidized under conditions that seek to minimize particle mixing.

17.7 DESIGN AND OPERATION OF LIQUID FLUIDIZED BEDS

17.7.1 Hydrodynamic Characterization of Flow in Fluidized/Expanded Beds and Bed Voidage

The voidage (ϵ) of a bed of particles is the fraction of the bed volume occupied by the interstitial space between the particles. Its value depends on the geometrical configuration of the beads, the pattern in which they are arranged within the bed, the size distribution of the particles, and the ratio of mean particle and contactor diameter. The bed voidage can be calculated using the following equation:

$$\text{Voidage } (\epsilon) = 1 - \frac{V_p}{V_b} \quad (17.7.1.1)$$

where V_p is the volume of the particles and V_b is the volume of the bed. The voidage of a packed bed is related to the sphericity of the particles, with a sphericity value of 1 for fully spherical particles. The bed voidage values can typically be in the range of 0.32 for a densely packed adsorbent, to 0.43 for a loosely packed adsorbent.³⁹ However, the voidage of a bed containing a range of particle sizes and geometrical shapes cannot be accurately predicted.

Therefore, an assumed value for ε_0 of 0.40 for a perfectly packed adsorbent bed is commonly found in chromatographic studies.⁴⁰ This value has also been applied throughout this study for all materials used.

17.7.2 Minimum Fluidization Velocity of Particles

The minimum fluidization velocity of the particles is achieved when the adsorbent becomes suspended in the liquid. This occurs when the drag forces exerted by the upward flow of the liquid phase are equal to the weight of particles in the liquid. Therefore, at minimum fluidizing conditions, it can be described by the following expression:

Drag by upward liquid flow = Weight of the particles – Buoyancy of the particles

This expression can be also presented as:

Pressure drop across the bed \times Cross section area of the bed = Volume of the bed \times Fraction of the particles \times Specific weight of the particles
or

$$\Delta P \times A_c = A_c \times H_{mf} \times (1 - \varepsilon_{mf}) \times [(\rho_p - \rho) \times g] \quad (17.7.2.1)$$

where ΔP is the pressure drop, A_c is the cross-sectional area of the column, and H_{mf} and ε_{mf} are the bed height and bed voidage at the minimum fluidization velocity (U_{mf}), respectively. Also, ρ_p is the density of the particles; ρ is the density of liquid phase and g is acceleration owing to gravity. Rearranging (17.7.2.1) gives:

$$\frac{\Delta P}{H_{mf}} = (1 - \varepsilon_{mf}) \times (\rho_p - \rho) \times g \quad (17.7.2.2)$$

However, on the basis of the relation between the pressure drop and the minimum fluidization velocity of particles, the point of transition between a packed bed and a fluidized bed was correlated by Ergun⁴¹ using (17.7.2.3). This is obtained by summing the pressure drop terms for laminar and turbulent flow regions

$$\frac{\Delta P}{H_{mf}} = 150 \times \frac{(1 - \varepsilon_{mf})^2}{\varepsilon_{mf}^3} \times \frac{\mu \times U_{mf}}{d_p^2} + 1.75 \times \frac{(1 - \varepsilon_{mf})}{\varepsilon_{mf}^3} \times \frac{\rho \times U_{mf}^2}{d_p^2} \quad (17.7.2.3)$$

where μ is the viscosity of the liquid and d_p is the diameter of the particle. The first term of the Ergun equation is linear with respect to the velocity and this will be dominant when the flow in the voids is laminar. Hence, (17.7.2.3) can be simplified to:

$$\frac{\Delta P}{H_{mf}} = 150 \times \frac{(1 - \varepsilon_{mf})^2}{\varepsilon_{mf}^3} \times \frac{\mu \times U_{mf}}{d_p^2}$$

when

$$\text{Re}_p = \frac{d_p \times \rho \times U_{mf}}{\mu} < 20 \quad (17.7.2.4)$$

The second term relates to turbulence. Therefore, (17.7.2.3) can be simplified to:

$$\frac{\Delta P}{H_{mf}} = 1.75 \times \frac{(1 - \epsilon_{mf})}{\epsilon_{mf}^3} \times \frac{\rho \times U^2}{d_p^2}$$

when

$$\text{Re}_p = \frac{d_p \times \rho \times U_{mf}}{\mu} > 1000 \quad (17.7.2.5)$$

In the intermediate region both terms have to be used. Therefore, the superficial velocity at minimum fluidizing conditions can be found by combining (17.7.2.2) and (17.7.2.3) and multiplying both sides by $\rho d_p^3 / \mu^2 (1 - \epsilon_{mf})$ to yield:

$$150 \frac{(1 - \epsilon_{mf})}{\epsilon_{mf}^3} \times \frac{\rho \times U_{mf} \times d_p}{\mu} + \frac{1.75}{\epsilon_{mf}^3} \times \left(\frac{\rho \times U_{mf} \times d_p}{\mu} \right)^2 = \frac{\rho \times (\rho_p - \rho) \times g \times d_p^2}{\mu^2} \quad (17.7.2.6)$$

If ϵ_{mf} is unknown, the following equation suggested by Wen and Yu⁴¹ can be used to determine the minimum fluidization velocity for the whole range of Reynolds numbers by the following assumption:

$$\frac{(1 - \epsilon_{mf})}{\epsilon_{mf}^3} \cong 11$$

and

$$\frac{1}{\epsilon_{mf}^3} \cong 14 \quad (17.7.2.7)$$

Hence, solving explicitly for U_{mf}

$$U_{mf} = \frac{\mu}{\rho \times d_p} \times \left[(33.7)^2 + 0.0408 \times \frac{\rho \times (\rho_p - \rho) \times g \times d_p^2}{\mu^2} \right]^{1/2} - 33.7 \quad (17.7.2.8)$$

Thus, at low particle Reynolds numbers (Re_p), (17.7.2.8) can be simplified to:

$$U_{mf} = \frac{d_p^2 \times (\rho_p - \rho) \times g}{1650 \times \mu} \quad (17.7.2.9)$$

Equation (17.7.2.9) was originally used to correlate the minimum fluidization velocity for gas–solid fluidization beds, but it has been successfully employed by Lan and co-workers⁴² for adsorbents in the field of direct recovery using liquid–solid systems (see Figure 17.5).

17.7.3 Terminal Settling Velocity of Particles

If a single particle is falling freely under gravity in an infinitely dilute suspension, it will accelerate until it reaches a steady-state velocity. This final velocity is known as the terminal settling velocity (U_t) and represents the maximum useful superficial velocity achievable in a

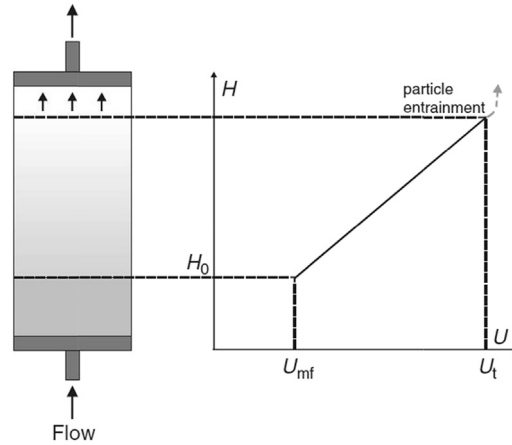


FIGURE 17.5 Operational window of fluidization velocities.

fluidized bed. Thus, the contained particles will be elutriated from the column if the superficial velocity is above U_t , the value of which can be predicted using the Stokes Equation (17.7.3.1). A wide range of particle terminal velocities for various Reynolds numbers were investigated by Kunii and Levenspiel.⁴³ They suggested that if the particles were assumed to be spherical and operated at a low particle Reynolds number ($Re_p < 0.4$), the Stokes equation was acceptable (see Figure 17.5). Therefore, the terminal velocity U_t can be expressed as:

$$U_t = \frac{d_p^2 \times (\rho_p - \rho) \times g}{18 \times \mu} \quad (17.7.3.1)$$

where d_p is the diameter of the particle and ρ_p and ρ are the density of the particle and liquid phase, respectively. Also, μ is the viscosity of the liquid phase and g is acceleration owing to gravity. The Stokes equation has been reported in the literature as being successfully used to predict terminal settling velocities of fluidized/expanded bed adsorbents.^{44,45}

Alternatively, the model of Shiller and Naumann is commonly used to predict the terminal velocity of a spherical particle:

$$Ga = 18Re_t + 2.7Re_t^{1.687} \quad 3.6 < Ga < 10^5 \quad (17.7.3.2)$$

where

$$Ga = \frac{\rho \times (\rho_p - \rho) \times g \times d_p^3}{\mu^2} \quad (17.7.3.3)$$

and

$$Re_t = \frac{\rho \times U_t \times d_p}{\mu} \quad (17.7.3.4)$$

where Ga is the Galileo number, Re_t represents the terminal Reynolds number, and d is the particle diameter. The model of Shiller and Naumann was successfully used to estimate

the particle terminal velocity by Thomas and Yates,⁴⁶ Jahanshahi and co-workers,^{47–72,74,75} and Shahavi and collaborators.^{66,70}

17.7.4 Degree of Bed Expansion

The degree of bed expansion contributes to the efficiency of fluidized bed/expanded bed adsorption as a composite function of liquid distribution, liquid and particle properties (size, shape, and density), and process conditions. Besides being an important design feature, the degree of bed expansion may be used as a quick and simple measure of bed stability.⁴⁸

The relation between superficial velocity (U) and bed voidage (ε) in a fluidized bed can be described by the classical correlation first postulated by Richardson and Zaki⁴⁹

$$U = U_t \varepsilon^n \quad (17.7.4.1)$$

where ε is the fluidized voidage and n is the Richardson–Zaki coefficient. It allows the calculation of the particle terminal velocity of any given suspension of uniformly dispersed spheres together with the liquid velocity required to perform a given expansion of a fluidized bed by the logarithmic plot of linear velocity against fluidized voidage. Thus,

$$\log U = \log U_t + n \times \log \varepsilon \quad (17.7.4.2)$$

The void fraction (ε) is estimated from the measured height of the expanded bed (H) and is a function of superficial liquid velocity. Thus,

$$\varepsilon = 1 - \frac{M}{\rho_p \times A_c \times H} \quad (17.7.4.3)$$

where M is the mass of particles. Also, the fluidized voidage can be determined as the total volume of particles (for a given bed) constant in both packed bed and fluidized bed configurations. Therefore,

$$A_c H_0 (1 - \varepsilon_0) = A_c H (1 - \varepsilon) \quad (17.7.4.4)$$

where H_0 and ε_0 are the packed bed height and voidage, respectively. Hence, by rearranging (17.7.4.4), the bed voidage at any fluidized bed height can be estimated using the equation:

$$\varepsilon = 1 - \frac{(1 - \varepsilon_0) \times H_0}{H} \quad (17.7.4.5)$$

The Richardson–Zaki coefficient (n) can be calculated from the following correlations

$$n = 4.65 + 20 \frac{d}{D} \quad \text{Re}_t < 0.2 \quad (17.7.4.6)$$

$$n = \left(4.4 + 18 \frac{d}{D} \right) \text{Re}_t^{-0.03} \quad 0.2 < \text{Re}_t < 1 \quad (17.7.4.7)$$

$$n = \left(4.4 + 18 \frac{d}{D} \right) \text{Re}_t^{-0.1} \quad 1 < \text{Re}_t < 200 \quad (17.7.4.8)$$

$$n = 4.4\text{Re}_t^{-0.1} \quad 200 < \text{Re}_t < 500 \quad (17.7.4.9)$$

$$n = 2.4 \quad \text{Re}_t > 500 \quad (17.7.4.10)$$

where D is the column diameter and Re_t is the particle Reynolds number based on the terminal velocity. The popularity of the Richardson–Zaki correlation in this field of study arises from its simplicity and good agreement with experimental data.^{48,50}

The operational window of a fluidized bed process is defined by the minimum fluidization velocity, U_{mf} at which a settled bed of adsorbent beads starts to fluidize and the terminal velocity (U_t) at which the bed stabilizes and adsorbent beads are entrained from the bed.

17.7.5 Matrices for Fluidized Bed Adsorption

Early work exploiting extensively cross-linked agarose adsorbents originally designed for conventional, packed bed processes demonstrated the principal of operation and the potential of fluidized bed adsorption for processing particulate feedstocks.³¹ However, these materials were not optimally suited because the combination of particle diameter and density occurred only at low flow rates (for example, 10–30 cm h⁻¹), which resulted in low overall productivity. Denser particles such as silica were more appropriate in this respect.⁵¹ However, a drawback of silica-containing material is the limited stability at high pH values, which makes it less suitable for biopharmaceutical production where alkaline conditions are commonly used for cleaning-in-place (CIP) and sanitization-in-place procedures.

The development of denser adsorbents enabled the use of higher flow rates and improved the stability of operation of expanded beds. Tailor-made adsorbents were produced using hydrophilic natural polymers such as cellulose, agarose, or synthetic trisacrylate-based materials. To enhance the particle density, heavy, inert filler materials have been incorporated during assembly. The resulting composite materials included cellulose-titanium dioxide and dextran-silica.⁵² Other materials reported for the fabrication of denser adsorbents were glass and zirconia. For example, Thömmes and co-workers⁵³ exploited custom-derived controlled pore glass particles for the purification of monoclonal antibodies. Zirconia-based materials exhibit a significantly higher density than silica. It has been demonstrated that even small particles (for example, less than 50 μm in diameter) may be fluidized at linear flow rates similar to those used for silica or density-enhanced agarose particles with a greater diameter.⁵⁴ In another approach, McCreath and colleagues developed perfluoropolymer particles that were derived with dye ligands for the affinity purification of dehydrogenases from disrupted baker's yeast.⁵⁵ The increased density of the support (2.20 g ml⁻¹) also allowed the use of comparatively small particles (50–80 μm) at an acceptable linear flow rate of 120 cm h⁻¹.

Agarose-based materials have been commercialized specifically for fluidized bed adsorption by increasing their specific weight with incorporated quartz or steel particles (STREAM-LINE).³⁷ The densities achieved have been exploited at 1.15 g ml⁻¹ for agarose-quartz and 1.3 g ml⁻¹ for agarose-steel composites. These materials are available with a range of ligand functionalities such as weak anion exchange (diethylaminoethyl, DEAE), strong anion exchange (quaternary ammonium, Q), weak cation exchange (carboxymethyl, CM), strong cation exchange (sulfopropyl, SP), chelating ligand (iminodiacetic acid for immobilized metal affinity chromatography), protein A (affinity purification of antibodies), and phenyl groups (hydrophobic interaction chromatography). More recently, so-called pellicular adsorbents

were defined as suitable for fluidized bed adsorption. These adsorbents are characterized by a dense core such as glass or stainless steel^{47,56} coated with a layer of porous material such as agarose. Such matrices promise high rates of adsorption/desorption owing to the absence of deep convective pores and the short diffusion distances within the thin porous layer that comprises the pellicle.

17.7.6 Column Design for Fluidized Bed Adsorption

To achieve a stable fluidized bed, the column has to fulfill some simple but important demands. A suitable liquid distribution is crucial to accomplish plug flow conditions within the bed and thus minimize particle dispersion. A prerequisite for the generation of an even velocity profile across the cross-section of a column is an evenly distributed pressure drop across the distributor at the column inlet. Pressure drop fluctuations lead to the development of channels, which are the most important influence on homogeneity in an adsorption process. Flow distribution can be achieved by using sieve plates, meshes, or a bed of glass ballotini.^{43,68,70} Bascoul and colleagues⁵⁷ investigated bed stability as a function of the distributor design, showing that channeling in the lower part of a fluidized bed owing to uneven flow distribution is reduced with increasing column length. This led to the conclusion that the fluidized bed itself serves as an effective flow distribution system. More recently, a novel distributor design was introduced that uses a stirrer in the bottom of the contactor to distribute the incoming feedstock. This configuration divides the fluidized bed into a limited, well-mixed zone at the bottom and a stable fluidized bed above it. Such contactors were included in the study presented here. Besides the demand for even flow distribution, the distributor has to enable the unhindered passage of particulates without becoming blocked or damaging shear-sensitive cells. Partial blockage of a distributor will cause channeling in the fluidized bed. Cell breakage in the flow distributor can lead to the unwanted release of intracellular compounds that may impair the purification process of an extracellular product for whole broths.

Another important factor that has a bearing on bed stability is the column verticality. Van der Meer and colleagues⁵⁸ demonstrated that even small deviations from vertical alignment lead to significant inhomogeneity of liquid flow. These findings were confirmed by Bruce and co-workers,⁵⁹ who found that this effect is more pronounced in small-diameter contactors. In their work, the dynamic capacity of a 1-cm column, used for the capture of glucose-6-phosphate dehydrogenase from unclarified yeast homogenate, was reduced by approximately 30% when misaligned by 0.185. However, a 5-cm contactor operated under similar conditions appeared to be unaffected.

17.8 EXPERIMENTAL PROCEDURE

In principle, the experimental protocol of fluidized bed adsorption does not deviate from packed-bed operations, but the main difference is the direction of the liquid flow. The sequence of steps of equilibration, sample application, wash, elution, and cleaning (CIP) is performed in an upward direction, although the last two might be undertaken in fixed-bed mode. During equilibration, the matrix is fluidized and a stabilized, fluidized bed is developed. Here, classification within the bed with regard to particle size of the adsorbent particles

may be determined by visual observation. At the same time, the matrix is primed for adsorption by the selection of a suitable buffer for product–adsorbent interactions. Subsequently, the feedstock is applied to the fluidized bed. Target proteins are adsorbed whereas cells, debris, and other particulates and contaminants pass through the bed. After sample application, residual biomass and unbound proteins are removed from the bed in a washing procedure. Elution may be performed either in packed-bed or in fluidized bed mode. A common procedure is to allow the adsorbent to settle and reverse the flow for elution. Here, the upper adapter is lowered to the top of the settled bed. On the other hand, maintaining a fluidized bed during elution prevents particle aggregation and thus facilitates subsequent cleaning of the adsorbent.⁶⁰ However, owing to the greater interstitial volume of the fluidized bed, the elution volume is increased compared with fixed-bed elution. After elution, the adsorbent is subjected to CIP procedures. These are important because the application of whole broth increases the contact of the adsorbent with nucleic acids, lipids, and cellular compounds, which are commonly removed or reduced in conventional primary recovery steps before fixed-bed column chromatography. Commonly used agents in CIP protocols are NaCl, NaOH, ethanol, acetic acid, urea, and guanidine hydrochloride.^{48,69,73}

17.9 PROCESS INTEGRATION IN PROTEIN RECOVERY

There is much current interest aimed at implementing processes that integrate the upstream and downstream operation for protein recovery.^{13,14,19} Although adsorption in fluidized beds provides considerable savings in cost and time over conventional purification techniques, it deploys a discrete operation with which the desired protein is captured at the termination of fermentation or once a cell suspension has been disrupted. The main disadvantage of this discrete recovery operation is the risk of detrimental effects on an unstable product associated during holdup periods.¹³ This may be defined as the time when the feedstock is harvested, preconditioned, and stored before being subjected to fluidized bed processing. The holdup period risks time-dependent product modification and/or inactivation by system antagonists including proteases, carbohydrates, harsh physical conditions,³ or product loss associated with protein–debris interaction. In addition, it has been reported that protein products are usually stabilized and less susceptible to protease degradation when they are adsorbed onto a chromatography solid phase. Therefore, a logical physical coupling of fluidized bed adsorption with upstream operations of fermentation or cell disruption might be predicted to gain additional benefits of product yield and quality by virtue of the immediate and direct sequestration of products from process feedstocks at the source.^{14,61,65,67}

However, the application of a multi-fluidized bed system in which each bed is sequentially operated online to the fermenter or disrupter to achieve a repetitive operation of this cycle could decrease the adsorbent inventory and increase the maximum batch size.

17.9.1 Interfaced and Integrated Fluidized Bed/Expanded Bed System

Fluidized bed recovery of protein from particulate-containing feedstock can be achieved using two methods: as an interfaced or integrated system.⁶² The interfaced system exploits a fluidized bed to capture the desired protein either at termination of fermentation or once

a cell suspension has been disrupted. In this system, the fluidized bed is normally operated in single-pass chromatography mode to achieve high adsorption efficiency. In contrast, the integrated fluidized bed system achieves the direct sequestration of target product from process feedstock at the source: for example, productive fermentation or immediately upon cell disruptate.⁵²

Direct product sequestration (DPS) is designed to minimize product degradation, which leads to higher product yield and improved molecular integrity.⁶³ An early application of DPS of protein products was demonstrated in which an extracellular acid protease produced by the oleaginous yeast *Yarrowia lipolytica* was continuously captured from productive fermentation. The authors reported that the development of such a technique increased the product yield by reducing the processing time and imposing a pseudo-constitutive state on the yeast. Similar advantages were noted with the DPS of α -amylase from fermentations of *Bacillus amyloliquifaciens* exploiting a manifold of fluidized beds.⁶⁴ In addition, Carmichael and co-workers⁶⁵ demonstrated the application of DPS in the recovery of tissue plasminogen activator from animal cell cultures (Chinese hamster ovary cells). The work of Hamilton and colleagues⁶² addressed the development of process intensification of DPS of acid protease produced by *Y. lipolytica*. Hamilton and co-workers,⁶¹ subsequently performed further investigations into the recovery of similar enzymes successfully from feedstock characterized with a high ionic condition without prior preconditioning (for example, dilution or dialysis). This exploited mixed-mode chemical ligands; as a result, the processing time was further shortened and overall operational efficiency increased.

During the purification of intracellular proteins, cell disruption by mechanical or biochemical means is the first step required in the process. However, it commonly initiates cellular and molecular degradation processes, analogous to those of natural cell death and lysis, owing to the disintegration of intracellular compartments that confine lytic enzymes.^{3,8} In addition, the generation of fine cell debris may promote electrostatic and/or hydrophobic product–debris interactions. Such adverse effects will compromise the yield and molecular fidelity of protein products, particularly when feedstocks are accumulated and processed in time-dependent batch operations. Proteolytic activity may be restrained by the addition of specific inhibitors. However, owing to the complexity and diversity of different host organisms, such measures are haphazard. Consequently, rapid processing (for example, by DPS at cell disruption) should minimize such degradation and enhance the yield and quality of even the most labile products.^{13,14} Here, instead of accumulating a disruptate in a holding tank, the product remains in its physiological environment, i.e., the intact cell, as long as possible and is exposed to the adsorbent immediately after its release from the cell in the disrupter. Contact times between the target molecule and the disruptate are thus minimal. Mechanical cell breakage in a bead mill has many attractive process characteristics including high disruption efficiency, high throughput and biomass loading, good temperature control, and unlimited scale-up for most bioprocesses. As a result of the operational characteristics of single-pass and continuous operation, the use of a bead mill is recommended as the ideal feedstock generator for direct sequestration of released products in a fluidized bed.

Baker's yeast suspension (20% ww/v original cells) was pumped to the bead mill at a flow rate of 280 cm h⁻¹ within the BRG 4.5 cm inner diameter contactor. Then, the disruptate from the mill was directly introduced to the pre-equilibrated fluidized bed containing ZSA II-CB and Macrosorb K4AX-CB.

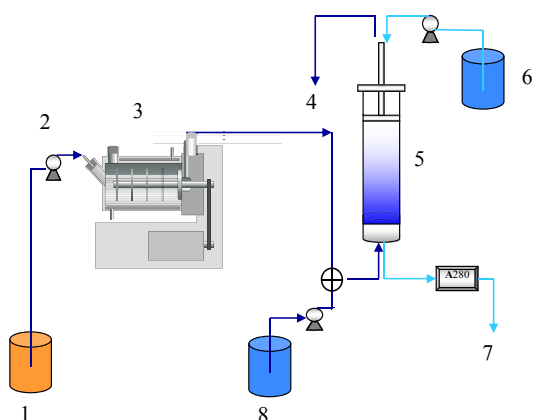


FIGURE 17.6 Experimental configuration for integrated bead milling and fluidized bed adsorption 1. Feedstock; 2. Peristaltic pump; 3. Bead mill; 4. Flow-through/waste; 5. Fluidized bed contactor; 6. Elution buffer; 7. Fraction collector/waste; 8. Loading buffer.

The experimental rig and process configuration for integrated bead milling and fluidized bed adsorption are shown in Figure 17.6.

NOMENCLATURE

ϵ Voidage
 V_p Volume of particles
 V_b Volume of bed
 A_c Cross-sectional of column area
 ΔP Pressure drop
 U_t Terminal settling velocity
 U_{mf} Minimum fluidization velocity
 H_{mf} Bed height at minimum fluidization velocity
 ϵ_{mf} Bed voidage at minimum fluidization velocity
 ρ_p Density of particles
 ρ Density of liquid phase
 G Acceleration of gravity
 μ Viscosity of liquid
 d_p Diameter of particle
 Ga Galileo number
 Re_t Terminal Reynolds number
 U Fluid superficial velocity
 H Expanded bed height
 M Mass of particles
 D Column diameter

References

1. Wheelwright SM. *Bio/Technology* 1987;5:789.
2. Asenjo JA, Patrick I. In: Harris ELV, Angal S, editors. *Protein purification applications*. Oxford: Oxford University Press; 1990.
3. Kaufmann M. *J Chromatogr B* 1997;699:347.

4. Harris ELV. *Protein purification methods: a practical approach*. Oxford: IRL Press; 1989.
5. Gilchrist GR, "Direct fluidised bed adsorption of protein products from complex particulate feedstocks". PhD thesis, University of Birmingham; 1996.
6. Walsh G, Headson D. *Protein biotechnology*. New York: John Wiley and Sons; 1994.
7. Hughes DE, Wimpenny JWT, Lloyd D. In: Norris JR, Ribbons DW, editors. *Methods in Microbiology*, vol. 5B. New York: Academic; 1971.
8. Middelberg APJ. *Biotechnol Adv* 1995;**13**:491.
9. Agerkvist I, Enfors S-O. *Biotechnol Bioengng* 1990;**36**:1083.
10. Vogels G, Kula M-R. *Chem Engng Sci* 1991;**47**:123.
11. Kula M-R, Schütte H. *Biotechnol Progr* 1987;**3**:31.
12. Schütte H, Kroner KH, Hustedt H, Kula M-R. *Enzyme Microb Technol* 1983;**5**:143.
13. Bierau H, Zhang Z, Lyddiatt A. *J Chem Technol Biotechnol* 1999;**74**:208.
14. Jahanshahi M, Sun Y, Santos E, Pacek AW, Franco TT, Nienow AW, et al. *Biotechnol Bioengng* 2002;**80**:201.
15. Lee S-M. *J Biotechnol* 1989;**11**:103.
16. Bell G, Cousins RB. In: Weatherley LR, editor. *Engineering process for bioseparation*. UK: Butterworth-Heinemann; 1994.
17. Kula M-R. *Bioseparation* 1990;**1**:181.
18. Roe SD. In: Verral MS, Hudson MJ, editors. *Separations for biotechnology*. Chichester: Ellis Horwood; 1987.
19. Lyddiatt A. *Curr Opin Biotechnol* 2002;**13**:95.
20. Chase HA. *J Chromatogr* 1984;**297**:179.
21. Kumar A, Galaev I Yu, Mattiasson B. *J Chromatogr B* 2000;**741**:103.
22. Denizli A, Piskin E. *J Biochem Biophys Meth* 2001;**49**:391.
23. Kopperschlager G, Bohme HJ, Hofmann E. *Adv Biochem. Engng* 1982;**25**:101.
24. Haff LA, Easterday RL. In: Eckstein F, Sundaram PV, editors. *Theory and Practice in affinity chromatography*. New York: Academic Press; 1978.
25. Skidmore GL, Horstmann BJ, Chase HA. *J Chromatogr* 1990;**498**:113.
26. Spalding BJ. *Bio/Technology* 1991;**9**:229.
27. Van Reis R, Leonard LC, Hsu CC, Builder SE. *Biotechnol Bioengng* 1991;**38**:413.
28. Anspach FB, Curbelo D, Hartmann R, Garke G, Deckwer W-D. *J Chromatogr A* 1999;**865**:129.
29. Datar RV, Rosen CG. In: Stephanopoulos G, editor. *Bioprocessing*. Weinheim: VCH; 1996.
30. Belter PA, Cunningham FL, Chen JW. *Biotechnol Bioengng* 1973;**15**:533.
31. Chase HA. *Trends Biotechnol* 1994;**12**:296.
32. Levenspiel O. *Chemical Reaction engineering*. New York: Wiley & Sons; 1999.
33. Burns MA, Graves DJ. *Biotechnol Progr* 1985;**1**:95.
34. Zhang Z, O'Sullivan D, Lyddiatt A. *J Chem Technol Biotechnol* 1999;**74**:270.
35. Thömmes J, Halfar M, Lenz S, Kula M-R. *Biotechnol Bioengng* 1995;**45**:205.
36. Karau A, Benken J, Thömmes J, Kula M-R. *Biotechnol Bioengng* 1997;**55**:54.
37. Hjorth R. *Trends Biotechnol* 1997;**15**:230.
38. Brown GG. *Unit operation*. New York: John Wiley and Sons; 1950.
39. Draeger NM, Chase HA. *Bioseparation* 1991;**2**:67.
40. Ergun S. *Chem Enginng Prog* 1952;**48**:89.
41. Wen CY, Yu YH. *AICHE J* 1966;**12**:610.
42. Lan JC-W, Hamilton GE, Lyddiatt A. *Bioseparation* 1999;**8**:43.
43. Kunii D, Levenspiel O. *Fluidisation engineering*. New York: John Wiley and Sons; 1969.
44. Sun Y, Pacek AW, Nienow AW, Lyddiatt A. *Biotechnol Bioprocess Engng* 2001;**6**:1.
45. Thomas CR, Yates JG. *Chem Eng Res Des* 1985;**63**:67.
46. Jahanshahi M, Pacek AW, Nienow AW, Lyddiatt A. *J Chem Technol Biotechnol* 2002;**78**:1111.
47. Chang YK, McCreath GE, Chase HA. *Biotechnol Bioengng* 1995;**48**:355.
48. Richardson JE, Zaki WW. *Trans Inst Chem Engng* 1954;**32**:35.
49. Tong X-D, Sun Y. *J Chromatogr A* 2002;**943**:63.
50. Finette GMS, Mao QM, Hearn MTW. *J Chromatogr A* 1996;**743**:57.
51. Morton PH, Lyddiatt A. In: Slater MJ, editor. *Ion Exchanger advances*. Elsevier Applied Science; 1992.
52. Thömmes J, Weiher M, Karau A, Kula M-R. *Biotechnol Bioengng* 1995;**48**:367.
53. Morris JE, Tolppi CG, Carr PW, Flickinger MC. *Abstr Pap Am Chem Soc* 1994;**207**.

54. McCreath GE, Chase HA, Lowe CR. *J Chromatogr* 1994;**659**:275.
55. Palsson E, Gustavsson PE, Larsson PO. *J Chromatogr A* 2000;**878**:17.
56. Bascoul A, Delmas H, Couderc JP. *Chem Engng J Biochem Engng J* 1988;**37**:11.
57. Van Der Meer AP, Blanchard CMRJP, Wesselingh JA. *Chem Engng Res Des* 1984;**62**:214.
58. Bruce LJ, Clemmitt RH, Nash DC, Chase HA. *Chem Technol Biotechnol* 1999;**74**:264.
59. Hjorth R. *Bioseparation* 1999;**8**:1.
60. Hamilton GE, Luechau F, Burton SC, Lyddiatt A. *J Biotechnol* 2000;**79**:103.
61. Hamilton GE, Morton PH, Young TW, Lyddiatt A. *Biotechnol Bioengng* 1999;**64**:310.
62. Morton P, Lyddiatt A. *J Chem Technol Biotechnol* 1994;**59**:106.
63. Burns M, Lyddiatt A. *Controlled fluidised bed protein recovery using hydrophobic matrices*. Rugby, UK: The IChemE Research Event, IChemE; 1996.
64. Carmichael IA, Al-Rubeai M, Lyddiatt A. *New developments and new applications in animal cell technology*. ESACT, Kluwer Academic Publishers; 1998.
65. Asghari F, Jahanshahi M. Fabrication and evaluation of low-cost agarose–zinc nanoporous composite matrix: Influence of adsorbent density and size distribution on the performance of expanded beds. *J Chromatogr A* 2012;**1257**:89–97.
66. Shahavi MH, Najafpour GH, Jahanshahi M. Hydrodynamic behaviour and biochemical characterization of a simple custom expanded bed column for protein purification. *Afr J Biotechnol* 2008;**7**:4336–44.
67. Asghari F, Jahanshahi M, Ghoreysy AA. Preparation and characterization of agarose–nickel nanoporous composite particles customized for liquid expanded bed adsorption. *J Chromatogr A* 2012;**1242**:35–42.
68. Jahanshahi M, Mosavian MTH, Otaghsara EST. Hydrodynamic characteristics and adsorption Particularity of Nanobiological feedstock along the bed height in a novel chromatography column. *Chromatographia* 2012;**75**:585–96. <http://dx.doi.org/10.1007/s10337-012-2235-3>.
69. Ebrahimpour M, Jahanshahi M, Khavarpour M. Purification of Nanoparticle Bioproduct in integrated Processes: Plasmid DNA separation and recovery. *Dyn Biochemistry, Process Biotechnol Mol Biology* 2011:78–80. Global Science Books.
70. Shahavi MH, Jahanshahi M, Najafpour GD, Ebrahimpour M, Hosenian AH. Expanded bed adsorption of Biomolecules by NBG Contactor: Experimental and Mathematical investigation. *World Appl Sci J* 2011;**13**(2):181–7.
71. Ebrahimpour M, Jahanshahi M, Hosenian AH. Adsorption Strategy of Plasmid DNA nanoparticulate: preparative purification by a simple custom expanded bed column. *J Chromatogr* 2010;**72**(P):383–91.
72. Jahanshahi M, Ebrahimpour M. Expanded bed chromatography as a tool for nanoparticulate separation: kinetic study and adsorption of protein nanoparticles. *J Chromatogr* 2009;**70**:1553–60.
73. Ebrahimpour M, Shahavi MH, Jahanshahi M, Najafpour GH. Nanotechnology in process biotechnology: recovery and purification of nanoparticulate bioproducts using expanded bed adsorption. *J Dyn Biochem Process Biotechnol Mol Biology* 2009;**3**(Special Issue 2):57–60.
74. Jahanshahi M, Najafpour GH, Ebrahimpour M, Hajizadeh S, Shahavi MH. Evaluation of hydrodynamic parameters of fluidized bed adsorption on purification of nano-bioproducts. *J Phys Status Solidi C* 2009;**6**(10):2199–206.
75. Jahanshahi M, Panahi H, Hajizadeh S, Moniri E. Boronate-containing copolymer grafted on Eupergit C as Matrix for Affinity Chromatography. *J Chromatografia* 2008;**68**(2):41–7;75:585–96.

SUBCHAPTER

17.11

Case Study: Biochemical Characterization of a Custom Expanded Bed Column for Protein Purification*

17.11.1 INTRODUCTION

Liquid fluidized bed adsorption (expanded bed adsorption) has emerged as an efficient method for the recovery of biological products from complex feedstocks. Expanded bed adsorption has demonstrated advantages over the traditional methods of recovery, e.g., circumventing the need for clarification of feedstocks before application to a fixed bed chromatography column.^{1,2} The hydrodynamic behavior of fluidized beds/expanded beds applied to chromatographic adsorption is different from the conventional liquid–solid fluidized beds. The conventional chemical engineering view of a fluidized bed is one in which there is a significant degree of mixing, both of the solid and the fluid phases: for example, in gas-fluidized systems.³ However, mixing in liquid fluidized systems is not as severe as in gas-fluidized ones. Here, the density differences between the solid and the fluid phase are comparatively small, and thus the bed shows a particulate behavior in which the bed can retain a uniform character. In a packed bed, the adsorbent beads are stationary and liquid flow through the bed approximates plug flow. In contrast, owing to the mixing of the adsorbent, a fluidized bed would be expected to show an inferior adsorption performance compared with the packed bed. Therefore, it is highly desirable to investigate the hydrodynamic performance and minimize the degree of mixing to mimic the adsorption characteristics found in a packed bed contactor with respect to capacity and resolutions.^{4,5}

Column (contactor) and solid phase designs have a major role in fluidized bed/expanded bed adsorption. The growth to full potential of applications for fluidized bed or expanded bed technology in biological product recovery may be considered to be currently limited by the availability of suitable adsorbents and columns in terms of efficiency and cost. The adsorbent design was extensively been studied in earlier publications.^{6–10} In the other words, such technology has been commercialized with customized contactor designs and extensive development programs required for their establishment. Such developments have invited re-examination of the simply designed fluidized bed contactor (Nanobiotechnology Group at Noshivani University of Technology referred to as the NBG contactor, as shown in

*This chapter was written with contributions from:

Mohammad Hassan Shahavi, Mohsen Jahanshahi, Biotechnology Research Lab., Faculty of Chemical Engineering, Noshirvani University of Technology, Babol, Iran.

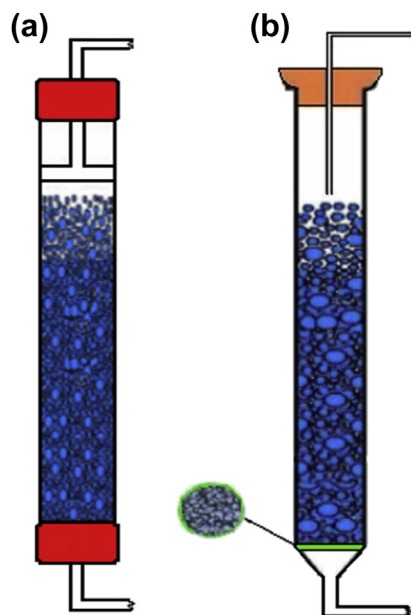


FIGURE 17.7 Representation of apparatus for expanded bed experiments. (a) Streamline column. (b) Custom-built NBG column.

Figure 17.7). The NBG contactor has the ability to retain adsorptive fractionation of protein products contained in particulate feedstocks, in respect of suitability for single-pass.

This case study summarizes the critical examination of the hydrodynamic performance of the NBG contactor and an equivalent commercial expanded bed contactor operated with Streamline™ DEAE adsorbent under various operating conditions. This investigation includes bed expansion tests, residence time distribution (RTD) measurements comprising determination of the Bodenstein number, and axial dispersion of the adsorbents across a range of fluid velocities. However, for the purpose of demonstrating the principle, the performance of adsorption of bovine serum albumin in the NBG column is investigated and compared with that of a commercial expanded bed column. The capture of egg albumin in batch binding experiments upon Streamline™ DEAE adsorbent and its expanded bed adsorption in both contactors is also demonstrated.

17.11.2 MATERIALS AND METHODS

17.11.2.1 Materials

Bovine serum albumin was commercially supplied by Sigma and egg albumin was purchased from Merck (Darmstadt, Germany). All reagents were supplied by Merck and Aldrich Chemical Company (Darmstadt, Germany); they were of analytical grade and

used as received. Streamline™ DEAE adsorbent was purchased from Amersham Biosciences (Piscataway, NJ 08855-1327, USA).

17.11.2.2 Adsorbent Contactors

Two types of contactors were used in this experiment. Streamline™ columns were purchased from Amersham Biosciences and adopted for studies of hydrodynamic and expanded bed recovery performance. In addition, custom-built devices fabricated by the NBG contactor, Nanobiotechnology Group (Babol University of Technology), which was equipped with a simple sintered glass distributor composed of a 100-mm mesh, were also used. Such contactors were composed of a glass column with a hemispherical inlet.

17.11.2.3 Bed Expansion Characteristics

Bed expansion characteristics were determined in expanded beds operated with buffer A (10 mM Tris/HCl containing 0.2% (w/v) sodium azide at pH 7.5). The adsorbent was repeatedly washed before use with equilibration buffer A and filtered until the pH and conductivity reached equilibrium. A given amount of adsorbent particles was transferred to the columns and allowed to sediment uniformly. The bed expansion of adsorbent was measured and recorded with increasing superficial liquid velocity through the inlet of the column. The superficial flow velocity was subsequently plotted against bed expansion expressed as the percentage ratio of expanded and settled bed heights (SBH).

17.11.2.4 Fluidized/Expanded Bed Adsorption

All fluidized bed adsorption experiments were undertaken according to a common protocol. Adsorbent was packed into the chosen contactor and equilibrated with buffer A. Before feedstock application, the bed was fluidized at 100% expansion ($H/H_o = 2$, where H and H_o represent expanded and SBHs, respectively) in equilibration buffer A. The experiment was continued in a single-pass operation with the application of serum bovine and egg albumin as feedstocks to the fluidized adsorbent at a given linear flow velocity. After feedstock application, the fluidized bed was washed with buffer A until A280 reached baseline values. Subsequently, product desorption was achieved in fluidized bed mode with 0.5 M NaCl in buffer A. Appropriate fractions were collected and assayed for protein content as described before.

17.11.3 RESULTS AND DISCUSSION

17.11.3.1 Bed Expansion

The bed expansion contributes to the adsorption efficiency as a composite function of liquid distribution, liquid properties (viscosity, density), particle characteristics, and the configuration of the column in terms of wall and distributor effects.^{11,12} The adsorbent expansion in the NBG contactor might be expected to exhibit unstable fluidization behavior because of the channeling generated by the simple distributor. This was not visibly apparent in the present study (see [Figure 17.8](#)). To estimate the variation of the bed expansion as a function of flow velocity throughout the bed, the Richardson–Zaki equation was used. The experiments were operated in buffer A and relevant graphs are shown in [Figures 17.8 and 17.9](#).

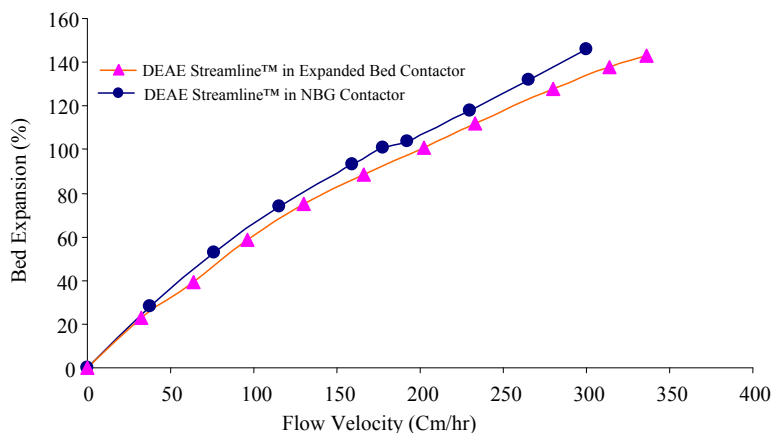


FIGURE 17.8 Bed expansion of the adsorbent as a function of linear flow velocity in expanded bed and NBG contactors.

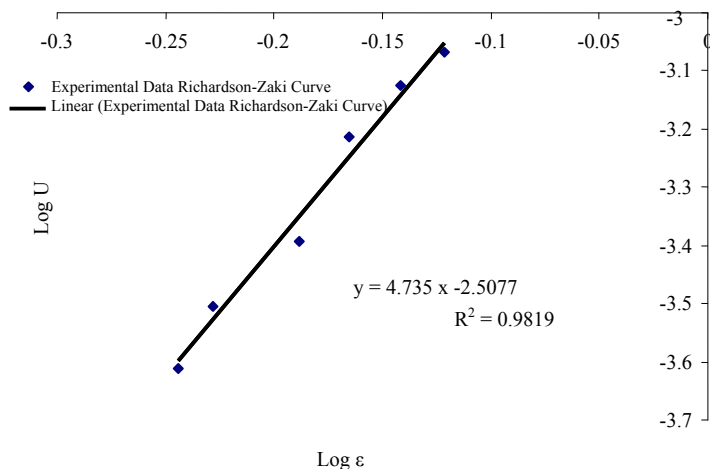


FIGURE 17.9 Flow velocity as function of bed voidage for calculation of Richardson–Zaki coefficient (n) and terminal velocity (U_t).

The theoretical terminal velocity was derived from the Shiller and Nanmann model. The experimental values of terminal velocity (U_t) can be determined by fitting data into the Richardson–Zaki equation. The values for the terminal velocity were derived from the equations mentioned earlier (bed expansion characteristics). A summary of bed expansion characteristics is presented in Table 17.1. Experimental values of the Richardson–Zaki coefficient determined here were about 4.7 and approximated the value of 4.8 commonly used in the laminar flow regime.^{13–15} The experimental values of the expansion coefficient and terminal velocity of the adsorbent in the NBG contactor agreed more closely with the results calculated from literature correlation than the corresponding values for the commercial contactor. There was a small difference between the experimental data and calculated data (Table 17.1)

TABLE 17.1 Experimental and theoretical values of expansion coefficient and terminal velocities for the adsorbent in the NBG contactor

Type of data	U_t (m/s)	U_m (m/s)	n
Theoretical data	3.25262 E-03	3.74482 E-05	4.74542
Experimental data	3.106 E-03	3.6762 E-05	4.735

attributed to the assumption of settled bed voidage ($\epsilon_0 = 0.4$) and the difference of particle size distribution in each of the beds. The discrepancies between these results are similar to those reported in the literature. For example, Thömmes et al. found that the calculated terminal velocity was about tenfold higher than that experimentally determined in the fluidized bed of controlled pore glass.¹⁶ That was because of the porous nature and irregular shape of the glass matrix.

17.11.3.2 Mixing of the Liquid Phase (Residence Time Distribution Experiments)

Measurement of the axial dispersion—that is, the deviation from plug flow movement of fluid elements in an adsorbent bed (both packed and fluidized)—is commonly performed by residence time distribution (RTD) analysis of step or pulse signals.¹⁷ This method was employed in the present research work, to characterize and compare the NBG contactor with a commercial expanded bed contactor. Measurements were made with regard to degree of axial dispersion and bed stability when materials were fluidized under similar conditions. The values of theoretical plate number (N), axial dispersion coefficient (D_{axl}), and Bodenstein number (Bo) were estimated and are summarized in Table 17.2.

Comparison of the results confirmed the superior hydrodynamic properties: that is, diminished mixing and stable fluidization throughout the bed. For example, the Bodenstein number of the adsorbent in the NBG, which represents the axial dispersion and fluidization behavior in the passage of fluid elements through the contactor, was as good as that of the commercial contactor.

Figure 17.10 summarizes the variation of D_{axl} with the degree of bed expansion for the adsorbent operated in buffer A. The D_{axl} curve increases with increased superficial flow velocity.^{18,19} This suggests that in a given contactor configuration, every individual adsorbent is characterized by a range of flow velocities at which the degree of axial dispersion is at a minimum. The measured Bo values were judged (Table 17.2); superior fluidization characteristics were exhibited that gave justification for further experimentation in the fluidized bed adsorption of bioproducts.

17.11.3.3 Equilibrium Kinetic Studies

A batch binding characteristics of Streamline™ DEAE was undertaken with egg albumin. The uptake of different concentrations of egg albumin upon the adsorbent is depicted as a function of different time scales in Figure 17.11. It can be seen from Panel A that the uptake of egg albumin occurs especially over the first minute of reaction. Panel B in Figure 17.11 indicates that proteins desorption approached a steady state value after approximately 5 min of reaction time.

TABLE 17.2. B_o and D_{axl} for different settled bed height (a) and for different expanded bed height (b)

(A)				
SBH	EBH	t (s)	D_{axl}	B_o
5	10	114.43	0.12579	8.400639
6	12	106.53	0.008893	9.519199
7	14	155.02	0.147457	16.60508
8	16	180.78	0.13098	18.946599
9	18	185.15	0.168619	20.58865
10	20	178.57	0.200093	18.36429
(B)				
SBH	EBH	t (s)	D_{axl}	B_o
6	8	342.21	0.000516	7.91374
6	10	122.66	0.003578	3.638651
6	12	105.13	0.003021	9.252633
6	14	91.568	0.004355	7.706067
6	16	41.161	0.023601	1.943883

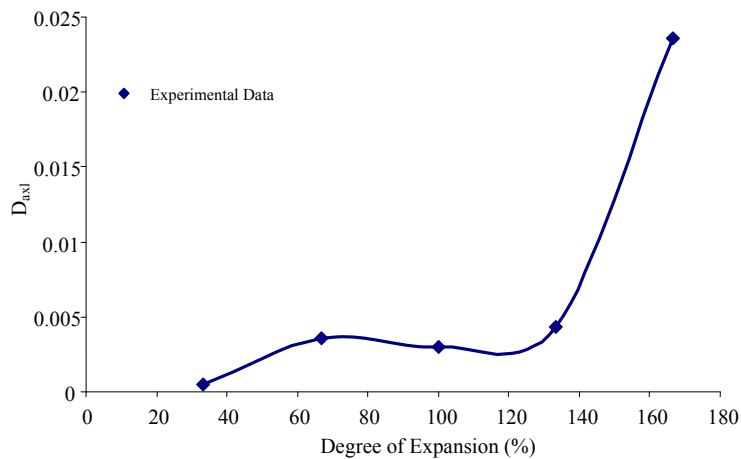
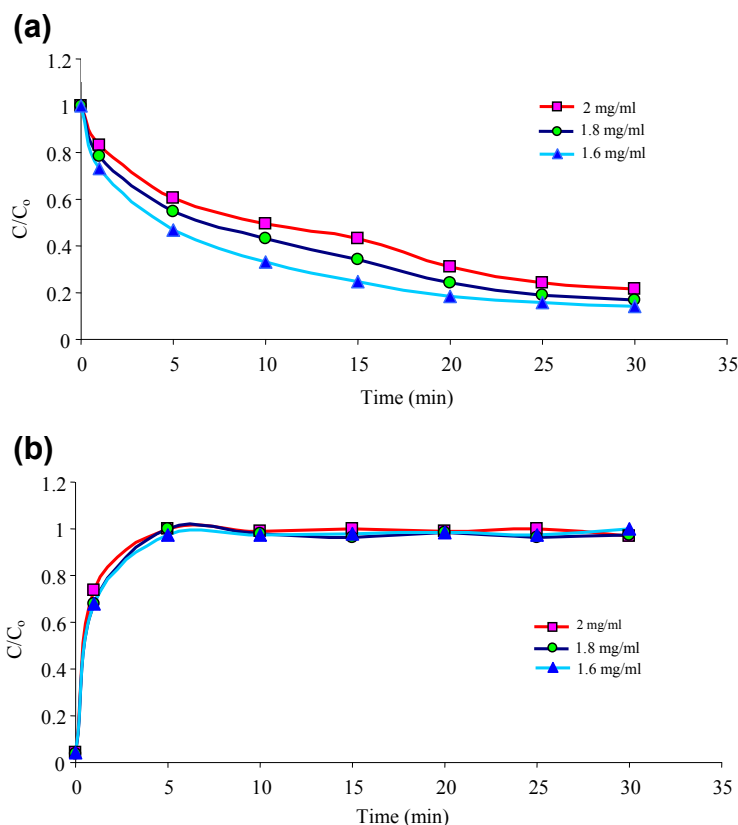


FIGURE 17.10 Axial dispersion coefficient as a function of bed expansion.

FIGURE 17.11 Batch binding of egg albumin to the streamline DEAE adsorbent. (a) Adsorbent. (b) Desorption.



Enhanced rates of binding and the attainment of higher binding capacities may be influenced by the lowered diffusion resistance to the attainment of saturation imparted by the Streamline™ DEAE, a standard adsorbent for expanded bed adsorption, and for good penetration of egg.^{18–21}

17.11.3.4 Expanded Bed Adsorption

The expanded bed adsorption performance of the adsorbent was investigated in the NBG contactor at different SBHs operated with bovine serum albumin and egg albumin at given flow velocities. As can be seen from Figure 17.12, the dynamic capacity (estimated from the protein challenge required to achieve 10% breakthrough of the protein, $C/C_0 = 0.1$) of SBH of 10 was the highest value recorded for the adsorbent under study, and the shape of all breakthrough curves closely approximated that of a packed bed of that material operated similarly with the same feedstock (data not shown).

This observation confirmed the relatively low degree of axial mixing and high stability of the fluidized bed in the NBG contactor. A small SBH exhibited a lower dynamic capacity and a shallower increase in product breakthrough, which could be attributed to channeling

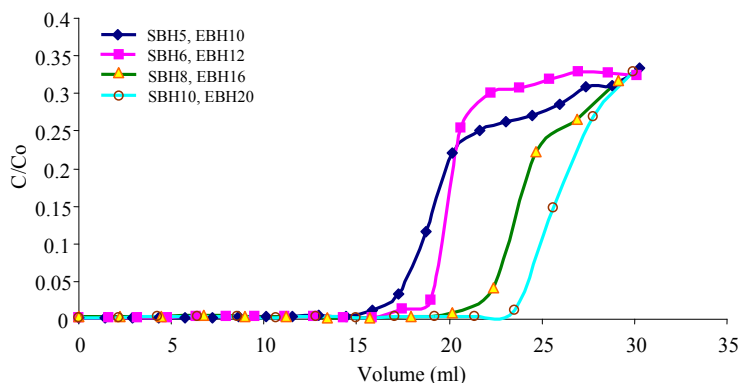


FIGURE 17.12 Breakthrough curve of egg albumin with Streamline™ DEAE adsorbent.

resulting from minor bed instabilities, as has been demonstrated before in hydrodynamic assessments. A full chromatogram of fluidized bed recovery of egg albumin also is displayed in [Figure 17.13](#).

In addition, a step-by-step fluidized bed adsorption of bovine serum albumin in the commercial column as well as in the NBG column was carried out. The step elution of Streamline™ DEAE in the commercial column resulted in broad peaks of protein concentration, whereas a similar step yielded a sharper peak for the NBG contactor such that the protein was eluted in a more concentrated form (see [Figure 17.14](#)). However, in this comparative experiment, the NBG contactor exhibited the lowest breakthrough and potential for foreshortening the overall operational time with respect to loading, washing, and elution stages, and might possess potential processing advantages by virtue of the distributor design.

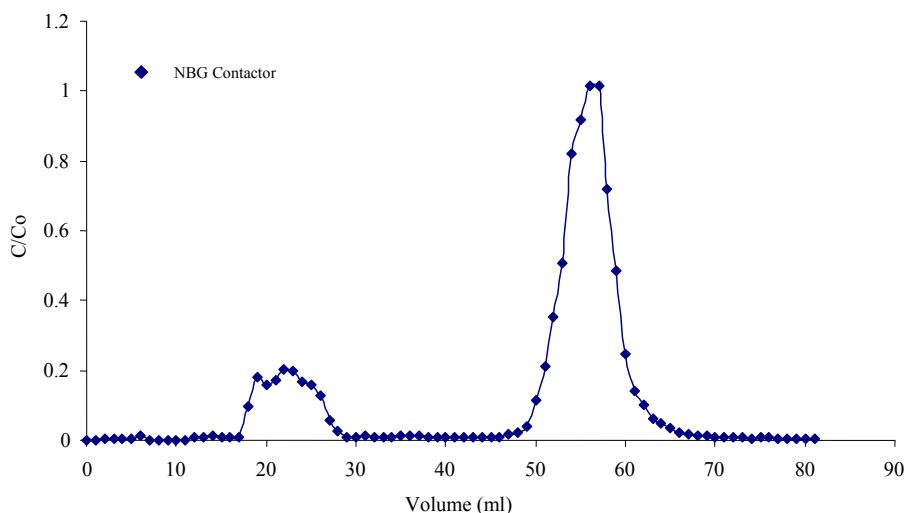


FIGURE 17.13 Full chromatogram of fluidized bed recovery of egg albumin in NBG contactor.

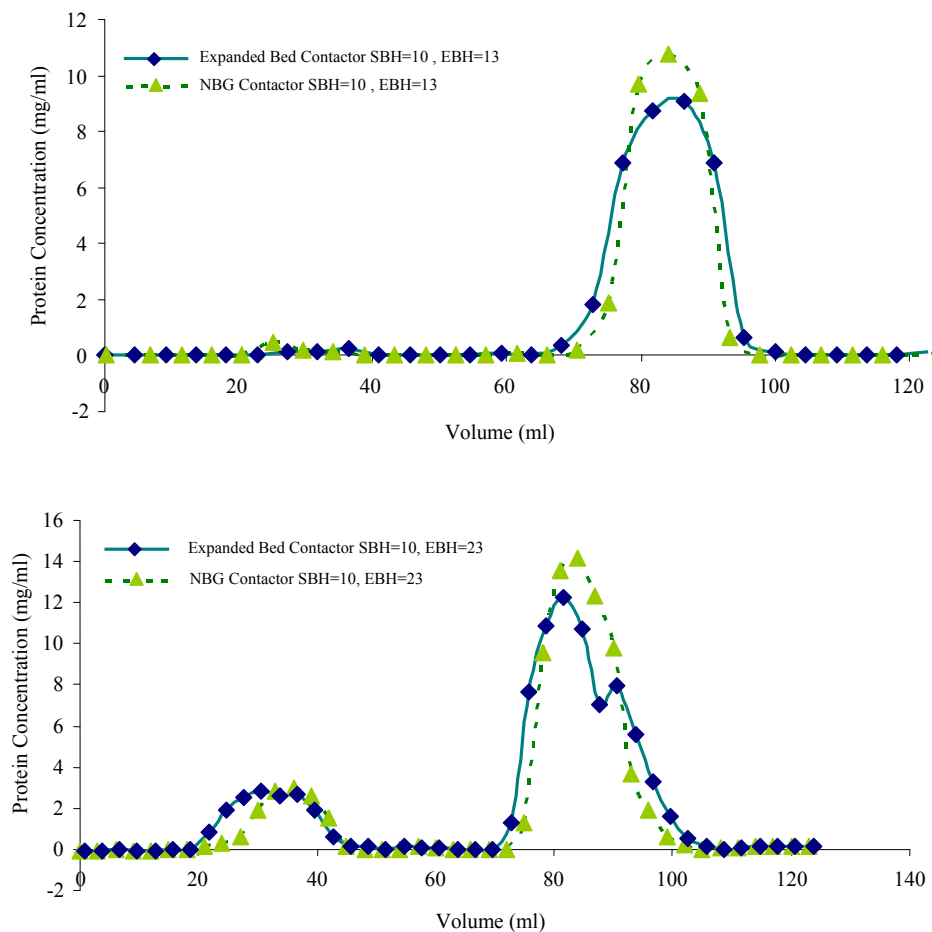


FIGURE 17.14 Full chromatogram of fluidized bed recovery of BSA in expanded bed and NBG contactors different expanded bed heights.

17.11.4 CONCLUSION

A simple unique fluidized bed contactor (NBG), which was equipped with a glass tube fitted with a simple sintered glass distributor composed of a 100-mm mesh, was prepared and used here. With respect to physical performance, the bed expansion response of NBG was similar to or better than commercial expanded bed contactor. In experiments undertaken to assess the hydrodynamic behavior of fluidized bed systems (estimation of N , D_{axl} , Bo , etc.), the performance of the NBG was relatively constant across a range of expanded bed height and fluid velocities. This study was completed with that of Streamline™ in different column diameters and SBH, which deteriorated within the same range of study. Batch binding studies of egg albumin adsorption upon Streamline™ DEAE indicated that this exhibited

apparently reasonable adsorption and capacity for the protein under common experimental conditions. In addition, adsorption and desorption equilibria were achieved in a relatively short contact time (see Figure 17.10). In fluidized bed experiments, the rapid achievement of baseline values of the feedstock in the effluents after the initiation of washing and elution steps confirmed and additional advantage of the NBG design (see Figure 17.13).

Furthermore, the ability to operate the adsorbent at flow velocities up to two or three times that of other column without diminution of adsorption or washing efficiencies because of its distributor is a clear practical advantage. It is believed that the simple, economic design of the NBG contactor compares favorably in hydrodynamic and biochemical performance with a commercial expanded bed contactor. It can be concluded from the work reported here that the prototype NBG contactor has many properties required as a column for protein purification and deserves further study in terms of refined geometric design, operational longevity, and suitability for validated manufacturing operations, which may be the subject of future publications.

References

1. Annelise S, Tetaud E, Merlin G, Santarelli X. LdARL-1 His-tagged recombinant protein: purification by immobilized metal affinity expanded bed adsorption. *J Chromatogr* 2005;**818**:19–22.
2. Balasundaram B, Harrison STL. Influence of the extent of disruption of Bakers' yeast on protein adsorption in expanded beds. *J Biotechnol* 2008;**133**:360–9.
3. Kuo JH, Yang CC. Mechanism of centrifugal filtration for separation of microbe/protein bio-suspension. *Chem Eng Proc* 2008;**47**:1647–55.
4. Jahanshahi M, Sun Y, Santos E, Pacek AW, Franco TT, Ninow AW, et al. Operational intensification by direct products sequestration from cell disruptates: application of a pellicular adsorbent in a mechanically integrated disruption-fluidized bed adsorption process. *Biotechnol Bioeng* 2002;**80**:201–12.
5. Bermejo R, Ruiz E, Acien FG. Recovery of B-phycoerythrin using expanded bed adsorption chromatography: scale-up of the process. *Enzyme Microb Technol* 2007;**40**:927–33.
6. Jahanshahi M, Pacek AW, Nienow AW, Lyddiatt A. Fabrication by three-phase emulsification of pellicular adsorbents customised for liquid fluidized bed adsorption of bioproducts. *J Chem Technol Biotechnol* 2003;**78**:1111–20.
7. Jahanshahi M, Zhang Z, Lyddiatt A. Subtractive chromatography for purification and recovery of nanobioproducts. *J Nanobiotechnol* 2005;**152**(3):121–6.
8. Jahanshahi M, Panahi H, Hajizadeh S, Moniri E. Boronate-containing copolymer grafted on Eupergit C as matrix for affinity chromatography. *J Chromatographia* 2008;**68**(2):41–7.
9. Sadat Taheri E, Jahanshahi M, Hamed Mosavian MT. Preparation, characterization and optimization of egg albumin nanoparticles as low molecular-weight drug delivery vehicle. *Part Part Syst Charact* 2012;**29**(3):211–22.
10. Jahanshahi M, Hamed Mosavian MT, Taheri Otaghsara ES. Hydrodynamic characteristics and adsorption particularity of nanobiological feedstock along the bed height in a novel chromatography column. *Chromatographia* 2012;**75**:585–96. <http://dx.doi.org/10.1007/s10337-012-2235-3>.
11. Asghari F, Jahanshahi M. Fabrication and evaluation of low-cost agarose–zinc nanoporous composite matrix: influence of adsorbent density and size distribution on the performance of expanded beds. *J Chromatogr A* 2012;**1257**:89–97.
12. Asghari F, Jahanshahi M, Ghoreyshi AA. Preparation and characterization of agarose–nickel nanoporous composite particles customized for liquid expanded bed adsorption. *J Chromatogr A* 2012;**1242**:35–42.
13. Davidson JF, Clift R, Harrison D. *Fluidisation*. 2nd ed. London: Academic Press; 1985.
14. Amersham Bioscience. *Expanded bed adsorption—principles and methods*. Uppsala, Sweden: Pharma Biotech; 1998 [Chapter 20].
15. Ebrahimpour M, Shahavi MH, Jahanshahi M, Najafpour GH. Nanotechnology in process biotechnology: recovery and purification of nanoparticulate bioproducts using expanded bed adsorption. *J Dyn Biochem Process Biotechnol Mol Biol* 2009;**3**(Special Issue 2):57–60.

16. Thömmes J, Weiher M, Karau A, Kula MR. Hydrodynamics and performance in fluidized bed adsorption. *Biotechnol Bioeng* 1995;**48**:367–74.
17. Levenspiel O. *Chemical reaction engineering*. 3rd ed. New York: John Wiley & Sons; 1999.
18. Ebrahimpour M, Jahanshahi M, Khavarpour M. Purification of nanoparticle bioproduct in integrated processes: plasmid DNA separation and recovery. *Dyn Biochem Process Biotechnol Mol Biol* 2011:78–80. Global Science Books.
19. Shahavi MH, Jahanshahi M, Najafpour GD, Ebrahimpour M, Hosenian AH. Expanded bed adsorption of biomolecules by NBG contactor: experimental and mathematical investigation. *World Appl Sci J* 2011;**13**(2):181–7.
20. Jahanshahi M, Najafpour GD, Ebrahimpour M, Hajizadeh S, Shahavi MH. Evaluation of hydrodynamic parameters of fluidized bed adsorption on purification of nano-bioproducts. *J Phys Status Solidi C* 2009;**6**(10):2199–206.
21. Shahavi MH, Najafpour GD, Jahanshahi M. Hydrodynamic behaviour and biochemical characterization of a simple custom expanded bed column for protein purification. *Afr J Biotechnol* 2008;**7**:4336–44.

Microbial Fuel Cells: A New Source of Power*

OUTLINE

18.1 Introduction	528	18.3.11 MFCs' Performance	543
18.2 Biological Fuel Cell	529	18.3.11.1 Conditions in the Anodic Chamber	544
18.3 Microbial Fuel Cell	531	18.3.11.2 Proton Exchange Membrane	544
18.3.1 MFC Construction	532	18.3.11.3 Conditions in the Cathodic Chamber	544
18.3.2 Active Biocatalysts	535	18.3.12 Applications of MFCs	545
18.3.3 Electron Transfer in MFCs	536	18.3.12.1 Electricity Production	545
18.3.4 Electron Transport in MFCs	538	18.3.12.2 Production of Biological Hydrogen	546
18.3.5 Use of a Mediator for Electron Transport	538	18.3.12.3 Biosensors	547
18.3.5.1 Using Artificial Mediators	538	18.3.12.4 Wastewater Treatment	547
18.3.5.2 Electron Mediators Generated by Self-producing Microbes	539	Acknowledgment	551
18.3.6 Challenges in MFCs	540	References	551
18.3.7 Calculations in MFCs	540		
18.3.8 Power Generation	541		
18.3.9 Overpotential in MFCs	542		
18.3.10 Coulombic Yield	543		

*This chapter was written with contributions from:

M. Rahimnejad, Biotechnology Research Laboratory, Faculty of Chemical Engineering, Noshirvani University of Technology, Babol, Iran.

18.1 INTRODUCTION

Energy plays a key role in humans' lives. One may have access to a source of heat and light using energy; in fact, energy can guarantee the economic status of countries.¹ Nowadays, fossil fuels are the main source of energy, and their pollution creates many problems for the living environment. Consequently, the emergence of appropriate, cheap, and clean alternatives is obviously important for the replacement of fossil fuels. The cause of rapid population is due to excessive fossil fuel consumption. As the energy crisis gradually affects and threatens the world, energy demands sustainable development.^{2,3}

Among the known resources of energy, electricity is the most desired and flexible form of energy.⁴ Considerable attention has recently been paid to renewable energy as an alternative to fossil fuels to reduce carbon dioxide emissions and eliminate global warming. However, most renewable energy technologies, particularly solar energy, are still not mature enough to compete with conventional energy based on fossil fuels. The preferable energy is electrical energy created by fuel cells.⁵ A fuel cell is a device that can directly convert chemical energy to electrical energy. The simple principle of a hydrogen fuel cell is illustrated in Figure 18.1. In the early nineteenth century, the concept of using fuel cells for power production was discovered by the German scientist Christian Friedrich Schonbein. Based on this concept, the first fuel cell was fabricated by a Welsh scientist and barrister Sir William Robert Grove in February 1839.^{6,7}

Because the cell does not follow the Carnot cycle theory, the efficiency of these cells was much higher than expected. Indeed, reactions took place in fuel cells could be considered

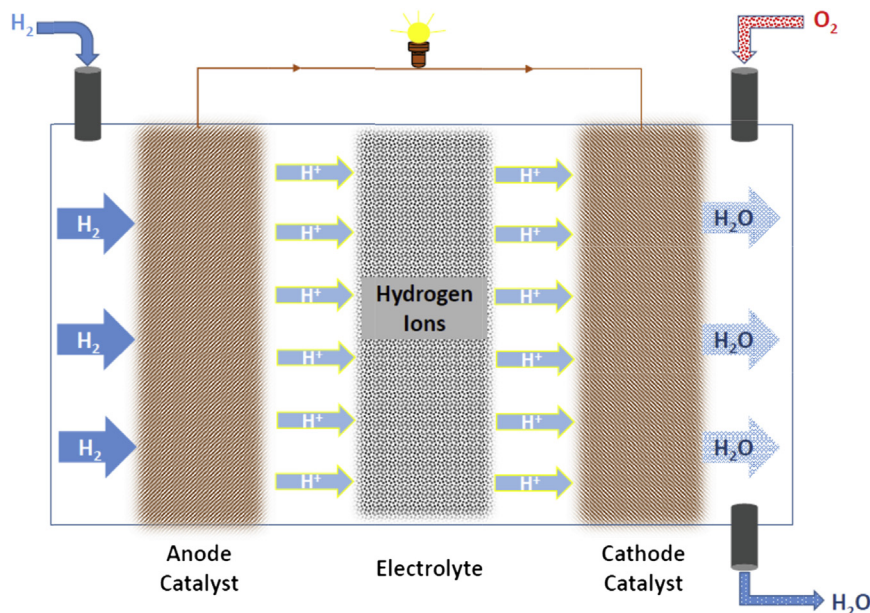


FIGURE 18.1 Schematic diagram of a fuel cell with a simple concept.

the reverse operation of water electrolysis. In other words, the final products of a reaction between hydrogen and oxygen are water, heat, and electricity.⁸ This type of cell cannot save energy, like batteries; they can only alter one kind of energy to another without consuming the materials inside the cell. Each fuel cell consists of three components: an anode electrode, a cathode electrode, and an electrolyte or membrane. Hydrogen is used as fuel in the cell and, after oxidizing in an anode electrode, a positive hydrogen ion and an electron are produced; then, protons and electrons pass through the electrolyte and external circuit, respectively. As a result, water is generated in the cathode by the reaction of oxygen, electrons, and hydrogen ions.^{9,10}

Fuel cells are classified and named based on their electrolytes:

1. Alkaline fuel cell
2. Phosphoric acid fuel cell
3. Polymer electrode membrane
4. Molten carbonate fuel cell
5. Solid oxide fuel cell
6. Biological fuel cell (BFC)
7. Formic acid fuel cell
8. Zinc–air fuel cell
9. Ceramic fuel cell

Fuel cells have different merits, such as:

- High efficiency
- High power
- Easy to transport
- Compatible with environmental rules
- System can be adjusted
- High energy density
- Flexibility toward fuels
- Increase production and decrease distribution
- Capability to combine with other energy production systems

Despite the large number of advantages, these cells have some demerits, such as the high cost of catalysts, corrosive electrolytes, and the harsh conditions of operation (high temperature and pressure).^{11,12}

18.2 BIOLOGICAL FUEL CELL

In light of the above-mentioned disadvantages of fuel cells and the recent energy crisis, BFCs are one of the latest emerging sustainable energy technologies that convert the chemical energy restored in substrates into electrical energy by means of active biocatalysts, such as microorganisms or enzymes, in various BFC configurations. In a BFC, electricity can be generated in a biological system. BFCs perform a similar function as nonbiological fuel cells do. Construction of BFCs is similar to that of a polymer electrode membrane with the exception that there are some differences in anodic reactions.¹³ But the major difference is the catalyst

TABLE 18.1 Comparisons of biological fuel cells with chemical fuel cells¹⁵

Characteristics	Biological fuel cell	Chemical fuel cell
Catalyst	Enzyme, microorganism	Metals
pH	7–9	Acid solution
Temperature	Environmental temperature	Over 200 °C
Electrolyte	Phosphate solution	Phosphoric acid
Capacity	Low	High
Efficiency	>50%	40–60%
Fuel type	Carbohydrate	Natural gas, hydrogen

used. The catalysis in a BFC is a microorganism or enzyme, and there is no need to use precious metals such as platinum.¹⁴ Use of BFCs also has other benefits:

- Do not require any catalysts
- Have high stability over a long duration
- Do not require any exchanger or condenser for the reactions
- Active biocatalysts are used
- Use various substrates as electron donors
- High efficiency

Table 18.1 compares BFCs with chemical fuel cells. BFCs use biocatalysts have the following benefits:

- Biocatalysts have the capability of operating in a low to moderate temperature range.
- Biocatalysts are cheaper than metal catalysts.
- Biocatalysts are reproducible and easily replaceable.

As stated earlier, a BFC is a device that converts biochemical energy to electrical energy. The concept of these units are that substrates are oxidized by microorganisms or enzymes, resulting in the production of electricity. **Figure 18.2** depicts the principal reactions that occur in BFCs.

Because the process theoretically does not follow the Carnot cycle, it is not feasible to obtain high efficiencies.¹⁶ BFCs often have two chambers.^{17,18} It is possible in some cases to eliminate the cathode chamber and expose the air cathode directly to the ambient air.¹⁹

BFCs are classified into three major categories.

- Microbial fuel cells (MFCs)
- Sedimentary MFCs
- Enzymatic MFCs

Photomicrobial cells and MFCs that make use of a variation of solid sludge can be classified under these three main categories.²⁰

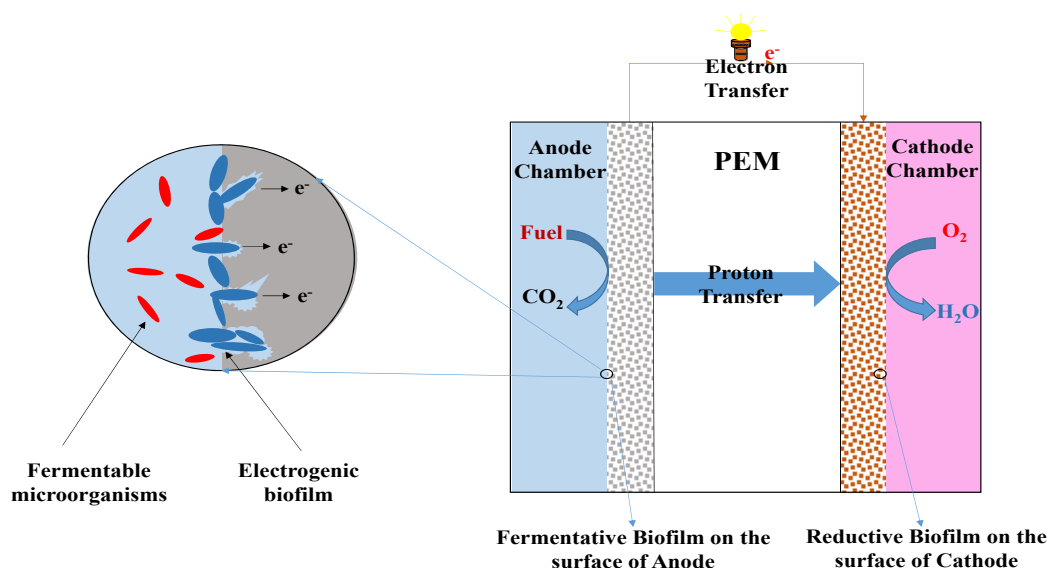


FIGURE 18.2 Schematic diagram of a biological fuel cell with a biochemical reaction in the anode and cathode compartments. PEM, proton exchange membrane.

18.3 MICROBIAL FUEL CELL

Active microorganisms in MFCs liberate electrons, while electron donors are consumed. In an anaerobic anode chamber, substrates such as carbohydrates are used; as a result, bioelectricity is produced in an MFC. Among electrochemical cells, MFCs bring new insight into electricity generation by different types of substrates and have attracted a huge number of scientists. Microorganisms are involved in reduction reactions. Certain microorganisms are capable of producing bioelectricity from reductive substances.^{21,22}

In 1911, Potter²³ was the first scientist to introduce the concept of an MFC. Logan and Regan²⁴ observed that bacteria can produce electrical current. Living cultures of *Escherichia coli* and *Saccharomyces* species were used to generate electricity in an MFC with a platinum electrode.²³ The research in this area was almost stopped for about 55 years after the first innovation; there was no advancement in MFC development.²⁵

No serious research on MFCs was practiced until later decades (the 1950s and early 1960s). The US space program encouraged scientists to develop MFCs as potential waste disposal systems and simultaneous power generators for use during space flights. This did not attract much attention until it was discovered that electron mediators could greatly surge current density and power output. However, the electron mediators had several disadvantages.²⁶

A big step was taken in the development of MFCs; Gil et al.²⁷ acknowledged that there was no need to use an artificial electron mediator to transfer produced electrons from the bacteria to the anode electrode. Mediators have the ability to accelerate the transfer of electrons to the anode. The outer layer of a large number of microbes are made of a nonconductive lipid

membrane, peptidoglycans, and lipopolysaccharides, which prevent the transfer of electrons to the anode. The ability of mediators to pass through the membrane and release electrons to the anode was also investigated.^{28–30}

Karube and his research team³¹ reported electricity generation using rice bran and glucose as substrates in an MFC. They used *Clostridium butyricum* as a biocatalyst for hydrogen production in the anode chamber. In the late 1970s, an extensive amount of work and investigations were accomplished by many scientists such as Allen and Bennetto.³² Allen and Bennetto publicized their work and tried to understand how fuel cells operate.¹⁵ Regarding the transmission of energy and electricity directly to electrodes, some valuable works have recently been demonstrated, such as the new finding of an effective path of connecting microorganisms to electrodes to increase the electron transmission efficiency. It was recently reported that *Rhodospirillum rubrum* is instantly able to transmit more than 83% of electrons produced from glucose oxide in Fe⁺³.³³

In 2007, the University of Australia introduced a sort of microbial cell that was used in experimental runs by the Foster Brewing Company. The MFC contained 10 l of fluid, which was fed by sewage as fuel. The waste was converted to carbon dioxide and water while producing electricity. The MFC, with a capacity of 600 gallons and power generation of about 2 KW, was considered as a great success.

The effect of a mixed culture medium and an incremental feeding rate on the power output of the system was recently studied by Rabaey and his coworkers.³⁴ They used wide sheet electrodes in their investigation. An efficiency of 89% was obtained at a feeding rate of 0.5 g l⁻¹ glucose per day.² Other researchers have conducted investigations using pure and mixed culture media.^{33,35,36} The electrical power output of the primary MFCs was not considerable (range of 1–40 mW/anode surface area).^{18,20} Today, scientists have greatly endeavored to obtain optimum power output. Logan, in Pennsylvania, has made many efforts toward this concept and is well known in this regard; power output of the MFC designed by his research team was primarily in the range of 150–10 mW/anode surface area, and they also have reported 500 mV power output.² Rahimnejad and his coworkers³⁷ improved MFC performance by fabricating a new stack. The maximum current and power generated in the stack of MFCs were 6447 mA m⁻² and 2003 mW m⁻², respectively.

Belgian scientists announced that they were able to produce 3600 mV per electrode surface area.³⁴

Briefly, electrical current produced by bacteria was observed by Potter²³ in 1911, and limited feasible results were obtained on this subject in the next 50 years.³⁸ Later, the attraction of fuel cells became stronger and the field of MFCs began to improve.³² The steep slope of MFC progress began in 1999,^{18,39} but the main interest in MFCs have increased in recent years. So many achievements have been gained and numerous articles and research have been published to date. The number of articles in the field of MFCs published by researchers from different countries from 1990 to 2013 is presented in Figure 18.3; these articles were identified by typing the key word *microbial fuel cell* in a Scopus search.

18.3.1 MFC Construction

MFC is a novel tool that can obtain bioenergy in the form of hydrogen and/or electricity directly from different organic and inorganic compounds while simultaneously treating biodegradable substrates or contaminants in wastewater. In MFCs, electrons are provided

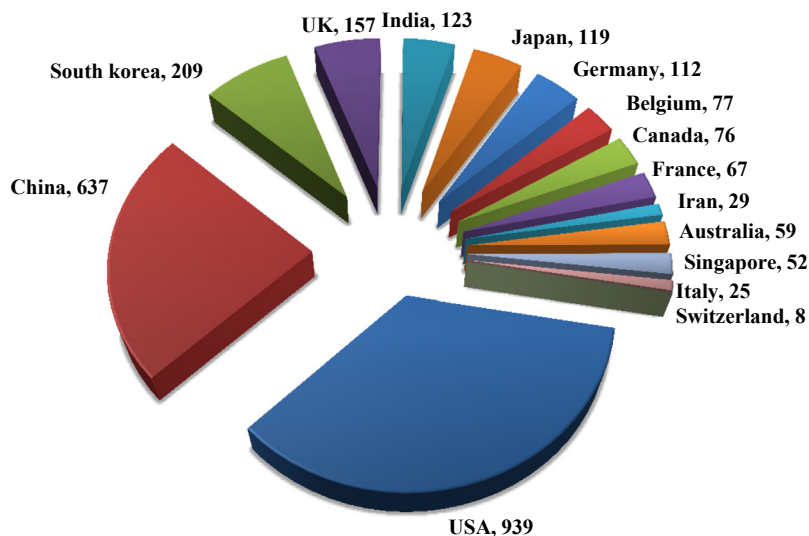


FIGURE 18.3 Comparison of the share of several countries in the distribution of articles on microbial fuel cells. Values shown in pie chart are numbers of articles.

from chemical bonds with the aid of active microorganisms.⁴⁰ In terms of construction, MFCs have different designs: single compartment, dual compartment, and stacked MFCs. Each design can be used for a specified purpose. In a single-compartment MFC, the cathode is directly exposed to air⁴¹ (see Figure 18.4). Therefore, there is no need to have an extra cathode chamber.

A dual-compartment MFC comprises anodic and cathodic chambers separated by a PEM. Figure 18.5 shows a dual-chamber MFC. Various types of materials are used; these are listed in Table 18.2. The materials used in MFCs affect on the performance of the devices. These days, carbon materials (carbon black, graphite, carbon paper, carbon cloth, etc.) are used as an anode electrode in most MFCs because of their good conductivity, stability in a microbial inoculums mixture, and surface area. Cathode catalysts have to be coated on the surface of the cathode to cause an oxygen reduction reaction (e.g., Pt).^{42,43} Also, some conductive polymers such as polypyrrole and polyaniline can be used in the cathode as support or as catalysts. The structure of supporting material significantly affects the performance of MFCs.^{44,45} Conductive nanofiller/polymer have recently been widely investigated in industries and academia.^{42,46}

For instance, the PEM has been found to play a major role in MFCs, in particular in dual-chamber MFCs, because it has the ability to separate the cathode and anode while facilitating the transfer of protons from the anode to the cathode. In stacked MFCs, several MFCs are connected in series and parallel.^{47,48}

Single MFCs were used by many scientists to generate power by means of pure or mixed cultures as active biocatalysts.^{14,34,49} The obtained results confirmed that the electricity and power generated from an individual MFC was too low to be used in low-consumption

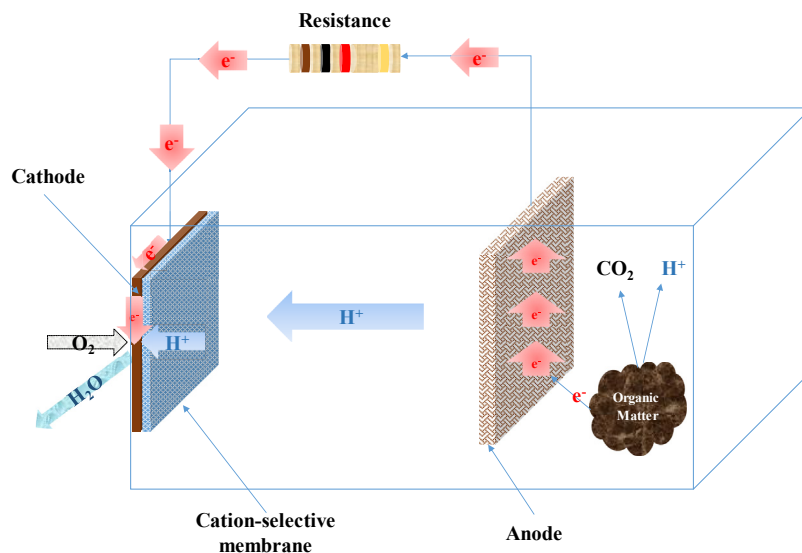


FIGURE 18.4 Schematic diagram of a single-compartment microbial fuel cell.

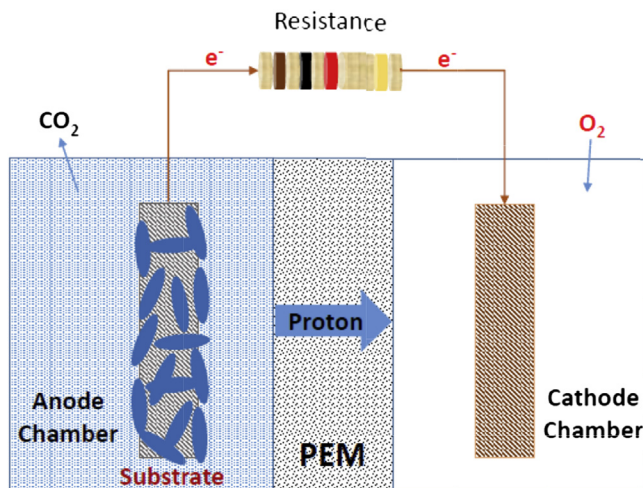


FIGURE 18.5 Schematic diagram of a dual-compartment microbial fuel cell. PEM, proton exchange membrane.

devices. Therefore, a number of individual MFCs have to be connected in a series or in parallel to produce enough power for a specific application. Any desired current or voltage can be achieved by a parallel or series connection of a few single cells. A connection of single MFCs connected in a series and/or in parallel is called a fuel cell stack.^{50,51}

TABLE 18.2 Basic components of biological cells with the material⁴⁷

Component	Material	Consideration
Anode	Graphite, plate graphite, carbon paper, carbon fabric, black platinum, Reticulated Vitreous Carbon (RVC) carbon, ...	Required
Cathode	Graphite, plate graphite, carbon paper, carbon fabric, black platinum, RVC carbon, ...	Required
Anode compartment	Glass, poly carbonate, Plexiglas	Required
Cathode compartment	Glass, poly carbonate, Plexiglas	Optional
Proton exchange system	Proton exchange membrane, Nafion, Ultrex, salt bridge, polyethylene, polystyrene	Required
Electrode catalyst	Platinum, black platinum, manganese oxide, ferric oxide, electron mediator fixed anode	Optional

18.3.2 Active Biocatalysts

The principles of BFCs are similar to that of other types of fuel cells. The main difference is that the microorganisms or enzymes are used as catalysts, and, consequently, there is no need to use expensive metal catalysts. The appropriate conditions for reaction are easily achievable. It is only required that the cell be maintained at a suitable temperature, barometric pressure, and neutral pH for the reaction to take place. The microorganisms are implemented as active biocatalyst for the reduction reactions. Certain microorganisms are capable of producing reductive substances in the anode compartment.

Many microorganisms are able to deliver the generated electrons via catabolism of organic matter to the anode electrode. Several pure cultures of bacteria are used as active biocatalysts for power production in MFCs,⁵² such as *Shewanella oneidensis*,^{53,54} *R. ferrireducens*,³³ *Geobacter sulfurreducens*,³³ *C. butyricum*,⁵⁵ *Pseudomonas aeruginosa*,⁵⁶ *Saccharomyces cerevisiae*,⁵⁷ and *Streptococcus lactis*.⁵⁸

Also, marine sediment soil, active sludge water, and sewage are natural resources of organisms that are used to generate power in MFCs. Typically, a mixed culture may be potent source of biocatalysts and allows the use of a wide range of substrates.^{47,59,60}

Microorganisms attached to the anode surface consume substrate and generate bioelectricity. There is no precise and exact method to transport the produced electron by microorganisms to the electrode surface, and little knowledge and information is available. Microscopic methods such as atomic force microscopy (AFM) and scanning electron microscopy images can be used to demonstrate the physical characteristics of the electrode surface and to examine the growth of microorganisms attached to the electrode's surface. Figure 18.6(a) illustrates the anode surface before use in an MFC. As it indicates, no microorganism was present on the anode before its use in the anode chamber. A piece of anode surface (1 × 1 cm) was cut off at the end of the batch process and the results of observations by photo- and electron microscope scanning are illustrated in Figure 18.6(b) at a 10,000-fold resolution. Figure 18.6(b) indicates that a uniform biofilm of

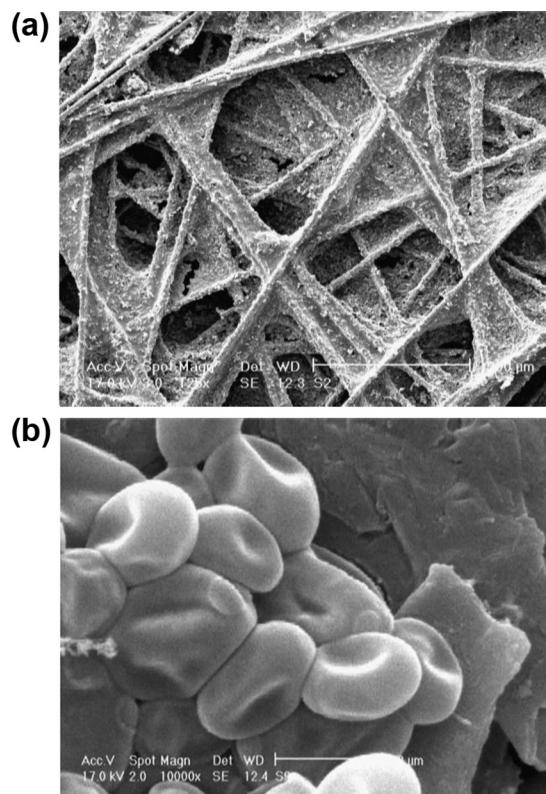


FIGURE 18.6 (a) Scanning Electron Microscopy image of the anode surface. (b) Biofilm developed on the anode surface; *Saccharomyces cerevisiae* was used as the active biocatalyst in the anode compartment of a dual-chamber microbial fuel cell.

microorganism—a colony of cultured yeasts—has been cultured on the external surface of the anode electrode. These attached active microorganisms can generate bioelectricity from substrate.

AFM also was applied to provide surface and morphological information of the electrode in the anode compartment mentioned above. [Figure 18.7](#) depicts the AFM images of the shape and surface characteristics of the graphite electrode. A piece of the anode electrode (1×1 cm) was analyzed by AFM before ([Figure 18.7\(a\)](#)) and after ([Figure 18.7\(b\)](#)) use in a dual-chamber MFC ($500\times$ magnification). These images demonstrate that microorganisms were growing on the graphite surface.

18.3.3 Electron Transfer in MFCs

In the past decade, most studies of microbial cells were restricted to academic articles and publications that merely considered MFCs as an alternative energy resource. Recent efforts by scientists resulted in greater power output. In future, research will be directed toward

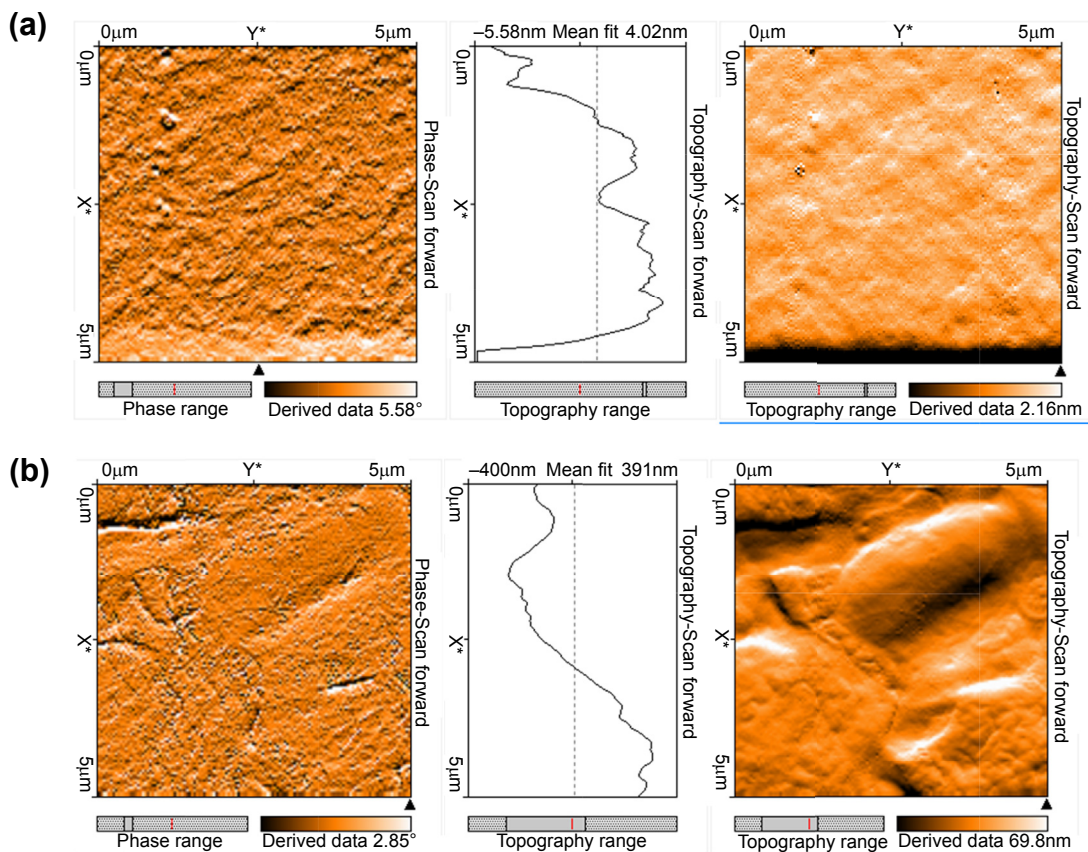
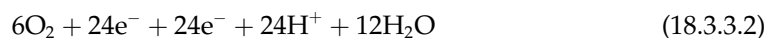
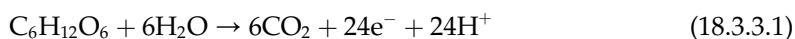


FIGURE 18.7 Atomic Force Microscopy image of a carbon paper electrode before (a) and after (b) use in a microbial fuel cell (MFC). *Saccharomyces cerevisiae* was used as an active biocatalyst in the anode compartment of a dual-chamber MFC.

understanding electron transport from the bacteria to the anode's surface. Electron transport in the anode chamber is the key point in understanding the theory behind MFC operation.⁶¹ There has been no precise and complete transport protocol for transmitting the produced electron by microorganisms to the electrode's surface, and limited knowledge and information are available.

As biocatalysts in MFCs, microorganisms consume different substrates as a carbon source in the anode chamber and produce electrons and protons. For example, glucose can be used in MFCs as an electron donor. The anodic and cathodic reactions take place at the anode and cathode, as summarized below:



From the above reactions, 24 mol of electrons and protons are generated by complete oxidation of 1 mol of glucose in an anaerobic condition. The key question here is, how does the produced electron reach the anode electrode? The performance of some MFCs has been increased by the addition of artificial electron mediators. Electron mediators are used to shuttle electrons from the broth to the surface of the anode electrode.

18.3.4 Electron Transport in MFCs

The main electron transport mechanism is direct transport of the produced electrons by certain components called nanowires. A nanowire is an electricity-conducting component that can transport the produced electron from the microorganisms to the surface of the anode electrode. Groby et al.⁶² reported the use of conductive components in soil bacteria (i.e., *Showanella* species). The component's conductivity was investigated using a Scanning Tunneling Microscope. Also, the existence of a conductive component has been proven through other species of organisms.^{63,64}

18.3.5 Use of a Mediator for Electron Transport

The electron mediator is the key and essential factor in the transportation of produced electrons by microorganisms to the anode's surface. The mediators are classified in two groups: self-generated mediators and artificial electron mediators.

18.3.5.1 Using Artificial Mediators

Some artificial mediators are occasionally used in transporting electrons to the electrode's surface. The electron carrier is capable of connecting the cell membrane and electron acceptors within the cells; it also eliminates the reduced state of cells and transfers electrons to the electrode's surface. The mediator is an essential part of MFCs that uses fermentation microorganisms, including *E. coli*, *Pseudomonas*, *Proteus*, *S. cerevisiae*, and species of *Bacillus*.⁵⁷ These bacteria are not capable of transporting the produced electrons to the electrode's surface by themselves. Prevalent electron carriers are thionine, benzyl viologen, 2,6-dichlorophenol-indophenol, 2-hydroxy-1,4-naphthoquinone, phenazines, phenothiazines, phenoxoazines, iron chelates, and neutral red.¹⁴

The mediator travels between the electrode and the bacterium while transporting the electrons. They grab the electrons from the bacteria and transport them to the anode's surface.^{14,57} Najafpour and his coworkers⁵⁷ utilized thionine, neutral red, methylene blue, and ferric chelate at several concentrations (50–600 $\mu\text{mol l}^{-1}$) as an electron shuttle in the anode chamber. They used *S. cerevisiae* as the active biocatalyst for power production. Park and Zeikus⁶⁵ investigated the interactions between bacterial cultures and electron mediators. The effect of thionine and neutral red as mediators of oxidation and reduction of energy carriers such as nicotinamide adenine dinucleotide (NAD^+) was investigated. The biomolecules NAD^+ and NADH are in oxidized and reduced forms, respectively. Several types of mediators were used to enhance the electron transport in MFCs.^{27,66}

A major problem in mediators is their toxicity and slight solubility, which in turn restrict their application in BFCs. Soluble redox mediators have been added to the anode chamber to

TABLE 18.3 Microorganisms and media used in MFCs for power production

Microorganism	Mediator	Substrate	Power density (mWm ⁻²)	Current density (mA m ⁻²)	Reference
<i>Proteus mirabilis</i>	Thionine	Glucose	—	191	35
<i>Saccharomyces cerevisiae</i>	Thionine	Glucose	60	436	57
	Neutral red	Glucose	190	1600	57
<i>Shewanella oneidensis</i>	Anthraquinone-2,6-disulfonate (AQDS)	Lactate	22.2	44.4	54
<i>Domestic wastewater</i>	Humic acid	Glucose	28	85	60
<i>Streptococcus lactis</i>	Ferric chelate complex	Glucose	49	102	58
<i>Domestic wastewater</i>	Humic acid	Acetate	123	589	60
<i>Mixed consortium</i>	Mediator-less	Glucose, sucrose	479	—	59
<i>Domestic wastewater</i>	Humic acid	Xylose	32	145	60
<i>Saccharomyces cerevisiae</i>	MB	Glucose	42	360	57
	Ferric chelate	Glucose	37	346	57
<i>Micrococcus luteus</i>	Thionine	Glucose	—	85	67

improve electron transfer. Several researchers have developed advanced anode materials by impregnating the anode with chemical catalysts.^{35,65} Therefore, suitable mediators to be used in BFCs must have the following characteristics:

1. Connect easily to the cell membrane
2. Transport the electrons easily to electrode
3. Guarantee a high rate of electrode reaction
4. Be soluble in anolyte
5. Not lead to toxicity or microbial decomposition
6. Be inexpensive and available

Table 18.3 lists examples of the cells with mediators accompanied by substrate and the microorganism used in each indicated system.

18.3.5.2 Electron Mediators Generated by Self-producing Microbes

Adding external media to cultivated mediator is not compulsory. Some microorganism produces mediators such as *Pyocyanine* or relevant compounds which play the role as mediators and transport the produced electrons to anode surface.⁶³ The obtained species of *Pseudomonas* in MFCs produce some material called phenazine which transports the produced electrons to the electrode. In some cases, electron plays the role of mediator in transporting the produced electrons to electrode surface.⁶⁸

18.3.6 Challenges in MFCs

The challenges with MFCs are low current and voltage generation; the maximum generated voltage, regardless of the resistance, is around 1.14 V. This value has been calculated on the basis of using NADH (-0.32) as the electron donor in the anode chamber and oxygen ($+0.82$) as the electron acceptor in the cathode chamber.⁵⁰ Moreover, the maximum voltage generated in an MFC so far was around 0.8 V when acetate was used as the substrate⁶⁹; this indicates limitations in obtaining the ideal voltage. Normally, the voltage generated in common MFCs using oxygen in the cathode chamber as the ultimate electron acceptor is around 0.5 V.^{70,71} In addition, obtaining desired electrical current in MFCs has its own challenges: the decrease of current caused by the inappropriate design of an MFC and the resultant resistance, limitations in transportation, and the extent of the conversion of the substrate to electrical current.^{14,50}

To resolve the above-mentioned challenges and obtain the desired voltage and/or electrical current, one may design MFCs as a stack and connect the cells in parallel or a series, depending on the demand. If higher voltage is required, one may connect the cells in a series or in parallel to increase the electrical current generated. Therefore, the desired voltage or electrical current can be obtained using this technique. Figure 18.8 illustrates the schematic of a constructed stack of MFCs.

18.3.7 Calculations in MFCs

In MFCs, substrates are oxidized by microorganisms and, as a result, protons and electrons are produced, which pass through the membrane or electrolyte and external circuit,

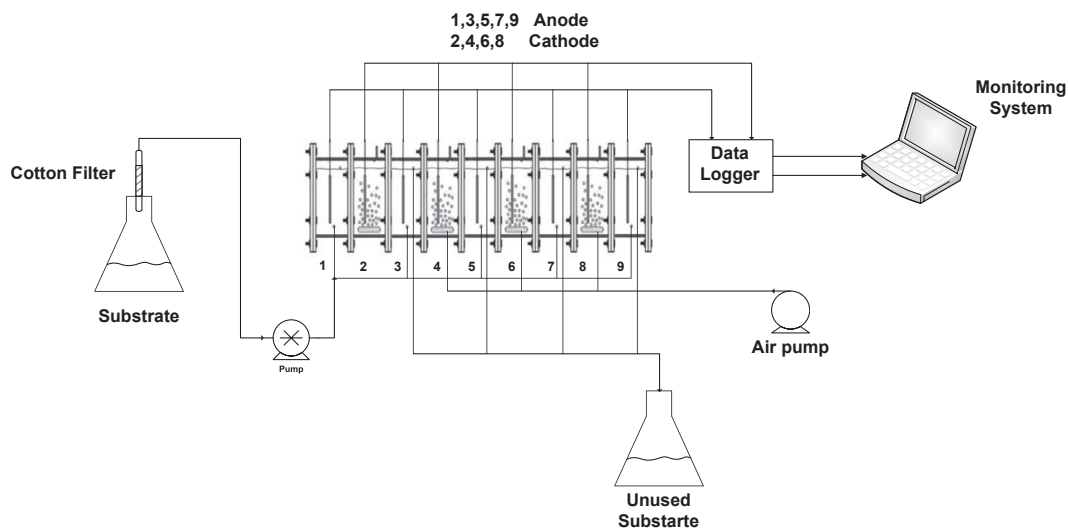
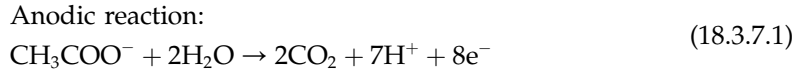


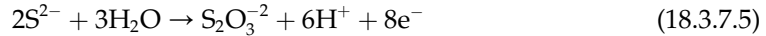
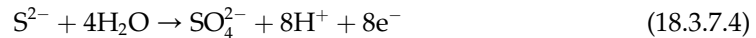
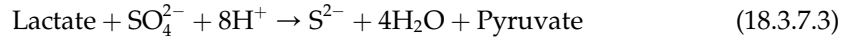
FIGURE 18.8 A schematic of a constructed stack of microbial fuel cells.

respectively. For instance, acetate could be used as a substrate; the typical reactions are stated below:



In these reactions the substrate breaks down into carbon dioxide and water, which are accompanying by electricity generated as a by-product.

The substrate is one essential biochemical factor affecting power generation in MFCs. MFCs are able to consume different sources of chemical matter for bioelectricity production. MFC technology recently was considered as a new method for wastewater treatment and simultaneous power production. For example, there are many substrates that contain sulfur compounds (sulfide, sulfite, SO_3^{2-} , S^{-1} , HS^{-1}). Sulfite-reducing bacteria (e.g., the microorganism *Desulfovibrio desulfuricans*) are among anaerobic microbes that use sulfite as the final electron acceptor⁷²; microorganisms use substrate (e.g., lactate) as an electron resource that results in elemental sulfur (S^{-2}). Reactions of carbon and sulfate reduction are presented in Eqns (18.3.7.3)–(18.3.7.5).



An MFC is unique in its ability to produce bioelectricity and treat wastewater at the same time. For nearly a decade, the use of wastewater as fuel in MFCs has been common practice among scientists to generate electricity.¹³ The benefit of utilization of wastewater for power production in MFCs is that it is free and the net carbon dioxide emission is acceptable.

18.3.8 Power Generation

The power output of MFCs (P_{cell}) can be calculated by the following expression:

$$P_{\text{cell}} = E_{\text{cell}} \int I \, dt \quad (18.3.8.1)$$

where E_{cell} is the cell potential and I is the electricity current produced. If the rate of electricity current is stable, one may get:

$$P_{\text{cell}} = E_{\text{cell}} I \quad (18.3.8.2)$$

The maximum electromotive force E_{emf} , which is generated by all types of batteries and fuel, can be calculated as follows:

$$E_{\text{emf}} = E^\circ - \frac{RT}{n f} \ln(\Pi) \quad (18.3.8.3)$$

where E° is the standard electromotive force, R is the universal gas constant, T is the absolute temperature in Kelvin, n is the number of transported electrons, f is the Faraday constant, the Π parameter equals the ratio of product activity to the power of the stoichiometric coefficient divided by the ratio of the reactant's activity to the power of their stoichiometry:

$$\Pi = \frac{\text{Products}^p}{\text{reactants}^r} \quad (18.3.8.4)$$

According to the International Union of Pure and Applied Chemistry, all reactions are written in chemical reduction so that reactors are always oxidative and products are reduced.



According to the International Union of Pure and Applied Chemistry, standard state is defined as 298 K and a chemical concentration of 1 M for fluids and 1 bar for gases. E° is calculated regarding hydrogen as the standard state and is defined as $E^\circ(\text{H}_2\text{O}) = 0$, which is called a normal hydrogen electrode. Therefore, the standard chemical potential is obtained by assuming $\Pi = 1$ relative to the hydrogen electrode.

For operational application of a biological cell, the power generation capacity must be considered. For a fuel cell, power density and volumetric power can be calculated using Eqns (18.3.8.6) and (18.3.8.7):

$$\text{Power density} = \frac{P_{\text{cell}}}{A} \quad (18.3.8.6)$$

$$\text{Volumetric power} = \frac{P_{\text{cell}}}{V_e} = \frac{A_e}{A} P_{\text{cell}} \quad (18.3.8.7)$$

where P_{cell} is the power obtained by the cell and A is the surface area of the cell.¹⁶

18.3.9 Overpotential in MFCs

In MFCs the measured voltage differs from the produced voltage. In other words, the difference between the measured voltage and the cell voltage, which is called overpotential, is caused by resistance in electron transmission and initial resistance. Overpotential is as a result of (1) activation losses; (2) bacterial metabolic losses; and (3) concentration losses. Overpotential of the system can be calculated using the following equation:

$$E_{\text{emf}} = E_C - E_A - \sum IR_e \quad (18.3.9.1)$$

where E_C and E_A are experimental potentials of the cathode and anode, respectively.

To obtain high voltage from a cell, the electromotive force of the cell must be maximal and ohmic resistance loss should be minimal. This resistance most often consists of the resistance of electron transmission to electrodes, connections, resistance in electron transmission through the PEM (if any), and cathodic and anodic electrolytes. Decrement in distance between electrodes, using of PEM with lower resistance and increment of conductivity in electrolytes, can decrease the amount of ohmic resistance lost.¹⁴

18.3.10 Coulombic Yield

However, power generation is the main goal of MFC operation, but extracting electrons stored in biomass and recovering as much as energy as possible from the system are important. The recovered electrons are called coulombic efficiency. In another definition, coulombic efficiency is the fraction of electrons recovered as current versus the total electrons in organic materials.

$$C_E = \frac{\text{Coulombs recovered}}{\text{Total coulombs in substrate}} \quad (18.3.10.1)$$

The coulombic yield is one of the most important factors in MFCs. Coulombic yield is, in theory, the product of generated coulombs in the MFC divided by the total coulombs that can be obtained as a result of substrate consumption; this is stated as follows:

$$C_E = \left(\frac{C_P}{C_T} \right) \times 100 \quad (18.3.10.2)$$

where C_P is the number of coulombs generated, which is obtained by integrating the electrical current against time, and C_T is the number of coulombs theoretically obtained from a carbon source; C_T can be estimated by the following expression:

$$C_T = (F \times b \times S \times V \times M^{-1}) \quad (18.3.10.3)$$

where F is the Faraday constant, b is the number of moles of electrons generated as a result of substrate consumption (24 mol of electrons were generated per mole of glucose in anaerobic conditions), S is the substrate concentration, V is the working volume of the anode chamber, and M is the molecular weight of the substrate. Thus, the coulombic yield in a batch process can be calculated via the stated equation:

$$C_E = \frac{M \int_0^t I \times dt}{F \times b \times V \times \Delta C} \quad (18.3.10.4)$$

An ampere is defined as the transfer of 1 C of charge per second, or $1A = 1C/s$. Thus, integration of the current obtained over time is the total coulombs transferred in the system. The coulombic yield in a continuous process based on substrate consumption and flow rate of the system can be calculated using the following expression:

$$C_E = \frac{M \times I}{F \times b \times q \times \Delta C} \quad (18.3.10.5)$$

where q is the flow rate of the substrate into the system.^{24,73}

18.3.11 MFCs' Performance

Different factors affect MFCs' performance, but PEM, the condition in the anodic and cathodic chambers, is considered one of the most important.

18.3.11.1 Conditions in the Anodic Chamber

Fuel or substrate as a source of nutrients and energy is one of the most important parameters in biological processes such as electricity production in MFCs. Fuel type and its concentration and rate are considerable factors that affect the power and current produced in MFCs. The effects of various types of substrates on MFCs' performance were previously investigated.^{74–76}

Use of the proper kind of microorganisms in the anodic chamber is also important. Many microorganisms are capable of transporting to the anode the electrons obtained by organic metabolism. Mixed culture of microorganisms from marine sediment soil, active sludge water, and sewage are rich natural resources of organisms for power production.⁴⁷

18.3.11.2 Proton Exchange Membrane

The separator between the anode and cathode compartments is one of the most important factors affecting MFC performance. The PEM is the most frequently used separator in dual-chamber MFCs because of its moderately high conductivity to cations and low internal resistance compared with other separators.^{77,78} Cation exchange membranes, also known as PEMs, are one of the most widely used separators and are designed for transferring protons in MFCs.⁷⁹ The performance of a PEM is studied based on its ability to transport produced protons from the anode to cathode; moreover, they must prevent the transfer of substances, oxygen, and minerals from the anode to cathode chambers.^{80,81} However, membrane type (PEM or cation exchange membrane) affects the performance of MFCs and has not been studied well. Poor proton transferability is one of the most recognized deficiencies of PEMs, which holds despite their various composition, internal resistance, and conductivity. There are some drawbacks:

1. PEMs are expensive. The estimated cost of a PEM is reported to be close to 40% of the total cost of a finished MFC.⁸²
2. The higher transfer ratio of cations to protons can prevent electrochemical reactions in the cathode, which result in lower cathode cell performance.
3. Chemical and biological fouling results in an increase in internal resistance, which in turn results in lower efficiency and performance of MFCs.

For long-term operation, membrane fouling can be considered as a result of biofilm formation on the PEM. Some scientists described that biofouling in dual-chamber MFCs has a negative effect on the MFCs' performance.^{83–85}

18.3.11.3 Conditions in the Cathodic Chamber

Oxygen is a suitable and common electron acceptor, and the output power is directly relevant to this factor. Different methods of increasing the amount of oxygen in cathodic solution were offered. Use of an air pump or proper oxidant can successfully surge the amount of oxygen, and subsequently the output power, as was investigated by many researchers.^{86,87}

Besides the advantages of MFCs, such as mild operation reaction conditions, some major developments must be done to enhance the power generated. Improvement of MFC performance using catalysts such as platinum in the cathode compartment was investigated, but these materials are generally expensive.¹³ The use of biocathodes, which can increase the

dissolved oxygen of solution, has recently attracted many scientists. Because of the low cost of biocathodes, their use in MFCs has recently gained interest. Algal biocathodes have the specific ability to enhance oxygen supply in the cathode compartment; hence there is no need for a mechanical aeration device.⁸⁸ In many studies, oxygen was used as the final electron acceptor at the surface of the cathode electrode.²⁷ Consumption of electrons and protons that are combined with oxygen forms water and ends this transfer cycle. Moreover, the use of biocathodes has been reported to reduce the charge transfer resistance of the cathode.⁸⁹ It was reported that dissolved oxygen in an MFC with an algae-assisted cathode was increased and subsequently produced power. In addition, the photosynthetic process of algae has been studied.^{88,90} The effect of biocathodes on MFCs' performance was studied in the Biotechnology Research Laboratory at the Babol Noshirvani University of Technology. Sulfide (1.5 g l^{-1}) was fed into an anode compartment as a substrate. Because of the need for proper growth and respiration of algae in the presence of sunlight, the cell was placed next to a laboratory window from the initial moment of cell operation. A data logger was set to record Open Circuit Voltage (OCV) until steady-state conditions were achieved. It was observed that, during the day, the cell voltage was increased until it reached a constant value. As the sun went down, voltage decreased, and this trend continued throughout the night. The best performance of the MFC and the maximum value of voltage, power, and current density were obtained between 14:00 pm and 16:00 pm, and the minimum values of these parameters were noted at 3:00 am until 4:00 am. The obtained results were relevant to values of dissolved oxygen in the cathode chamber, as was previously reported.⁹¹ Dissolved oxygen from the cathode solution before adding algae was 4.94 mg l^{-1} . It was observed that oxygen at the cathode increased, and so did cell voltage. The average values of dissolved oxygen at all days of the experimental period were 8.90 and 11.87 mg l^{-1} at 11:00 am and 13:00 pm, respectively. Between 14:00 pm and 16:00 pm, when the MFC generated maximum values of current and power, the average dissolved oxygen increased to 18.57 mg l^{-1} until 19:00 pm, when the sun went down and the dark phase began. This parameter decreased to 13.04 and 9.75 mg l^{-1} at 19:00 pm and 22:00 pm, respectively, and this value remained constant (7.20 mg l^{-1}) at approximately 3:00 am to 4:00 am. Therefore, there was a significant fluctuation in the value of the cell voltage (see [Figure 18.9](#)).

Also, the performance of an MFC may be enhanced by several important process parameters that are critical in the MFC's operation, such as (1) microbial electron transfer, (2) cell metabolism, (3) internal and external resistance, and (4) cathode oxidation. These important parameters greatly influence the transfer of generated electrons and MFC performance.⁹²

18.3.12 Applications of MFCs

The MFC is such a novel technology and has different applications, which can be classified into four major categories.

18.3.12.1 Electricity Production

As mentioned above, the MFC is a novel technology; it is able to generate electricity and can convert biochemical energy to electrical energy with the aid of microorganisms.

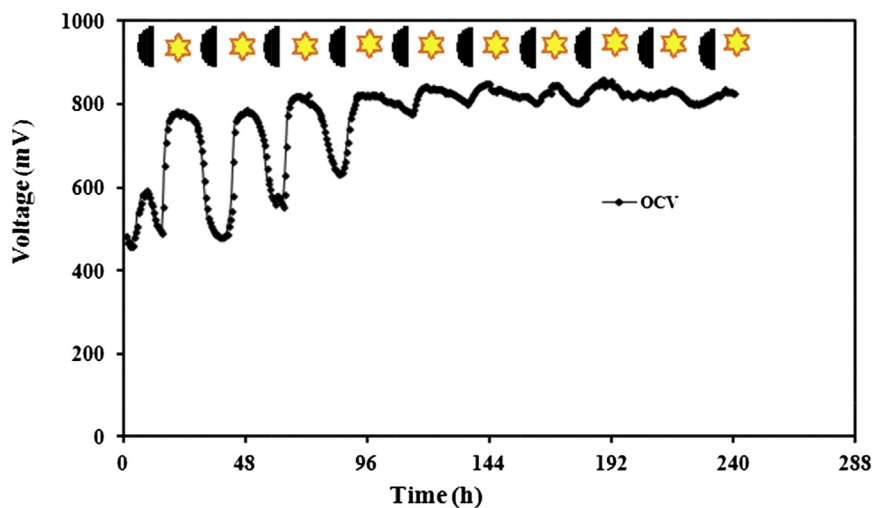


FIGURE 18.9 Open Circuit Voltage (OCV) of a microbial fuel cell in the presence of a biocathode. Sulfide (1.5 g l^{-1}) was used as the substrate in the anode compartment.

Regarding it does not follow the rules of the Carnot cycle, it has a high efficiency. However, electricity generated by MFCs is very low because of the slow rate of electron transport. A simple solution to this problem is to save the generated electrons in rechargeable devices and use them as needed. A group of capacitors were used to save energy in a robot called “Eco Bot I,” in which electricity was supplied by a microbial cell. MFCs also are suitable for low-energy systems and sensors. The electricity produced by cells is very low, but it is possible to get greater voltage by putting several MFCs in a series or in parallel.^{47,93} The constructed MFC could be used in low-energy appliances, for example, in low-energy lights such as light-emitting diode lights and digital watches, and successfully supply the required energy (see Figure 18.10).

18.3.12.2 Production of Biological Hydrogen

MFCs could be operated for hydrogen production instead of electricity generation. To achieve this goal, the cathode was maintained in anaerobic conditions and an external potential was used to decrease the thermodynamic barrier and subsequently increase the cathodic potential. In a normal state, a proton is produced in the anode and moves toward the cathode to bond with oxygen and form water. Hydrogen production from protons and electrons generated by microbial metabolism in MFCs is not thermodynamically acceptable.

Electrons and protons produced in the anode compartment bonded in the cathode to produce hydrogen. The external potential required for the MFC was 110 mV, which is much less than the direct electrolysis of water at a normal pH. The energy required for water to be directly electrolyzed is 1210 mV which is higher than that needed for MFCs. Also, part of the energy required for the production of biohydrogen is supplied by biomass oxidation in the anode. Microbial cells are capable of producing 8–9 mol H_2 /mol glucose, which seems

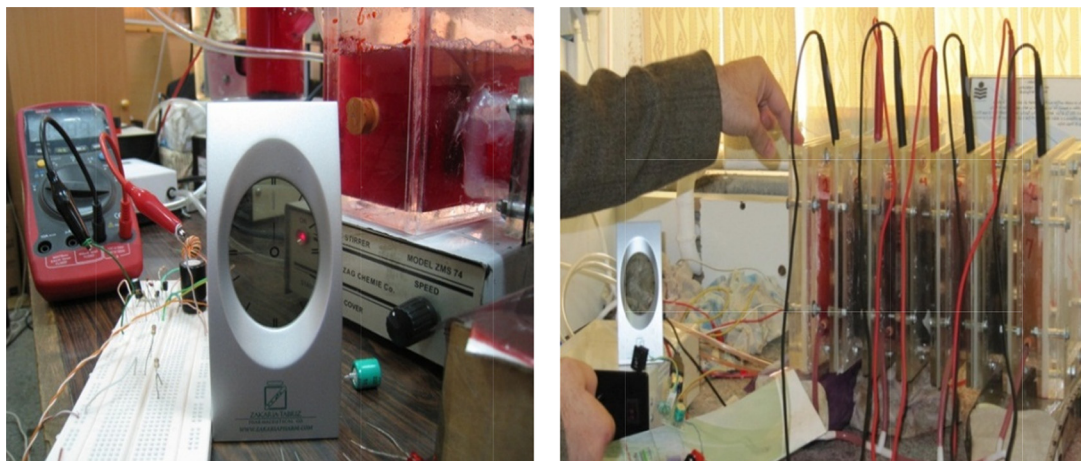


FIGURE 18.10 A constructed microbial fuel cell supplying the power required for low-energy appliances. a) Single chamber MFC for running digital clock. b) Lab scale MFC stack for running digital clock.

more reasonable compared with 4 mol H_2 /mol glucose in common fermentation at optimum operating conditions. To produce biological hydrogen using MFCs, it seems that there is no need for long-term oxygen in the cathode, which results in improved efficiency of the MFC. Another advantage of hydrogen production in MFCs is the ability to save gas and use it later.^{94,95}

18.3.12.3 Biosensors

Another application of MFCs is use as biosensors. The suitable coulombic efficiency of MFCs allows their use in biological oxygen demand (BOD) measuring sensors.⁹⁶ A suitable method of measuring BOD in a fluid current is to calculate the coulombic efficiency of the system. Several researchers have claimed that there is a liner relationship between the coulombic and BOD concentrations of the solution.⁴⁷

It has been reported that *Shewanella* sp., as biobased catalytic systems, are suitable to measure the BOD of wastewater. It can also help measure other materials.⁹⁷ Karube et al.⁹⁸ used MFCs as BOD measuring sensors in which hydrogen was generated by *C. butyricum* that was fixed on the electrode. Kim et al.⁹⁹ used MFCs to measure BOD. The developed system even worked for duration of 5 years without any process maintenance. Measurements of organic matter have been implemented by the use of MFCs in the detection system.¹⁰⁰

Chemical sensors are used to measure blood glucose and oxygen concentration in diabetic patients. The sensors also have been used to measure pulse, blood pressure, and other vital signs.¹⁰¹ Use of MFCs to measure lactate by *Shewanella putrefaciens* also has been reported. This biosensor was able to measure amounts of lactate up to 50 mM.¹⁸

18.3.12.4 Wastewater Treatment

Wastewater treatment is one of the most well-known and useful applications of MFCs. Conventional municipal wastewater treatment plants consist of numerous treatment units that may be different in the way they are placed, but in each setup achieving the maximum

efficiency is the most important issue. Several techniques for wastewater treatment have been proposed; however, in most of the approaches, too much time spent or high cost is the main obstacle. Also, a high level of operational processes is required in most treatment methods.⁴⁷

Clean water is an undeniable human right. A large amount of agricultural and industrial wastewater is produced annually. For example, annual animal manure production in the United States is approximately 580 million tons. To avoid water pollution and control odor, animal waste must be pretreated before it is disposed in the environment. Also, it must be considered that high nitrate and phosphate concentrations lead to water pollution.¹⁰²

In general, wastewater is divided into organic and inorganic wastes in terms of their ingredients. MFCs provide a new approach to electricity generation and simultaneous treatment of organic and inorganic wastes. When microorganisms oxidize the substrate in wastewater, electrons are released and a stable resource of electricity is created. Using MFCs to treat wastewater has been the center of attention since 1991. Urban wastewater is composed of a mixture of organic matter that can be used as fuel in MFCs.¹⁵ In addition, organic molecules such as acetate, propionate, and butyrate can also be converted to water and carbon dioxide. One of the desirable characteristics of such cells is that it allows the use of various waste types, including carbon dioxide and human waste.

In 1991, wastewater treatment by MFCs was started by Habermann and Pommer.¹⁰³ Afterward, many researches were involved in this area. Hygienic waste, food processing

TABLE 18.4 Power production with wastewater treatment by MFCs

Component eliminated	Maximum power	Anode material	Cathode material	Removal efficiency (%)	Location of removal	Reference
Chemical Oxygen Demand (COD)	371 mWm ⁻²	Graphite plate	Graphite plate	95	Anode chamber	94
COD	225 mWm ⁻²	Graphite plate	Graphite plate	92	Anode chamber	104
Carbon	34.6 Wm ⁻³	Granular graphite	Granular graphite	100	Anode chamber	106
COD	7.6 mW	Graphite felt	Graphite felt	90	Anode chamber	107
Dye	15.73 mWm ⁻²	Graphite plate	Graphite plate	93.15	Anode chamber	108
Nitrogen	34.6 Wm ⁻³	Granular graphite	Granular graphite	67	Cathode chamber	106
Copper	339 mWm ⁻³	Graphite plate	Granular graphite	96	Cathode chamber	109
COD	26 mWm ⁻²	Graphite plate	Graphite plate	80	Single chamber	19

wastewater, and swine wastewater were recycled as biomass sources for MFCs because of the rich nature of their organic matter.^{19,94,104,105} Table 18.4 lists MFCs that were experimented, to eliminate different pollutants and generate power.

MFCs also are used for treatment of inorganic wastes. Some inorganic components were commonly found in wastewater. Sulfide is one of the most prevalent and hazardous ions found in waste. Sulfide is generated in wastewater by the reduction of sulfate in sewage and pipes. This toxic ion can cause serious problems such as a bad smell, a negative impact on human health, and a corrosive environment for building materials such as concrete.¹¹⁰ Sulfide can be oxidized into different species of sulfur. Under certain reaction conditions and according to redox potential, 30 species of sulfur can be produced. Sulfur is the major component produced from sulfide oxidation and is not able to be oxidized again. The sulfur produced can only be oxidized by microbial catalysts.¹¹¹ The oxidation of sulfide and sulfur compounds in MFCs were extensively studied by a large number of research scientists.^{112–114}

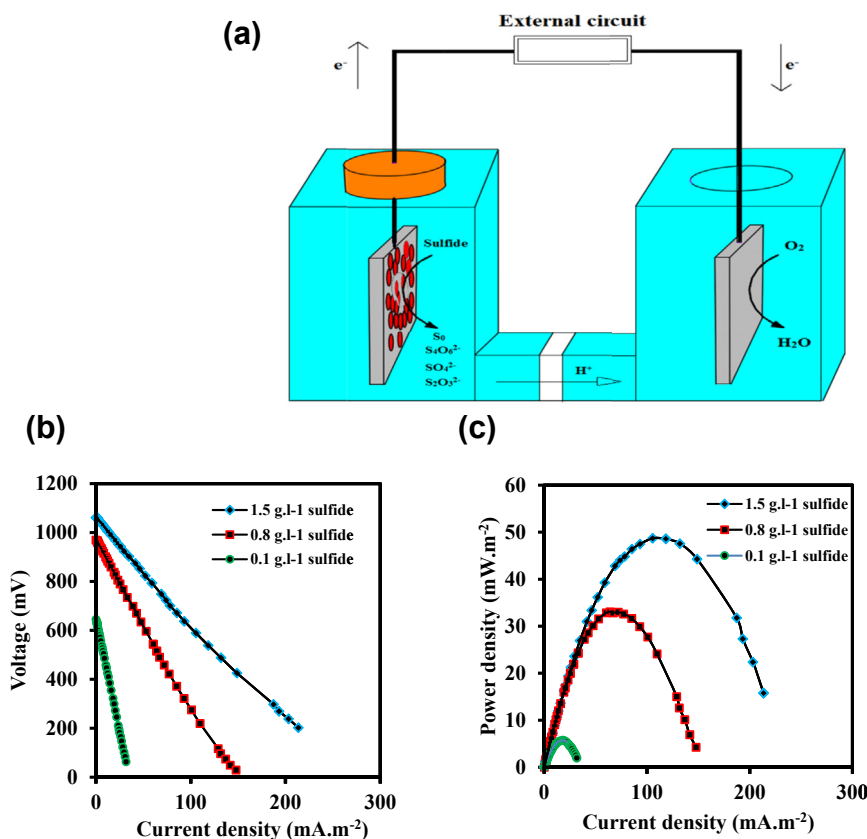


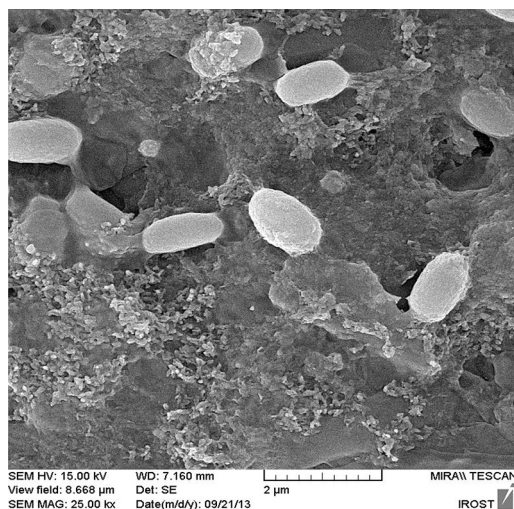
FIGURE 18.11 (a) Schematic diagram of a fabricated microbial fuel cell (MFC) for sulfide removal. (b) polarization and (c) power density curves of MFCs consist of 1.5, 0.8, and 0.1 $\text{g}\cdot\text{l}^{-1}$ sulfide as the substrate.

Simultaneous electricity generation and sulfide removal were investigated in our Biotechnology Research Laboratory.¹¹⁵ For this purpose, three different dual-chamber MFCs were operated. Mixed culture of microorganisms was used as biocatalysts and was collected from the anaerobic process tank operated in the wastewater treatment facility in Ghaemshahr, which is located in the north part of Iran. The influence of three different concentrations of sulfide (0.1, 0.8, and 1.5 gl^{-1}) on MFCs and their elimination was investigated. The maximum values of current and power density (231.47 mA m^{-2} and 48.65 mW m^{-2} , respectively) were acquired in the MFC with 1.5 gl^{-1} sulfide as the electron donor. In this system, sulfide was totally removed after 10 days. Figure 18.11 displays the schematic diagram, polarization, and power curves of the MFC at different sulfide concentrations, which were plotted when cell conditions became stable, and the maximum value of output power and current were determined.



Different images of the cells that have been fabricated at laboratory scale.

Microbial catalysis plays a significant role in sulfide removal and electricity generation in MFCs. SEM elucidated the formation of biofilm and attached bacteria on an anode electrode.



MFCs with biocathodes (SEM images from the outer surface of the anode electrode after use in an anode compartment).

Acknowledgment

The authors gratefully acknowledge the Biotechnology Research Center, Noshirvani University of Technology, Babol, Iran, for the facilities provided to accomplish this research.

References

1. Lewis NS, Nocera DG. Powering the planet: chemical challenges in solar energy utilization. *Proc Natl Acad Sci* 2006;**103**(43):15729–35.
2. Logan B. Biologically extracting energy from wastewater: biohydrogen production and microbial fuel cells. *Environ Sci Technol* 2004;**38**(9):160–7.
3. Mohan Y, Das D. Effect of ionic strength, cation exchanger and inoculum age on the performance of microbial fuel cells. *Int J Hydrog Energy* 2009;**34**(17):7542–6.
4. Daud WRW, Najafpour G, Rahimnejad M. Clean energy for tomorrow: towards zero emission and carbon free future: a review. *Iran J Energy & Environ* 2011;**2**(3):262–73.
5. Bard AJ, Faulkner LR. *Electrochemical methods: fundamentals and applications*, vol. 2. New York: Wiley; 1980.
6. Grote M. *Surfaces of action: cells and membranes in electrochemistry and the life sciences. Studies in history and philosophy of science part C: studies in history and philosophy of biological and biomedical sciences*; 2010.
7. Guo Q, Furukawa K, Sopher BL, Pham DG, Xie J, Robinson N, et al. Alzheimer's PS-1 mutation perturbs calcium homeostasis and sensitizes PC12 cells to death induced by amyloid peptide. *Neuroreport* 1996;**8**(1):379.
8. Timmers RA, Strik DP, Hamelers HV, Buisman CJ. Long-term performance of a plant microbial fuel cell with *Spartina anglica*. *Appl Microbiol Biotechnol* 2010;**86**(3):973–81.
9. Steele BC, Heinzel A. Materials for fuel-cell technologies. *Nature* 2001;**414**(6861):345–52.
10. Rahimnejad M, Ghasemi M, Najafpour G, Ghoreyshi A, Bakeri G, Hassani Nejad SK. Acetone removal and bioelectricity generation in dual chamber microbial fuel cell. *Am J Biochem Biotechnol* 2012;**8**(4).
11. Palmer I, Seymour CM, Dams RA. *Application of fuel cells to power generation systems*, 1995, Google Patents.
12. Blomen LJ, Mugerwa MN. *Fuel cell systems*. Plenum Publishing Corporation; 1993.
13. Rodrigo M, Canizares P, Lobato J, Paz R, Sáez C, Linares J. Production of electricity from the treatment of urban waste water using a microbial fuel cell. *J Power Sources* 2007;**169**(1):198–204.

14. Logan BE, Hamelers B, Rozendal R, Schröder U, Keller J, Freguia S, et al. Microbial fuel cells: methodology and technology. *Environ Sci Technol* 2006;**40**(17):5181–92.
15. Shukla A, Suresh P, Sheela B, Rajendran A. Biological fuel cells and their applications. *Curr Sci* 2004;**87**(4):455–68.
16. Bullen RA, Arnot T, Lakeman J, Walsh F. Biofuel cells and their development. *Biosens Bioelectron* 2006;**21**(11):2015–45.
17. Bond DR, Lovley DR. Electricity production by *Geobacter sulfurreducens* attached to electrodes. *Appl Environ Microbiol* 2003;**69**(3):1548–55.
18. Kim H, Hyun M, Chang I, Kim BH. A microbial fuel cell type lactate biosensor using a metal-reducing bacterium, *Shewanella putrefaciens*. *J Microbiol Biotechnol* 1999;**9**(3):365–7.
19. Liu H, Ramnarayanan R, Logan BE. Production of electricity during wastewater treatment using a single chamber microbial fuel cell. *Environ Sci Technol* 2004;**38**(7):2281–5.
20. Bond DR, Holmes DE, Tender LM, Lovley DR. Electrode-reducing microorganisms that harvest energy from marine sediments. *Science* 2002;**295**(5554):483–5.
21. Norbeck JM, Heffel JW, Durbin TD, Tabbara B, Bowden JM, Montano MC. *Hydrogen fuel for surface transportation*, vol. 160; 1996.
22. Larminie J, Dicks A, McDonald MS. *Fuel cell systems explained*, vol. 2. New York: Wiley; 2003.
23. Potter MC. Electrical effects accompanying the decomposition of organic compounds. *Proc R Soc London Ser B Contain Pap Biol Charact* 1911;**84**(571):260–76.
24. Logan BE, Regan JM. Electricity-producing bacterial communities in microbial fuel cells. *Trends Microbiol* 2006;**14**(12):512–8.
25. Park DH, Zeikus JG. Improved fuel cell and electrode designs for producing electricity from microbial degradation. *Biotechnol Bioeng* 2003;**81**(3):348–55.
26. Mokhtarian N, Wan Ramli W, Rahimnejad M, Najafpour G. Bioelectricity generation in biological fuel cell with and without mediators. *World Appl Sci J* 2012;**18**(4):559–67.
27. Gil GC, Chang IS, Kim BH, Kim M, Jang JK, Park HS, Kim HJ. Operational parameters affecting the performance of a mediator-less microbial fuel cell. *Biosens Bioelectron* 2003;**18**(4):327–34.
28. Williams RH. *Fuel decarbonization for fuel cell applications and sequestration of the separated CO₂*. Tokyo: United Nations University Press; 1998.
29. Yao H, Lim L, James R, Schieber M, Natarajan M. Surface aging of HgI₂ crystals studied by VASE and AFM. *Nucl Instrum Methods Phys Res Sect A: Accel Spectrom Detect Assoc Equip* 1996;**380**(1):26–9.
30. Rahimnejad M, Najafpour GD, Ghoreyshi AA, Talebnia F, Premier GC, Bakeri G, et al. Thionine increases electricity generation from microbial fuel cell using *Saccharomyces cerevisiae* and exoelectrogenic mixed culture. *J Microbiol* 2012;**50**(4):575–80.
31. Karube I, Matsunaga T, Tsuru S, Suzuki S. Biochemical fuel cell utilizing immobilized cells of *Clostridium butyricum*. *Biotechnol Bioeng* 1977;**19**(11):1727–33.
32. Allen RM, Bennetto HP. Microbial fuel-cells. *Appl Biochem Biotechnol* 1993;**39**(1):27–40.
33. Chaudhuri SK, Lovley DR. Electricity generation by direct oxidation of glucose in mediatorless microbial fuel cells. *Nat Biotechnol* 2003;**21**(10):1229–32.
34. Rabaey K, Lissens G, Siciliano SD, Verstraete W. A microbial fuel cell capable of converting glucose to electricity at high rate and efficiency. *Biotechnol Lett* 2003;**25**(18):1531–5.
35. Choi Y, Kim N, Kim S, Jung S. Dynamic behaviors of redox mediators within the hydrophobic layers as an important factor for effective microbial fuel cell operation. *Bull Kor Chem Soc* 2003;**24**(4):437–40.
36. Palmore GTR, Whitesides GM. Microbial and enzymatic biofuel cells. *Enzymatic conversion of biomass for fuels production* 1994;vol. 566:271–90.
37. Rahimnejad M, Ghoreyshi A, Najafpour G, Younesi H, Shakeri M. A novel microbial fuel cell stack for continuous production of clean energy. *Int J Hydrogen Energy* 2012;**37**(7):5992–6000.
38. Lewis K. Symposium on bioelectrochemistry of microorganisms. IV. Biochemical fuel cells. *Bacteriol Rev* 1966;**30**(1):101.
39. Kim BH, et al. Mediator-less biofuel cell. 1999, Google Patents.
40. Rahimnejad M, Najafpour G, Ghoreyshi AA. Effect of mass transfer on performance of microbial fuel cell. *Mass transfer chemical engineering processes* 2011;vol. 5:233–50.

41. Tardast A, Najafpour G, Rahimnejad M, Amiri A. Bioelectrical power generation in a membrane less microbial fuel cell. *World Appl Sci J* 2012;**16**(2):179–82.
42. Qiao Y, Li C, Bao S, Bao Q. Carbon nanotube/polyaniline composite as anode material for microbial fuel cells. *J Power Sources* 2007;**170**(1):79–84.
43. Yoshitake T, Shimakawa Y, Kuroshima S, Kimura H, Ichihashi T, Kubo Y, et al. Preparation of fine platinum catalyst supported on single-wall carbon nanohorns for fuel cell application. *Phys B* 2002;**323**(1–4):124–6.
44. Bezerra CWB, Zhang L, Lee K, Liu H, Marques ALB, Marques EP, et al. A review of Fe-N/C and Co-N/C catalysts for the oxygen reduction reaction. *Electrochim Acta* 2008;**53**(15):4937–51.
45. Lee K, Zhang L, Lui H, Hui R, Shi Z, Zhang J. Oxygen reduction reaction (ORR) catalyzed by carbon-supported cobalt polypyrrole (Co-PPy/C) electrocatalysts. *Electrochim Acta* 2009;**54**(20):4704–11.
46. Al-Saleh M, Sundararaj U. A review of vapor grown carbon nanofiber/polymer conductive composites. *Carbon* 2009;**47**(1):2–22.
47. Du Z, Li H, Gu T. A state of the art review on microbial fuel cells: a promising technology for wastewater treatment and bioenergy. *Biotechnol Adv* 2007;**25**(5):464–82.
48. RAHIMNEJAD M, et al. Nafion as a nanoproton conductor in microbial fuel cells. *Turkish J Eng Environ Sci* 2011;**34**(4):289–92.
49. Chung K, Okabe S. Continuous power generation and microbial community structure of the anode biofilms in a three-stage microbial fuel cell system. *Appl Microbiol Biotechnol* 2009;**83**(5):965–77.
50. Aelterman P, Rabaey K, Hai The Pham, Boon N, Verstraete W. Continuous electricity generation at high voltages and currents using stacked microbial fuel cells. *Environ Sci Technol* 2006;**40**(10):3388–94.
51. Cheng S, Liu H, Logan B. Increased power generation in a continuous flow MFC with advective flow through the porous anode and reduced electrode spacing. *Environ Sci Technol* 2006;**40**(7):2426–32.
52. Jung S, Regan JM. Comparison of anode bacterial communities and performance in microbial fuel cells with different electron donors. *Appl Microbiol Biotechnol* 2007;**77**(2):393–402.
53. Ringeisen BR, Ray R, Little B. A miniature microbial fuel cell operating with an aerobic anode chamber. *J Power Sources* 2007;**165**(2):591–7.
54. Ringeisen BR, et al. High power density from a miniature microbial fuel cell using *Shewanella oneidensis* DSP10. *Environ Sci Technol* 2006;**40**(8):2629–34.
55. Park HS, Kim BH, Kim HS, Kim HJ, Kim GT, Kim M, et al. A novel electrochemically active and Fe (III)-reducing bacterium phylogenetically related to *Clostridium butyricum* isolated from a microbial fuel cell. *Anaerobe* 2001;**7**(6):297–306.
56. Rabaey K, Boon N, Hofte M, Verstraete. Microbial phenazine production enhances electron transfer in biofuel cells. *Environ Sci Technol* 2005;**39**(9):3401–8.
57. Najafpour G, Rahimnejad M, Ghoreschi A. The enhancement of a microbial fuel cell for electrical output using mediators and oxidizing agents. *Energy Sources, Part A* 2011;**33**(24):2239–48.
58. Vega C, Fernández I. Mediating effect of ferric chelate compounds in microbial fuel cells with *Lactobacillus plantarum*, *Streptococcus lactis*, and *Erwinia dissolvens*. *Bioelectroch Bioener* 1987;**17**(2):217–22.
59. Rabaey K, Ossieur W, Verhaege M, Verstraete W. Continuous microbial fuel cells convert carbohydrates to electricity. *Water Sci Technol* 2005;**52**(1):515–23.
60. Thygesen A, Poulsen FW, Min B, Angelidaki I, Thomsen AB. The effect of different substrates and humic acid on power generation in microbial fuel cell operation. *Bioresour Technol* 2009;**100**(3):1186–91.
61. Liu H, Logan BE. Electricity generation using an air-cathode single chamber microbial fuel cell in the presence and absence of a proton exchange membrane. *Environ Sci Technol* 2004;**38**(14):4040–6.
62. Gorby Y, Yanina S, McLean J, Rosso K, Moyles D, Dohnalkova A, et al. Electrically conductive bacterial nanowires produced by *Shewanella oneidensis* strain MR-1 and other microorganisms. *Proc Natl Acad Sci* 2006;**103**(30):11358.
63. Reguera G, Nevin K, Nicoll J, Covalla S, Woodard T, Lovley D. Biofilm and nanowire production leads to increased current in *Geobacter sulfurreducens* fuel cells. *Appl Environ Microbiol* 2006;**72**(11):7345.
64. Reguera G, Pollina R, Nicoll J, Lovley D. Possible non-conductive role of *Geobacter sulfurreducens* pili nanowires in biofilm formation. *J Bacteriol* 2006;**189**(5):2125–7.
65. Park D, Zeikus J. Electricity generation in microbial fuel cells using neutral red as an electronophore. *Appl Environ Microbiol* 2000;**66**(4):1292.

66. Bennetto H, Delaney G, Mason J, Roller S, Stirling J, Thurston C. The sucrose fuel cell: efficient biomass conversion using a microbial catalyst. *Biotechnol Lett* 1985;7(10):699–704.
67. Choi Y, Jung E, Park H, Jung S, Kim S. Effect of initial carbon sources on the performance of a microbial fuel cell containing environmental microorganism *micrococcus luteus*. *Notes* 2007;28(9):1591.
68. Rabaey K, Verstraete W. Microbial fuel cells: novel biotechnology for energy generation. *Trends Biotechnol* 2005;23(6):291–8.
69. Liu H, Cheng S, Logan B. Production of electricity from acetate or butyrate using a single-chamber microbial fuel cell. *Environ Sci Technol* 2005;39(2):658–62.
70. Oh S, Logan B. Voltage reversal during microbial fuel cell stack operation. *J Power Sources* 2007;167(1):11–7.
71. Rahimnejad M, Mokhtarian N, Najafpour G, Daud W, Ghoreyshi A. Low voltage power generation in a biofuel cell using anaerobic cultures. *World Appl Sci J* 2009;6(11):1585–8.
72. Cooney MJ, Roschi E, Marison IW, Comminellis C, von Stockar U. Physiologic studies with the sulfate-reducing bacterium *Desulfovibrio desulfuricans*: evaluation for use in a biofuel cell. *Enzyme Microb Technol* 1996;18(5):358–65.
73. Jafary T, Najafpour G, Ghoreyshi A, Haghparast F, Rahimnejad M, Zare H. Bioelectricity power generation from organic substrate in a microbial fuel cell using *Saccharomyces cerevisiae* as biocatalysts. *Fuel Cells*, vol. 4; p. 1182.
74. Pant D, Van Bogaert G, Diels L, Vanbroekhoven K. A review of the substrates used in microbial fuel cells (MFCs) for sustainable energy production. *Bioresour Technol* 2010;101(6):1533–43.
75. Park D, Zeikus J. Impact of electrode composition on electricity generation in a single-compartment fuel cell using *Shewanella putrefaciens*. *Appl Microbiol Biotechnol* 2002;59(1):58–61.
76. Jafary T, Ghoreyshi AA, Najafpour GD, Fatemi S, Rahimnejad M. Investigation on performance of microbial fuel cells based on carbon sources and kinetic models. *Int J Energy Res* 2013;37(12):1539–49.
77. Kim J, Cheng S, Oh S, Logan B. Power generation using different cation, anion, and ultrafiltration membranes in microbial fuel cells. *Environ Sci Technol* 2007;41(3):1004–9.
78. Zhang X, Cheng S, Wang X, Huang X, Logan BE. Separator characteristics for increasing performance of microbial fuel cells. *Environ Sci Technol* 2009;43(21):8456–61.
79. Li W-W, Sheng G-P, Liu X-W, Yu H-Q. Recent advances in the separators for microbial fuel cells. *Bioresour Technol* 2011;102(1):244–52.
80. Min B, Cheng S, Logan B. Electricity generation using membrane and salt bridge microbial fuel cells. *Water Res* 2005;39(9):1675–86.
81. Deng Q, Li X, Zuo J, Ling A, Logan BE. Power generation using an activated carbon fiber felt cathode in an upflow microbial fuel cell. *J Power Sources* 2010;195(4):1130–5.
82. Rozendal RA, Hamelers HV, Rabaey K, Keller J, Buisman CJ. Towards practical implementation of bio-electrochemical wastewater treatment. *Trends Biotechnol* 2008;26(8):450–9.
83. Ter Heijne A, Hamelers H, De Wilde V, Rozendal R, Buisman C. A bipolar membrane combined with ferric iron reduction as an efficient cathode system in microbial fuel cells. *Environ Sci Technol* 2006;40(17):5200–5.
84. Chae KJ, Choi M, Ajayi FF, Park W, Chang IS, Kim IS. Mass transport through a proton exchange membrane (nafion) in microbial fuel cells. *EnergFuel* 2007;22(1):169–76.
85. Ghasemi M, Wan Daud WR, Ismail M, Rahimnejad M, Ismail AF, Leong JX, et al. Effect of pre-treatment and biofouling of proton exchange membrane on microbial fuel cell performance. *Int J Hydrogen Energy* 2013;38(13):5480–4.
86. Venkata Mohan S, Mohanakrishna G, Srikanth S, Sarma P. Harnessing of bioelectricity in microbial fuel cell (MFC) employing aerated cathode through anaerobic treatment of chemical wastewater using selectively enriched hydrogen producing mixed consortia. *Fuel* 2008;87(12):2667–76.
87. Rhoads A, Beyenal H, Lewandowski Z. Microbial fuel cell using anaerobic respiration as an anodic reaction and biomineralized manganese as a cathodic reactant. *Environ Sci Technol* 2005;39(12):4666–71.
88. González del Campo A, Cañizares P, Rodrigo MA, Fernández FJ, Lobato J. Microbial fuel cell with an algae-assisted cathode: a preliminary assessment. *J Power Sources* 2013;242:638–45.
89. Franks AE, Nevin K. Microbial fuel cells, a current review. *Energies* 2010;3:899–919.
90. Lobato J, González del Campo A, Fernández FJ, Cañizares P, Rodrigo MA. Lagooning microbial fuel cells: a first approach by coupling electricity-producing microorganisms and algae. *Appl Energy* 2013;110:220–6.

91. Walter XA, Greenman J, Ieropoulos IA. Oxygenic phototrophic biofilms for improved cathode performance in microbial fuel cells. *Algal Res* 2013;**2**(3):183–7.
92. Rahimnejad M, Bakeri G, Najafpour G, Ghasemi M, Oh S-E. A review on the effect of proton exchange membranes in microbial fuel cells. *Biofuel Res J* 2014;**1**(1):7–15.
93. Wilkinson S. “Gastrobots”—Benefits and challenges of microbial fuel cells in foodpowered robot applications. *Auton Robot* 2000;**9**(2):99–111.
94. Oh S, Logan BE. Hydrogen and electricity production from a food processing wastewater using fermentation and microbial fuel cell technologies. *Water Res* 2005;**39**(19):4673–82.
95. Liu H, Grot S, Logan BE. Electrochemically assisted microbial production of hydrogen from acetate. *Environ Sci Technol* 2005;**39**(11):4317–20.
96. Peixoto L, Min B, Martins G, Brito AG, Kroff P, Parpot P, et al. In situ microbial fuel cell-based biosensor for organic carbon. *Bioelectrochem* 2011;**81**(2):99–103.
97. Lovley DR. Microbial fuel cells: novel microbial physiologies and engineering approaches. *Curr Opin Biotechnol* 2006;**17**(3):327–32.
98. Karube I, Matsunaga T, Mitsuda S, Suzuki S. Microbial electrode BOD sensors. *Biotechnol Bioeng* 1977;**19**(10):1535–47.
99. Kim BH, Chang IS, Gil GC, Park HS, Kim HJ. Novel BOD (biological oxygen demand) sensor using mediator-less microbial fuel cell. *Biotechnol Lett* 2003;**25**(7):541–5.
100. Kumlanghan A, Liu J, Thavarungkul P, Kanatharana P, Mattiasson B. Microbial fuel cell-based biosensor for fast analysis of biodegradable organic matter. *Biosens Bioelectron* 2007;**22**(12):2939–44.
101. Hart JP, Abass A-K, Honeychurch KC, Pemberton R, Ryan S, Wedge R. Sensors/biosensors, based on screen-printing technology for biomedical applications. *Indian J Chem Sect A* 2003;**42**(4):709–18.
102. Ramalho RS. *Introduction to wastewater treatment processes*; 1983.
103. Habermann W, Pommer E. Biological fuel cells with sulphide storage capacity. *Appl Microbiol Biotechnol* 1991;**35**(1):128–33.
104. Min B, Kim J, Oh S, Regan JM, Logan BE. Electricity generation from swine wastewater using microbial fuel cells. *Water Res* 2005;**39**(20):4961–8.
105. Najafpour G, Rahimnejad M, Mokhtarian N, Daud W, Ghoreyshi A. Bioconversion of Whey to electrical energy in a biofuel cell using *Saccharomyces cerevisiae*.
106. Virdis B, Rabaey K, Yuan Z, Keller J. Microbial fuel cells for simultaneous carbon and nitrogen removal. *Water Res* 2008;**42**(12):3013–24.
107. Moon H, Chang IS, Jang JK, Kim BH. Residence time distribution in microbial fuel cell and its influence on COD removal with electricity generation. *Biochem Eng J* 2005;**27**(1):59–65.
108. Yadav AK, Dash P, Mohanty A, Abbassi R, Mishra BK. Performance assessment of innovative constructed wetland-microbial fuel cell for electricity production and dye removal. *Ecol Eng* 2012;**47**:126–31.
109. Tao H-C, Liang M, Li W, Zhang L-J, Ni J-R, Wu W-M. Removal of copper from aqueous solution by electro-deposition in cathode chamber of microbial fuel cell. *J Hazard Mater* 2011;**189**(1):186–92.
110. Zhang L, De Schryver P, De Gussem B, De Muynck W, Boon N, Verstraete W. Chemical and biological technologies for hydrogen sulfide emission control in sewer systems: a review. *Water Res* 2008;**42**(1):1–12.
111. Sun M, Mu Z-X, Chen Y-P, Sheng G-P, Liu X-W, Chen Y-Z, et al. Microbe-assisted sulfide oxidation in the anode of a microbial fuel cell. *Environ Sci Technol* 2009;**43**(9):3372–7.
112. Rabaey K, Van de Sompel K, Maignien L, Boon N, Aelterman P, Clauwaert P, et al. Microbial fuel cells for sulfide removal. *Environ Sci Technol* 2006;**40**(17):5218–24.
113. Lee C-Y, Ho K-L, Lee D-J, Su A, Chang J-S. Retracted: electricity harvest from wastewaters using microbial fuel cell with sulfide as sole electron donor. *Int J Hydrogen Energy* 2012;**37**(20):15787–91.
114. Cai J, Zheng P. Simultaneous anaerobic sulfide and nitrate removal in microbial fuel cell. *Bioresour Technol* 2012;**129**:224–8.
115. Izadi P, Rahimnejad M. Simultaneous electricity generation and sulfide removal via a dual chamber microbial fuel cell. *Biofuel Res J* 2013;**1**(1):34–8.

Biological Treatment*

OUTLINE

19.1 Introduction	558	19.11 Biological Nitrification and Denitrification	579
19.2 Organic Removal in Sustainable Microbial Growth	558	19.12 Biological Treatment Processes: Suspended and Attached Growth	586
19.3 Microbial Metabolism	559	19.12.1 Kinetics of Suspended and Attached Growth Processes	586
19.4 Microbial Growth Kinetics	561	19.12.2 Suspended Growth Processes	587
19.5 Growth Rate and Treatment Kinetics	562	19.12.3 Sludge Retention Time (SRT)	587
19.5.1 Nutrient Requirements	565	19.12.4 Biomass Concentration in System	589
19.5.2 Effects of pH and Temperature	566	19.12.5 Food to Microorganisms Ratio	590
19.6 Removal Mechanisms in Biological Processes	568	19.12.6 Effluent Substrate Concentration	591
19.7 Aerobic Biooxidation	569	19.12.7 Oxygen Requirements	592
19.8 Anaerobic Digestion	572	References	594
19.9 Abiotic Losses	576		
19.9.1 Adsorption	576		
19.10 Volatilization	578		

*This case study was partially written with contributions from:
 Roya Pishgar, School of Civil Engineering, Babol Noshirvani University of Technology, Babol,
 Mazandaran, Iran.

19.1 INTRODUCTION

In recent decades, great interests for biological treatment of wastewater have been developed. With appropriate considerations, all the biodegradable constituents present in various types of wastewaters are biologically treated. Grasping a profound understanding of the characteristics of each biological process enables engineers to devise the most appropriate treatment for certain objectives, helping them provide proper environmental conditions and efficient techniques.

Biological treatment methods employ aerobic, facultative, and anaerobic microorganisms to convert or oxidize organic matters and eliminate the oxygen demand of wastewater. As domestic sewage undergoes treatment biologically, dissolved and particulate biodegradable matters are transformed into acceptable end-products, while suspended and nonsettleable colloidal solids integrate to form biological floc or biofilm. Also, the conversion or complete removal of nutrients (i.e., nitrogen and phosphorous) and particular trace organic compounds can occur during biological treatment of domestic sewage. Furthermore, the organic and inorganic compounds existing in various industrial effluents are susceptible to biological degradation. Toxic constituents and compounds frequently found in industrial wastewaters may necessitate a pretreatment stage prior to discharging the industrial wastewater to a municipal collection system. Inhibitory concentrations of organic and inorganic pollutants in industrial wastewaters may hinder microbial growth by either slowing the biodegradation process or completely intoxicating the viable biological system. High concentrations of nitrogen and phosphorus available in agricultural irrigation wastewater, which have a stimulating effect on the growth of aquatic plants, can satisfactorily be degraded by various biological processes.¹

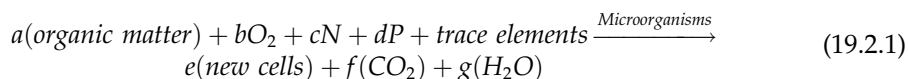
Considering the type of growth and retention of microorganisms in biological treatment systems, biological processes can be classified into two principal groups: suspended growth and attached growth processes. In suspended growth processes, microorganisms are maintained in suspension within the bulk liquid by suitable mixing techniques. Attached growth processes, also referred to as fixed-film or biofilm processes, are those biological treatment systems in which microorganisms are attached to solid-support or inert packing material (e.g., rocks, slag, specific ceramic or plastic packing). As microorganisms oxidize organic compounds and consume nutrients and certain inorganic constituents, harmless end-products and new cell tissues are produced, which can subsequently be removed by means of physical operations such as settling and gas stripping.

19.2 ORGANIC REMOVAL IN SUSTAINABLE MICROBIAL GROWTH

Microorganisms play the key role in biological treatment processes. Complete removal or significant reduction of the concentrations of biodegradable organic constituents in wastewaters can be achieved with proper microbial consortia; the mixed culture is either intrinsically present in the wastewater, or is introduced to the target wastewater by blending it with domestic sewage or biological sludge. However, pure cultures of organisms may be utilized in certain cases for removal of specific contaminants. In favorable environmental conditions,

microorganisms are capable of presenting high efficiency in destruction of pollutants, thus, producing an acceptable effluent. Several factors should be considered carefully to achieve a suitable environment for metabolism of the organisms; those factors include sufficient nutrition, the presence of inorganic anions and cations in concentrations lower than their threshold values for the organisms, proper pH, appropriate temperature depending on the presence of thermophilic or mesophilic organisms, adequate presence or complete absence of dissolved oxygen for respective aerobic and anaerobic systems, absence of toxicity and inhibition (which may occur due to the presence of certain concentrations of specific pollutants), and ample hydraulic and sludge retention time to allow the microorganisms to grow and complete their biochemical activities.²

The removal of organic constituents, identified as carbonaceous biochemical oxygen demand (BOD), in dissolved and particulate forms as well as stabilization of nonsettleable organic matters can be achieved by a variety of microorganisms, specifically bacteria. The living organisms contribute in degradation of organic substrate to simple end-products along with the production of additional new cells, until the substrate is completely removed. Equation 19.2.1 depicts aerobic biological oxidation as described above. The biomass will consequently endure the stage of endogenous respiration. In this stage, autooxidation of organics in the cells happens in order to supply requisite energy for maintaining the remainder of the cells; as a result, continuous and fractional decrease in living cell mass with respect to time is inevitable.^{1,3}



According to the above equation, microorganisms need to uptake some essential nutrients, i.e., carbon, nitrogen, and phosphorus sources together with some trace elements in appropriate concentrations, for accomplishing their metabolic activities. Water and wastewater treatment processes are mostly planned so the required carbon source is provided through consumption of target organic matter. Ammonia (NH₃) and phosphate (PO₄³⁻) are examples of nitrogen and phosphorus sources that are commonly used. The value of C:N:P ratio is a determining parameter for sound performance of biological treatment process; for aerobic systems, it should be in the range of 100:5:1 to 100:20:1.² Anaerobic processes, in contrast, require much lower nitrogen and phosphorus in compare to aerobic systems due to slow metabolism and gradual growth of anaerobic microorganisms. The optimal C:N:P ratio of 100:2.5:0.5 with increasing effect on methane yield has been reported.⁴

19.3 MICROBIAL METABOLISM

Understanding biochemical activities of microorganisms is of great necessity for correctly selecting and properly designing a biological treatment process for a special purpose. Microbial metabolism is characterized by the types of the sources of carbon and energy required for synthesizing new cells and transforming organic material to end products. Carbon and energy sources, also known as substrates, are two main factors for classifying the organisms in different categories (see Table 19.1).¹

TABLE 19.1 Classification of microorganisms with respect to their required sources of carbon and energy

Type of microorganisms		Carbon source	Energy source	Example
Heterotroph	Chemotroph	Organic compounds	Oxidation–reduction reactions	Protozoa, fungi, most bacteria
	Phototroph	Organic compounds	Light	Sulfur-reducing bacteria
Autotroph	Chemotroph	CO ₂	Oxidation–reduction reactions	Nitrifying bacteria
	Phototroph	CO ₂	Light	Algae, photosynthetic bacteria

Microorganisms need carbon for the synthesis of new cellular material that can be obtained from either organic matter or carbon dioxide. Depending upon which of these materials is utilized as a carbon source, microorganisms are divided into two principal groups: heterotrophs and autotrophs. Organisms, which are referred to as heterotrophs, uptake organic carbon in order to reproduce new biomass; on the other hand, organisms that gain their requisite carbon from carbon dioxide are identified as autotrophs. Deriving cell carbon from carbon dioxide necessitates an extra energy-consuming reductive reaction for releasing the carbon for the usage of autotrophs. Hence, a higher level of energy is required for the synthesis of autotrophic organisms in comparison to that of heterotrophs. This phenomenon leads to low growth rate, and thus, slight biomass yield for autotrophic organisms.¹

Light and chemical oxidation reactions are two disparate sources of energy for cell maintenance. Organisms capable of using light as their energy source are called phototrophs, while those organisms that elicit the needed energy from oxidation–reduction reactions are recognized as chemotrophs. Phototrophic and chemotrophic organisms can obtain their carbon for the formation of new cells from either organic matter or carbon dioxide. Therefore, phototrophs and chemotrophs that can live on organic carbon are also characterized as heterotrophs; however, if their cell carbon is extracted from carbon dioxide, they should be known as photoautotrophs or chemoautotrophs.¹ Some examples of each group of organisms are presented in Table 19.1. Chemical reactions, led by chemotrophs, are oxidation–reduction processes (or redox equations) where energy is produced by transferring an electron from an electron donor to an electron acceptor. As the electron donor is oxidized, the electron acceptor, which can be either organic or inorganic compounds, is reduced. If the electron acceptor is within the cell, endogenous metabolism occurs. Exogenous metabolism can happen when the electron is transferred to an agent outside the cell such as dissolved oxygen and nitrite/nitrate.¹

It is the nature of an electron acceptor in a redox reaction that determines if the metabolism of the organisms is respiratory or fermentative. Transferring an electron to an external electron acceptor, which is catalyzed by enzymes, is known as respiratory metabolism. Fermentation occurs when an internal electron acceptor is reduced. Compared to respiratory heterotrophic bacteria, strict fermentative heterotrophs are recognized as slow-growing organisms with low cell yield due to low energy originated from fermentation. According

TABLE 19.2 Respiration and metabolic functions of microorganisms

Type of organism	Affinity to electron acceptor	Electron acceptor	Metabolism
Aerobic	Obligate	Only oxygen	Respiratory
	Facultative	Oxygen, nitrite/nitrate (NO_2^- , NO_3^-)	Respiratory
Anoxic (denitrifying bacteria)		Nitrite/nitrate (NO_2^- , NO_3^-)	Respiratory
Anaerobic	Obligate	Only an internal electron acceptor	Fermentative
	True facultative	Internal electron acceptor, oxygen	Fermentative and respiratory
	Aerotolerant facultative	Only an internal electron acceptor, although insensitive to oxygen	Fermentative

to the type of electron acceptor, metabolic functions of microorganisms are presented in Table 19.2.

In aerobic and anoxic processes, energy is generated by transporting an electron to external electron acceptors, i.e., oxygen and/or nitrite and nitrate. The energy requirement of obligate aerobic bacteria can only be supplied by utilizing oxygen as an electron acceptor. In contrast, facultative aerobes are capable of adopting nitrite/nitrate as an electron acceptor that is devoid of oxygen. In anoxic processes, nitrite or nitrate play the role of the electron acceptor. Obligate anaerobic organisms are able to maintain their metabolic activity only in the absence of oxygen. However, facultative anaerobes can grow properly in either the presence or absence of oxygen. True facultative anaerobic microbes can switch to respiratory metabolism when the oxygen is present in the media. Aerotolerant anaerobes have the ability to live and function in the presence of molecular oxygen, showing comparatively no sensitivity to it; however, their metabolic activity is rigorously fermentative.¹

19.4 MICROBIAL GROWTH KINETICS

In biological treatment processes, substrate degradation depends on biomass growth and activity. With oxidizing organic compounds, a microbial community attains requisite cell carbon and energy for generating new cell tissues and reproduction. Hence, the dynamics of microbial growth and substrate utilization control the performance of biological treatment processes.

As it is previously described, four distinguishable phases can be identified in microbial growth curve cultured in batch reactor: lag phase, exponential growth phase, stationary phase, and death phase. After acclimating to new environmental condition during lag phase, the bacterial community represents a rapid growth and cells multiply exponentially. At this stage, namely exponential growth phase, the oxidation of organic matters leads to the formation of new cells and the production of end products. Subsequently, when substrate

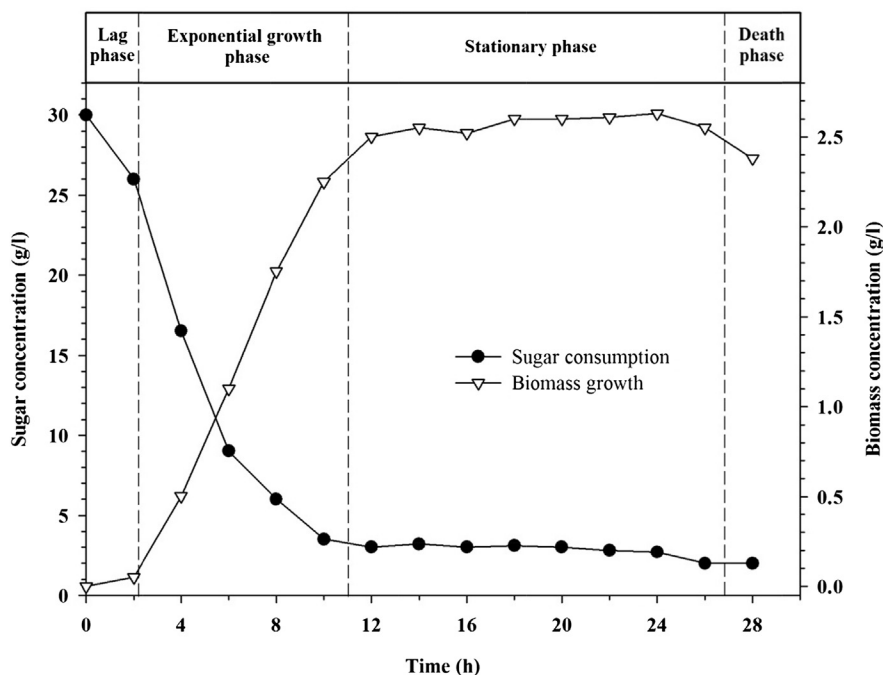


FIGURE 19.1 Growth curve of *Saccharomyces cerevisiae* in batch system. Biomass formation occurred as the sugar content of molasses was consumed.

concentration drastically decreases, biomass concentration remains relatively constant in the stationary phase. As the cell starts to go through endogenous respiration at the end of the stationary phase, the rate of growth and death rate counterbalanced in this stage. Complete depletion of substrate alongside toxic effects of dead cell residue and cell metabolites causes the remainder of the cells to become deactivated and, in consequence, death phase occurs. In this phase, exponential decrease in the concentration of living organisms often happens. The four phases of *Saccharomyces cerevisiae* in batch system with consumption of the sugar content of molasses are illustrated in Fig. 19.1. As the experiment was not continued in the death phase, the exponential decrease in cell concentration was not completely shown. However, the onset of endogenous respiration is very apparent.

19.5 GROWTH RATE AND TREATMENT KINETICS

The study of growth phases indicates the simultaneous occurrence of microbial growth and substrate utilization in the batch process. As the oxidation of organic or inorganic matters (i.e., electron donors) contributes to production of a new cell culture, the ratio of biomass produced to substrate consumed is referred to as biomass yield as given by Eqn (19.5.1).

$$\text{Biomass yield} = \frac{\text{g biomass produced}}{\text{g substrate consumed}} \quad (19.5.1)$$

The basic equation of microbial growth kinetics can be written based on biomass yield concept correlating cell growth to substrate utilization as follows:

$$\frac{dX}{dt} = Y_{X/S} \left(\frac{dS_{su}}{dt} \right) \quad (19.5.2)$$

where X is biomass concentration (g l^{-1}), t is time for relevant changes (d), Y is yield coefficient (g g^{-1}), and S_{su} is concentration of soluble substrate (g l^{-1}). It should be noted that, in the above equation, the changes in biomass concentration refer to an increase in cell concentration during the phase of exponential growth.

To obtain net biomass production rate, self-digestion of microorganisms during the death phase should be considered. Biomass decay can be described in proportion to the current biomass concentration. Therefore, the equation that relates the rates of cell growth and substrate depletion in batch and continuous processes can be summarized as follows:

$$r_{ng} = -Y(r_{su}) - k_d \cdot X \quad (19.5.3)$$

where K_d is endogenous decay coefficient (g VSS/g VSS.d). Net growth rate, r_{ng} , and substrate utilization rate, r_{su} substituted for dX/dt and dS_{su}/dt , respectively.

Biomass propagation in batch mode is proportional to the mass of microbial solids present in the system. So, specific cell growth rate, μ ($\text{g new cell/g cells.d}$) defines the cell growth in biological system with respect to biomass concentration as follows:

$$\frac{r_{ng}}{X} = \mu \quad (19.5.4)$$

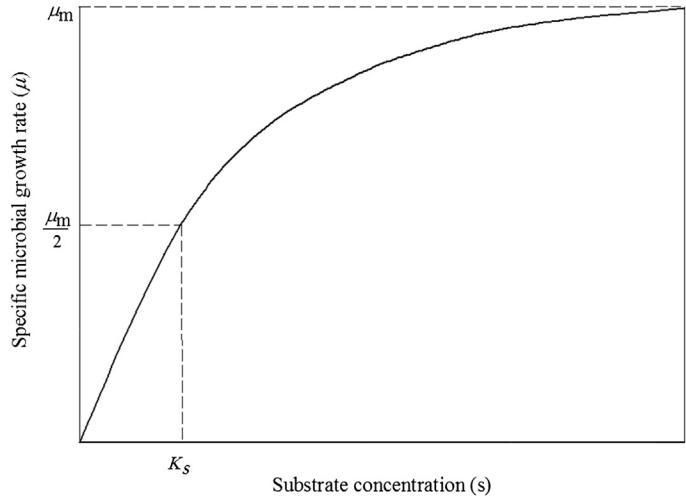
Monod proposed a model for the specific growth rate of bacterial cultures as the following, in which soluble substrate concentration is the limiting factor for microbial growth.⁵

$$\mu = \frac{\mu_m S}{K_s + S} \quad (19.5.5)$$

where μ_m is maximum specific cell growth rate ($\text{g new cell/g cells.d}$), S is substrate concentration in dissolved form (g l^{-1}), and K_s is half-velocity constant (g l^{-1}) that indicates the substrate concentration corresponding to one-half of the maximum specific cell growth rate ($\mu = \frac{\mu_m}{2}$). The K_s constant shows the affinity of microorganisms to the growth-limiting substrate. The low value of K_s denotes the suitability of the substrate for microbial growth because high microbial propagation happens on low substrate concentrations.¹⁻⁷ The plot in Fig. 19.2 shows cell growth rate versus substrate concentration schematically.

However, the Monod model is a simple equation that correlates the trend of microbial growth to substrate concentration. For specific conditions such as substrate inhibition, the Monod equation can be developed into a new model, namely the Haldane model, in order to show the inhibition effect on the cell growth. The Haldane model is mathematically termed as per the following relationship:

FIGURE 19.2 Typical specific microbial growth rate versus growth-limiting substrate concentration.



$$\mu = \frac{\mu_m S}{K_s + S + (S^2/K_i)} \quad (19.5.6)$$

where K_i is inhibition coefficient (g l^{-1}); it is the concentration of substrate in which cell growth is inhibited. The high value of K_i suggests that the organisms are not so sensitive to the target substrate and that the inhibition effect is observed in high concentrations of the substrate.

For modeling-dissolved substrate removal in the batch reactor, the Michaelis–Menten equation can be written by a combination of Eqns (19.5.2, 19.5.4 and 19.5.5):

$$r_{su} = -\frac{\mu_m X S}{Y_{X/S}(K_s + S)} \quad (19.5.7)$$

In Eqn (19.5.7), negative value denotes the decrease in substrate concentration due to its utilization. As the equation is used in mass balances, the presence of the negative sign is necessary. The term $(\mu_m/Y_{X/S})$ can be substituted for k , which represents the maximum specific substrate utilization rate (g substrate per g cell.d) as given below:

$$r_{su} = -\frac{kXS}{K_s + S} \quad (19.5.8)$$

According to relative values of K_s and S , Eqn (19.5.7) can be simplified to other expressions representing boundary cases. When substrate concentration is much higher in compare to K_s value ($S \gg K_s$), substrate depletion can be expressed as follows.

$$r_{su} \approx -kX \quad (19.5.9)$$

In this case, substrate removal is not dependent upon its concentration, and only the concentration of microbial solids influences substrate reduction; this is because of the low affinity of the organisms to the substrate.

For substrate concentrations much lower than K_s value ($S \ll K_s$), Eqn (19.5.7) will be written in the following simple form:

$$r_{su} \approx -kX \frac{S}{K_s} \approx k'XS \quad (19.5.10)$$

where $U = \frac{kS}{K_s}$ is defined as specific substrate utilization rate (g substrate per g cell.d). The value of $k' = \frac{k}{K_s}$ may vary for different wastewaters, which shows the ratio of specific substrate utilization rate per soluble substrate concentration (U/S).

Substrate concentration that is considered for the proposed rate expression is referred to an available substrate in dissolved form. However, soluble substrate constitutes a fraction of biodegradable organic matters in the wastewaters; in domestic sewage, the ratio of soluble organic material to total biodegradable organic matter varies between 0.02 and 0.05, and limited amounts of soluble organic matter in some industrial wastewaters can be observed. Organic compounds can be used just in dissolved form by the living organisms. Particulate substrates should, therefore, be hydrolyzed by extracellular enzymes made by bacteria to soluble substrates. Graddy and coworkers⁸ have proposed a model for the transformation of particulate substrate to soluble substrate based on biomass and particulate substrate concentrations as given below:

$$\frac{dS_{ps}}{dt} = -\frac{k_p(S_{ps}/X)X}{(K_x + S_{ps}/X)} \quad (19.5.11)$$

where S_{ps} is particulate substrate concentration (g l^{-1}), k_p is maximum specific substrate concentration transformation rate (g particulate substrate/g cell.d), X is biomass concentration (g l^{-1}), and K_x is half-velocity degradation coefficient (g g^{-1}). The term (dS_{ps}/dt) suggests the conversion rate of particulate substrate concentration to dissolved form.

19.5.1 Nutrient Requirements

In addition to carbon and energy sources, other nutrients are integrated to sound cell activity. Microorganisms need organic and inorganic nutrients for growing and synthesizing new cells as unavailability of those nutrients may limit the biomass growth. Microbial cells are composed of carbon, oxygen, nitrogen, phosphorus, and hydrogen: 50, 20, 12, 9, and 2% of cell dry weight, and the remaining 5% is related to ash and trace elements. Table 19.3 represents the major and minor inorganic nutrients plus main organic nutrients required for cell maintenance. Identified as growth factors, organic nutrients are of great necessity for cell growth due to their role as precursors of organic cellular material; however, they are not synthesizable compounds by organisms from carbon source.¹

Excess amounts of nitrogen and phosphorus are present in domestic sewage. In contrast, the paucity of these nutrients in numerous industrial wastewaters necessitates their addition as supplementary substrates. Pulp and paper, cotton textile, and cannery are examples of industries that generate effluents with a deficiency in nitrogen and phosphorus.³ An alternative method for improving the level of nitrogen and phosphorus in industrial wastes is diluting them with sewage, which saves in chemicals consumption (e.g., urea as a supplemental nitrogen source). Besides, it leads to moderating the characteristic of industrial wastewaters that

TABLE 19.3 Organic and inorganic nutrients essential for cell growth

Major inorganic nutrients	Minor inorganic nutrients	Main organic nutrients
Nitrogen (N)	Zinc (Zn)	Amino acids
Phosphorus (P)	Manganese (Mn)	Purines
Sulfur (S)	Molybdenum (Mo)	Pyrimidines
Potassium (K)	Selenium (Se)	Vitamins
Magnesium (Mg)	Cobalt (Co)	
Calcium (Ca)	Copper (Cu)	
Iron (Fe)	Nickel (Ni)	
Sodium (Na)		
Chlorine (Cl)		

makes simultaneous treatment of domestic sewage and industrial wastes feasible. As previously stated, the C:N:P ratio for aerobic biological treatment process should vary between 100:5:1 and 100:20:1. Based on BOD measurement as an index for organic compounds, the desirable ratio is 100:5:1 for BOD:N:P to achieve satisfactory cell synthesis and organics removal in biological processes. A nitrogen-limiting situation can lead to the accumulation of polysaccharide during cell synthesis, filamentous growth, and low efficiency in BOD removal.⁹

The age of biological sludge (θ_c) plus the amount of sludge withdrawn from the biological process determine nitrogen and phosphorus requirements. While age of the biomass (θ_c) increases, nitrogen and phosphorus contents of the biological sludge show a descending trend. The nitrogen and phosphorus contents of 12.3 and 2.6% in newly synthesized cells diminish to 7.1 and 1% in nonbiodegradable cell residue remained of autolysis, respectively; these content values are derived on the basis of volatile suspended solids (VSS). An extended sludge age (θ_c) denotes more recycling times rather than that of the systems with short age of the sludge. Sludge recycling ensures returning of surplus nutrients resulted from endogenous respiration to the system, leading to reduction in nutrient demand. While nutrient requirements of conventional activated sludge is BOD:N:P of 100:5:1, an extended aeration process requires N of 0.825 and P of 0.165 proportional to 100 unit of BOD₅ removed.³

19.5.2 Effects of pH and Temperature

The pH and temperature of the medium are two environmental conditions that should cautiously be controlled so that the favorable performance of biological process can be achieved. Microbial growth and activity are restricted by specific values of pH, and temperature as the optimum growth can only occur in a particular range of these parameters.

Bacterial culture can be divided into three general categories according to the optimal temperature for their growth: psychrophilic, mesophilic, and thermophilic. Psychrophilic bacteria function best in cold temperatures, i.e., 12–18 °C, while the temperature range of 25–40 °C is

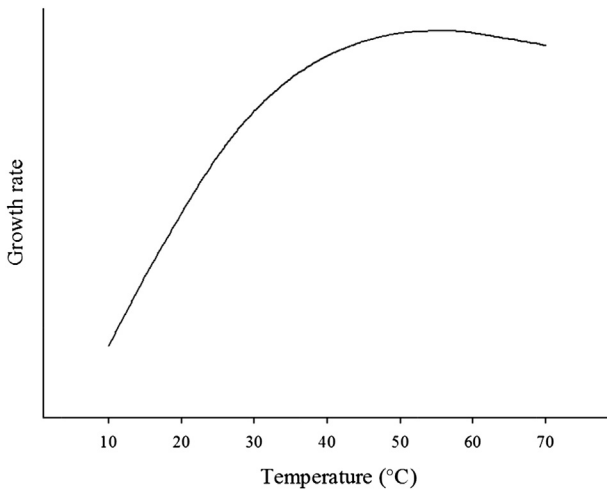


FIGURE 19.3 Typical response of mesophilic bacteria in term of growth rate to temperature changes.

optimum for the survival and growth of mesophiles. Maximum increase in growth and metabolism of thermophilic bacteria can be observed in high temperatures (55–65 °C). However, these microorganisms are capable of enduring a broader range of temperature, which varies between 10 and 30 °C, 20–50 °C, and 35–75 °C for psychrophilic, mesophilic, and thermophilic, respectively. As Fig. 19.3 depicts, every 10 °C increment in temperature up to optimum value highly influences the growth rate, making it twofold of the former quantity. In contrast, temperatures over the optimum value show an insignificant decrease in growth rate and the enzymatic and metabolic activity of organisms.

In addition to affecting microbial growth rate, the temperature influence on biological treatment processes in other aspects. As an example, gas transfer rate is subject to changes when the temperature varies. Also, the settling characteristics of biological solids depend on the temperature of the medium; a high temperature leads to intense convective currents in the liquid, which slow down the settling time of particulate matters. Hence, the reaction rate constants of a biological process should be corrected by the following relationship for specific temperature:

$$K_T = K_{20}\theta^{(T-20)} \quad (19.5.2.1)$$

Where K_T is the reaction rate coefficient at the specific temperature of T (°C), K_{20} is the reaction rate coefficient at the temperature of 20 °C, θ is the temperature activity coefficient, and T is the temperature of process (°C). For determining θ practically, no less than three separate experiments with bench-scale systems at different temperatures should be conducted.

Another growth-limiting factor is the pH of the environment. Bacteria can only survive within a pH of 6.5 and 7.5. The pH out of the limits of nine and four is lethal to most of the microorganisms. Anaerobic processes, specifically methanogenic bacterial cultures, are susceptible to the pH out of the limits of 6.6 and 7.6. Measures should be taken to control the pH in anaerobic treatment processes due to the accumulation of volatile fatty acids (VFAs) at the primary stages of the process. At the beginning of anaerobic digestion, the

number of fermentative and methanogenic bacteria does not counterbalance the VFAs because of low growth rate of methanogenics. Hence, VFAs produced by acidogens are not offset by VFAs utilized by methanogens; thus, an increase in pH primarily happens. The drop of pH value to below 6.6 is deadly for a methanogenic community that system can only recover to a satisfactory situation within weeks or even months. To maintain the required buffering capacity and avoid pH fluctuations, several compounds are added to the wastewater such as lime (Ca(OH)_2), sodium bicarbonate (NaHCO_3), soda ash (Na_2CO_3), sodium hydroxide (NaOH), ammonia (NH_3), and ammonium bicarbonate (NH_4HCO_3).^{1,10}

19.6 REMOVAL MECHANISMS IN BIOLOGICAL PROCESSES

The disposal of organic matters in biological treatment processes can happen either biologically or nonbiologically. The biological removal of organic compounds is achieved by aerobic or anaerobic biodegradation, also known as biotic loss. Nonbiological removal of organics (or abiotic loss), which includes adsorption and volatilization, may be even more important than biodegradation for some toxic and recalcitrant constituents. In the adsorption process, compounds adsorb to mixed liquor suspended solids (MLSS) in the bioreactor and will be discharged subsequently from the system along with the wasted sludge. Volatilization happens when organics are emitted to the surrounding atmosphere due to their high volatility. An organic compound can be removed by one or several of above mentioned mechanisms. As biodegradation occur, the organics can be degraded either in one of three main types of pathways; the organic compound can be oxidized as growth substrate, or it may be presented as electron acceptor and will be reduced. In the other case, the target compound does not incorporate in microbial metabolism, and it will be degraded through cometabolism, in which a nonspecific enzyme involves changing the structure of the compound. For toxic and recalcitrant organic materials, since complete biodegradation may not be possible, biotransformation to another organic compound with different a nature occurs. Although an innocuous end-product may be produced, it is possible that a constituent, which is equally or even more harmful than the original compound, is also produced.

As organic matters present in water and wastewater are comprised of a number of undistinguishable organic constituents with analogous characteristics, the determination of parameters indicating the total organic content of water and wastewater is of great necessity. Biochemical oxygen demand (BOD), chemical oxygen demand (COD), and total organic carbon (TOC) are principal parameters used for quantifying aggregate organic matter. However, some analyses are also specified for the purpose of measuring individual organic compounds. Laboratory testing methods, which contribute to measuring BOD, COD, and TOC content of water and wastewater, can determine gross concentrations of organic matter greater than 1.0 mg/l. Gas chromatography and mass spectroscopy, which have improved significantly in recent decades, can be used for quantifying trace organics within the limits of 10^{-12} – 10^0 mg l⁻¹. The dissolved oxygen (DO) required by microorganisms for biochemical conversion of organic material is referred to as biochemical oxygen demand (BOD), commonly reported as 5-day BOD (BOD_5). Despite a plethora of limitations that the BOD test endures, it is extensively used for designing wastewater plants; The BOD test can

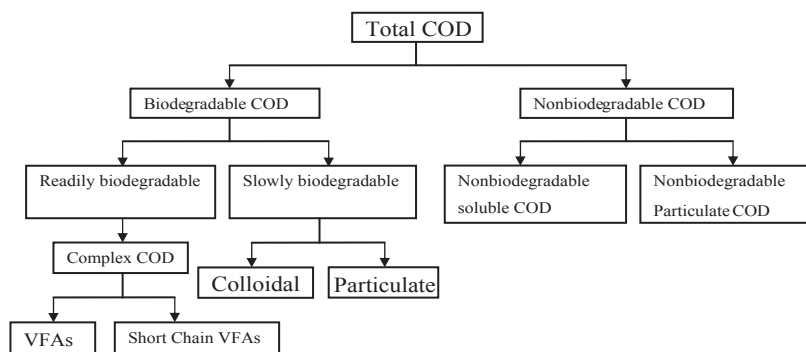


FIGURE 19.4 Various forms of COD in the wastewater.

evaluate efficiency of treatment processes, control effluent quality according to discharge limit permits, and quantify dissolved oxygen needed for biochemical oxidation of the organics. When ammonia is present in the wastewater, it can be oxidized to nitrite and further to nitrate. A large oxygen demand is required for the oxidation of ammonia to nitrate, which is also known as nitrogenous biochemical oxygen demand (NBOD); it can interfere in BOD associated with the decomposition of organic matter. Therefore, the nitrification reactions are suppressed in the BOD test by either adding chemicals or eradicating the nitrifying organisms, resulting in determination of carbonaceous BOD (CBOD). However, the CBOD test is only applicable to samples with low organic contents. In the case of applying the CBOD test to a sample withdrawn from an untreated wastewater containing high amounts of organic material, intensive error up to 20% may occur in the BOD value measurement. In the COD test, dichromate is utilized as reagent in acid solution in order to chemically oxidize the organic material present in the sample; equivalent oxygen for this purpose is known as COD. In compare to the BOD test, the COD measurement is preferred due to its completion within a shorter time (i.e., 2.5 h) rather than that of the BOD test (5 days or more). COD can be found in various forms in the wastewater (Fig. 19.4). Since there are various types of organic compounds present in domestic and industrial wastewaters, either biodegradable soluble chemical oxygen demand (bsCOD) or biochemical oxygen demand (BOD) is used as an index for determining the organic content.

19.7 AEROBIC BIOOXIDATION

Aerobic processes have been employed to reduce discharge of pollution into the water bodies. Pollution is not only identified as toxic and recalcitrant materials that adversely affect the health condition of living beings, but is also known as high concentrations of organics, discharged into water bodies from municipal and industrial sources. The degradation of organic compounds in receiving water causes the dissolved oxygen (DO) concentration to drop, possibly below the required quantity for aquatic life. In addition, the presence of suspended and nonsettleable colloidal solids can harm the limpidity of receiving water bodies. Regarding health concerns, the level of pathogens in water bodies, specifically originating

from domestic sewage, should be controlled as well. Toxic and recalcitrant organic materials are removable by suitable strategy as some of these materials are susceptible to aerobic biodegradation. Hence, an efficient biological treatment plant has to be designed to generate acceptable effluent, considering the different nature of constituents and compounds present in the wastewater.

Biological treatment process, termed as secondary treatment that is commonly preceded by a primary settlement, involve the removal of BOD. BOD removal occurs in a number of suspended and attached growth aeration treatment processes; the latter is also known as a fixed-film process. The most common technology associated with secondary treatment in municipal treatment plant is activated sludge unit operation. The U. S. EPA has regulated secondary treatment standards based on data obtained from publicly owned treatment works (POTWs) in practice (see Table 19.4). In those POTWs, a biological treatment concomitant with a physical operation contributed to the removal of biodegradable organic constituents and suspended and colloidal solids. Trickling filters and stabilization ponds are of those biological treatment processes that can also be employed as the principal process in certain facilities. However, these processes are not capable of consistently satisfying the regulated standards, even though a noteworthy decrease in BOD₅ and TSS occurs by these two processes. So, an alternate set of standards, called equivalent to secondary treatment standards, allows higher BOD₅, TSS, and CBOD₅ concentrations in the effluent of secondary treatment.

Microorganisms responsible for the aerobic oxidation of organic matters require sufficient contact time with the target wastewater; the contact time between the wastewater and the organisms is defined by sludge retention time (SRT). For achieving the most efficient

TABLE 19.4 Secondary treatment standards regulated and published by the U.S. EPA (Released in September 2010)^a

Effluent parameter	Unit	Average 30-day concentration	Average 7-day concentration
BOD ₅	mg l ⁻¹	30 (45 ^c)	45 (65 ^c)
TSS (total suspended solids)	mg l ⁻¹	30 (45 ^c)	45 (65 ^c)
pH (hydrogen ion concentration)	pH unit	Always within the limits of 6.0 – 9.0 ^b	
CBOD ₅ ^d	mg l ⁻¹	25 (40 ^c)	40 (60 ^c)
BOD ₅ and TSS removal (based on concentration)	%	≤85 (≤65 ^c)	—

^aFor the effluents of stabilization ponds and trickling filter, higher standard permit limits of 45 mg l⁻¹ and 65 mg l⁻¹ for 30-day and 7-day average are allowed, respectively. However, the quality of the receiving water body should not adversely be affected as a result of increased standards.

^bThe specified range should be carefully observed if the effluent pH is affected by industrial wastewater or supplementation of in-plant inorganic chemicals.

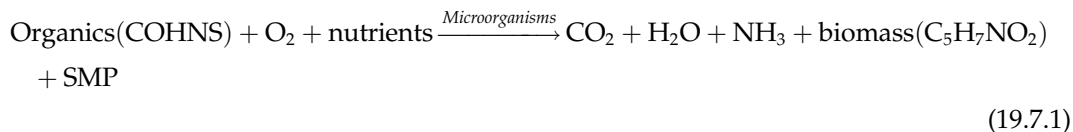
^cAlternate regulation, known as equivalent to secondary treatment standards, when trickling filter or stabilization pond, is employed in the secondary treatment stage.

^dIn the case of nitrification occurrence in a treatment process, BOD₅ cannot reliably represent the oxygen demand of the effluent. Carbonaceous BOD₅ (CBOD₅) permit limits can be set in lieu of BOD₅ for correctly indicating the effluent characteristics.

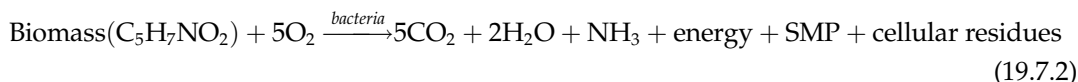
treatment, environmental factors should be in a favorable condition. Neutral pH is the best value for the removal of carbonaceous BOD; however, variation of pH between 6.0 and 9.0 can satisfactorily be tolerated by aerobic heterotrophs. Enough amounts of oxygen and nutrients should be available for the biochemical activity of the organisms. The preferable concentration of dissolved oxygen (DO) in a bioreactor is 2.0 mg l^{-1} ; however, the biodegradation rate shows slight changes in DO greater than 0.5 mg l^{-1} . While domestic sewage is rich in nutrients, i.e., N and P, industrial wastewaters may inherently encounter a shortage of nutrients. Therefore, adequate supplementation of N and P sources to industrial wastewaters should be considered in order to meet nutrient requirements for bsCOD treatment. Toxic compounds can partly or completely frustrate the microbial activity; the magnitude of the toxicity effect on aerobic autotrophs (ammonia-oxidizing bacteria) and methanogens is higher than the effect on heterotrophics bacteria. Different microorganisms can develop both in aerobic-suspended and attached-growth treatment processes, and thus contribute to the removal of organic matter. The mixed bacterial culture mainly consists of aerobic bacteria, and the remainder include protozoan, fungi, rotifers, nematodes, flatworms, and annelid worms.¹ By producing extracellular biopolymers, aerobic heterotrophic bacteria can be attached, and biological flocs or biofilm are formed in suspended or attached growth processes, respectively. The formation of biological flocs leads to improvement in the settling characteristics of microorganisms. So removal of free bacteria and suspended solids from treated liquid by gravity settling is feasible. The presence of protozoa is vital to aerobic biological treatment processes as they can be assumed as potential indicators of sound performance of the process; Long SRT and a DO concentration over 1.0 mg l^{-1} and devoid of toxicity effect are necessary for their stable activity. Protozoa contribute to effluent clarification as they uptake and consume free bacteria and colloidal particulate matters. The development of nuisance organisms under a specific loading rate and environmental condition leads to some problems in aerobic systems; two of which are bulking sludge and foaming that occur in activated sludge processes. Poor settling characteristics of biological flocs are responsible for bulking sludge, in which flocs are not favorably settled under gravity force. Hence, a considerable content of suspended solids in the effluent indicates poor operation of the treatment process. The development of foam on the surface of the activated sludge liquid is correlated by the presence of two bacteria genera: *Nocardia* and *Microthrix*; attachment of their hydrophobic surfaces to air bubble surfaces results in concentrated foam on the liquid in the activated sludge tank.

During aerobic biological oxidation, organic material is either oxidized or assimilated. More than half of organics are oxidized, providing requisite energy for metabolic activity of the bacterial community. The assimilation of the remainder of organic matter leads to the production of new cell tissues that may further be oxidized during autooxidation. The two following equations depict stoichiometry of aerobic biooxidation:

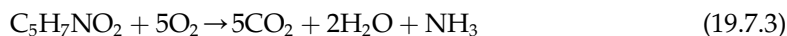
Oxidation and cell synthesis:



Endogenous respiration:



In Eqn (19.7.1), organic matter and oxygen serve as the electron donor and electron acceptor, respectively. The expression COHNS can substitute for organic matter, and SMP stands for a soluble microbial product that is defined as a nonbiodegradable fraction of organic matter appearing in the effluent as TOC or COD. $\text{C}_5\text{H}_7\text{NO}_2$ is the formula that demonstrates cell mass composition. In Eqn (19.7.1), biomass provides the redox reaction with the electron, while oxygen still plays the role of the electron acceptor. According to Eqn (19.7.2), 1 mol of $\text{C}_5\text{H}_7\text{NO}_2$ requires 5 mol of oxygen to be oxidized completely. Equivalent UBOD or COD of the cells is equal to 1.42 times the concentration of biomass in term of VSS.



Molecular weight of the cells = 113 g mol^{-1} , mw of $\text{O}_2 = 5 \times 32 \text{ g mol}^{-1}$

$\text{COD} = \frac{5 \times 32}{113} = 1.42 \text{ g O}_2/\text{g VSS}$; for complete oxidation of each unit mass organic compound, 1.42 units mass of oxygen is required. The determination of reaction rates, oxygen and nutrient requirements, and the amount of produced sludge are of primary concern for the design and operation of treatment plants. K and K' are rate coefficients, describing the biodegradability of organic matter and cell mass in the wastewater, respectively. In Eqn (19.7.1), the stoichiometric coefficient describes the fraction of organic matter that is biologically oxidizable to end products for generating energy. In fact, the stoichiometry can contribute to determining equivalent COD of biodegradable organic matter. The stoichiometric coefficient of the fraction of organics is oxidized, resulting in the synthesis of new cells. The sum of organics oxidized in order to produce energy and synthesize a new cell is approximately equal to the organics concentration in the influent while SMP is disregarded.

Total COD \sim COD oxidized for energy + COD oxidized for synthesizing new cell.

$$1 \sim a_1\text{COD} + a_2\text{COD} \quad (19.7.4)$$

For expressing biomass in term of VSS, COD of biomass that is equal to 1.42 g of O_2 per g of VSS should be substituted in Eqn (19.7.1):

$$1 \sim a_1\text{COD} + 1.42a_2\text{VSS} \quad (19.7.5)$$

19.8 ANAEROBIC DIGESTION

In the course of anaerobic digestion, the bioconversion of organic matters resulted in the production of methane and carbon dioxide. For the analysis of gas, GC is an analytical tool to define biogas composition. In its early stage, the anaerobic process would deliver hydrogen as a result of the hydrolysis of organic compounds occurring in the primary stage. This stage can be expanded by controlling the process parameters. A microbial fuel cell using wastewater as substrate is partially achieved for the primary treatment. In fact, seven clear

stages are identified in the entire biogas process as hydrolysis proceeds; specific bacteria or hydrogen reformers are discussed. As the pH of the culture dropped by acid forms, the concentration of organic acids gradually increases. Control of the pH and having defined ratio of C/N can assist the process by preceding methanogenic bacteria to lead the microbial pathway to methane formation. All biochemical reactions are catalyzed by a mix consortium of anaerobic bacteria that are fixed in a packed bed and fluidized biogranular hybrid systems. An investigation of the rate equation can help us to project microbial mass production rate, such as the Gompertz rate model, that is similar to the Logistic equation. Even the Monod rate equation can project the same expression with different assumptions. The material balance in early stage with the control of process parameter can achieve high hydrogen production; however, hydrogen generation in the anaerobic process is not a sustainable process since it would go through a pathway for bioconversion of an end product such as methane.

Anaerobic processes are advantageous over aerobic treatment methods due to reasons that are economically valued. Those reasons include low energy, reactor volume, footprint requirements, low biomass yield, and energy production in the form of biogas, which mostly consists of methane. Its application for treating high-strength and concentrated industrial wastewater has shown to be very cost-effective in comparison to aerobic processes because of the reduction in reactor volume and nutrient and energy requirement. Waste sludge and high-strength organic wastes primarily go under treatment in the anaerobic fermentation and oxidation processes. However, the recent treatment of dilute waste stream under anaerobic condition has been extensively reported. Since its effluent is not as high-quality as that of aerobic systems, it is the best anaerobic treatment that can be used along with aerobic processes; the application as a pretreatment step before discharging the wastewater into a municipal collection system or prior to an aerobic process is preferred.¹ Due to the high potential in killing pathogens, thermophilic anaerobic digestion operating in the temperature range of 50–70 °C has been of great interest alone or before mesophilic fermentation. One emerging process is temperature-phased anaerobic digestion (TPAD), which applies a short (2 days) 50–70 °C pretreatment step prior to 35 °C digestion in the main stage with sludge SRT of 10–20 days.^{11,12}

Organic matter is decomposed in the anaerobic process by going through three fundamental phases, i.e., hydrolysis, fermentation, and methanogenesis. In the case of the sound performance of the anaerobic process, the principal end products are methane and carbon dioxide. Figure 19.5 depicts the conversion flow of organic material to methane and carbon dioxide in the anaerobic process. In the hydrolysis phase, complex organic matter such as lipids and polymers are hydrolyzed and converted to simple organic matters or monomers. The conversion of particulate matter to soluble substances occurs in this phase. The end-products of this phase are accessible responsible for fermentation. In next step, i.e., fermentation is the phase in which acids and simple carbohydrates are decomposed and hydrogen, CO₂, and simple organic acids such as acetate, propionate, and butyrate are produced. This phase will continue until propionate and butyrate are also further converted to hydrogen and acetate. The principal products of fermentation process are H₂, CO₂, and acetate which are major substrates for methane formation.

Organic matter presenting as both an electron donor and electron acceptor causes this phase to be referred to as the fermentation phase. It is also termed as acidogenesis because of the production of simple organic acids in this phase. Depending on the nature of the

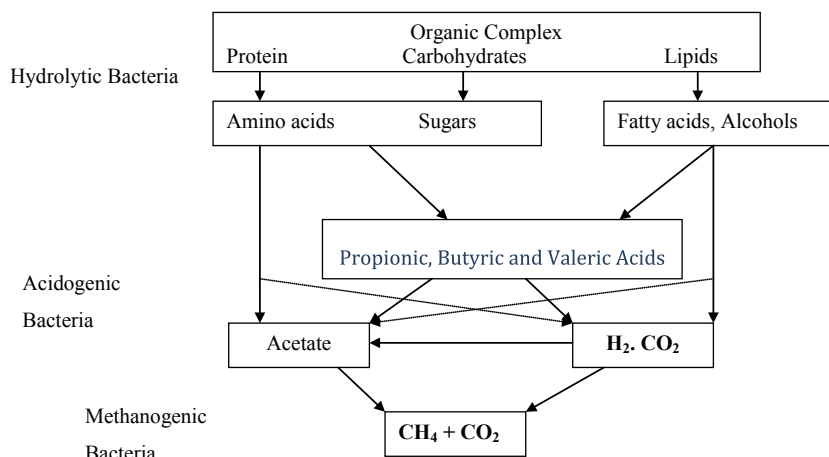


FIGURE 19.5 Biodegradation of organic matter in anaerobic process for biogas production.

organic waste, the anaerobic process may initiate from either hydrolysis or fermentation. Bacteria that perform hydrolysis and fermentation are of both facultative and obligate anaerobic groups. For instance, fermentation is the initial step for some industrial wastewaters. In the last phase, known as methanogenesis, a number of microorganisms are involved contribute to methane formation. Methanogens can be categorized into three groups: aceticlastic methanogens, hydrogen-utilizing methanogens, and acetogens; each group is in charge of specific reactions. As acetate is cleaved by aceticlastic methanogens, methane and CO_2 are formed from its methyl group and carboxyl group, respectively. Hydrogen-utilizing methane-formers oxidize hydrogen while CO_2 is reduced so as methane is produced. The third group, namely acetogens, uses CO_2 as an electron acceptor and H_2 as an electron donor to form acetate, which is further converted to methane. Methane-former organisms, classified as archaea, are of strict obligate anaerobes. The development of sulfate-reducing bacteria in anaerobic processes can be as troublesome as sulfide, which is toxic to methanogens that will be produced; the sulfides threshold concentration for biological treatment processes is 200 mg l^{-1} .² These organisms can reduce sulfate to sulfide, while they are classified into two groups, considering their electron donors. One group is capable of oxidizing a wide variety of organic materials to acetate when sulfate is reduced to sulfide. The second group consists of organisms that can consume fatty acids, especially acetate, in order to produce CO_2 alongside reducing sulfate to sulfide. To prevent sulfide toxicity, a controlled addition of iron instance in the form of ferrous or ferric chloride to the wastewaters containing sulfate is recommended since sulfate and iron react and thus, precipitate as iron sulfate.

The methanogens and acidogens establish a relationship based on mutual benefit, which is referred to as interspecies hydrogen transfer; as acidogens provide methanogens with substrates to utilize and survive, methanogens consume fermentation end products such as hydrogen, formate, and acetate to produce methane and CO_2 . With hydrogen consumption, its partial pressure will be kept extremely low. Therefore, the production of fermentation intermediate products (e.g., propionate and butyrate) decreases, and the fermentation reaction

equilibrium inclines to the formation of methanogenic substrates (i.e., acetate and formate). A disturbance in the process with adverse effect on methanogens activity causes a reduction in hydrogen uptake, leading to volatile fatty acids (VFAs) accumulation. As a result, the rate of the fermentation reaction will be decreased and a drop in the pH value likely may occur.

Since colloidal and particulate matters are converted to soluble compounds in the hydrolysis phase, the reaction rate of this phase determines the total quantity of the solid decomposed. However, it is the soluble substrate degradation kinetics that specifies the stability of the anaerobic process. The anaerobic process shows stable performance when VFAs concentration reduces as much to reach a possible minimum level. Due to the lower yield coefficient of methanogenic microbial community in comparison to acidogenic bacteria, the methanogens population should be available in sufficient number for guaranteeing the least VFAs content. Low yield and endogenous decay coefficients of methanogens, which are summarized in Table 19.5 are due to the low energy efficiency of the reactions they perform. Since the rate-limiting step in the anaerobic process is the methanogenesis phase, sludge retention time (SRT) of the anaerobic treatment is defined with the interval required for completing methanogenesis growth kinetics. The SRT requirement for methanogenesis stage in different temperatures is shown in Table 19.6; in which SRT for a practical suspended growth process is designated with safety factor (SF) of five. In the two initial phases, namely hydrolysis and fermentation, COD loss is not considerable because organic compounds have gone under chemical conversion only. Comparatively, significant removal in COD concentration happens in methanogenesis owing to organics conversion to methane and CO₂. Since no oxygen consumption occurs in anaerobic processes, COD removal can be demonstrated in term of the methane produced.

Anaerobic reaction is more sensitive to environmental factors such as pH and toxicity rather than the aerobic system. The optimal pH for anaerobic process is about neutral, which should be guaranteed with the supplementation of alkalinity. The pH values lower than 6.8 are lethal to methangens. Alkalinity addition is necessary because of the formation of high

TABLE 19.5 Typical yield and endogenous decay coefficients of methanogenic and acidogenic bacteria

Microbial group	Yield coefficient (gVSS/g COD)	Endogenous decay coefficient (gVSS/gVSS.d)
Acidogens	0.10	0.04
Methanogens	0.04	0.02

TABLE 19.6 SRT Requirement for completion methanogenesis phase and for suspended growth process

Temperature (°C)	SRT for methanogenesis phase (d)	SRT for suspended growth process with SF* = 5
20	7.8	40
25	5.9	30
30	3.2	15

* Safety factor.

amounts of CO_2 that constitute 30–35% of produced gases. The alkalinity requirement for anaerobic process varies, typically in the range of 3000–5000 mg l^{-1} as CaCO_3 .

In summary of anaerobic digestion, there are seven stages of microbial consortia; they are active for deposition of organic matters. At first, hydrolysis of organic complex may take place; then next stage would be the fermentation of sugars and organic acids, which would be the most possible fermentative activities of microbial agents. Anaerobic oxidation of long chain fatty acids and alcohols are the middle stage of digestion. Anaerobic oxidation of intermediate products is for the completion of the process. Acidogenic bacteria are active for acetate production from CO_2 and H_2 . For end products to be converted, bioconversion of acetate to methane occurs. Finally, methane production will be accomplished by the reminder of CO_2 and H_2 .

19.9 ABIOTIC LOSSES

In biological treatment processes, nonbiological removal or, in other words, abiotic losses including adsorption on biomass and volatilization, can occur alongside biodegradation.

19.9.1 Adsorption

Adsorption or partitioning of nonbiodegradable organic compounds onto mixed liquor suspended solids (MLSS) has been observed; however, adsorption cannot be accounted as the principal removal mechanism for the most organics. For instance, very low specific removal efficiencies have been reported for toluene (0.02%), ethylbenzene (0.19%), trichloroethane (0.83%), chloroform (1.19%), and carbon tetrachloride (1.38%) [1]. Slight specific removal efficiencies indicate that inconsiderable removal of compounds happens through adsorption compared with total treatment achieved. Some exceptions such as Lindane and other pesticides, nevertheless, demonstrate that although organics removal may not be able to be removed by biodegradation, significant adsorption can be detected. For toxic and recalcitrant materials, partitioning onto microbial cells is of great importance in comparison to biodegradation and volatilization.

Solids partitioning can be described by a general linear equilibrium relationship that is a modification of the Freundlich Isotherm model. It is applicable to the adsorption process with relatively low concentrations of organics in the liquid phase:

$$q = K_{sw}S \quad (19.9.1.1)$$

where q represents the ratio of quantity of organic absorbed (g) per absorbent mass (g), K_{sw} is partition coefficient that demonstrate the ratio of organic compound adsorbed in proportion to its liquid concentration $[(\text{g/g})/(\text{g l}^{-1})]$, and S is concentration of organic compound in solution (g l^{-1}).

Due to the relatively fast adsorption of organics in biological treatment processes, [Eqn 19.9.1.1](#) can be used for distinguishing the organics concentration in the liquid and solid phase. The hydrophobic nature of a target compound and solid adsorption characteristics is defining the magnitude of partition coefficient K_{sw} . Relatively large values of K_{sw} have been observed for the solids with high carbon content and high surface area. The K_{sw} values

can be defined as a function of the octanol–water partition coefficient of the organic compound as following:

$$K_{sw} = kK_{ow}^n \quad (19.9.1.2)$$

where K_{ow} is octanol/water partition coefficient in terms of $(\text{mg l}^{-1})_o/(\text{mg l}^{-1})_w$, k and n are the factors that vary between 1.38×10^{-5} and 4.3×10^{-7} (k) and 0.58 and 1.0 (n). Dobbes and coworkers¹³ proposed an equation to determining K_{sw} of biological solids in wastewater treatment processes:

$$\log K_{sw} = 0.58 \log K_{ow} + 1.14 \quad (19.9.1.3)$$

The octanol/water coefficient values for different organic compounds can be developed by measuring the concentration of the compound in the octanol/water two-layered mixture with octanol on top of the water layer. The organics with large K_{sw} value have been observed to be available in the octanol layer in high concentrations, resulting in high K_{ow} , which implies hydrophobicity.

For quantifying the amount of organic compound removed by sludge wasting, the ratio q in Eqn 19.9.1.1 can be written as the ratio of organic compound absorption rate onto the rate of sludge wasting:

$$q = \frac{r_{ad}}{r_{X,w}} \quad (19.9.1.4)$$

where r_{ad} and $r_{X,w}$ are daily rate of organics adsorbed onto solids (g d^{-1}) and solid wasted, respectively.

For an activated-sludge process under a steady-state condition, the quantity of sludge wasted per day can be estimated by the following equation:

$$r_{X,w} = \frac{X_T V}{\theta_c} \quad (19.9.1.5)$$

where X_T is mixed liquor suspended solids, MLSS (g l^{-1}); V is the volume of activated-sludge tank (l); and θ_c is sludge retention time, SRT (d).

Substituting Eqn 19.9.1.1 and 19.9.1.5 in Eqn 19.9.1.4, the rate of organic compound adsorbed per day can be expressed by the following equation:

$$r_{ad} = -\frac{X_T V K_{sw} S}{\theta_c} \quad (19.9.1.6)$$

Adsorption mechanism is important due to the transport and fate of organics, specifically toxic constituents, during subsequent sludge handling processes. Toxic compounds can disturb and possibly interrupt anaerobic reaction in the digester in which wasted sludge is processed. Toxicity of adsorbed compounds can also restrict land-disposal alternatives.

One of the principal methods of metal removal in biological treatment processes occurs through metal adsorption to and complexation with the microorganisms. Metal ions are adsorbed to negatively charged cell surfaces. In addition, metal complexation with carboxyl groups present in microbial polymers such as polysaccharides can happen as well. Moreover, metals can chemically be absorbed by protein-based materials available in the biomass. It is ascertained that Freundlich isotherm model can well describe metal removal in biological

treatment processes. A wide range of 50–9% for metal removal in biological processes has been observed; the exact removal efficiency is determined by several factors, including the initial concentration of target metal, the solids amount present in the bioreactor, and the sludge retention time (SRT).

19.10 VOLATILIZATION

Volatile organic compounds (VOCs) can be emitted to the surrounding atmosphere due to aeration. Air stripping can happen in various biological treatment processes such as trickling filter, aerated lagoon, and activated sludge. Depending on the particular VOC, air stripping and biodegradation may simultaneously contribute to its removal. Recently, the uncontrolled release of VOCs from wastewater collection and treatment facilities has been taken into consideration increasingly due to air pollution concerns.

The release of VOCs from the wastewater collection system and treatment plant is associated with two main mechanisms: volatilization and gas stripping. Volatilization indicates the partitioning of VOCs between the atmosphere and the wastewater. This procedure will continue until equilibrium concentration is achieved. It is the VOC concentration corresponding to in proportion to equilibrium concentration that controls the movement of a constituent, namely mass transfer, between two phases of gas and liquid. The greatest mass transfer can be observed when the VOC concentration in one of the two phases is far from the balanced concentration. Owing to the extremely low concentration of VOCs in the atmosphere, VOC's emission from wastewater to the surrounding atmosphere is the prevalent phenomenon. Furthermore, gas stripping of VOCs takes place when air is entered to the wastewater without force and intervention or introduced into it on purpose. VOCs' gas stripping is related to the variation of initial concentration in liquid phase and equilibrium concentration by mass transfer coefficient as given by Eqn 19.10.1:

$$r_{\text{VOC}} = -(K_L a)_{\text{VOC}}(C - C_s) \quad (19.10.1)$$

where r_{VOC} is rate of VOC volatilization and stripping ($\text{mg l}^{-1} \text{ d}^{-1}$); $(K_L a)_{\text{VOC}}$ represents the overall VOC mass transfer coefficient (d^{-1}); and C and C_s are the concentrations and saturation concentration of VOC in liquid (mg l^{-1}), respectively.

Several factors determine the percentage of VOC removed by stripping. Those factors include Henry's law constant; the biodegradation rate of the compound; the VOC's initial concentration; and the influent concentration of other organics, aeration methods, and power level in the aeration tank. For instance, benzene removal by stripping significantly varies when different aeration methods and various power intensities are adopted in the biological process. For wastewater with initial COD of 250 mg l^{-1} and influent benzene of 10 mg l^{-1} with diffused aerating system, percent of benzene stripping increases from three to 11 as the power level increase. Gas to liquid ratio governs the amount of VOC stripped when diffused oxygenation system is provided. As soon as bubbles of air are formed, mass transfer between gas and liquid phases initiates and continues until equilibrium condition. In most cases, slight gas injection volume result in the least amount of VOCs stripping. If surface aeration method is used, significant intensification in benzene stripping happens because of

infinite interface between the atmosphere and the wastewater. In this case, benzene removal by stripping increases to the range of 15–36% for the same power level. The components of the wastewater in question, particularly nonbiodegradable organics, affect the characteristics and the amount of biological sludge produced, and hence, the practical SRT can be changed. As a result, biodegradation share in VOC removal varies. When influent concentration of toluene increases from 0.1 to 40 mg l⁻¹, percent of toluene stripped in biological process with SRT of 3 days decreases from 17 to 15 percent. With further increase in influent toluene to 100 mg l⁻¹, toluene stripping reduces to the average amount of 14%. As the SRT is increased to 15 d with the initial toluene concentration of 40 mg l⁻¹, the amount of toluene stripped considerably diminishes to 5%.¹

To control VOCs stripping to the atmosphere, some strategies has been proposed, including source control in VOCs production, covering the various sections of the treatment facility, and eliminating the possibility of turbulence; it is proven that the release of VOCs at the points of turbulence is quite high in comparison to that of open surfaces. Providing cover on top of the treatment facilities necessitates the consideration of efficient off-gases treatment technologies. In addition, some problems are encountered in the case of supplying covering such as mechanical parts deterioration due to the corrosion and requirement of sufficient space for the entry of personnel for maintenance and repair purposes. Depending on the volume of gas to be treated plus the type of VOCs and their initial concentrations, disparate treatment techniques are suggested. Vapor-phased adsorption on carbon, macroreticular resin, or other VOC selective resins, thermal and catalytic incineration, combustion in a flare, boiler or process heater, and biofiltration are of the options for off-gas treatment. With increment in VOC inlet concentration, the order of off-gas treatment based on their efficiency in VOC removal is thermal incineration, catalytic incineration, carbon adsorption, and resin adsorption. For organics influent concentration of 20–90 ppmv, thermal and catalytic incinerations have shown a removal efficiency of 90–96%. As the VOCs concentration varies in the range of 5000–10,000 mg l⁻¹, resin adsorption depicts high capability in VOC control (i.e., 95–99% removal efficiency).¹

19.11 BIOLOGICAL NITRIFICATION AND DENITRIFICATION

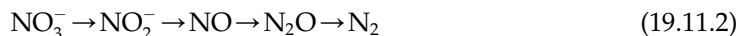
Biological nitrogen removal consists of two essential steps: nitrification and denitrification. The nitrification step involves ammonia (NH₄-N) oxidation to nitrite (NO₂-N), which is further oxidized to nitrate (NO₃-N) according to [Eqn 19.11.1](#). The denitrification process involves a series of reduction reactions for converting nitrate to nitrite to nitric oxide, nitrous oxide, and finally nitrogen gas (see [Eqn 19.11.2](#)). Nitrate reductive enzyme produced in a devoid or low concentration of DO helps in nitrate or nitrite reduction. The occurrence of the nitrification of all ammonia and organic nitrogen prior to denitrification is essential, because the product of the nitrification process (i.e., nitrate) is one of the fundamental components of denitrification reaction. So nitrification should be able to happen even in the worst condition, such as low temperature. Biological denitrification is a cost-effective alternative to costly ammonia stripping, chlorination, and ion exchange. Environmental concerns necessitate nitrogen removal for several reasons, including ammonia toxicity for fishes, ammonia effect on DO concentration in receiving water bodies, the possibility of eutrophication occurrence,

and water reuse applications, especially when effluents of wastewater treatment plants are used for recharging underground waters.

Nitrification reaction:



Denitrification reaction:



The nitrification process can be achieved in either a combined or separate system. Using a single-stage activated sludge process for conducting BOD removal and the nitrification process simultaneously is a common technique (Fig. 19.6a). However, when there is the possibility of toxicity and inhibition in the influent or high efficiency of nitrification is required, two sequential steps for BOD removal and nitrification are ideal. Figure 19.6b depicts a two-stage activated sludge process. In the two-stage activated sludge process, the first stage where BOD removal occurs is accomplished with short SRT, while the SRT of the following activated sludge system should be prolonged enough for the completion of nitrifying reactions. Long HRT and SRT required for the second stage indicate slow growth of nitrifying organisms compared to heterotrophic bacteria responsible for BOD removal. Optional bypassing of a fraction of influent wastewater to the second stage can be carried out for efficient flocculation and thus further clarification because of the low biomass yield of nitrifiers. Comparing these two systems, combined BOD and ammonia removal system is preferred due to less sensitivity to loadings fluctuations for a large aeration tank, lower production of wasting sludge, and better sludge settling characteristics. On the other hand, a separate nitrification system is more sensitive to loading fluctuations and a higher amount of sludge is produced that results in increased surplus sludge. In the attached growth process employed for nitrification, a large amount of influent BOD should be removed prior to the development and growth of nitrifying bacteria. Due to the difference in growth rates, heterotrophic bacteria that contribute to BOD removal populate in the top layers of the formed biofilm. Nitrifying organisms, in contrast, are established deep inside the fixed microbial film. Such an array of microbial growth can benefit live mass survival against potential toxicity and inhibition effects of substances present in the influent.

Nitrate removal, namely the denitrification process, occurs biologically in two approaches: assimilation and dissimilation, whereas in the latter, nitrate participates as the electron donor. Reduced nitrate to ammonia can be assimilated into biomass for synthesizing new cells when the cells do not access ammonia nitrogen ($\text{NH}_4\text{-N}$). In biological denitrification or dissimilating nitrate reduction, nitrate reduces to nitrogen gas where a variety of organic or inorganic compounds can be oxidized. On this basis, the activated-sludge denitrification process can be illustrated in two different flow arrangements, which are termed as preanoxic (substrate-driven) denitrification and postanoxic denitrification, shown in Fig. 19.6c and 19.6d, respectively. In preanoxic denitrification depicted in Fig. 19.6c, nitrate is reduced in a preceding anoxic zone, and nitrification occurs in a subsequent aeration tank. Organic compounds are the substrate of the denitrification process from which the name of substrate-driven denitrification has been derived, and nitrate produced in the aeration tank is returned to anoxic tank. Postanoxic denitrification is implemented so that BOD removal and nitrification are initially carried out, and then anoxic process for nitrate removal is implemented

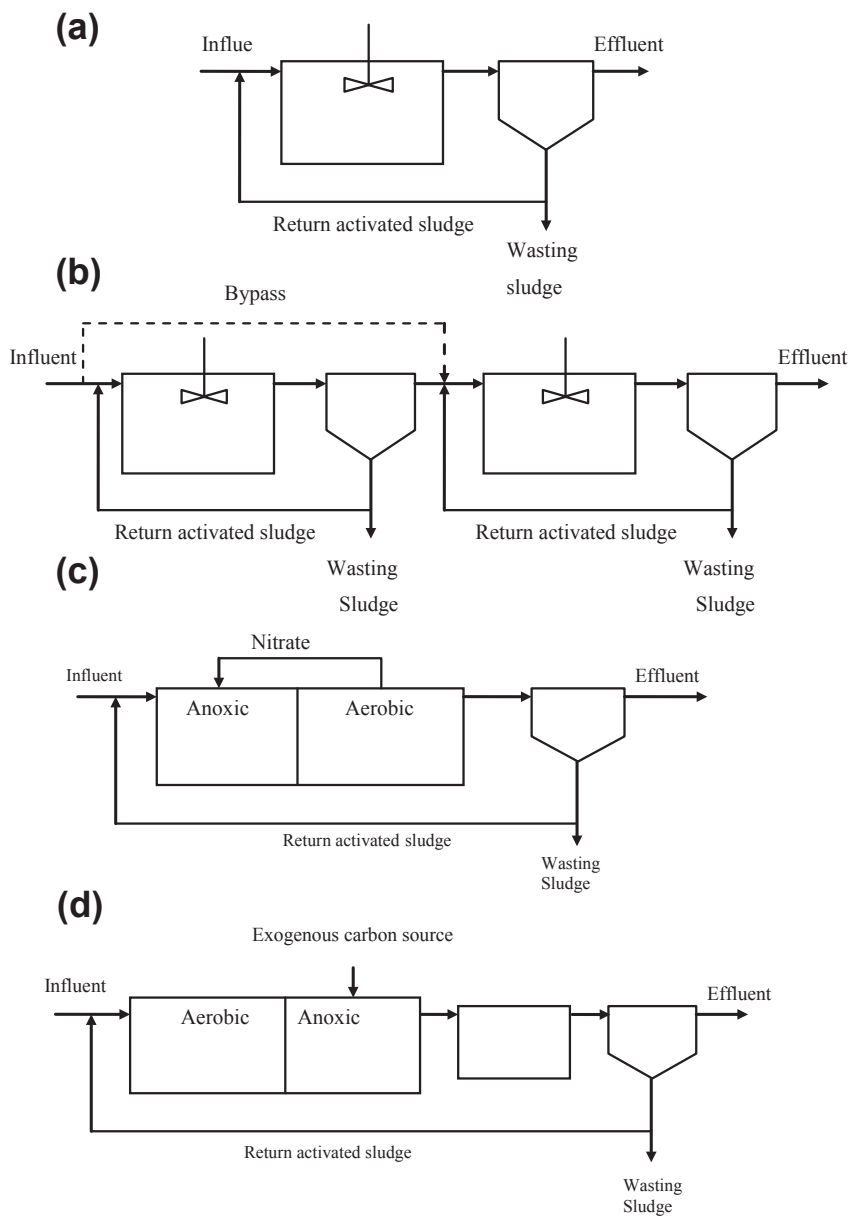
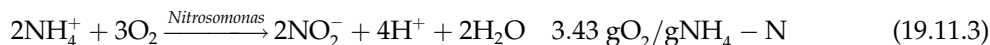


FIGURE 19.6 Process configuration for nitrification and denitrification: (a) single-stage activated-sludge nitrification system (b) two-stage activated-sludge nitrification system (a) preanoxic (substrate driven) denitrification (b) postanoxic (endogenous driven) denitrification.

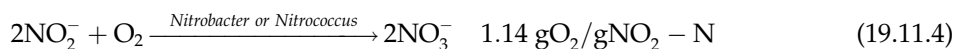
based on energy obtained from endogenous respiration. Owing to the low energy efficiency of endogenous respiration, postanoxic denitrification endures a slower reaction rate rather than preanoxic denitrification. To compensate for the slow reaction rate, an exogenous carbon source as methanol or acetate can be supplemented to the anoxic stage of the process.

The oxidation of the ammonia nitrogen in the nitrification process occurs through two energy-yielding steps:

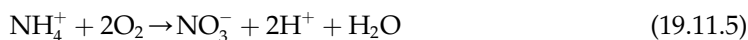
Ammonia nitrogen oxidation reaction:



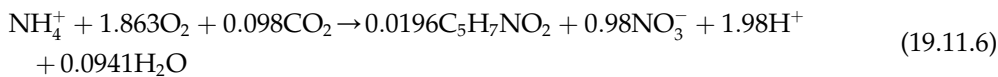
Nitrite nitrogen oxidation reaction:



The total ammonia oxidation to nitrate can be represented in a single equation stoichiometry as follows:



Considering the thermodynamics of biological reactions and free energy changes, ammonia oxidation can be illustrated as the following reaction with more accurate stoichiometric coefficients:



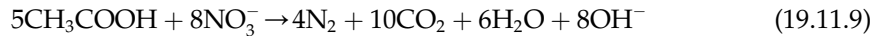
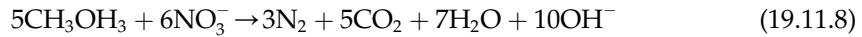
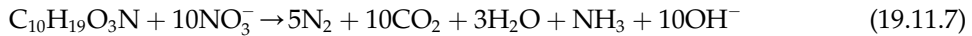
Nitrifying reaction requirements are summarized in Table 19.7. Based on the stoichiometry of biological nitrification, the oxygen demand for ammonia nitrogen ($\text{NH}_4\text{-N}$) oxidation to nitrate nitrogen ($\text{NO}_3\text{-N}$) is equal to 4.57 g of O_2 ; the amount of 3.43 g of required oxygen is assigned to nitrite production reaction (Eqn 19.11.3), and the remainder should be utilized for nitrite oxidation to nitrate (Eqn 19.11.4). According to Eqn 19.11.5, 4.25 g of DO is needed for the oxidation of 1 gram of ammonia to nitrate, and 7.07 g of alkalinity, as CaCO_3 should be supplemented for the compensating acidic effect of CO_2 produced. The difference between

TABLE 19.7 Oxygen and alkalinity requirements for nitrification process

Reaction requirement		Calculated stoichiometrically	Calculated bioenergetically ($f_s = 0.05$)	Actual amounts, obtained experimentally
Oxygen Demand (g O_2 /g N)	$\text{NH}_4 \rightarrow \text{NO}_2$	4.57	4.25	4.33
	$\text{NO}_2 \rightarrow \text{NO}_3$	4.34	—	3.22
	Total oxidation: $\text{NH}_4 \rightarrow \text{NO}_3$	1.14	—	1.11
Alkalinity (g as CaCO_3)		7.14	7.07	—

the values calculated by basic stoichiometry and thermodynamic principals of the reaction is related to not considering ammonia for synthesizing new cells in Eqn 19.11.5. Furthermore, the coefficients of Eqn 19.11.6 are achieved with the assumption of $f_s = 0.05$; the parameter f_s stands for the ratio of electron (e^-) moles of substrate used for cell synthesis to the electron (e^-) moles of the total substrate used, according to the thermodynamic concept of biological processes. In the design of biological nitrification processes, influent BOD and nitrogen concentrations, oxygen and alkalinity requirements, temperature, and the effect of inlet toxic substances should carefully be considered. Sources of carbon and phosphorus, along with trace elements (i.e., Ca, Cu, Mg, Mo, Ni, Zn) are required for nitrifying cell growth. Carbon in form of CO_2 can be obtained from the surrounding atmosphere, which will be sufficient with the consideration of the low reaction rate.

For the biological denitrification process, nitrate or nitrite serves as the electron acceptor, while a number of organic compounds can participate in this reaction as the electron donor. The typical electron donor depends on the configuration of the denitrification process. In pre-anoxic denitrification, the bsCOD or BOD of the influent wastewater is oxidized for the purpose of nitrite reduction. The bsCOD produced during endogenous respiration, which is commonly supplemented with exogenous carbon source like methanol, serves as the electron donor in postanoxic denitrification. Stoichiometry of biological denitrification can be observed in the following reactions where BOD of wastewater, methanol, and acetate are selected as electron donors, respectively. The term $C_{10}H_{19}O_3N$, as proposed by the U. S. EPA, is representative of the initial BOD of the wastewater in question.



Considering the above stoichiometry equations, it is observed that almost half of alkalinity consumed in the nitrification process (i.e., 7.14 g alkalinity as $CaCO_3$) is recovered in the denitrification process. The amount of 3.57 g of alkalinity as $CaCO_3$ is produced per each gram of nitrate reduced. The production of alkalinity in the denitrification process, hence, should be considered in the design of the biological nitrogen removal processes. The oxygen equivalents of nitrate and nitrite, which are useful parameters in estimating the total oxygen demand for designing an appropriate nitrification–denitrification process, are equal to 2.86 g O_2 /g NO_3-N and 1.71 g O_2 /g NO_2-N , respectively.

A sufficient amount of bsCOD or BOD should carefully be determined so that an adequate electron donor will be available in the nitrate removal reaction. Similar to aerobic oxidation where oxygen demand is related to biomass yield, the same concept can be applied to the denitrification process for estimating requisite bsCOD or BOD. On this basis, the following expression can be developed for calculating the required bsCOD per reduced nitrate nitrogen. Owing to long SRT needed for the completion of the denitrification reaction, the proposed expression is also applicable to the aerobic removal of bsCOD in particulate and colloidal forms:

$$g \text{ bsCOD}/g \text{ NO}_3 - N = \frac{2.86}{1 - 1.42Y_n} \quad (19.11.10)$$

TABLE 19.8 Microbiology of nitrification and denitrification process alongside the reactions' components

Name of reaction	Nitrification	Denitrification (anoxic reaction)
Type of organisms	Aerobic autotrophic	Facultative heterotrophic and autotrophic denitrifying bacteria Facultative heterotrophic and autotrophic nitrifying bacteria Anaerobic autotrophic nitrifying bacteria (Anammox process)
Bacteria genera	Nitrosomonas Nitrobacter, Nitrococcus	<i>Pseudomonas</i> (heterotrophic denitrifier) <i>Paracoccus pantotropha</i> (heterotrophic nitrifier) <i>Nitrosomonas europaea</i> (autotrophic nitrifier)
Carbon source	CO ₂	Organic materials
Electron donor	NH ₄ ⁺ , NO ₃ ⁻	Organic materials
Electron acceptor	O ₂	NO ₂ ⁻ , NO ₃ ⁻
Products	NO ₂ ⁻ , NO ₃ ⁻	N ₂ , CO ₂ , H ₂ O

The microbiology of the nitrification–denitrification processes is summarized in Table 19.8. Strict aerobic autotrophic bacteria from the domains of *Nitroso*- and *Nitro*-bacteria are capable of accomplishing nitrification. The most prevailing genera are *Nitrosomonas*, *Nitrobacter*, and *Nitrococcus*. The denitrification process is commonly accomplished by facultative heterotrophic or autotrophic bacteria. The most commonly found genera of heterotrophic denitrifying bacteria is *Pseudomonas*, which is capable of oxidizing a wide range of organic compounds such as hydrogen, methanol, carbohydrates, organic acids, alcohols, benzoates, and other aromatic compounds. Autotrophic denitrifying bacteria use hydrogen and reduced sulfur compounds as electron donors. On the other hand, heterotrophic and autotrophic nitrifying bacteria can also complete the nitrate reduction reaction under aerobic condition. A novel heterotrophic nitrifying bacterium capable of nitrate removal under anaerobic condition is also identified in mid-1990s. This organism conducts a process termed Anammox which stands for anaerobic ammonium oxidation. Anammox process involves oxidation of NH₄⁺ and reduction of NO₂⁻ with no need to carbon source, accomplishing simultaneous nitrification and denitrification. Denitrification rate in Anammox process under anaerobic condition has been found to be much faster (about six–10 times) than that of the reaction carried out by autotrophic denitrifying *N. europaea*.

In nitrification for temperatures lower than 28 °C, ammonia oxidation kinetics govern the nitrifying process, and hence, ammonia-oxidation saturation kinetics is the essence of the design procedure (see Eqn 19.11.11). As the temperature increases to values over 28 °C, the oxidation rate and kinetics of ammonia and nitrite should be accounted.

$$\mu_n = \left(\frac{\mu_{nm} N}{K_n + N} \right) - k_{dn} \quad (19.11.11)$$

where μ_n is specific growth rate of nitrifying organisms (g new biomass/g biomass.d), μ_{nm} represent maximum specific growth rate of nitrifying organisms (g new biomass/g biomass.d), N is nitrogen initial concentration (g l⁻¹ or mg l⁻¹), K_n is half-velocity coefficient where $\mu_n = \frac{\mu_{nm}}{2}$, and K_{dn} is endogenous respiration coefficient for nitrifying organisms

(g VSS/g VSS.d). The μ_{nm} value has been reported to be between 0.25 and 0.77 g VSS/g VSS.d at temperature of 20 °C. Due to the lower maximum specific growth rate of nitrifying organisms (μ_{nm}) compared with aerobic heterotrophic bacteria, long SRT is required for the nitrification process. Under a stable condition, the nitrite concentration in the activated-sludge nitrification process can decrease to under 0.10 mg l⁻¹, while the ammonia concentration varies from 0.50 to 1.0 mg l⁻¹. However, in the transient condition when the growth of nitrite-oxidizing bacteria is limited due to a shortage in the substrate concentration, the NO₂-N concentration of 5–20 mg l⁻¹ can be observed. The DO concentration of up to 3–4 mg l⁻¹ significantly affects the nitrification rate, while the increment in temperature enhances the reaction rate. A DO concentration below 0.5 mg l⁻¹ seriously frustrates the nitrification rate with a higher adverse effect on nitrite-oxidizing bacteria rather than the corresponding effect on the ammonia-oxidizing organism. This problem results in incomplete nitrification reaction, and thus, an accumulation of nitrite nitrogen (NO₂-N). In the denitrification process, microbial growth kinetics and substrate depletion are similar to those of aerobic biooxidation. Instead of oxygen, nitrate serves as the electron acceptor in the denitrifying reaction. For aerobic process, it is previously described that the soluble substrate concentration controls the soluble substrate utilization rate. The denitrifying rate is also dependent upon on initial nitrate concentration. For a determination of the substrate utilization rate, [Equations 19.11.12](#) can be modified to show the nitrate utilization rate in preanoxic denitrification. This modification should be accomplished to consider not the availability of solely denitrifying bacteria in the anoxic zone of the preanoxic denitrification process. The modification of the expression is carried out by multiplying the term η in [Eqn 19.11.12](#) as given in the following equation:

$$r_{su} = -\frac{kXS\eta}{K_s + S} \quad (19.11.12)$$

where η is the portion of denitrifying organisms in the biomass (g VSS/g VSS). Other parameters (i.e., k , X , S , K) are formerly described. Although the value of k in denitrification is much lower than that of the aerobic process, it is considered the same as that for aerobic oxidation; thus, the neglected effect on k is compensated by multiplying the term η in the expression for the substrate utilization rate. The value of η has been observed to be in the range of 0.2–0.8. The K_s value shows no difference with nitrate and oxygen as electron acceptors. In postanoxic denitrification, the microbial community exclusively consists of nitrate-reducing bacteria because influent BOD has been depleted significantly in the former aerobic zone. Therefore, consideration of the term η is not necessary anymore. Using methanol as an electron donor in the suspended-growth denitrification process, the requisite SRT is about 3°–6 d, which shows no variation with the SRT for aerobic systems.

Environmental conditions such as pH, toxicity, metals, and free ammonia (NH₃) concentration influence either nitrification or denitrification rates. The range of 7.5–8.0 is an optimum value for pH in nitrification process, which is practically maintained at 7.0 to 7.2. Due to the production of hydrogen ion in ammonia oxidation, the controlled addition of alkalinity in the form of soda, lime, soda ash, sodium bicarbonate, or magnesium hydroxide may be needed for balancing the pH. In contrast, the pH value is of less concern in denitrification owing to alkalinity produced in the nitrite reduction reaction. The variation of the pH value between 7.0 and 8.0 does not affect denitrification reaction rate; however, a decrease in the

pH value in the range of 6.0–7.0 results in a drastic reduction in the denitrification rate. Numerous organic and inorganic compounds such as phenolic compounds, benzene, amines, and proteins, and many other constituents show a toxic effect on the ammonia-oxidation reaction rate, whereas nitrifies can be identified as good indicators of availability of toxic organics, even at low concentrations in the wastewater. Metals like chromium, copper, and nickel, un-ionized or free ammonia (NH_3), and also un-ionized nitrous acid (HNO_2) inhibit the nitrification process.

19.12 BIOLOGICAL TREATMENT PROCESSES: SUSPENDED AND ATTACHED GROWTH

In this section, practical applications of various fundamental concepts that are discussed earlier are presented. As previously stated, biological treatment processes can be divided to suspended and attached growth systems, considering the method of growth and retention of organisms in the system. The principles of biological treatment can be generalized for the systems included in either group, but some distinctions will arise due to the difference in the microbial growth. Kinetics of these two major systems, design considerations, and biological processes are discussed in this section. The classification of various biological treatment processes into two main groups of suspended and attached growth systems are presented in Table 19.9. Attached growth treatment can occur naturally at lakes, river bottoms (sediments), and solids. Here, only engineered processes have been exemplified.

19.12.1 Kinetics of Suspended and Attached Growth Processes

Before discussing each biological process individually, modeling and kinetics of suspended growth and fixed-film processes are generally explained. In addition, design and operating parameters are introduced.

TABLE 19.9 Examples of suspended and attached growth biological processes

Suspended growth	Attached growth
Activated sludge processes	Trickling filter
Aerated lagoon	Rotating biological contactors (RBCs)
Waste stabilization pond	Submerged media beds
Aerobic sludge digester	(e.g., Downflow, upflow, and fluidized)
Anaerobic sludge digester	Wetlands
	Land treatment
	Infiltration processes

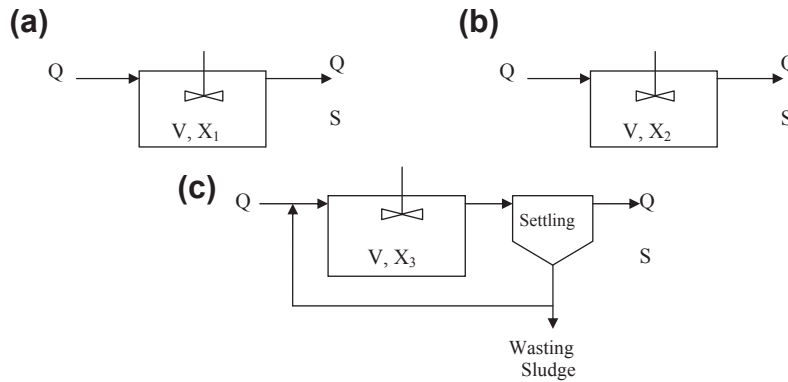


FIGURE 19.7 Different handling-solid approaches in suspended-growth wastewater treatment facility: (a) facultative system (b) flow-through without sludge recycling (c) flow-through with sludge recycling (V = volume, X = biomass concentration, S = substrate concentration).

19.12.2 Suspended Growth Processes

The handling of solids in suspended growth systems can be accomplished in three different methods as illustrated in Fig. 19.7. Power input level for keeping solids in suspension determines the type of handling solids, and thus, the type of system in use. With zero or low power input level, there is no control on solids in facultative systems, so the solids may either easily settle or discharge from the system along with the effluent. Flow-through systems without recycling have enough power input level to provide partial control of solids. Solids are maintained in suspension and fully leave the system in the effluent. In systems with recycling, the solids are completely controlled with a high power-input level. The solids are completely suspended in the bulk liquid and are not able to go out with the effluent. That fraction of solids, which should be returned to the system and the portion that it should be withdrawn from, are carefully determined. A settling unit operation helps to retain the solids in the system. In all three types discussed above, a steady state is eventually reached where solids produced and solids wasted are balanced, and no accumulation occurs. In facultative processes and flow-through systems without recycling, a steady-state condition naturally happens; in contrast, the determining factor for achieving the steady-state condition in systems with recycling is the amount of wasted sludge. Practical applications of the handling of solids types in wastewater treatment are shown in Table 19.10.

A flow-through system with sludge recycling is schematically considered as the model for the complete-mix activated-sludge process (see Fig. 19.8). To develop growth and substrate utilization kinetics, mass balance should be considered for each constituent in question (i.e., biomass and substrate) within the boundaries of a control volume.

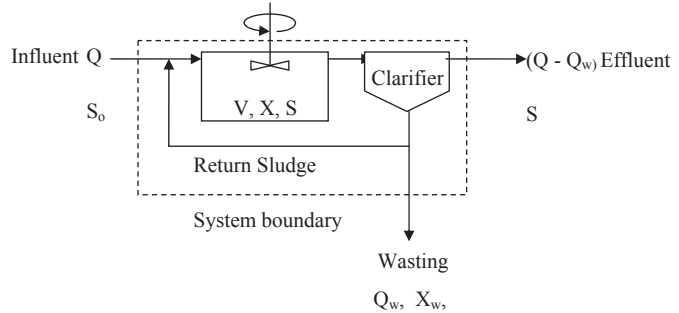
19.12.3 Sludge Retention Time (SRT)

Hydraulic retention time (HRT) shows the interval when wastewater is maintained in the system in order for being treated. For all three handling solids types, the hydraulic retention

TABLE 19.10 Practical applications of handling solids types in biological treatment processes

Facultative systems	Flow-through without recycling	Flow-through with recycling
Waste stabilization ponds	Sequence batch reactor (SBR)	Activated sludge processes
Facultative aerated lagoons	Fully aerobic, full-through lagoons	

FIGURE 19.8 Schematic flow diagram for activated-sludge process (V = volume, Q = flow rate, S = substrate concentration, X = biomass concentration).



time, t , can be determined by $t = V/Q$, where V represent the volume of the system (m^3) and Q is the influent flow-rate ($\text{m}^3 \text{d}^{-1}$).

The period for retaining biomass in the system is completely different from the system HRT. It is referred to as sludge retention time (SRT) or sludge age, and also known as mean cell residence time. Literally, the system SRT can be defined as total mass of solids in the system per total mass of solids lost per day.

$$\theta_c = \frac{\text{mass of solids in the system}}{\text{mass of solids lost daily}} \quad (19.12.3.1)$$

To mathematically establish an expression for the system SRT, a material balance for the biomass concentration across the control volume is considered:

$$\begin{aligned} \text{Biomass accumulation rate} &= \text{biomass inflow} - \text{biomass outflow} \\ &\quad + \text{biomass production} \end{aligned} \quad (19.12.3.2)$$

Using nomenclature shown in Fig. 19.8):

$$\frac{dX}{dt} V = QX_o - [(Q - Q_w)X_e + Q_w X_w] + r_{ng} V \quad (19.12.3.3)$$

where dX/dt is defined as rate of variation in biomass concentration in the reactor ($\text{g VSS m}^{-3} \text{d}^{-1}$); V is the aeration basin volume or, in general, reactor volume (m^3); X_o is influent biomass concentration (g m^{-3}); Q represents the influent flow rate ($\text{m}^3 \text{d}^{-1}$); Q_w is the wasting sludge flow-rate ($\text{m}^3 \text{d}^{-1}$); X_e is the effluent biomass concentration (g l^{-1}); and r_{ng} shows the net biomass production rate ($\text{g VSS m}^{-3} \text{d}^{-1}$).

Under the steady-state condition ($dX/dt = 0$) and with the assumption $X_o = 0$:

$$[(Q - Q_w)X_e + Q_wX_w] = r_{ng}V \quad (19.12.3.4)$$

By dividing Eqn 19.12.3.4 by V and X , the following expression yields where X represents the biomass concentration in the reactor:

$$\frac{[(Q - Q_w)X_e + Q_wX_w]}{XV} = \frac{r_{ng}}{X} \quad (19.12.3.5)$$

The term (r_{ng}/X) represents the inverse of sludge age. In addition, it equals to the biomass specific growth rate, μ , according to Eqn (19.5.4). So the SRT can be expressed by the following equations:

$$\theta_c = \frac{XV}{[(Q - Q_w)X_e + Q_wX_w]} \quad (19.12.3.6)$$

$$\frac{1}{\theta_c} = \mu \quad (19.12.3.7)$$

Equations (19.12.3.5) can also be written as the following by substituting Eqn (19.5.3) for r_{ng} in its right-hand side and $\frac{1}{\theta_c}$ for its left-hand side:

$$\frac{1}{\theta_c} = -Y \frac{r_{su}}{X} - k_d \quad (19.12.3.8)$$

Substituting Eqn (19.5.8) into Eqn (19.12.3.8) results in an expression that correlates the system SRT to effluent substrate concentration, S (g BOD or bsCOD m^{-3}) and biokinetic coefficients of growth and decay.

$$\frac{1}{\theta_c} = \frac{YkS}{K_s + S} - k_d \quad (19.12.3.9)$$

For facultative and flow-through systems, Eqn (19.12.3.6) can be simplified due to no sludge recycling as follows:

$$\theta_c = \frac{XV}{QX_e} \quad (19.12.3.10)$$

In flow-through systems with no sludge returning, the biomass concentration in the reactor completely escapes from the system with the effluent ($X = X_e$), therefore $t = \theta_c$. In systems with recycling, $X > X_e$, and thus $\theta_c > t$. For instance, the extended aeration process is a system that has much longer SRT (i.e., 20–30 d) in comparison to its HRT (e.g., $t = 0.5$ –3 d). Although settlement of a portion of inlet biomass concentration in facultative systems results in $\theta_c > t$, θ_c , the value is not accurately determinable due to a vague fraction of the biomass concentration that escapes from the system.

19.12.4 Biomass Concentration in System

An expression for the biomass concentration in the reactor can be developed by the following analysis.

Mass balance for substrate utilization:

$$\begin{aligned} \text{Substrate accumulation rate} &= \text{inlet substrate} - \text{outlet substrate} \\ &+ \text{Substrate utilization rate} \end{aligned} \quad (19.12.4.1)$$

Representing above expression in symbols:

$$\frac{dS}{dt} V = QS_o - QS + r_{su} V \quad (19.12.4.2)$$

where S_o is substrate concentration in the influent (g.l^{-1}).

Under steady-state condition, i.e., $dS/dt = 0$:

$$QS_o - QS = r_{su} V \quad (19.12.4.3)$$

Dividing Eqn (19.12.4.3) by Q and substituting the Eqn (19.5.8) for r_{su} .

$$S_o - S = t \left(\frac{XkS}{K_s + S} \right) \quad (19.12.4.4)$$

Solving Eqn (19.12.4.4) for $kS/(K_s + S)$ and substituting in Eqn (19.12.3.10), and then solving the resulted equation for X yields.

$$X = \left(\frac{\theta_c}{t} \right) \left[\frac{Y(S_o - S)}{1 + \theta_c K_d} \right] \quad (19.12.4.5)$$

Accordingly, the biomass concentration in the aeration basin is a function of the SRT, the HRT, the biomass yield, the endogenous decay coefficients, and the amount of substrate removed in the reactor ($S_o - S$).

19.12.5 Food to Microorganisms Ratio

The food to microorganisms (F/M) ratio is a process parameter used for design and controlling the operation of activated sludge processes, and it can be defined as given below:

$$\frac{F}{M} = \frac{\text{substrate inflow}}{\text{Mass of microbial community}} \quad (19.12.5.1)$$

Expressing it by symbolic method yields:

$$\frac{F}{M} = \frac{QS_o}{VX} = \frac{S_o}{tX} \quad (19.12.5.2)$$

In the F/M ratio, the substrate concentration can be considered in term of BOD_5 , BOD_u , COD, and the biomass concentration can be substituted in as MLSS or MLVSS.

In facultative systems such as aerated lagoons and stabilization ponds, the F/M ratio cannot be obtained because the denominator (i.e., cell mass in the system) cannot be determined due to settlement of a portion of microbial solids.

19.12.6 Effluent Substrate Concentration

If Eqn (19.12.3.9) is solved for the effluent substrate concentration S , an expression yields as given below:

$$S = \frac{K_s[1 + K_d\theta_c]}{\theta_c(Yk - K_d) - 1} \quad (19.12.6.1)$$

The above equation points out that substrate concentration in the effluent is only affected by the SRT and biokinetic coefficients of growth and decay, and is independent of influent substrate concentration.

Substrate (i.e., BOD or bsCOD) removal efficiency, which also indicates the process efficiency, can be defined by the following expression:

$$E, \% = \frac{S_o - S}{S_o} \times 100 \quad (19.12.6.2)$$

The specific substrate utilization rate U is equal to $(-r_{su}/X)$ and can also be correlated to the ratio F/M :

$$U = -\frac{r_{su}}{X} = \frac{Q(S_o - S)}{VX} = \frac{S_o - S}{tX} \quad (19.12.6.3)$$

Also,

$$U = -\frac{r_{su}}{X} = \frac{kS}{K_s + S} \quad (19.12.6.4)$$

Equations (19.12.6.3) can also be written in the following:

$$U = \frac{S_o - S}{S_o} \times \frac{S_o}{tX} \quad (19.12.6.5)$$

Substituting Eqn (19.12.5.2) and (19.12.6.2) into Eqn (19.12.6.5) yields:

$$U = \frac{(F/M)E}{100} \quad (19.12.6.6)$$

Substituting U for $(-r_{su}/X)$ in Eqn 19.12.3.8 gives another expression for obtaining the SRT as the following:

$$\frac{1}{\theta_c} = YU - k_d \quad (19.12.6.7)$$

Combining Eqn (19.12.3.8) and (19.12.6.7), the system SRT can also be defined as Eqn (19.12.6.8):

$$\frac{1}{\theta_c} = -Y \left[\frac{(F/M)E}{100} \right] - k_d \quad (19.12.6.8)$$

19.12.7 Oxygen Requirements

A mass balance on biodegradable COD (bCOD) reveals the oxygen requirement for a suspended growth wastewater treatment system (See [Eqn 19.12.7.1](#)). A fraction of the bCOD concentration is oxidized to end products (e.g., CO₂ and H₂O) during the wastewater treatment for generating energy. Almost the remainder of the bCOD concentration is used for synthesizing a new cell. Endogenous respiration also demands oxygen while its required concentration for this purpose depends on the system SRT.

$$\text{bCOD removed} = \text{bCOD utilized for energy} + \text{bCOD for biomass production} \quad (19.12.7.1)$$

In a steady-state condition, the rate of biomass production and biomass removed as wasted sludge is equal. Therefore:

$$\text{bCOD utilized for energy} = \text{bCOD removed} - \text{COD of sludge removed} \quad (19.12.7.2)$$

$$R_{or} = Q(S_o - S) - 1.42P_{wx} \quad (19.12.7.3)$$

where R_{or} is the oxygen requirement (kg d⁻¹), and P_{wx} shows biomass in terms of VSS, which is removed daily as waste sludge (kg d⁻¹).

EXAMPLE 1

The concentration of soluble organic in an aerobic lagoon has been defined by the following equation:

$$\frac{S_e}{S_o} = \frac{1 + bt}{aKt}$$

Where S_o is soluble organic concentration at initial condition (5000 mg l⁻¹) and S_e is soluble organic at effluent (50 mg l⁻¹), also given the kinetic data for biodegradable matters in the wastewater as $K = 65 \text{ d}^{-1}$, $a = 0.5$ dimensionless, and $b = 0.2 \text{ d}^{-1}$ with a flow rate of 25,000 m³ d⁻¹.

1. Calculate the size of lagoon with 2.5 m depth, if the lagoon is square in shape.
2. What would be the concentration of soluble organic after 3 days of aging in the lagoon?
3. How much oxygen is required for daily oxidation of the above wastewater?

The useful relations are:

$$\text{Biomass concentration: } X_v = \frac{aS}{1 + bt}$$

$$\text{Oxygen required: } O_2 = a S_r + 0.14X_v \cdot t.$$

$$S_r = S_o - S_e$$

Solution:

$$5000/50 = [1 + 0.2 t]/(0.5 \times 65 t)$$

$$t = 8 \text{ days}$$

$$\text{Volume of Lagoon is } V = 200\,000 \text{ m}^3$$

$$\text{Area } A = (L)(W) = 200\,000/(2.5) = 80,000 \text{ m}^2$$

$$\text{Set } L = 4W = 565 \text{ m, } W = 141.6 \text{ m}$$

$$S_e/5000 = [1 + 0.2(3)]/(32.5)(3)$$

$$S_e = 82.05 \text{ mg l}^{-1}$$

$$X_v = (0.5)(82.05)/[1+(0.2)(3)] = 26.6 \text{ mg l}^{-1}$$

$$\text{O}_2 \text{ required} = 0.5(5000 - 82.05) + 0.14(26.6)(3) = 2470.2 \text{ mg l}^{-1} = 2.47 \text{ g l}^{-1} = 2.47 \text{ kg m}^{-3}$$

$$\text{O}_2 \text{ required} = 2.47 (25,000) = 6.175 \times 10^4 \text{ kg day}^{-1}$$

PROBLEMS

1. In activated sludge process, three tanks in series are used in wastewater treatment plant. The arrangements are shown in Figure Q1. The analysis of CSTR in series is implemented for the treatment plant. Use all of the given information to define the MLVSS concentration in each tank. Biomass concentration is defined by the following equation:

$$X = \frac{Y(S_0 - S) + X_0}{1 + k_d(HRT)}$$

Given data:

$$V = 250 \text{ m}^3, S_0 = 1500 \text{ mg l}^{-1}, Q_0 = 5000 \text{ m}^3 \text{ d}^{-1}, Q_r = 1000 \text{ m}^3 \text{ d}^{-1}, X_r = 10,000 \text{ mg l}^{-1}$$

$$S_1 = 4 \text{ mg l}^{-1}, S_2 = 6 \text{ mg l}^{-1}, S_3 = 8 \text{ mg l}^{-1}, Y = 0.65, k_d = 0.1 \text{ d}^{-1}$$

2. A digester was loaded with an initial substrate concentration of $900 \text{ mg BOD}_L \text{ l}^{-1}$ and a final initial substrate concentration of $150 \text{ mg BOD}_L \text{ l}^{-1}$. The volumetric loading rate of the digester was $50,000 \text{ m}^3 \text{ d}^{-1}$. Assume constant operating temperature, 35°C .

Given Data: $\theta_c = 30 \text{ d}$, $Y = 0.2$ and $k_d = 0.03 \text{ d}^{-1}$

- a. What would be the amount of volatile solids (P_x) produced per day
- b. The volume of biogas produced per day
- c. Calculate the volume of the digester

Useful relations:

$$P_x = 3.15 \times 10^{-4} Q Y(S_0 - S)/(1 + k_d \theta_c)$$

$$\text{Volume of biogas} = 5.62[3.15 \times 10^{-4} Q (S_0 - S) - 1.42 P_x]$$

3. Reducing *Coliform* bacteria in the treated wastewater by chlorine solution represented by the following equation:

$$NA = N_0(1 + 0.23c_t t)^{-3}$$

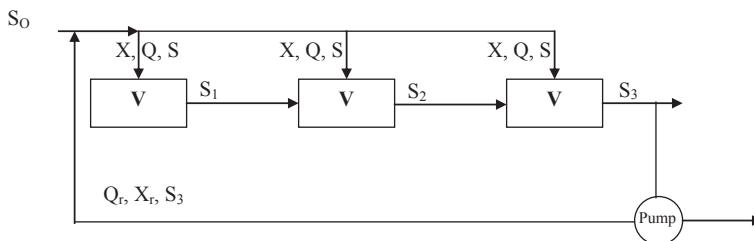


FIGURE Q1 Schematic Diagram of three stages of activated sludge process for parallel feeding of equal volume tanks in series with a recycle ratio.

Where N_A and N_0 show the number of coliforms at time t and t_0 respectively,

c_t represent the residual chlorine concentration.

The rate equation is expected to be $d N_A/dt$.

Using mass balance at steady state condition, calculate the volume of CSTR required for chlorination unit to achieve a 95% reduction of *Coliforms* in the treated effluent. Assume that in both cases that the remaining chlorine residual was 10 mg l^{-1} . The wastewater flow rate is $50 \text{ m}^3 \text{ min}^{-1}$.

4. The following data were obtained from four units of complete mix-activated sludge process for food processing wastewater. Determine the endogenous decay coefficient k_d and the maximum yield Y by using these data.

Unit no.	$X, \text{ g MLVSS d}^{-1}$	$r'_g, \text{ g MLVSS d}^{-1}$	$U, \text{ g BOD}_5/\text{g MLVSS d}$
1	18.81	0.88	0.17
2	7.35	1.19	0.41
3	7.65	1.42	0.40
4	2.89	1.56	1.09

5. Design a sedimentation basin for an aerated lagoon with a hydraulic detention time of 4 days and a liquid level above a sludge layer of 1.5 m. The sedimentation pond is cleaned every two years of operation.

Given data: $SS_i = 500 \text{ mg l}^{-1}$

$SS_e = 50 \text{ mg l}^{-1}$

$Q = 4000 \text{ m}^3 \text{ d}^{-1}$

$\text{BOD}_5 \text{ influent} = 330 \text{ mg l}^{-1}$

$Y = 0.65$

$k_s = 100 \text{ mg l}^{-1}$

$k = 6 \text{ d}^{-1}$

$k_d = 0.07 \text{ d}^{-1}$

The first-order BOD_5 removal rate constant $k' = 2.5 \text{ d}^{-1}$

- a. Determine lagoon's dimensions, mass of solids, volume, and surface area.
- b. Calculate outlet BOD_5 using lagoon relations for S/S_0 as a function of detention time.
- c. Calculate the biological solids (cells) produced using the following relation:

$$X = Y(S_0 - S)/(1 + k_d\theta)$$

References

1. Metcalf L, Eddy H, Tchobanoglous G, Burton FL, Stensel DH. *Wastewater engineering: treatment, disposal, and reuse*. 4th ed. McGraw-Hill; 2004.
2. Patwardhan A. *Industrial waste water treatment*. PHI Learning Pvt. Ltd; 2008.
3. Arceivala SJ. *Wastewater treatment for pollution control*. Tata McGraw-Hill Education; 1999.

4. Rajeshwari K, Balakrishnan M, Kansal A, Lata K, Kishore V. State-of-the-art of anaerobic digestion technology for industrial wastewater treatment. *Renew Sustain Energy Rev* 2000;**4**(2):135–56.
5. Monod J. The growth of bacterial cultures. *Annu Rev Microbiol* 1949;**3**(1):371–94.
6. Nuhoglu A, Yalcin B. Modelling of phenol removal in a batch reactor. *Process Biochem* 2005;**40**(3):1233–9.
7. Najafpour G, Younesi H, Syahidah Ku K. Ismail, Ethanol fermentation in an immobilized cell reactor using *Saccharomyces cerevisiae*. *Bioresour Technol* 2004;**92**(3):251–60.
8. Grady Jr CL, Daigger GT, Love NG, Filipe CD, Leslie Grady C. *Biological wastewater treatment*. IWA Publishing; 2011.
9. Eckenfelder WW. *Industrial water pollution control*. McGraw-Hill; 1989.
10. Rittmann BE, McCarty PL. *Environmental biotechnology: principles and applications*. New York: McGraw-Hill; 2001.
11. Riau V, De la Rubia M, Pérez M. Assessment of solid retention time of a temperature phased anaerobic digestion system on performance and final sludge characteristics. *J Chem Technol Biotechnol* 2012;**87**(8):1074–82.
12. Ge H, Jensen PD, Batstone DJ. Increased temperature in the thermophilic stage in temperature phased anaerobic digestion (TPAD) improves degradability of waste activated sludge. *J Hazardous Materials* 2011;**187**(1):355–61.
13. Dobbs RA, Wang L, Govind R. Sorption of toxic organic compounds on wastewater solids: correlation with fundamental properties. *Environ Science Technology* 1989;**23**(9):1092–7.

Biofuel Production*

OUTLINE

20.1 Biofuel Production and Global Scenarios	597	20.3 Processes and Technologies	609
20.1.1 <i>Historical Background</i>	597	20.3.1 <i>Bioethanol</i>	609
20.1.2 <i>Global Scenarios—Drives and Impacts of Biofuel Production</i>	598	20.3.2 <i>Biobutanol</i>	612
20.2 Feedstock for Biofuel Production	600	20.3.3 <i>Biodiesel</i>	613
20.2.1 <i>First-Generation Biofuel Feedstocks</i>	601	20.3.4 <i>Biohydrogen</i>	621
20.2.1.1 <i>Bioalcohol Resources</i>	601	20.3.5 <i>Biogas and Biomethane</i>	621
20.2.1.2 <i>Biodiesel Resources</i>	601	20.4 Intensification and Integration	622
20.2.2 <i>Second-Generation Biofuels</i>	602	20.4.1 <i>Reaction—Reaction Integration</i>	622
20.2.2.1 <i>Bioalcohol and Biogas Resources</i>	602	20.4.2 <i>Reaction-Separation Integration</i>	623
20.2.2.2 <i>Biodiesel Recourses</i>	602	20.4.3 <i>Separation—Separation Integration</i>	623
20.2.3 <i>Third-Generation Biofuel Resources</i>	607	20.4.4 <i>Energy Integration</i>	623
20.2.3.1 <i>Bioalcohol Resources</i>	607	20.5 Economic Perspective	624
20.2.3.2 <i>Biodiesel Resources</i>	608	References	625

20.1 BIOFUEL PRODUCTION AND GLOBAL SCENARIOS

20.1.1 Historical Background

In contrast to the general perception that biofuels are an emerging class of energy carriers, the history of biofuel production goes back to the sixteenth century, when biogas was first

*This chapter was written with contributions from:

Arash Mollahoseini, Biofuel Research Team (BRTeam), Karaj, Iran; Meisam Tabatabaei, Biofuel Research Team (BRTeam), Karaj, Iran and Agricultural Biotechnology Research Institute of Iran (ABRII), Karaj, Iran.

used by the Assyrians and then the Persians for the sake of urban welfare.^{1,2} A historical summary of biofuel production is provided in [Table 20.1](#).

20.1.2 Global Scenarios—Drives and Impacts of Biofuel Production

There has been much concern about the consequences of a massive increase in the world's population, because it has been estimated to reach 9–10 billion by the second half of the current century. Among the lack of resources may be food, health, and energy. On the other hand, conventional energy resources are depleted and their combustion has caused a serious threat to human health and the environment. Carbon dioxide, SO_x, and NO_x emissions are directly diminishing air quality and side effects such as acidic rain, the greenhouse effect, and consequently global warming have led to natural disasters. The main strategy chosen to deal with these emissions is to use alternative energy sources instead of further exploring fossil fuels, which are the main source of carbon emission.

Excluding the nuclear power, which is also accompanied by problems, alternative energy resources including geothermal power, wind power, water and ocean thermal power, and biofuels are main candidates to meet ever-increasing global energy demands. Among these new energy carriers, biofuels are the most promising in the transportation sector, where energy supply and availability are crucially important. Therefore, as mentioned earlier, owing to (1) growing energy demands, (2) dwindling fossil fuel resources, and (3) predictable and unpredictable environmental crisis and natural disasters related to climate change, advancing renewable energy and in particular biofuel production is an undeniable alternative.¹¹

The International Energy Agency defines renewable energy as “energy derived from natural processes which are replenished constantly and in its various forms, it derives directly or indirectly from the sun or from heat generated deep within the earth.” There have been debates regarding the official inclusion of hydropower plants and biomass under this definition.¹¹ Nevertheless, these two sources are generally accepted as renewable sources of energy as well.^{12,13} From the transportation sector's point of view, biomass and the resultant biofuels are the most important alternative fuels among all resources.¹⁴

To develop and extend biofuels, four main policies have been proposed: (1) financial and budgetary support through direct or indirect modes such as tax refunds; (2) trade measures and tariffs¹⁵ (tax regulations could severely hinder the promotion of biofuels if the policies are not sufficiently supportive)¹⁶; (3) a share of the transportation fuel market devoted to biofuels as a mandatory blend with fossil fuels or a precisely optional form^{17,18}; (4) helping market chain development, supporting the flow from the end user's side rather than the producer's side.¹⁹ [Table 20.2](#) summarizes supporting measures in different countries including the United States, the European Union, Brazil, China, Thailand, India, Indonesia, and Malaysia.²⁰

At the first glance, one may consider biofuels to be whole advantageous owing to their environmental benefits, such as diminished greenhouse gas emissions and their consequent

TABLE 20.1 Initial events of biofuels

Type of biofuel	Year of emergence	Pioneers	Region	Further notes	References
Biogas (biomethane)	Sixteenth century	Persians and Assyrians	The Middle East	<ul style="list-style-type: none"> In the seventeenth century, Van Helmont reported that a flammable gas was produced from decomposed organic materials. John Dalton and Humphrey Davy were the first scientists to independently realize the nature of the flammable gas as biomethane during the first decade of the nineteenth century. 	1,2
Biobutanol	1861	L. Pastor	France	Biobutanol production grew during World Wars I and II in many countries, but the use of biobutanol later dwindled owing to the high cost of feedstock.	3,4
Biodiesel	1853	E. Duffy and J. Patrick	—	In Germany in 1893, the development of Rudolf Diesel's prime model, a single 10-foot-long iron cylinder with a flywheel at its base, also had a significant role in the global introduction of biodiesel.	5,6
Biohydrogen	1939	H. Gaffron	US (University of Chicago)	Biohydrogen production was first reported in an algae, <i>Chlamydomonas reinhardtii</i> . In the twentieth century, A. Melis (University of California) explained that enzymes are responsible for biohydrogen production.	7,8
Bioethanol	1859	E. Drake	US	<ul style="list-style-type: none"> In an investigation funded by Eugen Langen, Samuel Morey and Nicholas Otto used bioethanol blends in internal combustion engines. Henry Ford also had an important role in the development of the bioethanol industry. 	9,10

positive impact on global warming. However, there are also drawbacks associated with the production and promotion of such energy carriers, including competition with the food market over raw materials, extra pressure on local water resources, and deforestation and the loss of biodiversity.^{21–23}

TABLE 20.2 Policies set by main global biofuels producers²⁰

Country	Target or mandate	Production incentives	Trade policy
European Union	Mandate: Minimum of 10% of transport fuel from renewable fuels by 2020.	Member states can apply tax reduction on biofuels as well as provide production incentives	Specific tariff of €0.192 l ⁻¹ of under-natured ethanol and €0.102 l ⁻¹ of denatured ethanol
United States of America	Mandate: 36 billion gallons of biofuel by 2022.	Tax credit of US \$0.45 per gallon (\$0.12 l ⁻¹) for ethanol blenders and US \$1.00 per gallon (\$0.26 l ⁻¹) for biodiesel blenders	Ethanol tariff of US \$.54/gallon (\$0.143 l ⁻¹) plus ad valorem duty of 2.5%. Ad valorem duty of 1.9% on biodiesel.
Brazil	Blending mandate for ethanol at 20–25%. Biodiesel use mandate set at 5% since 2010 (proposed to increase to 10% by 2020).	Tax incentives on fuel ethanol and biodiesel. Tax incentives on fuel flex vehicles.	Ad valorem duty of 20% on ethanol imported from outside the Mercosur area. Ad valorem duty of 14% for biodiesel.
India	Indicative 20% target for blending for both ethanol and biodiesel by 2017.	Minimum price mechanism for feedstocks. Tax incentives for ethanol and biodiesel.	Ad valorem duty of 28.6% on both ethanol and biodiesel.
China	Target of 12.7 Bnl ethanol and 2.3 Bnl biodiesel consumption in 2020. (15% of fuel consumption to be non-fossil fuel by 2020).	Production subsidies on ethanol and biodiesel.	Ad valorem duty of 5% on denatured ethanol and 40% on denatured ethanol.
Thailand	Ethanol: E20 mandatory since 2008. Biodiesel: B2 mandatory since 2008 and B5 since 2012.	Tax exemption for ethanol. Investments subsidies for ethanol plants. Soft loans for biodiesel.	—

This chapter reviews the historical background of biofuels and discusses the strategies used in biofuel production in different parts of the world. Moreover, biofuel production processes with a focus on innovations, intensification, and integration throughout the processes are explained. Finally, factors used in the economic tradeoff analysis of biofuel production are elaborated upon.

20.2 FEEDSTOCK FOR BIOFUEL PRODUCTION

One of the main factors to be considered in biofuel production is the raw material, i.e., the feedstocks used in the process. Not only is the final cost directly proportional to the price of

available feedstocks, a huge part of the process is related to different pretreatments required for different feedstocks. This means that by choosing or adopting the right feedstock, advantages such as high efficiency and low production cost, sustainable processes, and lower environmental issues could be gained simultaneously. Here, feedstocks are discussed from the viewpoint of different biofuel generations.

20.2.1 First-Generation Biofuel Feedstocks

First-generation biofuels are produced from edible seeds and plants. This group mainly consists of maize,^{24,25} wheat,^{26,27} sugarcane,^{28–30} sugar beet,^{31,32} cassava,^{33,34} and corn^{35–38} (used to produce bioalcohols (bioethanol and biobutanol)), as well as sunflower,^{39–41} soybean,^{42–44} rapeseed,^{45–47} and palm^{48,49} (used to produce biodiesel). These feedstocks are capable of being converted into biofuels (bioalcohols and biodiesel) by means of processes such as fermentation and transesterification, respectively.⁵⁰ Some of these feedstocks are introduced in the following.

20.2.1.1 Bioalcohol Resources

Sugarcane: Sugarcane belongs to the grass family (*Poaceae*); the tall grass-like plants have a height of 1.2–3 m. Sugarcane plants are propagated through the stem; sugar is synthesized through leaf chlorophyll via photosynthesis. Stored carbohydrates are in form of sugar in the long stems. Tropical conditions are most suitable for growing this plant. Sugarcane and sweet sorghum are the most important feedstocks for fermentative bioethanol production.

Sorghum: Sorghum, a genus of grasses with more than 30 species, is another edible plant; the grains produced are used to make cereals, snacks, bread, and porridge, whereas the residues can be used as animal feed. Ethanol derived from sweet sorghum is of high quality (low sulfur content and high octane number) and can therefore be used in gasoline motors as gasohol when blended with gasoline at ratios as high as 1:4.⁵¹

Corn: Corn is a major resource of bioalcohols. The largest producers of corn-based ethanol are the United States and Brazil.⁵² Bioethanol production processes might parallel coproduction or byproduction of other valuable products, i.e., distiller's dried grains, corn gluten feed, and corn gluten meal,⁵³ which could affect the economic viability of the process if properly used. Overall, the high starch content of corn and the fast development of cultivation and processing technologies make the plant a good option for bioalcohol production.

Wheat: A cereal grain originated from Eastern countries, wheat is produced worldwide. After corn and rice, wheat is the third most produced cereal. The starch in the seeds' structure could be hydrolyzed to monomeric sugar for fermentation into bioalcohols through relevant processes.

20.2.1.2 Biodiesel Resources

Soybean: Soybean oil contains five different fatty acids: oleic, palmitic, linoleic, linolenic, and stearic. Because of the high oil content (15–20%), this seed is a high-yield feedstock for biodiesel production.⁵⁴ A high degree of biodegradation, reduced toxicity, low emission, enhancement of lubricity, and improvement in the flashpoint all make soybean-derived biodiesel one of the best options for blending with diesel fuel.⁵⁴ Compared with rapeseed and

canola, soybean oil is said to possess lower oxidative stability.⁵⁵ Blending with petrodiesel fuel is regarded as a solution to make up for this drawback of soybean biodiesel.⁵⁶

Sunflower: Sunflowers originated in Central America. Extracted sunflower oil is one of the most frequently used oils for cooking. The remaining parts of seeds after oil extraction can be used as animal feed owing to their high nutrient content.^{57,58} From a physiological point of view, although the plant possesses deep taproots, it seems to be susceptible to drought.⁵¹

Palm oil: Palm oil is extracted oil from palm fruits, mostly exported by countries located in tropical regions such as Southeast Asian countries (Malaysia, Indonesia, and Thailand). Inexpensive palm oil production compared with canola, soybean, and rapeseed oil makes this feedstock a superior option from an economical point of view.⁵⁹

20.2.2 Second-Generation Biofuels

Because there are doubts about the environmental impact of first-generation biofuels on the one hand and their influence on food security and prices on the other, second-generation biofuels were developed.^{50,60–62} Such biofuels are driven from lignocellulosic resources, woody biomass and inedible seeds such as *Jatropha curcas*, as well as waste oil feedstocks, all of which are available at low prices. Residues generated in the food industry and during first-generation biofuel production can be used as substrates for second-generation biofuel production.

20.2.2.1 Bioalcohol and Biogas Resources

Lignocellulosic biomass: Lignocellulose is defined as plant residues composed of cellulose, hemicellulose, and lignin.⁶³ The complicated molecular structure of lignocellulosic materials makes them a challenging resource for biofuel production. They usually consist of 30–56% cellulose, 10–27% hemicellulose, and 3–30% lignin.⁶⁴ The complicated structure of such a feedstock makes pretreatment inevitable. Pretreated lignocellulosic biomass contains less lignin and the rigidity of the cellulosic polymers is also decreased. In fact, physical, chemical, physicochemical, and/or biological pretreatment makes the raw materials more accessible to enzymatic hydrolysis, which in turn leads to the higher production rate of fermentable sugars and resultant bioalcohols or biogas, i.e., biomethane and biohydrogen.^{64,65} Table 20.3 summarizes the lignocellulosic feedstocks used in recent investigations for biohydrogen and biomethane production.^{66–96}

20.2.2.2 Biodiesel Recourses

Jatropha: *Jatropha* is native of Mexico but is also found in many tropical countries in Asia and Africa. *Jatropha* is an inedible seed whose oil can be directly used as a fuel in adopted diesel engines or transesterified to be blended with petroleum diesel up to 25% without requiring significant variations in the diesel engine's system. The byproduct (filter cake) can be used as an energy source for the production process or as a fertilizer. *Jatropha* trees withstand harsh drought conditions and the seeds contain 27–40% oil. There are also claims stating that the plant resists diseases and pests.⁵¹ A comprehensive review of *Jatropha*'s properties can be found elsewhere.^{97,98}

TABLE 20.3 Lignocellulosic resources used for biohydrogen and biomethane production

Produced biofuel	Microorganism	Lignocellulosic feedstocks	Reactor operating condition	Process mode	Highest yield	Notes	References
Biohydrogen	Activated sludge	Corn stover	35 °C 5.5 pH	Batch	2.84–3.0 mol H ₂ (mol glucose) ^{−1}	Effect of different temperatures and reaction times also studied.	66
		Corn straw	55 °C pH 7	Batch	1.53 mol H ₂ (mol glucose) ^{−1}	Combination of acid pretreatment and microwave irradiation was better pretreatment compared with thermal acid pretreatment. Higher surface area and better particle size distribution of treated corn straw resulting from microwave irradiation led to higher accessibility to the substrate. (optimum: 0.3 N H ₂ SO ₄ , 45 min, 700 W).	67
		Wheat straw	pH 5.3 (self-stabilized) 70 °C	CSTR, UASB, and AF. Continuous stirred tank reactor, Up flow anaerobic sludge blanket, Anaerobic filter	212.0 ml H ₂ g ^{−1} sugar	Different reactor configurations led to different hydrogen production yields. Best result is for UASB reactor.	68
	Mixed microflora	Wheat straw	—	Batch	68.1 ml H ₂ g ^{−1} TVS	—	68
		Sweet sorghum stalk	36 °C	Batch	15.13–127.26 ml H ₂ /g TVS		69
		Poplar leaves	120 rpm 35 °C	Batch	15.04 –44.92 ml g ^{−1} poplar leaves		70

(Continued)

TABLE 20.3 Lignocellulosic resources used for biohydrogen and biomethane production—cont'd

Produced biofuel	Microorganism	Lignocellulosic feedstocks	Reactor operating condition	Process mode	Highest yield	Notes	References
		Beer residue	120 rpm 35 °C	Batch	53.03 ml g ⁻¹ dry beer Lees	Pretreatment of raw feedstock resulted in 17-fold improvement in reaction.	71
		Xylose	70 °C	CSTR	1.36 mol H ₂ mol ⁻¹ xylose	—	72
		Poplar leaves	120 rpm 35 °C	Batch	15.04–44.92 ml g ⁻¹ poplar leaves		70
	<i>Clostridium butyricum</i> CGS5	Rice straw	37 °C pH 7.5	Batch	0.76 mol H ₂ mol ⁻¹ hexose	—	73
	<i>Clostridium thermocellum</i> 27405	Corn stover and cellobiose feed	120 rpm 50 °C 6.8 pH	Two-step batch reactions	1.67 mol H ₂ mol ⁻¹ glucose and 1.64 mol H ₂ /mol glucose	Two-step process consisting of fermentation and electrohydrogenesis studied.	74
	<i>Clostridium beijerinckii</i> KCTC 1785	Food waste	150 rpm 35 °C 5.5 pH	Four anaerobic sequencing batch reactors	2.4 mol H ₂ mol ⁻¹ hexose	—	75
	<i>Enterobacter cloacae</i> IIT-BT 08	Rice straw (SM-A), bagasse (SM-b), and coir (SM-C)	6 pH	Batch	75.6 (mmol l ⁻¹ h ⁻¹)	—	76
	<i>Thermoanaerobacterium thermosaccharolyticum</i> W16	Corn stover	Variant pHs	Batch	2.24 mol H ₂ mol ⁻¹ hexose	—	77
	<i>C. butyricum</i> AS1.209	Corn straw	35 °C	Batch	68 ml H ₂ g ⁻¹ corn straw	—	78
	<i>C. butyricum</i>	Sugarcane bagasse	Incubation of organisms at 37 °C and 150 rpm	Batch	1.73 mol H ₂ mol ⁻¹ hexose	Optimum condition of 0.5% H ₂ SO ₄ and 60 min.	79
	<i>Caldicellulosiruptor saccharolyticus</i>	Sweet sorghum	pH 6.8 350 rpm	Batch	2.6 mol H ₂ mol ⁻¹ hexose	Effect of feedstock inclusion rate studied.	80

	<i>C. saccharolyticus</i> and <i>Thermotoga neapolitana</i>	Sweet potato peels	pH 5.4 90 °C 30–60 rpm	Batch	2.4–3.8 mol ⁻¹ H ₂ mol ⁻¹ glucose	Different reaction times and feed concentrations investigated.	81
	<i>Thermoanaerobacterium</i> sp.	Food waste	15 rpm 55–60 °C	Internal recirculation packed-bed reactor	45.54 ml g ⁻¹ volatile Solid	—	82
	Isolated microorganism from <i>Cellulomonas</i> sp., and <i>Cellulosimicrobium cellulans</i>	Rice husk, rice straw	37 °C 7.5 pH	Batch	17.24 mmol H ₂ g ⁻¹ glucose	Nine different microorganisms compared with each other; <i>C. butyricum</i> CGS5 showed best hydrogen production performance.	83
	<i>C. saccharolyticus</i> DSM 8903 and <i>T. neapolitana</i> DSM 4359	<i>Miscanthus</i>	—	Batch	2.9–3.4 mol H ₂ mol hexose	—	84
	<i>Cellulomonas</i> E3-01	Carboxymethyl-cellulose Xylan Sugarcane Bagasse	37 °C 7–7.5 pH		1.58 mol H ₂ mol ⁻¹ hexose 0.91 mol H ₂ mol ⁻¹ pentose 6.01 mmol H ₂ g ⁻¹ reducing sugar	Carboxymethyl-cellulose, xylan used with no pretreatment.	85
Biomethane	Mixed culture	54 different vegetables and fruit wastes	35 °C	CSTR	More than 90% yield (after 50 days of fermentation)	Methane yields and kinetics of different plant parts of same variety differed.	86
		Grass silage	35 °C pH 7.4–7.5	Batch	495 ml per g volatile solid	NaOH treatment hindered methane production by 15%.	87
		Office paper waste	35 °C	Batch	360,410 ml per g volatile solid	Acid treatment resulted in higher conversion of cellulose into biomethane.	88
	Digested cow manure	Wheat straw	55 °C	Batch	297 ml per g volatile solid	—	89

(Continued)

TABLE 20.3 Lignocellulosic resources used for biohydrogen and biomethane production—cont'd

Produced biofuel	Microorganism	Lignocellulosic feedstocks	Reactor operating condition	Process mode	Highest yield	Notes	References
		Maize silage	35 °C	Batch	410 ml per g _{volatile solid}	—	90
	Solid waste digester inoculum	Wheat straw		Batch	276 ml per g _{volatile solid}	Effect of fermentation reaction time and temperature on methane yield studied.	91
	Co-digested plant slurry	Maize drying up residue	40 °C	Batch	307 ml per g _{volatile solid}	Rice and barley straw, grape stalks, grape marcs, maize drying up residue, tomato skins and seeds, and whey also studied, showing lower efficiencies.	92
	Municipal solid waste digester inoculum	Paper tube residual	55 °C	Batch	493 ml per g _{volatile solid}	Steam explosion pretreatment resulted in 107% higher yield compared with untreated paper residuals.	93
	Inoculum taken from a thermophilic digester	Jose tall wheatgrass (wheatgrass)	50 °C pH 7	Batch	290 ml per g _{volatile solid}	Study included investigation of enzyme (N342) addition to two-step digesting procedure	94
	Mesophilic sludge from Gaobeidian wastewater Treatment system	Corn stover	35 °C	Batch	220 ml per g _{volatile solid}	—	95
	Anaerobic digester sludge	Sugarcane bagasse (<i>Saccharum officinarum</i>)	35 °C	Batch	72.1 l methane per kg ⁻¹ bagasse	Peroxide pretreatment of feedstock led to highest production (compared with calcium peroxide pretreatment)	96

CSTR, continuously stirred tank reactor; UASB, upflow anaerobic sludge blanket; TVS, total volatile solids; AF, anaerobic filter.

Caster: Caster is a drought-tolerant plant with deep tap roots; it originated in East Africa but is also cultivated in other parts of the world. Its reddish and purple seeds contain more than 40–50% oil. Just like other oily seeds' extracts, castor oil can be used individually as an engine fuel but the high viscosity might be a hindrance. Therefore, improvement of viscosity through transesterification could lead to an ideal diesel engine fuel made from castor oil.

Waste cooking oils and animal fats: Many articles in favor of biofuel production from waste cooking oil^{99–102} or animal fats^{103,104} assess the economics and tradeoff balances.¹⁰⁵ These articles also point to the many shortcomings of the feedstocks, such as high fatty acid and water content and other impurities.^{100,101} Nevertheless, because a great portion of the cost of biofuel production arises from the raw materials used, owing to their two- to threefold lower cost, these waste-oriented feedstocks are mostly preferred over fresh oils.¹⁰⁵ In another words, biodiesel produced from virgin vegetable oil would be roughly 50% more costly than biodiesel produced from waste cooking oils.¹⁰¹ The yield of transesterification for waste cooking oil is slightly lower than virgin oil, which is ascribed to the impurities contained, i.e., free fatty acids, water, and others.^{103,106}

Oily wastewaters: Wastewater from oil chemical plants is considered a raw material for biodiesel.¹⁰⁷ As a matter of fact, there are two ways though which biodiesel could be produced from oily wastewater recourses such as oil mill wastewater. The first way is to use the filtered oil and grease contained (usually < 5%) in the primary sledge; the second route is to apply secondary sludge as a resource for biodiesel production. More specifically, the second way would require collection of microorganisms formed during aerobic and anaerobic processes, followed by extraction of the microbial oil produced.¹⁰⁸ Transesterification could be performed by separation of lipids and oily streams from the sludge¹⁰⁹ or in situ, which means that the reaction would be conducted with the sludge and the separation processes would be postponed until the downstream stages.¹⁰⁸ The remaining sludge could be a good source for biomethane production.^{110,111}

20.2.3 Third-Generation Biofuel Resources

Third-generation biofuels are produced from microalgae and some other microorganisms such as cyanobacteria,¹¹² bacteria,¹¹³ fungi, and yeast.¹¹⁴ This could avoid competition between biofuel and food over resources and land. Consequently, concerns about the drawbacks and increased food prices would be diminished.¹¹⁵ In the same manner, using algal and microbial feedstocks offers advantages such as ease of cultivation with few observations required and the possibility of using saline waters, which are basically not used in agricultural practices.¹¹⁶

20.2.3.1 Bioalcohol Resources

Algae: Algae could be exposed to processes through which the intracellular sugars, starch, or cellulose could be extracted and fermented into bioethanol or biobutanol. Alternatively, the biomasses as a whole could be fermented to produce bioalcohols.^{117,118} Genetic engineering has also been used to produce bioethanol directly in these microorganisms.^{119,120} In fact, algae offer numerous advantages compared with other energy crops, including higher biomass productivity, best photosynthetic efficiency with highest CO₂ conversion and O₂ production, a liquid media requirement with easy handling, and a versatile/flexible cultivation environment.

Cyanobacteria: Owing to their unique photosynthetic properties, cyanobacteria are capable of converting up to 10% of the sun's energy into biomass. This is considerably higher than the 1% recorded by conventional energy crops such as corn or sugarcane, or the 5% converted by algae. Therefore, these photosynthetic microorganisms could be regarded as environmentally sustainable and economically effective feedstocks for the production of different types of biofuels including bioalcohols.¹²¹ Bioalcohol production through cyanobacteria could best couple energy production and the sequestration of industrial carbon dioxide emissions to reduce greenhouse gas pollution without competing with food production.¹²² In a recent study, Aikawa et al.¹²³ investigated direct ethanol production from *Arthrospira (Spirulina) platensis*, a fast-growing halophilic cyanobacterium that accumulates large amounts of glycogen. In their study, they used lysozyme and a recombinant amylase-expressing yeast strain to eliminate the need for biomass pretreatment and amylase hydrolysis. Through this innovative process, i.e., direct conversion process from *A. platensis* to ethanol, 86% of theoretical ethanol yield was achieved (6.5 g l⁻¹ with an ethanol productivity of 1.08 g l⁻¹ per day).

Apart from efforts to improve the bioprocess aspects of bioalcohol production from cyanobacteria, a number of investigations have focused on genetic and metabolic engineering of these organisms to improve alcohol yields and economize the production process. For instance, Gao et al.¹²⁴ strived to integrate photosynthetic biomass production and microbial conversion in an attempt to directly convert carbon dioxide into ethanol by the cyanobacterium, *Synechocystis* sp. PCC6803, into a single biological system. In their study, a mutant strain was constructed by genetically introducing pyruvate decarboxylase from *Zymomonas mobilis* and overexpressing endogenous alcohol-dehydrogenase while down-regulating the biosynthetic pathway of poly- β -hydroxybutyrate. Eventually, an ethanol production efficiency of 5.50 g l⁻¹ was achieved.

20.2.3.2 Biodiesel Resources

Oleaginous microorganisms (microorganisms with lipid content higher than 20%) useful for oil extraction and consequent biodiesel production could be categorized into a number of groups out of which the most important groups are as follows:

Algae and cyanobacteria: Both algae and cyanobacteria provide potential advantages for lipid-derived biofuel, especially biodiesel production, owing to their great capacity to convert carbon dioxide into lipids without competing for arable land necessary for agricultural oleaginous crops. Development in bioprocess engineering and increased knowledge of algal and cyanobacteria physiology has paved the way for their use in biofuel production including biodiesel.^{112,114} Comparatively, cyanobacteria are more advantageous organisms in terms of their faster cell growth, and the fact that they are naturally transformable. The latter increase the potential for cyanobacteria to be genetically engineered.^{125,126}

On the other hand, algae's ability to produce high amount of lipids makes algal feedstocks a great resource for biodiesel production. Compared with conventional first- and second-generation feedstocks such as rapeseed and soybean, algal resources have oil contents ranging between 20% and 80% (W/W)^{116,127} and a higher growth rate, and 49–132 times less area is required for their cultivation,¹²⁸ which is promising in the future of the world biofuel market.

Bacteria: Reaching a bulky biomass in only 12–24 h makes the bacterial species a fast-growing microorganism for biodiesel production, just like algae. There are few bacteria available that are inherently capable of producing lipid through a biological or metabolic

pathway. For instance, *Arthrobacter* sp. is a bacterium with an oil content as high as 40%.¹²⁹ Overall, some bacterial strains produce high amounts of lipid, but because these lipids are generated in the outer membrane, they are difficult to extract. As a result, biodiesel production from bacterial lipid resources is still not industrially feasible.¹³⁰

Yeast: Under certain cultivation conditions, different yeasts such as *Cryptococcus albidus*, *Lipomyces lipofera*, *Lipomyces starkeyi*, *Rhodospiridium toruloides*, *Rhodotorula glutinis*, *Trichosporon pullulan*, and *Yarrowia lipolytica* are capable of producing lipids.¹³¹ Analysis of the oil extracted from these yeast strains revealed that the main fatty acids in their structure are myristic, palmitic, stearic, oleic, linoleic, and linolenic. This means that the quality of the produced biodiesel could be equivalent to those obtained from chemically or enzymatically catalyzed seed oils.¹³¹

Despite all of the positive discussions revolving around third-generation biofuel feedstocks, critics question the capability of currently present algal resources to offer relative independency from petroleum fuels. In an article published by a group of top international algal fuel experts, they stated, "I do not (and cannot) refute that an ideal microalgal strain harboring an optimal combination of traits could be potentially found or even engineered, but that is yet to happen."¹³² That algal feedstocks are far from being used conventionally and from being relied on as biofuel raw material was mentioned by Singh and coworker.¹³³ They argued that algal fuel would reach a commercial stage in 2020. On the other hand, massive amounts of CO₂, P, and N as nutrients are required to grow algae, and different infrastructures such as aquatic environments and roads for accessibility are also crucial for the sustainable development of algal-based biofuel. If the problems of nutrition recycling, CO₂ supplementation (which is introduced as the bottleneck of the procedure), and energy recovery from the biomass are overcome, a small portion of petroleum-based fuels consumption could be replaced with algal-based biofuels.¹³²

Fourth-generation biofuels not only lead to sustainable energy production but also result in capturing and storing of CO₂. More specifically, biomasses that have absorbed CO₂ while growing are converted into fuel using the same processes as second-generation biofuels. However, this process differs from second- and third-generation production because at all stages of production, CO₂ is captured using processes such as oxy-fuel combustion followed by geo-sequestration by storing it in old oil and gas fields or saline aquifers. This carbon capture makes fourth-generation biofuel production carbon-negative because during this process more carbon is stored than produced. In other words, this system not only captures and stores carbon dioxide from the atmosphere, it also reduces emissions by replacing fossil fuels.¹³⁴ Classification and comparisons of different generations of biofuels are listed in Table 20.4.

20.3 PROCESSES AND TECHNOLOGIES

Here, different biofuel production processes are briefly discussed and recent advances and developed technologies are introduced.

20.3.1 Bioethanol

Bioethanol production processes consist of initial pretreatment, fermentation, and purification steps. Based on the feedstock used and the process implemented, pretreatment steps

TABLE 20.4 Classification and comparisons of different biofuels^{135–137}

Type of biofuels	First generation	Second generation	Third generation	Fourth generation
Feedstocks	Edible seeds and plants: corn, soybean, sugarcane, potato, wheat, rice, rapeseed, coconut, palm, sunflower	Lignocellulosic biomass, switchgrass, wood and forest wastes, agricultural and urban wastes	Microbial species, algae, fungi, yeast, cyanobacteria	Similar to those of first- to third-generations biofuels
Fuels produced	Bioethanol, biobutanol, biodiesel, methanol, mixed alcohols	Bioethanol, biohydrogen, biobutanol, biodiesel, methanol, mixed alcohols, Fischer–Tropsch gasoline, biomethane, dimethylether	Biodiesel, methanol, biohydrogen, biomethane	Green diesel, green aviation fuel, green gasoline
Production processes	Fermentation, transesterification	Pretreatment, enzymatic hydrolysis, fermentation, transesterification, anaerobic digestion, microbial photolysis	Transesterification, fermentation, photosynthesis, anaerobic digestion, microbial photolysis	—
State of the processes	Mature	Relatively new and not mature enough for cost reduction	Relatively new and not mature enough for cost reduction	Relatively new and not mature enough for cost reduction
Advantages	Environmental and social benefits Available feedstocks at large quantities	Close to meeting the claimed environmental benefits Available feedstocks in large quantities Low cost for feedstock	Low and sometimes no cost for feedstock	Carbon-negative
Disadvantages	Might potentially have a negative impact on biodiversity Contribute to higher food prices owing to competition with food	Lower conversion Lack of technological and research breakthrough	Lack of technological and research breakthrough Not yet commercially feasible	Technological and research efforts still ongoing Higher cost

vary, including milling, soaking, physiochemical/chemical/biological pretreatment, enzymatic saccharification (hydrolysis), and sterilization (cooking). The selection and sequence of these treatments are related to the feedstock used and its composition.

A major portion of bioethanol in the world is produced from cornstarch through wet and dry milling processes. In the former process, corn is first soaked in water, followed by grinding to increase the surface area while the outer parts (non-starch) are totally removed. Alternatively, corn could be ground without water, or dry milling. There are some differences between these methods. Dry-ground corn results in animal feed and bioethanol and has a higher yield and is consequently used more often in bioethanol production plants whereas

the wet-ground corn results in a series of products such as starch, corn gluten feed, corn gluten meal, and fructose corn syrup.^{138,139} The obtained slurry of cornstarch is fed into a bioreactor in which *amylase* enzyme is present. There are two types of *amylase* capable of being industrially used in hydrolyzing starch: *alpha-amylase* and *glucoamylase*. The differences between these two enzymes and their methods of hydrolyzing starch may be found elsewhere.^{139,140} Heating the system leads to the hydrolysis of starch and the production of glucose. Fermentation then takes place and ethanol, CO₂, and some other negligible products result. (Detailed information on the fermentation process are discussed in early chapters of this book.) Distillation columns or other separation units of operation are finally used to purify and concentrate the ethanol. Extra water in the produced alcohol is removed generally using molecular sieves. Figures 20.1 and 20.2 show a flowchart of the wet grinding and dry fermentation processes.

Producing alcohols from sugarcane is similar in principle to the process used for the corn as feedstock, but it does not involve the same pretreatment steps.¹³⁹ More specifically, the

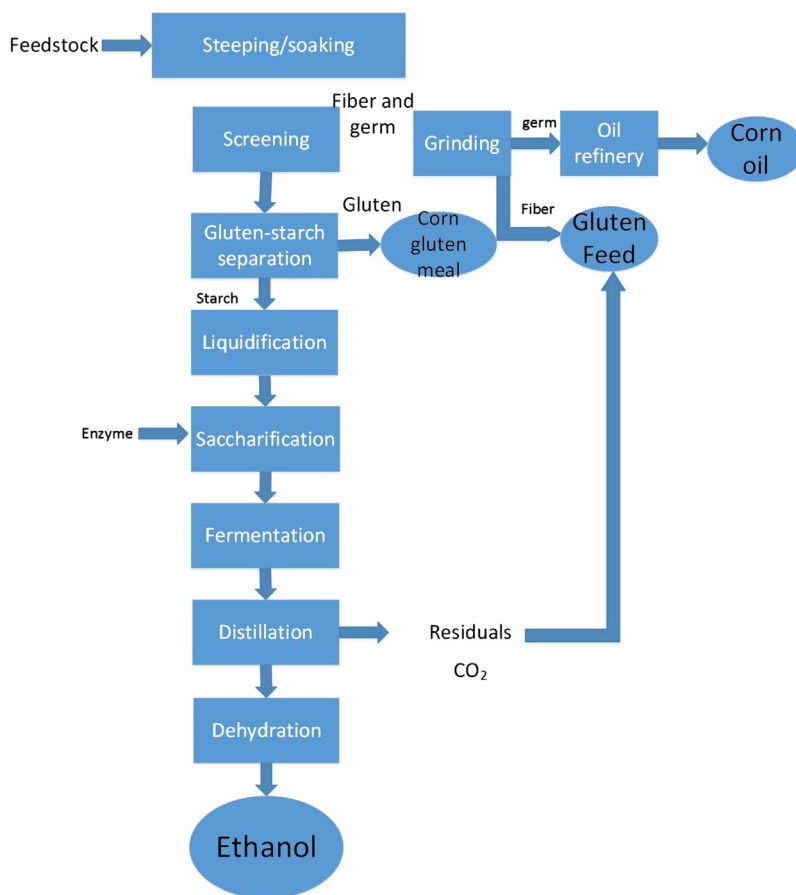


FIGURE 20.1 Wet grinding (milling) flowchart for bioethanol production.

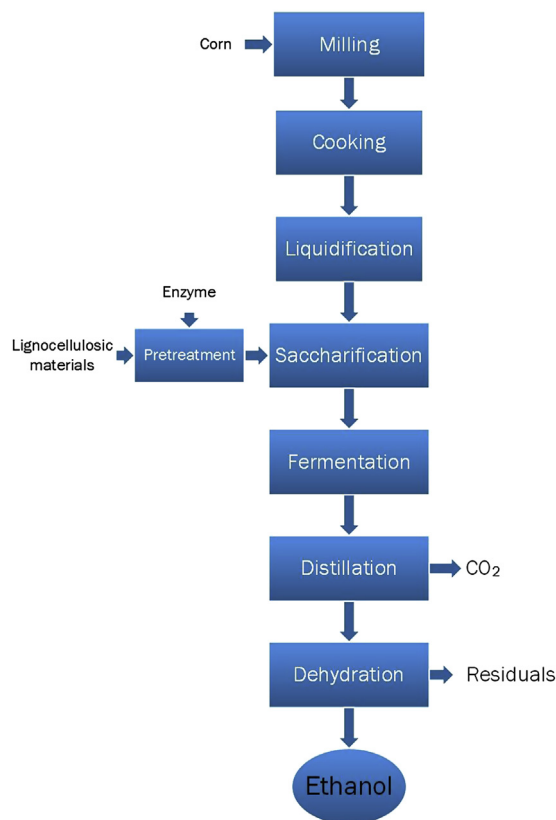


FIGURE 20.2 Dry grinding (milling) process flowchart for bioethanol production.

initial steps here consist of extracting sugar from the cane and removing the lignocellulosic portion or bagasse, filtering the sugar juice, and beginning the fermentation process.

20.3.2 Biobutanol

Petrochemical-based butanol production cost is heavily proportional to the propylene market and crude oil prices.^b Therefore, biobutanol production from renewable resources could be significantly important in the future of the energy market and transportation sector. This is basically because compared with bioethanol, biobutanol holds greater promise, such as its higher energy content (approx. 90% of gasoline) and because it does not absorb water like bioethanol. Traditionally, bio-based butanol is produced through an acetone–butanol–ethanol (ABE) fermentation process in which *Clostridia* species, namely *Clostridium acetobutylicum*, *Clostridium beijerinckii*, *Clostridium saccharobutylicum*, and *Clostridium saccharoperbutylacetonicum*, are used¹⁴¹ Each species best functions under specific conditions

^bThe petrochemical route to produce butanol is described as follows: hydroformylation of propylene leads to the formation of aldehyde. Hydrogenation of these aldehydes results in production of *n*-butanol.

and using a specific feedstock. Traditional butanol fermentation processes in use since the late 1950s have some disadvantages, which highlight the need to improve currently used processes while striving to develop novel processes:

- Using distillation as the separation unit operation, which consumes a high amount of energy.
- Toxicity of the produced biobutanol to microorganisms when its concentration rises.
- Phage contamination especially in large-scaled units.
- Several byproducts (acetone and ethanol) hindering the downstream purification processes.
- Low production yield.

On the other hand, the feedstocks used in the fermentation process are mainly starch and sugar, which as discussed previously, lead to competition over food resources.

There are a number of solutions to overcome these obstacles, such as finding new strains and genetically engineering currently used microorganisms to increase the efficiency of the process.^{142–145} Beside microbial enhancement and the replacement of traditional batch processes with continuous or semi-continuous ones, implementing more efficient and lower energy-demanding purification processes such as membrane separation technologies or nontoxic liquid–liquid extraction have improved the economic viability of biobutanol production.¹⁴¹ For instance, Liu et al.¹⁴⁶ introduced a new mixed matrix membranes incorporating zeolitic imidazolate frameworks (ZIF-71) particles into polyether-block-amide for biobutanol recovery from ABE fermentation broth by pervaporation. The membrane with 20 wt% ZIF-71 resulted in high *n*-butanol separation performance.¹⁴⁶

20.3.3 Biodiesel

Although vegetable oil can be used directly as fuel in diesel engines, the most important limitation lies in the fact that the high viscosity of vegetable oils results in poor atomization in the engine's combustion chamber, which eventually leads to other operational problems.¹⁴⁷ Among methods found to solve this problem, transesterification was reported to be more favorable owing to the simultaneous dilution of the oil and improvement of its other properties as a fuel.¹⁴⁸ Transesterification is a catalytic route to obtain biodiesel and the catalyst could be an acid,¹⁴⁹ base,¹⁵⁰ or both in homogeneous and heterogeneous forms,^{151,152} and enzymes.^{153–158}

Developments in the field of biofuel processing have led to numerous commercial biodiesel production technologies. Most existing production plants, operated either in batch or continuous mode, use transesterification reaction and homogeneous catalysts. Alkaline homogeneous catalysts such as sodium methoxide, potassium methoxide, sodium hydroxide, and potassium hydroxide are favorable because of their high yield and low residence time. What might decrease the efficiency of basic catalytic processes would be the side reactions required, such as neutralization as well as saponification and consequent entrapment of the produced biodiesel in the produced soap, which is intensified if the amount of soap created in the process is high.¹⁵⁹ Vicente et al.¹⁵⁹ compared the different alkaline homogeneous catalysts. According to their report, methoxides led to a high conversion rate of almost 98–99%, but their application was limited by their high price and high hygroscopicity;

therefore, sodium and potassium hydroxides are the most widely available choices with lower conversions of 85.9% and 91.6%, respectively. Although the rate of alkaline homogeneous catalysts is reported to be 4000-fold higher than acidic homogeneous catalysts,¹⁰⁰ their use is limited to feedstocks with less than 0.5 wt% free fatty acid content or acid values less than 1 mg KOH g⁻¹.^{160,161}

The mechanism of a base-catalyzed reaction is simple. Briefly, first the negative species (RO⁻) such as CH₃O⁻ attacks the carbonyl group, forming a tetrahedral intermediate. Afterward, the R₁COOCH₃ leaves and the new O–H bond is formed. The cycle goes on two more times so that all carbonyl groups are re-formed (Figure 20.3).

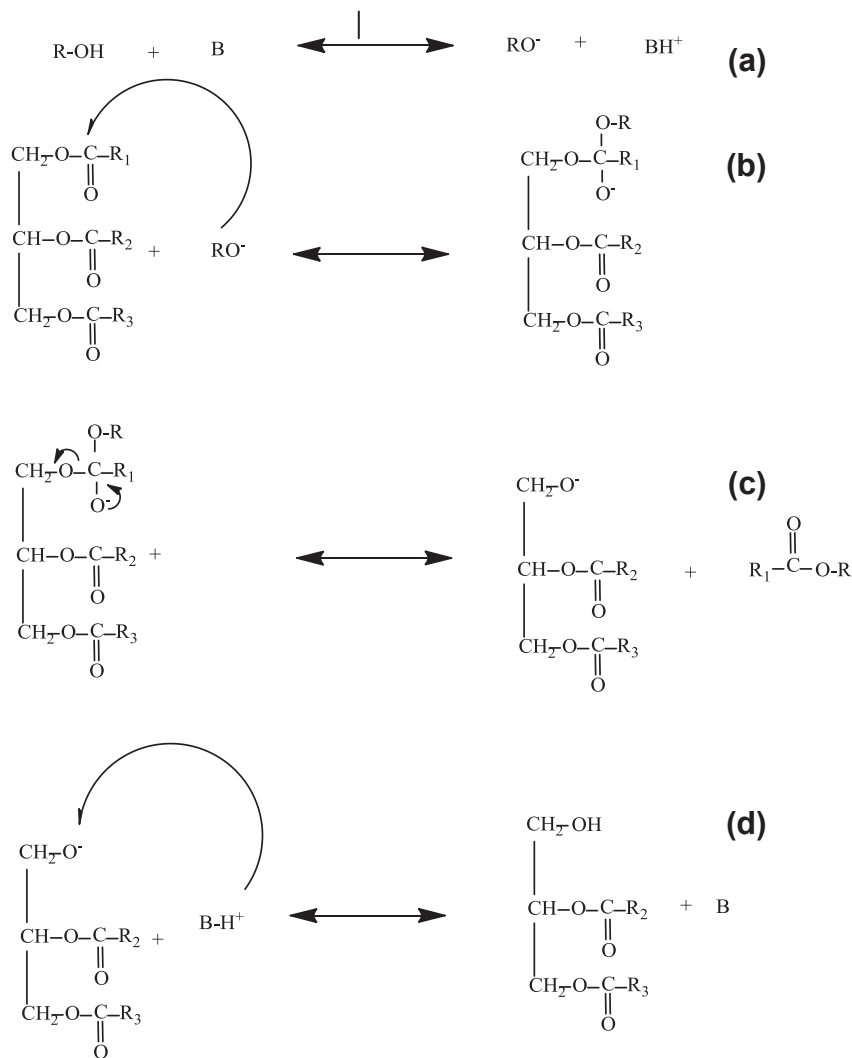


FIGURE 20.3 Schematic steps of base-catalyzed transesterification.

Homogeneous acid catalysts, on the other hand, resist the high FFA content of the feedstock and could catalyze both transesterification and esterification reactions simultaneously. Among the wide range of acids used, sulfuric acid (H_2SO_4) and hydrochloric acid (HCl) are most common. The higher yield of base catalysts and corrosion problems caused by acid catalysts, as well as the high oil to alcohol ratio requirement,^{162,163} have made the base-catalyzed process much more appealing to industrial plants. The mechanism of an acid-catalyzed reaction is shown in Figure 20.4. Briefly, H^+ attacks the carbonyl groups of the triglycerides. Then, the nucleophilic attraction of the alcohol used in the reaction resulted in the formation of a tetrahedral intermediate. The final step is the migration of proton and breakdown of the large molecule. This procedure takes place three times so that all carbonyl branches of the triglyceride are re-formed.

High costs of downstream purification occur and enormous amounts of wastewater are generated during such processes when homogeneous catalysts are used. Therefore,

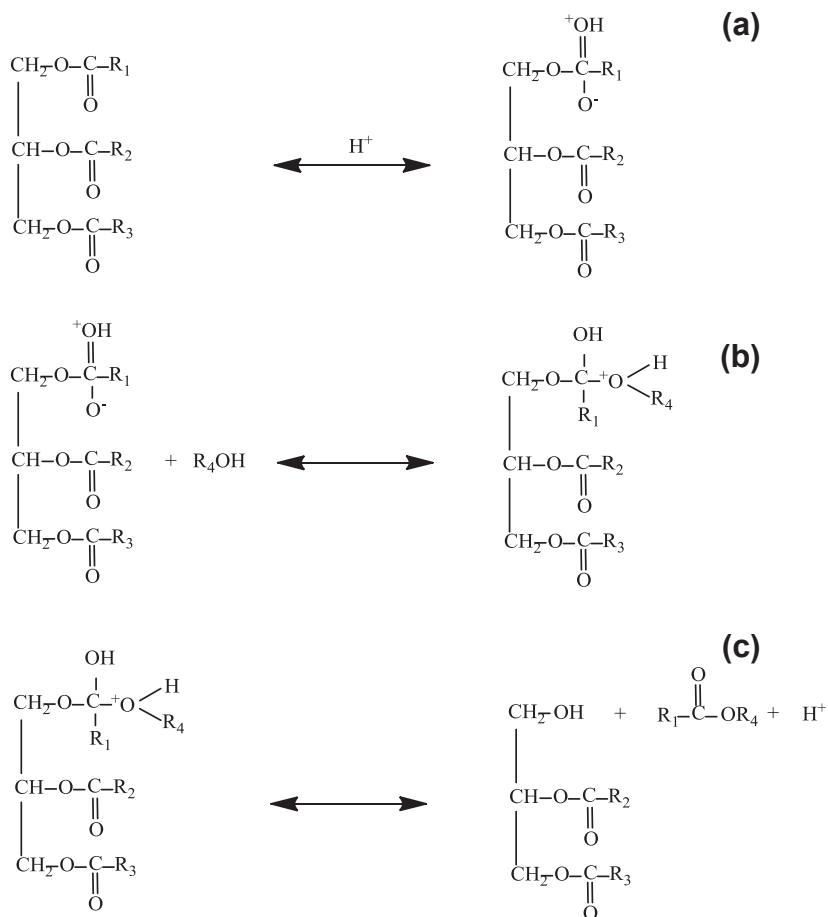


FIGURE 20.4 Schematic steps of acid-catalyzed transesterification.

heterogeneous catalytic procedures are more favorable in terms of the process costs. However, heterogeneous-catalyzed reactions also have serious drawbacks such as mass transfer limitation and longer residence time.¹⁵⁹

Overall, despite many achievements, the industrial production of biodiesel using homogeneous catalysts encounters major challenges: (1) Conventional continuous transesterification processes, as discussed earlier, need a longer residence time, resulting in increasing reactor volume, high capital cost, and a large footprint, and are difficult to control. (2) Moreover, the presence of FFA and water in the feedstock causes soap formation, leading to reduced reaction yield and the loss of biodiesel product via entrainment in the soap phase during the washing process. (3) Another Achilles heel of currently used technology is the water washing step applied in the process to remove remaining glycerol, soap, catalyst, methanol, or salts from the alkyl esters. As mentioned earlier (implementation of water washing), this results in the generation of highly polluting wastewater, but also, to reach to standards, the remaining water needs to be removed, which deteriorates the energy balance of the process. (4) Finally, the issue of equipment corrosion has been controversial in the field of homogeneous catalysts.^{164,165}

A solution to these problems is to apply the heterogeneous catalytic process. This process includes the easier step of product separation because no catalyst residues are dispersed in the product phase. Moreover, because no water is used in the purification step, the heterogeneous catalytic transesterification process is more environmentally friendly.¹⁶⁶ In addition, the catalyst is not consumed and is easily regenerated, which is favorable for the whole process.¹⁶⁷

Heterogeneous catalysts are also relatively tolerant to high FFA and water content.¹⁶⁸ Several heterogeneous catalytic processes have been studied that could be classified into the categories of metal hydroxides, metal complexes, metal oxides, and supported catalysts.¹⁶⁹ Despite its simplicity and efficacy, heterogeneous catalytic esterification has a number of major drawbacks, i.e., diffusion limitations resulting in a lower reaction rate.¹⁷⁰ Moreover, although the possibility of being tailor-made is considered an advantage, the preparation and reaction conditions for heterogeneous catalysts are energy intensive.¹⁷¹ In some cases, lower catalytic activity compared with conventional homogeneous catalysts, partial dissolution, and lowered surface active area in the form of an active bed or cylinder were reported as challenging issues.¹⁷²

The other catalytic route is enzymatic transesterification that uses lipase mostly in a bioreactor or membrane bioreactor. Enzymes can be spread in the reactor's solvent medium or immobilized on support for interaction with substrates. In the case of a membrane bioreactor, immobilization of biochemical catalysts can also be performed on the membrane's surface. The mode of reactors can be fed batch or batch as well as continuous processes.^{157,173,174} Immobilized enzymes are normally used in different types of reactors such as fixed or fluidized bed reactors, stirred tanks, and, as previously stated, membrane reactors. The operation mode and unit operation system depend on the type of enzyme and its stability in the system when facing conditions such as a high flow rate as well as pressure and shear tensions.¹⁷⁵ Membrane reactors are highly recommended for glycerol separation in enzyme-immobilized systems^{176–178}; however, the high cost of membranes and membrane reactors make fixed bed reactors a much more convenient option.¹⁷⁵

The conversion mechanism of triglycerides to biodiesel with enzyme (lipase) follows the ping pong Bi Bi model. According to a comprehensive study by Al-Zuhair and coworkers,¹⁷⁹ active sites containing acidic or basic groups conduct the re-formation of the species by donating or accepting protons. For enzymes such as lipase, the reactions are performed using hydroxyl (–OH) groups as acceptors of protons or nucleophile sites whereas amine groups are required to accept and release protons (Figure 20.5).

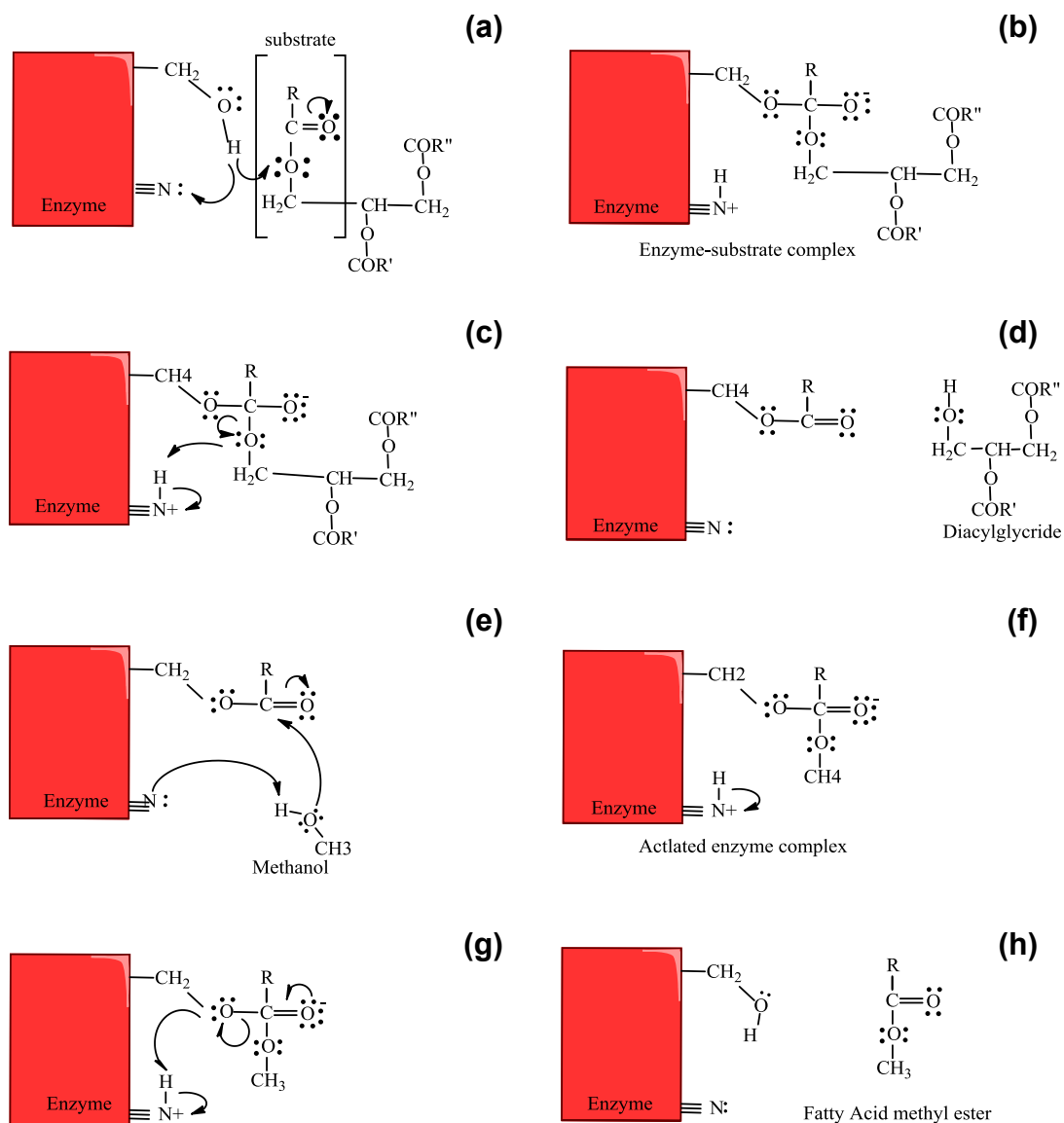
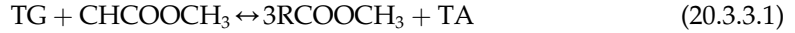
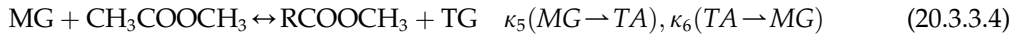
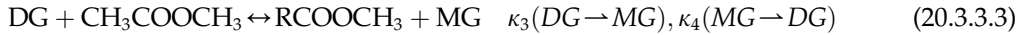
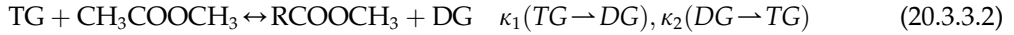


FIGURE 20.5 Schematic steps of enzymatic transesterification.

A report by Xu et al.¹⁸⁰ confirmed that there is a ping pong Bi Bi mechanism governing the reaction. Their simplified reaction kinetic hypothesis led to three consecutive second-order reactions (based on the intermediate species detected) that describe the transformation of triglyceride to FFA methyl ester. These reactions are shown in Figure 20.5 and Eqs (20.3.3.1–20.3.3.4).



Stepwise reactions:



Xu et al.¹⁸⁰ proposed the mechanism by taking some assumptions into consideration, including a negligible amount of water content and no hydrolysis reaction, no mass transfer resistance, and a concurrent action of enzyme on the acyl group.

$$\frac{d[\text{TG}]}{dt} = -\kappa_1[\text{TG}][\text{A}] + \kappa_2[\text{DG}][\text{ME}] \quad (20.3.3.5)$$

$$\frac{d[\text{DG}]}{dt} = \kappa_1[\text{TG}][\text{A}] - \kappa_2[\text{DG}][\text{ME}] - \kappa_3[\text{DG}][\text{A}] + \kappa_4[\text{MG}][\text{ME}] \quad (20.3.3.6)$$

$$\frac{d[\text{MG}]}{dt} = \kappa_3[\text{DG}][\text{A}] - \kappa_4[\text{MG}][\text{ME}] - \kappa_5[\text{MG}][\text{A}] + \kappa_6[\text{TA}][\text{ME}] \quad (20.3.3.7)$$

$$\frac{d[\text{ME}]}{dt} = \kappa_1[\text{TG}][\text{A}] - \kappa_4[\text{DG}][\text{ME}] + \kappa_3[\text{DG}][\text{A}] - \kappa_4[\text{MG}][\text{ME}] + \kappa_5[\text{MG}][\text{A}] - \kappa_6[\text{ME}] \quad (20.3.3.8)$$

$$\frac{d[\text{TA}]}{dt} = \frac{d[\text{ME}]}{dt} \quad (20.3.3.9)$$

$$\frac{d[\text{TA}]}{dt} = \kappa_3[\text{MG}][\text{A}] - \kappa_6[\text{TA}][\text{ME}] \quad (20.3.3.10)$$

After simplification:

$$\frac{d[\text{TG}]}{dt} = -\kappa_1[\text{TG}][\text{A}] + \kappa_2[\text{DG}][\text{ME}] \quad (20.3.3.11)$$

$$\frac{d[\text{TG} + \text{DG}]}{dt} = -\kappa_3[\text{DG}][\text{A}] + \kappa_4[\text{MG}][\text{ME}] \quad (20.3.3.12)$$

$$\frac{d[\text{TG} + \text{DG} + \text{MG}]}{dt} = -\kappa_5[\text{MG}][\text{A}] + \kappa_6[\text{TA}][\text{ME}] \quad (20.3.3.13)$$

As presented by Dossat et al.,¹⁸¹ this proposed simplified model is more suitable for batch and continuous scale-ups. Dossat and coworkers also reported the exclusion of *n*-hexane from the reaction medium. The organic solvent-free medium diminished disadvantages

such as toxicity, flammability, and a high cost while retaining all of the positive points.¹⁸¹ Based on the investigations into the effect of the reactant's concentration, it was shown that the inhibitory effect of alcohol, which was clear in the ping pong mechanism, could be lessened at a high concentration of substrates, i.e., triglycerides.¹⁸² A study by Al-Suhair¹⁸³ studied the same parameters for transesterification of waste cooking oil. The inhibitory effect of alcohol was more than with the other substrate. Cheirsilp and coworkers¹⁸⁴ also published efforts to find the best and the most holistic mechanism of enzymatically produced biodiesel from palm oil and ethanol. As claimed, the proposed model accounted for all of the concentration variations of different species beside the alcohol inhibitory effect.

Table 20.5 lists recent articles published on kinetics studies of enzymatic biodiesel production.

Beside catalytic procedures, there are other methods for performing transesterification, such as microwave irradiation,^{185–189} ultrasonic-assisted,^{190–194} and supercritical methanol,^{41,195–197} which can be used individually or coupled in a process. Figure 20.6 schematically presents the various steps involved in the conventional transesterification of an oil feedstock into biodiesel. Another alternative for the transesterification process is cracking of oils in the presence or absence of a catalyst.¹⁹⁸

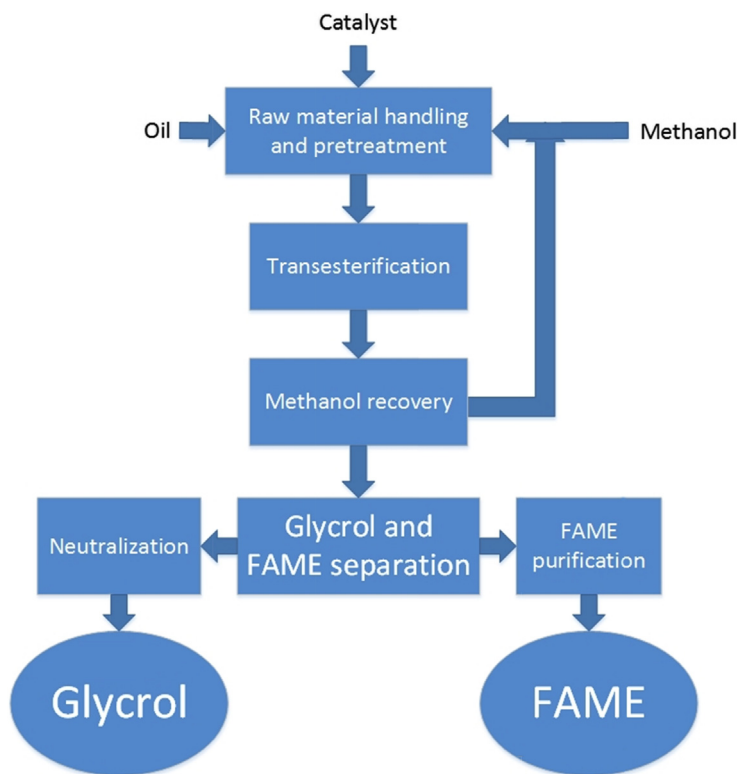


FIGURE 20.6 Schematic flowchart of biodiesel production.

TABLE 20.5 Kinetics studies reporting on enzymatic transesterification

[TG]	Enzyme	[A]	Base model for mechanism	Proposed equation	V_{\max}	Km [TG]	Km [A]	$K_{i \cdot A}$	$K_{i \cdot TG}$	References
Palm oil	Lipase (EC 3.1.1.3)	Methanol	Ping pong Bi Bi model	$\nu = \frac{V_{\max}}{1 + \left(\frac{K_{IA}}{[A]}\right) \left[1 + \left(\frac{[S]}{K_S}\right)\right] + \left(\frac{K_{IS}}{[S]}\right) \left[1 + \left(\frac{[A]}{K_A}\right)\right]}$	0.041 mol (cm min) ³	430 mol m ⁻³	350 mol m ⁻³	3.3×10^4 mol m ⁻³	4.45×10^4 mol m ⁻³	179
Soybean oil	Lipase (<i>Candida antarctica</i>)	Methyl acetate	Ping pong Bi Bi model	$\nu = \frac{V_{\max}[TG][A]}{K_S[A] \left(1 + \left(\frac{[A]}{K_A}\right)\right) + K_A[TG] + [TG][A]}$	1.9 mol min ⁻¹	1 mol	16 mol l ⁻¹	0.0455 mol l ⁻¹	—	180
Sunflower oil	Lipase (<i>Rhizomucor miehei lipozyme</i>)	Butanol	Ping pong Bi Bi model	$\nu = \frac{V_{\max}[TG][A]}{K_S[A] \left(1 + \left(\frac{[A]}{K_A}\right)\right) + K_A[TG] + [TG][A]}$	250 mMol min ⁻¹ g ⁻¹	5.4 mMol	55 mM	13 mM	—	181
Sunflower oil		Methanol	Ping pong Bi Bi model	$\nu = \kappa_6[E \cdot Bd] \frac{V_{\max}[S]}{1 + K_{IS} \left[\frac{[S]}{S}\right] + \frac{K_S}{[S]} \left(1 + \frac{[A]}{K_A}\right) + \frac{K_A}{[A]}}$	0.414 min ⁻¹	0.16 mol cm ⁻³	9.8×10^{-5} mol cm ⁻³	1.9 mol cm ⁻³	—	182
Waste cooking oil (from palm oil)	Lipase (<i>C. antarctica</i>)	Methanol	Ping pong Bi Bi model	$\nu = \frac{d[P]_i}{dt} = \frac{K[E]}{1 + (K_{IA}/[A]) [1 + ([S]/K_S)] + (K_{IS}/[S]i) \cdot [A]i/K_A}$	1.96 mol cm ⁻³ min ⁻¹	250 mol m ³	110 Mol/ m ³	3.5×10^4 mol m ³	2.8×10^4 mol m ⁻³	183

TG, triglyceride; A, alcohol; E, Enzyme; [], initial molar concentration; K_S , apparent Michaelis–Menten constant for triglycerides; K_A , apparent Michaelis–Menten constant for methyl acetate or alcohol; V_{\max} , initial maximum velocity of reaction; K_{IS} , inhibition constant of substrate, i.e., triglyceride; K_{IA} , inhibition constant of alcohol.

20.3.4 Biohydrogen

Owing to its high energy content ($122 \text{ KJ g}^{-1} \text{H}_2$) and almost zero emissions, biohydrogen is considered one of the best alternative energy carriers for petroleum-based fuels.¹⁹⁹ According to Chong et al.,²⁰⁰ biohydrogen can be produced through two different routes of photosynthesis and anaerobic acidogenesis processes (fermentation). Each process involves some microorganisms and feedstock. The hydrogen production yield by these processes depends on factors such as the type of microorganism, pH of the reaction environment,^{201,202} operation mode, operation temperature, both mesophilic (35°C)²⁰³ and thermophilic (50°C),²⁰⁴ and type and composition of the feedstock used.²⁰⁵ Feedstocks can be adjusted or optimized by adding nutrients.²⁰⁶

Dark fermentative biohydrogen production (which is the most frequently used process for biohydrogen production compared with light fermentation and photosynthesis²⁰⁷), can be performed using diverse groups of microorganisms that possess multi-enzyme systems, individually or through mixed cultures.¹⁹⁹ The process mainly consists of two steps: hydrolysis and acidogenesis. Organic acids and CO_2 are co-products of the process. From a hydrogen production aspect, mixed cultures of microorganisms are advantageous compared with monoculture ones. The possibility of investigating mixed feedstocks using continuous instead of batch processes and the likelihood of gaining higher yields owing to co-fermentation are advantages.¹⁹⁹ Just as in biomethane production, biohydrogen can be produced with mesophilic or thermophilic microorganisms. Higher hydrolysis activation levels, better pathogenic distribution, and a lower probability of contamination make extreme thermophilic ($70\text{--}80^\circ\text{C}$) pathways more attractive choices.¹⁹⁹ Increments in acetate production while eliminating butyrate, ethanol, and lactate may also explain the superiority of thermophilic microorganisms.²⁰⁸

During the anaerobic production mode, hydrogen is produced in the liquid phase and consumed by methanogenic microorganisms. To produce hydrogen efficiently in the gas phase, either these biohydrogen consumers must be eliminated or the reaction time should be shortened.^{209,210} The type of inocula, operating conditions, i.e., pH, temperature, hydrogen partial pressure, feed composition and nutrients, reactor residence time, and configuration affect parameters through the main process.²⁰⁷

20.3.5 Biogas and Biomethane

There are four main steps in biomethane production: hydrolysis, acidogenesis, acetogenesis/dehydrogenation, and methanation.^{211,212} As previously pointed out, from a residence time aspect, it is important to know what sort of feedstock is going to be consumed because the hydrolysis procedure depends on the molecular structure of the substrate. In fact, the duration of the conversion of conventional substrates increases according to the following order: carbohydrate (a few hours), proteins and lipids (a few days) and lignocellulose structures.²¹³ First, hydrolyzing and fermenting microorganisms attack the polymers and monomers. Microorganisms taking part in this step are anaerobes such as *Bacterioides*, *Clostridia*, and *Bifidobacteria*. During this step, acetate and hydrogen and varying amounts of volatile fatty acids such as propionate and butyrate are produced.²¹¹ Acetate and hydrogen are the byproducts of the hydrolysis step. Through the second step,

other anaerobic bacteria change the resultant compounds to short-chain organic acids, C₁–C₅ molecules (e.g., butyric, propionic, and acetic acids), alcohols, hydrogen, and carbon dioxide. At the third stage, products of the acidogenic phase are consumed as substrate by acetogenic bacteria, which produce hydrogen as a byproduct while acetic acid is also produced. High partial pressure of the hydrogen produced can hinder the rest of the bacteria's performance. Hence, hydrogen partial pressure is an operational condition that needs to be kept under certain levels. The fourth step involves the activity of a group of strictly anaerobic *archaea* called *methanogens* that perform methanation.²¹³ Microorganisms such as *Methanosarcina barkeri*, *Metanococcus mazei*, and *Methanosaeta concilii* are capable of converting either one or all of the produced materials into methane.²¹¹ The kinetics of the whole process is proportional to many parameters such as substrate, thermal and pH conditions of the fermenter, and the enzymes produced during the steps. A more detailed explanation of the metabolisms and kinetics of biomethane production can be found elsewhere.^{213,214}

Methanogenic fermentation can be performed using two modes of process: wet and dry digestion. Wet digestion includes the treatment of substrate with less than 10% solid content, which means that the media in the digester can be pumped and stirred. Dry digestion involves substrates with a solid content of 15% to 35%. A dry mode operation is usually set as a batch whereas the wet mode can be operated continuously.²¹³

20.4 INTENSIFICATION AND INTEGRATION

The integration of processes as a means to intensify production/purification processes leads to inevitable advantages such as a reduction in capital costs and energy use, decrement of utilities and structures, fewer process steps, lower physical volume, and, as the name clearly illustrates, a faster and intensified process and higher yields.^{215,216} According to a comprehensive chapter written by Sanchez et al.,²¹⁷ integration of bioethanol production processes can be classified into four main types: reaction–reaction integration, reaction–separation integration, separation–separation, and energy. The subject is discussed briefly here. Apart from the basic meaning of the “homogeneous” and “heterogeneous,” herein and during the description of process integration, processes with a reaction and separation/unit operation are called heterogeneous whereas processes with two reactions or two unit operations are referred to as homogeneous.²¹⁸

20.4.1 Reaction–Reaction Integration

Several examples of reaction–reaction integration are provided here for both first-generation ethanol based on starch, glucose, or biomass and second-generation ethanol from lignocellulosic resources. Homogeneous integration of ethanol production can be conducted during different steps of fermentation and biochemical transformation. A good example is integration of the detoxification section with pretreatment steps and fermentation. The idea of combining starch hydrolysis and glucose fermentation is the next homogeneous integration in bioethanol production (co-fermentation or simultaneous hydrolysis fermentation (SHF)). There are many routes by which this can be performed, such as conducting

both reactions in one reactor, finding one microorganism capable of doing both reactions, or genetically engineering one.^{219,220}

There are other homogeneous integration examples aside from the already commercialized SHF process, such as simultaneous saccharification fermentation, in which the degradation procedure of cellulose and the formation of polysaccharides are coupled with the fermentation of glucose. Although this integrated process leads to more convenient operating conditions and lower equipment requirements, the different optimum conditions (pH and temperature) of fermentation and degradation make the integrated process challenging to control.²²¹ Simultaneous saccharification and co-fermentation and consolidated bioprocessing (CPB) are two examples of integrated reaction–reaction ethanol production processes. The main difference between the CPB process and the others is the use of only one microorganism for the whole process.

20.4.2 Reaction-Separation Integration

Coupling separation with reactive processes may be considered a more practical integration owing to the significant lower cost of downstream separation and purification. Enzymatic hydrolysis joined to a separation process is the first instance offered in this category.²²² Membrane bioreactors with enzymes in the retentate side or immobilized on the membrane itself have been proven to act well because the catalytic activity is kept at a standard level while the enzyme is prevented from mixing with the products. The concept of a membrane reactor can also be used to remove ethanol from the culture broth, which shifts the reaction to a higher level as the inhibitory effects of alcohol are eliminated or decreased.²²³ Beside membrane reactors, the act of removing ethanol can also be carried out by other separation unit operations such as vacuum, vacuum distillation, membrane distillation, pervaporation, stripping, and solvent extraction.^{215,224–226}

20.4.3 Separation–Separation Integration

More recently developed separation technologies are the examples of the separation–separation integration mode, whose main purposes are to improve the level of purification and decrease the cost. The idea mainly consists of a membrane separation process coupled with an old one such as extraction or distillation.²²⁷

20.4.4 Energy Integration

The concept of energy integration in chemical engineering mainly comes from a technology called pinch, in which the heat streams of a process exchange energy values with others to minimize the energy demands of the process. With a more holistic viewpoint, energy integration can be defined as the generation and consumption of a process's electrical, mechanical, and thermal needs within the borders of the process itself. To this extent, there have also been other proposed types of technology. Cogeneration systems or combining heat and power generation and burning a portion of biomass are the examples of energy integration.^{228,229} In addition to the integration of these systems, the use of biofuels in CHP systems has been assessed.^{230–232}

Apart from these integration and intensification methods, there have been other integration strategies aimed at reducing the overall emission of biofuel production processes. Among those, carbon capture and storage (CCS) strategies have attracted a great deal of attention. Using CCS strategies, CO₂ from biofuel combustion or industrial processes can be captured, transported, and stored underground, in depleted oil and gas fields and deep saline formations. Therefore, CCS has a significant role in the global transition to a sustainable low-carbon economy.^{233–235}

20.5 ECONOMIC PERSPECTIVE

This section is devoted to a descriptive argument regarding the economic aspects of biofuel production. To begin, it is beneficial to highlight that each economic study has to consider all different aspects of a subject or to be holistic. There are four groups of aspects to be considered for biofuel production and use. The first is related to feedstock resources, which are known to be the most influential parameter on the final biofuel price.¹⁰⁵ This group mainly consists of factors such as land use and feedstock properties. The second group is the production process and technology,²³⁶ which cover upstream and downstream high-tech developments, operating and capital costs, and production capacity, i.e., the scale of the production plants. The third group, which is mostly neglected in economic studies, is byproducts.^{237,238} The fourth group is expense saved through the lessened amount of environmental contamination/emissions, and consequently through the savings of energy and money for human health care. To the best of our knowledge, until now, no published report has strived to put all of these data together.

Some of the data reported in the literature are presented here; the need to conduct holistic and comprehensive studies is strongly highlighted. According to a report by Demirbas, entitled “Political, economic and environmental impacts of biofuels: A review,”²³⁹ the final cost of a biofuel can vary based on the costs imposed by the conversion process, the scale of the production, and, of course, the feedstock used. For instance, bioethanol is more expensive compared with its petrochemical rival, gasoline, in most of the producing countries around the world. However, Brazil, which was previously introduced as the largest bioethanol producer in the world, owing to the large availability of cheap feedstock, i.e., sugar, has the most economic ethanol production. In fact, a bottom line must be considered in each country for oil prices below which biofuels cannot compete. For instance, whereas the oil price in the European Union must reach US \$70 so that bioethanol can be offered in a competitive environment, the price is said to be around US \$50–60 for the United States. For a country such as Brazil, with tropical weather and suitable conditions for providing raw materials, which reduce the main feedstock costs, the bottom line is reported to be US \$25 to US \$3/barrel of oil.

As expected, the size of the plant can also influence biofuel production costs. Larger-scale production plants can achieve lower final costs, which might be as high as 15–20% of the overall biofuel cost. A comprehensive comparison between different biofuels is offered in a book entitled *Biofuels—Global Impact on Renewable Energy*.²⁴⁰ The results of this comparison are summarized in Table 20.6. The comparison includes investment costs and process economies, all of which are based on the identical capacity of 45 MM gal biofuel per year. The data reported here were all obtained through simulations made with Aspen Plus software.

TABLE 20.6 Comparison between different biofuel production plants from an economic point of view²⁴¹

45 MM gal/yr biofuel	Corn ethanol	Sugarcane	Soybean diesel	Corn butanol	Corn stover ethanol (biochem)	Wood chips ethanol (thermochem)
Total production cost (M\$/yr)	74	58	121	88	64	58
Total project investment (M\$)	131	88	23	276	183	241
Production cost (\$/gal)	1.53	1.29	2.55	1.96	1.48	1.32
Energy density (BTU/gal)	76,330	76,330	119,550	99,837	76,330	76,330
Production cost with energy equivalent to gasoline(\$/gal)	2.33	1.95	2.48 (equivalent to gasoline) 2.74 (equivalent to diesel)	2.28	2.25	2.00

References

1. Rivard CJ. *Deploying anaerobic digesters: current status and future possibilities*. 1; 1996.
2. Abbasi T, Tauseef S, Abbasi SA. *Biogas energy*. Springer; 2011.
3. Qureshi N, Ezeji TC. *Biofuels, Bioprod Biorefin* 2008;**2**(4):319–30.
4. Zverlov V, Berezina O, Velikodvorskaya G, Schwarz W. *Appl Microbiol Biotechnol* 2006;**71**(5):587–97.
5. Lin L, Cunshan Z, Vittayapadung S, Xiangqian S, Mingdong D. *Appl Energy* 2011;**88**(4):1020–31.
6. Bajpai D, Tyagi V. *J Oleo Sci* 2006;**55**(10):487.
7. Happe T, Hemschemeier A, Winkler M, Kaminski A. *Trends Plant Sci* 2002;**7**(6):246–50.
8. Ghirardi ML, Zhang L, Lee JW, Flynn T, Seibert M, Greenbaum E, et al. *Trends Biotechnol* 2000;**18**(12):506–11.
9. Tomes DT. *Biofuels: global impact on renewable Energy, production agriculture, and technological advancements*. Springer; 2011.
10. Songstad D, Lakshmanan P, Chen J, Gibbons W, Hughes S, Nelson R. *Historical perspective of biofuels: learning from the past to rediscover the future*. *Biofuels*. Springer; 2011. p. 1–7.
11. Jordan-Korte K. *Government promotion of renewable energy technologies: policy approaches and market development in Germany, the United States, and Japan*. Springer; 2011.
12. Kaushal P, Abedi J. *J Ind Eng Chem* 2010;**16**(5):748–55.
13. Sørensen B. *Energy Policy* 1991;**19**(4):386–91.
14. Junginger M, Goh CS, Faaij A. *International Bioenergy Trade: History, status & outlook on securing sustainable bioenergy supply, demand and markets*. Springer; 2014.
15. Wiesenthal T, Leduc G, Christidis P, Schade B, Pelkmans L, Govaerts L, et al. *Renewable Sustainable Energy Rev* 2009;**13**(4):789–800.
16. Zhou A, Thomson E. *Appl Energy* 2009;**86**:S11–20.
17. Demirbas A. *Energy Convers Manage* 2008;**49**(8):2106–16.
18. Sorda G, Banse M, Kemfert C. *Energy Policy* 2010;**38**(11):6977–88.
19. Blanco Fonseca M, Burrell A, Gay SH, Henseler M, Kavallari A, Pérez Domínguez I, Tonini A. *Impacts of the EU biofuel target on agricultural markets and land use: a comparative modeling assessment, reference report by the joint centre of the European commission, institute for prospective technical studies*. 2010.
20. Blanco M, Adenauer M, Shrestha S, Becker A. *Methodology to assess EU biofuel policies: the CAPRI approach*. Institute for Prospective and Technological Studies, Joint Research Centre; 2012.

21. Gao Y, Skutsch M, Drigo R, Pacheco P, Masera O. *Appl Geogr* 2011;**31**(2):508–18.
22. Tschamntke T, Clough Y, Wanger TC, Jackson L, Motzke I, Perfecto I, et al. *Biol Conserv* 2012;**151**(1):53–9.
23. Ajanovic A. *Energy* 2011;**36**(4):2070–6.
24. Hertel T, Golub A, Jones A, O'Hare M, Plevin R, Kammen D. *Global land use and greenhouse gas emissions impacts of US Maize ethanol: the role of market-mediated responses*. Center for Global Trade Analysis, Department of Agricultural Economics, Purdue University; 2009.
25. Persson T, Garcia y, Garcia A, Paz J, Jones J, Hoogenboom G. *Agric Syst* 2009;**100**(1):11–21.
26. Grönröft A, Brosowski A, Meisel K, Müller-Langer F. *Sugar Ind-Zuckerind* 2013;**138**(4):208–14.
27. Erdei B, Galbe M, Zacchi G. *Biomass Bioenergy* 2013;**56**:506–14.
28. Zuurbier PJP, van de Vooren J. *Sugarcane ethanol: contributions to climate change mitigation and the environment*. Wageningen Academic Pub; 2008.
29. Quintero J, Montoya M, Sánchez O, Giraldo O, Cardona C. *Energy* 2008;**33**(3):385–99.
30. Goldemberg J, Coelho ST, Guardabassi P. *Energy Policy* 2008;**36**(6):2086–97.
31. Jaggard K, Townsend B. *Biofuel cropping systems: carbon, land and food*. p.138; 2014.
32. Langeveld J, Ven G V d, Vries SCD, Brink L V d, Visser CD. *Int J Sustain Dev* 2014;**17**(1):78–88.
33. Gheewala SH, Bonnet S, Silalertruksa T. *Bulbous plants: biotechnology*. p.177; 2013.
34. Dai D, Hu Z, Pu G, Li H, Wang C. *Energy Convers Manage* 2006;**47**(13):1686–99.
35. Torres CF, Munir F, Otero C, Hill Jr CG. *J Am Oil Chem Soc* 2002;**79**(8):775–81.
36. Mojović L, Nikolić S, Rakin M, Vukasinović M. *Fuel* 2006;**85**(12):1750–5.
37. Shapouri H, Duffield JA, Wang MQ. *The energy balance of corn ethanol: an update*. United States Department of Agriculture, Economic Research Service; 2002.
38. Bothast R, Schlicher M. *Appl Microbiol Biotechnol* 2005;**67**(1):19–25.
39. Ghobadian B, Rahimi H, Tavakkoli Hashjin T, Khatamifar M. *J Agric Sci Technol* 2010;**10**:225–32.
40. Mittelbach M. *J Am Oil Chem Soc* 1990;**67**(3):168–70.
41. Demirbas A. *Energy Convers Manage* 2007;**48**(3):937–41.
42. Di Serio M, Ledda M, Cozzolino M, Minutillo G, Tesser R, Santacesaria E. *Ind Eng Chem Res* 2006;**45**(9):3009–14.
43. Garcia CM, Teixeira S, Marciniuk LL, Schuchardt U. *Bioresour Technol* 2008;**99**(14):6608–13.
44. Ebrahimi S, Amini G, Younesi H, Najafpour GD. *Middle-East J Sci Res* 2012;**11**(10):1323–7.
45. Leclercq E, Finiels A, Moreau C. *J Am Oil Chem Soc* 2001;**78**(11):1161–5.
46. Kusdiana D, Saka S. *Fuel* 2001;**80**(5):693–8.
47. Li L, Du W, Liu D, Wang L, Li Z. *J Mol Catal B: Enzym* 2006;**43**(1):58–62.
48. Abdullah A, Salamatina B, Mootabadi H, Bhatia S. *Energy Policy* 2009;**37**(12):5440–8.
49. Foon CS, May CY, Liang YC, Ngan MA, Basiron Y. Malaysian palm oil board. *Palm Oil Dev* 2005;**42**:28–34.
50. Naik S, Goud VV, Rout PK, Dalai AK. *Renewable Sustainable Energy Rev* 2010;**14**(2):578–97.
51. Ndegwa G, Moraa V, Jamnadass R, Mowo J, Nyabenge M, Iiyama M. Potential for biofuel feedstock in Kenya. ICRAF Working Paper, 2011.
52. Balat M, Balat H. *Appl Energy* 2009;**86**(11):2273–82.
53. Farrell AE, Plevin RJ, Turner BT, Jones AD, O'hare M, Kammen DM. *Science* 2006;**311**(5760):506–8.
54. Kinney A, Clemente T. *Fuel Process Technol* 2005;**86**(10):1137–47.
55. Vasudevan PT, Briggs M. *J Ind Microbiol Biotechnol* 2008;**35**(5):421–30.
56. Mushrush GW, Beal EJ, Hughes JM, Wynne JH, Sakran JV, Hardy DR. *Ind Eng Chem Res* 2000;**39**(10):3945–8.
57. Petit H, Germiquet C, Lebel D. *J Dairy Sci* 2004;**87**(11):3889–98.
58. Chang J, Lunt DK, Smith SB. *J Nutr* 1992;**122**(11):2074–80.
59. Crabbe E, Nolasco-Hipolito C, Kobayashi G, Sonomoto K, Ishizaki A. *Process Biochem* 2001;**37**(1):65–71.
60. Mohammadi M, Mohamed AR, Najafpour GD, Younesi H, Uzir MH. *Sci World J* 2014;**2014**.
61. Mohammadi M, Najafpour GD, Younesi H, Lahijani P, Uzir MH, Mohamed AR. *Renewable Sustainable Energy Rev* 2011;**15**(9):4255–73.
62. Sharma Y, Singh B, Madhu D, Liu Y, Yaakob Z. Fast Synthesis of High Quality Biodiesel from 'Waste Fish Oil' by Single Step Transesterification. *Biofuel research journal* 2014;**3**:78–80.
63. Levin DB, Carere CR, Cicek N, Sparling R. *Int J Hydrogen Energy* 2009;**34**(17):7390–403.
64. Cheng C-L, Lo Y-C, Lee K-S, Lee D-J, Lin C-Y, Chang J-S. *Bioresour Technol* 2011;**102**(18):8514–23.
65. Sulaiman A, Hassan MA, Shirai Y, Abd-Aziz S, Tabatabaei M, Busu Z, et al. *Aust J Basic Appl Sci* 2009;**3**(3).
66. Das D, Veziroğlu TN. *Int J Hydrogen Energy* 2001;**26**(1):13–28.

67. Liu C-z, Cheng X-y. *Int J Hydrogen Energy* 2010;**35**(17):8945–52.
68. Kongjan P, Angelidaki I. *Bioresour Technol* 2010;**101**(20):7789–96.
69. Shi XX, Song HC, Wang CR, Tang RS, Huang ZX, Gao TR, et al. *Int J Energy Res* 2010;**34**(8):662–72.
70. Cui M, Yuan Z, Zhi X, Wei L, Shen J. *Int J Hydrogen Energy* 2010;**35**(9):4041–7.
71. Cui M, Yuan Z, Zhi X, Shen J. *Int J Hydrogen Energy* 2009;**34**(19):7971–8.
72. Kongjan P, Min B, Angelidaki I. *Water Res* 2009;**43**(5):1414–24.
73. Lo Y-C, Lu W-C, Chen C-Y, Chang J-S. *Bioresour Technol* 2010;**101**(15):5885–91.
74. Lalaurette E, Thammannagowda S, Mohagheghi A, Maness P-C, Logan BE. *Int J Hydrogen Energy* 2009;**34**(15):6201–10.
75. Kim JK, Nhat L, Chun YN, Kim SW. *Biotechnol Bioprocess Eng* 2008;**13**(4):499–504.
76. Kumar N, Das D. *Enzyme Microb Technol* 2001;**29**(4):280–7.
77. Cao G, Ren N, Wang A, Lee D-J, Guo W, Liu B, et al. *Int J Hydrogen Energy* 2009;**34**(17):7182–8.
78. Li D, Chen H. *Int J Hydrogen Energy* 2007;**32**(12):1742–8.
79. Pattrra S, Sangyoka S, Boonmee M, Reungsang A. *Int J Hydrogen Energy* 2008;**33**(19):5256–65.
80. Panagiotopoulos I, Bakker R, De Vrije T, Koukios E, Claassen P. *Int J Hydrogen Energy* 2010;**35**(15):7738–47.
81. Mars AE, Veuskens T, Budde MA, Van Doeveren PF, Lips SJ, Bakker RR, et al. *Int J Hydrogen Energy* 2010;**35**(15):7730–7.
82. Ueno Y, Fukui H, Goto M. *Environ Sci Technol* 2007;**41**(4):1413–9.
83. Lo Y-C, Saratale GD, Chen W-M, Bai M-D, Chang J-S. *Enzyme Microb Technol* 2009;**44**(6):417–25.
84. de Vrije T, Bakker RR, Budde MA, Lai MH, Mars AE, Claassen PA. *Biotechnol Biofuels* 2009;**2**(1):12.
85. Lo Y-C, Su Y-C, Cheng C-L, Chang J-S. *Int J Hydrogen Energy* 2011;**36**(21):13955–63.
86. Gunaseelan VN. *Biomass Bioenergy* 2004;**26**(4):389–99.
87. Pakarinen O, Tähti H, Rintala J. *Biomass Bioenergy* 2009;**33**(10):1419–27.
88. Xiao W, Clarkson WW. *Biodegradation* 1997;**8**(1):61–6.
89. Kaparaju P, Serrano M, Thomsen AB, Kongjan P, Angelidaki I. *Bioresour Technol* 2009;**100**(9):2562–8.
90. Bruni E, Jensen AP, Pedersen ES, Angelidaki I. *Appl Energy* 2010;**87**(7):2212–7.
91. Bauer A, Bösch P, Friedl A, Amon T. *J Biotechnol* 2009;**142**(1):50–5.
92. Dinuccio E, Balsari P, Gioelli F, Menardo S. *Bioresour Technol* 2010;**101**(10):3780–3.
93. Teghammar A, Yngvesson J, Lundin M, Taherzadeh MJ, Horváth IS. *Bioresour Technol* 2010;**101**(4):1206–12.
94. Romano RT, Zhang R, Teter S, McGarvey JA. *Bioresour Technol* 2009;**100**(20):4564–71.
95. Zheng M, Li X, Li L, Yang X, He Y. *Bioresour Technol* 2009;**100**(21):5140–5.
96. Rabelo S, Carrere H, Maciel Filho R, Costa A. *Bioresour Technol* 2011;**102**(17):7887–95.
97. Openshaw K. *Biomass Bioenergy* 2000;**19**(1):1–15.
98. Pramanik K. *Renew Energy* 2003;**28**(2):239–48.
99. Zhang Y, Dube M, McLean D, Kates M. *Bioresour Technol* 2003;**89**(1):1–16.
100. Kulkarni MG, Dalai AK. *Indu Eng Chem Res* 2006;**45**(9):2901–13.
101. Phan AN, Phan TM. *Fuel* 2008;**87**(17):3490–6.
102. Pazouki M, Zamani F, Zamzaman AH, Fahar M, Najafpour G. *World Appl Sci J* 2010;**8**(6):719–24.
103. Karmakar A, Karmakar S, Mukherjee S. *Bioresour Technol* 2010;**101**(19):7201–10.
104. Hillion G, Leporq S, Rouxel JJ, Stern R. Process for the production of esters from vegetable oils or animal oils alcohols. Google Patents, 1999.
105. Zhang Y, Dube M, McLean D, Kates M. *Bioresour Technol* 2003;**90**(3):229–40.
106. Marchetti JM. *Process Saf Environ Prot* 2012;**90**(3):157–63.
107. Pittman JK, Dean AP, Osundeko O. *Bioresour Technol* 2011;**102**(1):17–25.
108. Mondala A, Liang K, Toghiani H, Hernandez R, French T. *Bioresour Technol* 2009;**100**(3):1203–10.
109. Dufreche S, Hernandez R, French T, Sparks D, Zappi M, Alley E. *J Am Oil Chem Soc* 2007;**84**(2):181–7.
110. Francioso O, Rodriguez-Estrada MT, Montecchio D, Salomoni C, Caputo A, Palenzona D. *J Hazard Mater* 2010;**175**(1):740–6.
111. Jetten MS, Horn SJ, van Loosdrecht M. *Water Sci Technol* 1997;**35**(9):171–80.
112. Beetul K, Bibi Sadally S, Taleb-Hossenkhan N, Bhagooli R, Puchooa D. An investigation of biodiesel production from microalgae found in Mauritian waters. *Biofuel Research Journal* 2014;**2**:58–64.
113. Biello D. *Sci Am* 2010;**302**(4):21–2.

114. Tabatabaei M, Tohidfar M, Jouzani GS, Safarnejad M, Pazouki M. *Renewable Sustainable Energy Rev* 2011;**15**(4):1918–27.
115. Singh A, Olsen SI, Nigam PS. *J Chem Technol Biotechnol* 2011;**86**(11):1349–53.
116. Mata TM, Martins AA, Caetano NS. *Renewable Sustainable Energy Rev* 2010;**14**(1):217–32.
117. Adams JM, Gallagher JA, Donnison IS. *J Appl Phycol* 2009;**21**(5):569–74.
118. Harun R, Danquah MK, Forde GM. *J Chem Technol Biotechnol* 2010;**85**(2):199–203.
119. John RP, Anisha G, Nampoothiri KM, Pandey A. *Bioresour Technol* 2011;**102**(1):186–93.
120. Wargacki AJ, Leonard E, Win MN, Regitsky DD, Santos CNS, Kim PB, et al. *Science* 2012;**335**(6066):308–13.
121. Li Y, Horsman M, Wu N, Lan CQ, Dubois-Calero N. *Biotechnol Prog* 2008;**24**(4):815–20.
122. Paulo C, Estrada V, Di Maggio J, Diaz M. *Comput Aided Chem Eng* 2011;**29**:1366–71.
123. Aikawa S, Joseph A, Yamada R, Izumi Y, Yamagishi T, Matsuda F, et al. *Energy Environ Sci* 2013;**6**(6):1844–9.
124. Gao Z, Zhao H, Li Z, Tan X, Lu X. *Energy Environ Sci* 2012;**5**(12):9857–65.
125. Heidorn T, Camsund D, Huang H-H, Lindberg P, Oliveira P, Stensjö K, et al. *Methods Enzymol* 2010;**497**: 539–79.
126. Ruffing AM. *Engineered cyanobacteria*; 2011. landesbioscience.com.
127. Demirbas MF. *Appl Energy* 2011;**88**(10):3473–80.
128. Chisti Y. *Biotechnol Adv* 2007;**25**(3):294–306.
129. Wang C, Chen L, Rakesh B, Qin Y, Lv R. *Front Energy* 2012;**6**(3):266–74.
130. Meng X, Yang J, Xu X, Zhang L, Nie Q, Xian M. *Renew Energy* 2009;**34**(1):1–5.
131. Li Q, Du W, Liu D. *Appl Microbiol Biotechnol* 2008;**80**(5):749–56.
132. Klein-Marcuschamer D, Chisti Y, Benemann JR, Lewis D. *Biotechnol Bioeng* 2013;**110**(9):2317–22.
133. Singh J, Gu S. *Renewable Sustainable Energy Rev* 2010;**14**(9):2596–610.
134. Gray D, White C, Tomlinson G. *Increasing security and reducing carbon emissions of the US transportation sector: a transformational role for coal with biomass*; 2007.
135. Nigam PS, Singh A. *Prog Energy Combust Sci* 2011;**37**(1):52–68.
136. Awudu I, Zhang J. *Renewable Sustainable Energy Rev* 2012;**16**(2):1359–68.
137. Gupta VK, Tuohy MG. *Biofuel technologies: recent developments*. Springer; 2013.
138. Tomes D, Lakshmanan P, Songstad D. *Biofuels: global impact on renewable energy, production agriculture, and technological advancements*; 2010.
139. Onuki S. *Bioethanol: industrial production process and recent studies*; 2006.
140. Van Der Maarel MJ, Van Der Veen B, Uitdehaag J, Leemhuis H, Dijkhuizen L. *J Biotechnol* 2002;**94**(2):137–55.
141. Dürre P. *Curr Opin Biotechnology* 2011;**22**(3):331–6.
142. Lütke-Eversloh T, Bahl H. *Curr Opin Biotechnology* 2011;**22**(5):634–47.
143. Nielsen DR, Leonard E, Yoon S-H, Tseng H-C, Yuan C, Prather KLJ. *Metab Eng* 2009;**11**(4):262–73.
144. Shen CR, Liao JC. *Metab Eng* 2008;**10**(6):312–20.
145. Steen EJ, Chan R, Prasad N, Myers S, Petzold CJ, Redding A, et al. *Microb Cell Fact* 2008;**7**(1):36.
146. Liu S, Liu G, Zhao X, Jin W. *J Membr Sci* 2013;**446**:181–8.
147. Oh PP, Lau HLN, Chen J, Chong MF, Choo YM. *Renewable Sustainable Energy Rev* 2012;**16**(7):5131–45.
148. Ferella F, Mazzotti Di Celso G, De Michelis I, Stanisci V, Vegliò F. *Fuel* 2010;**89**(1):36–42.
149. Melero JA, Iglesias J, Morales G. *Green Chem* 2009;**11**(9):1285–308.
150. Kawashima A, Matsubara K, Honda K. *Bioresour Technol* 2008;**99**(9):3439–43.
151. Mohadesi M, Hojabri Z, Moradi G. biodiesel production using alkali earth metal oxides catalysts synthesized by sol-gel method. *Biofuel research journal* 2014;**1**:30–3.
152. Akia M, Yazdani F, Motae E, Han D, Arandiyani H. A review on conversion of biomass to biofuel by nanocatalysts. *Biofuel Research Journal* 2014;**1**:16–25.
153. Szczesna Antczak M, Kubiak A, Antczak T, Bielecki S. *Renewable Energy* 2009;**34**(5):1185–94.
154. Xu Y, Du W, Liu D, Zeng J. *Biotechnol Lett* 2003;**25**(15):1239–41.
155. Fjerbaek L, Christensen KV, Norddahl B. *Biotechnol Bioeng* 2009;**102**(5):1298–315.
156. Ranganathan SV, Narasimhan SL, Muthukumar K. *Bioresour Technol* 2008;**99**(10):3975–81.
157. Nielsen PM, Brask J, Fjerbaek L. *Eur J Lipid Sci Technol* 2008;**110**(8):692–700.
158. Hasheminejad M, Tabatabaei M, Mansourpanah Y, Javani A. *Bioresour Technol* 2011;**102**(2):461–8.
159. Vicente G, Martnez M, Aracil J. *Bioresour Technol* 2004;**92**(3):297–305.
160. Lam MK, Lee KT, Mohamed AR. *Biotechnol Adv* 2010;**28**(4):500–18.

161. Felizardo P, Neiva Correia MJ, Raposo I, Mendes JF, Berkemeier R, Bordado JM. *Waste Manage* 2006;**26**(5):487–94.
162. Jacobson K, Gopinath R, Meher LC, Dalai AK. *Appl Catal B: Environ* 2008;**85**(1):86–91.
163. Wang Y, Ou S, Liu P, Xue F, Tang S. *J Mol Catal A: Chem* 2006;**252**(1):107–12.
164. Canakci M, Van Gerpen J. *Trans ASAE* 1999;**42**(5):1203–10.
165. Carmo AC, de Souza LK, da Costa CE, Longo E, Zamian JR, da Rocha Filho GN. *Fuel* 2009;**88**(3):461–8.
166. Dossin TF, Reyniers M-F, Berger RJ, Marin GB. *Appl Catal B: Environ* 2006;**67**(1):136–48.
167. Chouhan A, Sarma A. *Renewable Sustainable Energy Rev* 2011.
168. Endalew AK, Kiros Y, Zanzi R. *Biomass Bioenergy* 2011;**35**(9):3787–809.
169. Zabeti M, Wan Daud WMA, Aroua MK. *Fuel Process Technol* 2009;**90**(6):770–7.
170. Mbaraka IK, Shanks BH. *J Am Oil Chemists' Soc* 2006;**83**(2):79–91.
171. Sharma YC, Singh B, Korstad J. *Fuel* 2011;**90**(4):1309–24.
172. Kurayama F, Yoshikawa T, Handa H, Furusawa T, Bahadur NM, Sato M, et al. *Bioresour Technol* 2012.
173. Ko MJ, Park HJ, Hong SY, Yoo YJ. *Bioprocess Biosyst Eng* 2012;**35**(1–2):69–75.
174. Machsun AL, Gozan M, Nasikin M, Setyahadi S, Yoo YJ. *Biotechnol Bioprocess Eng* 2010;**15**(6):911–6.
175. Jegannathan KR, Abang S, Poncelet D, Chan ES, Ravindra P. *Crit Rev Biotechnol* 2008;**28**(4):253–64.
176. Saleh J, Tremblay AY, Dubé MA. *Fuel* 2010;**89**(9):2260–6.
177. Gomes MCS, Arroyo PA, Pereira NC. *J Membr Sci* 2011;**378**(1):453–61.
178. Molinari R, Santoro ME, Drioli E. *Ind Eng Chem Res* 1994;**33**(11):2591–9.
179. Al-Zuhair S, Ling FW, Jun LS. *Process Biochem* 2007;**42**(6):951–60.
180. Xu Y, Du W, Liu D. *J Mol Catal B: Enzym* 2005;**32**(5):241–5.
181. Dossat V, Combes D, Marty A. *Enzyme Microb Technol* 2002;**30**(1):90–4.
182. Al-Zuhair S. *Biotechnol Prog* 2005;**21**(5):1442–8.
183. Al-Zuhair S, Dowaidar A, Kamal H. *Biochem Eng J* 2009;**44**(2):256–62.
184. Cheirsilp B. *Biochem Eng J* 2008;**42**(3):261–9.
185. Zhang S, Zu Y-G, Fu Y-J, Luo M, Zhang D-Y, Efferth T. *Bioresour Technol* 2010;**101**(3):931–6.
186. Azcan N, Danisman A. *Fuel* 2008;**87**(10):1781–8.
187. Perin G, Álvaro G, Westphal E, Viana L, Jacob R, Lenardão E, et al. *Fuel* 2008;**87**(12):2838–41.
188. Hsiao M-C, Lin C-C, Chang Y-H. *Fuel* 2011;**90**(5):1963–7.
189. Kumar R, Ravi Kumar G, Chandrashekar N. *Bioresour Technol* 2011;**102**(11):6617–20.
190. Kumar D, Kumar G, Singh C. *Ultrason Sonochem* 2010;**17**(5):839–44.
191. Mootabadi H, Salamatinia B, Bhatia S, Abdullah AZ. *Fuel* 2010;**89**(8):1818–25.
192. Veljković VB, Avramović JM, Stamenković OS. *Renewable Sustainable Energy Rev* 2012;**16**(2):1193–209.
193. Stavarache C, Vinatoru M, Maeda Y. *Ultrason Sonochem* 2007;**14**(3):380–6.
194. Kumar D, Kumar G, Singh C. *Ultrason Sonochem* 2010;**17**(3):555–9.
195. Demirbas A. *Energy Convers Manag* 2009;**50**(4):923–7.
196. Hawash S, Kamal N, Zaher F, Kenawi O, Diwani GE. *Fuel* 2009;**88**(3):579–82.
197. Song E-S, Lim J-w, Lee H-S, Lee Y-W. *J Supercrit Fluids* 2008;**44**(3):356–63.
198. Xu J, Jiang J, Chen J, Sun Y. *Bioresour Technol* 2010;**101**(14):5586–91.
199. Kongjan P, Kotay M, Min B, Angelidaki I. *Biotechnol Bioeng* 2010;**105**(5):899–908.
200. Chong M-L, Sabaratnam V, Shirai Y, Hassan MA. *Int J Hydrogen Energy* 2009;**34**(8):3277–87.
201. Ginkel SV, Sung S, Lay J-J. *Environ Sci Technol* 2001;**35**(24):4726–30.
202. Skonieczny MT, Yargeau V. *Int J Hydrogen Energy* 2009;**34**(8):3288–94.
203. Hawkes FR, Hussy I, Kyazze G, Dinsdale R, Hawkes DL. *Int J Hydrogen Energy* 2007;**32**(2):172–84.
204. Valdez-Vazquez I, Ríos-Leal E, Esparza-García F, Cecchi F, Poggi-Valardo HM. *Int J Hydrogen Energy* 2005;**30**(13):1383–91.
205. Pan C, Fan Y, Xing Y, Hou H, Zhang M. *Bioresour Technol* 2008;**99**(8):3146–54.
206. Van Ginkel SW, Oh S-E, Logan BE. *Int J Hydrogen Energy* 2005;**30**(15):1535–42.
207. Khanal SK. *Anaerobic biotechnology for bioenergy production: principles and applications*. p. 189–219; 2008.
208. Karadag D, Mäkinen AE, Efimova E, Puhakka JA. *Bioresour Technol* 2009;**100**(23):5790–5.
209. Chen C-C, Lin C-Y, Lin M-C. *Appl Microbiol Biotechnol* 2002;**58**(2):224–8.
210. De Vrije T, Claassen P. *Bio-methane & bio-hydrogen*. p. 103–23; 2003.
211. Weiland P. *Appl Microbiol Biotechnol* 2010;**85**(4):849–60.

212. Tabatabaei M, Sulaiman A, Nikbakht AM, Yusof N, Najafpour G. *Influential parameters on biomethane generation in anaerobic wastewater treatment plants*. InTech; 2011.
213. Deublein D, Steinhauser A. *Biogas from waste and renewable resources: an introduction*. John Wiley & Sons; 2011.
214. Grieder C, Mittweg G, Dhillon BS, Montes JM, Orsini E, Melchinger AE. *Biomass Bioenergy* 2012;**37**:132–41.
215. Cardona CA, Sánchez Ó. *J Bioresour Technol* 2007;**98**(12):2415–57.
216. Hahn-Hägerdal B, Galbe M, Gorwa-Grauslund M-F, Lidén G, Zacchi G. *Trends Biotechnol* 2006;**24**(12):549–56.
217. Sánchez OJ, Montoya S. *Production of bioethanol from biomass: an overview*. *Biofuel technologies*. Springer; 2013. p. 397–441.
218. Cardona C, Sánchez O. Analysis of integrated flow sheets for biotechnological production of fuel ethanol. *Energy* 2006;**31**:2447–59.
219. Zaldivar J, Nielsen J, Olsson L. *Appl Microbiol Biotechnol* 2001;**56**(1–2):17–34.
220. Lynd LR, Weimer PJ, Van Zyl WH, Pretorius IS. *Microbiol Mol Biol Rev* 2002;**66**(3):506–77.
221. Claassen P, Van Lier J, Contreras AL, Van Niel E, Sijtsma L, Stams A, et al. *Appl Microbiol Biotechnol* 1999;**52**(6):741–55.
222. Gan Q, Allen S, Taylor G. *Biochem Eng J* 2002;**12**(3):223–9.
223. Biofuels Al-Zuhair S. *Bioprod Biorefin* 2007;**1**(1):57–66.
224. O’Brien DJ, Roth LH, McAloon AJ. *J Membr Sci* 2000;**166**(1):105–11.
225. Mazubert A, Poux M, Aubin J. *Chem Eng J* 2013;**233**:201–23.
226. Esfahanian M, Ghorbanfarahi A, Ghoreyshi A, Najafpour G, Younesi H, Ahmad A. *Int J Eng-Trans B: Appl* 2012;**25**(4):249.
227. He H, Guo X, Zhu S. *J Am Oil Chem Soc* 2006;**83**(5):457–60.
228. Bolhàr-Nordenkamp M, Rauch R, Bosch K, Aichernig C, Hofbauer H, Kirtikara. K. 2nd RCETCE, Phuket, Thailand 2003. p. 567–572.
229. Obernberger I, Thonhofer P, Reisenhofer E. *Euroheat Power* 2002;**10**:1–17.
230. Eriksson G, Kjellström B. *Appl Energy* 2010;**87**(12):3632–41.
231. Dong L, Liu H, Riffat S. *Appl Therm Eng* 2009;**29**(11):2119–26.
232. Marbe Å, Harvey S, Berntsson T. *Energy* 2004;**29**(8):1117–37.
233. Lindfeldt EG, Westermarck MO. *Energy Procedia* 2009;**1**(1):4111–8.
234. Rhodes JS, Keith DW. *Biomass Bioenergy* 2005;**29**(6):440–50.
235. Pettersson K, Harvey S. *Energy* 2010;**35**(2):1101–6.
236. Shirazi MMA, Kargari A, Tabatabaei M, Mostafaeid B, Akia M, Barkhi M, et al. *Bioresour Technol* 2013;**134**:401–6.
237. Javani A, Hasheminejad M, Tahvildari K, Tabatabaei M. *Bioresour Technol* 2012;**104**:788–90.
238. Sulaiman A, Othman N, Baharuddin AS, Mokhtar MN, Tabatabaei M. *Procedia-Soc Behav Sci* 2014;**121**:35–43.
239. Demirbas A. *Appl Energy* 2009;**86**:S108. S17.
240. Tomes D, Lakshmanan P, Songstad D. *Biofuels: global impact on renewable energy, production agriculture, and technological advancements*. Springer; 2010.
241. Tao L, Aden A. *Vitro Cell Dev Biol-Plant* 2009;**45**(3):199–217.

Appendix

CONSTANTS AND CONVERSION FACTORS

Power	W	cal/s	kcal/h	Btu/s	Btu/h	lb _f ft/s	hp
1 W	1	0.239	0.8604	9.478×10^{-4}	3.412	0.7376	1.341×10^{-3}
1 cal/s	4.18	1	3.6	3.966×10^{-3}	14.276	3.086	5.611×10^{-3}
1 kcal/h	1.1622	0.2778	1	1.102×10^{-3}	3.966	0.857	1.559×10^{-3}
1 Btu/s	1055	252	907.78	1	3600	778	1.415
1 Btu/h	0.293	0.07	0.252	2.78×10^{-4}	1	0.216	3.93×10^{-4}
1 lb _f ft/s	1.356	0.324	1.167	1.285×10^{-3}	4.63	1	1.818×10^{-3}
1 hp	746	178.2	642	0.707	2540	550	1

Energy	J	cal	Btu	lb _f ft	Kw h	Hp h	erg
1 J	1	0.239	9.478×10^{-4}	0.738	2.778×10^{-7}	3.725×10^{-7}	1×10^7
1 cal	4.184	1	3.966×10^{-3}	3.086	1.162×10^{-4}	1.559×10^{-6}	4.18×10^7
1 Btu	1055	252	1	778	2.93×10^{-4}	3.93×10^{-4}	1.055×10^{10}
1 lb _f ft	1.356	0.324	1.285×10^{-3}	1	3.766×10^{-7}	5.05×10^{-7}	1.356×10^7
1 kw h	3.6×10^6	8.6×10^5	3412	2.655×10^6	1	1.341	3.6×10^{13}
1 hp h	2.68×10^6	6.42×10^6	2.54×10^3	1.98×10^6	0.7457	1	2.6845×10^{13}
1 erg	1×10^{-7}	2.39×10^{-8}	9.478×10^{-11}	7.376×10^{-8}	2540	3.72×10^{-4}	1

Pressure	Pa	bar	atm	Torr (mmHg)	Psi
1 Pa	1	1×10^{-5}	9.876×10^{-6}	7.5×10^{-3}	1.45×10^{-4}
1 bar	1×10^5	1	0.987	750	14.5
1 atm	1.013×10^5	1.013	1	760	14.7
1 Torr (mmHg)	133.3	1.33×10^3	1.316×10^{-3}	1	1.934×10^{-2}
1 Psi	6.9×10^3	1.488×10^{-5}	6.8×10^{-2}	51.7	1

PHYSICAL CONSTANTS AND CONVERSION FACTORS

Ideal gas law constant, <i>R</i>	8.314 J mol ⁻¹ K ⁻¹
	1.987 cal mol ⁻¹ K ⁻¹
	82.058 cm ³ atm mol ⁻¹ K ⁻¹
	8.317 erg g mol ⁻¹ K ⁻¹
	0.082057 L atm g mol ⁻¹ K ⁻¹
	62.361 L mmHg g mol ⁻¹ K ⁻¹
	0.0848 kg _f cm ⁻² L g mol ⁻¹ K ⁻¹
	998.9 mmHg ft ³ lbmol ⁻¹ K ⁻¹
	1.314 atm ft ³ lbmol ⁻¹ K ⁻¹
	1.986 Btu lbmol ⁻¹ R ⁻¹
	7.805 × 10 ⁻⁴ hp h lbmol ⁻¹ R ⁻¹
	5.819 × 10 ⁻⁴ kW h lbmol ⁻¹ R ⁻¹
	0.7302 atm ft ³ lbmol ⁻¹ R ⁻¹
	555 mmHg ft ³ lbmol ⁻¹ R ⁻¹
	10.73 Psi ft ³ lbmol ⁻¹ R ⁻¹
	1545.3 lb _f ft lbmol ⁻¹ R ⁻¹
	1.851 × 10 ⁴ lb _f in lbmol ⁻¹ R ⁻¹

CONVERSION FACTORS

Given a quantity	Multiply by	To get quantity
US gallons	3.785	Liters
Cubic feet	28.316	Liters
Meters	39.37	Inches
Kilograms	2.2046	Pounds
Ponds	453.59	Grams
Poise	0.1	g cm ⁻¹ s ⁻¹
Centipoise	0.01	Poise
Centipoise	0.001	kg cm ⁻¹ s ⁻¹
Centipoise	2.42	lb ft ⁻¹ h ⁻¹

Index

Note: Page numbers followed by “b”, “f” and “t” indicate boxes, figures and tables respectively

A

- A. aureus*, 3t
- A. wentii*, 3t
- ABE, *see* Acetone–butanol–ethanol
- Abiotic losses, 576–578
- ABRII, *see* Agricultural Biotechnology Research Institute of Iran
- Acetic acid, 13, 55t, 83–84, 313b–314b, 621–622
- Acetic acid fermentation process, 312–314
- Acetobacter*, 13
- Acetobacter aceti* (*A. aceti*), 312–314
- Acetobacterium*, 300t
- Acetobacterium woodii*, 83–84
- Acetone, 53, 58–59
- Acetone–butanol–ethanol (ABE), 612–613
- Acetyl CoA, 84
- Acid pH, 436
- Acidogenesis, 573–574
- Acidogens, 574–575
- Acidulent, 11–12
- Acrylamide polymers, 242
- Actinomycetes, 6–7
- Activated sludge, 70b, 76, 399–410, 580–582
- Activation energy, 28
- Activators, 28
- Adenine, 30–31
- Adenosine triphosphate (ATP), 29, 291–292, 318
- Adsorbent contactors, 518
- Adsorption, 115, 242, 576–578, *see also* Downstream processing
 - chromatography, 245
 - fixed-bed, 243–244
 - Freundlich isotherm, 243
 - ion-exchange, 242
 - langmuir isotherm, 243
- Aerated bioreactor, 70b, 225
- Aerated system, 70b, 195–196, 218–219
- Aerated tank, 78
- Aeration, 48, 53–56, 76, 199, 381–382, 427–428, 578
- Aeration tank, 78, 79f–80f
- Aerobacter aerogenes*, 131, 132f
- Aerobic
 - biological oxidation, 569–572
 - bioreactors, 53–54, 195–196
 - downflow process, 410
 - process, 561
 - wastewater treatment, 76, 410–415
- Aerobic culture, 57, 65b–66b, 69b–70b
- Affinity chromatography binding, 245
- AFM, *see* Atomic force microscopy
- Agar, 263, 293, 353, 353f, 442, 447–448
- Agaricus bisporus* (*A. bisporus*), 431–432
- Agarose, 245–246, 509
- Agarose-based materials, 509–510
- Aggregated mycelia, 204–205
- Aggregation, 116, 235
- Agitation, 53–57, 56t, 63, 134–137, 195, 199, 355, 365, 381
- Agitation speed, 56, 88f–89f, 95, 96f
- Agitator, 57–58
- Agitator power, 61, 63
- Agricultural Biotechnology Research Institute of Iran (ABRII), 597
- Aiba, 177t
- Air filtration, 405b
- Air sparger, 56–57
- Airlift
 - bioreactors, 196–197, 202
 - pressure cycle bioreactor, 195, 197
- Alcohols, 1–2, 9–10, 114
- Algae, 607–608
- Alginate, 268
- Alginic acid, 268
- Alkaloids, 239–240
- Alkanes, 431
- α -ketoglutaric acid, 14–15
- Alumina membrane, 483
- American Type Culture Collection (ATCC), 334
- Amino acid, 14–15
- Ammonia (NH₃), 559
 - nitrogen oxidation reaction, 582
 - removal, 461
- Ammonium bicarbonate (NH₄HCO₃), 567–568

- Ammonium fumarate, 260
- Amperometric biosensors, 118, *see also* Biosensors
- linear detection range, 122
 - LOD, 122
 - recovery time, 122
 - response time, 122
 - sensitivity, 123
 - sweeping potential *vs.* time, 119f
 - voltammetry, 118
- Amperometry, 117–118
- Amyl acetate, 239
- Amylases, 33–34
- Amyloletic enzyme, 424
- Anabolism, 218
- Anaerobic
- digestion, 572–576
 - production, 621
 - reaction, 575–576
- Anaerobic media, 295–301
- Anaerobic membrane bioreactor (AnMBR), 463
- Analyte, *see* Substrate
- Andrew substrate inhibition model, 93–94
- Andrews and Haldane model, 55t
- Angular velocity, 233–235, 382–383
- Animal fats, 607
- AnMBR, *see* Anaerobic membrane bioreactor
- Anode, 109–110, 535t
- Anodic chamber, 544
- Anoxic process, 561
- Antibiogram assay, 352–353
- Antibiotics, 346, 348
- antibiogram assay, 353
 - in batch process, 347
 - biological assay, 353
 - analytical method, 352–353
 - bioreactor design
 - and control, 355–356
 - specification sheet, 360t, 361
 - chemical agents, 347
 - detection, 352–353
 - experimental procedure, 352
 - fermenter
 - description, 352
 - dimension estimation, 356–357
 - herbal medicines, 347
 - inoculum preparation, 349–350
 - microorganisms and media, 349
 - oxygen transfer rate determination, 359–361
 - penicillin, 348–349
 - extraction, 352
 - filtration, 352
 - power input determination, 358–359
 - Reynolds number determination, 358
 - submerged culture, 354–355
- Antifoam, 62, 112–113, 199–200, 384
- Antigens, 4, 347
- Apoenzyme, 28
- Apparent Michaelis constant, 153, 176
- Aqueous two-phase partition, 500
- Arabinoxylanase, *see* β -glucanase
- Araboascorbic acid, 3t
- Arginine, 114, 116, 429t
- Arrhenius' law, 38, 40, 209
- Arsphenamine, 347
- Arthrobacter*, 14–15, 608–609
- Arthrospira platensis* (*A. platensis*), 608
- Artificial mediators, 538–539
- Ascorbic acid, 36t, 114
- Asparagines, 298
- Aspartase, *see* Aspartate ammonia lyase
- Aspartate ammonia lyase, 28–29
- Aspartic acid, 28–29
- Aspergillus niger* (*A. niger*), 363–365
- Aspergillus oryzae*, 6–7
- ATCC, *see* American Type Culture Collection
- Atomic force microscopy (AFM), 535–536
- ATP, *see* Adenosine triphosphate
- Attached growth, 586–594, 586t
- Attached growth process, 558
- Autoclave, *see* Closed system
- Autoclave operation, 449–450
- Autotrophic, 83–84, 584
- Auxotroph, 301
- Average biomass concentration, 141
- Azotobacter vinelandii*, 65b–66b
- ## B
- β -lactam antibiotics, *see* Penicillin
- Bacillus amyloliquefaciens*, 287t
- Bacillus polymyxa*, 351t
- Bacillus subtilis*, 3t, 351t, 352–353, 430
- Bacillus thuringiensis*, 2
- Background current, 118
- Bacteria, 567–568, 608–609
- culture, 566–567
 - media sterilization, 447–448
- Bacterial amylase, 3t
- Bacterial protease, 3t
- Bacteriophage, 8
- Bacteriostatic, 346
- Bacto-agar, 293
- Bagasse, 46–47, 611–612
- Baker's yeast, 10–11, 16–18, 17f, 420, 429
- batch experiment, 421
- Basal medium, 295

- Batch
 - adsorption, 500
 - citric acid fermentation, 371–373
 - culture
 - cell growth, 131
 - disadvantages, 140
 - kinetics of, 132–133
 - experiment
 - continuous ethanol fermentation experiment, 343
 - optical cell density, ethanol, and carbohydrate concentration, 342
 - fermentation, 278, 419–421
 - ethanol, 406b–407b
 - experiment, 340–341
 - glucose concentration, cell density, and ethanol production, 274f
 - kinetic model for, 274f
 - relative activities of *S. cerevisiae* in, 275f
 - yeast cell dry weight and optical density, 271
 - mixed reactor, 196
 - sterilization, 437–439
 - system, 90–91
- Batch Bioreactor, 84–88
- bCOD, *see* Biodegradable chemical oxygen demand
- Bed matrix, 245
- Bed voidage, 504
- Beer, 34, 194, 201, 238
- Beer's law, 337
- β -glucanase, 34
- β -lactam antibiotics, 346, 349
- Beverages, 1–2, 5–6, 330
- BFC, *see* Biological fuel cell
- Bioalcohol resources
 - first-generation biofuel, 601
 - second-generation biofuels, 602
 - third-generation biofuel resources, 607–608
- Bioanalytical assays, 114
- Bioassay, 352–353
- Biobutanol production, 612–613
- Biocatalysts, 535–536
- biocatalysts, active, 535–536
- Biochemical oxidation *Xanthomonas campestris*, 314b–317b
- Biochemical oxygen demand (BOD), 559, 568–569
- Biochemical reaction stoichiometry, 331–332
- Bioconversion, 11–12
- Biodegradable chemical oxygen demand (bCOD), 592
- Biodegradable polymer, 11–12
- Biodegradable soluble chemical oxygen demand (bsCOD), 568–569
- Biodiesel
 - production, 613–619, 619f
 - resources
 - first-generation biofuel, 601–602
 - second-generation biofuels, 602–607
 - third-generation biofuel resources, 608–609
- Bioelectricity, 531
- Bioelements, 114–115
- Bioethanol, 330
 - fuel benefits, 331
 - production, 462–463, 601, 609–612
 - dry grinding, 612f
 - wet grinding, 611f
- Biofilm, 259
- Biofilter, 3–4
- Bioflocs, 235–236
- Biofuel production, 462, 598
 - classification and comparisons, 610t
 - drives and impacts, 598–600
 - economic perspective, 624
 - events of, 599t
 - feedstock, 600–601
 - first-generation biofuel, 601–602
 - second-generation biofuels, 602–607
 - third-generation biofuel resources, 607–609
 - integration of process, 622–624
 - policies, 600t
 - processes and technologies, 609
 - biobutanol production, 612–613
 - biodiesel production, 613–619, 619f
 - bioethanol production, 609–612
 - biogas production, 621–622
 - biohydrogen production, 621
 - biomethane, 621–622
- Biofuel Research Team (BRTeam), 598–599
- Biogas
 - production, 621–622
 - resources, 602
- Biohydrogen production, 621
- Biological
 - catalysts, 30
 - fluorophores, 129
 - fouling, 464–465
 - hydrogen production, 546–547
 - process, 568–569
 - transport of oxygen, 217–218
 - mass transfer coefficient estimation, 218–221
 - mass transfer in aerated and agitated vessels, 221–223
- Biological assay, 114, 353
- Biological element, 114–115
- Biological fuel cell (BFC). *see also* Microbial fuel cell (MFC), 529–530
- Biological oxygen demand (BOD), 457–458, 547
- Biological transport of oxygen, 217–223
- Biological treatment, 558

- Biological treatment (*Continued*)
- abiotic losses, 576–578
 - aerobic biooxidation, 569–572
 - anaerobic digestion, 572–576
 - attached growth, 586–594, 586t
 - biological
 - denitrification, 579–586, 581f, 584t
 - nitrification, 579–586, 581f, 584t
 - growth rate, 562–568
 - microbial
 - growth kinetics, 561–562
 - metabolism, 559–561
 - organic removal, 558–559
 - principal groups, 558
 - removal mechanism in biological process, 568–569
 - suspended growth, 586–594, 586t
 - treatment kinetics, 562–568
 - volatilization, 578–579
- Bioluminescence, 104
- Biomass, 10–11
- balances, 141–142
 - concentration, 589–590
 - yield, 562–563
- Biomass composition, 106t
- Biomaterials immobilization, 115
- adsorption, 115
 - covalent binding, 116
 - cross-linking, 116
 - encapsulation, 115–116
 - entrapment, 115
- Biomethane, 621–622
- Biomolecules, 14, 28, 239–240, 538
- Bioprocess, 2, 3t, 9
- products, 10
 - biomass, 10–11
 - cell products, 11
 - modified compounds, 11
 - and services, 10t
- Bioprocess scale-up
- aerobic wastewater treatment, 410–415
 - applied calculation method for, 391b–394b
 - bioreactor design, 384–388
 - calculation, 396b–397b
 - dynamic model, 399–410
 - ethanol batch fermentation, 406b–407b
 - filter and air filtration, 405b
 - mass transfer coefficient calculation, 398b–399b
 - oxygen transfer rate, 399–410
 - power calculation, 394b–396b
 - power consumption calculation, 414b–415b
 - procedure, 376
 - for constant K_La , 377–378
 - for constant mixing time, 379–381
 - on physical concepts, 381–384
 - on shear forces, 378–379
 - stirred tank reactor chemostat *vs.* tubular plug flow, 388–399
 - vinegar production, 408b–410b
- Bioreactor design, 9, 53–54, 193–194, 384–388
- aerated and stirred vessels percentage distribution, 194t
 - airlift bioreactors, 202
 - biological transport of oxygen, 217–223
 - bubble column fermenter, 201
 - controlling probes, 105–106
 - CSTR fermenter design equations, 205–208
 - heat transfer, 203–205
 - performances, 195t
 - sensor characteristics, 106–107
 - specification sheet, 360t, 361
 - stirred tank bioreactor, 198–200
 - temperature effect on rate constant, 209
 - type of, 195–198
- Biosciences, 5
- Biosensors, 113, 547, *see also* Fermentation process control
- biological element, 114–115
 - biomaterials immobilization, 115–116
 - components, 114f
 - transducer, 117–118
- Biostat, 137
- Biosynthesis, 14, 55, 292–293, 346
- Biosystem, 105–106, 217–218
- Biotechnology, 2–5, *see also* Downstream processing
- advances in, 497
 - cell disruption, 498–499
 - Dyno Mill KDL-I, 499f
 - protein products, 497–498
 - protein purification, 500–501
- Biotic loss, 568
- Biotransformation, 11
- Blastospores, 354–355
- BOD, *see* Biochemical oxygen demand; Biological oxygen demand
- Bovine serum albumin (BSA), 425
- BP, *see* British Petroleum
- Bradyrhizobium*, 2
- Breakthrough point, 243
- Brevibacterium*, 3t, 14–15
- Brevibacterium lactofermentum*, 300t
- Brevibacterium* sp., 3t
- British Petroleum (BP), 426–427
- Broad spectrum, 351t
- Broth, 252b–253b
- Broth rheology, 106t
- BRTeam, *see* Biofuel Research Team

- BSA, *see* Bovine serum albumin
bsCOD, *see* Biodegradable soluble chemical oxygen demand
Bubble, 68–74
Bubble column, 384–388, 385b
 fermenter, 201
Bubble diameter, 60–61, 220, 221b–223b
Bubble residence time, 68
Bubble size, 56–57, 59, 220
Buoyant force, 68, 225
Butanol, 6–7, 240, 612–613
Butyl acetate, 239–240, 352
Butyric acid, 327b
- C**
Cake resistance, 231–233
Calcium alginate, 268–270
Calderbank and Moo-Young, 219
Candida lipolytica, 363–364
Candida rugosa (*C. rugosa*), 181–182
Candida sp., 302t, 303, 430t
Candida tropicalis (*C. tropicalis*), 431–432
Candida utilis (*C. utilis*), 6–7, 431–432
Capacitance, 105, 112–113
Capacitance foam detector, 113
Capacitance probes, 105
Carbohydrates, 2, 7–8, 15, 163b–165b, 267, 369
Carbon capture and storage (CCS), 624
Carbon dioxide, 6–7, 33–34, 56, 462, 598, 608
Carbon dioxide production rate, 56, 105
Carbon Monoxide, 84, 93, 98f
Carbon monoxide dehydrogenase (CODH), 84
Carbon sources, 5
Carbonaceous biochemical oxygen demand (CBOD), 568–569
Carboxy methyl cellulose (CMC), 116, 245–246
Carotenoid, 36t, 37
Carrageenan, 116, 288t
Carrier binding, 261
CAS, *see* Conventional activated sludge
Caster, 607
Catabolic pathway of glucose, 318
Catabolic repression, 165f
Catabolism, 7–8, 55, 318, 432–433
Catabolite, 196
Catabolite repression, 196
Catalysts, active, 30
Catalytic processes, 83–84
Cathode catalyst, 533
Cathodic chamber, 544–545
Cation exchange membrane, *see* Proton exchange membrane (PEM)
CBOD, *see* Carbonaceous biochemical oxygen demand
CCS, *see* Carbon capture and storage
Cell concentration, 84–85, 90–91, 134–137, 173
Cell density, 65b–66b, 69b–70b, 134–137, 141, 270, 476
Cell density monitoring, 419–420
Cell dry weight (CDW), 56, 79, 80f, 85, 131, 255, 339, 368
Cell harvesting, 143
Cell load, 137f
Cell morphology, 106t, 332–333
Cell optical density (COD), 54–55, 79, 129
Cell recycling, 143, 462
Cell respiration, 129, 217–218
Cell rupture, 57, 238
Cell suspension, 498–499, 499f, 511
Cell turbidity, 138f, 271
Cell wall, 6, 35, 346, 498–499
Cell(s)
 activities, 259
 concentration, 332
 disruption, 238–239, 498–499
 growth, 371–372
 in batch culture, 131
 phases, 131–132
 products, 11
 wall, 6
 weight, 368
 measurements, 339
Cellular composition, 106t, 428t
Cellulose, 34, 330, 430
Cellulose acetate, 116, 460t
Cellulose triacetate, 262
Centrifugal force, 200, 233–234
Centrifugation, 233–235
 centrifuge effect, 233–234
 theory of, 233–235
Centrifuge, 233–234, 239, 250b
Cephalosporin, 3t, 346, 350, 351t
Cephalosporine
 Cephalosporium acremonium, 3t, 351t
Ceramic membrane, 483, 486f
 alumina-coated on, 487f
 zirconia-coated on, 489f
Cheese, 1–2, 11–12, 34, 194
Chemical agents, 347
Chemical antifoams, 112
Chemical oxygen demand (COD), 457–458, 568–569, 569f
Chemical sensors, 547
Chemical sterilization, 451
Chemoautotrophs, 560

- Chemolithotroph, 83–84
Chemostat, 134–137
Chemostat bioreactor, *see* Continuous stirred tank reactor (CSTR)
Chemostat modification, 143
Chemotherapy, 347
Chen and Hashimoto, 176t
Chitin, 35
Chitosan, 115–116
Chromatography, 244–253
 principles of, 246–253
Chronoamperometry, 118
Cibacron Blue 3 GA, 500–501, 501f
CIP, *see* Cleaning-in-place
Circulation time, 106t
Citric acid, 2, 363–364, 369
 analytical method, 368–369
 experimental run, 369–371
 factors affecting mold growth, 365–367
 fermentation process, 365–367
 kinetic model in, 371–373
 processes for recovery, 369
 production, 324b–325b, 364–365, 367–368
 purification processes, 369
 seed culture, 367
 seeding inoculum, 367
Citric acid cycle, 84
Clean water, 548
Cleaning-in-place (CIP), 509
Clogging, 112, 196, 363–364
Closed system, 435–436
Clostridium acetobutylicum (*C. acetobutylicum*), 6–7
Clostridium butyricum (*C. butyricum*), 532
Clostridium ljungdahlii (*C. ljungdahlii*), 83–84
 CO substrate on, 96–98
 growth simulation, 90f
Clostridium species, 6–7
Clostridium thermoaceticum, 83–84
Clostridium thermocellum, 331–332
Clostridium thermohydrosulfuricum, 331–332
CMC, *see* Carboxy methyl cellulose
CO substrate, 96–98
CoA, *see* Coenzyme A
Coagulated milk, 3t
Coalescing systems, 61–62
Cobalamin (vitamin B12), 3t, 296t
COD, *see* Chemical oxygen demand
CODH, *see* Carbon monoxide dehydrogenase
Coenzyme A (CoA), 35–36
Coenzymes, 28, 35–37, 36t
Cofactors, 35
Collagen, 116
Competitive inhibitors, 31, 32f
Compressible cake, 232
Conductance, 105, 112t
Conductance probes, 105
Conductivity, 105, 112t, 117–118
Conductometry, 117–118
Conjugated enzymes, 147, 149–150, 153
Conservation of mass principle, 309–317
Consolidated bioprocessing (CPB), 623
Constant mixing time, 379–381
Constant power, 376–377
Continuous culture, 140
Continuous extraction column, 240–242
Continuous fermentation, 341–342, 419–421, 471f, 473, 474t
Continuous sterilization, 439–441, 440f, 446b–447b
Continuous stirred tank reactor (CSTR), 104, 105f, 381, 389b–391b
 fermenter
 design equations for, 205
 Monod model for chemostat, 205–208
Contois model, 176
Control unit, 104, 114f
Conventional activated sludge (CAS), 457–458
Conventional batch fermenter, 357f
Conveyer centrifuge, 233
Cooling coil, 349–350
Coomassie plus protein assay reagent, 425
Coomassie–protein reaction scheme, 425
Corn, 601
Corn steep liquor, 14–15, 18, 311b–312b, 348
Corn syrup crystallization, 8
Correction factors, 211b–214b
Corynebacterium glutamicum, 2
Cottrell equation, 120
Coulombic yield, 543
Coulter counter, 332
Covalent binding, 116, 284
CPB, *see* Consolidated bioprocessing
Critical dilution rate, 137, 142
Cross-flow, 459
Cross-linking, 116, 262
Crystallization process, 241, 253–255
CSTR, *see* Continuous stirred tank reactor
Current, 54, 108, 118, 332
 background, 119–120
Cyanobacteria, 608
Cyclic voltammetry, 118
Cyclic voltammogram, 119–120, 119f
Cysteine, 298, 428–429, 429t
Cytoplasm, 6
Cytoserine, 346

D

D-mannuronic acid, 268
 Dairy products, 1–2, 9, 11–12, 34
 DAP, *see* Diaminopimelic acid
 Death phase, 90–91, 131–132, 140, 179, 354, 561–563
 Death rate, 86, 139, 437
 Decanter, 233
 Decarboxylase, 29, 34, 608
 Denitrification, biological, 579–586, 581f
 Dermatophytic fungi, 351t
 Description of glycolysis, 319–326
 Detecting antibiotic, 352–353
 Detection, 112–113, 117, 352–353
 detection range, 122
 Dextran, 3t, 509
 Dextrin, 16, 245–246
 Dialysis, 228, 512
 Diaminopimelic acid (DAP), 14
 Diauxic growth, 165f
 Digestive enzymes, 30
 Dilution rate, 72, 139, 168t, 478–479
 maximum dilution rate, 134–137, 165b–166b, 214b–215b
 Dimensionless aeration rate, 211b–214b, 359
 3,5-dinitrosalicylic acid (DNS), 78, 337
 Dinucleotide, 7–8, 36t
 Direct conversion process, 608
 Direct product sequestration (DPS), 512
 Disadvantages of batch culture, 140
 Disc-stack bowl centrifuge, 235, 235f
 Disk turbine agitator, 58
 Dissolved carbon dioxide, 104–105, 106t
 Dissolved oxygen (DO), 54, 76, 109, 419, 568–571
 measurement, 54
 and control, 109–110
 probe, 54
 in SCP, 419
 Distillation, 174, 228, 330–331, 610–611, 623
 Divinyl benzene, 242
 Dixon plot, 189
 DNA, 35, 106t
 DNAligase, 35
 DNS, 270–271, 337, 472
 DNS, *see* 3, 5-dinitrosalicylic acid
 DO, *see* Dissolved oxygen
 DO measurement, 123
 DO probe, 54, 58, 109, 123, 419
 Double reciprocal plot, 145–146
 Doubling time, 6
 Dourado, 177t
 Down-comer, 202, 220–221
 Downstream processing, 11, 228, 497
 acid recovery by liquid–liquid method, 230f

cell disruption, 238–239
 centrifugation, 233–235
 and solvent extraction, 230f
 chromatography, 244–253
 conventional techniques, 501–502
 crystallization process, 253–255
 emerging technology for cell recovery, 238
 experimental procedure, 510–511
 FBA, 502–504
 filtration, 231–233
 flotation, 237
 freeze-drying, 255
 jacketed fermentation vessel, 229f
 liquid fluidized beds, 504–510
 process integration, 511–513
 for proteins purification, 498f
 sedimentation, 235–236
 DPS, *see* Direct product sequestration
 Draft tubes, 202
 Driving force for mass transfer, 58
 Dry heat sterilization, 450
 Drying, 228, 236, 449, 485, 488, 603t–606t
 Dual substrates, 147–152, 163b–165b, 178
 Dynamic model, 399–410

E

Eadie–Hofstee plot, 172f
 Effective mineral, 106t
 Effluent substrate concentration, 591
 Ehrlich ascites tumor, 287t
 EI, *see* Enzyme–inhibitor
 EIS, *see* Enzyme–inhibitor–substrates
 Electricity, 528, 545–546
 Electrochemical biosensor, 117–118
 Electrochemical detectors, 109
 Electrode, 54, 110–111, 113, 118
 Electrode response, 107
 Electrodialysis, 452, 469, 500
 Electrolyte, 54, 61–62, 109–110, 118, 231, 530t, 542
 Electromagnetic flow meters, 105
 Electron
 acceptor, 560
 beam sterilization, 451
 donors, 562–563
 mediator, 538–539
 transfer, 536–538
 transport, 538
 Elemental balances, 303–305
 Elemental composition, 291–293, 304
 Embden–Meyerhof–Parnas pathway (EMP), 318–326
 glycolysis, 319–326
 EMR, *see* Enzymatic membrane reactor

- Encapsulation, 115–116
Endocarditis infection, 347
Endomycopsis biospor, 40
Energy balance for continuous ethanol fermentation, 305–306
Energy integration, 623–624
Enterobacter aerogenes, 14
Entrapment, 115, 261–262
Enzymatic hydrolysis reaction, 181
Enzymatic membrane reactor (EMR), 181–182
Enzymatic rate equation, 187–189
Enzyme, 20
 activators, 30–31
 catalysts, 30–31
 classifications, 28–30
 coenzymes, 35–37
 deactivation, 37–38
 elementary reaction rate, 21–28
 inverse urea and inverse rate calculation, 24t
 linear plot, 24f
 Lineweaver–Burk plot, 25f–26f
 Michaelis–Menten rate constants, 24b–25b
 enzymatic reactions, 20
 enzyme-catalyzed reaction inhibitors, 31–33
 industrial application, 33–35
 kinetics, 182
 product inhibition study, 185–186
 rapid equilibrium system, 187
 substrate and product inhibitions analyses, 182–183
 substrate inhibition study, 183–185
 verification, 189–191
 leakage, 115
 effect of pH, 37
 production, 16, 20–21
 specific function, 30
 unit activities, 37
Enzyme activators, 30–31
Enzyme activities, 28, 33–34, 37, 40t, 45–46, 344
Enzyme Commission, 37
Enzyme kinetic model, 181–191
Enzyme kinetics, 182–186
Enzyme reaction kinetics, 145–146, *see also* Growth kinetics
 noncompetitive inhibition rate model, 153–172
 reaction mechanism with competitive inhibition, 152–153
 reversible reactions with dual substrate reaction, 151–152
 single enzyme with dual substrates mechanism, 147–151
Enzyme-catalyzed reactions inhibitors, 31–33
Enzyme-substrate (ES), 32
 Enzyme–inhibitor (EI), 185–186
 Enzyme–inhibitor–substrates (EIS), 32–33
 EPS, *see* Extracellular polymeric substance
 Equilibrium constant, 242
 Equilibrium kinetic studies, 520–522
 Ergosterol, 36t, 37
 Erythromycin, 3t, 15, 239–241, 351t
 ES, *see* Enzyme-substrate
 Escherichia coli (*E. coli*), 15, 260, 304–305, 334t, 538
 Essential amino acids, 14, 422, 428
 Estimation of mass transfer coefficient, 218–221, 381
 Ethanol, 330
 analytical method, 338
 fermentation, 278, 468
 batch fermentation, 406b–407b
 biofilm reactor use for ethanol production, 267
 continuous fermentation, 471f, 473, 474t
 experimental environment, 470–472
 immobilized biomass activity, 268
 using MBR, 470, 474–479
 membrane technology, 469
 in using *S. cerevisiae*, 267
 inhibition, 468
 production, 330–331
 immobilized systems for, 288–289
 2-ethoxyethanol, 185
 Evaporation, 113, 228, 342
 Exhaust gas, 105, 112, 349–350
 Exit gas, 56, 104–105
 Expanded bed adsorption, 518, 522–523
 degree of bed expansion, 508–509, 516
 Streamline™ DEAE, 522
 Exponential growth phase, 131–132, 333
 External loop, 195, 197–198, 202
 Extracellular polymeric substance (EPS), 464–465
 Extracellular polymers, 259
 Extraction of penicillin, 239–240, 352
- F**
F/M ratio, *see* Food to microorganism ratio
Faraday constant, 110–111, 541–543
FBA, *see* Fluidized bed adsorption
Fed batch, 18, 144, 413–415
Fed batch culture, 144–145
Fed-batch mixed reactor, 196
Fermentation, 7–8, 573–574
 fermentation-based products, 461–462
 media preparation for, 292–293
 anaerobic media preparation, 295–301
 medium formulation, 293–294
 minimal and standard media preparation, 301–303

- phase, 573–574
- process, 7–9
- Fermentation process application, 7–10, 356
 - batch
 - experiment, 342–343
 - fermentation experiment, 340–341
 - biochemical reaction stoichiometry, 331–332
 - bioethanol fuel benefits, 331
 - cell dry weight measurements, 339
 - continuous fermentation experiment, 341–342
 - ethanol
 - analysis analytical method, 338
 - production, 330–331
 - expected results, 343–344
 - growth and product formation kinetics, 333–334
 - inoculum preparation, 335
 - media sterilization, 342
 - optical cell density, 332–333
 - RI determination, 338
 - seed culture inoculation, 336–337
 - stock culture preparation, 334–335
 - yield calculation, 339
- Fermentation process control, 104, *see also* Biosensors
 - bioreactor
 - controlling probes, 105–106
 - sensor characteristics, 106–107
 - DO measurement and control, 109–110
 - foam detection and prevention, 112–113
 - pH/redox measurement and control, 110–111
 - temperature measurement and control, 108–109
- Fermenter, 9, 53–54, 194–195
 - description, 352
 - dimension estimation, 356–357
- Fick's law, 120
- FID, *see* Flame ionization detector
- Filamentous
 - form, 333
 - organisms, 293
 - shape, 6–7
- Film theory, 59, 91, 91f
- Filter aids, 231, 310b–311b
- Filter cake, 12, 231–232, 246b–247b, 310b–311b
- Filterability, 231
- Filtration, 231–233, 352
 - filter and air, 405b
 - hormone separation in gel, 252b
 - pressure drop, 231
 - sterilization with, 450
 - theory of, 231–233
- First-generation biofuel, 601
- feedstocks, 601–602
- Fixed-bed adsorption, 243–244, 502
 - Fixed-film or biofilm process, *see* Attached growth process
 - Flame ionization detector (FID), 472
 - Flat blades Turbine disk, 58
 - Flavin adenine denucleotide, 129, 500–501
 - Fleming, 15, 348
 - Flocculation, 195, 230–231, 580
 - Flotation, 237–238
 - Fluidized bed, 196, 518
 - Fluidized bed adsorption (FBA), 502–504
 - column design for, 510
 - matrices for, 509–510
 - Fluidized/expanded bed system, 503–504
 - hydrodynamic characterization, 504
 - interfaced and integrated, 511–513
 - Fluorescence, 117, 129, 130f
 - Fluorescence spectroscopy, 129–130
 - Fluorophase, 129
 - Fluorophore, 129
 - Flux, 58, 64, 123, 490
 - FO, *see* Forward osmosis
 - Foam
 - breaker, 112, 384
 - detection and prevention, 112–113
 - detectors, 112
 - level, 106t
 - Foaming, 104, 112, 199–200, 349–350
 - Food additive, 2, 14, 363–364, 429
 - Food stabilizer, 3t
 - Food to microorganism ratio (F/M ratio), 590
 - Forward osmosis (FO), 465–466
 - Four-bladed disk turbine, 200
 - Free enzyme, 20, 22, 31, 148, 150, 187–188
 - Free sites, 31–32, 148–149
 - Freeze drying, 229, 255
 - freeze drying/lyophilisation, 229
 - freeze-dried culture, 334
 - Freundlich isotherm adsorption, 243
 - Freundlich model, 243
 - Froude number, 63, 199, 384
 - Fuel cell, 528, 528f
 - classification, 529
 - merits, 529
 - stack, 533–534
 - Funda-foam system, 200
 - Fungi, 2, 6–7, 11–12, 349, 418–419, 607
 - Fungus *Fusarium*, 331, 431
 - Fusarium* sp., 331–332
- G**
 - GAC, *see* Granular activated carbon
 - Galactose, 462
 - Galileo number, 507–508

- Galvanic detectors, 109
 Gas analyzer, 109
 Gas bubble formation, 68–74
 Gas chromatography (GC), 244, 338, 568–569
 Gas dispersion, 56–58
 Gas flow rate, 201, 221b–223b, 357, 385b, 396b–397b
 Gas fluidized beds, 503
 Gas hold-up, 60–61, 68, 68b, 203–204, 211b–214b, 396b–397b
 Gas mixing patterns, 106t
gas oil flocc, 220
 Gas superficial velocity, 201, 357
 Gas–liquid system, mass transfer in, 59–60
 Gassed power, 61, 211b–214b, 380, 402b–404b
 GC, *see* Gas chromatography
 GDH, *see* Glutamic acid dehydrogenase
 Gel beads, 259–260
 Gel chromatography, 245
 Gel filtration, 228–229, 245–246
 Gel polarization, 550
 Gelatin, 262
 Ghose and Tyagi, 177t
 Glucolysis, 6–7, 320f
 Gluconic acid, 13, 309b–310b
Gluconobacter, 13
Gluconobacter suboxydans, 3t
 Glucose, 431
 isomerase, 34
 oxidase, 123
 Glutamic acid, 2, 3t, 9, 14–15
 Glutamic acid dehydrogenase (GDH), 14–15
 Glutaraldehyde, 110–111, 116, 262, 284
 Glycerol, 8–9, 14, 305–306, 330, 616
 Glycolysis, 319–326
 glycolytic, 7–8
 Graetz number, 204–205
 Graetz–Leveque equation, 204–205
 Gram-negative bacilli, 427–428
 Gram-negative bacteria, 346
 Gram-positive bacteria, 346
 Granular activated carbon (GAC), 460–461
 Grashof number, 218–219
 Gravitational force, 63
 Growth factors, 36, 292–293, 442, 565
 Growth inhibitors, 106t
 Growth kinetics, 129
 in batch bioreactor, 84–88
 batch culture, 131
 for continuous culture, 133–137
 growth phases, 131–132
 indirect measurements, 129
 fluorescence spectroscopy, 129–130
 specific growth rate, 130–131
 material balance for CSTR, 137–145
 unstructured kinetic model, 173–179
 Growth phase, 131–132, 354, 562–563
 Growth rate, 31, 54, 86, 130–131, 139, 174, 206, 254–255, 304–305, 371–372, 562–568
 Growth stimulants, 36, 131, 442
 Growth stoichiometry Elemental balances, 303–305
 Growth-limiting factor, 567–568
 Growth-rate limitations, 304–305
- ## H
- Hagglund, 177t
 Haldane model, 563–564
 Half-life, 11, 37–38, 278–279
 Hanes-Woolf, 183f–186f
 Hansford model, 178
 Heat evolution, 104
 Heat production, 108–109
 Heat transfer, 203–205
 Heat transfer coefficient, 203–205, 441–442
 Heating, 43, 231, 437, 449, 610–611
 Heating phase, 449
 Hemicellulase catalase, 11
 Hemicellulose, 330, 602
 Hemocytometer slide, 332
 Henry's constant, 92
 Henry's law, 59–60, 67, 96, 578–579
 Herbal medicines, 347
 Herbert, 177t
 Hetero-polymer, 330
 Heterofermentative organism, 6–7
 Heterogeneous catalysts, 616
 Heterogeneous nucleation, 253–254
 Heterogeneous systems, 20, 53–54
 Heterotroph, 301, 560
 Hexokinase, 28
 Hexose, 28
 High shear rate, 195
 High-pressure homogenizer (HPH), 498–499
 Hinshelwood, 176, 177t
 Histidine (His), 35–36
 Hollow fiber, 459, 463, 469
 Holoenzyme, 28
 holographic laser interferometry, 285–286
 Homofermentative organism, 6–7
 Homogeneous nucleation, 253
 Homogeneous phase, 20
 Homolactic fermentation, 11–12, 319
 Hormone, 4–6, 15, 228, 252b
 Hot plates, 441–442, 441f
 HPH, *see* High-pressure homogenizer

- Humidification, 228, 309b–310b
 Hydraulic retention time (HRT), 587–588
 Hydrochloric acid (HCl), 615
 Hydrodynamics, 517
 Hydrogen production, 621
Hydrogenase, 28–29, 129
 Hydrolases, 29–30
 Hyphae, 6–7, 367, 371–372
- I**
- Ibuprofen ester, 181–182, 182f, 185, 189
 ICR, *see* Immobilized cell reactor
 Immobilization
 of biomaterials, 115–116
 methods, 285t
 of microorganisms by covalent bonds, 284
 ethanol productivity, 288t
 growth and colony formation, 286–288
 microbial cells, 286t
 oxygen transfer to, 284–285
 studies of diffusion, 287t
 substrate transfer to, 285–286
 Immobilized cell reactor (ICR), 262, 468
 continuous fermentation of dual substrate, 264t
 electronic microscopic scanning, 271, 272f–273f
 ethanol detection, 271
 ethanol fermentation in using *S. cerevisiae*, 267
 biofilm reactor use for ethanol production, 267
 immobilized biomass activity, 268
 experimental reactor system, 268–270
 experimental setup, 269f
 properties and appearance of *Saccharomyces cerevisiae* beads, 270t
 experiments, 263
 glucose concentration determination, 270–271
 kinetic model for immobilized *P. acidipropionici*, 266t
 model test using *P. acidipropionici*, 265f
 rate model, 263–266
 statistical analysis, 271
 conversion *vs.* retention time, 276f
 glucose concentration, cell density, and ethanol production, 274f
 glucose consumption, 276f
 kinetic model for batch fermentation, 274f
 Lactobacillus bulgaricus beads, 277f
 percentage growth of immobilized cells, 275f
 relative activities of *S. cerevisiae*, 275f
 S. cerevisiae beads, 277f
 yeast cell dry weight and optical density, 271
 Immobilized enzymes, 616
 Immobilized microbial cells, 259–260, *see also*
 Microorganisms
 advantages and disadvantages, 262
 alternative methods, 261f
 batch fermentation, 278
 carrier binding, 261
 cross-linking, 262
 entrapment, 261–262
 ethanol production *vs.* retention time, 280f
 glucose concentration and, 281f
 evaluation, 272–278
 high concentration effect, 279–281
 reactor setup, 279
 relative activity, 278–279
 techniques, 260f
 Immobilized system, 195
 for ethanol production, 288–289
 ethanol productivity from, 288t
 Immunoglobulin C, 251b
 Impeller, 106t, 210, 376, 378–379, 386b–388b
 marine, 58
 tip velocity, 210, 376, 378–379
 Impeller flooding, 106t
 Impeller speed calculation, 386b–388b
 Impeller tip velocity, 210, 376, 378–379
 Inclined blade turbine, 57
 Inducers, 106t
 Industrial bioreactors, 202
 Industrial fermentation, 2
 Industrial microbiology
 amino acids production, 14–15
 Baker's yeast, 16–18, 17f
 bioprocess, 2
 products, 10–11
 biosciences, 5
 biotechnology, 2–5
 enzymes production, 16
 industrial fermentation, 2
 insulin production, 14–15
 lactic acid production, 11–12
 microbe functions, 5–7
 microorganisms, 1–2
 penicillin production, 15–16
 process fermentation, 7–9
 vinegar production, 13
 Inexpensive carbon sources, 418–419
 Inhibition, 148–149
 Inhibitors, 30–31
 Inoculum preparation, 335, 349–350
 Inorganic components, 549
 Inorganic membrane, 483–484
 Insulin production, 14–15, *see also*
 Penicillin—production
 Intensification and integration methods, 622
 energy integration, 623–624
 reaction-separation integration, 623

Intensification and integration methods (*Continued*)
 reaction–reaction integration, 622–623
 separation–separation integration, 623
 Interferon, 3t, 4–6, 228–229
 Intermediate enzyme–substrate complex, 150
 Intermig agitator, 58
 Internal-loop, 202
 International Energy Agency, 598
 Interspecies hydrogen transfer, 574–575
 Intracellular enzyme, 11, 228–229, 237, 503–504
 ion exchangers, 228–229, 243
 Ion-exchange adsorption, 242
 Ion-exchange chromatography, 244–246
 Iranian Research Organization for Science and
 Technology (IROST), 42, 470
 Irreversible, 20–21, 151–152, 464
 Isomerization, 29–30
 Isopropanol, 6–7, 271

J

Jacket, 203–205, 438–439, 499
 Jacketed bioreactor, 408b–410b
 Jatropa, 602
 Jerusaliwski, 177t
 Jin, 177t

K

“Kat”, 37
 Kinetic model, 173–179, 371–373
 Kinetic parameters, 24b–25b, 95, 97t, 165b–166b,
 183, 373
 Kinetics, 140–141, 151–152, 354–355, 586, 620t
 Kinetics of Growth, 84–88, 333–334
 Kinetics of reversible reactions, 151–152
Klebsiella aerogenes, 334t
 Koji bioreactor, *see* Static tray bioreactor

L

L-aspartic acid, 260
 L-glucuronic acid, 268
L. brevis, 11–12
L. casei, 11–12
L. delbrueckii, 11–12
L. helveticus, 11–12
L. manihotivorans, 11–12
L. paracasei, 11–12
L. plantarum, 11–12
 Lactase, 11
 Lactate, *see* Lactic acid
 Lactic acid, 11–12, 461–462
Lactobacillus bulgaricus, 3t, 11–12, 277f, 279
Lactobacillus delbrueckii, 3t, 11–12
Lactobacillus species, 6–7, 11–12

Lactose, *see* Whey
 Lag phase, 86, 88–89, 131, 133, 163b–165b, 278,
 561–562
 Lambert-Beer law, 129
 Laminar flow, 63, 204–205, 231–232, 448, 519–520
 Landfill leachate (LFL), 460–461
 Langmuir isotherm adsorption, 243
 Langmuir–Hanes, 274f, 278
 Leachate, 20–21, 460–461
 Leucine, 114, 298, 429t
Leuconostoc mesenteroides, 3t
 LFL, *see* Landfill leachate
 Ligase, 30, 35
 Light microscope (LM), 484
 Lignin, 34, 330, 423–424, 430, 602
 Lignase
 Lignocellulose, 602, 603t–606t
 biomass, 602
 Limit of detection (LOD), 122
 Linear detection range, 122
 Linear first-order differential equation, 265
 Linear-sweep voltammetry, 118
 Lineweaver–Burk
 equation state, 121–122
 plot, 25f–26f, 343
 Lipases, 41
 Lipid, 9, 26b, 262, 531–532, 608–609
 Lipopolysaccharide, 35, 262, 531–532
 Liquid chromatography, 337, 352–353, 369, 500
 Liquid fluidized bed adsorption, 516, 518, *see also*
 Nanobiotechnology Group contactor (NBG
 contactor)
 adsorbent contactors, 518
 bed expansion characteristics, 518
 bed voidage, 504
 column and solid phase designs, 516–517
 degree of bed expansion, 508–509
 FBA
 column design for, 510
 matrices for, 509–510
 hydrodynamic
 characterization, 504
 performance of NBG contactor, 517
 materials, 517–518
 particles
 minimum fluidization velocity, 505–506
 terminal settling velocity, 506–508
 Liquid gas mass transfer process, 411f
 Liquid level, 105, 113, 134–137, 381
 Liquid–liquid extraction, 240, 613
 LM, *see* Light microscope
 LOD, *see* Limit of detection
 Logistic equation, 90–91

- Logistic model, 88–89, 173–174, 372
 Loop bioreactor, 195, 197–198
 Low-temperature sterilization, 452
 Lux meter, 93, 95
 Lyophilization, 255
 Lyophilized, 228, 255
 Lysine, 2, 3t, 14–15, 262, 298, 429t
 Lysozymes, 30, 35
- M**
- Macrofloc, 235
 Maintenance, 42–43, 83–84, 547, 560, 565, 579
 Malic acid, 13
 Malt, 7–8, 34, 293, 299t, 420–421
 Malthus function, 86
 Mammalian cell, 196
 Manton–Gaulin homogenizer, 239
 Marine propeller, 63, 212f, 215b–217b
 Marine type, 58
 Mass balance for biological processes, 306–309
 Mass flow meter, 105
 Mass spectroscopy, 568–569
 Mass transfer
 in aerated and agitated vessel, 221–223
 coefficients, 61–62, 381
 limited process, 63–74
 phenomena, 91–93
 film theory for, 91f
 Material balance, 413–415
 Maximum dilution rate, 134–137, 165b–166b, 214b–215b
 MBR, *see* Membrane bioreactor
 Mechanisms of single enzyme, 147–151
 Media sterilization, 342
 Medium formulation, 293–294, 344
 MEK, *see* Methyl ethyl ketone
 Membrane, 465–466
 γ -alumina, 484–485, 491
 anisotropic membrane, 353
 ceramic membrane, 483, 492
 charged membrane, 577–578
 dense membrane, 481
 fouling, 463–465, 502, 544
 isotropic membranes, 352–353
 metal and liquid membranes, 353
 microporous membranes, 352
 nonporous membranes, 486f
 semipermeable membrane, 285t
 synthetic membranes, 242
 zirconia, 484
 Membrane bioreactor (MBR), 331, 457, 469, *see also*
 Ethanol—fermentation
 advantages, 457–458
 applications, 460–463
 configurations, 458–459, 459f
 development, 465–466
 ethanol production in, 480t
 materials and modules, 459
 membrane fouling, 463–465
 Membrane fouling, 463–465
 Membrane module, 181, 463, 465, 489
 Membrane reactor (MR), 455, 456f, *see also* Membrane
 bioreactor (MBR)
 Membrane separation, 181, 228, 457–458, 475–476,
 500, 623
Meningococci, 347
 Metabolic pathway, 31, 267, 318, 330, 608–609
 Metabolic rate, 129
 Metabolites, 2, 4, 84, 259, 348, 461–462
 Metal ions, 577–578
 Methane, 427–428, 431–432
 Methane-former organism, 573–574
 Methanogenic bacteria, 84, 293–294, 572–573
 Methanogenic fermentation, 622
 Methanogens, 574–575
 Methanogenesis, 573–574
 Methanol, 431–432
 Methionine, 298, 427–429, 429t
 Methyl ethyl ketone (MEK), 239–240
 Methyl isobutyl ketone, 239–240, 352
 Methylcellulose, 116
 Methylene blue, 332, 538
Methylophilus methylotrophus (*M. methylotrophus*),
 418–419
 MF, *see* Microfiltration
 MFC, *see* Microbial fuel cell
 Michaelis–Menten
 constant, 22, 24b–25b
 equation, 564
 illustration, 22f
 kinetic parameters, 182
 rate equation, 22, 25b
 Micro-fluidizer, *see* High-pressure homogenizer
 (HPH)
 Microbial
 biomass separation, 421
 catalysis, 550
 functions, 5–7
 growth, 561–562
 organic removal in, 558–559
 effect of substrate concentration, 88–91
 metabolism, 559–561
 population control, 436–437
 process, 375–376
 Microbial fuel cell (MFC), 530–531
 active biocatalysts, 535–536

- Microbial fuel cell (MFC) (*Continued*)
- applications, 545–550
 - with biocathodes, 551f
 - calculations in, 540–541
 - challenges in, 540
 - conditions
 - in anodic chamber, 544
 - in cathodic chamber, 544–545
 - construction, 532–534, 540f
 - coulombic yield, 543
 - dual-compartment, 534f
 - electron
 - mediator, 538–539
 - transfer, 536–538
 - transport, 538
 - overpotential in, 542
 - PEM, 544
 - performance, 543
 - power generation, 541–542
 - single-compartment, 534f
- Microbial protein (SCP), 3t
- Microbiological media, 442–450
- Microcapsuls, 115–116
- Micrococcus*, 14–15
- Micrococcus glutamicus*, 3t
- Micrococcus luteus*, 286t, 350, 539t
- Microfiltration (MF), 457
- cross-flow microfiltration, 457
- Micromonospora purpurea, 351t
- Microorganisms, 1–2, 259, 558, *see also* Immobilized microbial cells
- under anaerobic growth conditions, 267
 - for citric acid fermentation, 365
 - immobilization by covalent bonds, 284
 - ethanol productivity, 288t
 - growth and colony formation, 286–288
 - microbial cells, 286t
 - oxygen transfer to, 284–285
 - studies of diffusion, 287t
 - substrate transfer to, 285–286
 - and media, 349, 470
- Microsparger, 56–57
- Microtubules, 351t
- Microwave sterilization, 450–451
- Milk, 1–2, 11–12, 432, 442
- Milling, 8, 15, 486, 609–610
- Mineral ions, 106t, 301
- Ming, 176t
- Minimal media, 297t, 301–303
- Mixed culture, 330, 427–428, 550, 621
- Mixed inhibitors, 31
- Mixed liquor suspended solids (MLSS), 457, 568, 576
- Mixing, 57, 63, 503–504, 520
- Mixing time, 201, 379–381, 385–388
- Mobile phase, 244
- Modified chemostat, 143
- Molar flux, 58–60, 64, 67
- Molasses, 5, 8, 14, 311b–312b, 367–370, 561–562
- Molds, 6–7
- Molecular sieve chromatography, *see* Gel chromatography
- Monilla* sp., 331–332
- Monod
 - constant, 278
 - model, 563–564
 - rate equation, 74, 141
 - rate model, 71
- Monod kinetic, 165b–166b, 278
- Monosodium glutamate, 14–15
- Morphology, 5–6, 133, 204–205, 286, 485
- Moser, 175–176, 176t
- MR, *see* Membrane reactor
- Mucor*, 16, 331
- Mushroom, 418–419
- Mutants, 14, 348
- Mycelia, 217–218, 231, 233, 332, 349–350, 363–364, 379
- N**
- N-acetylglucosamine peptidoglycans, 35
- N-acetylmuramic acid, 35
- NAD, 106t
- NAD/NADH, 106t
- NAD⁺, *see* Nicotinamide adenine dinucleotide
- NADH, *see* Nicotinamide adenine dinucleotide hydrogenase
- NADPH, *see* Nicotinamide adenine dinucleotide phosphate
- Nanobiotechnology Group contactor (NBG contactor), 516–517
- adsorbent contactors, 518
 - bed expansion, 518–520
 - characteristics, 518
 - equilibrium kinetic studies, 520–522
 - expanded bed adsorption, 522–523
 - fluidized/expanded bed adsorption, 518
 - hydrodynamic performance, 517
 - materials, 517–518
 - mixing of liquid phase, 520
- Natural polymer, 5, 115, 330, 509
- NBG contactor, *see* Nanobiotechnology Group contactor
- NBOD, *see* Nitrogenous biochemical oxygen demand
- Neosphenamine, 347
- Nephelometry, 332–333

Nernst, 110–111
 Neutral pH, 570–571
 Newtonian fluids, 62–63, 203–204, 220, 386b–388b
 Niacin, 36, 36t, 428–429
 Nicotinamide adenine dinucleotide (NAD⁺), 538
 Nicotinamide adenine dinucleotide hydrogenase (NADH), 28–29, 129
 Nicotinamide adenine dinucleotide phosphate (NADPH), 14–15
 Nicotinic acid, 35–36, 294t, 296t–297t
 Nitrate removal, *see* Denitrification biological
 Nitrification, biological, 579–586, 581f
 Nitrite nitrogen oxidation reaction, 582
 Nitrobacter agilis, 259–260
 Nitrogen oxides (NO_x), 462
 Nitrogen source, 4, 42, 49, 175, 293, 369–370, 431–432
 Nitrogenous biochemical oxygen demand (NBOD), 568–569
 Nitrogenous compounds, 461
 Non-mechanical methods, 498–499
 Non-stirred, non-aerated system, 194
 Noncompetitive inhibition rate model, 153–172
 Noncompetitive inhibitors, 33f
 Normal hydrogen electrode, 542
 Novobiocin, 379, 502
 Nozzle, 43, 233, 352
 Nuclear power, 598
 Nucleic acids, 114, 292–293, 301, 428, 432–433, 510–511
 Nusselt number, 203–204
 Nutrient requirements, 565–566

O

Off gas composition, 106t, 313b–314b
 Off-gas analysis, 56
 Oily wastewaters, 607
 Online gas chromatography, 56
 Open system, 133–137
 Optical biosensor, 117
 Optical cell density, 332–333
 Optical density, 79, 104, 164t, 271, 419–420, 472
 Optimum dilution rate, 478–479
 Optimum pH, 37
 Organic
 acids, 263
 fermentation of dual substrate, 264t
 production rate in ICR, 265–266
 compounds, 580–582
 fouling, 465
 matter, 573
 micropollutants removal, 461
 removal, 558–559

Organisms, 560
 Osmosis membrane bioreactor (OSMBR), 465–466
 OTR, *see* Oxygen transfer rate
 OUR, *see* Oxygen uptake rate
 Overpotential, 542
 Oxidase, 11, 28–29, 123
 Oxidation
 and cell synthesis, 571
 enzymes, 28–29
 oxidation–reduction process, 560
 Oxidizing bacteria, 3t
 Oxidoreductase, 28–29, 123
 Oxygen, 544
 limitation, 419
 requirements, 592–594
 transport, 67–68, 347
 Oxygen consumption, 195t, 313b–314b, 575
 Oxygen demand, 217–218, 568–569, 582–583
 Oxygen transfer rate (OTR), 54–57, 76, 359–361, 378
 in activated sludge, 399–410
 aerated tank for pharmaceutical wastewater, 76–78
 in fermenter, 58–59
 Oxygen uptake rate (OUR), 54, 394b–396b
 Oxyhemoglobin, 35–36

P

Palm oil, 602
 Paraffins, 66b–67b
 Partial pressure, 58, 67, 93, 398b–399b, 621–622
 Particles
 minimum fluidization velocity, 505–506
 terminal settling velocity, 506–508
 Partition chromatography, 244–245
 Pasteur, 7–8, 11–12
 Pathway, 6–7, 318, 320f, 429
 PDMS, *see* Polydimethylsiloxane
 Peclet number, 218–219
 Pectinase, 34
 Pellagra, 36
 Pellicular adsorbents, 509–510
 PEM, *see* Proton exchange membrane
 Penicillin, 346, 348–349
 extraction, 352
 filtration, 352
 production, 15–16, 325b–326b
 Penicillin G, *see* Penicillin
 Penicillinase, 346
Penicillium chrysogenum, 3t, 15, 248b, 287t, 348, 351t
Penicillium griseofulvum, 351t
Penicillium notatum (*P. notatum*), 348
Penicillium, 6–7
 Pentose, 330, 337
 Peptidoglycan, 346

- Peptostreptococcus*, 294
Permeate, 116, 459, 461, 470–472, 481
Pervaporation technique, 469–472, *see also*
 Ethanol—fermentation
Petri dishes, 353, 448
Petrochemical-based butanol production, 612–613
Petroleum, 422
PFN metals, 293–294
pH, 110–113
pH/redox measurement, 110–111
Phagocytosis, 347
Pharmaceutical, 2, 4, 28, 78, 461–462
Phenylalanine, 564
Phialides, 350
Phosphatase, 29, 559
Phosphate, 29–30, 419–420, 548, 559
Phosphate buffer, 292–293, 301, 419–420
Phosphate isomerase, 29–30
Phospholipids, 116
Phosphorylation, 28, 320f
Photoautotrophs, 560
Physical agents, 436–437
Physical sterilization, 437
Piezoelectric, 117
Pigment, 129, 348
Pilot scale, 105, 210, 451
Plant, 105–106, 376–384
Plant cell, 2, 194, 428–429
Plate filters, 231
Plates, *see* Theoretical equilibrium stages
Platinum resistance thermometers, 108
Plug flow, 71f
Polarographic
 detectors, 109
 electrodes, 110
Pollution, 569–570
Polyacrylamide, 262
Polyacrylamide gel, 40, 245–246, 261–262
Polyacrylate, 116
Polyamide, 357
Polycarbonate, 116
Polydimethylsiloxane (PDMS), 469
Polyethylene dioxythiophene, 115
Polyethylene glycol-dextrose, 250b–251b
polylactatic acid, 11–12
Polymerase, 35
Polypyrrole, 115, 533
Polysaccharide, 9, 33–34, 235–236, 447, 465, 623
Polystyrene, 262, 448
Polysulfone, 116
Polytetrafluoroethylene (PTFE), 469
Polythionine, 115
Polyuronic acid, 268
Polyvinyl alcohol (PVA), 484, 489–490
Polyvinylidene fluoride (PVDF), 465
Porous ceramic support, 490–491
Portion coefficient, 242
Postanoxic denitrification, 580–582
Potential, 110–111, 118, 120, 268, 350, 418–419, 483
Potentiometric detector, 123
Potentiometry, 117–118
POTW, *see* Publicly owned treatment work
Power consumption, 63, 376–377, 414b–415b
Power generation, 541–542
Power input, 358–359
Power law, 204–205
Power number (Re), 380, 382
Prandtl number, 203–204
Preanoxic denitrification, 580–582
Precipitation, 229, 239–241, 369
Precursors, 37, 565
Pressure cycle bioreactor, 195, 197
Primary metabolites, 318
Principle of chromatography, 246–253
Probe, 43, 54, 105–106, 109, 349–350
Process control, 105–106
Process integration, 511–513
Product inhibition, 185–186
Product recovery, 228, 238–240
Product yields, 140
 of biomass, 73
 calculation, 339
 coefficient, 339
Production of penicillin, 15–16, 348–349
Products, 10t, 11, 117, 314b–317b, 497–498
Programmed autoclave, 448–449
Prokaryote cell, *Streptomyces*, 6–7, 346
Promoters, 28, 30–31
Propeller agitator, 58
Propioni bacterium, 302t, 303
Propionibacterium acidipropionici (*P. acidipropionici*), 263
 ICR kinetic model for immobilized, 266t
 model test using, 265f
Propionic acid, 9, 472
Prosynthetic groups, 35–36
Protease, 11, 31, 34–35, 511
Protein
 concentration, 424–425
 process integration in protein recovery, 511–513
 products, 497–498
 purification
 dye ligand pseudo-affinity adsorption, 500–501
 strategies overview, 500
Protein recovery, 503, 511–513
Protein synthesis, 14
Proteolytic activity, 512

Proton exchange membrane (PEM), 544
 "Pruteen" protein, 427–428
 "Pseudo-ligand" adsorption, 500–501
Pseudomonas aeruginosa, 259–260, 287t, 535
Pseudomonas bacteria, 584
Pseudomonas methylotroph, 3t
Pseudomonas sp., 3t, 334t, 428
 PTFE, *see* Polytetrafluoroethylene
 Publicly owned treatment work (POTW), 570
 Pulse, 118, 520
 Pump, 43, 113, 134–137, 268–270, 544
 Pumping, 18, 58, 210, 419–420
 Pure culture, 7–8, 88, 334, 442
 Purification factor, 242
 PVA, *see* Polyvinyl alcohol
 PVDF, *see* Polyvinylidene fluoride
 Pyruvate, 318–319, 320f

Q

Quasi-equilibrium system, *see* Rapid equilibrium system

R

Racemic, 182f, 181
 Racemic ethoxyethylbuprofen ester, 182, 182f
 Racemic ibuprofen esters Membrane reactor, 181, 182f, 189
 Rapid equilibrium system, 187
 derivation of enzymatic rate equation, 187–189
 Raschig rings, 263
 Rate model, 71, 160b–162b, 167b–169b, 176
 Rate of biomass production, 140–141
 Rate of formation, 139, 178
 Rate of product formation, 139–141
 Rayleigh number, 219
 Reaction mechanism Competitive inhibition, 152–153
 Reaction-separation integration, 623
 Reaction–reaction integration, 622–623
 Reactor weight, 106t
 Recombinant *E. coli*, 3t
 Recovery time, 122
 Redox, 110–111
 Redox equations, 560
 Redox potential, 104–105, 549
 Reduction enzymes, 28–29
 Refractive index (RI), 338
 Removal mechanism, 568–569
 Residence time, 71–72, 621–622
 Residence time distribution (RTD), 517, 520
 Respiration, 53, 55
 rate, 217–218
 respiratory metabolism, 560
 Respiration, endogenous, 572

Respiration quotient (RQ), 53, 55–56, 304
 Response time, 122
 Reverse osmosis (RO), 460–461
 Reversible, 20, 35–36, 151–152
 Reynolds number (*Re*), 63, 203–204, 358, 380
 Rheology, 106t, 378
Rhizobium, 2
Rhizopus, 41
Rhizopus oryzae, 42, 46t, 48t
Rhizopus oryzae PTCC 5176, 42
Rhodocyclus gelatinosus, 299t
Rhodoferrax ferrireducens (*R. ferrireducens*), 532
Rhodospirillum rubrum (*R. rubrum*), 84
 RI, *see* Refractive index
 Riccati equation, 86
 Richards, 221b–223b
 Richardson–Zaki coefficient, 508–509
 Riser, 202
 Rising bubbles, 69, 218
 RNA, 30, 106t
 RO, *see* Reverse osmosis
 Rotameter, 105
 Rotary drum filter, 231, 369
 Rotary drum vacuum filter, 231
 Rotating disk contactors, 240–242
 Rotational disk foam sensor, 113
 round per second (rps), 63
 RQ, *see* Respiration quotient
 RTD, *see* Residence time distribution
 Rushton turbine, 57

S

Saccharifications, 34, 330, 430, 623
Saccharomyces cerevisiae (*S. cerevisiae*), 16–18, 267, 305
 active and fresh beads, 277f
 properties and appearance, 270t
 relative activities, 275f
 Safety factor (SF), 575
 Salting, 254
 Saturation constant, 334
 SBH, *see* Settled bed heights
 Scale up, 210–217, 376–384, 396b–397b, 402b–404b
 Scale-up bioreactor, 376–384
 Scanning electron microscope (SEM), 271, 484
 Schnidt number, 218–219
 SCP, *see* Single cell protein
 Scroll conveyer centrifuge, 233
 Second-generation biofuels, 602–607
 Secondary metabolite, 1–2, 14, 371–372, 418–419
 Secondary treatment, *see* Biological treatment
 Sedimentation, 235–236
 Seed culture, 367, 419–421
 inoculation, 336–337

- Selectivity, 245–246
- Self-producing microbes, 539
- SEM, *see* Scanning electron microscope
- Sensitivity, 123
- Sensors, 105, 113–114, 547
- Separation factor, 476
- Separation–separation integration, 623
- Sephadex, 252b
- Serine, 29, 116, 298
- Settled bed heights (SBH), 518
- “Seudo-affinity” adsorption, 500–501
- Severly, 177, 177t
- SF, *see* Safety factory
- Shear, 57, 78, 195, 202, 378
- Shear forces, 378–379
- Sherwood number, 218–221
- SHF, *see* Simultaneous hydrolysis fermentation
- Shigella*, 347
- Sigma factor, 234
- Sigmoidal S-shaped curve, 106–107
- Simultaneous hydrolysis fermentation (SHF), 622–623
- Single cell protein (SCP), 10–11, 317, 418–419
- advantages, 432–433
 - analytical methods, 424–426
 - batch experiment, 421
 - batch fermentation, 419–421
 - continuous fermentation, 419–421
 - disadvantages, 432–433
 - DO in, 419
 - for experimental preparation, 433
 - media preparation for, 424
 - microbial biomass separation, 421
 - microorganism growth, 422
 - nutritional value, 428–429
 - organism, 429–432
 - petroleum, 422
 - petroleum-based, 418–419
 - processes, 426–428
 - production methods, 422–424
 - substrates for, 429–432
- Slant agar, 334, 335f
- Slow-acting electrode, 107
- Sludge retention time (SRT), 570–571, 575, 577–578, 587–589
- SmF, *see* Submerged fermentation
- SMP, *see* Soluble microbial product
- Soda ash (Na_2CO_3), 567–568
- Sodium alginate, 270
- Sodium bicarbonate (NaHCO_3), 567–568
- Sodium hydroxide (NaOH), 567–568
- Sodium potassium tartrate, 270–271, 337
- Sol–gel process, 483–484, 491, *See also* Zirconia-alumina membrane
- Solid handling, 228
- Solid-state fermentation (SSF), 20, 41
- Solids partitioning, 576
- Solubility, 54, 64, 109, 228, 538–539
- Soluble microbial product (SMP), 464–465
- Solvent extraction, 239, *see also* Downstream processing
- continuous extraction column process, 240–242
 - product recovery by liquid–liquid extraction, 240
- Sorbose, 3t
- Sorghum, 601
- Soybean oil, 601–602
- Spargers, 199–200, 384
- Specific death rate, 139, 443–444
- Specific growth rate, 72, 95, 130–131, 176, 205, 431, 563
- Specific oxygen uptake rate, 259–260
- Specific uptake rate, 95, 259–260
- Spectroscopy, 129–130, 568–569
- Spirulina* algae, 10–11
- Sporulation, 349
- SRT, *see* Sludge retention time
- SSF, *see* Solid-state fermentation
- Standard calibration curve, 426
- Standard media, 301–303
- Staniskis, 176t
- Staphylococcus aureus*, 348
- Staphylococcus aureus*, 15
- Starch, 426, 431
- Static tray bioreactor, 42
- Stationary phase, 244, 333
- Steady state, 54–55, 72–74, 77, 142, 206, 378, 473, 589, 592–594
- Sterilization, 435–436
- batch, 437–439
 - chemical, 451
 - continuous, 439–441, 440f, 446b–447b
 - death rate of living organism, 437
 - dry heat, 450
 - electron beam, 451
 - with filtration, 450
 - high-temperature, 442
 - hot plates, 441–442
 - initial medium contaminants, 444b–445b
 - low-temperature, 452
 - media for microbiology, 442–450
 - microbial population control, 436–437
 - microwave, 450–451
- Steroids, 2, 37, 239–240
- Stirred tank bioreactor, 198–200
- scale-up of, 210–217

Stirred tank reactor, 195
 Stirring, 63, 486, 488, 490
 Stock culture, 334–335, 447
 Stoichiometric coefficient, 162b–163b, 304, 317, 572
 Stoichiometric coefficients for cell growth, 317
 Stoke's law, 233–234
 Stokes equation, 506–507
Streptococcus thermophilus, 3t
Streptomyces, 3t, 231, 233, 299t, 351t
Streptomyces erythreus, 3t, 351t
Streptomyces fradiae, 351t
Streptomyces griseus, 351t
Streptomyces mediterranei, 351t
Streptomyces nodosus, 351t
Streptomyces olivaceus, 3t
Streptomyces orientalis, 351t
Streptomyces rimosus, 351t
Streptomyces sp., 299t
 Streptomycin, 16
 Styrene, 242
 Submerged culture, 349–350, 354–355
 Submerged fermentation (SmF), 41
 Substrate, 114
 balance, 142–143, 412–413
 concentration, 73, 389b, 390t
 gradients, 259
 inhibition study, 183–185
 Substrate balance, 133, 142, 206, 412–413
 Substrate inhibition, 88, 93–94, 182–183, 183f–184f, 468
 Substrate limitation, 145, 175
 Substrate-driven denitrification, *see* Preanoxic denitrification
 Sugar analysis, analytical method for, *see also* Fermentation process application
 mixed sugar analysis, 337–338
 quantitative analysis, 337
 Sugarcane, 601
 bagasse, 42
 Sulfide, 549
 Sulfonamides, 347
 Sulfur, 549
 Sulfur dioxide (SO₂), 462
 Sulfuric acid (H₂SO₄), 615
 Sunflower oil, 602
 Superficial gas velocity, 385
 Superficial velocity, 61, 506–507
 Supplementary nutrients, 13, 292–293, 424, 429
 Surface tension, 62, 112, 221b–223b, 436–437
 Suspended growth, 586–594, 586t
 process, 558, 587
 Synthesis gas (syngas), 83–84
 Synthetase, 30
 Synthol

T

TCA, *see* Tricarboxylic acid
 Technology for cell recovery, 238
 Teflon, 116
 Temperature control, 18, 43, 104, 335, 499
 Temperature-phased anaerobic digestion (TPAD), 573
 Terminal velocity, 69, 219, 506–507, 519–520, 519f
 Tessier, 175–176
 Theoretical equilibrium stages, 503
 Theoretical yield of ethanol, 141, 319
 Theory of centrifugation, 233–235
 Theory of filtration, 231–233
 Thermal biosensor, 117
 Thermal conductivity Rotating disk, 112
 Thermal mass flow meters, 105
 Thermistors, 108, 117
Thermoanaerobacter ethanolicus, 330
 Thermocouples, 108, 117
 Thermopiles, 117
 Third-generation biofuel resources, 607–609
 Threonine, 116, 298
 TOC, *see* Total organic carbon
 Toluene diisocyanate, 116
 "Toprina" protein, 427–428
 Total organic carbon (TOC), 568–569
 Tower fermenter, 104, 384
 Toxin, 6–7, 174, 178
 TPAD, *see* Temperature-phased anaerobic digestion
 Trace metals, 95, 292–293, 344, 350, 368, 427–428
 Trace minerals, 293–294, 429
 Transducer, 117
 electrochemical biosensor, 117–118
 optical biosensor, 117
 piezoelectric biosensor, 117
 thermal biosensor, 117
 Transesterification, 607
 acid-catalyzed, 615f
 base-catalyzed, 614f
 enzymatic, 617f, 620t
 Transferase, 29
 Transmembrane pressure, 457
 Transmitted output signal, 107
 Tray bioreactor, 20–21, 42, 46–47
 Tricarboxylic acid (TCA), 84, 363–364
 Trickle bed, 196
 Tris maleate buffer solution, 300t
 Tryptophan, 36
 Tuberculosis, 349
 Tubular module, 71, 268–270, 463
 Turbidimetric methods, 332–333
 Turbidity, 332–333
 Turbidostat, *see* Biostat
 Turbulent flow, 63, 379, 398b–399b, 414b–415b, 505

Tyrosinase, 20
Tyrosine, 20, 116

U

Ultrafiltration (UF), 457, 469
Ultrasonic, 112, 619
Ultrasound, 113, 238
Ultraviolet spectrophotometry (UV spectrophotometry), 337–338
Uncompetitive inhibitors, 32, 32f
Unloading phase, 449
Unstructured kinetic model, 173–179
Unstructured models, 84–85, 90–91, 174–175, 371–372
Upstream processing, 11
Urease, 20, 30
Uric acid, 429, 432–433
Uricase, 20, 432–433
Urinary tract infection, 347
Uronic acid, 268

V

Vaccines, 2, 4, 497
Vacuum phase, 448
Valine, 298
Van der Waal's forces, 115
Vancomycin, 346
Vaned disk, 212f
Verlhurst, 174
Verlhurst model, 174
Viability of cells, 106t
Vinegar, 13, 408b–410b
Vitamin, 37, 428–429
Vitamin A, 37
Vitamin D, 37
Void, 244, 268–270, 279, 286, 508
Volatile fatty acid (VFA), 567–568, 574–575
Volatile organic compound (VOC), 578
Volatile products, 174
Volatile suspended solids (VSS), 566
Volatilization, 578–579
Voltammetry, 118
Volterra extended model, 174
Volumetric flow rate, 68, 205, 210, 234, 382–383
Volumetric mass transfer coefficient, 359

W

Wash out, 207
Waste cooking oils, 607
Waste sludge, 573
Wastewater, 76, 78, 548, 587–588
Wastewater treatment, 463, 547–550, 548t
Water–Gas shift reaction, 83–84, 93–95
Weber, 220
Westerhoff, 177t
Wet digestion, 622
Wet steam, 435–436
Wheat, 601
Whey, 431
Whole cell, 11, 123, 259–260
Wine, 1–2, 13
Wolfe's mineral solution, 301t

X

X-ray diffraction (XRD), 488–489
Xanthan gum, 9, 314b–317b
Xanthan gum production, 314–317
Xanthomonas campestris, 204–205
Xylanase, 34
Xylose, 263, 337

Y

Yeast, 2, 6–7, 236, 271, 279, 293, 426–427, 609
Yeast and malt extracts (YM extracts), 420–421
Yeast and Rennet, 3t
Yeast peptone glucose media, 302t
Yield, 5, 14–15, 20, 23, 41, 65, 73, 140, 163b–165b, 218, 239–240, 268, 281, 323b–324b, 339, 370–371, 400b–401b, 478, 575t, 607
Yogurt, 1–2, 7–9
Yue, 176t

Z

Zeolitic imidazolate frameworks-71 (ZIF-71), 613
Zirconia-coated alumina membrane, 484, 490
 fabrication of inorganic membrane, 485f
 inorganic acids, 485
 materials, 485–489
 methods, 485–489
 results, 491–492
Zymomonas mobilis, 267, 330, 608